AVIATION IN THE XXI-ST CENTURY

INTERNATIONAL CIVIL AVIATION ORGANIZATION
NATIONAL ACADEMY OF SCIENCES OF UKRAINE
MINISTRY OF EDUCATION AND SCIENCE,
YOUTH AND SPORT OF UKRAINE
NATIONAL AVIATION UNIVERSITY

PROCEEDINGS

THE FIFTH WORLD CONGRESS
"AVIATION IN THE XXI-st CENTURY"

"Safety in Aviation
and Space Technologies"

Volume 1

September 25-27, 2012
Kyiv, Ukraine

INTERNATIONAL CIVIL AVIATION ORGANIZATION
NATIONAL ACADEMY OF SCIENCES OF UKRAINE
MINISTRY OF EDUCATION AND SCIENCE,
YOUTH AND SPORT OF UKRAINE
NATIONAL AVIATION UNIVERSITY

PROCEEDINGS

THE FIFTH WORLD CONGRESS
"AVIATION IN THE XXI-st CENTURY"

"Safety in Aviation
and Space Technologies"

September 25-27, 2012

Volume 1

KYIV 2012

COFOUNDER

- ✈ National Aviation Academy State "Azerbaijan Hava Yollari" Closed Join-Stock Company, Azerbaijan

- ✈ Georgian Aviation University, Georgia

- ✈ JSC "Civil Aviation Academy", Kazakhstan

- ✈ Nanchang Hangkong University, China

- ✈ Vilnius Gediminas Technical University, Lithuania

- ✈ The State School of Higher Education in Chelm, Poland

- ✈ Moscow State Technical University of Civil Aviation, Russia

- ✈ The International University of Logistics and Transport in Wroclaw, Poland

- ✈ Polish – Ukrainian Research Institute, Poland-Ukraine

* Authors are responsible for the content of the report

SYMPOSIA

CONTENTS

SYMPOSIUM 1. MODERN SPACE AND AVIATION TECHNOLOGIES

1.5. Problems of recovery controllability of the aircrafts

1.11 Computer systems

1.12. Mathematical modeling and numerical methods

A.I. Bogdanovych, PhD Engineering (Nation Aviation University, Ukraine)

ESTIMATION OF MODIFICATION ACTIVATION ENERGY "ШХ15" IN FUEL AVIATION "TC-l"

In the results realization of the tribokinetic tests of the "ШХ 15" in fuel aviation "TC-1" and according to experimental-calculate method of estimation of kinetic characteristics and activation energy of 2-nd stage triboreaction-mechanical-chemical modification E_{TC-1}^{M} =0.296 kj/mol. This is 3-4 time less than analogues value of activation energy modification "ШХ 15" in fuel aviation "PT" E_{PT}^{M} =0.921-1,354 kj/mol.

Setup of the problem. The development of modern aviation, military, automotive engineering is impossible without increasing the reliability, durability, productivity, cost-efficiency of machines, mechanisms and their units. These requirements are especially important in designing, manufacturing and operation of mentioned above items as well as in their operation. Increased reliability, durability and cost-efficiency of these items depend on the surface durability of their individual units. In it is turn, the surface durability (wear-firmness) of structural materials of triboconnections cannot be increased and the antiwear properties of fuel and lubricants cannot be improved without conducting of tribotechnical tests. But for conducting of such tests it's necessary to use universal, energy, integral and invariant criteria, at least in one of the value ranges of loads (P), speeds of sliding and temperatures. The criterion that meets all the above mentioned requirements is activation energy, which is the whole three stages of triboreaction [1]. This criterion is an energy criterion in fact, integral and universal in application, invariant in the normal mechanical-chemical wear range, i.e. in the range of structural adaptation of the triboconnection materials, which has been proved experimentally [1]. The kinetic characteristics and activation energy of 2-nd stage - mechanical-chemical modification (E^{M}) for the fuel aviation "PT" and hydraulic oil "АМГ-10" were also determined [2].

Aim of the work – determination of the kinetic characteristics activation energy of 2-nd stage triboreaction - mechanical-chemical modification (E^{M}) for the fuel aviation "TC-1".

Calculation - experimental part. Calculation-experimental part. For the achievement of aim i used of the tribokinetic tests to determine the kinetic characteristics and wear activation energy "ШХ 15" in fuel aviation "TC-1" ("ДСТУ 320.001249943.011-99") fuel "TC-1", a production of the Kremenchug oil - processing plant conducted on the friction machine "КИИГА-2" [3]. Both hard-phased elements were produced with ball-bearing steel "ШХ15" (ГОСТ 801-78). Tests conducted by axis load P=98,l H, speed of slide V_{ck}=l,18 m/c without excess pressure in the cell, at two temperatures: T_1=333°K and T_2=303°K. Then, with the help of instrumental microscope "МИМ-7" at 70-divisible increment the diameter of the spot wear of every ball, was measured in two interperpendicular directions and the arithmetic value of diameters of the spots wear d, the mean value d of thee of spots wear - d_c and mean value d_c of thee or more tests were calculated. According to the method of carrying of tribokinetic tests, I calculate the value of the wear of every ball, which is the geometric form of the ball segment, diameter the base of which is the diameter spot wear. The sum of the volume wear of third balls (summary volume wear of one test) and calculated the arithmetic mean value of summary value wear of three or more tests V_c. Results of these tests we bring into table 1.

The next stage of the tribokinetic experiment is to calculate the speed of reaction wear w:

$$N = \frac{\lg \omega_1/\omega_2}{\lg a_1/a_2}, \qquad (1)$$

where V_{Cti} and V_{Cti-1} -mean value of the summary wear of the tree balls at moment of time t_i and t_{i-1} respectively.

The results of these calculations of w for every interval of time Δt are brought into table 1. The order of the reaction wear N^P was calculated for the initial Δt_1 and last Δt_3 interval of time using the next formula:

$$\overline{w} = \frac{Z_{t_i} - Z_{t_{i-1}}}{\Delta t}, \qquad (2)$$

where w_1 and w_3- speed of wear for interval of time Δt_1 and Δt_3 respectively;

V_{C1} and V_{C3} - mean of the three balls for intervals of time Δt_1 and Δt_3 respectively.

Table 1

Characteristics of the surface destruction 3-nd of the stage triboreaction-wear

Temperature of the tests, T, °K	Time of the tests, t_i, $\times 10^3$, s	Mean values of summary volumes of wear of the 3th tests, $V_c \times 10^{-3}$, mm^3	Speed of wear for intervals of time, $\Delta t \times 10^6$, mm^3/s	Order of wear N^P for interval of time Δt	Constants of speed of wear $K^P \times 10^{-3}$, s^{-1}	Mean values K^P, K_s^P $\times 10^{-3}$, s^{-1}	Coefficient of deviation of the estimation of K^P, w,%	Graphical value of K^P
303	1,8	0,87934	-	0,84	-	0,47455	4,6	tg24,5°=0,4557
	2,4	1,18034	0,50167		0,48713			
	3,0	1,58446	0,67353		0,48722			
	3,6	2,07816	0,82283		0,44931			
333	1,8	0,91013	-	1,01	-	0,98132	8,3	tg43,5°=0,9490
	2,4	1,71737	1,3454		1,02565			
	3,0	2,9643	2,07821		0,88781			
	3,6	5,61713	4,42168		1,0305			

The results of the calculation of the order of reaction of wear N^P are also brought into table 1. The constants of speed of wear K^P I calculate with help of the final value of V_c in intervals of time Δt, i.e. using the formula:

$$K^P = \frac{\Delta V_C}{\Delta t \cdot V_{C\ ap.}} = \frac{w}{V_{C\ ap.}} \qquad (3)$$

where V_{Cap} - mean arithmetic value of V_C at beginning and at the end of the interval Δt.
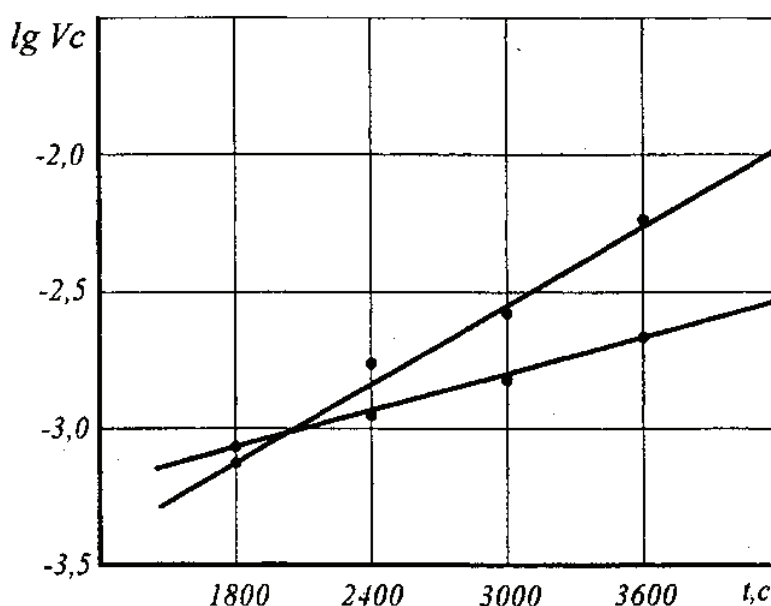
Fig.l Diagram of the dependence logarithm of mean values of summary volumes of wear of three balls in three tests (lgV_C) from of the tests (t): 1 - at 333°K, 2 - at 303°K.

The results of these calculations I also bring into table 1. I also bring the mean arithmetic values of K^P and coefficient of deviation of the estimation of K^P-W, which is calculated according to method of the calculations of measurement errors of the physical quantity [4].

Kinetic characteristics of 2-nd stage triboreaction determine to secondary structure concerning area:

$$\delta = \frac{S_{BC}}{S_K} 100\%, \qquad (4)$$

where $S_к = S_1 + S_2 + S_3$ - full area contact equal sum of wear areas third balls;

S_{BC} - secondary structure area, calculate to formula:

$$S_{BC} = S_K - \frac{\Delta V_{cp}}{\Delta t \cdot K^P \cdot h_{BC}}, \qquad (5)$$

where $\Delta V_{cp} = V_{cp\,ti} - V_{cp\,ti-1}$ – interval of meanings summary value wear of three balls according to two meanings interval Δt, $V_{cp\,ti}$- t_i and $V_{cp\,ti-1}$- t_{i-1} according to;

h_{BC} – thickness secondary structure or thickness mechanical-chemical modification.

Results of calculations. Results of calculations determined S_{BC} and δ according to equations (4) and (5), results of calculations of the order reaction modification (N^M) the constants of speed modification (K^M), coefficient of deviation of the estimation of the estimation of K^M – W^M bring into table 2.

Table 2

Kinetic characteristics of modification 2-nd of the stage triboreaction

Value						Mean values K^M, K_c^M x10⁻⁴, s⁻¹	Coefficient of deviation of the estimation of K^M, w_K, %	Graphical value of K^M
Temperature of the tests, T, °K	Time of the tests, t_i, x10³, s	Secondary structure area, S_{BC}, mm²	Secondary structure concerning area, δ, %	Order of modification for interval of time, N^M	Constants of speed of modification K^M x10⁻⁴, s⁻¹			
333	1,8	2,06505	89,814	$N_{1-3} = 0,79$	0,59626	0,61138	3,1 %	tg147⁰=0,613
	2,4	2,36979	86,478		0,63071			
	3,0	3,05082	83,449		0,59416			
	3,6	4,04623	80,163		0,62437			
303	1,8	1,77638	89,613	$N^M_{1-3} = 0,87$	0,60864	0,60721	2,5%	tg148⁰=0,601
	2,4	1,98882	86,480		0,59313			
	3,0	2,2321	83,425		0,59947			
	3,6	2,48635	80,341		0,62761			

For control of the correction of the of the determination of the kinetic characteristics of modification N^M and K^M, calculated by equations (1) and (3). I build the diagrams of the dependence of lgδ from time of the tests (t) (fig.2). The linear dependence of lgδ from t confirmed the order of the reaction $N^M \sim 1$ and set the value of K^M graphically, which is equal to the tangent of the angle of inclination of the straight line to the axis OX. This value of K^M is also brought into table 2.

Thus, knowing the value of K^M at both temperatures $T_1=333°K$ and $T_2=303°K$, according to the equation of Arrenius, the value of the modification activation energy (E^M) calculated:

$$E^M = \frac{RT_1T_2}{T_1-T_2} ln\frac{K_1^P}{K_2^P} = \frac{1,9144T_1T_2}{T_1-T_2} lg\frac{K_1^P}{K_2^P} = \frac{1,9144 \cdot 333 \cdot 303}{30} lg\frac{0,61138}{0,60721} = 0,296 \ (kj\,/\,mol\,),$$

where R – universal gas constant.
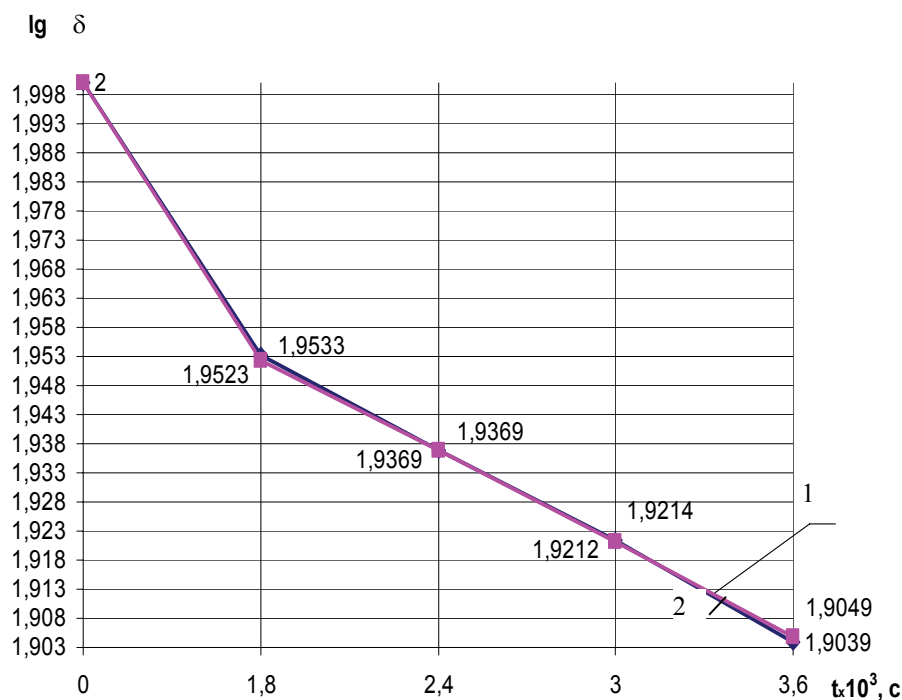
Fig.2 Diagram of the dependence lgδ from the time of the tests (t): 1 - at 333°K, 2 - at 303°K.

Conclusions

1. Results calculations of kinetic characteristics and modification activation energy confirmed adequacy of kinetic model normal mechanical-chemical wear and constructive of experimental-calculation method of estimation kinetic characteristics and activation energy of three stages triboreaction [1].

2. The established value of activation energy 2-nd stage triboreaction - mechanical-chemical modification "ШХ 15" in fuel aviation "ТС-1" (E^M_{TC-1} = 0,296 kj/mol) approximately 3-4 time less than analogous value E^M in fuel "РТ" (E^M_{PT} = 0,921...1,354 kj/mol) [2].

3. The established value of E^M_{TC-1}=0,296 kj/mol in the fuel "ТС-1" replenished the bank of data of modification of the steel "ШХ15" and antiwear properties of the fuel "ТС-1" and matrixical energy - activation criterion of estimation of construction materials, antiwear properties and modification of combustible - lubricant materials and combinations of these materials [5].

References

1. *Богданович А.И.* Кинетические и энергетико-активационные характеристики износостойкости и совместимости материалов трибосопряжений: автореф. дис. канд. техн. наук. - Киев, 1987.-20 с.

2. *Богданович О.І.* Використання енергії активації 2-ї стадії тріброеакції як критерій оцінки механо-хімічного модіфікування. – Вісник Харківського національного технічного університету сільського господарства ім. П.Василенка, вип. 39., Харків, 2005, с.141-148.

3. *Аксёнов А.Ф.* Трение и изнашивание металлов в углеводородных жидкостях. -М: Машиностроение, 1977.-147 с.

4. *Зайдель А.Н.* Ошибки измерений физических величин/ изд. перераб. и доп.-Л.: Наука, 1974.-108 с.

5. *Бершадский Л.И., Богданович А.И., Назаренко П.В.* Энергетико-активационный матричный критерий совместимости. В кн.: Триботехника - машиностроению: Тез. докладов Ш Моск.: научно-технической конференции (2-4 сентября 1987г.), М.,1987,с.67-68.

UDC 629.735.083

A.Tamargazin, Doctor Engineering, I.Linnik Ph.D. Engineering, M.Oleg, T.Kramarenko
(National Aviation University, Ukraine)

THE PROBLEM OF KEEP OF AIRCRAFT PARK AIRWORTHINESS
IN THE PROCESS OF THEIR OPERATION IN AIRLINES

The article deals with the problematic issues of status and development of Ukraine's aviation system, allowing to give an objective assessment of scientific and practical importance, the role and place of the most complex set of tasks on establishment and maintaining the airworthiness of aircraft operated by airlines of Ukraine, in order to ensure efficiency and safety.

The level of safety of civil aircraft (CA) is primarily determined by the efficiency of the existing system to maintain their airworthiness. The problem of airworthiness maintenance has been solved at all stages of formation and development of Civil Aviation, and is currently the focus of international aviation organizations and governmental authorities. At each stage, in accordance with the requirements of the time, a certain system of airworthiness maintenance of aircraft and the corresponding system of legislative, regulatory and technical documentation acted [1].

New economic relations in Ukraine, and consequently, a change of principles, rules and forms of state regulation and control in aviation led to a significant change in the requirements of the standardized security and monitoring to ensure airworthiness of aircraft at their manufacturing, testing and maintenance.

Current requirements of regulatory assurance and controls of aircraft worthiness implement in their development in a state of reliability, durability, capability, persistence, operational and maintenance manufacturability, testability, etc. However, the shape and content of the continuing airworthiness of aircraft in the process of continuous operation depends to a much greater degree on the strategies, methods, modes of maintenance and repair, the economic and institutional arrangements and other aspects guided on continuing of aircraft worthiness.

Of particular relevance the problem of maintaining the aircraft worthiness acquires in the present working conditions of air transport in Ukraine, which are characterized by: the formation of a large number of private airlines (over 60%), some of which do not have enough of their industrial and technological base, a significant amount of the aircraft, having the operating time and service life (over 70%), lack of budgetary financing for the maintenance of airworthiness, the lack of investment in fleet renewal, the imperfection of the governmental system of certification in aviation. The latter circumstance is connected to the fragmentation of aircraft technique certification itself and air transport facilities, the lack of unified methodology for creation of mantioned systems, as a result there is no implementation of a systematic approach to solving a complex interrelated set of tasks of ensuring the aircraft worthiness and maintenance.

Issues of maintaining airworthiness are contained in a number of other existing normative documents, regulations, standards, which, however, also aren't merged into a single system. However, there are no regulations addressed to the problems of maintaining the airworthiness of the direct statement, as provided in the ICAO documents [2,3].

It should be noted that the problem of securing and maintaining of aircraft worthiness is paid constant attention by aviation experts of organizations and companies of the aviation industry and civil aviation.

Systemic crisis, which is observed almost everywhere in the world and particularly in the former Soviet Union due to the changes in socio-economic structure, to a large extent has affected Ukraine's aviation. This becomes more important due to the fact that the country is situated in the extreme geographical and geo-economic conditions, and any activity in Ukraine is characterized by its proximity to the threshold, forbidden indicators of real threats to national security in the political, social, economic and military spheres. Any kind of manufacturing in our country requires much more expenses than in any other industrial area in the world. The severe climate leads to the fact

that the life and production requires a large expenditure of energy. The expenditures for energy, heat and energy resources make domestic products are generally non-competitive. And it will be more evident the more active participant will be Ukraine in the globalization process. Therefore, at each stage of historical development, we must be able to do what other can't do.

The Ukrainian aviation (Aviation Complex), in the times of the Soviet period, was separated into two independent, often competiting, vertically integrated structures (Aviaprom and Civil Aviation), and it made a hard way at its stages of transformation from the planning and distribution economy to the market one. A series of unsystematic solutions and the negative consequences of their implementation, defined as reforms, led aviation complex of Ukraine to the brink of collapse. Neither in pre-reform period nor during reforming was proclaimed only precise reconstruction programs, but even more or less distinct slogans.

In the absence of regular large orders from the Ukrainian airlines (as a consequence of the break between the Aviaprom and Civil Aviation), in the last decade they faced the unprecedented five times for the global practice of declining demand for passenger transport. The domestic aviation industry, designed to meet the needs of very different scales in the aircraft was forced to operate in a single mode of supply.

In the late 70's – early 80's of the previous century Aircraft industry was modernized with the introduction of new technologies, mastered the production of fourth generation aviation. Today, having missed a technological breakthrough, it remained at more than twenty years' prescription. At present the Ukrainian aviation industry, according to experts, is characterized by high levels of low-volume production and isolation from marketing outlets. At the present stage we are only beginning to talk about the uncertainty of the priorities of Ukraine's aviation system. But this prolonged consciousness took too much time.

In the aviation sector of Ukraine it is time to put an end to the flourishing of unqualified monopolism for the creation, improvement and development of "something". Lack of legal regulations, protecting governmental and social infrastructures, and research organizations of industry from unfair and unwarranted permanent structural and institutional reforms, is one of the main problems. Structural changes that occurred in the civil aviation of Ukraine for the past twenty years are characteristic example.

The inability of the aviation industry authorities systematically comprehend the current events makes one in the first place to focus on finding ways to move to the near goal, and not on output of long-term goals. The logic of the mechanical duplication of an uncomprehended experience of developed countries dominates above them. The inertia of this process turns the Ukrainian aviation on a path that is deprived of future prospects.

Today we are witnessing the conquest of our aviation market, which began after the introduction into the Ukrainian air force of western standards and regulations. The same scenario the United States used to seize the Chinese aviation market, starting with legal and regulatory environment - they translated into Chinese their own rules (FAR) and lobbied their adoption as Chinese national aviation regulations, after that they stepped to the mass supply of aviation technology (AT) on the China aviation market.

The repetition of the scenario is clearly evident in Ukraine, where is being introduced only western aviation technologies, at the same time the Western system of aviation standards not harmonized with Ukraine are actively implemented in practice. At the same time, these actions are fully supported by the state Department of Civil Aviation of Ukraine, which first of all must pursue the high goals of the national level.

Global problems are acting as sources of emergency situations leading to a crisis. In the thesaurus the word "crisis" is treated as a sudden drastic change in something, like an acute shortage or lack of something, as a difficult and dangerous situation. Exactly in the latter sense, the term "crisis" is most often used in the theory of risk management.

The most dangerous today is a systemic crisis, in which turned out to be Ukrainian aviation complex. This crisis has affected all structural areas, and they can not get out of it, taking only a few steps, or introducing reforms in one direction only.

Today the aviation system has no major goals and objectives that need to be system-forming. Some of its structural parts (artificially divided into Aviaprom and Civil aviation) solve their problems at the expense of solving the problem as a whole. Unregulated separate development of these structures has led to quite unexpected results. Now the Ukrainian Aviation entered the stage of a systemic crisis, in which the negative trends of the last twenty years begin to lead to new types of disasters. The disasters of the recent years have shown that the ordinary technical solutions or not adoption of the ones resulted in a long chain of reasons and effects that led to tragic consequences and great losses. It should be kept in mind that the reinforced efforts of the influence spheres of aviation market, both international and domestic, went mainly to the phase of technological and military confrontation, that is, in this situation, we can speak of a deterioration in the level of "technological safety", which determines the degree of protection of human, society, the objects and the environment from the risks associated with the ungrounded creation or not creation of technical systems, technological processes and materials ensuring the achievement of fundamental national interests. At the same time, scientists believe that technological security is becoming the assurance dominant of "anthropogenic safety."

The causes of this instability can not be explained merely by "human factor". Perhaps the time has come to solve the problems of personal liability for breaking the level of "technological safety."

Science at the present level may provide mechanisms for the development of security strategy, basing on the ideas of the risk theory. Overcoming the crisis requires a different level of monitoring and other mechanisms, management tools, use of other technologies. In order the new mechanisms play their role, both political will and constant systematic efforts not only researchers', but of many government institution are required.

Moreover now, it's hard to tell how efficient created the system and technologies will be, and how much efforts will require their refinement as needed.

Management is an integrated process. Actions (or lack thereof) in one direction usually affect the other direction. This relationship leads to the following: an improvement in one area can only be achieved at the expense of another. This happened between the Civil Aviation and Aviaprom, when the increase in traffic volume in the Civil Aviation was achieved through the elimination of the Ukrainian one and purchasing of foreign aircraft by Ukrainian airlines, i.e., in connection with the reform the interaction of airlines and aircraft manufacturers almost stopped. Companies Boeing and Airbus have expertly taken an advantage of this for their expansion in Ukrainian market, using their possibilities represented by the Ukrainian legislation. According to experts in relation to the penetration of western aircraft on the Ukrainian market the following trends and factors are observed:

– the secondary market of western aircraft, is basically, the aircraft of 80-90th of the last century, made in the USA, where has come a period of change of exploited aircraft model range, which coincided with the crisis;

– a powerful political and economic pressure and support (lobbying) by governmental and public finance institutions of U.S. and the EU, interested in the technical re-arming of their airlines;

– externally attractive, but in general, ruinous to the Ukrainian airlines, terms of aircraft delivery and the operation (leasing, hire purchase, discount);

– the lack of legislative barriers and non-tariff regulation in Ukraine on the way of penetration of the western aircraft production to the Ukrainian market;

– unsystematic (spontaneous) assumption of untrained base of used Western aviation equipment would destroy the already fragile single technical space of Ukrainian aviation industry;

– the introduction of mass production of the western aircraft will require solid investments to change the whole system of Ukrainian airworthiness and ground infrastructure;

– today's Ukrainian airports and airport structure is not ready for regular operation of western aircraft on the Ukrainian airfields, as noted by western manufacturers (Boeing);

– taken at exploitation the Western aircraft will require the replacement of Ukrainian legislative base which is not harmonized with western law, this will result in the destruction and collapse of a single technical space of Ukraine;

– to give western aircraft Ukrainian domestic market, which is a capacious market of regional aircraft, it means to put the country into a technological dependence on the West.

– the inability of the tariff regulation of the airplanes in terms of Ukraine's accession to the WTO, if there is no working mechanisms to tariff regulation.

Today a negative impact on the image of Ukrainian aviation has the absence of Agreements on Admission of Ukrainian Certificates of Aviation Equipment in the West, as well as facilitated in the 90's the mode of certification of the western aviation equipment in Ukraine. Where and who is responsible for this, including the relation to the state-developer? This is a prime example of political lobbying of western aviation equipment on the Ukrainian market in the absence of Ukrainian aviation support (political lobbying). In Western countries manufacturers of civil aviation receive an unlimited political, diplomatic and economic support of their governments, which, in order not to attract the WTO authorization, made it necessary to develop series of complex and specific financing measures. An example of political lobbying of the interests in the world is Boeing Company. The visit of U.S. President to India in summer of 2006 was an Indian order of passenger planes for 1.5 billion dollars to Boeing firm in late 2006.

It should be noted about the appeared problems with Western aviation technology at the Department of Defense related to ensuring the country's defense. This is due to the fact that the Soviet aviation technology has always been of dual-use, and now refunding of domestic airlines fleet is mainly due to the purchase of Western aircraft that can not always be applied in complex situations, such as the occurrence of man-made or climate disasters. And they are especially not suited for the tasks set before the civil aviation in the event of armed conflict. They have other characteristics of the landing, maintenance, placement of goods.

Solving the problem of providing the aviation security is fulfilled at three levels: International (global and regional – regions of the world); National (specific country, regional – regions of the country); Private (company or individual). These levels differ radically from each other by the set of problems and indicators that characterize them, as well as their goals. The objectives of the unit at a lower level may not only be different but be in conflict with the goals of the security unit of a higher level. We can observe the events, when the goals of airlines as to aviation equipment not coincide with the goals of the state at a strategic level, and regulatory institutions of civil aviation, following the airlines make decisions that lead to the destruction of the aviation complex of Ukraine. Being tactically justified for the commercial interests of airlines, the practice of importing of old western aircraft is contrary to the strategic interests of the state and passengers, whose lives and health are directly dependent on the state of the airlines' fleet.

Conclusion. In accordance with the ICAO rules the country of airplanes registration bears full responsibility for the airworthiness of aircraft, listed in its registry. Ukrainian aviation authorities dissociated themselves from all control for the airworthiness of the western production aircraft flying in Ukrainian airlines, having given their registration and legal regulation of operation not even to the western states but their colonies (for example, to the Bermudas, which is a protectorate of Britain, and where registered many of western production aircraft, flying in Ukrainian airlines).

The priority measures should be the improvement of the legal base through the supplement with rules of direct action, which should not have retroactive effect and worsen the conditions of the aviation system functioning. It should be considered the establishment of single regulatory environment through the gradual convergence of Ukrainian aviation legislation with that of Western (mainly European countries), make a gradual transition to single rules and regulations.

References

1. *Тамаргазін О.А.* Системи технічного обслуговування пасажирських літаків. – К.: КМУЦА, 2000. – 268 с.

2. ICAO DOC 9760 Airworthiness Manual Volume I – Organization and Procedures, 2001.–93 p.

3. ICAO DOC 9760 Airworthiness Manual Volume II – Design Certification and Continuing Airworthiness, 2001. – 326 p.

V.P. Royzman, Dr.Sc. (Khmelnitsky National University, Ukraine)

VIBRATION AND BALANCING OF AIRPLANES AIRCRAFT PROPELLERS BY LINEAR AND NONLINEAR CORELATIONS

The report gives methods of reducing vibrations by balancing propellers directly on the airplanes when running the engines with the working frequencies of rotation. The report shows the existence of another type of exciting force generating vibrations of every blade, its frequency is that of the first harmonic of the propeller. This excitation occurs during the so called "sloping" blowing around the rotating. Propeller when the air flow is going round the airplane in the directions perpendicular to the longitudinal axis of the plane.

One of the principal sources of vibrations and noise caused by the turboprop engine of an airplane passed on to the engine and further on to the airplane itself is that of an aircraft direct-drive propeller.

The exciting force of the aircraft propeller is generated by static, dynamic and aerodynamic imbalance of the blades thereof. The imbalances mentioned in the report make up forces and momenta the rotation frequency of which coincides with that of the propeller itself causing movement along a closed curve of the engine-motogondola installation with the frequency thereof coinciding with that of the first harmonic of the propeller. This movement is received by the vibrating sensors, inserted in the case of said engine as vibrations of the same frequency.

The report deals with the cause of coming about the above imbalances and methods of eliminating thereof. The emphasis is laid on the fact, that the effects of the above forces and momenta might be added or minimized by means of balancing.

The report shows the existence of another type of exciting force generating vibrations of every blade, its frequency is that of the first harmonic of the propeller. This excitation occurs during the so called "sloping" blowing around the rotating. Propeller when the air flow is going round the airplane in the directions perpendicular to the longitudinal axis of the plane.

Such Interaction of the rotating aircraft propeller with the air flow is observed during the evolution of the airplane especially during its slipping turbulences lifting off when taking off as well as in the moments of touching down when landing with the airplane wearing upon its undercarriage or in case of a strong lateral wind.

The generation of the above vibrations is shown in fig.1, according to which during one revolution of a blade rotating with the velocity **W** of the propeller's shaft, which is blown around by the air flow **V**, said blade during the first half of its revolution "runs away" from the flow so that its fibers with the dot. **A** plotted upon then are stretched out during bending; of the blade and those with the dot. **B** are shrunk. During the second half of the revolution said bland "runs upon" the flow and fibers with the dot. **A** plotted thereupon are shrunk and those with the dot. **B** - are stretched out.
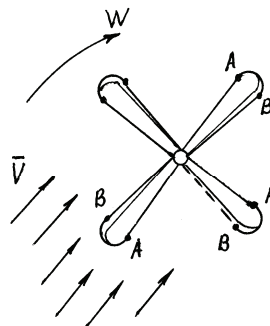
Fig. 1. Diagram showing generating vibrations in a blade during the
"sloping" blowing around the propeller

Thus during one revolution of the propeller's shaft every of the blades thereof performs one complete bending vibration. This phenomenon grows dangerous when the proper frequency of the blades vibration is near to that of the propeller's rotating (taking into account the centrifugal tension during the rotation), inasmuch as in practice there occurred breaks up of blades during the flight and (or) deformations of the redaction gearbox parts.

The proper frequency of the blades vibrations during the propeller's rotation was measured by throwing upon them rubber balls weighted 10H.

The experimentally measured tensions in the "sloping" blowing around reached for some airplanes up to 100MPa and more and may damage the material of the blades.

The report gives methods of reducing vibrations by balancing propellers directly on the airplanes when running the engines with the working frequencies of rotation, A. special emphasis is laid on methods of providing for two starts using experimental masses and a marker of position of said blades relating to the vibrating sensor as well as three starts but without the above marker. The vibrating sensor is mounted on such a place of the engine's case, where the dependence of said vibrations on the weight of the load inserted in the propeller is the nearest to the linear.

The balancing based on linear correlation is carried on as follows:

1. In case of said engine functioning with the working frequency of rotation the vibrations and signal of the marker thereof are registered upon the tape of the oscillograph.

2. In the place of the propeller independent on the angle of blowing around an experimental load is inserted with the above measurements being repeated.

3. From the vibrations vector $\overline{A}_2$ (fig. 2) in case of using said experimental load the above vector A_1 is subtracted in case of initial imbalance. Then vector $\overline{A}_2 - \overline{A}_1$ gives the value of said vibrations from the experimental load P_{exp}. The weight of the balancing load P_{bal} is measured according to the formula

$$P_{bal} = P_{exp} \frac{\overline{A}_1}{\overline{A}_2 - \overline{A}_1}.$$
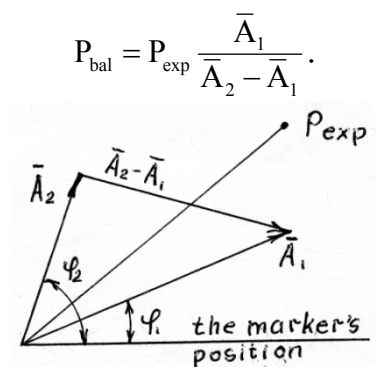
Fig 2. Vectors plotted when defining said balancing load

The place of inserting said balancing load is defined between the position P_{exp} and the vector of vibrations $\overline{A}_2 - \overline{A}_1$ by the phase difference. If the dependence of the amplitudes and the vibrations phases of the engine on the experimental loads inserted in the aircraft propeller are far from the linear, the balancing is repeated with the start with said experimental load being regarded as an initial and that with the balancing load – mas experimental.

Said balancing was carried on for various types of aircraft propellers, engines and airplanes providing for reducing several times their vibrations according to the first propeller harmonic.

References

1. Левит М.П., Ройзман В.П. Вибрация и уравновешивание роторов авиадвигателей. Машиностроение, Москва, 1970г.

M.N.Regulsky, Ph.D. Engineering, A.D. Pogrebniak, Ph.D. Engineering,
(S.P. Tymoshenko Institute of Mechanics, NAS, Ukraine),
O.I.Yurchenko, O.S.Tugarinov, Ph.D. Engineering,
(National Aviation University, Ukraine)

CALCULATION-EXPERIMENTAL METHOD OF SHELL STRUCTURES LIFE ESTIMATION

In this work, calculation-experimental method of the large-sized shell structures fatigue life estimation is covered. The life calculations are made based on the interpretation of the shell fragments fatigue test results using the statistical model, initial data for which are life distribution function parameters of fragments or model samples.

Introduction. The experience of creation of critical structures operating at alternating loads shows, that at the final stage of experimental engineering development, researchers always strive to get experimentally supported estimates of fatigue resistance characteristics, as it is admitted, first of all, in the aircraft industry, and also other machine building industries. However, full-size field fatigue tests performance for the large-sized structures causes serious difficulties of both technical and economical character.

In many cases, the difficulties that occur are overpassed using the tests of the structure fragments, containing potentially hazard areas and limiting the entire structure strength. Based on the results of such tests and their appropriate interpretation, the methods of calculation-experimental estimation of various large-sized structures types are developed.

Generalized stages of development of the large-sized shell structures life prediction calculation-experimental method using an approach, involving componentwise fatigue tests, come to the following sequence:
– prediction or identification of potentially hazard areas in the structure (by calculation or experiment);
– separation of the fragments containing hazard areas from the structure, considering the possible load application diagrams during tests;
– selection of the forms and sizes of test samples, for which either natural fragments or model samples may be used, which configuration is obtained by the fragment form optimization;
– selection of the loading diagram at tests and development (if needed) of the specialized test procedures;
– comparative analysis of the stress and strain state in the area of predicted failure of the structure and test sample (fragment);
– actually, fragment fatigue tests at selected loading conditions (basic experiment);
– test results interpretation to predict the structure life, and possible error estimation.

The structures, allowing the componentwise tests (with appropriate fragments cut or special production) may include, for example, some types of the case thin-slab structures [1,2], frame and truss structures [3], and also those that contain a number of identical components [4].

In the work [5], the implementation of abovementioned generalized stages is shown at development of calculation-experimental method of fatigue life prediction of the circular concentrator cylindrical shells, loaded with axial distributed forces of cyclical character. The method idea is that the shell is fragmented along the generating lines and the fragments life is tested at cyclical tension-compression, having provided the same ratio of stresses from the axial force and wall bending moment as occur at the fragments operation inside integral shell. The fragments (model samples) test results are the initial statistical data for the scale effect calculation and thus, obtaining probabilistic fatigue resistance characteristics of the large-sized circular concentrator shells.

Method implementation and main calculation ratios. Cylindrical shell with the circular stress concentrator under the action of axial linear loads of cyclical character is examined.

A peculiarity of its loading in the concentrator area is the bending moments initiation, caused by unilateral wall thickness change because of circular recess or belt. In the concentrator area the shell is loaded with axial linear load T_x and longitudinal line bending moment M_t, approximate value of which is determined by multiplication of the longitudinal force T_x by the semidifference of major and minor shell wall thicknesses. To the effect of the same loads, the fragment or model sample must be exposed at testing (Fig.1). As a coupling parameter between the hazard area stress state of the model sample and shell, the bending coefficient K_b, is admitted, which determines the bending and tension ratio in the concentrator area and is equal to the maximum bending and tension (compression) stresses ratio in section of the concentrator diametral symmetry plane in the shell or model sample (points 1 and 3 in Fig. 1a).
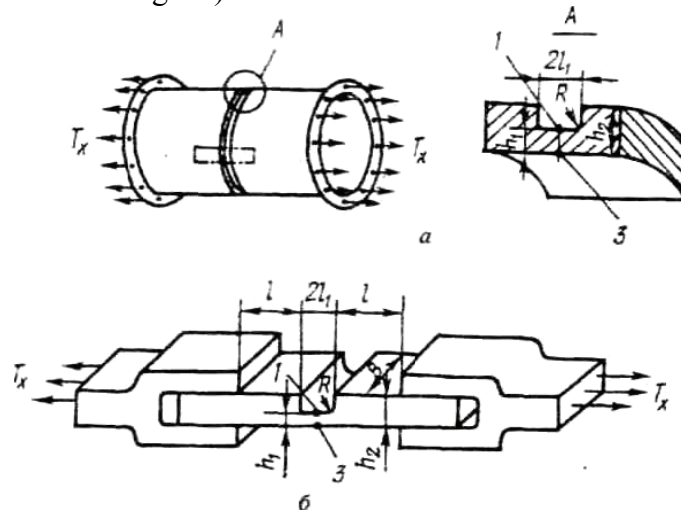
Fig. 1 The circular concentrator shell (*a*) and its fragment (model sample) in grips (*b*), loaded with axial linear load T_x

Comparative analysis of the concentrator area stress state in the shell and model sample showed, that having provided the balance of axial linear loads T_x and bending coefficients K_b for the shell and model sample, it is possible to reach the stress state identity by the first primary stress and the first primary stress gradient, i.e. by those stress state factors that have a determining influence on fatigue characteristics.

If to see the shell as a system, containing a number z of the same simultaneously operating fragments, in this case the event is of interest that at some constant level of the stress amplitude σ_a (or axial linear load T_x), a failure of at least one of the shell fragments will occur during its number of cycles running N_R^{ob}. This event is identified starting from the limit shell state occurrence and is registered by the first fatigue macrocrack occurrence. It is supposed, that the fragment or model sample limit state in basic experiment must be registered by the same size crack occurrence (0,5…1,5 mm). The stage of fatigue crack development in this case is not examined, which is specific for a number of critical structures.

At the uniform axial linear load distribution along the shell perimeter (all the fragments are loaded the same), formula of transfer from the fragments life distribution function to the shell life distribution function has the following form [5,6]:

$$P^{ob}\left(N_R^{ob}\right)=1-\left(1-P^{fr}\left(N_R^{fr}\right)\right)^z, \qquad (1)$$

where $P^{ob}\left(N_R^{ob}\right)$ – value of the shell life distribution function at the constant level of axial linear load amplitude T_x; $P^{fr}\left(N_R^{fr}\right)$ – value of the fragment life distribution function, correspondent with the same argument value (i.e. $N_R^{ob}=N_R^{fr}$) and the same T_x level; z – number of the shell fragments; N_R^{ob} and N_R^{fr} – numbers of cycles before the shell and fragment failure, respectively.

Predicted shell lives are determined using the function, reciprocal to the shell lives distribution function $P^{ob}\left(N_R^{ob}\right)=f\left(N_R^{ob}\right)$, i.e.:

$$N_R^{ob} = f^{-1}\left(P^{ob}\left(N_R^{ob}\right)\right). \qquad (2)$$

Registration of the ratios (1)-(2), expressing mathematical formulation of the examined shell life statistical model, supposes independence of events, consisting fatigue failure sites generation in various shell fragments, which corresponds with abovestated shell limit state formulation.

Fragment lives distribution characteristics data at the several cyclical load levels, enable to create predicted shell fatigue curves based on the failure probability parameter.

Results of the method experimental approval. Experimental procedure for identification of fatigue life of the model samples, shell fragments and available size shells, tested to approve the calculation-experimental method of fatigue life prediction for the circular concentrator cylindrical shells, have been already particularized in [5,7]. Here, we will stop only on the findings and main conclusions based on performed tests.

Predicted and experimental lives comparison was performed for the shells with circular concentrator made of alloy AMr6, which configuration and sizes are shown in Fig.2. As the test samples in the basic experiment, the natural fragments were used, cut from the shell and fatigue tested at symmetrical load cycle with the nominal stress amplitude $\sigma_a = 65$ MPa, under which in this case we mean the quotient of axial linear load division by the minor fragment or shell wall thickness i.e. $\sigma_a = T_x/h_1$ (Fig.1).

The estimates for parameters of empirical shell fragments life log distribution according the ten samples test results were: mean life log $lg\,N_R^{fr} = 4,54$ and meansquare life log deviation $S\,lg\,N_R^{fr} = 0,26$.

For the purpose of the method approval, three shells were tested at the same as for the fragments symmetrical cycle nominal stress amplitude $\sigma_a = 65$ MPa. At that, both shells and fragments were tested at the bending coefficient value $K_b = 2$.

Because of the limited tested shells number, only mean predicted (50%-ly) and experimental lives were compared.
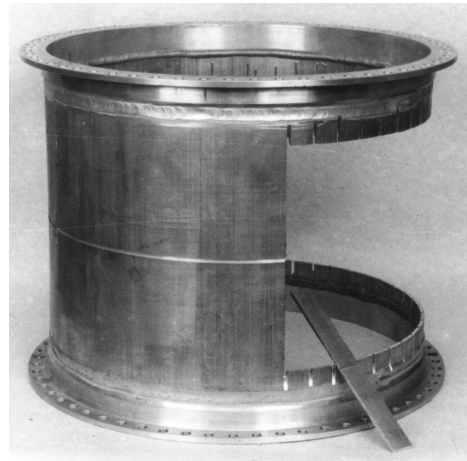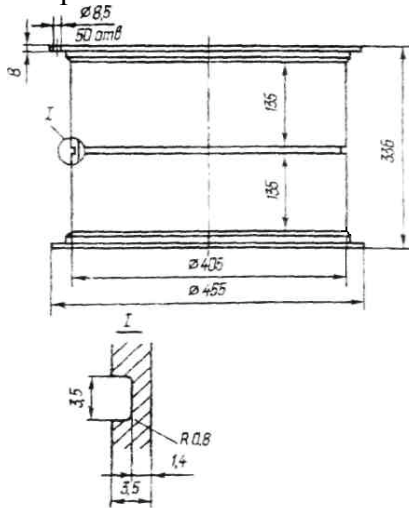
Fig.2 Geometrical parameters of the tested shells, photo of the cut shell and its fragment.

In Fig. 3, a log normal approximation of the fragment lives distribution function (1) is shown, and also the shell lives distribution function (2), created in accordance with the formula (1) at the shell fragments number $z = 51$ (fragment width is 22 mm). Ibid, a point estimation of the experimental shell lives with 90% confidence interval is marked (3).

As is evident from Fig.3, the result of prediction does not contradict to the experimental data. The difference between predicted and experimental shell life (at antilog comparison) was 32%, specifically: predicted life – cycle $N_R^{ob} = 8875$, experimental – cycle $N_{Re}^{ob} = 12980$, which may be admitted as wholly satisfactory, taking into account an experimental results variation, specific for fatigue test.

In terms of the possible application of abovestated method, the most important moment is approach or "probability convergence" of predicted shell life and model sample life values for the small-scale failure probability. The experience of performed tests showed that the prediction adequacy of fatigue resistance characteristics would be higher exactly for the small failure probabilities, which is especially significant for the large-sized expensive structures of critical designation.
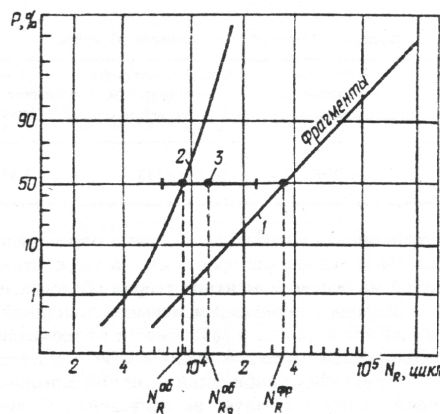
Fig.3 Experimental and predicted shell lives comparison at the failure probability P =50%: 1 – log normal approximation of the fragment lives distribution; 2 – predicted shell lives distribution function; 3 – point estimation of the shell lives mean log with 90% confidence limits.

Conclusions. Calculation-experimental method of the large-sized shell structures fatigue life prediction was developed, allowing to consider main calculation and technology factors, influencing the structure fatigue resistance characteristics, taking into account their interaction, by means of the tests of the shell fragments (model samples), containing potentially hazard failure areas.

Experimental approval of the developed method showed, that the results of the shell lives calculation prediction do not contradict to the experimental data.

The findings of the shell fatigue lives prediction in the form of distribution functions allow to perform evaluation of reliability and also resource, corresponding to the normed failure probability.

References

1. *Почтенный Е.К.* Прогнозирование долговечности и диагностика усталости деталей машин.– Минск : Наука и Техника, 1983. – 246с.

2. *Коростылев Л.И.* Об усталостной прочности некоторых очагов концентрации напряжений корпусных конструкций // Строительная механика корабля: Сб. науч. тр. – Николаев : НКИ, 1990. – С. 16-21.

3. *Данилин А.И., Комаров В.А., Усольцев С.М.* Проектирование имитатора отсеченной части конструкции при проведении прочностных испытаний // Прикладные проблемы прочности и пластичности. Анализ и оптимизация деформируемых систем / Всесоюзн. межвуз. сб. – Горьковский университет, 1988. – Вып. 39. – С. 83-90.

4. *Калюта А.А., Рудзей Г.Ф.* Регрессионный анализ усталостных характеристик образцов сварных соединений из титановых сплавов // Проблемы машиностроения и надежности машин. – 2004. – № 6. – С. 41-45.

5. *Регульский М.Н.* Прогнозирование характеристик сопротивления усталости цилиндрических оболочек с кольцевым концентратором // Проблемы прочности.– 1998. – №6. – С. 23-31.

6. *Болотин В.В.* Ресурс машин и конструкций М. : Машиностроение, 1990. – 448 с.

7. *Регульский М.Н.* К вопросу испытаний на усталость конструктивных элементов несимметричного профиля при осевом нагружении // Проблемы прочности. – 1995. – №5-6. – С.62-68.

V.I. Burlakov, PhD. Engineering, O.V. Popov, PhD., Engineering, D.V. Popov
(National Aviation University, Ukraine)

MANAGEMENT PROCESSES OF TECHNICAL OPERATION OF COMPLEX OBJECT IN CONDITIONS WITH FUZZY SOURCE INFORMATION

Creation of management information by technical maintenance of aviation techniquis is directed on the increase of reliability the functional systems of aircraft courts and to the decline of expenses on his technical service. Considerable influence renders an effective management this group of expenses as on economic so on a technical constituent the use of aviation techniquis on purpose.

Adaptive control can be presented as a teaching process, which contains a decision-making process, his realization and teaching on the basis of the got experience to the methods of more effective activity in the future.

By an alternative to the strict quantitative going near the decision of task on forming of the programs of technical service there is rational combination of high-quality purposeful engineering analysis on the choice of methods of technical exploitation and works on technical service with the quantitative methods of ground of periodicity of works, which mathematical models, describing influence of frequency of implementation of these works on safety of functional systems, are developed for. The choice of methods of technical exploitation and composition of works on technical service can be executed with the use of engineering analysis of influence of descriptions of reliability of the functional systems and their elements on safety, regularity and economic efficiency of air courts by the logical charts of making a decision. The offered method is developed in development of the indicated high-quality approach and allows formal to analyse influence of concrete types of failures of elements (and functional systems on the whole) on safety and regularity of flights. The basic differences of the offered method from MSG-3 consist in the following:

- the division of possible types of failures is made on the degrees of danger and influence on regularity of flights;

- the choice of methods of technical exploitation and works is provided on technical maintenance of every element on each of the examined possible types of his failures;

- the clear division of the stages of analysis of types of failures of the functional systems and types of failures of its elements is made in accordance with the accepted methodology of security of wares of aerotechics analysis;

- the formal account of functional meaningfulness of failures of elements of the functional systems and frequency of failures of elements is provided.

Thus, the purpose of development is maximal harmonization of methods and technologies of forming and certification of the programs of technical maintenance of air courts, applied in Ukrainian practice, and their foreign analogues.

The analysis of the most characteristic mathematical models of prophylaxis shows that they allow estimating influencing of measures on the management by the state of the system only on separate descriptions and properties of technical devices, at assumptions which not fully reflect the external environments of AT wares.

So, in many cases, descriptions of the faultless systems and elements determine in a function only one periodicity of implementation aircraft maintenance, here plenitude maintenance and control is not taken into account. In other cases of description of faultlessness express depending on plenitude and periodicity only one stage of exploitation, and it means on the very limited part of technical resource of item. In practice in most cases takes place multistage maintenance and every mode differs by the value of plenitude control and periodicity of leadthrough.

For the complex account of influence on descriptions and objects properties of exploitation, managing influences, development of new methodological approach to the management by the state of wares of aviation techniquis (AT) is required, allowing defining the optimum managers of influence taking into account all operating factors.

The management by a volume, modes and periodicity of implementation works on condition of providing the set level of capacity of AT wares with the purpose of minimization expenses is an optimization task. During optimization of technical service maintenance it is necessary to come from structural and operating properties of AT wares.

The complete volume of maintenance works makes the great number Q, which is broken up on the row of under great number Q_i are maintenance modes (operative, intensive labor, repairs), different in a number of the controlled parameters $-\Pi_i$, by character of maintenance works and periodicity of their implementation. Regulations works are executed repeatedly and include:

- continuous control of the state of AT wares in the process of application on the great number of parameters $\Pi_н$;

- leadthrough of works on providing of flight Q_B and control of the technical state on parameters $\Pi_П$;

- periodic control the state of AT on the great numbers of parameters $\Pi_{P1};\Pi_{P2};....\Pi_{Pi};....\Pi_{Pк}$ and leadthrough of prophylaxis restorations works after working off the wares of certain works $\Delta t_{p1};\Delta t_{p2};....\Delta t_{pi};....\Delta t_{pк}$ or duration of exploitation $\Delta \tau_{pi}$ in a volume Q_{pi}. Major repairs of AT are conducted after working off the useful life resource R or (failures of wares) in a volume Q_{Ri}.

The difficult systems of AT in the process of exploitation form the countable set of the states:
$$H = \{H_0 H_1 H_2 ... H_q\} \tag{1}$$
where H_0 is under great numberof the capable of working states,

H_q – down state.

Intermediate the states $H_j (j = 1, q - 1)$ are caused by the failures of separate elements or their great number, which reduce efficiency work of the system, but does not cause the loss of their capacity.

The complete control for all states H makes the great number $\Pi_N = \{\Pi_1 \Pi_2 ... \Pi_N\}$, however to carry out global verification not always possibly, and not always expediently, in connection, with what use the system of verifications Π_i on certain parameters $(\Pi_П; \Pi_н; \Pi_{Pi})$.

For realization of process control of change properties and descriptions objects of exploitation it is necessary to define the possible managers of influence and to optimize organization of their leadthrough at the set limitations for the receipt of the required values of output vector H^T at minimum operating costs.

One of distinctive descriptions of complex objects (CO) is a presence of plenty of independent entry and output parameters, characterizing the state of the system ambiguous appearance. The construction of adequate model at plenty of entrance variables requires high-cube base of knowledge, the amount rules of products in which exponentially increases with the increase of entrances the model, that reduces quality of fuzzy logic intervening.

In this case on the stage of generation base of knowledge, consisting of fuzzy logical rules, it is expedient to operate the concrete not parameters of the system, but classes of its states. It, in most cases results in diminishing of volume the base of knowledge, and accordingly to the increase of management exactness.

Consequently management of complex objects must be carried out not on it parameters, but on the states [1]. Thus, in system of automatic management (SAM) CO there is a task of authentication of the state of complex object of management on it looked after parameters.

When the state of object can be presented as a vector of numbers, determining the geometrical location of consisting space the coordinates of which are signs description of the state, it is talked about the clusterization of the state [2].

The group of the states of object, formative in space descriptions compact in a manner area, is named a cluster. Realization of method of clusterization in the intellectual system (IC) is determined the mutual spatial location of clusters in space. If set about clusters, proper different classes, far enough from each other, it is possible to take advantage of classification on some from birth-certificates. Among the great number of algorithms of clusterization most known algorithm of ISODATA and algorithm of maxmin distance [3]. During work with complex objects clusters can be recovered and have the washed out scopes, which takes a place as a result of incomplete or fuzzy information about the state of object. The methods of breaking up the space of problems, operating concepts theories of fuzzy sets, are used in this case [4].

Multicriteria problems have a characteristic feature, the above all difference of which consists in that no single point of view is, and there is the great number of effective decisions, or decisions optimum on Pareto. On Pareto such alternatives which in transition from one alternative to other the values of one or a few criteria can not become better without worsening of even one criterion will be optimum. Determination of great number on Pareto narrows the initial great number of decisions, that it diminishes vagueness. If some additional information about a task is absent, the subsequent narrowing of great number of Pareto by formal methods is impossible.

If criteria and their values get out taking into account a cooperatively, as a result general interest of group of criteria is put higher than interests of every separate criterion, the choice is optimum on Pareto [5].

If criteria and their values get out taking into account a cooperatively, as a result general interest of group of criteria is put higher than interests of every separate criterion, the choice is optimum on Pareto [6].

Every alternative $v^i \in V$ there is the set of parameters

$$v_{(i)}^i = V^i\left(v_1^i, v_2^i, ..., v_n^i\right), \quad i = 1, 2, ..., n \tag{2}$$

that and an alternative can be examined as vector in measurable space of parameters.

The improvement of the system of estimations takes place by the change of parameters V_j^i, and acceptability of these changes is estimated by a criterion. Formal consideration task of choice begins since composition of great number of alternatives is certain. The question of theoretical analysis and complication of such analysis can substantially depend on that, how the successfully entered great number the V objects taken for alternatives.

The multicriteria model of decision-making optimum individual is set as vectorial criterion in a kind, which scalar functions which are certain on V and measure the internals of decision on a certain scale are components. In general case they incompatible. On foundation $K(v)$ it is needed to choose the decisions the best in the certain understanding.

A not separate alternative and not pair of alternatives which need to be compared, and all great number of variants, which the "best" variant gets out from, is the argument of algorithm of choice.

Construction of the generalized criterion is based on that the generalized internals of alternatives are estimated by distance between an ideal and examined alternative and than less this distance, the best alternative. How ideal take an alternative which a vector answers

$$v(t) = \left[v_1(t_0), v_2(t_0), ..., v_m(t_0)\right] \tag{3}$$

where the maximal values are components for maximized and minimum values for the minimized criteria of optimum, which are achieved on the great number of alternatives V.

Distance between two alternatives s and t certainly in ordinary evklyds understanding

$$D_{S1} = \left[\sum_{j=1}^{n} \left(U_j^S - U_j^t \right)^2 \right]^{\frac{1}{2}} \tag{4}$$

so, that $D_{st} = D_{tS}$ and $D_{SS} = 0$.

In this expression the generalized criterion can be formulated in a kind:

a) most absolute deviation from an ideal alternative for criteria, parts of one dimension:

$$F = W\left[v_1(t), v_2(t), ..., v_m(t) \right] = max \left| v_i(t_0) - v_i(t) \right|, \tag{5}$$

б) most relative deviation from an ideal alternative for criteria, parts of different dimension

$$F = W\left[v_1(t), v_2(t), ..., v_m(t) \right] = max \left\{ \frac{v_j(t_0) - v_i(t)}{v_i(t_0) - v_i^{min}(t_0)} + \frac{v_i(t) - v_i(t_0)}{v_i^{max}(t) - v_i(t_0)} \right\}, \tag{6}$$

For the grant of evenness of influencing of each of criteria on the final value of integral criterion it is necessary to level turn-downs values of criteria by the down-scaling and taking them to the range [1; 0].

Selection of great number of base alternatives, determinate measure for their comparison and setting of the system of advantages between them - are foundation of decision-making the best. The selection of this great number will shorten the subsequent analysis and will decrease the amount of calculations for the processes control of technical exploitation.

Conclusion

For realization of process control of change properties and descriptions objects of exploitation it is necessary to define the possible managers of influence and to optimize organization of their leadthrough at the set limitations for the receipt of the required values of output vector at minimum operating costs.

It should be noted that in the known models of optimization of plenitude and periodicity of prophylactic measures on the management by the state of difficult objects of exploitation development poliparametric method of optimization not is completed until now.

Referents

1. *Лохин В.М., Захаров В.Н.* Интеллектуальные системы управления: понятия, определения, принципы построения / Сб. научн. статей «Интеллектуальные системы автоматического управления / Под. ред. И.М. Макарова, В.М. Лохина. - М.: ФИЗМАТЛИТ, 2001. с. 25–38.

2. *Дуда Р., Харт П.* Распознавание образов и анализ сцен. - М.: Мир, 1976.

3. *Сокал Р.Р.* Кластер-анализ и классификация: предпосылки и основные направления // Классификация и кластер / Под ред. Дж. Вэн Райзина. -М.: Мир, 1980. С. 7-19.

4. *Леоненков А.В.* Нечеткое моделирование в среде MATLAB и fuzzyTECH. – СПб.: БХВ-Петербург, 2003.

5. *Заде Л.А.* Размытые множества и их применение в распознавании образов и кластер-анализе // Классификация и кластер / Под ред. Дж. Вэн Райзина. -М.: Мир, 1980.

6. *Мелихов А.Н., Бернштейн Л.С., Коровин С.Я.* Ситуационные советующие системы с нечеткой логикой. - М.: Наука, 1990. 272 с.

7. *Ногин В. Д.* Принятие решений в многокритериальной среде: количественный подход.– М.: ФИЗМАТЛИТ, 2002.–144с.

UDC 629.735.017.1:629.735.33(043.2)

A.A. Tamargazin, Doctor Engineering, O.S. Yakushenko, Ph.D Engineering,
P.O. Vlasenko, postgraduate student
(National Aviation University, Ukraine)

FORMING OF INSTALLERS FOR AIRLINE'S FLEET RELIABILITY CONTROL AUTOMATED SYSTEM

Expediency of creating the reliability control automated system is approved on the basis of analysis of questions related to airline's fleet reliability control. General structure and main functions of automated system are considered. Content of software installers that could be used for installing to company's server, system administrator, expert and operator workplaces is described.

Problem

One of the most effective modern means for supporting, controlling and optimizing maintenance and technical activities of airline is the reliability control system of aircraft functional systems and components.

The general reliability control circuit of airline park consists of data collecting, data processing and control actions. Initial data for reliability control is faults and failures detected by pilots or during maintenance process, unscheduled components removal, flight delays and cancellations, scheduled maintenance reports, flying time of airplane mainstay products and components, scheduled check and check reports. On the base of these data the reliability parameters estimation, control and monitoring is provided. The prognostication of reliability parameters, analysis and control of components life state, preparation of evidence info are conducted. Control of Airline Maintenance Program and Reliability Program is provided by making the necessary changes in Maintenance program. These changes are made for increasing (saving) the reliability and reducing costs for maintenance, airworthiness and flight safety necessary level support.

Information concerning only flight or maintenance personnel comments is put in Logpage. For a large company that has 20-30 aircraft there are 4000 - 6000 Logpages. Airlines need to process information for three last years at least. Firstly this work should be done by some persons and the results of this work must be given to appropriate workers of the Airline. Secondly this work can not be done with a high quality without special software even if it would be done with a significant staff.

All this data points to necessity of creating specialized automated system for reliability control of aircraft park and mainstay products (plane, engine, auxiliary power unit, propeller, gear) of airline.

Research and publications analysis

In recent years numerous papers such as [1-4], which focusing on the creation of automated systems pay much attention to development of reliability control methodologies and methods. But not enough papers pay attention to development of software for automated systems. Also, taking in account that these automated systems must agree with international and national Authorities requirements and regulations (ICAO, the State Department of Aviation Transport of Ukraine) and airline manufacturers. Herewith the requirements and procedures of these organizations are constantly improving and changing.

Taking into account this the aim of this paper is to consider questions connected with development of the general structure of reliability control automated system at the airline level.

General structure of reliability control automated system of Airline fleet

Automated system that can provide simultaneous work of some users with information should be based on the use of relational database management systems. Such systems are designed to work in local networks and in the Internet. They include:

- the database (a file or files on hard disk that contain data);
- server (standard software system for database management, which is installed on the server computer and provides database control);
- ODBC - drivers (Open Database Connectivity, a software interface for databases accessing) that are installed on each computer of end users and provide interaction of application (automated system) with the server;
- automated system software.

Possible structure of such system is shown on Figure 1.

Fig. 1. The structure of reliability control automated system of Airline fleet

Main functions of reliability control automated system of Airline fleet and purpose of it's main modules

Analysis of stated information shows that the automated system should provide at least three fundamentally different groups of functions for operation with the database:
- entering of data;
- creation of output forms, reports and their expert analysis;
- maintenance of automated systems database.

Thus software installer should provide four types of system installation:
- database server, that should be installed only at one computer (usually at network server computer);
- operators' workplace;
- experts' workplace;
- system administrator's workplace.

At all workplaces except server computer should be installed ODBC-drivers. At the server these drivers are installed only in case if both database software and end user software are installed there. Such variant of installation is possible for example if automated system and database are installed at one personal computer.

Key features of software that is installed at operator's workplace should provide input to the system and modification of the following information:
- failures and faults detected on the airplane by crew or maintenance staff;
- flight delays;

1.1.20

- flight cancellation (by technical reasons);
- delay maintenance;
- corrective actions of maintenance personnel;
- types of airline's aircrafts and their characteristics;
- airline's aircrafts and their characteristics;
- monthly fling time of aircraft;
- long time maintenance;
- periodical maintenance and checks of functional systems (high altitude starting of auxiliary power unit, check of auto landing system);
- codifiers and classifiers of systems.

Key features of software that is installed at expert's workplace should provide analyzing of processed input data:
- samples of specified type failures for determined period;
- reliability parameters for the whole aircraft park, individual airplanes and for individual systems;
- flight delays and cancelations;
- summary report of the aircraft operation;
- summary report of the engines operation;
- failures of individual components;
- long time maintenance;
- periodic checks of individual systems;
- contextual search of information;
- batch creation of reports for aircraft manufacturer and Department of Aviation Transport.

Key features of software that is installed at administrator's workplace should provide such database control functions:
- creation/deletion of users, controlling of information access rights (view parts of database, information modifying, records deleting);
- system database maintenance (cleaning, reindexing, analyzing of database and its tables);
- the database backup and restore of the database from a previous backups;
- change of database structure and features;
- service functions.

Conclusions

The analysis of the main functions of reliability control automated system of Airline fleet was conducted. Reasonable dividing of functions to the parts depending on operation (expert, operator, administrator) was considered.

References

1. *Кучер О.Г.* Контроль та аналіз стану надійності систем і агрегатів повітряних суден в експлуатації/ Кучер О.Г., Власенко П.О.// Наукоємні технології. – 2010. – № 1. – С. 15–26.

2. *Кучер О.Г.* Експлуатаційна надійність авіаційних двигунів. Її контроль та аналіз в авіакомпанії/Кучер О.Г., Власенко П.О.// Авиационно-космическая техника и технология. – 2011. – № 9(86). – С. 108–115.

3. *Кучер О.Г.* Модель експлуатаційної надійності повітряних суден/ Кучер О.Г., Власенко П.О. // Наукоємні технології. – 2010. – № 2. – С. 10–17.

4. *Кучер О.Г.* Порівняльний аналіз показників надійності і ефективності іноземної та вітчизняної техніки/ Кучер О.Г., Власенко П.О.// Наукоємні технології – 2009.- № 2.– С. 9-17.

5. *Хоменко А.Д.* Работа с базами данных в Delphi. 3 изд./ Хоменко А.Д., Гофман В.Э.// - СПб.: БХВ-Петербург, 2005. -640 с.

6. *Князьков П.В.* Анализ и обеспечение надежности воздушных судов гражданской авиации в процессе их эксплуатации СПб.: 2001. -110 с.

UDC 629.735.083:519.68(045)

L.A. Zhuravlova, PhD Engineering, V.V. Matsuk, bachelor, A.V. Plakhotnuk, bachelor
(National Aviation University, Ukraine)

MODELING OF AN AIRCRAFT MAINTENANCE DEPARTMENT CAPACITY

The paper presents the model of evaluation of an aircraft maintenance department capacity on conditions, when the time of waiting is restricted, and when it is not restricted. The specific aim was to determine the optimum work schedule that satisfies increasing maintenance labor requirements with the minimum cost and highest efficiency.

In general, aviation management expressed three concerns to be taken into account: (1) the current excessive overtime to cover weekends and unplanned maintenance; (2) the seven-day maintenance requirement associated with the flight schedule, which is active during the weekends; (3) the significant increase in scheduled maintenance workload due to changes in both the maintenance program and the flight schedule. Aircraft maintenance requirements can be broadly classified as follows: Scheduled maintenance: including pre-flight, post-flight, daily and phase checks, calendar time changes, time limited component changes, in addition to A, B, C, and D checks (periodic aircraft PM/inspection programs of increasing intensity). Unscheduled maintenance: to handle unplanned problems reported by flight or maintenance crews. Special maintenance: as required to satisfy special instructions or directives by the manufacturer, Aviation Administration of the country, and aviation management.

In many cases the flight line maintenance had been operating on a five-day (Saturday-to-Wednesday) schedule, with two full eight-hour shifts per day. The line was experiencing excessive overtime, especially during the weekends where it has to support an increasing number of flights. The purchase of some new aircraft, more frequent maintenance checks, and additional flights to new destinations increases the pressures on aircraft maintenance. In this situation it is necessary to estimate the current capacity of a maintenance crew and to determine the best schedule of aircraft maintenance to respond to these challenges. The modeling is the best way to provide the effectiveness of a maintenance crew. The model is based on the analysis of labor demands, overtime statistics, current schedule, current workforce size, and other relevant statistics. (Table 1 and Table 2 shows the working parameters of the model.

Table 1

Input data

Value	Parameter description	Value name
λ	intensity of receipt of units on replacement	*lamb*
μ	intensity of replacing the units by maintenance crews	*mu*
n	total number of maintenance crews	*n*
t_{och}	Aircraft average time of waiting in turn	*toch*

Table 2

Settlement parameters

Value	Parameter description	Value name
α	Ratio of specified intensity of receipt of units on replacement to the intensity of replacing the units by maintenance crews	*alfa*
P_0	Probability of the situation, when all maintenance crews are vacant	*P0*
P_{zan}	Probability of the situation when all maintenance crews are occupied	*Pzam*
M_0	Average length of the turn of expectation	*M0*
T_{sr}	Average time of waiting of units replacement	*Tsr*
M_{obs}	Average number of units under replacement, including the units waiting for the turn	*Mobs*
M_{vil}	Average number of vacant maintenance crews	*Mvil*

Value	Parameter description	Value name
k_{pr}	Coefficient of idle time	**kpr**
M_{zan}	Average number of maintenance crews occupied by replacement of unites	**Mzam**
k_{zav}	Coefficient of workload	**kzav**
v	Intensity of waiting	**nu**
β	Normalized intensity of waiting	**beta**
r	Number of airplanes waiting in queue	**r**
K	Number of airplanes which may come for maintenance work	**K**
N_{och}	Number of airplanes waiting for the maintenance work	**Noch**
P_{vid}	Probability of refusal to maintain by reason of restricted idle time	**Pvidm**
n_{zan}	Average number of maintenance crews occupied by maintenance works	**nzan**
n_{vil}	Average number of vacant maintenance crews	**nvil**
k_{pr}	Coefficient of idle time	**kpr**
P_{obs}	Probability of implementation the maintenance work for each incoming airplane	**Pobs**

The process of the model design takes into consideration three subjects relevant to the study: aircraft regular maintenance procedures, maintenance staffing and personnel scheduling.

Information on aircraft maintenance processes and policies may be obtained by interviewing the concerned people, gaining insights and experience-based points of view on problems and possible solutions. For each shift, data must be collected on the current schedule, current workforce size, and average overtime hours per month. Information was also gathered on each shift's daily manpower requirements, relation to the flight schedule, and relation to the other shift. Other relevant statistics were also collected. In addition to interviews, sources of data included: weekly flight schedules; weekly maintenance planning schedules; weekend work schedules; yearly maintenance projections; employee time sheets; maintenance work log books; and company manual on work schedules.

The applied workforce capacity estimation technique is given below.

I. Maintenance department capacity on the condition that the time of waiting is unlimited:
1. Ratio of specified intensity of receipt of units on replacement to the intensity of replacing the units by maintenance crews: $\alpha = \dfrac{\lambda}{\mu}$.

2. Probability of the situation, when all maintenance crews are free: $P_0 = \dfrac{1}{\sum\limits_{i=0}^{n}\dfrac{\alpha^i}{i!} + \dfrac{\alpha^n}{(n-1)!\,(n-\alpha)}}$.

2. Probability of the situation when all maintenance crews are occupied: $P_{zan} = P_0 \dfrac{\alpha^n}{(n-1)!\,(n-\alpha)}$.

3. Average length of the turn of expectation: $M_0 = P_{zan}\dfrac{n\alpha}{(n-\alpha)^2}$.

4. Average time of waiting of units replacement: $T_{sr} = P_{zan}\dfrac{1}{(n\mu-\lambda)}$.

5. Average number of units under replacement, including the units waiting for the turn:
$$M_{obs} = M_0 + \dfrac{nP_0}{(1-\dfrac{\alpha}{n})} + P_0\sum_{i=1}^{n}\dfrac{a^i}{(i-1)!}.$$

6. Average number of vacant maintenance crews: $M_{vil} = P_0\sum\limits_{i=1}^{n}\dfrac{n-i}{i!}\alpha^i$.

7. Coefficient of idle time: $k_{pr} = \dfrac{M_{vil}}{n}$.

8. Average number of maintenance crews occupied by replacement of unites: $M_{zan} = n - M_{vil}$.

9. Coefficient of workload: $k_{zav} = \dfrac{M_{zan}}{n}$.

II. Maintenance department capacity on the condition that the time of waiting is limited

1. Intensity of waiting: $\nu = \dfrac{1}{t_{och}}$. Reduced intensities: $\alpha = \dfrac{\lambda}{\mu}$, $\qquad \beta = \dfrac{\nu}{\mu}$.

2. Probability of the situation, when all maintenance crews are vacant (no airplanes for the maintenance work):

$$P_0 = \frac{1}{\displaystyle\sum_{i=0}^{n} \frac{\alpha^i}{i!} + \frac{\alpha^n}{n} \sum_{r=1}^{K} \frac{\alpha^r}{\displaystyle\prod_{j=1}^{r}(n+j\beta)}},$$

where r – number of airplanes waiting in queue; K – number of airplanes which may come for maintenance work.

3. Number of airplanes waiting for the maintenance work: $N_{och} = \displaystyle\sum_{r=1}^{K} \frac{r\alpha^{n+r}}{n!\displaystyle\prod_{l=1}^{r}(n+l\beta)} P_0$.

4. Probability of refusal to maintain by reason of restricted idle time: $P_{vid} = \dfrac{\beta}{\alpha} N_{och}$.

Average number of maintenance crews occupied by maintenance works:

$$n_{zan} = P_0 \sum_{i=1}^{n} \frac{\alpha^i}{(i-1)!} + nP_0 \sum_{r=1}^{K} \frac{\alpha^{n+r}}{n!\displaystyle\prod_{q=1}^{r}(n+q\beta)}.$$

5. Coefficient of workload: $k_{zav} = \dfrac{n_{zan}}{n}$. Average number of vacant maintenance crews: $n_{vil} = n - n_{zan}$.

6. Coefficient of idle time: $k_{pr} = \dfrac{n_{vil}}{n}$.

7. Probability of implementation the maintenance work for each incoming airplane: $P_{obs} = 1 - P_{vid}$.

The MATLAB program:

```
%program maintenance crew capacity
clear all;
 %Input data
lamb=input('\n INPUT INTENSITY OF COMING AGREGATES lamb=');
mu=input('\n INPUT INTENSITY OF REGL WORKS mu=');
n=input('\n INPUT NUMBER OF MAINTENANCE TEAMS n=');
toch=input('\n INPUT THE TIME OF WAITING toch=');
K=input('\n INPUT TOTAL NUMBER OF AIRCRAFT K=');
r=input('\n INPUT NUMBER OF WAITING AIRCRAFT r=');
%1. INTENSITY OF WAITING
nu=round(1/toch); fprintf('\n\n\n INTENSITY OF WAITING nu=%f',nu);
%2. REDUCED INTENSITIES
alfa=lamb/mu; beta=nu/mu; fprintf('\n REDUCED INTENSITIES alfa=%f  beta=%f',alfa,beta);
%3. PROBABILITY THAT TEAMS ARE FREE
sum1P0=0; for i=0:n
 sum1P0=sum1P0+(alfa^i)/factorial(i);
 end
prodP0=1; for j=1:r
prodP0=prodP0*(n+j*beta);
end
sum2P0=0; for r=1:K
sum2P0=sum2P0+(1/prodP0);
 end
P0=1/(sum1P0+(((alfa^n)/n)*sum2P0));
 fprintf('\n PROBABILITY THAT TEAMS ARE FREE P0=%f',P0);
%4. AVERAGE NUMBER OF WAITING AIRPLANES
prodNoch=1; for l=1:r
```

```
   prodNoch=prodNoch*(n+l*beta);
 end
Noch=0;  for r=1:K
Noch=Noch+((r*alfa^(n+r))/((factorial(n))*prodNoch));
 end
fprintf('\n Average number of waiting airplanes Noch=%f',round(Noch));
%5. PROBABILITY OF REFUSE
Pvid=(beta/alfa)*Noch;
 fprintf('\n Probability of refuse Pvid=%f',Pvid);
%6. AVERAGE NUMBER OF WORKING TEAMS
sum1nzan=0; for i=1:n
sum1nzan=sum1nzan+((alfa^i)/factorial(i-1));
 end
prodnzan=1; for q=1:r
prodnzan=prodnzan*(n+q*beta);
 end
sum2nzan=0; for r=1:K
sum2nzan=sum2nzan+((alfa^(n+r))/((factorial(n))*prodnzan));
end
nzan=P0*sum1nzan+n*P0*sum2nzan;
fprintf('\nAVERAGE NUMBER OF WORKING TEAMS nzan=%f',round(nzan));
%7. KOEF OF OCCUPATION THE TEAMS
kzav=nzan/n;
fprintf('\n KOEF OF OCCUPATION THE TEAMS kzav=%f',kzav);
%8. AVERAGE NUMBER OF FREE TEAMS
nvil=round(n-nzan);
fprintf('\n AVERAGE NUMBER OF FREE TEAMS nvil=%d',nvil);
%9. KOEF OF IDLE TIME
kpr=nvil/n;
fprintf('\n KOEF OF IDLE TIME kpr=%f',kpr);
%10. PROBABILITY OF PERFORMING THE REGLAMENT WORKS
Pobs=1-Pvid;
fprintf('\nPROBABILITY OF PERFORMING THE REGLAMENT WORKS Pobs=%f',Pobs);
```

Conclusions

By using a unique modeling technique, it is possible to estimate the required number of workers and optimize the maintenance schedule. It gives the opportunity to determine the optimum work schedule that satisfies increasing maintenance labor requirements with the minimum cost and highest efficiency.

Referents

1. *Бусленко Н. П.* Моделирование сложных систем / Н. П. Бусленко. – М.: Наука, 1978. - 400 с.

2. *Комаров А.А.* Методическое пособие по расчету периодичности проведения работ на авиационной технике.-К.:КМУГА, 1995.-48 с.

3. *В. Н. Спиридонов* Моделирование сложных технических объектов: состояния и переходные функции/http://www.nbuv.gov.ua/portal/Soc_Gum/Vamsu_tekhn/2010_1/Spy_nov.htm

4. *Бразилович Е.Ю.* Модели технического обслуживания сложных систем: Учеб. Пособие. -М.:Высш. Школа.-1982.-231 с.

5. Инженерно-авиационная служба и эксплуатация летательных аппаратов. Задачник-справочник / под. ред профессора *Максимова Н.А.*-К.:КВВИАУ, 1975.-228 с.

UDC 002:004:629.735.03(045)

L.A. Zhuravlova, PhD Engineering, E.A. Sapeliuk, PhD Engineering
(National Aviation University, Ukraine)

FUZZY MODEL OF ASSESSMENT OF THE EFFICIENCY OF INFORMATION SOURCES IN THE FRAME OF AN AIRCRAFT GAS TURBINE ENGINE OPERATIONAL SPACE

The paper is devoted to the problem of investigating the information sources in the frame of the operational space of an aircraft gas turbine engine. The fuzzy model of information source efficiency is given.

Introduction. To provide a complete aircraft gas turbine system-level intelligent model, the strategy of problem domain investigation should be applied. Traditionally, simulation software development has followed the top–down structured design approach, which applies the method of functional decomposition to establish the problem domain structure. The configuration of an aircraft gas turbine engine problem domain can be represented as the set of information modules. Each of these module to be considered as the information source or/and the information receiver. From a structural view point, a gas turbine engine problem domain is the information space, which consists of internal and external information sources. Essentially the gas turbine engine - as the assembly of engine components-inlet, fan, compressors, combustor, duct turbine, shafts and nozzle – is the source of internal information flows. The external sources are all other objects, which generate the information flows for the needs of engine operation. In order to provide the efficiency of an aircraft gas turbine engine operation, it is necessary to investigate, classify and unify all data, which are taken from both internal and external information sources.

Characteristics of information sources. An aircraft gas turbine engine operational space involves different classes of information sources, which generate the information flow. They are: design bureau, manufacturing plants, operators, laboratories of reliability and diagnostics, aviation administration, aircraft overhaul plants, research and development institutions, maintenance and repair enterprises, environmental factors. The set of information source characteristics makes it possible to evaluate its efficiency. The main characteristics of an information source are given below.

Architecture of information source (IS) reflects the form and structure of manufacturing process, which involves clusters of material (also hardware and software), time and human resources.

Content of IS reflects the type of data massage (or massages) as the set of information resources, which is generated by exactly concrete information source. The level of information uncertainty is estimated for different types of content.

Volume of IS is the amount of information, which it generates per time unit.

Coverage of IS is evaluated by the number of customers, to which it permanently transfers the information messages.

Quality of IS is evaluated by such parameters as timeliness, reliability, credibility, importance, utility and entropy.

Adequacy of IS is estimated as the degree of correspondence between real and expected properties of IS. The adequacy is determined by peritentity, relevance, completeness and exactness of information massages, which it transfers.

It is obvious, that characteristics of IS (as physical object) mostly become formed by its information resources. Conformably, the characteristics of information flows are determined by the IS characteristics. All these characteristics are of different physical nature, different evaluating methods, different scales of evaluation, different methods of records presentation, expect different techniques of processing etc. However, the aggregation of all characteristics makes it possible to generate the integrated IS characteristic – IS efficiency.

Generating of IS integrated characteristic may be implemented by the use of linguistic variables.

Fuzzy model. The layout of linguistic variable "IS effectiveness" is shown on Figure 1.
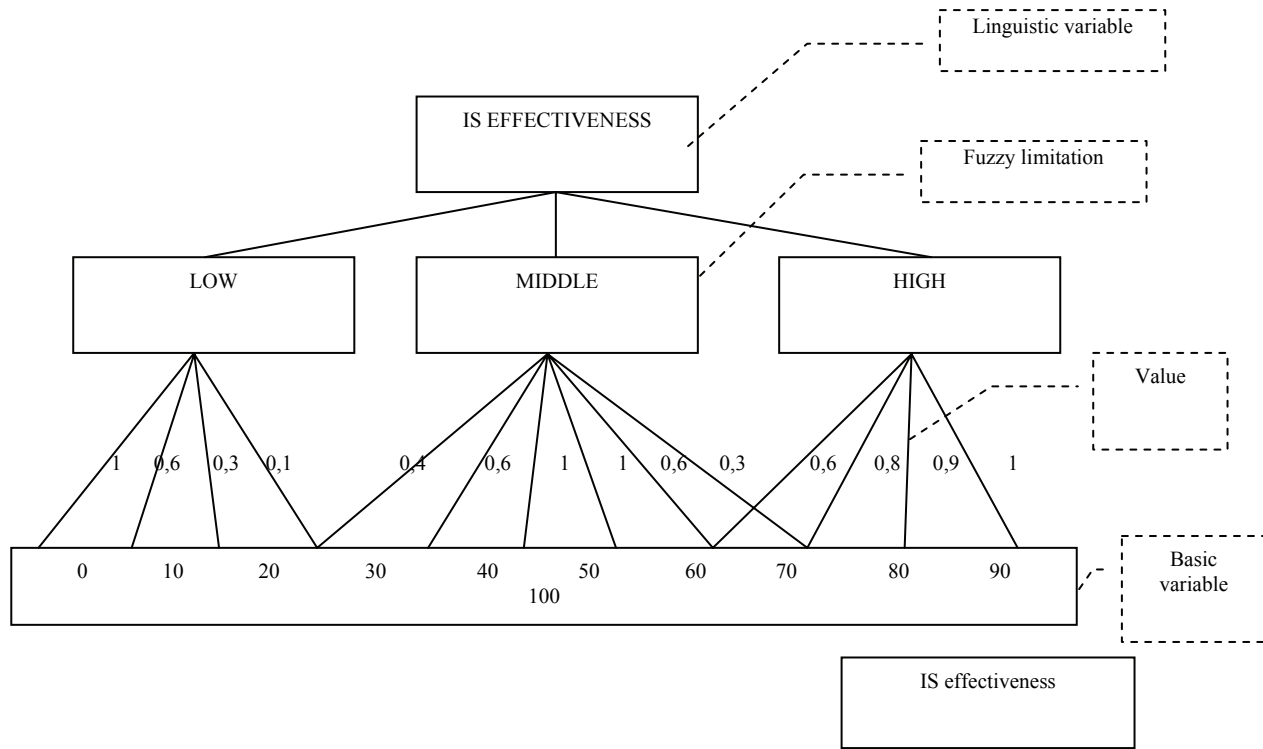
Figure1.- Linguistic variable "IS effectiveness"

Information sources of an aircraft gas turbine engine operational space for convenience can be classified as high-performance IS, low-performance IS and middle-performance IS. It is obvious, that IS performance is not stable value. It depends upon the actual values of IS information resources and characteristics in every point of time. For instance, one of the key reasons of IS effectiveness decreasing is its aging. That is why the monitoring of IS characteristics is urgent.

For the purpose of monitoring the term-sets of key IS characteristics to be defined. Evaluating values of the basic variable "IS effectiveness" are represented as the set of scale points:

$$E=\{0\ 10\ 20\ 30\ 40\ 50\ 60\ 70\ 80\ 90\ 100\}.$$

Tem-set of linguistic variable "IS effectiveness" (corresponding $E_{\textit{н}}$ – low effectiveness, E_{c} – middle effectiveness i $E_{\textit{в}}$ – high effectiveness):

$$A=\{\ (x_1|\mu_1),\ (x_2|\mu_2),\ (x_2|\mu_2),\ ...\ (x_{10}|\mu_{10})\},$$

where x_i – base variable value; μ_i - membership function.

Monitoring values of different IS are given in Table 1.

Than

$$E_{\textit{н}} = \{\ (0|1),\ (10|0,6),\ (20|0,3),(30|0,1)\ (40|0),\ (50|0),\ (60|0),\ (70|0),\ (80|0),\ (90|0),\ (100|0)\},$$

$$E_{c} = \{\ (0|0),\ (10|0),\ (20|0),(30|0,4)\ (40|0,6),\ (50|1),\ (60|1),\ (70|0,6),\ (80|0,3),\ (90|0),\ (100|0)\},$$

$$E_{\textit{н}} = \{\ (0|0),\ (10|0),\ (20|0),(30|0)\ (40|0),\ (50|0),\ (60|0),\ (70|0,6),\ (80|0,8),\ (90|0,8),\ (100|1)\}.$$

The IS effectiveness evaluation technique involves some stages. The first stage: fuzzification – generating the linguistic variables of key IS characteristics. Second stage: definition of actual values for each IS for the current situation, and membership functions determination (Figure 2).

The third stage: the aggregation of fuzzy sets of all IS parameters and generating the integrated characteristic – IS effectiveness.
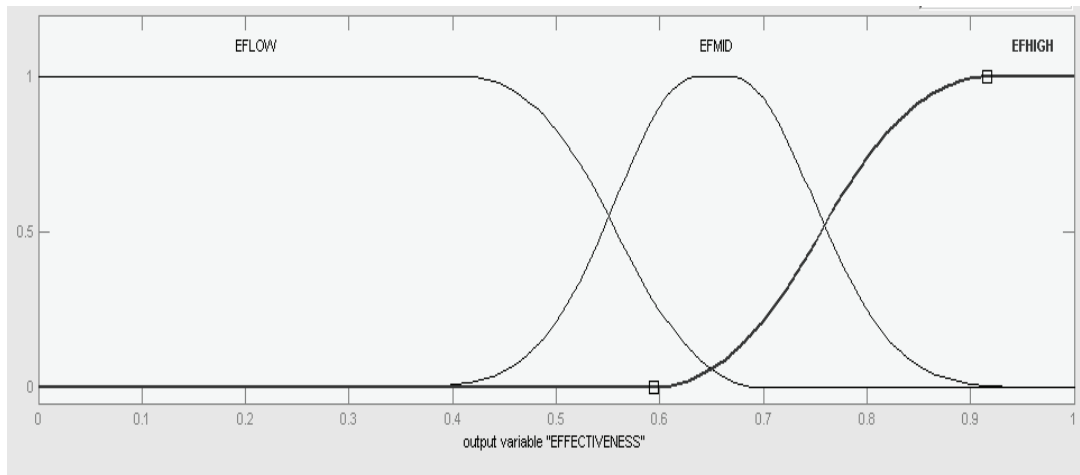
Figure 2 - Membership functions

The fuzzy model of IS efficiency assessment in the frame of an aircraft gas turbine engine operational space is implemented in computing environment of MATLAB Fuzzy application. The main goal of the modeling is to estimate the integral efficiency of total information support of an

Table 1

Characteristics of information sources of aviation gas turbine engine operational space

Information source	Effectiveness	Architecture	Content	Volume	Coverage	Quality					Adequacy
						timeliness	credibility	importance	utility	entropy	peritentity, relevance, completenes exactness
Design beaureu	0,65	M/0,9	3/0,7	0,4	0,3	0,6	0,7	0,9	0,9	0,1	0,9
Plant-manufacturer	0,55	P/0,5	3/0,7	0,8	0,3	0,6	0,7	0,9	0,6	0,4	0,5
Operator	0,35	P/0,5	3/0,5	0,9	0,3	0,3	0,3	0,6	0,6	0,1	0,5
Laboratories of reliability and diagnostics	0,43	M/0,9	3/0,5	0,9	0,3	0,6	0,7	0,6	0,4	0,4	0,2
Aviation administration	0,85	P/0,5	3/0,5	0,9	0,9	0,3	0,9	0,9	0,4	0,4	0,5
Aircraft overhaul plants	0,49	P/0,5	3/0,5	0,9	0,3	0,3	0,3	0,6	0,6	0,4	0,5
Research and development institutions	0,34	P/0,5	3/0,5	0,4	0,3	0,3	0,3	0,4	0,4	0,1	0,2
Maintenance and repair enterprises	0,76	P/0,5	3/0,5	0,9	0,3	0,6	0,9	0,9	0,6	0,8	0,9
Environmental factors	0,4	P/0,1	3/0,5	0,4	0,9	0,3	0,3	0,9	0,9	0,1	0,2

aircraft gas turbine engine process of operation on the basis of real values of efficiency of all information sources.

Input signals of the fuzzy model are actual values of ISs characteristics. The ranges of input data are determined by membership functions of each IS elements of the term-set. The concrete value of each input signal is specified with the help of rule viewer (Figure 3).

For instance, Figure 4 demonstrates the results of modeling session, which gives the opportunity to define the zones of both high and low efficiency, and, properly, define the unwanted combinations of IS characteristics. (*a* – dependence of the efficiency on the IS architecture and content; *b* – dependence of the efficiency on the IS architecture and volume).
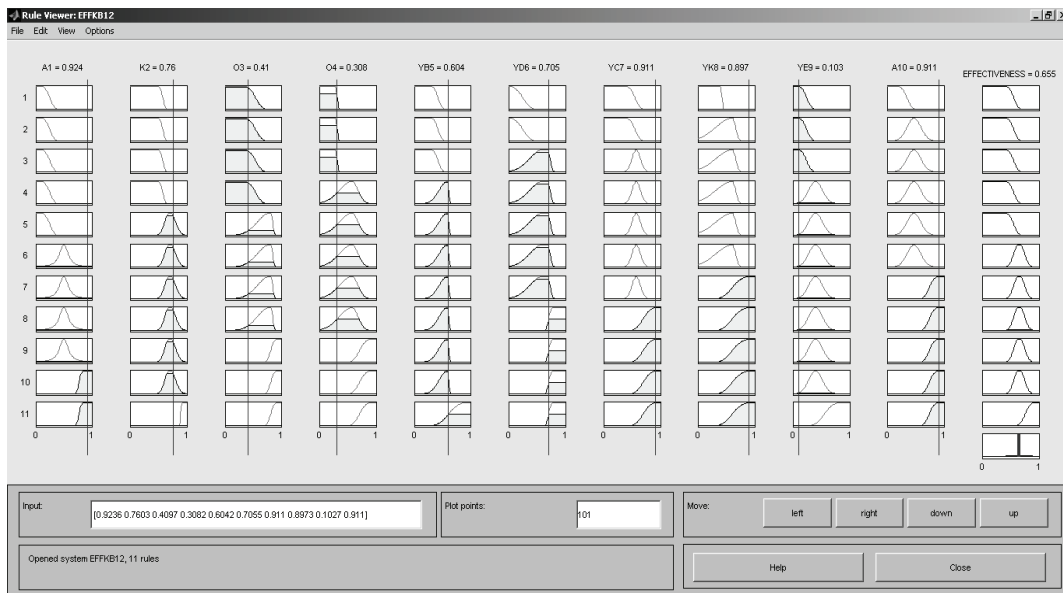
Figure 3 - Fuzzy system rule viewer
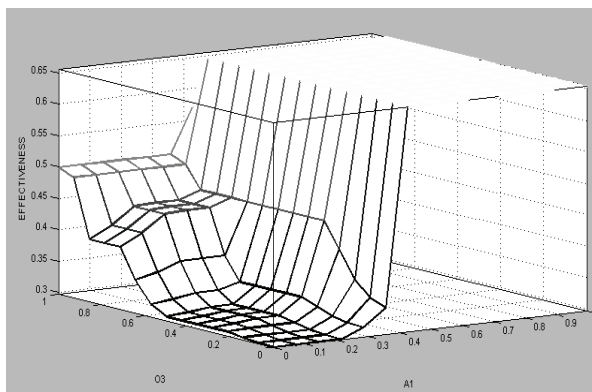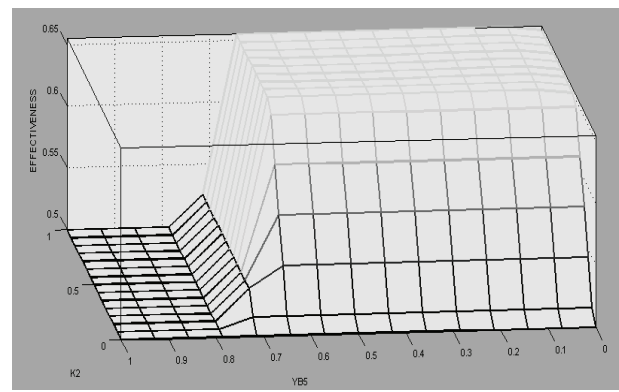
a   *b*

Figure 4 - Zones of high and low efficiency

Conclusions

The proposed fuzzy model can be used for the investigation of information space characteristics of complex technical object operational space – aviation gas turbine engine, for instance. It gives the opportunity to define the optimal strategy of information flows and information sources control, and generate the most complete and effective information support of aviation gas turbine engines process of operation.

References

1. Aircraft TELE-MAintenance and Support through intelligent resource management / http://www.ist-world.org/ProjectDetails.aspx

2. Fuzzy Logic Toolbox™ 2. User's Guide.- © COPYRIGHT 1995–2008 The MathWorks, Inc.

3. *Riid A.* Transparent Fuzzy Systems: Modeling and Control / www.mathworks.com

UDC 621.923

O. Sydorenko, PhD Engineering, V. Variukhno, PhD Engineering, E. Evsyukov
(National Aviation University, Ukraine)

THE INCREASING OF TRIBOTECHNIC CONNECTIONS RESOURCE OF AEROTECHICS BY THE METHOD OF DETONATION SPRAYING

Scientific researches in this direction are conducted with the purpose of perfection of process of detonation spraying and development of new composition materials on the basis of Fe with the purpose of increase the resource of aerotechics details.

Introduction. Construction of airplanes, helicopters, and aviation engines (AE) has a large nomenclature of details which work at high temperatures, in aggressive environments, at the considerable and different, by a sign, loadings of the friction which operate on their surface. The properties of materials and surfaces are the most important factors, impacting the operational reliability and service life of elements, which work in friction conditions. Hence, the development of technologies of shaping the hard-wearing blankets during the processes of manufacturing and restoring the weared-out units, is the most actual problem. Thus proceeding in awaiting-parts and aggregates on occasion can be compared to their production of new details, and losses, related to insufficient wear proofness, may arrives the considerable sizes. One of perspective methods of increase the resource and reliability of wares which work in the conditions of friction, is the usage of coverings. Among the methods of flame spraying of coverage's the most perspective is a detonation method. It is explained large force of tripping of coverage with basis (to 200 MPa), small porosity, small temperature of heating of detail (to 150°C) which does not cause structural change. The purpose of this work is an estimation of damages and study of features of proceeding in geometrical forms with the purpose of increase the operating properties of details which work in the conditions of friction, detonation method of spraing of wear proof coverings.

Research of detonation coverage's. Scientifically grounded choice of protective and fastening coverage's of surfaces of details allows considerably to increase longevity and capacity of details and constructions at the economy of all kinds of energy resource, that allows to shorten the consumption of awaiting-parts and economize scarce materials sharply.

In aviation industry at strengthening and proceeding of the friction surfaces usually are used the materials on the basis of Ni-Cr-Co-Al-Y with the different admixtures of other metals or connections. Also well proved the ВКНА (КХН, ЭИ) material. But, such materials are cost enough and it is expedient to use them for a production and proceeding in details which work in extreme external environments and which cost enough in a production [1,2].

Counting on a large price in proceeding the details by cost materials, the considerable nomenclature of details which work in the conditions of friction must be rejected. Such approach is economic unprofitable, that is why the priority is direction of development of composition coverage's on the basis of Fe «metal connection - metal ligament», inexpensive and practical in the conditions of exploitation.

Research of detonation coverage's is conducted on the basis of Fe with addition of different alloying elements (nitrides, borides, carbides of boron, silicon and other materials) by a wear. For comparison the some permanent was probed and materials with coverage of hard-alloy mixture VK-20 [3,4],Tested on a machine, developed in NAU, on the pair of standards with these coverages with the previous polishing of coverage to the roughness of surface of P=1-1,25 mkm (with the imitation of the real terms of exploitation: to amplitude of vibromoving 0,1 and 1,0 mm, frequency 30 Htz, the temperature +25°C but at enhanceable temperatures +120-150°C, the base of tests 210 and 510 cycles, as dependence of the gravimetric and linear tearing from the time of tests).

During tests a task to set dependences of change the coefficient of friction and intensity of wear of existent materials and offered material on the basis of Fe from the specific loading and sliding speed, was put (Figure 1, 2).
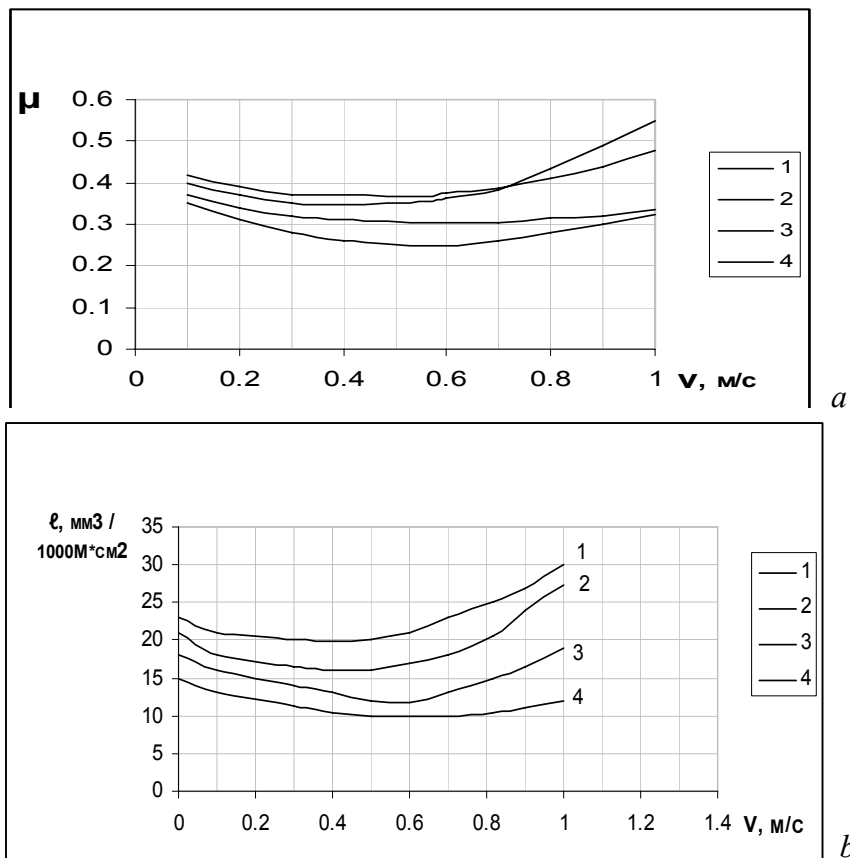
Figure 1. Dependence of coefficient of friction (*a*) and intensity of wear (*b*) from speed of sliding (at the specific loading of 1.0 MPa: 1-steel of U12a; 2-X18H9T; 3-Fe-C-Cr-Al-B; 4- VK-20
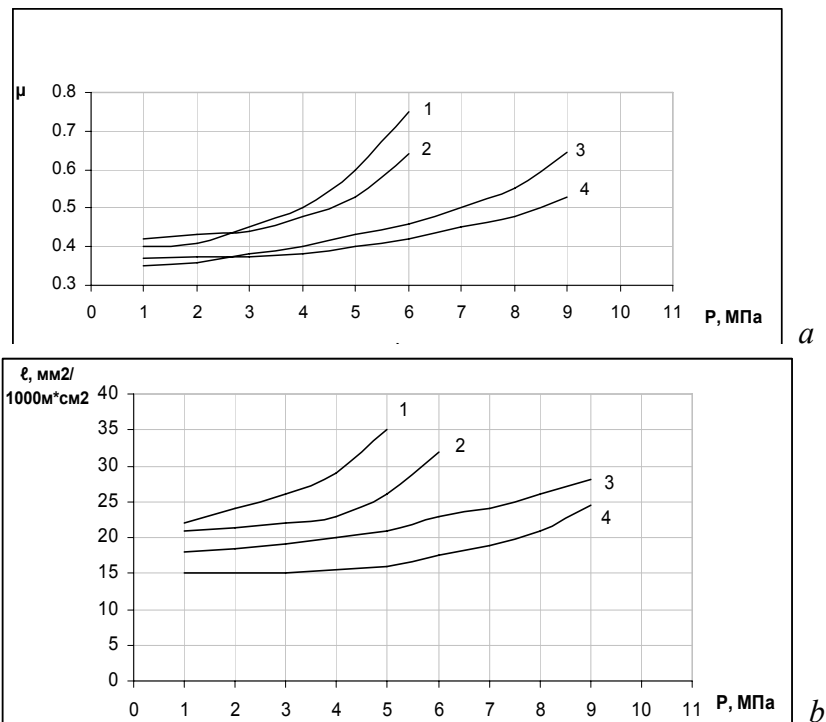
Figure 2. Dependence of coefficient of friction (*a*) and intensity of wear (*б*) is on the specific loading (at speed of sliding 0,1 m/s: 1-steel U12a; 2-X18H9T; 3-Fe-C-Cr-Al-B; 4- VK-20

As evidently from the resulted dependences, the material of coverage on the basis of Fe has some greater coefficient of friction and speed of wear at identical sliding speed and specific loading than coverage from the alloy VK-20. However at less speeds and loadings their indexes are practically identical. That, it is possible to draw a conclusion, that for the large nomenclature of

1.1.31

wares which work at the small moving and speeds, such as plungers of hydraulic and fuel aggregates, slide-valve pair of executive mechanisms, labyrinth packing's, and others like that, the use of cheap material of coverage on the basis of Fe for strengthening and renewal is economic advantageous.

It is found out in the process of research, that the basic retentive factors, which limit the realization of potential possibilities of technologies of gas-thermal covering at renewal and defence of frictionunits against the wear, is absence of conceptual approach to the problem of creation the coverages, workings in the conditions of friction and possessing high resistance to the wear. Realization of such approach allows to change a structure and properties of coverages in necessary direction, and to create the coverages with the beforehand set properties for different external environments.

In accordance with this, the scientific issue of the day, which was decided in this work, is an increase of wearproofness of detonation coverages on the base of development and application of positions of their capacity management.

The followings tasks decided for realization of the put purposes:
- determination of optimum composition and structural components of the coverages;
- conformities to the law of tribosystems capacity management of wearproof coverages depending on descriptions of coveraging materials;
- optimization of technologies of preparation and overcoating;
- application of the complex methods of research the structure and properties of composition coverages.

Such method of forming the composition coverages, their causing and forming of functional properties, which are proper the spectrum of ladening (to the expluatation conditions) allowed to create methodology of forming the gradient coverages, which conformities to the law of decline the intensity of wear, increases of thermal and inoxidizability, are underlaid.

Conclusions

Scientific researches in this direction are conducted with the purpose of perfection of process of detonation spraying and development of new composition materials on the basis of Fe with the purpose of increase the resource of aerotechnics details. The offered materials and technologies can be used for renewal and strengthening of surfaces of friction pairs not only in aviation industry but also at car repair service production and machine tool industry.

References

1. *Фень Е.К., Малишкін В.В., Дмитренко В.М.* Зміцнення та володіння деталей авіаційної техніки жаростійкими покриттями. В зб. праць III Міжнародної науково-технічної конференції АВІА-2001, К., НАУ, 24-26 квітня, 2001, Т.1.

2. *Малышкин В.В., Ходак Н.А., Дмитренко В.Н., Лубяный В.В.* Повышение сроков эксплуатации деталей авиационной техники путём восстановления размеров их геометрических форм и упрочнения газо-термическим напылением жаростойкими покрытиями. В сб. трудов IV Международной научно-технической конференции АВИА-2002, К., НАУ, 23-25 апреля, 2002, Т.1.

3. *Варюхно В.В., Сидоренко О.Ю., Євсюков Є.Ю., Машинська Н.В.* Методика розрахунку ресурсу та прогнозування довговічності деталей машин при навантаженні тертям. Вісник НАУ: Сб. наук. пр. – Київ: НАУ, 2011. – № 4. – С.103-105.

4. *Подчерняева И.А., Щепетов В.В., Варюхно В.В., Евсюков Е.Ю.* Закономерности изнашивания покрытий на основе композиционной керамики. Современные проблемы подготовки производства, обработки, сборки и ремонта в промышленности и на транспорте: Материалы 11-го Международного научно-технического семинара (21-25 февраля 2011). К.: АТМ, 2011. – С.210-212.

UDC 621.646:629.735.03

U.N. Rikunich, A.E. Sitnikov, PhD Engineering, E.I. Barilyuk
(Public Company «Kiev Central Bureau of Valve Design», Ukraine)
H.I. Zayonchkovskiy, Doctor Engineering (National Aviation University, Ukraine)

METHODOLOGICAL ASPECTS OF PERFORMANCE RESERVES CHOICE OF SMALL SOLENOID VALVES

Methodical aspects of performance reserve selection of compact solenoid valves were considered. Changes in the technical condition of parts and assemblies of valves during the process of wear-out under operating loads were taken into consideration.

Implantation of scientifically proven methods of performance reserve selection of compact electromagnetic valves during the design process gives the ability for realization most of the actions aimed at valve design enhancing and meet the safety requirements even during the stage of project documentation development. This allows significantly reduce the time and increase the effectiveness of design process of modern compact electromagnetic valves for aerospace industry.

As accumulated valve design experience shows, problem of necessary operational safety index guarantying depends on solving next pair of tasks: guarantying the fatigue strength of valve structural elements and assuring the parametrical reserves of valve work capacity.

As a research object the pneumatic valve with double-positioned polarized electromagnet was chosen (fig. 1), which is widely used in aerospace devices because of low energy consumption level required for its operation. For the valve operational changes evaluation the longevity test was conducted. Five valve samples were put on the test until their complete failure.
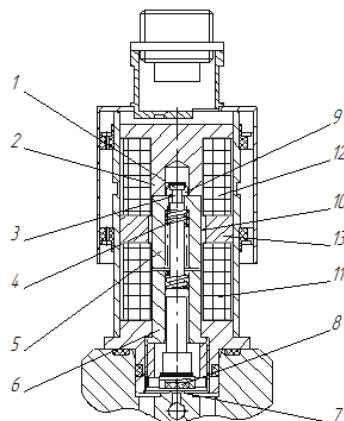
Fig. 1. Structural sketch of the valve with double-positioned polarized electromagnetic actuator:
1 – rod head; 2 – electromagnet case, 3 – rod neck; 4 – buffer spring; 5 – slider; 6 – bottom stop; 7 – saddle; 8 – valve; 9 – retainer; 10 – sectionalizer; 11 – closing winding; 12 – opening winding; 13 – constant magnet

Conducted longevity test of sample valves showed that during the operating time there is a small decrease of voltage U_{open} and time t_{open} and small decrease of U_{close} and time t_{close}. Also significant decrease of valve length movement χ_{valve} because of the position change of slider 5 relatively to the retainer 9 and rod 1. The reason of the position change is circular wear on the terminate edge of the slider and plastic deformation of elements of the valve electromagnetic actuator agile system (in first case – rod neck 3). When χ_{valve} decreases up to the critical level (0,1 mm) then the rod failure takes place.

Obtained experimental functional valve parameters (FP) change dependencies from operating time were put in the base of engineering methodic for predicting operational changes of FP in compact electromagnetic valves during lifetime. Further development of this technique is the methodic of determination and scientifically proven parametric work efficiency of compact electromagnetic valves and its implantation in designing process of JSCB "Kiev Central Valve

Design Bureau".

Under the work efficiency by y_i functional parameter (FP), we will bear in mind the difference $\Delta y_i(t)$ between normalized $[y_i]$ value in requirements specification and its achievement $y_i(t)$ at the operational time t, i.e.:

$$\Delta y_i^{PR}(t) = [y_i]_U^{SR} - y_i \text{ (when it is limited from above)} \quad \text{or}$$

$$\Delta y_i^{PR}(t) = y_i - [y_i]_B^{SR} \text{ (when it is limited from below).}$$

Under the valve work efficiency $\eta_{y_i}(t)$ by its y_i FP, we will bear in mind the relation of y_i parameter and normalized $[y_i]$ value in requirements specification.

$$\eta_{y_i}(t) = \frac{[y_i]_U^{RS}}{y_i(t)} \text{ (when it is limited from above)} \quad \text{or}$$

$$\eta_{y_i}(t) = \frac{y_i(t)}{[y_i]_B^{RS}} \text{ (when it is limited from below).}$$

Worked out methodic allows, even on the early stages of design process, to determine by its output functional parameters $\Delta y_{i0}^{PR}(t_0)$ and corresponding work efficiency coefficients $\eta_{y_{i0}}(t_0)$ such valve work efficiency that will guarantee during whole operational lifetime of the valve the interposition of its FP in legitimate range given by the requirements specification with probability $[P_{yi}]^{RS}$.

Determination of electromagnetic valve parametric work efficiency reserves by their main output parameters is based on probabilistic assessment of possibility for the valve functional parameter to transgress the admissible bounds in any time moment during the operational lifetime.

At that following assumptions were made:

- valve functional parameter $y_i(t)$ change during its normal lifetime is a random process with normal distribution (this assumption is proven by the research results stated in [1]);

- deterministic base (mathematical expectation value $m_{y_i}(t)$) change of y_i functional parameter can be approximated with monotone increasing (or steadily decreasing) power function from operation time t:

$$m_{y_i}(t) = m_{y_{i0}} + ct^\alpha$$

or in dependence from the quantity of triggering block-cycles $n_{b.c.}$:

$$m_{yi}(n_{b.c.}) = m_{yi0} + k(n_{b.c.})^\beta,$$

where c and k – are the coefficients that determine the change speed of mathematical expectation value $m_{y_i}(t)$ of y_i functional parameter correspondingly to the operating time t or the number of triggering block-cycles $n_{b.c.}$; α, β – corresponding coefficients of the power function.

Another case of the power function is when $\alpha = 1$ (or $\beta = 1$) and mathematical expectation value linear low change is considered.

Based on normal distribution law of parametric valve failures during lifetime, lets evaluate the non-failure operation probability of $n_{b.c.}$ trigger cycles:

$$P_{y_i}(t,n) = F(u_{y_i}); \quad u_{y_i}(t) = \frac{[y_i]_U^{RS} - m_{y_{in}}}{S_{y_{in}}} = \frac{[y_i]_U^{RS} - m_{y_{in}}}{m_{y_{in}} v_{y_{in}}}, \text{ if } y_i \leq [y_i]_U^{RS} \text{ or} \qquad (1)$$

$$u_{y_i}(t) = \frac{m_{y_{in}} - [y_i]_B^{RS}}{S_{y_{in}}} = \frac{m_{y_{in}} - [y_i]_B^{RS}}{m_{y_{in}} v_{y_{in}}}, \quad \text{if } y_i \leq [y_i]_B^{RS}, \qquad (1, a)$$

where $F(u_{yi})$ – is the sign of the normal distribution function; u_{y_i} – fractile of the normal distribution of y_i parameter; $m_{y_{in}}$, $S_{y_{in}}$ and $v_{y_{in}}$ – evaluations of mathematical expectation, standard deviation

and variation coefficient of y_i valve functional parameter after nb.c. trigger cycles. Equations (1), (1, a) are called in literature sources as "equations of connection" [1]. Lets examine a case, when y_i valve functional parameter steadily increases during lifetime because of the influence of operational loads and is limited from above by the maximal value of $[y_i]_U^{RS}$. In that case work efficiency start coefficient of brand new valve will be determined as

$$\eta_{y_{i0}} = \eta_{y_{in}} + \Delta\eta_{y_{in}} ,$$

where $\Delta\eta_{y_{in}}(t) = f(n_{b.c.})$ – valve work efficiency decrease by y_i functional parameter, caused by the valve operational changes during operation.

Considering the "equation of connection" (1), after correspondent transformations it is possible to obtain following equation for choosing the start work efficiency reserve of the designed valve:

$$\Delta\eta_{y_{i0}} = 1 + [u_{yi}]^{RS}(v_{y_{i0}} + \Delta v_{y_{in}}) + \frac{[y_i]_U^{RS} \cdot (m_{y_{in}} - m_{y_{i0}})}{m_{y_{in}} \cdot m_{y_{i0}}} . \tag{2}$$

In case, when y_i mathematical expectation change is close enough to linear, i.e. $m_{y_{in}} \approx m_{y_{i0}} + k_{y_i}(n_{b.c.})$, then

$$\Delta\eta_{y_{i0}} \cong \frac{[y_i]_U^{RS} \cdot k_{y_i}(n_{b.c.})}{(m_{y_{i0}})^2 + m_{y_{i0}} \cdot k_{y_i} n_{b.c.}} = \frac{[y_i]_U^{RS} \cdot k_{y_i} n_{b.c.}}{m_{y_{i0}}(m_{y_{i0}} + k_{y_i} n_{b.c.})} . \tag{3}$$

Similarly we can obtain equations for determining valve work efficiency by y_i functional parameter if during lifetime there is monotone decreasing of that parameter and its minimal value is limited by $[y_i]_U^{RS}$ from below. So we have:

$$\Delta\eta_{y_{in}} = \frac{k_{y_i} n_{б.ц}^{\beta}}{[y_i]_{\text{н}}^{ТЗ}} ; \tag{4}$$

$$\eta_{y_{i0}} = \frac{1}{1 - [u_{y_i}]^{ТЗ} \cdot v_{y_{in}}} + \frac{k_{y_i} n_{б.ц}^{\beta}}{[y_i]_{\text{н}}^{ТЗ}} . \tag{5}$$

Thus for determination the designed valve parametric work efficiency reserves it is necessary to know following statistic data:

- initial value of mathematical expectation $m_{y_{i0}}$ and variation coefficient $v_{y_{i0}}$;

- data about predicted values of $m_{y_{in}}$ and $v_{y_{in}}$ in the process cross-section, which corresponds to lifelength $n_{b.c.}$;

- data about the character of functional parameter changes during lifelength $m_{y_{in}} = f(n_{b.c.})$

That required statistical data is determined as exploitation summary of experimental samples of the designed valve. Experimental resourse tests of the considered electromagnetic valve type had shown that cane segment of the moving-contact assembly of the valve is the critical component that limits the resource of the valve. That cane segment of the moving-contact assembly of the valve is the rod, which works in conditions of substantial cyclic impulse loads.

Conducted researches had shown that for such cases of load it is reasonable to use energy evaluation of work efficiency of valve cane segments. It has been estimated that fatigue defects accumulation process in parts of the electromagnetic valve which work under substantial cyclic dynamic loads is directly connected with the value of relative kinetic energy of valve moving-contact assembly E_{valve}^{MCA} .

The condition of the designed valve work efficiency through the specific kinetic energy of the valve moving-contact assembly can be written as:

$$E_{valve}^{MCA} \leq [E_{valve}^{MCA}]^{RS} ,$$

1.1.35

where $\left[E_{valve}^{MCA}\right]^{RS}$ – is the permissible level of the kinetic energy of the valve moving-contact assembly which is given in requirement specification as n^{RS}.

The following analytical dependency that allows to determine the electromagnetic valve cane segments fatigue strength reserve was obtained:

$$\eta_E \approx 1{,}414 \cdot [u]^{RS} \cdot v_{E_{valve0}} + 1, \qquad (6)$$

where $[u]$ - normal reciprocal distribution; $v_{E_{кл0}}$ - variation coefficient of the parameter E_{valve0} in the initial cross-section of the process.

For determining the level of specific kinetic energy of the electromagnetic valve moving-contact assembly, when necessary non-failure probability of the valve cane segment during its operation, we can use the following equation

$$\left(E_{valve}^{MCA}\right) = \frac{\left[E_{valve}^{MCA}\right]_{np}^{RS}}{1{,}414 \cdot [u]^{RS} \cdot v_{E_{valve0}} + 1} . \qquad (7)$$

For the purposes of practical implementation of developed methodic for determining the fatigue strength of electromagnetic valve cane segments we obtained experimental dependencies of maximal rod trigger cycles before its total failure from the level of specific kinetic energy of moving-contact assembly for different structural materials: 08Х18Н10Т (fig. 2), ВТ1-0, АК4-1.
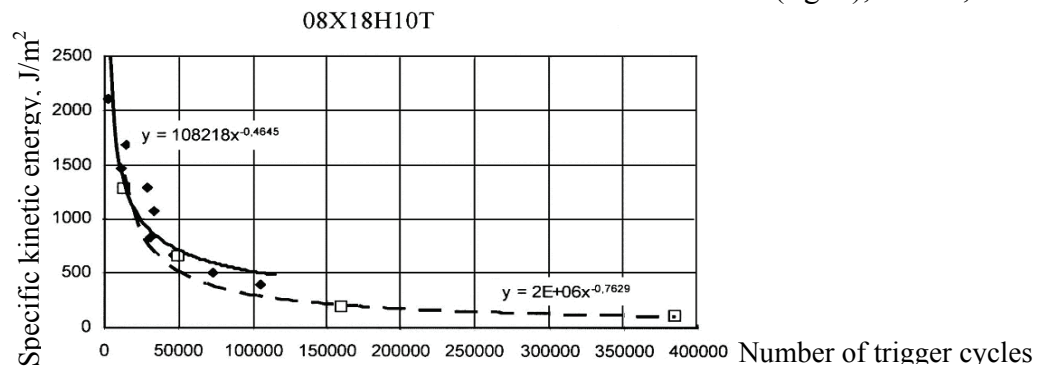
Fig. 2. Dependency of maximal rod trigger cycles before its total failure from the level of specific kinetic energy of moving-contact assembly of the electromagnetic valve

Conclusions. 1. An algorithm for determining the compact electromagnetic valve work efficiency reserve was created. This algorithm takes into consideration features of valve technical changes during operational lifetime.

2. Analytic dependencies (2) - (5) for determining parametric work efficiency reserves of electromagnetic valve were obtained. These dependencies allow choosing necessary parameters of the designed valve simultaneously meeting the demands of requirements specification.

3. Analytical dependency (6) for determining the coefficients of fatigue strength of cane segments of moving-contact assembly of the valve has been proposed. This dependency is based upon experimentally obtained dependency of the valve trigger quantity before the total cane segment failure from the level of contact-moving assembly of the electromagnetic valve.

4. An engineering methodic has been developed for determining the work efficiency reserves of the compact electromagnetic valves. This methodic is implemented in the design process of public company «Kiev Central Bureau of Valve Design».

References

1. Надежность трубопроводной пневмогидроарматуры / *В.В.Хильчевский, А.Е.Ситников, В.А.Ананьевский.* – М.: Машиностроение, 1989. – 208 с

UDC 662.75(045)

S. Puzik, PhD Engineering, A. Hvozdetskyi, O. Puzik, B. Ostrovskyi, engineer
(National Aviation University, Ukraine)

THE FULL-SIZED TEST-BENCH FOR DIAGNOSTICS AND PURIFICATION OF AVIATION FUEL

It was detected that the purification of aviation fuel and lubricating materials problem is little known. It was revealed the absence of multifunctional experimental test-benches for solution this issue. Proposed for using projected and produced stand, which was embrace not only for diagnostics but for cleaning aviation fuel and lubricating materials

The problem defined. Questions of increasing reliability and durability of aircraft exploitation, the ways of economy of aviation fuel and lubricating materials (FLM) inseparably related with aviation liquids cleanness. Notion «clear» liquid is conditional. Should be considered that liquid is «clear» if size and amount of contamination particles don't affect for efficiency of aircrafts fuel systems.

Further increasing of air transport efficiency exploitation related with providing required level of aviation FLM.

At present required levels of aviation FLM cleanness in aircraft systems, in airports FLM warehouses and stands of civil aviation repair plants is achieved due to traditional filters with using filtration (porous) partition. These filters, together with a range of advantages have significant deficiencies: small mud capacity, high hydraulic resistance, complication restoration of filter elements etc. This complicates its using.

Together with traditional filters considerable attention in our country and abroad is paid to force cleaners as a purification tools which depends on power field classified so: electrical, centrifugal, magnetic and gravitation [1].

Research results. Force cleaners compensate for the above mentioned deficiencies of traditional filters and have high mud capacity, law hydraulic resistance, absence of variable filter elements. But its characterized by some deficiencies: demand power sources (all cleaners except gravitation), weight, dimensions. Simultaneously insufficient researches amount in this liquid's purification area needs search the force cleaners' perfection ways [2], for what the full-sized test-bench for diagnostics and purification of aviation fuel was created. Furthermore, stand is intended for researches of technological processes with FLM, namely internal surface's purification of tank. The principal scheme of stand is shown in Fig. 1.

Fuel from tank RGS-60 *18* removed by pump type SCL-20-24A *9*, *44*, which was set on special foundation for prevention pump's vibration influence on stand. In a case, when cranes *56* and *57* closed, fuel is pumped through filters' system *5*, *49*, *52*; in a case, when crane *54* closed, fuel is pumped through force cleaner *53*. There where set manometers for control differential pressure on filters system and gravitation cleaner.

Pumped fuels' contamination control carried by liquids' control instruments PKZg-902 *32*, *37*, which were set after forcing and before suction pipeline. The technical characteristics of PKZg-902 are:

- sensitivity (lower limit of diameter of particle, which are registered) — 3 (mkm);
- consumption of working fluid through the instrument — 200–450 cm^3/min;
- the maximum acceptable concentration of particles in 1000 cm^3 — 100 000 (pc);
- measurement error of particle size (relatively the reference exciter) — ± 25 %;
- counting particles error — ± 25 %;
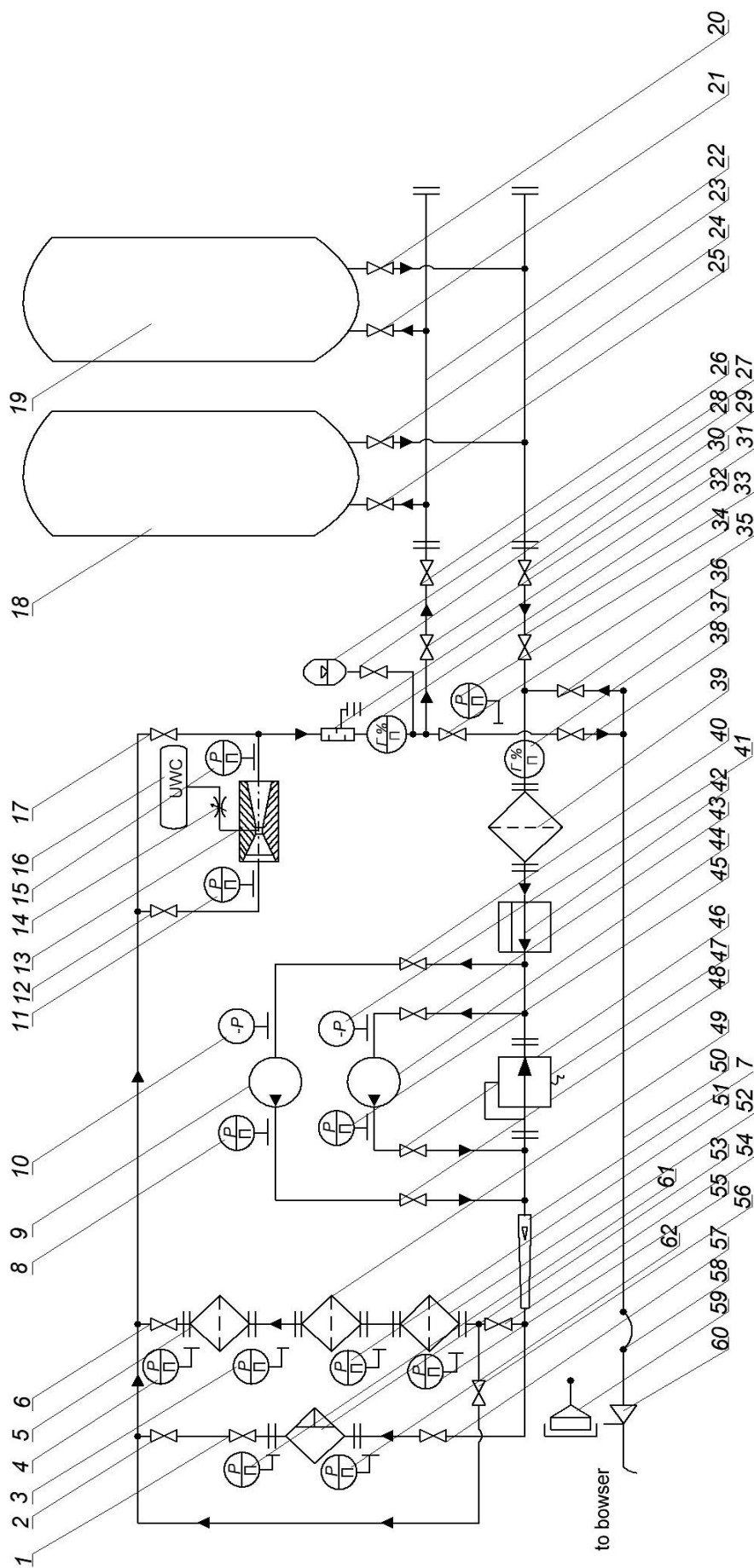
Fig. 1. Principal scheme of the full-sized test-bench for diagnostics and purification of aviation fuel

1, 2, 6, 12, 17, 20, 21, 23, 25, 26, 28, 29, 30, 33, 35, 36, 38, 40, 43, 46, 48, 54, 56, 57 — cranes; *3, 4, 11, 15, 34, 51, 55, 61,62* — manometers; *5* — filter TF-10 with TFB 8D2.966063 or AFB-1, AFB-5; *7* — flow indicator; *8, 45* — differential pressure gauges; *9, 44* — pumps SCL-20-24A; *10, 41* — pressure-vacuum gages; *13* — confuzor-diffuser type nozzle; *14* — dosing throttle; *16* — forecastle with unwatercrystallization (UWC) liquid; *18, 19* — tanks RGS-60; *22* — forcing pipeline; *23* — suction pipeline; *27* — hydraulic shock absorber GA-2; *31* — induction neutralization of fuels' static electricity (INSEP); *32, 37* — liquids control instrument PKZg-902; *39* — filter FGN-60 (120) with FE-670-15-I (3 pc), FE-2000-15-I (1 pc); *42* — contaminations' introduction instrument; *47* — protective bypass valve SPPK 4-16; *49* — filter-separator ST 500-2M with PBFV-1200M (1 pc) in part of EVK-300-5M (4 pc.), ES-300A (4 pc); *50* — pipeline to tanker; *52* — filter TF-10 with case TFCh-16K and FE-055M (6 pc), FE-170-I (6 pc); *53* — force cleaner; *58* — dispensing hose; *59* — tip of lower fuelling NNZ-4; *60* — dispensing crane RP-40

1.1.38

- the maximum acceptable pressure of working liquid — 3 kg/cm^2;
- necessary for instrument supplying voltage — 220 V;
- frequency — 50 (Hz);
- dimensions — $355 \times 355 \times 420$ mm;
- mass — 7 кг

Before cleaning system, which is research, was set vibration flow indicator *7*, which allows determining temperature, density and quantity of pumping liquid. It called Coriolis flow indicator, in which movable transformation element doesn't rotate, only provides continuous oscillation with constant or periodically damped amplitude under external influence [3].

After filter FGN-60, -120, *39* was set contaminations' introduction instrument *42*, by which pollution entered in dosing amount for more exact research of fuel cleaning during its pumping through stand.

For adding UWC liquid crane *17* was closed and open crane *12*, directing the fuel flow through mixing unit. In unit construction considered, that in local dosing instruments pressure in trunk pipelines is more than introduction of UWC liquid. Through dosing throttle *14* UWC liquid from forecastle *16* by gravity gets into throat of confusor-diffuser nozzle, where due to the above mentioned considerable difference of pressure and thus under influence of hydrodynamic cavitation, mixing with fuel and uniformly distributed by volume of output from diffuser [4]. Pressure at the inlet and outlet of the nozzle controlled by manometers *11* and *15*.

Pump SCL-20–24A *9, 44* is as suction, centrifugal-vortex type. Case made of aluminium alloy. At the top of the case are suction and force pipes.

Horizontal steel tank RGS-60 *18, 19* intended not only for fuel storage but for research purification of its internal surface.

Conclusions

Therefore, full-sized test bench allows:

1. Introduce contamination to aviation fuel in various concentration for research of efficiency its purification by filters and cleaners.

2. Conduct research on diagnostics and purification of fuel in a wide range pumping, temperature and pressure.

3. Dosage add UWC liquid in a fuel.

4. Research purification of tank's internal surface by different methods.

References

1. *Пузік С.О.* Методичні аспекти проблеми очищення авіаційного палива силовими очисниками / *С.О. Пузік, В.С.Манзій* // Препринт. — К.: НАУ, 2010. — 45 с.

2. *Пузік С. О., Гвоздецький А. В.* Спосіб очищення реактивних палив шляхом осадження часток забруднень Пат. 67429 України, МПК C10G 31/00. — №201017538 Заявл. 15.06.2011; Опубл. 27.02.2012, Бюл. №4. — 5 с.

3. *Пузік С.О.* Розробка гравітаційного очисника авіаційних палив. Автореф. дис. канд. техн. наук. — К.: КМУЦА, 1999. — 20 с.

4. *Ланецький В.Г.* Спосіб змішування протикристалізаційної рідини в авіаційному паливі від замерзання води / *В.Г. Ланецький, С.О. Пузік, О.С. Пузік, І.О. Ліпко, О.О. Ліпко* // Пат. 31646 України, МПК B01F 5/00. — №200802124, Заявл. 19.02.2008; Опубл. 10.04.2008, Бюл. №7. — 5 с.

V.S. Boutko Ph.D. Engineering (National Aviation University, Ukraine)

TRANSIENT PROCESS OPTIMIZATION OF PRESSURE STABILIZATION DEVICE OF AXIAL PISTON PUMP

Given materials are dedicated to pressure stabilization quality analysis of transient process & dynamic characteristics investigation of pressure regulating devise of axial-piston positive displacement pump.

Introduction

In hydro kinematic schemes of many modern pumps that are used in civil aviation the substantial lack is a very high open-loop gain. That is why it is necessary to introduce throttles of small cross-section area in series to the main hydraulic line (Figure 1).
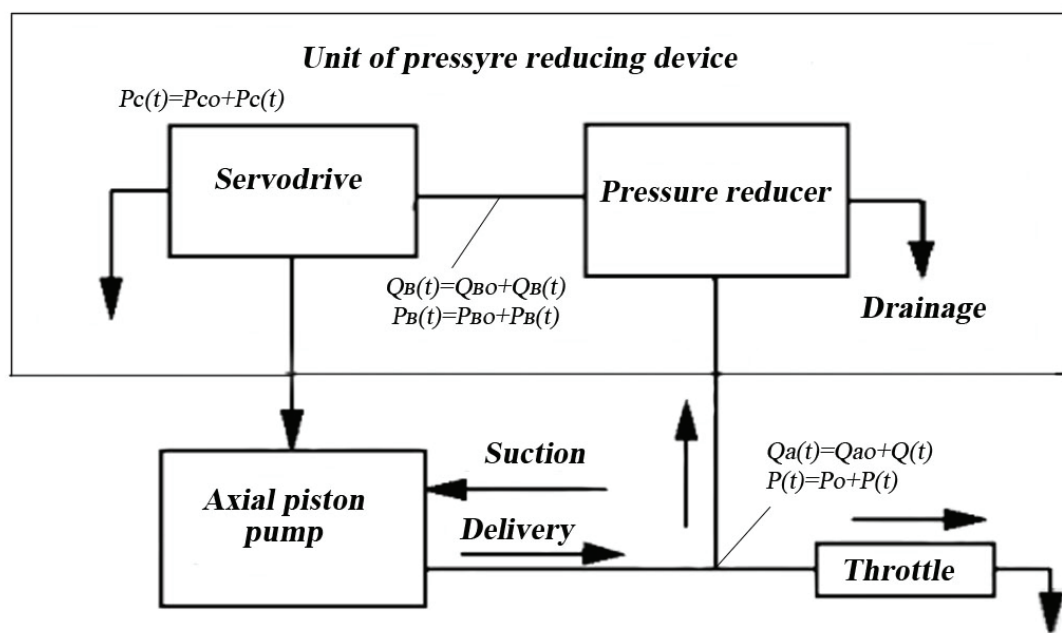
Figure 1 - The operational block diagram

The undamped natural frequency is of sufficiently high value, but the open-loop damping ratio is too law. An appreciable amount of open-loop damping is desirable in order to reduce the effect of variations in the load damping on the stability of the closed-loop system. The system can be stabilized affectively with great open-loop damping ratios or law value of position-feedback gain.

Statement of the problem

Purpose of this work is to study the principles of improving the quality of optimization of the damping properties of automatic device, stabilization of volumetric pump pressure, which provides minimum over shots in addition to the effective suppression of pressure oscillations in the delivery of the pump.

Creation and analysis of mathematical models

To improve the dynamic properties of the system the automatic stabilizer has been applied with hydraulic pressure reducer. It is very important for the dynamics of the system, that according to the coefficients of damping, and coefficients of gain of direct control chain the pressure reducer works actively because it includes the mathematical description and adds the additional parameter - coefficient of pressure drop (describes the pressure decreasing with the fluid flow rate increasing to

the servo drive of the automatic stabilizer). But additional including of the throttle in the servo system line reduces the quality of the system transient performance.

In analyzing the dynamic behavior of this system it is necessary to assimilate the characteristics of each of its components to a comprehensive characterization of the system. In this case, mathematical equations and block diagrams are used to represent the complete system.

For the estimating dynamic properties of the system and the pressure regulator in particular the transfer functions of the piston moving (1) and of the pressure change in the regulator (2) has been obtained.

The transfer functions has been derived by the compilation of the linearized equations: continuity equations, force equations for the piston motion in the servo system and in the pressure-reducer, the slide motion of the sensitive part of the system and the constraint equations of fluid flow and pressure drops.

The transfer functions of the linear model of the system, after the Laplace transforms becomes:

The transfer functions of the piston displacement (TFD)
$$W_y(S) = \frac{Y(S)}{\Phi(S)} = \frac{A_0}{a_3 S^3 + a_2 S^2 + a_1 S + a_0} \tag{1}$$

The transfer function of the pressure in the delivery line of the system (TFP)

$$W_p(S) = \frac{P(S)}{\Phi(S)} = \frac{(b_3 S^3 + b_2 S^2 + b_1 S + b_0) B_0}{a_3 S^3 + a_2 S^2 + a_1 S + a_0}, \tag{2}$$

where $\Phi(s)$ — the Laplace transform of the unit step change on the load throttle; $Y(s)$ and $P(s)$ - the Laplace transforms of the original functions of y(t) (the servo piston motion) and p(t) (pressure change on the throttle), respectively; a_3, a_2, a_1, a_0, b_3, b_2, b_1, b_0, A_0, B_0 - constants that define dynamic properties of the pump.

Optimization of the transfer function TFD is having been done by the way keeping the uniformity of the amplitude frequencies characteristics and linear phase characteristics in the widest band of frequencies. Fulfillment of the condition of uniformity of the amplitude (Figure.2) denotes the Nyquist diagram approximation to a circle at least in its lower half part for the not lower than third order dynamic systems.
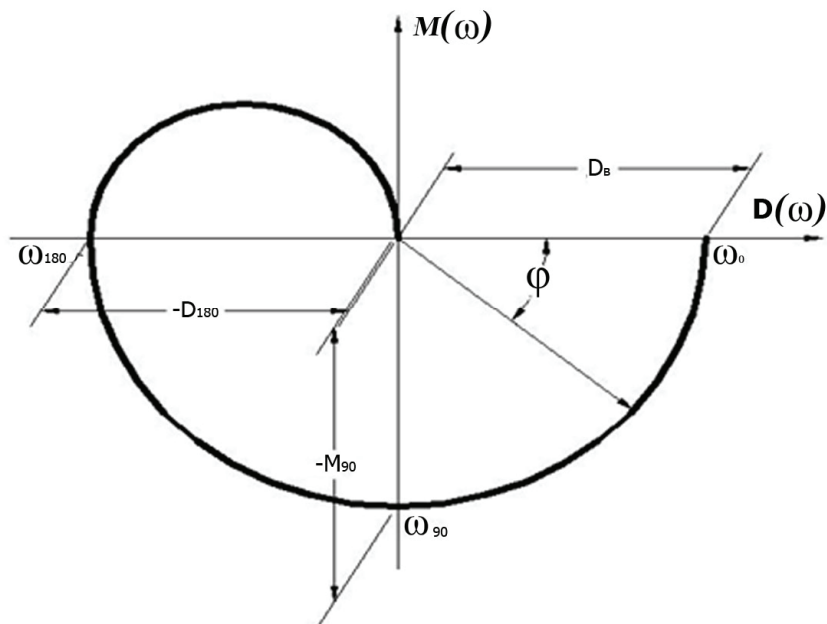
Figure 2 - Polar plot- Nyguist diagram

Function TFP (3) is presented in the form of the complex variable by means of the frequency method after transformation by substituting $s = j\omega (j = \sqrt{-1})$ operator into it:

$$W_y(j\omega) = \frac{A_0}{a_0 - a_2\omega^2 + j(a_1\omega - a_3\omega^3)} = D_{(\omega)} + jM_{(\omega)} \tag{3}$$

where

$$D_{(\omega)} = \frac{A_0 a(\omega)}{a^2(\omega) + b^2(\omega)}; \ M_{(\omega)} = \frac{A_0 b(\omega)}{a^2(\omega) + b^2(\omega)}$$

are the real and imaginary parts of TFP, respectively.

At phase shift on 90 $°\left(\omega t = \frac{\pi}{2}\right)$; $a_{(\omega)} = a_{90} = 0$ at the first particular frequency $\omega^2 = \omega_{90}^2 = \frac{a_0}{a_2}$. Therefore, the real part of the TFP in the polar plot-Nyquist diagram passes through zero.

At the second particular frequency TFP $\omega^2 = \omega_{180}^2 = a_1/a_3 \ ; b_\omega = 0$,

The optimum ratio of the kinematics of the servo drive and its damping

The ratio of actuator kinematics is equal to the ratio of the increment of the coordinate of the piston (y) to the increment of the variable operating volume (V). This ratio, together with the flow rate gain of the slider valve, (k_3) defines a straight chain amplification of the dynamic system of the pump servo drive. The addition of the throttle servo line reduces the speed of the dynamic system and therefore cannot serve as a means of improving the quality of transient processes.

The connection in series of the pressure reducer greatly increases the possibility of optimization of the parameters with a slight complication of the pump design.

From the second condition of optimization, assuming that

$k_b^2 k_c^2 \ll m^2 k_y^2 + 2mk_y k_b k_c$ we will obtain $k_{opt} \approx \frac{\sigma^2}{2 - \sigma^2}\left(\frac{F^2 + Ck_c}{k_y} - \frac{mk_y}{\sigma^2 k_c}\right)$.

The optimum quality factor of the dynamical system of the transfer function $W_y(s) = \frac{Y(s)}{\Phi(s)} = \frac{A_0}{a_3 s^3 + a_2 s^2 + a_1 s + a_0}$ depends mainly on the gain ratio of the servo drive (k_h) and the degree of pressure reduction (λ).

The optimum gain ratio of the servo drive kinematics with the additional assumption is determined by:

$$k_{opt} \approx \frac{\sigma_0}{F}\left(\lambda + \frac{k_n C_{зол}}{\lambda к_3 f_3}\right)\sqrt{\frac{(F^2 + Ck_c + k_b k_y)^3}{mk_c}} . \tag{4}$$

Since the analytical optimization of output parameter (delivery pressure of the pump) is very difficult to obtain because of the third-order polynomial numerator TFP, then the TFD function is being optimized.

According to the results of TFD, optimization the major parameters of a dynamical system: the circular natural frequency (ω_c), damping vibration (η) and exponent decrease may be identified.

From physical conditions the integration constants C1, C2, C3 of the piston displacement $y(t)$ may be determined:

$$y(t) = C_1 e^{rt} + C_2 e^{nt}\cos(\varpi_c t) + C_3 e^{nt}\sin(\varpi_c t). \tag{5}$$

Direct determination of the transition function of pressure TFP is being estimated similarly but according to the new constants, which can be calculated from the equation:

$$p(t) = D_1 e^{rt} + D_2 e^{nt}\cos(\varpi_c t) + D_3 e^{nt}\sin(\varpi_c t). \tag{6}$$

The transition pressure function TFP is defined by means of basic $y(t)$ (5) using the connection between the TFD and the TFP:

$$P(s) = \frac{C_{зол}}{\lambda F k_3 k_3} \beta(s) Y(s), \qquad (7)$$

where $\beta(s) = b_3 S^3 + b_2 S^2 + b_1 S + b_0$ is a polynomial of third degree with respect to the differentiation operator.

Constant value D can be estimated like:

$$D_1 = \varphi_1 C_1; \; D_2 = \varphi_2 C_2 + \varphi_3 C_3; \; D_3 = \varphi_2 C_3 - \varphi_3 C_2;$$

Analysis of the simulator results of transient functions $y(t)$ and $p(t)$ are shown in Figure. 3.
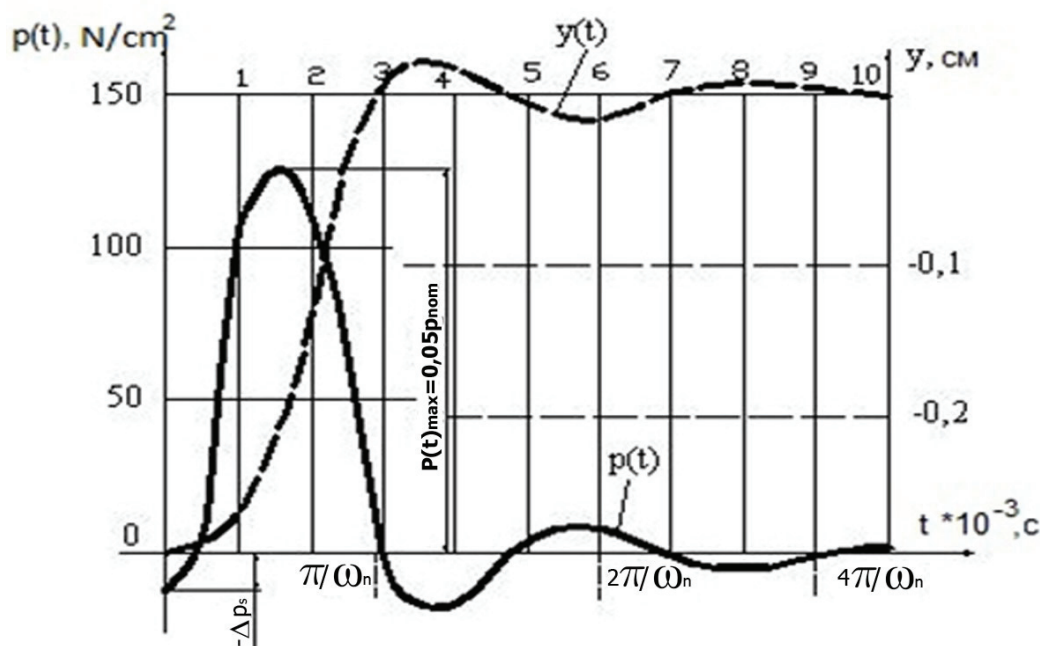
Figure 3 - Transient response

Conclusions

1.   For $y(t)$: small overshoot of the first half wave (overshoot less than 5% of full piston stroke); the intensive damping of the oscillations (not more than 2 half-wave); small time of regulation (with not more than 0,005s. in the passed band).

2.   For $p\,(t)$: the maximum overshoot pressure during acceleration of the piston, intensive damping; maximum overshot not exceed 5% of the nominal pressure at the step function of the pump delivering of 0.1 of nominal.

References

1.   *Р. Дорф, Р. Бишоп*, Современные системы управления, пер. с англ. Б.И. Копылова.- М.: Лаборатория Базовых знаний, 2004.-832с.

2.   *Халфман Р.* Динамика, пер. с англ., Главная редакция физико-математической литературы из-ва «Наука», М.:-1972.-568с.

3.   *Д.Н. Попов* «Динамика и регулирование гидро- и пневмосистем». Учебник для машиностроительных вузов. М., 1976.

4.   *Ч. Филлипс, Р. Харбор* Системы управления с обратной связью. М.: Лаборатория базовых знаний, 2001-615с.

UDC 620.179.1

S.R. Ignatovich, Sc.D., M.V. Karuskevich, Ph.D., T.P. Maslak, Ph.D.
(National Aviation University, Ukraine)
Jean-Bernard Vogt, Sc.D., Ingrid Serre, Ph.D. (Université Lille1, France)

APPLICATION OF THE LIGHT MICROSCOPY AND ATOMIC FORCE MICROSCOPY FOR QUANTITATIVE FATIGUE DAMAGE ASSESSMENT

As a result of the repeated loading the deformation relief appears and grows on the surface of pure metals and alloys. The deformation relief is a system of extrusions, intrusions and persistent slip bands. Intensity of the deformation relief increases cycles by cycles and depends on the level of the applied loads. The possibility of the relief and fatigue analysis by the light microscopy and atomic force microscopy is shown in this paper.

Introduction. Forming of the surface deformation relief under cyclic loading is a result of the dislocation movement. Deformation relief can be explored at the different scale levels. On the surface of the aluminum deformation relief can be observed by the light microscopy under the relatively small magnification. Optical methods allow to analyze the process of the relief nucleation and development as an development of the plane images. Additional tool for the analysis of relief images is a fractal geometry. Atomic force microscopy at the moment is a most power method for the investigation of the deformation structures. It allows to explore relief components from the nano to meso scale levels and exhibits the advantage to measure accurately the *z*-coordinate during the scanning of the surface in the *x* and *y* directions with a resolution of the order of nm.

The interest to the wide investigation of the deformation relief on the surface of alclad aluminium alloy D16AT is caused by proved relationship between the relief parameters and the process of fatigue accumulation. These researches have been carried out at the National Aviation University [1, 2]. The practical result of the researches is a concept of a new fatigue sensor, based on the possibility to monitor fatigue by the parameters of the sensor's surface state [3, 4].

Proposed approach to the fatigue life assessment by the parameters of the deformation relief needs creation of the phenomenological model of the relief development. Thus the necessity of the further researches with advanced methods is determined.

Application of the light microscopy to the investigation of cyclically deformed metals surface. The main volume of deformation relief data has been obtained in result of the fatigue testing of the constructional aluminum alloy D16AT specimens. The western analog of the alloy is a 2014 T3 alloy. The regimes for fatigue testing have been selected to correspond the real loading conditions of the aluminum parts of the aircraft fuselage and wing.

Deformation relief may be observed under the magnification from x200…to x 300. Such enlargement gives the images with homogenous surface structure even near the stress concentrators.

Saturation of the surface by the extrusions, intrusions, persistent slip bands changes cycle by cycle monotonically as it shown in fig. 1. The specimen has been tested by cyclical tension with maximum stress $\sigma_{max} = 147,0$ MPa, stress ratio $R = 0$.

a)   b)   c)   d)
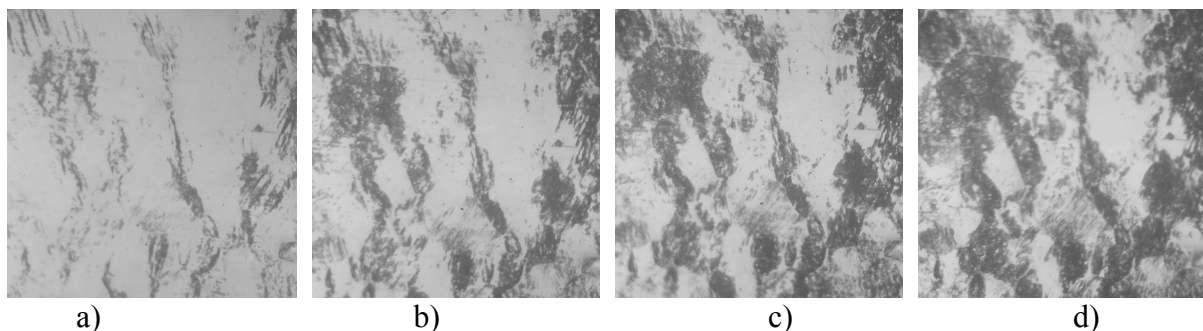
Fig. 1. Images of the deformation relief: a) $N = 30\ 000$ cycles (1,9% of life); b) $N = 100\ 000$ cycles (6,3 % of life); c) $N = 200\ 000$ cycles (12,6 % of life); d) $N = 400\ 000$ cycles (25,2% of life)

On the photos obtained with magnification x350 (fig. 1) one can reveal known features of fatigue: slip bands, extrusions, intrusions.

The share of slip bands on the observed area decreases with increase of cycle's number, intrusions and extrusions becomes the preferable structures.

The images of cyclically loaded specimen surfaces have been processed by special software. The program saves the surface images in bmp format and gives the possibility to determine the proposed damage parameter D quantitatively. Such parameter is estimated near the stress concentrator on the area approximately 0,09 mm^2. Damage parameter D is equal to the ratio of the surface area with deformation tracks (PSBs) to the total checked surface in the observed spot.

Fractal dimension is considered as an additional parameter of the deformation relief.

The search of the additional criteria for the deformation relief quantitative description leads to fractal geometry [5], which is wildly used nowadays at solving the material science problems.

Fractal geometry is a mathematical concept that describes objects of irregular shape. Some natural geometrical shapes, that can be irregular, rough or fragmented, can be described using concepts of fractal geometry as long as the requirement of self-similarity is satisfied. The latter term implies that the geometrical features of an object are independent of the magnification or observation scale. Nowadays there are a lot of methods of the fractal dimensions calculation for the nature objects. One of the most widespread is a "box counting" method. This method allows calculation of the definite types of fractal dimension.

The first possible type of fractal dimension is fractal dimension of the boundaries of deformation relief spots. This type of fractal dimension is designated as Dp. For some fractals the most informative parameter is a fractal dimension of the ratio of perimeter to area. It is known, that this ratio characterizes the shape of objects, and for the regular geometrical figures this parameter is constant value and doesn't depend on the object size. At the paper [6] this type of fractal dimension was successfully used for the description of the clouds shape. Correspondent fractal dimension for the clusters of deformation relief will be further called Dp/s. For the data processing the special software has been developed [1-4].

Fractal dimensions of the deformation relief clusters contours as well as the fractal dimensions determined by the ratio of perimeter to area exceed topological dimension of the line and are within the range of 1 to 2. In fig. 2 the graphs of the proposed surface relief parameters D and Dp/s evolution under fatigue are presented. The loading by cyclical bending have been conducted under the maximum stresses 147,0 МПа; 173,2 МПа; 234,5 МПа with stress ratio R=0.
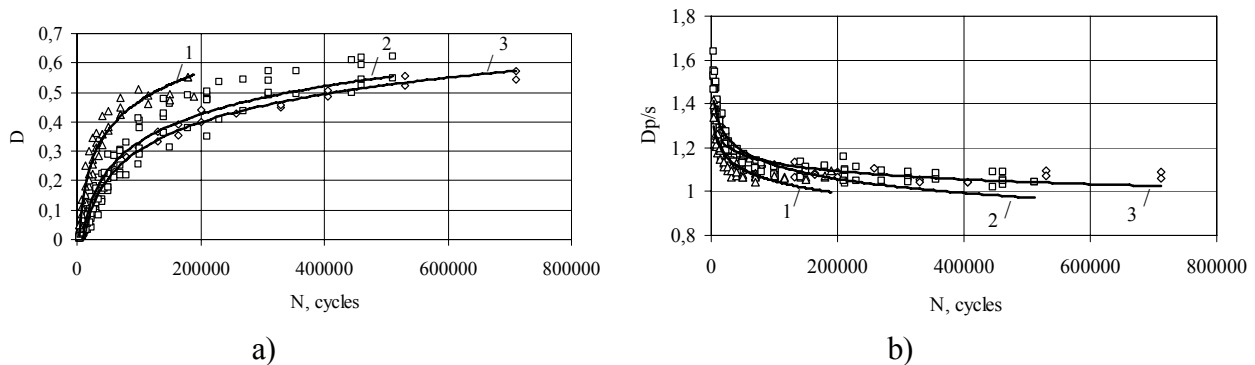
Fig. 2. Evolution of the damage parameter D (a) and fractal dimension Dp/s (b) under fatigue:
1) σ_{max} =234,5 MPa; 2) σ_{max} =173,2 MPa; 3) σ_{max} =147 MPa; R=0

Both diagrams points out the monotonic character of the selected parameters evolution. The regression analysis of the data points to the possibility to predict residual life ($N_{R,}\%$) of the specimens by the multiple regressions of view:

$$N_{R,}\%=A - B*D - C*D_{p/s}.$$

1.2.2

As it is seen from fig. 2 both relationships have clear expresses stages of the saturation. The saturation can take up to 80 % of the life to the crack initiation. Obviously, the achievement of the saturation by the clusters of the deformation relief points to the stoppage of the new grains involvement into the process.

Nevertheless, it is clear that the damage continue to grow after the point of the parameters *D* and *Dp/s* saturation. Thus, to reveal features of the damage on the deformed metal surface the advanced methods are necessary. The analysis of current methods of the surface morphology investigation shows that one of the most perspective method is an Atomic Force Microscopy.

Application of the Atomic Force Microscopy (AFM) for the deformation relief analysis.

AFM has been employed for the determination of cyclic plasticity partition in a duplex stainless steel, an alloy that contains an equivalent fraction of austenite and ferrite. The alloy has been fatigued in the low cycle fatigue regime, under strain control ($\Delta\varepsilon_t$ = 1.6%) by using a symmetrical triangular waveform and a strain rate of $4 \cdot 10^{-3}$ s^{-1}. Under this condition, both phases have been reported to be covered by fatigue slip markings suggesting they accommodate the cyclic plasticity. However, the role of each phase and their interaction in the mechanism of cyclic deformation accommodation is poorly documented.

The evolution of the stress amplitude with number of cycles is reported fig. 3a in log scale and fig. 3b with the fatigue life fraction in a linear scale.
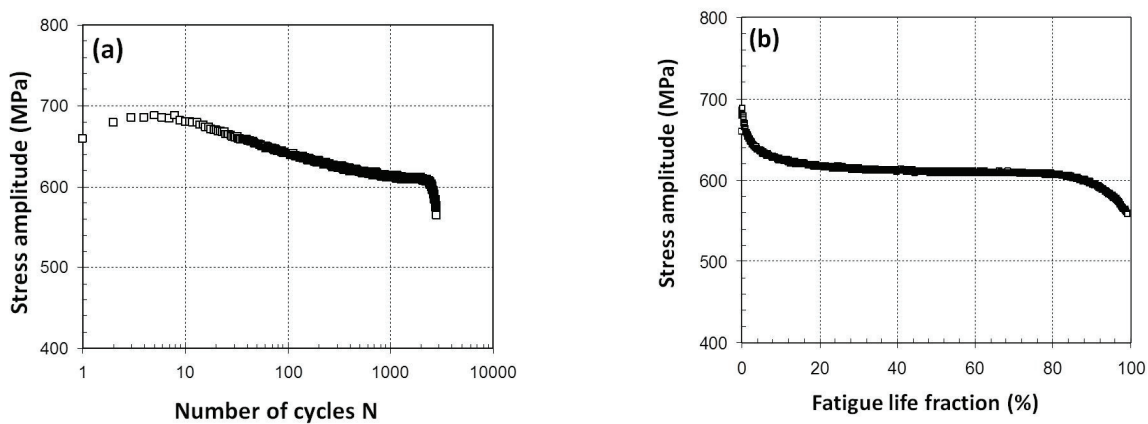
Fig. 3. Evolution of the stress amplitude with the number of cycles N (a) and with the fatigue life fraction (b) during cycling at $\Delta\varepsilon_t$=1.6%

The response consists in a cyclic hardening period during 5 cycles followed by a cyclic softening up to about 1 000 cycles where the material tends to be stabilized. Therefore, interrupted fatigue tests were carried out on a same specimen at 0.15% (5 cycles), 3.5% (100 cycles), 25% (730 cycles) and 60% (1680 cycles) of the fatigue life N_f for observations at AFM. In order to study the surface evolution, AFM observations were performed at room temperature in air using a Digital III Atomic Force Microscope in tapping mode with a Veeco anisotropic pyramidal tip MPP-11100.

Identification of slip markings.

At first, the high resolution of AFM images allows us to distinguish the different slip markings according to their morphology as follows. The different morphologies and their classification appear on the AFM micrograph taken after 60% of the fatigue life (fig. 4).

In the austenitic phase of the duplex stainless steel, slip markings can be classified into three different types according to their morphologies and their average height. The slip markings consist of rectilinear slip lines (height less than 20nm), ribbon like extrusions (height between 20nm to 75nm and up to 100nm) or a mixed morphology (extrusion beginning along the slip lines) [7].

However, in the ferritic phase, the classification is a little bit more complex because the formation of slip markings originates not only from the bulk properties of the ferrite but is also assisted by the neighbouring austenite. The former are curvilinear slip traces (less than 10nm in height), as observed in a previous work on monotonic behaviour of DSS [8], located at the interior

of the ferrite grains while the latter appear as straight slip lines near the α/γ boundaries (continuation of the PSM in γ). Other persistent slip markings more typical of cyclic deformation were observed and can be separated into three groups: rectilinear band-like extrusions and curvilinear cord-like extrusions (height between 15nm to 50 nm) and "highly rugged areas" areas frequently located at the phase boundaries which extrusions heights with the higher values can reach up to 100nm.

Relief evolution during cyclic deformation in austenite

Surface modifications start to develop early in fatigue life (near 40% of active grains after 5 cycles). The grain activity almost increases during the very first 3.5% of N_f and then evolutes at a moderate rate for the rest of the fatigue life (fig. 5a). The straight slip lines with a mean height step between 10 and 20nm, probably formed during the first quarter of cycle, is the main feature of the slip markings after 5 cycles. Slip localisation in these lines transforms them progressively into extrusions. The formation of the so called extrusions occurs by a local displacement of matter in the slip line giving rise to the mixed morphology. Increasing the number of cycles results in well formed extrusions. After 100 cycles (3.5% N_f), the slip markings have a double height distribution, 25-45nm and 15-20nm, which correspond respectively to the well formed extrusions and to the slip mixed bands. Further cycling results in the growth of extrusions up to 75nm at 25% of the fatigue life, more than 100nm at 60% of the fatigue life [7]. Slip traces corresponding to a secondary slip system are observed at 60% of fatigue life in few grains in areas close to the grain boundary (19% of the active grains). At this level of the fatigue life, little and irregular intrusions are detected running parallel to one side of the extrusions, but AFM is not the most suitable tool for direct evaluation of their depth from the metallic surface.
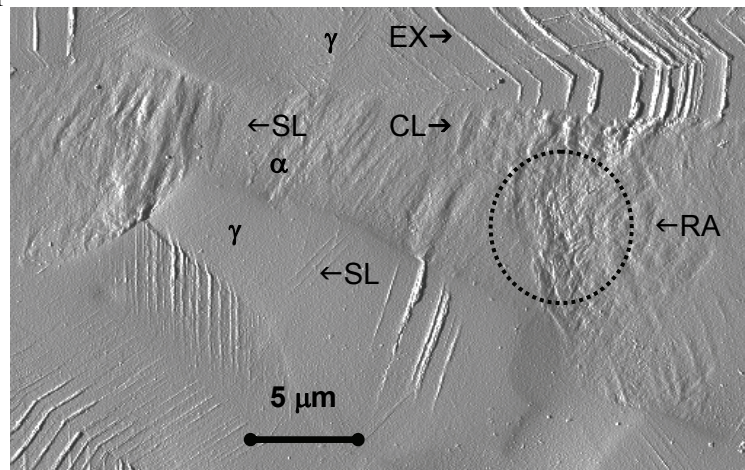
Fig. 4. AFM (signal error) micrographs with almost all kinds of slip markings: SL: slip line, CL: cord like extrusion, EX: ribbon like extrusion, RA: rugged area

Relief evolution during cyclic deformation in ferrite

As opposed to observations in austenite, the surface activity in ferrite during the first percentages of the fatigue life is weak. The surface feature, mainly consisting of slip lines, is nearly similar after 5 cycles (0.15% of the fatigue life) and 100 cycles (3.5% of the fatigue life) where less than 25% of ferrite grains are activated (fig. 5b). Occasionally, extrusion emergences which height was irregular (between 17 and 26nm) were observed [7]. A real activity in ferrite seems to occur after 25% of the fatigue life where the band like extrusions, the cord like extrusions and the highly rugged areas (HRs) can be easily identified. 80% of ferrite grains are active after 60% of the fatigue life but it was observed that inside a given grain highly rugged areas could be sided with undeformed material zones. It is interesting to note that in both phases slip bands are growing during cycling (fig. 5c), even in austenite though ferrite accepts to contribute later in the fatigue than austenite.

The detailed AFM study of surface relief in DSS cycled at $\Delta\varepsilon_t$=1.6% allows us to conclude that the two phases of the DSS contribute to the cyclic plastic deformation. In terms of stress

evolution, the initial hardening-softening period up to 25% of the fatigue life reflects a self-austenitic response related to well formed extrusions. From that point, a real contribution of the ferritic phase seems to take place even though topographic changes are noticeable since 3.5% of the fatigue life. This allows concluding that the cyclic accommodation by the two phases is a progressive process in which ferrite compensates the vanishing action of austenite in the accommodation mechanism.
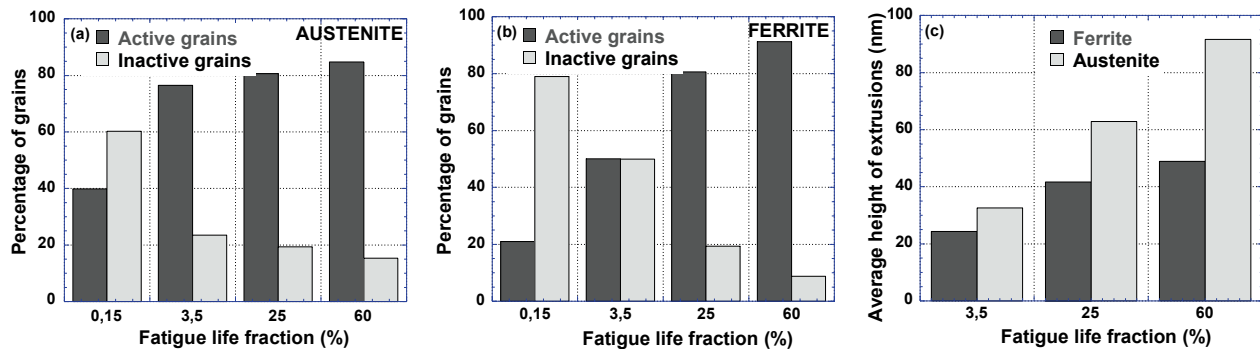
Fig. 5. Evolution of the plasticity partition vs. fatigue life fraction in terms of active and inactive grains in austenite (a) and in ferrite (b) of the DSS and in terms of extrusions average height in α and γ grains

Conclusions

Deformation relief on the surface of cyclically deformed metals can be considered as an indicator of the accumulated fatigue damage.

One of the efficient methods for the deformation relief analysis is a light microscopy. Intensity of the deformation relief and fractal dimension of the relief's clusters allows determining quantitatively fatigue damage especially on the early stages of fatigue.

Creation of the phenomenological model of the deformation relief forming and evolution requires investigation of the process on different scale levels.

Atomic force microscopy can be considered as a perspective tool to collect data for adequate model of the deformation relief.

References

1. *Karuskevich M.V., Korchuk E.Yu., Yakushenko A.S., Maslak T.P.* Estimation of the accumulated fatigue damage by saturation and fractal dimension of the deformation relief // Strength of materials - Vol. 40. - № 6. – P. 693-698.

2. *Karuskevich M., Karuskevich O., Maslak T., Schepak S.* Extrusion/intrusion structures as quantitative indicators of accumulated fatigue damage // International Journal of Fatigue. – 2012. – № 39. – P. 116–121.

3. *Karuskevich M.V.* Fatigue life prediction by the structurally sensitive damage indicator // Proceeding of NAU. – 2012. – № 1. – P. 139–143.

4. *Karuskevich M.V., Maslak T.P., Siedametova G.S.*, Fatigue sensor for structural health monitoring // 5th Int. conf. on structural health monitoring of intelligent infrastructure (SHMII-5): 11-15 December 2011.–Cancún, Instituto de Ingeniería, UNAM, México. – Poster presentation №5.

5. *J. Feder.* Fractals. - New York: Plenum Press. – 1988.

6. *S. Lovejoy.* Area-perimeter relation for rain and cloud areas. - Science, 216. – 1982. – P. 185 – 187.

7. *Vogt J.-B., Salazar D., Proriol Serre I*, Partition of cyclic plasticity in the 25Cr-7Ni-0.25N duplex stainless steel investigated by atomic force microscopy, Chapter 8 in Duplex Stainless Steels Ed. I. Alvarez-Armas and S. Degallaix-Moreuil, ISTE Ldt and John Wiley & Sons, 2009.

8. *Serre I., Salazar D., Vogt J.-B.*, AFM investigation of surface relief in individual phases of deformed duplex stainless steel // Materials Science Engineering A – 2008 - Vol. 492 – P. 428–433.

UDC 629.735.083.2/ 03:620.179.1(045)

S.R. Ignatovich, Dr. sc. ing. (National Aviation University, Ukraine)
N.I. Bouraou, Dr.sc.ing. (National Technical University of Ukraine "KPI", Ukraine)
M.V. Karuskevich, Ph.D. (National Aviation University, Ukraine)

STRUCTURAL HEALTH MONITORING OF AIRCRAFT IN OPERATION

The analysis of current trends in aircraft structural health monitoring systems is presented. The new approach for accumulated fatigue assessment is described. The main idea of the proposed methodology consists in possibility to assess metal fatigue by the parameters of the surface deformation relief. Main damage parameters are indicated. The conceptual design of inboard computer- aided fatigue monitoring system is shown.

Introduction. Modern aircraft is a very complex and expensive product. To provide efficient economic operation the service life should not be less than 30 years and 40…80 thousands of flights [1].

The cost of aircraft maintenance is about 25 % of total operational costs [2]. Taking into account the huge world aircraft fleet it is clear, that the reduction of the maintenance cost directed on the operational safety is a very actual and important problem for aircraft manufacturers and operators.

The damage tolerance concept is based on the possibilities to inspect and monitor growth of the defects [3,4]. In other words it means the necessity of structural health monitoring for individual craft and correspondent assessment of residual life. The task can be solved by the application of advanced tool methods of nondestructive inspection.

Methodology of the aircraft state assessment and prognosis of residual life is based on the interpretation of current data from inspected parts obtained by the gages, sensors, transducers, etc.

Important information for structural health analysis is delivered by the stress-strain gages. These data allow identification of the history of loading and predict failure.

Thus, data about loading and accumulated damage complement each other and are mutually dependent.

For the solution of the aircraft life prognosis problem the development of the intelligent diagnostic system is more realistic and economically efficient way of research and development activity. The important branches of such systems are the systems of Structural Health Monitoring (SHM) [5].

The aim of the presented paper is to ground actuality, necessity and perspectives of the development and application of the aircraft systems for accumulated fatigue analysis and prognosis of the residual service life.

Modern trends of SHM systems application in aviation. SHM systems are under intense development during past two decades. First systems were proposed for the bridges, sky-scrapers, etc. After these initial stages of research and developments, SHM became the subject of aviation manufactories and authorities.

In 90th Airbus proposed "intelligent" airframe technology, which includes the development and implementation of smart structure technologies [6].

In 2007 the Aerospace Industry Steering Committee (AISC), which consists of industry, military, government, regulatory and academic organizations started activity on providing the implementing SHM for commercial and military aerospace applications. Airbus views SHM as key to its "intelligent structure philosophy" and Boeing has identified it as an emerging technology that may provide significant improvements in operational efficiencies [7].

SHM presumes implementation of different kinds of sensors to assess influence of stress-strain conditions and environment on strength and fatigue of aircraft components [8, 9].

The final aim of SHM is a building a nervous system for aircraft (fig.1). SHM technologies can give operational personal complete information about what is going on in an aircraft's structure whenever it is needed [6, 8].
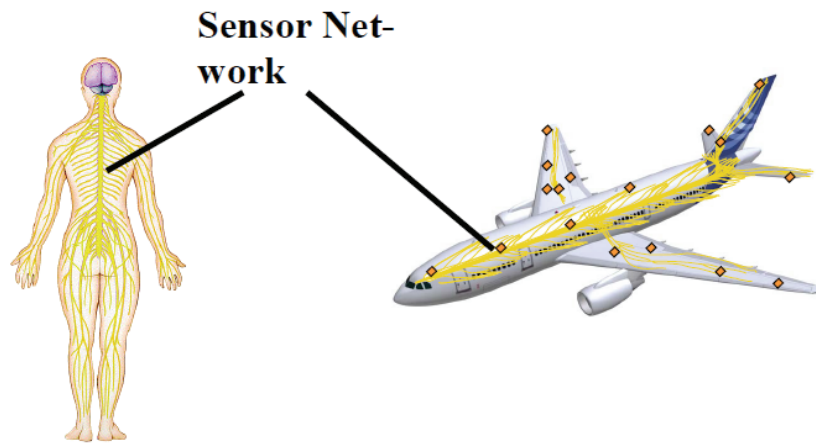
Fig. 1. SHM is the imitation of the human nervous system

In the future, aircraft airframes will implement technologies in a step-by-step way, which will give aircraft structures self-adaptive, self-monitoring and "self-healing" characteristics. Corresponded research and technology programs in these technological areas are ongoing.

It is expected that implementation SHM into the new airframe designs may be used to increase the allowable stress level by more than 15%, while keeping the inspection interval constant [6].

Monitoring of the loading and damage. Key components of SHM systems are the sensors, registering appearance and growth of the defects under the operation. At the moment a set of different sensors have been created [10, 11]. More efficient were proved to be sensors based on the measurement of electrical resistance, surface roughness, martensitic transformation, fatigue fuses, oxide film sensors, etc. At the same time some methods of the direct inspection should be mentioned here: acoustic emission, ultrasonic, etc.

One of the most advanced methods is an application of the fiber Bragg-based sensors. Optical strain gauges are in any applications. These sensors are based on so-called fiber Bragg gratings. Such a Bragg grating uses a great many reflection points at regular spacing. At each of these points, part of the radiated light is reflected. The reflected light interferes and generates a reflection peak. This peak shows a characteristic wavelength which is dependent on the spacing of the reflection points [12].

Lamb wave methods [12] recently can be considered as a more reliable way to locate damage in the composite materials. These techniques have been implemented in a variety of approaches, including the use of separate actuators and sensors to monitor transmitted and/or reflected waves, and multipurpose patches which both actuate and sense. Each of these techniques offers their own unique advantages in detecting certain types of damage.

Besides the information about stress-strain state the online data concerning accumulated fatigue damage, nucleation of fatigue cracks are necessary for residual service life prediction. The methods of acoustic emission, Lamb wave techniques, acoustoultrasonic sensors in some cases are used successfully.

Monitoring of the exhausting of aircraft service life. According to the statistic collected by the aircraft manufactures and operators the fatigue remains one of the more major types of the operational damage. Approximately 31% of airframe defects are the fatigue cracks [8]. That is why the problem of fatigue monitoring takes an important place in SHM systems.

Fatigue sensors may be attached to the aircraft parts. Being subjected to the operational spectrum of loads the sensor changes the physic and mechanical property itself and indicates history of loading and accumulated fatigue damage.

Among the existing sensors the roughness sensors should be separated as a special subgroup [10]. The features of the roughness evolution essentially growth if the surface of the sensors covered with the layer of easily plastically deformed metal, for example by the pure aluminium. As a result of the cyclical loading the deformation relief develops on the aluminium surface.

Optical registration with computer analysis of the digital images of the deformation relief allows quantitative assessment of the relief and correspondent fatigue damage of the component under the operational loading.

Two possible kinds of the surface relief sensors are: a) foil sensors, and b) sensors made of alclad aliminium alloy.

Foil sensors are made of pure aluminium. Sensors can be attached by glue to the inspected part of the airframe [13, 14]. The disadvantage of the application of this type of sensors is a big labour input, complexity of the attachment, problems with transmission of loads to the sensor from structure.

The fatigue sensor made of alclad aliminium alloy has been proposed at National Aviation University. The same idea is used. The deformation relief is considered as an indicator of fatigue. For the sensor manufacturing the alloys are used: D16AT, V95A, 2024T3, 7075T6 [15].

In some cases the direct diagnostic of fatigue damage by the parameters of deformation relief is possible. For this purpose the local area near the stress concentrator should be prepared by polishing to provide of the possibility to investigate surface by optic. Such method is appropriate to parts made of alclad alloy [15,16].

As additional characteristic for deformation relief analysis the parameters of roughness are proposed [17].

Mentioned above approach has resulted in a new methodology for aircraft structural health monitoring system and to the development of experimental inboard sample [18] (fig. 2)
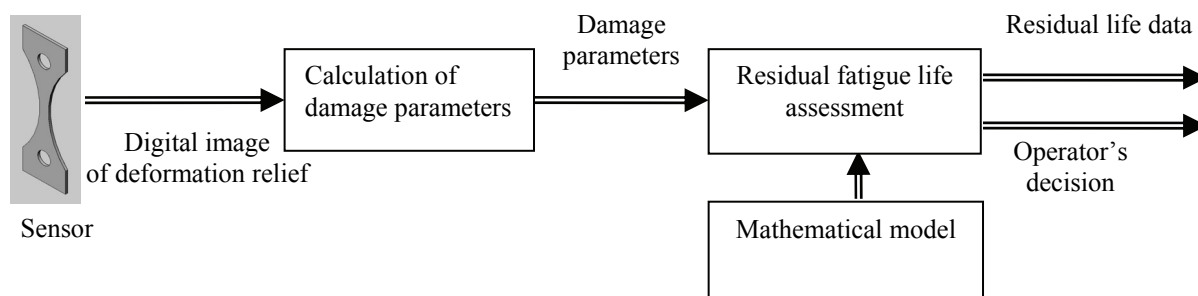
Fig. 2. The scheme of inboard fatigue monitoring system

Conclusions

As a result of the wide spectrum of research and development efforts conducted at the National Aviation University the new methodology for aircraft fatigue monitoring is created.

At the moment the experimental sample of inboard monitoring system can be designed and tested on real aircraft structure.

References

1. Peter B. The global airline industry/ B. Peter, A. Odoni, C. Barnahart. – West Sussex (UK): John Wiley & Sons Ltd, 2009. – 509 p.
2. Giurgiutiu V. Active sensors for health monitoring of aging aerospace structures. [Электронный ресурс] / SPIE's 7-th Int. symp. on smart struct. and materials, 5-9 March 2000, Newport Beach, CA. − Режим доступа к информации: http://www.me.sc.edu/Research/lamss/pdf/ CONFERENCES/C55_SPIE-00-3985-32_numbered.pdf.
3. Шанявский А. А. Безопасное усталостное разрушение элементов авиаконструкций / А.А. Шанявский. − Уфа : Монография, 2003. − 802 с.
4. Kuchemann J. Aircraft design: synthesis and analysis/ J. Kuchemann. − Stanford : Desktop Aeronautics Inc., 2001. − 570 p.
5. Бурау Н.И. Мониторинг жизненного цикла авиационной техники: проблема и основные пути ее решения / Н.И. Бурау, В.В. Аврутов// Современные методы и средства

неразрушающего контроля и технической диагностики: мат. 14 ежегодной межд. конф., 13-18 октября 2006 г., Ялта. – УИЦ «НАУКА. ТЕХНИКА. ТЕХНОЛОГИЯ», 2006. – С. 18-19.

6. Speckmann H. Structural Health Monitoring: a contribution to the intelligent aircraft structure. [Электронный ресурс]/ H. Speckmann, H. Roesner // Proc. 9th European NDT Confer. (ECNDT), 25-29 Sept., 2006, Berlin, Germany. − Режим доступа к информации: http://www.ndt.net/article/ ecndt2006/doc/Tu.1.1.1.pdf.

7. Airbus and Boeing back structural monitoring. [Электронный ресурс] / Flightglobal. Aircraft. − Режим доступа к информации: http://www.flightglobal.com/articles/2007/ 02/20/ 212184/ airbus-and-boeing-back-structural-monitoring.html.

8. Bartelds G. Aircraft structural health monitoring, prospects for smart solutions from a European viewpoint/ G. Bartelds // NLR TP 97489: National Aerospace Laboratory NLR − Amsterdam, 1997. − 13 p.

9. Boller C. Fatigue in aerostructures − where structural health monitoring can contribute to a complex subject. [Электронный ресурс] / C. Boller, M. Buderath // Philos. Transact. Royal Soc. − Режим доступа к информации: http://rsta.royalsocietypublishing.org/content/ 365/1851/561.full.

10. Rajic N. Methods of Early Fatigue Detection / N. Rajic, K. Tsoi // DSTO Aeronautical and Maritime Research Laboratory (DSTO-NT-0059). − Melbourne, 1996. − 31p.

11. Игнатович С.Р. Виброакустическая диагностика усталостной поврежденности образцов из алюминиевого сплава / С.Р. Игнатович, Н.И. Бурау, С.С. Юцкевич // Авиационно-космическая техника и технология. − Харьков: ХАИ, 2007. −№ 9 (45). − С. 124−128.

12. Staszewski W. Monitoring on-line integrated technologies for operational reliability – MONITOR / W. Staszewski // Air and Space Europe. − 2000. − V.2, N4 – P. 67-72.

13. Nagase Y. Fatigue gauge utilizing slip deformation of aluminium foil / Y. Nagase, T. Nakamura, Y. Nakamura // JSME international journal. Ser. 1, Solid mechanics, strength of materials. – 1990. − Vol. 33, №4, − P. 506−513.

14. Zasimchuk E. Single crystals as an indicator of fatigue damage/ E. Zasimchuk, A. Radchenko, M. Karuskevich // Fatigue Fract. Eng. Mater. Struct. − 1992. − Vol. 15, N 12. − P. 1281−1283.

15. Карускевич М.В. Зразок-свідок втомного пошкодження авіаційних конструкцій / М.В. Карускевич, Д.М. Костенюк, Є.В. Каран // Вісник Інженерної академії України. – 2009. − №3-4. – С. 219-224.

16. Карускевич М.В. Оптичний контроль накопиченого втомного пошкодження / М.В. Карускевич, Д.М. Костенюк, Є.В. Каран // Вісник НАУ. – 2009. − № 2. – С. 48-51.

17. Ignatovich S.R. The fatigue damage control of Al-clad alloy D16AT by characteristics of deformation relief on surface / S.R. Ignatovich, S.S.Yutskevych // Mechanical Fatigue of Metals: Abstr. XV Intern. Colloq. (XV-ICMFM), 13 – 15 September 2010 / Ed. by D. Rozumek & E. Macha. – Opole: Opole University of Technology, 2010. – P. 25.

18. Игнатович С.Р., Карускевич М.В., Бурау Н.И., Краснопольский В.С. Перспективы использования бортовых автоматизированных систем контроля выработки усталостного ресурса авиационных конструкций // Вісник Тернопільського Національного технічного університету: спеціальний випуск. Ч. 2, 2011 – С. 136-143.

V.V. Astanin, Sc.D., O.A. Tamargazin, Sc.D., O.I. Olefir, Ph.D., G.O. Shchegel, Ph.D.
(National Aviation University, Ukraine)

DESTRUCTION OF AVIATION ENGINE ELEMENTS OF COMPOSITE MATERIALS AT IMPACT LOADS

The need to reduce the weight of aircraft power plants leads to increased use of composites at their manufacture. Energy absorbing properties of a representative of the family of three-dimensionally fiber-reinforced composite materials based on glass fibers and polymer matrix at high-speed impact loads in the range of impact velocities of 200...1600 m/s and critical ranges of the material penetration velocities are studied.

Introduction

Modern aircrafts must meet the increasingly stringent requirements of weight reduction, increase of efficiency ensuring a high level of security at the same time. This leads to attempts of replacement of an increasing number of metal components of aircraft propulsion systems to manufactured with usage of composite materials ones [1, 2]. Such materials must possess specialized properties, suitable for the respective operating conditions of aircraft engines. There are two main groups of parts and engine components, which material is subject to different requirements.

The first group consists of the loaded with extremely high temperatures details of the internal motor tract, namely the working elements of the combustion chamber, turbine and exhaust cone. The details of these units should be rationally produced of metal and ceramic composites as they perform excellent characteristics of heat resistance. The second group includes load-bearing elements of the power plant working channel operating in less intensive thermal conditions, as well as all auxiliary propulsion units, which are external with respect to the main channel of a gas engine. These elements include [3]:

- sound-absorbing panels and casings forming the gas channel and representing the box-type structures with perforated surfaces;

- power panels and casings, which are box-type structures that perform the role of load-bearing units in engine elements;

- single-layer structures performed as unified load-bearing or connector elements, enclosures and cases.

Fiber-reinforced composites based on polymer matrix are well suited just for production of such elements allowing to achieve high levels of strength, provided the optimal selection of the type of material and its reinforcement. Such materials allow achievement of significant benefits in reducing the weight of the structure, but require careful examination and verification of their properties under conditions of every type of loads occurring in the operating conditions of air vessels. Given the high risk and devastating consequences, as well as a high probability of occurrence of impact loads, the study of the properties and behavior of advanced composites for application in aircraft engines under the action of impact is a problem primary importance.

Methods

The role of fiber reinforcement of composite materials consists in perception of the load and in absorption of the correspondingly applied energy up to the maximum level possible without breaking. Therefore ensuring of an optimal redistribution of load among the possibly greater number of fibers of the material plays an urgently important role. Effective redistribution leads to increased strength of the composite-material as of a unified structure at the same strengths of fibers and matrix individually.

In this regard, highly loaded and responsible parts of aircraft engines working also under impacts are intended to be produced of three-dimensionally fiber-reinforced composite materials. This is especially true due to the fact that fiber-reinforced composite elements are predominantly

shells of different kind. Impacts usually take place in the direction perpendicular to the shell surface or at an angle to it that increases the importance of realizing the three-dimensional fiber reinforcement. The described situation determined the choice of the researched representative of the family of three-dimensionally fiber-reinforced composite materials based on glass fibers and polymer matrix as an object of study.

The amount of energy that the material can absorb depends on the method and rate of the load application. Thus, the energy absorbing properties and strength of material depend on the velocity of interaction. Therefore, the material impact tests were carried out first of all at different values of such parameter as impact velocity. The other conditions of the collision remained unchanged during the experiments.
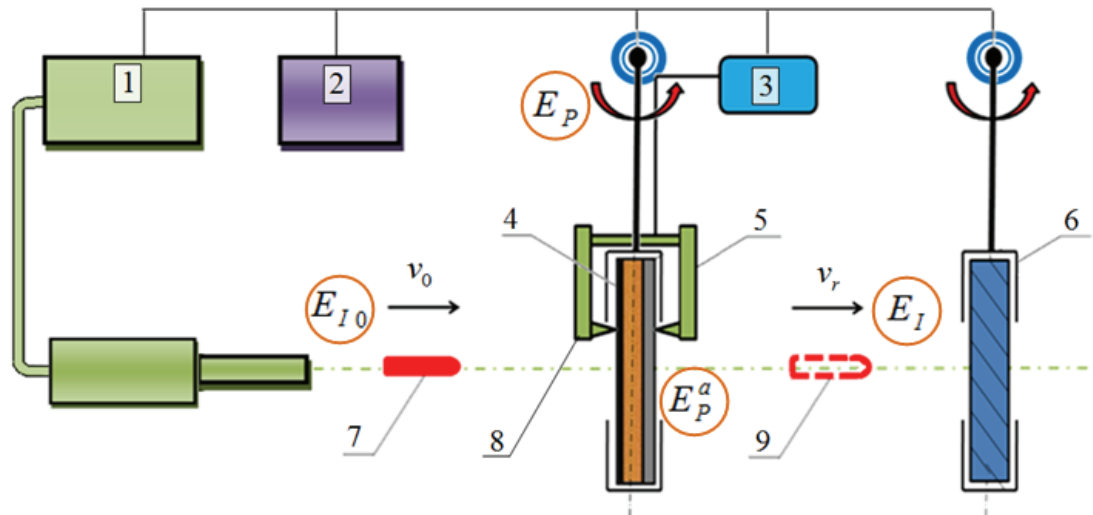
Fig. 1. Principal scheme of the impact testing system: 1 – combustion chamber, 2 – diaphragm unit, 3 – acceleration tube, 4 – control unit, 5 – carriage, 6 – working gas supply unit; 7 – power switching and pressure control unit; 8 – ignition unit; 9 – power supply unit

Structurally, the more advantageous arrangement of the experiment during an impact test of material samples is a test scheme according to which the sample is stationary fixed at the beginning of the impact. The required impact velocity is achieved through acceleration of the impactor taken as a non-deformable rigid body. This allows to easily control the kinetic energy that is introduced into the initial system of interacting bodies, as well as to place all the necessary recording equipment directly on the specimen mounting frame. In the carried out tests the attention was given to analysis of the energy absorbed during the collision by the tested material. Exactly this parameter characterizes the material protective properties that allow preserving the other parts and structure assemblies of the engine from damage caused by hitting bodies or formed fragments.

Principal scheme of the experiment and appropriate impact testing system is shown in fig. 1. More information about the realized test complex for the study of impact strength «aSTanin» («Acceleration System for Testing of Anti-damage Innovations») can be found in [4, 5].

It is also necessary to note that a great number of three-dimensionally fiber-reinforced materials are in fact conventionally considered to be so. This is due to the complexities of creating three-dimensional structures of interlaced fibers. In these cases, there is only binding of individual material layers in the direction of the third axis.

Results

The research allowed determining the characteristic for the material under study ranges of impact velocities, which are followed by the same type of material sample reaction and the type of damage formed. At minimum collision velocities only slightly noticeable forming of deformation cavities of small size is observed without damage of fibers and deeper lying layers of material. It can be assumed that this damage is superficial and does not lead to significant loss of strength.

Velocities of about 300 m/s are critical for the material and are accompanied by the transition from non-through penetration of the sample to cross-cutting (fig. 2). Thus, the limit of protective capabilities of the material to absorb impact energy is reached.
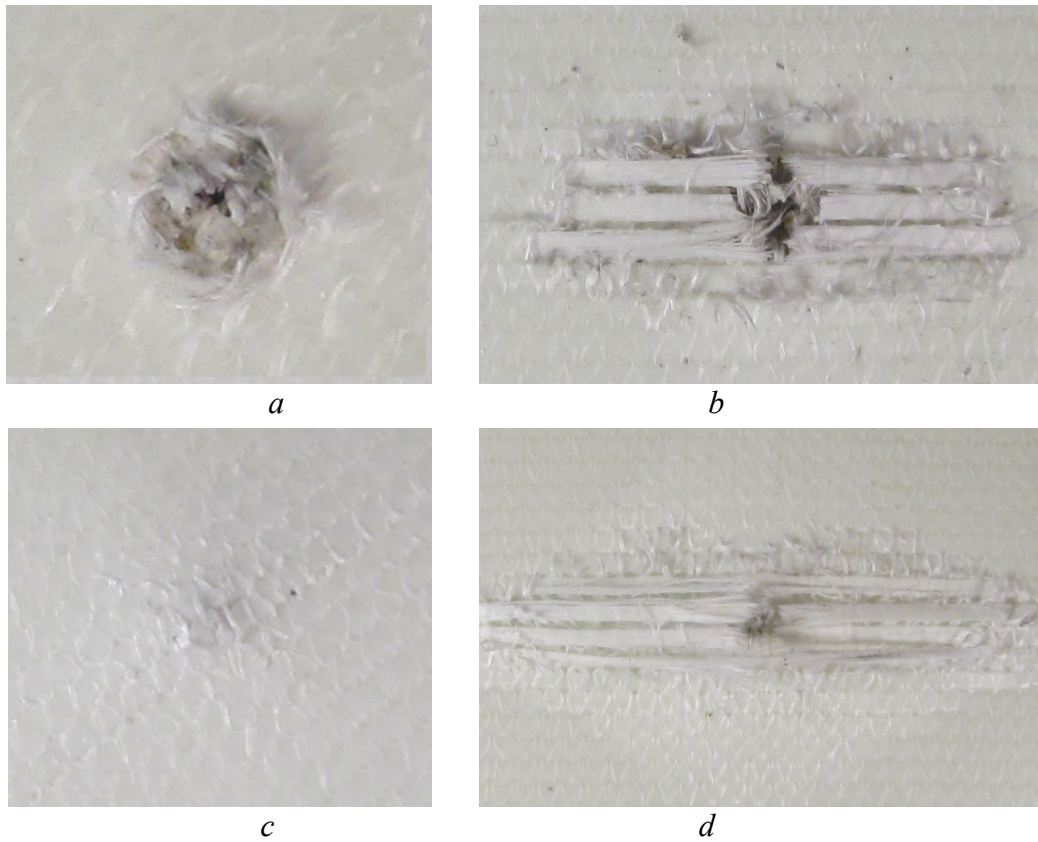
Fig. 2. Damaged front (top) and dorsal (bottom) surface of the sample material at the critical velocity of the almost cross-cutting specimen penetration (*a, c*) and at higher perforating impact velocity (*b, d*)

Non-through damage of the specimen is accompanied by intensive cracking along the fiber-matrix boundaries, fiber breakage, delamination of the layers. At high impact velocities these effects are considerably amplified.
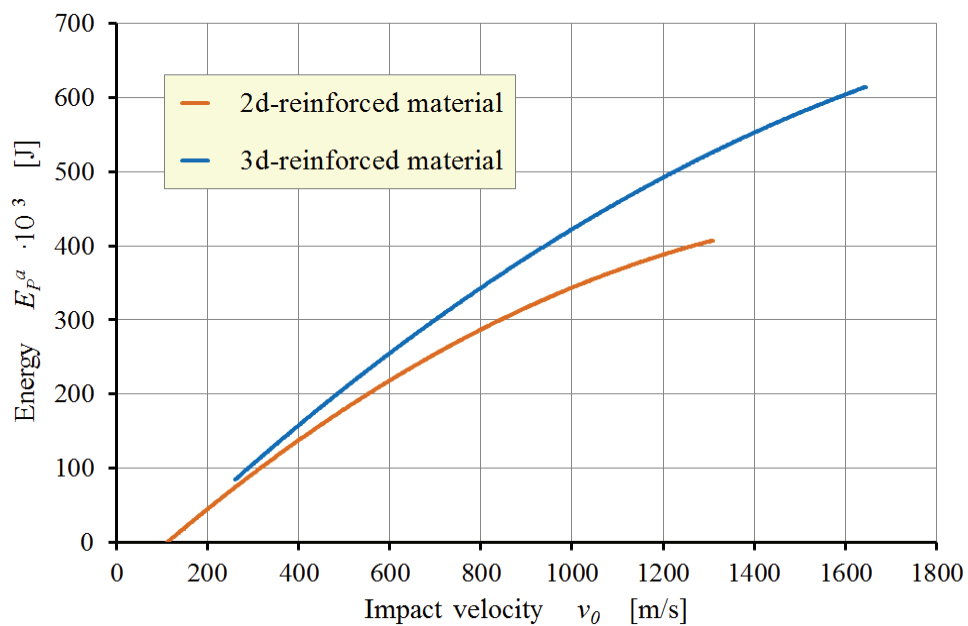
Fig. 3. Absorbed by the sample material energy according to the impact velocity

1.2.12

A characteristic feature of the sample penetration is formation of elongated damage area in each layer of material, which stretches in the direction of primary reinforcing fibers. This effect is explained by the peculiarities of fiber reinforcement lattice and weak coupling between the fibers along the perpendicular direction, i.e. in the case of the investigated material, insufficient reinforcement in the third direction for the aim of impact load perception.

The impact energy absorbed by the sample was calculated on the basis of the recorded values of the initial velocity of the impactor and its mass and velocity of the impactor after penetration, as the difference between its initial and residual kinetic energy. In addition, the calculation took into account the energy perceived during the impact interaction by the bearing structure supporting the specimen.
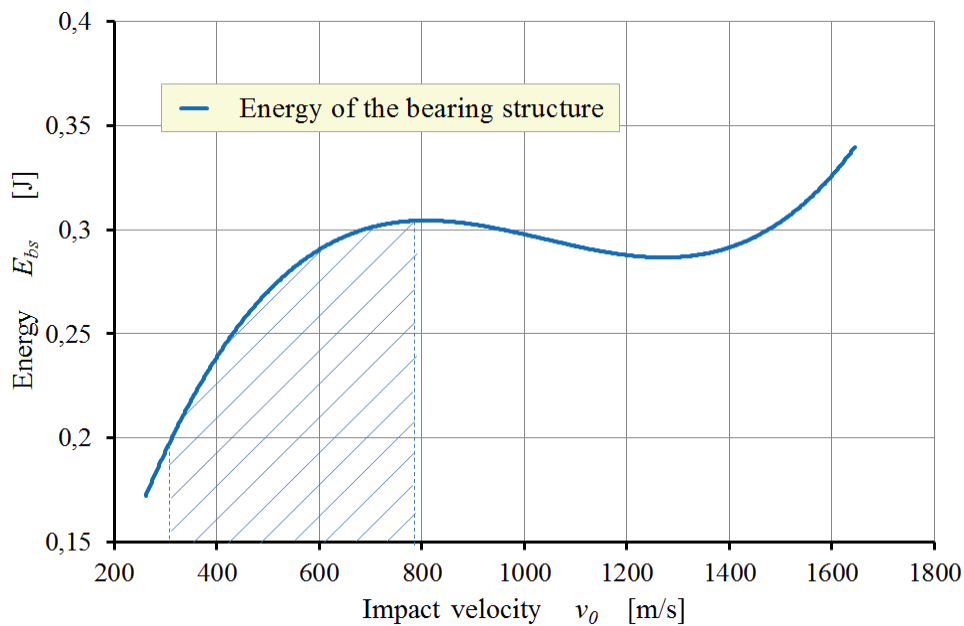
Fig. 4. Perceived by the bearing structure energy according to the impact velocity

The resulting values of energy absorbed by the sample material depending on the impact velocity are shown in fig. 3. These data are compared to those obtained previously for material of the same thickness, made on the basis of glass fibers and polypropylene matrix earlier described i.e. in [6]. The difference between the two materials is the type of reinforcement, namely presence or absence of reinforcing fibers in the third direction perpendicular to the plane of the sample.

An important result of the study is determination of the transferred to the supportive bearing structure energy during the impact interaction (fig. 4).

The presented curve illustrates a pronounced non-linearity of the dependence. The energy transferred to the main bearing structure continues to increase in the range of velocities higher than the ballistic limit of the material marking the start of its through-out perforation (the shaded region in fig. 4). This leads to conclusion that the region designates the range of increased energy absorption capabilities in this range of velocities. More detailed tests of the samples may allow studying this effect taking into account the duration of the process of impact interaction during the time of the impacting bodies contact.

Discussion

Analysis of the results of the carried out tests allows resuming that the higher energy-absorbing performances of the three-dimensionally reinforced composite material compared to the two-dimensionally reinforced one can be explained with the higher specific content of fibers per unit area, which interacts with the impactor, together with the fibers better binding due to their interlacing and not only due to composite matrix. Thus not only the reinforcement type and specific fiber volume play role, but also uniformity of arrangement of the fibers that form a unit three

dimensionally reinforced lattice cell and reciprocal aspect ratio of this cell and the size of the impacting object.

In addition it can be concluded that, in contrast to the reinforcement type and consequently the way of fiber location in the material designed for use under tension and compression, material intended for work under impact should possess not only enhanced reinforcement in the third direction perpendicular to the main shell plane, but also improved connection between the fibers not only due to redistribution of the load through the matrix material, but also due to plexus of fibers of different directions together.

These measures allow the use of composite materials of reduced percentage of reinforcing fibers in more critical details and thus further reduction of the structural weight of aircraft engine and raising the quality of its operation [2, 7].

Summary

Carried out researches of samples of three-dimensionally reinforced composite material based on glass fibers and polypropylene matrix have shown perspectivity of their use for manufacturing of structural components of aircraft propulsion systems as compared to two-dimensionally reinforced composite materials of the same type. Velocity ranges of impact interaction are determined, which are characterized with improved energy-absorbing properties that allow heightening of the effectiveness of the material usage in manufacture of protective structural elements of aircraft engines.

Reference

1. *Михеев С.В., Строганов Г.Б., Ромашин А.Г.* Керамические и композиционные материалы в авиационной технике. – Москва: Альтекс, 2002. – 276 с.

2. *Кулик Н.С., Тамаргазин А.А., Линник И.И.* Показатели качества функционирования авиационных ГТД // Авіаційно-космічна техніка і технології: Зб. наук. праць. – Харків: Нац. аерокосмічний ун-т "Хар. авіац. ін-т", 2002. – Вип. 34. – С.4-7.

3. *Рубцов С.М.* Применение современных полимерных композиционных материалов в элементах и узлах газотурбинных авиационных двигателей. Диссертация к.т.н. – Пермь, 2009. – 148 с.

4. *Astanin V.V.* Impact deformation and fracture of hybrid composite materials / *V.V. Astanin, G.O. Shchegel* // Strength of Materials. – 2011. – Vol. 43, No. 6. – p. 615-627.

5. *Astanin V.V.* Characterising failure in textile reinforced thermoplastic composites by electromagnetic emission measurements at medium and high velocity impact loading / *V.V. Astanin, G.O. Shchegel, W. Hufenbach, A. Hornig, A. Langkamp* // International Journal of Impact Engineering (May 2012), doi:10.1016/j.ijimpeng.2012.05.001.

6. *Shchegel G.O.* Modellierung des Verhaltens von Mehrkomponen-Verbundmaterialien bei Hochgeschwindigkeitsbelastung. Dissertation zur Erlangung des akademischen Grades Dr.-Ing. – Dresden, 2011. – 138 с.

7. *Ромашин А.Г., Викулин В.В., Мухин Н.В.* Прогрессивные технологии и полимерные композиционные материалы для авиационной и ракетно-космической техники XXI века // В сб.: Теория и практика технологий производства изделий из композиционных материалов и новых металлических сплавов (ТПКММ). Тр. 4-й междунар. конф., Москва, 27-30 авг. 2003. – Москва: Знание, 2004. – с. 532-543.

UDC 539.43:669.717

A.I. Radchenko, Ph.D., S.S. Yutskevych, Ph.D., V.M. Panteleev
(National Aviation University, Ukraine)

ASPECTS OF METAL FATIGUE PROCESS UNDER TWO-BLOCK LOADING TESTS

In this paper was described the results of fatigue tests of some metals and alloys under variable amplitude with two blocks cycles in statistic aspects. It is shown, that test results has low coefficient of determination for liner dependences and test data should be represented as correlation field. The correlation field is a result of two processes with specific tendencies. This effect is considered within the bounds of synergetic discretely-likelihood fatigue model.

In National Aviation University were carried out large in statistic aspect fatigue test for estimation of dependence between prior cyclic loading and residual durability of metal and alloys. Specimens were tested at two stresses by two types of tests. For first type of researches were used method when a specimen with stress concentrator firstly was fatigue tested under one stress level σ_1 for n_1 cycles and then under second stress level σ_2 it was loaded up to fracture (n_2) (Fig. 1a). For second type of researches a smooth specimen firstly was fatigue tested under stress level σ_1 for n_1 cycles and then a stress concentrator in the form of hole was drilled. It changed stress distribution near stress concentrator and fracture zone was localized.

Special attention was paid to loading amplitude stability and material properties assurance. For this purposes the specimens were manufactured from the same sheet of metal and hole concentrators were drilled by one operator and the same tools.

Fatigue test loading regime was the same and operation of test machine was controlled periodically. Cycling loading was performed as cantilever bending with constant amplitude with 25 Hz frequency. These arrangements directed on spread of fatigue test results decreasing. The specimen draw is represented on Fig.1b.
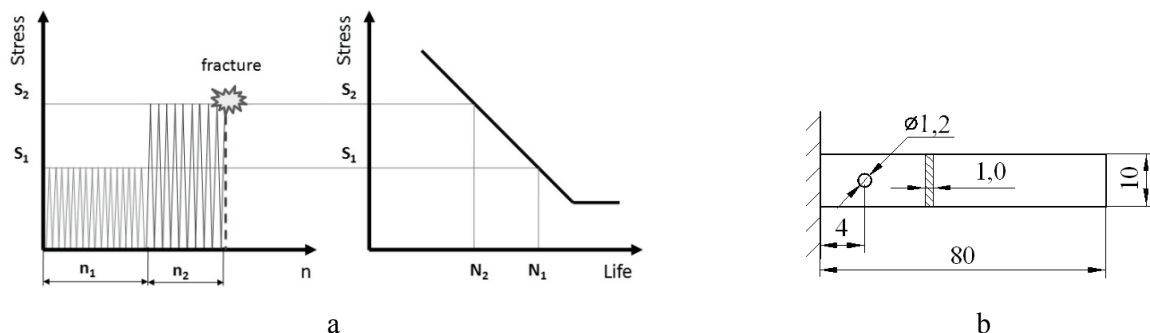
a   b
Fig.1 Fatigue test loading in compare with S-N curve (a) and specimen draw (b)

In this article the results of technical pure copper and steel 12H18N10T will be discussed. The test data are represented in the form of semilog diagrams on Fig.2. and Fig. 3. The typical features of the diagrams are:

1. Linear dependences of n_2-n_1 results have low coefficient of determination R^2: $R^2 = 0.093$ for cooper and $R^2 = 0.233$ for 12H18N10T steel. It makes impossible to apply Miner's Rule for the test results in general.

For the next explanation of n_2-n_1 diagrams it will be used "correlation field" term instead of "dependence";

2. The presence of residual durability n_2 sharp increasing (for example, on Fig. 3 for n_1 equal $1 \cdot 10^3$; $4 \cdot 10^3$ cycles and so on), that are connected with metal hardening and residual durability n_2 decreasing (for example, on Fig. 3 for n_1 equal $0,8 \cdot 10^3$; $3,8 \cdot 10^3$ cycles and so on).

Detailed analysis of the data allows to single out regular occurrence in the correlation fields. There are fatigue process bifurcations that are characterized by rapid residual durability n_2 changes occurred after definite number of n_1 cycles. points.
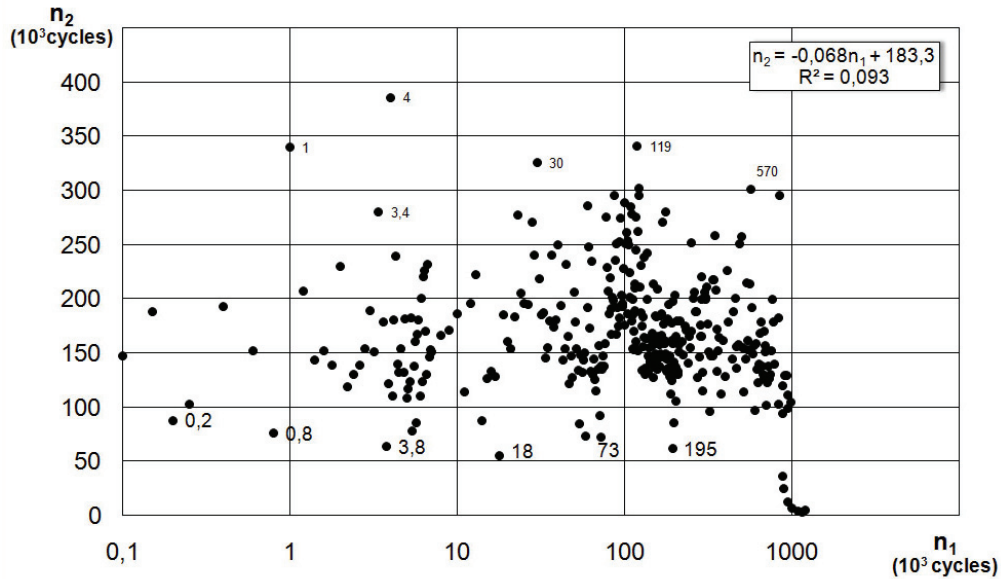
Fig. 2. n_1 vs. n_2 correlation field for copper
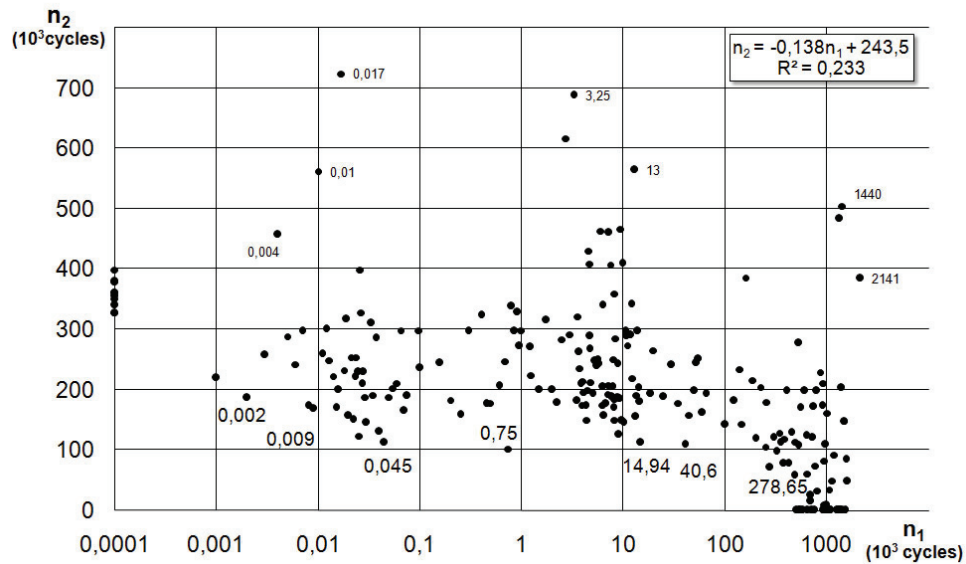
Fig. 3. n_1 vs. n_2 correlation field for 12H18N10T steel

Appearance of bifurcation points is described by V. Ivanova recurrent relationship [3]:

$$\frac{n_1(i)}{n_1(i+1)} = \Delta^{\frac{1}{2^{i-1}}} , \tag{1}$$

where n_1 – number of cycling loads, that determined time of bifurcation points appearing;
i – sequence number of bifurcation points;
Δ – metal fracture universal constant, that can be calculated as

$$\Delta = \frac{L}{H_0} \cdot \frac{G}{E} , \tag{2}$$

L – Latent heat of fusion;
H_0 – change in enthalpy under heating from 0 degrees K to fusion temperature;
E и G – modulus of elasticity and shear modulus with 0 degrees K.
For iron metal fracture universal constant $\Delta = 0,108$ and for cooper – 0,168.
Ivanova's law could be applicable on the incubation period before crack initiation and useful for a model that could explain behaviour of material under fatigue.
The main ideas of developed model are:

1. Prior cyclic loading – residual durability correlation field has irregular shape that is caused by residual durability n_2 sharp increasing (spikes) presence. Spikes constellation is characterized by spikes series cascade. Each series is formed according Ivanova's recurrent relationship.

Number of cycles up to first spike for every r-series is called Basic Bifurcation point (NBBr). The value of NBBr depends on specimen material, thermomechanical treatment, mode of deformation, levels of cycling loads, design and manufacture factors, environmental and so on. Next spikes position in the series is described by Eq. 1.

2. Series of spikes origin can be explained by microplastic deformation process in different grains on certain oriented plane;

3. Metals fatigue process should be considered as a composition of two processes: high-frequency process on a nanoscale level (within a separate slip plane of grain) and low-frequency that is proceeding on mezo- and macroscale levels.

High-frequency process is caused by fatigue process bifurcation points in various crystallographic planes and it is characterized by spikes in correlation fields.

4. Discrete spikes for every stress level organize a totality of few cascade of series.

For example, on the Fig. 4 three series with 4 spikes are shown: I-series (■-dots with numbers inside) II-series (▲-dots with numbers inside) and III-series (●-dots with numbers inside). On diagram n_{20} is mean value of results with follow condition: the specimens are tested only under σ_2 stress level or, in other words, with $n_1=0$.

For every series it is possible to find appropriate spikes in n_1-n_2 diagram. But for I-series and III-series spikes №4 haven't coincidence with spikes of correlation field by reason of tests absence with appropriate n_1, and the same situation with single spikes S_1, S_2, S_3: a lack of test data makes it impossible to find other spikes according to Eq.1.

The high frequency process is connected with plastic deformation evolution at different scale levels in according to V.Panin's theories [4,5].

The low frequency process of metal evolution is caused by successive defect substructure changes. On Fig. 4 data points of low frequency process are marked by bubbles (○).

During low frequency process it is carried out principles of successive, selforganize substructure realization by reason of definite microplastic deformation scale level achievement [5].

Metal fatigue behaviour under low frequency process is described by many authors as stages of fatigue. Mechanism of substructure evolution has been well studied experimentally and by instrument methods [3].

Evolution rearrangement of defect structure under microplastic deformation process flows in according to synergetic principles at the micro-, meso- and macroscale levels. This rearrangement allows to mark out system of fatigue process stages and use generalized S-N curve.

In our case material residual durability research tests showed some characteristic fatigue stages. Theses stages boundaries are characterized by minimum residual durability n_2* or "drops" (D_1, D_2, D_3 on Fig. 4).
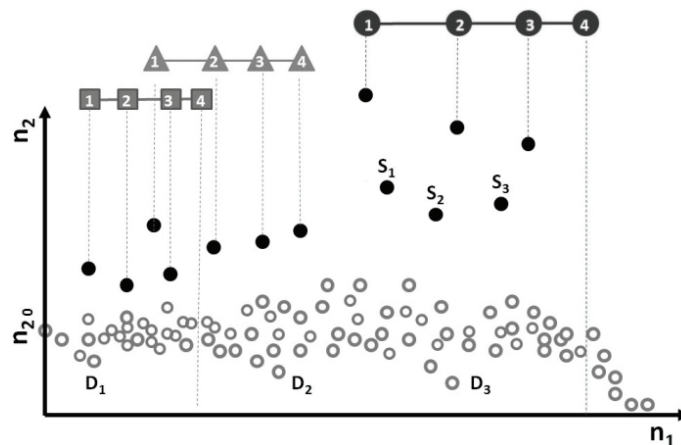
Fig.4. Conventional correlation field for prior cyclic loading – residual durability

Analysis of low frequency process test result shows close correlation between number of prior cyclic loading up to drops (n_1^*) and their position numbers (Num) in correlation field.

In correlation fields for each drop was set position number from 1 to 6 for copper (Fig. 2) and from 1 to 8 for 12H18N10 (Fig. 3). The dependence between position number and n_1^* are shown on semilog diagrams (Fig. 5). It's necessary to note that there are a lot of evolution process observations that could be described by logarithmic law (e.g. cell enlargement, mollusc and so on).

$$\text{Log } n_1^* = 0{,}614\,\text{Num} + 1{,}715$$
$$R^2 = 0{,}995$$

$$\log n_1 = 0{,}741\,\text{Num} - 0{,}423$$
$$R^2 = 0{,}991$$

a   b
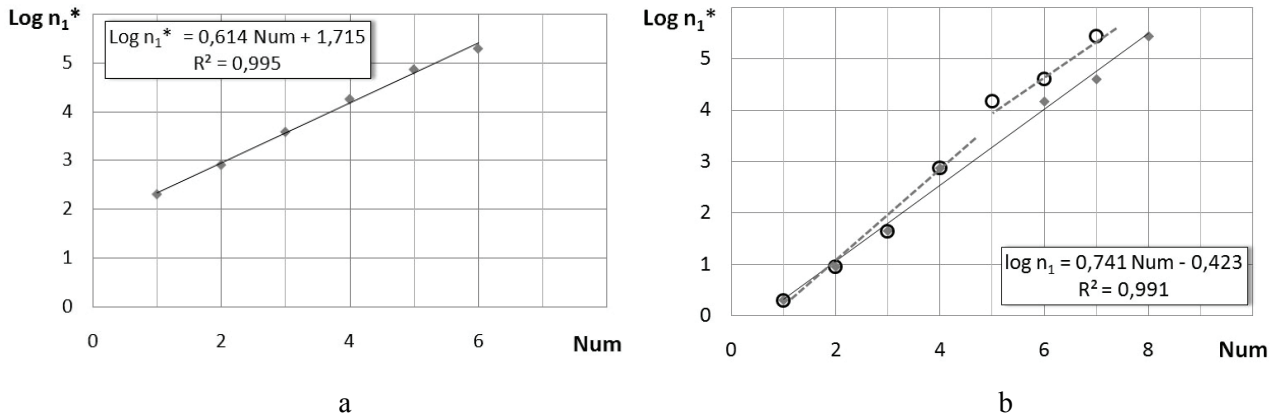
Fig. 5. Position number vs. log n_1^* diagrams for copper (a) and 12H18N10 steel (b)

The diagram for 12H18N10 steel was built for two assumptions:
- a lack of test data makes it impossible to find drop n_1^* with position number Num=5 (Fig. 5.b ♦-dots)
- it is bend in line after drop Num=4 (Fig. 5.b ○-dots) that could be explained by fatigue process mechanism changing and should be proved by new fatigue tests.

Summary

Fatigue process dividing on evolutional (low frequency) and discrete (high frequency) processes is conditional, but it is more convenient for analysis and represents evolution process at different scale levels.

Discussed results allow to estimate next aspects of metal fatigue process under two-block loading tests:

1. Correlation field of fatigue test results has number of spikes that could be inadvertently accepted as random test errors. But durability spikes are represented real process in metal and fatigue process and could be described as component of high frequency process.

2. Low part of correlation field envelope that represent minimal residual durability value has minimum residual durability "drops".

In our opinion, further correlation field envelope low part researches will make it possible to increase accuracy of residual durability prediction.

References

1. *Radchenko A.I.* Details and structure elements lifetime exhaustion discretely-likelihood model, Questions of aircraft structure service life and durability, Kiev 1982, p.3-12 (in Russian)

2. *Radchenko A.I.* Discretely-likelihood model of fatigue fracture, VII all-USSR metal fatigue conference, Institute for metallurgy of A.A. Baikov (1982), p. 90-93 (in Russian)

3. *Ivanova V.S., Terentev V.F.* Nature of fatigue, Metalurgiya, Moscow (1975) (in Russian)

4. *Panin V.E., Lihachev V.A., Grinyaev Yu.V.* Deformation structural lavels of solid body, Nauka, Novosibirsk (1985) (in Russian)

5. *Panin V.E.* Synergetic pronciples of physical mesomechanics, Theor. Appl. Fracture Mech., V. 37, No. 1–3, (2001), p. 261.

UDC 621.22

O.M. Boltenkova («Voronezh State University of Engineering Technology», Russia)

SHAPING MACHINE OF HIGH RESOURCED PIPELINE ELEMENTS

The description of the major parts and units, as well as modes of operation of the shaping machine of high resourced pipeline elements.

As part of a modern aircraft, especially important is the usage of high-resource pipeline in thin-walled structures. Typically, such pipeline is made from the uniform elements, which includ shortly-bend and stage fittings, tees, adapters, made from titanium, aluminum alloys and corrosion-resistant steel. The elements of the pipeline listed above should have a wall thickness of 0.4 to 1.5 mm and a diameter of 32 to 160 mm. [1].

One of the most rational way of making such pipeline elements is a hydromechanical stamping of billets with the usage of elastic pressure environment, providing high yield and low flying weight.

When shaping the unified elements of seamless pipe and longitudinal pipe pieces in order to avoid goffer and breaks the material it is necessary to compensate for the amount of elastic filler during stamping:

- In shaping tees - an excess of an elastic material is removed;
- While stamping adapters - stir up the missing filler;
- While bending steeply curved and stepped through the curved nozzle pushing creek - gradually increase the pressure filler, so that after the shaping it has reached the required value.

All these problems can be solved using machine for forming pipe fittings elements on the basis of universal hydraulic press *2* PYE-160 (Fig. 1) containing the forming cylinders *3* and *4* with the established and the associated additional telescopic hydraulic cylinders. By specifying the kinematics for each of the cylinders during the process of deformation of round billet and maintaining a certain ratio between the rates of movement of hydraulic cylinder piston rods of hydraulic cylinders and additional shaping, you can achieve the optimal value of the volume, and, consequently, the pressure inside the flexible filler tube stock and exclude the presence of a stamped for rejection details in the form of ripples, tears, scuffs and scratches.
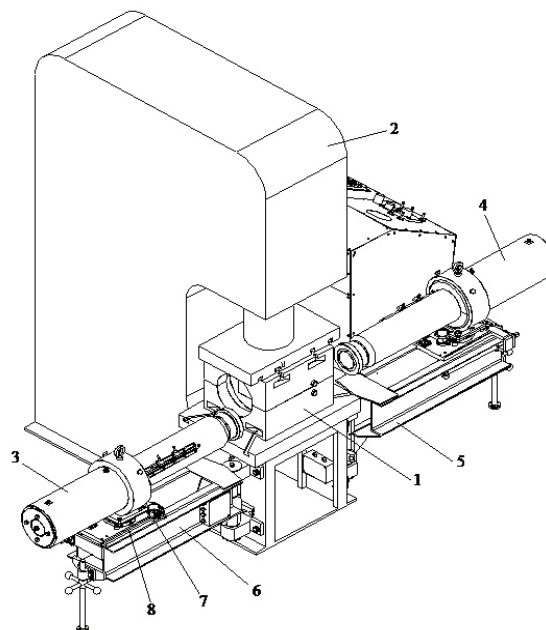
Fig. 1. Major parts and components machine for forming pipe fittings elements:
1 – container; 2 – press PYE-160; 3, 4 – cylinders forming; 5,6 – brackets; 7 – rotation mechanism;
8 – longitudinal movement mechanism

Working process on the machine for forming pipe fittings elements is as follows:

1.   <u>While shaping of the tees:</u>

On the table of press *2* it is placed a container *1* with a detachable pre-assembled matrix for shaping tees. With the rotation mechanism *7* and the longitudinal movement mechanism *8* and the brackets *5*, *6* cylinders forming *3* and *4* are set in one line. After that, the upper part of the container is attached to a movable boom press *2*, and rises above the plane of the connector. Flanges forming cylinders *3*, *4* plants in the annular grooves of the container *1*. Cylinder backwater bottom of the outlet tee is exposed at right angles to the axis of the tube blank (depending on the type of stamped tee).

After closing the top and bottom of the container *1* a process of deformation of the pipe blank begins by means of hydraulic cylinders with additional axial punches precipitation with simultaneous creation of the internal pressure of an elastic filler.

After formation of the transition zone between the workpiece and the outlet pipe tee stems more cylinders begin to move away in the opposite direction to the axial sediment tube stock. Thus, the excess amount of elastic filler is extruded from the cavity of tube stock, and, consequently, the pressure is stabilized by an elastic filler. Thus, one can avoid a tee for rejection in the form of corrugations and ruptures. To limit the tensile stress in the challenge of shaping the tee at its bottom part of the force transmitted to the hydraulic cylinder backwater. On reaching a given height allotment process is an axial precipitation stops, the pressure in the cylinders is reset and after opening the container *1* and pushing a stamped tee backwater hydraulic cylinder, the finished product is extracted from the matrix detachable.

2.   <u>During the shaping of adapters:</u>

All of the press *2* setting up are similar to those described above, except backwater hydraulic cylinder, which in this process remains untapped, and, with the difference that in the container *1*, a detachable set matrix, designed for shaping adapters. After closing top and bottom of the container *1* a process of deformation of the pipe blank begins by means of hydraulic cylinders with additional axial punches precipitation with simultaneous creation of the internal pressure of an elastic filler.

After the draft tube stock by a specified amount of additional hydraulic cylinder rods start to move in a direction coinciding with the axial draft tube stock. Thus, the missing volume of the elastic filler is injected into the cavity of the tubular billet and the elastic pressure filler takes the optimal value.

After reaching the final value of the pressure in the cylinders precipitation dropped after opening the container *1*, and a stamped detachable adapter is extracted from the matrix.

3.   <u>In the bending steeply curved pipes pushing:</u>

On the table of press *2* it is placed split matrix for bending steeply curved pipes. With the rotation mechanism *7* and the longitudinal movement of mechanism *8* and the brackets *5*, *6* shaping cylinders *3* and *4* are set at a certain angle in accordance with the required geometric parameters of the steeply curved pipe. After that, the upper part of the matrix is attached to the moving crosshead press *2*, and rises above the plane of the connector. Flanges forming cylinders *3*, *4* plants in the annular grooves of the matrix. Tube billet with the established elastic filler and covered with grease is placed in a cylinder forming a sleeve *3*, the body which had been previously raised over the bottom part of semi-matrix. After the plant cylinder flange forming an annular groove 3 in the matrix. At the front end of tube stock set of elastic washers installed and tightened retaining the punch ball, the force which is transmitted an additional hydraulic cylinder.

After closing the top and bottom of the container *1* begins the process of pushing the plunger push the tube blank with a given back pressure, which increases smoothly ball retaining plunger, depending on the achieved bending angle. At the end of the process of formation pressure in the cylinders is reset and after expansion of the matrix stamped steeply curved pipe for rejection without the detachable extracted from the matrix.

Conclusion: machine for high-resource items piping shaping is a versatile tool for the production of tubular components of pipeline systems of modern aircraft without a reason for rejection. Kinematic diagram of the apparatus provides the optimal value of the volume of an elastic filler, thereby expanding technological capabilities, satisfy the equipment due to the receipt of special-and hyperfine-wall elements of the pipeline and increase their quality.

References

1. *Давыдов О.Ю., Егоров В.Г., Кочегаров А.И.* Определение параметров штамповки раздачей крутоизогнутых и ступенчатых патрубков // Заготовительные производства в машиностроении №2, 2010. С. 17-22.

UDC 551.511.6(043.2)

N.I. Delas, Ph.D., V.A. Kasyanov, Doc. of Tech. Sc., T.V. Shypytiak.
(National Aviation University, Ukraine)

ENTROPY APPROACH TO THE ATMOSPHERIC TURBULENCE ANALYSES

From the point of view of flight safety ensuring it is important to have information about distribution of the number of atmospheric turbulent vortexes, their size sand intensity. We have to dispose information about nature of influence of some parameter turbulence. A "Limit-Hyperbolic Distribution law" (LHD) was proposed and can be a good alternative to the existing statistical hypotheses.

The modern imagination about turbulent flows is based on the cascade model [1] (Richardson cascade). In accordance with this concept energy of external enters at the turbulence flow through the vortexes of the largest scale. Then as a result of consequent subdivision of the vortexes their evolution passes through the three typical steps: long wavelength interval, inertial interval (of Kolmogorov) and dissipative interval. At last the energy is being dispersed under action of viscous dissipation.

Like so, in turbulent flows dynamics longscale vortexes play key role. Their appearance is stipulated by combination of unique atmospheric and physical factors, and bears independent character. This probability of sum of events equals to the product of their particular probabilities: $f(x_1 + x_2) = f(x_1) \cdot f(x_2)$. Correspondent functional equation has solution $f(x) = e^{-x}$. Normalization depends on specific conditions. Exponential distribution of number of large vortexes on their energies (intensities) has been stated for tropic cyclones and also tornado and convective thermals, more about this in detail in the article [2].

Inertial interval is being characterized with developed isotropic structure of turbulent vortexes. Influence of viscous dissipation is supposed to be negligibly small. In this interval energy spectrum is described successfully with known Kolmogorov formula: $E_K = const \cdot K^{-5/3}$, where $K = 2\pi / l$ – wave number, l – liner scale of pulse. This formula has been found from dimension reason [3].

In view of such conventional division into intervals, the numerical simulation of turbulent flow is currently the most common was the "method of large eddy simulation" or LES-method (Large Eddy simulation). On the point of view of flight safety the most critical is inertial interval of atmospheric turbulence with developed structure of vortexes appears, because it corresponds to the typical dimensions of plains.

To describe statistical properties of pulses of wind velocity in the limits of inertial interval Gaus probability density function often is used, or Raleigh distribution (if X and Y are independent random values Gaus distributed, of equal variance σ^2, then random value $Z = \sqrt{X^2 + Y^2}$ is distributed accordance with Raleigh distribution:

$$f(x;\sigma) = \frac{x}{\sigma} \cdot \exp(-\frac{x^2}{2\sigma^2}), \qquad (1)$$

where $x \geq 0$, $\sigma > 0$.

Nevertheless important requirement for application of this distribution has to be independence mentioned above, which can't be count correct, because the evident statistical link between the individual vortexes. This link is stipulated by nature of cascade process as basement of turbulent energy exchange. Correctness of this statement is verified with empirical data (fig. 1) given in [4] found by Dopler sound method of atmospheric turbulence with coherent lidars (Light Identification, Detection and Ranging (LIDAR) – technology of obtaining and processing of information about remote objects with help of active optical system using light reflection and its dispersion in transparent and semitransparent medium):

$\rho(A_S) / \rho_{max}$ $\qquad\qquad\qquad\qquad$ $\rho(P_S) / \rho_{max}$
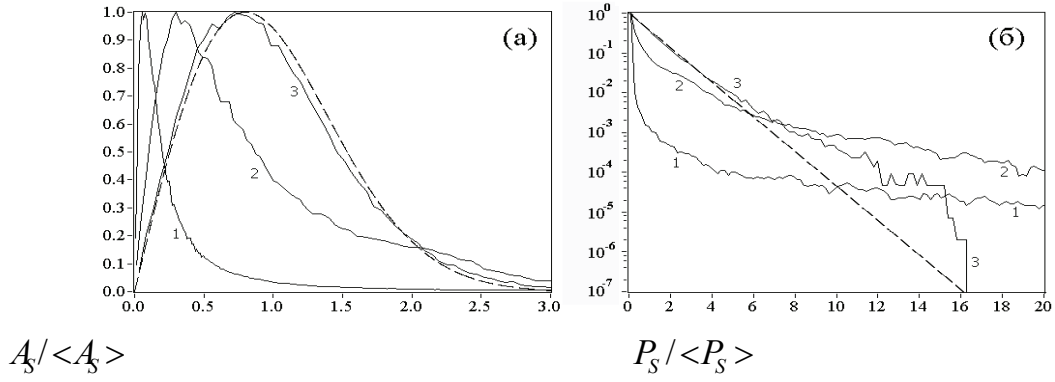
Fig.1. Probability density functions of amplitude A_S and power P_S of echo signal (graphs 1, 2, 3 corresponds to the cases of focusing of beam on the distances 10, 50, 100 meters). Raleigh distribution (a) and exponential distribution (b) are shown with the dashed line.

We have to pay our attention to the circumstance that the empirical functions in difference with the dashed line have brightly evident "heavy tails", which are typical for power distributions [5]. The main idea of this work can be expressed as a following statement: distribution of number of turbulent vortexes (as minimum into inertial region) with respect to the energy bearing by them is subjected to the principle of maximum entropy proposed by Janes [7]. Using this principle authors found "Limit-Hyperbolic Distribution law" (LHD) [6] which could give good alternative to other statistical hypothesis. Law connects the probability density distribution of "entropy carrier" number with amount of this individual energy:

$$\frac{f(\varepsilon)}{f(\varepsilon_*)} = \frac{\varepsilon_*}{\varepsilon} \cdot \exp(1 - \frac{\varepsilon_*}{\varepsilon}) , \qquad (2)$$

where ε_* and $f(\varepsilon_*)$ – coordinates of maximum point of this dependence. Taking into account that velocity of turbulent pulses have square-law link: $\varepsilon \propto v^2$, we can possibility to write formula:

$$\frac{f(v)}{f(v_*)} = \frac{v_*^2}{v^2} \cdot \exp(1 - \frac{v_*^2}{v^2}) \qquad (3)$$

The diagram of this function is given on the fig. 2.
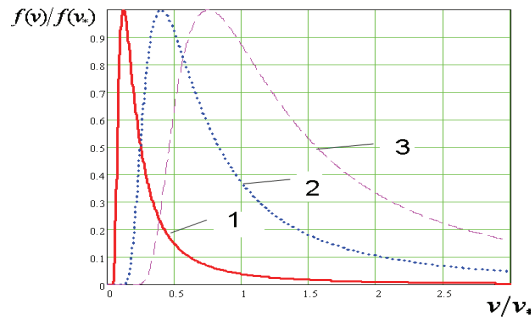
Fig. 2. Limit-Hyperbolic law of Distribution (LHD) of probability density of turbulent pulses as a function of their velocity

As it is seen the law of LHD enough lightly corresponds to the empirical distributions shown on the previous figure. Differences in tail region for the third curve (fig. 1), that was obtained for the largest distance most likely connected with measurement error. This supposition confirms in indirect way abrupt downward change of correspondent curve (3-b) on the right fig. 1.

In contradistinction to the Raleigh distribution (1) which often has to be chosen as a statistical hypothesis in order to describe turbulent pulses, proposed in this paper LHD law was found from physical presupposition.

As it was already sad in the basement of this Law have been put "principle of maximum entropy" for distribution of limited amount of resources between given set of "media resources". It

turn out to be that LHD-Law sufficiently, describe other objects, were similar division of resources have place, for example, distribution of lengths of fatigue splits.

Important property of LHD-Law is scale invariance of its scope with different values ε_* and $f(\varepsilon_*)$ (fig. 3):
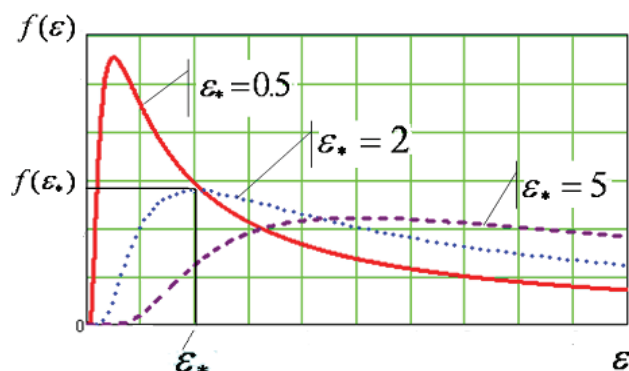
Fig. 3. Dependence of LHD-Low diagrams on parameter ε_*

Existences of scale invariance property of LHD-Law allow using for description of objects of fractal type.

Conclusions

According to empirical data, distribution of probability density of large-scale vortexes (cyclones, hurricanes, tornados) and distribution for small scale vortexes bear different type. Uniqueness of appearance of large-scale object implies their relative independence. Because of this their distribution is nearly exponential.

Middle scale vortexes are products of cascade transformation of more big vortexes into less big ones. Available energy is distributed between vortexes of different size, which can not be considered independent. Due to this reason the use of Gaus distribution or Raleigh distribution into this region of vortexes size is not valid.

Proposed by authors "Limit-Hyperbolic Distribution law" (LHD) tightly corresponds to the experimental data. This distribution is found on the base of maximum entropy principle [7]. It gives possibility to determine the link between parameter ε_* and $f(\varepsilon_*)$ with integral characteristics of flow region.

References

1. *Фриш У.* Турбулентность: Наследие А.Н. Колмогорова [Текст] : пер. с англ. — М. : Фазис, 1998. — 360с.

2. Функции распределения вероятности для циклонов и антициклонов в период 1952-2000 гг.: инструмент для определения изменений глобального климата [Текст] : доклады Академии Наук. — 2007. — Т.413, №2. — С.254-256.

3. *Цитович, В. Н.* Развитие представлений о плазменной турбулентности [Текст] / В. Н. Цитович // Успехи физических наук. — 1972. — Т.108, вып. 1. — С.143-176.

4. *Смалихо, И. Н.* Ветровое зондирование когерентными доплеровскими лидарами [Текст] : автореферат диссертации на соискание ученой степени доктора физико-математических наук : 01.04.05 / И. Н. Смалихо ; [Институт оптики атмосферы им. В. Е. Зуева СО РАН] . — Томск, 2011. — 39 с.

5. *Делас, Н. И.* Негауссово распределение как свойство сложных систем, организованных по типу ценозов [Текст] / Н. И. Делас, В. А. Касьянов // Восточно-евроро-ейский журнал передовых технологий. — 2012. — №3/4. — С. 27-32.

6. Делас Н. И. Предельно гиперболический закон распределения в самоорганизованных системах [Текст] / Н. И. Делас, В. А. Касьянов // Восточно-евроро-ейский журнал передовых технологий. — 2012. — №4/4. — С. 38-43.

7. *Jaynes E.T.* Information Theory and Statistical Mechanics. I and II – Phys. Rev. №2, №4, 1957.

UDC 533.694.73

E. Udarcev, Doc. of Tech. Sc., O. Shcherbonos, Ph.D., S. Alekseenko
(National Aviation University, Ukraine)

THE ORGANIZED VORTEX FORMATION AT THE EDGES OF THE WING AS A WAY TO IMPROVE THE AERODYNAMIC CHARACTERISTICS AT SUBSONIC SPEEDS

The way to improve the aerodynamic characteristics with vortex generators (VG) longitudinal vortices on the leading edge in the direct flow, and on the trailing edge of the reverse flow. It is shown that VG at the leading edge to increase lift and the critical angle of attack due to exposure to large-scale vortices are static or dynamic flow separation.

Introduction.

The most important task in terms of safety is to ensure the aircraft stability and control at the exit at large angles of attack at which the upper surface of the airfoil flow separation develops in the form of large-scale vortices altering the pressure distribution along the chord of the wing and leading to a drop in the lift, increased drag, the change damping and formative moments in the wake Karman.

Large-scale vortices are formed on the surface of the wing are the result of viscous-inviscid interaction and depend on the viscosity of the medium and on the pressure distribution on the wing. In the two-dimensional formulation of the study of dynamic stall on the wing is a very approximate model. Prospective studies are three-dimensional flows, the vortex interaction and active influence on them in various ways. One way is to destroy the influence of stable vortex flow on the upper wing surface, which develops at the boundary of the viscous-inviscid flow interaction in the flow around the wing.

It is known that the distinguishing feature of large-scale vortices that arise in the separation region is their high sensitivity to external perturbations [1, 2]. It turned out [3] that by means of longitudinal vortices generated at the leading edge of the wing with numerous inflows of small size can be controlled over a tear-off calendar blocks destroying large vortices, which leads to improved aerodynamics of the wing, substantially increasing the critical angle of attack.

Office of separated flows using vortex is used for many years active in the design of an effective lengthening of the wings of various influxes (VG) at the edge of the wing [4] or the vortex generating "teeth" on the wing span.

Vortex structure for optimum aerodynamic performance improvements can be specially shaped contoured front edge of the wing, depending on the critical velocity, the optimal step between VG and depending on the characteristics of the airfoil and the flow regimes, the Reynolds and Strouhal number for the oscillations of the wing.

Vortex formation at the leading edge of the wing can produce the effect of increasing the lift, increased suction force, the increase of the critical angle of attack changes the longitudinal momentum. In order to achieve a certain goal should be to use a different configuration VG to form one "vortex slat."

Studies of small disturbances in the tear-off of the wing vortices has been studied in [5, 6, 7], how to control flow separation are protected by patents [8, 9].

The work of Novosibirsk scientists to study the vortex structure separated flows are summarized in the thesis Pavlenko AM [5]. Attention is drawn that the tear-off eddies are three-dimensional large-scale nature, which essentially defines the physical picture of the flow. In this paper we propose a method of local influence on the vortex structure of separated flow projections on the upper surface of the edge of the wing, leading to turbulence in the flow and the local blowing within the region of failure of discrete jets as a way to destabilize the vortex structures of the separated flow. As a result, states that the protrusions in the form of ribs or cones, point blowing creates an obstacle in cross-currents of failure, which in turn lead to a significant change in flow pattern.

In the work of Polish scientists influence the results of discrete jet blowing on separated flows. The basic function Cy = f (α), Cx = f (α), mz = f (α), obtained in a wind tunnel at Re = 10^6, M = 0.05-0.1 for the profile of NACA0012.

Canadian scientists have studied the flow characteristics of fin whale is not the leading edge build-up. The results showed that the growths on the leading edge of the fin in the steady state leads to a substantial change in the aerodynamic characteristics. This is the closest to the research topics discussed in this article [7].

Formulation studies of the effect sag VG on the front edge of the wing, on the integral aerodynamic characteristics.

The study VG on the aerodynamic characteristics at high angles of attack was carried out in subsonic wind tunnels in the static and dynamic changes in the angle of attack.

In the static mode, the weight of research conducted various VG on the front edge of the wing in a wind tunnel UTAD NAU-2 at up to 30 m / s, numbers, Re = 2 * 10^5. model of the wing span 400 h 150 mm, thickness profile with = 16%. With a clean wing flow separation occurs at 18^0 with the fall of the lift by 40%.

We investigated the following characteristics VG Fig. 1. b = 30-70% c, H = 20-60% c, s = 8-110% c. results of changing the lift shown in Fig. 2, the polar Fig. Three. characteristic that the maximum quality of the wing with VG unchanged compared with the smooth wing that can be developed to explain the suction force on the leading edge. The torque characteristics vary more stable Fig. 4. Study of pressure distribution showed that significantly change the characteristics of flow separation as in the direct blasting, and at the back with a blasting VG on the trailing edge.

The main research interest is the model of light weight unmanned aircraft Fig. 5 with a wingspan of 1.7 m in the flight configuration with the polar plane with VG is shown in Figure 6, and aileron effectiveness is demonstrated in Fig. 7.

Conclusion:

VG on the wing leading edge high-performance tool to increase the critical angle of attack, the optimization of the vortex and the slat to increase the maximum lift coefficient.

VG not lead to a substantial change in the most advantageous angle of attack and aerodynamic qualities.

VG on the leading edge of the wing is not promising for use in unmanned aerial vehicles operated in the turbulent atmosphere.

VG on the leading edge are useful when used on wind turbine Darrieus type.

References:

1. Брыленов А.П., Жарнова Г.М., Занин Б.Ю. Отрыв потока на прямом крыле при повышении внешней турбулентности. Ученые записи Цаги Том XXXV, №1-2. 2004.

2. Павленко А.М. Изучение вихревой структуры отрывных течений и методов управления отрывом на моделях крыльев при малых числах Рейнольдса. Автореферат диссертации. Новосибирск 2011.

3. Іщенко С.О. Методи та засоби керування поздовжніми вихровими структурами та їх дослідження (НДР №503-ДБ08). Київ: НАУ, 2010.

4. Бюшгенс Г.С. Аэродинамика, устойчивость и управляемость сверхзвуковых самолетов. М.: Наука, Физматлит, 1998.

5. Бюшгенс Г.С. Аэродинамика и динамика полета магистральных самолетов. М.: Наука, Физматлит, 1995.

6. Andszej Krzysiak. Applikation of a new concept of air jet vortex generators for flow control. Transaction of the institute of aviation. Warszawa 2011.

7. Stanway M.J. Hydrodynamic effects of leading tubercles on control surfaces and flapping foil propulsion. Massachusetts Inst. Tech. 2008.

8. Занин Б.Ю. Козлов В.В. Способ управления отрывом потока. Патент Р.Ф. №2328411. 2008.

9. Щербонос О.Г. Ударцев Є.П. Генератор вихорів. Патент України №67743. 2012.
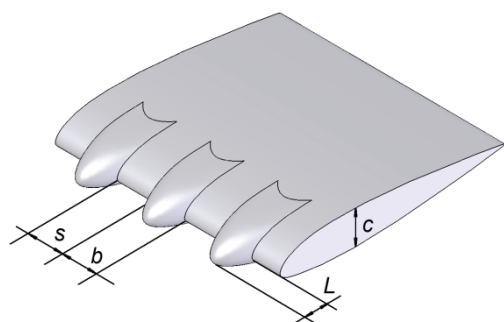
Fig.1
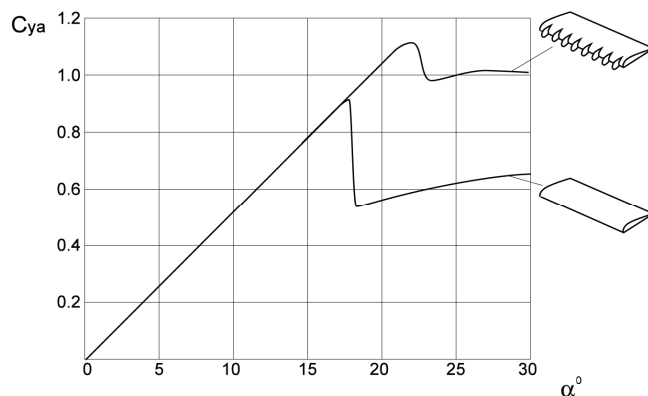
Fig.2
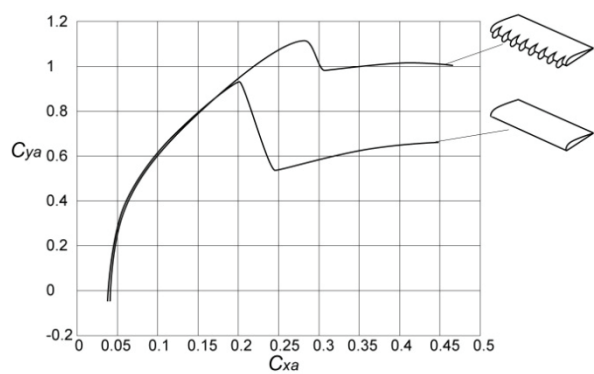
Fig.3
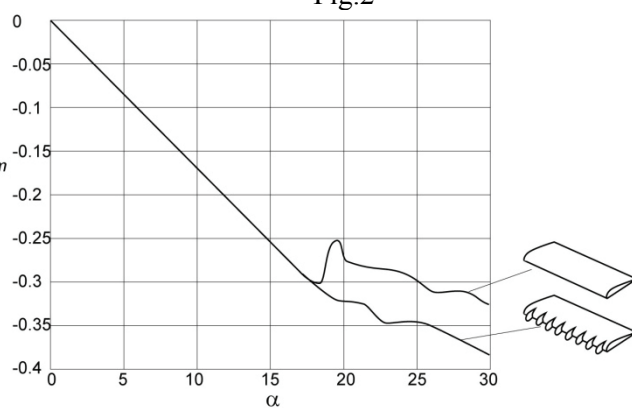
Fig.4

Fig.5
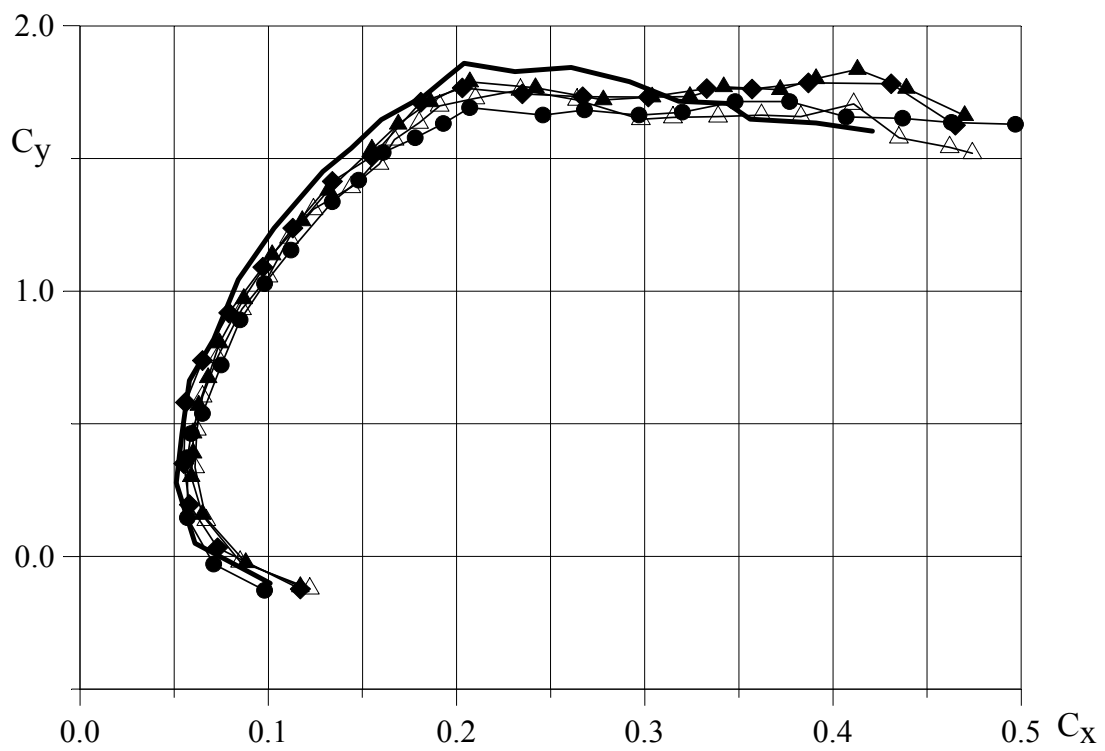
Fig.6
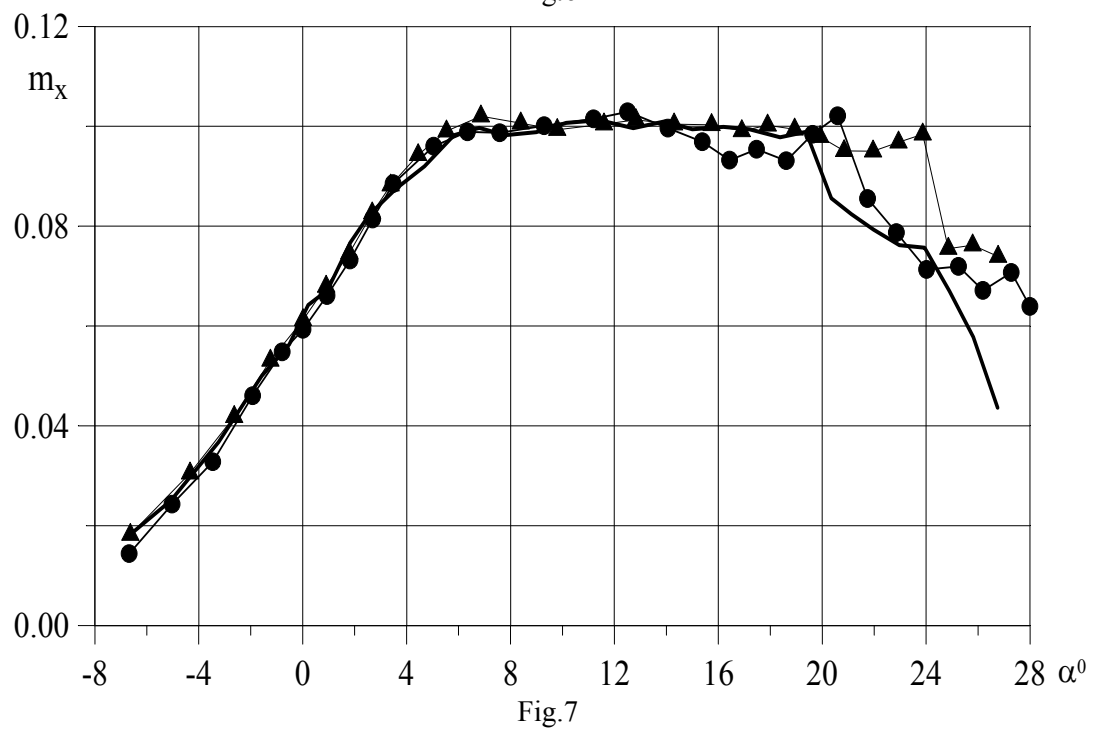
Fig.7

1.3.7

N. Yurchenko Ph.D., P. Vynogradskyy Ph.D., Yu.Paramonov,
V.Tsymbal, A.Koshil, K. Kuzmenko
(Institute of Hydromechanics NASU, Ukraine)
R. Pavlovskyy Ph.D., A. Zhdanov Ph.D.
(National Aviation University, Ukraine)

OPTIMIZATION OF AERODYNAMIC FACILITY FOR INTERDISCIPLINARY RESEARCH

Design, parameters and functional features of the Aerodynamic Complex for Interdisciplinary Research are discussed. The objective of the Complex enhancement and its engineering solutions improving operational capabilities and experimental potential are described.

Introduction

Aerodynamic Complex for Interdisciplinary Research (ACIR) is a key part of the Laboratory for Advanced Aerodynamics and Interdisciplinary Research of the Institute of Hydromechanics (IHM NASU). ACIR aims at studies of a wide variety of aerodynamic problems based on novel developments in the field of flow control such as applications of plasma discharges generated by microwave (MW) radiation. The latter defines the multidisciplinary nature of investigations conducted in cooperation with Moscow Radio-Technical Institute (MRTI RAS). The created research complex enables thorough investigations of the flow around various types of single models and cascades for conventional flow conditions and for those in presence of MW radiation.

The ACIR was designed and manufactured in 2005 by the combined efforts of IHM, NAU and MRTI specialists in the framework of joint projects funded by the European Office of Aerospace Research. The ACIR key part is the low-turbulence wind tunnel. During first stages of its exploitation, it showed a number of shortcomings related basically to certain inconsistencies between the electrodynamic requirement to the uniformity and intensity of MW field and the aerodynamic requirements to flow quality and efficiency of operation. The complex transfer from NAU to IHM in 2011 was accompanied with its significant upgrade to avoid the deficiencies, to extend operational free-stream velocities and to broaden a range of research problems.

1. Composition and functionality of ACIR

The ACIR is based on the wind tunnel with an axial fan and flow speed control system, and MW radiation and protection systems. The complex includes the three-component strain gage balance, 25-point pressure measurement subsystem and two-channel hot-wire anemometer. The measurement process is controlled with the Data Acquisition and Control System (DAS)

Primary ACIR features at the time of its deployment in NAU were:

- air flow velocity, $U_0 = 1.7\text{-}39.0$ m/s at turbulence level of $\varepsilon < 1\%$;
- conventional studies of boundary layers over flat and curved surfaces;
- measurements of aerodynamic loads on the model in a wide range of angles of attack;
- generation of MW radiation around a test model in accordance with certain parameters to satisfy requirements of the developed boundary-layer control approach;
- MW protection of operators and measurement equipment.

1.1 Wind tunnel

A direct-flow wind tunnel with a closed type test section of 0.31 x 0,6 x 0,8 m (width x height x length) is designed to study both separate aerodynamic profiles like airfoils or turbine blades and turbine blade cascades. The wind tunnel is made of metal and consists of an input device, intake nozzle, Eiffel chamber with a test section, diffuser, fan and exhaust nozzle. A metal screen was

installed at the entrance to the nozzle and the original devices for protection from microwave radiation. Front mesh was installed on the entrance to the nozzle, performed the role of deturbulized screen.
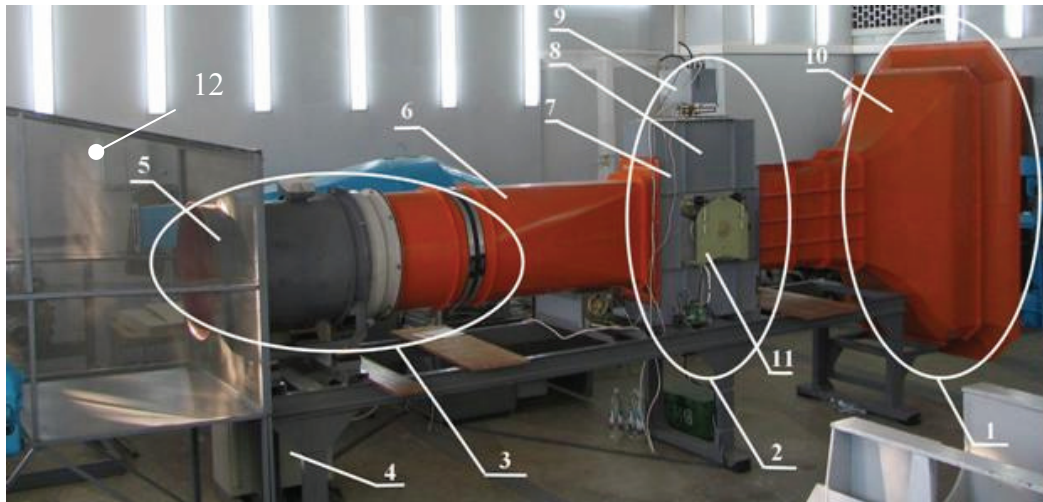
Fig. 1 Wind tunnel complex equipped with the microwave-generation and protection systems for automated measurements of aerodynamic coefficients
1-3 parts which has been modified, 4 – fan control system, 5 – exhaust system, 6 – diffuser, 7 – test section, 8 – Eiffel chamber and MW-radiation system, 9 – magnetron, 10 - intake nozzle,11 – strain gage

1.2 The flow measurement system

The system provides a measurement of dynamic pressure in the working section, temperature, humidity and barometric pressure at the ACIR, calculation of these data the density of the air flow regime in the working section, velocity of the flow in the working area and the calculations of Reynolds number.

Measurement of temperature, barometric pressure and relative humidity is made by meteorological station "troposphere - G» which is linked to the DAS. Measurement of dynamic pressure, static pressure is carried out by pressure differential in the intersection at the entrance to the nozzle at its widest part and at the outlet nozzle to the working part. To do this, 4 holes is made at the two sections in the walls of the nozzle, which is connected to two collectors. The outputs of these collectors are connected to the precision laboratory pressure sensors.

1.3 MW generating system and protection against radiation

The system consists of: magnetron with horn antenna which is situated on the upper side of the Eiffel's chamber, and two regulated power source: a source of constant power of 1.5 kW and pulse source with pulse power up to 7 kW at an average power of 1.0 kW. The microwave generation system and of protection from itself was developed in MRTI according to specifically design and features of ACIR. The system was iterative optimized to provide sufficient intensity of the electromagnetic field form low-power generator and its uniformity in the working area during the measurement.

1.4 The 3-component strain gage balance

The 3-component strain gage balance is implemented on three tensoconverters BA-1005 production association "Veda" (Ukraine) with three tensoconverters Scaime CPJ (France). On scales mounted mechanism for changing the angle of installation models (alpha mechanism) and incremental electric transducer to measure the position of the model. Balance measurements of three components of the full load model in the vertical plane, which allows to calculate the value of

lifting force, the resistance and pitch moment model. Alpha provides a mechanism for establishing a model from any angle to the oncoming flow in the range 0-360 ° with the management of RUI or manually from the console. Measuring the angle of the model is carried out with an error of not more than 0,1 °.

1.5 *Drainage measurement system*

The system includes a block of 25 pressure transducers MPXV-5004 the company Freescale and stabilized power supply and is designed to measure the pressure distribution on the model.

1.6 *Hot-wire measurement system*

The system includes two channels of hot-wire anemometers constant temperature control unit. The system provides a measurement of static and dynamic properties of the flow (average velocity and turbulent fluctuations) around the model or in the empty working section. Transmission of commands for configuring of hot-wire anemometers of RUI to control units via interface USB/RS232.

2. Modernization of Aerodynamic Facility for Interdisciplinary Research

2.1 *Shortcomings of the ACIR first configuration*

Conducted in MRTI calculations showed that for greater uniformity of the electromagnetic field in the zone model of the optimal width of the working parts should be 0.28 m, as was designed and constructed a new work of specified width. Its installation required a change in shape of the nozzle flow and the first section of the diffuser. Analysis of nozzle geometry, made while carrying AKMD to IHM, showed that the inner contour of the nozzle was significantly distorted as a result of errors in the design and as a result of purely manufacturing defect.

During the research was also conducted visualization of air movement in the input device and around it in the external space, which showed that the area near the entrance pipe can create a whirlwind caused by the disruption of the flow of sharp edges incoming rastrubu wind tunnel. Whirlwind pass through a metal grid in the nozzle where the fall in the working part, where they are cause nonstationarity, non-rectilinear flow significantly affects the data of the experiment.

Analysis of fans settings showed that due to undervalued and extended the diameter of the fan rotor hub fairing flow rate to the fan exceeds the flow rate in the working section, resulting in undue loss of full pressure. Sam had a bad fan profiled blade with a large axial gap, which also reduced its efficiency and created a great acoustic sound. According to the calculations, performed on the results of measuring the full and static pressure before and fan and power consumption was found that the efficiency of the fan at maximum capacity is 48%.

Therefore, during installation at the Institute of Hydromechanics ACIR decided to upgrade wind tunnel, which included the following.

1. To improve conditions for entry into the inner flow path of wind tunnel before the nozzle was set to soothing chamber permanent section length of 400 mm, inside of which was mounted honeykomb ocellated square section with sides of 40 mm and length 160 mm. Before honeykombom was established guard and calming at the junction with the nozzle chamber - one optimized for the hydraulic resistance.

2. For input devices such as phonograph with sharp edges was mounted "collar" of glass fiber plastic, which ensures smooth flow of external rotation flow in front of the running part of wind tunnel.

3. The internal contours of the nozzle (Fig. 3) were smoothed to avoid the closed angle (pos. 6 in Fig. 3) as potential vyhoroutvoryuvachiv and close to the curve Witoszynskyj. Large volumes filled with foam, and puttied and sanded. At the entrance to the work of completed smoothly connect the nozzle of a new path narrower workingparts.
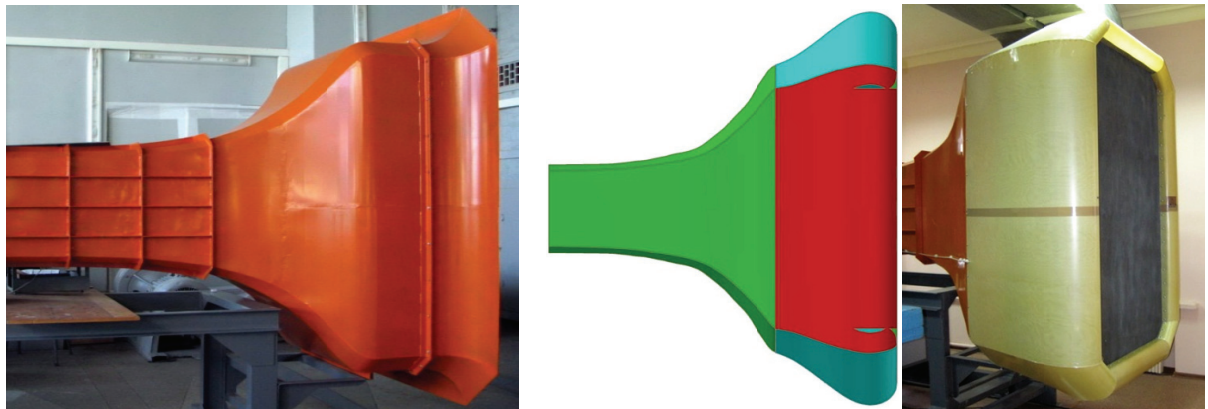
Fig. 2 Remodeling of the wind-tunnel intake nozzle: (1) initially manufactured nozzle; (2) stage of the design to improve the flow quality; (3) newly fabricated nozzle with the protecting/smoothing grid
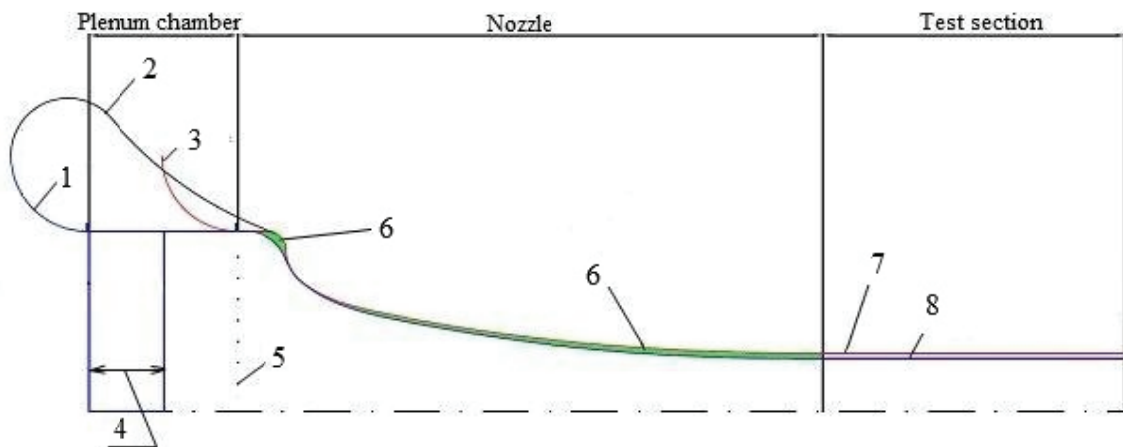
Fig. 3 Comparison of the wind tunnel contours before and after modernization
1 - new intake, 2 – intake fillet, 3 - old intake, 4 – honeycomb, 5 – deturbullzing screen, 6 – polyurethane foam, 7 - old test section contour, 8 – new test section contour

4. Assembled new working part, which is made of 20-mm steel plate and has a valid geometry. The upper and lower walls of the working parts are made of perforated longitudinal grooves of the degree of perforation of 18%, which reduces the impact of borders on stream flow and bearing configurations bluff bodies. Working hatch for access to the interior of the working parts significantly increased, providing greater convenience during installation model.

5. Similarly nozzle part, made smooth connection of the working part of the first section of the diffuser, which was also wider than the new working part.

6. According to the results of measurements of head loss in the running of the compiled and installed a new fan AZN 710/350 firms Novenco (Fig. 4), which has a larger outer diameter, built fairing bushings and aerodynamically profiled blades. Efficiency of the new fan reaches 91%. To connect the old with the new diffuser fan diffuser installed larger diameter spacer, and for the reduction of output for fan speed set off an external diameter of the diffuser at the outlet 900 mm.

7. The results of the complete loss of pressure and increased diameter of the original diffuser allowed to abandon the complex exhaust device (pos. 12 in Fig. 1) and replace it with a simple grid, stretched on the back flange of the original cone.

(a)   (b)   (c)
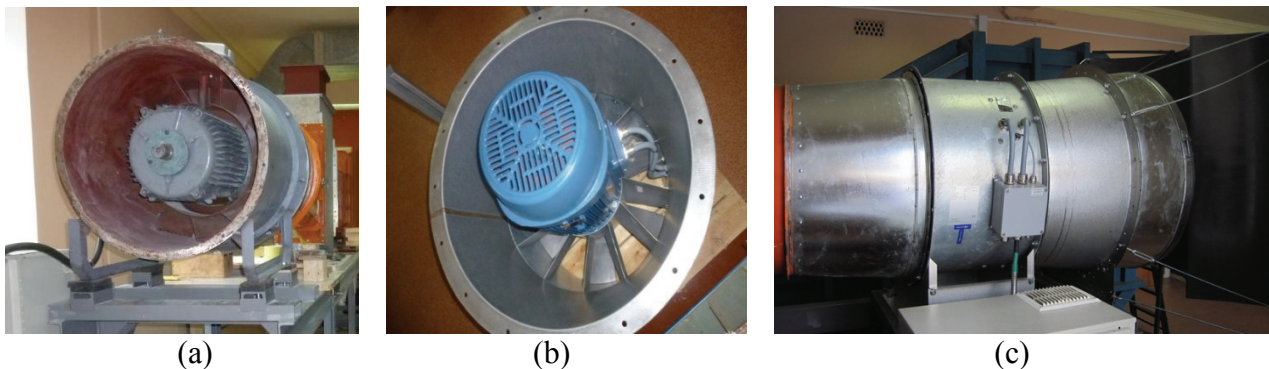
Fig. 4. (a) – Old fan VOE-6.3 U2, (b) – axial fan of Novenco AZN 710/350, (c) – the new air-gas channel

Results of modernization is made possible to obtain the following results:

  ➢ maximum speed in an empty wind tunnel exceeds 70 m/s and in a pipe with an installed model poorly streamlined body the maximum size (cylinder diameter 106.6 mm length 200 mm) - over 65 m/s;
  ➢ in the most difficult case to model power consumption not exceeding 21.5 kW, which indicates the correctness of calculations fan;
  ➢ level of turbulent flow decreased, as indicated by the increase of critical Reynolds number for cylinder with 3h105 to about 3.7h105 found in experiments carried out;
  ➢ maximum noise level significantly decreased and it is estimated not to exceed 85 dB;

Summary

Optimization of Aerodynamic complex for interdisciplinary research has provided a significant increase of maximum flow rate while maintaining maximum power consumption. The level of turbulence and acoustic noise level decreased. This enables larger numbers of subjects Reynolds models and reach the area by the critical Reynolds numbers for the cylinder that provides experiments in field conditions that were previously unavailable to AKMD.

References

1. Aerodynamic facility with MW-Systems for Flow Control Based on Localized Plasma Generation, *P. Vynogradskyy, N. Yurchenko, R. Pavlovsky, O. Zhdanov*, 2008, AIAA Paper -2008-3939.
2. Initiated Surface Microwave Discharge as an Efficient Active Boundary-Layer Control Method, *V. L. Bychkov, I. I. Esakov, L. P. Grachev, A.A. Ravaev, K.V. Khodataev, N.F. Yurchenko*, 2009, AIAA-2009-889.
3. Impact of Spanwise Arrays of Plasma Discharges on Aerodynamic Performance, *N. Yurchenko, N. Rozumnyuk, Yu. Paramonov, V. Tsymbal, P. Vynogradskyy, A. Zhdanov*, 50th AIAA Aerospace Sciences Meeting, 2012, AIAA-2012-1029.

AKNOWLEDGEMENTS

UDC 629.735.015

N. Yurchenko Ph.D., P. Vynogradskyy, Ph.D., K. Kuzmenko
(Institute of Hydromechanics, Ukraine)
R. Pavlovskyy Ph.D., A. Zhdanov Ph.D.
(National Aviation University, Ukraine)

MICROWAVE-INDUCED STREAMWISE WORTEX GENERATION IN AERODYNAMIC COMPLEX FOR INTERDISCIPLINARY RESEARCHES

The results of experiments of flow over aerodynamic models in the field of microwave radiation were described in the article. The choice and construction features of the plasma-initiated model is presented in this paper relatively to experimental tasks

Introduction

The main part of the Aerodynamic Facility for Interdisciplinary Research is the wind tunnel of an open-return type with closed type test section with following sizes: (width, height, length).

Fig.1 The microwave generation system

Wind tunnel includes the following systems: the flow measuring system, the 3-component strain gage balance, the pressure distribution system, the microwave generation system. The recent total modernization of the facility, which applied for every element of facility, was made accordingly to recommendations of Moscow Radio Technical Institute (MRTI) to improve the conditions of microwave radiation. The sizes of the test section were changed in place of installation and improved protection of staff from dangerous radiation.
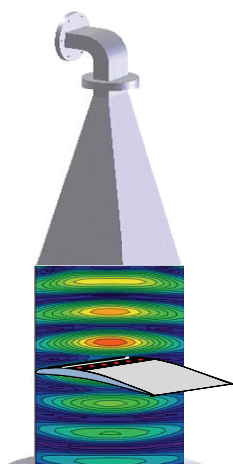
1. The microwave generation system

The system includes: magnetron with horn antenna and two regulated power sources which are situated on the upper side of the Eiffel chamber. Power supplies consist of: a source of constant power of 1.5 kW and pulse source pulse power up to 7 kW at an average power to 1.0 kW. The industrial generator of microwave radiation has a wavelength of $\lambda_{mw} = 12.24$ cm, which is the most absorbed in water. So, it requires the protection of operators and measurement system from itself. The microwave generation system and protection from microwave radiation were developed by MRTI and based on the

Fig. 2 . Cross-sectional of the model with the plasma initiators

construction and features of the AFIR test section. The system was iterative optimized to provide sufficient intensity and uniformity of the field from low-power generator in the test section during the measurement.

The principle of the system is shown in Figure 1. The researched profile radiated from the horn is situated in the field of radiation. Horn is installed on top of the model, the mirror is situated from below of the profile. The cross array of plasma initiators is made on the upper side of the model. When model located in the radiation field it will create a point-discharges of plasma. This transversely mounted plasma-generator array generates a streamwise vortices which is changed a boundary-layer structure. In Figure 2 shows the cross-section of model, with the specified direction of the MW-radiation and position of the initiators relative to it.

2. Experimental models

The model consists of two main parts (Fig. 3.4): 105º degrees cylindrical pipe segment with 6 mm thick made of polyvinylchloride, which sets the basic contour of the model. The second part is a metal insert with 2 mm thickness, where the plasma generators are situated. This metal plate is mounted on the basic polyvinylchloride segment by 8 countersunk screws. There are four transverse insertions within the model for holding its cylindrical shape and provide sufficient rigidity during experiment. They are glued to the basic cylindrical pipe for additional fixation in their positions. There is a holder in the middle of the model, which is base for all the elements of the model. Including twenty-four drainage tubes, in which the signal coming from holes on the model to the pressure sensors. Step of the receiving holes on the surface of the model is 15º. Discharge on the model of the plasma initiators is obtained through the transversely mounted plasma-generator array.

Fig. 3 The test model

Fig. 4. Fabrication of the airfoil-type model with actuators of localized plasma discharges

Requirements to the model materials are also basically the same supplemented with the requirement

of radio-transparency:

- Low thermal conductivity and high dielectric properties of the basic (body) material;
- Sufficiently high insulating and strength properties of a surface layer, its high-quality processing to provide a smooth surface;
- Long-term thermal resistance of the construction in localized areas of plasma initiators.

3. Aerodynamic measurement using microwave radiation

It was made a large number of models which differed in principle of plasma generation, and design since the beginning of the experiment. These models have different geometrical parameters, configuration, different space between initiators, different surfaces for initiators installation, initiators location place. The experimental problem was formulated in accordance with previously obtained data related to the study of the behavior of a prototype model. So there were chosen the following parameters of the model: curvature of the surface of the cylinder diameter D = 90 mm; free-stream velocity U_0 = 10-40 m/s; distance between generators is z = 10 mm (Fig. 4.) A further step z was chosen by taking into account the favorable effect of aerodynamic characteristics

obtained by mechanical vortex generators and electromagnetic requirements of MRTI. Relatively to linear arrangement of the array of generators, which create a stable burning of plasma discharges on the fixed distance from each other.
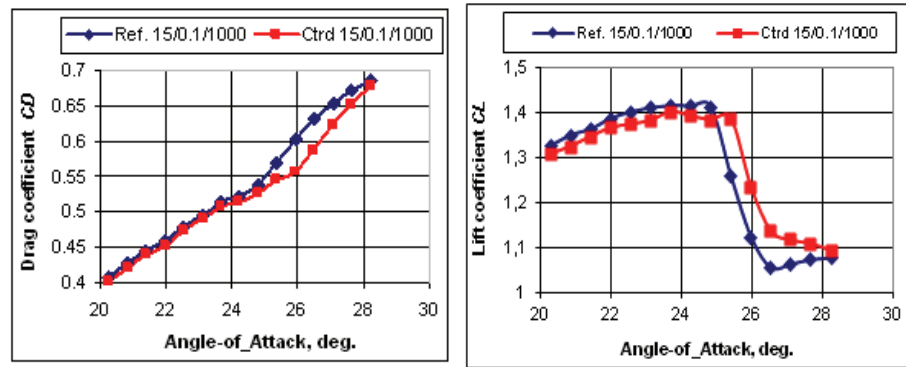
Fig. 5 Lift and drag coefficients for reference (Ref.) and plasma-controlled (Ctrd) models, U_0= 15 m/s, MW pulse mode: f=1000 Hz, t=0.1 s

To follow results of numerical simulation, various modes of MW system operation were considered. Results of measurements (Fig. 5) and of numerical simulation are in a good agreement confirming the conclusion about the need of a correct choice of MW radiation parameters. The spanwise array of localized plasma discharges can improve the aerodynamic performance, lift coefficients having been found to be more sensitive to the parameters of plasma-initiating MW radiation.

To provide higher stability of generation and behavior of MW-initiated plasma discharges prototype model was preliminarily tested in MRTI.

All information about the experiment and the obtained parameters come to the Data Acquisition and Control System (DAS), from which operator manages and conducts the experiment.

Data Acquisition and Control System makes it possible to carry out the following measurements: remote control of model position in the working chamber (setting of different values of the angle of attack), measurement according to the plan of the experiment, control of the radiation system, measurements and calculations (e.g. calculation of aerodynamic coefficients, pressure distribution on the model surface, a graphical representation of results).

Data Acquisition and Control System consists of matching hardware and software parts. One of it function is the development of new subprogram for the vector representation of the pressure distribution on the model surface during the experiment. Example of graphical window shown in Fig. 6, with a clearly visible of presentation of results and efficient analysis of measurement process. This can greatly improve the program of research, reduce the number of test runs and increase more detailed measurements at critical points.

Results of the experiment are shown in the Fig. 5. The pressure distribution on the cylinder's surface with mounted plasma initiators are illustrated on the Fig. 6. The pressure distribution is shown with the plasma initiators and without them, for better comparison of initiators activity.

MW-radiation influences on the model from the top, at the same time position of initiators was changed relative to the flow axis. In Fig 5. We see a variation in lift and drag coefficients for reference (Ref.) and plasma-controlled (Ctrd) models.
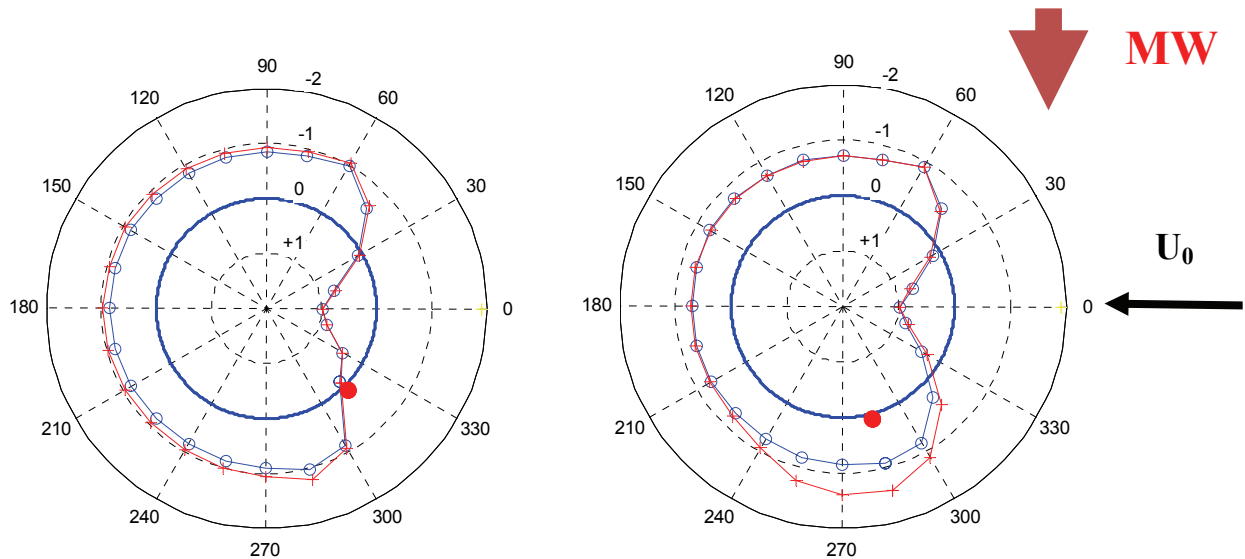
Fig. 6 Pressure distribution over the plasma-controlled circular cylinder model in a crossflow: $Re_D = 1.23 \times 10^5$; t= 60 µs; F =500 Hz; (a) θ = 45°; (b) θ =75°

Summary

MW energy distribution in a wind-tunnel test section was investigated. Further development of models design and technology will be in conjunction with the Moscow Radio Engineering Institute to increase the lifetime of plasma initiators during the experiment in wind tunnel. Modernization of AFIR changed conditions for interdisciplinary research through the changes of complex elements.

References

1. Improvement of the turbine blade performance based on the flow instability and receptivity analysis, *N. Yurchenko, R, Rivir*, 2000, proc. 8th Int. symposium on transport Phenomena and Dynamics of Rotating Machinery (ISROMAC-8), Honolulu, U.S.A., pp. 300-306

2. Control of the profile aerodynamics using streamwise vortices generated in a boundary layer, N. *Yurchenko, R. Rivir, R, Pavlovsky, P. Vinogradsky, A. Zhdanov*, 2003, proc. World Congress "Aviation in the XXI-st Century", Kyiv, Ukraine.

3. MW-generated point plasma discharges as a novel approach to boundary-layer control, *N. Yurchenko*, 2008, AIAA-2008-1388.

4. Aerodynamic facility with MW-Systems for Flow Control Based on Localized Plasma Generation, *P. Vynogradskyy, N. Yurchenko, R. Pavlovsky, O. Zhdanov*, 2008, AIAA Paper -2008-3939.

5. Initiated Surface Microwave Discharge as an Efficient Active Boundary-Layer Control Method, *V. L. Bychkov, I. I. Esakov, L. P. Grachev, A.A. Ravaev, K.V. Khodataev, N.F. Yurchenko*, 2009, AIAA-2009-889.

6. Impact of Spanwise Arrays of Plasma Discharges on Aerodynamic Performance, *N. Yurchenko, N. rozumnyuk, Yu. Paramonov, V. Tsymbal, P. Vynogradskyy, A. Zhdanov*, 50th AIAA Aerospace Sciences Meeting, 2012, AIAA-2012-1029.

Aknowledgements

UDC 629.7.07.4:612.881

I.B. Kuznetsov, Doctor of Science ("Training center" St. Petersburg, Russia)

SCIENTIFIC BASIS FOR INTERACTION OF PILOT WITH FLIGHT PARAMETERS INDICATION SYSTEM AT THE AIRCRAFT HANDLING

Process of distribution and visual attention change-over by pilot is described. Results of theoretical and experimental results are generalized by formulation of basic principles for reading of information by pilot through optic canal. Methodology of formation by pilot of interaction with display information at the aircraft handling according to the instruments is formulated.

Introduction

Statistical analysis of safety of flights of civil aviation aircrafts (AC) continues to show significant number of aviation accidents and catastrophic air crashes connected with incorrect activity of air crew. Generalization results of analysis of emergency flights allows for conclusion that in majority of cases spatial disorientation is the basic reason of crashes [1]. Considering the AC handling as the steering controls action determined by information obtained by the pilot from equipment in the AC cabin it is obvious that skill of correct distribution and change-over of visual attention (DCVA) at the instruments is directly interconnected with emergency events. That is why neither implementation of new navigation and landing systems nor plane control automation or equipping of pane with modern integral instruments with the most perfect indication reduced requirements to the skill of pilot to obtain the necessary information in time. Therefore, development of scientifically based DCVA principle and on the basis of it – models and technique of reasonable DCVA at flights according to the instruments – has important industrial meaning in the flights safety provision.

Typical DCVA schemes offered before are developed by method of subjective generalization of experience of flights according to the instruments of pilots-trainers for AC with electromechanical indication [2]. Presented number of DCVA routes depending on the stage of flight and tasks solved by pilot is measured in tenths which currently significantly complicates their successful mastering and application in connection with absence of theoretical basis required for flight within the established DCVA limits. Common to these techniques is optimization of instruments used at DCVA, creation of attention reserve at the pilot for the case of abnormal (emergency) situation and rigid adherence to the stages of flight and piloting tasks being solved. These schemes do not consider constructional features of presentation of information at the "glass cabins" and are not proved by objective theoretical DCVA principles as well as are not confirmed by experimental studies. Exactly because of reasons stated above solution of task did not gain further development at the modern level. Results obtained before call into doubt possibility of creation with application of them of effective technique for training of pilots in DCVA in the process of modern AC flight operation that is why it is necessary to study the essence of pilot's interaction with display information which is an objective reflection of the flight dynamics.

Study task description

It is proposed at solution of task on DCVA principles detection at the flights according to the instruments within established operating limits to consider the model of pilot as tracking system (TS). Possibility of TS theory methods application for determination of pilot's visual and motoric activity characteristics required for AC stabilization at the reference trajectory is based upon the fact that for AC stabilization the pilot shall with established accuracy track the dynamics of controlled disturbed flight parameters (FP) and inhibit through stabilizing control FP disturbances in some frequency range, i.e. actually reproduce with established accuracy random function which describes FP deviation from its values at the reference trajectory. That

is why it is necessary to set the required frequency of pilot's referencing to FP and formulate DCVA principle at instrument flying.

Theoretical studies

Basic provisions determining optimal routes of pilot's DCVA at instrument flying can be based on the study and analysis of whole spectrum of dynamic characteristics of certain information parameters presented to the pilot as well as constructional features of their realization at the AC instrumentation console. This postulate determines the role of pilot in the AC control process. The pilot as transfer member in the form of tracking dynamically self-adjusting system through optic canal records at the input deviations from parameters set according to the frequency of controlled parameters changing with formation of control signals in the circuit between instrumental information field and controls first of all on the basis of dynamics and statics of information field readings and operational flight plan.

Tracking system (TS) operation which tracks some process x(t) is described by integral convolution equation [3, 4]:

$$x(t) - \int_0^t k(t-s)x(s)ds = f(t), \tag{1}$$

where: t is time;

k(t) is function which characterizes TS response to the input signal (function of TS response to input δ-impulse, k(t)=0, at $t \le 0$);

$\int_0^t k(t-s)x(s)ds$ is the process reproduced by TS under the process being tracked x(t)

(TS output);

$x(t) - \int_0^t k(t-s)x(s)ds = f(t)$ is the TS error desynchronization between TS input

and output signal.

Main TS objective is in ensuring of set process tracking accuracy x(t), i.e. in mathematical description and technical realization of such core k(t) of equation (1) at which:

$$|f(t)| \le C \quad \text{for} \quad \forall t \in [0, +\infty] \quad , \tag{2}$$

where C is maximum allowable TS error.

If the function x(t) is random then TS error f(t) at any specific time will be a random value that is why planned quality of TS operation which tracks the random process shall have probabilistic form:

$$P\big(|f(t)| \le C \quad \forall t \in [0, +\infty]\big) \ge p \quad , \tag{3}$$

where: p is set threshold process tracking probability x(t) with accuracy C determined from operational requirements.

For TS which tracks standard random process under set quality of its functioning required frequency of information loading into TS is determined. For such control at the set value of error variance D analytical type of spectrum of control frequencies necessary for reproductive performance can be described by the following equation:

$$D = 2 \int_0^{\omega_0} S(\omega)\sin^2 \psi(\omega)d\omega + 2 \int_{\omega_0}^{+\infty} S(\omega)d\omega, \tag{4}$$

where: S is spectral density;

ω is frequency;

ψ is phase characteristic.

Required frequency can be determined with usage of standard formula:

$$D_f(\omega_0) = 2 \int_{\omega_0}^{+\infty} S(\omega)d\omega \leq D \quad . \tag{5}$$

At that value ω_0 equal to the TS core spectrum width k(t) is the requirement to the technical realization of TS being under consideration: the bigger the value ω_0 is the more frequency components of input signal shall be accurately tracked by TS. By reference to practically important consideration in relation to minimization of pilot's visual load TS core spectrum width k(t) shall be selected as minimum possible one from frequencies ω_0 which ensure established quality of TS operation. Such minimum core spectrum width k(t) is equal to:

$$\overline{\omega} = \inf \left\{ \omega_0 \middle| D_f(\omega_0) \leq D, \quad \omega_0 \geq 0 \right\} \quad . \tag{6}$$

where: $\psi(\omega)$ is phase-frequency characteristic (PFC) of TS actuator;

D is maximum value of TS error variance f(t) at that planned quality of TS operation is ensured.

Frequency $\overline{\omega}$ can be called theoretically as required TS frequency in its technical realization. At that, formulas (5) and (6) allow for determination of required TS frequency under spectral density of its input signal.

Formally, to present the pilot's activity in the form of TS it is enough to determined not the frequency частоту $\overline{\omega}$ but minimum informative for pilot frequency of controlled process tracking x(t) which is determined by minimum allowable for recovery under discreet reference system frequency for tracking of function with limited frequency ω_0 with Fourier spectrum width which under sampling theorem [4] makes up $2\omega_0$ rad/s or ω_0/π Hz.

Obtained conclusion on value ω_0/π Hz as minimum required process tracking frequency x(t) remains reasonable for calculation of minimum required frequency of pilot's visual references to FP x(t) for its stabilization within operating limits therefore it is also equal to ω_0/π Hz. At that target of pilot in the task for AC stabilization is not the recovery of FP deviations x(t) under discreet system of its values – references withdrawn at visual references to FP and formation of such FP deviations dynamics at which probability of falling of FP deviations f(t) not compensate by stabilizing control outside of operating limits does not exceed the value 1-p. But for complete inhibition of frequency component of disturbed FP deviations x(t) having frequency τ Hz the pilot shall supply to the input of corresponding control element sinusoidal controlling action with the same τ Hz frequency. To form such sinusoidal controlling action the pilot shall at the period of function with frequency τ Hz perform double change of direction of his action onto control element. Each change of direction of pilot's action onto control element shall be preceded by visual reference of pilot to FP because selection of new control parameters and monitoring of FP response to the change of control is carried out by the pilot based on the visual information on FP dynamics. Therefore, minimum frequency of pilot's visual references to this FP required for of disturbed FP harmonic component inhibition with frequency τ Hz (as well as for inhibition of all its harmonic components with lower frequencies) equals to 2τ Hz – doubled frequency of required stabilizing control.

Experimental study

To obtain the answer to questions connected with pilot's DCVA optimization at AC piloting at different stages of flight, determination of degree of individuality in the piloting technique and extent of pilot's DCVA influence at AC steering according to the instruments the author performed the study of subjective opinion of pilots of the following AC types: A-320, B-737, B-767, An-148 and Tu-204 [5]. During the process of expert questioning the pilots were charged with similar tasks on DCVA depending on various modes of landing approach. Results obtained did not provided with possibility of optimum routes determination and DCVA principles formulation

therefore development of experimental technique which allows with application of special technical tools for performance of registration of pilot's visual activity at modern AC piloting became the important stage of study.

Possibility of pilot's DCVA instrumental study is based upon the fact that pilot's sight is moving in jerking manner with stops at some points – piloting parameters and then quickly moves to another point. At that perception and processing of piloting information is carried out namely at that points of fixation where the sight stops. That is why the task for determination of optimum technical tool which allowed for conduction of corresponding measurements in the modern AC cabin was solved and appropriate experimental flights technique was developed [6]. The author performed experimental flights on complex simulator of plane Ty-204 with six degrees of movability and liquid-crystal display equipment. Total duration of flight experiment was seven days with participation of six experienced AC command pilots; at that, 123 minutes of registration of DCVA routes of pilot which performs pilots were recorded. As a result of experiment the following is established:

1. FP number in DCVA cycle of pilot which performs piloting is the parameter of piloting technique (flight experience) which is not seen expressly, is not fixed by AC objective control, is absent in the norms (criteria) of piloting technique and is not evaluated subjectively by the pilot performing monitoring in the process of AC crew training and examination. This parameter has dominating influence onto accuracy of piloting in complicated and emergency conditions of AC flight operation.

2. Minimum time of FP fixation by pilot at AC with FP electronic indication system is not more than 0.2 s; at that information fixed in the form of visual image is processed by the pilot within 0.4 s.

3. In the process of DCVA of pilot which performs piloting main parameter is not the time of presence of pilot's sight at FP but FP number in DCVA cycle.

4. Availability of inverse dependence of FP number in DCVA cycle and instrument flying accuracy. The bigger number of FP is present in DCVA circuit the worse the piloting accuracy parameters are and the higher the probability of aviation accident is.

5. Misrepresentation by majority of pilots of DCVA routes correction at flights in various piloting conditions.

6. Pilot's DCVA routes shall be closed; they shall start and end at the same instrument (FP). For electromechanical instruments such reference instrument is horizon indicator or flight director and for AC with electronic indication system parameters located in the center of screen (command bars) are the reference.

7. Closed DCVA route of pilot's sight movement shall include except the reference one not more than two FP (instruments); at that priority is given to one parameter (DCVA cycle with two routes).

8. If DCVA route will be chaotic or will consist of three instruments (parameters) and more – practically always there will be present non-controllable invisible for pilot fallings of controlled parameter outside of operating limits.

Conclusions

Theoretical studies and results of experimental flights allow for formulation of the following conclusions and generalizations:

1. Main characteristics of process of pilot's interaction with FP indication system at control of flight trajectory and stabilization on it are determined by AC aerodynamic performance and set accuracy of piloting which define sequence (frequency of references) and route of sight which on the basis of experimental data practically coincide with theoretical values calculated under minimum frequencies of pilot's visual references to FP required for piloting task completion [1].

2. Structure of pilot's visual activity especially at the most difficult stages of flight (at landing approach, flying according to the duplicate instruments, flying at equipment failure) is determined by availability of basic instrument which visualizes tangage, tilting and deviations from course and

glidepath which accrues about 60% of pilot's visual load with instrumental information and reference FP in the form of command signals [2, 5].

3. Pilot's visual control of FP with doubled frequency of this FP changing theoretically guarantees established amount of AC stabilization within operating limits for this FP deviation and absence of non-controllable FP falling outside of AC operating limits [2, 7, 8].

4. Visual routes of pilots which successfully performed the flight task with observation of set flying limitations and procedures ensured allowable time of absence of the sight fixation at controlled FP that resulted in availability of two (less frequently three) instrumental cycles with beginning and ending at reference FP [7, 8].

References

1. *Kuznetsov I.B.* Principles of pilot's attention distribution determined by aerodynamic performance and accuracy of piloting.// Journal "Polet" No. 9. 2011. - P. 26-31.

2. *Kuznetsov I.B.* Experimental studies of pilot's visual activity at piloting of AC with electronic information display system.//Scientific bulletin of Moscow State Technical University of Civil Aviation (MSTUCA) No. 172 (10) – M.: MSTUCA, 2011. - P. 120-126**.**

3. *Zorich V.A.* Mathematical analysis. – M.: Nauka, 1984. – Part II. – 640 p.

4. *Krasnov M.L. et al*. Functions of complex variable. Operational calculus. Theory of stability. M.: Nauka, 1981. – 303 p.

5. *Kuznetsov I.B*. Study of pilot's attention distribution at instrument flying.// Journal "Polet" No. 1. 2012. - P. 22-27.

6. *Kuznetsov I.B.* Videooculographical methods of pilot's activity study// Journal "Information and control systems" No. 1(56)/2012. - P. 79-83.

7. *Kuznetsov I.B., Stolyarov N.A.* Formation of basin principles for pilot's interaction with instrumental equipment.// Journal "Polet" No. 7. 2011. - P. 22-27.

8. *Kuznetsov I.B.* Methodological basics of pilot's training in distribution and change-over of attention at instrument flying.// Scientific bulletin of MSTUCA No. 177 (3) – M.: MSTUCA, 2012. - P. 97-104**.**

L.I. Grechykhyn, doctor of phys.-math. sciences, prof.
(Minsk State Higher Aviation College, Minsk, Belarus)
N.G. Kuts, Ph.D., docent
(Lutsk National Technical University, Lutsk, Ukraine)

HEAT PUMP WITH THE MOBIUS SCREW

It was developed a molecular-kinetic theory of the screw with the surface of Mobius, which allowed a computer simulations in different conditions of its use. It was considered the possibility of the direct and reverse mechanization of the screw with the surface of Mobius. It presents data of the computer simulation to clarify the optimal shape of the working screw with a surface of Mobius as a heat pump.

Introduction. In aviation are widely used pulling and pushing air screws. Their use is due to the fact that they allow more efficient air travel then the jet-powered aircrafts. The main disadvantage of the air screws is their strong glaciation.

Aim and objectives. The positive or negative quality of the air screws has not become sufficient justification. In this regard, there was objective to transform the negative effect of the working screws into their positive quality. This aim required to solve the following tasks: - to determine the operating conditions of screws of different designs and to find the optimal shape for maximum traction with minimum energy consumption; - to develop a theory, which allows the computer simulation in different conditions of its use; - to consider the possibility of mechanization of the screw; - to conduct the computer simulations to clarify the optimal shape of the screw with a working surface of Mobius as a heat pump.

The main part. The optimal shape of the screws with the surface of a Mobius. To reduce the frontal resistance with increasing traction, in the works [1, 3] is proposed a screw with the surface of a Mobius. Various screws with the surface of Mobius are shown in Fig. 1. It is possible to rotate such screw at high speeds without fear of its destruction. The width of the strip, rolled into the surface of Mobius, by computer simulation is set such as to provide maximum traction with minimum frontal resistance for a given aircraft with a given engine capacity. Analysis of the screw Shpady is described in [4-6]
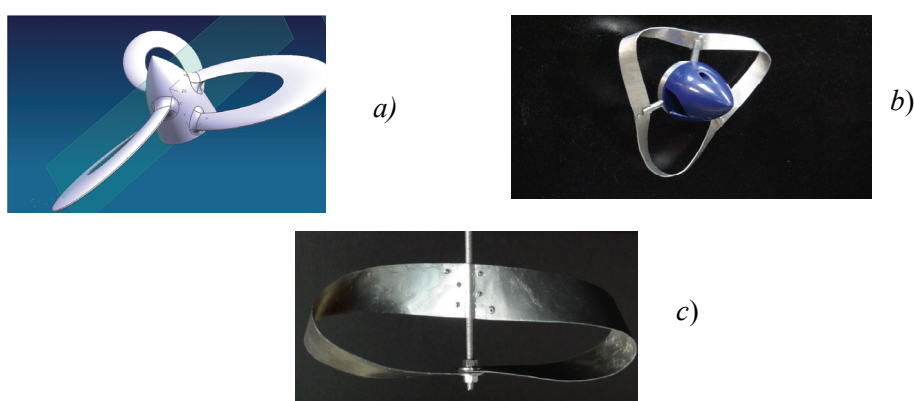
Fig.1. The screws with the surface of a Mobius:
a) –screw of Shpady; b) – screw of Grechyhyn; c) – screw of Narushevitch

In this work it is analyzed the screw with the surface of Mobius, offered by Narushevytch. The front edge of the Narushevytch's screw is an ellipse in which the semi-major axis a is a semi-diameter of the circular swept surface of the screw, and the minor axis b - is the distance between the front and rear edge along the axis of rotation. If to direct the X-axis along the rotation axis and the Y-axis perpendicular to the axis of rotation with the center between the front edge on axis and

the Y-axis perpendicular to the axis of rotation with the center between the front edge on the axis of rotation, the screw of Mobius in these coordinates has the form

$$y = b\sqrt{1 - \frac{x^2}{a^2}} \ . \tag{1}$$

Let's consider the theory of the operation of the screws with the surface of a Mobius, placing it in a way shown in Fig.1., using the general approach developed in [3-6]. It should be taken into account the formation of a zone of rarefaction behind his back side and the mechanism of filling the area with ambient air. Screw of Narushevytch shown in Fig. 1, interacts with the ambient air with its four planes. The front part of the screw is formed from the upper and lower surface, and the back part of the – from the outer and rear surface. Each of these surfaces has its own aerodynamics.

1. *The upper surface of the front part of the screw.* The interaction angle of the upper surface of the screw with the ambient air for the linear part without rounding (without mechanization of blades), shown in Fig. 2, will be measured relative to the direction of motion, i.e. relative to the thrust vector. In such reckoning the angle of twist of the front part of the wing varies from 90^0 to 45^0. Then along the Y-axis the twist angle is
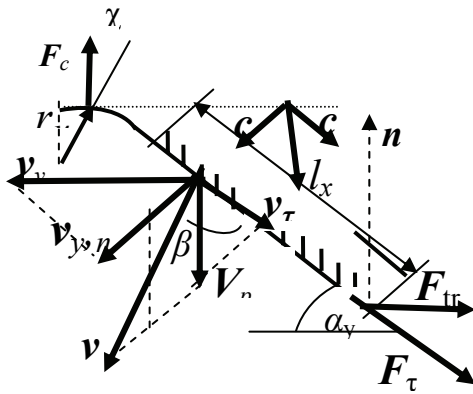
Fig. 2. Scheme of interaction between the molecules of air and the upper surface of the front part of the screw
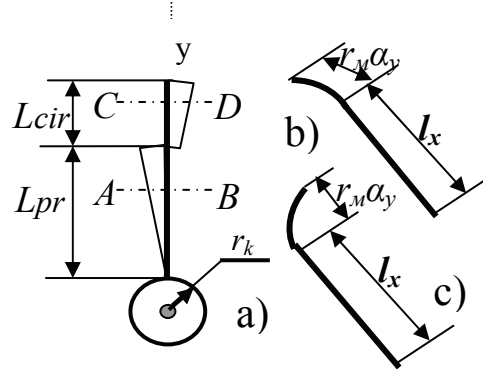
Fig. 3. Blade of the screw with a straight (b) and reverse (c) mechanization: a) - a general view of the plane of rotation, b) – view of AB; c) - view of CD

$$\alpha_y = \frac{\pi}{2} - \frac{\pi}{4}\frac{y}{a} \ . \tag{2}$$

The countdown for the Y-axis is performed in the radius of spinner and ends at a distance, where begins opposite mechanization of the screw blades, equal to L_{pr} (Fig. 3). At some distance y in the element Δy with the width of the strip of the surface of Mobius l_x, ambient air molecules will be taking an impact normally to the surface of the screw. The magnitude of the impact is determined by the speed with which the screw rotates and by the mass of air, which had interacted with the surface element $\Delta S = l_x \Delta y$ of a linear field of the width of the screw blades. Based on Fig. 2 the mass of air involved in the interaction,

$$\Delta m = \rho_\infty v l_x \Delta y \cos(\alpha_y - \beta)\Delta t \ . \tag{3}$$

here ρ_∞ – density of the ambient air, v_y, v_{II} – respectively, the linear speed of rotation of the screw and the speed of air flow, which is formed by screw, or the speed of the screw relative to the ambient air, and

$$v = \sqrt{v_y^2 + v_{II}^2 + 2v_y v_{II} \cos\alpha_y} \ - \tag{4}$$

And for the angle β after simple transformations we obtain

$$\beta = arctg\left[\sqrt{\left(\frac{2v}{v_{II} + 2v\cos\alpha_y}\right)^2 - 1}\right] \ . \tag{5}$$

1.3.23

The change of momentum $\Delta p_1 = \Delta mv \cos(\alpha_y - \beta)$ leads to a force of impact

$$\Delta F_1 = \frac{\Delta p_1}{\Delta t} = \rho_\infty v^2 l_x \Delta y \cos^2(\alpha_y - \beta)\sin\alpha_y \qquad (6)$$

And the moment of forces $\Delta M_1 = \Delta F_1 y$.

The resultant moment of force and the power of the front of the screw of Mobius, formed only by a linear upper surface, respectively are

$$M_1 = \int_{r_k}^{L_{pr}} \rho_\infty v^2 l_x \cos^2(\alpha_y - \beta)\sin(\alpha_y) y \, dy; \quad N_1 = M_1 \omega, \qquad (7)$$

here $\omega = 2\pi f$ - a circular frequency and f – a linear speed of the screw, r_k – a radius of the spinner, L_{pr} – a length of the front of the screw with a direct mechanization.

The flow of air that rushes along the upper surface of the front of the screw, moves with the speed $v_\tau = v \sin(\alpha_y - \beta)$ and goes along the surface of the screw, creating a gas-dynamic pressure at a distance y from the axis of rotation $\Delta T_1 = 0,5\rho_\infty v_\tau^2$.

Such pressure creates an additional force moment, which reduces power consumption from the energy source and is

$$W_2 = \int_{r_k}^{L_{pr}} \Delta T_1 l_x \sin(\alpha_y) y \, dy. \qquad (8)$$

The same flow creates the reactive thrust, made by the upper surface of the front part of the screw

$$F_{T,2} = \frac{1}{2}\int_{r_k}^{L_{pr}} \rho_\infty v^2 l_x \sin^2(\alpha_y - \beta)\sin(\alpha_y) \, dy, \qquad (9)$$

creating a moment of force and consuming the corresponding power

$$W_2 = \frac{1}{2}\int_{r_k}^{L_{pr}} \rho_\infty v^2 l_x \sin^2[\alpha_y - \beta)]\sin(\alpha_y) y \, dy; \quad N_2 = M_2 \omega. \qquad (10)$$

2. *The bottom surface of the front of the screw.* Behind the bottom surface of the front side of the screw the shedding flow is formed. In the area of shedding flow arises a region of rarefaction. The pressure in the rarefied region is following [5]

$$P_\theta = P_\infty \exp\left(-\frac{m_a v_y^2}{2k_B T_\infty}\right). \qquad (11)$$

Here m_a - an average weight of air molecules, k_B – the Boltzmann constant, and T_∞ - an environment temperature.

In the bottom area of the front side of the screw with the increasing of rotation in the mean free path, arises a complete vacuum, which is filled with molecules of air at a speed of sound at ambient temperature, determined by the Laplace's formula

$$c = \sqrt{\frac{kR_\varepsilon T_\infty}{\mu}}. \qquad (12)$$

k - a ratio of indexes of heat capacity at the const. volume and the const. pressure and for air - 1,4; R_ε – the gas const. 8,31 J and μ – a molar weight of the air ~ 0,029 kg/mol.

The general scheme of the interaction of air with the bottom surface of the front of the screw is shown in Fig. 4. Behind the screw is formed the rarefaction zone, which is being filled with the airflow with sound speed normally to the surface and to the interface plane of rotation of the screw relative to the environment (upper dashed line) in Fig.3. The resulting flow speed based on the theorem of cosines $v_{rez.} = \sqrt{2}c$.

The air flow to the lower surface of the front part of the screw will be

$$J_3 = \frac{1}{4}n[c - v\cos(\alpha_y - \beta)], \qquad (13)$$

here $n = P_e / k_B T_\infty$ - concentration of air particles in the shedding flow zone.
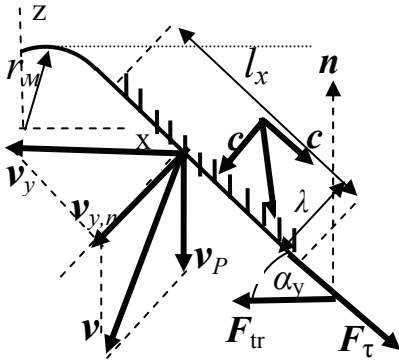
Fig. 4. The scheme of interaction between the molecules of air and the upper surface of the front part of the screw

The mass of air which will interact with the surface element ΔS for the time Δt to the underside of the front of the screw

$$\Delta m_3 = J_3 m_a \Delta t = \frac{1}{4}\rho_e\big[c - v\cos(\alpha_y - \beta)\big]\Delta S \Delta t . \qquad (14)$$

In the process of interaction of this air mass with an element of surface ΔS at a distance y to the screw will be given impulse

$$\Delta p_3 = 2\Delta m_3 [c - v\cos(\alpha_y - \beta)]. \qquad (15)$$

As a result, it will arise the force of influence on this element of the surface, by the value of $\Delta F_3 = 2\Delta m_3[c - v\cos(\alpha_y - \beta)]/\Delta t$. In the normal component of the force we consider the linear velocity of the screw element $v_y = 2\pi f r_y$, which reduces the magnitude of the flow velocity of air molecules to the lower surface of the front part of the screw. Then

$$\Delta F_3 = 0,5\rho_e\{c - v\cos(\alpha_y - \beta)\}^2 \sin(\alpha_y)\Delta S , \qquad (16)$$

The resulting force towards the rotation helps to increase the speed, and therefore relieves the power consumption from on-board power source. The resultant active force normally to the surface on its element ΔS at a distance from the axis of rotation y is

$$\Delta F_3 = \frac{P_e}{2k_B T_\infty} m_a \{c - v\cos(\alpha_y - \beta)\}^2 l_x \sin(\alpha_y)\Delta y. \qquad (17)$$

Under the influence of such force there comes a moment of force $\Delta M_3 = \Delta F_3 y$,

The resultant moment of force, due to the shock effect of the air molecules on the lower surface of the front part of the screw perpendicular of the normal to the axis of rotation:

$$M_3 = \int_{r_k}^{A-L} \frac{P_e}{2k_B T} l_x m_A \{c - v\cos(\alpha_y - \beta)\}^2 \sin(\alpha_y) y dy . \qquad (18)$$

Along the surface arises a flow of air with a speed of sound.

Applying Bernoulli's law, we obtain the force and moment of force, which change the traction and the power consumption of the screw from the onboard power source, respectively:

$$F_3' = \int_{r_k}^{A-L} \frac{P_e}{2k_B T} m_a c^2 \sin(a_y) l_x dy;$$

$$M_3' = \int_{r_k}^{A-L} \frac{P_e}{2k_B T} m_a l_x \, c^2 \sin(a_y) y dy \qquad (19)$$

The resultant moment of force $M_{3,pe3.} = M_3 - M_3'$. If it is positive, then the screw will draw power from the onboard source, and if it is negative, then it will go completely in the operation of the heat pump and will start additionally to spin and consume energy from the environment, equal to $N_1 = M_{3,rez.}\omega$.

Such situation is quite possible, but difficult to implement. It's necessary to look for the other approaches. The tangential component of the velocity of air flow after the screw creates a reactive force of the propeller thrust. The resultant traction is created by both the upper and lower surfaces of the front of the screw. Then

$$X_a = \int_{r_k}^{L_{np.}} \big[\rho_\infty v^2 \sin^2(\alpha_y - \beta) + \rho_e(c - v\cos(a_y - \beta))^2\big]\sin\alpha_y y dy. \qquad (20)$$

Here $\rho_e = P_e m_a / k_B T$ - density of the air flow in the area of shedding flow.

The front part of the screw with the surface of Mobius creates in the inner region between two surfaces the zone of rarefaction, in which the pressure is determined by the formula (9). Under such

pressure is performed the compression of the front and rear blades of the screw with a surface of Mobius. The longer the blades are apart, the faster the central region between the blades is filled with ambient air and as a result the tightening force between the blades is removed. That means that the screw works more efficiently. These properties of the Mobius screw previously had not been studied in detail and therefore often received a negative result in its application.

That's why, the Shpadi screw blades are separated by the largest possible distance from each other, as it is possible to construct. The result was a positive effect. The resulting power consumed by a screw and the produced thrust are formed by a linear surface of the front side of the screw. Let's have a look at the similar situation for the back of the screw.

3. *The back of the screw.* The angle of twist for the external and the rear surface of the back of the screw with the surface of Mobius relative of the normal to the axis of rotation is

$$\alpha_y' = \frac{\pi}{4}\frac{y}{a}. \tag{21}$$

All formulas obtained for the front of the screw will remain the same for the back of it, just the angle α_y is replaced by the angle α_y'. For the outer surface of the back of the screw the force point of resistance to rotation, and the expended power is

$$M_4 = \int_{r_k}^{L_{pr}} \rho_\infty v^2 l_x \cos^2(\alpha_y' - \beta)\sin(\alpha_y')y dy; \quad N_4 = M_4\omega. \tag{22}$$

To the rear surface of the back side of the screw the force point of increase of rotation and expended power for this is

$$M_5 = \int_{r_k}^{L_{pr}} \frac{P_\text{в}}{2k_B T}l_x m_A\{c - v\cos(\alpha_y' - \beta)\}^2 \sin(\alpha_y')y dy; \quad N_5 = M_5\omega.. \tag{23}$$

Tractive force will be

$$\Delta X_a = \int_{r_k}^{L_{pr}} 2\pi\left[\rho_\infty v^2 \sin^2(\alpha_y' - \beta) + \rho_e c^2\right]\sin\alpha_y' y dy. \tag{24}$$

To increase the lift and to reduce frontal resistance of the aircraft wing is used different machinery. The most reasonable application to the screw is the "Kruger tooth." Let's consider such mechanization applied to the screw of Mobius, in the forward direction at the site L_{pr} and in the opposite direction at the site L_{ob}. The location of these sites along the screw blades is shown in Fig.3. In the first case appears a concentration of air flow to the axis of rotation and the screw thrust increases, and in the second case the air flow is directed from the axis of rotation of the screw and the screw thrust is reduced. Therefore, the inverse mechanization applies not only to the screws, but also to the fans and turbines. However, this is not always justified.

The mechanization of the screw with the surface of Mobius. To increase the thrust consider mechanization, caused by the bend radius of the frontal edge of the screw blades. This design of the screw blade directs the concentration of air flow to the axis of rotation behind the screw. In Fig. 3 and Fig. 4 is shown such mechanization by bending the frontal edge of the screw blade of radius r_M. The speed of incoming airflow v_Π increases the mass of gas, moving along the surface of the blade. This increases the tangential velocity of the airflow, which determines the strength of the screw thrust. The size of the radius of the bend, which captures air, is determined as follows

$$\varsigma \approx r_M[1 - \cos(\alpha_y)]. \tag{25}$$

On each element of bend surface the speed of the air has its normal and tangential components, which are respectively

$$v_{M,n} = v\cos(\alpha_y'' - \beta''); \quad v_{M,\tau} = v\sin(\alpha_y'' - \beta''), \tag{26}$$

Here the angle α_y'' is changed from α_y to zero and determined in accordance with Fig. 4 as follows:

$$\alpha_y'' = arctg\left[\sqrt{(r_M/z)^2 - 1}\right]. \tag{27}$$

Then the mass of air, which interacts with the element of the bend surface, is

$$\Delta m = \rho_e v \cos(\alpha_y'' - \beta'') \Delta l\, \Delta y \Delta t , \qquad (28)$$

here $\Delta t = \Delta l / v_{M,\tau}$ and Δl – an element of arc length on the bend.

Bending radius varies from zero to r_0 along the screw blade, which is set at a distance from the axis of rotation of the screw equal L_{pr} (Fig. 3), and at each distance from the axis of rotation

$$r_{\scriptscriptstyle M} = \frac{r_0}{L_{pr}} y . \qquad (29)$$

The normal component of air velocity determines the impact effect of air on the screw blade $F_{y\partial.}$, and the tangential one determines the centrifugal force of pressure on the blade $F_{\scriptscriptstyle U}$ and the pressure force due to Bernoulli's law $F_{\scriptscriptstyle B}$. Integral values of the moments of the forces acting on the element of area of the bend, taking into account the effect of the flat surface facing the flow, of the front of screw are:

$$M_6 = \int\limits_{r_\kappa}^{L_{pr}} dy \int\limits_{r_M \cos\alpha_y}^{r_M} \rho_\infty v^2 \cos^2(\alpha_y'' - \beta'') \sin\alpha_y''(L_{np} + z)dz;$$

$$M_7 = \int\limits_{r_\kappa}^{L_{pr}} dy \int\limits_{r_M \cos\alpha_y}^{r_M} \frac{1}{r_M}\rho_\infty v^2 \sin^2(\alpha_y'' - \beta'') \sin(\alpha_y'')(L_{np} + z)dz^2; \qquad (30)$$

$$M_8 = 0,5 \int\limits_{r_\kappa}^{L_{pr}} dy \int\limits_{r_M \cos\alpha_y}^{r_M} \rho_\infty v^2 \sin^2(\alpha_y'' - \beta'') \sin(\alpha_y'')(L_{np} + z)dz.$$

If you set the width of the screw blade $h = f(y)$, then at each distance from the axis of rotation of the linear part of the blade is reduced and is $l_x = h - r_{\scriptscriptstyle M}\alpha_y$. In addition to traction (20) is added the value

$$\Delta X_a'' = \int\limits_{r_\kappa}^{L_{pr}} \rho_\infty [v \sin(\alpha_y'' - \beta'')]^2 l_x \sin(\alpha_y'')dy . \qquad (31)$$

In the area of shedding flow behind the bottom surface of the blade of the screw front the torques are calculated by the formulas

$$M_9 = \int\limits_{r_\kappa}^{L_{pr}} dy \int\limits_{r_M \cos\alpha_y}^{r_M} \rho_e [c - v\cos(\alpha_y'' - \beta'')]^2 \sin\alpha_y''(y + z)dz;$$

$$M_{10} = \int\limits_{r_\kappa}^{L_{pr}} dy \int\limits_{r_M \cos\alpha_y}^{r_M} \frac{1}{r_M}\rho_e [c - v\sin(\alpha_y'' - \beta'')]^2 \sin(\alpha_y'')(y + z)dz^2; \qquad (32)$$

$$M_{11} = 0,5 \int\limits_{r_\kappa}^{L_{pr}} dy \int\limits_{r_M \cos\alpha_y}^{r_M} \rho_e [c - v\sin(\alpha_y'' - \beta'')]^2 \sin(\alpha_y'')(y + z)dz.$$

The resultant thrust with straight mechanization and using (31) will be

$$\Delta X_a = \int\limits_{r_k}^{Lpr} 2\pi dy \int\limits_{r_M \cos\alpha_y}^{r_M} \left[\rho_\infty v^2 \sin^2(\alpha_y'' - \beta'') + \rho_e c^2\right] \sin\alpha_y''(y + z)dz . \qquad (33)$$

At some distance from the axis of rotation the screw blade edge is bent in the opposite direction. In this part of the screw on the outside the airflow moves away from the screw, and on the inner side arises a zone of dilution of a relatively large volume, and air is directed along the axis of rotation almost with the speed of sound and, therefore, increases the traction with a decrease in power consumption.

Reverse mechanization of the screw blade. Fig. 5 shows the reverse mechanization of the screw blade. For such a blade a linear region of the front and rear parts of the screw interacts with the ambient air as described above without significant changes. Bend area is streamlined by the air from the normal and tangential velocities, respectively, equal to

$$v''_n = v\cos(\alpha'''_y - \beta''');$$
$$v''_\tau = v\sin(\alpha'''_y - \beta''') \quad , \tag{34}$$

The presence of such velocities in the bending leads to an impact, centrifugal effects, due to the action of the Bernoulli`s law. Calculations of the integral action of all these forces are carried out according to formulas (30) and (31), but with their own values α'''_y and β'''.

In the area of shedding flow situation is more complicated. The impact to the linear region of the element of the blade surface for the front side of the screw is determined by formulas (11) - (20), and for the back side of the screw - by the formulas (21) - (24). In the area of the bend in the situation with the reverse mechanization is more complicated. When rotating of the screw in the breakaway zone the air molecules strike the blade surface normally with speed of sound. The velocity decreases by a normal component of the velocity of flow from the reverse side. Therefore $v'_n = c - v\cos(\alpha'''_y - \beta''')$, and the tangential component $v'_\tau = c\cos(\alpha_y - \alpha'''_y)$.

The angle β' is determined by the formula (5), angle $\alpha'''_Y = arctg\left(\dfrac{\sqrt{r_M^2 - z^2}}{z}\right)$.

In Fig.5. Scheme of position of the bending radius (1) on the front edge of the screw with the surface of a Mobius

The impact effect to the surface element of the bend will give the value

$$\Delta F_{yд.} = 2\rho_e \left[c - v\cos(\alpha'''_y - \beta''')\right]^2 \Delta z \Delta y . \tag{35}$$

The centrifugal force and the force due to Bernoulli's law, respectively

$$\Delta F_{ц} = \rho_e \left[c - v\cos(\alpha'''_y - \beta''')\right] c\cos(\alpha_y - \alpha'''_y)\frac{\Delta z^2}{r_M \sin\alpha'''_y}\Delta y; \tag{36}$$

$$\Delta F_{Б} = 0{,}5\rho_e \left[c\cos(\alpha_y - \alpha'''_y)\right]^2 \Delta z \Delta y$$

To obtain the integral values of forces defined by (35) and (36), we integrate them along the Z axis and the axis Y.

Additional traction force in this amount will be

$$\Delta X''_a = \int_0^{L_{ob}} \rho_e (c - v\sin\alpha'''_y)^2 \zeta \, dy . \tag{37}$$

The mass of air, which interacts with the bend radius area, is

$$\Delta m = \rho\sqrt{v_y^2 + v^2}\,\Delta z \Delta y \Delta t \cos(\chi) , \tag{38}$$

here $\Delta t = r_y \cos\alpha_y / v_y$ and $\chi = arctg(v/v_y)$.

The radius of bend area varies from zero to r_0, which is set at a distance from the axis of the screw rotation equal to the length of the blade, and at each distance from the axis of rotation, is determined by:

$$r_y = r_M + \frac{c\,y}{L_{ob.}} , \tag{39}$$

The angle of twist varies along the Y-axis in the following way: for the front side of the screw and to the back side of the screw

$$\alpha_y = \frac{\pi}{2} - \frac{\pi}{4}\frac{L_{pr.} + y}{a} , \tag{40}$$

$$\alpha_y = \frac{\pi}{4}\frac{L_{pr.} + y}{a} . \tag{41}$$

The upper side. Air mass Δm gets momentum $\Delta p = \Delta m v_y$. Then the impact effect of air molecules on the screw blade creates a retarding force

$$\Delta F'_{y\partial} = \rho\sqrt{v_y^2 + v^2}\, v_y \cos^2(\beta_y)\cos(\chi)\Delta z \Delta y, \tag{42}$$

here angle $\beta_y = arctg\left(\dfrac{\sqrt{r_y^2 + z^2}}{z}\right)$ and angle $\chi = arctg(v/v_y)$. The same mass of air has a centrifugal

acceleration and acts on the bend of the edge of the screw blade with the force

$$\Delta F'_{L\!I} = \rho\sqrt{v_y^2 + v^2}\, v_y \cos\beta_y \cos(\chi)\Delta z^2 \Delta y / r_y, \tag{43}$$

The presence of a tangential air flow leads to a force caused by the law of Bernoulli

$$\Delta F'_{E} = 0.5\rho v_y^2 \sin(\beta_y)\cos(\beta_y)\Delta z \Delta y. \tag{44}$$

As a result, the screw blade overcomes only the force of impact, and centripetal force and gas-dynamic pressure on the contrary help to the rotation of the screw. To obtain the resultant acting of these forces on the $\Delta S = l_x \Delta y$, it should be taken the integral along the axis Z from $r_y - \zeta$ to r_y.

$$\Delta F_1 = \int\limits_{r_y-\zeta}^{r_y}\left(dF'_{y\partial.} - dF'_{L\!I} - dF'_{E}\right), \tag{45}$$

The torque about the axis of rotation $\Delta M'_2$, here a – the size of the screw blade

$$\Delta M'_2 = \int\limits_{L_{np.}}^{a} \Delta F_1 (L_{np.} + y)\cos(\alpha_y)dy, \tag{46}$$

The flat side of the blade is experiencing the impact effect of air molecules and the hydrodynamic pressure, due to Bernoulli's law. For these forces we obtain:

$$\Delta F_{2,y\partial.} = \rho\sqrt{v_y^2 + v^2}\, v_y l_x \cos^2(\alpha_y)\Delta y;$$
$$\Delta F_{2,E} = 0.5\rho v_y^2 \sin^2(\alpha_y) l_x \Delta y. \tag{47}$$

Here l_x – a linear part of the screw blade, which is determined $l_y = a - r_y \alpha_y$.

The resulting force $\Delta F_2 = \Delta F_{2,y\partial.} - \Delta F_{2,E}$ creates a torque about the axis of rotation, namely

$$\Delta M''_2 = \int\limits_{L_{np.}}^{a} \Delta F_2 \cos(\alpha_y)(L_{np.} + y)dy.. \tag{48}$$

The lower side. Behind the lower side arises a zone of rarefaction. Filling the zone of rarefaction occurs simultaneously in two directions, namely from the top surface, swept by screw and normal to the surface of the screw with speed of sound. The normal and tangential velocity of the air molecules will have the form $v_n = c - v_y \sin(\beta); \quad v_\tau = v_y \cos(\beta), \quad \beta = arctg(\sqrt{r^2 - z^2}/z)$

The impact effect of the air molecules on the lower side of the front of the screw will be

$$\Delta F''_{y\partial.} = \rho(c - v_y \sin\beta)^2 \sin\beta \Delta z \Delta y, \tag{49}$$

Here $\rho = \rho_\infty \exp\left(-\dfrac{m_a v_y^2}{2k_E T}\right).$

Similarly, for the centrifugal force and the force of hydrodynamic pressure, we obtain

$$\Delta F''_{L\!I} = \rho c^2 \sin^3(\beta)\Delta z^2 \Delta y / r_y;$$
$$\Delta F''_{E} = 0.5\rho c^2 \sin^3(\beta)\Delta z \Delta y. \tag{50}$$

The force of the impact and the centrifugal force are acting in one direction and speed up the rotation of the screw, but the force due to the action of the Bernoulli`s law prevents rotation of the screw. If we integrate all the acting forces on the bend along the axis Z, we obtain the resultant force on the element of area of the screw blade $\Delta S = l_x \Delta y$

$$\Delta F_3 = \int_{r-\zeta}^{r} (-dF''_{y\partial.} + dF''_{\mathcal{U}} + dF''_{\mathcal{B}}). \tag{51}$$

Under the influence of such force arise the torques about the axis of rotation

$$\Delta M''_3 = \int_{L_{np.}}^{a} \Delta F_3 \cos(\alpha_y)(L_{np.} + y)dy.. \tag{52}$$

On the linear part of the underside of the blade the air produces a shock impact with the speed of sound and creates a hydrodynamic pressure in accordance with the law of Bernoulli. Then

$$\Delta F_{4,y\partial.} = \rho[c - v_y \sin(\alpha_y)]^2 \sin(\alpha_y)\Delta z \Delta y;$$
$$\Delta F_{4,\mathcal{B}} = 0.5\rho c^2 Sin^3(\alpha_y)\Delta z \Delta y. \tag{53}$$

These forces are mutually opposite. Their resultant force is $\Delta F_4 = -\Delta F_{4,y\partial.} + \Delta F_{4,\mathcal{B}}$

The resulting force also creates a torque about the axis of rotation of the blade

$$\Delta M''_4 = \int_{L_{pr.}}^{a} \Delta F_4 \cos(\alpha_y)(L_{pr.} + y)dy.. \tag{54}$$

Taking the integral over the entire length of the blade h, we get the full force of the impact of air flow on the blade and hence the total moment of force about the axis of rotation

$$X_a = \int_{L_{pr.}}^{a} \cos(\alpha_y)(dF_1 + dF_2 + dF_3 + dF_4); \quad M_a = \int_{L_{pr.}}^{a} \cos(\alpha_y)(L_{np.} y)(dF_1 + dF_2 + dF_3 + dF_4). \tag{55}$$

For the back side of the screw blade are implemented front and back surfaces, for which there are own forces in contact with the air. The twist of the back side of the screw blade is determined by (41), and the bending radius is determined by (40). Otherwise the air interacts with the front and the back surfaces in different ways.

With the help of computer simulation it is necessary to choose the size of the screw with the surface of Mobius, through a combination of the size of forward and the size of backward mechanization, for a certain type of engine to provide maximum traction and minimum consumption from external power source.

In Table 1 and Table 2 are shown the results of theoretical calculation of the screw characteristics. The resistance of the screw at the rotation speed of 2800 r/min, the magnitude of thrust and the power consumption from energy source depending on the total radius of the screw (the screw parameters are: the maximum bending radius of 20 mm, the width of the blade - 30 mm, the radius of spinner - 16 mm, the ratio of the length of the reverse mechanization to the total radius of the screw - 0.05)

Table 1

Param eters	The total radius of the screw, mm					
	150	200	250	300	350	400
T_a, kG	8,8/13,1	15,6/21,0	24,1/30,7	34,3/41,8	46,1/54,4	59,3/68,3
X_a, kG	86,0/81,2	143,9/135,7	210,7/1984	283,5/266,5	359,3/337,2	435,5/408,4
N, h.p	3,3/4,8	10,3/12,7	23,3/26,7	44,3/48,8	75,4/81,0	118,8/125,2

Table 2

Parameters	The frequency of rotation of the screw, r/min					
	500	1000	1500	2000	2500	3000
T_a, kG	3,0/11,3	7,8/15,6	12,6/19,9	17,2/24,2	21,6/28,3	25,8/32,2
X_a, kG	268,8/253,0	256,2/242,0	243,0/230,0	230,8/217,8	218,2/205,8	205,8/193,6
N, h.p.	-0,8/0,13	0,4/2,0	3,7/6,0	9,3/12,1	17,3/20,5	27,8/31,4

The resistance of the screw, the magnitude of thrust and power consumption from energy source, depending on the frequency of rotation of the screw (the screw parameters are: the total radius of the screw - 250 mm, the maximum bending radius -- 20 mm, the width of the blade - 30

mm, the radius of spinner - 16 mm, the ratio of the length of the reverse mechanization to the total radius of the screw - 0.05) with the surface of Mobius and the presence of direct and reverse mechanization depending on the radius of swept surface and the screw speed in the mode of the fan and at the forward movement when a version of the pulling or pushing screw is implemented.

The results of the first version are listed above the line and below the line is the second version of the forward velocity of 60 km/h. Based on the data of Table 1 and Table 2 we obtain, that for the above engine the screw of Mobius is the most suitable in the presence of direct and inverse mechanization with the general radius of 250 mm. The other parameters of the screw are given in the name of Tables 1 and 2.

The effect of changes in power consumption of a screw of Mobius with direct and inverse mechanization depending on the bending radius is shown in Fig. 6, and in Fig. 7 - on the ratio of length of the inverse mechanization to the total length of the radius of the screw. In the first and second cases the power of consumption is reduced with a slight fall of the screw thrust. A more noticeable drop in power consumption occurs when increasing of the length of inverse mechanization of the Mobius screw. Here the power of consumption may be negative. This means that such screw will act as a heat pump. So far as the power of consumption in the rotation of the
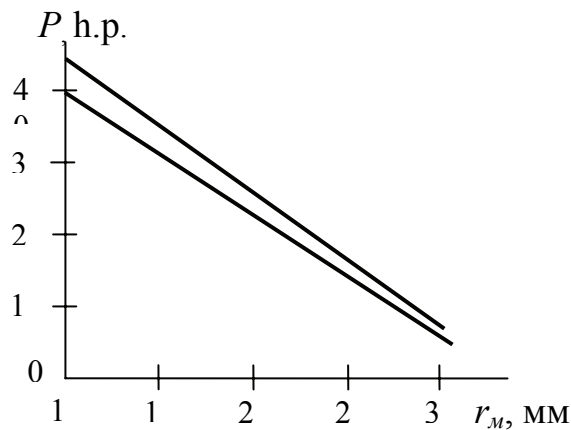
Fig. 6. The dependence of the power consumed by the screw, the maximum value of the radius of the bend at a speed of rotation of 2800 r/min: L = 250 mm, rc = 16 mm, h = 30 mm
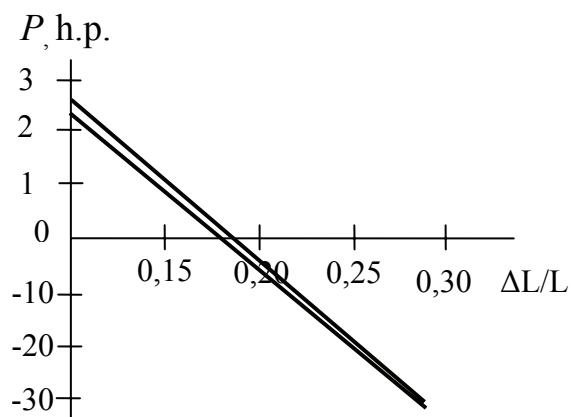
Fig. 7. The dependence of the power consumed by the screw, the ratio of the lengths of direct and inverse at a speed of rotation of the mechanization 2800 r/min: $L = 250$ mm, $r_{\kappa} = 16$ mm, $h = 30$ mm and $r_{M} = 20$ mm

screw is determined mainly by acting on of the air from the back of the blade, where the rarefaction zone is implemented, every molecule of air, striking the surface of the blade, due to elastic collision, gives off a part of its energy. The air in this area, moving along the surface of the blade, leads to a marked cooling of the blades. The effect of cooling of the blades is sufficiently known. However, the explanation for this phenomenon previously has been given purely qualitatively, without a strict justification of convective heat exchange with ambient air.

Conclusions. The investigations revealed the following:

1. The air screw with a Mobius surface is more economical than the usual blade screws put into practice. 2. The direct mechanization by bending the edges of the screw blade allows for a certain speed of rotation of the screw, to transfer the screw with the surface of the Mobius to the mode of a heat pump. 3. The inverse mechanization transfers the screw with the surface of Mobius to heat pump mode of operation with a significant decrease in the frequency of rotation of the screw. 4. The joint use of the direct and inverse mechanization of the screw with a surface of Mobius allows, for smaller size and lower speed of rotation of the screw, to provide maximum thrust at a given engine power and a speed of the aircraft.

References

1. Shpady A.L., Timofeev V.F. Unhelical propellers / Problems of training for civil aviation: proceedings of the international scientific-practical conference on 20-21 November 2008: the scientific publication // Red. Ushakov N.U. - Ulyanovsk: UVAU GA, 2008. P. 40-43.

2. Grechykhyn L.I., Laptsevych A.A., Kuts N.G. Power base of unmanned aerial vehicles / Energetic - Mn. BNTU, № 3, 2011. P. 64-78.

3. Grechykhyn L.I., Laptsevych A.A., Kuts N.G. Aerodynamics of aircraft. - Mn. IOOO "Law and Economics", 2012. - 285 p.

4. Grechykhyn L.I. The molecular-kinetic theory of aircraft rowing screw. / Sat materials I International Youth Conference "Civil aviation: the twenty-first century" Ulyanovsk: USTU, 2009. P. 18-24.

5. Grechykhyn L.I., Sakharuk D,A,, Syvashko A.B., Tsanava A.A. Energy propeller Unmanned Aerial Vehicle. The theory, laminar flow/Energy. Proceedings of the institutions of higher education and energy organizations of the CIS, 2010, № 4. P. 59-68.

6. Grechykhyn L.I., Sakharuk D,A,, Syvashko A.B., Tsanava A.A. Energy propeller Unmanned Aerial Vehicle. Experimental studies, for shedding / Energy. Proceedings of the institutions of higher education and energy organizations of the CIS, 2010, № 5. P. 61-65

7. Grechykhyn L.I. Nonequilibrium optical emission of air and spacecraft / Doctoral Dissertation. Minsk, BPI, 1987. - 327 p.

L.I. Grechikhin, Prof. A.A. Laptzevitch, Ph.D.
(State Air Force College, Minsk, Republic of Belarus)

GENERAL AERODYNAMICS

Below please find a short summary of the analysis of a number of aerial vehicle elements, such as high-lift wing devices, aircraft propellers, commanding elements and on-board power sources.

Introduction: The Heavy Lift Unmanned Aerial Vehicles development is focused on the subject of substantial increase in range and airborne time. The priorities are focused on Unmanned Aerial Precision Locator and Strike systems. The PLS current tasks demand that the UAV should be able to fly tens and sometimes hundreds thousand kilometres. Thus, the aerial vehicle (AV) aerodynamics design, command systems and on-board power supply system requirements are fairly rigid:

- AV drag should be minimized and the aerodynamic lift should be maximized;
- AV should be able to continue the flight with its engines switched off over a long period of time, i.e. should have parachute properties;
- AV weight and size should be decreased;
- AV engines (electrical or thermal) should produce more than 1000 kW of power;
- AV engines should have long service life;
- AV engines should be equipped with the automatic diagnostics system, so to be able to make an informed decision regarding AV automated mode flight;
- AV flight control by pilot or ground pilot should be kept to a bare minimum enabling the use of on-board AI;
- AV should be protected from any external interference.

To satisfy all the requirements listed above proved to be almost impossible. However, certain solutions were offered and those we shall examine now.

AV drag and aerodynamic lift.

The power produced by AV engines during the flight is used solely to counter the drag. The aerodynamic lift appears as a result of interaction with the static atmosphere. It lifts up weighing hundreds of tons AV to the altitude of 10 km and more. For example, the amount of energy used to lift up the TU-134 aircraft to the 10 km altitude is approximately $4,12 \cdot 10^9$ Joules. The aircraft reaches the altitude of 10 km in 25-35 minutes using roughly 1.96-2.75 MW of power (263-369 thousand horse power). These are fairly sizeable energies. The aircraft is required to be able to produce an aerodynamic lift of at least 42 tons in order to escape the planet's gravity. Where would an aircraft source so much energy? If we consider the aircraft as an open power system that interacts with the surrounding environment, then the energy is sourced from the environment, from its internal energy. The earth atmosphere is cooled down as a result of such interaction (the principal of a thermal pump).

Because the aircraft is an open system, the Lomonosov's law of conservation and transformation of the energy is applicable. While taking into the account the law of transformation of energy and considering the interaction with the environment from the point of view of molecular-kinetic theory the following issue have been discussed:

1. how the airframe drag is created
2. why mainly the aircraft wings create the aerodynamic lift of a sizeable proportions

It has been determined that the most economical type of wing would be the elliptical one, and the decrease in the air drag depends on the separate flow.

Example: Picture 1. Calculations of the air drag and the aerodynamic lift functional

connection for the aircraft with elliptical wing at the speed of 100 km/h. At the given speed the lift increases and the drag decreases. When the angle of attack reaches 30 degrees it drops down to the negative value. This means that when the engines of an aerial vehicle with elliptical wings are switched off the angle of attack increases sharply and the drag decreases. For some time the aircraft continues to fly without significant reduction in speed. It implies that elliptical wing has parachute qualities.
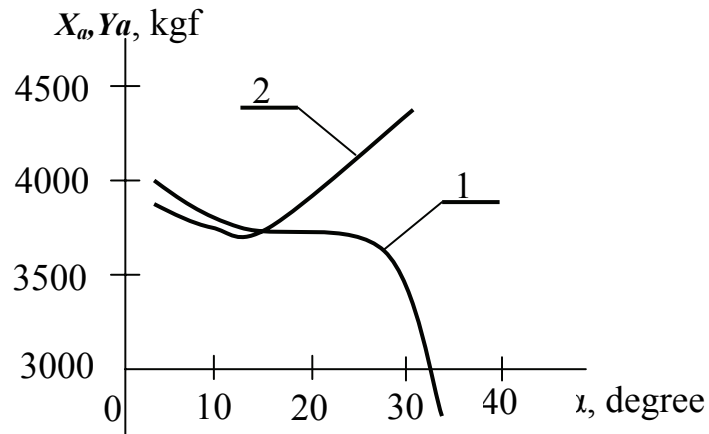
Picture 1. Functional correlation between the angle of attack of the elliptical wing and 1) the drag, 2) the lift. Y - kilogram-force, X - degree

The paradox appears at the speeds greater than 180 km/h and the angles of attack greater than 30°. The aircraft with elliptical wings transforms into a thermal pump and its speed actually increases after the engines were switched off.

Use of propellers in aviation (air-screws)

In subsonic aircraft the air propellers are used convert the rotary motion from piston engine shaft to provide propulsive force. Lately, the air-propellers with an inverse plane (Möbius plane) with various configurations are closely studied.

Functional correlation between the rotation speed and power intake and thrust power is shown on the Picture 2 for the 12 cm propeller blade with 3.5 cm width at the speed of 180 km/h, high-lift and regular wing. The main features of an air-screw with Möbius plane are as follows:

- The air-propeller contains the ribbon with leading edge bent at a given radius. The radius of a leading edge is varying from zero to its maximum value on the outer surface of the air-propeller. The ribbon is folded around the Möbius circle and is fastened normal to the axis of rotation on one end and normal to the disk plane on the other.
- The leading edge radius of the propeller ribbon increases the transformation ratio practically indefinitely, depending on the rotation speed. Once over the activation energy threshold the air-propeller starts functioning as a thermal pump unit.
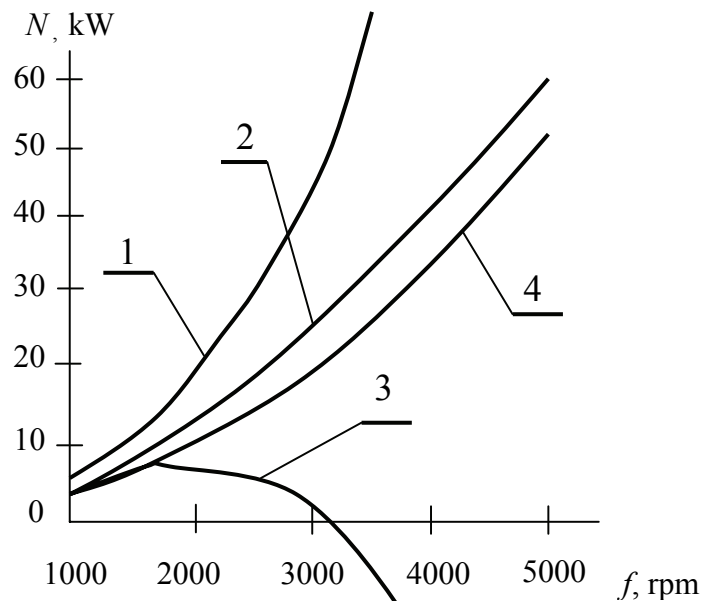
Picture 2. Functional correlation between rotation speed and 1- the intake for wing without optimisations 2- the thrust power for wing without optimisation 3- the intake for high-lift wing 4- the thrust power for high-lift wing

High-lift wing aerodynamics

The necessity for the drag and the wing lift control is most evident when the aircraft manoeuvres, especially during the take off and the landing time. There are devices available for optimisation of a take off and a landing. The design of the aircraft high-lift wing transforms it into a complex mechanical system. Wing slats and leading edge flap are located on the leading edge of the wing, while ailerons, flaperons, flaps and diving brake are located on the trailing edge. Swirl plates, interceptors and lift spoiler are located on the upper part of the wing. Molecular-kinetic theory allows to calculate the impact of each and every optimisation device.

Example: Picture 3. Calculations of the drag and the lift for a tilt flap (slender wedge 3 cm to 6 mm wide). When increasing the flap deflection angle up to 10° there are no changes in the drag. For deflection angle of more than 10° there is a sharp increase in drag and dramatic reduction in total lift of this particular wing. It follows that flaps should not be installed along the entire length of the wing. Generally, they are installed as few separate blocks. To increase the angles of flaps is dangerous. These angles should not be used at all when the attack angles reach the value of 10-12° and the flap deflection angles are about 20-30°. If the wing with the flap is placed in aerodynamic tube, the drag and the lift seem to increase. In reality the situation is opposite. The results obtained in air-tubes led to incorrect interpretation of the experimental data obtained during the flight of the aircraft with pilot controlled flaps.
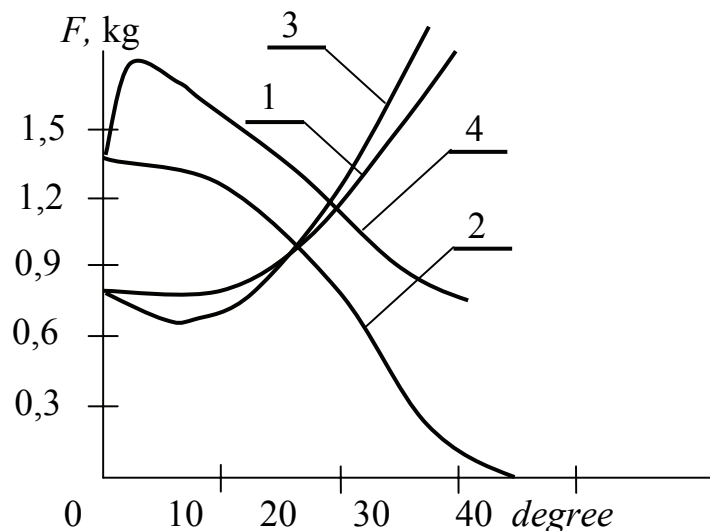
Picture 3. Functional correlation between the deflection angle of the wing element and 1- the drag with tilt flap 2- the lift with tilt flap 3- the drag with slot flap 4- the lift with slot flap

Aerodynamics of the aircraft command elements

Aircraft stable flight is defined by equal-zero sum of all forces and torques. The aircraft position in space is determined by the speed of flight and the aircraft position relative to the velocity vector. Four elements should be controlled during the aircraft flight in a given direction: 1) the speed (the path of gas alteration) 2) the ailerons, elevons, interceptors and flaps 3) the altitude control 4) the rudder. The advantage of molecular-kinetic theory when used for aircraft control analysis will be discussed using the aileron as an example.

Calculations of the aileron forces and torques are performed only for one aileron. For the whole aircraft the total will be calculated by integrating the obtained values along the Z axis relative to the centre of gravity.

The main aileron force is the one that appears as a result of the air molecules blow impact on the aileron back surface.

Picture 4 shows the changes in forces that build up when the aileron deflects up and down at the attack angle of 10°. When the aileron deflects up it results in sharp decrease of a force (2-3 times), and when it deflects down - a sharp twofold increase. Therefore when the attack angles values are fairly big the differential aileron control is used (for example, +10° down and 30° up).

Ailerons are needed for side control of the aircraft movement in space. Even the smallest aileron angle deflection should result in substantial changes in the banking angle. The requirements state clearly that minimal efforts should be used in order to control the flight mode of an aircraft when aileron angle deflects. Small angle of aileron deflection should result in fairly big momentum of couple impact. Therefore all ailerons are located in a furthest possible points from the aircraft centre of gravity. This rule is implemented in all types of aircraft.

For small angles of aileron deflection the resulting angle of aircraft deflection is relative to the air current and may become negative. The condition known as aileron reversal, which may led to a spinning dive.

1.3.36
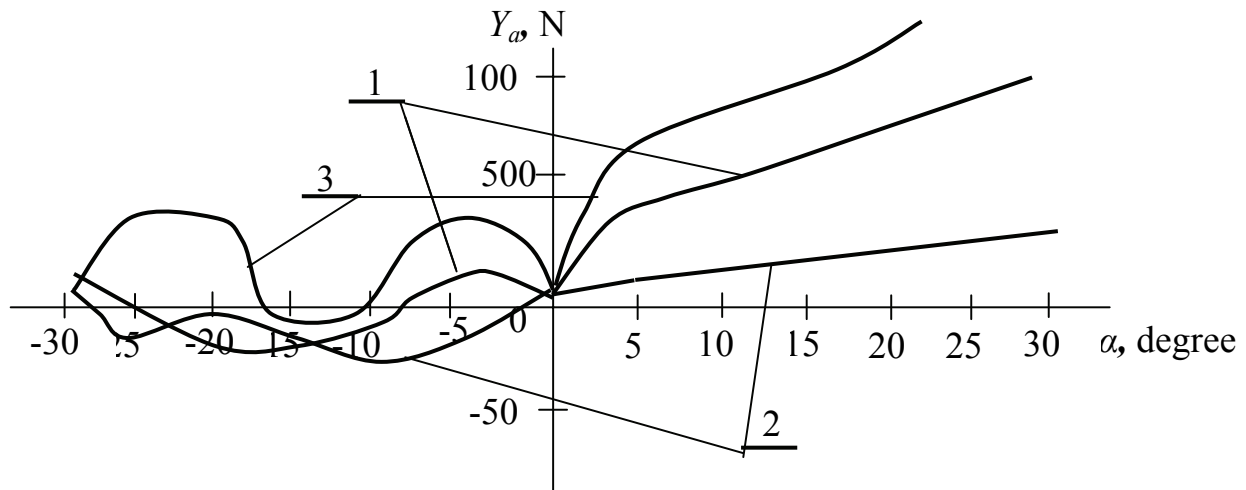
Picture 4. Functional correlation between aileron angle deflection and banking angle when 1- the attack angle is 0°, 2- the attack angle is 10° deflection down and 3- the attack angle is 10° deflection up.

On-board power sources.

   Both automotive and aircraft industries use the hybrid power systems extensively. Thermal pump units should gain a much wider use along with currently employed thermal and electrical engines. Stirling engines, ventilators, turbine and compressors all may be used as the thermal pumps. The prospective development of the ferrite based magnetodynamics MG set looks quite promising.

Conclusion. The main path of the aircraft evolution lies in development of aerial vehicles with elliptical and grilled wings, vortex AV and powered para-gliders. The thermal pump units will be widely included in on-board power systems.

1.3.37

A.V. Bondar, E.S. Plakhotniuk
(National Aviation University, Ukraine)

EVALUATION OF THE STABILITY DERIVATIVES IN A LONGITUDINAL, LATERAL AND TRANSVERSE MOTION OF THE UNMANNED AERIAL VEHICLE IN THE CURVILINEAR FLIGHT WITH ROTATION

The results of evaluation of the stability derivatives in the longitudinal, lateral and transverse movement of the curvilinear flight to the rotation of the example of unmanned aerial vehicle

Evaluation of stability derivatives in the longitudinal and lateral movement of unmanned aerial vehicle is required to determine the dynamic stability and control characteristics, the development of automatic control systems, mathematical modeling of the flight simulator for use in equipment and certification.

In Fig. 1 shows a general view adopted for the calculation scheme unmanned aerial vehicle. As the figure shows this aircraft is a unit normal scheme with a high wing, vertical tail fin of the two. Therefore, to assess the stability of the derivatives in the longitudinal and lateral movement in the curvilinear flight to the rotation will use the well-known approach to the classical scheme of the aircraft.
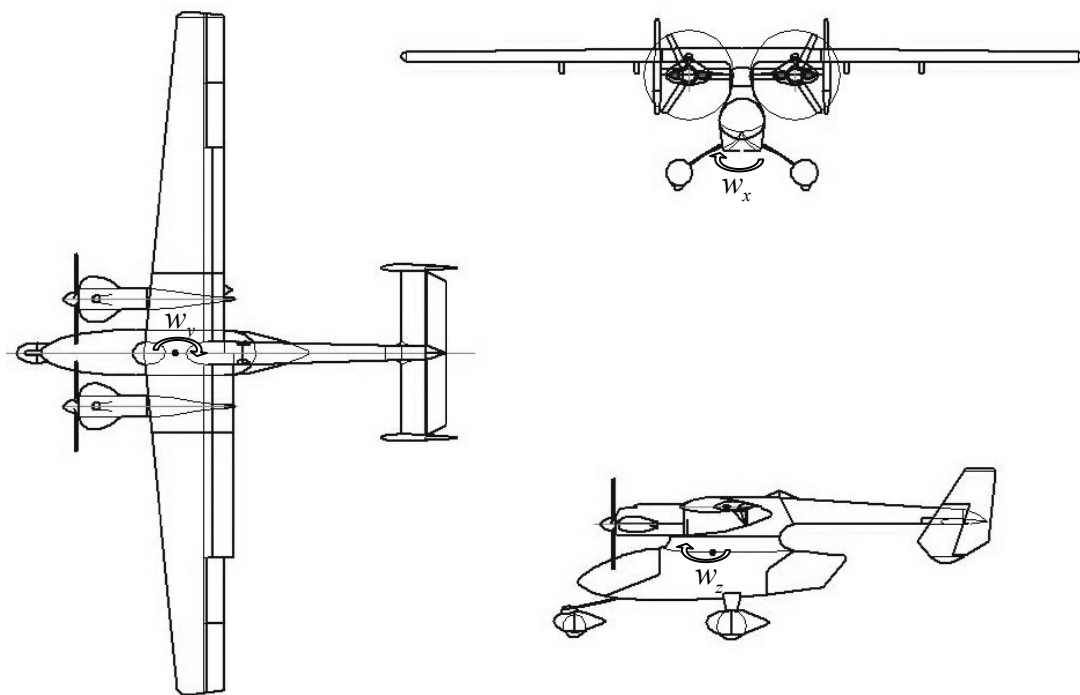
Fig. 1. The General view of the unmanned aerial vehicle

To determine the aerodynamic derivatives of unmanned aerial vehicle used by the classical approach [1] and the formulas of [2], [3].

The paper presents the results of calculations of the following derivatives:

$m_{z\,кр.}^{\overline{w}_z}$ - a wing;

$m_{z\,Г.О.}^{\overline{w}_z}$ - a horizontal tail;

$m_z^{\overline{w}_z}$ - the resulting damping factor;

$m_z^{\overline{\dot{\alpha}}}$ - derivative of pitching moment on $\dot{\alpha}$;

$m_y^{\overline{w}_y}$ - yaw damping coefficient;

$m_x^{\overline{w}_x}$ - roll damping coefficient;

$m_x^{\overline{w}_y}$ - roll damping during rotation.

The coefficients are determined without taking into account the wing propellers blowing at various angles of attack, flap and elevator. The results are shown in Fig. 2 (a-f) without blasting. The developed program allows you to analyze the influence of various factors on the magnitude of the coefficients.
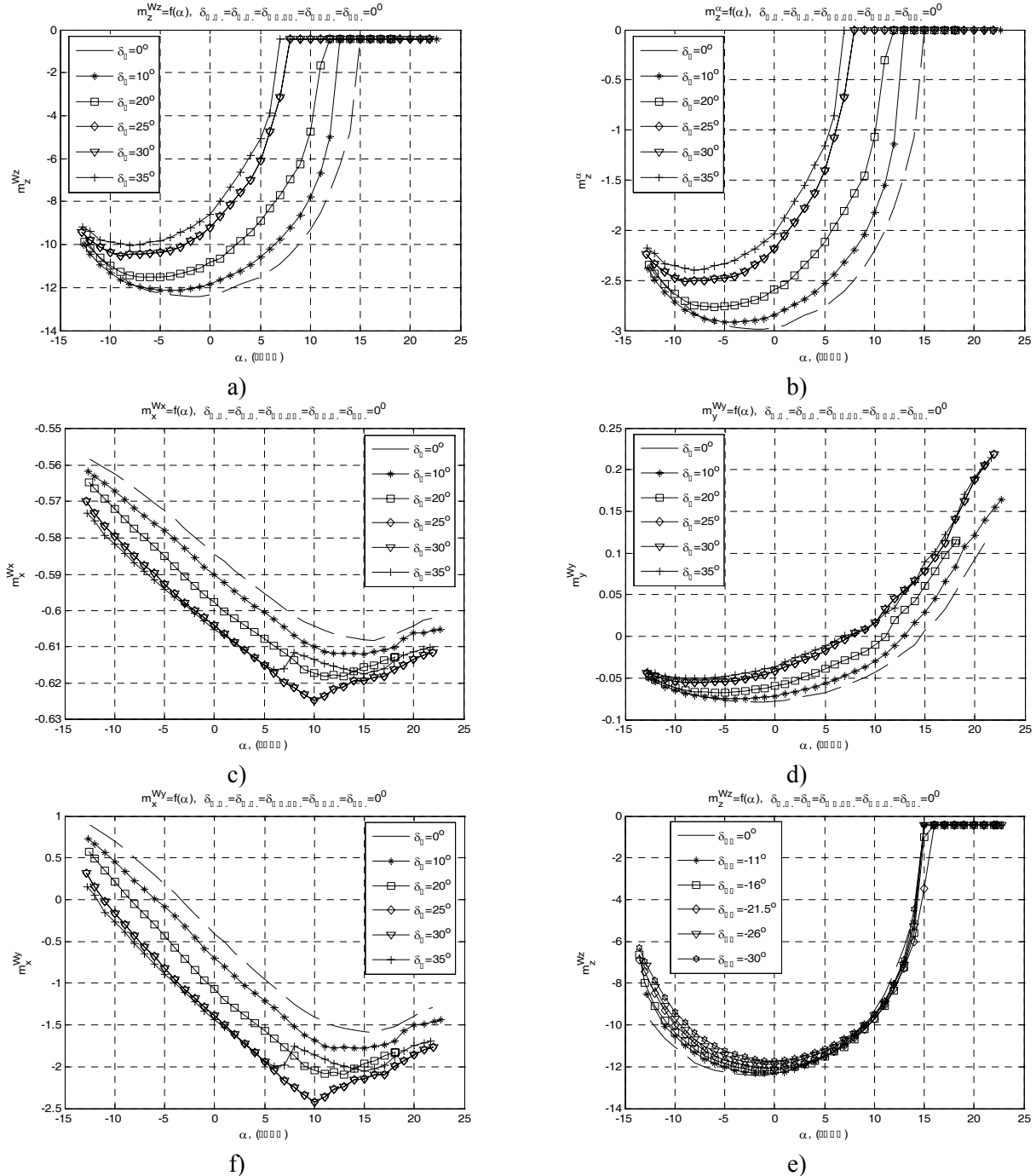
Fig. 2. Depending on changes in the stability of the derivatives of the angle of attack in the flap and elevator

Here is an example of estimating the coefficients of the stability derivatives in the longitudinal, lateral and transverse movement of the curvilinear flight with rotation. The initial data for the calculation shall use the following: $c_y^\alpha = 5.02(1/\text{рад})$; $\overline{x}_T = 0,249$; $\lambda = 10,8$; $\chi = 4,3°$;

$c_{\text{Г.О.}}^{\text{б}} = 4{,}3(1/\text{рад})$; $S_{\text{Г.О.}} = 0{,}56(\text{м}^2)$; $L_{\text{Г.О.}} = 2{,}25(\text{м})$; $S = 3{,}34(\text{м}^2)$; $b_A = 0{,}57(\text{м})$; $B = 0{,}55$; $a = 0{,}075$; $S_{BO} = 0{,}7(\text{м}^2)$; $L_{BO} = 1{,}936(\text{м})$; $l = 6(\text{м})$; $k_{BO} = k$; $\lambda_{BO} = 1{,}4$; $\chi_{BO} = 30°$; $\alpha = 6°$; $\eta = 1{,}72$; $B = 0{,}55$; $D = 3{,}99$.

We consider two cases of flight conditions, taking into account the first case of blowing tail propellers propulsion of the aircraft, the second without blowing (engine failure). For both cases the adopted altitude 3000 (m), speed is equal to 34.8 (m / s). The following are calculated values derived resistance:

1) taking into account the propellers blowing ($c_x = 0{,}08$; $c_y = 0{,}97$; $k_{_3} = 0{,}8$):

$m_{z\,\text{кр.}}^{\overline{w}_z} = -0{,}44$;

$m_{z}^{\overline{\alpha}} = -2{,}98$;

$m_{z\,\Gamma.O.}^{\overline{w}_z} = -9{,}96$;

$m_{y}^{\overline{w}_y} = -0{,}06$;

$m_{z}^{\overline{w}_z} = -12{,}39$;

$m_{x}^{\overline{w}_x} = -1{,}98$;

$m_{x}^{\overline{w}_y} = -1{,}23$

2) without blowing propellers ($c_x = 0{,}07$; $c_y = 0{,}83$; $k = 0{,}66$):

$m_{z\,\text{кр.}}^{\overline{w}_z} = -0{,}44$;

$m_{z}^{\overline{\alpha}} = -2{,}69$;

$m_{z\,\Gamma.O.}^{\overline{w}_z} = -8{,}99$;

$m_{y}^{\overline{w}_y} = -0{,}06$;

$m_{z}^{\overline{w}_z} = -11{,}23$;

$m_{x}^{\overline{w}_x} = -1{,}78$;

$m_{x}^{\overline{w}_y} = -1{,}05$

Conclusions

1. Shown method for estimating stability derivatives in the longitudinal, lateral and transverse movement of unmanned aerial vehicle flight in the curvilinear to the rotation can be used to profit the design of new unmanned vehicles;

2. The obtained results of calculations on the example of a specific unmanned aerial vehicle made it possible to establish the range of variation of stability derivatives;

3. The analysis of the results, which gave the opportunity to show the nature of the relationship between derivatives and the stability of the parameters of motion device;

4. These results agreed well with results obtained by other authors [1], [2], [3].

References

1. *Лебедев А.А., Чернобровкин Л.С.* Динамика полета беспилотных летательных аппаратов. Учебное пособие для вузов. М., Оборонгиз, 1962. - 548 с.

2. *Остославский И.В., Калачев Г.С.* Продольная устойчивость и управляемость самолета. – М.: Государственное издательство оборонной промышленности, 1951. – 367 с.

3. *Остославский И.В., Стражева И.В.* Динамика полета. Устойчивость и управляемость летательных аппартов. – М.: Машиностроение, 1965. – 468 с.

4. Беспилотные летательные аппараты. Методики приближеннях расчентов основных параметров и характеристик. /Под редакцией *Силкова В.И.* – К.: ЦНИИ ВВТ ВС Украины, 2009.– 302 с.

UDC 533.694.73

V. Zhila, Ph.D.
(National Aviation University, Ukraine)

THE ENERGY ESTIMATION OF THE BIOT-SAVART LAW FOR THE AERODYNAMIC PROBLEMS

Analysis of additional energy, which is taken by the stream when straight vortex of finite dimensions exist in it was made. Conclusion of unlimited additional energy of flow and contradiction of this to the physical view. Was marked that the formula bio-Sawara can be correctly applied only for stationary problems.

Introduction.

Almost in any science, there are assertions, which are used as indisputable truths that do not require proof. In such a situation, there is nothing strange, this corresponds to the axiomatic approach to construction of any theory. The need to rethink these claims generally occurs when you attempt to more in-depth study of the phenomenon. A striking example of such rethinking can serve the refutation of Aristotle's assertion that heavy body falls down to the ground faster than light body, which was made by Galileo. It means well-known experience of Galilei on Pisa tower. The importance of this refutation for the further development of mechanics was unquestionable.

Without pretending to parallels with the great Galileo, in this article the author presents his attempt to analyse the validity of application of formula Biot-Sawart in problems of aerodynamics. The importance of the considered topic is determined by the widespread using of this formula and the practical meaning of the results.

The apparent excessive detail in the application of widely known facts is caused by the desire of the author to provide an opportunity for objective criticism of his analysis, since the expected conclusions of the extremely responsible.

The problem consideration

The problem arose when an attempt is made to interpret the induced drag of the finite span wing from energy point of view. To explain the approach, consider the elementary vortex scheme of the finite span wing shown in Figure 1. Idea of analysis is as follows.

1. In the relative translation motion of the finite span wing length of elements of its vortex scheme, which are directed along the flow direction, during time unite   are increased on the value $\Delta x = V_\infty \cdot 1$.

2. The additional length Δx of the elements of the vortex scheme of the finite span wing induce in the space additional speed. This additional speed is increasing the kinetic energy of the flow ΔE_k (if we accept that the wing relative to the observer is steady and the medium is moving with the speed of relative motion). The only source of this energy is the energy of the transmitted to the stream by the wing. This allows you to write equality $X_i \cdot \Delta x = \Delta E_k$ or equivalent $X_i \cdot V_\infty \cdot 1 = \Delta E_k$. These expressions and reflect energy meaning of inductive resistance X_i.

3. Let's calculate additional kinetic energy associated with increasing the length of the element of the vortex scheme (such as trailing vortex of the finite span wing) Δx. As a basis, take the scheme in Figure 2, which is classical and is considered in any textbook on aerodynamics [1, 2].

In accordance with the scheme, according to the formula of Biot-Sawart, dv_i is the velocity induced at an arbitrary point *A* by infinitely small segment $d\overline{s}$ of the vortex with strength Γ, and is determined as

$$dv_i = \frac{\Gamma}{4 \cdot \pi} \cdot \frac{\overline{r} \times d\overline{s}}{r^3} . \qquad (1)$$

Well known [1], that for the segment AB (fig. 3) of straight linear vortex with strength Γ at an arbitrary point M is induced the speed, whose module is determined by the formula

$$v_i = \frac{\Gamma}{4 \cdot \pi \cdot r_0} \cdot (\cos\theta_1 - \cos\theta_2), \qquad (2)$$

which is the result of application (1) to the scheme on Figure 3.
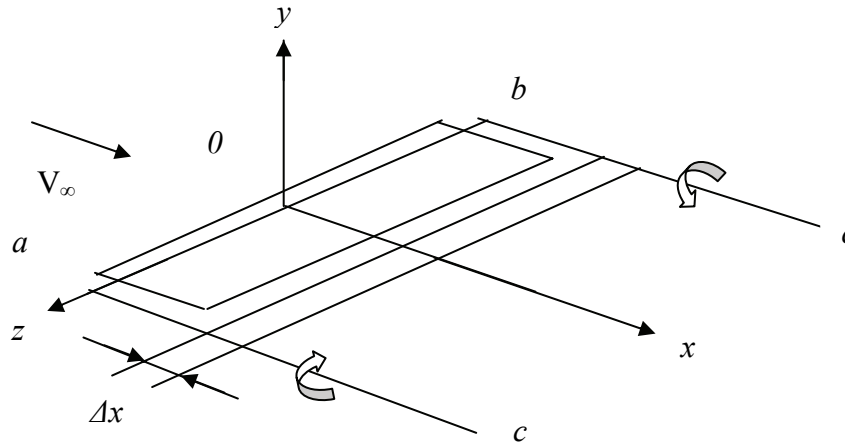
Fig. 1. The simplest vortex scheme of the finite span wing.
ab-bound vortex, ac, bc-trailing vortices, V_∞ -relative velocity of fluid flow.
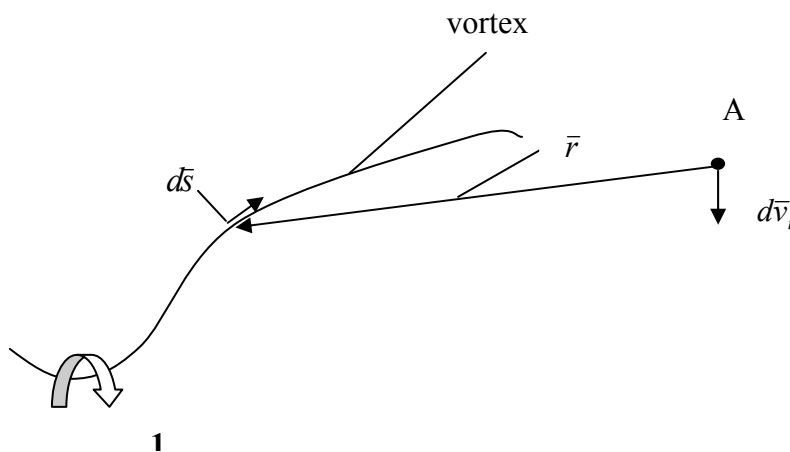
Fig. 2. Illustration scheme for Biot-Sawart formula.
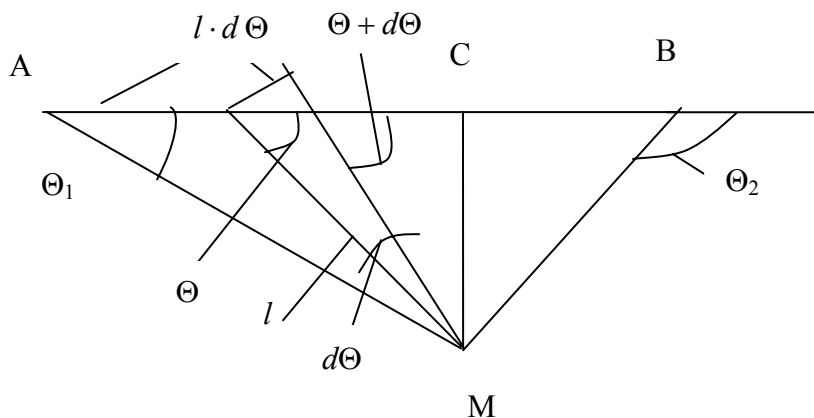
Fig. 3 Scheme of the segment of the straight vortex.

1.3.42

For all points, which are situated on a circle of radius r_0 at fixed values θ_1, θ_2, the formula (2) will give the same value of the inductive speed. With this speed, you can associate an elementary volume $dW = 2 \cdot \pi \cdot r \cdot dr \cdot dx$. This is the volume of the ring with rectangular cross section (see fig. 4). All particles in this volume are moving with the same velocity modulus. In this case, one may speak about "kinetic energy of inductive motion" rings. Value of this energy

$$dE_{ki} = \frac{dm \cdot v_i^2}{2} \tag{3}$$

where dm is the mass of the liquid contained in the ring.

$$dm = \rho \cdot dW = 2 \cdot \pi \cdot r \cdot dr \cdot dx \tag{4}$$

(2) and (4) (3) becomes a

$$dE_{ki} = \frac{\rho \cdot \Gamma^2}{16 \cdot \pi} \cdot \frac{(\cos\theta_1 - \cos\theta_2)^2}{r} \tag{5}$$
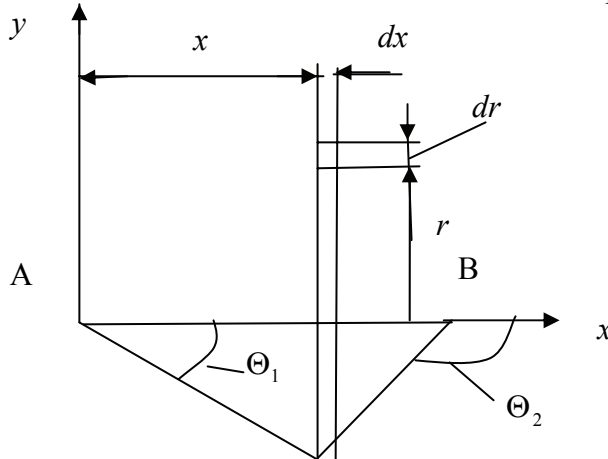
Fig.4. Chart for the calculation of kinetic energy of "inductive motion".

A chart on fig.3 we use for determination of corners θ_1 and θ_2 as functions of parameters of r and x. As a result of replacement in (5) θ_1 and θ_2 expression (5) will accept the kind of corresponding functions of parameters of r and x:

$$dE_{ki} = \frac{\rho \cdot \Gamma^2}{16 \cdot \pi} \cdot \left\{ \frac{x^2}{(x^2+r^2)\cdot r} - \frac{2\cdot x \cdot (x-l)}{\sqrt{x^2+r^2}\cdot\sqrt{(x-l)^2+r^2}\cdot r} + \frac{(x-l)^2}{[(x-l)^2+r^2]\cdot r} \right\} \cdot dr \cdot dx \tag{6}$$

In the expression (6) letter l means the length of segment AB of the vortex.

If integrate the last expression on r in limits from zero to infinity and on x - from minus infinity to plus infinity (in accordance with fig.4), then we will obtain that additional kinetic energy got by the stream as a result of inducing in it additional speeds by the segment AB of straight line vortex . We will write down expression for the calculation of the indicated integral.

$$E_{ki} = \frac{\rho \cdot \Gamma^2}{16 \cdot \pi} \cdot \int_{-\infty}^{+\infty} \int_0^{+\infty} \left\{ \frac{x^2}{(x^2+r^2)\cdot r} - \frac{2\cdot x \cdot (x-l)}{\sqrt{x^2+r^2}\cdot\sqrt{(x-l)^2+r^2}\cdot r} + \frac{(x-l)^2}{[(x-l)^2+r^2]\cdot r} \right\} \cdot dr \cdot dx \tag{7}$$

The integral in the last expression is the improper integral, therefore the first question on that it is necessary to answer at the analysis of expression is convergence of integral.

Reasons that an integral is improper integral two: first is an endless value of speed at $r=0$ and infinity limits of integration on the variables of r and x.

The first reason can be removed, entering the radius of vortex, which physically reflects restrictions the area of vortex cross-section. After introduction the radius of vortex - r_v r at integration will be changed from r_v to ∞, excluding the infinity values of inductive speeds.

Let's transform internal integral in expression (7), with taking into account r_v.

1.3.43

$$\int_{r_v}^{\infty} \frac{1}{r} \cdot \left[\frac{x \cdot \sqrt{(x-l)^2 + x^2} - (x-l) \cdot \sqrt{x^2 + r^2}}{\sqrt{x^2 + r^2} \cdot \sqrt{(x-l)^2 + r^2}} \right]^2 \cdot dr \qquad (8)$$

When x and l are fixed, integrand is positive and restricted, i.e. it is less or equal $A \cdot r^{-2}$, where A is some positive finite number. Definite integral of last expression exist, finite and is restricted by the meaning of integral

$$A \cdot \int_{r_v}^{\infty} r^{-2} \cdot d\,r = A \cdot r_v^{-1} \qquad (9)$$

If (9) substitute in (7) expression with meaning infinity will be obtained.

As the additional attestation that integral (7) is the improper integral can be used its numerical estimation based on the numerical analysis.

Sense of this analysis was to take to the numeral calculation of values of double integral at the successive increase of limits of integration. At expansion of limits of integration the numerical value of integral increased constantly, arriving at a ninth order, after that the expansion of the limits of integration was shut-down. The got result is not proof that a double integral goes away to infinity in the classical sense, but can serve as evidence of unlimited growth of kinetic energy of "inductive motion". The last result conflicts with limit nature of aerodynamic drag in general and induced drag in particular.

Conclusion:

The conducted analysis allows to assert that for the induction by the vortex of finite sizes the field of speeds determined by the Biot-Savart law unlimited energy is required, and it conflicts with the real physical terms.

The reason of the indicated contradiction can be kinematic approach that was used for proving of Biot-Savart law and did not reflect energy relations.

At infinitely long existence of whirlwind with him it is possible to link unlimited energy, that justifies application of Biot-Savart law in the stationary tasks of aerodynamics.

Taking into account fact, that there are large number of numerical methods of aerodynamic calculation (method of discrete vortices, panel methods), which are based on using Biot-Savart law and, according declaration of the authors, give the results, which good correspond with experiment results, it is necessary to investigate deep the conditions of comparison these results.

References

1.Фабрикант Н.Я. Аэродинамика. Изд-во "Наука", Москва, 1964.

2. John D. Anderson, JR Fundamentals of aerodynamics, Second Edition, McGrow-Hill, Inc, 1991.

UDC 629.736.072.8: 681.3

V.V. Kabanyachyi, Ph.D.
(National Aviation University, Ukraine)

FORCE CUEING FOR PILOT TRAINING

A force cueing problem in flight simulators is formulated and solved on the bases of integrated system approach. Components of the problem are shown. An optimal technology of force cueing is described.

Formulation of the problem. A flight simulator is a basic technical mean of pilot training in normal and abnormal flight conditions. A motion system is one of the main components of flight simulator. It is a source of information about state and movement of aircraft, about functioning of its systems, about both maneuverable and disturbance movement, about critical flight regimes and abnormal situations, etc.

A motion perception is a first stage of piloting act. It is a complex mental process. The motion perception is based on a stimulus set that perceived by some physiological systems. Force cues are a source of advancing and warning information. They don't demanding a processing and identification. Force cues keep constantly and actively a pilot knowledge about a state, attitude, character of the aircraft movement in the space, its controllability and functioning of systems. They inform the pilot even in a case if the movement isn't perceived by other physiological systems. The motion perception on a basis of force cues is a determining, genetically older and the most reliable. In the case of force cueing absent a pilot technique in the flight simulator differs from the pilot technique in the aircraft.

A learning efficiency of flight simulators depends substantially on its fidelity level and in particular on a motion system fidelity level. Due to the high cost of the motion system the problem of improving the quality of force cueing to improve the learning properties of flight simulators is actual problem.

Analysis of recent researches and publications. As shown in [1], methodically the force cueing represents itself a difficult problem. Due to constructive and economic factors it isn't possible practically to achieve in flight simulators a full quantitative reflection of sensation dynamics and the motion perception. The force cueing represents a closed process. It consists not in a reproduction of aircraft movement, but in use of special control laws. This control laws synthesize a control signal. The synthesis is based on kinematics parameters of an aircraft movement and on a force cueing technology which used. The control law synthesizes such control signal that characteristic signs of the force cue would be in certain limits close to an actual at the same controls.

Statement of problem. Traditional technologies of force cueing (a high-frequency filtering, a nonlinear optimum filtering, a quasioptimal control, digital controllers, etc.) are insufficiently effective. So they demand to use motion platforms with length jacks not less than 2 m. A high cost of motion system and a growth of requirements to them do very actual a problem of more effective force cueing technologies development. It was not possible to solve this problem within a theoretical mechanics framework [2]. If force cues are represented with an accuracy which lies within a perception threshold and motion perception particularities are not taking into account then force cues can differ from an actual and false force cues can arise over available limitations. Researches show that it is possible to receive a force cueing high fidelity only on a basis of effective utilization of motion platform available resources. It is necessary to do under a careful coordination of aircraft movement information with laws of functioning, limitations and dynamics of physiologic systems with which the pilot feel, perceive and interpret movement. At the same time it is necessary to take into account following. First, the motion perception in an actual flight conditions is formed in a process of continuously varying forces field. The motion platform movement creates a movement sensation with breaks in some movement phases. Secondly, only the physiological

processes don't determine a mechanism of pilot movement perception. It is connected still with piloting tasks and a psychophysiological perception of all movement information.

Presentation of the main material. A cyclic law control was developed for effective decision of force cueing problem. It passed approbation in some flight simulators [3, 4]. On a base of integrated system approach the cyclic control law integrates movement perception peculiarities of person (operator) [5], piloting peculiarities [6], an account of characteristics, available (structural and energy) resources of motion platform. It is necessary to do under a careful coordination of aircraft movement information with laws of functioning, limitations and dynamics of physiologic systems with which the pilot feel, perceive and interpret movement. A necessity of system approach usage is caused by a fact of system-forming factor existence – a force cueing fidelity (which is understood as a sufficient degree of closeness of simulated force cues to actual ones). It is possible to formulate a mathematical statement of force cueing problem only on its basis. For high quality of force cueing it is necessary [1]:

* To simulate characteristic signs of force cue (character, perception time, direction, intensity and duration);

* Both the character and duration of force cue should correspond to actual;

* A mismatch of force cues perception times on aircraft and on flight simulator should be smaller as it is possible and to be within limits which depend on requirements of force cue fidelity;

* Both the intensity and duration of force cues should be proportional to actual;

* For effective utilization of platform displacement working range the force cues are simulated only when pilot perceives them and current motion parameters of motion platform allow doing this.

Motion system creates following force cueing:

1. Linear and angular dynamic force cues along longitudinal, vertical, lateral, roll and yaw degrees-of-freedom created by linear and angular motion platform movements;

2. Linear static force cues along longitudinal and lateral degrees-of-freedom created by pitch and roll motion platform movements;

3. High frequency force cues (vibrations and shocks).

Dynamic force cueing is main component of force cueing. A developed force cueing method build upon implementation of control cycle created autonomous motion platform movement which characteristic signs are perceived by pilot as aircraft motion characteristic signs caused by same control inputs.

The cyclic control law consists in a following. A pilot movement perception has physiological and psychological peculiarities. So ties between force cues and its characteristic signs are essentially nonlinear. For its representation the simulated model of motion perception [6] has been developed. This model, which is suitable for effective utilization in the force cueing, represents physiological, psychological peculiarities of person force cues perception. It describes quantitatively correctly a correlation between the force cue and characteristic signs. It estimates a force sensation depending on movement kinematics parameters: $\ddot{\Omega} = a_0\dddot{s} - a_1\dot{\Omega} - a_2\Omega$, where Ω, $\dot{\Omega}$, $\ddot{\Omega}$ is a movement perception function (a motion is perceived only in the case if this function exceeds a perception threshold), its first and second derivatives; a_0 a_1, a_2 are coefficients of motion perception model (they represent dynamics of motion perception from a force cue acting); $\dddot{s}$ is a force cue (an acceleration).

With the purpose of coincidence of force cue perception time in the aircraft and in the flight simulator the motion platform should begin the movement earlier (time t_1), than the pilot will perceived this movement in the aircraft (time t_2). The pilot will perceive the force cue in the flight simulator after finishing of forecast period $\Delta\tau = t_2 - t_1$. The forecasting is used for the beginning of motion platform movement in a proper time. It provides the coincidence of force cues perception times in the aircraft and in the flight simulator. The forecasting allows reducing a time delay practically to zero. A forecast motion perception function $\overline{\Omega}$ (a forecasted value of motion perception function during time $t + \Delta\tau$) is calculated for this purpose:

$\overline{\Omega} = \dot{\Omega} + \Delta\tau \ddot{\Omega} + 0{,}5\Delta\tau^2 \dfrac{d}{dt}(\ddot{\Omega})$, where $\Delta\tau$ is a forecast time of motion perception function. The coincidence of force cue perception time in the aircraft and in the flight simulator is achieved by a choice of corresponding value of forecast time $\Delta\tau$. The perceived force cue intensity is defined by a calculated derivative of forecast function of aircraft motion perception $\dot{\overline{\Omega}}$: $\dot{\overline{\Omega}} = \ddot{\Omega} + \Delta\tau \dfrac{d}{dt}(\ddot{\Omega})$.

The forecast function sign of aircraft motion perception defines the force cue direction: $sign\overline{\Omega}$.

A task of a final state control synthesis had been solving for a program control calculation. It was based on using of control function. This control function provides a motion platform movement from an initial phase state to a final one. It is optimal because a number of final conditions equals to order of differential equations system, which describes the motion platform movement. Along linear degrees of freedom the pilot perceives an acceleration derivative. So a fourth time derivative of motion platform displacement is used as the control function for avoiding of false force cues appearance. The control function includes a program and feedback components. For achievement of force cueing high fidelity all motion platform phase coordinates (from a displacement to a fourth time derivative of motion platform displacement) are kept in limits, which provide a normalized fidelity of motion platform movement. Analytic dependencies between motion parameters and characteristic signs in the aircraft and in the flight simulator were determined according to estimation by pilots of force cueing fidelity.

A motion cycle consists from four phases: a racing, a following, a braking and a homing action. In the racing phase the motion platform is leaded out on a preset acceleration derivative according to an optimal program. The acceleration derivative provides the force cue perception in a preset time and with a preset intensity and duration. For desired force cue creation in the following phase the motion platform moves with a constant acceleration derivative up to a preset acceleration. In the braking phase the motion platform movement creates an earlier then in a real flight an adaptation to the motion platform movement in the following phase. The bracing phase begins if it is possible to brace the motion platform movement with an acceptable motion quality for minimum time. It consists from two stages. The first stage ends if the motion platform movement achieves a preset bracing acceleration. The second stage ends if the motion platform movement achieves a zero velocity and a preset terminal motion platform displacement. At the homing action motion parameters are kept within a certain threshold to avoid an appearance of false force cues.

Signs of motion perception functions of aircraft and flight simulator should coincide in two cases. First, it takes place in the racing phase if function modules of motion perception in the aircraft and in the flight simulator are lower than the perception threshold and if the function module of forecast motion perception in the aircraft has achieved or has exceeded the perception threshold. Second, it takes place in the racing and in the braking phases if function modules of motion perception in the aircraft and in the flight simulator exceed the perception threshold. Signs of motion perception functions of aircraft and flight simulator can't coincide in the braking and in the homing action phases. They can't coincide in such case. On the one hand, function modules and forecast functions of aircraft motion perception exceed the perception threshold. On the other hand, the function module of motion perception in the flight simulator is lower than the perception threshold. In other words:

$$sign\Omega_{Fs} = \begin{cases} sign\Omega_A & \left|\overline{\Omega}_A\right| \geq \Omega_t, \left|\Omega_A\right| < \Omega_t, \left|\Omega_{Fs}\right| < \Omega_t; \\[2mm] & \left|\Omega_A\right| \geq \Omega_t, \left|\Omega_{Fs}\right| \geq \Omega_t; \\[2mm] \pm sign\Omega_A & \left|\overline{\Omega}_A\right| \geq \Omega_t, \left|\Omega_A\right| \geq \Omega_t, \left|\Omega_{Fs}\right| < \Omega_t, \end{cases}$$

where Ω_{Fs}, Ω_A are motion perception functions of flight simulator and aircraft, $\overline{\Omega}_A$ is the forecast function of aircraft motion perception, Ω_t is the motion perception threshold.

It is natural to use a cost function as a criterion for force cueing estimation. This function estimates a coincidence mistake of motion perception in the aircraft and in the flight simulator:

$$J(u) = \int\limits_0^T \left[\Omega_A(t) - \Omega_{Fs}(t,u)\right]^2 dt \left\|\Omega_A(t)\right\| > \Omega_t.$$

So a problem of force cueing is come to a control synthesis, which minimizes this cost function:

$$J^*(u) = \min \Rightarrow u^*(t)$$

$$s \in s^*$$

$$q \in \Omega_q$$

$$\text{sign}\Omega_{Fs} = \begin{cases} \text{sign}\Omega_A & \left\|\overline{\Omega}_A\right\| \geq \Omega_t, \left|\Omega_A\right| < \Omega_t, \left|\Omega_{Fs}\right| < \Omega_t; \\ & \left|\Omega_A\right| \geq \Omega_t, \left|\Omega_{Fs}\right| \geq \Omega_t; \\ \pm \text{sign}\Omega_A & \left\|\overline{\Omega}_A\right\| \geq \Omega_t, \left|\Omega_A\right| \geq \Omega_t, \left|\Omega_{Fs}\right| < \Omega_t, \end{cases}$$

where u is the control; s is the motion platform displacement; s^* is the motion platform displacement working range; q is a characteristics vector of motion platform; Ω_q is an allowable range of motion platform characteristics definition, that is an limited area, within which is provided a normalized quality of motion platform movement.

Conclusions

Decision of force cueing problem includes:

– Researches of motion platform characteristics with a purpose of characteristics set definition q, which allow to estimate a motion platform validity to the force cueing, and their normalization, that is a definition of allowable range of motion platform characteristics definition Ω_q;

– An optimization of motion platform control for an expansion of motion platform working ranges and for an improvement of force cueing fidelity;

– A determination of ties between movement parameters of aircraft and motion platform, a development of force cueing effective technologies, which increasing a degree of conformity between force cues in the aircraft and in the flight simulator, and due to this an improvement of force cueing fidelity.

The mathematical statement allows establishing a general criterion dependencies and also quantitative ratios, which are necessary for a force cueing optimization and the motion platform control, characteristics normalizations and a designing of motion platforms.

References

1. *Кабанячий В.В.* Імітація акселераційних діянь на авіаційних тренажерах// Вісник НАУ. – К.: НАУ. – 2001 р. – №2. – С. 96-102.

2. *Александров В.В., Садовничий В.А., Чугунов О.Д.* Математические задачи динамической имитации полета. – М.: МГУ. – 1986. – 181 с.

3. Программная реализация в цифровом варианте циклического закона управления (ЦЗУ-6) шестистепенным динамическим стендом в составе авиационных тренажеров неманевренных самолетов Ту-204, Ил-96-300. – М.:МГА. – 1989. – 163 с.

4. Исследования ДС6-1,5 и реализация ЦЗУ в составе имитатора акселерационных воздействий ИПС-74ТК-200: Отчет о НИР/ КМУГА, № ГР 0195U025224. – К., 1998. – 130 с.

5. *Кабанячий В.В.* Оптимальна функція початку сприйняття акселераційних діянь з обмеженнями// Вісник НАУ. – К.: НАУ. – 2001 р. – №3. – С. 85-88.

6. *Сотников Д.А., Кабанячий В.В.* Модели восприятия движения маневрирования самолета и их использование в задачах имитации движения на авиационных тренажерах// Безопасность полетов. – К.: КИИГА. – 1986. – С. 77-83.

T.V. Shypytiak, Grad. Stud.
(National Aviation University, Ukraine)

SAFETY IN TERMS OF SUBJECTIVE ANALYSIS

This article represents alternative approach to the flight safety, in particular "human factor". An approach is based on the principle of maximum entropy. Some results of modeling were presented.

The role of the "human factor" in the aviation devoted a large number of publications, for example: [1-5] and a lot of ICAO documentation: [6,7,8,9]. The problem of safety is becoming increasingly important due to the growth of air traffic. Therefore requires the development of new alternative approaches to the study of safety, in particular, the role of human factors. In this paper considers the problem of decision making in many alternative situation within the framework of subjective analysis [10].

The aircraft and its crew are considered as an active system that interacts with the external environment, and the main element of it is person who has decision-making. The fact that the aircraft is the latest generation of increasingly automated and, in principle, can make flights without pilot intervention, does not eliminate the problem of the "human factor", and, consequently, the aircraft with the crew does not turn into a passive system. Today aircrafts are increasingly automated and, in principle, can make flights without pilot intervention, but it does not eliminate the problem of the "human factor", and, consequently, the aircraft with the crew does not turn into a passive system. There are many examples from the recent past, when the wrong decisions lead to serious consequences - accidents and disasters.

The method of investigation, which is offered, can be called "information entropy". It is based on the variational principle of Jaynes [11].

In this work, we will focus on those examples, when the pilot is forced to solve the problem of selecting the set of alternatives. And with increasing degree of automation of flight control, the relative proportion of these cases will increase. Suppose that the choice of decision is related with the distribution of preferences on a set of alternatives $\sigma_i \in S_a, (i \in \overline{1, N})$. Distribution of preferences on S_a, as the set S_a itself, each time has a "personal media". You can talk about the unconditional and conditional preferences.

Quantitative measure of the relative "strength" of preference is denoted by $\pi(\sigma_i)$, $\pi(\sigma_i \mid \sigma_j)$ and called substantive preferences when it comes to choosing a product from a set, or management strategies for resolving of flight situations. The distributions $\pi(\sigma_i)$, $\pi(\sigma_i \mid \sigma_j)$ are very similar to probability distributions, but are not.

We assume that the preference parameters are normalized:

$$\sum_{i=1}^{N} \pi(\sigma_i) = 1; \quad \sum_{i=1}^{N} \pi(\sigma_i \mid \sigma_j) = 1; \quad \forall i \in \overline{1, N} \tag{1}$$

A quantitative theory of preferences becomes informative if it is possible to construct a quantitative image of the preferences. This problem is solved by postulating the following principle: each time the distribution of preferences to maximize a certain criterion, a priori, "founded" in the human psyche.

The principle that we are a priori "imposing" the human psyche is called the "principle of maximum subjective entropy." By means of subjective entropy value:

$$H_\pi = -\sum_{i=1}^{N} \pi(\sigma_i) \cdot \ln \pi(\sigma_i) \qquad H_\pi \geq 0 \tag{2}$$

For the distribution $\pi(\sigma_i \mid \sigma_j)$:

$$H_{\pi_j} = -\sum_{i=1}^{N} \pi(\sigma_i \mid \sigma_j) \cdot \ln \pi(\sigma_i \mid \sigma_j) \qquad H_{\pi_j} \geq 0 \qquad (3)$$

Entropy $H_\pi, (H_{\pi_j})$ are the measure of uncertainty. If $\pi_i = \dfrac{1}{N}(\forall i \in \overline{1, N})$, so there is maximum uncertainty $H_\pi = H_{\pi\max} = \ln N$ and conversely if distribution $\pi(\sigma_i)$ is singularly ($\pi_i = 0 \quad \forall i \neq j$ and $\pi_j = 1$ if $i = j$) then $H_\pi = 0$.

Assume that the efficiency of the system described by the function:

$$E_\pi = \sum_{i=1}^{N} \pi(\sigma_i) \cdot F(\sigma_i, \alpha, \beta, ...) \qquad (4)$$

The function F will call "cognitive function", which contains the exogenous information (relative to resources, utilities, probabilities, subjective probabilities), and endogen information about the subject (endogenous parameters α, β).

It is assumed that the distribution $\pi(\sigma_i)$ maximizes the function:

$$\Phi_\pi = -\sum_{i=1}^{N} \pi(\sigma_i) \cdot \ln \pi(\sigma_i) + \sum_{i=1}^{N} \pi(\sigma_i) \cdot F(\sigma_i, \alpha, \beta, ...) + \gamma \cdot \sum_{i=1}^{N} \pi(\sigma_i) \qquad (5)$$

Here the second term represents the weighted preferences $\pi(\sigma_i)$ of a number of cognitive functions. In this case the value E_π is not defined in advance, therefore (4), not be regarded as an isoperimetric condition.

The third term, by contrast, is a consequence of the isoperimetric constraint (1).

Looking for a maximum Φ_π of $\pi(\sigma_i)$, we find:

$$\pi(\sigma_i) = \frac{e^{F(\sigma_i, \alpha, \beta, ...)}}{\sum_{q=1}^{N} e^{F(\sigma_q, \alpha, \beta, ..)}} \qquad (6)$$

We call this distribution, following the terminology of Stratanovich [13] canonical. The essence of the variational principle reduces to the defined display on the S_a set of cognitive functions in the set $\pi(\sigma_i)$. The variational principle was proposed by Jaynes [11] in 1956-57 for problems of physical kinetics, and is formulated for the probability distribution $p(\sigma_i)$. The essential difference is that in this case it is used to determine the distribution of preferences that are not probabilities.

In the special case cognitive function may represent a probability of achieving a particular result at a resolution of the problem $(\sigma_i \to \sigma_j)$ or the subjective probability [12]. Thus, the postulation of Jaynes variational principle applied to the distributions of preferences provides a quantitative model, which makes it possible to solve several problems associated with predicting the behavior of the subject, in certain conditions, the investigation has already happened, for example, accidents, development of conflict situations, and so etc.

Entropy thresholds and thresholds distinguish ability preferences

An important hypothesis of subjective analysis is the assumption of the existence of entropy thresholds and the thresholds of the distinguish ability of alternatives. Introduction of entropy threshold leads to the fact that the entropy gets the space structure. In addition, opens the way for experimental observation of the evolution of preferences and parametric identification of their distributions.

Consider the evolution of entropy H_π in the event of a problem situation (Fig. 1):
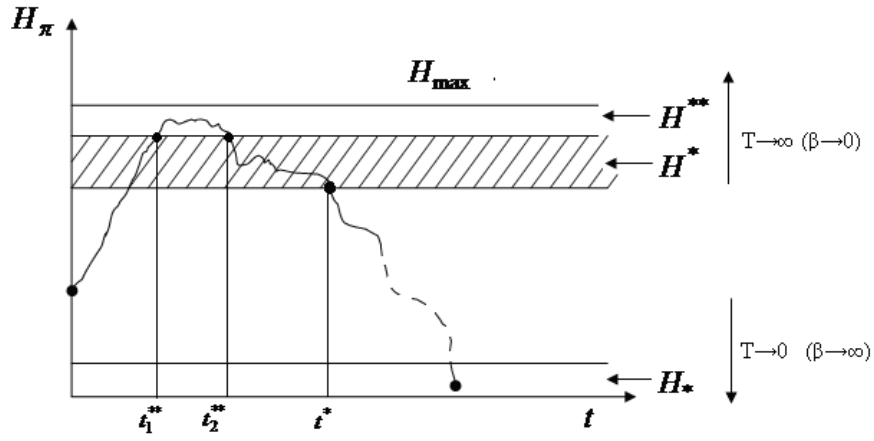
Fig. 1. Change of entropy with time

If the problem is complicated and paired with risks, the entropy increases, and may enter the area $H^{**} \leq H_\pi \leq H_{max}$. This uncertainty is extremely high - the state of mental chaos (stress, hysteria). With time the psyche calms down, and the entropy is in the region $H^* \leq H_\pi \leq H^{**}$. This area can be called the area of "freedom" or area "debate." Here is a meaningful comparative analysis of alternatives, more information content, resulting in the entropy decreases and crosses the "top - down" threshold H^* - the threshold of "decision". The area $H^* \leq H_\pi \leq H_*$ is called a domain of "necessity." Here is the structuring of the system, further reducing uncertainty and realization decisions already taken. Finally, the entropy can enter the area $0 \leq H_\pi \leq H_*$. This is an area we define as a situation in which "there is no escape." In this sense, our system is not transitive. There is a kind of "zombiing" of the subject.

Apparently, there are certain thresholds distinguish ability of alternatives. The necessary conditions for making a decision are the following: $H_\pi \leq H^*$; $H_\pi < 0$, velocity of information presentation should not exceed 50 bits / sec.

Speed perception and understanding of information subject that arises in the active system can not be above a certain level. This fact should be reflected in the mathematical models generating benefits that develop in Jaynes variational principle. Define the information flow rate q (t) as follows relation:

$$q(t) = \frac{dH_\pi}{dt} = -\sum_{i=1}^{N}\left(\ln \pi_i + 1\right)\cdot \dot{\pi}_i \qquad (7)$$

in turn:

$$\frac{d\pi_i}{dt} = \pm\beta\cdot\pi_i\cdot\left(\dot{F}_i - \sum_{j=1}^{N}\dot{F}_j\cdot\pi_j\right) \qquad (8)$$

The assumption of the presence of the marginal rate of perception of information is reduced to the following conditions:

$$\frac{d\pi_i}{dt} = \begin{cases} \frac{d\pi_i}{dt}, if & \left|q_p\right| < q_p^* \\ 0, \ if & \left|q_p\right| \geq q_p^* \end{cases} \qquad (9)$$

On this model performed parallel calculations of subjective and objective entropy, besides the condition:

$$\begin{cases} \dfrac{dH_\pi}{dt} = \pi_i - \sum_{i=1}^{N}\left(\ln\pi_i + 1\right)\cdot\dot{\pi}_i \ if \ \dfrac{dH_p}{dt} < q_p^* \\ \dfrac{dH_\pi}{dt} = 0 \qquad\qquad\qquad\qquad if \ \dfrac{dH_p}{dt} \geq q_p^* \end{cases} \qquad (10)$$

Here are some results of mathematical modeling advantages.

1.3.51

On the fig.2 depiction change of preferences and entropy with time. At some moment in time speed of change entropy exceeds a certain threshold, leading to the stop of preferences. At this time the subject can not perceive information and therefore not able to further distinguish the alternatives and make decisions. The only way out of this situation is to reduce the rate of change of entropy.
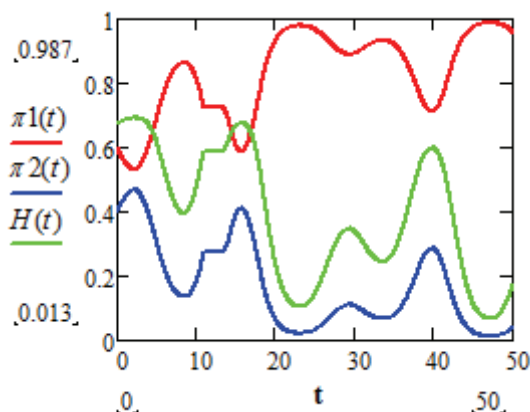
Fig.2. Changing preferences and entropy with time.

Conclusions

In this paper we propose an alternative approach to modeling the growth of the "human factor" in aviation. The approach is based on a priori assumptions, postulated, in particular, on the principle of maximum subjective entropy. Using this principle can make up for the shortcomings of statistical data.

References

1. Энциклопедия безопасности авиации [Текст] / Н. С. Кулик, В. П. Харченко, М. Г. Луцкий и др.; под общ. ред. Н. С. Кулика – К. : Техника, 2008. – 1000 с.

2. *Безпека авіації [Текст] / В. П. Бабак, В. П. Харченко, В. О. Максимов та ін.; під заг. ред. Бабака В. П. — К. : Техніка, 2004. — 584 с.*

3. *С. Р. Молер, М. Олнатт, М. К. Стриклер мл. и др.* Ошибки пилота: человеческий фактор [Текст] : пер. с англ. – М. : Транспорт, 1986. – 262 с.

4. Безопасность полетов [Текст] : учебник для вузов / Р. В. Сакач, Б. В. Зубков, М. Ф. Давиденко и др. ; под. об. ред. Р. В. Сакача. – М. : Транспорт, 1989. – 239 с.

5. *Жулев, В.И.* Безопасность полетов летательных аппаратов [Текст] / В. И. Жулев, В. С. Иванов. – М. : Транспорт, 1986. – 224 с.

6. Руководство по обучению в области человеческого фактора. Doc 9683-AN/950 [Текст]. – Утв. Генер. Секретарем. – Издание первое. – Канада, Монреаль, ICAO, 1998. – 370с.

7. Человеческий фактор в системе мер безопасности гражданской авиации. Doc 9808-AN/765 [Текст]. – Утв. Генер. Секретарем. – Издание первое. – Канада, Монреаль, ICAO, 2002. – 120с.

8. Сборник материалов «Человеческий фактор» №16. Кросскультурные факторы и безопасность полетов. Циркуляр ИКАО 302-AN/175 [Текст]. – Утв. Генер. Секретарем. – Канада, Монреаль, ICAO, 2004. – 52 с.

9. Руководство по управлению безопасностью полетов. Doc 9859-AN/474 [Текст]. – Утв. Генер. Секретарем. – Издание второе. – Канада, Монреаль, ICAO, 2009. – 318 с.

10. *Касьянов, В. А.* Субъективный анализ [Текст] / В. А. Касьянов. – К. : НАУ, 2007. – 512 с.

11. *Jaynes, E. T.* Information Theory and Statistical Mechanics [Text] / E. T. Jaynes // Phys. Rev. – 1957. – №4. – P. 620-630.

12. М. де Гроот. Оптимальные статистические решения [Текст]: пер. с англ. — М. : Мир, 1974. — 491 с.

13. Стратонович, Р. Л. *Теория информации [Текст] / Р. Л. Стратонович. — М. : Сов. радио, 1975. — 424 с.*

Piotr Strzelczyk, DSc. Eng. Rzeszow University of Technology, Poland
Tomasz Muszyński, MSc. Eng. Technical Sciences of PWSZ in Chelm, Poland

EXPERIMENTAL INVESTIGATION OF A VARIABLE GEOMETRY DUCTED PROPELLER.

The paper presents preliminary results of experimental research on the variable geometry ducted propeller. The purpose of present work is broadening area of application ducted propellers by use of variable geometry shrouds. The paper contains description of test setup and initial tests results for some selected geometries of intakes and exit nozzles in comparison with an open propeller. The results confirmed the assumption that for each flight speed, the variable geometry duct propeller can be more efficient than a free propeller.

Introduction

Researches, conducted for decades by scientific research institutes and leading aviation industry companies, concerning development of ducted propellers succeeded in application of ducted propellers in two velocity ranges. The first range contains velocities over Ma 0,6: turbofan jet engines mastered entirely market of airliners and subsonic army aircraft. There exist designs of powerplants employing free propellers for flights in such velocity range like Piaggio Avanti, An 70 with D-27 Motor-Sich propfans, Tu-95 with turbo CRP powerplant. However, due to plenty of limitations of such propulsion, they are a minority-merely a fraction of percent of these with turbofans. Second range of application spreads from 0 to 40 m/s. Ducted propellers are used in airships and hovercraft, where high thrusts at small   advance ratios are desired. High thrusts at low advance ratio is There are no serial-produced manned aircraft of velocities below Ma 0,6, using ducted propellers nowadays. Only about 50 RFB Fantrainer 400/600 and 200 Edgley Optica EA-7 airplanes, were made. The question is why ducted propellers are applied for low and high speeds but no for intermediate range?

Background of the problem the current technology status

Propeller duct designs for low and high velocities are based on different criteria, thus nozzle shapes arappears as a result of compressibility effects. Moreover, duct, significantly increases effective aspect ratio of blade, so outer part of blade can be much more loaded. Hence higher thrust from the propeller-disc area can be derived obtained with significantly reduced noise level in comparison with open propellers. Lower ducted propeller diameter causes that blade tip speed also much lower. For low velocities, acceleration nozzle is applied. Increasing airflow velocity in nose section is accompanied by pressure drop, which causes additional thrust. Thanks to additional thrust derived from duct, ducted propeller provides more thrust with the same engine power. Many tests confirmed thrust growth in comparison to free propeller for low flight velocities[1],[2],[3],[5],[6]. The investigations indicate static thrust growth for ducted propellers compared to free propellers, depending on design was from several percent for fixed pitch propellers to 39% for variable pitch propellers. Ducts applied nowadays, are of fixed geometry. Fixed duct geometry must be designed, likewise fixed propeller pitch, as compromise for take-off and cruise conditions. The basic conclusion from available reports and articles is statement, that it is impossible to create universal propeller duct geometry which would be simultaneously proper for static thrust and cruise conditions.

Suggested problem solution, and range of research work

The natural solution seems to be, similar to variable pitch propeller: a duct with shape which can vary with speed. However, this task is much more structurally sophisticated than in case of variable pitch propeller. It was assumed, that no exchangeable duct inlets and outlets will be applied, because derived solutions will be unable to obtain realistic variable geometry. The first, and as it turned out to be, the most laborious stage, was development of construction variant which would be applicable for practical use. Application of s not taken into account, because they are still

in tests phase. Many construction variants of inlets and outlets, of aircraft with and without thrust vectoring were analyzed as well as solution models occurring in nature. Much more effort required development of inlet, because the solutions applied in supersonic aircraft were not suitable for low velocities. A separate problem was controlling of the geometry itself. Application of typical high velocities solutions was too sophisticated, expensive and in this case unnecessary, because of significantly lower forces occurring in such wind tunnel velocities. The choice of geometrical dimensions was based on stats and using results from reports and articles available. During design the emphasis was put on good manufacturability of structure and low level of drag for cruise speed, it was assumed that high thrust for low velocities will be assured by high angle (more than 15 degrees) of inlet contraction. Basing on statistical data and assumed conditions main duct dimension was established, i.e. duct length/diameter ratio of 1,1:1 and relative duct airfoil thickness lower than 10%. Other geometrical parameters of model were analyzed including backlash dimension between duct and propeller blade tip gap, from [4], was concluded that backlash dimension has significant influence on ducted propeller performance, from others in turn e.g. concerning hovercraft operations was concluded that it should not be too low because of threat of easy blade damage, so it was assumed 1% of propeller blade diameter. Initially the duct consisted of 128 elements, after number of tests it was managed to simplify it by using biomimetic elements-overlapping, pressing and sealing each other "feathers" –inspired by birds' tails, so that the structure covering elements number was reduced to 64. Variable geometry duct inlet and outlet control system consists of 32 spherical joints coupled through linkages with two independent collars- one for inlet, one for outlet. Collars twist causes linkages angle change relative to transversal plane, thus changing duct inlet or outlet flare angle. Variable geometry duct designing and execution was the most laborious stage till now, there were many attempts using sheets of paper, composites and duralumin, for different geometries, using different types of hinges and geometry control systems.

Fig.1 Duct configuration for low airflow velocities.
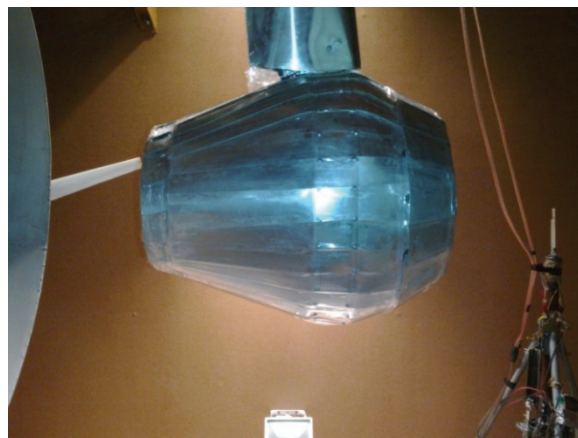
Fig.2 Duct configuration for high airflow velocities.

Both thrust and torque was measured using beam strain gauges. Engine was attached to outer part of bearing, ability to rotate was withdrown by scales system. Pressure difference measurement was executed by stagnation total pressure tubes. Airflow velocity-dynamic pressure measurement using Prandtl tube. Pressure sources was connected to digital manometer. Rotational speed measurement was conducted with opto-isolator, temperature and humidity were measured by portable mini-weather station. For the experiment purposes computer measuring system in modular version was used, operating in DasyLab environment. This enabled conducting an experiment according to modern metrology requirements. Sampling frequency was at 10000 Hz, packet size 4096 samples. Initial piloting measurements were conducted, and subsequently selected and measured 33 the most hopeful settings. The range of intake adjustment varied from diameter of 238mm to 405mm which corresponds accordingly 60-175% of propeller circle area. The range of

outlet adjustment varied from diameter of 187mm to 382mm which corresponds accordingly 37-155% of propeller circle area. Measurement was conducted for 10 days during 2 months (February, May) meanwhile the pressure, humidity and temperature were changing, so that the results will be converted to ISA conditions and subsequent to other dimensionless quantities distinctive for propellers. The purpose of experimental research was examination of influence of duct geometry change on powertrain aerodynamic characteristics and expanding an area of ducted propellers application to velocities uneconomical so far. The experiments were conducted in TA 1000 wind tunnel located in Institute of Aerodynamics and Fluid Mechanics, Rzeszów University of Technology.

Results of hitherto research

Information about particular geometries aerodynamic characteristics were retrieved, e.g. about coefficient of thrust change for different outlet geometries and constant intake diameter and for opposite situation. The highest static thrust was obtained for widest possible intake flare and medium outlet flare, which is consistent with ducted propellers theory [7]. The tunnel front section flow-round velocity increase, being an airfoil, by means of propeller work and also forward speed increase causes occurrence leading edge of this airfoil significant velocity increase, thus significant underpressure results in resultant force directed forward creating additional thrust. Slight extension of channel behind propeller plane of rotation is used to decelerate outlet stream, thus energy loss is much lower. The setting 0,67/0,63 succeeded in highest zero thrust speed, higher than zero thrust speed for the propeller itself. The results are in stage of rendering yet, but initial conclusions can be derived. For examined powerplant and particular settings, the relationship between static thrust producing ability and high speed thrust is inversely proportional: the higher the static thrust growth, the higher the drag and lower powerplant total thrust for the highest thrust geometry setting. Through the change of geometry setting it is possible to improve thrust for greater advance ratio.
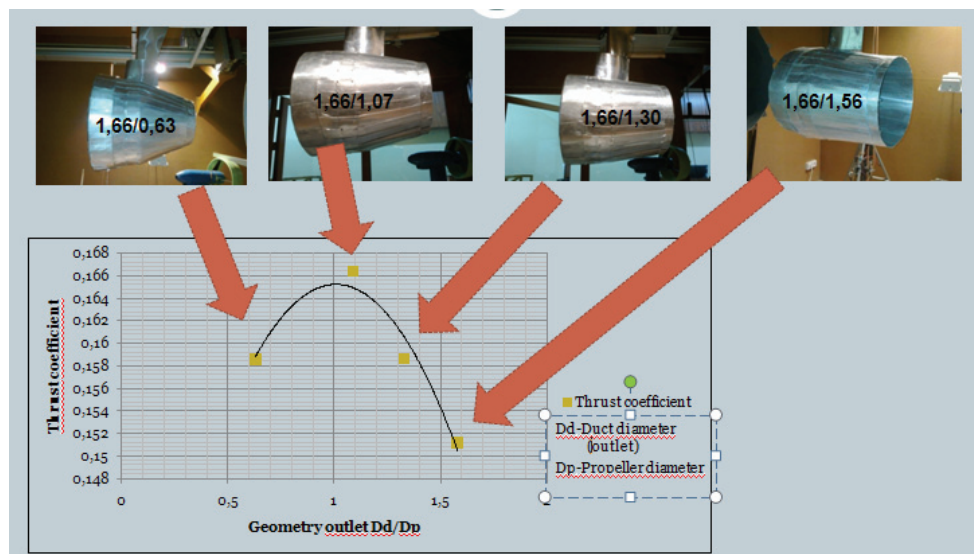
Fig.3. The value of thrust coefficient for increasing outlet diameter and constant inlet diameter (166% of propeller disc area) for 5 m/s.
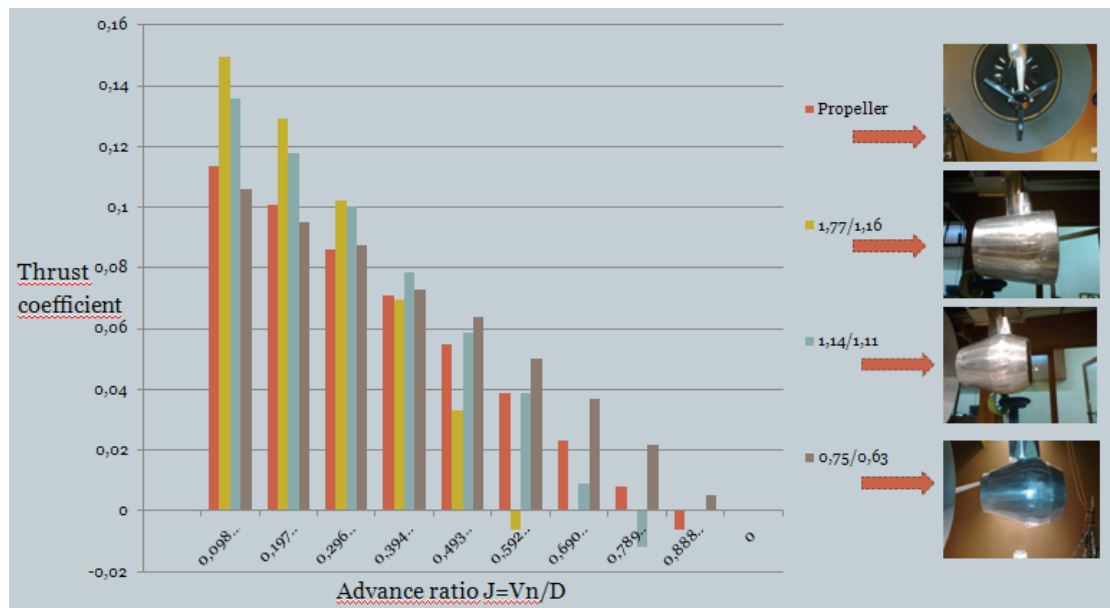
Fig. 4. Dependence of the thrust coefficients of the advance ratio.

Numerical flow study were conducted by finite volumes method using commercial pack Ansys/Fluent. There is planned numerical study continuation in Interdisciplinary Modeling Center of Warsaw University (ICM). In order to determine optimum calculations conditions there are conducted comparative analysis for the sort of mesh-type used: nonstructural, structural, hybrid flow model and the manner of boundary layer mapping, model of turbulence. To generate calculation meshwork software ICEM CFD was used. In the majority of fuselage flow simulations already conducted the meshwork of "boundary layer" type was generated with elements of PRISM type. In domain area meshwork with TETRA type elements was used, transition between boundary layer and fuselage surrounding space was executed with PYRAMID elements type. Numerical studies will be conducted for several model configurations, the first stage for the duct itself, without any propeller, not before achieving similar results with those experiential the propeller using the FAN feature will be added. It allows in simple manner to render the flow caused by work of featured element not requiring its particular shape. This condition is defined by adding momentum at propeller disc. The changr om fomentun was proportional to featured step of pressure.
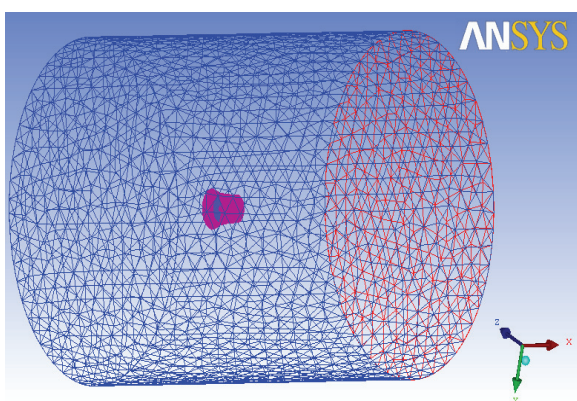
Fig.5 Calculation domain
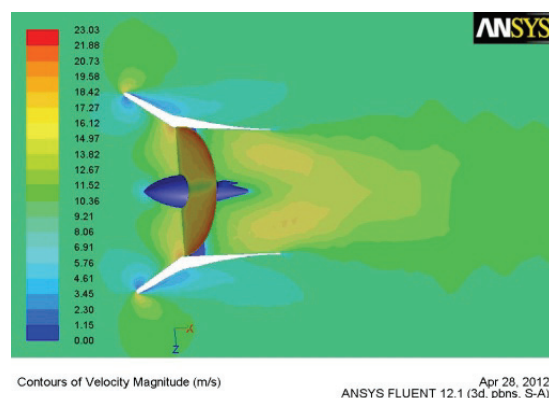
Fig.6 Contours of velocity magnitude   for model 1,6/1,05
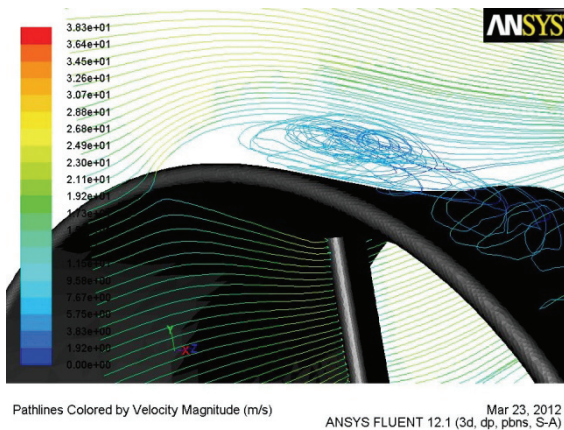
Fig.7 Contours of velocity magnitude for model 1,6/1,05
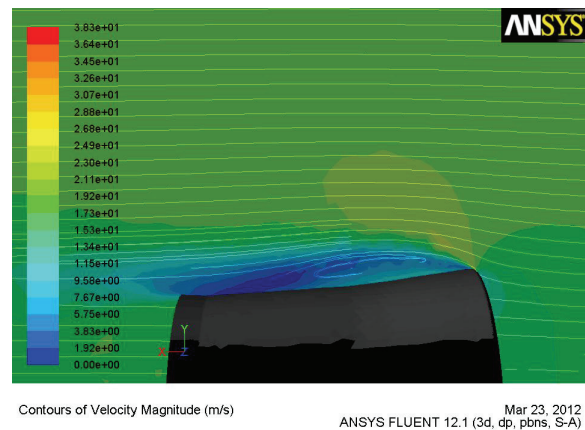
Fig.8 Pathlines for model 1,6/1,05.

Pressure distribution can be used to determine local covering tension e.g. essential covering wall thickness assessment or after implementing additional procedures, to conduct fluid-structure interaction (FSI) analysis of the whole construction.

Conclusion

Our research shows, that variable duct geometry has significant influence on powerplants aerodynamic characteristics change and can be the fastest way to improve efficiency/economy of powerplants nowadays. Progressive development of designing methods as well as construction technologies enables creating more and more sophisticated devices. The advanced designing systems using fluid-structure interaction analysis and shape-memory materials works have significant influence on development of such powerplants. Moreover, constantly growing possibilities of this solutions application-the market of short, medium range and GA aircraft is the fastest growing. As well as modern army V/STOL UAV designs also use ducted propellers due to higher power load capability of small propeller and higher efficiency for low flight velocities. The implementation in the real case is not too difficult and should be performed as soon as possible, because of the large potential benefits. Furthermore, this solution can be easily modified so as control of thrust vector would be possible and that expands the area of application of this solution.

References

[1] R. Lewandowski, *On possibility of Propulsion by Ducted Propeller*, Technika Lotnicza i Aastronatyczna ,Warszawa No. 1 1983, Poland (in Polish)

[2] Neal & W.E. Slack, NRCC Aeron.Rep. LR-445 „Static and low forward Speer tests on several six-foot diameter tractor and pusher ducted propellers" Ottawa, November 1965.

[3] K. Szafran, *The Laboratory Experience of Fan Propeller Unit Power for Unmanned Airship,* Warsaw Institute of Aviation, Proceedings of Conference Scientific Aspects of UAV's, May 07 − 09, 2008, Warsaw, Poland

[4] A. Akturk, C. Camci, *Tip clearance investigation of a ducted fan used in VTOL UAVS,* Proceedings of ASME Turbo Expo Turbine Technical Conference, June 6-10, 2011, Vancouver, Canada

[5] S.C. Roberts, Trecom Technical Report 64-41, The Marvel projects, MSU 1964

[6] T. Taylor, 'Experimental investigation of the effects of some shroud design variables on the static thrust characteristics…", LTL,Washington 1958, USA

[7] P. Strzelczyk, „Selected Problems of Propeller Aerodynamics", OW PRz", Rzeszów 2009, Poland (in Polish)

MSc. Eng. K. Grzegorczyk, D. Galas, E. Wajszczak
(Institute of Aviation Warsaw, The State School of Higher Education in Chełm, Poland)

ISSUE OF ICING IN AVIATION. STUDY WITH USE OF NUMERICAL SIMULATION.

Although over 100 years have passed since Wright brothers' first flight, icing has not been discovered entirely yet. We have divided our essay into 4 parts. First introduces the receiver to the meteorological aspect of icing. Second part is devoted to physics aspect of ice accretion. Third and fourth parts describe icing with mathematical models and present a numerical simulation. We have completed our presentation with results of numerical simulation.

1. Introduction

Icing is a process of creation of an ice layer on a surface (e.g. of an aircraft). It can result in change of aerodynamic characteristics of aerodyne or worse in damage of the engine. The most exposed parts to icing are: leading edges of wings and stabilizers, engine inlets, leading edges of propeller blades and rotors. Also other parts like: outer antenna, windshield or struts.

It is generally accepted that aircrafts which moves faster than 1000 km/h (540 kts) are practically resistant to icing due to frictional heat.

Considering causes of icing we will distinguish: direct sedimentation of ice crystals or snow, freezing of supercooled water droplets when they hit the aircraft surface and water vapor sublimation on the surface of the aircraft.

Classification of icing which is the most obvious and important for aviation study is due to shape of ice, therefore we can encounter:

- Ice with a shape of profile. It appears when the temperature is below -20°C and the cloud is not very watery. When the droplets hit the airplane, they freeze immediately and they do not change the shape of the airfoil (Figure 1). With small droplets ice accretion appears in the vicinity of the leading edge. With bigger ones the range of icing will grow. It's the most dangerous kind of ice accretion.
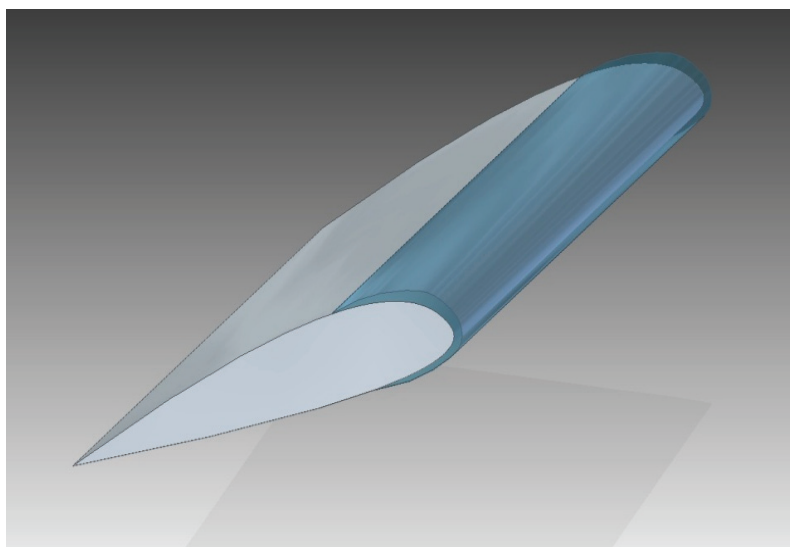
Figure 1. Ice with a shape of the profile

- Ice with a shape of a block. This type of icing forms in the temperature about -5°C or lower when the cloud is very watery and an aircraft is moving with low speed. The droplets hitting leading edge do not freeze therefore they are blown further where they do freeze (Figure 2). It is less dangerous type of icing because vibration on flying airplane shatter the ice which in consequence falls off.
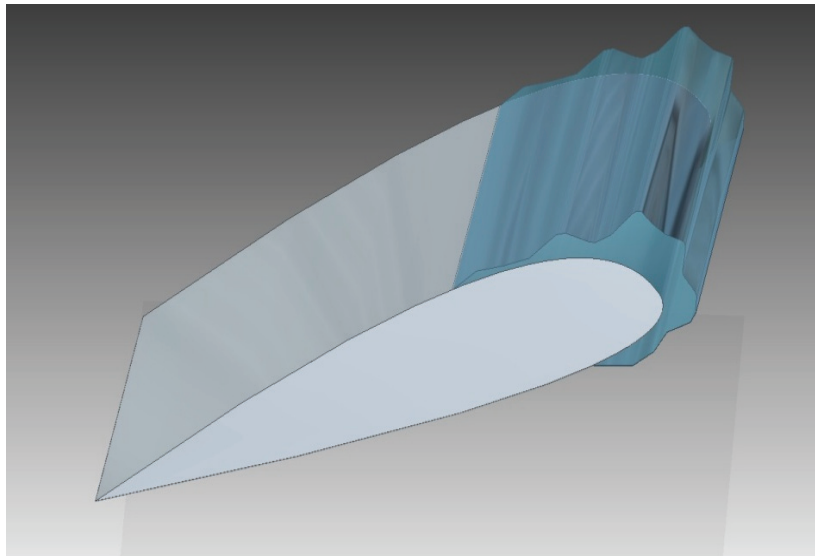
Figure 2. Ice with a shape of a block

- Hoarfrost. It is possible to encounter it when the cloud has small rate of watery or through sublimation of water vapor when the sky is cloudless. When an aircraft is rapidly descending from high altitude (the surface of the airplane is colder than outside air temperature), there is a perfect situation for creation of hoarfrost. The thickness of the ice layer is normally slight and it doesn't change aerodynamic properties significantly, however it remains dangerous due to reduction of visibility from the cockpit (Figure 3).
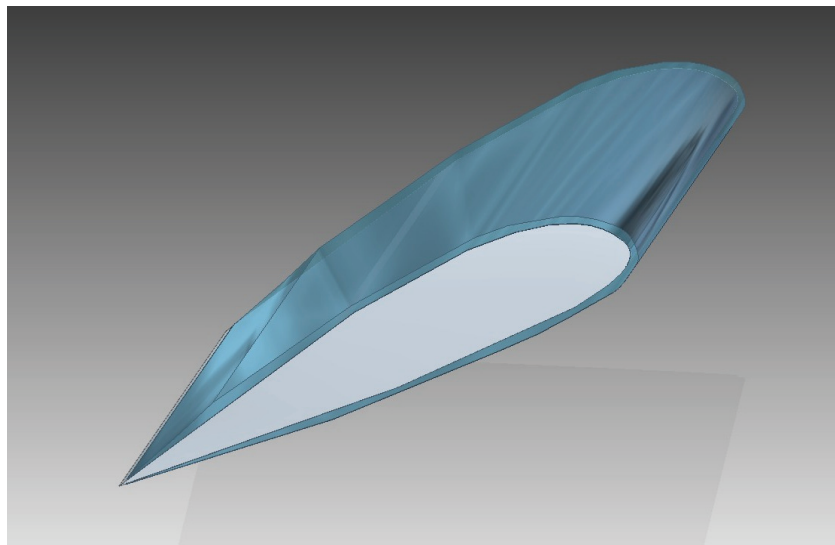
Figure 3. Hoarfrost

The speed of ice accretion provides other classification:
- Trace – intensity of ice accretion is slightly bigger than rate of loss due to sublimation.
- Light – speed of ice accretion does not exceed 0,5 mm/min. It is assumed that this type of icing poses danger to flights in icing environment exceeding 1 hour.
- Moderate – the velocity is between 0,5 – 1 mm/min. With that rate of accretion it
- affects also flight of short duration.
- Severe – with intensity between 1 - 2 mm/min de-icing
  systems aren't efficient enough.

It is relevant that preceding division is approximate, therefore moderate conditions of icing for one aircraft could be severe for another.

According to ice structure we can name:

- Clear ice (glaze ice) – it occurs in the temperature -20˚C - 0˚C, in watery clouds, from droplets which freeze the moment they hit the surface. It is quite dense and hard, therefore it is very difficult to remove.
- Rime ice – the temperature for this type of icing is below -10˚C, in clouds formed by ice crystals or supercooled droplets with diameter of 0,5 mm. Most common characteristics of rime ice are crystal structure, roughness of surface and lower density than clear ice due to content of air bubbles.
- Mixed ice – it is a combination of two above types of icing. It occurs in cumulus clouds (especially Cb clouds) where it is easy to find strong mixing of small and large water drops in the temperature of about -10,0°C. It is also possible to encounter in Ns clouds.
- Hoarfrost – it is homogeneous layer on the aircraft's surface. Besides increase in drag, it causes reduction in visibility.

Icing is so hazardous because of consequences which it has in aviation. Among numerous effects we have decided to emphasize:

- Ice accretion on leading edges of an aircraft disturbs the aerodynamic shape of wing. It results in reduction in lift, increase in drag, weight, stall speed or fuel consumption which is the worst from ergonomic point of view.
- In conditions of severe icing rate of ice accretion may amount to 1,25 cm/min. That would result in loss of stability due to irregular distribution of weight. Furthermore ice on propeller may cause engine vibration. The moment it falls off it might damage skin of an aircraft.
- As a result of icing it is possible to clog pressure sources (alike static and total inputs). Obviously that would have impact on instruments' readings (airspeed indicator, altimeter and vertical speed indicator).
- Deposition of ice causes (as mentioned) limitation in visibility from cockpit or precludes retraction of undercarriage.

2. Physics of phenomena

Considering icing from physical aspect is extremely complicated task due to multiplicity of processes which occur in ice zone. Furthermore there are phenomena with contrary qualities of great power. However we can name 3 basic conditions for ice creation:

- Water occurrence in the atmosphere
- Transport of water to profile i.e. aircraft movement, fluid movement around an airfoil or diffusion
- Dissipation of heat leading to water freezing

Basic processes seem to be obvious but fragmentary issues are far more complex. To fragmentary issues we can include:

- Deflection of air stream induced by airfoil movement towards surrounding air
- Water uptake by profile.
- Undercooling of water droplets in liquid state. Small water droplets remain in liquid state even in -40˚C.
- Kinetic heating of air. It occurs in a zone where the biggest air accumulation exists i.e. leading edge. It is remarkable that this process opposes to icing but still leading edges are the most susceptible to ice accretion.
- Kinetic heating produced by droplets. Water drops hitting the surface transfer their kinetic energy.
- Convective exchange of heat. It occurs between surface of aircraft and flowing air stream.
- Water evaporation or ice sublimation located on surface of profile. This phenomenon contributes to heat dissipation.
- Heat emission related to crystallization (freezing of water which hits the surface).
- Heat emission related to friction. It is especially important when considering high speed flow.

The phenomena mentioned above are not the only ones which have impact on icing but they are considered as the most essential.

Another aspect which complicates consideration of icing is the necessity of knowledge from many fields of classic physics like atmospheric physics, meteorology, thermodynamics, aerodynamics and flight mechanics. With simplification of the process itself it is possible to consider the phenomena basing on fundamental laws and physical dependencies:

- First law of thermodynamics. The change in the internal energy of a system is equal to the amount of heat exchanged with surroundings and the amount of work performed on or by the system. To simplify the problem – the temperature is a measure of the internal energy of a system. Considering icing using the first law of thermodynamics it is possible to explain kinetic heating of air. In the stagnation point the kinetic energy of air particles is converted into the internal energy which increases the temperature.
- Temperature. As mentioned above we may define it as a measure of the internal energy of a system. The temperature lower than the water freezing temperature is an indispensable condition for icing occurrence.
- Normal physics conditions. Normal temperature is equal to the ice melting temperature in normal pressure. It provides a reference point to physics conditions in which icing occurs.
- Specific heat. According to the definition it is a measure of the amount of energy per unit mass required to raise the temperature by one degree Celsius. Analyzing icing it is important to remember that water has high specific heat.
- Isentropic gas transformation. In case of that transformation it is practicable to establish precisely the relation between variations in density, pressure and temperature of the considered system. For example if we have 100% increase in pressure, it will cause 60% increase in density and 21% increase in absolute temperature. Considering 5% decrease in the temperature of melting that would mean 13,5 K drop. It is substantial for process of icing.
- Relation between the velocity of gas stream and variation in the temperature and pressure. Taking into account first law of thermodynamics and having decrease in gas speed, we will encounter increase in the temperature and other way round. Pondering the isentropic gas transformation, we may designate changes of particular parameters.
- Continuity equation. If liquid or gas flows through a tunnel with variable cross-section, mass flow remains constant. Considering flow around the airfoil like upper surface we encounter the biggest growth of speed. Thus an increase in the speed is observed, there is also decrease in the internal energy and hence decrease in the temperature.

Other factors should also be taken under consideration: water phase transitions (which has even bigger specific heat than water itself - crystallization of one water drop supplies heat enough to warm few other drops), humidity (cold air can hold smaller amount of water vapor than warmer one), saturation pressure (under the ice layer is bigger than the one you may find above the water layer). From above facts we may come to conclusion that unsaturated air for water might be oversaturated for ice. That would explain why ice occurs on airfoil without water presence in the atmosphere in the liquid from. Another factor which should not be omitted is water droplet uptake (which grows with increasing drop diameter and flow speed while decreases with increase in distance from leading edge). Very important process is convective heat exchange. It is a basic way of interchange heat between profile and surroundings. Moving fluid collects and carries the energy from the body of higher temperature to the one with lower energy. For the aircraft performing the flight in supercooled atmosphere the amount of lost heat by convection increases with rising speed and decreasing dimensions. It explains why ice grows at first on antennas as well as small and protruding elements. In order to define icing scientist had introduced icing coefficient β. It is ratio of water amount that forms ice layer to all the water captured by the surface.

3. Mathematic icing models

Bilanin model. It's a mathematical model of ice growing in time according to cloud watery, temperature and icing coefficient.

Dietenberger model. It is a mathematical model which describes changes of lift coefficient C_z, drag coefficient C_x and critical angle of attack α_{cr} in correlation to type and intensity (p) of contamination also maximum camber of its surface structure (k). We may apply Dietenberger model with assumptions: ice layer appears at the whole leading edge (p=1), wing chord equals MAC (mean aerodynamic chord), $k=\delta_l=\delta_{l\ max}(t)$, a and b coefficients are selected depending on considered profile and contamination type.

Messinger model for icing. In this consideration fundamental is the law of conservation of energy for equilibrium of temperature in isolated, unheated surface exposed to icing. Model has several limitations including: icy surface in Messinger model is smaller than the real one; base is isolated; model does not imply heat dissipation by the system, therefore the only method of balancing the energy is to create the hidden heat. In practice we would encounter ice growing.

4. Numerical simulation

For our simulation we used ICEM program for creating structural mesh and FLUENT as analysis system from ANSYS package. Type of our simulation was 2D. We used airfoil of ATR72 with average chord of 2,255 m. The following parameters were set: air velocity V=50m/s, density $\rho=1,225$ kg/m^3, angle of attack $\alpha=0$ °. The computational domain dimensions were as follow: length - 22m , height - 20m, semi circle with radius of 10m from leading edge side. Mesh type for both cases was quad and number of cells was around 30 000. Structural mesh with boundary layer for clean airfoil is displayed in figure 4.
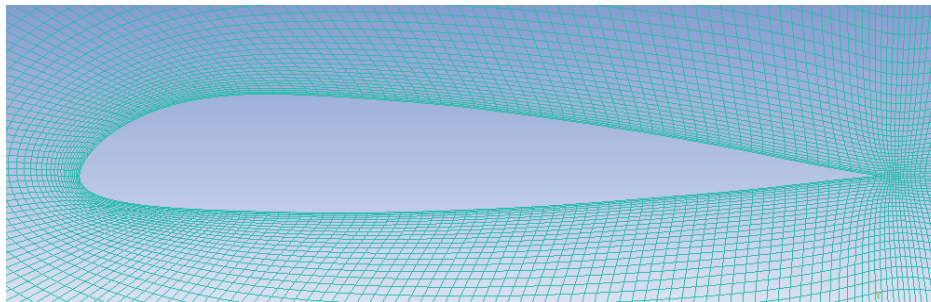
Figure 4. Structural mesh for clean airfoil

Results which we obtained are presented below:

Airfoil	Drag	Lift
Clean	100%	100%
With ice accretion	212,729%	92%
Difference	+ 112,729%	-8%

We observed significant degradation of aerodynamics characteristic of the airfoil. Drag increased significantly by 112,729% and lift decreased noticeably by 8%. Distribution of pressure around both profiles is displayed in figures 5 and 6. Comparing both illustrations we clearly see that area of low pressure over clean airfoil is larger than the one over the airfoil with ice. What is more, area of high pressure in stagnation point is significantly greater for airfoil with ice. Both of this observations explain the degradation of performances.
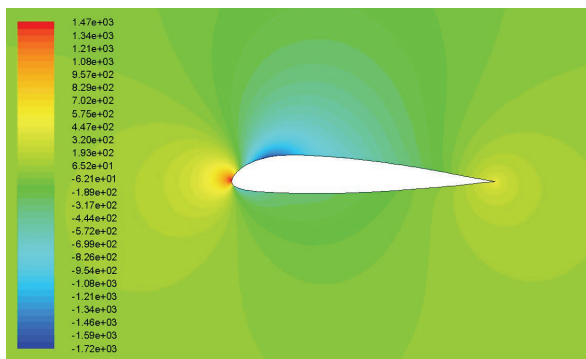
Figure 5. Pressure distribution over clean airfoil
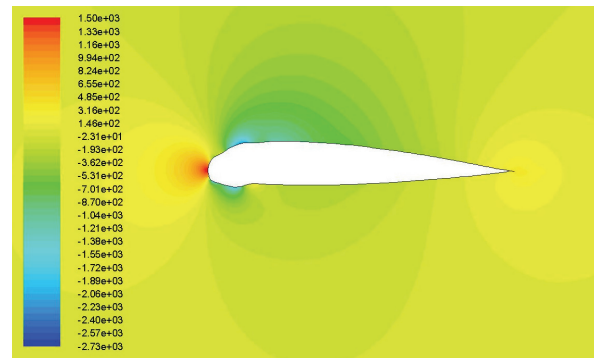
Figure 6. Pressure distribution over airfoil with ice

5. Conclusion

Our study confirmed that icing is a very complicated phenomenon. Over the years since the beginning of aviation icing proved to be extremely dangerous. Even though the aeronautical industry is one of the most developmental branches, the 100% efficient method of counter-acting ice influence has not been discovered yet. Because of that every pilot should respect unpredictability and strength of nature and therefore when it is possible avoid the known icing conditions.

References

1. Extension to the Messinger Model for Aircraft Icing. *T.G. Myers*
2. Modelowanie i symulacja numeryczna dynamiki obladzanego samolotu w fazie wznoszenia, *M.Sc. Mohamed Bajash Ghaleb Al-Sharabi*
3. Meteorologia dla pilotów, *Szefostwo służby hydrometeorologicznej sił zbrojnych RP*
4. Meteorology, JAA ATPL Training, *Jeppesen Publication*
5. Principles of Flight, JAA ATPL Training, *Jeppesen Publication*
6. Numerical simulation of ice accretion on multiple-element airfoil sections, *S.J. Jacobs, J.M. Hospers, H.W.M. Hoeijmakers*
7. Oblodzenie samolotu: Part I Przyczyny, wpływ na wykonywanie operacji powietrznych, *dr inż. pil. H. Jafernik, dr inż. pil. J. Kozuba*
8. Meteorologia, *Aeroklub Polskiej Rzeczpospolitej Ludowej*
9. Meteorologia dla potrzeb szybownictwa, M.T. Schimidt
10. Zjawisko oblodzenia w układzie zasilania silnika lotniczego lekkiego samolotu, *J. Weinar, Z. Bonca*
11. Podstawy aerodynamiki i mechaniki lotu, *A. Abłamowicz, W. Nowakowski*
12. Oblodzenie statków powietrznych, Chapter II Fizyka zjawisk oblodzeniowych statków powietrznych, *dr hab. inż. Andrzej Panas, dr hab. inż. Grzegorz Kowaleczko*
13. Wybrane zagadnienia z aerodynamiki i mechaniki lotu, *ppłk pil. dr inż. Ireneusz Smykla*
14. Airfoil Coordinates Database, *http://www.ae.illinois.edu/m-selig/ads/coord_database.html*

UDC: 621. 537.611.

A.P. Kudrin, PhD Engineering, professor (National Aviation University, Ukraine)
M.N. Svirid, PhD Engineering, associated professor (National Aviation University, Ukraine)
L.B. Pryimak, post-graduate (National Aviation University, Ukraine)

RENEWAL TRIBOMAGNETIC MECHANISM WITH PARAMAGNETIC MODIFICATOR USING

In the article it is determined, that when magnetic field acts on the working environment, protective tape, which appears on the friction surface has higher level of capacity than at a friction without magnetic field influence. It is set, that in the case with paramagnetic tin powder in oil composition, at the magnetic field influence on a working environment at the friction, the greatest renewal level is at S-S-N-N magnetic field direction and equals 1,5...3,5 mkm/km

Machines service life increasing straightly depends on the effective and rational using tribopairs, that shows up in support of it calculation parameters and such cases gathers over 80%. In many cases details of weighing in a few kilograms change a size from 10 to 300 microns, pass to the state of unserviceable, but the main it's part is fully working. Thus, the most perspective way of mechanism capacity support will be it's renewal and it is desirable in the conditions of unhandless technologies.

Thus, perspective direction of renewal in the exploitation process problem decision is the most not studied way of the magnetic-field energy using for the change of the system state to the reparation level. Taking into account, that lubricating materials are component part of tribosystem, the study of friction knot tribological parameters becomes perspective by the magnetic field influencing the on oil.

The tasks of this work are:

- determination of the magnetic field influence on lubricating materials;
- friction surfaces renewal conditions studing by the magnetic field influence on the lubricating materials.

So, as tribomagnetic renewal technologies include for itself intercommunication of working environment, oil with working materials (products of wear, oil modificators), then in the process of friction micromagnit processes will be realized in the wear products particles, that magnetize and design properties of magnetic liquid that consists of oil and wear products.

Work mechanism of magnetic liquids, that consist of magnetized metallic powder small particles, the nearest represents the friction knot work conditions in lubricating environments and surfaces wear processes under the action of force magnetic lines. [1-3]

Choosing the magnetic phase substances of wear products and oil solution liquid basis, by the quantitative correlation it is possible to varied by tribomagnetic constituent properties in wide limits, for example, magnetized of working environment and degree of it's changing under the magnetic field action.

Researches were conducted with the help of tribological complex [4] with the speeds 0,5 m/s, 1 m/s and 1,5 m/s, loading changed from 0,1 to 5 MPa. ШХ15 served as a standard and ЛС59-1 – as a rider, working environment: М10Г2$_к$ (mineral) and 5W40 (synthetic) motor oils. For quicklier study of paramagnetic material influence mechanism on the friction conditions of ferromagnetic standard on a diamagnetic rider oil modificator, tin paramagnetic powder was used.

It is known that paramagnetic by the action of magnetic field is displaced in the area of magnetic lines positive gradient. So, tin, which is paramagnetic, powder using, for tribomagnetic renewal of ШХ15 steel friction surface by adding of this powder to the working environment, namely in М10Г2к and 5W40 oils, and wear researches during different directions of magnetic lines [5] and different magnetic induction size enable by quicklier method to define system tribological parameters.

According to the tasks researches conducted at different magnetic field directions in accordance with which on fig. 1. the friction surfaces topographies are got with the tribological complex using [4]. Superficial descriptions of ШХ15 steel on the rider ЛС59-1 in treated by the magnetic field environments of М10Г2к and 5W40 with tin powder addition by the chosen direction of magnetic lines [5] and size of magnetic induction are present on fig. 1. are specify on superficial descriptions difference.

М10Г2к

a)　　　　b)　　　　c)　　　　d)

5W40

e)　　　　f)　　　　g)　　　　h)

Without　　S-N　　　　S-N- S-N　　　S- S -N-N
magnetic field
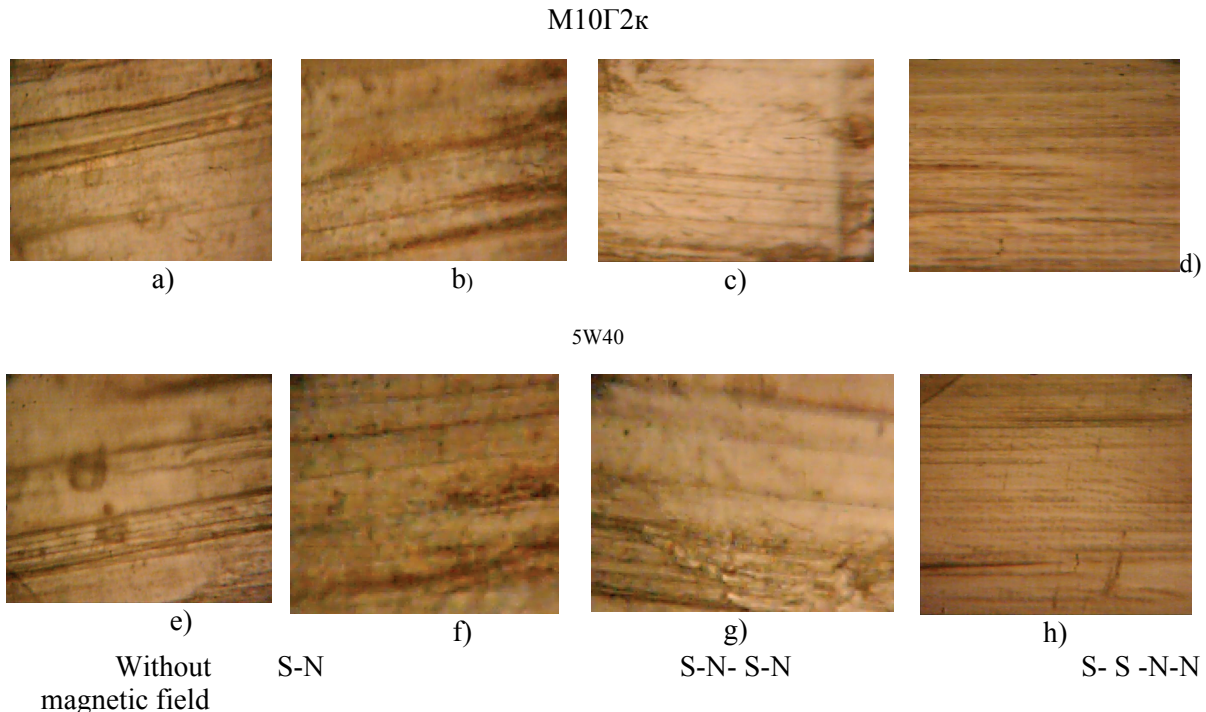
Fig. 1. ШХ15 standards friction surfaces topography on the rider ЛС59-1 in treated by the magnetic field environments of М10Г2к and 5W40 with tin powder addition with different direction of magnetic lines and size of magnetic induction

In the case of friction without magnetic field influence (fig.1a) and e) paramagnetic tin arbitrarily displacing in oil and constantly gets on the friction surface. Protective tapes in this case are the thickest (l0…20 microns), and the level of renewal is the greatest 1,8…3,8 mkm/km (fig.2.).

Surfaces, which are presented on fig 1b) and 1f) appear as a result of oil treatment by the the field with S-N directions and characterized by the presence of greater amount of protective tapes and less roughness (R_a =5…8mkm) than on fig 1a) and 1e), it is explained by the magnetic field influence on a paramagnetic tin (by magnetic induction 0,15 T). Created tapes on surfaces are characterized by the renewal 1,2…3 mkm/km (fig. 2).

a)　　　　　　　　　　　　　　　b)
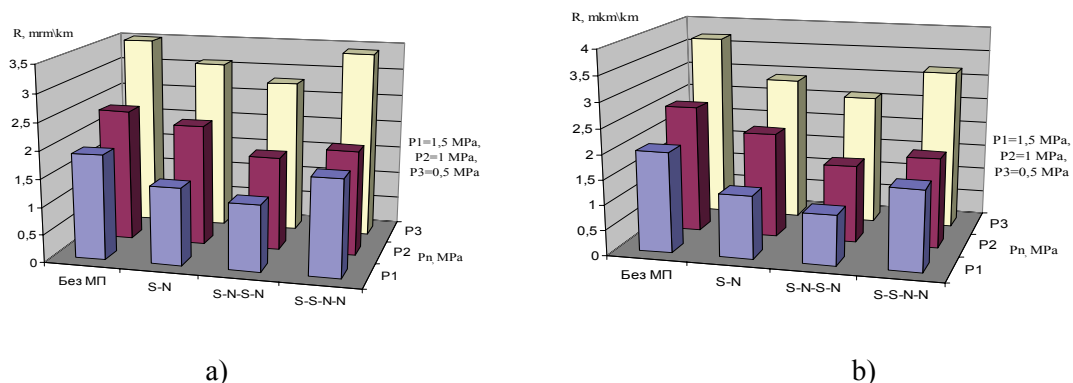
Fig. 2. Tribological parameters of feromagnetic ШХ15 steel on diamagnetic ЛС59-1 1 in the environments a) М10Г2к and b)5W40 with tin paramagnetic powder addition under the magnetic field action due to the load

1.4.2

Using S-N-S-N magnetic field direction with magnetic induction 0,3 T, tin is in the magnetic field zone influence, which is far from the friction surface. But some it's percent will get on the friction surface, but it's amount for the friction surface renewal is not considerable, that is why created protective tapes have a small thickness (fig of 1c) and 1g), and renewal is 0,8…2,5 mkm/km.

Tribologichni parameters of ШХ15 steel feromagnetic on diamagnetic ЛС59-1 1 in the environments of М10Г2к and 5W40 with tin paramagnetic powder addition under the magnetic field action are presented on fig 2.

During use of force lines direction in accordance with S-S-N-N direction, paramagnetic tin comes out from the magnetic field action area in a working environment, thus, the products amount for protective tapes formation is greater (fig. 1d) and 1h), accordingly the renewal level is higher (fig. 2). On fig. 1d) and 1h) the friction surfaces are shown at magnetic field S-S-N-N direction and magnetic induction 0,3 T, that more intensive covered by the protective tapes. Reason of it is that according to this magnetic field direction tin partly came out from the magnetic field action zone in an oil environment. Then tin gets on the friction surface where accepts active part in creation of protective tapes. Thus, it is needed to notice that renewal level is higher and equal 1,5…3,5 mkm/km (fig.2).

However, if to talk about quality of protective tapes, it is evident that when magnetic field influences on a working environment, protective tape, which creates on the friction surface more thin, but it's tribological quality is better (fig. 1b and 1f): 1,5..2mkm), it is more elastic and has a higher level of capacity than without magnetic field influence, which thicker (fig. 1a) and 1e): 4…6 mkm), but peels very quickly, as is not elastic, thus, owning the low level of capacity. Proof of it are researches on «micron-alpha» device, noncontact 3d profilograf [6], that show surfaces topography and tapes thickness analysis during renewal with the paramagnetic tin using without magnetic field action (fig.3a) and during S-N-S-N magnetic field direction (fig. 3b).

a)

b)

Fig. 3. ШХ15 steel friction surface profilography on diamagnetic ЛС59-1 1 in М10Г2к environment with tin paramagnetic powder addition a) without magnetic field, b) б) S-N- S-N magnetic field direction

1.4.3

On the friction surface, which is presented on fig.3a), without magnetic field influence it is evidently character of created protective tapes the thickness of which is 1,6 mkm, and the area of their surface coverage arrives to 40%.

It is evidently from fig. 3b, that the tapes at an magnetic field action have considerably lower power potential. Surface is characterized by topographical tapes with the thickness 0,6…0,8 mkm on 80% area. Elasticity of protective tape rises considerably, that evidently from its property evenly cover the friction surface roughness.

Thus, during magnetic field acting on oils, tape which appears on the friction surface has higher level of capacity than without magnetic field influence.

Conclusions:

1. It is determined, that when magnetic field acts on the working environment, protective tape, which appears on the friction surface has higher level of capacity than at a friction without magnetic field influence.

2. It is set, that in the case with paramagnetic tin powder in oil composition, at the magnetic field influence on a working environment at the friction, the greatest renewal level is at S-S-N-N magnetic field direction and equals 1,5…3,5 mkm/km.

References

1. Трибология. Исследования и предложения: Опыт США и стран СНГ/Под ред. В.А. Белого, К. Лудемы, Н.К. Мышкина. - М.: Нью-Йорк, 1993.

2. Белый А.В., Карпенко Г.Д., Мышкин К.Н. Структура и методы формирования износостойких поверхностных слоев. - М.: Машиностроение, 1991. 45с.

3. Розман Г.А. Строение и свойства вещества (учебное пособие), Изд. 2-е, переработанное. Псков, изд-во ПГПИ, 2001. - 292 с., рис. 131, табл 12.

4.Свирид М.М., Паращанов В.Г., Занько С.М., Задніпровська С.М., Приймак Л.Б., патент на корисну модель: Пристрій для дослідження матеріалів на тертя та зношування, UA 36600 GO1N 3/56, 27.10.2008.

5. Свирид М.Н., Кудрин А.П., Приймак Л.Б. Трибологические параметры сталей в обработанных магнитным полем смазывающих материалах. - ХНУ, Проблеми трибології. 2012. – №1 – С. 22-24.

6. Игнатович С.Р., Закиев И.М., Борисов Д.И., Закиев В.И., Методика исследования физико-механичесеих свойств поверхностных слоїв материалов при усталости с использованием многофункционального прибора «Микрограмма» / Авиац.-косм. Техника и технология: - Х.: ХАИ. – Вып.8(16).- 2004.-С.103-166.

UDC 621.891

M.N. Svirid, PhD Engineering, associated professor (National Aviation University, Ukraine)
E. Waise, PhD Engineering, professor (Technical University in Kielce, Poland)
V.V. Lubjanij, PhD Engineering, professor of NAU (National Aviation University, Ukraine)
G.A. Volosovich, PhD Engineering, professor of NAU (National Aviation University, Ukraine)

FRICTION PAIR TRIBOMAGNETIC PROPERTIES IN THE EVENLY DIRECTED MAGNETIC FIELD

In the article it is defined that during using of permanent magnets fields and electromagnets, energy of force lines ignores resistance of environment, that is why it is possible by their action to replace the electric parameters of technological processes. General actions of both renewal mechanisms considerably activate a process that becomes, as researches show, more attractive and perspective.

Large attention was always spared for operating reliability and problem of machines and mechanisms longevity. An increase of wearproofness is an actual task that can be decided on the base of deep scientifically-reasonable decisions. Repair and renewal of precessions pairs working details of pumps differ in high labour intensiveness, exactness of details making, that in a turn affects a price. The prospected knot is a cylinder-piston by hard requirements on admittances to 3-5 microns.

Technical progress complicates the machines work terms, the specific loadings and tribopairs exploitation terms increase [1], so aspiration to decrease weight of aggregate is important task. Process of exploitation requires the increase of tribopair work, extension of resource due to the choice of rational method of renewal. Now there are many methods of renewal of the presented mechanisms. Unhandless renewal technology of machines knots becomes actual because that decreases the price of machines life resource.

Increase of renewal manufacturability of plunger pumps friction precession surfaces by impulsive magnetic field by handless technologies using working liquids.

Research tasks: to determine influence of even impulsive magnetic field on materials and their composition elements at the triboknot ununstable state; to define the parameters of renewal terms of friction surface in current ressistence oil environments.

Longevity of power aggregates of pumping over mechanism in a great deal depends on tribopair , piston – cylinder, work that must support the technical parameters of all mechanism.

Using of impulsive magnetic-field for renewal of friction pairs allows to carry out renewal with friction knot handless, that considerably abbreviates the resources expense.

The object of scientific researches processes passing between the friction surfaces of physical object, a cylinder and a piston.

In obedience to technology of researches [2] due to chart finger-plane on a machine with recurrently-forward motion researched the processes of wear intensity at a friction without greasing. For activation of researches in the magnetic field applied modifiers, as powders, with different magnetic properties. Preparation of specimen surface of was conducted by a mechanical method, grinding on an abrasive micronic hide, than washed by alcohol and weighed on the analytical scales АДВ-200М with accuracy 10^{-4} grammes.

A specimen was placed in the removable tip of friction machine and set loading - 3,5 MPa, velocity of recurrently-forward movement is 0,12 m/s, in the center of the rider , length of that which was 33 мм. Material of specimen was steel 45 hard-tempered on martensite, and a rider alloy of ЛС59-1composition-metal. A working environment was oil М10Г2к. An experiment was conducted with direction of magnetic-field such as S/N, N/S and without influence of magnetic-field. In the process of every separate experiment in the zone of friction added powder modifier: ferromagnetic class nickel (to 20 мкм), paramagnetic tin (to 20 мкм) and diamagnetic zinc(to 40 мкм). The size of magnetic induction folded 0,15 T.

Basis of friction process is formation of protective tapes on the working surface and condition of their existence without non-destructive for a long time, under the action of external forces. There is the superficially-deformation loading of material at recurrently-forward motion (RFM), shake a structure, that considerably lowers the capacity of all friction knot. Loading renders predominating influence on the tribology parameters of interactive surfaces. Elements of environment or air, and also materials entering in the composition of friction knot. Loading renders predominating influence on the tribology parameters of interactive surfaces. Secondary structures appear as a result.

During oil modifying by ferromagnetic powder nickel friction pair without magnetic field (fig.2 - 17, 18) wore out to 48 mkm / km (fig. 1), that is explained by that powder of nickel in the process of deformation considerably becomes stronger, arriving at hardness 200 HB, that more than hardness of tin and less than hardness of specimen surface. That is why nickel works as an abrasive friction constituent on the tin surface. A specimen, having hardness almost in five times higher, carries out the role of hard surface that assists powder trowelling. During magnetic field presence (fig. 2 - 5, 6, 11, 12) specimen added in weight (1-5 mkm/km), and rider wore out (45-60 mkm/km), that is why as ferromagnetic pulled in the field and comes to specimen from 65Г, and rider operates as an abrasive, that is explained by the considerable increase of magnetic field force by ferromagnetic powder nickel, that strengthens specimen magnetic field, value of which equals 5000 ... 8000.

Properties of diamagnetical materials in magnetic field are characterized by the displacement of them toward the negative gradient of the directed action of force lines. During oil modification by zinc in the conditions of friction-sliding on the specimen surface the conglomerates of zinc are spread (fig.2-1) that decreases a wear (fig. 1) considerably. Under the magnetic field influence there are moving of tribotapes constituents that determine the terms of friction pair existence. A rider has the double constituent of influence on the friction plane from the side of the modified powder of zinc, that darts out from the steel friction zone on a tin composition-metal and displacement from the friction plane of tin constituents. That is why during oil modifying by zinc (fig.2 – 2,8) rider had a wear to 4 mkm/km during S/N magnetic field direction and 28mkm/km during N/S. At presence of magnetic field (fig.2 - 1, 7) on specimen friction surface passes the renewal process 4,7-12 mkm/km
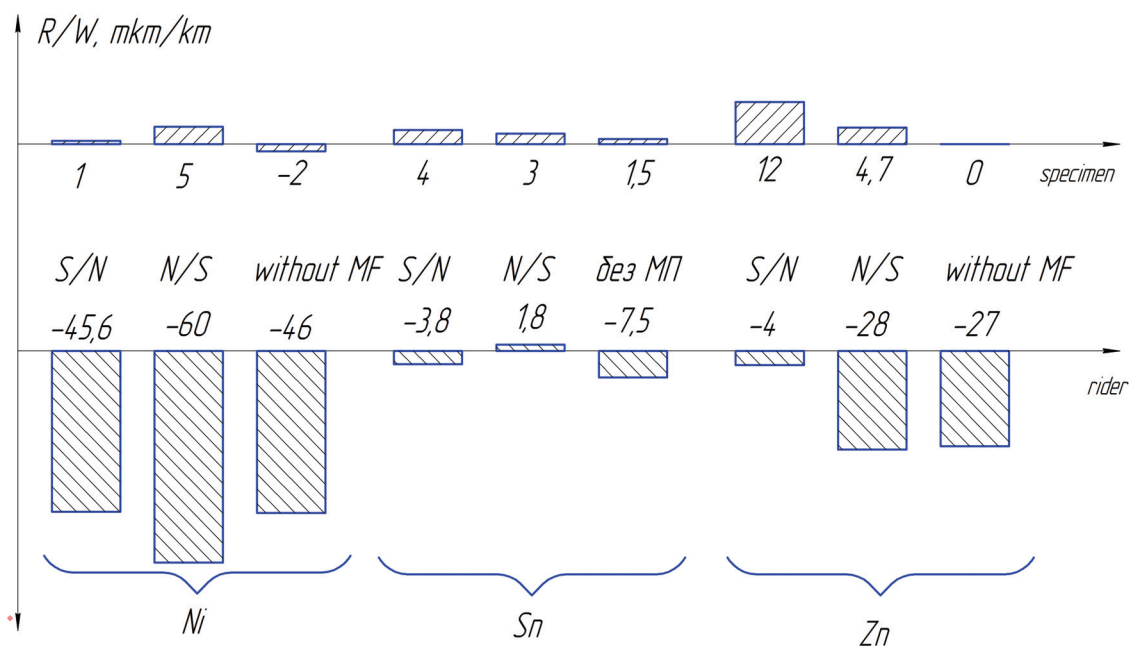
Fig. 1. A diagram of tribological parameters in the magnetic field in the environment of М10Г2к

The renewal conditions are explained by the mechanical constituent of powder trowelling process on the friction surface, and without a presence Mmagnetic field action specimen wear equals to zero (fig. 2 - 13, 14).

Oil modification by the paramagnetic tin powder is characterized by the renewal conditions of specimen friction surface, so as tin hardness far fewer, than in steel 65Г and in composition-metal C59-1, in addition, paramagnetics are place always in magnetic field. During N/S magnetic field direction (fig.2 - 9, 10) the renewal process of both friction surfaces is explained by the general action of deformation constituent and direction of positive magnetic gradient.

S/N

1

3

5

2

4

6

Diamagnetic

Paramagnetic
N/S

Ferromagnetic

7

9

11

8

10

12

Diamagnetic

Paramagnetic
Without magnetic field

Ferromagnetic

13

15

17

1.4.7
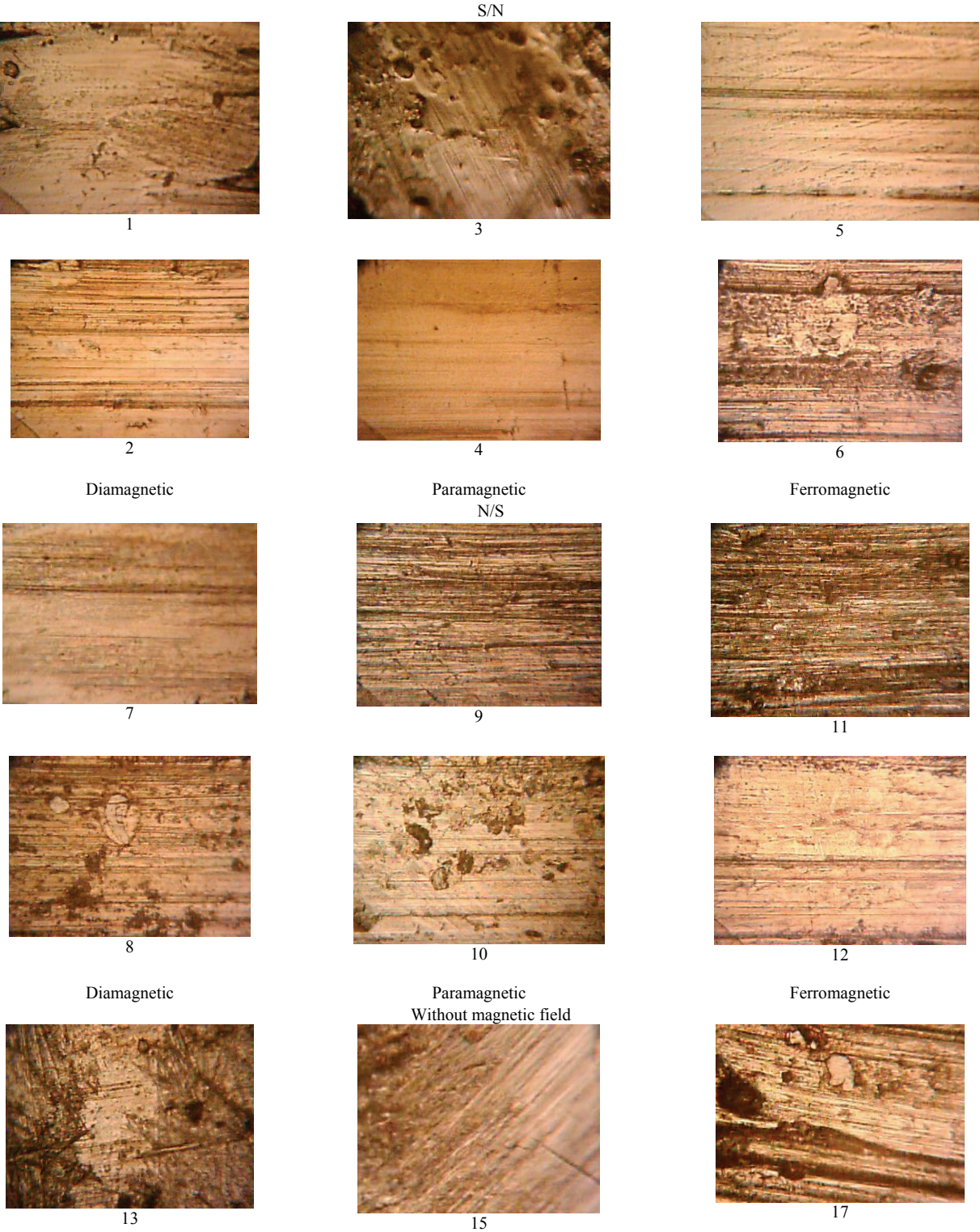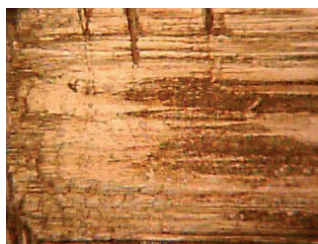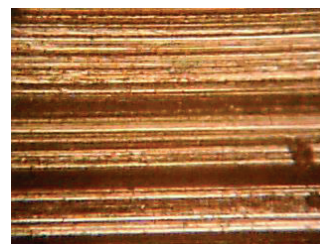
14	16	18
Diamagnetic	Paramagnetic	Ferromagnetic

Fig. 2. Friction surfaces topographies

The friction mechanism is stipulated by properties of nanoparticles that accumulate in conglomerates, it decreasees their general internal energy, with the further placing between the surfaces of friction as the reason wear decreasees considerably.

Conclusions:

Thus, triboelectrochemical technologies give possibilities of tribosystem state power control, improvement of machines reliability parameters indexes and decline of service charges, including repair. The most widespread technologies defects connect with the electric charges moving, declining of working liquid resistance. These facts decline technological charges on an equipment and make a lower prime price to the products.

During using of permanent magnets fields and electromagnets, energy of force lines ignores resistance of environment, that is why it is possible by their action to replace the electric parameters of technological processes. General actions of both renewal mechanisms considerably activate a process that becomes, as researches show, more attractive and perspective.

References

1. *Костецкий* Б.И., Носовский И.Г., Бершадский Л.И., Караулов А.К. Надежность и долговечность машин /под ред. Б.И. Костецкого. — К.: Техника, 1975. - 408 с.

2. *Патент* на корисну модель № 45574, МПК G01N 3/56. Пристрій для дослідження матеріалів на тертя та зношування при зворотно-поступальному русі / Свирид М.М., Кудрін А.П., Задніпровська С.М., Ловейко М.Г., Морозова І.В. Заявлено 29.07.2009; Опубл. 10.11.2009, Бюл. № 21.

UDC: 621.891 (042.2)

M.V. Kindrachuk, Dr. of Tech. Sci, professor (National Aviation University, Ukraine)
O.V. Tisov (National Aviation University, Ukraine)

WEAR APPLICATION OF Co-TiC CEMENTED CARBIDES FOR GAS TURBINES

The work offers a solution of urgent theoretical and practical problem of increase of wear resistance of GTE blades top shrouds contact faces by Co–TiC cemented carbides with combined micro and macro hardening. High strength of an alloy helps it to resist plastic deformations arising due to action of tangential force. Accompanied by generating of friction induced surface structure with positive gradient of mechanical properties provides to Co-TiC cemented carbides perfect wear resistance at high temperature operation

Introduction. Developments in aerospace engineering were always accompanied by increase of fuel combustion temperature, thus improving fuel efficiency or increasing thrust of the engine [1]. But it also increases loading of turbine elements, especially of rotor blades and decreases service life of the engine by causing more rapid loss of surface material due to wear [2]. Particularly blades top shrouds contact faces should be mentioned. The point is that nickel-based alloys, used to produce blades, have poor wear resistance. Plastic deformations of material surface layer due to friction cause a rise of oxidation and fatigue wear.

To solve the problem application of Co-TiC cemented carbides to cover top shrouds contact faces is proposed. They have higher melting point (1320–1340°C) then majority of used today nickel-based alloys. Their high temperature creep resistance is provided by carbide fraction +0.5…1 μm by a mechanism, similar to γ´ precipitate at nickel alloys. Carbide grains -20…+5 μm withstand wear thus reducing stresses in matrix material and preventing surface layer plastic deformations.

Current work is devoted to experimental investigation of their high temperature fretting wear resistance.

Experimental facilities and materials. For experiment ring-to-plane wear test with ring reciprocal rotating motion was used. Applied relative displacement – 120 μm, frequency – 30s⁻¹, number of displacements per test – 5×10^6, specific load – 30 MPa. Temperature ranged from 300 °C to 1050 °C, what was provided by circular electric furnace. Applied relative displacement, specific load temperature values are close to operating conditions of engine D-36. Specimens of powder alloys for wear test where produced by hot-vacuum-sintering process. Cutting them on ready-to-soldering parts was performed by spark cutting in oil bath. After preparation, they where jointed to the holders by high temperature solder with melting point 1240–1270°C [3]. The view of soldered to holders specimens is given on fig. 1.
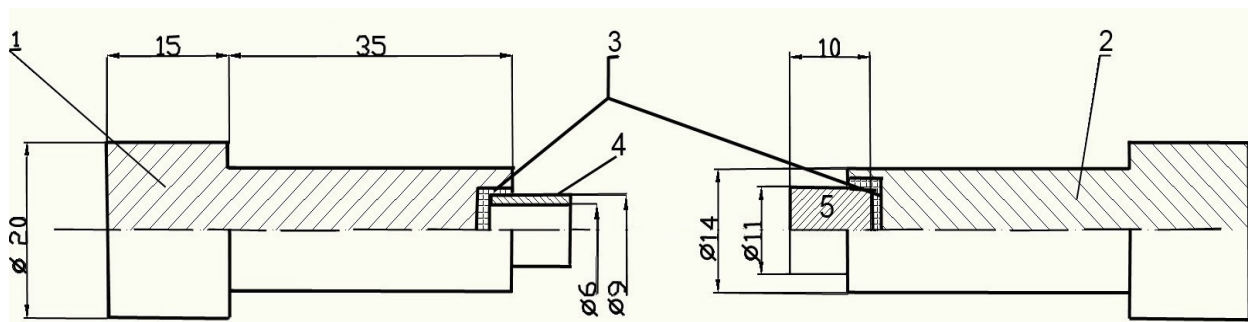
Fig. 1. Diagrammatic representation of specimens: 1, 2 – holders, 3 – solder, 4 – movable specimen, 5 – fixed specimen

TiC powders for sintering where prepared by high-energy ball milling with separation of +20 μm grains. Titanium carbides in quantity 50 % vol. (alloy P-76) have been cemented by cobalt. To increase high temperature properties of the binder it was additionally alloyed by 20–24 % (mass.) of chromium and by 3–4 % (mass.) of aluminium and iron. Wear test results were

compared with Co-TiC cast alloy containing 30% vol. of carbides (alloy P-69 [4]) and industrial eutectic alloy XTH-62 [5, 6], which contains up to 20 % vol. of NbC. To determine wear resistance linear wear of specimens was measured (ref. 6). After wear test specimens were detached from holders and their cross-sections were made in order to determine plastic deformation of sublayer (fig. 2).

a   *b*
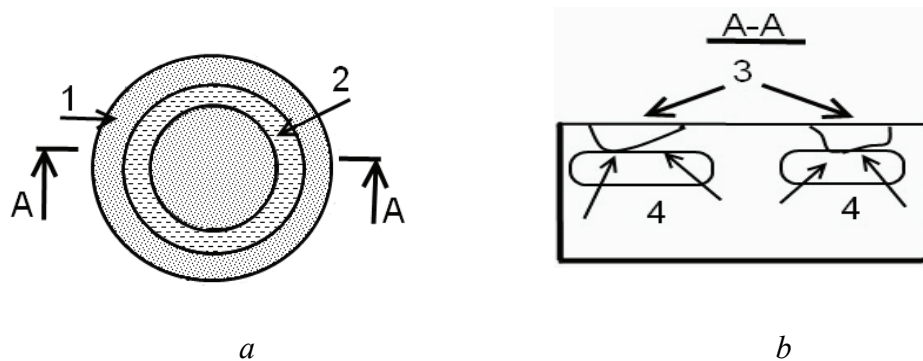
Fig. 2. Specimen top (a) and section (b) views: friction surface (1), wear scars top
(2) and cross-section (3), surface deformation analyzed area (4)

Structural aspect. Both cast alloys structure is obtained due to crystallization of carbides solution in cobalt. As far as titanium (niobium) and carbon are introduced as separate phases, it takes some time to full reaction running. The primary carbides solidification starts much earlier then that of binder. This process runs until the level of solubility of carbides in liquid phase. This leads to significant growth of their size (up to 30 μ*m*) and irregular distribution through the alloy. The cracks in these grains are clearly seen (fig. 3, *a*). As volume ratio of carbides in binder increases, TiC and NbC grain growth up to 60μm (fig. 3, *b*). It is also necessary to mention, that 30% vol. of carbides in eutectic alloys is limiting and require elaborate manufacturing procedures due to high viscosity of a melt.

During binder solidification smaller (secondary) grains of 0.5–2 μ*m* size appear. Their quantity is predetermined by solubility level of carbides in molten cobalt and can hardly be changed significantly without additional heat treatment.

Powder alloy P-76 (ref. 4) (fig. 3, *c*) is characterized by uniform carbides distribution through the alloy. Grain size varies from 0.5 μ*m* up to 20 μ*m*

a   *b*   *c*
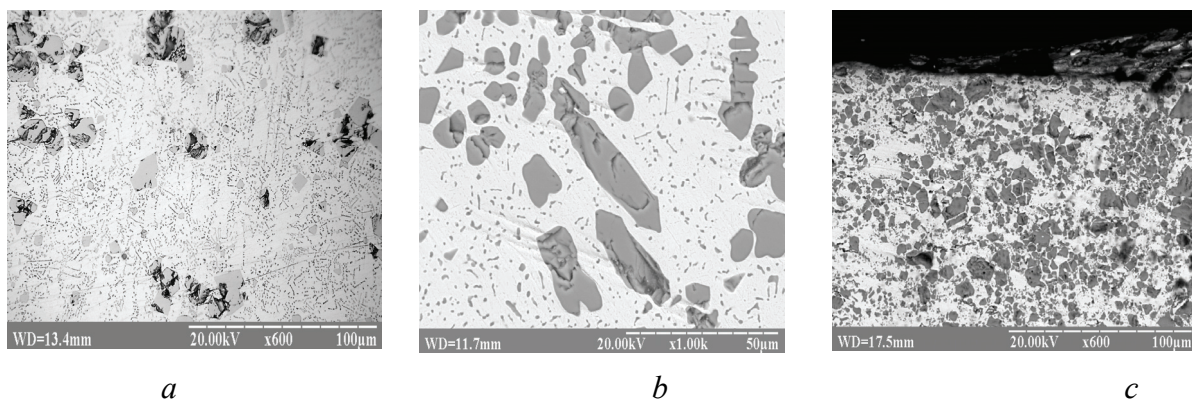
Fig. 3. Microstructure of cast alloys XTH-62 (*a*), P-69 (*b*) and cemented Co-TiC
carbides (*c*)

Pore size seldom rises to critical (6–12 μ*m*) [7], it's density is as high as 97% of theoretical. Pores in powder materials cause failure initiation and are strongly unwanted [8].

Experimental results. Wear test showed an advanced wear resistance of Co-TiC cemented carbides. Their linear wear is much less then of other tested materials what can be compared using fig. 4. Top view of wear scars analyses gives a conviction in wear of XTH-62 alloy due to intensive oxidation (fretting-corrosion). On its friction surfaces thick and porous oxide layer is formed. It is destructed on actual
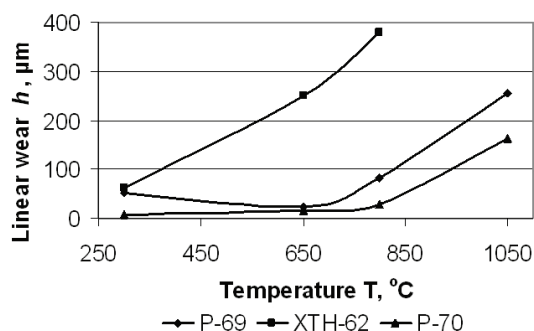
Fig. 4. Wear chart of investigated materials

contact areas, as a result contact of two unprotected by oxide layers metallic surfaces becomes possible (bright areas on fig. 5, *a*). Analyses of bright areas on wear scars helps to make conclusion about their formation as a result of fatigue wear. It is proved by surface "terracing" (fig. 5, *b*) which is typicalfor this kind of wear. High loads due to friction cause plastic deformations of sublayer (fig. 5, *c*). Taking into account these two simultaneous processes it can be deduced that friction-caused plastic deformation rapidly increases chemical activation of cobalt-based solid solution resulting in high oxidation and fatigue wear rate.

Similar behavior was observed at analyzing of P-69 alloy. Despite lower wear it's surface is also deformed. It can be clearly seen on fig. 5, *d*. Plastic deformation causes high strain in surface layer. This leads to destruction of friction-induced surface oxide films (fig. 5, *e*). It can be explained both by high external loading and plastic deformations of sublayer. The letter is proved by fig. 5, *f*.

Results of P-76 powder alloy testing differ a lot from eutectic. At high temperature it forms a discrete surface structure. It represents a mixture of bright and dark fields (fig. 5, *g*). Size of the letter varies from 100 up to 300 μm. Friction-induced surface structures were analyzed for chemical composition using scanning-probe microscope REMMA 106N. It has proved that different fields (dark and bright) are being formed by different oxides: bright fields contain up to 50% (mass) of chromium and 4–6% (mass) of aluminum, dark fields contain up to 46% (mass) of titanium and almost free of chromium and cobalt. Material of both fields contain about 40–48 % (mass) of oxygen. By this it may be proved, that dark fields are formed by titanium oxides on areas of continuous friction contact, what is partially proved by their dimensions. Bright fields are formed on "friction-free" areas. On microlevel friction-induced film is smooth, with no signs of fatigue wear or cracks (fig 5, *h*). Cross-section of specimens under wear scars (fig. 5, *i*) proves absence of sublayer plastic deformation.

a, × 40

b, × 500

c, × 600

d, × 40

e, × 500

f, × 2500

P-76
(T = 1050° C)

g, × 80   h, × 1000   i, × 2000
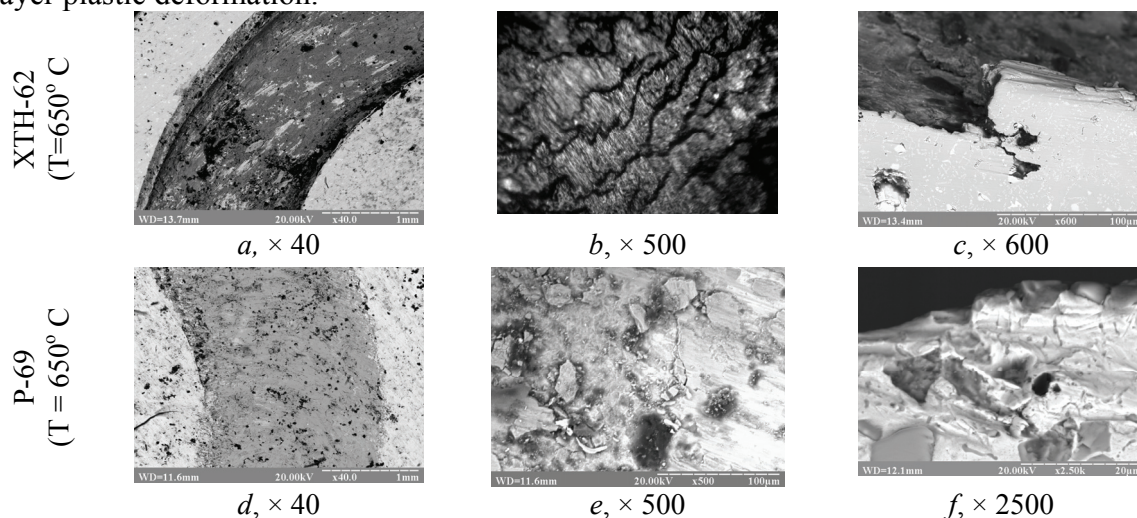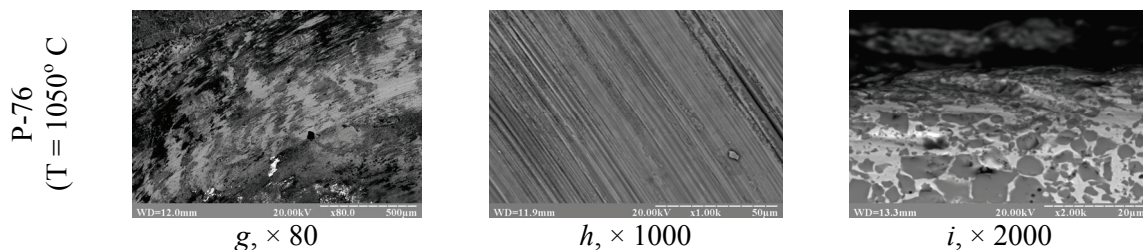
Fig. 5. The morphological details of investigated alloys wear scars and sublayers

Discussion. Plastic deformation of sublayer is important factor which causes intensive fatigue and oxidation wear. Also heated metal is "extruded" (fig. 5, *c*) from the most loaded contact areas. Thus, to increase wear resistance of material it is necessary to avoid plastic deformations of sublayer. Use of 50 % (vol.) of TiC is efficient to solve this task. High temperature causes oxidation of both binder and filler. During this process fine and submicron TiO_2 worn particles are formed (fig. 6). High temperature (up to 1050 ^{o}C), small size of particles activate grain boundary

diffusion, and high pressure on friction areas leads to their sintering due to capillary forces [9] over binder oxide layer thus forming friction induced structure with positive gradient of mechanical properties. Even if not sintered, TiO_2 particles are not removed from contact area during fretting-wear test. Their hardness is less then hardness of binder oxide layer and they may perform a function of solid lubricant.

Fig. 6. Formation of fine and submicron TiO_2 worn particles

Conclusions:

Use of powder metallurgy methods allows controlling of carbides grain size and their distribution through the alloy. Precisely balanced volume ratio of carbides makes it possible to reduce plastic deformations and to decrease wear of Co-TiC cemented carbides. Oxidation of TiC surface leads to appearance of fine and ultra-fine TiO_2 powder. Simultaneous action of high temperature and pressure in contact area make them sintered to the matrix oxides layer, thus gradient friction-induced structure is formed. Results of wear tests performed in close-to-operating conditions showed an advanced wear resistance of Co-TiC cemented carbides. It makes them prospective for gas turbines wear applications.

References

1. *Sims C. T*. Superalloys II. Metallurgia, Moscow, 1986, Vol. 1, Chapt. 1. *[C.T. Sims, N. S. Stoloff, W. C. Hagel]* (In Russian).

2. *Dukhota O. I*. Proc. Int. conf "Modern Problems of Tribology", Kiev, May, 2010 National Aviation University, p. 146. *[O.I. Dukhota, T.S. Cherepova, O.V. Tisov and V.I. Vovk]* (In Ukrainian).

3. *Peichev G. I*. Wear resistant alloys for GTE contact surfaces. J. of Engine Building 2 (2006) p. 191 *[G.I. Peichev, A. K. Shurin, L. J. Ivshchenko, V. E. Zamkovoy, N. V. Andreychenko]* (In Russian).

4. *Dukhota O. I*. Investigation of high temperature fretting-wear resistance of cobalt-based composite alloys. J. Problems of Friction and Wear, 53 (2010) p. 196-197. *[O.I. Dukhota and O. V. Tisov.]* (In Ukrainian).

5. *Shurin A. K*. Engineering of alloys for gas turbine blades top shrouds hardening. Service Life and Safety Problems at maintenance of Constructions and Machines, The E.O.Paton Electric Welding Institute, Kiev, 2009, p. 641 *[A.K. Shurin and T. S. Cherepova.]* (In Russian).

6. *Dukhota O. I*. Composite alloys for gas turbine engines top shrouds contact faces hardening. J. Problems of Tribology, 4 (2010) p. 102. *[Dukhota, M. V. Kindrachuk, O. V. Tisov, T. S. Cherepova.]* (In Ukrainian).

7. *Shubert W. - D*. Modern Hardmetals, V.N. Bakul Institute for superhard materials, Kiev, 2008, p. 207.

8.. *Miner R. W*. Effects of fine porosity on the fatigue behaviour of a powder metallurgy soperalloy Met. Trans. A J. Vol. 12, 2 (1981) 265. *[R. W Miner, R. L. Dreshfield.]*

9. *Gessinger G. H.*. Powder metallurgy of superalloys. Metallurgia, Cheliabinsk, 1988, Chapt. 1, p. 60. *[G. H Gessinger]* (In Russian).

UDC: 620:619.1

O.V. Bashta, PhD. (National Aviation University, Ukraine)

MICRO CRACK PROPAGATION BEHAVIOR IN ALUMINIUM ALLOY Д-16АТ

Effects of microstructure and grain size on fatigue behaviors such as fatigue strength, crack initiation and propagation behaviors were discussed. Data about lengths of microcracks (MC) which appear during a loading before revealing of a macrocrack, growth rates of cracks and kinetics of growth MC are obtained.

Essence of a problem. Accumulation and association of dissipated short cracks concerns one of leading mechanisms of damageability and realisation of a limiting condition of it designs, it is necessary to consider at forecasting of their resource.

For metals micron-sized microcracks formation and coalescence occur in the plastic zone as a result of dislocation-activity and stress concentration.

To understand such fracture behaviors, it is necessary to establish a method to detect microcracks which are undetectable by the existing technologies. Microscopically, fracture can be classified into shear and tensile separation. When a macrocrack propagates, microcracks coalesce three-dimensionally in front of the macrocrack, and fracture resistance (toughness) varies depending on whether the coalescence process is of shear type or tensile type. In efect, it is necessary to classify both microscopic and macroscopic fractures into shear and tensile types, and the formation speed of microcracks can serve as an evaluation parameter of ductility and brittleness.

For macroscopic understanding of fractures, it is necessary to define the propagation of the main crack associated with the material structure. As the main crack often propagates non-uniformly, it is necessary to define the length corresponding to the non-uniform propagation of the crack.

It is known, that process of fatigue of metals is localised in a blanket [1]. With increase in quantity of cycles in all materials the characteristic strip structure - strips of the steady localised shift develops. The substructure in sliding strips can be different depending on material type. Borders of strips and especially their joints often become places of fatigue cracks origin. Transformations in dislocation arrangement which are realised in the course of fatigue tests, have character of "phase transition" in a defective subsystem and occur, as a rule, at achievement of certain ("critical") density of dispositions.

Thus microcracks in plastic materials arise in steady strips of sliding. Therefore the surface is a data carrier about dynamics of exhaustion of carrying ability of constructional elements. Estimation of the blanket condition is considered as a way of fatigue damage diagnostics.

One of fundamental features of multiple destruction of materials is the multystage. Each stage of the destruction process is characterised by separate dimensional level. At each stage there is an origin and growth of the dispersed defects (cracks, pores). Thus transition from a stage of destruction with lower dimensional level of damages on following on which damages have the big sizes, occurs by accumulation of defects in limiting concentration. Such scheme of destruction is inherent practically in all constructional materials and arises at various kinds of power interaction [2].

Stages of damageability at fatigue failure can be write down, as [1-3].: the Stage 1 - accumulation of separate micropores and microcracks statically distributed in volume of metal; stage 2 - development of cracks on borders of grains, twinnings and sliding strips; stage 3 - development of the main crack in a material, with existing system of microcracks.

One of displays of the machine details damage at a cyclic loading is presence of disseminated on the limited surface area the short cracks. Destruction of materials, is caused by the continuous in time processes of cracks origin, growth and association, it is considered universal [4], is called as plural and is characteristic for many damaging factors, for example, for fatigue [5-7], cyclic creep and corrosion.

The quantity of experimental data on plural destruction is very limited. It is connected with labour of input identification and complexity of supervision at the behaviour of a considerable quantity of small defects on a surface of samples.

At presence on the limited area of a surface or in material volume even a small amount of microcracks (MC) which sizes is in an interval $0,1... 10^3$ the micron [1-7], always exists final probability of their association. Association of MC carries danger of sudden occurrence of macroscopical defect. Therefore the initial estimation of a limiting condition at a stage of development MC should be made taking into account the factor of association of dissipated defects.

Technique and essence of experiment. Nondestructive evaluation comprises the steps of (1) detecting the presence of defects in materials, (2) locating the position, (3) classifying the type, (4) determining the size and shape of each defect, (5) clarifying the mode of cracking and other characteristics, (6) determining the mode of fracture by considering external load and environmental conditions, and judging the degree of the severity of the defects by using an analysis based on fracture mechanics, (7) making an ultimate judgment on acceptability or, in other words, implementing material screening, and then, (8) for materials that have proved acceptable, evaluating its safety factor and service life. Here, the steps (1) to (5) for detecting defects are in the category of nondestructive test and inspection, while nondestructive evaluation includes the steps (6) to (8) as well. In applying such nondestructive evaluation, therefore, it is necessary not only to enhance the accuracy of nondestructive inspection techniques for detecting defects but also to consider (1) undetectable defects, (2) correspondence between the size of the detected defects and the size of defects leading to fracture, (3) fracture models (representing formation, growth and coalescence processes of micro defects).

The detection of microcracks is indispensable to non-destructive evaluation. Although various microcrack-detection methods, including X-ray, ultrasonic, microfocus X-ray based on electromagnetic equipment, high-frequency ultrasonic and ultrasonic microscope are being developed, it is still impossible to detect internal defects finer than several tens of microns, and there is no method to evaluate the mode of fracture. Although electric resistance, ultrasonic and acoustic emission analyses are used for the detection of microcracks.

Standard corset specimens cut out from sheet aluminum alloy Д-16АТ with the thickness of 1,3 mm with a plating layer, the average grain size on the plating layer is 47 μm. They were loaded on hydro-pulsating machine MUP - 20. The maximum loading in the minimum section was equaled to 250 MPa at frequency of a loading of 11 Hz. A loading cycle - sinusoidal, zero. The base of tests was not less 10^5 cycles. In the present study the fatigue tests were carried out in laboratory air (temperature 16–25 ^{0}C, humidity 40–70%).

After the next stage of a loading the specimen tacked away from loading machine and parameters of microcracks were measured, further the specimen passed the next loading.

The program of tests of specimens on a low-cycle fatigue included research of accumulation processes and development of short cracks before occurrence of a macrocrack, their association and definitive destruction of the specimen.

Identification of cracks, definition of their co-ordinates on the specimen surface sand measurement of it sizes was carried out visually by means of microscope MMP-4 ЛОМО and with application an eyepiece of a micrometer with which it is completed microhardnessmeter ПМТ-3.

After the control of a surface of the specimen the gain of quantity and length of cracks for a stage of tests, density of cracks on the surface area, growth rate of cracks was estimated.

For each microcrack was defined it growth speed $\Delta h = \Delta l / \Delta N$, where Δl - a gain of length of a crack for ΔN loading cycles.

Experimental data and their discussion. Figure 1 shows the relation between the crack length 2a of main cracks and the relative number of cycles to fracture cycles $N=N_f$ for two specimens in both alloys. From the figures, the crack propagation curves showed almost similar tendency in both alloys. Plural number of cracks occurred at each specimen, but crack didn't coalesce each other during the fatigue process and each main crack propagated individually. The

cracks initiated at very early stage from inclusions near surface, but they propagated very slowly during the early stage.

Process of accumulation of multiple damage can be characterised as formation at first a considerable quantity of small cracks, their gradual growth, and already then their gradual, and subsequently avalanche merges in cracks with much big sizes. The size of the microcracks arising in superficial plated layer of aluminum alloy Д-16АТ proportional to size of structural elements of a material.
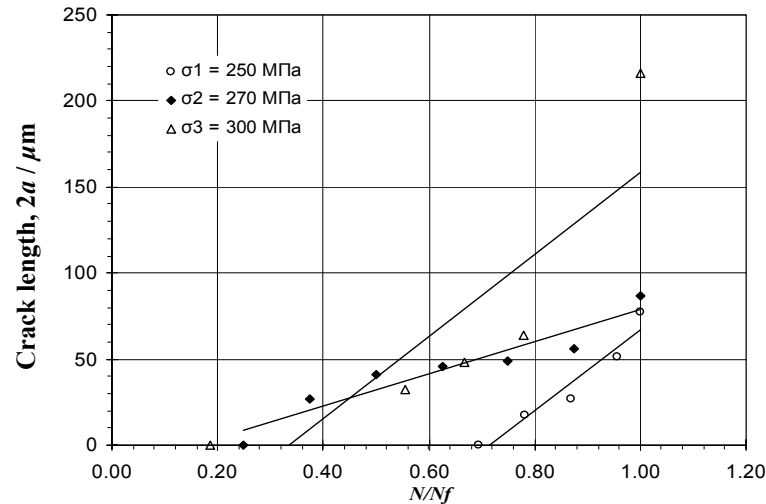
Fig. 1 Relation between crack length $2a$ and ratio of number of cycles to failure $N=N_f$.
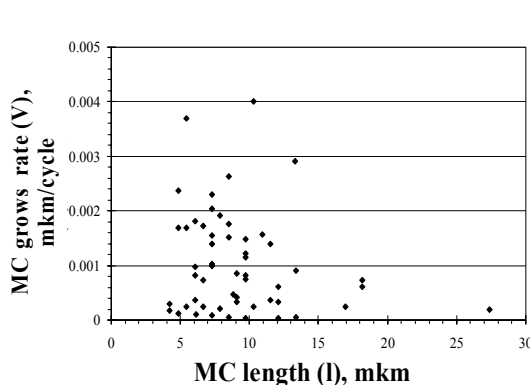
Fig.2. Dependence of the MC grows rate to their length
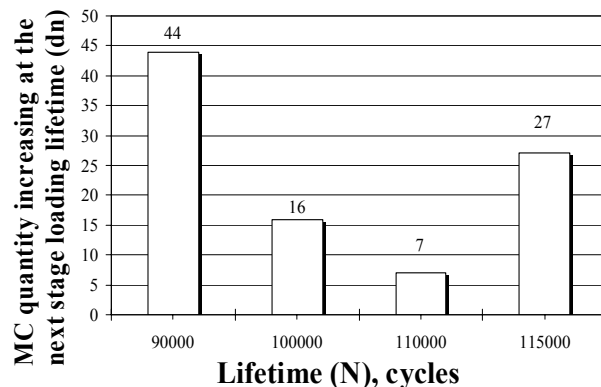
Fig.3. Dependence of the MC quantity increasing to the next stage loading lifetime

Thus microcracks which arise on steady strips of sliding in the middle of grain, extend within grain with certain speed then meeting structural barriers in the form of border of grain they stop or become such that do not extend. Thus a share of cracks which do not grow, or have very small growth rate - considerable (fig. 4). After the crack will overcome border of grain speed of its growth increases, except own growth also at the expense of association with the next cracks (fig. 3). On the basis of the examined laws it is possible to draw a conclusion on casual character of MC growth rate (fig. 2).

From dependence on fig. 3 follows, that with an operating time, the quantity of new MC arising for surfaces of the specimen decreases up to a stage before destruction. It confirms the fact of prevalence of process of association MT on the big operating time.
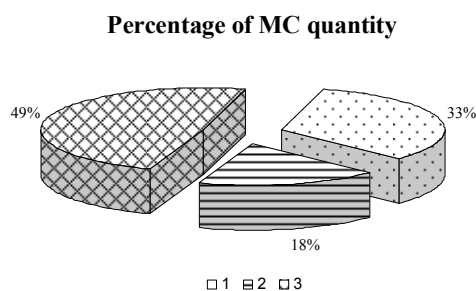
Fig.4. Percentage of MC quantity: 1 – $\Delta h=0$; 2 – which are disappeared; 3 – which are growing nonstop
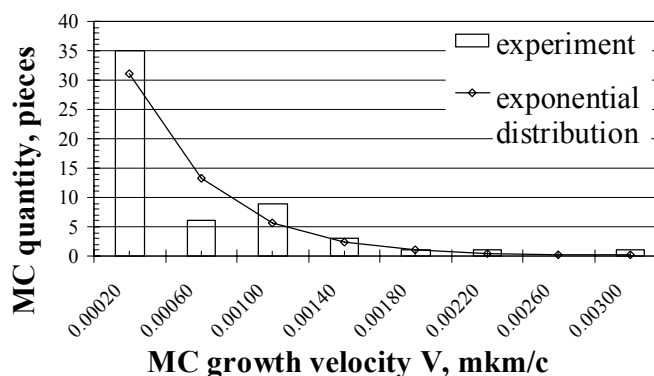
Fig.5. Dependence of the MC quantity to their growth velocity

At a cyclic loading dependence of dissipated microcracks quantity from quantity of cycles of a loading as a rule is linear. Thus the final stage of the damage connected with formation of cracks of higher dimensional level, is characterized by reduction of quantity of dissipated defects because of their intensive association. In some cases it leads to reduction of speed of accumulation of cracks and a deviation of corresponding dependence on the linear.

Conclusions

The question of MC growing is investigated. Namely growth rate of cracks and a kinetics of MC growth. Thus received, that on a surface of the specimen the part of cracks grows with constant speed, a part - in steps, the part does not extend, and the part from them disappears, i.e. so-called "healing" MC (fig. 3) is observed.

At statistical processing of empirical histograms of crack quantity to their speeds distribution it has been received, that the given distributions are approximated by the indicative law (fig. 4).

The major factor defining destruction at multiple damaging, is association of dispersed cracks, especially at a finishing stage which makes, approximately, 30 % from the general durability. At this stage of growth of the largest crack it is carried out exclusively at the expense of its association with other cracks along a distribution trajectory.

References

1. *Немец Я.* Развитие усталостных трещин // Проблемы прочности. – 1988. – № 7. – С. 9–18.

2. *Ботвина Л.Р.* Кинетика разрушения конструкционных материалов. - М.: Наука, 1989. - 232 с.

3. Механика разрушения и прочность материалов. Справочное пособие в 4-х томах. / Под общей ред. В.В. Панасюка. – К.: Наукова думка, – 1988 – 1990. –Т. 4: Усталость и циклическая трещиностойкость конструкционных материалов. / *О.Н. Романив, С.Я Ярема и др.*, – 1990, – 680с.

4. *Школьник Л.М.* Скорость роста трещин и живучесть металла. - М.: Металлургия, 1973.-216 с.

5. *Suh C. M., Kitagawa H. (1986)* Crack growth behaviour of fatigue microcracks in low carbon steels. Fatigue Fract. Eng. Mater. Structures. - 9, № 6. - P. 409-424.

6. *Игнатович С.Р., Кучер А.Г., Якушенко А.С., Башта А.В.* Моделирование объединения рассеянных поверхностных трещин. Сообщение 1. Вероятностная модель объединения трещин // Пробл. прочности. – 2004. –№2. – С. 21–32.

7. *Gao N, Brown M.W., Miller K.J.* Crack growth morphology and microstructural changes in 316 stainless steel under creep-fatigue cycling // Fatigue Fract. Eng. Mater. Structur. - 1995. - 18, № 12. - P. 1407-1422.

UDC: 623.746

V.M. Kindrachuk, Dr., (Institute for Materials Research and Testing, Berlin, Germany)
B.A. Galanov, Dr., V.V. Kartuzov, Dr.
(Frantzevich Institute for Problems of Materials Science, Kyiv, Ukraine)
M.V. Kindrachuk, Dr., (National Aviation University, Kiev, Ukraine)

ON CONTACT SURFACE (NANO) INDENTATION TANGENTIAL DISPLACEMENTS THEORETICAL ACCOUNTING

Elastic contact between a non-ideal Berkovich indenter and a half-space is investigated. The derived mathematical model of the contact allows for tangential displacements of the boundary points of the half-space. The tip of the blunted indenter is simulated as a smooth surface. The boundary element method is implemented in the model for numerical simulation of nanoindentation.

Introduction. Indentation is a widely used tool in the study of mechanical properties of materials, such as hardness H and elastic modulus E on the micro- and millimeter scales. For the analysis of material on the smaller scale a nanoindentation technique has been developed. However, the results gained by the nanoindentation test are more complicated to interpret. A number of factors have to be taken into account, since they are highly relevant on the nanometer scale. These can be the roughness of contacting surfaces, non-planar surface of samples, non-ideal shape of indenters *etc*. Therefore, a more careful examination of exactly what these effects cause on the interpretation of nanoindentation is required.

In respect to development of its mathematical model, indentation is a subject of the contact mechanics. Hertz presented the first theory of mechanical contact more than a century ago [1]. It is restricted to frictionless contact between elastic bodies and smooth surfaces. Hertz considered only the normal displacements on the surface of solids. However, it is known [2, 3] that the Hertzian formulation of the contact problem causes the incompatibility of the strains in the area around the contact. It was shown in [2] that the mentioned incompatibility of the strains depends strongly on whether the formulation of the contact problem takes into account the free tangential displacements on the contact surfaces. The tangential displacements were firstly accounted for in the works of Galanov [2, 4] and later in the works of Soldatenkov [5] and Argatov [6]. The two-dimensional wedge indentation of an elastic half-plane was considered in the work of Georgiadis [7]. He showed analytically, that a singularity in the contact stress at the wedge apex did not occur after accounting for tangential displacements. However, the boundary integral equation method was suggested for more general and difficult contact problems.

In the present work we develop the refined model of the three-dimensional contact problem, which accounts for both the tangential displacements on the contact surface of samples and for the bluntness of the indenter tip. We consider the indentation of half-spaced samples by the widely used Berkovich indenter. A rigid indenter is assumed. Therefore, there are elastic tangential displacements only on the surface of the sample. The other hypotheses of the Hertzian formulation remain without changes. The method of non-linear integral boundary equations (NIBEs) is applied to formulate the problem [8, 9]. The numerical solution of NIBEs is carried out by means of the boundary element method.

The analysis of nanoindentation by an ideal Berkovich indenter is a complicated problem itself, since the Galin-Sneddon solution is invalid in this case [10]. It is clear, that an investigation of nanoindentation by a non-ideal Berkovich indenter is even more intricate problem. However, fundamental relations for general three-dimensional schemes of nanoindentation by indenters of non-ideal shapes were derived [11], where the indenter shape near the tip was approximated by homogeneous functions. It was shown, that degrees of the shape functions for blunted indenters vary between 1 (cone or pyramid) and 2 (elliptic paraboloid tip). An approximation of the indenter bluntness by the homogeneous functions with the degree 2 is used in the present study, in order to derive a numerical solution for the load-displacement curves of nanoindentation.

The mathematical model presented in this work is formulated in a dimensionless form. This has two advantages. First, the model is valid both for elastic micro- and macro-contacts. Second, the simulation of nanoindentation data becomes more convenient, since the results of numerical solutions of the dimensionless problem can be easily rescaled to match conditions of a real experiment.

Table of symbols

O, x_1, x_2, x_3	Cartesian coordinate system
M, N	Points on the plane $x_3 = 0$
R_{MN}	Distance between points $M(x_1, x_2)$ and $N(\xi, \eta)$
r	Distance between point M and the origin O, $r = \sqrt{x_1^2 + x_2^2}$
h	Displacement of the indenter
$f(x_1, x_2)$	Gap between the indenter and the specimen before deformation
γ	Angle between Ox_3 and $O'E$, depends on the position of M (see Fig. 1)
R	Radius describing the shape of the blunted indenter tip, depends on the position of M
β	Indenter parameter, $\beta = \cot 65^\circ = 0.466$
d	Bluntness of the indenter tip
r_c	Distance between the origin O and the contour of the orthogonal projection of the bluntness to the plane $x_3 = 0$
S	Orthogonal projection of the contact region on the plane $x_3 = 0$ after deformation
Ω	An arbitrary area in the plane $x_3 = 0$ containing the contact region
$v(M), M \in \Omega$	Unknown function in the integral boundary equation
P	Force applied to the indenter in the direction normal to the flat surface of the specimen
$P_0(h)$	Dimensionless compression force
E_i, υ_i	Young's modulus and Poisson's ratio respectively of the diamond indenter
E_s, υ_s	Young's modulus and Poisson's ratio respectively of the sample
$K(M, N)$	Kernel of the integral operator

Model equations. We use the mathematical model of a unilateral contact between the Berkovich rigid indenter and an elastic half-space (sample). The indenter with the equation of the surface $x_3 = -f(x_1, x_2)$ is pressed by the force P to a boundary of the contacting sample (see Fig. 1). The sample is considered as a positive half-space $x_3 \geq 0$. The origin O of Cartesian coordinates, x_1, x_2, x_3, is put at the single point of the initial contact between the indenter and the sample. The contact region S is an orthogonal projection of the contact between the sample and the lateral surface of the indenter on the plane $x_3 = 0$ after deformation.

a   *b*
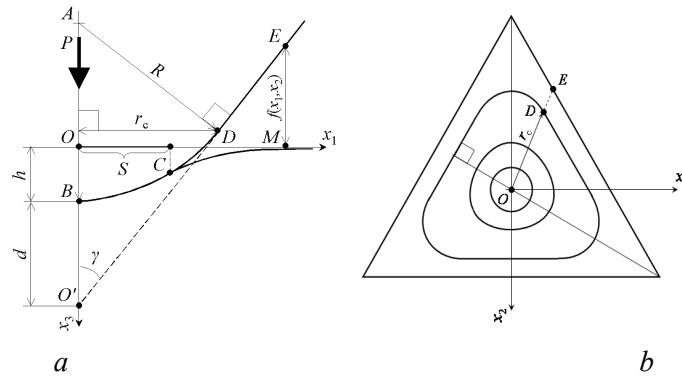
Fig. 1. (*a*) Geometry of the simulated blunted indenter, *BCDE*, and of the ideal Berkovich indenter, *O'DE*. The segment *BD* is the arc of the circle with the centre *A* and radius *R*; *d* is the bluntness of the indenter tip. *OB* is the displacement of the indenter, which causes the contact *BC* with the sample. (*b*) Cross section of the simulated blunted indenter. The contour lines correspond to various positions of *D*

The bluntness of the Berkovich indenter is modelled in the same way as in the previous paper [12] in which arcs of different curvature form the surface of the bluntness, see Fig. 1(*b*). All these arcs lie in the planes containing the axis Ox_3. Before deformation, the bottom end of each arc coincides with the origin O in such a way, that the surface of the bluntness is smooth in the vicinity of the origin O. The upper end of each arc lies on the surface of the Berkovich indenter, so that a smooth transition from the blunted shape ($r \le r_c$) to the pyramidal one ($r > r_c$) occurs. The distance, r_c, is that between the origin, O, and the projection of the upper ends of the arcs to the plane $x_3 = 0$, *i.e.* r_c defines the contour of the orthogonal projection of the bluntness to the plane $x_3 = 0$. The condition of the smooth transition yields the relations [12]:

$$r_c = R \cdot \cos\gamma,$$
$$R = d \cdot \frac{\sin\gamma}{1 - \sin\gamma}, \tag{1};$$

where: R is the radius describing the shape of the blunted indenter, as shown in Fig. 1, *a*; d is the bluntness of the indenter tip. Let us introduce the function $s(M) \equiv s(x_1, x_2) = \frac{\sin\gamma}{1 - \sin\gamma}$, where (x_1, x_2) are the coordinates of the point M lying on the plane $x_3 = 0$. Since γ lies in the range $\left[65°; 76.8° \right]$, then $s(x_1, x_2)$ ranges from 9.67 to 36.8 respectively.

The set of NIBEs [8; 9] (with an unknown function $v(M)$, $M \in \Omega$, and displacement h) is applied to formulate the model:

$$\mu v^-(M) + \lambda \iint_\Omega K(M, N) v^+(N) dS_N = h - f(M), \quad M, N \in \Omega,$$
$$\iint_\Omega v^+(N) dS_N = P, \tag{2};$$
$$\mu, \lambda > 0.$$

Here $v^+(M) = \sup\{v(M), 0\}$ is the contact pressure and $v^-(M) = \inf\{v(M), 0\}$. The function $\left(-\mu v^-(M) \right)$ defines the gap between the indenter and the specimen after deformation and μ is an arbitrary positive parameter. The indenter is rigid, so λ is defined only by the elastic constants of the sample $\lambda = \frac{1 - \upsilon_s^2}{\pi E_s}$. For the region Ω we further assume $\Omega = \{M : h > f(M)\}$. The kernel $K(M, N)$ of the integral operator in (2) accounts for the normal (in the direction Ox_3) and for the tangential (in the plane $x_3 = 0$) displacements of the half-space on the contact surface. If only the blunted shape of the indenter is contacting, then:

$$K(M, N) = \frac{1}{R_{MN}} - \frac{\varepsilon}{R} \cdot \frac{x_1^2 + x_2^2 - (x_1 \xi + x_2 \eta)}{R_{MN}^2} \tag{3};$$

where (x_1, x_2) and (ξ, η) are the coordinates of the points M and N lying on the plane $x_3 = 0$; $2\varepsilon = \frac{1 - 2\upsilon_s}{1 - \upsilon_s}$. The first term in (3) corresponds to the normal displacements of the contact surface. The second one allows for the tangential displacements on the contact surface, which are induced by the surface of the bluntness.

We consider further the contact between the bluntness of an indenter and a sample. This contact occurs if the contact region $S = \{M : v(M) \ge 0\} \subseteq \Omega$ lies within the orthogonal projection of the bluntness to the plane $x_3 = 0$, *i.e.* $\{M : v(M) \ge 0\} \subset \{M : r \le r_c\}$. As follows from Fig. 1, this condition is satisfied if $h < d$. Indeed, let us define $r_{contact}$ as the distance between the origin O and the contour of the contact region S. As is seen from Fig. 1, $r_{contact} \le \sqrt{2hR}$. According to (1) $r_c = R \cos\gamma$. Then,

$$\frac{r_{contact}}{r_c} \le \frac{\sqrt{2hR}}{R \cos\gamma} = \sqrt{\frac{2h}{d \cdot s(x_1, x_2) \cdot \cos^2\gamma}} < \sqrt{\frac{2}{1.8} \cdot \frac{h}{d}} < \sqrt{\frac{h}{d}}.$$

On the assumption of $r \le r_c$ one has the following expression for the function $f(M)$:

$$f(M) = R - \sqrt{R^2 - r^2}. \tag{4};$$

However, if $h < d$, then $\left(\dfrac{r}{R}\right)^2 \ll 1$. Therefore the function in (4) can be approximated as:

$$f(M) = \frac{r^2}{2R}.$$
(5);

The function $f(M)$ in (2) and defined further in (5) is not the paraboloid as in the Hertzian problem, since R depends on M accordingly to (1).

Before starting the numerical calculations, the system (2) is reformulated in a dimensionless form [15]. The derivation of the final formula for the load-displacement diagram:

$$P = \frac{\sqrt{2d}}{\lambda} \cdot P_0(h) \cdot h^{3/2} \tag{6};$$

To obtain the function $P_0(h)$, the numerical solution of the set in (B.1) at different values of the mutual approach h is necessary.

Results and discussion. The tangential displacements influence the load-displacement curves (6) only via the dimensionless compression force $P_0(h)$. Therefore, it is enough to consider this function to comprehend the relations between tangential displacements and the indentation behavior of different materials.

As can be seen from (B.1), the equation used for determination of the dimensionless contact pressure U^+ and therefore of $P_0(h)$ includes the displacement h, the parameter of the indenter bluntness d and the Poisson's ratio υ_s of the sample material. Moreover, all these quantities are included only in the term which accounts for tangential displacements. Hence, the influence of the properties of the sample being indented on the value arising tangential displacements is determined by the Poisson's ratio of the sample material υ_s and does not depend on its Young's modulus.

If $\upsilon_s = 0.5$ ($\varepsilon = 0$ for a perfectly incompressible material) then the term accounting for the tangential displacements in (B.1) is zero and tangential displacements do not arise during indentation. This result is well-known from the literature [13]. In this case the function $P_0(h)$ does not depend on the displacement h. Its value P_0 is determined by the shape of the indenter. The resulting load P in (6) is proportional to $h^{3/2}$.

Otherwise, if $\upsilon_s < 0.5$ ($\varepsilon > 0$), then tangential displacements occur and the relation $\varepsilon \cdot \sqrt{\dfrac{h}{d}}$ determines their magnitude. The resulting load P is no longer proportional to $h^{3/2}$.

To quantify the effect of tangential displacements on the load-displacement curves, the set (B.1) was solved numerically and the function $P_0(h)$ obtained at various values of the Poisson's ratio ($\upsilon_s = 0 - 0.5$) of the sample material. We have set the indenter parameter as $\beta = 0.466$. The solution for $P_0(h)$ is given in Fig. 2(*a*). The black points correspond to the numerical solutions. Fitting the data set in Fig. 2(*b*) by $P_0(h) = P_0 + b \cdot \left(\dfrac{h}{d}\right)^{\gamma}$ yields the curves with parameters that are listed in table 1.

The dimensionless compression force, $P_0(h)$ at $\upsilon_s = 0.5$ is $P_0 = 1.277$ and obtained by the numerical solution of (B.1). Therefore, the dependences of $P_0(h)$ and $P(h)$ on the displacement h can be approximated by:

$$P_0(h) \approx P_0 + b(\upsilon_s) \cdot \sqrt{\frac{h}{d}}, \tag{7}$$

$$P(h) \approx \frac{\sqrt{2d}}{\lambda} \cdot P_0 \cdot h^{3/2} + \frac{\sqrt{2}}{\lambda} \cdot b(\upsilon_s) \cdot h^2,$$

where $b(\upsilon_s)$ is a function depending on Poisson's ratio of the sample material, $b(0.5) = 0$.
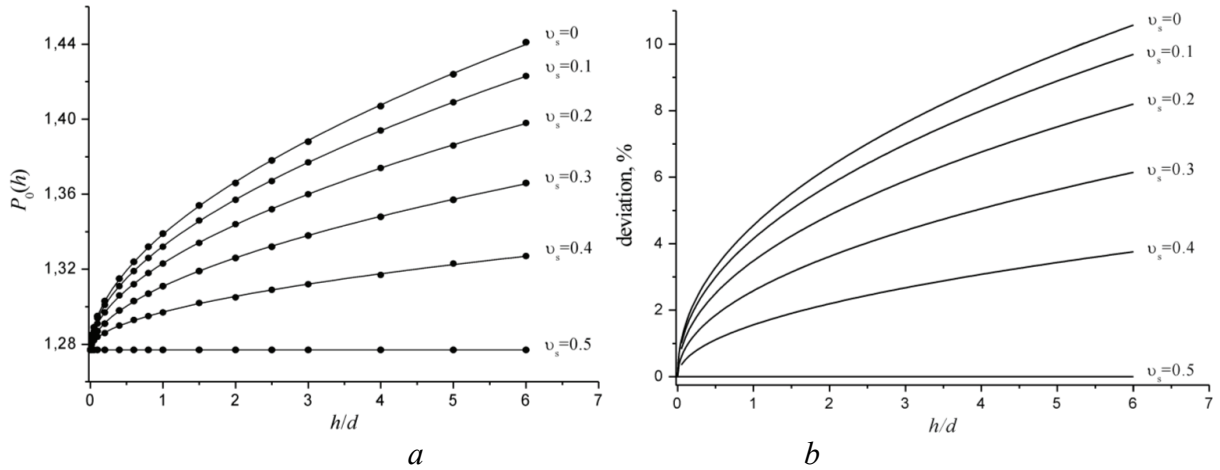
Fig. 2. Dimensionless compression force as a function of the indenter displacement for the samples with different Poisson's ratios (*a*). The relative deviation of the load determination, see (*8*), indicates the influence of the tangential displacements on the determination of the load at a given displacement (*b*).

The values of the parameters *b* and χ which yield the best-fit of the dimensionless compression force (black points in Fig. 2(*a*)) by the function $P_0 + b \cdot \left(\frac{h}{d}\right)^{\chi}$

υ_s	$b\,(10^{-2})$	$\chi\,(10^{-1})$
0	6.17 ± 0.08	5.41 ± 0.02
0.1	5.56 ± 0.08	5.37 ± 0.03
0.2	4.63 ± 0.07	5.32 ± 0.03
0.3	3.38 ± 0.05	5.34 ± 0.02
0.4	2.03 ± 0.05	5 ± 0.03
0.5	0	0

It should be noted, that if the tangential displacements in the model are neglected, then the dimensionless compression force $P_0(h) = P_0 = 1.277$, regardless of the value of Poisson's ratio υ_s. Neglecting tangential displacements one gets smaller values for the dimensionless compression force and consequently a smaller value of the load compared to the values calculated when accounting for tangential displacements. The deviation of the dimensionless compression force (7) is $b(\upsilon_s) \cdot \sqrt{\frac{h}{d}}$ and the deviation of the load (6) is $\Delta P \approx \frac{\sqrt{2}}{\lambda} \cdot b(\upsilon_s) \cdot h^2$. Hence, the load discrepancy growth is approximately quadratic as the displacement increases.

Let us introduce the relative deviation of the load determination $dev = \left(P(h) - P_{no\,TD}(h)\right)/P(h)$, which occurs if tangential displacements are not considered. Accordingly to (7) the relative deviation can be estimated as:

$$dev = \frac{P(h) - P_{no\,TD}(h)}{P(h)} \approx \frac{b(\upsilon_s) \cdot \sqrt{\frac{h}{d}}}{1.277 + b(\upsilon_s) \cdot \sqrt{\frac{h}{d}}} \qquad (8);$$

where $P(h)$ is the load calculated according to (6) with allowance for tangential displacements; $P_{no\,TD}(h)$ is the load calculated accordingly to (6) with the constant value of $P_0 = 1.277$, *i.e.* without the allowance for tangential displacements (further the model neglecting tangential displacements). The dependence of the relative deviation function (8) on the

dimensionless displacement of the indenter is shown in Fig. 2(*b*) for various values of Poisson's ratio υ_s of the sample material. It is seen, the discrepancy in determination of the load accumulates as the displacement increases.

Conclusions:

The frictionless indentation of an elastic half-space (sample) by the rigid Berkovich indenter of non-ideal shape is investigated. The formulation doesn't neglect the tangential surface displacements, coupling them with the normal surface displacements. The derived mathematical model of the elastic contact is based on a set of non-linear integral boundary equations.

It is shown that the dependence of the load on the indenter displacements consists of two terms. The first term is caused by the normal surface displacements and is proportional to $h^{3/2}$. The second term results from the tangential displacements and is approximately proportional to h^2. This term vanishes if Poisson's ratio of the sample approaches 0.5. The value of the second term can achieve 5 % of the total load, at displacements of the indenter comparable with the value of the parameter of the indenter bluntness.

References

1. *Hertz H.* 1882 J. reine und angewandte Mathematik 92 156 – 71.
2. *Galanov B. A.* 1982 Dokl. Akad. Nauk Ukr. SSR 7 36 – 40.
3. *Galanov B. A., Grigor'ev O. N.* 1986 Strength Mater. 18 1330 – 7.
4. *Galanov B. A.* 1983 Izv. Akad. Nauk SSSR, Mekh. Tverd. Tela 6 56 – 63.
5. *Soldatenkov I. A.* 1994 Izv. Ross. Akad. Nauk, Mekh. Tverd. Tela 4 51 – 61.
6. *Argatov I. I.* 2004 J. Appl. Mech. Tech. Phys. 45 118 – 23.
7. *Georgiadis H. G.* 1998 Comput. Mech. 21 347 – 52.
8. *Galanov B. A.* 1993 J. Math. Sci. 66 2414 – 8.
9. *Galanov B. A.* 1985 J. Appl. Math. Mech. 49 634 – 40.
10. *Borodich F. M., Keer L. M.* 2004 Int. J. Solids Struct. 41 2479 – 99.
11. *Borodich F. M., Keer L. M. and Korach C. S.* 2003 Nanotechnology 14 803 – 8.
12. *Kindrachuk V. M.* 2006 Nanotechnology 17 1104 – 11
13. *Johnson K. L.* 1985 Contact Mechanics (Cambridge: Cambridge University Press).
14. *Landau L. D., Lifshitz E. M.* 1986 Theory of elasticity. In Course of Theoretical Physics, 7 (NY: Pergamon Press).

UDC: 621.891

A.A. Kornienko, Ph.D. engineer, assistant professor (National Aviation University, Ukraine)
S.V. Fedorchuk, senior teacher (National Aviation University, Ukraine)

STRUCTURE OF COMPOSITE ELECTROLYTIC COATINGS WITH EUTECTIC FILLER DESIGNED FOR OPERATION AT ELEVATED TEMPERATURES

The investigations of structure, elements distribution and microhardness of areas: matrix-transition area-particle of composite electrolytic nickel-based coatings are carried out. As a filler of composite coatings the powder of wear proof eutectic alloy designed for operation at elevated temperatures is used.

Introduction. An effective solution to the problem of increasing the heat and wear resistance of parts made from construction materials is the formation on them of wear-resistant composite layers hardened by high-melting borides and carbides with using eutectic reaction between them since the high-temperature strength and thermal stability is determined by their structure and phase state. This solution has been successfully realized thanks to using composite electrolytic coatings (CEC), composed of a ductile metallic matrix and wear-resistant powdered filler [1]. The paper [2] shows that the phases TiB_2, CrB_2 and VC are characterized by chemical compatibility, strong connection and are in stable equilibrium with metal base (steel 12X18H9T) at elevated temperatures (up to $0,9T_{melt}$). Such alloys are suitable to work in friction units at simultaneous action of chemically active medium and elevated temperatures without lubrication. Therefore the present work aim is to develop the composite electrolytic coatings hardened by eutectic fillers for operation at elevated temperatures and investigate their structure.

Experimental procedure. Composite electrolytic coatings were produced through silting of strengthening especially designed to operate at elevated temperatures eutectic powders [3] with electrolytic nickel. The fractions of particles were ranged from 50 to 80 μm and were deposited onto the horizontal cathode under impulse stirring of the electrolyte at a current density of 5-10 A/dm^2. The heat treatment of samples with coating was vacuum annealing at temperatures 950 ºC and 1250 ºC. The structure was investigated with optical microscope "Неорнот 21" and scanning electron microscope "РЕММА-102-02", microhardness – ПМТ-3, element composition – energy dispersive spectrometer "Link 860/500".

Results and discussion. The structure of matrix-filled CEC nickel – eutectic fillers is shown on Fig 1.

a   *b*
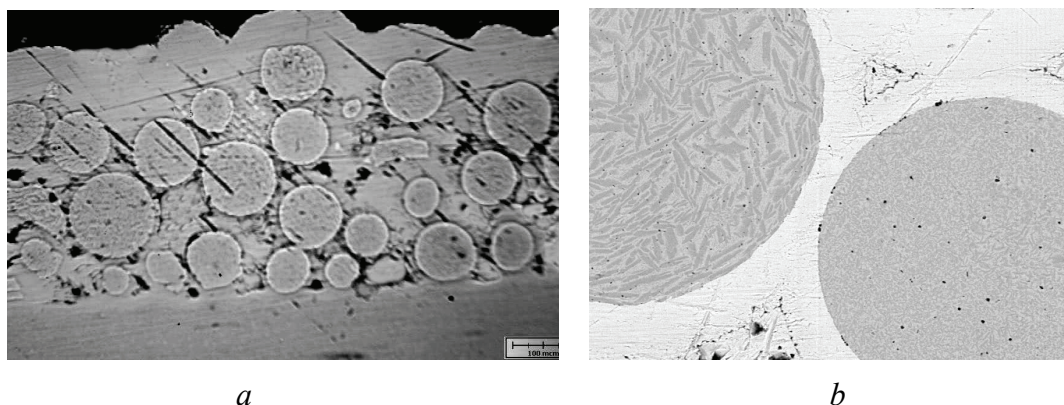
Fig. 1. The structure of CEC nickel – eutectic fillers without heat treatment:
$\times$ 100 (*a*); $\times$ 600 (*b*)

The coating consists of nickel matrix with fillers of eutectic powders. So long as particles of eutectic powder are electroconducting fillers the obtained coating is characterized by small porosity about 5%.

Preparatory tribological tests shown insufficient high wear resistance of obtained coating due to low adhesive bond of coating with substrate layer in raw state and low cohesive resistance due to porosity (Fig. 1, *a*) and absence of interaction between matrix and fillers (Fig. 1, *б*), that results in chipping of filler particles under investigation.

Therefore is necessary to perform heat treatment of the CEC by vacuum annealing.

The two variants of heat treatment temperature conditions were chosen: 1 – without remelting of coating at temperature 950 ºC, that is about 80 % of melting temperature (equalizing is 30 min and cooling with kiln); 2 – with remelting of coating at temperature 1250 ºC (equalizing is 30 min and cooling with kiln).

The metallurgical studies of boundary area filler – matrix for samples after heat treatment at temperature 950 º C showed that the eutectic crystals have equal sizes (Fig. 2, *b*) due to eutectic recrystallization and the dissolution of obvious interface (Fig. 2).

a   *b*
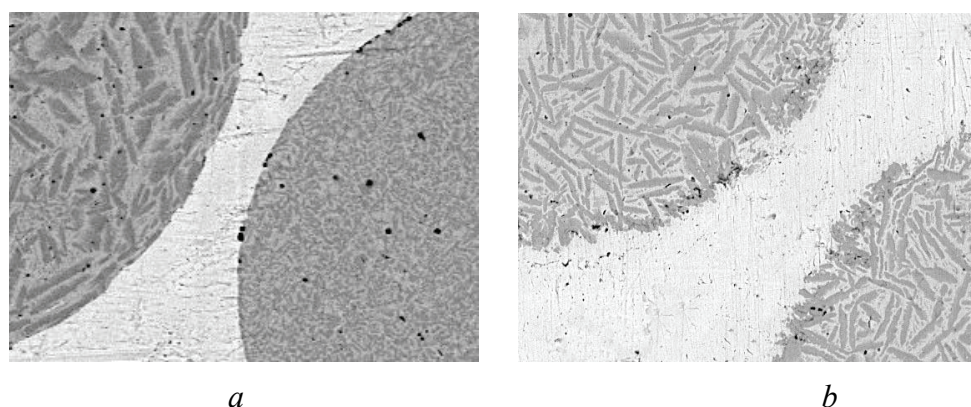
Рис. 2. The structure of CEC nickel – eutectic fillers, × 1000: *a* – without heat treatment; *b* – after heat treatment at temperature 950 ºC without coating remelting

The investigation of coatings chemical composition analysis (table 1) by X-ray spectrum analysis showed, that the heat treatment results in changing of chemical composition of coating components due to interdiffusion between matrix and filler, structure and phase transformation. Thus the transitional area between matrix and filler with increased content Ti, Cr, Fe in contrast to chemical composition of boundary area filler – matrix for samples before heat treatment was appeared, at that there isn't the essential changing of filler chemical composition.

Table 1

Chemical composition of CEC

Element, %	matrix			boundary area			filler		
	without heat treatment	after heat treatment at 950 ºC	after heat treatment at 1250 ºC	without heat treatment	after heat treatment at 950 ºC	after heat treatment at 1250 ºC	without heat treatment	after heat treatment at 950 ºC	after heat treatment at 1250 ºC
Ti	0,08	0,09	0,14	0,10	0,17	0,19	0,24	0,23	0,21
Cr	0,03	2,9	12,1	0,67	8,3	22,11	26,91	28,63	23,09
Fe	0,44	8,37	35,05	1,72	33,68	47,02	63,03	61,71	51,01
Ni	99,45	88,64	52,71	97,51	57,85	30,68	9,82	9,43	25,69

Fig. 3. The structure of remelted CEC after heat treatment at temperature 1250 ºC, × 200

After heat treatment at temperature 1250 ºC the coating is remelted (Fig. 3), but there are areas with different chemical composition (табл. 1), that for convenience may be considered as matrix, transitional area and filler.

The heat treatment hardened matrix. Thus the microhardness measurements before and after heat treatment for different coating areas shows (table 2) that the microhrdness of nickel matrix was increasing after heat treatment due to matrix alloying by filler elements and nickel recrystallization. At that the transitional area between matrix and filler with increased microhardness ($H\mu$=4,5–5,5 GPa) was appeared.

Table 2

Microhardness of CEC, GPa

Heat treatment of coating	Without heat treatment	After heat treatment at 950 ºC	After heat treatment at 1250 ºC
Matrix	3,0–3,2	3,3–4,0	4,0–4,7
Filler	8,1–8,9	6,7–7,5	6,0–6,5

The microhardness of filler after heat treatment is less due to recrystallization of eutectic powders at temperature 950 °C (Fig. 2 *a*, *b*) and remelting at temperature 1250 °C with appearing of eutectic and solid solution of iron and nickel (Fig. 3).

Conclusions:

The heat treatment of CEC of system nickel – eutectic alloy without remelting and with remelting significantly changes the structure and the element allocation of coating areas: matrix, boundary area, filler. As a filler the especially designed to operate at elevated temperatures eutectic powder was used. The heat treatments (vacuum annealing at temperatures 950 ºC and 1250 ºC) are used for increasing matrix mechanical properties, adhesive and cohesive strength. Besides, the heat treatment at temperatures higher than forecast working temperatures of friction units allows avoiding uncontrolled structural change inside coating under action of working temperatures, since the developed coatings are planned to use for operation for friction units at elevated temperatures.

The work needs further elaboration. The next stage of research will be the tribological investigations of developed CEC in conditions of room temperature and especially elevated temperatures.

References

1. *Лучка М.В., Киндрачук М.В., Мельник П.И.* Износостойкие диффузионно легированные композиционные покрытия. – К.: Техника, 1993. – 143с.

2. *Кіндрачук М.В.* Вплив структури евтектичних плазмових покриттів на їхні триботехнічні властивості в широкому діапазоні температур / М.В. Кіндрачук // Фізико-хімічна механіка матеріалів. –№4. – С.66–71.

3. Пат. 27849 Україна, МПК C23C 8/02. Зносостійкий сплав / В.Є. Панарін, М.В. Кіндрачук, Джамаль Ібрагим Мансур, С.В. Федорчук, В.В. Погоріла. Заявл. 21.08.07; опубл. 12.11.07, Бюл. №11, 2007.

UDC: 621.78(043.2)

V. Kravtsov, PhD, professor (National Aviation University, Ukraine)
M. Sadegy, postgraduate (National Aviation University, Ukraine)

BIFURCATIONAL LOSS OF STABILITY OF UNDERLAYMENTS OF FRICTION AT QUASYSTATIC LOADS

The method of determination of steady forms of equilibrium is examined after the loss of stability. These processes can arise up at a friction on the borders of underlayments. For research the method of decision of usual differential equalizations is used, that is based on joint application of method of continuation on a parameter and method of Newton. There is possibility to determine the great number of decisions after the loss of stability.

At research of the intense condition of basic surfaces or their microscopic roughnesses often it is necessary to define behaviour of investigated elements at loss of stability. Thus there can be a great number of supercritical forms after the loss of stability. In these cases it is necessary to possess a mathematical model by means of that it is possible to define the critical loading and possible supercritical forms of equilibrium.

For overcoming of this problem methodology of numeral research of nonlinear deformation of resilient elements is offered, that uses the known decisions of Lagrange and Euler. This methodology describes an equilibrium and deformation of resilient element, his external and internal geometry [1]. We will describe a research method briefly.

We will enter and is $\bar{n}$, $\bar{b}$, $\bar{\tau}$ - natural trihedron with the single coordinates of main normal and tangent; u,v,w - coordinates of movable trihedron; $\bar{F}$, $\bar{M}$ - are vectors of internal efforts and moments; p, q, r - curvatures in relation to the coordinates of movable trihedron; x, y, z - coordinates of independent variable of s.

We will present the system of resolvent equalizations that describe deformation of resilient element, in a kind

$$\mathbf{x'}=\mathbf{f}(\mathbf{x},s,\lambda), \tag{1}$$

here a $\mathbf{x}(s)=(F_u(s),F_v(s),F_w(s),p(s),q(s),r(s),\tau_x(s),\tau_y(s),\tau_z(s),$

$n_x(s),n_y(s),n_z(s),b_x(s),b_y(s),b_z(s),x(s),y(s),z(s))^T$ – vector of position (m=18), f–vector-function of right parts of the system of equalizations; λ – parameter of intensity of loading (a derivative marks a stroke on s). A parameter λ can be both actual and formal, that represents quantitative descriptions of task.

On this basis the system of differential equalizations is got in borders $0 \le s \le S$, where the independent variable of s changes. This system of equalizations has the general eighteenth order. The presence of six first integrals

$$|\bar{\tau}| = 1, \ |\bar{n}| = 1, \ \bar{\tau}\bar{n} = 0, \ \bar{\tau}\times\bar{n} = \bar{b} \tag{2}$$

allows to decrease her order to twelfth. Methodology of decision of task, that is examined, based on sharing of method of continuation on a parameter and method Newton. The presence of six first integrals allows to decrease her order to twelfth. On verge of $s = 0$ interval of $0 \le s \le S$, where the variable of s changes six independent extreme conditions and six equalizations are set connections that appear the first integrals. For arrangement of the system of equalizations it is enough on verge of $s = S$ to set six independent extreme conditions $\bar{\psi}[\bar{x}(s)] = 0$. In these equalizations $\bar{\varphi},\bar{\theta},\bar{\psi}$ designate vectors-functions that have a dimension equal six.

Branching of decision $\mathbf{x}_0(s)$ at $\lambda=\lambda_0$ maybe only then, when at the $\mathbf{x}_0(t),\lambda_0$ corresponding linearized task has a non-trivial decision. That making sure, that it takes place, is necessary to investigate the extended $m \times (m + 1)$ matrix

$$[\mathbf{b}_C(\mathbf{C}_0,\lambda_0),\mathbf{b}_\lambda(\mathbf{C}_0,\lambda_0)]. \tag{3}$$

If the grade of this matrix is equal *m*, then there will be the unspecial minor key of order of *m*. According to a theorem about a non-obvious function, equalization $b(C,\lambda)=0$ can be decided in relation to components C and λ, corresponding to this minor key, expressing them through a remaining component. This decision will give in a vinicity (C_0,λ_0) an only continuous curve in (*m* + 1)- measure (C,λ) space, passing through (C_0,λ_0). If the grade of the made matrix less than, than *m*, then equalization of branching can have a few decisions near-by (C_0,λ_0). For their construction it is necessary to decide the task of theory of branching. In a general view she is formulated so:

1. To find $\mathbf{x}_0(s)$, λ_0, there is branching at that.

2. To define a number and directions of branching $(\mathbf{x}_0(s), \lambda_0)$ off decisions.

3. To build and investigate branching off decisions in a vinicity $(\mathbf{x}_0(s), \lambda_0)$.

One of methods of decision of this task is decomposition of function $\mathbf{b}(C,\lambda)$ in a limit row of Taylor in a vinicity (C_0,λ_0). He can be got, if has $\mathbf{b}$ necessary derivatives in a point (C_0,λ_0), that exist in case that $\mathbf{f}(\mathbf{x},s,\lambda)$ and $\mathbf{B}[\mathbf{x}(s,\lambda,C),\lambda]$ have corresponding derivatives on $\mathbf{x}$ and λ in a point $(\mathbf{x}_0,\lambda_0)$.

For the construction of close equalizations of branching it is necessary to take into account in correlation (3) members of higher-orders. Thus, at adding to him elements the second order, it will look

$$\frac{\partial b(C,\lambda)}{\partial C}\delta C + \frac{\partial b(C,\lambda)}{\partial \lambda}\delta\lambda + \frac{1}{2!}\frac{\partial}{\partial C}\frac{\partial b(C,\lambda)}{\partial C}\delta C\delta C +$$

$$+ \frac{\partial}{\partial \lambda}\frac{\partial \mathbf{b}(C,\lambda)}{\partial C}\delta C\delta\lambda + \frac{1}{2!}\frac{\partial}{\partial \lambda}\frac{\partial \mathbf{b}(C,\lambda)}{\partial \lambda}\delta\lambda^2 \approx 0. \qquad (4)$$

At the calculation of derivatives of vectorial function $\mathbf{b}(C,\lambda)$ it is necessary to differentiate a vectorial function $\mathbf{B}[\mathbf{x}(s,\lambda,C),\lambda]$, that depends difficult character on these variables. Therefore for the construction of close equalization of branching (3) it is necessary to dispose functions

$$\frac{\partial \mathbf{x}(s,C,\lambda)}{\partial C}, \frac{\partial \mathbf{x}(s,C,\lambda)}{\partial \lambda}, \frac{\partial}{\partial C}\frac{\partial \mathbf{x}(s,C,\lambda)}{\partial C}, \frac{\partial^2 \mathbf{x}(s,C,\lambda)}{\partial \lambda^2}, \frac{\partial}{\partial \lambda}\frac{\partial \mathbf{x}(s,C,\lambda)}{\partial C}.$$

We will enter denotations:

$$\frac{\partial \mathbf{x}(s)}{\partial C} = \mathbf{Y}(s), \frac{\partial \mathbf{x}(s)}{\partial \lambda} = y_\lambda(s), \frac{\partial}{\partial C}\frac{\partial \mathbf{x}(s)}{\partial C} = \frac{\partial \mathbf{Y}(s)}{\partial C} = \mathbf{Z}(s),$$

$$\frac{\partial}{\partial \lambda}\frac{\partial \mathbf{x}(s)}{\partial C} = \frac{\partial \mathbf{Y}(s)}{\partial \lambda} = \mathbf{Z}_\lambda(s), \frac{\partial^2 \mathbf{x}(s)}{\partial \lambda^2} = \frac{\partial \mathbf{y}_\lambda}{\partial \lambda} = \mathbf{Z}_\lambda(s). \qquad (5)$$

For the construction of three-index functional matrix of *Z(s)* it is necessary to differentiate both parts of equalization (5) on a size $\mathbf{C}$

$$\frac{d}{ds}\left(\frac{\partial \mathbf{Y}}{\partial \mathbf{C}}\right) = \mathbf{f}_x\frac{\partial Y}{\partial C} + \left\{\mathbf{f}_{xx}\frac{\partial x}{\partial C}, Y\right\}$$

or taking into account denotations that were accepted before

$$\frac{dZ}{ds}= \mathbf{f}_x\, Z + \{\mathbf{f}_{xx}, Y, Y\}. \tag{6}$$

Thus, the matrix of $Z(s)$ can be got by the decision of task Cauchy for equalization (5) with the initial conditions of $Z(0) = 0$. Уравнения для $\mathbf{Z}_\lambda(s)$ и $z_\lambda(s)$ получаются так же, но выглядят следующим образом Equalizations for $\mathbf{Z}_\lambda(s)$ and $z_\lambda(s)$ turn out similarly, but look like the following

$$\frac{dZ_\lambda}{ds}=\mathbf{f}_x Z_\lambda + \{(\mathbf{f}_{xx}\mathbf{y}_\lambda+\mathbf{f}_{x\lambda})\} \quad (\mathbf{Z}_\lambda(0) = 0), \tag{7}$$

$$\frac{dz_\lambda}{ds}=\mathbf{f}_x\mathbf{z}_\lambda+\mathbf{f}_{\lambda\lambda}+ \{(\mathbf{f}_{xx}\mathbf{y}_\lambda+\mathbf{f}_{x\lambda}),y_\lambda\} \quad (z_\lambda(0) = 0).$$

The decision of the system of nonlinear algebraic equalizations (7) can be got by the separation of roots with subsequent clarification by the method of Newton. For this purpose variations $\delta\lambda$ must be appropriated small positive $\delta\lambda = p$ or negative $\delta\lambda = -p$ value (p - small positive number) and at set $\delta\lambda$ from the system of m equalizations(4) to find the m component of vector . On occasion, when at the construction of decision of the system (4) the method of Newton meets badly, more comfortable as the independently varied parameter to choose one of components δC_i of vector $\delta\mathbf{C}_i$ and from the system (4) to find other components $\delta C_i \ (i\neq j)$ and $\delta\lambda$. Thus, if the system (4) does not have decisions or among roots there are multiple, it is necessary to decrease a size p, in equalizations of branching to take into account next members of decomposition and calculation to repeat. Further on a parameter it is possible the method of continuation to continue a bifurcational decision on each of branch. At the decision of the applied tasks the stage related to the construction of matrices-functions $\mathbf{y}_\lambda(s), Y(s), Z(s), Z_\lambda(s), z_\lambda(s)$ on large intervals $0\leq s\leq S$ appears most labour intensive. For these aims the numeral methods of decision of tasks Cauchy are used: method of Runge-Kutt of fourth order or method of Everhart of the eleventh order.

Conclusions:

At research of behavior of construction after the loss of stability often there are situations, when a few continuations of decisions that is directed on different branches from bifurcational points are possible. Them can be a few and on branches. At the construction of great number of positions of branches, that come from the point of bifurcation especially important the task of separation of steady branches appears from unsteady. For this purpose it is possible to take advantage of the known theorem of Lagrange-Dirichlet : if in position of the isolated equilibrium of the conservative mechanical system with ideal and stationary connections her complete potential energy has minimum, then this position of equilibrium is steady.

This theorem sets the sufficient terms of equilibrium of the conservative systems. According to her for proof of stability of equilibrium of the deformed system it is enough to make sure in that the sum of potential energy of resilient deformation and potential energy of external potential forces has in the examined position minimum. For the system with one degree of freedom, characterized generalized coordinate of q, determination of minimum decides elementaryly.

References

1. *Кравцов В.И.* Механика гибких глубоководных систем. - Киев.: Наук. думка, 1997. - 256 с.

UDC: 621.891

A.P. Danilov, postgraduate (National Aviation University, Ukraine)

MECHANISM OF GRADUAL AND SUDDEN FAILURES OF FRICTION KNOTS

The paper presents a brief overview and introduced a mechanism of gradual and sudden failure of tribological systems. It is shown that the phasing defines a partial and reversible destruction of the tribological behavior of structures, and sudden failures of the complete and irreversible destruction of these structures.

Failures of nodes in the friction of antifriction systems largely determine the reliability and safety equipment, they are limited resources, are the cause of accidents and disasters, and therefore, topical study of the mechanism and regularities of the failure modes in tribological systems, research in this direction.

Disclaimer - the event consisting in the violation of health facility. The efficiency is characterized in such a state of the object at which the values of all its parameters correspond to the requirements of normative-technical documentation.

To determine the numerical values of the majority of reliability required by the statistical data to calculate the number of failures that occurred in different periods of products.

Depending on the nature of changes in the basic parameter of the system before the occurrence of failures divided by the gradual and sudden [1].

Phasing out - it is a random event, consisting in a slow change in the output parameter and the law-it outside of the established requirements of normative-technical documentation. The reason for phasing in tribology is the wear of friction higher than the permissible value. Wear can be represented as the sum of independent variables on the interval τ, which isat $t \gg \tau$, according to the central limit theorem, is normally distributed and can be represented as:

$$I(t) = \langle i \rangle \; t \; \pm \; \tau\sigma \; \eta \; (t/\tau)^{1/2} , \tag{1}$$

where $I(t)$ –wear, $\langle i \rangle$ -the time-average value of wear, σ - standard deviation of the wear rate, η - a Gaussian variable with zero mean and unit variance.

From (1) the average wear rate $\langle i \rangle$ is defined as:

$$\langle i \rangle = I(t)/t \; \pm \; \sigma \; \eta \; (t/\tau)^{-1/2}$$

Time to reach limiting wear, as well as wear at fixed time are normally distributed and can therefore be calculated.

In the traditional mechanistic approach, the primary method of research in tribology is the analysis - a division of the elements, and the wear and tear is seen as variants of microcutting, cohesive, fatigue and brittle fracture surfaces of solids or chemical films formed. The following types of mechanical wear: abrasive, fatigue, corrosion, mechanical, fretting corrosion, cavitation, etc.

Sudden failure - this is a random event, which is equally likely to happen any moment, and which consists in an abrupt change of the parameter. In the state of tribology sudden failure can occur at any moment, and then, with a different probability to return to normal state, or refusal to develop a process that ends with an anomalously high value of wear, seizure, breakage or fire initiation [2].

Sudden failure determines the safety of technical systems. It can be caused by a sharp change in the external influencing factors. Such failure may also occur due to the gradual accumulation of damage that can not be detected in advance to use the available technical means, for example, lubricant starvation - the sudden destruction of the bearing cage, etc.

It was also found that the anti-friction system homogeneous with respect to only a small number of features of the process of failure. These signs tell about destruction of the tribological structures, which is reversible at wear and irreversible in case of failure [3]. In the real friction nods

failure is developing in the time intervals from several hours to several tens of hours. This allows us to detect a process failure at an early stage and prevent the dangerous consequences. Sudden failures are determined by frequency of occurrence of abnormal conditions in the tribological contact, that is, a sequence of discrete events. The use of time spent in this state as a temporary measure and interprets the probability to combine the two streams (gradual and sudden failures) into a coherent whole: the discrete and continuous. In this case the random variables, such as failure rate, time to reach the maximum allowable value of wear, time to first failure and mean time between failures is used as a measure, and the probabilities of these states – as the characteristics of the processes of failure.

In the study of rare events, the property of the function $(1+x)^{1/x}$, which lies in the fact that as $x \to 0$, this quantity tends to the limit $e \approx 2{,}718$. If the probability of failure of the friction hour operation is ρ, then the probability that the failure does not appear within n hours is

$$1-(1-p)^n = 1-(1-p)^{-1/p(-np)}$$

If $p \to 0$ then $-p \to 0$, $(1-p)^{-1/p} \to e$ means. For sufficiently small p

$$1-(1-p)^n \approx 1-e^{-np} = 1-e^{-\alpha}; \ \alpha = np \qquad (2)$$

Equation (2) differs from 0 or 1 in the case where α is bounded, then there does not tend to 0 or to ∞. This means that the number of trials must be of the order $1/p$, or p is of the order of the twentieth $1/n$. If you are using as a measure of continuous time t, expressed in hours when the probability of failure at the twentieth hour $p = 10^{-4}$ of work, we need experiments of at least 10^4 hours. The probability that in the n series of tests for rare events happens m times gives the Poisson formula.

$$p_m = \frac{\alpha^m}{m!} e^{\alpha}$$

This formula is used for large, but finite u, substituting np instead of α. After the initial phase of the running steady stream of refusals is the simplest Puassov's flow, that is, it satisfies the conditions of stationarity, the lack of effects and the ordinary. Probability of failure of $P(t)$ and probability of failure $Q(t)$ represented by laws:

$$P(t) = \exp(-\lambda t) \qquad (3)$$

$$Q(t) = 1 - \exp(-\lambda t) \qquad (4)$$

By law,(3)distributed the probability that the distance in time between successive moments of failure would be greater than t, the mean time to failure in a steady stream of $T_{cp} = 1/\lambda$ is determined statistically, the expression (3) takes a discrete frequency of occurrence of failures in a homogeneous ensemble of a large amount of friction in a continuous time the probability of failure of any node of the ensemble. It appears the property of ergodicity time probabilities, which in this case is the fact that the probability of failure of one system is equal to the relative number of failed systems of the ensemble. The probability of failure does not depend on history, but only on the characteristics of tribosystem λ and the length of time interval. For example, for a single node of friction $\lambda(t) = 10^{-4}$ at any 10 hours of operation $P(t) = 0{,}99$, and for 100 hours - correspondently in a large ensemble for 10 hours signs of failure will be 0.1%, and 100 hours of 1% of total the number of anti-friction components.

Stability of stationary states in open systems is associated with formed under nonequilibrium conditions, the dissipative structures. In tribosystem surface layers after the break-in are made up of particles from the atomic to microscopic dimensions, which have a high level of excess free energy. The desire to minimize the free energy leads to the spontaneous emergence of coagulation-condensation bonds between particles and between particles and solid surfaces. Exchange links with friction is accompanied by dissipation of mechanical energy and entropy production. The boundary conditions given by the speed and load conditions to prevent the emergence of the free energy

minimum and a maximum entropy. The impact of flows of energy and matter leads to the emergence of dissipative structures in which the consolidating role played by the desire for excess free energy minimum, and the mobility of information and communication between elements of the structure provides entropy.

As a sign of failure used: temperature raise, violation of the friction surface state, changing the acoustic and vibration spectra, and the availability of the products of wear metal particles of visible size (> 100 mkm) [4].

Aircraft gas turbine engines are diagnosed by changes in vibration characteristics: frequency, amplitude, velocity, acceleration, arising from the wearing of the rotor element and bearings. The signals of vibration sensors evaluate the mean value and variance of these characteristics. For each type of engine their critical level is approved.

In the operation of aircraft critical parameters were refined dispersion of metal particles in the products of wear and tear, changes in the size and number of particles in the development of failure. In the normal state of wear products composed of ultrafine particles of oxides, sulfides, phosphates, coke, tar, metal-polymer, cermets and other final products of physicochemical transformations in contact. The appearance of metal particle sizes up to 4 microns corresponds to the negligible probability of failure, with particles ranging in size from 4 to 15 microns. put on the motor-controlled operation, if the particle size is more than 15 microns, the object is removed from service. The use of spectral analysis was the next stage of development of diagnostics, for example, the engine is serviceable if the concentration of metal in the oil does not exceed: Fe-14, Al-10, Cu-10, Sc-10, Pb-7 g / m Experience has shown that a wide variety of materials, operating conditions, type of aircraft and engines, anti-friction system homogeneous with respect to a small number of signs of failure. This can be explained by the same mechanism of failure processes in different systems.

Conclusions:

The probability of failure in the tribological system determines the state of self-generated in the tribological contact structures of dissipative type. Gradual failures determine the wear – the destruction of multiple reversible tribostructures. Wear on the time interval τ is the independent variable, so for the time t >> τ as the sum of independent uniform variables has a normal distribution that is predictable in a probabilistic sense.

Sudden failures are distributed over time with constant probability, and therefore unpredictable. In tribological systems, sudden failure determines the rapid irreversible destruction of tribostructures, which leads to abnormally high wear, seizure or fire. Moment of occurrence of state failure is sudden, and therefore to prevent the failure is possible by identify this condition as early as only possible. To do this, it is necessary for each tribosystem to identify signs of failure, methods of technical diagnostics.

References

1. *Y.K. Velichko.*, Theory of Reliability / Y.K.Velichko., V.G.Koronin / / MGA KIIGA, Kiev. 1971.-120-c.

2. *E.A. Kulgavy*Tribosystem in random environments / EA Kulgavy / / Problems of Tribology. Vol. № 3. - 2004. - P.8-12.

3. *E.A. Kulgavy*Tribological characteristics and their application / EA Kulgavy / / Problems of Tribology. Vol. № 3. - 2003. - S. 51-61.

4. *L.P. Lozitsky* Practical diagnostics of aircraft gas turbine engines / LP Lozitsky, V. P Stepanenko, VA Studenikin / /:-M.: Transport, 1985. - 102 p.

UDC: 621.891

Y.L. Khlevna, postgraduate (National Aviation University, Ukraine)

MECHANISTIC AND ATOMIC-MOLECULAR APPROACH TO THE TRIBOSYSTEM RUNNING-IN PROCESS

This paper presents a brief analysis of the study of running-in process. It discrepancy mechanistic ideas of running-in process submitted by atomic-molecular model of the tribological contact. With the help of the Boltzmann transport equation exponential expression returned to running-in. The basic characteristics of running-in are determined.

Any tribological system can be in one of three states: evolution - on the stage of running-in, stationary - mode, normal operation and abnormal - status failure [1].

The initial surface quality obtained by the processing machine parts, has the characteristics usually different from those of working condition, which is formed during the operation. The transition from initial state to the work called running-in that occurs during the initial wear [2].

The initial period of work is a complex mechanical, physical and chemical phenomenon. Many studies on this question in different units, suggests that this technological operation plays an important role in enhancing security and improving economic performance in operation, as in the manufacture of new parts so the repair.

In most works the authors aim to develop optimal methods of running-in. But there is no perfectly defined influence of external and internal factors on the process. The goal is to get running-in friction surface such actual contact area that can withstand operating loads. Those mutual treatment combinations to sustainable tribological wear. Realization of this goal is possible to determine the mechanism of tribological system running-in (TS). However, now this goal is not sufficiently developed. Most work is considered mechanistic approach to running-in of TS. But steady work is defined as the surface layers of friction pair created at running-in. The purpose of this paper is to analyze the mechanism running-in, taking into account both mechanistic and atomic-molecular approach to studyinf of trybosystem.

Analysis of the mechanistic ideas of running-in process. Evolutionary stage is divided into two phases: 1) intensive running-in at the macro level, 2) at the micro level. Initially, the important role played by roughness, plastic deformation, load system [3].

Plastic deformation of the surface layers of tribosystem elements cause irreparable damage. Damage to individual structural components (mainly solid phase), located in some areas of friction pairs; damage in most of the friction surface. At the same surface is an active surface layer, followed by a subsurface layer. Thickness of the active particles from micron to tens of microns, and subsurface - a few millimeters. Layers represent the only group of frictional interaction of contacting bodies. Regardless of the mode of friction material and the active surface layer is involved in physical and chemical triboreaktion. In some cases, provides maximum lubrication regime [4].

If plastic deformation occurs in the thin surface layers of easily moving, the work conjugated pair of passes without bully. This is facilitated by specially printed cover with soft metals, with layers of solid lubricants, polymer coating, or use self-lubricating alloys, composite materials. Features of self-lubricating materials include the interaction of the soft phase and solid matrix during elastic and plastic deformations. Using heterogeneous alloys with a soft phase in the process running-in most intensively than stationary period is squeezing this phase due to differences boundaries yield components and different degrees of plastic deformation at stresses above the yield stress of the matrix and the soft phase. Formed by the transfer of metal with a soft phase thin protective film can create a kind of fortified area on the mating surfaces.

One of the main conditions for the completion of running-in was considered to be the initial transition technology to operational roughness. Experimental studies [2, 5] showed that after running-in on the friction surface roughness is formed, regardless of the source obtained by machining, and depends only on the conditions of wear. Is the work [2, 6], which examined only the

roughness formed during running-in, and confirmed the legality of using the term "equilibrium roughness.» The value of the equilibrium roughness depends on the load applied to the friction, sliding speed and friction properties of materials couples [6]. The surface changes its roughness to achieve minimum friction coefficient corresponding to the minimum energy friction. Initial roughness mainly affects the time running-in [7]. Regularities of formation and the calculated equilibrium roughness characteristics are given in papers IV Krahelsky etc.

Investigation of changes in microhardness during running-in [8] showed that the period of running-in ends after reaching by the surface some level of deformation. Running-in of tribological system at modes that are close to critical (according to I. Karasik on "seizure limit") is a decrease with time of Sommerfeld parameters and coefficient of friction on dependence of Hersi-Shtribek. Thus the range of load and speed regulation does not go beyond semifluid grease. Depending on the type of pair friction bearing capacity is very different.

Changing the properties of the deformed surface is caused by the nature of friction characteristics of conversion of mechanical energy into heat. The process of adjustment of friction pairs during running-in is power, as it proceeds with the absorption or release of energy contacting surfaces. [3].

Atomic-molecular approach to the process of running-in. From the standpoint of thermodynamics, on the evolutionary stage of the atoms located at the interface of two phases, are "special" as on the status of asymmetrical force field and in their energy states. Indeed, a new surface requires the expenditure of work on breaking ties, much of which accumulated in the form of excess potential energy of interphase boundary [1].

However, as shown by NA Boucher, is self Tribology system as a result of structural adaptability in friction. In shaping the flows of matter plays a crucial role transport processes and self-organization, leading to the formation of dissipative structures trybolohycheskyh contact type. The mechanism of formation of these structures is determined by the organizing influence of nonequilibrium conditions on the flow of matter [1]. Formation of flows of matter in the tribological contact is determined by transport phenomena at the atomic level.

In coordination number equal to eight lattice, surface atoms have seven to one due to internal atoms and solids from one to seven free bonds, the energy which creates excess surface energy of solids. In the contact between a surface atom and atoms of counterbody may be formed from one to seven ties. If the number of bonds with atoms of counterbody exceeds the number of internal connections, then the relative motion of solids, an atom is transferred to another surface. When friction is continuous transfer of atoms between the surfaces, the active atoms enter into chemical bond with atoms of counterbody and oil. Interatomic contact is not seen in terms of real physical object and as a result of the dynamic redistribution of the probability density of electron states, due to which, there are electrical forces of attraction, repulsion or neutral condition.

On the evolutionary stage the tendency to free energy minimum dominates. In the contact is aggregation of particles that are transferred, the internal flow of materials aimed at forming tribistructure and increase its volume and flow of matter from the system decreases until it reaches a stationary level. In steady state tribostrukture fluktuates near the average value for one part of matter fluctuations obtained from the system as a product of wear, and tribostrukture is restored.

Thus, during running-in formed tribological structure, then the process of fluctuation in stationary mode with constant mean and variance, excessive growth is limited entropy, and the lower level – the free energy [1]. Formula for rate of wear it = dI / dt and wear I (t), as a function of time t, is:

$$i_t(t) = (i_0 - < i_t >)\exp(-t/T) + < i_t > \qquad (1)$$

$$I(1) = (i_0 - < i_t >)T[1 \; i_t - \exp(-t/T)] + < i_t > t \qquad (2)$$

where i_0 and $<i_t>$ - primary and secondary stationary value rate of wear: T - relaxation time running-in; I (t) - wear.

Replacing in formulas (1) and (2) the time t on the path of friction l, we obtain a formula to describe the intensity of wear and wear i_1 I (1) by way of friction. Exhibitors on the left side

describe the evolutionary process running-in while playing running-in evaluate the relaxation time T, and the contribution running-in to wear - functional $I_0 = (i_0 - \langle i_t \rangle) \, T \, [1 \, i_t - \exp(-t/T)]$. On the evolutionary stage of running-in of tribosystem moving from a state that is set in the state of technology, which is determined by the process.

Conclusions:

While traditional mechanistic approach, the mechanism running-in determine deformation and fracture of surface layers of contacting solids. This is not the real conditions of tribological contact in antifriction systems. Released all types of fracture surface appearance of metallic particles in the wear products are considered as signs of failure.

In no equilibrium conditions of tribological contact in the exchange with the environment matter, energy, particles are formed in a dissipative structure type, which form the level of tribological processes.

Applying the Boltzman transport equation, the analytical expression for the evolutionary process running-in exponential type was obtained. The main characteristics are running-in running-in time and wear on the initial stage.

Managing characteristics level is possible with the help of external factors (increased loading in progress) and internal (structure of solids and oils).

References

1. *Кульгавый Э. А.* Триботехнические характеристики и их применение // Проблемы трибологии. Вып.№3. – 2003. – С. 51-61.

2. *Костецкий, Б.И.* Качество поверхности и трение в машинах / Б.И. Костецкий, Н.Ф. Колисниченко. – Киев : ТЕХНiКА, 1969. – 214 с.

3. *Денисова Н.Е., Шорин В.А., Гонтарь И.Н., Волчихина Н.И.,Шорина Н.С.* Триботехническое материаловедение и триботехнология:учеб. пособие/Под общей редакцией Н.Е.Денисовой. –Пенза: Изд-во Пенз., 2006. –248с

4. *Панкрашев А. С.* Интенсификация процессов приработки цилиндро-поршневой группы отремонтированных дизельных двигателей путем финишной обработки гильз цилиндров антифрикционными материалами – автореферат кандидата технических наук 05.20.03 Санкт-Петербург-Пушкин 2010, 20с.

5. *Комбалов, В.С.* Влияние шероховатости твердых тел на трение и износ / В.С. Комбалов. – М. : Наука, 1974. – 112 с.

6. *Ящерицын, П.И.* Технологическая наследственность в машиностроении / П.И. Ящерицын, Э.В. Рыжов, В.И. Аверченков. – Минск : Наука и техника, 1977. – 221 с.

7. *Дроздов Ю.Н.* Обобщенные характеристики для оценки износостойкости твердых тел // Трение и износ. Т.1. -1980. -N 3. С.417-424.

8. *Карасик, И.Н.* Прирабатываемость, закономерности и методы оценки влияния приработки и изнашивания на триботехнические характеристики опор скольжения: Дисс . доктора техн. наук: И.Н. Карасик. М., 1983. – 450 с.

UDC: 621.179

A.P. Kudrin, PhD, professor, M.N. Svirid, PhD Engineering, associated professor,
V.G. Paraschanov, A.Y. Yakobchuk
(National Aviation University, Ukraine)

STRUCTURAL CHANGES OF THE FRICTION SURFACES DUE TO ACTION OF PULSE MODULATED CURRENT

The problems of restoration of precision friction pairs in the environment with high electrical resistance are discussed. The triboelectrochemical restoration modes in the PEG environment were determined.

Introduction. The increasing of durability of any machines in the 30 ... 40% is equivalent to a similar increase in production, which leads to the extrication of huge financial, material and labor resources. At the same time, the durability of machines, which is defined as the ability to save workingability up limit state, most often is determined by wear of friction surfaces, i.e. change of their size due to wear, and is not corresponded with the breakage of the separate parts due to the low strength ones. The increased wear is the reason for shocks and vibration, and as a result can lead to accidents. Often the failure of multi-ton aggregate is caused by wear and loss of workingability of small detail, while the wear can be measured by parts of millimeter. Thus, the renovation of the friction surface, which can be some microns, is the most progressive method for increasing of element's wearability. The use of electrochemical technology, for spraying of thin coatings, is the most economically reasonable, but it is necessary to use the electroconductive environment for them, which significantly increases the corrosion component of the system.

Fig. 1 shows that in the gear pumps there are friction pears of steel-steel (gear), steel-brass, steel-aluminum. Such a wide spectrum of friction pears significantly complicates the electrochemical restoration of surfaces.

To develop the technologies, which will provide to conduct electrochemical material transition in the environment with a high level of electrical resistant.

We will us polyethylene glycol (PEG) 400 with the concentration 75% in the water, and which is surface active environment.

It is important to determine the electrical current parameters, which will provide electrochemical reaction.

The physical meaning is to introduce the conditions when the PEG will conduct electrical current. Fig. 2 shows that the environment electrical conductivity, which has high resistant density about 1 MOm/sm^2, completely prevents the passage of direct current.
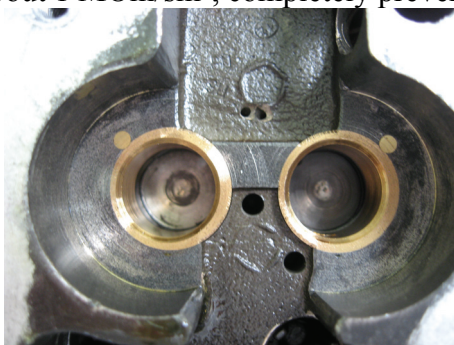
Fig. 1. The element of gear pump.
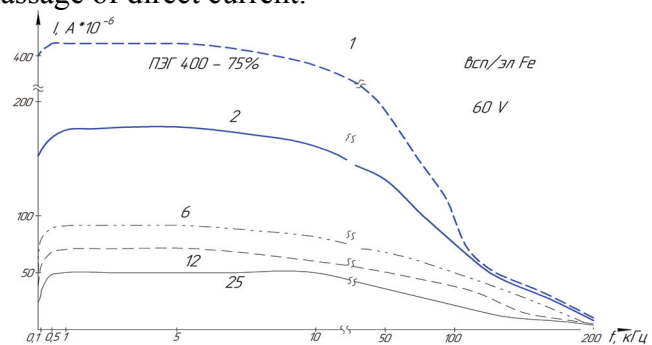
Fig. 2. The diagram of changing of the current in the environment of PEG-400-75 depending on the current frequencies with the auxiliary iron electrode. 1 – alternating current, 2 – through the diode, 6 – interruption of 6 Hz., 12 – interruption of 12.5 Hz, 25 – interruption of 25 Hz

To determine the electrochemical parameters of the environment, the current of various

frequencies from 20 Hz to 200 kHz and voltage of 60V was passed through PEG-400-75 (Fig. 2). Fig. 2 shows that at wide range of electrical current frequency, current force can be very different from $40*10^{-6}$A to $50*10^{-6}$A depending on other current parameters. It is important, that However, the current force decreases in the electrolyte of PEG depend on current frequency. It is important, that half-wave current (curve 2) almost in 2 times greater if the current has same parameters and the interruption of 6 Hz.

Experimental facilities and materials. The tribological investigations were carried out with the help of special test machine [1], test conditions were: speed – 0.5 m/s, 1 m/s and 1.5 m/s, and he load was varied from 0.1 to 5 MPa. The specimen was made of steel 45 hardened to martensite, counterface – glass, working environment – PEG-400-75, additional electrode – Fe.

For the investigation and according to electrochemical properties of working liquid, the current of 1 kHz frequency was passed throw friction zone. From experience, the greatest vibration signal arisen at frequencies from 1 kHz to 5 kHz, which characterizes a large component of deformation. According to this, electrical current of 1 kHz frequency was applied to the addition electrode. In this situation, thick tribo-films are formed on the surface of steel 45. The thickness of this film up to 15 μm (fig. 3) and can full up to 70% of friction zone, the friction coefficient was 0.06…0.08.

According to literature data deformation activity of the metal surface occurs at the 1 ... 8 Hz of pulsed electric current and takes influence on a crystal lattice formation [2]. The main direction of the investigation is the action of impact of dual directional component of the frequency of electric current on deformation characteristics of the surface material at friction. According to [3] the structure of surface tribological films is more hard-working at the action of pulsed electric current.

Was investigated tribological parameters of friction pair in the conditions of pulsed electrical current of 1 kHz frequency and interruption of 6 Hz. In this conditions the thickness of tribological films are 1…2.5 *μm* and can full up to 90% of friction zone, the friction coefficient decreases to 0.03 (fig. 4).

Fig. 3. The topography of steel 45 surface, when the pulsed electrical current of 1 kHz frequency is applied and additional electrode **Fe** is used

Fig. 4. Friction surface of steel 45, when the pulsed electrical current of 1 kHz frequency and interruption of 6 Hz is applied and additional electrode **Fe** is used

Experimental results Experimentally was determine that triboelectrochemical processes on the friction surface are present at rectified one-period current in combination with additional electrode **Fe**. Topography of the friction surface is shown on the fig. 4.

Vibration component was used as one of the additional parameter of surface friction wearing process monitoring. Was indicated that vibration signal, during friction process, is characterized by current force decreasing at high frequency. Fig. 5 shows that curves №4 and 0 are correspondent to tribological films formation which are present on fig. 3. Here indicates that if the current is 16 Hz frequency, the film can be broken and thes process is characterized by increasing of vibration force from -35 to -45 dB. The application of electrical current interruption of 6 Hz is characterized by curves №2 and 3. The force of vibration signal is much decreased up to -40…-50 dB for the frequency up to 5 kHz and up to -80…-90 dB for the frequency 10…20 kHz. Curve №1 characterizes frequency parameters of testing machine in friction mode, but without installed friction pair.

The transition of iron electrons from additional electrode to friction surface is achieved due to increasing of current frequency up to 1 kHz. Dates of electrical current resistant, according to diagram of fig.2, are substituted into the formula instant power from the voltage change $I\,p\,(t) = U^2(t)\,/\,R$ or current change $p(t) = I^2(t)/R$
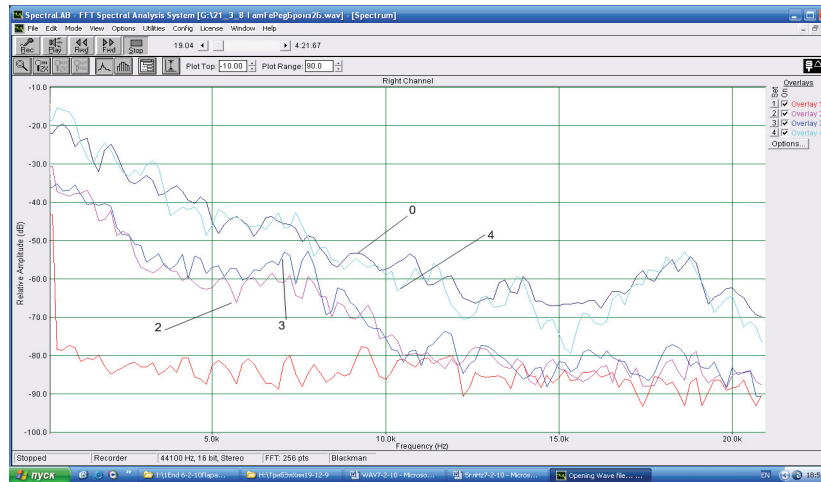
Fig. 5 Parameters of frequency signal of input frequency 1000 Hz (№ 0 i 4) and the signal 1000 Hz, which is modulated by interruption of 6 Hz

We can see that the power is inversely proportional to R (active resistant), but capacitive resistance is directly proportional to $f\,(Xc=nf)$ frequency.

Given that the friction surface is micro-condenser, then with increasing frequency of resistance will decrease. Therefore, in this zone will be current at high frequencies. Thus, the carrier frequency of 1 kHz is optimal.

Analyzing friction conditions of steel 45 by the glass in PEG environment, and surface films characteristics, we can say:

- friction at action of signal of 1 kHz is characterized by very rough tribological films to 8 ... 15 mm thick (Fig. 3), which are distributed on the 70% of friction zone;

- if the electrical signal to modulate, i.e. to interrupt of 6 Hz (Fig. 4), is formed tribological films, which have a thickness of 0,5 ... 2 µm. Thin films are characterized by flexibility and greater adhesion to the surface.
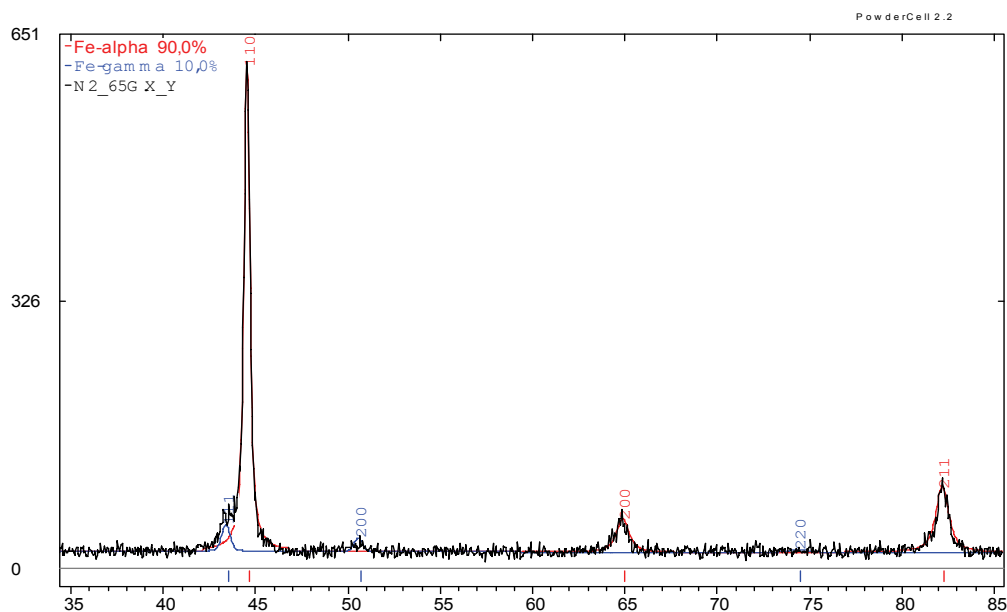
Fig. 6. X-ray analysis of the friction surface of steel 45 on glass

X-ray analysis was made with the help of monochromatic CuK_α and measured on the

diffractometer ДРОН-УМ1. At 1 kHz frequency of signal, was indicated the change of size of crystal lattice from 2.8669 Å to 2.8678 Å *Fe-alpha* phase. In addition there is up to 10% *Fe-gamma* with parameter of crystal lattice 3.6010 Å (fig.6). For austenitic steel are forming mostly single-phase crystallization at austenitic γ-Fe with face-centered crystal (FCC) and preserving reshetkoy ee do with cooling cryogenic temperatures.

The restructuring of the crystal lattice in the *Fe-gamma*, under the influence of electric signal 1kHz and duty interruption of 6 Hz changes the state of the material. A number of another phase – high-alloyed ferrite (δ-Fe crystal with body-(BCC) lattice) is usually in the alloy is from 0 to 10%. The formation of γ-Fe has a different solubility of carbon associated with the large size of the pores in the center of a cell γ-iron, and the introduction of the carbon lattice is distorted so the need for greater dissolution raise the temperature, according to the diagram Fe-C.
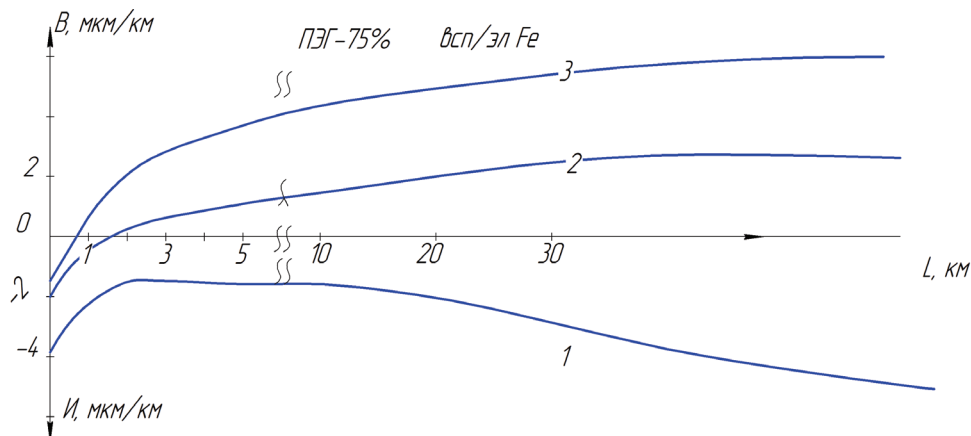
Fig. 7. Tribological parameters of friction pair of steel 45 on ЛС59-1 in the conditions of frequency modulation of electrochamical signal. 1 – half-wave one-way rectified current 1kHz; 2 – two-half-wave one-way rectified current 1kHz; 3 – two-half-wave one-way rectified current 1 kHz interrupted of 6 Hz

Conclusions:

To investigate the actual performance was measured the wearability of friction pair of on steel 45 ЛС 59-1 among the 75% polyethylene glycol concentration in the water with an additional electrode **Fe**. Fig. 7 shows that the process of tribological restoration is by using of two-half-wave one-way rectified current 1 kHz interrupted of 6 Hz. This wear is reduced almost 2 times (Fig. 7).

Thus, the impact of the modulated signal is 1kHz interrupted of 6 Hz change the structure of the friction surface, which increases almost 3 times its strength at friction due to compression of the crystal lattice.

References

1. *Свирид М.М.* Пристрій для дослідження матеріалів на тертя та зношування // Патент на корисну модель 36600, G01N 3/56. Заявка u200809663, 23.07.2008. Опубл. 27.10.2008, Бюл. 20, 3 с. *[Свирид М.М., Занько С.М., Задніпровська С.М., Паращанов В.Г., Приймак Л.Б.]*

2. *Белый А.В.* Структура и методы формирования износостойких поверхностных слоев. - М.: Машиностроение, 1991. 45с. *[Белый А.В., Карпенко Г.Д., Мышкин К.Н.]*

3. *Влияние* электрического импульса на условия трибоэлектрического восстановления Свирид М.Н., Кравец И.А., Волосович Г.А., Бородий В.Н., Приймак Л.Б. Проблеми тертя та зношування №54 2010 135-142

UDC 621.78:669.15(045)

V.I. Dvoruk, doctor of technical sciences, prof. (National Aviation University, Ukraine),
E.P. Puhachevska, assistant (National Aviation University, Ukraine),
S.S. Belykh, postgraduate (National Aviation University, Ukraine)

ABRASSIVE WEAR RESISTANCE AND STRUCTURE OF ALLOYING STEELS

The correspondence order between rheological parameter and abrasive wear resistance of alloying steels of different structural classes after heat treatment in wear conditions by fixed abrasive has been found. It denotes necessity of rheological and kinetic approach to strength base of nature and its wear resistance mechanism.

The scientifically reasonable solution of abrasive wear resistance problem by steel structure control is actual tribology's assignment. Its solution is possible only in case of creation theoretical base. Almost all theories of abrasive wear resistance [1-6 and others] denote main role of strength factor in nature and mechanism of abrasive wear. But there is no one thought about it according strength theory. Mostly the generally accepted statistic of strength concept [7] is considered as main. According to it material destruction is critical action which happen at attaining strength boundary by actual stress [1-5]. So, strength boundary is material physical constant. However, it's not real, because strength boundary depends from a lot of factors and universal laws describing material work by any conditions are absent, so, such factor is conditional [8]. Another lack of statistical approach is taking into account time factor influence only trough accessory factors (for example, moisture absorption from air, deformation and relaxation processes, etc.), while direct action of this factor in destruction mechanism is unaccounted.

The kinetic strength theory hasn't such lacks [7]. According to this theory destruction is considered as thermofluctuation process, which cannot be characterized by strength boundary.

As there is no generally adopted viewpoint on nature and mechanism of abrasive wear resistance, the new wear resistance concept has been proposed [9,10]. It's base is kinetic and rheological imagination about link between destruction processes and deformation one at abrasive wear resistance. Pointed conception is result of superposition and application in dialectic unity of rheological and kinetic strength concepts to abrasive destruction description.

The rheological concept considers destruction not as statistic critical action but as kinetic process developing in time. From kinetic concept viewpoint, destruction phenomenon is conglomeration process in time of thermoclutch crack of interatomic bonds. So, there is hierarchy between this approaches that gives foundation for their superposition. According to proposed [8] physical model abrasive destruction is sequence of actions of wear particle separation which are created due to development of primary lateral horizontal cracks to their intersection with working surface, secondary lateral cracks, vertical wedge-shaped cracks, etc. The rheological parameter $R = \dfrac{K_{IC}}{\sqrt{h_\Pi}}$, where K_{IC} is metal destruction viscosity and h_Π is dimension of plastic area at crack peak is considered as wear resistance criterion. This value is a factor index of correlation between processes of destruction and deformation, which according to its physical essence characterizes strength from creation of lateral cracks on boundaries of plastic zones at peaks of vertical wedge-shaped cracks. The destruction viscosity K_{IC} in mentioned criterion is rheological and energetic characteristic at the same time [11]. It takes into account strength and plastic properties of metal simultaneously. The last fact is important because there is functional connection between abrasive wear resistance and strength-plastic characteristics of steels of different structural classes [12]. But in comparison with standard characteristics of strength and plasticity which are conditional and take into account middle properties of metal at wear, the index K_{IC} estimates local properties near crack top and "connects" with plane-strain condition in set zone. So, destruction viscosity is fundamental characteristic of metal strength to destruction.

It is accounted necessity of comparative assessment of obtained results with known regularities at steel choice for experiment conduction. Therefore it were chosen such steel grades which are widely researched in other scientific thesis [6,12,14]. The mentioned steels are heat treated for the purpose to expand range of change of researched properties. The heat treatment was consist of steel hardening at optimal for each steel temperature and tempering at temperature 493 K, 693 K, 893 K. This is give possibility to analyze influence of structural state after steel tempering on its properties.

The tribotechnical tests of steels are conducted by methods and methodics which are used at work [13]. The mechanical, tribological and rheological properties of steels are shown in table 1.

The research objects were dependences of steel wear resistances at abrasive wear from its rheological characteristics: destruction viscosity K_{IC}, dimension of plastic area in crack peaks h_{Π}, rheological parameter R.

The research results allow to systematize data about link between rheological properties and steel wear resistance (Fig.1).

Table 1

Mechanical, rheological and tribothecnical properties of steels

Steel grade	Structural class	Heat treatment mode, K		HRC_e	δ_e, MPa	K_{IC}, $MPa\sqrt{m}$	h_{Π}, m	$R_3 \cdot 10^4$, MPa	$\varepsilon \cdot 10^2$, kg^{-1}
		Hardening	Tempering						
95Х18	Martensite	1293-1343, oil	493	62	1800	10	$9,33\cdot10^{-9}$	10,4	16,45
			693	58	1300	12	$5,5\cdot10^{-8}$	5,1	8
			893	40	800	15	$1,4\cdot10^{-7}$	4	6,28
40Х	Perlite	1123-1153, oil	493	49	1850	9,6	$8,29\cdot10^{-8}$	3,44	5,4
			693	39	1420	12	$1,56\cdot10^{-7}$	3,03	4,76
			893	24	850	14	$2,84\cdot10^{-7}$	2,66	4,16
110Г13Л	Austenite	1293-1343, water	493	18	616	17,2	$2,14\cdot10^{-7}$	3,72	5,82
			693	17	415	20,7	$3,59\cdot10^{-7}$	3,45	5,43
			893	16	360	25	$5,4\cdot10^{-7}$	3,33	5,23
Н18К9М5Т	Maraging	1113-1133, oil	493	33	1070	12,9	$2,34\cdot10^{-7}$	2,66	4,17
			693	49	1400	11,8	$1,79\cdot10^{-7}$	2,78	4,37
			893	47	1500	14,8	$2,92\cdot10^{-7}$	2,74	4,3
Р18	Carbide	1563-1583, oil	493	59	1150	12,7	$3,25\cdot10^{-8}$	7,08	10,6
			693	62	1320	11,8	$1,6\cdot10^{-8}$	9,4	14,5
			893	65	1600	10,8	$6,1\cdot10^{-9}$	13,8	21,7

It is observed individual tendencies of change of rheological indexes at tempering for each steel class. For steel of martensite class the K_{IC} and h_{Π} increase and R decrease with tempering temperature rising (Fig.1, a).

The character of change of rheological indexes for steel of perlite class is the same as for steel of martensite class, but rising K_{IC}, and h_{Π} and falling R is happen not so intensive (Fig. 1, b).

Following decrease of change intensiveness K_{IC}, h_{Π} and R at saving its characteristics is observed in austenite steels (Fig.1, c).
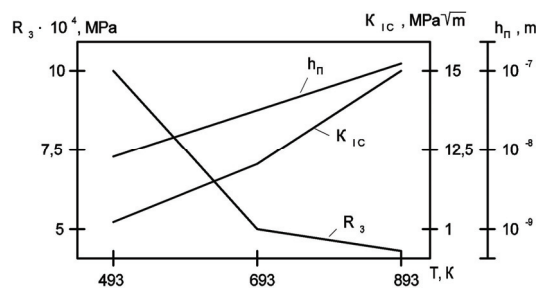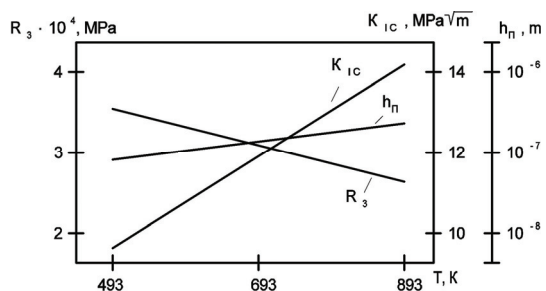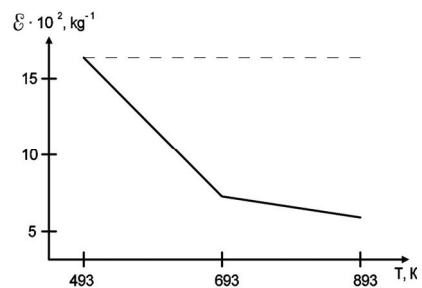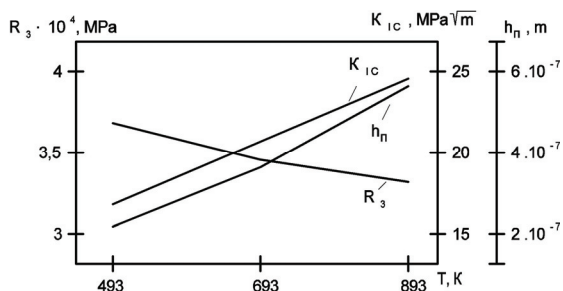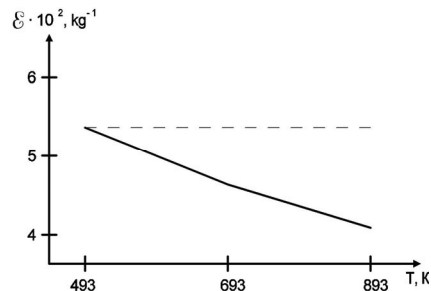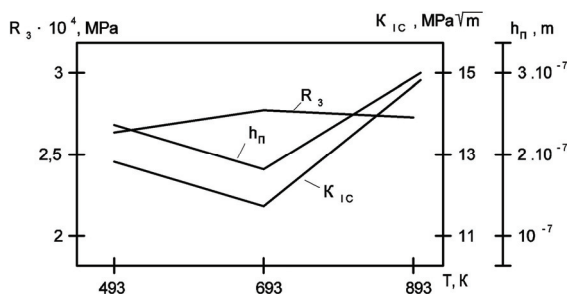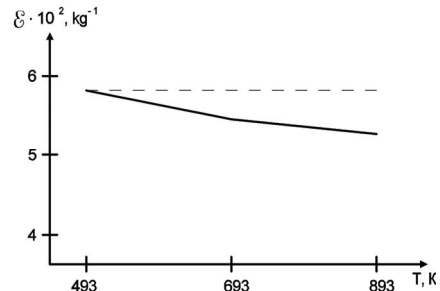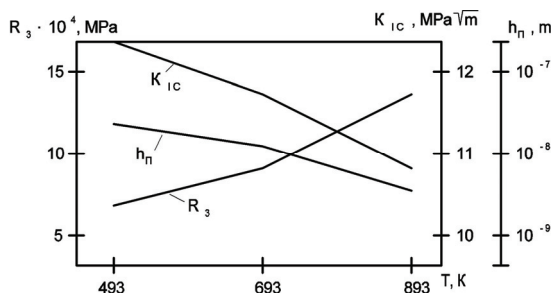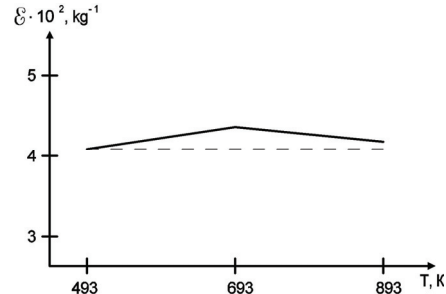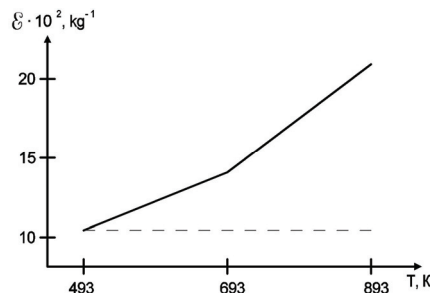
Fig.1 - Dependence of rheological properties (I)
and wear resistance (II) from tempering temperature for steels:
a – 95X18; b – 40X; c – 110Г13Л; d – Н18К9М5Т; e – P18

1.4.41

The differ character of rheological properties change is fixed at steels of maraging class. By rising tempering temperature up to 693 K K_{IC} and h_{Π} falls and R insignificantly rises. Further tempering temperature increasing lead to rise K_{IC} and h_{Π}, and R shows tendency to decresing y (Fig.1, d).

The rheological properties K_{IC} and h_{Π} decrease and R increases in steels of carbide class at tempering temperature rise (Fig.1, e).

The comparison of dependences of rheological properties and wear resistance from tempering temperature (Fig.1) shows its complete correspondence for steels of all classes. It is observed direct correspondence between rheological parameter R and wear resistance ε and inverse relation – between destruction viscosity K_{IC}, dimension of plastic area h_{Π} and wear resistance ε.

So, it have been developed for the first time the correspondence law between change of rheological parameter and abrasive wear resistance depending from steel tempering temperature.

The most important for abrasive wear resistance is rheological parameter for each steel class independently from tendency of change and interconnection of destruction viscosity indexes and dimension of plastic area. The complete correspondence of set dependences is observed between change of rheological parameter and wear resistance of steels in all interval of tempering temperatures.

The rheological parameter in each structural steel class defines level and tendency of change its wear resistance at tempering. The value of rheological properties and wear resistance is stipulated mainly by chemical composition of steel.

Data about numerical values of rheological properties which provide maximal wear resistance in each structural class can be obtained from table.

The highest wear resistance has carbide steel P18. It is achieved due to the highest value of rheological parameter.

The maraging steel H18K9M5T has low rheological parameter, as a result, low wear resistance. The same can be said about austenite steel 110Г13Л, its wear resistance approximately equal to wear resistance of steel H18K9M5T.

The greatest change of rheological parameter after tempering at temperature 893 K in relation to its value after tempering at temperature 493 K is observed in martensite steel 95X18 (decreasind in 2,6 times) that is accompanied by corresponding decrease of its wear resistance.

At transfer from steel of martensite class to steels of another structural classes – perlite, austenite and maraging, mentioned effect decreases firstly up to practically zero level in maraging steel, after that at transfer to carbide steel it is happen inversion – the value of rheological parameter after tempering at temperature 893 K increases in relation to its value after tempering at temperature 493 K. These results allows to open general viewpoint of change of wear resistance and rheological parameter of steel of different structural classes, show change tendency of tribotechnical and rheological properties of steels at different tempering temperatures, correlate advantages and disadvantages of steels of each class taking into account its maximal wear resistance and rheological parameter.

Conclusions

It has been established as result of conducted researches:

1. The alloying steels of different structural classes are subjected to such correspondence law: the wear resistance of steels grows with increasing rheological parameter. So, the rheological and kinetic approach should be used at strength base of nature and mechanism of abrasive wear resistance.

2. The change tendency of rheological indexes at tempering depends on structural class of steel. It can be growing, nonmonotonic or falling character with tempering temperature increase.

3. The value of rheological parameter and wear resistance of steels of different structural classes is defined by ratio of intensity of destruction viscosity change and dimension of plastic area at set tempering temperature.

References

1. *Хрущов М.М., Бабичев М.А.* Абразивное изнашивание / М.: Наука, 1970. – 251с. – Библиогр.: С. 242 – 247.

2. *Кащеев В.Н.* Абразивное разрушение твердих тел. / М.: Наука, 1970. – 247 с. – Библиогр.: С. 237 – 245.

3. *Тененбаум М.М.* Сопротивление абразивному изнашиванию / М.: Машиностроение, 1976. – 270 с. – Библиогр.: С. 263 – 268.

4. *Брыков Н.Н.* К вопросу о закономерностях сопротивляемости сталей и сплавов абразивному изнашиванию // Проблеми трибології: - 1997. - № 4. – С. 13 – 20.

5. *Брыков М.Н.* Основы теории износостойкости железоуглеродистых сплавов при абразивном изнашивании // Проблеми трибології: – 2007. – № 2 – С. 46 – 56.

6. *Виноградов В.Н.* Абразивное изнашивание / В.Н. Виноградов, Г.М. Сорокин, М.Г. Колокальников: – М.: Машиностроение, 1990. – 224 с.: ил., табл. – Библиогр.: С. 217 – 219.

7. *Регель В.Р.* Кинетическая природа прочности твердих тел / В.Р. Регель, А.И. Слуцкер, Э.Е. Тамашевский: – М.: Наука, 1974. – 560 с.: ил., табл. – Библиогр.: С. 536 – 560.

8. *Латишенко В.А.* Диагностика жест кости и прочности материалов / Рига: Зинатне, 1968. – 320 с.: – Библиогр.: С. 274 – 299.

9. *Дворук В.И.* Научные основы повешение абразивной износостойкости деталей машин / К.: КМУГА, 1997. – 101 с. – Библиогр.: С. 95 – 99.

10. *Дворук В.I.* Реолого-кінетична концепція абразивної зносостійкості та її реалізація в керуванні працездатністю механічних трибосистем: Автореф. дис. доктора техн. наук / НАУ. – К., 2007. – 40 с.

11. *Хеккель К.* Техническое применение механики разрушения / М.: Металлургия, 1974. – 64 с. – Библиогр.: С. 92 – 93.

12. *Сорокин Г.М., Малишев В.Н.* Аспекты металловедения в природе механического изнашивания // Трение и знос. – 2005. – Т. 26, № 6. – С. 598 – 607.

13. *Дворук В.I., Герасимова О.В.* Вплив структурного стану на абразивне руйнування сталі // Проблеми тертя та зношування: Зб. наук. праць. – К., 2007. – № 47. – С. 82 – 94.

14. *Сорокин Г.М., Албачагиев А.Ю., Медляев И.А.* Некоторые аспекты выбора и создание износостойких металлических материалов для условий абразивного изнашивания // Трение и износ. – 1990. – Т.11, № 5. – С. 773 – 781.

V. Egorov, PhD, S. Zhachkin, PhD, I. Fomenko, a postgraduate student
(PLC "Research Institute of automated means of production and control", Voronezh, Russia)

EFFECT OF THE TRIBOELECTROCHEMICAL TREATMENT ON THE QUALITY OF THE SURFACE

The quality of the surface after preliminary triboelectrochemical treatment depends on the share of electrical discharge machining (EDM) and electrochemical (ECM) components of the process. Their ratio is able to vary to achieve the optimal values of the roughness of the machined surface, changing the technological parameters of treatment.

The single transition formation of lightweight flange made from pipe billets with the degree of circumferential strain within 28% became possible by increasing the plasticity of titanium alloys by the preliminary triboelectrochemical treatment. The triboelectrochemical treatment does not only improve the plasticity characteristics of alloys, but also changes the qualitative parameters of the machined surface.

The triboelectrochemical treatment is a complex interaction of electrochemical, electrocontact, EDM and mechanical components of processing [1]. When material is processed by the cathode-brush the quality of the surface layer depends on the ratio of the processing components and technological parameter of the treatment: a linear velocity of rotation of the tool, an operating voltage, a number of bunches of pile in the cathode-brush.

The value of the roughness parameter of the surface machined by the triboelectrochemical treatment depends on the ratio of electrochemical treatment and EDM. Surface roughness was investigated with use of profilograph-profilometer model 201 manufactured by the factory "Calibre" and the double microscope MIS-11. The data of the dependence of roughness parameter on the share of the electrochemical removal of material during processing are shown in Table 1.

Table 1

Share of the electrochemical removal, %		Roughness parameter R_a, μm
electrochemical treatment	EDM	
61,5	27,0	0,9 – 1,1
51,0	32,0	1,1 – 1,5
44,5	35,0	1,1 – 1,5
31,0	40,0	1,2 – 1,7

The prevalence proportion of EDM leads to the increase of roughness. The height of the irregularities in the processing depends on the pulse energy [2]:

$$R_{z(EDM)} = K_н A_u^p ,\qquad (1)$$

where R_z – the roughness of the machined surface, which characterizes the average depth of profile (holes), μm,

$K_н$ – the coefficient depending on the treatment regime, the electrode material, the working environment, etc. ($K_н =1..3$),

A_u – the pulse energy, J,

p – the exponent, which depends on the treatment regime ($p=0,3..0,4$).

After the preliminary triboelectrochemical treatment surface acquires the shape with recesses in the form of holes, similar to the form of micro-relief after the EDM, which determines the surface roughness. The equation (1) for the depth of roughness profile, taking into account spherical form of hole, assumes the view:

$$R_{z(\text{ЭЭО})} = K_{\text{и}} U_{\text{и}} I \frac{2\arccos\phi/R}{\omega},$$

where U_u – the operating voltage, V,

    I – the amperage, A,

    $\varnothing$ – the sectional diameter of the metallic pile cathode-brush ($\varnothing$=0,05..0,15 mm),

    R – the radius of a working area, mm,

    ω – the angular velocity of the cathode-brush rotation, rad/s.

The formation of surface microrelief with ECM depends on the composition, temperature, flow rate of the electrolyte, the structure of the billet material. These factors have little effect the anodic dissolution process, but due to the selective dissolution of different structure and physical and chemical properties of separate phases of the machined surface intergranular erosion are observed, which determines the surface roughness.

The rate of electrochemical dissolution is the sum of the partial dissolution rates of separate phases and blocks of grains of different structure [3]:

$$i = \sum_{1}^{n} i_n \, .$$

The depth of intergranular erosion is determined by the difference of anodic dissolution rate of separate phases:

$$\sum_{1}^{n} i_n = \frac{U\eta\lambda_t}{\sum_n (\rho_n)\delta} \cdot \frac{100}{\sum (K_n/\varepsilon_n)},$$

where i_n – the linear rate of dissolution of n-phase, mm/s,

    U – the operating voltage, V,

    η – the current output,

    λ_t – the specific conductivity, S/m,

    ρ_n – the density of n-phase, kg/m^3,

    δ – the size of the interelectrode gap, mm,

    K_n – the mass content of n-phase in the alloy, %,

    ε_n – the electrochemical equivalent of n-phase, g/A·s.

When billets are machined by the method of surface treatment [4], the size of interelectrode gap is determined by the downforce of the electrodes:

$$\delta = \sqrt{\frac{P}{k \cdot \mu \cdot n}}, \tag{2}$$

где P – the downforce of the electrodes, N,

    μ – the dynamic viscosity of the electrolyte, Pa·s,

    n – the rotational speed of the cathode-brush, rev/min,

    k – the estimated coefficient, which depends on the material and the diameter of the cross section of the metal cathode-brushes pile.

Taking into account the equation (2), we have:

$$\sum_{1}^{n} i_n = \frac{U\eta\lambda_t\sqrt{k \cdot \mu \cdot n}}{\sum_n (\rho_n)\sum (K_n/\varepsilon_n)\sqrt{P}} \, .$$

The depth of the layer of material, removed during the time τ, is equal to:

$$R_{z(ECM)} = \frac{100 U\eta\lambda_t \sum_n \varepsilon_n \sqrt{k \cdot \mu \cdot n}}{\sum_n (\rho_n K_n)\sqrt{P}} \cdot \tau \ (\text{μm}).$$

The value of the roughness parameter of the surface, treated by a brush-cathode, is determined by the difference in the rates of formation craterlets with EDM and anodic dissolution of the surface layer:

$$R_z = R_{z(EDM)} - R_{z(ECM)}.$$

The depth of microrelief irregularities of surface machined by the triboelectrochemical treatment is characterized by an equation:

$$R_z = K_u A_u^p - \frac{100 U \eta \lambda_t \sum_n \varepsilon_n \sqrt{k \cdot \mu \cdot n}}{\sum_n (\rho_n K_n) \sqrt{P}} \cdot \tau \ (\mu m).$$

The value of the parameter of roughness Ra of a surface, machined by the triboelectrocemical treatment, depends on the continuity of the cathode-brush pile (Fig. 1), as this option of processing effects duration and contact area of the tool with the workpiece. The value of the roughness parameter decreases with increasing number of bunches of metal pile. Tab. 2 contains the empirical data of the ratio of the pulse duration and duty cycle depending on the diameter of the cathode-brush and the number of sections of the pile to obtain the optimal values of the roughness parameter (R_a=0,9..1,5 μm).

Table 2

Cathode diameter, mm	Number of sections, p	Pulse duration, $\cdot 10^{-4}$ s	Duty cycle
11	6	3,00	1
13	7	2,60	
15	6	2,40	
16	5	2,36	
18	5	2,20	
20	5	2,00	
11	4	3,00	2
13	4	3,60	
15	4	2,40	
16	3	2,36	
18	3	2,20	
20	3	2,00	
11	3	3,00	3
13	3	2,60	
15	3	2,40	
16	3	2,36	
18	3	2,20	
20	3	2,00	

The tab. 2 shows if pulse duty cycle value increases by more than 2 the roughness parameter of surface, machined by the preliminary triboelectrochemical treatment, does not depend on the continuity of the cathode-brush pile.

The quality of the surface of the workpiece after triboelektrochemical treatment depends on the rotation speed of the tool. When a billet made from alloy VT1-0 was processed the increase of the linear speed of the cathode-brush rotation from 5.7 to 25 m/s resulted in a decrease of the roughness parameter R_a from 2 to 0.9 microns. The dependences of changes in the quality of the machined surface on the linear velocity of tool rotation are shown in Fig. 2, 3.
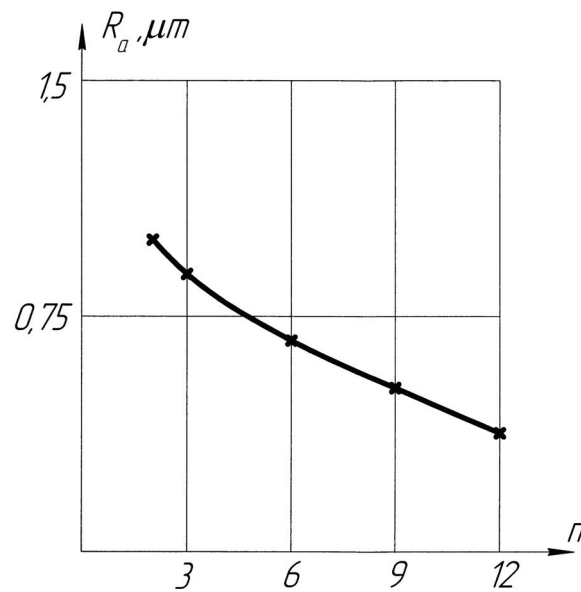
Fig. 1. The dependence of the change of the roughness parameter on the number of pile bunches in the cathode-brush: R_a - the roughness of surface after triboelectrocemical treatment, n - number of the bunches of metal pile in the cathode-brush
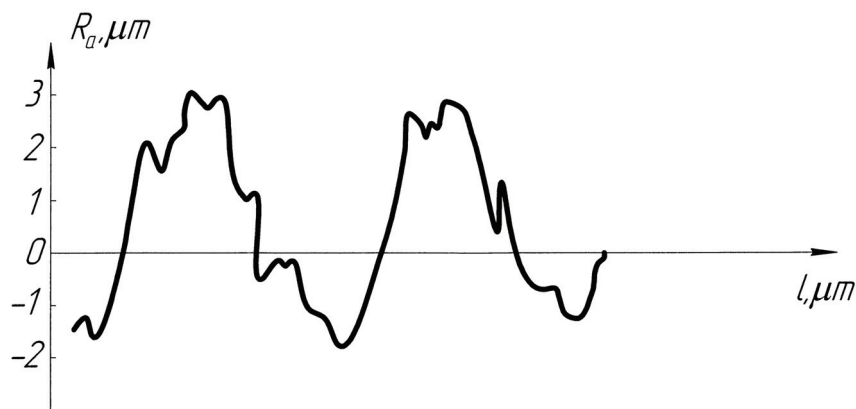
Fig. 2. The view of a profilogram of the surface at a cathode-brush linear speed being 5,7 m/s
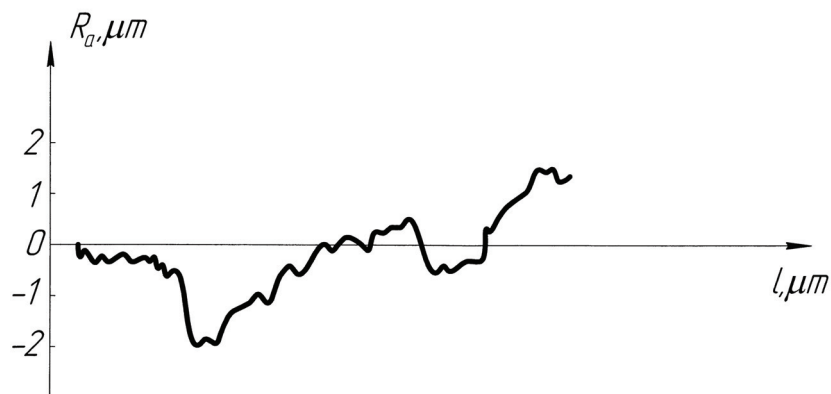
Fig. 3. The view of a profilogram of the surface at a cathode-brush linear speed being 25 m/s

Operating voltage at which carried out the preliminary triboelectrochemical treatment, also effects the value of the roughness parameter of the machined pipe billet surface. The increase of voltage led to an increase of EDM share and consequently to the deterioration of surface quality. With the excess of the operating voltage value being 7.5 V, the value of the machined surface roughness parameter increased sharply (Fig. 4). The surface microrelief acquired deepening in the form of craters typical for the EDM.
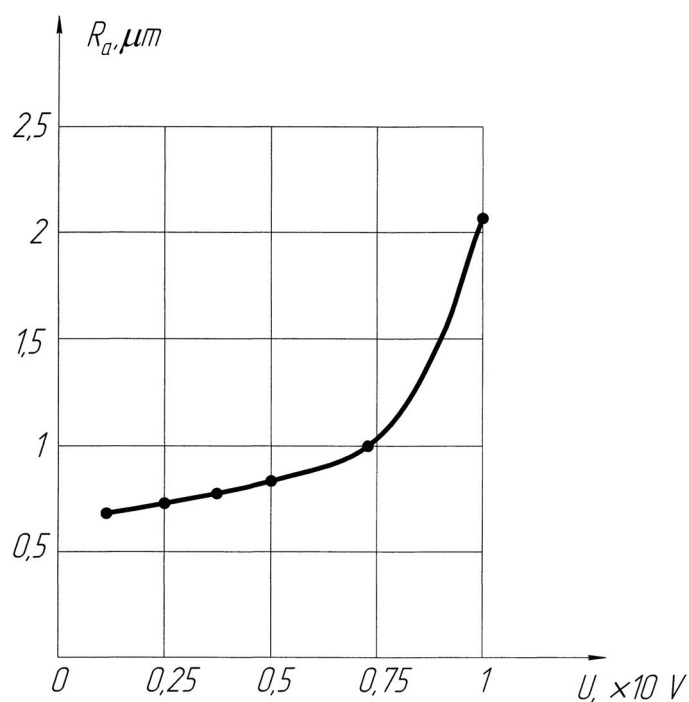
Fig. 4. The dependence of the roughness parameter Ra on the operating voltage U

The dependence of the parameter of surface roughness after the triboelectrochemical treatment on the technological parameters has the form of the regression equation:

$$R_a = 0{,}49 + 0{,}5U - 0{,}18\tau - 0{,}13n + 2{,}5\delta + 0{,}1I .$$

Processing should be performed by low energy pulses, following with high frequency, to obtain the surface with small roughness parameter. This is achieved by using cathode-brushes with a certain number of pile bunches, increasing the linear velocity of the tool rotation and preserving of the operating voltage within 7.5 V.

The optimal process parameters of the triboelectrochemical treatment allow to improve plastic properties of pipe billets material and to provide high quality of the machined surface. Small values of surface roughness parameter of the product prevent the formation of undesired stress concentrators during exploitation and as a consequence, the development of fatigue cracks. The high quality of the surface after the triboelectrochemical treatment optimal regimes is beneficial to fatigue resistance and cyclic durability of the titanium pipeline elements.

References

1. *Жачкин С.Ю., Егоров В.Г., Фоменко И.В.* Реология поверхностного слоя титанового сплава при обработке ТЭХО. – В межвуз. сб. науч. тр.: Обеспечение качества продукции на этапах конструкторской и технологической подготовки производства. Вып. 7. – Воронеж: ВГТУ, 2011. – С. 53 – 58.

2. *Немилов Е.Ф.* Справочник по электроэрозионной обработке материалов. – Л.: Машиностроение. 1989. – 164 с.: ил.

3. *Смоленцев В.П.* Технология электрохимической обработки внутренних поверхностей. – М.: Машиностроение. 1978. – С. 115 – 128.

4. А.с. 1443297 СССР, МКИ4 В23 Н5/06. Способ поверхностной обработки / *Аракелян Б.В., Смоленцев В.П.*

UDC 621.7.043

V. Egorov, PhD, S. Zhachkin, PhD, I. Fomenko, a postgraduate student
(PLC "Research Institute of automated means of production and control", Voronezh, Russia)

EFFECT OF THE TRIBOELECTROCHEMICAL TREATMENT ON THE OPERATIONAL CHARACTERISTICS OF FLANGE JOINTS

Using of titanium alloys, sensitive to high cyclic loads, in the aircraft industry increased requirements on finishing technology. The preliminary triboelectrochemical treatment contributes to the increase of the fatigue strength and cyclic durability of the pipeline systems elements.

The preliminary triboelectrochemical treatment of billets made of titanium alloys has a significant impact on the operational characteristics of lightweight flanges. The triboelectrochemical treatment increases the homogeneity of the surface layer and approximates its physical and chemical properties to the properties of the material in the entire bulk. The preliminary treatment of the cathode-brush provides the increase of ductility of titanium alloys before the process of dieing and prevents formation of brittle gas-saturated layers. All of the abovementioned improves the billets surface quality and prevents the appearance of unwanted stress concentrators on it. As a result, the triboelectrochemical treatment of the billets made of titanium alloys improves its plastic properties, increases the resistance to the appearance and spread of fatigue cracks, what is beneficial to the longevity and reliability of products.

When the lightweight flanges are pressed (Fig. 1), axial residual macrostresses accumulate in the zone of maximum plastic strain, i.e. in the ridge, which negatively impacts on the endurance of products. The preliminary triboelectrochemical treatment is intended to align the residual stresses throughout the wall thickness of pipe billet before forming to ensure homogeneity of the material flow and to prevent rejection.

Fig. 1. The lightweight flange of 50 mm in diameter made of titanium alloy PT-7M

The investigation of residual stress distribution across the wall thickness of pipe billets and products was carried out by the method of electrotensometry with sequential grazing of strained layers by the electrochemical method. The results of calculations by the method of Davidenkov [1] are presented in charts 2 - 5.
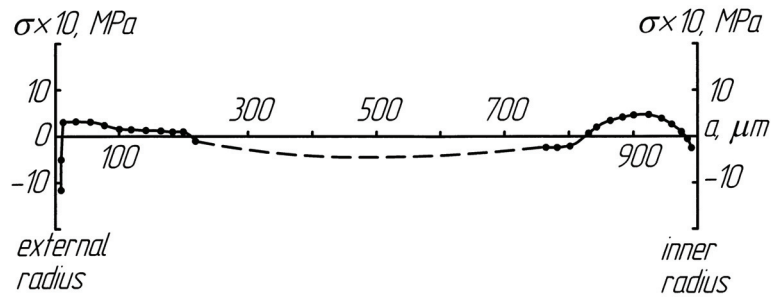
Fig. 2. The graph of distribution of residual stresses throughout the pipe wall thickness ø 50 mm in a state of delivery: a - the wall thickness of the pipe billet

The character of the distribution of residual stresses throughout the wall thickness of the workpiece in a state of delivery (Fig. 2) indicates that there is a slight defective gas-saturated layer at the surface of pipes.
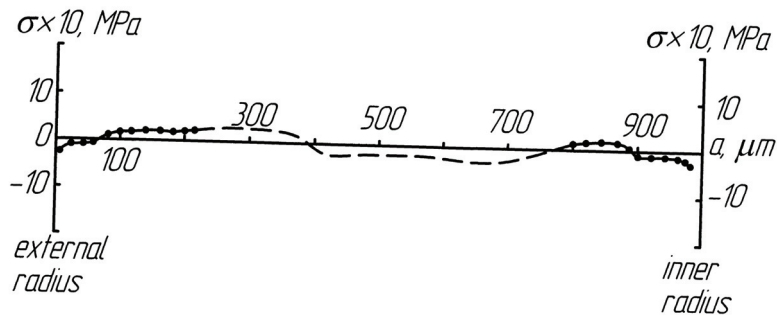
Fig. 3. The graph of distribution of residual stresses throughout the pipe wall thickness ø 50 mm after the triboelectrochemical treatment of the outside: a - the wall thickness of the pipe billet

The reduction of residual stresses on the outside of the workpiece to the level of 15 - 20 MPa is caused by removing of a thin layer of material from the surface of the pipe billet by the triboelectrochemical treatment on the external diameter (Fig. 3). The preliminary triboelectrochemical treatment before the formation evens out the residual stresses across the entire wall thickness, which contributes to the uniformity of plastic deformation.
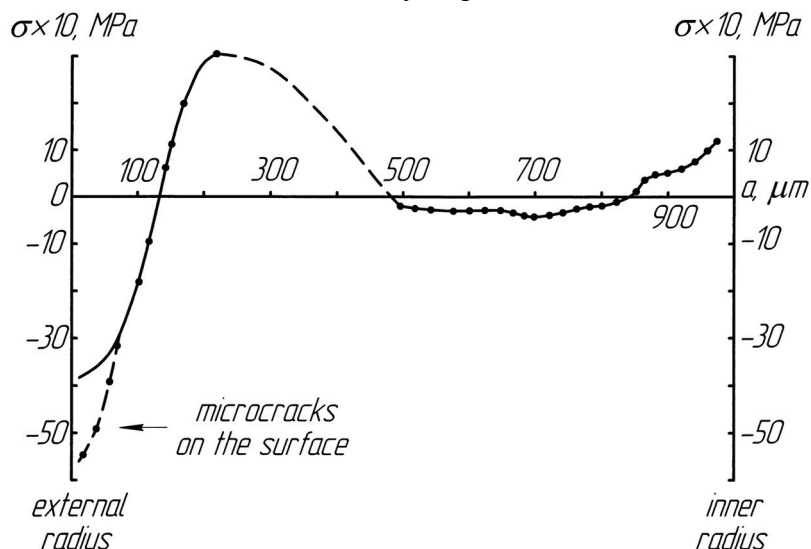
Fig. 4. Graph of distribution of residual stresses throughout the wall thickness of the ridge flange with the condiional pass 50 mm without the triboelectrochemical treatment (conditional strain 20%): a - the wall thickness of the flange

When the flanges are pressed by the flexible filler with conditional relative deformation 20% without the application of the preliminary triboelectrochemical treatment, the residual compressive stresses being 550 MPa were found on the external radius of the corrugation (Fig. 4), which exceeds

the yield strength of the material (σ_y = 380 MPa). The formation of microcracks net (or microcavities) on the outside of the corrugation is the cause of this excess, which is methodical experimental error in the determination of residual stresses arising from the increase of the electrochemical etching speed of the defective surface (a priori assumed that the etching rate is constant in the experiment).

The residual tensile stresses acting on the inner radius of the flange corrugation reach 120 MPa and become compressive at a depth of 150 μm (Fig. 4).

The distribution of the residual stresses throughout the flange wall thickness has changed significantly after the preliminary triboelectrochemical treatment of workpieces and the subsequent formation. The compressive residual stresses acting on the outside radius of the corrugation are 80 - 100 MPa while the tensile residual stresses acting on the inner radius are 400 - 420 MPa, what is approximately equal to the yield strength (Fig. 5).

Thus, the preliminary triboelectrochemical treatment provides the favorable conditions of plastic deformation along with the redistribution of residual stresses, which compensates pulsating loads, experienced by the pipeline systems of aircraft, through the wall thickness of the finished product.
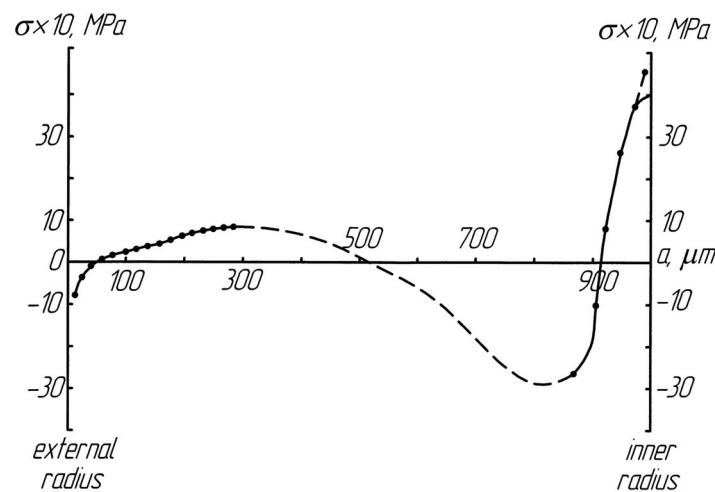
Fig. 5. The graph of the distribution of residual stresses through the wall thickness of the flange ridge with the conditional pass 50 mm with the preliminary triboelectrochemical treatment (conditional strain 20%): a - the wall thickness of the flange

The batches of lightweight flanges are made in accordance with the following technological schemes for research of the influence of the triboelectrochemical treatment on the durability:

1. The pipe billets of 50 mm in diameter made of titanium alloy PT-7M (the state standard 19807-91) were processed with a brush-cathode in the following regime: the operating voltage U = 7,5 V; the time of the treatment τ = 30 s; the current density i_a = 150 A/cm^2; the rotational speed of the cathode-brush V = 2200 rev/min, the material of the brush-cathode pile - copper MM-1 (ТУ 16-705.492-2005). Then the lightweight flange ridge with the degree of deformation - 20% was pressed by the cold plastic deformation method by the flexible filler with axial compression.

2. Billets of PT-7M were not exposed to the preliminary triboelectrochemical treatment, the formation of corrugation was happening in a few transitions with the consistent application of the deformation by the 8 – 10 % and intermediate annealing. The selected flange batches were annealed in the following regimes:

550°C – 0,5 h in the titanium foil in the air;
550°C – 0,5 h in vacuum;
650°C – 2 h in vacuum;
750°C – 2 h in vacuum.

The formed lightweight flange batches were tested for endurance to the appearance of cracks on the test machine URM-I with the frequency of the loading 40 Hz and of axial compression force

P_{max} = 3700 N (370 kg · s) corresponding to the torque of a clamp M_t = 5 N · m (50 kg · s · cm). If lightweight flanges withstood 2 million cycles, the tests were continued with the increased axial compression force P_{max} = 5000 N (500 kg · s). The test results are shown in Table 1.

Table 1

The test results of flanges

№ the sample	Characteristics of the sample	Axial force P, kg·s		The number of cycles stable to failure	Nature of the destruction	The average number of cycles stable to failure
		P_{max}	P_{min}			
1	annealing 650°C, in vacuum 2 h	370	35	950 000	longitudinal crack	563 100
2		370	40	285 000	crack	
3		370	40	470 500		
4		370	40	547 000		
5	annealing 550°C, in the titanium foil in the air 0,5 h	370	50	125 000	crack	155 300
6		370	45	200 000		
7		370	50	141 000		
8	annealing 550°C, in vacuum 2 h	370	50	230 000	crack	319 400
9		370	50	265 000		
10		370	45	463 200		
11	annealing 750°C, in vacuum 2 h	370	50	250 000	crack	299 600
12		370	50	269 000		
13		370	45	380 000		
14	The triboelectrochemical treatment	370	40	2 000 000	no cracks	1 876 700
15		370	50	2 000 000		
16		370	50	2 000 000		
17		370	45	1 070 000	microcrack	
18		370	50	2 000 000	no cracks	
19		500	50	2 013 000	microcrack	
20		500	50	2 054 000		

The experimental data showed that the flanges, exposed to the preliminary triboelectrochemical treatment, withstood the destruction up to 1,876,700 cycles in average with a load of 500 kg. The flanges, exposed to the various regimes of heat treatment, withstood the destruction from 155,300 to 563,100 cycles. It means the treatment of workpieces by cathode-brush increases the number of cycles stable to failure from 3.3 to 12 times.

The conclusions

1. The treatment of workpieces by the cathode-brush removes the surface gas-saturated layers evening out the residual stresses across the wall thickness of the pipe billet, which allows avoiding the earlier plastic flow of the surface layer material in the process of the cold deformation in comparison with the core.

2. The application of the triboelectrochemical treatment before forming increases ductility of the pipe billet material, redistributes residual stress across the wall of the finished product, creating a the surface tension on the inner surface for compensating of the pulsating pressure of the working environment in the pipeline systems of aircraft.

3. The preliminary triboelectrochemical treatment of the inner billets surface can increase the number of cycles of the lightweight flanges steadeness to the destruction from 2.2 to 12 times in comparison with the flanges, which are used with the application of heat treatment.

References

1.*Фридман Я. Б.*. Механические свойства металлов. Ч. 1. – М.: Машиностроение. 1974. – 472 с.

V.N. Kazak, Ph. D., Prof., A.G. Ogyr, Post-g. student
(National Aviation University, Ukraine)

SYNTHESIS OF A TRAFFIC MANAGEMENT SYSTEM ON THE HELICOPTER ALTITUDE

When operating the helicopter take off, as well as stabilization of a given height hanging apparatus there is a need for control problems of the center of mass position of the helicopter in a vertical plane. The presented control algorithm ensures the required characteristics of a closed system when changing altitude helicopter.

Theoretical studies of the dynamics of controlled helicopters and practice development and use of automatic piloting helicopters found that the design of control loops angular motion and the motion of the center of mass can be performed separately.

Problems controlling the position of center of mass of the helicopter in the space are solved under the assumption that the automatic stabilization system designed by the angular position. It is assumed here that the internal rotational motion of the control loops have a much greater speed than the outer contours of controlling the position of center of mass. Synthesis of control laws for the outer contours is performed on the equations of motion of the center of mass.

The equations of motion of center of mass of the helicopter at the height of the form [1]:

$$\dot{H} = V \qquad m\dot{V} = P(H,\varphi) + Y(H,V) - G, \tag{1}$$

where H - the height, V - velocity of change in altitude, G - weight of the helicopter, m - its mass, Y - aerodynamic drag force, $P(H, \varphi)$ - lift the rotor, depending on the altitude H and the pitch φ.

The aerodynamic drag force is directed against the velocity vector and defined as follows:

$$Y(H,V) = \begin{cases} -c_x(H)S\dfrac{\rho V^2}{2}, V \rangle 0 \\ c_x(H)S\dfrac{\rho V^2}{2}, V \langle 0 \end{cases} \tag{2}$$

where c_x – coefficient of drag machine, S – area of its cross section, ρ – density of air at this altitude.

The dependence of the lift from the rotor pitch φ is nonlinear and is approximated by:

$$P(H,\varphi) = \chi G p(H,\varphi)$$
$$\chi \rangle 0 \tag{3}$$

where χ – coefficient of traction stock with respect to the weight of the helicopter.

Nonlinear function:

$$p(H,\varphi) = c_1(H)\varphi^2 + c_2(H)\varphi^3$$
$$c_1, c_2 \rangle 0 \tag{4}$$

The coefficients c_1, c_2 depend on the altitude. With minor changes H can be made permanent.

For the control of the object function is φ - pitch rotor. Controlled variable is the H - height of the helicopter. In this case, equation (1) becomes:

$$\ddot{H}(t) = F(H, \dot{H}, \varphi) \tag{5}$$

$$F(H, \dot{H}, \varphi) = \frac{1}{m}(P(H,\varphi) + Y(H,\dot{H}) - G)$$

The ultimate goal of management is considered the conclusion of the helicopter on a constant height H^0 = const. Thus it is necessary that the process $H(t) \rightarrow H^0$ may largely correspond to the solution of equation:

$$\ddot{H}^{*}(t) + \beta_1 \dot{H}^{*}(t) + \beta_0 H^{*}(t) = \beta_0 H^0$$

$$\beta_1 = 2\frac{\zeta}{\tau_H}, \beta_0 = \frac{1}{\tau_H^2}$$

(6)

where τ_H – the time constant for the controlled variable H.

From control theory it is known that the best results are achieved with transient damping coefficient $\zeta = \sqrt{2}/2$. In this case, the transition process $t_H \approx 3\tau_H$, and the magnitude of the overshoot $\sigma \approx 5\%$.

The figure 1 shows a block diagram of a control loop center of mass motion of the helicopter at an altitude.
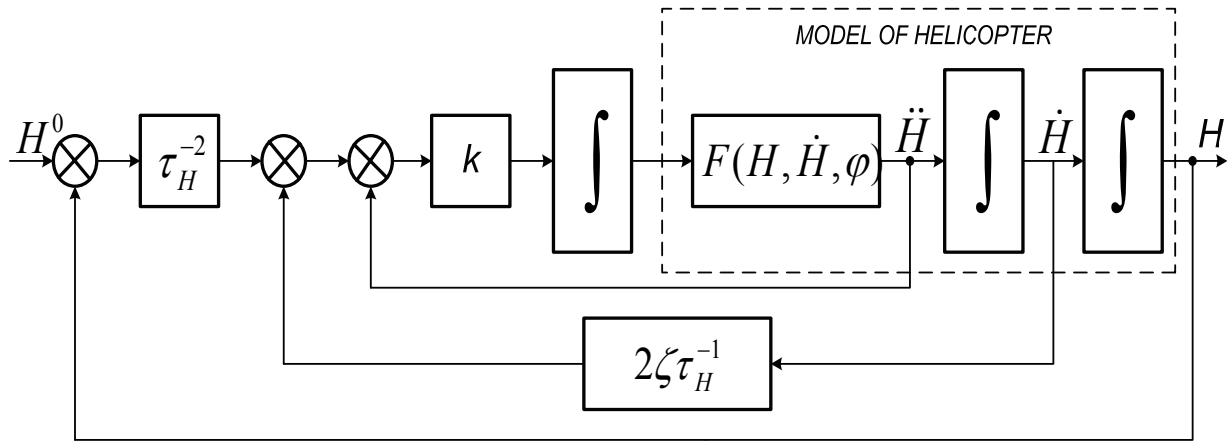
Fig. 1. The block diagram of a control loop center of mass motion of the helicopter on the height

To calculate the control function φ used in the system of measuring height H, and its rate of change $\dot{H}$ and of acceleration $\ddot{H}$.

Based on the general form of the control algorithm to accelerate, as described in [2], the control function $\varphi(t)$ is calculated by the relations:

$$\dot{\varphi}(t) = k\left[F^{*}(H, \dot{H}) - \ddot{H}\right]$$

$$F^{*}(H, \dot{H}) = \frac{1}{\tau_H^2}(H^0 - H) - 2\frac{\zeta}{\tau_H}\dot{H}$$

(7)

Here F^{*} is the required acceleration of the height at which the trajectory is realized, the reference given by the equation system (6).

With the proper gain k in the forward loop system constructed algorithm provides error testing $\delta_H(t) = H^0 - H(t)$ of the law, which is defined by equation (6) designated trajectory [3].

Expression (7) for the deviations are of the form:

$$\dot{\delta}_{\varphi} = k\left[F^{*}(\delta_H, \dot{\delta}_H) - \ddot{\delta}_H\right]$$

$$F^{*}(\delta_H, \dot{\delta}_H) = -\frac{1}{\tau_H^2}\delta_H - 2\frac{\zeta}{\tau_H}\dot{\delta}_H$$

(8)

For small deviations δ_H can be taken $F_0^0 = 0$. Under this condition, the homogeneous equation has the form:

$$\frac{1}{kF_{\varphi}^0}\dddot{\delta}_H + \ddot{\delta}_H + 2\frac{\zeta}{\tau_H}\dot{\delta}_H + \frac{1}{\tau_H^2}\delta_H = 0$$

(9)

,

which describes the process of changing $\delta_H(t)$ the actual height deviations from the assigned values of H^0.

From (9) shows that in the case $kF_\varphi^0 \to \infty$ of a deviation $\delta_H(t)$ will be determined by the differential equation:

$$\ddot{\delta}_H^* + 2\frac{\zeta}{\tau_H}\dot{\delta}_H^* + \frac{1}{\tau_H^2}\delta_H^* = 0 \tag{10}$$
,

which follows from (6), if there is to take $\delta_H^*(t) = H^0 - H^*(t)$.

As a result, the control algorithm would be:

$$\dot{\varphi} = \frac{N}{\tau_H F_\varphi}(F^* - \ddot{H}),$$

$$F^* = \frac{1}{\tau_H^2}(H^0 - H) - 2\frac{\zeta}{\tau_H}\dot{H} - \frac{\tau_H}{N}(F_0\dot{H} + F_1\ddot{H}) \tag{11}$$

This control algorithm (11) has a variable options F_φ, F_0, F_1 linearly dependent on the coordinates of the state of H, $\dot{H}$ and the control function φ.

In this equation, which describes the process of changing the height $H(t) \to H_0$ in the control loop with the given algorithm has constant coefficients and linear

$$\dddot{H} + \frac{N}{\tau_H}(\ddot{H} + 2\frac{\zeta}{\tau_H}\dot{H} + \frac{1}{\tau_H^2}H) = \frac{N}{\tau_H^3} \tag{12}$$

With an appropriate choice of N in the system can be implemented the required degree of approximation of $H(t) \to H^*(t)$. If $\tau_H N^{-1} \to \infty$ in equation (12) takes the form (6). In this case, theoretically, we have $H(t) = H^*(t)$ [4].

Conclusion

The practical usefulness of the algorithms traffic control center of mass of the helicopter can be determined by studying the dynamics of the system in different modes of flight. However, one can expect that the control algorithm (7) with constant parameters will provide the required characteristics of a closed system in which the dynamic properties of the managed object in a wide range. This assertion is based on the fact that the system is managed to accelerate. Therefore, the closed circuit has low sensitivity to changing parameters.

References

1. *Батенко А. П.* Управление конечным состоянием движущихся объектов. – М.: Сов. Радио, 1977. – 257 с.

2. *Крутько П. Д.* Обратные задачи динамики управляемых систем6 нелинейные модели. – М.: Наука. Гл. ред. Физ.-мат. лит., 1988. – 574 с.

3. *Palett, E. H. J. and Coyle, S.*, Automatic flight control, Blackwell Science, 1993 (4th edition)

4. *Bramwell A. R. S. Bramwell's* Helicopter Dynamics / Bramwell A. R. S., Done G., Balmford D. – Oxford : Butterworth-Heinemann, 2001. – 373 p.

UDC 621.396.93(045)

Alekseeva Irina, Lemesh Sergey, Petrova Valentina
(National Technical University «KPI», Ukraine)
Liliya Novachuk, post-graduate student (National Aviation University, Ukraine)

HANDOFF IN HETEROGENEOUS WIRELESS DATA NETWORKS

In this paper the effects of handoff decision algorithms on the performance in a heterogeneous network is presented. A moving-in–moving-out scenario is introduced for vertical handoff in hybrid wireless networks to characterize intertechnology roaming between two networks with substantially different data rates. This creates an overlay-underlay situation in which the MT has a preference to connect to the overlay network to access a substantially higher data rate. As a result, the algorithms for moving out and coming in the overlay network would be different. At the end of the paper are given conclusions.

1. Moving-in moving-out scenario. The moving-in–moving-out scenario introduced in this section is used for the analysis of roaming between two networks with substantially different data rates. This handoff scenario is depicted in Fig. 1, in which the data services of underlay cellular networks are augmented by a high-data rate overlay service such as a WLAN in a dynamic and seamless manner. As shown in the figure, the lower speed underlay network covers the entire area while the higher speed overlay network only covers a small hot spot in the middle of the area of the coverage of the underlay network. Between the area of full coverage of the overlay network and the remaining coverage area of the underlay network there is a transition region for which the overlay network has partial coverage due to the shadow fading characteristics of the radio channel. Since the algorithms and performance in this scenario are not symmetric, this scenario can be further divided into two separate cases:

1. Moving-in: from underlay cellular network (e.g., GPRS or UMTS) to overlay network (e.g., WLAN or WiMAX)

2. Moving-out: from overlay network to underlay network.
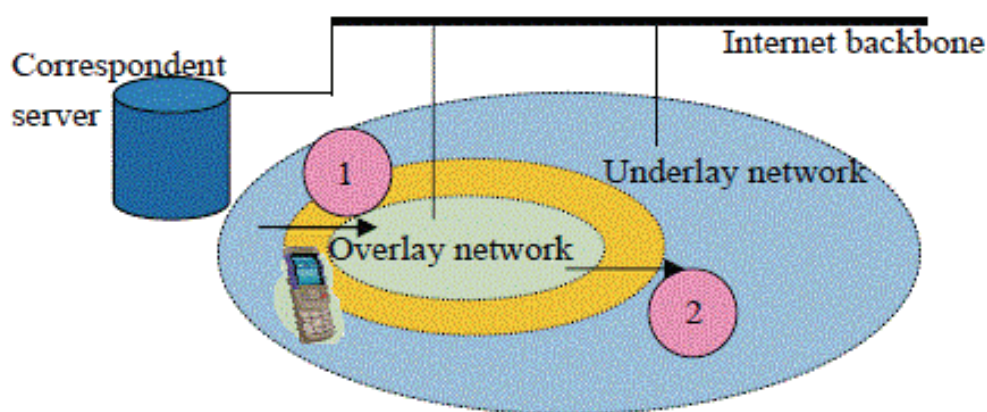
Fig. 1. Scenarios for Inter-technology handoff.

For the design of a handoff decision algorithm, this scenario provides a completely different environment than the Manhattan micro-cellular scenario. In the Manhattan micro-cellular scenario, the handoff decision algorithm has no specific preference to connect to a wireless point of connection because all points of connections provide the same service. Therefore, the handoff decision is made by processing the vector of received signal strengths from all base stations. In the moving-in moving-out scenario, the MT has a preference to connect to the overlay network, and the decision is made based on the received signal strength from the overlay network wireless point of connection only. In the Manhattan micro-cellular scenario, the ideal location for handoff is the

midpoint between the wireless points of connections. In the moving-in moving-out scenario, we do not know the ideal location for the handoff.

2. Throughput analysis for the traditional handoff algorithms.

In homogeneous networks, pure power based handoff generates a lot of unnecessary handoffs back and forth between wireless points of connection. In heterogeneous network access, some amount of ping-pong can be tolerated in favor of maximizing the overall mean throughput. The effective data rates in overlapping radio cells can be noticeably different. Therefore it may be beneficial to try to utilize this difference in data rates already in the transition region, thus maximizing the benefits of making a vertical handoff.

For analysis purposes, we consider two simple handoff algorithms: one based only on received signal strength and one based on a dwell timer with received signal strength. The performance of these algorithms is analyzed in the transition regions of moving out scenarios. The objective in this analysis is to determine what factors are important during the handoff and how they influence the handoff decision.

3. Performance in moving-in scenario.

As a numerical example, we compare the difference in gain in throughput for dwell-timer and power based handoff algorithms to find out their sensitivity to the handoff delay in the moving out scenario. Performance is measured as mean throughput during moving-in transition in proportion to the ratio of the effective data rates. The dwell-timer is used only when making a vertical handoff from WLAN to cellular to persist in the higher effective data rate system.

It is assumed that in the moving-in scenario the dwell-time is no longer than the total sojourn time in the hot spot. Fig. 2 shows how an increase in the dwelltimer is affecting the throughput in comparison with the power based handoff algorithm where the handoff decision is based solely on the received signal power level and the predefined threshold value. The mobile terminal velocity is a constant 5 m/s. The ratio of the effective data rates is 5 corresponding to, e.g., UMTS-WLAN roaming. The figures show five different cases where handoff delay is varied from 100ms up to 4s. The zero dwell-timer is equal to the power based case but it is not shown in the figures due to the logarithmic scale chosen for the dwell-time axis. The results show that it is not beneficial to increase the dwell-time beyond a certain point with small velocities, as it affects the throughput in the defined transition region. This is the case with both small and large handoff delays and it is more severe with the small delays. This can be explained by the fact that a long dwell-time excludes data from the slower network, assuming that only one NIC receives data during the transition at a time. When the ratio of the effective data rates is low (5 or less), the use of a longish dwell-timer blocks data that could have been received from the cellular data interface. Increasing the velocity makes the transition region shorter (it is traversed in a shorter period of time), which directly decreases the number of collected time samples within the transition region and thus results in lower mean throughput in the transition region.

Clearly, the use of a dwell-timer has limited value in such conditions, and the maximum value of the dwell-time is around 200-300 ms. The fact that the ratio of the effective data rates is quite low, indicating that the difference between the effective data dates of the overlapping systems is not considerable, naturally lessens the potential of using the dwell-timer in the scenario used, in comparison to a simple power (RSS threshold) based handoff algorithm. In fact, with high handoff delay (more than 1 s), the added value of using a dwell-timer becomes negligible. Only in the case of a higher than pedestrian velocity and with low vertical handoff delay does the dwell-timer provide a small additional gain in mean throughput.

When the ratio of the effective data rates is low, the use of the dwell-timer has little or no value. It can even decrease the mean throughput and cause unwanted disruption in the data traffic. Thus in practice the value of the dwell-timer should be kept at a minimum, yet aiming at a gain in mean throughput to the extent that it is possible, taking into consideration the application requirements for parameters such as maximum allowed delay and number of retransmitted packets.
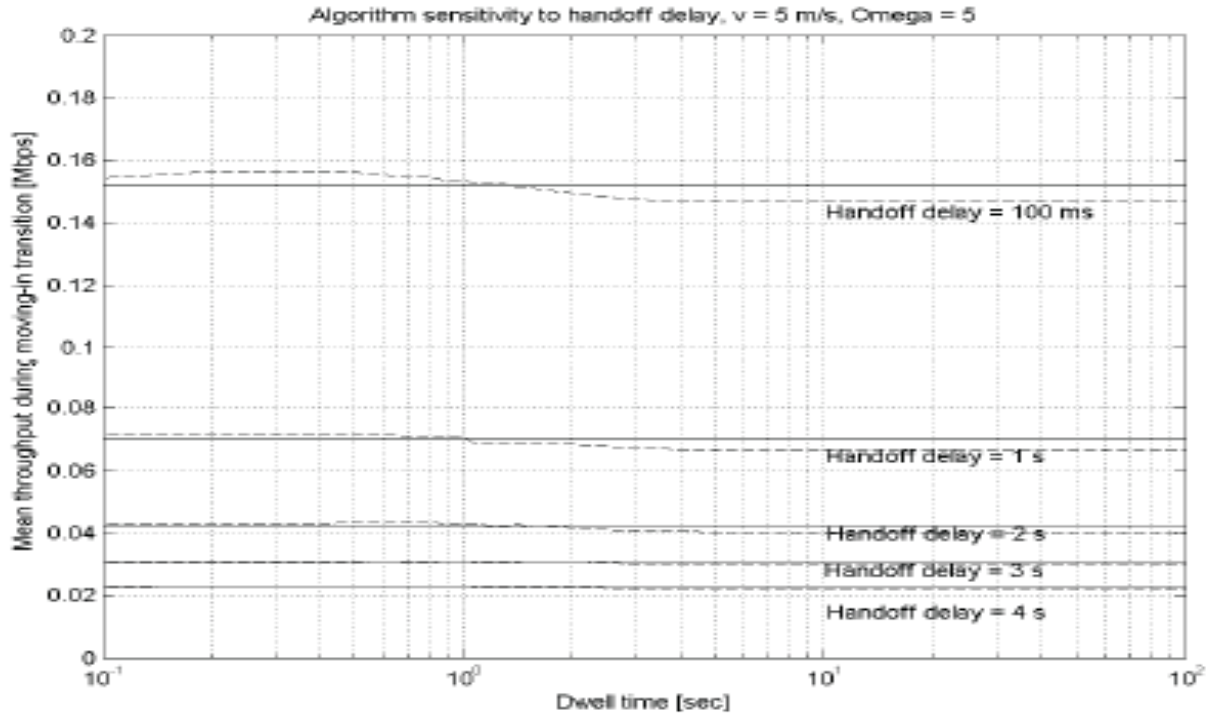
Fig. 2. Comparison of the power and dwell-timer based handoff algorithms in the moving-in scenario with different handoff delay values (100 ms … 4 s). $\Omega = 5$ and mobile velocity of 5 m/s.

Fig. 3 presents throughput performance comparisons when the ratio of the data rates is 20, corresponding to, e.g., GPRS-WLAN roaming. It can be immediately noticed that the dwell-timer is now very effective, especially with low handoff latencies and higher mobile velocity.

This can be explained with the increased difference in the effective data rates. It is no longer beneficial to visit lower speed networks due to the penalty in time that performing the handoff incurs. A higher velocity translates into a shorter transition region in time, resulting in fewer RSS samples with a static sampling rate.

A higher mobile speed increases the importance of collecting all possible RSS samples during the transition, thus making a difference in comparison to the power (RSS threshold) based handoff algorithm. Increasing the dwell-timer without a limit is not reasonable for a real application, and the dwell-timer must naturally have a finite value.

In our simulation model, the maximum value can be increased to very high values. This simply indicates that the mobile terminal is persisting in the overlay network from the first RSS sample it can access. Maximum gain in mean throughput is reached with a dwell-timer value of around 1 s. As a numerical example, in Fig. 3 we see that when the MN velocity is 5 m/s, the ratio of the effective data rates is 20, and the vertical handoff delay is 100 ms, gain in mean throughput with a 1 s dwelltimer is more than 10 % (125 kB/s -->144 kB/s) over the power based algorithm.

One can note a clear difference between the results presented in Fig. 2 and Fig. 3, indicating a trend for the benefits of using a dwell-timer when the ratio of the effective data rates is high.

The overlaying hotspot provides a theoretical data rate higher than 1 Mbps at the edge of the hotspot cell. In general, the dwell-timer based handoff algorithm seems to be less sensitive to an increase in velocity than it is to an increase in handoff delay. In other words, the increase in handoff delay seems to lessen the potential of using a dwell-timer in the moving-in scenario.
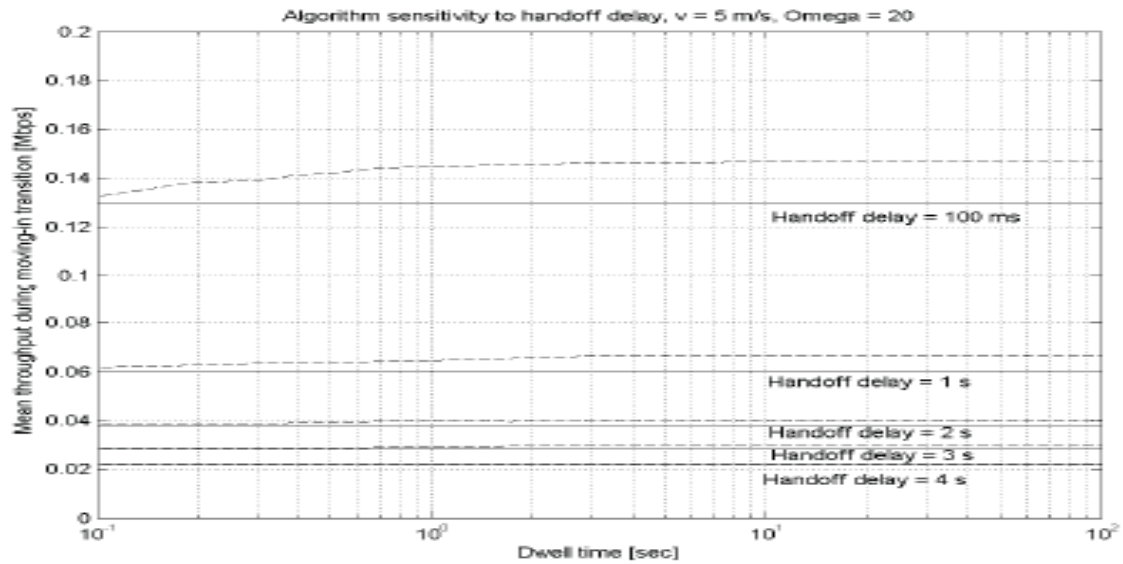
Fig. 3. Comparison of the RSS and dwell-timer based handoff algorithms in the moving-in scenario with different handoff delay values (100 ms … 4 s). $\Omega = 20$ and mobile velocity of 5 m/s.

The increase in velocity seems to increase the potential of getting more gain in mean throughput by using a dwell-timer in the moving-in transition, compared with the power (RSS threshold) based handoff algorithm.

Conclusion

Results for handoff algorithm sensitivity to the handoff delay and the velocity of the mobile terminal in the moving-out scenario are shown in Fig. 2 and Fig. 3. Similarly to the moving-in scenario, a dwell-timer is used only when making a vertical handoff from WLAN to cellular. While in the moving-in scenario the transition region ends after the handoff to WLAN is executed for the last time and handoff delay Δ has past, in moving-out one must consider when the dwell-timer ends. In the moving-in scenario, the dwell-timer ends when the MN sojourns in the WLAN cell, so it does not matter if it is longer than the transition region. But, in the moving-out scenario, the dwell-timer extends beyond the transition region. We refer to this phenomenon as the *post transition effect*. Results in Fig. 2 and Fig. 3 clearly illustrate how the increased dwell-timer suddenly decreases mean throughput in the moving-out transition region.

References

1. Ylianttila M, Mäkelä J, Krishnamurthy P & Pahlavan K (2000) Intertechnology mobility testbed. Proc. Finnish Wireless Communications Workshop, Oulu, Finland, 1: 38-43.
2. Ylianttila M, Mäkelä J & Pahlavan K (2005) Analysis of handoff in a location-aware vertical multi-access network. Elsevier J Comp Networks 2,185-201.
3. Zeng H & Chlamtac I (1999) Handoff traffic distribution in cellular networks. Proc. Wireless Communications and Networking Conference, (WCNC), 413-417.
4. Zhou J & Sun N (2006) A Seamless Handoff Scheme for Mobile IP. Proc. IEEE Vehicular Technology Conference, (VTC), 2: 927-931.

UDC 629.735.33-519 (045)

V.M. Kazak, Ph.D., prof., O.K. Gorbach, Post-g. student
(National Aviation University, Ukraine)

UNMANNED AERIAL VEHICLE WITH AEROSTAT ATTRIBUTE

The main features of aerostat and their characteristics are analyzed. Design of solar powered hybrid unmanned aerial vehicle with aerostat attribute is proposed. Aerostat lift value and necessary power value for horizontal flight, takeoff and landing of the hybrid UAV are calculated.

Balloons, gliders and dirigibles were the first aircrafts, which raised human in air [1]. Today despite the fact that the type of aircraft lighter than air with the propulsion system has given way to familiar to us planes and helicopters, most recently in the world are actively reviving the idea of airship as an alternative mode of transport because of its safety, environmental friendliness and versatility. Advances in technology allowed us to use not flammable hydrogen but an inert helium to fill the airship. Modern airships seem more attractive for use in various fields because of their efficiency and environmental friendliness. They can be equipped with internal combustion engines, electric motors and solar panels, nuclear engines. According to the developers of the Russian airship "BARS", there is 8-10 times lower cost of passengers and cargo transportation by "BARS" than by the aircraft [2].

Attempts to get rid of the dirigible's shortcomings have led to the appearance of combined airships that use not only the aerostatic force of helium, but also the airscrew thrust to create the lift force. Therefore an interest in aerostatic aerial vehicle (AAV) developed, which have great potential to achieve high performance. Enhancing of airplane performance with the help of features of dirigible is proposed in paper. Application of combined method of creating lift force promises to mix the positive features of the airship and airplane and eliminates their special shortcomings. Hybrid of airplane and airship allows to combine the maneuverability of the airplane with the airship fuel economy.

Development of modern membrane materials to accommodate the gas (that is lighter than air, eg helium) is equally important to create AAV because of its considerable leakage through the membrane. Previously, all the gas in dirigible stationed in the membrane of a single volume and with a simple wall of oiled or varnished cloth. Subsequently, membranes were made of rubberized fabric or other (synthetic) single-layer or multilayer materials to prevent leakage of gas and increase their service life. The volume inside the membrane began to divide into sections. Fiberglass is a promising material now to make membrane of dirigible [3].

The global trend of development and implementation of renewable and more environmentally friendly energy sources shows that one of the most promising areas in the development of aircraft is to develop a solar powered UAV. Photovoltaic cells generate electricity to power electric engines and airborne equipment. It was created near one hundred UAV various dimensions that uses solar in all over the world to nowadays [4]. Thus, activity of such aircrafts developers and the possibility of combining the merits of different type of aircrafts make a promising development of UAV hybrid class.

Problem formulation. The aim of the article is to analyze the main current publications on the development of AAV and aircraft that equipped with photovoltaic cells. The main subject is to identify the basic parameters of the hybrid UAV with aerostat attribute used photovoltaic cells. Also perform calculation of the lift force that consist of aerodynamic forces and lift force of gas lighter than air and necessary power value for horizontal flight, takeoff and landing of the hybrid UAV.

The main part. Analysis of previously created constructions of the hybrid airship (without airfield airplanes with aerostatic unloading), showed that they are "flying wing" of mixed type, the main part of which is disc-shaped center wing section. It serves to accommodate the lifting gas. The wing panel installed at the edges and also it has a tail unit. This design reduces lateral windage of

aircraft. The presence of such elements as airplane wing and tail unit can provide the necessary stability and control in horizontal flight.

Design proposed of a hybrid UAV typed as "airplane-dirigible" with combination of aerodynamic lift force and the lift force of gas, and solar powered electric propulsion unit is shown in Fig. 1.
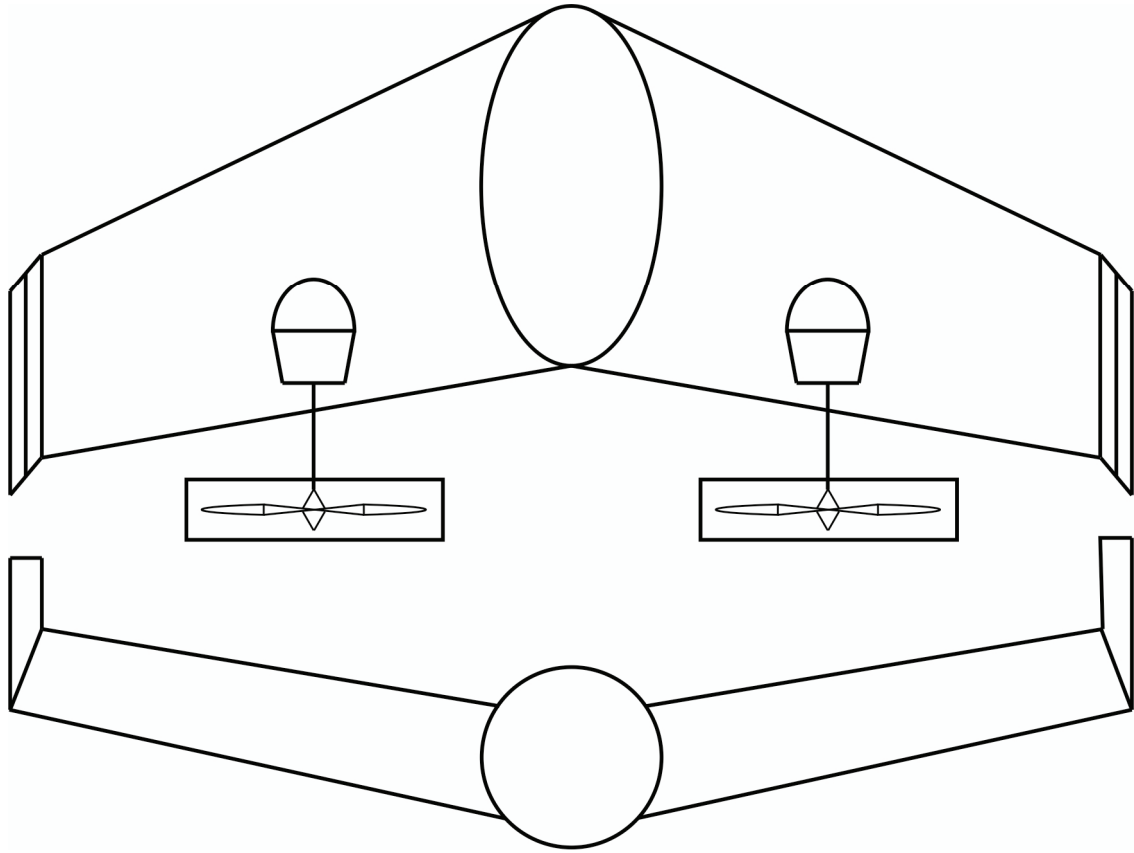
Fig.1. Design of hybrid UAV typed "airplane-dirigible".

Aerostatics is based on the law of Archimedes. On any item that is in the atmosphere, acting lift force equal to the weight of air displaced this object. As known Power of Archimedes for the balloon is equal to:

$$F_A = (m_a - m_g) \cdot g \text{'}$$
(1)

where m_a – weight of air, displaced aerostat membrane, m_g – weight of gas in membrane, $g = 9.81$ м/с^2 – free fall acceleration.

Weight m_a and m_g expressed in terms of the gas density and membrane volume:

$$m_a = \rho_a \cdot V$$
$$m_g = \rho_g \cdot V$$
(2)

where V – membrane volume, ρ_a, ρ_g – respectively, the density of the ambient air and the gas density inside the membrane.

We can obtain the relation between density, pressure and temperature from the equation of Clapeyron-Mendeev, taking into account the fact that ratio of any gas is the ratio of universal gas constant R to the it molecular mass:

$$\rho_a = \frac{p \cdot M_a}{R \cdot T_a} \tag{3}$$

$$\rho_g = \frac{p \cdot M_g}{R \cdot T_g}$$

where p – pressure of ambient air, T_a, T_g – respectively temperature outside air and temperature inside membrane, R_a and R_g – respectively gas constant of air and gas.

Finally aerostat lift force taking into account (2) and (3) receive from (1):

$$F_A = \frac{V \cdot p \cdot g}{R} \cdot \left(\frac{M_a}{T_a} - \frac{M_g}{T_g} \right) \tag{4}$$

We use specific lift force to compare the lift force efficiency of one cubic meter of various gas. Specific lift force is:

$$f_A = \frac{F_A}{V} = \frac{p \cdot g}{R} \cdot \left(\frac{M_a}{T_a} - \frac{M_g}{T_g} \right) \tag{5}$$

The values of gas constant are given in Table. 1.

Table. 1.

Gas constant

Parameter	Air	Helium	Hydrogen
Molar mass, kg/mol	0,0289644	0,004	0,002
Gas constant, J/kg K	287	2079	4158

We obtain the specific value after divide the right and left sides of (5) by g. It indicates how many pounds can raise 1 m³ of a gas under certain conditions. Calculations of the specific lift force value for various gases are given in Table. 2 in terms of international standard atmosphere (ISA), which is used by ICAO in calculations of aircrafts movement:

pressure p_0=101325 Pa,
temperature ambient air T_0=15 °C,
altitude H_0=0 m,
hunidity f=0%,
rate of temperature drop L=0,0065 K/km,
universal gas constant R = 8,31447 J/mol K.

Table. 2.

Specific lift force values for various gases in terms of ISA.

Ges temperature, °C	Specific lift force, kg/m³		
20	air	helium	hydrogen
40	0,021	1,057	1,140
60	0,098	1.068	1,145
80	0,165	1,077	1,150
100	0,225	1,085	1,154
120	0,279	1,093	1,158
140	0,370	1,099	1,168

As we can see from the analysis of the data in Table. 2. specific lift force of helium and hydrogen are almost equal. It gives an advantage to helium over hydrogen for wider use because of the explosion hazard of the last one.

It is also necessary to evaluate the effect of altitude on the specific lift force. We analyze the dependence of air pressure, temperature and density at the height compared to the MSA. To calculate these parameters at a certain height in the troposphere (the lower part of the atmosphere,

within 8-18 km depending on latitude, in our case, we consider up to 3 km, where linear decrease in temperature is the main property) will be used the following relations:

temperature at altitude h above sea level:

$$T = T_0 - L \cdot h \tag{6}$$

pressure at altitude h above sea level:

$$p = p_0 \cdot \left(1 - \frac{L \cdot h}{T_0}\right)^{\frac{g \cdot M}{R \cdot L}} \tag{7}$$

We calculate density by substituting the appropriate temperature values T and pressure p at a given altitude h in (3).

It has already been considered in detail the influence of the major factors on the aerostat lift force. Sometimes it is necessary to assess the impact on the aerostat lift force of such a parameter as humidity. At 100% humidity and ambient temperature of 20 degrees the lift force is reduced by 1% compared to the absolutely dry air, and at 40 degrees, this decrease will amount to 3%. It would give reducing lift force by 15...20 kg for aerostat class AX-7 [Таланов А.В. Все о воздушных шарах. М, Изд. Астрель, 2002]. As we can see the influence of humidity has a little effect on small UAVs.

Modern photovoltaic elements, including, of Ukrainian origin have 15-20% efficiency. The emergence of thin film GaAs, multilayer GaInP/GaAS/Ge photovoltaic cells with efficiency up to 24-32% can get from one square meter of surface of 200 - 300 W power. The relative weight of photovoltaic cells is about 5g/W. It is no obstacle in their use of UAVs as a power source. Therefore, the use of photovoltaic cells as a power source UAV as alternative inexhaustible energy sources is a good prospect.

Using photovoltaic cells as the main-board DC power supply require UAV to equip with batteries for the accumulation of electrical energy during the day and electric power supply for equipment and propulsion at night. Modern sealed chemical power sources, for example, based on Li-ion, have relative characteristic "power-weight" about 250 Whr/kg. It allows their use as a power source in small UAVs.

Conclusion

The analysis of the main current publications on the development of AAV and aircraft by using photovoltaic cells is conducted. Design of solar powered hybrid unmanned aerial vehicle with aerostat attribute is proposed. The basic parameters of the hybrid UAV typed unmanned aerial vehicle with aerostat attribute using photovoltaic cells are designed. The calculations aerostat lift force and power necessary for horizontal flight, takeoff and landing UAV hybrid are done.

References

1. *Кулик М.С., Казак В. Н., Гусинін В.П.* «Дирижаблі», Ч.1, – Киев: НАУ, 2005. – 184 с.
2. *Яшина Г. А.* «Дирижабли шаг в будущее», - Федеральное интернет-издание, 2010. - http://www.kapital-rus.ru/articles/article/176532
3. *Бойко Ю.С.* «Воздухоплавание в изобретениях», - М., 1999. – 352 с.
4. *Noth A.* "Design of solar powered airplanes for continuous flight", - Zurich, 2008. – 196 p.

S.V. Enchev, PhD, S.S. Tovkach, post-graduate student
(National Aviation University, Ukraine)

METHOD OF MULTIFRACTAL FORMALISM FOR ANALYSIS INFORMATION IN ELECTRONIC CONTROL SYSTEMS AIRCRAFT GAS TURBINE ENGINES

Considered the foundations of the continuous wavelet-transform-based multifractal analysis theory and the information necessary for diagnosis gas turbine engines. It explains generalizations of a multifractal concept to irregular functions, better known as the method of wavelet transform modulus maxima; it discusses the efficiency of the multifractal formalism in the investigation of nonstationary processes and short signals.

Introduction. It is known that among the faults and failures of gas turbine engine make up a significant part of the parametric, consisting of the disparity between the values of the parameters controlled by the engine specification standards. To control and prevent similar failures are used parametric methods of diagnosis, based on special processing and analysis thermo gas dynamic values and other parameters measured at the engine running [1]. Assessment of the technical state of engines as the flight and ground applications, operating conditions is carried out, usually for a limited amount of information, which is due to small number of staff monitored parameters. This significantly limits the efficiency of parametric methods of diagnosis based on the identification of mathematical models of the workflow engine. Therefore, current research is to improve the efficiency of diagnostic methods, including the method of multifractal formalism for the analysis of information in electronic control systems of aircraft gas turbine engines.

Stating the problem. The theory of fractals and multifractals [2] is currently widely used to describe self-similar and complex scaling properties observed in various physical systems [2,3]. Fractals are geometric objects (lines, surfaces, and bodies) that have a jagged shape and exhibit some degree of similarity (repetition) in a wide range of scales. The repetition can be complete (regular fractals) or might show some elements of randomness (random fractals). The structure of random fractals on a small scale is not identical to the structure of the entire object, but their statistical properties coincide and self-similarity persists after averaging over statistically independent realizations of the object.

A single quantity – the Hausdorff dimension or scaling exponent – is sufficient to statistically describe a fractal. It describes the preservation of both the geometry and the statistical properties under scaling. But many effects in physics, chemistry, biology, and other sciences exist that require generalizations of a fractal-like idea to more complex structures with additional scaling exponents. These structures are often characterized by a set of coefficients, and the Hausdorff dimension is just one of them. Complex fractals, called multifractals, are important because they most often occur in nature, while simple, self-similar objects only idealize real phenomena. In practice, the multifractal approach means that the object under study can be divided into parts each of which has its own self-similarity properties [4]. Signals recorded in natural experiments are also important representatives of this class, and the existence of a precise mathematical approach to the analysis of complex structures of processes is undoubtedly valuable for a large number of practical problems. Simple or monofractal processes (for example, a $1/f$ noise or a Wiener random process) are homogeneous in the sense that their scaling parameters remain the same on any scale. The spectrum of such signals, $S(f) \sim f^{-\beta}$, does not change in a large frequency range, i.e., β is a constant. A multifractal process can be decomposed into regions with different local scaling properties. Consequently, describing such a process requires a large number of coefficients. In particular, the multifractal process spectrum cannot be described by a power law with a single exponent β. Several known attempts to generalize the multifractal concept to functional signal dependences exist. One such attempt is based on the method of structure functions, which is often used in various fields of research. This approach is most popular in the study of strongly developed turbulence [3]. In the

early 1990s, Muzy, Bacry, and Arneodo [2, 4] proposed a more advanced method of the "wavelet transform modulus maxima" (WTMM), which has significant advantages: the possibility of analyzing a wide range of singularities and their derivatives, smaller errors in computing the scaling characteristics, etc. The WTMM method has been successfully applied in studying the structure of inhomogeneous processes of various kinds. It is based on wavelet analysis [4], which is also called a mathematical microscope due to its ability to preserve good resolution on multiple scales. The WTMM method, which we consider below, was proposed by Muzy, Bacry, and Arneodo and is based on the continuous wavelet transform. This method is attractive because it allows considering both singular measures and singular functions and is much more universal in studying multi-scale properties of objects than the previously developed methods. Wavelets are often interpreted as a generalization of classical algorithms for covering a set by spheres, cubes, etc. Because the basis functions of the wavelet transform are well localized (soliton-like), they provide an effective mathematical method for analyzing nonstationary processes.

Because many processes in nature belong to the multifractal class, the multifractality property can be considered a very general rule of nature; this phenomenon merits study and description itself. Moreover, this study is practically valuable due to the possibility of developing new methods of analysis for experimental data based on the WTMM method and applicable to the solution of multiple problems. We note that few methods for processing nonstationary data exist. If the properties of a process change even in extremely short time intervals, then classical random process analysis algorithms can lead to errors in interpreting the results. The set of universal tools, applicable independently of stationarity, includes the interpretation based on the analytical signal concept, the detrended fluctuation analysis, and the wavelet analysis [5]. The multifractal method discussed in this paper is another instrument for this task. Although the WTMM method uses a wavelet analysis in intermediate calculations, it would be incorrect to regard this method as a part of wavelet analysis: it is a combination of two separate theories, the theory of wavelets and the theory of multifractals, which has profound similarities with statistical thermodynamics. Such a combination of two separate theories gives new opportunities to solve applied problems.

The method of wavelet transform modulus maxima. The WTMM method studies irregular behavior of a function $g(x)$ in two stages. In the first stage, the wavelet transform is performed in accordance with equation

$$W(a, x_0) = \frac{1}{a} \int_{-\infty}^{\infty} \psi\left(\frac{x - x_0}{a}\right) g(x) dx . \qquad (1)$$

The result of the wavelet transform can be interpreted as a surface in a three-dimensional space (Fig. a). The most important information is contained in the "skeleton" – the lines of local extrema of the coefficient surface $W(a, x)$, which are sought at each a (Fig. b).
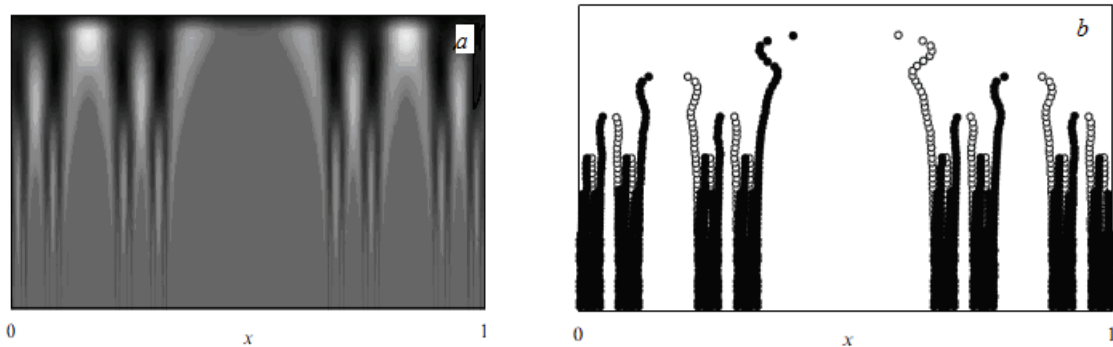
Figure: a – A projection of a wavelet transform on to the ax plane. Larger values of the wavelet coefficients $W(a, x)$ correspond to darker regions; b - Lines of the local extrema of the $W(a, x)$ coefficient surface; the minima are white circles and the maxima are black circles

The choice of the basis functions is determined by the type of information to be extracted from $g(x)$. A necessary condition is that the selected wavelet have the smoothness not less than that of the signal. Regarding the choice of the parameter m in

$$\psi^{(m)} = (-1)^m \frac{\partial^m}{\partial x^m} \left[\exp\left(-\frac{x^2}{2} \right) \right], \qquad (2)$$

we note that on one hand, increasing m allows ignoring large-scale polynomial contributions (that is, removing the trend) and analyzing small-scale variations of the function, but on the other hand, multiple differentiation leads to an increase in the number of lines of local extrema of the wavelet coefficients and to a large number of additional lines occurring at a small scale. Those lines are too short to conduct estimates of power dependences like $W(a, x_0) \sim a^{h(x_0)}$ as $a \to 0$ and become obstacles in a numerical study of the singularities.

As pointed out in [2, 5], the wavelet transform is constructed such that $W(a, x)$ is a regular function even if $g(x)$ is irregular. All the information about a possible singularity of $g(x)$, including its localization x_0 and exponent $h(x_0)$, is reflected in the asymptotic behavior of the coefficients $W(a, x)$ for small a. If the coefficients diverge at small scales, then g has a singularity at x_0 and the Holder exponent can be found by plotting equation $W(a, x_0) \sim a^{h(x_0)}$ in a double logarithmic scale and calculating the slope of $\ln W(a, x_0)(\ln a)$. If the coefficients $W(a, x)$ are close to zero in the vicinity of x_0 on a small scale, then g is regular at that point. An important observation in computing the Holder exponent is that the sought characteristics are theoretically independent of the choice of the wavelet transform basis functions, which allows introducing a universal (in some sense) analysis of local irregularities (although the wavelet representation, of course, depends on the chosen basis).

The first step of the WTMM algorithm concludes with the selection of a skeleton. The analysis of the selected lines of local extrema and the local maxima of the wavelet transform moduli theoretically allows computing the Holder exponent, i.e. analyzing the singularities of $g(x)$. But this approach is only approximate; with an increase in scale, the influence of neighboring singularities increases, leading to various errors. In multifractal theory, it is preferable to perform calculations based on the so-called partition functions $Z(q, a)$ that allow obtaining more reliable estimates of the sought characteristics. Therefore, the second step of the WTMM method consists in constructing the partition functions as

$$Z(q, a) = \sum_{l \in L(a)} |W(a, x_l(a))|^q , \qquad (3)$$

where $L(a)$ is the set of all lines of local maxima of the wavelet-coefficient moduli that exist on scale a, and $x_l(a)$ characterizes the position of the maximum belonging to the line l. In this case, the use of the modulus of the wavelet coefficients ensures the stability of the method. Without that (using phase information), the method would not allow obtaining a stable solution. We note that in general, considering the maxima can lead to difficulties related to the stability of the method (it is better to operate with averaged values). Nevertheless, the wavelet transform procedure itself uses coefficients computed within a frequency - time window, which already provides averaging. Definition (3) does not work for negative q, because it is possible to have a situation where $W(a, x_l(a)) = 0$. In practice, therefore, another formula is used,

$$Z(q, a) = \sum_{l \in L(a)} \left(\sup_{a' \le a} |W(a', x_l(a'))| \right)^q . \qquad (4)$$

which means selecting the maximum value of the wavelet-coefficient modulus along each line on scales less than the given value of a. According to [4], the relation

$$Z(q, a) \sim a^{\tau(q)}, \qquad (5)$$

holds, where $\tau(q)$, to be determined for some q from the slope of $\ln Z(q, a)(\ln a)$, is called the scaling exponent. Varying the powers q in constructing partition functions (4) yields a linear dependence $\tau(q)$ for monofractal objects $(H = d\tau / dq = const)$ and a nonlinear dependence

$\tau(q) = qh - D(h)$ with a large number of Holder exponents $h(q) = d\tau/dq \neq const$ in the case of multifractals. For some values of q, the scaling exponents $\tau(q)$ have a simple interpretation [4]. Thus, there is a dependence between $\tau(2)$ and the exponent β in the spectral power density function $S(f) \sim 1/f^\beta$:

$$\beta = 2 + \tau(2). \tag{6}$$

Furthermore, because the spectral density function is related to the correlation function by the Fourier transformation, the known β allow determining the rate of decrease of correlations $\psi(\tau) \sim \tau^{-\gamma}$, i.e., the exponent γ. The dependence between the basic quantities used within the WTMM method is determined by the Legendre transform

$$\begin{cases} h = \dfrac{d\tau}{dq}, \\ D(h) = qh - \tau(q), \end{cases} \tag{7}$$

Compared to the method of structure functions, the multifractal analysis based on the wavelet transform allows investigating singularities at negative q. The partition functions $Z(q, a)$ for $q < 0$ characterize the scaling properties for weak singularities (small fluctuations), and for $q > 0$, for strong singularities (large fluctuations).

Conclusion. Multifractal formalism based on wavelet analysis, in comparison with traditional methods of studying the structure of the signals (such as correlation analysis) makes it possible to explore the more subtle characteristics. This method shows sensitivity to the dynamics on different scales from weak singularities (small fluctuations) to strong singularities (large fluctuations). The basis of the analysis of the wavelet transform is a tool very well suited for studying the properties of self-similarity (in terms of wavelet coefficients then stepped behavior of their higher moments when zooming). The method is well suited for solving physics problems, since it operates with intuitive features. In particular, the singularity spectrum provides information on the one hand, the correlation properties of the process (which are among the basic characteristics of the theory of stochastic processes) and on the other hand, the degree of homogeneity of the signal, which is a quantitative measure of the width of the function of the generalized fractal dimension D_q.

Therefore, it is possible to improve the quality of the electronic control system by modifying the algorithms and complexity management, and improved diagnostics, enter accounting experience and technical condition of the engine. This method allows you to diagnose damage in the early stages when they are not visible at the external review. Further development of this area will detect defects and their place of deployment, reducing operating costs and allow the most efficient use of engines.

References

1. *Климентовский Ю.А.* Системы автоматического управления силовыми установками летательных аппаратов / Учебное пособие // Под ред.. д.т.н. Митраховича М.М. – К.: КВIЦ, 2001. – 400 с.

2. *Павлов А. Н.* Мультифрактальный анализ сложных сигналов / А. Н. Павлов, В. С. Анищенко // Успехи физических наук. – 2007. – Т. 177, вып. 8. – С. 859 – 876.

3. *Schroeder M.* Fractals, Chaos, Power Laws: Minutes from an Infinite Pardise (New York: W.H. Frecman, – 1991) [Translated into Russian (Moscow Izhevsk: RKhD, –2001, – p. 440)].

4. *Meyer Y.* Wavelets: Algorithms and Applications (Philadelpha, Pa.: Society for Industrial and Applied Mathematics, – 1993, – p. 214)

5. *Пахомов Г.И., Пахомов Ю.Г.* Применение вейвлетов для обработки сигналов // Вестник ПГТУ. Электротехника, информационные технологии, системы управления / Г.И. Пахомов, Ю.Г. Пахомов. – Пермь: Изд-во Перм. гос. техн. ун-та, 2007. – 86 с

UDC 681.14 (045)

F. Geche PhD, V. Kotsovsky, PhD (Uzhorod National University, Ukraine)
A. Batyuk, PhD (Lviv National University, Ukraine)
D. Shevchuk, PhD (National Aviation University, Ukraine)

THE RECOGNITION OF DISCRETE PATTERNS AND SIGNALS IN THE NEURAL BASIS

The method of real time synthesis of four-layered neural schemes for the recognition of Boolean vectors is studied in the paper. Also studied is the efficiency of the working of these schemes dependent upon the values of the tolerance matrix indices used in the recognition schemes synthesis

Introduction. The methods of the neural technologies are very powerful and useful for solving different applied tasks in information theory, time series forecasting and pattern recognition. The synthesis procedure consists of two main levels. In the first level we must elaborate efficient methods of the synthesis of one threshold device with many inputs. The number of inputs depends on actual task conditions. The second level is connecting the neural elements into one logical schema. The configuration of this schema must provide the realization of needed mapping. The classical threshold synthesis methods (approximation methods, iterative methods) aren't efficient in practice if the neuron have large numbers of inputs. So the development of new methods of synthesis of threshold elements of neural schemas is a very important task nowadays. In the given investigation we proposed the method of tolerance matrices for the synthesis of one threshold element. These nets can be successfully used in solving the problem of real task classification and object recognition encoded by Boolean vectors [1-4].

The synthesis of the recognition scheme. Let $K_1, K_2, \ldots, K_t$ be the learning sample for object classes $K_1', K_2', \ldots, K_t'$| Classes K_i', K_j' $(i \neq j)$ and subsets $K_i \subset K_i'$, $K_j \subset K_j'$ $(i \neq j)$ can have non-empty intersection. Let us consider the task of the neural scheme synthesis assigning for several objects d from $\bigcup\limits_{i=1}^{t} K_i'$ one of the object classes K_i' if the learning sample is thus defined:

$$K_1 = \left\{ \left(\alpha_{11}^{(1)}, \ldots, \alpha_{1n}^{(1)} \right), \left(\alpha_{21}^{(1)}, \ldots, \alpha_{2n}^{(1)} \right), \ldots, \left(\alpha_{k_1 1}^{(1)}, \ldots, \alpha_{k_1 n}^{(1)} \right) \right\},$$

$$\ldots\ldots\ldots\ldots\ldots\ldots\ldots\ldots\ldots\ldots\ldots\ldots\ldots\ldots\ldots\ldots\ldots\ldots\ldots$$

$$K_t = \left\{ \left(\alpha_{11}^{(t)}, \ldots, \alpha_{1n}^{(t)} \right), \left(\alpha_{21}^{(t)}, \ldots, \alpha_{2n}^{(t)} \right), \ldots, \left(\alpha_{k_1 t}^{(t)}, \ldots, \alpha_{k_1 n}^{(t)} \right) \right\},$$

where $\alpha_{ij}^{(r)} \in \{0,1\}$.

We use the neural scheme with three neural device layers and one logical output block which detects the membership of the specified object d to one of the object classes $K_1', K_2', \ldots, K_t'$ [4].

The algorithm of the synthesis of the recognition scheme.
Step 1. Let $\{K_1, \ldots, K_t\}$ be the learning sample, set $s = 1$ and go to step 2.
Step 2. Build the set

$$A_s = K_s \cup \left(Z_2^n \setminus \bigcup\limits_{i \neq s} K_i \right) \tag{1}$$

and find an arbitrary p-cover of the set K_s with the fixed indices $j_{1s}, j_{2s}, \ldots, j_{r_s s}$ in the set A_s, that is $P_{A_s}\left(K_s; \mathbf{b}_1^s, \ldots, \mathbf{b}_{r_s}^s \right) = \mathbf{b}_1^s p\left(\mathbf{b}_1^s A_s \right) \cup \mathbf{b}_2^s p\left(\mathbf{b}_2^s A_s \right) \cup \ldots \cup \mathbf{b}_{r_s}^s p\left(\mathbf{b}_{r_s}^s A_s \right)$.

Search out the structure vector $\left[\mathbf{w}_{ms}; T_m^s \right]$ for the characteristic function f_m^s of the set $\mathbf{b}_m^s p\left(\mathbf{b}_m^s A_s \right)$ $(m = 1, 2, \ldots, r_s)$ following the above-mentioned algorithm. On detecting the first-layer structures $\left\{ \left[\mathbf{w}_{1s}; T_1^s \right] \ldots, \left[\mathbf{w}_{r_s s}; T_{r_s}^s \right] \right\}$, search out the second-layer weight vector $\mathbf{v}_s$ and go to step 3.

Step 3. If $s < t$ then set $s = s + 1$ and go to step 2, otherwise the synthesis of the scheme is finished.

Note 1. *P*-cover $p_{A_s}\left(K_s; \mathbf{b}_1^s, ..., \mathbf{b}_{r_s}^s\right)$ of the set K_s in A_s with the fixed indices $j_{1s}, ..., j_{sr_s}$ is not detected unambiguously. Therefore we can select minimum, maximum or any other *p*-cover.

If we want to select the *p*-cover unambiguously, then we should define the learning sample (the set of Boolean vectors for the testing of the recognition scheme) and select for it the optimal *p*-cover of the set K_s in A_s with the fixed indices $j_{1s}, ..., j_{sr_s}$ with the property of minimizing the error for this learning sample for fixed η. The step-by-step changing of the value of $\eta \in (0, 1)$ helps us to search out the optimal value η^* and respective optimal indices $j_{1s}^*, ..., j_{r_s s}^*$ of the *p*-subsets.

Note 2. Subject to the technical condition of first-layer neuron realization (the maximum absolute value of weights) we can detect the index j_{ms} of the tolerance matrix corresponding to the given calculation. Following the above-mentioned algorithm the maximum absolute value of the weights of the block s is equal to $2^{j_{ms}-1} + 1$. Therefore the bounds at components of structure vectors are defined by the indices of the tolerance matrix.

Note 3. If we set $j_{1s} = 1, ..., j_{sr_s} = 1$ we should obtain the simple classifier.

Let us consider the example of the synthesis scheme. Let us have the receptive fields 3×3. Set the following learning sample and specify two classes. We thus encode these binary images. The first three components of vector are filled on the basis of the first line of the receptive field. If the corresponding cell contains "*", then the component of vector is equal to 1. If the cell does not contain "*", then it is equal to 0. Next we fill following components on the base of second and third rows.

Let us write the codes of respective binary images in the learning sample classes $K_1; K_2$ of the classes K_1', K_2'

$$K_1 = \begin{cases} \mathbf{b}_1^1 = (010111010), \\ \mathbf{b}_2^1 = (010011010), \\ \mathbf{b}_3^1 = (010101010), \end{cases} \qquad K_2 = \begin{cases} \mathbf{b}_1^2 = (111010010), \\ \mathbf{b}_2^2 = (110010010), \\ \mathbf{b}_3^2 = (011010010). \end{cases}$$

We find the maximum *p*-cover for K_1', K_2' with the maximum indices and synthesize the recognition scheme. According to the algorithm, on building the *p*-set $p\left(\mathbf{b}_1^1 A_1\right)^{\sigma_{11}}$, where $\sigma_{12} = \begin{pmatrix} 1 & 2 & 3 & 4 & 5 & 6 & 7 & 8 & 9 \\ 3 & 4 & 5 & 1 & 2 & 6 & 7 & 8 & 9 \end{pmatrix}$, we can use all vectors from Z_2^9 except $(101011000)^{\sigma_{11}}$, $(101001000)^{\sigma_{11}}$, $(100011000)^{\sigma_{11}}$. So:

$$p\left(\mathbf{b}_1^1 A_1\right)^{\sigma_{11}} = (L_2 \ 0...0) \triangle \left(L_2^*(1) \ 0...0\right) \triangle \left(L_3^*(1) \ 0...0\right) \triangle ... \triangle \left(L_9^*(1) \ 0...0\right). \tag{2}$$

We can write (2) at matrix notation

$$p\left(\mathbf{b}_1^1 A_1\right)^{\sigma_{11}} = \begin{pmatrix} 000000000 \\ 100000000 \\ 010000000 \\ 001000000 \\ 000100000 \\ 000010000 \\ 000001000 \\ 000000100 \\ 000000010 \\ 000000001 \end{pmatrix}$$

The maximum p-cover of the learning sample K_1 of the class K_1' in A_1 contains the only subset, that is

$$P_{A_1}(K_1; \mathbf{b}_1^1) = \mathbf{b}_1^1 p(\mathbf{b}_1^1 A_1).$$

On the basis of decomposition (8) we build the vector $\mathbf{u}_{11} = (u_1^{11}, u_2^{11}, \ldots, u_9^{11})$:

$$u_1^{11} = -1, \ u_2^{11} = u_1^{11} - 1 = -2, \ u_3^{11} = u_2^{11} + (1-1) = -2, \ldots, u_9^{11} = u_8^{11} + (1-1) = -2 \, .$$

Then we define the weight vector $\mathbf{w}_{11} = \mathbf{b}_1^1 (\mathbf{u}_{11}^{\sigma_{11}^{-1}}) = \mathbf{b}_1^1 (-2,-2,-2,-1,-2,-2,-2,-2) = (-2,2,-2,1,2,2,-2,2,-2)$ and the threshold $T_1^1 = ((\mathbf{b}_1^1 \oplus \mathbf{g}^{\sigma_{11}^{-1}}), \mathbf{w}_{11}) = ((0,1,0,1,1,1,0,1,1), \mathbf{w}_{11}) = 7$. So, we look for the first-layer neuron of the first block with the structure $[(-2,-2,-2,1,2,2,-2,2,-2); 7]$.

Similarly we can build the vector structure of the neural element of the second block of the first layer.

$$p(\mathbf{b}_1^2 A_2)^{\sigma_{12}} = \begin{pmatrix} 000000000 \\ 100000000 \\ 010000000 \\ 001000000 \\ 000100000 \\ 000010000 \\ 000001000 \\ 000000100 \\ 000000010 \\ 000000001 \end{pmatrix},$$

where $\sigma_{12} = \begin{pmatrix} 1 & 2 & 3 & 4 & 5 & 6 & 7 & 8 & 9 \\ 1 & 3 & 2 & 4 & 5 & 6 & 7 & 8 & 9 \end{pmatrix}$. Here we can use all vectors from Z_2^9 except $(101011000)^{\sigma_{12}}$, $(101001000)^{\sigma_{12}}$, $(100011000)^{\sigma_{12}}$. In this case the maximum p-cover of the learning sample from the class K_2' in A_2 with the maximum index coincides with the set $\mathbf{b}_1^2 p(\mathbf{b}_1^2 A_2)$, that is

$$P_{A_2}(K_2; \mathbf{b}_1^2) = \mathbf{b}_1^2 p(\mathbf{b}_1^2 A_2).$$

The above-mentioned algorithm $\mathbf{u}_{12} = (-1,-2,-2,-2,-2,-2,-2,-2,-2)$,

$\mathbf{w}_{12} = \mathbf{b}_1^2 (\mathbf{u}_{12}^{\sigma_{12}^{-1}}) = (1,2,2,-2,2,-2,-2,2,-2)$ and $T_1^2 = ((\mathbf{b}_1^2 \oplus \mathbf{g}^{\sigma_{12}^{-1}}), \mathbf{w}_{12}) = 7$. Then, the neuron of the second block has the structure $[\mathbf{w}_{12}, T_1^2]$.

Then we substitute K_s in place of B_s in (6) and find $v_1^1 = 1$, $v_1^2 = 1$. Thereby, the synthesis of the recognition scheme is finished. The first-layer neuron of block 1 can be activated only if input vectors belong to

$$P_{A_2}(K_1; \mathbf{b}_1^1) = \mathbf{b}_1^1 p(\mathbf{b}_1^1 A_1) = \{(010111010), (010011010), (010101010), (110111010),$$
$$(000111010), (011111010), (010110010), (010111110), (010111000), (010111011)\},$$

and these vectors cannot activate the first-layer neuron of block 2. Therefore, the recognition scheme reckons the following images to class K_1'.

These images correspond to the set
$$P_{A_2}(K_2; \mathbf{b}_1^2) = \mathbf{b}_1^2 p(\mathbf{b}_1^2 A_2) = \{(111010010), (011010010), (110010010),$$

$(101010010), (111110010), (111000010), (111011010), (111010110), (111010000), (111010011)\}$.
Concerning the others binary images the recognition scheme doesn't make a decision because $F_1 = 0$ and $F_2 = 0$.

If we realize the synthesis of the recognition scheme for above-mentioned classes of binary images concerning minimum p-covers with the minimum indices then we should have

$$p\left(\mathbf{b}_1^1 A_1\right)^{\sigma_{11}} = p\left(\mathbf{b}_1^2 A_2\right)^{\sigma_{12}} = \begin{pmatrix} 000000000 \\ 100000000 \\ 010000000 \end{pmatrix}$$

and $P_{A_1}\left(K_1; \mathbf{b}_1^1\right) = K_1$, $P_{A_2}\left(K_2; \mathbf{b}_1^2\right) = K_2$. The first-layer neurons would have the following structures:

(Block 1): [(−1,1,−1,1,1,1,−1,1−1);4], (Block 2): [(1,1, 1,−1,1,−1,−1,1−1);4] with the recognition scheme being the simple classifier.

Note 1. If the probabilities p_i of the occurrence of the vectors of classes $K_1', \ldots, K_t'$ are not equal then the recognition scheme is thus modified: in the fourth layer $\max\{F_i\}$ is changed by $\max\{p_i F_i\}$, $i = 1, \ldots, t$.

Conclusion

1. The developed method of the synthesis of four-layered neural network works in real time and can be useful for the recognition of the object classes encoded by Boolean vectors of very large length.

2. This method provides the searching procedure for optimal values of parameters of the recognition schema that can improve its precision.

3. The method of the synthesis includes different constrains on the value of the first layer weight vectors. It is very important for the technical realizations.

References

1. Гече, Ф. Е. Представление и классификация изображений в пороговом базисе / Ф. Е. Гече, А. В. Ануфриев // Кибернетика, К. – 1990. – №5. – С. 90-96.

2. Батюк, А.Є. Синтез высокопроизводительных специализированных структур для анализа и обработки изображений в пороговом базисе: Гл. 4 / А. Е. Батюк, В. В. Грицык, Ф. Э. Гече [и др.] // Параллельная обработка информации: монография. В 5 т. Т. 5 / [авт. коллектив]: ред.: Б. Н. Малиновский, В.В. Грицык. -- К.: Наук. думка, 1990. – С. 319-363.

3. Гече, Ф. Бульові нейрофункції і синтез розпізнавального пристрою у нейробазисі / Ф. Гече, В. Коцовський, С. Ковальов, А. Батюк // Вісник Національного університету "Львівська політехніка". Комп'ютерні науки та інформаційні технології. – Львів, 2007. – № 598. – С. 44-50.

4. Журавлев, Ю. И. Об алгебраическом подходе к решению задач распознавания или классификации / Ю. И. Журавлев // Пробл. Кибернетики, М.. – 1978. – Вып. 33. – С. 5-68.

UDC 621.396.93(045)

Alekseeva Irina, Kovshyk Anastasiya, Prishepa Tatyana
(National Technical University «KPI», Ukraine)
Tachinina Elena, PhD (National Aviation University, Ukraine)

THE USE OF WIRELESS SENSOR NETWORKS FOR MONITORING AND CONTROL OF TRANSPORT NETWORKS BASED ON SDH TECHNOLOGY

This paper examines and analyzes the possibility of using wireless sensor network technology to monitor and control the transport network based on technology SDH. Analyzes the components of the sensor networks, their architecture and routing protocols. Describes the technology of wireless sensor networks based on standard 802.15.4/ZigBee. At the end of the paper are given conclusions

Recently, the role of innovative technologies to solve the challenges of monitoring and control of transportation networks is growing. One of the latest developments in this area includes wireless sensor networks (WSN). This paper discusses key aspects of the development of wireless sensor networks and the technology of the network for the assessment of the critical object.

The use of low-cost wireless control options opens up new areas for application of telemetry and control systems, such as:
- Replacement of cables in systems;
- Early detection of possible failures of actuating mechanisms for control of parameters such as vibration, temperature, pressure, etc.;
- Control of the access to the systems of the facility;
- Monitoring of the perimeter of the facility;
- Controls on the movement of personnel in the territory of the enterprise;
- Automatization of the control inspection and maintenance;
- Monitoring of the environmental parameters of the environment.

1. **The components of the wireless sensor network.**

Wireless sensor network consists of a miniature computing devices – motes, real sizes of which are typically less than one cubic inch. At mote there are placed the CPU, memory - flash and swift, digital to analog and analog-digital converters, an radio-frequency transceiver, a small power supply, and sensors. Sensors can be very diverse: from the most common measuring temperature, pressure, light level, to specialized, can measure, for example, the level of background radiation and the content of CO_2.

Motes are used for collecting and processing sensor data. One of the advantages of WSN technology is self-organization and the ability to heal itself, which is especially important in the monitoring of strategic sites. Data transmission over the network is stages from one device to another. Routes of transmission are generated automatically so that in finite number of hops across the network data from each mote were transferred to the gateway, which has a connection to the corporate network. In the event of failure of one or more nodes, the network structure is changed so that information from all working motes could be obtained from the gateway.

The ability to deploy networks in difficult conditions, lack of physical communication and the minimum size of sensor devices make the WSN technology extremely flexible. However, there are a number of specific requirements to the functionality of the WSN, which must be considered. One of the main requirements is to implement mechanisms for changing the structure of the network, focused on the external conditions, such as the quality of communication between nodes, which in turn gives rise to the task of assessing the quality of communication or, more generally, "the cost of connection."

The most energy intensive operation for motes is to transfer data in a wireless environment. Because the energy-efficient form the transmission is a key factor for service life extension term, as it is almost entirely dependent on battery life. In networks with multi-link messages forwarding nodes perform the functions of both the sender and the router. Therefore, the failure of some sites

due to lack of nutrition can cause significant changes in the topology of a further reorganization and redirection of packets across the network, which in turn will mean more energy consumption. Thus, the effective management of energy resources is an important aspect of motes operation of wireless sensor networks. However, too strict energy conservation is the negative side, reducing the quality and speed of data transfer, which is unacceptable in some applications.

2. **Communication protocols.**

Communication protocols must satisfy several requirements at once. The problem is solved at different levels of users: the physical, MAC-level, routing level. At the physical level, the main goal is to reduce the energy consumption associated with sending data packets.

The main idea of MAC-level is to "make" mote as long as possible to be in sleep mode, which is characterized by disconnecting from the power of the majority of devices belonging to the spendthrift. Finally, the main concern of the level of routing is to build effective multi-link transmission routes messages from a mote-sender to receiver (usually a gateway).

Data collecting of the wireless sensor network can be done in different ways depending on the purpose of the network. Taking into account the different ways of using online resources, wireless sensor networks can be divided into classes depending on the type of operation and type of the target application:

- Proactive networks. The nodes of the network periodically turn on their sensors and transmitters, remove the evidence and pass them on to the base station. Thus, they make "snapshots" of their environment with some frequency and are usually used for applications that require regular monitoring of certain values.

- Reactive networks. Reactive network nodes with a certain periodicity remove evidence, however, do not pass it, if the data fall within a certain area of normal readings. At the same time, information about the sudden and sharp changes in the readings of sensors and their output outside the range of normal values immediately transmitted to the base station. This type of network is designed to work with real-time applications.

- The hybrid networks. This is a combination of the two types, where the sensor nodes are not only taken periodically send data, but also to respond to sudden changes in the values.

3. **Architecture of wireless sensor networks.**

The development of simple and energy-efficient algorithms for wireless sensor networks has led to the emergence of different architectural solutions. There are two types of architecture wireless sensor networks: homogeneous and hierarchical (cluster). The homogeneity of the network means that all nodes perform the same function in the collection, processing and transmission of information. This approach allows for optimal routing. Data transfer occurs at the most convenient route, which allows savings of important resources such as energy (the channel is on the route with the highest amount of energy) and time (the transfer takes place by the shortest route).

For critical data transfer can be arranged on the most reliable way. Aggregation of data, if necessary, is as following message to the base station. However, the formation of such an organization network links between nodes occurs spontaneously, leading to clashes and the emergence of packet delays associated with the output from hibernation sites are selected on the transmission path.

An alternative approach is a hierarchical routing. It is based on dividing the network into areas, called clusters. Within each cluster there is a router - a node that is responsible for collecting information from around the cluster, its processing and onward transmission. The rest of the cluster mote carry only data collection and transmission of the router.

Thus, the nodes in the hierarchical networks are not equal. First, the aggregation occurs on the router, and second, sending the aggregated data can then be carried out only by routers. Thus minimizes transmission delays, since routers are always available. Clashes of the packages excluded due to the centralized method of creating links. However, this does not provide optimal routing of data paths. In addition, the mote acting as a router, spends much more energy, which leads to rapid depletion of its battery. There are architecture, involving the use of a router is physically isolated

reel, with large reserves of energy and computing power, but this approach is applicable only for a narrow range of applications.

4.   Technology of wireless sensor networks based on standart 802.15.4/ZigBee.

Today, the technology of wireless sensor networks based on standards 802.15.4/ZigBee is the only wireless technology, which can be used to solve the problem of monitoring and control are critical to the battery life of sensors.

ZigBee network operates in license-free 2.4 GHz band and is focused on the transfer of small amounts of information from many sources, including a battery-operated. Scope of ZigBee network extends from the home automation (lighting control, home appliances, audio-video equipment) to build systems to monitor large industrial facilities (eg, temperature control and vibration motors, collecting sensor data flow of electricity, gas and water, fire and security survey sensors). ZigBee technology is based on two independent solutions.

Standard IEEE 802.15.4-2003 determines the physical parameters of the transmitter to build a network of small amounts of data.

The range of frequencies - 868 MHz, 915 MHz, 2.4 GHz, the number of frequency channels 1-16, type of modulation - QPSK and BPSK. This also applies to the so-called medium access protocol (MAC-level), which describes the structure of RF packages and determines the number of addressable devices.

It also describes the mechanisms of verification and validation of the integrity of the received data, procedures for assessing the quality of the channel and the ability to avoid collisions (the restriction on the simultaneous operation of multiple transmitters).

There are transceiver chip based on the standard IEEE 802.15.4 that can be successfully used in data transmission systems that do not have anything to do with technology ZigBee.

Specification of ZigBee stack defines what properties should have a device which is constructed from a network, how to package information is transmitted from one node to another, as a new device connects to the network and who is the chief, and who is subordinate. Specification of ZigBee stack is not a program, it is only a set of rules under which the program should be developed for a specific microcontroller. For the organization of physical connection with the construction of networks of ZigBee transceiver chip used standard IEEE 802.15.4.

Thus, ZigBee is a software add-in, based on the 802.15.4 standart, which defines the range of frequencies and radio format.

Conclusions.

Recently, the role of innovative technologies to solve the challenges of monitoring and control of transportation networks is growing. One of the latest developments in this area includes wireless sensor networks (WSN).

Wireless sensor network consists of a miniature computing devices – motes, real sizes of which are typically less than one cubic inch. At mote there are placed the CPU, memory - flash and swift, digital to analog and analog-digital converters, an radio-frequency transceiver, a small power supply, and sensors. Sensors can be very diverse: from the most common measuring temperature, pressure, light level, to specialized, can measure, for example, the level of background radiation and the content of CO_2.

Data collecting of the wireless sensor network can be done in different ways depending on the purpose of the network.

Taking into account the different ways of using online resources, wireless sensor networks can be divided into classes depending on the type of operation and type of the target application: proactive networks, reactive networks and hybrid networks.

The development of simple and energy-efficient algorithms for wireless sensor networks has led to the emergence of different architectural solutions. There are two types of architecture wireless sensor networks: homogeneous and hierarchical (cluster).

Today, the technology of wireless sensor networks based on standards 802.15.4/ZigBee is the only wireless technology, which can be used to solve the problem of monitoring and control are critical to the battery life of sensors.

The use of low-cost wireless control options opens up new areas for application of telemetry and control systems for SDH technology, such as:

- Replacement of cables in systems;
- Early detection of possible failures of actuating mechanisms for control of parameters such as vibration, temperature, pressure, etc.;
- Control of the access to the systems of the facility;
- Monitoring of the perimeter of the facility;
- Controls on the movement of personnel in the territory of the enterprise;
- Automatization of the control inspection and maintenance;
- Monitoring of the environmental parameters of the environment.

The use of wireless devices to create a dispatch system that provides the operator instant access to information about the state served by the facilities.

References

1. IEEE Std 802.15.4-2003. Part 15.4: Wireless Medium Access Control (MAC) and Physical Layer (PHY) Specifications for Low-Rate Wireless Personal Area Networks (LR-WPANs). 1 October 2003.

2. Cordeiro C.M. Ad hoc & sensor networks Theory and Applications / C.M. Cordeiro, D.P. Agrawal. – Singapore: World Scientific Publishing Co., 2006.

3. Mainwaring A., Culler D., Polastre J., et al. // Proc. of the 1st ACM international workshop on Wireless sensor networks and applications. Atlanta. ACM, 2002. P. 88.

4. Бурдонов И.Б. Операционные системы реального времени / И.Б. Бурдонов, А.С. Косачев, В.Н. Пономаренко. – М.: CITForum, 2006. – 347 с.

UDC 65.011.3:656.71(045)

V. Vovk PhD (National University of Food Technologies, Ukraine)
M. Vasilyev, post-graduate student (National Aviation University, Ukraine)

PREVENTION OF OCCURRENCE OF FAILURE SITUATIONS IN AIRPORT USING EXPERT SYSTEM

In the article reasons of extra situations are analyzed in air-port. The main tasks of airport services are analyzed. It is offered count of functioning of airport services in extra weather terms.

Failure situation means a result of influence of perturbations on process which leads to deviations from fixed plan of flight service.

ICAO determine following weather conditions which may cause failure situations:
− ice- temperature is below 0 C degrees;
− freeze;
− overcold rain;
− high winds;
− rain which causes unreliable adherence with Flight Strip;
− fog or low visibility;
− snow.

Flying operating service of Aircraft AC includes following types of flight support:
− airdrome support of flights executes by airdrome service of airport and includes complex of methods aimed for supporting for permanent operating readiness of airdrome elements. For executing of technology operation for technician support of airdrome involved the base of airdrome service with complex of buildings and necessary equipment;
− for radio and lighting support of flights automatic system of air traffic control, radio systems and navigation aids, radar, radio range systems of landing, lighting equipment of airdromes, communication means e.c.;
− organizing, planning and support of AC traffic on air routes and in field of airdrome is responsibility of Air Traffic Control Service (ATCS) in defined for it areas (field lies to the territory of airdrome upon which in air field maneuvering of AC is exercised). One of the main buildings of ATCS- air traffic control tower which provide air traffic control in areas of limit lines; AC traffic control; airdrome special purpose auto transport control; radio and lighting aids control and control for their functioning;
− providing of controllers of AC with radio connection aids and control for traffic of AC and also keeping these aids in repair are in obligations of radio equipment and connection service. Same functions regarding lighting aids execute service of light providing of flights;
− meteorological support of flights consists from timely informing of commanders, air staff and officers of ATCS about changes of weather conditions in area of airport;
− expert system- is computer program which operates with experience in defined subject area for working out of recommendations or handling of problems;
− system besides executing of calculate operations forms defined reasons and resumes basing on experience it has;
− during solving of problems heuristic and approximate methods are basic which in contrast to algorithmic not always guaranty success. Heuristic essentially is rule of thumb which in machine type is some experience got by man within accumulation of practical experience of handling the similar problems. Such method are approximate in those type as first they do not need estimated initial information and second there are defined level of confidence (or not confidence) that offered handling is correct.

Expert System has within acceptable time find solution which would be not worse which con offer specialist in this subject area.

Expert System is designed taking into account cooperation with different users for which it's operation should be transparent as far as possible.

Note- Expert System consists from experience in defined subject area, accumulated in result of practical activities of human (or humanity) and us it for solving of problems, specific for this area. By this expert systems differs from another "traditional" systems

Main criteria of access to experience are logic adequateness, heuristic power and naturality, notation organicity.

Present AC among technical products are most complicated in architecture and dangerous machines in operation. During design of AC and automatic systems for it's supporting it is necessary maximum reduce part of "Life Cycle Product" according to international standard ISO 9004.

As far as many processes in automatic systems of taking off and landing of planes go with random deformations so tasks handling this problem should be with consideration of probable deviations. Ignoring of stochastic parameters at design of automatic system of all weather taking off and landing of planes may cause sufficient errors and even to crashes.

Integration of acclimatization methods of all weather taking off and landing of planes may be considered as system which is a part of international standard methodology (ISO 9004) of "Life Cycle of Products".

So solving this problem it is possible to claim that at present it is very important and actual.

Subject of research is systems of aviation field. For achieving of fixed aim following tasked were handled:

1. Design of system of automatic engineering of processes of all weather taking off and landing of planes:

- analyze of problems of all weather taking off and landing of planes and problems on operating of airport during bad weather;

- design of mathematic models of all weather taking off and landing of planes;

- optimization of processes of all weather taking off and landing of planes;

- developing of principles of organizing of services and departments of airport.

2. Modeling of Expert Evaluation during all weather taking off and landing of planes:

- analyze of main meteorological elements defining terms and technical requirements for developing automate system;

- forming of base of experience about meteorological elements and their influence on all weather taking off and landing of planes;

- organizing of dialog among traffic control service and another services of the airport

- developing of module of distant refilling and correction of experience base about meteorological elements;

Structure of ES has following components:

−experience base which has many products, assigned by alphabet and system of basic products (formal rules of outputs);

−data store (data base);

−interpreter, solving of task defined for it;

−linguistic processor, releasing cooperation of EX with user (expert) on natural and professional languages, graphic language, tactile influence;

−experience getting components;

−explaining part of component, answering the questions of user;

ES operated in two modes: getting experience mode (by experience Engineer from experts) and in mode of handling of task by user.
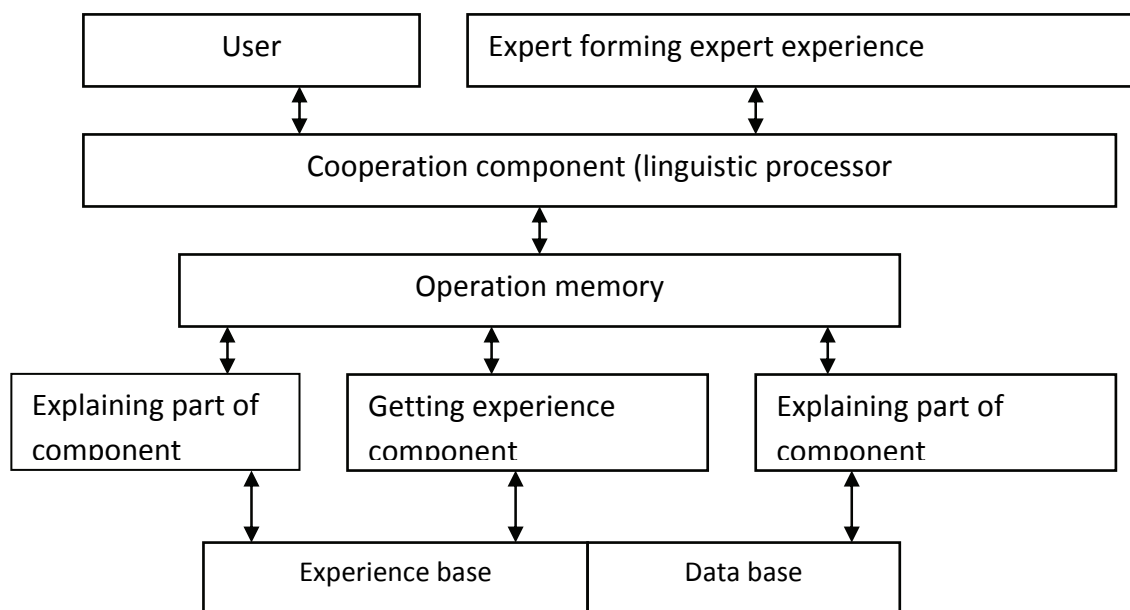
Fig. 1. ES General structure Scheme

Expert systems are applied as effective aid of analyze of poor formalized and difficult algorithmic tasks for recognizing of objects and classifying of conflicts, terms of their release, search for helpful and optimal activities in terms of different conflicts fig.1. Technologies of expert systems allow to find solutions at shortage of initial data about the object of control, to identify strategies and actions of opponent in conflict situations, to proceed meaning content of large volume data and on base of it to form optimal decisions and management. One of the main directions of applying of expert systems in management is conception of casual management, which realize not only control of the object, its parameters and structure but also to each class of situations appearing at functioning of system decision for control is defined.

Conclusion

For effective management of the airport in failure situations, decreasing of economic losses of airlines from bad weather conditions it is reasonable to use expert systems. It will allow to take optimal managerial decisions, to decrease layup time of the aircrafts, to organize lines for taking off and landing according to fixed criteria and to control the activities of airport services for arrangement of the airport during failure situations.

References

1. *Вдовин А. А., Чугаев Ю. Г., Кулицкий Т. П., Махарев Э. И.* Комплексная автоматизированная система управления эксплуатационным предприятием // Транспорт, 1986г. – 174с.

2. *Сапожников Г. В.* Об имитационном моделировании оперативного управления работой аэропорта //Техническая эксплуатация летательных аппаратов и авиадвигателей. – Рига: РКИИГА,1980г. – С.64-72.

3. *Смммирнов Н. Н.* Методика анализа эффективности процессов технической эксплуатации самолетов в эксплуатационных авиапредприятиях. – М.: Воздушный транспорт, 1978г. – 61с.

4. *Запорожець В. В., Шматко М. П,* Аеропорт: організація, технологія безпека // К.: Дніпро 2002р. – 168с.

UDC 681.586.5(045)

L. Afanasyeva (National Technical University «KPI», Ukraine)
N. Kravchuk, PhD (National Aviation University, Ukraine)

EXAMPLES OF CONSTRUCTING A MATHEMATICAL MODEL OF THE PRIMARY SIGNALS OPTIMAL FILTERS IN TELECOMMUNICATION SENSOR-BASED SYSTEMS

The model examples of optimal filtering noised measurements in telecommunication systems with optic lines have considered. It is suggested the algorithm for selection signal to background noise. Possible options for constructing an optimal filter for different forms of output are considered on the example.

Introduction. Problem of filtering signals and images in autocorrelation noise always was relevant in various fields of science and technology. Practical importance has included the analysis images of geophysical fields and remote sensing data and the tasks of medical diagnostics.

Problems of determining the state of the system after the measurement often take place in practice. Measurements are always accompanied by random errors, so it's incorrectly talk about the definition of the system. The evaluation by statistical processing of measurement results should be viewed [1].

Problem. The purpose of this study is to build analytical mathematical models of processing noisy sensor measurements in telecommunication systems (TS) to improve the accuracy of measurements and the corresponding ability to perform specified functions of TS in transfer data with certainty for a long time.

An example of optimal filtering to handle noisy sensor measurements of optical telecommunication systems and fiber optic lines were seen and proposed structure of the algorithm filtering.

Linear Kalman-Byusi filtering theory was extended to the case of cyclic optimal filtering of an obstacle to observations for which at each cycle a linear shaping filter described by the differential equation Gulko - Novoseltsev [2].

A method of construction of analytical mathematical models of optimal filtering signals of sensors includes the following stages.

1)   Based on the fact that the signal is represented as a sum of sinusoids of frequencies ω_0 with random or unknown amplitude and phase and stationary random function with covariance function $k(\tau) = De^{-a|\tau|}(\cos \omega_1\tau + \frac{a}{\omega_1}\sin \omega_1|\tau|)$, with its additive mixture of noise, which has a covariance function $k_1(\tau) = D_1 e^{-a|\tau|}$ have the following differential equation

$$\dot{Z}_1 = Z_2, \dot{Z}_2 = -\omega_0^2 Z_1,$$

-where $Z_1(t)$ - Sinusoidal signal and $Z_2(t)$ - its derivative.

2)   Stationary random function $Z_3(t)$ be considered as forming the filter output signal, described by equations

$$\dot{Z}_3 = Z_4, \dot{Z}_4 = -b^2 Z_3 - 2aZ_4 + V,$$

where $b^2 = a^2 + \omega^2$, and V - white noise with intensity $v = 2Dab^2$.

3)   The observed signal is determined by the formula

$$X = Z_1 + Z_3 + U,$$

U - noise with the covariance function $k_1(\tau) = D_1 e^{-a|\tau|}$.

4)   Thus we have a system of four-dimensional state vector described by the equation $\dot{Z} = a_1 Z + a_0 + \psi V$ at $a_0 = 0$:

$$a_1 = \begin{bmatrix} 0 & 1 & 0 & 0 \\ -\omega_0^2 & 0 & 0 & 0 \\ 0 & 0 & 0 & 1 \\ 0 & 0 & -b^2 & -2a \end{bmatrix}, \quad \psi = \begin{bmatrix} 0 & 0 \\ 0 & 0 \\ 0 & 0 \\ 1 & 0 \end{bmatrix}.$$

Shaping filter for noise U described by equation $\dot{U} + \alpha U = V_1$, де V_1 - white noise with intensity $v_1 = 2D_1\alpha$.

5)   The signal observed miss by back system that is forcing part of the first order transfer function $s + \alpha$. As a result we get signal X_1 with a white noise. Have:

$$X_1 = \dot{X} + \alpha X = \dot{Z}_1 + \alpha Z_1 + \dot{Z}_3 + \alpha Z_3 + V_1 = \alpha Z_1 + Z_2 + \alpha Z_3 + Z_4 + V_1,$$ defined as
$X = b_1 Z + b_0 + \psi_1 V$ at $b_1 = \begin{bmatrix} \alpha & 1 & \alpha & 1 \end{bmatrix}$, $b_0 = 0$, $\psi_1 = \begin{bmatrix} 0 & 1 \end{bmatrix}$

6)   From the formula $\beta = (Rb_1^T + \psi v \psi_1^T)(\psi v \psi_1^T)^{-1}$ finds
$\beta = Rb_1^T v_1^{-1}$.

$$\beta = Rb_1^T v_1^{-1} = \begin{bmatrix} R_{11} & R_{12} & R_{13} & R_{14} \\ R_{12} & R_{22} & R_{23} & R_{24} \\ R_{13} & R_{23} & R_{33} & R_{34} \\ R_{14} & R_{24} & R_{34} & R_{44} \end{bmatrix} \begin{bmatrix} \alpha \\ 1 \\ \alpha \\ 1 \end{bmatrix} * \frac{1}{2D_1\alpha} = \begin{bmatrix} \beta_1 \\ \beta_2 \\ \beta_3 \\ \beta_4 \end{bmatrix},$$

where $\beta_p = \dfrac{\alpha R_{p1} + R_{p2} + \alpha R_{p3} + R_{p4}}{2D_1\alpha}$ $(p = 1,2,3,4)$.

7)   Error covariance matrix R, in this case has the form

$$\dot{R} = \begin{bmatrix} 0 & 1 & 0 & 0 \\ -\omega_0^2 & 0 & 0 & 0 \\ 0 & 0 & 0 & 1 \\ 0 & 0 & -b^2 & -2a \end{bmatrix} R + R \begin{bmatrix} 0 & -\omega^2 & 0 & 0 \\ 1 & 0 & 0 & 0 \\ 0 & 0 & 0 & -b^2 \\ 0 & 0 & 1 & -2a \end{bmatrix} -$$

$$- \frac{R}{2D_1\alpha} \begin{bmatrix} -\alpha^2 & \alpha & \alpha^2 & \alpha \\ \alpha & 1 & \alpha & 1 \\ \alpha^2 & \alpha & \alpha^2 & \alpha \\ \alpha & 1 & \alpha & 1 \end{bmatrix} R + \begin{bmatrix} 0 & 0 & 0 & 0 \\ 0 & 0 & 0 & 0 \\ 0 & 0 & 0 & 0 \\ 0 & 0 & 0 & 2Dab^2 \end{bmatrix}$$

Consider the application of the above methods in case of interference U with exponential-cosine covariance function $k_1(\tau) = D_1 e^{\alpha|\tau|} \cos \omega_2 \tau$. Random function with the covariance function may be seen as the result of converting white noise V_1 with intensity $v_1 = 2D_1\alpha$ shaping filter with transfer function $(s + \gamma)(s^2 + 2\alpha s + \gamma^2)$, where $\gamma^2 = \alpha^2 + \omega_2^2$. Differential equations of this filter has the form $\ddot{U} + 2\alpha\dot{U} + \gamma^2 U = \dot{V}_1 + \gamma W_1$. The inverse system is represented by parallel connection of boosting links with first-order transfer function $s + 2\alpha - \gamma$ and aperiodic chain with transfer function $2\gamma(\gamma - \alpha)/(s + \gamma)$ (fig.1).
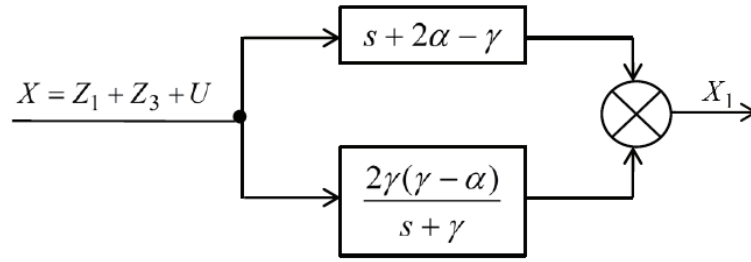
Fig. 1. The scheme of the return system

As a result of converting the system signal that is observed $X = Z_1 + Z_3 + U$ will receive the signal

$$X_1 = (2\alpha - \gamma)(Z_1 + Z_3) + \dot{Z}_1 + \dot{Z}_3 + Z_5 + V_1 =$$
$$(2\alpha - \gamma)(Z_1 + Z_3) + Z_2 + Z_4 + Z_5 + V_1,$$

where Z_5 determined by the differential equation

$$\dot{Z}_5 = 2\gamma(\gamma - \alpha)(Z_1 + Z_3) - \gamma Z_5.$$

The result is a system five-dimensional state vector described by the equation $\dot{Z} = a_1 Z + a_0 + \psi V$ at $a_0 = 0$:

$$a_1 = \begin{bmatrix} 0 & 1 & 0 & 0 & 0 \\ -\omega_0^2 & 0 & 0 & 0 & 0 \\ 0 & 0 & 0 & 1 & 0 \\ 0 & 0 & -b^2 & -2a & 0 \\ 2\gamma(\gamma - \alpha) & 0 & 2\gamma(\gamma - \alpha) & 0 & -\gamma \end{bmatrix}, \quad \psi = \begin{bmatrix} 0 & 0 \\ 0 & 0 \\ 0 & 0 \\ 1 & 0 \\ 0 & 0 \end{bmatrix}.$$

The observed converted signal is determined by the formula $X = b_1 Z + b_0 + \psi_1 V$, at $b_1 = \begin{bmatrix} 2\alpha - \beta & 1 & 2\alpha - \beta & 1 & 1 \end{bmatrix}$, $b_0 = 0$, $\psi_1 = \begin{bmatrix} 0 & 1 \end{bmatrix}$.

Constructed for this system Kalman-Byusi filter, we obtain the optimal filter. Matrix gain β is a matrix-column of elements

$$\beta_p = \frac{(2\alpha - \gamma)(R_{p1} + R_{p3}) + R_{p2} + R_{p4} + R_{p5}}{2D_1 \alpha} \quad (p = 1, \ldots, 5).$$

The equation of covariance matrix [3] in this case has the form

1.5.29

$$\dot{R} = \begin{bmatrix} 0 & 1 & 0 & 0 & 0 \\ -\omega_0^2 & 0 & 0 & 0 & 0 \\ 0 & 0 & 0 & 1 & 0 \\ 0 & 0 & -b^2 & -2a & 0 \\ 2\gamma(\gamma-\alpha) & 0 & 2\gamma(\gamma-\alpha) & 0 & -\gamma \end{bmatrix} R +$$

$$+ R \begin{bmatrix} 0 & -\omega_0^2 & 0 & 0 & 2\gamma(\gamma-\alpha) \\ 1 & 0 & 0 & 0 & 0 \\ 0 & 0 & 0 & -b^2 & 2\gamma(\gamma-\alpha) \\ 0 & 0 & 1 & -2a & 0 \\ 0 & 0 & 0 & 0 & -\gamma \end{bmatrix} - \frac{R}{2D_1\alpha} \times$$

$$\times \begin{bmatrix} (2\alpha-\gamma)^2 & 2\alpha-\gamma & (2\alpha-\gamma)^2 & 2\alpha-\gamma & 2\alpha-\gamma \\ 2\alpha-\gamma & 1 & 2\alpha-\gamma & 1 & 1 \\ (2\alpha-\gamma)^2 & 2\alpha-\gamma & (2\alpha-\gamma)^2 & 2\alpha-\gamma & 2\alpha-\gamma \\ 2\alpha-\gamma & 1 & 2\alpha-\gamma & 1 & 1 \\ 2\alpha-\gamma & 1 & 2\alpha-\gamma & 1 & 1 \end{bmatrix} R + \begin{vmatrix} 0 & 0 & 0 & 0 & 0 \\ 0 & 0 & 0 & 0 & 0 \\ 0 & 0 & 0 & 0 & 0 \\ 0 & 0 & 0 & 2Dab^2 & 0 \\ 0 & 0 & 0 & 0 & 0 \end{vmatrix}.$$

Conclusions

Treated output signals' sensors of TS contains useful signal against the background of various types of interference (noise) at each cycle of cyclic optimal filter. Herewith, in the general case the same range of barriers is presented throughout the interval of the main frequency range and superimposed on the spectrum signal. Under these conditions was obtained the analytical mathematical models of optimal filters that allows quickly and with a given reliability to detect the end of each cycle evaluation signal to background noise of any complexity, with the ability to use on cycle assessment of simplified mathematical models of noise.

References

1. *Ivanov A.B.* Контроль соответствия в телекоммуникациях и связи. Измерения, анализ, тестирование, мониторинг/ Ivanov A.B. – М.: Cyrus Systems, 2000. –375 с.

2. *Pegachev V.S.*Стохастические дифференциальные системы. Анализ и фильтрация./V.S. Pegachev, I.N. Sinicin. – 2-е изд., доп. – М.: Наука. Гл. ред. Физ.-мат. Лит., 1990. – 632 с.

3. *Pegachev V.S.* Теория вероятностей и математическая статистика. / V.S. Pegachev – М.: Наука. Главная редакция физико-математическойлитературы, 1979. – 496 с

J. Zaharchenko post-graduate student (National Aviation University, Ukraine)

AUTOMATIC ALLOCATION OF PROJECT RESOURCES MODERNIZATION OF AVIATION TECHNICS BASED ON GENE EXPRESSION PROGRAMMING ARTIFICIAL IMMUNE SYSTEMS

In work the decision of a problem of search of the best distribution of resources between projects is considered with the help clonal immune algorithm. The method of task decision of management considered in article projects of aviation technique modernization offered on the basis of immune algorithms allows shows achievement of necessary authenticity of planning results of conducting of its modernization and validity of practical recommendations of the conditions of vagueness of financing

In modern conditions the market constantly makes new more rigid demands to the aviation techniques (AT), that requires its continuous improvement. From the account of constant ageing of aviation park and economic crisis modernization of existing aviation park and continuation of its service life is one of the ways satisfaction these requirements.

AT modernization is understood as restoration obsolete (in the functional relation) its samples by replacement of a design, element base, materials or manufacturing techniques for the purpose of improvement characteristics and increase of efficiency use.

Modernisation of aviation park resolves, unlike purchase of new samples of AT, to finish the out-of-date technics for level which meets modern requirements, at expenses 10 times the smaller. Therefore AT modernisation is a priority direction of the majority countries of the world, even such as the USA, Russia, Great Britain, France, etc. Widely known in the world are such military planes as bombers B-52, B-1, Tu - 95, fighter F-16, MiG-29, etc. that as a result of reusable modernisation are on arms more than 30 years and meet modern requirements. Many civil passenger planes also constantly pass modernisation for satisfaction to ICAO requirements.

Many civil transport and passenger airplanes also pass modernisation for the purpose of satisfaction to requirements ICAO. So, for example, the world's largest transport airplane AN-124 as a result of modernisation considerably expands the functionality and starts to meet modern requirements ICAO. After modernisation take-off mass of airplane AN-124-100M-150 reaches 402 T., its load-carrying capacity is increased to 150 T. And considerably many taktiko-technical characteristics improve. The airplane is equipped with modern air complexes and systems, among which: system of the prevention of collision of airplanes in air TCAS-2000, system of zone navigation BRNAV, an early warning system of collision with earth TAWS (TTA-12), etc.

One of the unsolved problems of methods of modernization is the task of project management modernization and the formation of optimal blood pressure (rational) plan its implementation. This problem is an important upgrade for AT, from the solution of which depends on the effectiveness of its implementation, as well as unjustified consumption of resources.

One of the important tasks of planning the modernization of aircraft is the allocation of resources between the various power companies, which will be upgrading its fleet, according to all the necessary stages of the modernization program. The result is a planning schedule for the entire process, served as a schedule of works according to the power company by type of aircraft subject to the terms of the program of modernization. It should develop a calendar standards to ensure uniform upgrade aircraft in a given period of existing facilities with a maximum load of them and minimize the costs of resources.

To solve this problem was applied algorithm clonal selection artificial immune systems.

Serve schedule works as a data array where the first line contains the name of work. Each work has the following attributes: start date, end date used resource.

Table 1

Example of an array schedule

Work1	Work2			WorkN
Date starting work1	Date starting work2			Date starting workN
Date ending work1	Date ending work2			Date ending workN
Resource1 Resource2 Resourceμ	Resource1 Resource3 Resourceμ-1			Resource2 Resource3 Resourceμ

There are arrays indicating the dependencies between jobs "predecessor-successor" and an array of project resources.

Table 2

Example of an array of work relationships

Work	W ork1	W ork2		Wo rkN
Follow er	W ork2	W ork4 W ork12		

Table 3

Example of an array of resources

Reso urce1	Reso urce2	...	...	Reso urceμ

Using Table 2 and Table 3 arrays forming control rules, which impose restrictions on the appointment time getting started, depending on the dependence of "predecessor-successor" and use of resources and ensure a "correct" schedule.

In this formulation the construction schedule is proposed to find that option work schedule, which would minimization time period to wait between work and as a result - reduce the total time duration of the project.

For an optimal or near optimal schedule is proposed using evolutionary algorithms artificial immune systems that are based on incomplete fingering options.

Clonal selection algorithm of artificial immune systems for the construction project schedule modernization AT:

Step 1: Create a set of timetables for the array of Table 1, where the beginnings of work are set randomly, taking into account control rules derived from Table 2 and Table 3.

Step 2: compute the total length of each schedule and ranking conducted by the growth (in the first place are options for calendar plans with the lowest total of the project.)

Step 3: bleed a number of "best" schedule and procedure for the cloning of artificial immune systems is a certain number of copies selected timetables.

Step 4: There is a change in each of the options multiplicate timetables (changing the beginning of work) with directions to get better at all time (or at least not worse) version of the project schedule.

Step 5: A re-ranking choices received timetables.

Step 6: Checking condition stops the algorithm. If you are - krok8 otherwise - krok6.

Step 7: With a set of timetables reserve a certain number of the best, others are replaced by a set of options for timetables generated random sample kroku1. We come to kroku2.

Step 8: With the final set of options timetables selected the best (with the lowest total of the

project). This option is accepted as optimal.

However, given the specific task scheduling projects of modernization of aircraft and their difference from the discrete manufacturing projects proposed use multyhromosomu antibodies from curtailment of expression by means of programming.

In the task parallel-serial work, where each job must be executed on one or more machines, and should be considered precursors of operations (in some cases followers), assign priorities proposed additional level of work (if there is no work of predecessors, or if the work-predecessors been fulfilled, the work gets highest priority - becomes available for execution).

For this project we identified the modernization of JSC main components of the aircraft maintenance and operation of data nodes. By defining the types of activities that require certain work units for execution, select the number of combinations of-work, which will operate our schedule.

Structure of expression includes the submission of antibodies alphabet characters, consisting of two subsets:

- Functional {+} (where "+" means the possibility of parallel work, "" - follow-up)
- Terminal (combined work).

Additionally, proposed to add neprohramuyemu part. It belongs to the set priorities of work, which will determine the list of works at some time point and the availability of resources for work at this time point.

In general, the antibody will look like:

Head						Tail						Priority of works				Availability of resources			
-	+	+	...	+	-	17M2	25M3	...	...	...	37M2	0	1	1	0	1	1	0	0

Figure 1. A general view of the antibody in the form of expressive programming

The overall algorithm of the schedule:

Step 1: creating random sets of schedules

2nd step: calculating the length of the project for each schedule. N Selection of the best and change all the other so that their duration was less than or equal to the selected

Step 3: selection of the best m in length and replace all other new random.

4th step: test conditions stop the algorithm (given initial parameters)

5th step: if the condition is not fully known check, go back to step 1, otherwise - step 6

6-th step of the schedule established alternatives to choose the best option

Conclusion

In this paper, the proposed solution of the problem of optimal allocation of project resources modernization of aircraft based on gene expression programming artificial immune systems. A combination of algorithms expression programming and clonal selection allows you to get the "right" project schedule updating, who at the same time is optimal for distribution of resources.

References

1. *Dasgupta D.* Artificial Immune Systems and Their Applications/ Dasgupta D., Publisher: Springer-Verlag, Inc., January, 1999. – 306 p.

2. *De Castro L. N.* Artificial Immune Systems as a Novel Soft Computing Paradigm./ De Castro L. N., Timmis J. // Soft Computing Journal, vol. 7, Issue 7, July 2003. – P.526-544

3. *Литвиненко В.І., Самков О.В., Захарченко Ю.А, Четирін С.І.* Оптимізація розподілу фінансів між проектами в умовах невизначеності на основі імунного алгоритму. // Зб. Наук. праць. - Севастополь: СВМІ ім. П.С. Нахімова, 2008 р. – №1(14). – С. 15–21.

4. *Самков О.В., Захарченко Ю.А.* Застосування алгоритму клонального відбору для побудови планів модернізації авіаційної техніки // Автоматика. Автоматизация. Электротехнические комплексы и системы. – Херсон, ХНТУ. - №1(23). – 2009. – С.110-114.

Lysenko Alexander PhD (National Technical University «KPI», Ukraine)
Kirchu Pavel PhD (National Aviation University, Ukraine)

THE METHOD OF OPERATIVE SYNTHESIS OPTIMUM ON ENERGY COSTS OF A CONTROL LAW AN AEROPLATFORM FOR TELECOMMUNICATION SYSTEMS ON THE BASIS OF UAV

The thesis is devoted development of a method of operative synthesis of an optimum control law on energy costs small UAV the airborne type which is used in the capacity of a high-altitude relay aeroplatform, in the conditions of presence of indefinite parametric and stochastic perturbations of large intensity.

A key element of new broadband wireless access systems, operating in a metropolis, mountainous or rough terrain, as well as in combat and emergency situations is a high-rise located aeroplatforms with her special telecommunications equipment. Applications for such systems was sized UAV aircraft type to achieve the following advantages: relatively low cost of implementation, small compact performance, a short period of time required for the deployment of communication systems in a given area. Controlled movement of the platform in space allows to realize the desired quality of customer service through increased connectivity throughout the network and the application of deterministic multiple access protocols, providing remote intelligence collection or removal of sensors sensor networks. However, the specific property such as facility management aeroplatform (OC) is the fact that it operates in unstable weather conditions, heavy traffic air vehicles, and of intense stochastic external disturbances. This leads to the fact that the spatial position aeroplatform varies indefinitely in a wide range, which negatively affects the performance quality of telecommunications systems. For such systems the best way to manage aeroplatform is the method of structural and parametric synthesis of adaptive control laws.

Despite significant advances in the theory of efficient synthesis of optimal control laws - for tall aeroplatform remains the indeterminacy solutions to develop simple and fast algorithms for operational aqueous synthesis of control laws, which maintain the stability and quality sys-tem control in an uncertain modified OK, the presence of intensive external stochastic disturbances, reduced energy available UAV, and allowing to support quality functioning telecommunication system in the specified limits. Therefore extremely important is the task of developing a method of synthesis of optimal adaptive control law for the energy consumption pinpoint UAV aircraft type which is used as a high-altitude aeroplatforms for telecommunication systems.

1. Mathematical formulation of the problem

Formulate a mathematical formulation of the problem of this study. Let the control object is described by the equation of state:

$$\dot{X} = A(t)X(t) + B(t)U(t) + \eta(t);$$
$$Y = CX(t) + \xi(t), \tag{1}$$

where - $X \in R^n$ state vector; $U \in R^n$ - vector control; Y - vector measurements of fluctuations A (t), B (t) - n xn and n x m matrix parameter; η and ξ - vector of noise disturbance and noise measurement. The opportunity dimension or restore all-th vector of OK, so $X_B = X(t)$. Using the algorithm, consider the problem of OC desired dynamics while minimizing energy consumption in control. Coveted dynamics OC with minimum energy consumption for control will be set using the reference model.

$$\dot{X}_M = A_M X_M(t) + B_M R(t), \tag{2}$$

where $X_M \in R^n$ - state vector of the reference model - vector of input actions.
Formalizes target control, requiring that

$$\lim_{t \to \infty} E(t) = 0, \tag{3}$$

where $E(t) = X(t) - X_M(t)$ - the error system (1) and (2). Thus, the problem concerns the synthesis of adaptive systems with explicit reference model. Do not let on, OC affect measurable disturbance (set of) R = R (t), disturbances are not measured by N = N (t) and control of U = U (t). Observations of available output variables of the object $X_B = X(t)$ behavior of the object management depends on a number of independents parameters which denote ζ. Given a set of possible Ξ
values ζ, which defines the allowable class object and disturbances. Given target managem (3), which defines the desired behavior OK. You must synthesize algorhythm control that uses the measured or calculated on the basis of measurement values that are independent of, and providing for each reach the destination domain. ζ vector consisting of coefficients of equations that constitute the mathematical description (1) OC, as well as coefficients defining changes in external disturbances (environmental conditions). In addition, vector-ζ included abstract parameters that describe disturbance caused by inaccurate description OK. Then The problem can be formulated as follows.
Formulation 1: Find a control algorithm

$$U(t) = U_t(X(t), U(t), \Theta(t), R(t)), \tag{4}$$

$$\Theta(t) = \Theta_t(X(t), U(t), \Theta(t), R(t)), \tag{5}$$

which provides management to achieve goals (13) in the system (11), (12), (14), (15) for each $\zeta \in \Xi$. Here $\Theta(t)$ - vector of parameters of the regulator. In certain control algorithms (14), (15) to consider restrictions on the movement of UAV parameters identified above, namely restrictions on the maximum and mini-most the roll and pitch angles, as well as restrictions on the height of flight.
The generalized procedure for the synthesis of adaptive control algorithm with reference model comprises the following steps: Step 1: Problem synthesis, Phase 2 Synthesis of the optimal reference model; Step 3 Synthesis of optimal observer (Kalman filter) Step 4 Select the structure of the regulator (the synthesis of the main circuit) Stage 5 Select the custom settings; Step 6 Select the algorithm adaptation. Stage 7- rough, Step 8 Configure the adapter.
In step 2 is considered in detail the procedure for optimal synthesis of continuous and discrete reference model. In the synthesis of optimal (in terms of energy costs on management) reference model used linear quadratic optimal regulator used to adjust the dynamics of the object control (UAV). For the synthesis of optimal square-ungulate regulator considered nominal linear stationary model deterministic object management in the form of state space. Then the problem of optimal regulator is defined as the problem of finding the optimal control u (t) on the interval [t0, tf], such that a minimum value of the following function:

$$J_0(x(t_0), t_0) = \int_{t_0}^{t_f} [x(t)^T \Psi x(t) + u(t)^T \Phi u(t)] dt + x(t_f)^T \Psi_f x(t_f), \tag{6}$$

and where Ψ is R^{nxn} and a Φ_f is R^{nxn} - inherently symmetric-definite matrix, and Φ is R^{nxn} - inherently symmetric definite matrix. To achieve the desired quality of the transition process reference model is considered in detail the procedure for choosing the matrix coefficients Ψ and Φ.
As for the application of adaptive control law is necessary to know the full state vector is OK in the third stage is synthesized optimal observer status. As is known by the application of the synthesis Optimal observer status is action on the object of white noise as a stochastic perturbation. The underlying stochastic perturbation acting on the UAV in flight is turbulent wind, and he is white

noise. Therefore, application of optimal synthesis of an observer to describe the object controls at the state space as a serial connection is forming a filter that describes the action of turbulent wind on the UAV, and models of deterministic object management, which includes a model consistent with union executive mechanisms of object. Entries forming filter disturbance uncorrelated white noise, and output have color noise that characterize turbulence of the atmosphere. Then input the extended object in state space will disturbance white noise, which is essential application of optimal synthesis of observer status, and directly on the object will do color noise that characterizes the effect of turbulence. In American practice, standardized model of the forming filter. To describe the turbulent wind model is used Dryden MIL-F-8785C.

Block diagram of adaptive system subject is shown in Fig 1. In the algorithm specified external disturbances w1 and w2 measurement noise of sensors can be considered as a random shift parameter, which must track the path of adaptation and adjusts the matrix parameters of the regulator to achieve the objectives of control E (t) → 0. For ensure optimal performance of adaptive control systems in UAV conditions of intense external stochastic perturbation is used for the synthesis procedure of optimal adaptive control system with an explicit reference model based on the method of gradient descent algorithm called the gradient descent rule changes the vector of coefficients Custom regulator Θ, which is given by equation adapter type
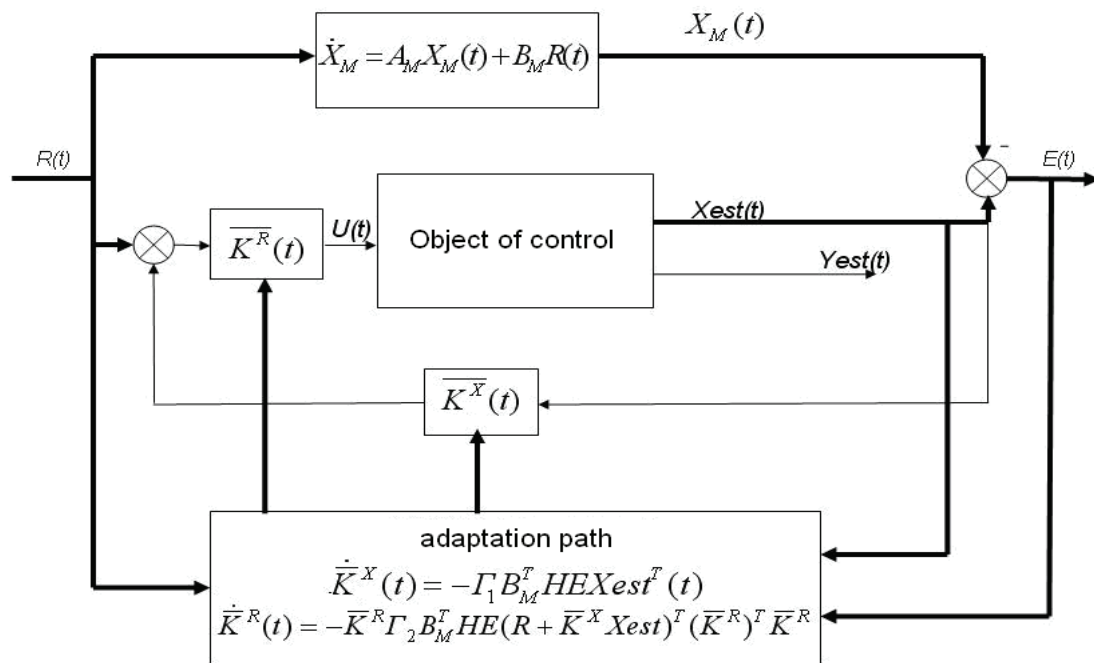
Figure 1. Block diagram of optimal adaptive control system

As a result, algorithm configuration matrices $\overline{K}^X(t)$ and $\overline{K}^Y(t)$

$$\dot{\overline{K}}^X(t) = -\Gamma_1 B_M^T \mathrm{HE}(t)X^T(t),$$
$$\dot{\overline{K}}^R(t) = -\overline{K}^R \Gamma_2 B_M^T \mathrm{HE}(t)(R + \overline{K}^X X(t))^T (\overline{K}^R)^T \overline{K}^R. \tag{7}$$

As quality control processes depends on the accuracy of estimation of state vector X then there is the problem of periodic identification parameter for calculation of parameters of optimal Kalman filter, which estimates the state vector of UAV. The result of the adaptation circuit control system is the calculation of matrix coefficients of the feedback coefficient matrix K^X and K^R in every time, so as to reduce the error between output and reference model output OK to zero. Therefore, given the consistency equation model and the object, in which are defined by contour approximation matrix of coefficients and parameters are known matrix reference model - it is possible to calculate the matrix parameters of the object domain A and B.

Equation of the identification process will be as follows:

$$B = B_M (K_*^R)^{-1}, \quad A = A_M - B_M (K_*^R)^{-1} K_*^X, \tag{8}$$

Identification procedure is conducted periodically. When calculating the matrix parameter control system remembers the importance of matrix coefficients of K^X and K^R and by hypothesis stationarity on identifying control law is fixed, according to which the adaptive controller is used currently. The same procedure takes place in the state where the observers at the time of calculation of the updated parameters of the optimal observer is stored and used the previous value. Using the method of computer modeling identified optimum time between the procedure of identification that is 20 s. for the facility management which meets the stated requirements for quality management processes.

Conclusions

Developed cyclic combined optimal adaptive control system UAV, with periodic identification procedure to configure the optimal observer status in flight allowed to provide the following indicators of quality control in terms of intense external disturbances and uncertain modified UAV:

- In the longitudinal channel for pitch angle control mode, the maximum deviation of steering wheels height is 25 degrees. The transition process in pitch angle is aperiodic character without static error, the transition process is 4. At the maximum angle of pitch deviation in velocity is - 0.2 m / s. For speed control mode transition processes for u is also aperiodic nature and stability of height error is 1%.

- In the side channel mode coordinated turn overflow on the corner of the course is 10%. If you change the course of 1 °, the maximum deviation of roll angle and is 1 °. Overshoot of slip angle is 15%. The results of the reference models for longitudinal and lateral channel comply with the terms of flight aeroplatforms based UAV.

- Support for accuracy assessment of the state vector aeroplatforms our level when errors on angular and spatial position relative to the nominal value not exceeding respectively 0.1 and at 2m.

References

1 *Лисенко О.І.* Синтез оптимальної траєкторії руху та закону керування аероплатформою для телекомунікаційних систем на базі безпілотного літального апарата/ О.І. Лисенко, П.І. Кірчу, С.В. Валуйський // Автоматика – 2010 : 17-та міжнар. конф. з автоматичного управління, 27–29 вересня 2010 р. : матеріали конф. – Харків, 2010. – Т. 2. – С. 52.

2. *Lyseko A.I.* Synthesis of the optimal observer of the state for the UAV adaptive control system / A.I. Lyseko, P. I. Kirchu // The 4rd world congress «Aviation in the XXI–st Century», «Safety in Aviation and Space Technology», 21–23 September 2010. – K., 2010. – Vol. 1. – P. 16.45–16.48.

3. *Лисенко О.І.* Підвищення структурної надійності радіомереж із самоорганізацією / О.І. Лисенко, П.І. Кірчу, С.В. Валуйський // Військова освіта та наука: сьогодення та майбутнє, : VI міжнар. науково-практична конф. ВІ КНУ ім. Т. Шевченка, 25–26 листопада 2010 р. : тези доп. – К., 2010.– С. 370-371.

4. *Лисенко О.І.* Визначення основних обмежень параметрів руху БПЛА, які використовуються в якості аероплатформ для безпроводових тимчасових мереж / .І. Лисенко, П.І. Кірчу // Проблеми телекомунікацій: П'ята міжнар. наук.-тех. конф., 19-22 квітня 2011 р.: збірник тез. – К., 2011. – С. 33.

UDC 621.313 (045)

N. D. Krasnoshapka, PhD, V.V. Tihonov, PhD, T.A. Mazur, PhD
(National Aviation University, Ukraine)

IMPROVEMENT THE ENERGY CHARACTERISTICS OF INDUCTION MOTORS

The article deals with ways to improve the energy performance of induction motors through the use of massive ferromagnetic shields of squirrel-cage rotor's winding outside the boundaries of the working air gap

In today's environment of constant growth in energy prices are actual questions of energy efficiency equipment. Almost half of the produced electrical energy is converted into mechanical energy by electric motors. The most common among them are induction motors (IM) with a squirrel-cage rotor. They have the smallest mass-clearance index and the cost. Also they are the most reliable and simple in operation, compared with other types of electrical machines. However, for this type of electromechanical converter is characterized by relatively low dynamic and energetic performance in start-up modes.

Scientists have proposed various solutions to improve the energy performance of induction motors, which work with frequent starts. These solutions allow increasing the amount of rotor's circuit resistance during start-up. One of these solutions might be the use of massive ferromagnetic shields squirrel-cage rotor's winding outside the boundaries of the working air gap [1].

In the induction motor with massive ferromagnetic shields should lengthen the rods of rotor windings. This design allows us to place the shields under the frontal parts of the winding and does not require increasing the axial length of the machine.

Figure 1 shows a sketch of design of induction motor with two-end shields and short-circuited rings [5], where 1 – a three-phase stator winding, 2 – lengthen parts of the rotor rods, 3 – short-circuited ring, 4 – ferromagnetic disc shields, 5 –rotor of the induction motor.
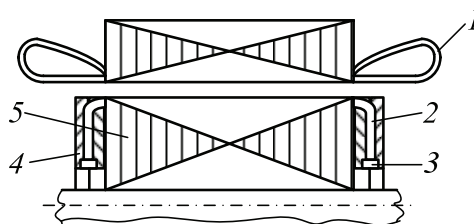
Fig. 1. Sketch design of induction motor with two-end
ferromagnetic screens parts of the rotor windings

Features of the electromagnetic processes that occur in the rotor circuit with a shielding of the parts of short-circuited winding, caused by the appearance of an additional electromotive force in the rotor circuit. This additional electromotive force created by the joint action of the magnetomotive force (MMF) of the rotor's winding currents and the eddy currents of ferromagnetic screens.

This electromotive force is proportional to the rotor circuit current. According to the law of electromagnetic induction it is directed against the reasons that caused this force.

We call this an electromotive force is equivalent introduced. Equivalent introduced electromotive force increases with the rotor slip. However, it significantly limits the current at high rotor slip. This leads to a limitation of magnitude of the current consumed by the induction motor from the power network.

Figure 2 shows the comparison for the mechanical and current characteristics of the induction motor 4A160S2У3 model (dashed line) and modified (solid lines) performance.

The second version of the technical solutions that will improve the start-up and operating characteristic of the motor is the use of an induction motor with dual squirrel cage and a variable magnetic flux.
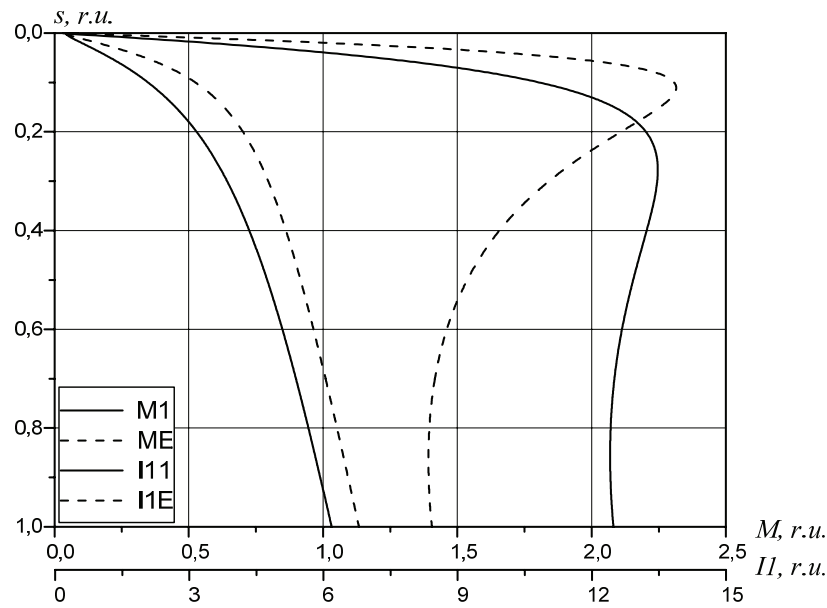
Fig. 2. Mechanical and current characteristics of an induction motor

Figure 3 shows a sketch of the proposed construction of an induction motor. Induction motor (Figure 3) has a stator magnetic circuit (1) with the slots (2) on the inner (3) and outer cylindrical surfaces, which posted a three-phase toroidal winding (4). Magnetic laminated shunt (5), which is located on the outer cylindrical surface of the stator package has slots (6) on the inner surface, the axes of which coincide with the axes of the stator slots.
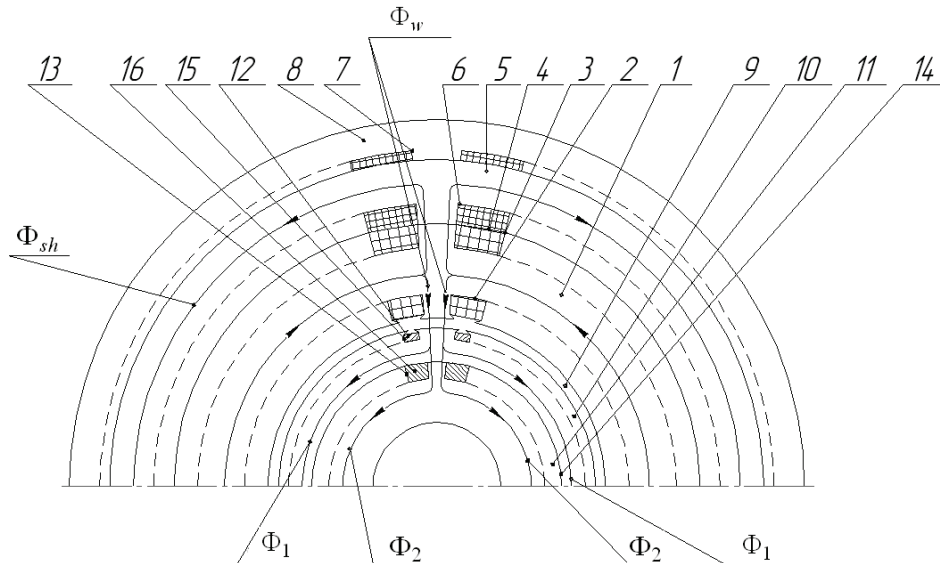
Fig. 3. Sketch design of an asynchronous motor with dual squirrel cage and variable magnetic flux

Bias winding (7) of the toroidal type 7 is placed in the slots (6) of the magnetic shunt and on the outer surface of the body (8). In the package bore of the stator is placed the rotor (9).

The rotor is made in the form of two short-circuited rotors (10) and (11). Between the surfaces of the first rotor (11) and the inner surface of the second rotor (10) placed the cylinder (14) of non-magnetic alloy. Axis of (13) of the second rotor and the slots (12) of the first rotor are coinciding. The slots of the second rotor are smaller section than the slots of the first rotor. Second winding of the rotor (15) made of brass or bronze, the first winding of the rotor (16) made of copper.

When you turn the motor in a network (start-up), the current consumed by the winding (4) of the stator (Fig. 3) is much higher than the motor rated current. As a result, the current in the magnetizing winding (7) is increases. The magnetic shunt under these conditions is saturated and the value of the magnetic flux becomes equal to $\Phi_{sh} = \min$, a $\Phi_w = \max$.

Increasing the working flux Φ_w leads to the fact that significantly increases the flow of Φ_2, which is closed through the yoke of the first rotor (11), and the second rotor yoke (10) using a

minimum bias current in the coil (7) is saturated. Increasing the flow of Φ_2 at start, leads to the fact that due to excessive short-circuited winding reactance (16) over the short-circuited winding reactance (15), significantly increases the current in the winding (15). Thus, in the start-up mode of the motor mechanical characteristic is shifted into the region of high slip

With increasing speed induction motor, the input current of the motor is reduced and the current in the magnetizing winding (7) drops.

The magnetic shunt is unsaturated and the magnetic flux Φ_1 in the rotor is closed through the yoke of the second rotor (10). That is, in the mode of minimum load the electromagnetic torque created by the interaction of the magnetic flux of the working current, which flows through the short-circuited winding with a large active resistance. Induction motor has a mechanical characteristic, shifted to the right.

By increasing the current in the bias winding (17) we can observ an increase in the magnetic resistance of the shunt (5), which leads to an increase in magnetic flux (Φ_2), which is closed through the first rotor yoke. Therefore, in the creation of the electromagnetic torque of the induction motor starts to attend short-circuited winding (16), which has low resistance. The mechanical characteristics of an induction motor starts to drift to the left to decrease the slip and speed of the induction motor is increases.

For the case of the maximum current in the magnetizing winding, mechanical characteristic is shifted to the left, as the moment due to the interaction of magnetic flux from the short-circuited winding currents (16), which have a low resistance. The phenomenon of redistribution of the current characteristic of the start mode is not observed. That is, the frequency of the EMF and current in the windings of the rotor is small and, hence, small values of reactance and their role is insignificant.

So, the change current in the bias winding can improve starting performance and allows a wide range of changing speed of induction motor.

Conclusions

In modern systems of electric drives to limit the starting current value is most often used the soft starter. The principle of operation of these devices is based on reducing the applied voltage during start-up.

However, the use of soft starter systems leads to a significant reduction of starting torque, which is proportional to the square of the applied voltage. The use of induction motors with high starting torque allows you to expand the application range of these devices especially when motor powered from independent power sources.

The use of massive ferromagnetic screens for the rotor windings can improve the dynamic and energetic parameters of IM in the starting modes by increasing the value of starting torque.

The proposed design of IM with a double squirrel cage and the stator with the magnetic shunt allows you to improve starting performance and makes smooth change of motor speed in a wide range possible. By choosing the parameters of the rotor windings can achieve frequency control from start up to the nominal mode.

References

1. *Борисенко В.Э.* Алгоритм расчета рабочих и пусковых характеристик асинхронного двигателя с частотно-зависимыми параметрами ротора / В.Э. Борисенко, Н.Д. Красношапка //Тр. Научного центра Военно-Воздушных сил. – 1997. – Вып. 1. – С. 183–186.

2. *Копылов И.П.* Математическое моделирование электрических машин: [Учеб. для вузов] / И.П. Копылов. – М.: Высш. шк., 2001. – 327 с.

3. *Вольдек А.И.* Электрические машины / А.И. Вольдек. – Л.: Энергия, 1974. – 840 с.

4. А.С. №1835594 Асинхронный двигатель / В.В. Тихонов // 1991.

UDC 621.396.946(045)

A. Lysenko, PhD, S. Valuiskyi
(National Technical University «KPI», Ukraine)
N. Kravchuk PhD (National Aviation University, Ukraine)

THE OPERATION EFFECTIVENESS INCREASE OF WIRELESS SENSOR NETWORKS BASED ON UAVs

The ways to improve the operation efficiency of wireless sensor networks with the rapid and unpredictable movement of mobile subscribers are described

Emergency natural and man-made disasters and military conflicts that are increasingly taking place in our world, resulting in complete or partial failure of the ground infrastructure, including telecommunications facilities (base stations of cellular communication, microwave and satellite stations, cable lines etc.). Rapid communications in units of rescue crews and other mobile services in these situations are possible through the deployment of wireless sensor networks (WSN) with mobile components. Mobile subscribers (MS) of such networks are equipped with sensors for different purposes, are free to move in a given area and connect with each other directly - in the zone of radio visibility, or with relay packets through neighboring nodes (ie acting as routing), forming a so multihop networks of arbitrary structure (Fig. 1). Increasing coverage of WSN is probably by a hierarchical spatial organization of network using telecommunications aeroplatform (TA) at various levels, which act as repeaters, linking together remote subscribers. Particularly important application of telecommunication aeroplatform based on miniature unmanned aerial vehicles (mUAVs), which are more efficient and economic as opposed to large aeroplatform (Global Hawk, Predator etc) [1,2].
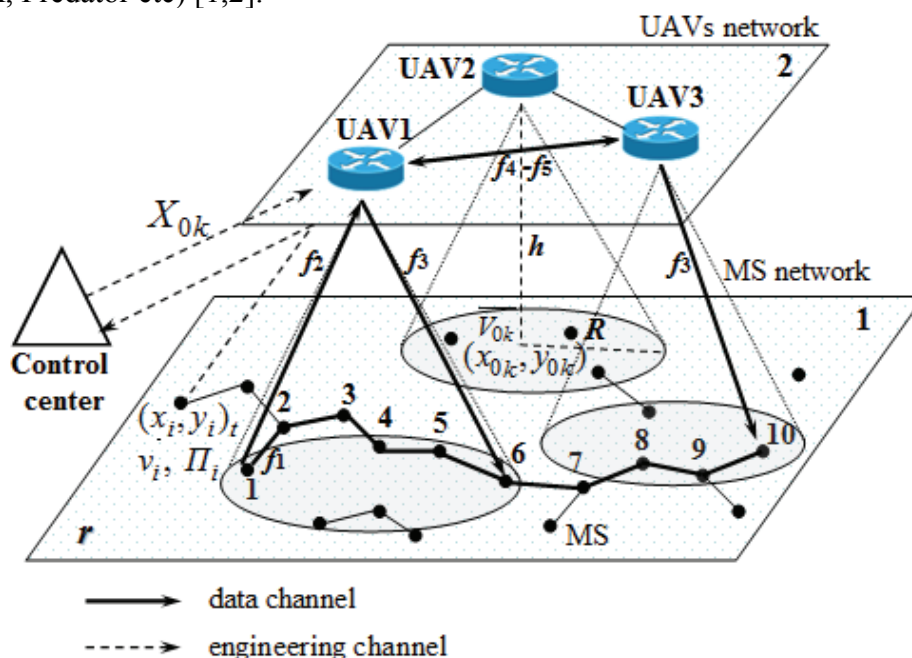
Fig. 1. The arhitechture exemple of WSN based on UAVs

Topology of such mobile radio networks is dynamic and constantly evolving and thus requires an effective control system (CS) that could quickly respond to structural and functional changes, providing certain management objectives. These objectives can be provision of structural connectivity, quality of data routes between subscribers (functional connectivity), increased throughput of network, reducing energy consumption and others. Managing parameters in this case may be the followings: transmition power, direction of ground and airborne antennas, load, position of nodes, etc. Not solved enough problem today is the optimal real-time control of

telecommunication aeroplatforms (UAVs) positions to increase throughput of network with simultaneous provision of structural and functional connectivity of mobile subscribers. Proposed methods and models today, which are placed in the CS of UAVs topology (location), solve just the problem of structural connectivity provision of disjoint network components, excluding the capacity limit of channel resources, load distribution and service of packets in the network nodes. Also, most methods just solve the static problem, without considering the nature of MS mobility and UAV maneuverability, and therefore subject to improvement.

In this paper was proposed a method of increasing wireless sensor networks throughput with the placement control of telecommunication aerial platforms (UAVs) in view of the rapid and unpredictable movement of mobile subscribers [3]. The difference of developed method from existing is that first proposed to combine mathematical models of connectivity estimation and quality of service of mobile subscribers, as well as an advanced search algorithm of quasi-optimal placement of telecommunication aerial platforms (UAVs), into a single computational procedure. Improvement of search algorithm consists in the fact that managed to avoid the exhaustive search of UAVs position (X_0) variants by the use of developed set of rules (Fig. 2), which help to select such variant of network connectivity, which increases network throuhput and also reduces the computation time. Detailed description of the method, advanced mathematical models and algorithms is given in [3].
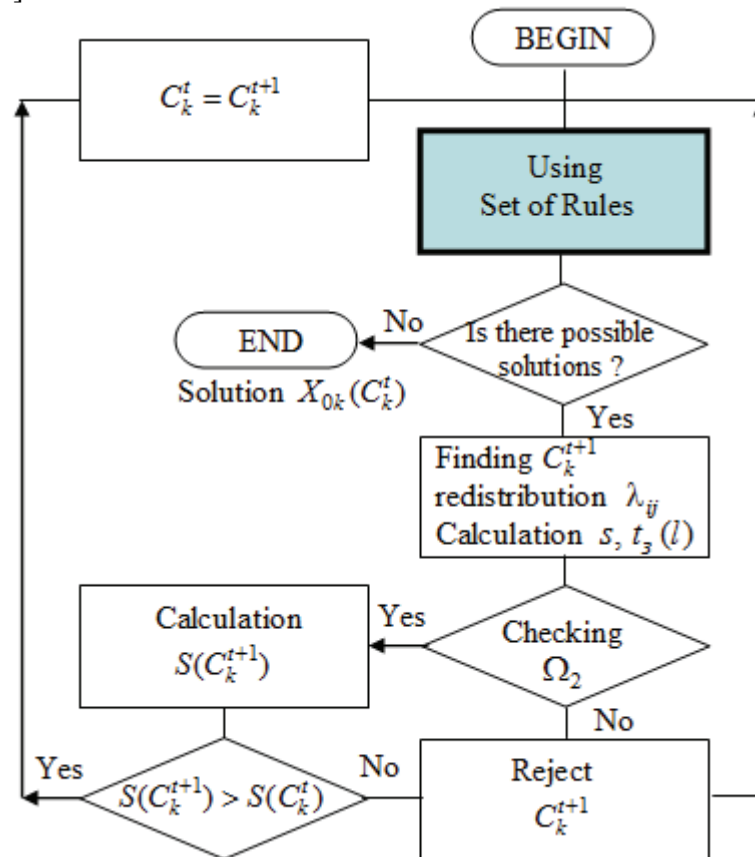
Fig. 2. The scheme of improved search algorithm of quasi-optimal placement of UAVs

It was examined existing ruls and on their basis was developed new and modified rules and appropriate control actions (procedures for finding quasi-optimal placement of UAVs in space).

All rules were classified into three groups: 1) to provide requirements for network connectivity (Ω_1); 2) to provide requirements for performance parameters (Ω_2); 3) to increase network throughput.

Here's an example of several rules, one for each group.

Rule 1. If the number of connectivity components (disconnected subgraph) of network graph more than 1, then telecommunication aeroplatform (UAV) should be placed so as to connect a larger number of connectivity components.

Rule 2. If the average transmission delay (number of relays) in some routes more than necessary, while telecommunication aeroplatform (UAV) should be placed so as to reduce the number of relays in route.

Rule 3. If you want to increase network throughput, telecommunication aeroplatform should be placed so as to cover the maximum number of congested nodes.

Simulation of operation of WSN based on UAV performed on a computerized environment MAPLE. This used the following input data: number of mobile subsribers $N = 140$; number of UAVs $K = 5$; size of MS area $r = 10000 \times 10000$ m^2; transmition radius of MS $d = 600$ m; transmition radius of UAV $R = 1500$ m, the shortest path search algorithm - Dijkstra, MS movement velocity 2 m/s. All other data is given in [3].

In this paper was considered three variants of control system of UAVs position:

CS1 - base control system (covering the maximum number of nodes);

CS2 - control system based on method of exhaustive search;

CS3 - control system based on proposed method (set of rules).

Sequence of the proposed method evaluation was following:

1) setting of network topology randomly and placing UAVs by CS1, CS2 and CS3 (Fig. 3);

2) calculation of network throughput S(C) for each CS. Determination of CS2 and CS3 win against CS1 and reliability of the results of each method relative to exhaustive search (Fig. 4,5);

3) calculation time of finding a solution for the proposed method (CS3) and the method of exhaustive search (CS2) and comparing the values of the duration of MS connectivity.

Analyzing charts according to the network throughput vs total load under different control systems, we can see that traffic in the range 500 ... 2000 packets during normalized packet transmission time T proposed system of UAV position (CS3) far outweigh the base system (CS1) and other ranges of all CS almost equally ineffective.

Therefore evaluated effectiveness of proposed method allows the following conclusions:

1) the average gain of the proposed method (CS3 relatively CS1) under the random generation of 100 variants of the original topology is 10-12%;

2) the mean deviation value of network throughput (for CS3) with respect to the method of exhaustive search (CS2) is 5-7%;

3) the average time a solution for CS3 is units/tens of seconds as opposed to units/tens of minutes for CS2, that under average duration of connectivity between MS 348 s, allows control UAVs position in real time.
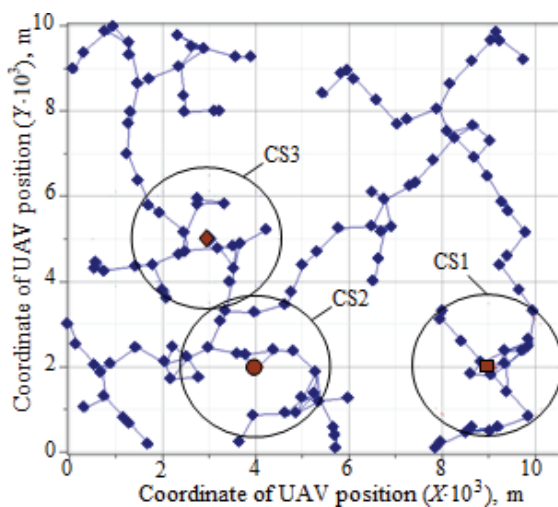
Fig. 3. The initial network topology with UAV deployment by CS1, CS2 and CS3
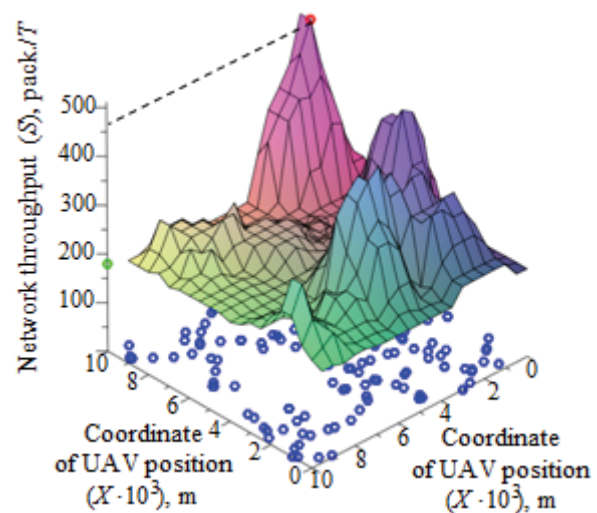
Fig. 4. Dependence of network throughput from location coordinates of one UAV (under CS3)
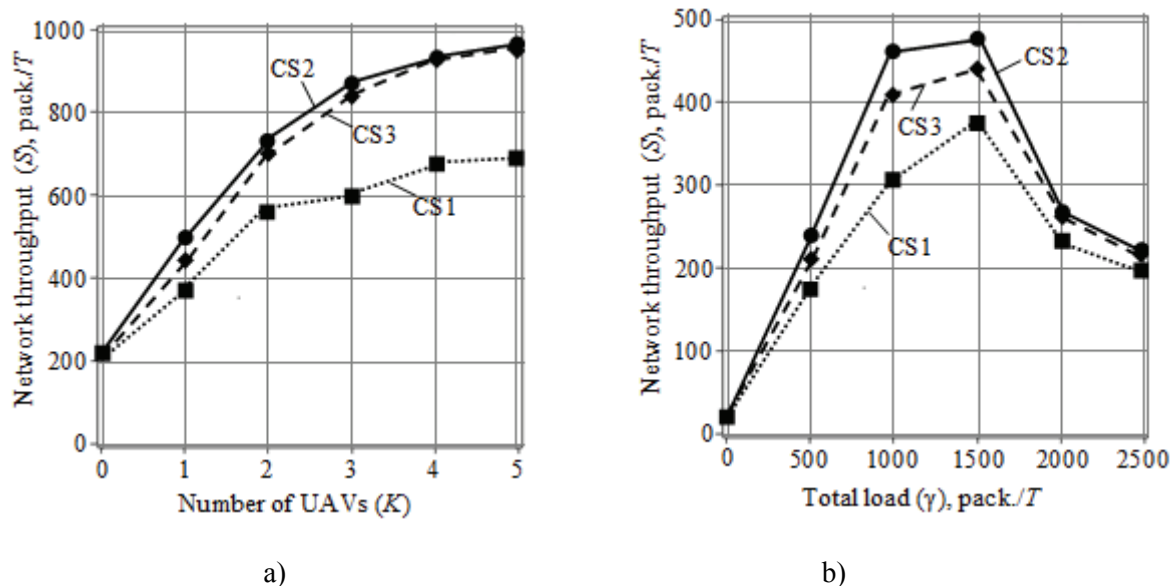
Fig. 5. Dependence of network throughput from the number of retired UAVs (a) and the total load (b) under different control systems of UAVs deployment

Conclusions

The paper is devoted to the important scientific and technical task, which is to develop a method of increasing wireless ad-hoc networks throughput with the placement control of telecommunication aerial platforms in view of the rapid and unpredictable movement of mobile subscribers. The difference of developed method from existing is that first proposed to combine mathematical models of connectivity estimation and quality of service of mobile subscribers, as well as an advanced search algorithm of quasi-optimal placement of telecommunication aerial platforms, into a single computational procedure. Application of the method allows to increase the network throughput to 10-12% in comparison with existing methods. Deviations of sub-optimal solutions from optimal, received by exhaustive method, are not more than 5-7%.

References

1. *Han Z.* Smart deployment/movement of unmanned air vehicle to improve connectivity in MANET / Z. Han, A. L. Swindlehurst, K. J. R. Liu // IEEE Wireless
Communications and Networking : conference, April 3-6 2006 : proceedings. – Las Vegas, 2006. –
P. 252–257.
2. *Lysenko O.* The optimal control of UAV network topology / O. Lysenko, S. Valuiskyi, O. Panchenko // Aviation in the XXI-st century – Safety in Aviation and Space Technologies: fourth world congress, 21-23 September 2010: proceedings. – Kyiv, 2010. – P. 1637–1640.
3. *Valuiskyi S.* Method of increasing wireless ad-hoc networks throughput with the placement control of telecommunication aerial platforms: the dissertation … candidate of technical sciences: 05.12.02 / Valuiskyi Stanislav. – Kyiv, 2012. – 128 p.

Iryna V. Prohorenko, assistant, Yuriy T.Guz, PhD
(National Aviation University, Ukraine)

INFORMATION CONNECTIVITY OF EDUCATIONAL INFORMATION

The problems of informative connectivity of portions of educational information, which are related to maintenance of the modules of educational disciplines, are examined. Considered questions of assessment of connectivity modules disciplines of the curriculum and optimization of the sequence of presentation of training modules

Main aspects of the problem. Educational information is presented in the form of software disciplines which the curriculum is a sequence of more or less related to the content regarding topics and sections. Improving the content and temporal structure of the educational process (EP) is associated with the analysis of logical relationships, both within the academic disciplines and between disciplines. The main structural elements in terms of EP content are didactic invariants which form the basis of its hierarchy. Number of educational information will define the concept of teaching through invariant. Didactic invariants are the main contents of teaching modules.[1] They generally form a hierarchical structure of the content of EP in which some information is implemented connectivity [2]. Structuring of subjects, both in terms of meaningful and in time, it seems like the problem of studying the connectivity information between elements. To this end, proposed some mathematical models for two types of communication of educational information. In this work the simple block diagrams connectivity teaching blocks out of which later can be built more complex. Will be considered two types of possible schemes:

- the minimum system of two teaching blocks (subjects) between which there is rigid and non-rigid connection;

In non-rigid connection may appear more than two levels of learning. In this case a big role will play choice of scale and efficiency of the apparatus. Consider approach to the Shannon information connectivity of two random variables, or two groups of random variables [3]. It is based on the following links: firstly, fundamental role of quantitative measures of uncertainty – entropy; secondly, probabilistic description of random media. Information is understood as a change in uncertainty, amount of information - the difference between quantitative measures of uncertainty before and after receiving information [3]:

$$I_{xy} = H_x - H_{x|y} \tag{1}$$

It is the connectivity information values x and y. In the full sense, it can be interpreted, as the amount of information contained in the y about x.

The amount of information (1) was introduced by Shannon. He also showed the value of this quantity in information theory. Using the known relation:

$$H_{x|y} = H_{xy} - H_y \tag{2}$$

can be written formula (1) as follows:

$$I_{xy} = H_x + H_y - H_{xy} \tag{3}$$

Entropies H_x, H_y, H_{xy} are defined using the following formula:

$$H_\xi = MH(\xi) = -\sum_\xi P(\xi)\ln P(\xi) \tag{4}$$

where M : - expectation.

Number of information connectivity of two random variables has the form:

$$I_{xy} = M[H(x) + H(y) - H(x,y)] = M \ln \frac{P(x,y)}{P(x) \cdot P(y)} \tag{5}$$

There are also equivalent forms of writing:

$$I_{xy} = M \ln \frac{P(x|y)}{P(x)} = M \ln \frac{P(y|x)}{P(y)} \qquad (6)$$

Besides the average entropy H_ξ there is random entropy $H(\xi) = -\ln P(\xi)$ and and can be introduced random connectivity information [5]:

$$I(x,y) = H(x) + H(y) - H(x,y) = \ln \frac{P(x,y)}{P(x) \cdot P(y)} = \ln \frac{P(x|y)}{P(x)} \qquad (7)$$

Consider the case in the study of two servings of educational information (two "blocks" or theme) with two types of connection (Fig. 2 a, b).
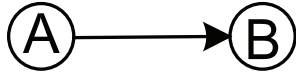
Fig.2 a) hard link   Fig.2. b) no hard connection

When a rigid connection (Fig.2.a) assimilation of pieces of information B is not possible without the assimilation of pieces of information A. When not-rigid connection piece of information B can be learned without learning pieces of information $\overline{A}$. In this case, we consider non-rigid connection (Fig.2.b.).
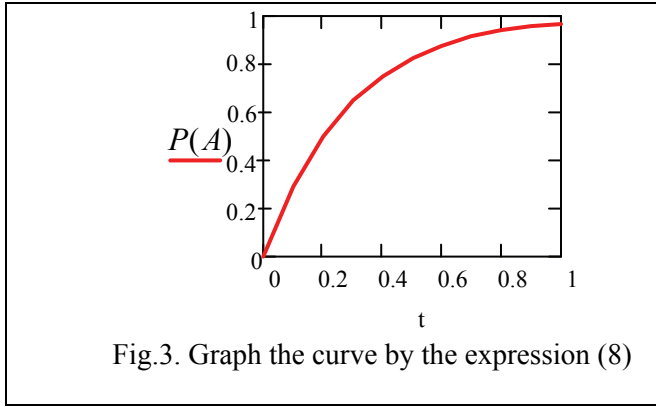
Fig.3. Graph the curve by the expression (8)   Fig.4. Graph of the logistic curve by the expression (9)
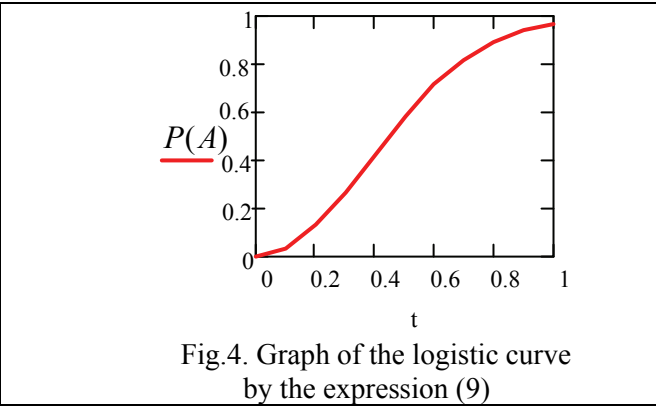
Consider two models depending $P(A)$ on time t.

$$P(A) = 1 - e^{-a \cdot t_1} \qquad (8)$$

$$P(A) = 1 - e^{-a \cdot t_1^2} \qquad (9)$$

A more realistic is a model (9) because the acquisition of information is no at small time. We use the model (8), the probability of assimilation in the portion B under the condition that piece of information A is assimilated, is:

$$P(B/A) = 1 - e^{-b \cdot t_2} \qquad (10)$$

Probability of undigested $\overline{A}$:

$$P(\overline{A}) = 1 - P(A) = e^{-a \cdot t_1} \qquad (11)$$

Then the probability of assimilation piece of information B on condition that piece of information

$\overline{A}$ is not assimilated:

$$P(B/A) = (1 - e^{-b_2(T - t_1)}) \qquad (12)$$

The total probability of assimilation B is:

$$P(B) = P(A) \cdot P(B/A) + P(\overline{A}) \cdot P(B/\overline{A}) \qquad (13)$$

Substituting the expression (11-12) we get:

$$P(B) = (1 - e^{-a \cdot t_1})(1 - e^{-b_1(T - t_1)}) + e^{-a \cdot t_1}(1 - e^{-b_2(T - t_1)}) \qquad (14)$$

Then the probability of simultaneous assimilation of A and B will be:

$$P(A \wedge B) = P(A) \cdot P(B/A) = (1 - e^{-a \cdot t_1})(1 - e^{-b_1(T-t_1)}) \qquad (15)$$

And information connectivity between A and B [2]:

$$I_{A,B}^* = \ln \frac{P(B/A)}{P(A) \cdot P(B/A) + P(\overline{A}) \cdot P(B/\overline{A})} = \frac{1 - e^{-b_1(T-t_1)}}{(1 - e^{-a \cdot t_1})(1 - e^{-b_1(T-t_1)}) + e^{-a \cdot t_1}(1 - e^{-b_2(T-t_1)})} \qquad (16)$$

Options a, b_1, b_2 depend on how the complexity of issues A and B and as the level of analytical abilities of the student.

b_1 – used in the assimilation of pieces of information A;

b_2 – used in the non-assimilation of pieces of information $\overline{A}$.

Similar calculations were carried out according to (10).

In the second stage was conducted the identification parameters. For this identification were taken statistics from the data module control students' first and second courses of Mechanics and Energy Department. Based on the data we obtained the assimilation pieces of information from time. It becomes clear how to divide time between the two portions of educational information to its assimilation was qualitative. According to expression (8) has been identified parameters a, b_1, b_2 and obtained the following data (table 1.1).

Table 1.1

Probabilities learning information

101 Група						
$P(A) = 0.33$	$P(\overline{A}) = 0.66$	$P(B/\overline{A}) = 0.125$	$P(B/A) = 1$	$a = 0.756$	$b_1 = 9.798$	$b_2 = 0.284$
102 Група						
$P(A) = 0.87$	$P(\overline{A}) = 0.13$	$P(B/\overline{A}) = 0$	$P(B/A) = 1$	$a = 3.849$	$b_1 = 9.798$	$b_2 = 0$
103 Група						
$P(A) = 0.3$	$P(\overline{A}) = 0.7$	$P(B/\overline{A}) = 0.093$	$P(B/A) = 0.89$	$a = 0.673$	$b_1 = 4.696$	$b_2 = 0.212$
104 Група						
$P(A) = 0.43$	$P(\overline{A}) = 0.57$	$P(B/\overline{A}) = 0$	$P(B/A) = 0.83$	$a = 1.061$	$b_1 = 3.77$	$b_2 = 0$
105 Група						
$P(A) = 0.57$	$P(\overline{A}) = 0.43$	$P(B/\overline{A}) = 0.17$	$P(B/A) = 0.88$	$a = 1.592$	$b_1 = 4.424$	$b_2 = 0.396$

In Table 1.2 were shown the results of probabilistic optimization temporal structure of the discipline of theoretical physics.

Table 1.2

Comparative analysis of the optimal time allocation discipline (theoretical physics) on the module with a non-rigid connection

Group	t_{np}	t_{opm}	Probability learning pieces of information $\Delta P(B)$ %	Weeks	Weeks
101		0.76	7.5		12
102		0.65	3		11
103	0.53	0.59	3	9	10
104		0.61	3		10
105		0.61	5		10

Fig.5. Probability of learning educational information B from the time for a non-rigid connection.

Consider how to change the time for learning with rigid connection.

Comparative analysis of the optimal time allocation discipline
(theoretical physics) on the module by rigid connection

Group	t_{np}	t_{opm}	Probability learning pieces of information $\Delta P(B)$ %	Weeks	Weeks
101		0.71	7		12
102		0.65	3		11
103	0.53	0.66	7	9	11
104		0.61	3		10
105		0.61	2		10

Fig. 6. Probability learning portion of educational information B from the time for a rigid connection

Similar calculations were carried out according to (9). Research results of optimization of probabilistic temporal structure of the discipline theoretical physics for logistic curve.

Comparative analysis of the optimal time allocation discipline
(Theoretical Physics) in modules with nonrigid connection

Group	t_{np}	t_{opm}	Probability learning pieces of information $\Delta P(B)$,%	Weeks	Weeks
101		0.91	4		15
102		0.84	12		14
103	0.53	0.84	53	9	14
104		0.83	47		14
105		0.83	36		15

1.5.48
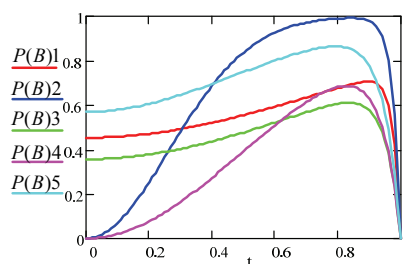
Fig. 7. Probability learning portion of educational information B from the time for a rigid connection. Consider how to change the time for learning linkage.

<div align="right">Table 1.5</div>

Comparative analysis of the optimal time allocation discipline (theoretical physics) on the module by a strong connection

Group	t_{np}	t_{opm}	Probability learning pieces of information $\Delta P(B)$ %	Weeks	Weeks
101		0.92	50		15
102		0.84	12		14
103	0.53	0.86	52	9	14
104		0.83	48		14
105		0.83	39		14
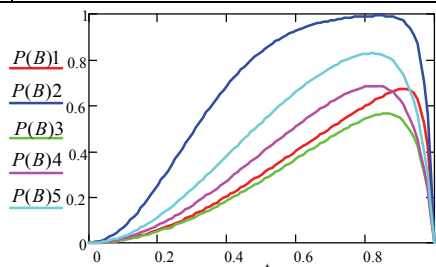
Fig. 8. Probability learning portion of educational information B and time for a hard connection.

These tasks are simplified, but they contain the basic meaning of the problem. They show that you can use cumulative statistics as a result of the Bologna system; these problems show that in almost all cases there are reasonable solutions. When data problem solved, we can say that you need to do to optimize a training course. Proposed to issue data in the form of recommendations to the research methodology of training in terms of subjective analysis.

Conclusion

The developed approach of forming modules of subjects on the basis of formal problems in information connectivity modules allowing subjects to supplement and partially eliminate the drawbacks of existing methods based on a modular approach and will improve the efficiency of EP as a result of this approach. Provides optimizing the allocation of time resources regard to the importance of information, which is determined by expert estimates.

References

1. *Касьянов В.А.* Субъективный анализ [Текст] / Касьянов В.А. – К.: НАУ, 2007. – 512 с.

2. Сетевые методы планирования и организации учебного процесса[Текст]/ А.А.Овчинников, В.С. Пучинский, Г.Ф. Петров.– М.: «Высшая школа», 1972.– 157с.

3. *Стратанович Р.Л.* Теория информации [Текст] / Р.Л. Стратанович. – М.: Сов. радио, 1975. – 424 с.

4. *Шеннон К.Е.* Работы по теории информации и кибернетике [Текст] / К.Е. Шеннон. Пер с анг. Под ред. Р.Л. Добрушена, О.Б. Лупанова М., ИЛ. 1963. – 832 с.

5. *Яглом А.М., Яглом И.М.* Вероятность и информация [Текст] / А.М. Яглом, И.М. Яглом. – М.: Наука, 1973.– 512 с.

UDC 629.735.015.7.2:656.7.08 (045)

D. Shevchuk, Candidate of Engineering, E. Tachinina, Candidate of Engineering
(National Aviation University, Ukraine)
Y. Tachinin, Design engineer (Antonov Company)

THE CONCEPT OF CONTROL RECONFIGURATION TO RESTORE THE AIRPLANE CONTROLLABILITY AND STABILITY AT FAILURE SITUATIONS

The possibility of application of system methods of reconfiguration of controlling surfaces for restoration of controllability and stability of the airplane in the conditions of sudden origin of a abnormal situation in flight is justified in the article. The structure and functional charts of the purposed configurable control system are provided.

Introduction. The efficiency of aviation use is inseparably linked with a problem of flight safety which successful solution defines the perspectives of development both civil, and military aviation to a considerable degree. Complexity of the flight safety problem solution continuously increases in connection with increase of intensity of aviation use and extension of it functional tasks. The current situation in flight is characterized first of all by the flight conditions and modes, the functional status of crew, operability of aviation systems, and aerodynamic status of the wings. As a result of action of unfavorable external factors and degrading internal processes the abnormal flight situation can appear. It is subdivided into four types: minor, difficult, emergency, catastrophic situation [1]. The extremely high transience of development of a abnormal situation (AS) requires the instantaneous interference in a situation for decision-making directed on restoration of controllability and stability of the airplane and by that prevent of transition of the current flight situation in the catastrophic.

In this article a class of possible failures is restricted to failures (damages) of controls and actuators. This class of failures is rather widespread: so, according to the article [2], 20 % of cases of airplanes crashes are connected to failures damages of auto flight control system (AFCS), and mainly with failures and damages of drives of steering organs. In [3] it is marked that the principal cause of unreliability of AFCS of the modern airplanes are failures of controls. The failures of actuators and controls should be considered together as they by results of appearance are often indistinguishable one from other: the actuator failure normally leads to fixing of the appropriate control surface in some position, the control surface failure (jamming) leads to such result; reduction due to actuator degradation, as well as reduction of the controlling surface owing to ingestion of mechanical or biological object, leads to reduction of efficiency of appropriate control unit.

Traditional approach is application of instrumental redundancy (reservation). However thereof the mass and airplane overall dimensions are increase that restricts universality of this approach. Therefore there is a question of search of more effective methods of preventing of development of AS in flight. Development of system methods of reconfiguration of control surfaces for restoration of the airplane controllability in the conditions of sudden AS in flight can become one of such directions.

Main part. As reconfiguration we will understand the control redistribution on controls for the purpose of creation of necessary control forces and moments for restoration of airplane controllability and stability in the conditions of AS origin in flight. Implementation of reconfiguration is possible for the airplanes with redundant controls. So, in [4,5] it is marked that for high-maneuverable airplanes with the decreased static stability, quitting on critical values of attack angle, for successful reconfiguration in case of failures eight independent governing bodies are necessary at least. The modern and perspective high-maneuverable airplanes possess a large number of governing bodies: elevons (section with independent control of each section), front horizontal empennage, spoilers, rudders, turning nozzles, etc.

In the airplanes developed earlier, there are no means of automatic implementation of reconfiguration, these functions are completely laid to the pilot. Therefore the result of reconfiguration completely depends on experience and ability of the pilot though essentially reconfiguration would allow to prevent 70 % of cases of incidents due to failures of actuators and controls (this inference is made in [2] based on the analysis of the flight incidents which were taking place in the USA).

In [6, 7] two examples of successful and unsuccessful implementation are given by the pilot of reconfiguration. In the first case the left section of the elevator of the Delta L1011 airplane appeared is clamped in situation 19° in case of take-off. The pilot prevents failure by reconfiguration. The second case is connected to DC-10 airplane failure on May 25 1979 in Chicago, called loss of section of the flap of the airplane. The subsequent simulation of a situation showed that the pilot could avoid failure by means of reconfiguration.

In this regard it is expedient to put at a development stage of AFCS of airplanes in system of means of automatic implementation of reconfiguration. In this direction in 1994 the U.S. Air Force laboratory of flight dynamics began development of the SRFCS program (Self-Repairing Flight Control System) [2] which purpose is implementation by development of AFCS of the modern and perspective airplanes of the actions providing reconfiguration and diagnosing of system and directed finally on reliability augmentation, fail safeties, survivability. The SRFCS program provides two basic approaches [2]. The first is connected to the automatic reconfiguration, the second with creation of the expert diagnostic systems making recommendations to the pilot depending on the developed flight situation.

Development of methods and models of reconfiguration of controlling influences aboard the plane in the conditions of origin special situations in flight operation [4] is devoted. For reconfiguration of controlling influences in case of failures of drives and governing bodies two approaches [4] are used: parametric and structural.

Parametric change of feedback factors of the executive mechanisms taking into account a technical status of the airplane, for improving of efficiency of their functioning.

Structural – control redistribution between operational governing bodies for recovery of acceptable characteristics of controllability and stability in the conditions of AS in flight.

On fig. 1 the simplified structure chart of reconfigured management system is provided.

The reconfigured control system of considered type assumes execution of three interdependent procedures:

- determination of response characteristics of the airplane in the course of flight execution;
- estimation of a technical status of the capital aircraft equipment, and also integrity of external contour of the airplane;
- formation of controlling signals on executive bodies of the airplane with use of information received by means of the first two procedures.

Let's suppose that movement of the airplane is described by a differential equation:

$$\dot{x} = F(x, a, q, u, t) + \xi_x \qquad (1)$$

where: x - n-dimensional state vector of object defined in space X, a - r-dimensional vector of parameters accepting values from a A-set and defined by properties of the environment; q - vector of integrity of external contour of the airplane in the flight, considering influence of standard damages on aerodynamic properties of the airplane, and the m-dimensional vector of controlling influences created by reconfigured management system and belonging to the set U; t - the current time belonging to a segment $[t_0, t_\kappa]$ on which AS in flight is defined; ξ_x - n-dimensional vector of uncontrollable perturbations (noise, measurement noises etc.); F - n- the-dimensional vector function of the specified arguments known, according to the assumption, on the basis of theoretical and pilot studies.
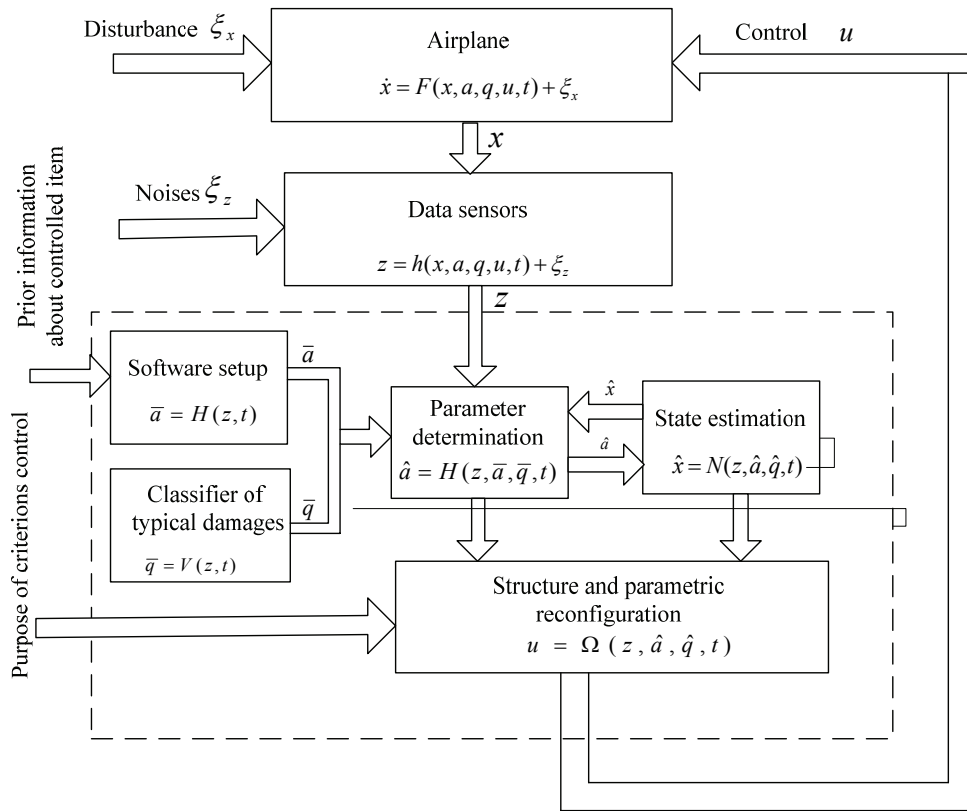
Fig. 1. The simplified structure diagram of configurable control system

Observation over movement of the airplane is carried out by means of a complex of the sensors measuring components of a status of object and control, and also integrity of its external contour in flight:

$$z = h(x,a,q,u,t) + \xi_z \qquad (2)$$

where: z - l-dimensional vector of observations in space Z, ξ_z - l-dimensional vector of the additive noises distorting indications of sensors; h - l-dimensional vector function of the specified arguments known on the basis of theoretical and pilot studies of sensors of information. Results of measurements arrive in reconfigured management system where are used for determination of response characteristics of the airplane and optimum (suboptimal) estimation of its status.

The following stage of functioning of the offered reconfigured management system is process of parametric identification of response characteristics of the airplane in the conditions of AS origin in flight which in a general view is described by the operator:

$$a = H(z,\overline{a},\overline{q},t) \qquad (3)$$

Thus, in considered structure it is necessary that identification is carried out in some neighborhood of program value of a vector of parameters. In the course of identification the reconfigured management system considers the factors influencing dynamic properties of the airplane (unfavorable external factors and degrading internal processes).

On the basis of signals of sensors and estimates of parameters of object it is carried out optimum (or suboptimal) estimation of a status of the object, allowing substantially to increase accuracy of information on a vector:

$$x = N(z,a,q,t) \qquad (4)$$

where: x - n-dimensional vector of an assessment of parameters of a vector x.

Total procedure of reconfigured management system is optimization of controlling impacts on airplane executive bodies on a basis, set the purposes of control and criteria of optimization for

preventing of development of AS in flight. The operator describing formation of a vector of optimum controls, looks like:

$$u = \Omega(z, a, q, t) \qquad (5)$$

The optimality criterions created beforehand, define a measure, leaning on which control algorithm selects an optimum way of achievement by object of the given status. The structure of the operator depends on a method of the job of the purpose of the control, minimized criteria and a choice of a method of the optimization, to AS had time development in flight, and also an aerodynamic status of external contour of the airplane.

Conclusion

Let's formulate the main outputs on this article.

1. Failures of actuators and controls lead normally to the following consequences: proportional lowering of efficiency of a control unit; fixing of a control unit; in some position (maximum, minimum, zero), lowering of efficiency of appropriate control unit due to reduction of the area of a control surface as a result of ingestion of mechanical or biological object.

2. In the conditions of redundancy of controls the task of reconfiguration can be essentially decided.

3. The algorithm of creation of the offered reconfigured control system contains the following stages:

-   formulation of optimality criterions;
-   development of a mathematical model of the airplane taking into account corrections which enters in AS control process;
-   synthesis of laws and models of control reconfiguration;
-   algorithm elaboration of adaptation (setup) of laws of control on modes of functioning of the airplane flight-navigation equipment;
-   implementation of the received laws and reconfiguration models by means of on-board computers.

References

1. Нормы лётной годности гражданских самолётов СССР. (НЛГС - 3). Межведомственная комиссия по нормам лётной годности гражданских самолётов и вертолётов СССР – 3-е издание. – 1984. – 464с.

2. *Eslinger R.A., Chandler P.R.* Self-repairing flight control system program overview // Proc. IEEE National Aerospace and Electronics Conf., 1988. V. 2. P. 504-511.

3. *Ostroff A.J., Hueschen R.M.* Investigation of control law reconfigurations to accommodate a control element failure on a commercial airplane // Proc. American Control Conf., 1984. V. 3. P. 1746-1754.

4. Системні методи відновлення живучості літальних апаратів в особливих ситуаціях у польоті : монографія / В. М. Казак. – К.:Вид-во Нац. авіац. ун-ту «НАУ-друк», 2010. – 284 с.

5. *Глумов В.М., Земляков С.Д., Рутковский В.Ю., Силаев А.В.* Алгоритмическое обеспечение отказоустойчивости систем автоматического управления // АиТ. 1988. - N° 9. С. 3-33.

6. *Napolitano M.R., Swaim R.L.* A new technique for aircraft flight control reconfiguration // Proc. AIAA Guidance, Navigation and Control Conf., 1989. Pt. 1. P. 1-9.

7. *Bonnice W.F., Wagner E., Motyke P., Hall S.* The application of the detection filter to aircraft control surface and actuator failure detection and isolation // Proc. AIAA Guidance, Navigation and Control Conf., 1985. P. 732-740.

V. Novikov, L. Afanaseva (National Technical University «KPI», Ukraine)
M. Vasilyev, post-graduate student (National Aviation University, Ukraine)

FUZZY LOGIC APPLICATION FOR QUEUE MANAGEMENT FOR TCP/IP NETWORKS

In this paper investigated an influence of different queue management and congestion avoidance techniques as a RED, A-RED, PI and REM for quality parameters in TCP/IP network. Fuzzy Logic Controller (FLC) was proposed to increase quality parameters

Introduction. Development of broadband technologies and the growing popularity of various Internet services lead to a permanent increase speed data channels and therefore needs to increase available bandwidth. As a result of uneven growth of bandwidth overload occur in some sections of the network. Traditional mechanisms for managing queues and prevent congestion (RED, A-RED, PI, REM) cannot cope with traffic management with complex dynamics, high nonlinearity and load changes, which leads to the appearance of congestion and global synchronization of TCP flows. This in turn reduces the effective data rate and affects the quality parameters, such as the percentage of lost packets, delay and delay variation.

Analysis of research and publications. Using classical mechanism DropTail to manage TCP traffic rise to the phenomenon of global synchronization, when the buffer overflow router simultaneously reset all the packages that come, and all TCP transmitters reduce TCP-box, and then sync it to increase, causing new overload. To counter this phenomenon was developed by RED mechanism that drops packets with probability, the average queue length, which linearly increases with RED mechanism still is the most common in routers, although many researchers stated its drawbacks [2-4]. They also developed modified RED (for example, Adaptive RED), to improve productivity, but management remains linear at the base. The analysis of existing mechanisms of bursts showed that the control system based on linear dependence is difficult to track the dynamics of complex nonlinear process, which is the load, generated current applications based on TCP connections.

Problem. For queue management in TCP / IP networks has been proposed a method of using a controller based on fuzzy logic FLC (Fuzzy Logic Controller).Regulators of FLC decision to change the current value of the probability dropping / marking package P_drop, adopted on the basis of input variables: the current value error queue length and its change Q_error d_error for the measurement and the corresponding set of rules that uses peer reviews. For input variables calculated value of membership function μ, that is, the degree of confidence that the input variable belongs to the fuzzy (linguistic) variable, such as "GREAT", "SMALL", "AVERAGE". Membership functions are chosen so that the sum of all the functions of input variable was equal to unity. To analyze the proposed method has been developed following simulation model and conducted simulation using controller based on fuzzy logic FLC Management courses in network TCP / IP.

Simulation. Simulation was conducted using the software package NS-2 [5]. To assess the quality parameters at the various control mechanisms in turn conducted modeling congestion in the channel between the two routers (velocity in the channel 15Mbyt / s, 120ms delay), through which passed multiservice traffic of 3 types:

- long TCP sessions created 100 simultaneous FTP applications:

- short time TCP session HTTP applications created with the intensity of 50 new connections per second;

- UDP traffic at a constant speed of 128 kbit / s full duplex to create a noise the mechanism of turn.

We used the implementation of TCP NewReno with enabled explicit congestion notification ECN (Explicit Congestion Notification) [6] for signaling by router to transport layer of a possible

overload in the channel by installing a marker CE (Congestion Expe rienced) in the header of IP packets instead of dropping packets. In the case of UDP traffic packets looked like at the moment of overload.

Time simulation is 100 seconds. At the initial time is 100 FTP sources start transmission. To simulate the dynamics of d time 40 seconds 50 FTP sources stops transmission, and at time 70 seconds again restores the transfer FTP sources with different time delays in the channel to the router, it is uniformly distributed in the range from 1 to 9 ms.

In the mechanism of Fuzzy Explicit Marking (FEM) [4] a fuzzy controller input parameters used in the error value queue (the difference between current value and the set) and the measured values of the previous errors. Unlike FEM we have been proposed as the second input parameter controller FLC use the ratio of the received packet to the maximum amount transferred by the interval measurement.

The ratio of the intensity of flows may more accurately reflect the dynamics of the size of the queue. In this simulation frequency measurements regulator FLC was set 10 ms and the maximum magnitude of change likely dumping during the measurement. For the RED mechanism set minimum and maximum threshold dropping 100 and 300 packets respectively, and the maximum probability of dropping 1/30.

Simulation results. Simulation results are presented in Table 1.

Table 1.

Simulation results for a given queue length 200 packets

The mechanism of turn	Size of turn Average. /Average square deviation of packets	Characteristics of traffic						
		Joint channel		FTP		CBR/UDP		HTTP
		Packets loss, %	Ratio of the channel	Packets loss, %	Speed Mbit/s	Packets loss, %	Delay of jitter, ms	Packets loss, %
FLC	198/77	1.01	0,994	0.55	12.28	9	217 6,1	1.84
FEM [4]	189/51	0.6	0,993	0.15	12.28	8	211/5,5	1.4
RED	181/ 65	0.59	0,993	0.58	12.26	3	208/5,5	0.54
A-RED	189/127	0.68	0,989	0.62	12.20	3.1	213/5.4	0.75
PI	240/145	0.68	0,978	0.61	12.06	3.2	235/4.8	0.76
REM	202/96	0.44	0,989	0.6	12.19	0.31	218/4,9	0.09
DropTail	449/79	3.7	0,995	2.93	12.39	2.6	332/5,7	5.3

Analysis of simulation results shows that using the mechanism Drop Tail significant losses due to buffer overflow occur at short HTTP connections, and using control with fuzzy logic (FLC

and FEM) TCP connection with minor losses, dropped packets in the main protocol UDP, which does not have control mechanisms of transmission.

An REM allows the smallest loss, but the turn has significant variations and channel utilization less. An FEM demonstrates the most resistant of all (the smallest standard deviation), and the mechanism FLC is less stable place, but rather the average value corresponds to a given length.

Conclusions

For queue management in TCP / IP networks has been proposed a method of using a controller based on fuzzy logic FLC. According to method carried out using simulation software package NS-2. The method of management courses with the regulator based on fuzzy logic FLC unlike FEM mechanism is less stable place, but rather the average value corresponds to a given length.

References

1. *Kucheryaviy E.A.* Управление трафиком и качество обслуживания в сети Интернет. - СПб.: Наука и Техника. 2004.

2. *May M. Bolot J.. Diot C, Lyles B.* Reasons not to deploy RED. IWQoS '99. Seventh International Workshop on Quality of sendee, 1999.

3. *Fengyuan R. Yong R.. Xiuming S.* Design of fuzzy logic controller for active queue management. Computer Communications 25. - 2002. - Pp. 874-883.

4. *Chrysostomou C. Pitsillides A. Sekercioglu Y.* Fuzzy explicit marking: A unified congestion controller for Best-Effort and Diff-Serv networks. Computer Networks 53. - 2009. - Pp. 650-667.

5. The Network Simulator. NS-2 - http://www.isi.edu/nsnam/ns

6. *Ramakrishnan K., Floyd T. Black D.* The Addition of Explicit Congestion Notification (ECN) to IP, RFC-3168, Sep. 2001.

UDC 629.735.064.5: 621.316.722: 064.53 (045)

V. P. Zakharchenko, Ph. D., V.V. Kozub, Post- G. student
(National Aviation University, Ukraine)

MAKING THE MATHEMATICAL MODEL OF VOLTAGE REGULATION OF THE AIRCRAFT'S POWER SUPPLY SYSTEM AND RESERCH OF STATIC AND DYNAMIC PROCESSES

In this thesis questions of automatic control of three-phase AC power supply system of the aircraft, making and researching of the dynamic model of aircraft contactless generator with a thyristors voltage regulator in static and dynamic modes are discussed.

Statement of the problem.
The process of development of the power supply systems of an aircraft is accompanied by a tightening of requirements to maintain the voltage level of accuracy. Increasing the accuracy of voltage regulation leads to rise reliability of aircraft equipment during operation and reduce the weight of the power supply systems in the design, by reducing the mass of the network, if the voltage regulator works more correct, the greater the voltage drop can expect in the network, and hence cross-section and mass of the network are smaller. Reducing the error voltage regulation near from 2 to 1% can reduce equipment weight by 2-4%. That effects on the economic production of the power supply systems. For example, in [1] states that series of 1000 aircraft will release extra income of 5,5million dollars, if the weight of the equipment reduces only 1 kg per 1 airplane.

The disturbances in the power supply systems appear due to changes of the loads and frequency of the rotor of generator, and they are the reason of the generator voltage deviations from the set values. Any load changes from zero to its nominal value and the range of rotor speeds of the DC and AC generator variables in 1,2-2,5 and more.

The present level of development of the avionics requires to ensure the quality of electrical energy. Analysis of problems in the development, production, certification and operation of the power supply systems of the aircraft shows the existing contradiction between demandings [2,3,4] to the effective functioning of such systems and capabilities of aircraft constructing companies to work on these requirements. This problem is discussed not only for the process of real aircraft operation but for the processes of creation new types of power supply systems for new aircrafts. The requirement of electrical energy are held in State Standard 19705-89, and according to it the loads changes in shown range should be equal to the parameters shown below (see *Table*).

The voltage at the terminals of the generator can deflect more than the permissible level if we do not held special measures. Therefore, power supply systems use special automatic voltage regulation. On most modern aircrafts synchronous generators are main source of the alternating current, and the stabilization of the voltage level is held by the means of automatic control in the chain of excitation.

Table

The values of steady-statethree-phase AC voltage constant frequency of the power supply system

Measurement point	Phase voltage, V			The average value of three-phase voltage, V		
	The power supply systems work modes					
	normal	*unnormal*	*emergency*	*normal*	*unnormal*	*emergency*
At the receiver	*108–119*	*100–127*	*104–122*	–	–	–
At the point of regulation	–	–	–	*111–118*	*105–125*	*112–120*

For each of the power supply system modes of GOST 19705 - 89 specific requirements for changes in the parameters of electric power are defined.

AC primary subsystems parameters are:
- Even dividing of loads between the phases in the three-phase system;
- The minimum phase angle of the vectors of the voltage;
- Unbalanced voltages in the uneven loads in the different modes of the power supply system;
- Factor for recurrent modulation pulse load;
- Wave form in constant voltage mode;
- The presence of voltage pulses on the bus for trips receivers, etc.

As it can be seen from the above the list of parameters of quality of electric power on board the aircraft, in general, they belong to the dynamic parameters of assessing the quality of its regulation, that is, the quality of transient processes in the power supply system. It may be noted the validity of this approach (as a quantitative assessment of the quality of the transition process in any system) is always more objectively described as the perfection of the system, and the degree of wear of the elements during operation. That is why there arises the problem of choice and justification of the most efficient method of assessing the dynamic properties of the aircraft as the power supply system that is created and those already in operation.

To evaluate the dynamic and static characteristics of the system voltage regulation (a transitional process, the error in the steady state, etc.) we need to analyze a mathematical model of the system. During the analysis the influence of individual elements of the regulating system for its stability is revealed, areas of possible values of its parameters are identified, high quality of transients are ensured. Firstly, you must create a mathematical model of the system for further evaluation, which is the purpose of this thesis.

Formation of a dynamic model of the aircraft's synchronous generator begins with the preparation of the equations of motion of the system that depends on the type of synchronous generator and the type of voltage regulator.

Realization of assessment methodology of quality of the dynamic system of transitional characteristic contains the following actions::
- making of a dynamic model of the "generator - regulator";
- preparation of equations for the dynamics of aircraft's power supply system in the form:

$$\left(a_3 p^3 + a_2 p^2 + a_1 p + a_0\right)\Delta U = \left(b_3 p^3 + b_2 p^2 + b_1 p + b_0\right)\Delta f , \qquad (1)$$

where ΔU - the relative change in voltage; Δf - the relative importance of the main perturbation (changes in DC generator's speed or synchronous generator load changes or other options depending on the type of aircraft's power supply system);
- development of the block diagram of automatic regulation system;
- assessment of static errors ΔU (according to [3]) and refinement of the coefficients of equation (1):

$$\Delta U = b_0 / a_0 \Delta f ;$$

- determination of the characteristic equation roots of the automatic frequency regulation system and automatic voltage regulation system.

As an example, the most promising system is contactless synchronous generator with thyristor voltage regulator [5].

In this system (shown in Pic. 1) the correction and stabilizing-regulating devices are not taken into account, we distinguish three basic levels:
- synchronous generator G;
- booster B;
- thyristor voltage regulator TVR.
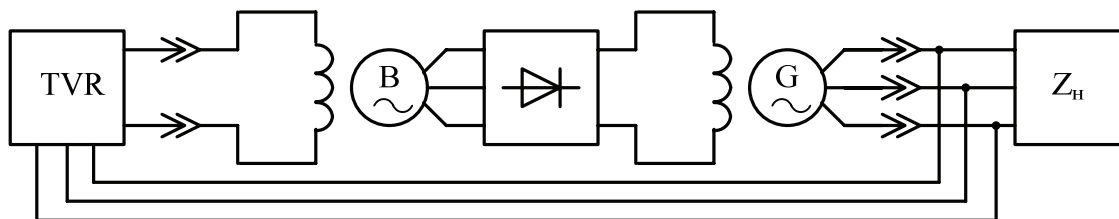
Pic. 1. Principal scheme of the automatic voltage regulation system with the help of the thyristor regulator

The purpose of research - the definition of the static characteristics of the system at an early stage of operation (error, overshoot) and dynamic characteristics, agreed with State Standard 19705-89, within the coordinates of the voltage and time (the majorant and minorant) for the determination of the transition process and steady-state entry into the tube of tolerances in specified time period.

Conclusions

The main indicators of the quality of the transient voltage regulation of the contact less genetator are time management and the magnitude of the overshoot.

The most accurate time control and the magnitude of the overshoot can be determined from the curve of the transition process, obtained by solving the equations of motion of the system (2). Approximately quality of transition and adjustment time can be estimated directly from the coefficients of the characteristic equation of the third order (5) on the basis of D. Braslavsky diagram [8] or by using a standardized chart of I.Vyshnegradsky, and taking into account the requirements of GOST 19705-89, as shown in [9] we can obtain a quantitative assessment necessary to verify compliance with the requirements of the system [3], consistent with the requirements of ICAO.

References

1. *Sindeev I.M., Savelov A.A.* Aircrafts' power supply systems – M.: Transport, 1990. – 296 p.

2. State Standard 19705–81. Aircrafts' and helicopters' power supply systems. – M.: Stand. publ., 1981. – 45 p.

3. State Standard 19705–89. Aircrafts' and helicopters' power supply systems. – M.: Stand. publ., 1989. – 45 p.

4. Russian State Standard 54073–2010. Aircrafts' and helicopters' power supply systems. – Used from 2011–01–01.

5. *Terehov V.M.* Elements of automatic electric drive. – M.: Energoatom publ., 1987. – 224p.

6. *Zakharchenko V.P., Vorobyov V.M., Kichigin A.A.* Assessment of on-board dynamic systems quality under transitional characteristics / / Actual problems of automation and information technology. – 2003. – V. 9. – P. 149–157.

7. Automatic control theory / Edited by *A.A.Voronov*. M.: High school, 1986. - 367 p.

8. *Zakharchenko V.P., Panov V.I.* Assessment of dynamic properties of the aviation energy sources with the help of computing appliances. – K.: KIUCA, 1984. – 36 p.

9. *Braslavskyu D.A.* Evaluation of regulation time with the help of the coefficients of the characteristic equations // Works of MAI, Issue 75. – M.: Defencepubl., 1957.

Vladimir S. Eremenko, PhD, Prof., Yuriy V. Kuts, D.E., Prof.,
Svetlana V. Shengur, post-graduate student,
Evgeniy F. Suslov, post-graduate student
(National Aviation University, Ukraine)

CIRCULAR STATISTICS IN ACOUSTIC FLOW DETECTION

Experimental tests of signals obtained by the acoustic impedance flaw detection method are described. Phase shifts differences sample circular variances from defect and defect-free signals are compared. Received results can be applied for further researches.

1. Introduction

Statistical processing of circular data signal measurement results is the main purpose of the paper. The number of tasks which can be solved by statistical circular analysis methods in different areas is expanding. Geodesy, cartography, geography, geology, location, navigation, physics, astronomy, energy, meteorology, biometrics, engineering, metrology, psychology, biology, medicine − it is not a complete list of random circles measuring and methods of circular data processing applications. It also could be used for information signals analyzing in different application of nondestructive testing.

Today composite materials are widespread in aerospace industry. The main reason of it is possibility to reduce weight of an aircraft but keep mechanical strength as well. Usually those materials use in construction of elevation rudders, wings, nose cone, leading-edge flaps, fuselage segments etc. However because of complex process of components fabrication and significant difference in mechanical characteristics of constituents they are liability to different defects.

There are many methods of non-destructive testing of composite materials such as ultrasonic testing, heat monitoring and acoustic testing which differ from each other by equipment cost and methodology complexity. One of the most widely used is impedance method based on evaluation of special parameter of construction could mechanical impedance which is in turn depends on defect presence in controlled zone. This method uses special piezoelectric sensor for transforming impedance into changing of electric signal which analyzing in flaw detector.

Contemporary flaw detectors use magnitude of signal obtained from the sensor as main information parameter but several other characteristics could be used for diagnostic decision-making [1,2]. The main tasks of the signal processing methodology described in this paper is phase characteristic obtaining, and phase shifts differences computation with the next sample circular variance computation using the sliding window and applying finding values as information parameters in impedance testing.

2. Input data

As an input data there are packages of signals received for two different composite material types: with the defects $u_{1d}(t)$ and $u_{2d}(t)$ and defect-free $u_{1df}(t)$ (Fig. 1) and $u_{2df}(t)$.

Characteristics of executed signals:
– samplings f_1=5 MHz and f_2=10 MHz;
– number of signals in a package:
  – for composite I: 11 points with 50 signal per point;
  – for composite II: 2 points with 31*5 signals per point (31 sensor contact with the surface of composite material per point with receiving 5 signals for each contact $u_{2d}(t)$ та $u_{2df}(t)$);
– number of points in the signals: $n1$=16323 та $n2$=15542.
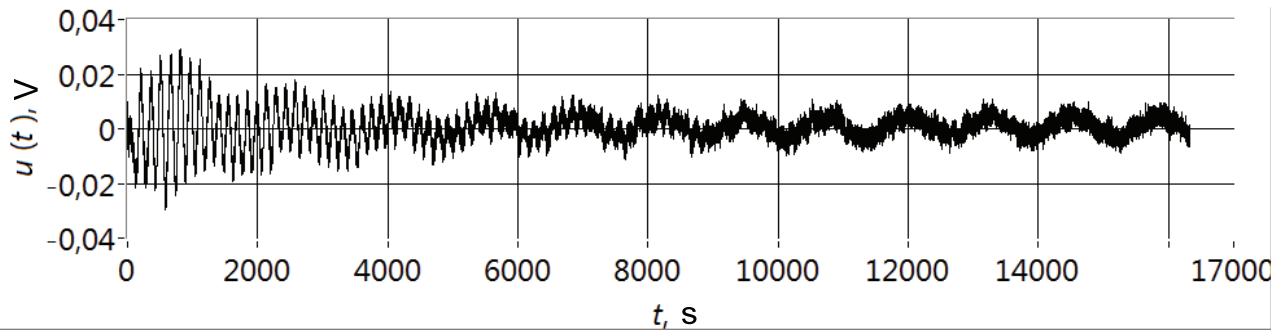
Figure 1 – Input defect-free signal $u_{1df}(t)$

3. Experimental part

The sequence of the experiment:

1)   formation of sliding window size of ~ 3 periods, witch are 480 and 900 points for $u_1(t)$ and $u_2(t)$ respectively;
2)   Hilbert transform application $\mathbf{H}[u(t)]$ for in-window signal area;
3)   phase characteristics $\Phi_1(j)$ та $\Phi_2(j)$ obtaining (Fig. 2):

$$\Phi(j) = 2\pi f j t T_s + \varphi_0 + \xi(jT_s), \tag{1}$$

where T_s – sampling period;

     f – signal frequency;

     φ_0 – initial phase.

4) linear trend (Fig. 2) obtaining

$$\Phi(t) = 2\pi f t + \varphi_0 \tag{2}$$

by method of least squares, according to which:

$$\varphi_0 = 2\frac{(2n+1)\sum\limits_{j=1}^{n}\Phi(j) - 3\sum\limits_{j=1}^{n}j\Phi(j)}{n(n-1)} \tag{3}$$

and

$$f = 3\frac{2\sum\limits_{j=1}^{n}j\Phi(j) - (n+1)\sum\limits_{j=1}^{n}\Phi(j)}{\pi T_{\text{Д}}n(n+1)(n-1)} \tag{4}$$
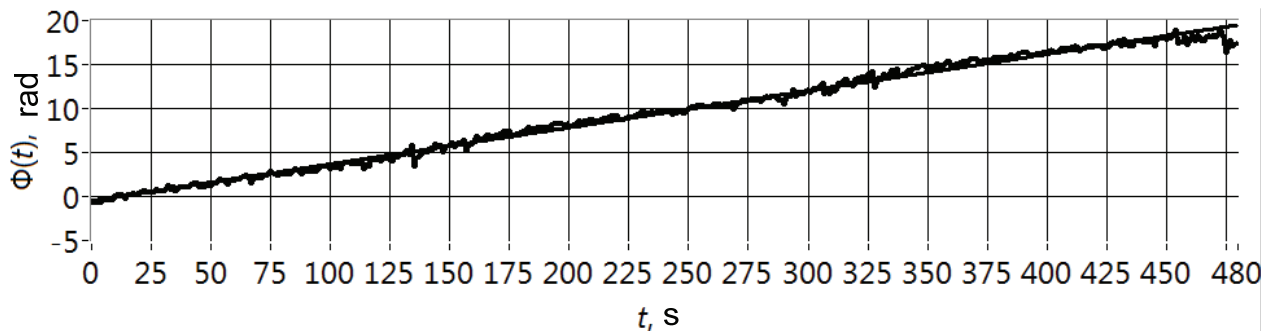
Figure 2 – Picture of the phase characteristics and linear trend for $t \in [3000...3480]$ section of defect-free signal $u_{1df}(t)$ in sliding window length 480 points

5) phase shifts differences $\theta_j = [\Phi(j) - \Phi(t)]$ computation (Fig. 3);

1.6.2

6) computation the circular variances V_{d} and V_{df} for phase shifts differences according to:

$$V = 1 - r = 1 - \sqrt{C^2 + S^2}\,,$$ (5)

where

$$C = \frac{1}{n}\sum_{j=1}^{n}\cos\theta_j\,, \quad S = \frac{1}{n}\sum_{j=1}^{n}\sin\theta_j\,;$$ (6)

7) statistics accumulation with subsequent averaging values of circular variance for defect-free $u_{\mathrm{1df}}(t)$ та $u_{\mathrm{2df}}(t)$ and defect $u_{\mathrm{1d}}(t)$ та $u_{\mathrm{2d}}(t)$ signals;
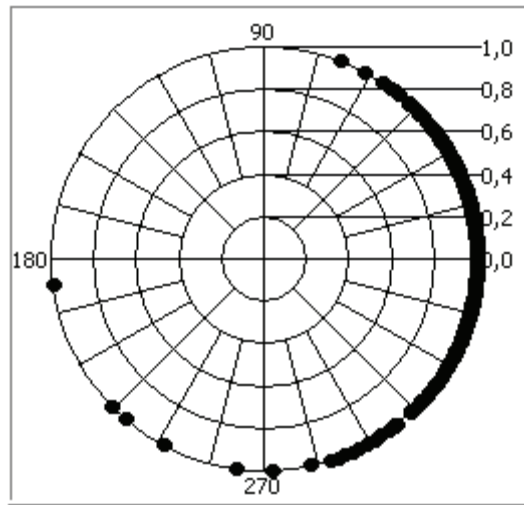
Figure 3 – The unit circle phase shifts differences displaying for $t \in [3000...3480]$ section of defect-free signal $u_{\mathrm{1df}}(t)$ in sliding window length 480 points

8) calculating the ratio of circular variance of the two defect-free signals and circular variance defect-free signal to the circular variance of the defect signal;
9) results graphical displaying.

Figure 4 represents graphs resulted from comparison circular variance of the two defect-free signals $V_{\mathrm{df}}^{(1)}/V_{\mathrm{df}}^{(2)}$ and circular variance defect-free signal to the circular variance of the defect signal $V_{\mathrm{d}}/V_{\mathrm{df}}$.

a

1.6.3

b
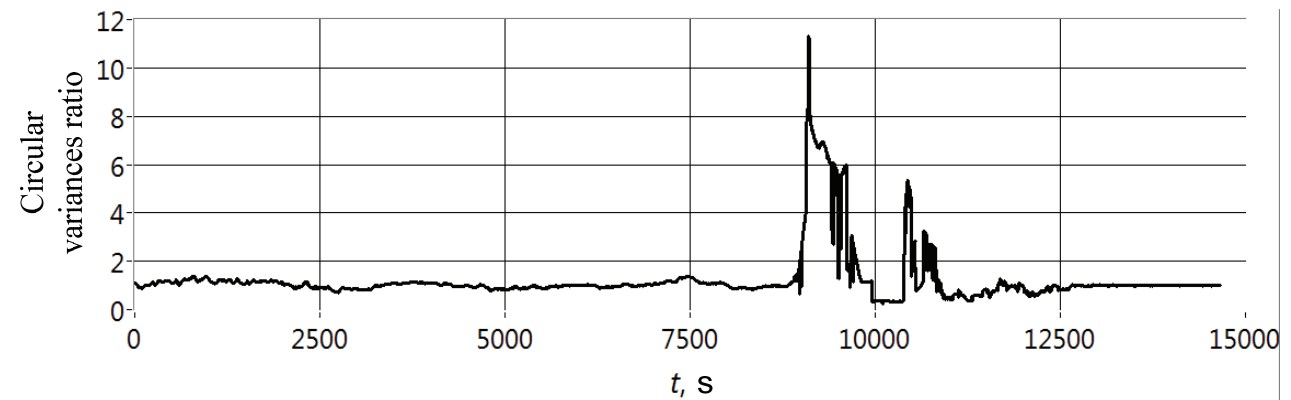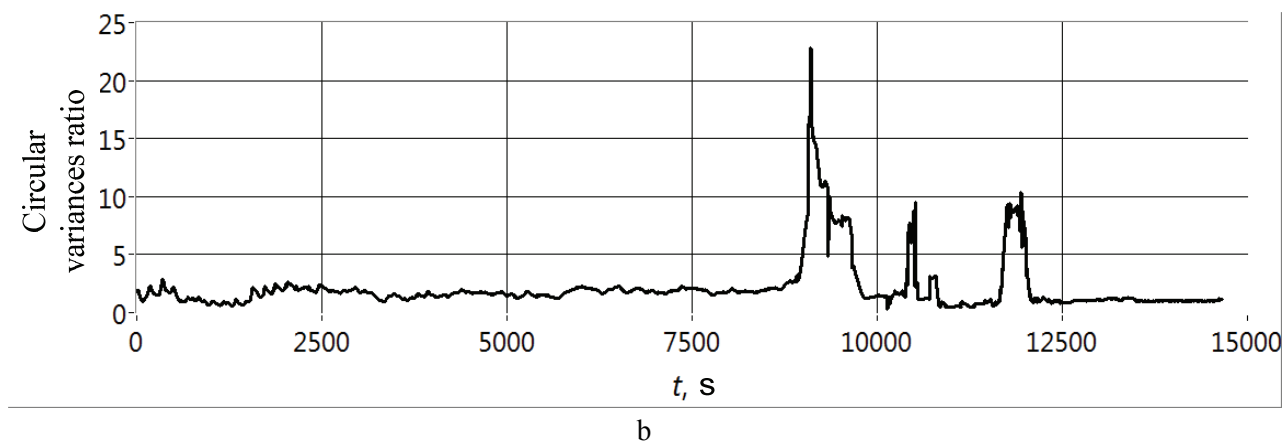
Figure 4 – Graphic relations of two defect-free signals circular variance $V_{\mathrm{df}}^{(1)}\big/V_{\mathrm{df}}^{(2)}$ (a) and circular variance defect-free signal to the circular variance of the defect signal $V_{\mathrm{d}}\big/V_{\mathrm{df}}$ (b)

According to the research we can conclude that the value of signals phase shifts differences circular variance of composite material defective zone comparatively more than defect-free zone one. This confirms the feasibility of circular statistics methods applying during acoustic detection of the composite material and the aircraft structural detail and gives rise to further researches.

4. Conclusions

1. Defect and defect-free signals obtained by the acoustic impedance flaw detection method are tested.

2. The value of signals phase shifts differences circular variance of composite material defective zone comparatively more than defect-free zone one.

5. References

1. *Еременко В.С.* Использование преобразования Гильберта для анализа сигналов импульсных импедансных дефектоскопов / В.С. Еременко, А.М. Овсянкин, Е.Ф. Суслов // Фізичні методи та засоби контролю середовища, матеріалів та виробів (серія). Вип. 12: електромагнітний, ультразвуковий та оптичний неруйнівний контроль. Збірн. наук. праць: – Львів: ФМІ ім. Г.В.Картпенка НАНУ, 2007 – С. 286 – 289.

2. *Еременко В.С.* Современные информационные технологии в системах неразрушающего контроля / В.С. Еременко, Е.В. Монченко, Б.Н. Налєсний, Е.Ф. Суслов // Вісник інженерної академії України. 2007, № 3-4. С. 113 – 116.

3. *Куц Ю. В.* Характеристика кутових вимірювань при статистиках малого обсягу / Ю. В. Куц, С. В. Шенгур, Л. М. Щербак // Системи обробки інформації. – 2010. – Вип. 4(85). – С.92-95.

4. *Fisher N.I.* Statistical analysis of circular data. Cambridge: Cambridge University Press, 2000.–277 p.

5. *Куц Ю. В., Шенгур С.В.* Програмний комплекс для моделювання та статистичного опрацювання результатів кутових та фазових спостережень // Вісник інженерної академії України. – 2010. – Вип. 3-4. – С.93-97.

6. *Куц Ю.В., Щербак Л.М.* Статистична фазометрія. – Тернопіль: Вид-во Тернопільського державного університету ім. І. Пулюя, 2009. – 383 с.

7. *Mardia K.V.* Statistics of Directional Data / K.V. Mardia and P.E. Jupp – London: Academic Press Inc., 1972 – 415 p.

UDC 006.91

Yuriy V. Kuts, D.E., Prof.,
Aleksey V. Dergunov, post-graduate student,
Svetlana V. Shengur
(National Aviation University, Ukraine)

CIRCULAR DATA POINT AND INTERVAL EVALUATION

The paper represents methods and the software for modeling and statistical proceeding of some common circular data analysis tasks. These tasks include computation of sample circular estimates such as mean direction, median, mode, variance, range, trigonometric moments, skewness, kurtosis and their confidence intervals

1. Introduction

According to national and international standards measurement results must include accuracy characteristics. The most widespread of them are expanded uncertainty or confidence interval [1].

The currency of this issue is caused by expanding number of tasks which can be solved by statistical circular analysis methods in such areas as economy, meteorology, geodesy, physics etc. Besides the most well-known packages for engineering calculations such as MathCad, MatLab, LabView do not contain functions for solving problems of statistical circular measurements data processing. Furthermore these program packages do not contain random circular data generators with circular distributions − von Mises, wrapped distributions family etc. For these reasons the possibilities of computer measurement experiments with random circles are limited.

Statistical processing of circular data measurement results software development is the main purpose of the paper.

According to the purpose of the paper, the software must provide:
1. Different probability densities random circular data simulation.
2. Hypothesis tests on von Mises, wrapped normal and uniform distributions.
3. The main circular sample statistical estimates computation.
4. Confidence interval estimation for circular mean and median directions.

2. Circular Sample Statistical Estimates

1. The main circular sample statistical estimates are [2, 3]:
2. The sample circular mean direction:

$$\bar{\theta} = \{\operatorname{arctg}\frac{S}{C} + \frac{\pi}{2}\{2 - (\operatorname{sign}S)\cdot[1 + \operatorname{sign}C]\};\qquad(1)$$

3. The mean resultant length:

$$r = \sqrt{C^2 + S^2}.\qquad(2)$$

4. Sample circular variance:

$$V = 1 - r.\qquad(3)$$

5. Sample standard deviation:

$$\sigma = \sqrt{-2\ln(1-V)} = \sqrt{-2\ln r}.\qquad(4)$$

6. A sample circular median direction $\bar{\theta}$ of angles $\theta_1,...,\theta_J$ is any angle θ such that half of data points lie in the arc $[\theta, \theta + \pi)$, and the majority of the data points are nearer to θ than to $\theta + \pi$.

7. The circular range is the length of the smallest arc which contain all the observations.
8. Mode − angle with the maximum data concentration around.
9. Skewness [2, 4]:

$$g_1 = b_3(\overline{\theta}_1)/V^{3/2} = r_2 \sin[\overline{\theta}_2(0) - 2\overline{\theta}_1]/V^{3/2} . \tag{5}$$

10. Kurtosis:

$$g_2 = [r_2 \cos[\overline{\theta}_2(0) - 2\overline{\theta}_1] - (1-V)^4]/V^2 . \tag{6}$$

11. Trigonometric moment:

$$T_u(\alpha) = \frac{1}{M} \sum_{j=1}^{M} e^{iu(\theta_j - \alpha)} . \tag{7}$$

3. Confidence Interval Estimation

Wide known methods of confidence interval obtaining are based on preliminary estimation of standard uncertainty and ratio coefficient for known probability density function. Often such distribution based on the results of previous measurements taken close to Gaussian. If the measurement results data is sufficient it checks for Gaussian distribution by one of the known criteria's. However in non priori information case it is impossible to taste sample on distributions and such approach can lead to significant errors in measurement results accuracy estimation.

Developed software includes confidence interval obtaining by traditional method, circular analogue of Chebishev inequality method, and methods with Johnson distribution and bootstrap technology application for circular data.

3.1. Traditional method

Traditional method provides obtaining of sample circular mean direction $\overline{\theta}$, standard deviation σ and Student coefficient. Confidence interval is obtaining considering the hypothesis of wrapped normal distribution as:

$$\overline{\theta} \pm t_{n,P}\sigma \tag{8}$$

3.2. Circular analogue of Chebishev inequality method

Circular analogue of Chebishev inequality method is used when random circle distribution is unknown. Method based on circular analogue of Chebishev inequality application [2]. Applying Chebishev inequality to the random variable $\sin([\theta - \overline{\theta}]/2)$ gives

$$P\left(\left|\sin\left((\theta - \overline{\theta})/2\right)\right| \ge \varepsilon\right) \le V/2\varepsilon^2 . \tag{9}$$

Confidence interval for mean direction can be obtained as:

$$\overline{\theta} \pm 2\arcsin\left(\varepsilon\sqrt{V/2}\right) \tag{10}$$

3.3. Method based on Johnson distribution application for random circle confidence interval obtaining

The Johnson distribution system is based on three possible transformations of a normal random variable. They are known as Johnson SL (lognormal), Johnson SU (unbounded) and Johnson SB (bounded), corresponding to exponential, logistic, and hyperbolic sine transformations. All three can be written as [5]:

$$z = \gamma + \eta\tau(x; \varepsilon, \lambda);$$
$$\eta > 0, \ -\infty < \gamma < \infty, \ \lambda > 0, \ -\infty < \varepsilon < \infty \tag{11}$$

where z is a standard normal random variable, τ is the transformation, and γ, η, ε and λ are scale and location parameters.

Johnson curves empirical distribution approximation depends on distribution family selection, computation of the parameters estimates and empirical probability function obtaining [6]. Confidence interval obtaining depends on computation of the inverse function for the probability density function $f(\theta)$ and estimation of symmetrical quantiles corresponding to given probability:

$$\left(\theta_{q/2}\right)\bmod 2\pi,\ \left(\theta_{1-q/2}\right)\bmod 2\pi\,, \qquad (12)$$

where q is the confidence level.

An empirical probability density function can also be useful for obtaining the mode, median and moments of given orders – the mean direction, standard deviation, skewness, kurtosis.

3.4. Bootstrap methods for circular statistical estimates and their confidence intervals obtaining

A class of computer-intensive statistical procedures called the bootstrap methods has a wide application for assessing the variability of a point estimate in situations where more usual statistical procedures are not valid and/or not available (e.g. the sampling distribution of a statistic is not known). The authors reviewed the parametric and non-parametric bootstrap methods for circular mean direction, median and their confidence interval limits estimation. The base algorithm of non-parametric bootstrap for an empirical distribution quantile estimate obtaining consists of following steps [7]:

1. Sampling with replacement a set of circles $\Theta' = \{\theta_1',...,\theta_n'\}$ from the original $\Theta = \{\theta_1,...,\theta_n\}$, $\theta_i \in [0,2\pi),\ n = \overline{1,N}$.

2. Computation of the quantile estimate θ for $\Theta' = \{\theta_1',...,\theta_n'\}$.

3. Repeating steps 1, 2 B times drawing a bootstrap distribution $\theta_1,...,\theta_B$.

4. Obtaining 2,5th and 97,5th percentiles from $\theta_1,...,\theta_B$ for 95% confidence interval.

Parametric bootstrap assumes the original circular data sample $\Theta = \{\theta_1,...,\theta_n\}$ from a distribution of a known form, a.g. von Mises $VM(\mu, k)$ distribution, where μ and k are known. With this assumption μ and k are estimated by μ and k from $\Theta = \{\theta_1,...,\theta_n\}$ and then each bootstrap sample is obtained by simulation from the $VM(\mu, k)$ distribution [4].

4. Modules of Software for Circular Measurement Data Modelling and Statistical Proceeding

Based on described methods the software for circular data simulating and statistical proceeding is developed. It consists of four main modules:

The input module provides an opportunity to keyboard input or loading from the text file and also generation random circles samples in accordance with the probability distribution functions – wrapped normal, von Mises, wrapped Cauchy, cardioid, wrapped Levy etc., – and given parameters (figure 1).

The module of statistical estimates and their accuracy characteristics obtaining with traditional methods application.

The module of statistical estimates and their accuracy rates obtaining with Johnson curves approximation of empirical circular distributions application.

The module of statistical estimates and their accuracy characteristics obtaining with bootstrap methods application (figure 2)
.
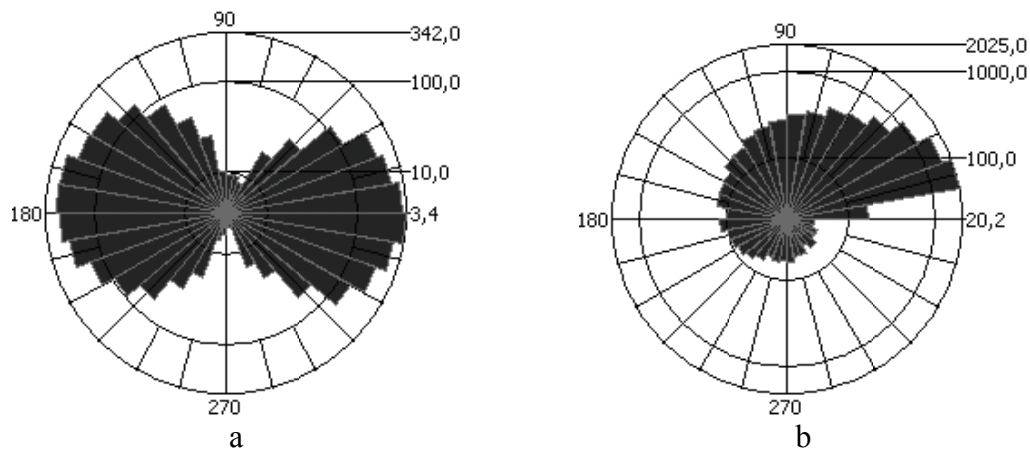
Figure 1 – Rose histogram: a – two Mises distributions; b – wrapped Levi distribution
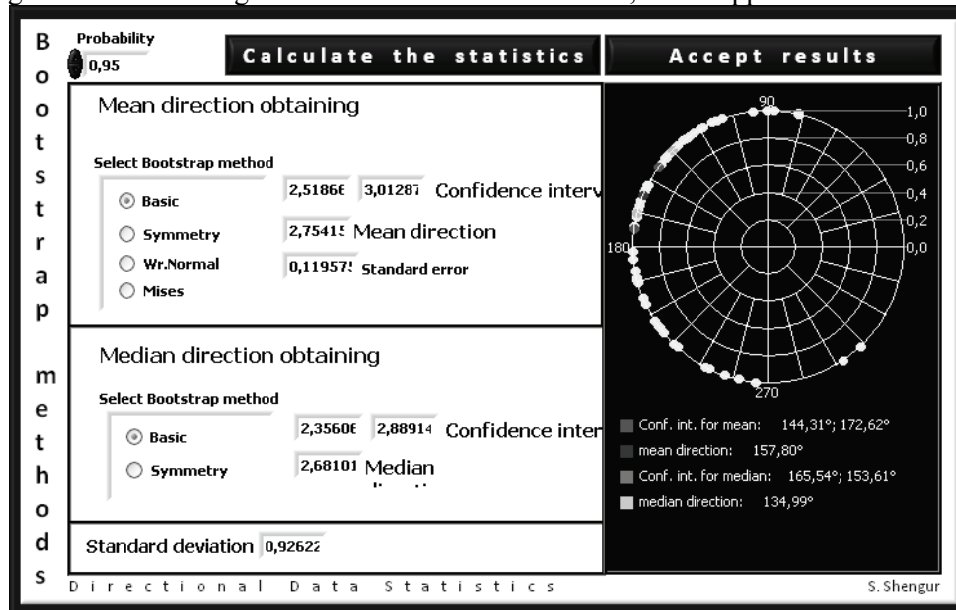
Figure 2 – The front panel of the module of statistical estimates and their accuracy characteristics obtaining with bootstrap methods application

4. Conclusions

Considered methods of circular data measurement results can be applied in such tasks as radar signals decoding, targets point's center of gravity definition, signal to noise ratio increasing in signal detection tasks.

Software for simulating and statistical processing of measurement circular data is discussed. It can be applied for:

1. Probability densities random circular data simulation: von Mises, wrapped normal, wrapped Cauchy, wrapped Levy, cardioid etc.

2. Obtaining the main statistical estimates – mean direction, mode, median, trigonometric moments, skewness, kurtosis, rate, standard deviation, variance etc.

3. Estimation of confidence interval limits for the mean direction and median based on traditional methods, Chebishev and bootstrap methods for unknown circular distribution.

4. Estimation of confidence interval limits for random circle based on Johnson curves empirical distribution approximation.

5. Displaying the results of simulation and processing on circular diagrams.

Developed software programs have such fields of application as circular measurement data statistical processing and computer experiments with random circles.

5. References

1. Guide to the Expression of Uncertainty in Measurement (GUM): First edition. – ISO, 1993. – 101p.

2. *Mardia K.V.* Statistics of Directional Data / K.V. Mardia and P.E. Jupp – London: Academic Press Inc., 1972 – 415 p.

3. *Jammalamadaka, S. Rao.* Topics in circular statistics / S. Rao Jammalamadaka, A. SenGupta. – Singapore: World Scientific Publishing Co. Pte. Ltd., 2001 – 322 p.

4. *Fisher N.I.* Statistical analysis of circular data. Cambridge: Cambridge University Press, 2000. – 277p.

5. Systems of frequency curves generated by methods of translation/ *Johnson N.L.*, – Biometrica, vol. 36, 1949, pp. 148-176.

6. *Khan G., Shapiro S.* Statistic models in engineering problems – M.: Mir, 1969. – 396 pp.

7. *Bradley Efron* (1982). The jackknife, the bootstrap, and other resampling plans, In Society of Industrial and Applied Mathematics CBMS-NSF Monographs, 38.

UDC 621.114.32

V.S. Eremenko, candidate of technical science,
A.V. Pereidenko, postgraduate student,
P.A. Shegedin, postgraduate student
(National Aviation University, Ukraine)

NONDESTRUCTIVE TESTING OF HONEYCOMB PANELS VIA ART-2 AND FUZZY-ART NEURAL NETWORKS

Usage of ART-2 and Fuzzy-ART neural networks for classification of defects in honeycomb panels were introduced and investigated. This article describes the algorithm of information signal processing in nondestructive testing of honeycomb panels via ART-2 and Fuzzy-ART neural networks. Results of practical usage of the special developed system for diagnostics technical condition of honeycomb panels were represented.

The existing methods of nondestructive testing of composite materials in most cases estimate a change of only one parameter of sensor informative data signal for a decision-making about a defect presence. Methods based on the estimation changes of a set of parameters can improve the nondestructive testing effectiveness, but require special algorithms for constructing decision rules.

Unfortunately, under the control of composite materials there are complex, nonlinear hyperplanes of diagnostic characters, and there is limited number of defects samples which used for classifier training. In this case it is impossible to make such classification which will provide the linear separation in the space of diagnostic characters. And this may lead to incorrect classification and decrease the reliability of nondestructive testing. To improve the reliability of nondestructive testing it is necessary increase the number of diagnostic characters, i.e. increase diagnostic characters space dimension. But, increasing of the diagnostic characters space dimension leads to situation when classification via linear hyperplanes becomes impossible or too cumbersome because of the lack of initial data and high dimension of input vectors. This also makes it difficult to create an approximation model, reduces calculation speed of separating hyperplanes, and increases the cost of hardware and software to implement the corresponding algorithms.

An alternative method of data processing and construction of decision rules for multiparameter nondestructive testing of composite materials is to use artificial neural networks. For nondestructive testing, artificial neural network allows to provide signals recognition (classification) obtained from the sensors during control. It also preserves important information about regular dependence of an informative signal's shape and the state of an object under control. This allows the neural network correctly classify new previously unknown signals, accumulate information and expand neural network knowledge about the range of possible defects without losing any information obtained earlier. Usage of such methods makes it possible to achieve high noise immunity, significantly reduce dependence on external factors, and provide high efficiency control. Systems of nondestructive testing based on neural networks can improve the reliability of control, reduce cost of system implementation, reduce hardware and software costs, and improve its performance.

There are a lot of publications which describe issues of neural networks effectiveness for signals registration and recognition (classification), the technical state recognition of an object under control and classification of possible defects, cluster analysis, etc. To choose the optimal architecture of a neural network, which will be used in the information-measuring system of nondestructive testing of products from composite materials, it was investigated such neural network architecture as the Kohonen network [1,2], the multilayer perceptron [3], the special hybrid neural network [4,5] and neural networks of adaptive resonance theory (ART): ART-2 [6-8] and Fuzzy-ART [9,10]. Based on the received results it was concluded to use neural networks ART-2 and Fuzzy-ART as a basis of composite materials technical state classifier. These neural networks allow to get the best accuracy of the nondestructive testing of honeycomb panels [8,10].

ART neural network [11] is a vector classifier which contains two layers of neurons (bottom-up layer or comparison layer and top-down layer or recognition layer). During the classification

process, the input signal is processing according to the weights of the neurons in comparison layer of an ART-network. The signal is then fed to a recognition layer where the competitive search of the one single winning neuron (the neuron with an active output signal) is performed. Winner neuron is a neuron whose weight vector lies closest to the input vector (signal). This neuron, that becomes active under the influence of the input signal, is corresponding to a particular class (pattern), which formed in the memory of neural network and could include an input signal. On the next stage a feedback signal from the winner neuron in the recognition layer comes back together with weights of an appropriate neuron to the comparison layer In the comparison layer input signal is checked for compliance with the pattern in the network memory. If this pattern does not correspond to the input signal, the activity of the winner neuron in the recognition layer must be suppressed and the search phase for the new winner neuron (pattern) in the network memory should be performed again but without suppressed neuron. The algorithm is repeated until correct pattern is not found or all neurons in the recognition layer are not suppressed. If all neurons in the recognition layer are suppressed, then it means that the input signal belongs to the new pattern. This new pattern was not registered by neural network earlier and it didn't similar to any of the previously registered patterns, stored in the network memory. In this case, the neural network will generate a new class and will provide a new neuron in the recognition layer. If during the search phase correct pattern (appropriate neuron with the corresponding weights) is found in the recognition layer, then the search phase stops and neural network generates as its output a signal that corresponds to one of the existing classes. Weights of the winning neuron in the recognition layer will be adapted according to appropriate network teaching rules [6,7,9]. So desired signal pattern in network memory will in more general form describe the group of signals which belong to the appropriate class.

At the department of information-measuring systems of the National Aviation University a special system of nondestructive testing of composite materials by low-velocity impact [12] was developed. For information signal processing ART-2 and Fuzzy-ART neural networks were used. Classification of defects with the developed system is performed by analyzing changes of the registered signals shape, forming in the memory of neural network desired informative signal patterns which correspond to non-defect parts of controlled samples and comparing registered signals with generated patterns.

For the system testing were used:
- two samples (S1 and S2) of honeycomb panels from wings of aircraft type An-70 with artificially formed defects (defects 1-5). The following types of defects were under control: peeling skin on the inside of the filler cladding; control was made from the outside of the cladding;
- one sample (S3) of a fiberglass with honeycomb filler PSP-1 and additional composite VKV-9, with an adhesive compound on the adhesive film VK-41 with artificial defect (defect 6). The following types of defects were under control: peel outer skin of the aggregate.

During the nondestructive testing of described samples for each sample and each area (without defect and with different defects) 250 realizations of the informative signals were obtained (Fig. 1). For diagnostic samples state data signal's shape was analyzed because its change allows determining presence of defect in honeycomb panel and performing classification its type with high reliability.

During the control process registered signals were given one by one in a casual order to the system entrance. After an appropriate signal was given to system, it was removed from input samples collection. This procedure was repeated until the input samples collection became empty. Thus, the system during the process of nondestructive testing automatically formed its own base of possible classes (defects).
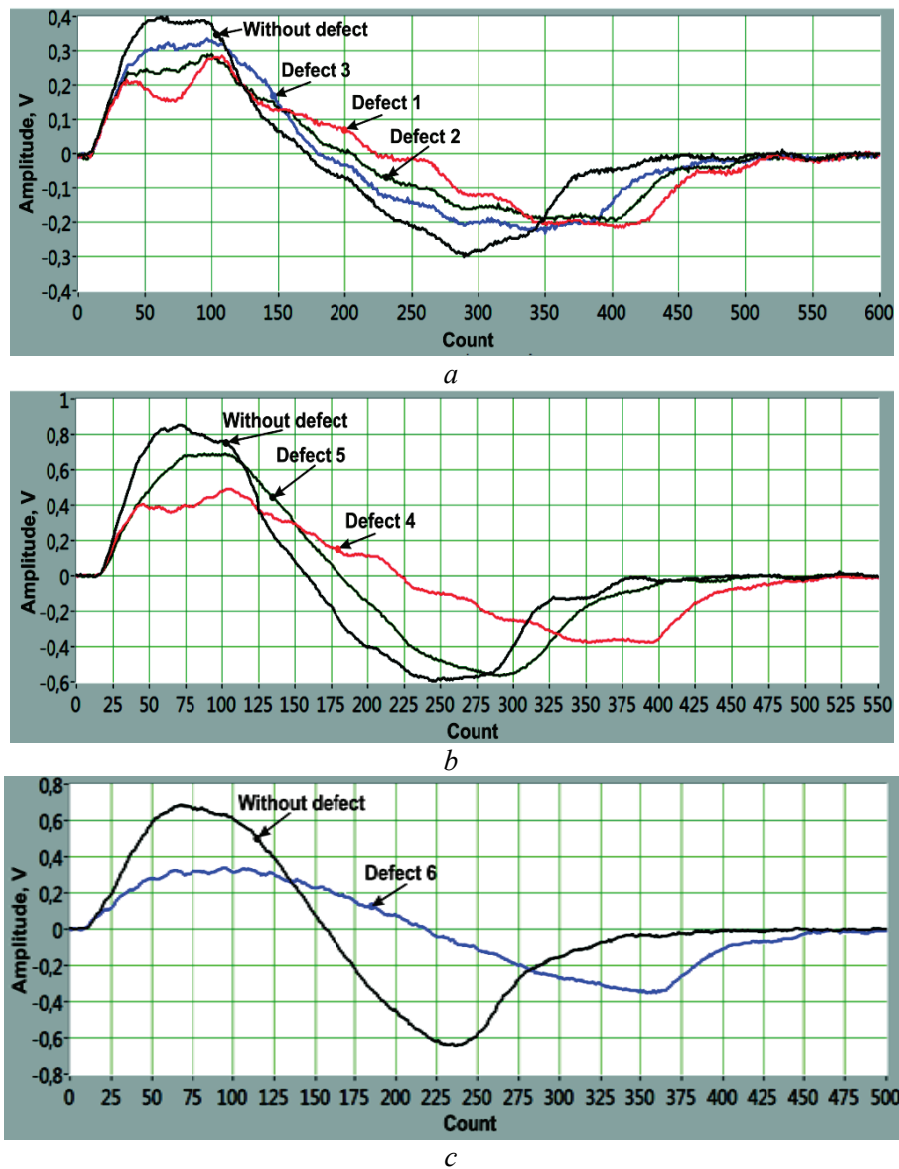
Fig. 1 Informative signals which were obtained from areas without defects and areas with
different defects during non-destructive testing of honeycomb panel samples S1(*a*), S2(*b*) and S3(*c*)

After the system has formed it data base the verification of the nondestructive testing reliability via described system had been performed. For these purposes for each area were obtained 100 new signals and these signals were given to the system for classification. Obtained results of the nondestructive testing reliability of products from composite materials using described system based on ART-2 and Fuzzy-ART neural networks presented at Fig. 2.
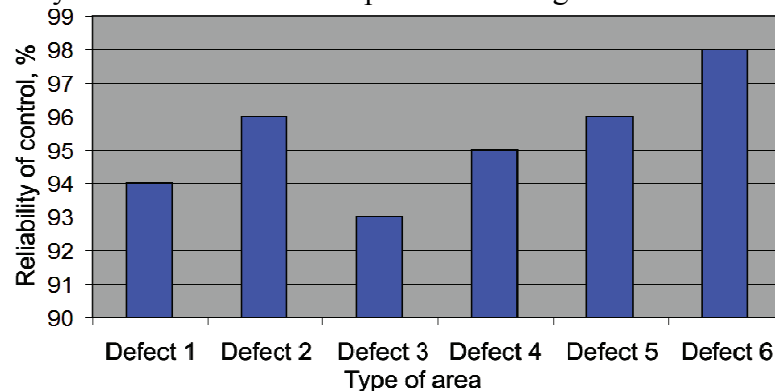
Fig. 2 Reliability of composite materials control using the nondestructive testing system based on
ART-2 and Fuzzy-ART neural networks

1.6.12

Based on these results, it should be noted that the described system of nondestructive testing based on ART-2 and Fuzzy-ART neural networks could detect and classify subsurface defects in honeycomb panels with high reliability and accuracy, as well as defects that are located on the back side of the cladding with an area larger than 2 cm^2 and with thickness of composite panel equal to 12.8 mm. The reliability of the nondestructive testing via described system is more than 93%.

References

[1]   *Pereidenko A.V.* Investigation of cluster analysis algorithms for solving nondestructive testing tasks/ *A.V. Pereidenko, V.S. Eremenko* // East European journal of advanced technologies. −2010. −№1/5(43). – P. 40-43. (In Ukrainian)

[2]   *Pereidenko A.V.* The system of cluster analysis of nondestructive testing products from composite materials / *A.V. Pereidenko, V.S. Eremenko, V.A Rogankov* // Knowledge-intensive technologies. −2010. −№3. – P. 73-77. (In Ukrainian)

[3]   *Pereidenko A.V.* The system of defects classification based on artificial neural networks / *A.V. Pereidenko, V.S. Eremenko, J.O. Pavlenko* // Bulletin of the National Technical University of Ukraine "Kyiv Polytechnic Institute". Series 'Instrument Engineering'. – 2010. – №40. – p. 72-80. (In Ukrainian)

[4]   *Pereidenko A.V.* Demerit rating system based on artificial neural networks / *A.V. Pereidenko, Y.V.Kuts, V.S. Eremenko* // "Days of nondestructive control 2010": matetials of XXV National Conference with International participation "Defektoskopiya'10", June 13-17, 2010.: proceedings – Sophia,2010. − p.469-475. (In Russian)

[5]   *Pereidenko A.V.* The system of standardless diagnosis of composite materials based on hybrid neural network. / *A.V. Pereidenko, V.S. Eremenko, E.F. Suslov, P.A. Shegedin* // " Educational, scientific and engineering applications in LabVIEW and National Instruments technology": materials of the 9th international scientific conference, December 3-4, 2010.: proceedings − Moscow,2010.−P. 207-212. (In Russian)

[6]   *Carpenter G.A.* ART 2: Stable self-organization of pattern recognition codes for analog input patterns / *G.A. Carpenter, S. Grossberg* // Applied Optics. – 1987. – №26. – P. 4919-4930.

[7]   *Carpenter G.A.* ART 2-A: An adaptive resonance algorithm for rapid category learning and recognition / *G.A. Carpenter, S. Grossberg, D.B. Rosen* // Neural Networks. – 1991. – №4. – P. 493-504.

[8]   *Pereidenko A.V.* Uses of the modified ART-2 neural network architecture in the nondestructive testing system of products from composite materials / *A.V. Pereidenko, V.S. Eremenko, O.V. Monchenko* // "Modern methods and instruments of nondestructive testing and technical diagnosis": materials of 19th International Conference, October 3-7, 2011.: proceedings – Gurzuf, 2011. – p. 81-84. (In Ukrainian)

[9]   *Carpenter G.A.* Fuzzy ART: Fast stable learning and categorization of analog patterns by an adaptive resonance system / *G.A. Carpenter, S. Grossberg, D.B. Rosen* // Neural Networks. – 1991. – №4. – P. 759-771.

[10] *Pereidenko A.V.* System Of Standartless Diagnostic Of Cell Panels Based On Fuzzy-ART Neural Network / *A.V. Pereidenko, V.S. Eremenko, V.O. Rogankov* // " MRRS-2011": Proceedings of the Third Microwaves, Radar and Remote Sensing Symposium, August 25-27, 2011: proceedings. – Kyiv, 2011. – p. 181-183.

[11] *Carpenter G.A.* A massively parallel architecture for a self-organizing neural pattern recognition machine / *G.A. Carpenter, S. Grossberg* // Computer Vision, Graphics, and Image Processing. – 1987. – №37. – P. 54-115.

[12] *Eremenko V.S.* Detection of impact damage honeycomb panels using low-velocity impact / *V.S. Eremenko, V.M. Mokijchuk, A.M. Ovsankin* // Technical diagnostics and nondestructive testing. – 2007. –№1. – P. 24-27. (In Russian)

S.F. Filonenko, Doctor of Engineering, Professor
O.P. Kosmach, junior researcher (National Aviation University, Ukraine)

LAWS OF CHANGE OF ACOUSTIC EMISSION TIME PARAMETERS AT DESTRUCTION OF COMPOSITE MATERIAL BY SHEAR LOAD

The regularities of change of acoustic emission time parameters at change of loading speed and heterogeneity of physical-mechanical properties of composite material were determined. The laws of change of acoustic emission time parameters at destruction of composite material were established.

Introduction

Composite materials (CM) are widely used in aviation, space equipment; any kind of transport; and other types of machinery because of the number of advantages. They have rather high physical-mechanical characteristics, are resistant to the influences of different kinds of environments, etc. For research of destructions of this materials are widely use traditional methods and methods which have high sensitivity to processes which are developing in structure of materials at their loading. One of the such methods of research, control and diagnostic of condition of equipment with CM is acoustic emission method (AE). At the same time, significant complications in interpretation of AE information which get registered, leads to complications of practical usage AE methods in control and diagnostic. In this case acquire great significance of the theoretical research of processes acoustic radiation which are directly connected with research of destruction processes in CM. For the last decade, one of the widely-distributed conceptions which use for research of destruction processes of CM is presented as a fibre bundle model (FBM) [1–4].

First direction connected with research of damageability of CM. According to this direction, destruction of CM interpret like the process continuous accumulation of damage. Herewith analyze parameter of damageability which characterize deviation of characteristics of elasticity from their initial values, that is observing the extent of damageability of material in total. Other direction connected with research of laws of destruction of CM elements in case of continuous it running with according redistribution of stresses on unbroken elements [1–4].

According this conception it is supposed that the loss of the bearing capacity of CM appears to be a consequence of the destruction of its fibres or elements. Destruction of CM is considered to be the process of the consecutive destruction of its fibres or elements. The most researches of destruction processes of CM directed to investigation of the regularities of its change for continuously condition of its running.

Most theoretical and experimental researches were devoted to the destruction process of CM under the conditions of uniaxial load. Such research allowed analytic expressions to be obtained for the number of fibres that remain in the evolution of the destruction process of CM. The correlations which were obtained characterize the processes of destruction and acoustic radiation only in the approach to the full destruction of the CM. At the moment of the destruction of the CM, all research functions have rupture. Such ambiguity does not allow a mathematic expression to be obtained for the description of the AE signal.

In articles [5, 6] was obtained the analytical expression of AE signal which formed at destruction of elements by shear load. Was accepted what distribution of threshold levels of elements destruction are independent and even with borders [0, 1].

According to the model [5, 6] the regularities of change of AE parameters depends from factors which connected with loading conditions, geometrical size of elements and its physical-mechanical characteristics. Certainly what determination of influence of this factors on AE signals and laws of change of their time parameters is very important for creation of AE methods of control and diagnostic of equipment and units with CM.

Results of researches

In articles [5, 6, 7] was shown what at shear loading of CM continuous of destruction process of elements agree with continuous AE signal which was formed. Herewith AE signal represent like video pulse which characterized by rapid increase of leading edge and relaxed decrease in amplitude on the trailing edge. The results of such modeling of destruction process of CM are shown in form of plot of AE signal $\widetilde{U}(t) = U(t)/U_0$ in relative units in Fig. 1. All parameters which come to expression $U(t)$ [5, 6, 7] set to dimensionless values and time presented in normalize values.

While modeling loading speed of CM $\widetilde{\alpha}$ was set to dimensionless value $\widetilde{\alpha}=100$. Value of destruction start time for speed of load $\widetilde{\alpha}=100$ is $\widetilde{t}_0=0,001$. Threshold stress of destruction (in relative units) for value $\widetilde{\alpha}$ and time of start destruction of CM elements was calculated according methods in articles [5, 6]. For accepted time $\widetilde{t}_0$ of start destruction of CM elements threshold stress is equal $\widetilde{\sigma}_0 \approx 0,087$. While modeling was accepted what value of parameters υ_0, r and g in relative units are equal to: $\widetilde{\upsilon}_0=1000000$, $\widetilde{r}=10000$, $\widetilde{g}=0,1$.
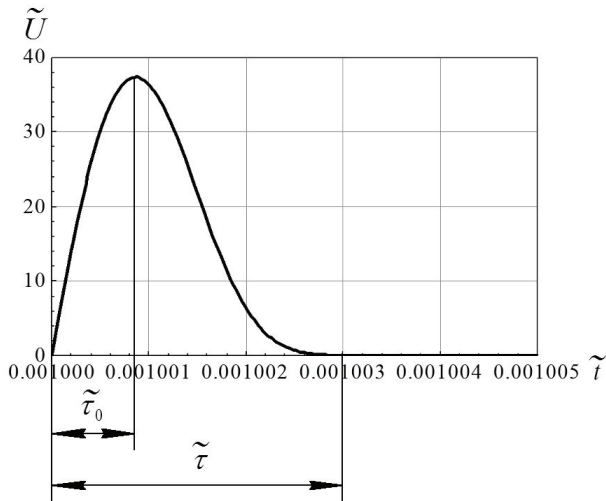
Fig. 1 – Time parameters of acoustic emission signal which form at destruction of elements of composite material by shear load. Values of modeling parameters: $\widetilde{\alpha}=100$; $\widetilde{\sigma}_0 \approx 0,087$; $\widetilde{g}=0,1$; $\widetilde{t}_0=0,001$; $\widetilde{\upsilon}_0=1000000$; $\widetilde{r}=10000$

From received results it is apparent what formed AE signal is video pulse. Such video pulse can characterized by such time parameters (fig.1), namely: duration of leading edge τ_0 and duration of signal τ. Assuredly what change in values of model parameters will influence on the regularities of change of destruction process of CM and time parameters τ_0 and τ of formed AE signals.

According to model it can be seen that, if the destruction process is taking place, the quantity of the remaining elements and the characteristics of the AE signal depend on the quantity of initial elements, speed of the load, physical and mechanical characteristics of the CM, and geometrical sizes of its elements.

Lets research the influence of loading speed and the heterogeneity of physical-mechanical characteristics of CM on law of change of time parameters of formed AE signals.

While research the influence of loading speed on time parameters of formed AE signals we will assume what we observe same CM which have same geometrical sizes of its elements and same physical-mechanical characteristics. While research the influence of heterogeneity of physical-mechanical characteristics of CM on time parameters of formed AE signals we will assume what we observe CM which have same geometrical sizes of its elements and constant speed of load.

The speed of load influence on speed of change of equivalent stress and condition the change of speed of destruction process of CM what was shown in [5, 6, 8]. This results from calculations the laws of quantity change of elements at destruction of CM by shear load according to model of destruction in [5]. In article [6] was shown the results of modeling of AE signals in time (in relative units) for speeds of load $\widetilde{\alpha}$ which changed in range from 100 to 500 with increment step $\Delta\widetilde{\alpha}=50$.

Herewith the values of parameters $\widetilde{\sigma}_0$, $\widetilde{\upsilon}_0$, $\widetilde{r}$ and $\widetilde{g}$ were accepted equal: $\widetilde{\sigma}_0 \approx 0,087; \widetilde{\upsilon}_0 =1000000; \widetilde{r}=10000; \widetilde{g}=0,1$. Lets define the values of time parameters of formed AE signal for each accepted value of loading speed and build the law of their change.

The laws of change of time parameters of formed AE signals from speed of load in relative

units are shown in fig.2. From fig.2 we can see what with increase the speed of load by shear load the duration of leading edge and duration of AE signal are reduce. Such reduce of duration of leading edge and duration of AE signal have nonlinearity laws of change. Processing of received data showed what with increase $\tilde{\alpha}$ in 5 times, that is from 100 to 500, duration of leading edge of formed AE signals reduce in 18,37 times and their duration reduce in 2,97 times. The reduction of values of time parameters of formed AE signals show increasing of speed of destruction process of CM elements. Besides, an increase in deformation speed leads to the transformation of the form of the AE signal. Its form gradually approaches the signal of a triangle waveform.
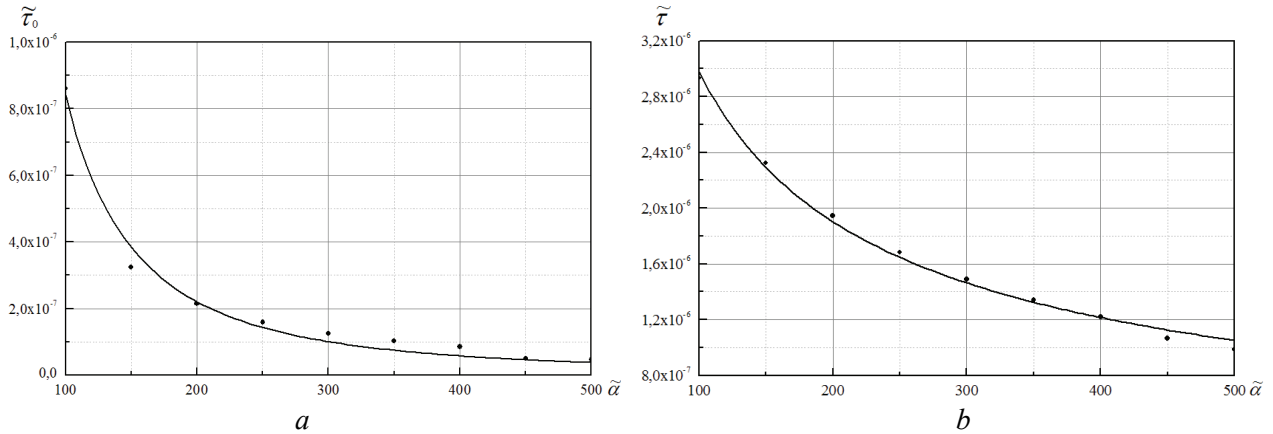
Fig. 2 – Dependence of change in duration of leading edge $\tilde{\tau}_0$ (*a*) and duration $\tilde{\tau}$ (*b*) of acoustic emission signals in relative units at change of speed of load $\tilde{\alpha}$ of composite material by shear load. Speed of load $\tilde{\alpha}$ takes values in range $\tilde{\alpha}$ =100…500 with increment step $\Delta\tilde{\alpha} = 50$. $\tilde{g}$ =0,1, $\tilde{\sigma}_0$≈0,087, $\tilde{\upsilon}_0$ =10^6, $\tilde{r}$ =10^4

Lets define the laws of change of time parameters of AE signals at change of heterogeneity of physical-mechanical characteristics of CM . Parameter *r* is connected with the sensitivity of the material to stress and characterises the dispersibility of its strength properties. For material with small dispersibility of characteristics *r*>>1. While modeling the AE signals in relative units the values of parameter $\tilde{r}$ will change in range from 10^4 to 2x10^4 with increment step $\Delta\tilde{r}$ =1000. We will suppose what the load of CM has constant speed. It value equal $\tilde{\alpha}$ =const=100. While modeling the parameters $\tilde{\sigma}_0$, $\tilde{\upsilon}_0$ and $\tilde{g}$ accept same as earlier, that is: $\tilde{\sigma}_0$≈0,087; $\tilde{\upsilon}_0$ =1000000; $\tilde{g}$ =0,1.
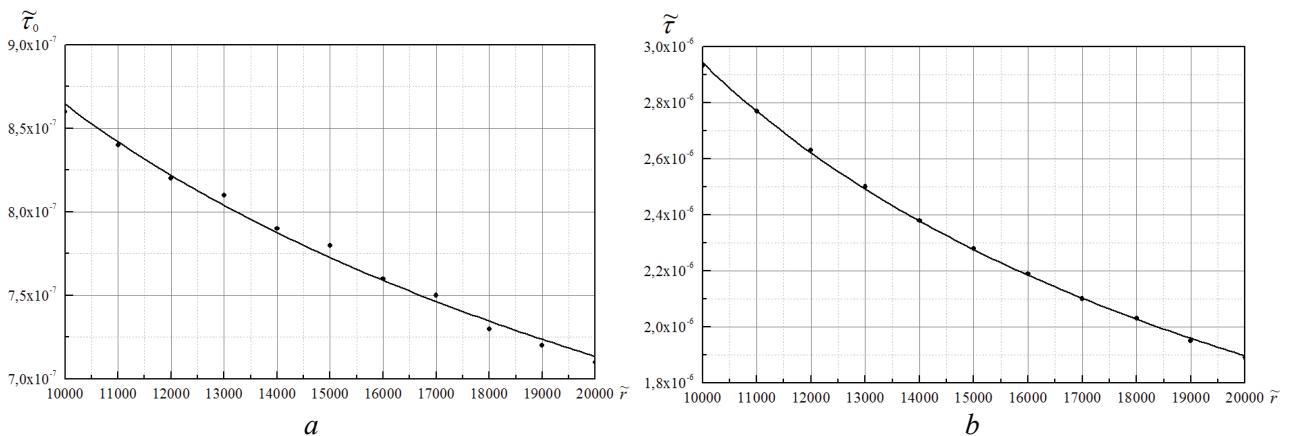
Fig. 3 – Dependence of change in duration of leading edge $\tilde{\tau}_0$ (*a*) and duration $\tilde{\tau}$ (*b*) of acoustic emission signals in relative units at change the values of parameter $\tilde{r}$. Parameter $\tilde{r}$ take values in range from $\tilde{r}$ =10000…20000, $\tilde{\alpha}$ =100. $\tilde{g}$ =0,1, $\tilde{\sigma}_0$≈0,087, $\tilde{\upsilon}_0$ =10^6

Lets define the values of time parameters of formed AE signal for each accepted value of parameter $\tilde{r}$ and build the law of their change. The laws of change of time parameters of formed

AE signals from heterogeneity of physical-mechanical characteristic of CM (parameter $\tilde{r}$) in relative units are shown in fig.3.

From fig.3 we can see what with reduce of CM heterogeneity (increase values of parameter $\tilde{r}$) the duration of leading edge and duration of AE signal are reduce. Such reduce of duration of leading edge and duration of AE signal have nonlinearity laws of change.

Processing of received data showed what with increase $\tilde{r}$ in 2 times, that is from 10^4 to $2x10^4$, duration of leading edge of formed AE signals reduce in 1,21 times and their duration reduce in 1,51 times. The reduction of values of time parameters of formed AE signals related with reduce time of destruction process of CM elements at constant speed of it load.

Received results showed what the largest influence to change of time parameters of AE signals (duration of leading edge and duration of signal) at destruction of CM have speed of load.

Conclusion

The results of research are showing what change the speed of load and heterogeneity of physical-mechanical characteristics influences on speed of destruction process of CM and time parameters of formed AE signals.

The continuity of the destruction process is accompanied by the formation of a continuous AE signal. The AE signal is characterised by accelerating increase leading edge of the amplitude and gradual fall on the trailing edge.

Was determined what increase the speed of load led to reduction of duration of leading edge and duration of formed AE signals. With reduce of CM heterogeneity the duration of leading edge and duration of AE signal are reduce. In both cases such reduce of duration of leading edge and duration of AE signal have nonlinearity laws of change and with high agreement can be described by power function.

References

1. *Hemmer P. C.* The Distribution of Simultaneous Fiber Failures in Fiber Bundles/ *P. C. Hemmer, A. Hansen* //J. Appl. Mech. – 1992. –vol.59. –№4. – P.909–914.

2. *Kun F.* Extensions of Fibre Bundle Models/*F. Kun, F. Raischel, R.C. Hidalgo, H.J. Herrmann* //Modelling Critical and Catastrophic Phenomena in Geoscience. Lecture Notes in Physics–2007.–vol.705.–P.57–92.

3. *Pradhan S.* Energy bursts in fiber bundle models of composite materials /*S. Pradhan, C. Hemmer* //Phys. Rev. E.–2008.–vol. 77.–№1.–4 p.

4. *Kovács K.* Pagonabarraga Critical ruptures in a bundle of slowly relaxing fibers /*K. Kovács, S. Nagy, R. C. Hidalgo, F. Kun , H. J. Herrmann*// Phys. Rev. E.–2008.–vol. 77.–№3.–8 p.

5. *Филоненко С.Ф.* Модель сигнала акустической эмиссии при разрушении композиционного материала под действием поперечной силы/ *С.Ф. Филоненко, В.М. Калита, А.П. Космач, Т.Н. Косицкая* // Технологические системы.–2010.–№ 2.–С.23–32.

6. *Філоненко С.Ф.* Моделювання сигналів акустичної емісії при руйнуванні композиційних матеріалів під дією поперечної сили /*С.Ф. Филоненко, О.П. Космач, Т.М.Косицька*//Вісник НАУ.–2010.–№2.–С.85–93.

7. *Філоненко С.Ф.* Акустична емісія при навантаженні композиційних матеріалів/ *С.Ф. Філоненко, В.М. Каліта, О.П. Космач* // Вісник НАУ. – 2010. – № 1.–С.133–141.

8. *Филоненко С.Ф.* Влияние неравномерности процесса разрушения композиционного материала на сигналы акустической эмиссии/ *С.Ф. Филоненко* // Технологические системы.–2011.–№1(54).–С.24–31.

V.V. Kovalchuk, V.A. Gromov, Alex. Alex. Panchenko
(Mylitary Academy, Odessa, Ukraine)
O.Yu. Shepel (National Aviation University, Ukraine)

CALCULATION PROCEDURE FOR THE QUANTUM ELEMENTS ROBOT'S NANOSYSTEMS

Calculations of structural phase transitions B1 - B2 under pressure in halcogenids Alkali Land Metals are carried out on the basis of approach of the local functional density theory, using as adjustment designing of amendments to potential by means of the electronic density received in self-coordinated calculation using approximation of local density. The results has interest for robot's nanosystems.

The standard calculation procedure of the energy of zoned structure E_k (for example, [1]) is used. In special points of Brillion's zone equation the secular was solved

$$\left[\frac{1}{2}\left(\vec{k}+\vec{g}\right)^2 - E_n\left(\vec{k}\right)\right]C_{n,\vec{k}}(\vec{g}) + \sum_{\vec{g}'} W(\vec{k}+\vec{g},\vec{k}+\vec{g}')C_{n,\vec{k}}(\vec{g}') = 0, \qquad (1)$$

where $C_{n,\vec{k}}(\vec{g})$ are factors of decomposition of pseudo-wave function as a number of plane waves

$$\varphi_{n,\vec{k}} = \sum_{\vec{g}} C_{n,\vec{k}}(\vec{g})\left|\vec{k}+\vec{g}\right\rangle, \qquad (2)$$

n is then number of a zone, k is a wave vector in the first Brilluon's zone, g, g' - are vectors of a return lattice. The Furies-image of potential $W(k_1, k_2)$ includes Furies -images potentials such as: W_H - Hartree, W_{xc} - exchange-correlation, W_{BHS} [2] - pseudo-potential which is named as Bachelet - Hamann – Schlüter.

Full energy using the density functional theory (DFT) is represented as

$$E = \frac{1}{N}\sum_{\vec{k}} E_{\vec{k}} - E_H + E_{xc} + E_{es} + \alpha_1 z, \qquad (3)$$

where N is a number of atoms of various grades in an elementary cell, energy Hartree

$$E_H = \frac{\Omega}{2}\sum_{\vec{g}}\frac{4\pi}{g^2}\left|\rho(\vec{g})\right|^2, \qquad (4)$$

The exchange-correlation contribution is the following

$$E_{xc} = \Omega\sum_{\vec{g}}\left[\varepsilon_{xc}(\vec{g}) - W_{xc}(\vec{g})\right]\rho(\vec{g}), \qquad (5)$$

where Ω is the volume of an elementary cell, $\varepsilon_{xc}(g)$ is the density of exchange -correlation energy, $\rho(g)$ is a Furies -image of electronic density, z is the average number of the valent electrons on atom, E_{es} is electrostatic energy.

Non Coulomb part of electron-ionic interaction is the following

$$\alpha_1 = \lim_{\vec{g}\to 0}\left\{W_{BHS}^{loc}(\vec{g}) + \frac{8\pi z}{\Omega g^2}\right\}. \qquad (6)$$

The local density functional theory (LDFT) is the standard approximation methods of calculation of exchange-correlation energy (5). And the same lacks of this approach [3] are well-known. From the point of view of research of polymorphism we shall note some of them: underestimation of the forbidden zone; understating of parameters of a lattice; different influence LDFT on the calculation of different conditions, that especially strongly affects the size of the forbidden zone and details of a structure of electronic zoned structure. Some lacks are peculiar directly LDFT, others result from DFT.

Recently a number of methods both avoiding application LDFT is offered, and trying to remove existing lacks of frameworks LDFT. Among the last we shall note self-action corrected (SAC) pseudo-potentials [4]. SAC eliminates not physical self-action of every electron and reduces

energy filled orbitals. Received in this approach power functional is noninvariant at unitary transformation filled orbitals it is possible to design a set of decisions too. Thus p-orbitals of an anion practically do not change, however d-orbitals of a cation can strongly be changed. It is necessary to note, that distortion of zoned structure is connected as with p-d-hybridization, which wrong estimates using LDFT, and to a wrong calculation of s-conditions which form a bottom of a zone of conductivity. Special interest can be shown to halcogenids of calcium because in Ca still there are no d-electrons. Calculation results sometimes to bad enough convergence of results in settlement circuits both not taking into account, and taking into account elimination of p-d-hybridization.

Thus, the iterative decision of the equation (1) insufficiently precisely describes the located conditions because of not physical self-actions. Entering SAC pseudo-potentials [5]:

$$V_{ps}^{SIC} = V_{BHS} - V_H\left[\rho^{at}\right] - V_{xc}\left[\rho^{at}\right],$$ (7)

unitary repeat calculation for electronic density of separate atoms ρ^{at}. Such pseudo-potentials cannot be used in solid-state calculations because of long interaction of Coulomb tails which should be compensated to introduction additional composed $1/r_{loc}$, which shifts a power scale and it is taken into account only in area $r < r_{loc}$.

The addition of additional contributions to pseudo-potential, which action could be counted "is destroyed" in part or completely application LDFT further it is modeled by fit procedure. These contributions are designed from the electronic density received in LDFT-calculation. On each step of iterative procedure the density changes in view of correction factor which depends on volume of an elementary cell. That part which in [5] is received from nuclear calculations is modeled and kept r_{loc} as the second fitting parameter.

For research of polymorphism the self-coordinated calculation in 80 points for each connection in an interval 0,4 Ω_0 - 1,2 Ω_0 with a step 0,01 Ω_0 where Ω_0 is the experimental volume of an elementary cell in structure B1 was carried.

Results of calculation were adjusted under the equation using Berch's condition

$$P = \frac{3}{2}B_0\left[\left(\frac{\Omega_0}{\Omega}\right)^{7/3} - \left(\frac{\Omega_0}{\Omega}\right)^{5/3}\right],$$ (8)

where P is pressure, B_0 is the volumetric module of compression at P=0, Ω is the volume of an elementary cell, Ω_0 is the volume of an elementary cell at P=0.

In structure B1 the calculation of Ω_0 and B_0 are adjusted under the corresponding experimental information, in structure B2 parameters determined full energy E_{tot} and B_0.

Table 1 represents equilibrium volumes of elementary cells Ω_0, volumetric modules of compression B_0, deviations $\Delta\Omega_0$ and ΔB_0 from the corresponding experimental values, arising basically because of the limited word length of the parameters, full of energy E_{tot} and volumes of elementary cells at phase transition B1-B2 for structure B1. Table 2 contains the same data for structure B2. Results of calculation of polymorphism are resulted in Table 3. Deviations only with known experimental data (see [6,7] where are resulted as well results of calculations of other authors) are specified.

Designations of volumetric characteristics: $\Omega_{0\,B1}$, $\Omega_{0\,B2}$ - equilibrium volumes of elementary cells in structures B1 and B2; $\Omega_{pt\,1}$, $\Omega_{pt\,2}$ - volumes at pressure of phase transition in corresponding structures are geven

$$\Delta\Omega = \Omega_{0\,B1} - \Omega_{0B2};$$
$$\Delta\Omega_{B1} = \Omega_{0\,B1} - \Omega_{pt\,1};$$ (9)
$$\Delta\Omega_{B2} = \Omega_{0\,B2} - \Omega_{pt\,2}.$$

References

1. *Kovalchuk V. V.* Cluster modidfication of the semiconductor's heterostructur Kiev: Hi-Tech Press.- 2007.-1 309 p.

2. *P. Blaudeck, Th. Freuenheim, D. Porezag, G. Seifert, E. Fromm,* Calculation of molecules, clusters and solids with DFT-LDA scheme // J. Phys. Condens. Matter 4, p. 6368-6371 (1992).

3. Encyclopedia of Computational Chemistry, Eds. P. Schleyer, H. Schaefer, N. Handy. Wiley, New York, 1998, p. 10-455.

4. *M.W. Schmidt, K.K. Baldrige, J.A. Boatz* et al., General atomic and molecular electronic structure system // J. Comp. Chem. 14, p. 1347-1363 (1993)

5. *E.F. Vansant, P. Van der Voort, K.C. Vrancken,* Characterisation and Chemical Modification of Silica Durfaces. Elsevier, Amsterdam, 1995.

6. *J.R. Chelikowsky, J.C. Phillips,* Chemical reactivity and covalent-metallic bonding of Si_n^+ (n=11-25) clusters // Phys. Rev. Lett. 63, p. 1655-1656 (1989).

7. *J.M. Garcia-Ruiz, E. Louis, P. Meakin, L.M. Sander,* Growth patterns in physical sciences and biology / In: NATO ASI Series B: Physics 304, Plenum, New York, 1993.

Table 1.

Results of calculation in structure B1.

Connection	Ω_0, (a.u.)^3	$\Delta\Omega_0/\Omega_0$, %	B_0, GPa	$\Delta B_0/B_0$, %	E_{tot}, Ry	Ω_{pt}, (a.u.)^3
CaO	98,12	+4,3	113,01	0,0	-17,071	72,44
SrO	115,59	-0,3	90,29	-0,8	-16,996	90,02
CaS	155,91	+0,1	63,78	-0,3	-10,830	113,30
SrS	183,92	-0,1	57,90	-0,2	-10,537	149,93
BaS	219,28	-0,2	52,65	+1,3	-11,056	197,13
CaSe	175,21	-0,1	53,70	+5,3	-9,870	126,65
SrSe	205,25	-0,1	44,62	-0,8	-9,685	167,86
BaSe	242,81	+0,1	39,18	+0,5	-9,357	215,83
SrTe	249,34	+0,1	40,77	+1,9	-8,638	206,17
BaTe	289,42	-0,1	38,03	+0,1	-8,430	263,15

Table 2.

Results of calculation in structure B2.

Connection	E_{tot}, Ry	B_0, GPa	Ω_0, (a.u.)^3	Ω_{pt}, (a.u.)^3
CaO	-17,029	138,74	84,62	64,85
SrO	-16,972	120,32	101,65	84,59
CaS	-10,790	59,68	138,66	99,70
SrS	-10,517	65,65	158,64	131,89
BaS	-11,045	44,74	195,12	173,44
CaSe	-9,832	46,71	158,09	111,32
SrSe	-9,671	59,94	183,39	155,88
BaSe	-9,349	37,85	220,56	194,96
SrTe	-8,631	49,27	235,61	200,27
BaTe	-8,424	46,14	265,09	243,79

Table 3.

Pressure of phase transitions B1-B2 and changes of volumes at phase transitions (in %)

Connection	p_{tr}, GPa	$\Delta p_{tr}/p_{tr}$, %	$\Omega_{pt1}/\Omega_{0\,B1}$	$\Omega_{pt2}/\Omega_{0\,B1}$	$\Delta\Omega/\Omega_{pt1}$	$\Delta\Omega/\Omega_{0\,B1}$	$\Delta\Omega_{B1}/\Omega_{0\,B1}$	$\Delta\Omega_{B2}/\Omega_{0\,B2}$
CaO	63,65	+1,0	73,8 (-0,8%)	66,1 (-1,6%)	10,5	7,7	26,2	23,4
SrO	37,38	+3,8	77,9 (-4,4%)	71,5 (+0,1%)	8,3	6,4	22,1	18,8
CaS	38,34	+3,6	73,7	64,0	12,0	8,7	27,3	28,1
SrS	17,82	-1,0	81,5	71,7	12,0	9,8	18,5	16,9
BaS	6,73	+3,5	89,9 (+0,3%)	79,1 (+2,3%)	12,0 (-12%)	10,8	10,1	11,1
CaSe	33,45	-1,6	72,3	63,5	12,0	8,6	27,8	29,6
SrSe	13,21	-5,6	81,8	76,0	7,1	5,8	18,2	15,0
BaSe	5,83	-2,8	88,9	80,3 (-8,5%)	9,7 (-30%)	8,6	11,1	11,6
SrTe	11,20	-6,7	82,7	80,3	3,9	2,4	17,3	15,0
BaTe	4,51	-6,0	90,9	84,2 (-7,2%)	7,4 (-44%)	6,7	9,1	8,0

UDC 621:004.89:005.8

I.A. Osaulenko, candidate of technical science
(Cherkassy State University B. Khmelnitsky Named, Ukraine)
V.M. Ilchenko, candidate of technical science (National Aviation University, Ukraine)

DECISION SUPPORT SYSTEMS USING IN PRODUCT LIFECYCLE AND PROJECT MANAGEMENT

Annotation. In this paper the different aspects of the decision making in design described. The questions of the decision support systems creating and using for the project management considered. The structured diagram of the project's initialization presented. The features of the consensus making analyzed. The conception of the consensus support system proposed.

The large scale projects realization in aviation industry, machine-building and many other sectors requires the participation of many actors, using different sources and much time. One of the important problems is the assuring of the interaction of the customer with executer. Another questions connected with optimal manufacturing allocation, coordination procedure elaboration, approving the works schedule and distribution of the responsibility.

Now many significant results of the studies on preproduction advanced. The different stages of this process are more or less formalized. So, CAD/CAE-systems using in design of the high technological production already became a standard. The CALS-technologies development caused the implantation of unified specification, data exchange formats and business-process description.

The aviation industry is one of the leaders in the manufacturing application and improving of this approach. For example, we can consider the conception of the system's design and refinement of the aviation engines. It consists of systems analysis and model's building, decision's searching area definition, algorithms of generalized project procedure execution's formation, project tree building, structures elements and they model's libraries formation, development and using, parallel works planning, technology of experience accumulation and application etc. Obviously, two groups of the tasks may be accentuated in this case. One of them connected with modeling of the physical processes and construction of the engine. Another supposes the Decision Support System's (DSS) creation for the choice of the embodiment of the engine and point-to-point synthesis of the models with continuous addition and improving.

In spite of many business partners existing, one of the features of aviation industry is sufficiently stable staff of the projects members. It gives the possibility of the direct description of the works consecution with Structured Analysis and Design Technique (SADT) using. This methodology allow to determine the accurate connection between the entrances and exits of every process, control influences and necessary sources. As a sources can consider employees, equipment, information, including data from DSS-system. The SADT-models allow to obtain the required level of decomposition. Advanced models mean for using not only on the stage of designing and manufacturing, but during exploitation, repairing and modernization.

In general, the specificity of the applying technology, equipment and software do the entry of new enterprises into the sector of the aircraft assemblies manufacturing very difficult. For many other branches, including machine-building, instrument-making, IT-industry, robotics, this restrictions are less rigid. As a result, the enterprises and firms have more opportunities for initialization of the common projects. But at the same time, the uncertainty in planning and works increases in connection with many different variants appearing.

In this case not only technical and technological factors determinate the success of the projects. The organization and information preproduction becomes more important. The innovation structures, such as technological parks and business-incubators, contribute to application of the new ideas. Also, the role of the structures, which specialized on engineer consulting, grows. Obviously, the creation of the regional technological nets is very available too.

For the better interaction of the companies the regional project office may be created. Of course, every subject makes a decision about the participation in each project singly. But in the case

course, every subject makes a decision about the participation in each project singly. But in the case of high uncertainty the aid of the special-purpose computer system may be perfectly advisable. Thereby, the task of the decision supporting is sufficiently actual, we can not guarantee the good results without its solving.

On of the most perspective approach connected with creation distributed DSS for the project decision in design and manufacturing of the high technological production. So, the important problem of the firm, which acted in high-tech sphere, is quickly increasing of information content, that circulated both inside of the company and interplant. At the same time, we need to take into account the dynamics of the data domain and necessity of the parts consensus achieving.

Nonrational decision making may be caused by the untimely entrance of information, using of the reductive approach for the problems, imperfect information processing or neglecting by the opinion of the different level's specialists. Also, the reason of hardship may be connect with insufficient attention for the group decision making procedures.

For the DSS, oriented on innovation projects, very actual the tasks of the achievable technical level, pay-off investment period and degree of risk. The possibility of the better coordination and standard project operation using is important too.
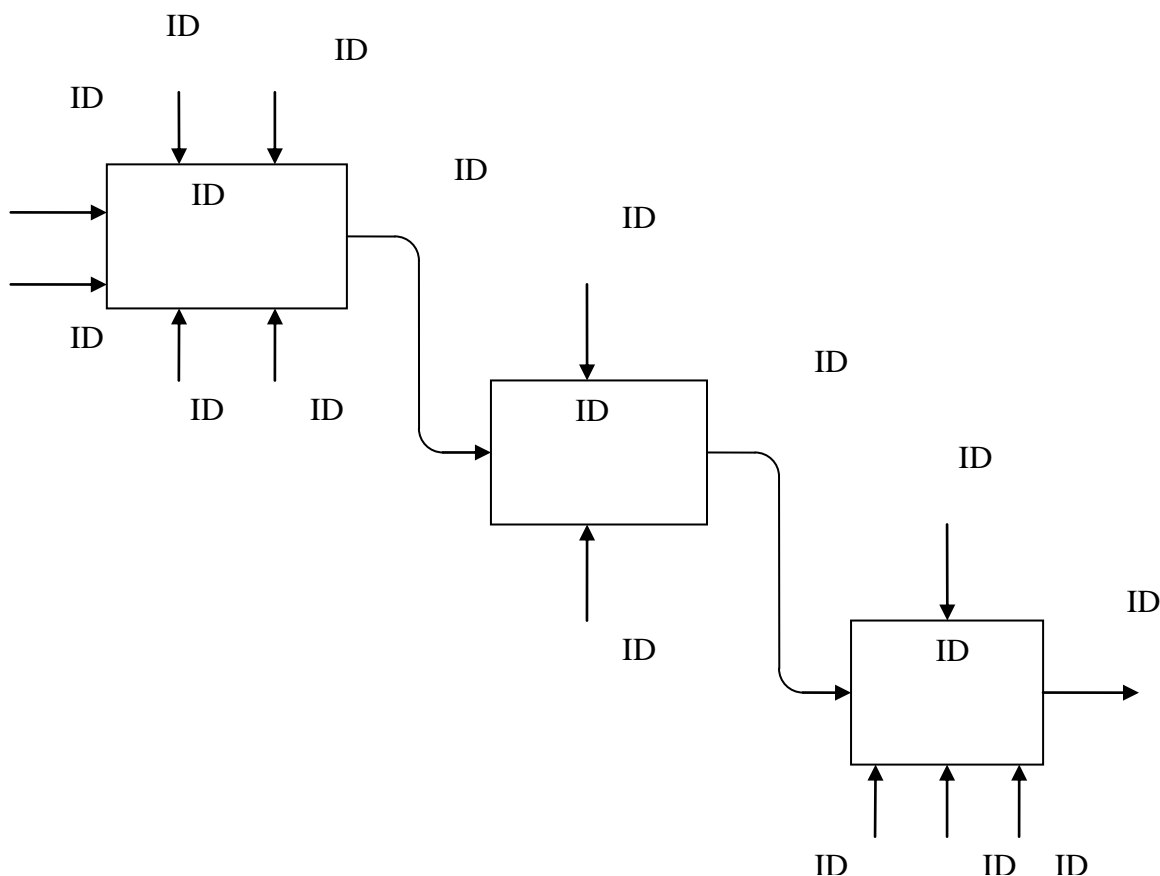
Fig. 1. Structured diagram of the process common project's initialization

An example of the process, connected with innovation production's creation, shown in Fig 1. As we can see, the DSS is used at the different stages. At first, it will be help to receive correct estimate of the current state. The next step supposes the determination of the priority and the perspective projects describing. Later the participants of the future projects are clarify themselves and they responsibilities are become known.

In this context we ought to draw attention on the organization of interaction dialogue. The first task consist in the organization of data exchange of one distant user with another. The second problem lied in the program realization of the explanation by system its conclusions. The demand of the explanation is very important, because it substantially ensure the making consensus.

The problems of the agreement includes different aspects. On of them connected with special

formalizing of the negotiations and they results. The main idea of the next aspect is the ensuring of the confidence in the business relations. Also important questions connected with the profit, which will receive every participant of the project. Moreover, the DSS ought to include the integrated database, in which the experience of the previous projects formalized.

For solving of the problem of the consensus making, we need to better understand the reasons, which have an influence on the participant's position, when he is concordant with another participant or with some viewpoint. As the theory of unforced interaction asserts, his opinion depends on the internal condition, external information and history of the relation with another participants. History in this context serves as statistic characteristic, that shows parameters of interaction in the past. For example, if one of the participants in most cases was concordant with another, that probability of the making consensus again is sufficiently high.

So, the DSS, in additions to data domain of the project, ought to take into account many others questions, which define the interaction of the project participants. The special module consisting of DSS for the solving of the considered tasks may be created. This module may be named Consensus Support System (CSS) and will include the procedures of the participant's reaction prediction in the different cases, forming of the optimal project command in compliance with adjusted criteria, defining the responsible for the negotiations. Also the CSS will contain the database of the typical situation and the base of knowledge. The base of knowledge will include the rules of reaction of every participant on the typical situation and other's opinion. Obviously, both bases constantly ought to increase. Moreover, all known algorithms of the group decision making need to realize in the system.

For the large scale projects, which consist of many stages and need of a long time, the necessity of the agreement's searching may emerge not only before the start of the project. If the intermediate results deviate from the plan, the correction action also need in consensus. Besides, the projects of creating some constructions, for example, at the time of the force-majeure, may not foresee the all speciality of the following exploitation of this object after the putting into operation. So, the CSS ought to support the decision on the different stages of the object's lifecycle.

The CSS is distributed system. It means, that the system ought to have the discretionary access control. Obviously, the central project office will have the full access. The access rights of another users are essential to confine. All this rightly for the DSS as a whole.

The creating DSS ought to use client-server architecture, to have the open interface with CAD/CAM, PDM/PLM, ERP/CSRP-systems, to work in real-time operation mode, to use Web-technologies, to work with remote work places, to have high data security and human-engineered interface. The system will use existing network, but may be necessary to set some parameters.

The effectiveness of the purposed DSS may be estimated by different parameters. The qualitative methods connected with the searching of the dependence on the management quality and project results. The quantitative methods allow to define such parameters as the response duration, channel capacity, quantity of users, memory size etc. Obviously, the organizational aspect of the system's using is very important, but the reliability of the hardware and software is significant too. Hence, all this factors ought to consider in complex.

Conclusions

On base of the executed analysis the most imported aspects of the decision making in the sphere of product lifecycle and project management defined. The features of the problems in the different sectors, which solving need to use decision support system, described. Obviously, the projects of the design and manufacturing high-tech production in the distributed system require the perfection of the existing approaches. One way of this goal achievement is the better interaction of the project participants. This is especially actual for the large scale projects. For the supporting of the project decision the theory of the unforced interaction purposed to use. On basis of this theory conception of the consensus support system suggested. The demands for the advanced system determined. Evidently, the following researches will be connected with formalization of the presented conception and creation of the appropriate models.

K.Y. Ohrimenko, c.t.s., honorable professor of ChDTU, A.V. Manziura
(Cherkassy State Technological University, Ukraine)
K. Eichhorn (K.K. Ohrimenko), c.t.s., docent.
(German Society of International Cooperation, Germany)
D.P. Ornadsky, c.t.s., docent.
(National Aviation University, Ukraine)

THE ERROR ACCURACY OF THE OUTPUT LINK OF ASSOCIATED MOVEMENTS OF THE KINEMATIC CHAIN

The accuracy probabilistic assessment method of a kinematic chain for screw displacement formation of a differential spacing terminal link at simulation modeling taking into account the equipartition law of random numbers is considered.

The helical surfaces of differential spacing find a wide application in various transporters, extruders and other mechanisms where either positioning accuracy achievement or high-speed conditional change of a terminal segment on the example of industrial robots manipulators is required. The solution of a research problem of kinematic accuracy of kinematic chains of differential spacing helical motion in this article is considered on the example of the general purpose lathe. For helical surface cutting of a differential spacing one of possible pitch control mechanisms is in addition entered into the construction of the machine axis drive.

The mathematical model of shaping at the helical surface generation of differential spacing in matrix form looks like:

$$\overline{r_0} = \prod_{\ell=1}^{n} A_{o\ell} \cdot \overline{r_\ell} = \begin{vmatrix} \cos\theta & -\sin\theta & 0 & 0 \\ \sin\theta & \cos\theta & 0 & 0 \\ 0 & 0 & 1 & 0 \\ 0 & 0 & 0 & 1 \end{vmatrix} \times \begin{vmatrix} 1 & 0 & 0 & 0 \\ 0 & 1 & 0 & 0 \\ 0 & 0 & 1 & z \\ 0 & 0 & 0 & 1 \end{vmatrix} \times \begin{vmatrix} 1 & 0 & 0 & x \\ 0 & 1 & 0 & 0 \\ 0 & 0 & 1 & 0 \\ 0 & 0 & 0 & 1 \end{vmatrix} \cdot \overline{r_\ell}, \quad (1)$$

where $\overline{r_0}, \overline{r_\ell}$ – respectively the equations of an ideal treated surface and the tool in a vector form, $\prod_{\ell=1}^{n} A_{o\ell}$ – product of shaping motion array of moving coordinates connected to elements of a kinematic chain; $x, z -$ coordinate of in-out and longitudinal machine axis, $z = A_n x^n + A_{n-1}x^{n-1} + ... + A_2 x^2 + A_1 x + A_0$ – a polynomial n-ht degree, defining the function type of curve scan of the differential spacing helical line.

Using Lagrangian interpolation polynomial at a tabular coordinate assignment

$$L_n(x) = \sum_{i=0}^{n} y_i \frac{(x-x_1)(x-x_2)...(x-x_{i-1})(x-x_{i+1})...(x-x_n)}{(x_i-x_0)(x_i-x_1)...(x_i-x_{i-1})(x_i-x_{i+1})...(x_i-x_n)}, \quad (2)$$

we come to the system of algebraic equations defining a polynomial ratio for the functional dependence of curve scan of any kind set by coordinates numerical values. The curve scan of the helical line of differential spacing can be created by sections fitting of straight lines and curves in junction points from a condition of set laws of movement taking into account values of speed and acceleration. Structurally-kinematic and kinematic schemes of the general purpose lathe with the pitch control mechanism to the offered configuration are considered in fig. 1.

According to the kinematic scheme of the machine fig. 1a, the equation of kinematic balance of an axis drive elements taking into account the additional pitch control mechanism looks like:

$$1об.шп. \cdot \frac{60}{60}\frac{30}{45}\frac{40}{86} \cdot \frac{86}{64}\frac{28}{28}\frac{28}{35}\frac{35}{35}\frac{20}{30}\frac{30}{35} \cdot 12\frac{22}{30} \cdot 12\frac{36}{12}\frac{32}{15}\frac{36}{16} \cdot u_{\text{д}} \cdot \frac{28}{28}\frac{18}{40}\frac{15}{48} \cdot 12 = p_{\text{н.в.}}$$

Fig. 1 - a) Kinematic scheme of the general purpose lathe; b) Block kinematic diagram of the general purpose lathe

The kinematic chain contains 33 links from which $z_1,...,z_4$ - links of spindle group, $z_5,...,z_{11}$ - group of replacement wheels; $z_{12},...,z_{28}$ - group of links of differential spacing cutting; $z_{29},...,z_{33}$ - separatory group. For determining of influence of each link in error formation of a cut pitch on the basis of the transfer relations of the kinematic balance equation the numbers of turns of each chain elements for one turn of the motion screw are defined.

For the accuracy assessment of positioning of kinematic chain terminal links of industrial robots manipulators similarly to the shaping accuracy of helical surface from an error effect of each element of kinematic chain of an axis drive the method of statistical tests is used. As opposed to the research of A.V. Levashov and A.S. Pluzhnikov [1,2] in this research [3,4] on the basis of the equipartition law of probability density of random quantities the statistical method of simulation modeling is applied. The vector nature of operating errors of kinematic chain elements, taking into account the direction, is estimated by quadratic means. The developed determination technique of the greatest accumulated error of a helical surface cutting pitch considers its importance for each of discrete intervals within one turn of the motion screw and all links of the additional kinematic chain. It allows to determine the influence of each element of a kinematic chain in limits as of one turn of the motion screw, and at repeated passes from a condition of a statistical sample of a kinematic chain on output accuracy. Setting discrete values of turn of the motion screw on $9°$ and repeating this procedure during a turn, we will receive a statistical sample of a set of discrete values of the pitch cumulative error of a kinematic chain. The received sample allows to get probabilistic value of a differential spacing of a cut helical surface. The pitch total cumulated error of a cut s helical surface at turn of the motion screw on each $9°$ is calculated with the accounting of all links on a formula, micron:

$$\Delta p_{\Sigma} = \sum_{i=1}^{33} \left(\Delta p_{\Sigma 1} + \Delta p_{\Sigma 2} + ... + \Delta p_{\Sigma 33} \right), \qquad (3)$$

where the cumulative error of each i-th of a link changes according to the harmonic law:

$$\Delta p_{\Sigma} = \sum_{i=1}^{33} \left[A_i \sin\left(k_i \varphi_j + \psi_i \right) \right] + \delta T_{\Sigma i}. \qquad (4)$$

In this formula $i-$ the number of a kinematic chain link; A_i – the amplitude value of kinematic accuracy standard of i-th of a link depending on a rotation angle of the motion screw; φ_i – rotation angles of the motion screw; ψ_i – phases shift of errors i-th link; k_i – the number of turns of a gear i-th link at turn of the motion screw on the selected angle; $\delta T_{\Sigma i}$ – a permissible variation of the helical line of the motion screw for a rotation angle φ_i.

Within carried-out research the angle of phase shift ψ_i is a random variable which accepts different values for each i-th turn of the motion screw. Shift of phases is defined as $\psi_i = 360° \cdot C$ and changes in limits $0 \div 360°$, where C – the numbers of equipartition in the interval $0 \div 1$ which are programmatically oscillated by the generator in the form of pseudo-random numbers.

From a condition of cutting modes calculation the spindle rotation frequency is accepted 1500min^{-1}. The fragment of calculation dependence compiling technique for determining of the total cumulative error of a pitch of a cut thread at turn of the screw on $9°$ within the first turn out of forty intervals of the motion screw turn, we will present in the form:

$$\Delta p_{\Sigma 9°} = 0{,}625 \sin\left(0{,}6 \cdot 9° + 360 \cdot 0{,}9355\right) + 0{,}625 \sin\left(0{,}6 \cdot 9° + 360 \cdot 0{,}3973\right) +$$
$$+ 0{,}625 \sin\left(0{,}6 \cdot 9° + 360 \cdot 0{,}23955\right) + 0{,}625 \sin\left(0{,}4 \cdot 9° + 360 \cdot 0{,}2133\right) +$$
$$+ 0{,}625 \sin\left(0{,}4 \cdot 9° + 360 \cdot 0{,}9035\right) + 0{,}625 \sin\left(0{,}25 \cdot 9° + 360 \cdot 0{,}4693\right) +$$
$$+ 0{,}625 \sin\left(0{,}25 \cdot 9° + 360 \cdot 0{,}3275\right) + 0{,}625 \sin\left(0{,}25 \cdot 9° + 360 \cdot 0{,}7653\right) +$$
$$+ 0{,}625 \sin\left(0{,}25 \cdot 9° + 360 \cdot 0{,}9115\right) + 0{,}625 \sin\left(0{,}2 \cdot 9° + 360 \cdot 0{,}7013\right) +$$
$$+ 0{,}625 \sin\left(0{,}2 \cdot 9° + 360 \cdot 0{,}555\right) + 0{,}625 \sin\left(0{,}2 \cdot 9° + 360 \cdot 0{,}0877\right) +$$
$$+ 0{,}625 \sin\left(0{,}15 \cdot 9° + 360 \cdot 0{,}0159\right) + 0{,}625 \sin\left(0{,}15 \cdot 9° + 360 \cdot 0{,}8933\right) +$$
$$+ 0{,}625 \sin\left(0{,}15 \cdot 9° + 360 \cdot 0{,}6235\right) + 0{,}625 \sin\left(0{,}1 \cdot 9° + 360 \cdot 0{,}3493\right) +$$
$$+ 0{,}625 \sin\left(0{,}1 \cdot 9° + 360 \cdot 0{,}8475\right) + 0{,}625 \sin\left(0{,}95 \cdot 9° + 360 \cdot 0{,}8453\right) +$$
$$+ 0{,}625 \sin\left(0{,}95 \cdot 9° + 360 \cdot 0{,}2315\right) + 0{,}625 \sin\left(0{,}08 \cdot 9° + 360 \cdot 0{,}9813\right) +$$
$$+ 0{,}625 \sin\left(0{,}08 \cdot 9° + 360 \cdot 0{,}1755\right) + 0{,}625 \sin\left(0{,}05 \cdot 9° + 360 \cdot 0{,}3573\right) +$$
$$+ 0{,}625 \sin\left(0{,}05 \cdot 9° + 360 \cdot 0{,}795\right) + 0{,}625 \sin\left(0{,}03 \cdot 9° + 360 \cdot 0{,}5733\right) +$$
$$+ 0{,}625 \sin\left(0{,}03 \cdot 9° + 360 \cdot 0{,}3435\right) + 0{,}625 \sin\left(0{,}03 \cdot 9° + 360 \cdot 0{,}2293\right) +$$
$$+ 0{,}625 \sin\left(0{,}03 \cdot 9° + 360 \cdot 0{,}3675\right) + 0{,}625 \sin\left(0{,}02 \cdot 9° + 360 \cdot 0{,}9253\right) +$$
$$+ 0{,}625 \sin\left(0{,}02 \cdot 9° + 360 \cdot 0{,}5515\right) + 0{,}625 \sin\left(0{,}014 \cdot 9° + 360 \cdot 0{,}2613\right) +$$
$$+ 0{,}625 \sin\left(0{,}014 \cdot 9° + 360 \cdot 0{,}2955\right) + 0{,}625 \sin\left(0{,}009 \cdot 9° + 360 \cdot 0{,}8373\right) +$$
$$+ 0{,}625 \sin\left(0{,}009 \cdot 9° + 360 \cdot 0{,}9995\right) + 0{,}9 = 1{,}8598, \ micron$$

Where $A_i = 25/40 = 0{,}625$ micron (25 microns – standard of kinematic accuracy of a gear for diameter of a separatory circle $d = 125$ mm; 40 – the number of intervals within a screw turn through $9°$); 0,6, 0,4,…, 0,08,…,0,009 – numbers of turns of each link of a kinematic chain for turn of the motion screw on $9°$; 0,9 microns – the pitch cumulative error limit of the motion screw at turn on $9°$ according to the standards of accuracy.

The reliability of the total cumulative error assessment is reached at the expense of increase in a statistical sample of calculation of 5 hundred passes of a helical surface cutting for dependence.

$$\Delta p_{\Sigma r} = \sum_{i=1}^{500} \Delta p_i . \tag{5}$$

The carried-out calculations allow to draw the histogram of value distribution range of the accumulated error where all dispersion values range $\Delta p_{\Sigma max}$ is divided into sixteen categories

$\left(a_{i-1}, a_i\right)$ with the length of Δa and the number of hits m in i-th category is counted up. The total accumulated error of a pitch for 500 passes, allows to define a mathematical expectation of the greatest accumulated error $\Delta p_{\Sigma 500} = \Delta p_1 + \Delta p_2 + \Delta p_3 + ... + \Delta p_{500}$, micron:

$$M\left|\Delta p_{\Sigma \max}\right| = \sum_{1}^{500}\left(\Delta p_{\Sigma}\right)_r \Big/ 500 \text{, micron.}$$

Some values of specific influence of separate links on the cumulative error of the kinematic chain, calculated according to the formula f. (7) are presented in the table.

$$E_i = \frac{M\left|\Delta p_{\Sigma \max}\right| - M\left|\Delta p_{\Sigma \max}\right|_i}{M\left|\Delta p_{\Sigma \max}\right|} \cdot 100\% . \qquad (7)$$

Процент влияния	E_1	E_2	E_3	E_4	E_5	E_6	E_7	E_8	E_9
%	2,94	2,93	2,76	2,91	2,92	2,94	2,96	2,94	2,93
Influence percent	E_{10}	E_{11}	E_{12}	E_{13}	E_{14}	E_{15}	E_{16}	E_{17}	E_{18}
%	2,9	2,93	2,92	2,95	2,68	2,9	2,92	2,94	0,001
Influence percent	E_{19}	E_{20}	E_{21}	E_{22}	E_{23}	E_{24}	E_{25}	E_{26}	E_{27}
%	3,02	2,86	2,89	2,87	2,94	2,92	2,92	2,96	2,88

According to four groups of links of a kinematic chain, their influence made for: spindle – 11,77 %; groups of replacement wheels – 20,54 %; groups of the wheels providing differential spacing cutting – 49,76 % and separatory group – 14,73 %.

Conclusions

The developed technique allows to calculate the cumulative error of a cut helical surface of a differential spacing and by analogy of positioning accuracy of a terminal function element of the industrial robot manipulator depending on a kinematic error of wheel gear and the pitch control mechanism.

The technique of simulation modeling is considered on the example of cumulative error determining of one and repeated turns of the motion screw. The specific influence on helical surface forming accuracy of each separate link of a thread-cutting kinematic chain is found.

With use of computer means the offered technique can be used at design of kinematic chains of drives and will allow to standardize the helical surface cutting accuracy of a differential spacing or the point-to-point accuracy of terminal links of industrial robots manipulators.

References

1. *Плужников А.С.* Расчёт точности зубо-резьбообрабатывающих станков. ЦБТИ, М.:1968, 75 с.

2. *Левашов А.В.* Основы расчёта точности кинематических цепей металлорежущих станков. М.: Изд. Машиностроение,1966, 212с.

3. *Охрименко К.Я., Манзюра А.В., К. Eichhorn (К.К. Охрименко).* Исследование оценки точности кинематической цепи станка при нарезании винтовых поверхностей постоянного шага. К.: Вістник інженерної академії України №2, 2011, С.245-250.

4. *Ohrimenko K.Y., Eichhorn K.K., Manziura O.V.* Simulation modelling of accumulated error of discrete drive kinematic chain. The fourth world congress "Aviation in the XXI-st century" – 2010, С.15.1-15.4.

UDC 004.056.5(045)

B.E. Zhurilenko, scientist doctor,N.S. Pelikh, graduate student
(National Aviation University, Ukraine)

CALCULATION AND RELIABILITY OF TECHNICAL INFORMATION SECURITY

A model of calculation the reliability of complex of technical information security (CTIS) depending on the number of hacking attempts is created. Justified the necessity of using multileveled CTIS. A model of calculation the degradation of CTIS for the period of time since the development to the commissioning is created.

With the proliferation of information technology, organizations are becoming increasingly dependent on information systems, and, consequently, more vulnerable to security threats. The network architecture of the distributed computing environment, came where the security depends on all items, as well as for its breach was sufficient to gain access to one of them.

The urgency of the problems of information technologies is the avowed that is confirmed by the large number of court cases regarding misconduct of information with restricted access. The companies often have multi-million dollar losses as a result of insufficient protection of sensitive information. However, the analysis of statistical data on violations said about problems in this area, which in most cases are caused by flawed design and insufficient reliability of information security systems.

Today, the need for information security is not in doubt. Any system of information security (SIS) must include adequate countermeasures of external and internal threats. Without a doubt, it to be a SIS complex, but at the same time, should involve the emergence of threats specific to an information system. At the stage of designing a CTIS that combines in one or more SIS, you need to identify and consider:

– size of the best financial investments;
– substantiation of the use of multilevel SIS;
– the degree of degradation and the prospect of CTIS in time.

For the company which designs CTIS, the prime interest has the sum of the financial investment in this system and the size of the theoretically possible losses with the full protection of the lack of available information. In addition of particular interest are the financial costs and the size of the general damages in case of hacking SIS [1].

Figure 1 includes calculation of reliability of CTIS [2] depending on the attempts of hacking, provided that the investment in the SIS are equal the value of the information that is provided by a large defensive team or the effectiveness of SIS on the unit. The reliability of the CTIS view as defined by the number of attempts of hacking, with each next does not depend on the results of the previous ones. Determine the reliability of CTIS on m hacking attempt by the formula:

$$P(x) = (p_{xall})^{m-1} \cdot p_x = (\frac{x}{H+x})^{m-1} \cdot \frac{H}{H+x} \tag{1}$$

where, p_{xall} is the value of reliability of CTIS;
m is a successful attempt to break into CTIS;
H is the financial loss in the absence of CTIS;
x is the investments to SIS at the level of reliability of p_x;
p_x is a level of reliability at the level of investment.

Figure 1 presents the results of calculation of reliability of CTIS $P(x)$ by the formula (1). In calculation curves $P_m(X)$ and $P(m)$ fully match.
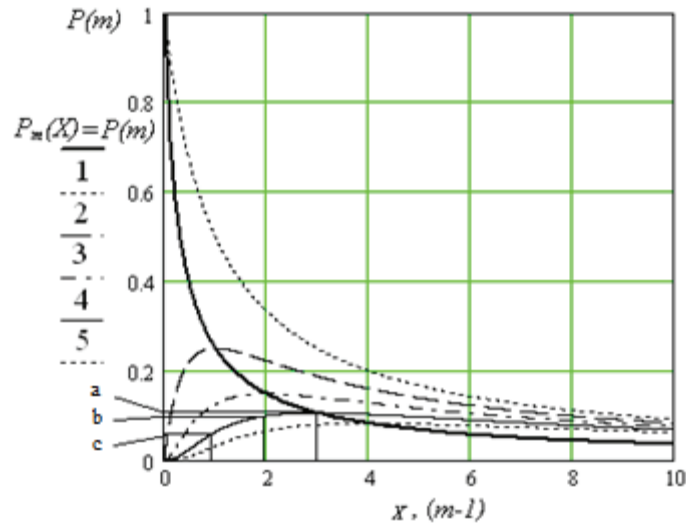
Figure 1 – the calculation of reliability of CTIS *P(m)* depending on the *m* hacking attempts: 1 when *m* = *1*; 2 when *m* = *2*; 3 when *m* = *3*; 4 – when *m* = *4*; 5 when *m* = *5*; *X* = *x/H* – the value of financial loss; *P_m(X)* is the curve, which determines the maximum value of reliability depending on the size of investments in SIS; *a, b, c* – the probability of *4, 3, 2* hacking attempts with the amount of investments in SIS which was calculated for 4 attempts at hacking.

Since the curve (fig. 1) is with the cost to breaking with the fourth attempt, the maximum probability of hacking have to spend *x* = *3H*. It is obvious that with this level of investment, the probability of hacking on the first attempt is minimal in comparison with the second (point b, fig. 1) and third (point b, fig. 1) attempts, for which the probability of hacking will increase. Opposite, if you invest in CTIS, it will be more optimally the required cost for hacking with the fourth (point a, fig. 1) attempt, the probability of hacking will diminish, according to the curve, which is the maximum *(x* = *4H)* in the direction of increasing *x*. In this case, the probability of hacking protection on the fourth attempt will diminish depending on the investment.
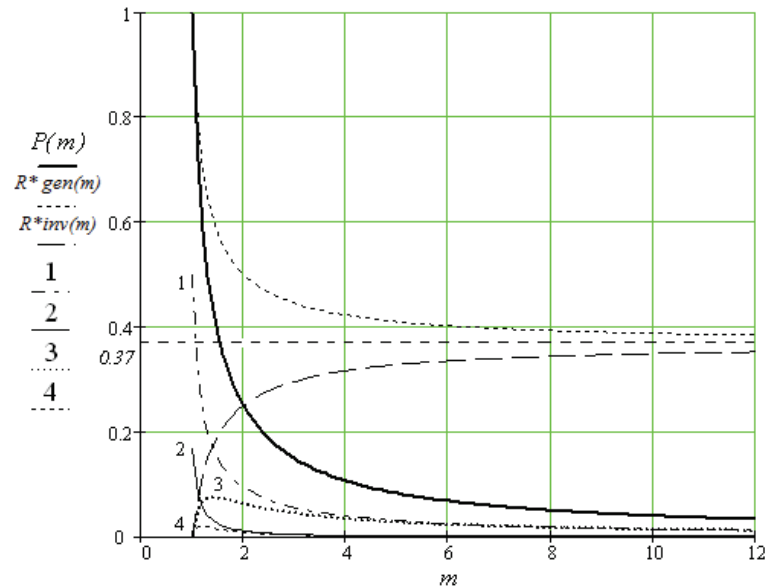
Figure 2 – the calculation of reliability of CTIS when using the multilevel SIS; *P (m)* is the curve, which determines the maximum value of CTIS depending on the attempts of hacking *m ≥ 1*; *R* gen (m)* is the quantity of the risk of losses in the full SIS hacking; *R* inv (m)* is the quantity of the risk of loss of investments in SIS;
1 – Quantity of the risk of losses when hacking two-leveled SIS *R* gen (m1,m2)*;
2 – Quantity of the risk of losses when hacking three-leveled SIS *R* gen (m1,m2, m3)*;
3 – Quantity of risks loss of investments in two-leveled SIS *R* inv (m1,m2)*;
4 – Quantity of risks loss of investments in three-leveled SIS *R* inv (m1,m2, m3)*.

1.6.30

In Figure 2 there are the results of calculations which prove that the use of one-leveled CTIS is totally ineffective, because even with endless investment in upgrading of CTIS it can't guarantee the sufficient level of reliability. Minimum number of SIS that can be used to achieve the required level of reliability must be at least two. The use of multilevel protection allows you to increase the reliability of the CTIS with the same investment.

In table 1 there are the numerical values of CTIS that show the reliability of it hacking and general damages or loss investment only. The calculations are carried out for $m1 = m2 = m3 = 2$, i.e. hacking at each level from the second attempt. A justification for this assumption is related to the fact that the maximum probability of loss of investment arises from the first to the second hacking attempts. So we can assume that for multilevel CTIS the calculation of hacking into the second attempt for each level is sufficient. Unlike the case of one-leveled CTIS, the probability of losing the investment for the nested SIS hacking at the endless attempts is reduced to zero. It should be noted that the increase in the size of the investment in SIS reduces not only the probability of complete loss, but also the most investment.

Table 1 – the numerical values of CTIS that show the reliability of it hacking and general damages or loss investment only.

The amount of security levels	The probability of losses	$m_1 = m_2 = m_3$									
		1	2	3	4	5	6	7	8	9	10
2	$R^*_{gen}(m_1,m_2)$	0,5	$9,4 \cdot 10^{-2}$	$5,5 \cdot 10^{-2}$	$3,9 \cdot 10^{-2}$	$3,0 \cdot 10^{-2}$	$2,5 \cdot 10^{-2}$	$2,1 \cdot 10^{-2}$	$1,8 \cdot 10^{-2}$	$1,6 \cdot 10^{-2}$	$1,4 \cdot 10^{-2}$
	$R^*_{inv}(m_1,m_2)$	0	$6.3 \cdot 10^{-2}$	$4,4 \cdot 10^{-2}$	$3,3 \cdot 10^{-2}$	$2.7 \cdot 10^{-2}$	$2,2 \cdot 10^{-2}$	$1,9 \cdot 10^{-2}$	$1,7 \cdot 10^{-2}$	$1,5 \cdot 10^{-2}$	$1,3 \cdot 10^{-2}$
3	$R^*_{gen}(m_1,m_2,m_3)$	$1,7 \cdot 10^{-1}$	$1,0 \cdot 10^{-2}$	$3,8 \cdot 10^{-3}$	$2,0 \cdot 10^{-3}$	$1,2 \cdot 10^{-3}$	$8,0 \cdot 10^{-4}$	$5,8 \cdot 10^{-4}$	$4,3 \cdot 10^{-4}$	$3,4 \cdot 10^{-4}$	$2,7 \cdot 10^{-4}$
	$R^*_{inv}(m_1,m_2,m_3)$	0	$7,8 \cdot 10^{-3}$	$3,3 \cdot 10^{-3}$	$1,8 \cdot 10^{-3}$	$1.1 \cdot 10^{-3}$	$7,5 \cdot 10^{-4}$	$5.5 \cdot 10^{-4}$	$4,1 \cdot 10^{-4}$	$3,3 \cdot 10^{-4}$	$2,6 \cdot 10$

Also important is the level of reliability of CTIS in time [3] taking into account the degradation of CTIS since the development to the commissioning. The reliability of CTIS in time is indicated by the following formula:

$$(t_0 + t) \cdot p'(t) = f(t) \tag{2}$$

where, t_0 is the time since the creation of the CTIS till the start of using;
t is the time within which the information is protected;
$p'(t)$ is the level of reliability of CTIS in time;
$f(t)$ is any positive function.

With the expression (2), we can say that for reliability CTIS function protection risks $f(t)$ while increasing time for t must be at least constant. The decreasing of $f(t)$ in time means that CTIS is not reliable and it must be replaced. The increasing of $f(t)$ over time means the CTIS is more efficient [4].

Thus, if CTIS is not certified in time for the assessment of the degradation it is necessary to consider the case where $f(t) = const$, which provides the lowest possible reliability in time. At the same time, the expression (2) can serve as a criterion of reliability SIS in time. If you know the $p'(0)$ at $t = 0$ and probability $p'(t_1)$ after some time $t = t_1$, you can infer about the level of reliability of CTIS. Condition $f(t) = const$ responses the minimum required level of reliability of CTIS in time.

Figure 3 shows the dependency of probability of hacking CTIS $P_m(t)$ with time and the number of attempts to break into the m attempt. On graph you can see that when increasing the hacking attempts the time required for this is reduced and, as a result, with the same level of reliability decreases the reliability of hacking CTIS for another attempt.
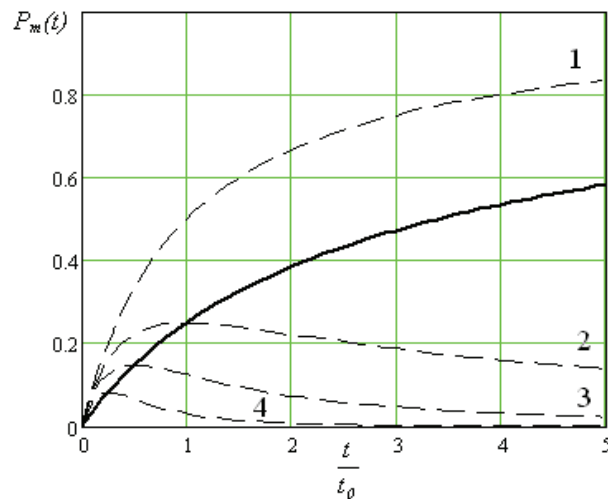
Figure 3 – the dependency of probability of hacking $P_m(t)$ from t/t_0 with
α ≈ 1: curve 1 is the one attempt hacking to $m = 1$, the curve 2 – two attempts $m = 2$, curve 3 – three attempts $m = 3$, curve 4 - after five attempts at $m = 5$.
Continuous line corresponds to the $P(t)$ is the maximum probability of hacking.

Conclusions. This article merges the results of the previous research on the Techniques and improving the reliability of CTIS. Definitely highlights that, according to the authors, played an important role in the development of any of the CTIS, namely, the level of reliability of CTIS depending on the number of attempts of hacking, of the feasibility of the use of multi-level CTIS that provide solid protection of sensitive information, as well as the optimum performance of the necessary investments for the development of CTIS. Cited research make it possible to count the optimal settings CTIS on the stage of development in order to identify and ensure the optimum level of reliability.

References

1. *Домарев В.В.* Безопасность информационных технологий. Системный подход / - К.: ООО ТИД "ДС", 2004. – 992с.
2. *Журиленко Б.Е., Николаева Н.К., Пелих Н.С.,* Оптимальные финансовые затраты и основные критерии построения или модернизации комплекса технической защиты информации // Правове, нормативне та метрологічне забезпечення системи захисту інформації в Україні: Науково-технічний збірник. Випуск 1 (22) – Київ, КПІ НДЦ «Тезіс», 2011. с.33-43
3. *Журиленко Б.Є.* Оцінювання деградації стійкості комплексної системи захисту інформації в часі // Вісник НАУ: науковий журнал. – Київ, НАУ, 2007. - №1(31). - с.67-69.
4. *Журиленко Б.Е., Николаева Н.К., Пелих Н.С.,*Оценка стойкости технической защиты информации во времени // Захист інформації: науково-технічний журнал. №1(54) – Київ: НАУ, 2012. с.104-108

G.Sokolovska, Engineer, L. Scherbak, Doctor of Technical Sciences
(National Aviation University, Ukraine, Kiev)

TASKS OF VIBRODIAGNOSTIC OF MECHANISMS AND SYSTEMS IN AVIATION

Consider such areas of vibrodiagnostics of mechanisms and systems in aviation such as functional, test and simulation. For each of the areas described their main tasks.

Introduction. Provision of reliable and failure operation of mechanisms and systems in aviation is an actual scientific and technical problem. Important role in solving this problem playing methods and means of vibration diagnosticsenabling timely for the tests to detect defects in them that have arisen.

It is known[1-3], that the vibration diagnostics is scientific and technical direction of the research division and of general technical diagnostics, which include theory, methods and means of detecting and finding defects in the objects of a technical nature on the basis of analysis of oscillatory processes in the system diagnostics. Source of information about the characteristics of the oscillation process is the vibration signal generated objects under investigation.

The main purpose of vibration diagnostics in aviation - improving reliability of objects during their operation, preventing possible damage, accidents, marriage, etc. Diagnostic information can also be used to predict the future work of the objects.

Considered in this paper main challenges of vibrodiagnostics and are offered along with traditional areas of diagnosis, such as functional or test, develop areas of simulation (computer) diagnosis.

Problems of functional vibrodiagnostics based on the formation, registration and analysis of vibration signals emitted by the object during its operation. Object types in aviation diagnosed functional, are the following:

- aircraft engines, including piston, air-jet and rocket;
- motors for various purposes;
- gears;
- rolling and sliding;
- other working mechanisms.

Effective solution of the vibrodiagnostics largely depends on the rational choice of diagnostic features, ie vibrational characteristics of the processes are most sensitive to match the appearance of the defect. The most common methods of functional diagnostics based on:

- pre-recorded vibration signal, including filtration, separation of temporal and spectral windows, the decomposition into additive independent components in order to improve its information;
- obtaining and analyzing the statistical characteristics of vibration signals as realizations of a random process is most sensitive to changes in the technical condition diagnosed object and using them as diagnostic indicators, including measurement of autocorrelation and cross-correlation function, time intervals and moments of disorder processes;
- comparative analysis of statistical characteristics of vibration signal in the normal and defective functioning of the object.

Tasks test of vibrodiagnostics based on the impact on the test object with a certain standard of the interventions, called the test. Impact test parameters are specially selected so that, on the one hand, improve information and sensitivity of diagnostic features, on the other hand, does not cause a system diagnosed irreversible change its condition. To test diagnostics upon in cases where the object does not emit vibrations during operation, is subject to vibrations generated by other objects, or if the recording and analysis of vibration characteristics in difficult operating conditions. Typical

test objects of vibrodiagnostics - aircraft construction, pipelines, core design and farms, and other multi-connection.

Methods of test vibrodiagnostics mainly same as the method of functional vibrodiagnostics, and for its intended purpose, they are non-destructive testing methods.

In general, when comparing of these two lines of research, the number of areas of functional vibrodiagnostics much more in comparison to the number of uses of the test vibrodiagnostics. Last mainly used in various types of tests, including tests on a shaker before the step operation of the facility.

Tasks of simulation vibrodiagnostics. The development of modern information technology for simulation of complex hardware and software systems, the widespread use of computer technology make it possible to create a new line of vibrodiagnostics - simulation (computer) modeling vibration diagnostics. It should be noted that in recent years the accumulated results of the solutions of the functional and diagnostic testing can be used as a basic foundation of knowledge of simulation vibrodiagnostics, and known problems vibroidentification[1-3] are an integral part.

The main tool of simulation vibrodiagnostics is coduct computer diagnostic experiment, analysis of the results and decisions. Note that the main problem simulates of vibrodiagnostics based on the development and justification of information support, which includes:

- the physical and mathematical models of the objects that form the primary and displaying the main characteristics of the functioning of vibration signals;
- models of vibration in general random fields as a function of time, space and random arguments;
- a sequence of diagnostic features as the statistical characteristics of vibration signals more fully reflect the dynamics of the objects under study;
- statistical methods for determining the sequence of diagnostic features, mainly in digital processing of vibration signals;
- algorithms and software of the computer diagnostic experiments.

The implementation of the information management in computer diagnostic experiment is usually performed during the design, testing a variety of laboratory, pilot and prototype developed object and the stage setting, certification and transfer of the facility.

In the future, based on the results this test facility operation, information provision is adjusted and used as to ensure its reliable operation, as well as to predict the outcome of certain time intervals in order to extend the life of the object.

As noted above, part of the simulation are the problems of vibro identification. For solving such problems have accumulated some experience and can briefly mention some of the known results.

So, for exampleis determined the solution of constructing a model of the object according to its dynamic behavior under certain external vibration effects.

There are two types of identification problems:

- *structural identification* - identification of the object based on the results of its vibration testing;
- *parametric identification* - determination of the parameters of the mathematical model (eg, the coefficients of differential equations) describing the dynamic behavior of the object.

It should be borne in mind that the parameter identification is possible if the structure of the object is known.

In problems of vibrodiagnostics is widely used methods of parametric identification. For example, defining the operation of the facility in its rejection of the basic parameters of their initial values corresponding to the defective (defect-free) state of the system, in fact, solve the problem of vibrodiagnostics, ie establish the fact of the defect, its location and size. Thus, the method of identification solved the problem vibrodiagnostics.

Depending on the mathematical model used to describe the dynamics of the controlled object, methods vibrodiagnostics be subdivided into linear and non-linear. Called linear vibrodiagnostics

such problems, the mathematical formulation of which leads to linear differential equations (ordinary or partial). Therefore, the methods of the linear vibrodiagnostics applicable to non-destructive testing of only those objects for which the fundamental simplicity of the linear vibration theory are valid in practice. It should be borne in mind that in the linear vibration diagnostics, only a limited number of motion parameters can be used as diagnostic features (resonant frequency spectrum of the object, the logarithmic decrement, amplitude and waveforms), characterized by the same low sensitivity.

The dynamics of real objects diagnosis in most cases described by the nonlinear integral-differential equations. Therefore, diagnosis of such objects it is advisable to approach based on nonlinear.

Conclusion. Based on the problems considered functional testing and simulation vibrodiagnostics can be concluded in the diagnostic systems in aviation.

- Potential opportunities of diagnostic systems determined by the selection of the diagnostic signal and information technology. Vibration signal contains sufficient diagnostic information for using modern information technologies to detect a faulty node machine, determine the type and depth of the defect and give the long-term forecast of its development.
- The most effective technical diagnostics, both stationary and portable, are based on computer equipment and technology. It is these tools allow you to use all the features of the promising methods of obtaining information, such as spectral analysis, and statistical analysis of the envelope of the recognition of the state.
- Promising methods of diagnosis in the first place, should include the rapidly developing methods of diagnosing and predicting the technical condition of vehicles on a one-off units measuring vibration or noise. They can be used effectively not only portable diagnostic systems, and monitoring systems with a limited number of the fixed-vibration and noise.
- Significant expansion of applications of monitoring and diagnostics of machines by signals of vibration and noise is possible if production of inexpensive automatic diagnosis, does not require any diagnostic training. .

References

[1] Aleksandrov A.A. Vibration and vibration diagnostics ship electric / A.A. Alexandrov, A.V. Barkov, N.A. Barkov, V.A. Shafransky. - L.: Shipbuilding, 1986. - 380 p..

[2] Balitsky F.Y. Vibroacoustic diagnosis of incipient defects / F.Y. Balitsky, M.A. Ivanov, A.G. Sokolova, E.I. Hamsters. - Moscow: Nauka, 1984. - 186 p.

[3] Marchenko B.G., Myslovich M.V. Vibrodiagnostics bearing units of electric cars. - Kiev: Naukova Dumka, 1992. - 190 p.

UDC 006.06:331.108(076)

I.P. Belokur, Doctor of Technical Sciences, Y.O. Gordonna, graduate
(National Aviation University, Ukraine)

CERTIFICATION OF PERSONNEL PROFESSIONAL ACTIVITIES ON NON-DESTROYING TESTING

The questions of the competency assessment of staff performing non-destroying testing processes and diagnosis of aerospace engineering at its certification.

Modern aerospace engineering requires availability of a wide range of qualified staff, certified by the organizations being independent from the education system. In the situation of competition the firm (enterprise) personnel should be trained well enough and the team should be built well enough to ensure the required quality of production (services) of the organization in such a market situation when the consumer's requirements and his/her expectations are being raised gradually. To ensure all the above, there is an information needed on the personnel ability to work efficiently enough, as well as whether (s)he meets the selected organization strategy; whether the personnel is able to change to meet the requests set by the competition environment; whether (s)he accepts changes positively. When they employ anyone, they employ not only a skilful professional but a person with his/her own character, inclinations, habits and fortune.

An international experience of enterprises provides evidence for the fact that no less then 20% of their general expenses is allocated for their personnel training and certification. Personnel certification provides an opportunity to the staff to provide documentary evidence by an independent organization of their skill level and the level of their workmanship in a current situation, and that will enhance their chances for employment or opportunities for their job promotion and mobility at the labour market.

One of the important directions in the area of quality management of aeronautical engineering (AE) is the enterprises' willingness to introduce the International and European standards. It assists greatly in advancing the internal organization of production, the AE industrial processes as well as processes of its servicing and renewal, and, as a result, it makes a positive impact on aircrafts (AC) safety and on the indicators of the enterprise's economic activities.

In the ISO 9001-2001, JAR-145, Standards requirements of Aircraft Guidance of the Inter-State Aviation Committee and European 'Procedures on certification of aircrafts and other aeronautic engineering outputs and components', there have been general methodological guidelines formulated on the quality management system (QMS) for AC production and servicing. The relevant chapters are devoted to practical issues of introducing the process approach to the AC quality management and to the personnel certification. The legal framework of the AC quality management system includes legal acts, documents enacted by the authority regulating the civil aviation activities, standards, branch procedure manuals, technological guidelines, technical conditions etc.

The novelty of approaches to QMS establishing is in orientation of managing the enterprise activities on satisfying the consumer's requests to the outputs quality, applying the process approach in managing the activities related to quality assurance, creating the conditions for regular improving of outputs and advancing the QMS.

Personnel engaged into functional areas having impact on quality, plays the central role in quality system implementation. Whatever modern the quality systems would be, there always a human standing beside them with his wishes and unwillingness, ability or inability to work efficiently. New conditions of the quality system functioning require sufficient changes in training personnel while considering new social-psychological interests.

It's necessary to remember that quality management is, in the first instance, management of human resources and their activities. Therefore, there should be a certain personnel management system existing at the enterprise which should foresee the process of evaluation of a worker's

performance of his/her duties – i.e., certification. While obtaining the certificate on competence, the specialist is the subject to technical observance by the certification authority according to the order of implementing the control over the certified personnel. The certificate availability proves that the specialist meets the qualification requirements (there is certain knowledge, abilities and skills). At the same time, while certification there a necessity occurs to evaluate the correspondence of the specialist with the character of a job performed. It is advisable to explore availability of personality accentuations. A German psychologist and psychiatrist Karl Leonhard developed and described classification of the personality accentuations where he has identified the following ten main types of accentuations: demonstrative; pedantic; hyperthymic; dysthymic, cyclothymic; ecstatic; sticking; excitable; anxious; emotive. The personality traits are divided into the core and additional ones. The core personality traits are the heart of the personality; they identify its development and mental health. Each of us has own identity image, i.e., some traits are accentuated. It's necessary to state that classification of personality accentuations is a classification of not pathologies but extreme variants of a norm. While having a successful development, accentuated persons can have much more creative potential than those non-accentuated – there is only a need to direct it into the right channel.

Description of the personality accentuations with the recommendations re: where they will be of the most of their use is provided in the manual prepared by us for the National Aviation University 'Certification of personnel'. As the experience of conducting activities on non-destroying control evidences, the specialists with a certain level of qualification according to the requirements of DSTU No 473 or EN 4179, tend to have two opposite motivation tendencies – striving for success (achievement motive) and longing to avoid failures (motive to avoid). Information about the personality motives allows during the process of professional-psychological certification making prognosis re: person's activity at a certain workplace. Diagnostics and evaluation of the achievement motive are of particular importance here. When some people have prevalence of striving for success, for high outcomes in making conclusions re: quality of a controlled object, the others have longing to avoid failures or mistakes while making decisions on control outcomes.

A personality's own assessment of his/her chances for success has a sufficient impact on his/her motivation to professional activities. The more a person believes in success, the more efforts (s)he tends to put into achieving the goal set. Assessment by the personnel of their own abilities can be the subject for exploration in the interviewing process. Successes which they had in the past form the faith in their own strengths, in their own efficiency. Failures in the past destroy one's faith. Subjective value of success defines the motivation for achievement (longing for success). The fact of how intensive a person will work in a specific area directly corresponds with the meaning that a personality puts into achievements in non-destroying control and technical diagnostics. While certification, there is a need to identify additionally how the job applicant imagines his/her activities at a new job placement or while controlling new components, details and joints; what kind of success (s)he might achieve; what personality meaning this success carries for him/her, what is the value of it for him/her etc.   Content analysis of the personality language (oral or written one) is quite an efficient one. In a person's language there are judgments, expressions identified which evidence the availability of a person's motive for success achievement. Thus, availability of the achievement motivation can be evidenced by positively formulated statements which do not express any apprehensions or uncertainty re: possibility to achieve the goal, and, on the contrary, there is a longing for a success expressed ('I would like', 'I plan', 'I strive for' etc). Based on the certification outcomes, human resources management services at the enterprise conduct staff recruitment and its development by means of developing the incoming information – job descriptions, qualification requirements and system of criteria which ensure personnel adaptation. Besides, they ensure personnel development (professional training, re-training, advancing qualification to ensure functions of the above organization, coordination and control, job promotions) with development of methodological recommendations on the above process practical realization.

Assessment of outcomes of specialists' professional activities is made for a certain period of time, according to the developed methodology of generalized outcomes assessment and managerial decisions on the outcomes obtained, and the mechanism for selecting candidates for the reserve to promote and to advance their professional qualification along with the conditions of the core and extra remuneration of labour.

Advancing qualification of the certified personnel at present conditions became an objectively necessary element for production activities, and it is considered to be not as a wish but as a required form of the above activities. The specialist's unwillingness to advance his/her qualification is considered to be an industrial discipline violation, with all the relevant consequences.

As there is a current tendency of increase in the national economics development speed, and the level of awareness has been enhanced amongst enterprises managers re: the important impact which the level of professionalism of the specialists on non-destroying control has on the above, there is an increase in their professional training observed at present. To ensure it, according to the order of the Ministry of Labour and the Ministry of Education of 26.03.2001 No 127/151, there have been recommendations developed re: the mechanism of stimulating enterprises personnel in order to strengthen its interest in on-going advancing its skills and knowledge. There were recommendations developed re: creating and functioning of regional associations of enterprises of different forms of ownership on the issues of professional training of staff at enterprises, with arranging professional training at their working places, according to the recommendation which has been adopted by the General Conference of the International Labour Organization. In the latter there is a cooperation foreseen, in case of necessity, with the International Labour Office on providing personnel with the opportunities for training and gaining experience which they are not able to receive at home, or business trips of qualifies experts from one state to other to assist in education organization, obtaining text books, exchange of qualified personnel and information on training issues.

Personified training of staff on non-destroying control and technical diagnostics ensure advancing its competence, development of knowledge on methods and means used while operating.

The competence module directly depends on the content of works under way. The competence shortcomings become clear after the audit of intellectual luggage, i.e., the knowledge audit. This becomes the basis for conclusions on the specialist's competence shortcomings on specific kinds or methods of control, theoretic knowledge or practice skills.

Decisions on how to fill in the competence gaps can be found via training – both personified and general one – for all the personnel on dimensions, control and tests. While doing this, they come out of the fact that the specialists' training and the personnel stability is an essential principle.

CONCLUSIONS: The certification of the stuff who works in the sphere of non-destroying testing and technical diagnostics assess his qualifications, and take into account its accentuation and motivation of the professional activities.

References
1. Білокур І.П. Сертифікація персоналу. Навчальний посібник.
– К.:«НауДРУК». 2009: -225 с.
2. Балабанова Л.В. Управління персоналом: Навч. посібник / Л.В. Балабанова, О.В. Сардак. – К.: Професіонал, 2006. – 512 с.
3. Борисова Е.А. Оценка и аттестация персонала. –СПб: : Питер, 2003. – 288с.: ил. – (Серия «Теория и практика менеджмента»).
4. Профессиональный отбор персонала / Под ред. И.А.Волошиной и В.Л. Шкаликова. М., 2001.

UDC 004.56.5(045)

M.G.Lutsky, Ph.D, associate professor (National Aviation University, Ukraine)
K.O. Kurin (National Aviation University, Ukraine)

TECHNOLOGY OF COMPRESSION OF IMAGES IS ON BASE OF METHOD OF CODING OF BINARY SEQUENCES DUE TO THE AMOUNT OF BIT CHANGES

The method of compression of images on the base of coding of binary sequences due the amount of bit changes is offered. The prototype of structure of coder is formed. The choice of method of transformation of component of image and method of coding of transforms is proved

Introduction. The modern computer systems apply graphics intensively. Some actions carried out by the system, for example loading and sending of files, also represented graphicly. Most programs offer to the user a graphic interface (GUI), what considerably simplifies work of user and allows easily to interpret the got results. Computer graphics are used in many areas of everyday activity at converting of difficult arrays of data into a graphic reflection. So the graphic images are extremely important, but they require the large amounts of memory. Animation which also is widely used in computer additions requires the even greater amounts of memory. All of these explains importance of compression of images.

Among the most widespread coders of compression of images are algorithms JPEG and JPEG-2000, that were developed by the Joint Photographic Experts Group for the compression of colorful images. Both these algorithms are based on the methods of coding, which take into account statistical surplus of information.

These algorithms of compression have the next failings [1]:
-     possible losses of information, which arises up on the stages of transformation and quantum of component of image;
- dependence of efficiency of compression from the characteristics of the source;
- at a compression in the mode without losses the insufficient values of degree of compression are provided (for natural images ratio averages 3).

The aim. A research purpose is development of technology of compression of images on the base of coding methods, based on principle different from statistical, in order to increase the efficiency of methods of compression of source with simultaneous minimization of additional distortions in a rebuild informative structure.

Forming of prototype of coder. Lets form the prototype of technology of compression of images on the base of the structure of algorithms of JPEG and JPEG-2000 [2] (Image. 1).
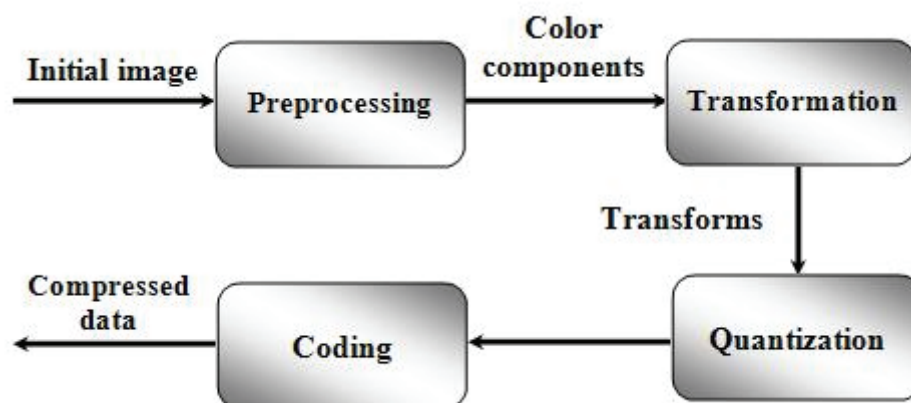
Image 1. Prototype of technology of compression of images

lets pass from a formal prototype to concrete realization of coder.

The first stage is – preprocessing. The coloured image turns into the format of presentation with a model RGB. In the offered technology the compression of data the transition from the colour model of RGB to the model of YUV is not used. This technology of compression does not foresee

the use of procedure of enlargement of pixelsls, which results in the considerable losses of quality of image.

Pixels of each component era grouped into blocks 8×8, that is called segments. The segmentation of matrix of image is provided to decline of amount of operations on processing of data in and to increase of degree of coherentness of the processed information.

The second stage – transformation. In article [2] with a purpose to prove the choice of algorithm of transformation of matrix of image there was provided the research of existent procedures of analytical transformations from the condition of their influence on the statistical structure of image.

The got results allowed to make a conclusion, that from point of achievement of the greater winning from a subsequent coding, the use of discrete wavelet transformation (DWT) has the biggest advantage.

The simplest method of description of discrete wavelet transformation use the multiplication of matrices [3]. One of most popular wavelets, the wavelet of Dobeshi, is based on four coefficients c_0, c_1, c_2, c_3:

$$c_0 = \frac{1+\sqrt{3}}{4\sqrt{2}}, \quad c_2 = \frac{3-\sqrt{3}}{4\sqrt{2}},$$

$$c_1 = \frac{3+\sqrt{3}}{4\sqrt{2}}, \quad c_3 = \frac{1-\sqrt{3}}{4\sqrt{2}}.$$

Matrix W of transformation:

$$W = \begin{pmatrix}
c_0 & c_1 & c_2 & c_3 & 0 & 0 & 0 & \ldots & 0 \\
c_3 & -c_2 & c_1 & -c_0 & 0 & 0 & 0 & \ldots & 0 \\
0 & 0 & c_0 & c_1 & c_2 & c_3 & 0 & \ldots & 0 \\
0 & 0 & c_3 & -c_2 & c_1 & -c_0 & 0 & \ldots & 0 \\
0 & 0 & 0 & 0 & \ldots & 0 & 0 & \ldots & 0 \\
0 & 0 & \ldots & 0 & 0 & c_0 & c_1 & c_2 & c_3 \\
0 & 0 & \ldots & 0 & 0 & c_3 & -c_2 & c_1 & -c_0 \\
c_2 & c_3 & 0 & \ldots & 0 & 0 & 0 & c_0 & c_1 \\
c_1 & -c_0 & 0 & \ldots & 0 & 0 & 0 & c_3 & -c_2
\end{pmatrix}.$$

During practical realization DWT is calculated as work multiplication of matrices WPW^T, where P – initial 8×8 matrix of pixels.

The third stage – quantum. After the calculation of all coefficients of DWT their quantum is provided. Every number from the matrices of coefficients of DWT is divided by the special number – coefficient of quantum from the table of quantum, and a result rounds to nearest whole.

The table of quantum accepted by default for JPEG is used.

As on this stage the quantized segments contain negative values, it is useful to form the matrices of signs by rule:

$$sign_{i,j} = \begin{cases} 0, \to com_{i,j} \geq 0; \\ 1, \to com_{i,j} < 0. \end{cases}$$

$sign_{i,j}$ – element of matrix of signs, which gives information about a sign of component $com_{i,j}$.

$i = \overline{0, L-1}$, $j = \overline{0, C-1}$, L and C – amount of rows and columns raster of image accordingly.

The fourth stage – coding of transforms. As it was already mentioned, the most widespread today technologies of compression of images – JPEG and JPEG-2000 – provide the high degrees of compression due to reduction of visual surplus and the next statistical coding of component of ortogonal transformations. For the coding of the quantized transforms the statistical methods of compression – codes of Haffmen (for the standard of JPEG) and arithmetic codes (JPEG-2000) –

are used. In article [5] the lacks of the use of this class of code methods for the compression of images were discussed, and it was suggested to plug in technology of compression a coding method which uses the different from statistical algorithms method of coding of transforms of image – method of coding on the base of the amount of bit changes in binary sequence (ABC).

This method of coding refers to the class of structural methods[1] which provide the removal of structural surplus on the basis of value of structural signs: an amount of changes from '1' to '0' $p_{1\to0}$ and an amount of changes from '0' to '1' $p_{0\to1}$. At the same time combination $p_{0\to1}$ та $p_{1\to0}$ determines another sign which characterizes a binary sequence – number of structural group S. Parameter S also determines the general amount of changess between '0' and '1' in a sequence [5].

Each of 64 numerical values of the quantized transform presents as a 8-bit binary number (every segment is a parallelepiped with length 8 bits and a width and height equal the dimension of segment 8×8). Every segment consists of eight layers.

On image 2 the principle of spatial structure of image is represented.

Segment 1,8

	64	65	66	67	68	69	70	71
8	60	3	1	1	0	0	0	0
9	6	3	0	0	0	0	0	0
10	14	4	1	0	0	0	0	0
11	3	2	0	0	0	0	0	0
12	0	0	0	0	0	0	0	0
13	0	0	0	0	0	0	0	0
14	0	1	0	0	0	0	0	0
15	0	0	0	0	0	0	0	0
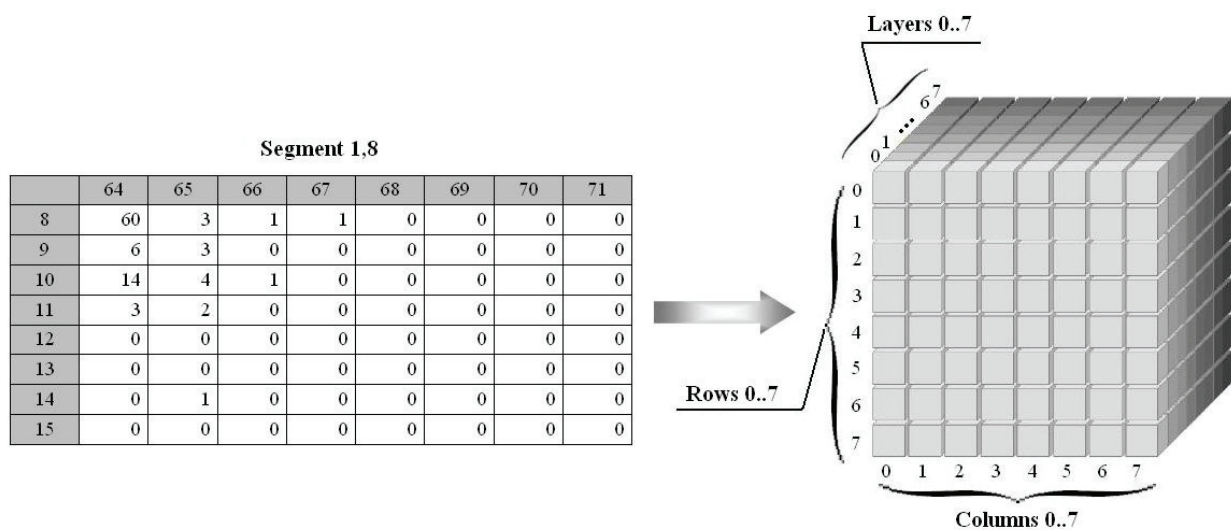
Image 2. Graphic model of spatial structure of image

The task of this stage is to form the sequence number with an ABC method for each of layers of segment on the base of exposure of structural surplus taking into account the structural signs. Thus for a segment 8 codes-numbers will be formed.

The coding procedure takes place in the next stages:

1. Zigzag scan-out. The use of this method of read-out of binary information is expedient, as it will provide reduction of amount of bit changes in a sequence.

2. Forming of array S_ar with the values of structural sign – amounts of changes between binary elements.

3. A calculation of values of sequence numbers for binary sequences of the bit layers of image.

The fifth stage – additional compression. On this stage the coding of sequence numbers with the method of RLE is used with the purpose of increase of degree of compression of source image.

Also on this stage with the same principle the coding of content of array of signs $sign$ is provided $sign$.

Conclusion

The scientific novelty of research, described here, consists in the following:
The prototype of structure of coder is formed.
The choice of method of transformation of component of image and is proved
The choice of method of coding of transforms is proved

The method of compression of images on the base of coding of binary sequences due the amount of bit changes is offered.

References

1. *Юдін О.К.* Методи структурного кодування даних в автоматизованих системах управління / О.К. Юдін. – К.: НАУ, 2007. – 210 с.

2. *Юдін О.К.* Використання аналітичних перетворень в задачах стиснення зображень / К.О. Курінь, О.К. Юдін, О.І. Варченко // Наукоємні технології. – К.: Вид–во Нац. авіац. ун–ту «НАУ–друк», 2011. – № 13(7). – С.64-69.

3. *Воробьев В.И.* Теория и практика вейвлет-преобразования / В.И. Воробьев, В.Г. Грибунин. – СПб.: ВУС, 1999. – 203 с.

4. *Селомон Д.* Сжатие данных, изображений и звука / Д. Селомон. – М.: Техносфера, 2006. – 386 с.

Юдін О.К. Метод кодування двійкових послідовностей за кількістю бітових переходів / К.О. Курінь, О.К. Юдін // Наукоємні технології. – К.: Вид–во Нац. авіац. ун–ту «НАУ–друк», 2011. – № 14(8). – С.64-69.

UDC 519.711/.72

A.Ja. Beletsky, Doctor of Technical Sciences, O.I. Volivach, R.Ju. Kandiba, D.A. Navrotsky
(National Aviation University, Ukraine)

MATRIX ANALOGUES OF THE DIFFI-HELLMAN PROTOCOL

The presents a comparative analysis of several matrix analogs of Diffi-Hellman algorithm, namely, Yerosh-Skuratov and Megrelishvili protocols as well as alternative protocols based on irreducible polynomials (IP) and primitive Galois or Fibonacci matrices. A matrix is defined as primitive one, if the sequence of its powers in the ring of residues by modulo IP forms a sequence of maximum length (m-sequence).

Introduction

Diffi-Htllman algorithm (DH algorithm, protokol) [1] assumes that two subscribers - Alice and Bob both know the public keys p and q where p is a large prime number, and q is a primitive root. Subscriber Alice generates a random big number a, computes $A = q^a \bmod p$ and sends it to Bob. In turn, Bob generates a random big number b, computes $B = q^b \bmod p$ and sends it to Alice. Then subscriber Alice raises number B received from Bob to her random power a and calculates $K_a = B^a \bmod p = q^{ba} \bmod p$. Subscriber Bob acts similarly, calculating $K_b = A^b \bmod p = q^{ab} \bmod p$. It is obvious that both parties receive the same number K, because $K_a \equiv K_b$. Then Alice and Bob can use this number K as a secret key, e.g. for symmetric encryption because a foe who intercepts numbers A and B faces with virtually unsolvable (in a reasonable time) the problem of calculation K, under the condition that numbers p, a, and b were chosen big enough.

Yerosh-Skuratov Protocol

In order to form a secret encryption key in the public network by subscribers Alice and Bob, the authors [2] propose to use DH protocol in the cyclic group of matrices $\langle M \rangle$, and the matrix M is considered as public information. It is assumed that Alice generates a random index x, calculates the matrix M^x and sends it to Bob. In turn, Bob generates a random index y, calculates the matrix M^y and sends it to Alice. Then both subscribers raise the matrices obtained from a partner in their secret powers and calculate the sheared matrix (encryption key) $K = M^{xy} \equiv M^{yx}$. The matrix M must be a high-order matrix (at least 100); so, the authors assert (by the way, without a proof), cracking key has invincible complexity. However, in [4] it has been proved that Yerosh-Skuratov protocol can easily be cracked based on the generalized Chinese remainder theorem.

Megrelishvili Protocol

The essence of the protocol [3] is following. Binary initialization vector V and primitive matrix M of order n are accepted as a public key. Subscriber Alice generates a random index x, calculates the vector $V_a = V \cdot M^x$ and sends it to Bob. In turn, Bob generates a random index y, calculates the vector $V_b = V \cdot M^y$ and sends it to Alice. Then Alice computes the key $K_a = V_b \cdot M^x = V \cdot M^{y+x}$, and Bob computes the key $K_b = V_a \cdot M^y = V \cdot M^{x+y}$. It is quite obvious that using such data exchange protocol, both parties receive the same private key K because $K_a \equiv K_b = K$. The algorithm of generating the matrices in Megrelishvili protocol is fairly simple and can be explained by the following calculation scheme

$$M_1 = 1, \quad M_3 = \begin{bmatrix} 1 & 0 & 1 \\ 1 & M_1 & 0 \\ 0 & 1 & 0 \end{bmatrix}, \quad M_5 = \begin{bmatrix} 1 & 0 & 1 & 0 & 1 \\ 1 & & & & 0 \\ 0 & & M_3 & & 1 \\ 1 & & & & 0 \\ 0 & 1 & 0 & 1 & 0 \end{bmatrix}, \ldots \tag{1}$$

As it follows from (1), the matrices M_i, $i = 1, 2, \ldots$, are matrices of odd order only that can cause some difficulties when they are used in cryptography. This shortcoming was remediated by replacing matrices of type (1) by primitive matrices of an arbitrary order that is synthesized based on the so-called generalized Gray transforms [5]. The essence of these transforms is explained below. The matrix form of direct (for simplicity denoted by number 2) and inverse (denoted by number 3) classical Gray transforms (codes) [6] can be presented in the form:

$$2 := \begin{bmatrix} 1 & 1 & 0 & 0 \\ 0 & 1 & 1 & 0 \\ 0 & 0 & 1 & 1 \\ 0 & 0 & 0 & 1 \end{bmatrix}; \qquad 3 := \begin{bmatrix} 1 & 1 & 1 & 1 \\ 0 & 1 & 1 & 1 \\ 0 & 0 & 1 & 1 \\ 0 & 0 & 0 & 1 \end{bmatrix}; \tag{2}$$

where as an example, the order of the matrix n is set $n = 4$.

Matrices (3), which we call left-sided Gray transform matrices, are in correspondence with the right-sided transform matrix defined by the following relations:

$$4 := 121 = 2^T; \quad 5 := 131 = 3^T, \tag{3}$$

where

$$1 := \begin{bmatrix} 0 & 0 & 0 & 1 \\ 0 & 0 & 1 & 0 \\ 0 & 1 & 0 & 0 \\ 1 & 0 & 0 & 0 \end{bmatrix} \tag{4}$$

is the matrix (operator) of the inverse permutation?

The set of operators (2) - (4), supplemented by the operator 0, or e (identity matrix), forms a complete set of simple Gray operators. From the elements of simple Gray operators, one can form so-called composed Gray codes (CGC) generated by the product of simple (elementary) Gray codes.

Table 1.

Gray Composite codes delivering
binary matrices property of primitiveness

The order of the matrix (n)			
32	64	128	256
2244424	22533435	2425535	22533435
2442224	22534335	2433534	22534335
12242253	24334225	2435334	24334225
12242443	25224334	22524224	25224334
12252242	222524424	22533334	2222535224

The simplest examples of CGC 121 and 141 can be seen in (3). Both simple and composed Gray codes have a number of remarkable properties. Firstly, the corresponding transformation matrices are nondegenerate and, therefore, are reversible. Secondly, there are simple inversing algorithms for CGC. And, finally, there are "crypto-order" CGC which have the property of primitiveness. Examples of such codes are given in Table 1.

Suppose *M* is a primitive binary matrix generated by the CGC *G*. With respect to such matrices, the following assertion can be easily proved by the test method.

Assertion. The primitiveness of matrices M is invariant to the group of linear transformations Ω *of the CGC G generating matrix M and transformations of similarity* Π *over these matrices.*

The Ω-group includes the following operators: cyclical shift, assess statement, inversion and conjugation as well as arbitrary combinations of these operators. Transformation Π forms matrix M_p which is similar to M and determined by the relation

$$M_p = P \cdot M \cdot P^{-1},$$

where *P* is a permutation matrix.

Alternative Protocols

This section proposes two options for alternative matrix protocols of secret key exchange on the open channel of communications. The procedure for the formation of the encryption key *K* in the first version of the protocol is based on the use of two public and one private key for both subscribers. As a public key a binary initialization vector *V* of *n* order and any irreducible polynomial (IP) φ_n of *n* order are chosen. Private keys are primitive (forming) elements ω of the Galois field $GF(2^n)$ over the IP φ_n, from which the subscribers (Alisa and Bob) form the primitive secret transformation matrices G_{φ_n, ω_a} and G_{φ_n, ω_b} respectively. The element ω of the field $GF(2^n)$ is primitive over IP φ_n, if the minimum rate *e*, at which $(\omega^e \equiv 1) \bmod \varphi$ assumes the value $e = 2^n - 1$.

Matrix $G_{\varphi, \omega}$ we call Galois matrices. The synthesis of algorithm for such matrices is explained on a concrete example. Let's IP $\varphi_8 = 100101101$, and the generating element (GE) of subscriber Alisa $\omega_a = 111$. We obtain

$$A = G_a = \begin{bmatrix} 1 & 1 & 1 & 1 & 0 & 1 & 1 & 1 \\ 1 & 1 & 1 & 0 & 1 & 1 & 0 & 1 \\ 1 & 1 & 1 & 0 & 0 & 0 & 0 & 0 \\ 0 & 1 & 1 & 1 & 0 & 0 & 0 & 0 \\ 0 & 0 & 1 & 1 & 1 & 0 & 0 & 0 \\ 0 & 0 & 0 & 1 & 1 & 1 & 0 & 0 \\ 0 & 0 & 0 & 0 & 1 & 1 & 1 & 0 \\ 0 & 0 & 0 & 0 & 0 & 1 & 1 & 1 \end{bmatrix}. \tag{5}$$

According to (5), the procedure of filling in the matrix G_a is carried out under the following scheme. First, the GE ω_a is arranged in the bottom row of the matrix. The elements of this row in the left from the GE elements are filled with zeros. Subsequent rows of the matrix (in the direction from bottom to top) are produced by a shift of previous lines. If left element of shifted line is 0, then the cyclical shift by one bit to the left (circular scrolling clockwise). In the case where the left element of shifted line is 1, the conventional shift of the line on one bit to the left and 0 is written to the vacant right element in line. Digit capacity of these lines is one bit more than the order of the matrix. The vectors corresponding to these lines are given to the residue modulo IP φ_n that returns them the capacity, which coincides with the order of the matrix *n*. Subscriber Bob forms similarly the Galois matrix $B = G_b$ using his primitive generating element ω_b.

The introduced Galois matrices have some interesting properties. First, the matrix product is commutative, i.e. $A \cdot B = B \cdot A$. At the same time, secondly, if at least one of the GEs is not a primitive of the IP, the commutative property of matrices is lost. Based on the above properties of Galois matrices a key exchange protocol was proposed.

We consider that initialization vector V and the IP φ are known. Alice chooses a secret primitive over φ GE ω_a, forms a Galois matrix A, calculates the vector $V_a = V \cdot A$ and sends it to Bob. In turn, the subscriber Bob selects a primitive GE ω_b, forms a matrix B that calculates the vector $V_b = V \cdot B$ and sends it to Alice. After that, both parties multiply vectors obtained from the partner, in own secret Galois matrix. Thus, a shared secret key K will be formed by the fact that the product of primitive Galois matrices over the same IP φ is commutative, and this implies the identity

$$K_a = V_b \cdot A = V \cdot B \cdot A \quad \equiv \quad K_b = V_a \cdot B = V \cdot A \cdot B .$$

Instead of Galois matrices G, Fibonacci matrices F can be used in the protocol with the same success. Fibonacci matrices are associated with Galois matrices by equation

$$F \xleftrightarrow{\perp} G, \quad \text{or} \quad F = G^\perp; \quad G = F^\perp ,$$

where $\perp -$ means the operator of right transposition, i.e. transposition with respect to the auxiliary diagonal matrix.

In the second alternative embodiment of the protocol the secret key K is computed in two rounds. In the first round, which repeats the above-considered first version of the protocol, a common to both subscribers secret binary vector of n-th order V_p is formed. On the basis of this vector, Alice and Bob compute the common permutation matrix P. One can propose different ways of constructing matrices P. Let us consider one of them. Let's $n=8$ and N is the decimal equivalent of the vector V_p. The task is to create permutation matrix P_8 of order eight for value N. Choose one or another way of numbering elements of matrices P_8 from 0 to 63. Calculate the value $n_8 = N \bmod 64$ and write 1 in that element of the matrix, whose number is equal n_8. After that, delete from the matrix P_8 the row and column, which contains 1. We obtain a matrix P_7 of 7-th order, whose elements are numbered from 0 to 48. Find the value $n_7 = N \bmod 49$, which is determined by the location 1 of the matrix P_7 and, consequently, in the matrix P_8. Following the proposed method, one can simply construct a permutation matrix P of any order.

Let proceed to the second variant of the encryption keys protocol. This protocol uses two public keys, which are the initialization vector V, and the irreducible polynomial φ, and also two private keys. These keys are generated by Alice and Bob as a random primitive over IP φ GE ω and υ. The protocol runs in two rounds. In the first round based on public keys V, φ and secret GE ω network operators calculate the total permutation matrix P. The second round is performed in the following order. Alice chooses a primitive over φ GE υ_a, forms Galois matrix A_υ, then similar matrix $A_p = P \cdot A_\upsilon \cdot P^{-1}$, computes a vector $V_a = V \cdot A_p$, and sends it to Bob. In turn, Bob chooses a primitive over φ GE υ_b, forms Galois matrix B_υ, then similar matrix $B_p = P \cdot B_\upsilon \cdot P^{-1}$, computes a vector $V_b = V \cdot B_p$ and sends it to Alice. After that, both parties multiply vectors obtained from partners on their secret similar Galois matrix. Thus, the shared key K will be generated due to the fact that the matrices A_p and B_p maintain the properties of primitiveness and commutativity of primary matrices A_υ and B_υ, respectively.

Results

The article analyzes the known matrix algorithms for exchanging encryption keys between subscribers of a network of open communication channels. The algorithms are based on the modified asymmetric Diffi-Hellman protocol (DH). The essence of the modification is reduced to replacing the large prime numbers of DH algorithm by assurance nondegenerate primitive binary matrices of high order. Methods of synthesis of these matrices are proposed based on both the generalized Gray codes, and irreducible polynomials. New key exchange matrix protocols have been developed. The protocols developed are superior for cryptographic strength to known cryptographic protocols, particularly Yerosh-Skuratov and Megrelishvili protocols described in this paper.

Conclusions

The proposed variants of vector-matrix protocols for exchanging by cryptographic keys on open communication channels have a good prospect to be applied for symmetric encryption in computer networks protected from the substitution of data, providing the necessary level of protection of private keys from unauthorized access. These protocols can make a strong competition to more resource-intensive RSA protocol.

References

[1] Diffi W., Hellman M.E. New Directions in Cryptography / / IEEE Transactions on Information Theory, v. IT-22, no. 6, Nov. 1976, P. 644-654.

[2] Yerosh I.L., Skuratov V. Addressing message transmitting using matrices over GF (2) / / Problems of Information Security. Computer Systems, 2004, № 1. - P. 72-78. (In Russian)

[3] Megrelishvili R. P., Chelidze M. A., Besiashvili G. M. Unidirectional matrix function - high-speed Diffi – Hellman's analog - Collection of materials 7th MK "Internet - Education - Science - 2010". - Vinnitsya: VNTU, 2010. - P. 341-344. (In Russian)

[4] Rostovtsev A. G. On the Matrix Encryption (criticism Yerosh-Skuratov cryptosystem). Available from: www.ssl.stu.neva.ru / psw / crypto / rostovtsev / Erosh_Skuratov.pdf (In Russian)

[5] Beletsky A. Y., Beletsky A. A., Beletsky E. A. Gray Conversion. The monograph in 2 volumes / V.1. Fundamentals of the theory. - Kiev: NAU Publishing House, 2007. - 506 p., Volume 2. Applied aspects. - Kiev: NAU Publishing House, 2007. - 644 p. (In Russian)

[6] Gray F. Pulse code communication. - Pat USA, № 2632058, 1953.

UDC 004.56(045)

M.B. Gumen, Ph.D, associate professor (National Aviation University, Ukraine)
K.O. Kurin (National Aviation University, Ukraine)

A METHOD OF CODING OF BINARY SEQUENCES BASED ON THE AMOUNT OF BIT CHANGES

The expedience of the use of structural code in the tasks of compression of dat is proved. The structural signs of binary sequences are defined. The rule of determination of amount of binary sequences which form structural groups is is described. The rule of calculation of sequence number of binary sequence based on the amount of bit changes is described.

Introduction. An idea of compression of data is fully natural, it appears up in an ordinary language as different reductions. Main reason to use the compression of data consist in the necessity to transmit and keep information in communication systems with most efficiency. In some sense the task of compression of data consists in a selection from the stream of information of his most meaningful and unique part which will allow to rebuild all initial information.

In connection with a permanent intensive progress of computer graphics the certain area of theory of compression is developed stormily – algorithms of compression of images.

The most compact presentation of information according to the known theory information work of Claude Shennon [1] is determined as entropy – numerical description which determines the lower limit of possible compression. This characteristic gives a quantitative estimation of information which is contained in a message, on the basis of his statistical descriptions.

However lately in an information theory the new unprobabilistic methods of estimation of information quantity appeared. It is explained by that fact that biggest part of informative processes are not statistical and their content can not be estimated only from positions of probabilistic information theory [2]. It defines the necessity of unprobabilistic methods of determining the amount of information and their adequate usage.

In basis of statistical methods a compression lies estimation of probabilities of appearance of elementary characters in the array of information, which determines the variable length codes, which are compared with these characters.

The most widespread today technologies of compression of images – JPEG and JPEG-2000 – provide the high degrees of compression due to reduction of visual surplus and the next statistical coding of component of ortogonal transformations. For the coding of the quantized transforms the statistical methods of compression – codes of Haffmen (for the standard of JPEG) and arithmetic codes (JPEG-2000) – are used. For these methods of coding next failings are typical [3]:

– the amount of machine operations, which is taken on processing of the transformed images can make to 70% from from the general amount of operations of procedure of their compression;

– the amount of operations that are necessary for implementation of statistical code for transforms formed on with the DCT and DWT, makes to 80% from the total amount of operations which is expended on the image compression;

– the parallel processing of statistical codes is difficult enough to realize;

– at processing of high-coherent images the degree of compression goes down sharply;

– a statistical code will not provide the additional compression of transform under a condition of presence of series of zeros of small lengths.

The aim. Therefore the aim of this research is development of coding method, which is based on principle different from statistical descriptions of information message, taking into account possibility of its usage in technology of compression of images.

Main part. Among the technologies of compact presentation of information the class of methods of compression, based on the removal of structural surplus by the detection of structural dependences in binary sequences according some sign, are selected. They are known as methods of structural coding [3].

Lets consider such structural signs of binary sequences: an amount of changes from '1' to '0' $p_{1 \to 0}$ and an amount of changes from '0' to '1' $p_{0 \to 1}$. In a table 1 binary sequences with the length $n = 4$ bits are shown. For each sequence the values of structural signs $p_{0 \to 1}$ and $p_{1 \to 0}$ are defined. We will mark that the analysis of values of structural signs is provided taking to account that an additional low bit is entered to a binary sequence (in a table selected grey). We will name such sequence extended.

It is obvious that binary sequences which is have the identical values of structural signs can be grouped in structural groups. In a table 1 structural groups are selected different tints of grey.

Table 1

Value of sequence numbers and structural signs for binary sequences
with length $n = 4$ btits

№	Binary sequence	Structural signs		Number of structural group	A sequence number is in a structural group
		$p_{0 \to 1}$	$p_{1 \to 0}$		
0	00000	0	0	0	0
1	00001	1	0	1	0
2	00010	1	1	2	0
3	00011	1	0	1	1
4	00100	1	1	2	1
5	00101	2	1	3	0
6	00110	1	1	2	2
7	00111	1	0	1	2
8	01000	1	1	2	3
9	01001	2	1	3	1
10	01010	2	2	4	0
11	01011	2	1	3	2
12	01100	1	1	2	4
13	01101	2	1	3	3
14	01110	1	1	2	5
15	01111	1	0	1	3

Thus a coding will consist in the appropriating to sequences its sequence number in this group. A value of sequence number will be less than than decimal value of binary sequence. Due to it a compression will be provided.

In a table 2 the values of number of binary sequences in structural groups and values of structural signs, which determine them, for the sequences of different length are defined.

Table 2

An amount of binary sequences in structural groups ($n = 4$ **)**

Structural signs		Number of structural group	An amount of sequences is in a structural group
$p_{0 \to 1}$	$p_{1 \to 0}$		
0	0	0	1
1	0	1	4
1	1	2	6
2	1	3	4
2	2	4	1

It is obviousl that values with which a binary sequence $A = \{a_1, a_2, ..., a_n\}$ will be encoded depends on length of binary sequence n and values of structural signs $p_{0 \to 1}$ and $p_{1 \to 0}$. At the same time combination $p_{0 \to 1}$ та $p_{1 \to 0}$ determines another sign which characterizes a binary sequence – number of structural group S. Parameter S also determines the general amount of changess between '0' and '1' in a sequence. The values of S, $p_{0 \to 1}$ та $p_{1 \to 0}$ are connected by next correlations:

$$p_{0 \to 1} = \left[\frac{S+1}{2} \right]; \tag{1}$$

$$p_{1 \to 0} = \left[\frac{S}{2} \right]; \tag{2}$$

$$S = p_{1 \to 0} + p_{0 \to 1}. \tag{3}$$

This allows to find out next conformities:

1. For a sequence with the length n a bit the amount of structural groups will make $n+1$.

This statement can be easily proved, considering limitations which are imposed on the value of structural signs:

- amount of changess from '0' to '1' $p_{0 \to 1}$ for a sequence with the length n bit taking into account expansion will lie in a range $0.. \left[\frac{n+1}{2} \right]$;

- amount of changess from '1' to '0' $p_{1 \to 0}$ for a sequence with the length n bit taking into account expansion will lie in a range $0.. \left[\frac{n}{2} \right]$;

- $p_{1 \to 0} + p_{0 \to 1} \leq n$;

- due to that an extended binary sequence always starts with a zero the amount of changes from '0' to '1' can not exceed amount of changess from '1' to '0';

- it is obviousl, that because of dependence between $p_{0 \to 1}$ end $p_{1 \to 0}$ a difference between the values of these signs can not exceed 1.

Taking into account these limits on the value of structural signs it is possible to claim, that the general amount of possible combinations will make:

$$2 \times (\left[\frac{n+1}{2} \right] + 1) - 1 = n + 1.$$

2. for every structural group S ($S \in 0..n$) the amount $N(S,n)$ of sequences in a group, and the range of sequence numbers with which the sequences will be encoded is determined as an amount of methods which it is possible to place S changes between '0' and '1' on n positions in the extended sequence with length $n+1$ bit, and is calculated with formula:

$$N(S,n) = \binom{n}{S} = \frac{n!}{S!(n-S)!}. \tag{4}$$

So the value of sequence number of binary sequence $A = \{a_1, a_2, ..., a_n\}$ in a structural group is a function of length n of binary sequence and number S of structural group. Lets designate this value as $NUM(A,S,n)$.

Procedure of determination $NUM(A,S,n)$ it is possible to carry out by a construction of code tables, similar to the table 1, and by a next search in them of proper sequence numbers $NUM(A,S,n)$ for the set binary sequence. On a receiving side procedure of decoding will be completed in a similar way – in obedience to the got values n and S the code tables will be built, and by value of $NUM(S,n)$ a necessary binary sequence will be defined.

But such principle of code seems to be inadvisable. Therefore a next task will be a search of mathematical model which will describe the rule of calculation of value of sequence number $NUM(A,S,n)$ for a binary sequence $A = \{a_1, a_2, ..., a_n\}$ due to the value of structural sign S.

Sequence number $NUM(A,S,n)$ for a binary sequence $A = \{a_1, a_2, ..., a_n\}$ with the length n a bit due to the value of structural sign S is calculated with a formula:

$$NUM(A,S,n) = \sum_{i=0}^{n-1}(a_{i+1} - a_i)\frac{(n-i)!}{l_i!(n-i-l_i)!} - a_n. \tag{5}$$

l_i - amount of remaining changes between '0' and '1' elements of binary sequence at the position between a_{i+1} та a_i:

$$l_i = l_{i-1} - |a_i - a_{i-1}|; \quad l_0 = s; \quad a_0 = 0.$$

Conclusion

The scientific novelty of research, described here, consists in the following:
- the expedience of the use of structural code in the tasks of compression of data is proved;
- the structural signs of binary sequences and their limitations are defined;
- the rule of determination of amounts of binary sequences, which form structural groups due to the structural signs is described and well-proven;
- the rule of calculation of sequence number of binary sequence in a structural group by value of amounts of transitions between the binary elements of sequence is described;

The got results allow to make a conclusion about expedience ofsubsequent usage of the offered method of coding of binary information in technologies of compression.

References

1. *Урсул А.Д.* Нестатистические подходы в теории информации / А.Д. Урсул // Вопросы кибернетики. – 1967.– №2.– С.88-93.
2. *Шеннон К.* Работы по теории информации и кибернетике / К. Шеннон. – М.: Изд-во иностр. лит-ры, 1963. – 793 с.
3. *Юдін О.К.* Методи структурного кодування даних в автоматизованих системах управління / О.К. Юдін. – К.: НАУ, 2007. – 210 с.

UDC 651.928(045)

V. A Shvets, PhD; V. V. Shestakova (National Aviation University)

THE USE OF FINGERPRINTS IN THE ELLIPTIC CURVE CRYPTOSYSTEMS

Proposed the use of fingerprints as the primary source for cryptographic systems on elliptic curves, as well as methods for detection of characteristic fragments reflecting fingerprints.

Entry. In recent years cryptosystem needed, based on elliptic curves (technology ECC - Elliptic Curve Cryptography), are widely used in comparison with classical cryptosystems. Improvement of the technology involved in standardization bodies such as NIST (National Institute of Standards and Technology), IEEE (Institute of Electrical and Electronics), ANSI (American National Standards Institute) ANSI (American National Standards Institute) and others.

One of the areas of number theory and algebraic geometry - the theory of elliptic curves over finite fields - has found application in modern cryptography. The main reason for this is that the elliptic curves (EC) over finite fields have virtually inexhaustible source of finite Abelian groups that are convenient for computation and have a rich structure [1].

Elliptic Curve Cryptosystems belong to the class of public-key cryptosystems. Their security is usually based on the difficulty of solving the problem of discrete logarithm in the group of points of an elliptic curve over a finite field. These are all due to their high reliability of comparison with other algorithms. There are persistent cryptoalgorithms for EC based on difficulty decomposition of large integers, when EC is set over a finite ring assembly in the module, but they are rare. However, it should be noted that the reliability is a relative notion related to the notion of the best known algorithm cracking system. With regard to the EC cryptosystem is an algorithm Silver-fallen-Hellman, Pollard and others. In the absence of information about some EK (secret key), these algorithms are subject to exponential time. In addition, the time that has elapsed since the first publication of the cryptosystem to EC (1985-1986 gg. Koblyts N., W. Miller), a significant drop in resistance algorithms EC has not happened. Whereas, the stability of RSA, based on the factorization problem, decreased approximately by one order per year. All this demonstrates the high reliability algorithms EC. Cryptosystems on EC can be effectively used for digital signatures and key exchange. Already the previous standard ANSI X9.62, which offers developers create powerful principles of digital signature based on the use of EC. Note that the security of such systems digital signature based not only on the stability of the algorithm at the EC, but also the stability of the used hash function. Do not forget about the requirements for the random number generator. And yet, today cryptosystem on EC is the most promising asymmetric cryptosystems.

In many ways, the EC is a natural and convenient analogue of multiplicative groups of fields, since the choice of EC is characterized by greater freedom of choice than a finite field. Elliptic curves are described by cubic equations, the general form of:

$$y^2 + axy + by = x^3 + cx^2 + dx + e, \qquad (1)$$

where a, b, c, d and e are real numbers satisfying certain simple conditions. To use the elliptical cryptography is not required to set the parameters that define the elliptic curve, ie the set of parameters for cryptographic protocol. Elliptic curve defined constants and equation (1).

If there is a curve for a given set of parameters using two methods:
• Choose a random curve, then use the algorithm counting points.
• Select a point, and then construct a curve on these points, using the technique of multiplication.

Traditionally, the source for generating keys cryptosystems EC used a random number generator. But as the source, you can use the biometric system.

Analysis of existing research. In the scientific literature source to generate key cryptosystems EC used a random number generator and no information about the other primary sensors. However, biometric characteristics of man is special and unique, so as primary sources of possible use of biometric systems.

The aim of this work to provide a solution on how to use fingerprint as the primary source for EC cryptosystems.

Most of the research. For example, we construct a graph of EC given by the equation $y^2 = x^3 + 3$.

a)   b)
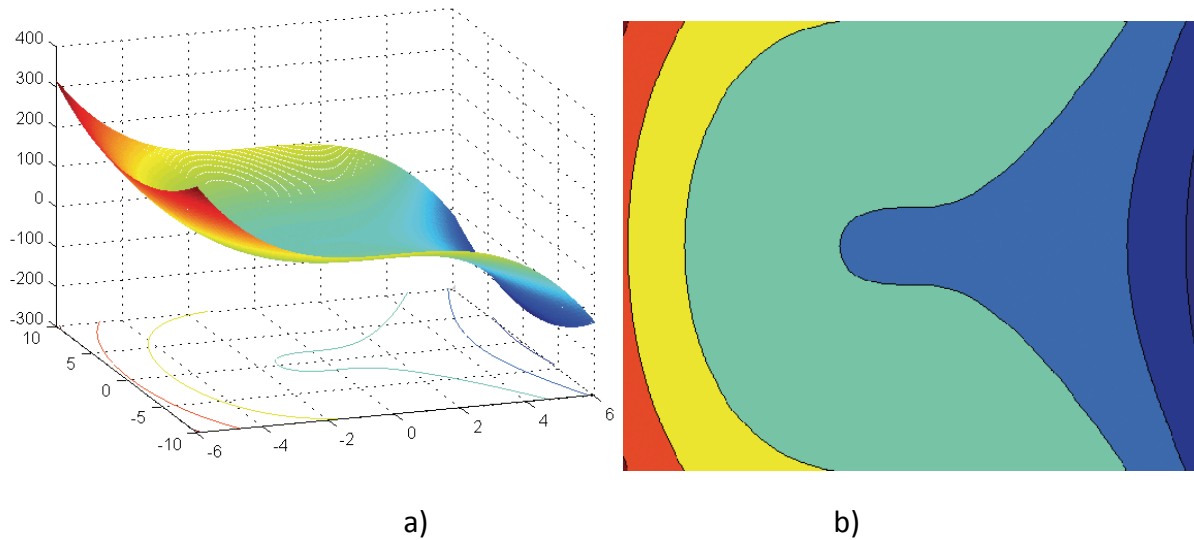
Figure 1. Schedule EC a) and its contour surface on XY plane b).

Here's fingerprint is obtained from the scanner (Figure 2.).

If we consider the papillary photography print and schedule of EC (Figure 1. b), we can say that papillary lines can be described by the EC with a certain set of parameters.

So a fingerprint can be generated by any set of points. Fingerprint always reliable, it can not lose, can not record in a notebook, and remember, received a fingerprint kit is not necessary. That is one of the sources in finding the EC can serve as a fingerprint used in biometric technologies.

Figure 2. Picture fingerprint.

To use the fingerprint cryptosystem to solve several problems:

- Convert fingerprint with shades of gray in two color black and white;
- To image processing, eliminate some point and breaks in papillary figure;
- Convert papillary lines to a thickness of 1 pixel;
- Identify characteristic fragment on the print;
- Approximated by this fragment and find the equation of the EC;
- Interpolate in integers EC and generate a key.

When scanning the fingerprint and performing authentication and user identification and verification key is added a number of problems:
- Interpolation in integers and image reconstruction fragment;
- Identifying and deciding on the authenticity of the fragment and confirmation key.

In addressing these objectives, we will use the library of image processing package MatLab (IPT).

Effectively remove noise in the image, you can use the operation circuit [2], which is an erosion, dilation applied to the result:

$A \cdot B = (A \oplus B) \ominus B$,

and release, which is defined as the erosion of A by B, followed by results performed dilatation on B:

$A \circ B = (A \ominus B) \oplus B$.

As a result of these actions were taken all the points that prevent and eliminated gaps in papillary lines thus obtained treated fingerprint (Figure 3).

For thinning papillary lines apply function bwmorph the library IPT, this feature reduces binary objects or images to form separate lines which have a thickness of only one pixel (Figure 4).

Figure 3. Processed fingerprint.   Figure 4. Thinned and inverted fingerprint.

Thus, the resulting image is a fingerprint that can be used as a source for selection of EC.

Choose your printout fragment (Figure 5.a) And hold its approximation by points obtained in integers interpolates EC. The result of the interpolation is shown in Figure 5.b.
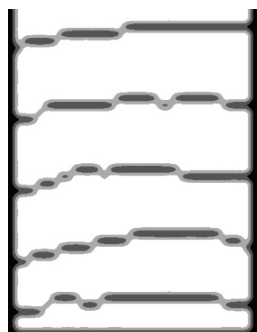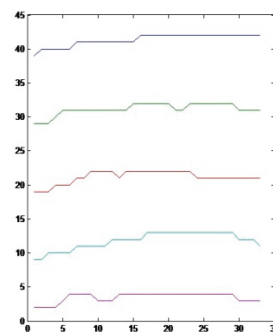
a)   b)

Figure 5. A fragment of fingerprint a), the result of interpolation b).

The figure shows a complete coincidence fragment fingerprint and calculated EC, ie have a fingerprint can calculate many EC or choose papillary line and calculate the EC point.

1.7.16

Repeated scanning exactly replicate fingerprint impossible, but you can not repeat itself imprint, and its fragments, as it was shifted imprint and papillary pattern does not change. Then it is necessary to solve the problem of detecting copy of the reference fragment for fingerprints.

As a reference fragment take images obtained by interpolation EC (Figure 5 B).

Consider two methods to identify the location of the fragment to the newly introduced print.

"The method of matching." We will "drag" selection throughout the matrix and count the number of matches (differences), black and white dots. If all the points are the same, then differences should ideally be 0.

Number display the differences in a graph (Fig. 6).

In Fig. 6 that there is a clear minimum, which means that the second matrix print reference fragment present first matrix.
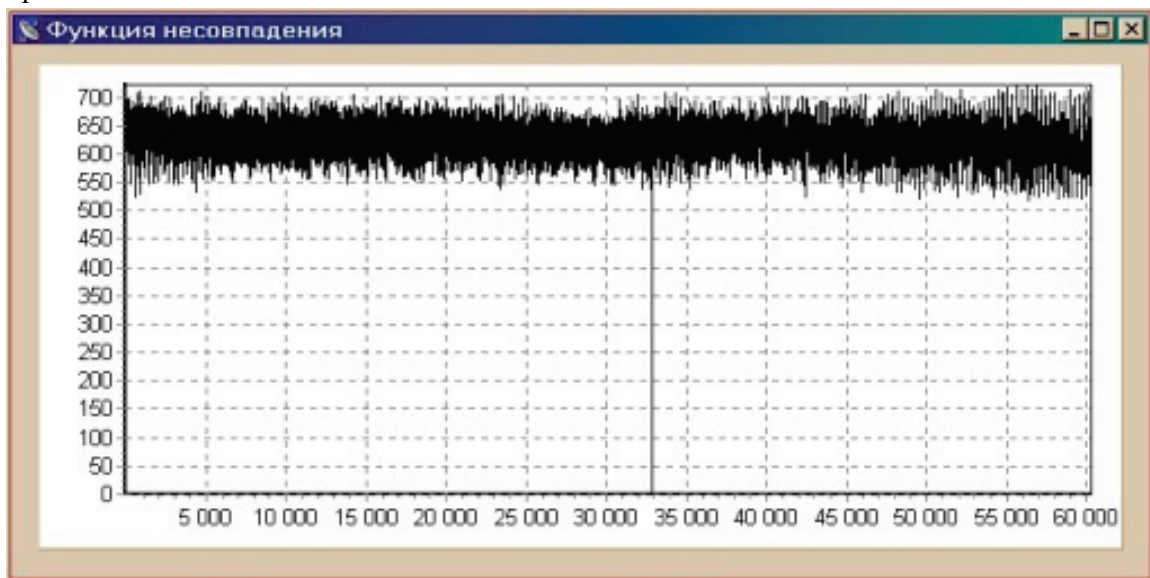
Figure 6. Figure discrepancies fragments.

So you can spend authenticate and verify key generation.

The second method that can be used - finding a more complex relationship between the two reflections, such as finding the correlation function of the reference fragment of a second fingerprint, which can be called "correlation-coordinate method" (Figure 7.).
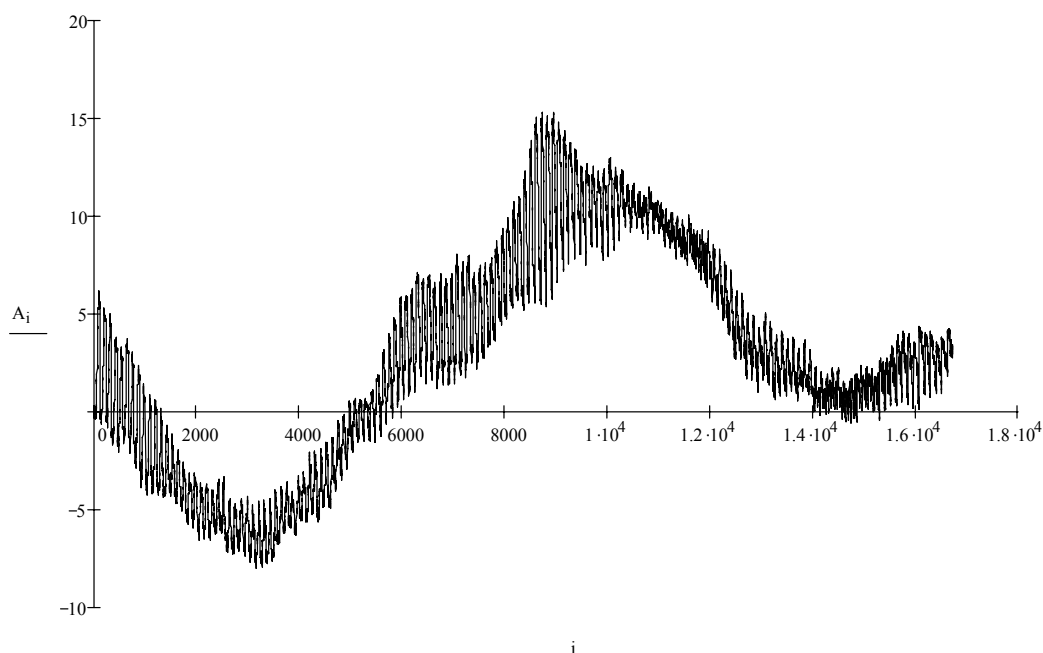
Figure 7. Correlation function of the reference fragment on fingerprint.

Maximum correlation function indicates the presence of the reference fragment fingerprints entered a second time.

Analyzing these results it can be argued that both methods can be of practical use for the detection of characteristic fragments for fingerprints entered several times. I would like to note that the "matching method" is more accurate and sensitive to the "correlation-coordinate method."

With the first, you can calculate the location coordinates inside the image prints and other parameters, while the maximum of the correlation function has no explicit maximum, so using it can be judged only on the availability of the reference fragment on another imprint.

Conclusions

The proposed solutions suggest the possibility of using fingerprint as the primary source for EC cryptosystems.

When processing a fingerprint can be a set of points for calculating EC. Following the discovery of a fragment fingerprint to authenticate and key generation with the use of elliptic curves.

References

1.   Алгоритмические основы эллиптической криптографии / *А. А. Болотов, С. Б. Гашков, А. Б. Фролов и др.* – М.: МЭИ, 2000. – 100 с.

2.   Цифровая обработка изображений в среде MATLAB / *Р. Гонсалес, Р. Вудс, С. Эддинс* – М.: Техносфера, 2006. – 616 с.

UDC 004.056.32

B.Y. Korniyenko, Ph.D. , O.K.Yudin, D. Sc. (National Aviation University, Ukraine)

THE DEVELOPMENT AND IMPLEMENTATION OF ENTERPRISE INFORMATION SECURITY POLICY

The basic principles of information security policy enterprise, its development and effective implementation. Certain key legal, institutional and engineering aspects of information security policies of the enterprise.

In practice in information security systems understand the physical maintenance of the safety, integrity, availability, confidentiality, accsssuracy and timeliness of information and guaranteed performance tools used for input, storage, processing and transmission.

The problem of information security is comprehensive, its solution should be a combination of legislative, administrative, organizational and program-technical measures.

Consequently, policy information security company - is a set of formal (approved or traditionally generated) rules governing the functioning of the information security [1]. Information Security Policy of the company provided selected class security systems and a set of organizational and administrative measures. Creating a security policy is one of the first requirements for information security organization as a whole and separately for each system that functions in the enterprise. This is due to the fact that is now widely used electronic means, thriving electronic eavesdropping, hacking, electronic fraud, espionage, etc.

The aim of the study is to describe the main principles of information security policy of the enterprise, its development and effective implementation.

The main purpose of information security policy - to ensure the safety of information and communication resources enterprise network by implementing the most efficient and optimal cost of security, minimize the level of information risks in order to prevent damage to the company [2].

The establishment of information security policy including already operating facilities information space of the enterprise and information network, including hardware, software and network security. This is due to the fact that the introduction of the system in operation, you can not avoid infringement established and maintained the level of information security and, of course, necessary to provide protection for creating an information system.

You must accept the legal basis for policy, as the legislative level involves the development and introduction of legislation, regulations and other regulations governing information security in computer systems at the state level.

Organizational (management) level involves the development and monitoring of comprehensive measures to support specific mode of information security of automated systems. The main objective is to develop an organizational level integrated security policy, organization of its effective implementation at the sites of automation. With regard to personnel working with automated systems, security policy must necessarily contain complex internal regulatory, organizational and operational controls, which include the methods of selection and placement of personnel, their training and development, ensuring discipline in the workplace. Organizational level necessarily must include measures of physical protection of premises and equipment from the threat of various origin .

To maintain information security mode are particularly important programmatic and technical measures that are based on a set of measures to ensure the physical safety of data, control the reliability of information processing, data protection against unauthorized access and use, check the most important in terms of information security events from to identify the sources of threats.

The required reliability, maintenance and security achieved in developing and using various mechanisms to ensure the reliability and security when processing data that affects the effectiveness of the policy.

Politics is the control mechanism under the existing risk and should be designed and developed in response to existing and potential risks. Thus, the full implementation of the risk assessment should be the first stage of the process of creating policy. Risk assessment should identify the weakest areas of the system and should be used to determine future goals and remedies.

Information security policy serves as a document or a multi-tiered system of documents that define the security requirements, the system measures or procedures, staff responsibilities and control mechanisms to ensure information security company. In security policy document recommended the following sections make:

1. The introductory section that confirms concerns management of information security problems.

2. Organizing a section that describes the units, commissions, groups of persons responsible for work in the field of information security.

3. Classification section that describes the physical and information resources of the enterprise and the necessary level of protection.

4. Staffing section that describes the security measures personnel.

5. Section that highlights the physical protection of information.

6. Section management that describes the approach to the management of computers and computer networks data transfer.

7. The section states that the rules of differentiation of access to information.

8. Section that describes measures to ensure continuous operation of the enterprise (access to information).

Effective information security policy defines the necessary and sufficient set of security requirements. It has minimal effect on productivity, adapts business processes, supported by management, positively perceived and executed employees.

Recommendations for the development and implementation of effective name

Accounting major factors that influence the effectiveness of name, determines the success of its development and implementation. The following recommendations are basic principles of effective name.

Information Security Policy - product of collective creativity. Recommended to include the working group following employees of the organization:

- Senior manager;
- Manager, responsible for implementing and monitoring compliance with information security policy;
- An employee of the legal department;
- Officer personnel;
- Representative of users;
- Technical expert;
- Experts on information security policy.

Continuity of learning

Training users and administrators of information systems is essential for the successful implementation of information security policy. Only conscious compliance information security policy leads to a positive result. Learning is realized by introducing everyone with the name under painting, publication name, mailing users newsletters, seminars and presentations, as well as individual advocacy violators information security policy requirements. If necessary for safety violators imposed sanctions foreseen name and internal regulations.

Continuous monitoring and responding to security breaches

Control of information security policy regulations can be done through scheduled inspections in the framework of the audit information security.

Politics should have not recommended, but mandatory. Responsibility for policy violation must be clearly defined. Violation of the name must be provided for specific disciplinary, administrative penalties and liability.

Continuous improvement of security policies

Name is not set phrases and forever established truths. You should not try to solve by implementing information security policy once all problems information security. The policy is the result of concerted decisions that determine the basic requirements for information security and reflect the current level of understanding of the problem at the company. In order to remain effective name should be periodically adjusted. Must be defined responsibility for supporting name to date and are intended intervals of revision. Policy should be simple and clear. Avoid complications that make policy unworkable. For this reason, it should not be long.

Supporting the company's management

At the implementation stage name crucial support company management. Information security policy into effect by order of the board chairman of the enterprise and the process of its implementation should be located in his control. In the name should be spelled out clearly concerns matters of leadership information security. From the coordinator of the working group on the management of the organization's name should be explained the risks that arise in the absence of the name, as prescribed in information security policy measures of information security must be economically justified.

Conclusions

Thus there is a general method of construction and implementation name, which would provide a reliable flow of information and its direct integrity, availability, confidentiality and authenticity. The most complete security can be ensured only through an integrated approach to this issue. You must constantly monitor new developments in this area.

Information security policy of the enterprise is part of a comprehensive information security system, so its design, implementation and realization of a very important task for information security department. Critically important condition for success in the field of enterprise is the organization of work and the creation of conditions for the implementation and support of high priority to information security.

References

1. Golubtschenko O.L. Polityka informacijmoji bezpeky. – Lugansk.: Vidavnyztvo SNK im. V.Dalia. - 2009. – 300 s.

2. Gmurman A.I. Informacionnaja bezopasnost – M.: «BIT-M». - 2004. –387 s.

UDC 003.26:621.39:530.145

O.K.Yudin, Doctor of Science, Professor
O.Veselskaya, Graduate
(National Aviation University, Kyiv, Ukraine)

CRYPTOGRAPHIC OF **WIRED EQUIVALENT PRIVACY** PROTOCOL AND HOW IT CAN BE IMPROVE

In the article the quality of information security in wireless networks by using WEP encryption scheme and RC4 symmetrical streaming algorithm was studied. The tips and ways to improve the security of information are given.

Introduction. In September 1999 IEEE-SA Standards adopted two wireless networks: 802.11b - 2,4 GHz, 11 MB and 802.11a - 5 GHz, 54 MB. Since wireless network quickly spread to all spheres of human activity, such as trade, education, health, etc. An important factor in the spread of wireless networks and turn them into existing networks is the need for access to essential business applications and resources 24 hours. a day and need to use the basic services and personal data away from the user. In addition, interoperability was facilitated by independent testing organizations such as Wireless Ethernet Compatibility Alliance (WECA) [1]. Security of wireless networks - is the biggest drawback that hinders total replacement of wired networks. Today, wireless networks IEEE 802.11 There are several generations of standards and protect:WEP, WPA, WPA2 (IEEE 802.11i); using authentication protocols IEEE 802.1x; using VPN (Virtual Private Network) to build a secure network for sharing data [3]. **Problem**. The research within this paper seeks to analyze security of wireless networks using optional encryption scheme WEP (Wired Equivalent Privacy). The objectives of this study are: research quality protection that provides encryption scheme WEP; research productivity WEP depending on the methods of its implementation and the possible methods of raising, research reliability symmetric streaming algorithms RC4; recommendations and possible methods for improving information security in wireless networks using WEP.

Analysis methods of protection WEP. Encryption scheme WEP is optional, however, despite this, is the mechanism of the first generation of secure interaction between peers and protection of data in wireless networks. The main objectives *WEP* are: restrict access to unauthorized users that do not have corresponding WEP- key; prevent decryption of data encrypted with WEP, with no WEP-key. WEP is a symmetric encryption mechanism. If WEP enabled, the transmitter takes the contents of the frame, which is only useful information and runs the encryption algorithm on it. Then the original contents of the frame is replaced with the data obtained after the implementation of the encryption algorithm. Personnel data are encrypted link with WEP-bit in the control field MAC-header. The recipient of the encrypted data frame passes through the frame is identical to the encryption algorithm as the sender. As a result, the output we get the original frame, which is transmitted to the upper levels, according to the hierarchical model of OSI [3]. Productivity WEP depends on the type of implementation - software or hardware, as well as the particular device. Some devices can achieve performance, only 2-3% worse than without encryption. However, very often, especially when program implementation is sensible decrease network performance WEP uses the stream cipher RC4, which was proposed by Ron Rivest from RSA Data Security, Inc. (RSADSI). Encryption algorithm RC4 - a symmetric stream cipher that supports keys of different lengths. Symmetric cipher - a cipher that uses an identical key for encryption and decryption. It differs from the block ciphers that process a fixed number of bytes. Key - is some information which is available in both the sender and recipient. RC4 allows different key length - up to 256 bits. In IEEE 802.11b selected key length of 40 bits. However, some manufacturers also support 128-bit key and attach the device to work with the key length. RC4 algorithm has the following properties: adaptability for hardware and software (SW), which means using it only computational primitive operations used by conventional processors, compact in terms of key size, and especially beneficial for processors with bitwise-oriented processing, low memory requirements, to implement the algorithm on devices with limited memory, simplicity and ease of implementation. Algorithm of RC4 is built like any stream cipher based on parameterized key

generator of pseudorandom bits from a uniform distribution (Gaussian normal distribution). Key length is usually from 5 to 64 bits. The maximum key length - 256 bits [2]. RC4 algorithm consists of two parts: 1.Creating a keys (sometimes called the extension key) 2. Encryption Algorithm.

Creating keys. RC4 key is a sequence of bytes of arbitrary length, which is based on the initial state of the cipher S - permutation of all 256 bytes. At the beginning of the algorithm, S is filled with successive values from 0 to 255 K and filled key (at necessarily to fill the entire array of key repeats). Then every regular element S_j exchanged places with element numbered i, the number of which is determined by the key element of K, and thus part of the sum of numbers of elements, which exchange took place in previous iterations, ie. $j = S_i + K_i + j$. **Encryption algorithm.** Another element of the pseudorandom permutation S_i all bytes exchanged with the element S_j, where $i = (i + 1)$ mod 256, and $j = (j + S_i)$ mod 256. Structure encrypt the message is: the original text is taken from a file, the key sequence according to the WEP encryption scheme can be either 5 or 13 characters, respectively; key can consist of small and large letters of the alphabet and Arabic numerals, key sequence generated by the generator of pseudorandom numbers stored in the file, the original message is encoded using the RC4 algorithm to demonstrate the application is stored in the file in two formats: a symbolic and hexadecimal. Standard IEEE 802.11 provides two mechanisms for selecting key for encryption and decryption frames. The first mechanism is based on establishing four keys by default. Keys default should be known to all stations wireless subnet. The advantage of using the default keys is that if the station received the keys, it can carry data sharing secret with all other stations subnet. The disadvantage of using this mechanism is that keys are available to all stations, and therefore quite likely to hacking or unauthorized receipt. The second mechanism that provides a standard IEEE 802.11, allows stations to communicate with each other on certain different keys («key mapping»). It is probably more secure form of work, as fewer stations known key. However, the distribution of keys is problematic if the number of stations in the network is large enough [1]. IEEE 802.11 defines two types of authentication methods: open system authentication and authentication with distributed (shared) key. Successful implementation phases of authentication and connection allows wireless node successfully enter the wireless network. When authentication with public key authentication whole process is an open text provided standard. If authentication with the distributed key in the authentication process used encrypted messages. WEP header and tail attached to the encrypted body frame. Most key by default, which should be used to decrypt the frame becomes the KeyID title shot with initialization vector. The ending contains Integrity Check Value (ICV) for controlling the correctness of the transmitted frame. Key length is usually divided by the length of WEP key and initialization vector length. For example, 64-bit key consists of 40-bit WEP-key, which is kept secret, and the 24-bit initialization vector [3]. **Disadvantages secure IEEE 802.11 and possible ways to overcome them.** The most important drawback is the lack 802.11 best way to key distribution. Statistical distribution that is defined in the standard specification, is available in pure form for large networks and for long stretches of time. Also, it is difficult to keep a secret key if the network should have access unauthorized users. Another drawback of the statistical distribution of the keys is that the passive monitoring of data streams in the network for a long time, possibly amass enough information about the key that will decrypt the message easily. Excluding this shortcoming needs to create dynamic key distribution schemes, their constant updating and assigning keys not to the node network, and the user (unauthorized user to know only their own key, and if it is widespread third party was available only to its traffic) . Another important drawback is that there is only 802.11 authentication process the client and authentication server is not available. This makes it possible to attack the network by feeding it unauthorized servers and redirect data traffic to them. Another vulnerable point data standard to them IEEE 802.11 has its own encryption algorithm RC4, which is implemented in WEP. And although the company RSA Data Security stated that the code has immunity to the methods of linear and differential crypto analysis is highly nonlinear and its algorithm does not use short cycles, its reliability has been questioned because of unauthorized disclosure of program text that used this code, but it directly threatened the security of wireless networks using WEP as an encryption scheme [1]. In this paper, Jovan Holicha that concerned the reliability analysis indicated the algorithm was noted that the sequences generated by RC4, not suitable methods of statistical analysis. But, on the other hand, for units that are larger than the size of the internal memory of the generator, there is always a linear statistical weakness or the so-called

"linear model." Such a model can be effectively determined using the method of linear sequential circuit approximation (ALPS). Linear statistical weakness - is a linear relationship between the bits gamut performed with a probability different from 1/2. In practical terms linear model J. Holicha can be used for selection in encryption generator RC4 among other cryptosystems as well as for determining word algorithm. In 2000 he published an article Flyuera C. and D. Mc Gre devoted to statistical analysis of stream generator RC4, in which were used in the work of J. Holicha for finding the value of the component S-box. Estimated time of this method is, where n - the portion of bits in the output stream, the length of the original sequence that is required for the statistical weakness of RC4, Such a model can be effectively determined using the method of linear sequential circuit approximation (ALPS). In 2000 he published an article Flyuera C. and D. Mc Gre devoted to statistical analysis of stream generator RC4, in which were used in the work of J. Holicha for finding the value of the component S-box. Estimated time of this method is, where n - the portion of bits in the output stream, the length of the original sequence that is required for the statistical weakness of RC4, approximates 2^{30}. The received result specifies essential weakness of the generator and a possibility of restoration of parameters i and n. Possible ways of increase of stability RC4 to breaking is the increase of length of a key up to the maximal value in 256 bytes and realization of its dynamic variation, used for enciphering messages, but it, in turn, will negatively affect throughput of the wireless data link. An alternative method of overcoming of weaknesses in the diagram of enciphering WEP is use of tunneling through a wireless network (IPSec, SSL / TLS). However, there are decisions, which do a wireless network safe in itself (WPA, WPA2) [3].

Conclusion

All attacks on WEP cipher based on deficiencies RC4, such as the possibility of collisions initialization vectors and frame. For all types of attacks to carry out the interception and analysis of data frames wireless network. Depending on the type of attack, the number of frames that need to crack WEP, different. After the adoption of the 2004 IEEE 802.11i standard WEP encryption scheme is considered outdated and one that does not provide reliable protection of your wireless network, but continues to be widely used as a means of protection and support equipment manufacturers to wireless networks in hardware and software implementations. I should say that WEP should be used only in the home and small enterprise networks, where it is processed classified information, according to the Law of Ukraine "On information". Following the regulations of Ukraine in the field of technical and cryptographic security. Thus, the use of WEP encryption scheme as a protocol for securing wireless networks may only be used in automated systems (AS) class 2 [5]. According to Sun TPI 2.5-005-99 WEP corresponds to the standard functional profiles of security in the computer system (CS), which is part of the AU class 2 with special requirements for privacy and confidentiality and integrity of information processed: 2.K.1 and 2.KTS.1. Thus, WEP encryption scheme without additional protection can be used in networks where sensitive information is handled with security classification "For Official Use Only," according to the Sun TPI 1.1-003-99, et al. Confidential information is defined directly owns that information as to require additional protection [4].

References

1. A. Proletarian, IV Baskakov, DN Chirkov, G. Fedotov, A. Bobkov, V. Platonov. Wireless Networks Wi-Fi. - M.: binomial. Laboratory known, 2007. - 216 p.

2. Behrouz A. Forouzan. Kryptohrafyya and safety of networks. Textbook. - M.: binomial. Laboratory known, 2010. - 784 p.

3. M. Maxim, D. wormwood. Safety Wireless Networks. - M.: Company AyTy; MQM Press, 2004. - 288 p.

4. Sun TPI 1.1-003-99 Terminology in the field of information security in computer systems from unauthorized access.

5. Sun TPI 2.5-005-99 Classification automated systems and standard functional profiles machined protection of information from unauthorized access.

UDC 004.728

A.Tikhomirov, Doctor of Science, Professor
(International Informatization Academy, Moscow , RF)
A.Trufanov, PhD, Professor
(Irkutsk State Technical University, Irkutsk, RF)
A.Caruso, Doctor of Science, Professor
(Court of Auditors, Regional Chamber of Control , Milan, Italy)
A.Rossodivita, Medical Doctor, Professor
(San Raffaele Hospital Scientific Foundation, Milan, Italy)
R.Umerov, Postgraduate
(National Aviation University, Kyiv, Ukraine)
Z.Umerova, Postgraduate
(Crimean Engineering and Pedagogical University, Simferopol, Ukraine)

DISASTER MANAGEMENT IN CONDITIONS OF GOVERNANCE FAILURE: ZEROING IN ON NETWORK MODELS

The need in strong cooperation and collaboration among all entities and actors while countering disasters has been considered. Proposed Comprehensive Network Lace as an end-to-end description of major categories of interactions for sets of entities using a multilayer variety of complex networks has been applied to model counteracting operations in conditions of poor state and social governance.

Introduction. In order to counteract disasters and emergencies it is necessary to build cooperation and collaboration among all entities and actors. While this headquarters and field teams of rescues feel need of supporting State power at the place of an event.

Cooperation and collaboration, i.e. information sharing and integration based on new ICT approaches are of value for the most sensitive fields:

- Disaster Medicine
- Intelligence Services

US State power for Intelligence:

Catalyst program will support IC information sharing and integration objectives

Information Sharing: Office of the Director of National Intelligence. 2010 Data Mining Report. For the Period January 1, 2010 through December 31, 2010

ODNI Civil Liberties and Privacy Office (CLPO) works closely with the ODNI Office.

CLPO has been considering how advanced technologies, employed in accordance with proper laws and policies, enable sharing and use of information while protecting privacy and civil liberties.

Haiti Earthquake case demonstrated lack of a State power and concomitant difficulties for international rescuers which had encountered with. Thus the problems in the Disaster field are not only of Natural and Technological aspects but those of Social and Political.

 It has been a time to explore the role of State power impact on national and international counteracting Global Disasters and Emergencies. One of the modern and fruitful analysis instruments for complicated social and group processes is Complex Network modeling.

In any discipline the large number of participants - subjects, objects, actors - and their relationships (interactions) suggests that such a set (chain) of interacting entities itself has some common fundamental features.

These network properties of the set, depend on its structure, rather than on internal contents of individual entities.

While math graph theory studies structural properties, interdisciplinary intersection has formed a new filed : theory of networks.

Applications of the theory of networks find themselves wherever there is a network, i.e everywhere.

Examples of meaningful and relevant networks are:

Internet; WWW; Network Governance, Economic Network, Social Networks, Knowledge Networks; Political networks, TV networks, National and local transportation routes (air, rail, water, metro, bus, tram); Electrical network; Communications (postage, telephone); Thermal network water supply and sanitation; Trade networks; webs of nervous system; intelligence networks; terrorist networks.
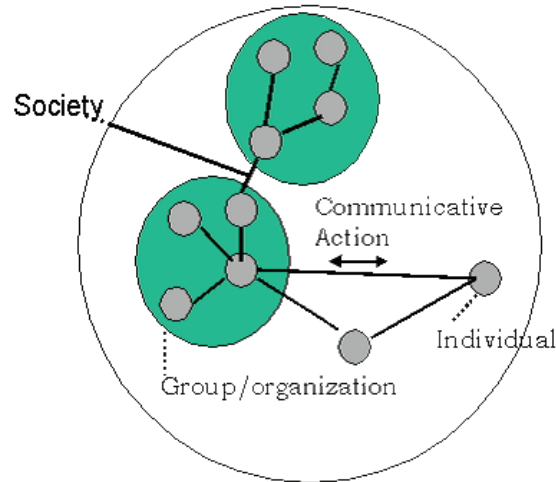
Fig. 1. Subjects and objects of networks

US State power for the National Security. Discovery of unknown terrorism relationships: Office of the Director of National Intelligence. 2010 Data Mining Report. For the Period January 1, 2010 through December 31, 2010

National Counterterrorism Center (NCTC) uses network analysis tools to discover relationships between Known and Suspected Terrorists (KST) and their associates.

A new program known as DataSphere will enhance data fusion and entity resolution, as well as discovery of unknown relationships. DataSphere, enables analysis of the activities of terrorists such as their communication networks and travel.

Advances in theory and practice of networks. Graph Theory originated in the moment when Leonhard Euler, Swiss, German and Russian mathematician, decided to prove that a passerby can not get around Konigsberg (modern Kaliningrad), using only one each of the seven city bridges.

Its key conclusion is: structural characteristics of graphs (networks) define a potential for their use. The first example of using the methods of modern algebra in graph theory accounts for the work of the physicist Gustav Robert Kirchhoff, in 1845 he formulated so called Kirchoff's laws to calculate voltages and currents in electrical circuits. Mathematician Dénes Kőnig published in 1936 a book titled "Theory of finite and infinite graphs" - the first textbook in the field of graph theory.

Introduction of probabilistic methods in graph theory, especially in research of Paul Erdős and Alfréd Rényi on asymptotic probabilities of graphs created another branch known as theory of random graphs.

Modern complex systems are attributed by high number of elements, which can reach tens and hundreds of thousands, and irregular ties.

The term "complex" is the best for such systems and their network models with non-trivial topological properties.

Resilience of network architecture is one of the major problems of building effective complex social, biological, technical and other systems.
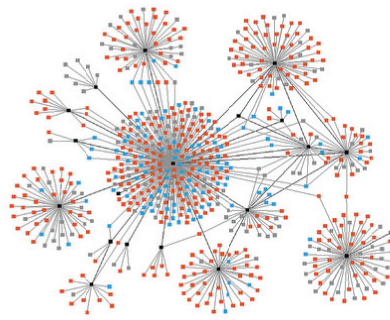
Fig.2. Integrated complex networks

Graphical representation of [A.-L. Barabási, R. Albert, H. Jeong. Mean-field theory for scale-free random networks. Physica .1999, A 272, P. 173-187] bypassed the whole world, and is widely used to demonstrate the exponential (a) and scale-free (b) networks.
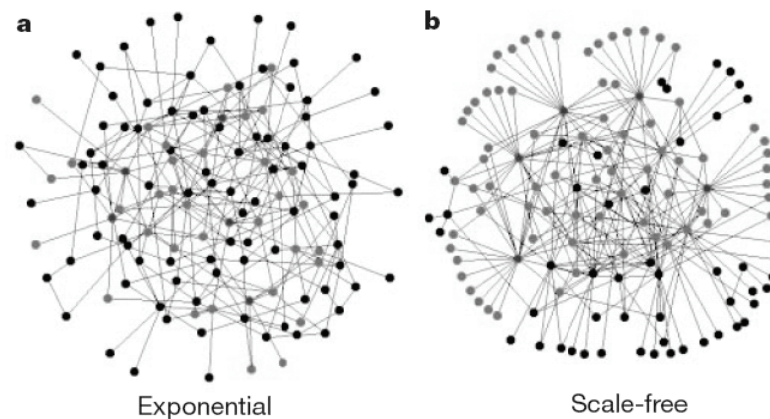
Fig.3. Graphical representation of network

Complex Network tools have been successfully applied to understanding and counteracting such threats as infection diseases spread and terrorist activity. Contrary another significant utilization of Complex Network approach is to develop good governance, management and organizational processes in international, national and corporation landscapes.

Problems and limits of applicability of current network models. Complex Network ideas have been steadily and successfully applied to the analysis of metabolic and genetic regulatory networks, in developing reliable scalable networks of wired and wireless communications, for development of vaccination strategies in fight against diseases, as well as a wide range of other practical issues.

However, neither in public nor in the corporate governance these ideas have not been applied widely and significantly. Many problems of modeling of organizational structures and cross-sectoral governance are resolved, the issues of control of complex networks continue to be complex and daunting.

This can be seen in the discussion of various approaches in directing of the Internet Governance Forum network (IGF)

Most biosocial systems are characterized by some degree of inequality of individuals, so that part of the system, individuals differ in their (Bio) Social ranks. Set of ranks-hierarchy- forms special relationships and their correspondent performance – hierarchical one. Hierarchical and egalitarian structures in many biosocial systems coexist and continually interact with each other.

Often one and the same biosocial system is considered by researchers and practitioners from different points of view : depending on the preferences the focus is either hierarchy with domination and subordination, or presence of equal relations in the system.

Researchers constantly faces with the competing nature of networks and their contrasting.

Many distributed systems, particularly cellular networks, computer networks and the Internet possess developed topologies and are based on complex and diverse social processes.

According to the founder of the technology of World Wide Web T. Berners-Lee, the next step in the development of the World Wide Web can be a GGG "Giant Global Graph'. Berners-Lee believes that such a graph, in contrast to a network of computers and the WWW, linking documents, interconnected people and, based on semantic technologies that provide users with services of higher class than the existing one.

Comprehensive networks as a new approach in studying of huge and especially complex systems. The concept of Comprehensive Network Lace CNL is based on an end-to-end description of major categories of interactions for sets of entities (subjects and objects) using a multilayer (multi-level) variety of complex networks.
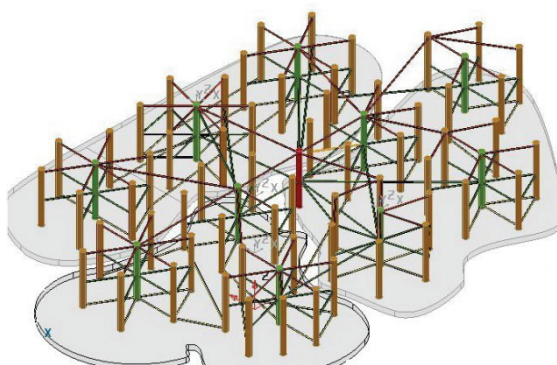
Fig.4. The approach of pair interactions of subjects (actors) in a separate thematic layers (TL)

The core of the approach is binary interactions of entities (actors) in a separate thematic layers (TL). In simple words, graph is a set of points (for convenience, the image - on the plane) and linked in pairs by lines, the CNL – is a set of points in the different thematic planes and corresponding joint lines.
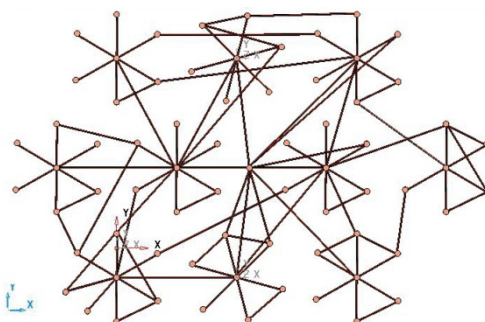
Fig.5. The sets of points and lines of communication

Actor of the Lace in a Comprehensive Network is a stem, stems attach the nodes of networks of different thematic layers (TL)
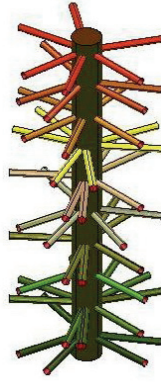
Fig.6. Lace actors in the CNL-trunks, stems attached network nodes different thematic layers (TL)

A classic graph has no two distinct edges connecting the same pair of vertices (nodes), in a Lace the number of links connecting a pair of stems might be multiple to the number of layers.
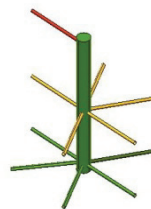
Fig.7. Thematic layers (TL) in the social system to determine the relations between family members, classmates, members of one the organization and department, superiors and subordinates-mi; colleagues in the same domain, and so on.

Thematic layers in a social system are defined by relationships between: 1. relatives; 2. classmates; 3. employees of one organization and agencies, superiors and subordinates; 4. colleagues in one subject area; 5. neighbors and childhood friends; 6. countrymen; 7. coreligionists; 8. friends on interests; 9. business partners; 10. random acquaintances.

Based on a Comprehensive Network Lace Scope in this work we propose a novel 3 Layer model of public connections for diverse State regimes for further simulation, quantitative assessment, and practical implementation in countering Global Disasters by international and interdisciplinary teams.

Principal findings and results. Based on a Comprehensive Network Lace Scope in this work we propose a novel 3 Layer model of public connections for diverse State regimes for further simulation, quantitative assessment, and practical implementation in countering Global Disasters by international and interdisciplinary teams.
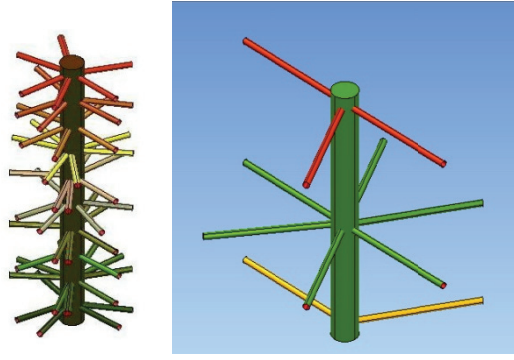
Fig.8. Third layer of government regulation

Traditionally the process of Emergency Management involves four phases: mitigation, preparedness, response, and recovery.

Contrary to known hierarchical layer application for Knowledge Acquisition and Information Sharing this new model describes an overall national Society Network by division that into the next three layers:

-Formal (State), as hierarchical governments structures

-Informal (presented by different long time sustainable link groups)

-Informal (acquaintances with short term links-so called weak ties)

The approach considers ambiguously communications between actors which are on different levels of hierarchy in a Comprehensive Network (eg information exchange, is modeled in several streams of information, formal and informal, from the more meaningful stem in a given hierarchy to peripheral one).

Summary. According to each of these layers –Severely State Formal, Sustainable Group Formal-Informal , and Severely Informal ones- we watch ONE of 3 types of Network topologies: hierarchical, scale –free, or random respectively.

Fig.10. Three types of network topologies

Mapping brings the next of CNL illustrations in case of State power degradation.

Information exchange is supported by diverse links, formal and informal, for different power State status.

New metrics to assess an imbalance of formal and informal structures of social control, has been proposed:

1) M_c- moments of centralities for the node i and the centrality C (degree centrality, betweenness centrality, or closeness centrality):

$$M_{Ci} = (\sum_{j \neq i} C_j \cdot L_{ij})/(n-1)$$

L_{ij} – the path length between nodes i and j, n - number of nodes   (stems) in the network;

2) Nodes $I_{\min,C,t}$ of thematic layer t, for which the moment of centrality C

 have minimal value in the layer t;

3) Shift of t_2 in t_1:

$$S_{Ct1,t2} = (\sum_{jt2 \neq i} C_{jt2} \cdot L_{IminCt1,jt2})/(n-1)$$

$L_{\text{Imin, Ct1, jt2}}$ is a path length between (a node for which the time of the centrality of C has a minimum value within layer t1) and jt2 (a node in layer t_2), t_1, t_2 $\in$t;

4) Set (vector) of centralities for a stem: [C_d, C_b, C_c];
5) Set (vector) centrality moments for a stem : [M_{Cd}, M_{Cb}, M_{Cc}];

References

1. M.Aminova, A.Caruso, A.Rossodivita, A.Tikhomirov, A.Trufanov, R.Umerov. State Failure as a Factor in International Global Counteracting Medical Opeations: Network Modelling / World Congress on Disaster and Emergency Medicine, Beijing, China, 2011.

2. А.Россодивита, А.Труфанов, Р.Умеров / Новые аспекты применения IT-рычагов (доктрин, моделей, инструментов) в противодействии глобальным угрозам. - К.: Информацио Консорциум, 2010. - 64 с.

3. R.Laporte, A.Trufanov. Information Security Approaches to Provide Social System Continuity in Conditions of Chemical, Biological, Radiological and Nuclear Threats. In "Strengthening National Public Health Preparedness and Response for Chemical, Biological, and Radiological Agents Threats". C.E.Cummings and E.Stikova (Eds.) IOS Press, 2007. Pp.45-52];

4. A.-L. Barabási, R. Albert, H. Jeong . Mean-field theory for scale-free random networks. Physica A 272, ,1999,p. 173–187.

5. F.Galindo, M.Guidotti,V.Gulevich,E. Gursky, S.Kolesnikov, S. Koptilov , R. Laporte, F.Linkov, M. Ranghieri,A. Rossodivita , E. Shubnikov , E. Stikova, A. Trufanov , and N.Vinograd. Information Sharing in Knowledge Society. Collection of Absracts, ASI "Preparing Regional Leaders with the Knowledge, Training and Instruments for Information Sharing and Decision-Making against Biological Threats and Pandemics", November, 30 - December 8, 2008, Milan, ITALY, p.12-15

6. Tikhomirov A.A., Trufanov A.I. Hyper-complex networks: new models for socio - economic and bio-social processes interpretation. [Electronic resource]. Available from: <http://www.pitt.edu/~super1/lecture/lec43841/index.htm>

A.Rossodivita, Medical Doctor, Professor
(San Raffaele Hospital Scientific Foundation, Milan, Italy)
A.Trufanov, PhD, Professor
(Irkutsk State Technical University, Irkutsk, RF)
R.Umerov, Postgraduate
(National Aviation University, Kyiv, Ukraine)

SOME NEW IN IT-LEVERAGES (DOCTRINES, MODELS, TOOLS) TO PROVIDE

In the paper are considered chaotic international environment impedes the process. Randomness, even with reservations (though sometimes very serious) is recognized by all researchers and associated with unresolved security problems. Problems of psychological and ethical character.

Introduction. Information exchange is the paradigm of all living things.

The modern technology of information exchange is thoroughly describes in 7-layer OSI model [1]:

OSI Model

	Data unit	Layer	Function
Host layers	Data	7. Application	Network process to application
		6. Presentation	Data representation, encryption and decryption, convert machine dependent data to machine independent data
		5. Session	Interhost communication
	Segments	4. Transport	End-to-end connections and reliability, Flow control
Media layers	Packet	3. Network	Path determination and logical addressing
	Frame	2. Data Link	Physical addressing
	Bit	1. Physical	Media, signal and binary transmission

However, a genuine knowledge transfer process is more complex than technological one only. It includes numerous operations and mechanisms. And where advanced knowledge is really shared, there is a significant breakthrough in science or practice. Only a few examples of this – the project "Large Hadron Collider» LHC European Centre for Nuclear Research [2] or treatment of Alzheimer's disease [3].

But currently one of the main features of information exchange – chaotic international environment impedes the process. Randomness, even with reservations (though sometimes very serious) is recognized by all researchers and associated with unresolved security problems. While the governments exits, public and personal safety will not be total nor absolute, but remain a relative and always depend on political will of "rulers". Surely, relationships are not limited to intergovernmental cooperation, and international politics is not simply foreign political activities of governments . But it might be a mistake to underestimate the role of the governments which continue to play in assessing the challenges and opportunities of the outer world, to adapt the nation to the international environment, to preserve its identity, the promotion of values, in other words, the national security in the broadest sense of the term. This is especially true in today's globalizing

world, where the "economization, informatization and the democratization of international relations creates unprecedented opportunities for development, but also make the system more vulnerable to terrorism, weapons of mass destruction may have information weapons" [4].

Niehl de Grasse Tizon, chairman of the Council of the Planetary Society: "If people ever die because of the catastrophic collision, it will be the greatest tragedy in the history of the universe. Not because we do not have enough brain power to protect themselves, but because we do not have enough foresight. The dominant view, which will replace us in a post-apocalyptic Earth may be interested in looking at our fossil skeletons in the museum of natural history, why the Big-Homo sapiens foresaw no better than the notorious dinosaurs with pea-brains in ".

Michael Crichton, author of "The strain Andromeda", "Jurassic Park" and "Victims". Creator of the television series ER:

"Sometime in the 21 century our complete folly of self-deception to face with our growing technological power. One area where this happens will be a meeting point of nanotechnology, biotechnology and computer technology. The common factor is that all three - is the ability to produce self-replicating objects in the environment."

"Nobody does anything until then, until it is too late. We put a traffic light at the intersection only after there will be crushed by a child. "

"They did not understand what they are doing. I am afraid that this inscription is carved on the grave of mankind.

Sensitive area of information exchange of information security. The very subject area overgrown with numerous myths [5].

With the collapse of the rigid bipolar structure with the poles of the USSR-USA, determines the degree and nature of the involvement of factors not only in the "high" (the security concerns, war and peace), but also "low" politics (covering issues of cultural exchanges, scientific and professional contacts ...), the invasion of new active participants in both these areas has become a truly result in a vast nature.

Thus, in addition to traditional international factors, States and international institutions, to involve new members, such as sub-structures, transnational corporations, NGOs, various associations, stable groups (up to the Mafia) and prominent individuals. But perhaps even more impressive are the changes we are making today in the nature and status of international relations involved in these kinds of temporary associations and "unorganized" individuals. This participation becomes a source of pure chance in the field of international relations and entail a transition from a situation of risk inherent in the Cold War, to a situation of doubt and associated One might specify the following developing and effective IT-tools countering global threats:

– Mass- Media
– Any information transport systems that carry cultural, ethical and moral components,
– Affordable and adequate language in the Investment Bank, supported by glossaries, dictionaries, including as general technical and mathematical sublanguages, especially graphics tools, as new language support for the exchange of information (mapping).
– Complicated complex social network, and within network models not only of hierarchical, but also random and scale-free nature [7].
– A global, flexible network of alert-tracking-information support, coordination, anti-training and employment specialists counter global threats to mankind [8].

For implementation of the new IT-leverage in countering global threats it seems useful to organize international interdisciplinary non-governmental portal.

While optimizing the network for information exchange with international portal, one should apply a more effective organization of information. Optimization is considered as removing the limitations of traditional methods of government to citizen services. In particular, this limited time period for the implementation of transactions, which in this case coincides with the working hours of most businesses, companies, organizations, while the network is needed around the clock to respond. To optimize the field is and to allow free public access to the resources of the portal. First of all, this decision purely technical issues - arrangement of public access points. A good example is

the system of the Australian state of Victoria MAXI, became the winner of various awards. MAXI - a single unit of public services, available not only to desktop computers with Internet access, but also in 50 stalls, as well as by phone 24 hours a day, 7 days a week, 365 days a year [9]. The system provides transactions between local government and individuals and legal persons. It was found that about 40% of transactions running through MAXI, carried out after working for government officials time. The benefits for citizens is obvious. But in countering global threats greatly reduced the problem of time trouble time to respond effectively. This approach reengineering IT-management tools due to the human factor. [10]

There are a number of problems of psychological and ethical character. High rate of introduction of electronic forms of information exchange should adequately correspond to the rate of psychological adjustment, which is especially important in countries with underdeveloped information infrastructure, which dictates the preservation for a long time, a parallel off-and online services. This is a fairly lengthy process. It requires changing the culture of relationships and changes in the forms of interaction, development of new habits all the actors [11].

Thus, the principle of the portal is the concept of management coordination, based on potential of information and telecommunication technologies and values of an open civil society, characterized by economic efficiency, openness, both for the initiatives, and for public scrutiny. The architecture of the portal assumes the inherent embodied in the concept of modularity: P2G, (Portal to government) - Government portal; P2B, (Portal to business) - portal business; P2C, (Portal to citizens) - citizens portal.

References

[1] http://en.wikipedia.org/wiki/OSI_model;

[2] http://en.wikipedia.org/wiki/LHC;

[3] G. Kolata. Rare Sharing of Data Leads to Progress on Alzheimer's. The New York Times, Published: August 12, 2010, (http://www.nytimes.com/2010/08/13/health/research/13alzheimer.html?pagewanted = 1 & _r = 1 & th & emc = th).

[4] E-government. UA - first steps. Alexander Brahms. 04/02/2002. http://www.ain.com.ua/politeconomia/2002/02/04/970.html;

[5] R. Laporte, A. Trufanov. Information Security Approaches to Provide Social System Continuity in Conditions of Chemical, Biological, Radiological and Nuclear Threats. In Strengthening National Public Health Preparedness and Response for Chemical, Biological, and Radiological Agents Threats ". C. E. Cummings and E. Stikova (Eds.) IOS Press, 2007. Pp.45-52];

[6] Allan. 1994. P. 65;

[7] A.-L. Barabási, R. Albert, H. Jeong. Mean-field theory for scale-free random networks. Physica A 272, 1999, p. 173-187.

[8] A. Rossodivita. "Creating a global network to respond to global Threat and training in an interdisciplinary approach, willingness responding to global threats "

[9] The system of the Australian state of Victoria MAXI;

[10] F. Galindo, M. Guidotti, V. Gulevich, E. Gursky, S. Kolesnikov, S. Koptilov, R. Laporte, F. Linkov, M. Ranghieri, A. Rossodivita, E. Shubnikov, E. Stikova, A. Trufanov, and N. Vinograd. Information Sharing in Knowledge Society. Collection of Absracts, ASI "Preparing Regional Leaders with the Knowledge, Training and Instruments for Information Sharing and Decision-Making against Biological Threats and Pandemics", November, 1930 - December 8, 2008, Milan, ITALY, p.12-15;

[11] A. Rossodivita, F. Galindo, E. Gursky, R. LaPorte, F. Linkov, E. Shubnikov, E. Stikova, A. Trufanov,; N. Vinograd. Interagency Collaboration Topology for Counteracting Global Threats International Preparedness & Response to Emergencies & Disasters. 11-14 January 2010 Hilton, Tel Aviv, Israel, Program and Book of Abstracts, p. 78.

UDC 519.816

Gulak N.K., Ph.D. (NAU, Ukraine)

METHODS OF ANALYSIS AND PERFECTION OF THE ORGANIZATIONAL AND INFORVATIVE PROVIDING OF FAST OF CUSTOM SERVICE

The basis of the system of support of acceptance of decisions (SSAD) was going. The structure's scheme of local SSAD was appearing. The means of construction was describing and the principal matter of the stage of construction SSAD for operation personnel of the custom.

The perspective reference points of development of custom organs of Ukraine must be based on front-rank information technologies and to allow to perfect the organizational and informative base of activity of custom organs.

The basic directions of researches in custom service:

- creation of program-information's complex «Data-base home and foreign scientific researches on custom business»;

    - reformation of structure and optimization of activity of custom service;

    - perfection of the informative providing of activity of custom service.

The method of choice of rational structure of the system of support of acceptance of decisions for the operative personnel of fast of custom service (FCS).

The system of support of acceptance of decisions (SSAD) for custom service of Ukraine is the distributed system including the aggregate of local SSAD, each of which executes the functions. The model structure of local SSAD is resulted on figure 1.

From all job mix of planning of distributed SSAD we will select two most essential tasks – choice of PC and distributing of functions between local SSAD.

The basic criteria of choice were: cost, productivity, volume of operative and of long duration memory, ergonomic.

The decided task behaves to the class of tasks of multicriterion optimization. For the decision of task a lexicographic method was chosen as most simple and requiring to minimum expert information about the preference of criteria.

Distributing of functions between local SSAD is enough the model task of planning of the difficult technical systems. With the purpose of minimization of the temporal expenditures related to the exchange by information between local SSAD and the cost of apparatus must concentrate in the local SSAD function, having maximal intercommunication.

Methods being based on the scission of counts are the most effective methods of decision of similar tasks.

The task of distributing of functions between local SSAD is presented as a task of the integer linear programming.

A task can be interpreted as a task of scission of the eventual oriented count in which to the tops the volume of memory is put in accordance, by the occupied definite function, and great number of arcs – algorithmic tie-up of functions. Decisions of task consist of scission of count on sub columns satisfying to the terms of minimum of function having a special purpose and limitations.

For the decision of task are developed heuristic algorithms being based on the directed search of lines and elements of matrix of tie-up of tops of count with the maximal degree of tie-up.

The resulted methods allowed to set the requirements to the personal computers for the single system of management of custom service of Ukraine and distribute functions between the elements of this system.

We will consider the problem of method of choice of rational model of representation of knowledge (MRK) for realization of base of knowledge.
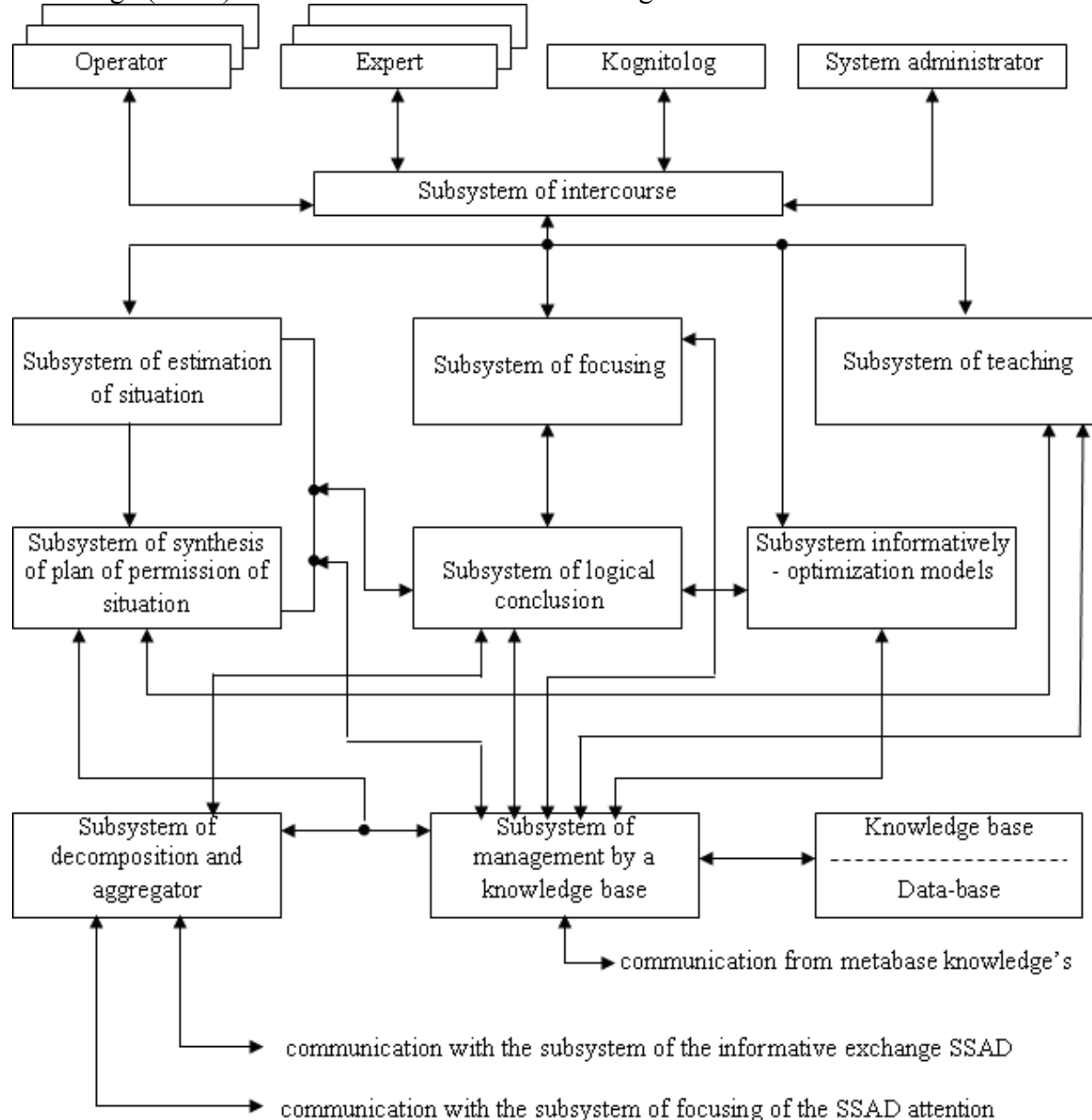
The Fig. 1

Essence of problem of knowledge representation consists of their formalization, i.e. in setting of knowledge's to on a formal language. The row of base MRK and their modifications is known (products models, a neuron and synoptically networks, frames, hybrid models and etc). each of models takes advantages and failing, therefore there is the scientific task of the rational choice MRK.

The offered method is based on application of expert estimations and includes next stages.

First stage. By an experimental way the importance of indexes of the MRK quality is determined.

For determination of importance of indexes of quality exists about 20 methods.

From considering of simplicity and comfort of application by us the method of the own vectors Ueya, being based on application of matrix of pair comparisons of indexes, was chosen. As a result of expert estimation the indexes were well-organized as follows:

$$C_2 > C_1 > C_5 > C_4 > C_3 > C_7 > C_6$$

For estimation of co-ordination of opinions of experts concordats was calculated. He turned out equal 0,75, that speaks about good co-ordination.

Second stage. It is determined by the degree of accordance to each to the MRK set indexes . The data presented in table were got as a result.

Third stage. Choice of model of knowledge representation for the SSAD realization. For the decision of multi-criterion task of optimization the method of languish- graphic organization, essence of which was set forth above, was applied**.**

As a result of decision of task expedience of application was shown in SSAD hybrid frame - products model of knowledge representation.

For the SSAD realization on a basis the frame - to the production model a practical method, including forming of knowledge base of every local SSAD, selection of operations of processing of knowledge's, is developed, test tuning of the system.

The got results were fixed in the basis of task of requirements to local SSAD, providing informative support of acceptance of decisions by the personnel of custom service.

Conclusions

Method of synthesis of optimum structure of distributed SSAD on the basis of the use of aggregate - decomposed approach which includes:

heuristic algorithm for the decision of task of distributing of functions between local SPPR, that is based on the close method of scission of counts;

method of choice of PC for realization of the system of support of acceptance of decisions on the basis of application of lexicographic method of multi-criterion optimization;

method of optimum organization of functioning of distributed SSAD in the conditions of large load.

The novelty of method consists in realization of aggregate - decomposed approach for the decision of task of the nonlinear mathematical programming by its decomposition on some private tasks of synthesis of the SSAD elements and organization of its functioning.

References

1.*Nilp*. Blackboard systems. The blackboard model of problem solving. AT Magazine, 1986, vol.7 p.p. 38-53.

2.*Wei T.H.* The algebraic foundations of ranking theory Theses. Cambridge, 1952, 35p.

3.*Saaty Thomas L* Eigenweinghtor an logarithmic lease sguares // Eur. J. Oper. Res. – 1990. – V.48. - # 1. – P. 156-160/

4. *Герасимов Б.М.* Системы поддержки принятия решений: проектирование, применение, оценка эффективности /Б.М. Герасимов, Н.М. Дивизинюк, И.Ю. Субач – Севастополь, СНИЯЭиП, 2004. – 320 с.

5. *Герасимов Б.М.* Принцип побудови й перспективи застосування інтелектуальних систем / Б.М. Герасимов, О.К. Оксіюк, Н.К. Гулак // Науково-технічна інформація. – 2006. - №2. – С. 48-52.

6. *Попов Э.В.* Экспертные системы: решение неформализованных задач в диалоге с ЭВМ /Э.В. Попов – М.: Наука, 1987 – 288 с.

UDC 004.056.5(045)

V.S. Vasilenko, PhD; A.V.Chunarova, PhD; A.V. Chunarov
(National Aviation University, Ukraine)

THE EFFECTIVENESS OF METHODS OF CODING IN ENSURING THE INTEGRITY OF INFORMATION IN MODERN INFORMATION SYSTEMS

In the article the analyses of existing methods of noise-immune channel coding of secure information networks. Defined quantitative evaluation of effectiveness of the use of the code with conditional residues provided to increase the integrity and accuracy of information that is stored, transmitted and processed in a modern information networks.

Relevance. Today, the process of accumulation, storage and transfer of information and communication systems and networks (ICSN) occur under the influence of both intentional and random noise. These noise of natural or artificial character can distort stored and processed data, i.e., violate basic properties of information, namely the confidentiality, integrity and availability. In this regard, noise-immune coding occupies a special place among the methods and facilities of fight against threat of violation of basic properties of information. Noise-immune coding is performed in order to protect information against random and deliberate noise in the transmission and storage of information in modern ICSN. To solve problems of transmission and protection of information in real communication systems is necessary to end the use of different techniques and tools and the application of noise-immune coding helps to effectively use the communication channels for reliable protection of the transmitted and stored information.

Statement of the problem. Increasing the speed of data transmission in the communication channel carries a number of random and deliberate noise on distortion of information that is stored, transmitted and processed in a modern information networks. This leads to the urgency of the development and use of new techniques that allow you to detect and correct such noise. In these conditions, special attention deserve the noise-immune codes which, unlike the cryptographic encryption and compression, to effectively deal with the random and deliberate noise in the channel.

Noise-immune coding given two main tasks:
− improving the efficiency and reliability of secure information systems and networks;
− increasing the level of security of these systems and networks.

Using the methods of noise-immune coding to achieve stability and security information ICSN allows to control functions and storage of information and ensures the correctness of these processes, but also provides protection against unauthorized actions and distortion. In this regard noise-immune coding necessarily imply further recovery and identification of information in the original form, suitable to be used in the processing and decision-making quality. Flawless recovery will reduce the likelihood of errors in decision making.

We can provide other benefits need to use noise-immune coding ICSN: reliable processing and storage, fighting grouping errors in secure systems and networks, information security in the transfer of public keys, etc.

The **purpose** of this article is to conduct a comparative analysis of existing methods of noise-immune channel coding data streams protected ICSN.

Comparative analysis of modern methods of noise-immune coding. Modern networks are widely used existing redundant codes with error detection (they only detect the error) and codes of the correction (these codes identify errors and fix it). For different types of noise in the communication channel there are different in their structure and redundancy design - noise-immune codes. Usually code redundancy is within 10 ...50%, or a little more. Block codes are widely used for quick detection and convolution codes for correcting single error. The most common among the block codes are codes of parity check, matrix codes, Hamming codes, cyclic (for example, Bose-Chaudhuri-Hocquenghem and Reed-Solomon codes). There is also a class of residual codes, including the code with conditional residues, residual-Hamming code (RH-code), residual-matrix

code (RM-code) [1, 2]. Classification of modern methods of the noise-immune coding.

Also modern noise-immune codes are classified into generalized and binary. ***Binary code*** - a code that are designed to detect (detection and correction) unitary errors. ***Generalized code*** designed to detect (detection and correction) packet distortion (multiple errors) with multiplicity b, which use coding and decoding algorithms, similar to the corresponding binary algorithms, but with respect to the generalized b - bit character.

Operations on generalized characters are performed to some of the modules, that searched the smallest residue or remainder of dividing the operation result for a module. This gave the opportunity to distinguish the corresponding generalized from binary codes to enter in their name the word "residue" that talk about code conditional residue, residue-Hemming, residue-matrix, residue-recurrent (RR) codes. It should be noted that residues-cyclic codes known as Reed - Solomon codes - on behalf of the authors of these codes [3, 4].

At this time, the types of noise-immune coding differ from each other in the following characteristics: relative speed, redundancy, identifying and correcting capability, structure, functionality, energy efficiency, etc. When choosing the type and use of noise-immune coding to improve the reliability and integrity of information flows ICSN must be taken into account: the distribution of errors in the communication channel; acceptable probability of error in the code combination; complexity algorithms for coding.

One of major factors of a choice of a code is character of distribution of mistakes in a liaison channel which defines correcting capacity of such code. Mistakes arising in actual liaison channels are dependent and tend to a grouping (packing), that is there are repeated mistakes. However, the majority of currently available methods of *noise-immune* coding a direction on revealing and updatings only unitary mistakes and completely lose the sense at occurrence of repeated batch mistakes.

The basic characteristics of methods of *noise-immune* coding. Further for carrying out of an assessment of efficiency of existing methods of coding it is necessary to define their characteristics on which they will be comparable. It is possible to carry the following to the basic characteristics [1]:

1. Relevancy of a code, or length of a base code word which includes information symbols (*m*) and verifying, or control, bats (*k*). Certainly relevancy of a code is drunk with the sum

$$n = m + k \qquad (1.1)$$

2. Relative speed of a code - *R* is the attitude of number of information symbols in a code combination m to impressiveness of a code *n*:

$$R = m/n \qquad (1.2)$$

3. Redundancy of a code is the attitude of number of control symbols in a code combination *k* to impressiveness of a code *n* and shows correcting capacity of a code:

$$K = 1 - m/n = 1 - R \qquad (1.3)$$

4. *Probability of occurrence of symbolical mistakes in a channel with the coding* Pc:

$$Pc = Q\left(\sqrt{\frac{R \cdot E_c}{N_0}}\right), \qquad (1.4)$$

where $Q(x) = \dfrac{1}{\sqrt{2\pi}} \displaystyle\int_{x}^{\infty} \exp\left(\dfrac{-u^2}{2}\right) du$ − integral of mistakes, $\dfrac{E_c}{N_0}$ − The attitude of energy of the coded bit to spectral density of capacity of noise in a channel.

Further we shall result an assessment of efficiency of use of currently available methods of *noise-immune* coding with objective of integrity of the information. For comparison the most widespread methods of *noise-immune* coding which are used for integrity by transfer and storage of the information (tab. 1.1-1.2) have been chosen. In the table methods of block coding (Hamming code, CRC-32, CRC-64 and a matrix code) with objective of revealing of mistakes and a class residual codes on the basis of revealing and correction of packages of mistakes are shown. We shall lead the comparative analysis of a code of conditional surpluses with existing methods of *noise-*

immune coding / decoding of information streams and we shall show efficiency of application from the point of view of integrity of the information dataflow.

Let's define an assessment of efficiency of use of a code of conditional surpluses from conditions of maintenance of reliability and integrity of code designs and to increase of protection of the information in modern ICSN. For an assessment of quality of a code of conditional surpluses the probability of occurrence of symbolical mistakes by frequency rate t from the set parity a signal / noise in a channel has been calculated.

From the received analytical and graphic dependences, it is possible to draw following conclusions:

−first, use of a code of the conditional rests in problems of integrity allows to reduce quantitative values of probabilities of occurrence of symbolical mistakes has decreased from 1,02 to 2,82 times for a code of the conditional rests in comparison with known methods;

−secondly, at use of a code of conditional surpluses redundancy depending on the used noiseproof code has decreased from 2 up to 13,4 times that has allowed to reduce complexity of realization of a code

−thirdly, relative speed of a code at use of a code of the conditional rests has increased from 1,01 up to 1,11 times.

Conclusions

In article the comparative analysis of existing methods of *noise-immune* channel coding of information streams ICSN. Carried out researches have shown, that application of residual codes allows to raise integrity and reliability of the information, is stored, passed and processed in modern information networks. Thus it is shown, that at use of a code of the conditional rests there is a reduction of probabilities of occurrence of symbolical mistakes and the further full elimination of distortions in a report of information from conditions of occurrence of repeated mistakes that raises efficiency and reliability of functioning ICSN from conditions of an increase of probability of the information dataflow.

That is, there is a reduction probability of occurrence of symbolical mistakes and full elimination of distortions in a report of information. Use of the given code allows to detect and correct repeated mistakes and to eliminate distortions. Also, there is an increase of speed of data transmission, an increase of the possible dataflow, savings of a strip of frequencies ICSN.

References

1. *Скляр Б.* Цифровая связь. Теоретические основы и практическое применение / Пер. с англ. – М.: Изд. дом Вильямс, 2004. – 1104 с.

2. *Юдін О.К.* Кодування в інформаційно-комунікаційних мережах – Монографія. К.: Книжкове видавництво НАУ, 2007. – 302 с.

3. *Василенко В.С.* Узагальнені завадостійкі коди в задачах забезпечення цілісності інформаційних об'єктів в умовах природних впливів / В.С. Василенко // Правове, нормативне та метрологічне забезпечення системи захисту інформації в Україні. –2006. – Вип. 2 (13) – С. 144 −159.

4. Пат. 67988 Україна, МПК Н03М 13/00 Спосіб забезпечення цілісності інформації на базі завадостійкого коду умовних лишків/ Василенко В.С., Василенко М.Ю., Чунарьов А.В.; заявник та патентовласник Нац. авіац. ун-т. – u201110207; заявл. 19.08.2011; опубл.12.03.2012, Бюл. №. 5 – 4 с.

5. *Чунарьов А.В.* Забезпечення цілісності інформаційних ресурсів на базі методів завадостійкого кодування/ А.В.Чунарьов, М.Ю.Василенко // Наукоємні технології: наук.-техн. конф. студентів та молодих учених (Київ, 11–12 листопада 2011 р.) – К.: Вид-во Нац. авіац. ун-ту «НАУ-друк», 2011. – С.11.

UDC 003.26:621.39:530.145

S.O. Gnatyuk, PhD, Associate Professor
O.G. Korchenko, Doctor of Science, Professor
(National Aviation University, Kyiv, Ukraine)

COMMERCIAL QUANTUM INFORMATION SECURITY SYSTEMS

In this paper the qualitative analysis of existed quantum information security systems is carried out. Their prospects and difficulties of implementation in modern information and communication systems are showed. In addition, the main results of projects to develop quantum information security systems are given.

Introduction. The main features of information security (IS) are confidentiality, integrity and availability (named CIA-model) [1]. Only providing these all gives availability for development secure information and communication systems. *Confidentiality* is the basic feature of IS, which ensures that information is accessible only to authorized users who have an access. *Integrity* is the basic feature of IS indicating its property to resist unauthorized modification. *Availability* is the basic feature of IS that indicates accessible and usable upon demand by an authorized entity. One of the most effective ways to ensure confidentiality and data integrity during transmission is cryptographic systems. The purpose of such systems is to provide key distribution, authentication, legitimate users authorisation and encryption. *Key distribution is one of the most important problems of cryptography*. This problem can be solved with the help of such methods [1-2]: a) Classical information-theoretic schemes; b) Classical public-key cryptography schemes; c) Classical computationally secure symmetric-key cryptographic schemes; d) Trusted Couriers key distribution; e) Quantum key distribution (QKD) [1-3]. The main advantage of last method is information-theoretic security. No one classical method gives that possibility. That's why IS systems using QKD are very effective and prospect. The main purpose of this paper is the analysis of existed quantum IS systems, their prospects and difficulties of implementation in modern information and communication systems.

Review of commercial quantum IS systems. The world's first commercial quantum IS system was *QPN Security Gateway (QPN-8505)* [4] proposed by MagiQ Technologies (USA). This system (fig. 1 a) is a cost-effective IS solution for governmental and financial organizations. It proposes VPN protection using QKD (up to 100 of 256-bit keys per second, up to 140 km) and integrated encryption. The QPN-8505 system uses BB84, 3DES and AES protocols. The Swiss company Id Quantique offers a systems called *Clavis*^{2} (fig. 1 b) and *Cerberis* [4]. Clavis^2 uses a proprietary auto-compensating optical platform, which features outstanding stability and interference contrast, guaranteeing low quantum bit error rate. Secure key exchange becomes possible up to 100 km. This optical platform is well documented in scientific publications and has been extensively tested and characterized. Cerberis is a server with automatic creation and secret key exchange over a fibre channel (FC-1G, FC-2G and FC-4G). This system can transmit cryptographic keys up to 50 km and carries out 12 parallel cryptographic calculations. The latter substantially improves the system's performance. The Cerberis system uses AES (256-bits) for encryption and BB84 and SARG04 protocols for QKD. Main features are future-proof security, scalability: encryptors can be added when network grows, versatility: encryptors for different protocols can be mixed and the last is cost-effectiveness: one quantum key server can distribute keys to several encryptors.

Toshiba Research Europe Ltd (Great Britain) recently presented another quantum IS system named *Quantum Key Server* [6]. This system (fig. 1 c) delivers digital keys for cryptographic applications on fibre optic based computer networks. Based on quantum cryptography it provides a failsafe method of distributing verifiably secret digital keys, with significant cost and key management advantages. The system provides world-leading performance. In particular, it allows key distribution over standard telecom fibre links exceeding 100 km in length and bit rates

sufficient to generate 1 Mb per second of key material over a distance of 50 km – sufficiently long for metropolitan coverage. Toshiba's system uses a simple «one-way» architecture, in which the photons travel from sender to receiver. This design has been rigorously proven as secure from most types of eavesdropping attack. Toshiba has pioneered active stabilisation technology that allows the system to distribute key material continuously, even in the most challenging operating conditions, without any user intervention. This avoids the need for recalibration of the system due to temperature-induced changes in the fibre lengths. Initiation of the system is also managed automatically, allowing simple turn-key operation. It has been shown to work successfully in several network field trials. The system can be used for a wide range of cryptographic applications, e.g., encryption or authentication of sensitive documents, messages or transactions. A programming interface gives the user access to the key material.

| a) | b) | c) |
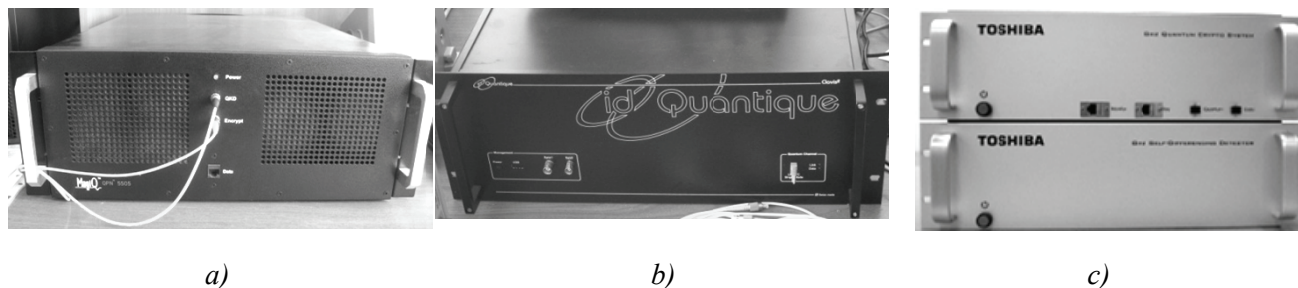
Fig. 1. Most popular commercial quantum IS systems

Another British company, QinetiQ, realised the world's first network using QKD – *Quantum Net (Qnet)*. The maximum length of communication lines in this network is 120 km. Moreover, it is a very important fact that Qnet is the first quantum IS system using more than two servers. This system has six servers integrated to the Internet.

Main projects in QKD. In addition the world's leading scientists are actively taking part in the implementation of projects (to develop quantum IS systems) such as SECOQC (Secure Communication based on Quantum Cryptography), EQCSPOT (European Quantum Cryptography and Single Photon Technologies) and SwissQuantum [1]:

1) SECOQC is a project that aims to develop quantum cryptography network. The European Union decided in 2004 to invest € 11 million in the project as a way of circumventing espionage attempts by ECHELON (global intelligence gathering system, USA). This project combines people and organizations in Austria, Belgium, the United Kingdom, Canada, the Czech Republic, Denmark, France, Germany, Italy, Russia, Sweden and Switzerland. On October 8, 2008 SECOQC was launched in Vienna. During the SECOQC the seven most important quantum IS systems have been developed or refined. Among these QKD systems are *Clavis²* and *Quantum Key Server* described above and also: 1) The coherent one-way system (time-coding) designed by GAP-Universite de Geneve and idQuantique realizes the novel distributed-phase-reference coherent one-way protocol; 2) The entanglement-based QKD system developed by an Austrian-Swedish consortium. The system uses the unique quantum mechanical property of entanglement for transferring the correlated measurements into a secret key; 3) The free-space QKD system developed by the group of H. Weinfurter from the University of Munich. It employs the BB84 protocol using polarization encoded attenuated laser pulses with photons of 850 nm wavelength. Decoy states are using to ensure key security even with faint pulses. The system is applicable to day and night operation using excessive filtering in order to suppress background light; 4) The low-cost QKD system was developed by John Rarity's team of the University of Bristol. The system can be applied for secure banking including consumer protection. The design philosophy is based on a future hand-held electronic credit card using free-space optics. A method is proposing to protect these transactions using the shared secret stored in a personal hand-held transmitter. Thereby transmitter's module is integrated within a small device such as a mobile telephone, or personal

digital assistant, and receiver's module consists of a fixed device such as a bank asynchrone transfer mode.

2) The primary objective of *EQCSPOT project* is bringing quantum cryptography to the point of industrial application. Two secondary objectives exist to improve single photon technologies for wider applications in metrology, semiconductor characterisation, biosensing etc and to assess the practical use of future technologies for general quantum processors. The primary results will be in the tangible improvements in key distribution. The overall programme will be co-ordinated by British Defence Evaluation and Research Agency and the work will be divided into eight workparts with each workpart co-ordinated by one organisation. Three major workparts are dedicated to the development of the three main systems: NIR fibre, 1.3-1.55 μm fibre and free space key exchange. The other five are dedicated to networks, components and subsystems, software development, spin-off technologies and dissemination of results.

3) One of the key specificities of the *SwissQuantum project* is to aim at long-term demonstration of QKD and its applications. Although this is not the first quantum network to be deployed, it wills the first one to operate for months with real traffic. In this sense, the SwissQuantum network presents a major impetus for the QKD technology. The SwissQuantum network consists of three layers: *a) Quantum Layer.* This layer performs Quantum Key Exchange; *b) Key Management Layer.* This layer manages the quantum keys in key servers and provides secure key storage, as well as advanced functions (key transfer and routing). *c) Application Layer.* In this layer, various cryptographic services use the keys distributed to provide secure communications.

There are also many practical and theoretical research projects concerning the development of quantum IS systems in research institutes, laboratories and centres such as Institute for Quantum Optics and Quantum Information, Northwestern University, SmartQuantum, BBN Technologies of Cambridge, TREL, NEC, Mitsubishi Electric, ARS Seibersdorf Research and Los Alamos National Laboratory.

Conclusion. This paper presents a review of modern commercial quantum IS systems, their analysis from viewpoint of prospects and difficulties of implementation in modern information and communication systems. Quantum IS systems are rapidly developing and gradually taking their place among other means of IS. Their main advantages are a high level of security and some properties, which classical means of IS do not have. One of these properties is the ability always to detect eavesdropping. Quantum IS systems therefore represent an important step towards improving the level of data security. However, many theoretical and practical problems must be solved for practical use of these systems in existing information and communication systems.

References

1. Quantum secure telecommunication systems / *[Oleksandr Korchenko, Petro Vorobiyenko, Maksym Lutskiy, Yevhen Vasiliu, Sergiy Gnatyuk]* // Telecommunications Networks: Current Status and Future Trends / edited by *Jesus Hamilton Ortiz.* — Rijeka, Croatia : InTech, 2012. — P. 211-236.

2. *Korchenko O.* Modern quantum technologies of information security against cyber-terrorist attacks / *O. Korchenko, Ye. Vasiliu, S. Gnatyuk* // Aviation. Vilnius: Technika, 2010. — V. 14, No. 2. — P. 58-69.

3. *Korchenko O.* Modern directions of quantum cryptography / *O. Korchenko, E. Vasiliu, S. Gnatyuk* // «AVIATION IN THE XXI-st CENTURY» — «Safety in Aviation and Space Technologies»: IV World Congress: Proceedings (September 21–23, 2010) — K. : NAU, 2010. — P. 17.1-17.4.

4. QPN Security Gateway (QPN-8505) [Electronic resource]. 13.07.2012, Available from: <http://www.magiqtech.com/MagiQ/Products.html>.

5. Cerberis Encryption Solution. [Electronic resource]. 13.07.2012, Available from: <http://idquantique.com/products/cerberis.htm>.

6. Quantum Key Server. Toshiba Research Europe Ltd. [Electronic resource]. 13.07.2012, Available from: <http://www.toshiba-europe.com/research/crl/QIG/quantumkeyserver.html>.

V.Y. Kovtun, Information Security PhD
A.O. Okhrimenko, Post-Graduate Student
(National Aviation University, Kyiv, Ukraine)

PARALLELIZATION OF SOFTWARE IMPLEMENTATION OF INTEGER MULTIPLICATION

In this paper there are considered several approaches for the increasing performance of software implementation of integer multiplication algorithm for the 32-bit & 64-bit platforms via parallelization. The main idea of algorithm parallelization consists in delayed carry mechanism using which authors have proposed earlier [11]. Proposed approaches for parallelization allows increasing the total algorithm computational complexity, as for one execution thread, but decrease total execution time on multi-core CPU.

Introduction. Public key cryptosystems have a long history from first publication of Diffie and Hellman [1], which initiates basis to modern cryptosystems, for example algebraic curve cryptosystems. The increasing of software and hardware implementation of public key cryptosystems is the most important among the actual tasks to public key cryptosystems developing. Arithmetic operations in rings and fields of integer form the basis of public key cryptosystems the whole of germination time. Integer multiplication operation is the main operation in ring or field arithmetic. Thus, the increasing performance of public key cryptosystems may be achieved via increasing performance of integer multiplication operation in ring or field arithmetic. Well known, that software implementation of any algorithm depends from the architecture of hardware platform. Such CPU evolution goes to increasing a CPU clock frequency. But after the reaching of physical limitation accent moves to increasing of execution threads. The task of algorithm parallelization of arithmetic operations for integers is not new [2, 3], in these papers there are considered Montgomery multiplication and integers arithmetic for implementation on NVIDID GP GPU [2, 3]. Further evolution this line for other arithmetic algorithms allows to find more effective parallelization technique for the different hardware platforms. There are several well-known parallelization techniques: OpenMP [4, 5] for the general purpose CPU; OpenCL [6] for general purpose CPU and for GP GPU NVIDIA & AMD; Intel Threading Building Block [7] for the general purpose CPU; NVIDIA CUDA [8] for GP GPU NVIDIA; AMD Accelerated Parallel Processing (APP) [9] for GP GPU AMD.

We consider algorithms for integer multiplication and approaches for their parallelization with OpenMP technology. OpenMP technology was chosen because it supported by most modern C++ compilers for variety hardware platforms (Intel C++ Compiler, GCC C++ Compiler, Microsoft C++ Compiler). OpenMP makes it easy to implement parallelism in existing C++ programs. Other mentioned technologies are more cumbersome and less obvious, but the main idea is not change of proposed parallelization approach.

Modified Comba. Earlier, in paper [11], authors proposed a modified algorithm Comba [10] – Modified Comba, with delayed carry technique. Using 64-bit variables for storing 32-bit variables allows to get rid of keep in mind a carry from high part of 32-bit variable after the each arithmetic operation. A brief analysis of Modified Comba algorithm [11], and show main difference with prototype – Comba algorithm [10] and work out in details on Modified Comba potentialities.

The idea of delayed carry, previously described in Modified Comba Algorithm [11], has prompted authors on capability of parallel addition values in columns

$$r_0 = \sum_{k=0}^{2n-1} \mathrm{Lo}\big(a_i \cdot b_j\big) \mid k = i+j, 0 \le i, j < n \quad \text{and} \quad r_1 = \sum_{k=0}^{2n-1} \mathrm{Hi}\big(a_i \cdot b_j\big) \mid k = i+j, 0 \le i, j < n .$$ In the

classical Comba algorithm, this approach is not feasible due to fact what addition operations with carry have connectedness. The fact of carry absence in sum accumulation for Modified Comba Algorithm allowing to say about isolatedness of sum accumulation operation, which allows to execute accumulation loop on step 2 and 3 in parallel standalone (independent) threads.

Notice, after the finishing sum accumulation in all standalone threads, still need to make an adjustment (to take in accordance a carry) $r_1 = r_1 + \mathrm{Hi}(r_0)$, $r_2 = r_2 + \mathrm{Hi}(r_1)$ and compute result $c_i = \mathrm{Lo}(r_0)$. The delayed carry mechanism allows formulating several approaches to the Modified Comba Algorithm parallelization: parallel execution (in two parallel threads) of loops in the step 2 and 3 with further final result correction. We will call it Modified Comba 2x; parallel execution (number of parallel threads) of iterations in loops in step 2 and 3 with further intermediate results (from parallel threads) merging. We will call it Modified Comba Mx.

Modified Comba 2x algorithm. The algorithm contains two loops in step 2 and 3, which read elements $a_i^{(32)}$ and $b_j^{(32)}$ of corresponding arrays with further writing results of multiplication $a_i^{(32)}$ and $b_j^{(32)}$ to elements $c_k^{(32)}$. Note, indexes k in loops in step 2 and 3 do not repeat while writing to elements $c_k^{(32)}$. This allows to say about data independence in these loops and ability of parallel loops execution by the parallel technique. It will be observed, both loops in step 2 and 3 use common temporary variables r_0, r_1 and r_2. Moreover, variables r_0 and r_1 keep values which use in loop in step 3 after the loop in step 2 finished.

Thus, after the finishing loop in step 3 it will require make an correction of results of loop execution in step 3 – to take into account results of execution loop in step 2 (results keep in temporary variables r_0, r_1 and r_2). See, while loops on steps 3 and parallelization, each thread should works with own private temporary variables rl_0, rl_1 and rl_2. Global variables r_0 and r_1 will be used only for the possible carry transfer from rl_0, rl_1 loop in step 2 to further correction of results accumulation in loop in step 3. Let's consider Modified Comba algorithm parallelization via OpenMP into two threads.

Algorithm Modified Comba 2x. Integer multiplication with OpenMP supports two threads.

Input: *integers* $a, b \in \mathbf{GF}(p)$, $w = 32$, $n = \log_{2^w} a$, $nk = 2n-1$. ***Output:*** *integer* $c = a \cdot b$.

1. #pragma omp parallel sections private($r_0^{(64)}, r_1^{(64)}$) begin

1.1. #pragma omp section begin

1.1.1. $rl_0^{(64)} \leftarrow 0$, $rl_1^{(64)} \leftarrow 0$, $rl_2^{(64)} \leftarrow 0$.

1.1.2. For $k \leftarrow 0$, $k < n$, $k{+}{+}$ do

1.1.2.1. For $i \leftarrow 0$, $j \leftarrow k$, $i \leq k$, $i{+}{+}$, $j{-}{-}$ do

1.1.2.1.1. $(uv)^{(64)} \leftarrow a_i^{(32)} \cdot b_j^{32}$. 1.1.2.1.2. $rl_0^{(64)} \leftarrow rl_0^{(64)} + v^{(32)}$, $rl_1^{(64)} \leftarrow rl_1^{(64)} + u^{(32)}$.

1.1.2.2. $rl_1^{(64)} \leftarrow rl_1^{(64)} + \mathrm{hi}_{(32)}\!\left(rl_0^{(64)}\right)$, $rl_2^{(64)} \leftarrow rl_2^{(64)} + \mathrm{hi}_{(32)}\!\left(rl_1^{(64)}\right)$.

1.1.2.3. $c_k^{(32)} \leftarrow \mathrm{low}_{(32)}\!\left(rl_0^{(64)}\right)$, $rl_0^{(64)} \leftarrow \mathrm{low}_{(32)}\!\left(rl_1^{(64)}\right)$, $rl_1^{(64)} \leftarrow \mathrm{low}_{(32)}\!\left(rl_2^{(64)}\right)$, $rl_2^{(64)} \leftarrow 0$.

1.1.3. $r_0^{(64)} \leftarrow rl_1^{(64)}$. 1.1.4. $r_1^{(64)} \leftarrow rl_2^{(64)}$.

#pragma omp section end

1.2. #pragma omp section begin

1.2.1. $rl_0^{(64)} \leftarrow 0$, $rl_1^{(64)} \leftarrow 0$, $rl_2^{(64)} \leftarrow 0$.

1.2.2. For $k \leftarrow n$, $l \leftarrow 1$, $k < nk$, $k{+}{+}$, $l{+}{+}$ do

1.2.2.1. For $i \leftarrow l$, $j \leftarrow k-l$, $i < n$, $i{+}{+}$, $j{-}{-}$ do

1.2.2.1.1. $(uv)^{(64)} \leftarrow a_i^{(32)} \cdot b_j^{32}$. 1.2.2.1.2. $rl_0^{(64)} \leftarrow rl_0^{(64)} + v^{(32)}$, $rl_1^{(64)} \leftarrow rl_1^{(64)} + u^{(32)}$.

1.2.2.2. $rl_1^{(64)} \leftarrow rl_1^{(64)} + \mathrm{hi}_{(32)}\left(rl_0^{(64)}\right)$, $rl_2^{(64)} \leftarrow rl_2^{(64)} + \mathrm{hi}_{(32)}\left(rl_1^{(64)}\right)$.

1.2.2.3. $c_k^{(32)} \leftarrow \mathrm{low}_{(32)}\left(rl_0^{(64)}\right)$, $rl_0^{(64)} \leftarrow \mathrm{low}_{(32)}\left(rl_1^{(64)}\right)$, $rl_1^{(64)} \leftarrow \mathrm{low}_{(32)}\left(rl_2^{(64)}\right)$, $rl_2^{(64)} \leftarrow 0$.

#pragma omp section end

#pragma omp parallel sections end

2. $r_0^{(64)} \leftarrow r_0^{(64)} + c_n^{(32)}$. 3. $r_1^{(64)} \leftarrow r_1^{(64)} + \mathrm{hi}_{(32)}\left(rl_0^{(64)}\right) + c_{n+1}^{(32)}$. 4. $t^{(64)} \leftarrow \mathrm{hi}_{(32)}\left(rl_1^{(64)}\right)$.

5. For $k \leftarrow n+2$, $k < nk$, $k{+}{+}$ do

5.1. $t^{(64)} \leftarrow t^{(64)} + c_k^{(32)}$. 5.2. $c_k^{(32)} \leftarrow \mathrm{low}_{(32)}\left(t^{(64)}\right)$. 5.3. $\mathrm{low}_{(32)}\left(t^{(64)}\right) \leftarrow \mathrm{hi}_{(32)}\left(t^{(64)}\right)$.

5.4. $\mathrm{hi}_{(32)}\left(t^{(64)}\right) \leftarrow 0$. 6. $c_{nk}^{(32)} \leftarrow \mathrm{low}_{(32)}\left(r_0^{(64)}\right)$.

7. Return (c).

After the finishing execution of the parallel threads in step 1.1 and 1.2, it is require correcting in steps 2-6 the result of thread in step 1.2 via carry transfer from result in other thread in step 1.1. Special attention deserves an algorithm with parallelization on multiply threads.

Modified Comba Mx algorithm. In detailed consideration of Modified Comba algorithm, it is easy to note, what iterations in loops in steps 2 and 3 do not depend on one another.

The exclusions are addition accumulation results and carry from current iteration to only that addition and carry results after the current iteration to further iteration processing in steps 2.2 and 2.3. By the entering individual local variables for the sum accumulation may be correctly performs parallel sum accumulation in iteration in steps 2 and 3. For these purposes in algorithm Modified Comba Mx declared two arrays $r0_i^{(64)}$ и $r1_i^{(64)}$, $i = \overline{0,\, 2n-1}$. Easy to see, that this approach allows to variate number of parallel threads without algorithm modification in whole.

Algorithm Modified Comba Mx. Integer multiplication with OpenMP supports multiply threads. ***Input:*** *integers* $a, b \in \mathbf{GF}(p)$, $w = 32$, $n = \log_{2^w} a$, $nk = 2n-1$. ***Output:*** *integers* $c = a \cdot b$.

0. $l \leftarrow 1$.

1. #pragma omp parallel private ($r_0^{(64)}, r_1^{(64)}$) reduction (+ : l) begin

2. #pragma omp for nowait begin

2.1. For $k \leftarrow 0$, $k < n$, $k{+}{+}$ do

2.1.1. $rl_0^{(64)} \leftarrow 0$, $rl_1^{(64)} \leftarrow 0$. 2.1.2. For $i \leftarrow 0$, $j \leftarrow k$, $i \le k$, $i{+}{+}$, $j{-}{-}$ do

2.1.2.1. $(uv)^{(64)} \leftarrow a_i^{(32)} \cdot b_j^{32}$. 2.1.2.2. $rl_0^{(64)} \leftarrow rl_0^{(64)} + v^{(32)}$, $rl_1^{(64)} \leftarrow rl_1^{(64)} + u^{(32)}$.

2.1.3. $r0_k^{(64)} \leftarrow rl_0^{(64)}$, $r1_k^{(64)} \leftarrow rl_1^{(64)}$.

#pragma omp for end

3. #pragma omp for nowait begin

3.1. For $k \leftarrow n$, $k < nk$, $k{+}{+}$ do

3.1.1. $rl_0^{(64)} \leftarrow 0$, $rl_1^{(64)} \leftarrow 0$, $rl_2^{(64)} \leftarrow 0$. 3.1.2. For $i \leftarrow l$, $j \leftarrow k-l$, $i < n$, $i{+}{+}$, $j{-}{-}$ do

3.1.2.1. $(uv)^{(64)} \leftarrow a_i^{(32)} \cdot b_j^{32}$. 3.1.2.2. $rl_0^{(64)} \leftarrow rl_0^{(64)} + v^{(32)}$, $rl_1^{(64)} \leftarrow rl_1^{(64)} + u^{(32)}$.

3.1.3. $r0_k^{(64)} \leftarrow rl_0^{(64)}$, $r1_k^{(64)} \leftarrow rl_1^{(64)}$. 3.1.4. $l{+}{+}$.

#pragma omp for end

#pragma omp parallel end

4. $rl_0^{(64)} \leftarrow r0_0^{(64)}$. 5. $rl_1^{(64)} \leftarrow r1_0^{(64)}$. 6. $c_0^{(32)} \leftarrow \text{low}_{(32)}\left(rl_0^{(64)}\right)$. 7. $rl_1^{(64)} \leftarrow rl_1^{(64)} + \text{low}_{(32)}\left(rl_0^{(64)}\right)$.

8. $rl_2^{(64)} \leftarrow \text{hi}_{(32)}\left(rl_1^{(64)}\right)$. 9. $rl_0^{(64)} \leftarrow rl_1^{(64)}$. 10. $rl_1^{(64)} \leftarrow rl_2^{(64)}$. 11. $rl_2^{(64)} \leftarrow 0$.

12. For $k \leftarrow 1$, $k < nk$, $k{+}{+}$ do

12.1. $rll_0^{(64)} \leftarrow r0_k^{(64)}$. 12.2. $rll_1^{(64)} \leftarrow r1_k^{(64)}$. 12.3. $rl_0^{(64)} \leftarrow rl_0^{(64)} + \text{low}_{(32)}\left(rll_0^{(64)}\right)$.

12.4. $rl_1^{(64)} \leftarrow rl_0^{(64)} + \text{hi}_{(32)}\left(rl_0^{(64)}\right) + \text{hi}_{(32)}\left(rll_0^{(64)}\right) + \text{low}_{(32)}\left(rll_1^{(64)}\right)$.

12.5. $rl_2^{(64)} \leftarrow rl_2^{(64)} + \text{hi}_{(32)}\left(rl_1^{(64)}\right) + \text{hi}_{(32)}\left(rll_1^{(64)}\right)$. 12.6. $c_k^{(32)} \leftarrow \text{low}_{(32)}\left(rl_0^{(64)}\right)$.

12.7. $rl_0^{(64)} \leftarrow rl_1^{(64)}$. 12.8. $rl_1^{(64)} \leftarrow rl_2^{(64)}$. 12.9. $rl_2^{(64)} \leftarrow 0$. 13. $c_{nk}^{(32)} \leftarrow \text{low}_{(32)}\left(rl_0^{(64)}\right)$.

14. Return (c).

Comparison with other algorithms. Parallelization efficiency may be evaluated by the comparison of average time execution of software implementations for proposed parallel algorithms with single thread Modfied Comba algorithm [11], for 1 million iterations for different integers bit-length. Performance measurement of software implementation is performed for the arrays with 32-bit machine words, which allows estimate performance of implementations in common (in whole, in all). The Modified Comba 2x, Mx and single thread Modified Comba are implemented in C++ and compiled with Intel C++ Compiler XE 2011 in Microsoft Visual Studio 2005 in Release Win32 target with Maximize Speed option and SSE2 supports.

In table 1 show the performance measurement results for different software implementations for 1 million multiplications and different CPU for specified arrays with 32-bit words length.

Table 1. Performance timing of different integer multiplications algorithms implementations

CPU	Algorithm	Count of 32-bit words / ms											
		3	4	8	16	32	48	64	96	128	192	256	384
Intel Dual Core T2130	Cmb*	16	16	46	187	702	1544	2652	5786	10246	22988	40206	90002
	Cmb* 2x	202	202	219	328	546	966	1591	3758	5381	13194	20508	49173
	Cmb* Mx	281	297	343	464	889	1544	2417	5332	8234	17935	33203	72519
Intel Core2 Duo T7200	Cmb*	16	16	46	156	484	1015	1734	3766	6719	14703	26063	57735
	Cmb* 2x	234	172	187	235	422	703	1125	2157	3641	7812	13531	29859
	Cmb* Mx	266	281	297	406	719	1235	1844	3593	6015	12891	22500	49625
Intel Core2 Duo E6400	Cmb*	0	16	31	94	328	688	1172	2515	4500	9843	17438	38610
	Cmb*	78	93	93	125	266	453	719	1672	2438	5265	9547	20281

	2x												
	Cmb* Mx	141	141	172	250	453	781	1218	2735	4047	8688	16000	34578
AMD A83510 MX	Cmb*	16	16	31	156	452	921	1576	3682	6537	14212	24133	51480
	Cmb* 2x	187	187	209	250	421	687	1061	2075	3416	7472	13072	28205
	Cmb* Mx	359	375	390	437	593	826	1185	2075	3276	6755	11404	24804
Intel Core i7-2600	Cmb*	0	16	16	78	249	546	936	2044	3525	5554	13884	30872
	Cmb* 2x	124	109	109	156	266	484	764	1622	2605	3635	9734	21902
	Cmb* Mx	172	156	203	234	312	421	609	1139	1794	7831	6334	13089

Try to analyze the results of experiments showed in table 1. The low-end CPU Dual Core T2130 showed superiority two thread implementation Cmb* 2x over single thread implementation Cmb* on integers with length in 32 word and Cmb* Mx over single thread implementation Cmb* on integers with length in 48 word. Note, Cmb* Mx showed worst performance then Cmb* 2x.

CPU Core2 Duo T7200 has better performance then CPU Dual Core T2130, in accordance with this Cmb* 2x leaded Cmb* on integers with length in 32 word and Cmb* Mx leaded Cmb* on integers with length in 48 word. Note, as in previous case, Cmb* Mx showed worst performance then Cmb* 2x. This behavior may be clearly explained via higher core performance of Core2 Duo T7200 in comparison with Dual Core T2130. Special attention should the mobile CPU AMD A83510 MX, which shows the superiority Cmb* 2x on integers with length in 32 words and Cmb* Mx on integers with length in 48 words. In addition, implementation of Cmb* Mx leads the Cmb* 2x on integers with length in 96 words. These results allow us to safely say, what Cmb* Mx may be efficiently used in computers with multiprocessors and multi-core CPUs. The desktop with Core2 Duo E6400 shows the comparatively results with Core2 Duo T7200: Cmb* 2x shows the superiority over single thread implementation of Cmb* on integers with length in 32 words and Cmb* Mx shows the superiority over single thread implementation of Cmb* on integers with length in 128 words. This behavior may be explained by the higher core performance of Core2 Duo E6400 in comparison with Core2 Duo T7200. The desktop with Core i7-2600 CPU shows the best results in comparison with other: so due to high performance of cores the superiority of Cmb* 2x and Cmb* Mx over single thread Cmb* shows on integers with length in 48 words.

The effect of execution Cmb* Mx on CPU with 4 cores and 8 execution threads appears in explicit superiority not only on Cmb* but also on Cmb* 2x. A further increasing the integers length showed a significant superiority Cmb* Mx over Cmb* 2x.

From Table 1 clearly shows that the effect of parallelism begins to appear while multiplication of integers with length more than 32 words. This is connected with significant penults (miscellaneous charges) in new work thread creation in one multiplication operation. These penults (miscellaneous charges) are commensurable with penults (miscellaneous charges) on multiplication by itself. This undesirable effect may be getting rid (avoiding) via preliminary working thread creation, before it carries out all arithmetics operations in library initialization stage. As well, it is worth to observer on: the effect from parallelization appears on the greater bit-length of integer if faster CPU is using. It is evidence by the results of measurements on CPU: Intel Core i7-2600 and AMD A83510 MX.

Conclusion. Results of experiments and theoretical investigations, which made in this paper, allow to say that: 1. Modified Comba algorithm proposed by authors may be efficiently parallelized. Modified Comba 2x algorithm in 1.5 times and Modified Comba Mx algorithm in 2 times is in excess of single thread algorithm. 2. The parallelization benefits appear on 1024 bit (on 32 word with 32-bit), this allow to say about a large penults (miscellaneous charges) on new parallel thread creation. These penults (miscellaneous charges) may be compensate in the arithmetic library on

initialization stage. 3. The OpenMP implementation (support) in GNU gcc C++ Compiler on Debian Linux 6.0 x86-64 and Microsoft C++ Compiler in Visual Studio 2005, 2008 and 2010 on Windows XP x86 and Windows 7 x86-64 is much the worst when Intel C++ Compiler XE 2011 on Windows 7 because C++ programs have much worst performance (they do not described in this work).

In software implementation, large time on new thread creation and large time on delay before thread destruction are mainly responsible for the worst performance (GNU gcc C++ Compiler on Debian Linux 6.0 x86-64 and Microsoft C++ Compiler in Visual Studio 2005, 2008 and 2010).

Further, authors see an application of parallelization technique to other arithmetic operation algorithms in rings and fields such as reduction and inversion for the enhancing performance of public key cryptosystems, like cryptosystems on algebraic curves. The necessity of these researches speaks results obtained by the authors of [12] via using CUDA technology in the implementation of elliptic curve cryptosystem.

References

1. *Diffie W., Hellman M. E.* New directions in cryptography // IEEE Transactions on Information Theory, vol. IT-22, pp. 644–654, 1976.

2. *Selçuk Baktir and Erkay Sava*. Highly-Parallel Montgomery Multiplication for Multi-core General-Purpose Microprocessors. // Cryptology ePrint Archive. –Report 2012/140. –2012. –16 p. [Electronic resource]. 13.07.2012, Available from: <http://eprint.iacr.org>.

3. *Pascal Giorgi, Thomas Izard, Arnaud Tisserand.* Comparison of Modular Arithmetic Algorithms on GPUs // In Proc. International Conference on Parallel Computing (ParCo 2009). - Vol19. –Lyon, France. -2009. –pp. 315-322.

4. The OpenMP API Specification for Parallel Programming. [Electronic resource]. 13.07.2012, Available from: <http://openmp.org>.

5. OpenMP in Visual C++. [Electronic resource]. 13.07.2012, Available from: <http://msdn.microsoft.com/en-us/library/tt15eb9t.aspx>.

6. Khronos OpenCL API Registry. [Electronic resource]. 13.07.2012, Available from: <http://www.khronos.org/registry/cl/>.

7. Intel Threading building blocks for open source. [Electronic resource]. 13.07.2012, Available from: <http://threadingbuildingblocks.org/>.

8. NVIDIA CUDA. [Electronic resource]. 13.07.2012, Available from: <http://www.nvidia.ru/object/cuda_home_new_ru.html>.

9. AMD Accelerated Parallel Processing (APP). [Electronic resource]. 13.07.2012, Available from: <http://developer.amd.com/sdks/ AMDAPPSDK/samples/showcase/Pages/default.aspx>.

10. *Comba P. G.* Exponentiation cryptosystems on the IBM PC // IBM Systems Journal. – Vol. 29(4). -1990. -pp. 526–538.

11. *Kovtun V., Okhrimenko A.* Approaches for the performance increasing of software implementation of integer multiplication in prime fields // Cryptology ePrint Archive. –Report 2012/170. –2012. –9 p. [Electronic resource]. 13.07.2012, Available from: <http://eprint.iacr.org>.

12. *Giorgi P. Izard T, Tisserand A.* Comparison of Modular Arithmetic Algorithms on GPUs. [Electronic resource]. 13.07.2012, Available from: <http://hal-lirmm.ccsd.cnrs.fr/lirmm-00424288/fr/>.

UDC 003.26:621.39:530.145

S.O. Gnatyuk, PhD, Associate Professor
T.O. Zhmurko, Postgraduate Student
(National Aviation University, Kyiv, Ukraine)

ASSESSMENT OF RANDOMNESS FOR TERNARY SEQUENCES IN QUANTUM CRYPTOGRAPHY

In this paper the analysis of contemporary situation in information security is carried out. Tests for assessment pseudorandom ternary sequences are represented for more effective applying them in modern quantum technologies.

Introduction. Recent research has shown that classical cryptography gives a cause to look for new outlooks [1]. For instance, all public-key cryptosystems rely on the factorization difficultness of large integers. However, the discovery by Peter Shor (1994) a polynomial algorithm allowing fast factorization of integers with a quantum computer destroys previous confidence in reliability of classical cryptography. Therefore, contemporary society needs to find a new option to secure information, which became essential and very expensive resource. One possibility is using quantum cryptography (QC) instead of classical [3]. QC lies at the intersection of information theory, classical cryptography and quantum mechanics. In addition to this, the security of information using methods of QC is guaranteed by the laws of quantum physics (non-cloning theorem - impossibility duplicate an unknown quantum state, impossibility of taking a measurement without perturbing the system, impossibility simultaneously measure the polarization of a photon in the vertical-horizontal basis and simultaneously in the diagonal basis, etc.).

QC currently includes such areas as quantum key distribution, quantum digital signature, quantum secret sharing, quantum stream cipher, quantum secure direct communication (QSDC) [2]. Considerable interest among the scientific community causes protocols of QSDC characteristic feature of which is the absence of any cryptographic transformations (thus solved the problem of the distribution of encryption keys). One of the most common QSDC methods is ping-pong protocol that does not require a large amount of quantum memory and is especially popular in studies of modern scientific world.

Randomness is very significant in providing information security. Random sequences are applying anyway in every security system. However, binary random sequences are studied at a high level. Nevertheless, ternary or trinary sequences (analogous to a bit, although it contains 0, 1, 2), which is more advisable to use in QC protocols (particularly in ping-pong protocol), are badly highlighted. Besides, the existence of the assessment tool is low-to-nonexistent. Therefore, methods of assessing ternary pseudorandom sequence need to be considered. <u>The main aim of this paper</u> is to show development of methods for the generation and evaluation of randomness such sequences.

For today, exists a number of different valuation techniques for binary pseudorandom sequences, for example:
- graphics tests;
- NIST Statistical test Suite;
- methods of testing RIPE;
- methods of testing FIPS 140-2 (NIST PUB FIPS 140 2);
- Methods D. Knuth (Stanford University, USA);
- The system of statistical tests DIEHARD J. Marsalya (Florida Statement University, USA);
- System CRYPT-S H. Hustavsona and others. (Kuyndslandskyy technologyical University, Australia);
- methods of statistical testing generators of pseudorandom sequences I. Gorbenko, A.

Poti (Kharkov military university, Ukraine), and so on.

However, in the analyses of these techniques there is no possibility to estimate the ternary pseudorandom sequences. Consequently, tests have been developed.

Before evaluating, first necessary to form a pseudorandom ternary sequence. Accordingly generator of such sequence was developed, a detailed description of it is represented in [3].
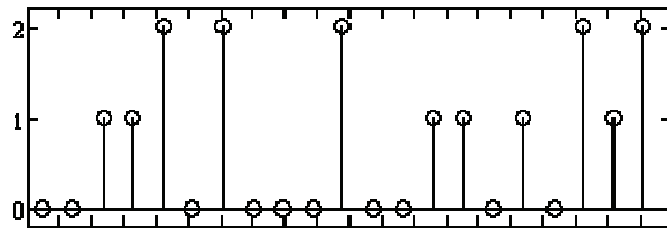
1.   Fig. 1. Graphical view of the ternary pseudorandom sequence

Frequency Tests. This test carries a proportionate assessment of zeros, ones and twos (for unbalanced ternary sequence). Specifies whether the number of zeros, ones and twos in the sequence is about the same as in really random in sequence. The result of this test is a histogram of occurrences of zeros, ones and twos in trytoviy sequence shown in Fig. 2 and a report in the form of a table that contains the frequency of occurrence and the deviation the average value.
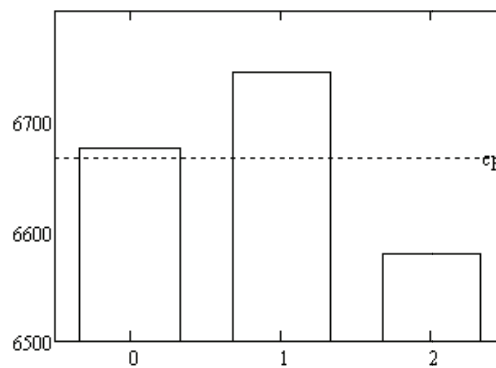
2.   Fig. 2. Frequency Tests Histogram

The assessment series test. Attention in this test focused on the total number of episodes in the entire sequence. The purpose of the test to determine whether the total number of runs of ones, twos and zeros of various lengths is such that expected from a random sequence. In the particular case of this test determines whether the oscillation between zeros and twos units are very fast or very slow.
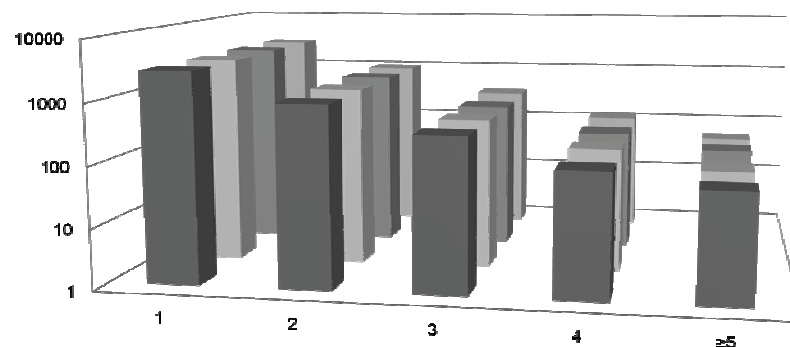
3.   Fig. 3. Histogram for series test
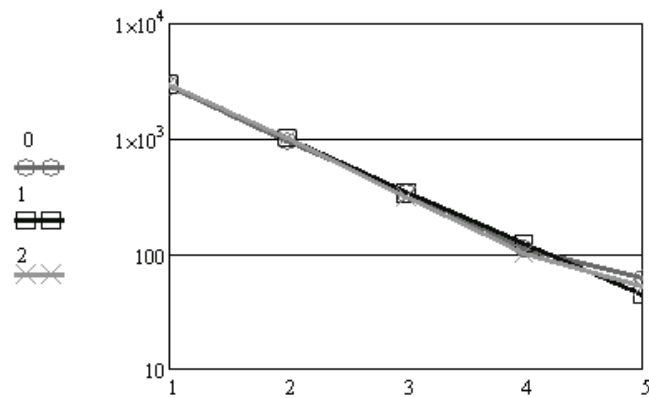
4.   Fig. 4. Comparative schedule

Spectral test . To search for periodicities in ternary sequences obtained spectra using FFT on samples from the generated sequence.
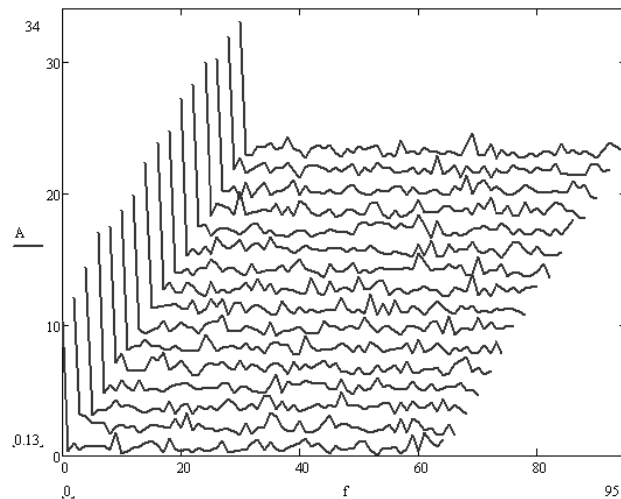
Fig. 5. Spectral test

Conclusion. This paper presents few tests, which help experts of QC qualitatively assess ternary sequences, witch more advisable to use in pin-pong protocol (QSDC). Analysis revealed no information about the ternary pseudorandom sequence, while binary random sequences are studied at a high level. Therefore was developed ternary pseudorandom sequences generator. Also was developed tests by which information security experts can evaluate suitability this sequences to use in quantum cryptography protocols to improve the effectiveness of their usage.

References

1. Quantum secure telecommunication systems / *[Oleksandr Korchenko, Petro Vorobiyenko, Maksym Lutskiy, Yevhen Vasiliu, Sergiy Gnatyuk]* // Telecommunications Networks: Current Status and Future Trends / edited by *Jesus Hamilton Ortiz.* — Rijeka, Croatia : InTech, 2012. — P. 211-236.

2. *Korchenko O.* Modern quantum technologies of information security against cyber-terrorist attacks / *O. Korchenko, Ye. Vasiliu, S. Gnatyuk* // Aviation. Vilnius: Technika, 2010. — V. 14, No. 2. — P. 58-69.

3. *Korchenko O.* Modern directions of quantum cryptography / *O. Korchenko, E. Vasiliu, S. Gnatyuk* // «AVIATION IN THE XXI-st CENTURY» — «Safety in Aviation and Space Technologies»: IV World Congress: Proceedings (September 21–23, 2010) — K. : NAU, 2010. — P. 17.1-17.4.

D.M. Grabinskyi, Postgraduate student
(National Aviation University, Kyiv, Ukraine)

SOFTWARE COMPLEX CERTIFICATION OF CRYPTOGRAPHIC KEYS

This article presents the main advantages of using digital signatures. The qualitative analysis of existed Ukrainian certification authority is carried out. Describes the steps to create public and private keys based on biometric features of a person (the iris). A scheme of generating key pairs digital signature by the algorithm RSA is showed.

The evolution of global communication in business and daily life resulted to the appearance a new field of relations, the subject of which is the electronic exchange of data. Three main features perform this data exchange: without use of digital signatures (DS); using DS issued by unreliable organization; using digital signatures issued by reliable organization - Certification Authority (CA) key [1].

Certificate authority is an organization that provides digital signature services:

- provision for use of DS;
- assistance in generating public and private keys;
- provide information about current, canceled and blocked public key certificates;
- time-stamping services;
- consulting and other services [2].

The use of digital signatures in electronic documents has several advantages that allow:

- replace in electronic documents traditional stamp and signature;
- improve and reduce the price in procedure of preparation, delivery, recording and storage of documents, to guarantee authenticity of documents;
- greatly reduce the movement of documents, accelerate and facilitate the process of sighting a single document by several persons;
- use the same means of DS in the exchange of information with all ministries, departments and administrations in Ukraine;
- verify the integrity of documents;
- ensure confidentiality of electronic document exchange.

The main difference between the DS and the usual signature is the fact that the first has no dependence on physiological characteristics of its owner. This feature is prevents the compare DS in legal status with the usual signature. Therefore, there is the problem of finding ways to improve methods of DS key generation. One solution of this problem is the use of biometric characteristics of a person to generate key information. Such keys are appropriate for use in government, where critical information resources circulate that require a higher level of protection.

In the course of the work was performed investigation of all Certification Authority of Ukraine. These include: Co.Ltd «Ukrainian Certification Center», Co.Ltd «Inter Metl», Co.Ltd «Art-Master», PJSC «Communication fund center», JSC «Public key infrastructure», Co.Ltd «National depository of Ukraine» and other. They provide basic services for the creation and maintenance of DS. The procedure of creating keys also similar and provided by hardware and software generators. Input parameters for them are random values of system clock or combination of numbers, which introduces a future owner DS. Therefore, by this methodology, a public and secret key depend on this data combination and not in any way depends on the physiological characteristics of its owner, as it happens with the handwritten signature. Further, in this letter will describe the methodology of generating keys for DS based on biometric characteristics of a person, that completely exhaust this problem.

Typical CA consists of the following: 1) CA workstation security administrator; 2) CA workstation administrator of certification; 3) CA application server; 4) CA database; 5) CA

workstation administrator of registration; 6) module of key generation; 7) CA open directory certificates; 8) server TSP; 9) Call-center software [5]. All these components interact with each other during the key generation procedure, however just key generation module is responsible for the formation of public and secret keys. Thus, using human biometric data for key generation will be carried out by improving not only the key generation module, but the whole CA.

All human biometric images are divided into static images limited with informative and dynamic images with unlimited informative. Static images of biometric data inherent the human body from birth, have limited value and may not be interchangeable by their owner [3]. Dynamic biometric images have unlimited informative and can be easily changed by theit owner. Therefore, to create a key information appropriate to use static biometric images. Among the list of all static images (cursive handwriting, keyboard handwriting, voice, fingerprint, iris, DNA and others) the best criteria of uniqueness, permanence, ease of measurement and stability corresponds picture iris. This biometric parameter is unique to every person. It is form in the first half year of life and remains unchanged until his death (iris changes related illnesses).

Traditionally biometrics is used for authentication users prediction of unauthorized division in the mode of placing of them to the information generators [4]. However, the used of biometric information systems for cryptographic protection of information, namely the possibility of using biometric data to generate cryptographic keys became an topical question recently.

In general, the process of transformation of human biometric cryptographic keys may be written as follows. Obtained from camera image (Figure 1) is subject to the process of segmentation: determined centers and radii of the pupil and iris [6].
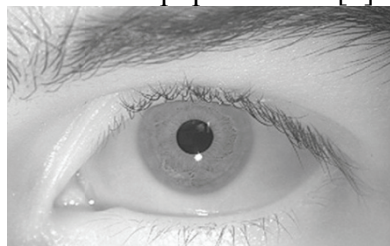
Fig.1. The resulting image obtained by scanning the iris

At this stage, eyelids and eyelashes can interfere with image processing, which cover part of the iris. They cause a group error. The article also suggested the use of Reed-Solomon's codes to correct errors (not binary cyclic codes that allow correct errors in blocks of data). Additionally, you can narrow down the area of the iris and process area, directly adjacent to the apple of the eye, where the probability of imposing of eyelids much lower. In Figure 2 shows an example of image segmentation module processed.
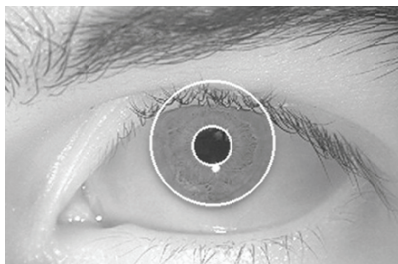
Fig.2. Images processed segmentation module

The next step is the separation of the iris from other parts of the image. It uses edges (by analyzing the first derivative) and further approximation limits iris simple geometric objects. Circumference pupil and iris outer boundary is located using Hough's transform. The next step is to normalize the image when the image is converted from polar coordinates to Cartesian. As a result of the algorithm is obtained images of size 512 by 64 pixel (Figure 3).

Fig.3. Images in a Cartesian coordinate system

Next, the resulting images are converted into binary sequence which attached to the timestamp of generate key pair. The resulting binary sequence is input for hash function GOST R 34.11-94 for reducing the size biometric key to 256 bits. Then this 256 bits key (secret biometric key) put to the input of sustainable generator of pseudorandom sequence and removed from the output sequence of pseudorandom numbers. From the resulting sequence of RSA algorithm is the creation of the secret and public keys.

As a result, generation got a pair of open and secret keys for DS scheme RSA. This sequence key generation for RSA scheme is shown in Figure 4.
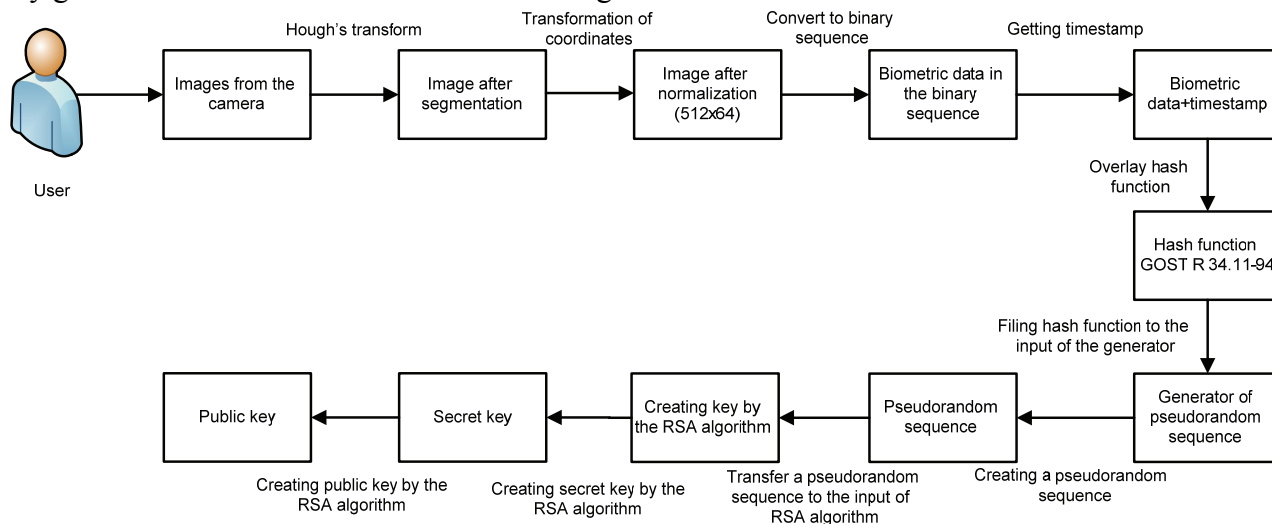
Fig.4. The scheme generation pair of keys digital signature

According to the above-described algorithm, it also allowed generation public and secret keys of electronic DS based on iris.

Conclusion. This article presents the main services provided by national CAs and the main advantages of using digital signatures in the electronic exchange of data. Also, carried out research allowed to determine the difference between regular and digital signatures through which was proposed scheme of key generation based on biometrics individual. From all the list of static biometrics of human for generating stable key information was chosen the iris as the most runoff, unique, sustainable and easy to collect characteristics. On the base of this choice was proposed a scheme of generating key pairs digital signature by the algorithm RSA. Thus, the proposed model of generation key information can be used in CA to improve the security level of electronic keys and equalizing the legal status of regular and digital signature.

References

1. Grabinskyi D. Software complex certification of cryptographic keys / D. Grabinskyi, S. Gnatyuk // Scientific and Technical Conference "Information Technology Security" (ITS-2012) (September 21–23, 2010) — K. : NAU, 2012. — P. 54.

2. Gorbenko Y. The infrastructure of the Digital Signature in Ukraine: problems of formation and development prospects // Information and analytical journal Carte Blanche - №6. – 2009. – P. 26-35.

3. Dodis Y. Fuzzy Extractors: How to Generate Strong Keys from Biometrics and Other Noisy Data. //Proceedings from Advances in Cryptology / Y. Dodis, L. Reyzin, A. Smith. - EuroCrypt. — 2004.

4. Kornyushin P. Construction of biometric authentication systems using a generator key sequences based on fuzzy data / P. Kornyushin, S. Goncharov, E. Kharin // Materials of the 50th All-Russian scientific conference. — Vladivostok: Pacific Naval Institute, 2007. — V.2. — P. 112-115.

5. System of cryptographic information security "code-X.509" [Electronic resource]. 19.03.2011, Available from: <http://www.cipher.kiev.ua/product_cipherx509.html

6. Secure biometric authentication signature [Electronic resource]. 15.04.2011, Available from: <http://www.slideshare.net/LiloSEA/ushmaev-cse-finalized>.

UDC 004.056.5(079.2)

V.V. Vasianovich, postgraduate
(National Aviation University, Ukraine)

DIGITAL IMAGE PROCESSING

The development of biometric person identification technologies caused by increase of amount of information, which is needed to be protected. That's why a new fingerprint recognition method, which is based on presence in the system some coefficients of the polynomial, was decided to be worked out. The identification of the fingerprint is based on the correlation coefficient, which is got in the end.

Matlab R2008a software was used for the implementation of the fingerprint recognition method.

The incoming fingerprint image (pict. 1) is coming to the input of the program. After this the incoming image is converted to the binary code to make it black and white (pict. 2).

Pict. 1. The incoming fingerprint image

Pict. 2. Digital fingerprint image

Now the digital fingerprint image is possible to be converted in the single-pixel curves system. As a result, we can see the image on the pict. 3.

After this the received image is filtered for reducing noise level and blur. The next step is cutting the snippet from the filtered fingerprint image for its further processing. The size of the snippet is random. The snippet of the fingerprint image is showed on pict. 4.

Further, the fingerprint recognition algorithm is to represent the cut snippet in matrix form and to make processing of it. The matrix form of the snippet is showed in table 1, where in the left column there are Y coordinates of every curve, and in the right column – X coordinates.

Pict. 3. Filtered fingerprint image

Pict. 4. Fingerprint image snippet

The coordinates of the curves of fingerprint snippet

Y	X
6	1
16	1
26	1
36	1
43	1
5	2
16	2
26	2
36	2
43	2
…	…

After finding the coordinates of "ones" we are to divide the curves from each other. The dividing algorithm looks like: the first X coordinate and the first Y coordinate are the initial coordinates of the first curve. Then the first X coordinate is compared with the second. If they are equal, the second X coordinate and the second Y coordinate are the initial coordinates of the second curve. Then the cycle is repeated. But if the next X coordinate differs from the previous, X and Y coordinates are the second coordinates of the first curve and so on. As a result, there are five arrays of the coordinates.

After finding the coordinates of each curve on a fingerprint snippet, we can plot the curves that exactly match the given snippet (pict. 5). The snippet is a matrix of values, each element of which is the cell, the size of which is one pixel, that's why the plot looks like broken curves. To make curves smoother, we are to make the approximation of each curve by least squares method, to get the coefficients of the polynomial, which will be interpolated after and the new plot will be got. As a result there are the coefficients of polynomial of degree four for each curve (table 2).

Then, using the coefficients of polynomial, interpolation is performed. As a result there are five arrays of interpolated values.
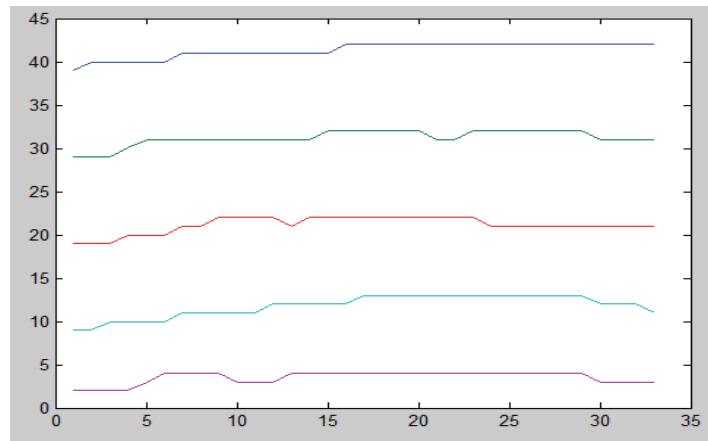
Pict. 5. The plot of the curves of the snippet

The coefficients of the polynomial values

a1	-0,0000	0,0001	-0,0066	0,2388	39,1593
a2	-0,0000	0,0020	-0,0523	0,6608	28,1148
a3	0,0000	-0,0009	-0,0007	0,4064	18,2634
a4	-0,0000	0,0005	-0,0118	0,3345	8,6824
a5	-0,0000	0,0018	-0,0463	0,5639	1,1369

These interpolated values are rounded to the nearest value. After this we can get the plot of rounded interpolated functions (pict. 6).
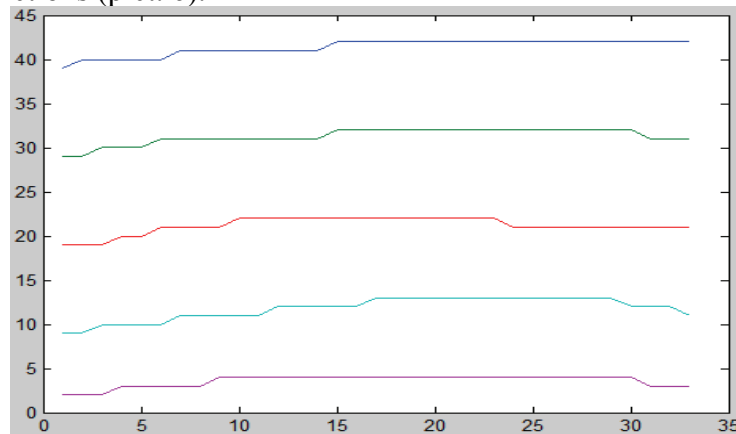
Pict. 6. The plot of rounded interpolated functions

As we can see the plot of rounded interpolated functions is almost equal to the plot of the curves of the snippet. So, we can say that the plot is built right.

Description of activities carried out above is that they allow us to ignore the fingerprint image. That is, after these actions there are no need to store the fingerprint image, it's enough to store the polynomial coefficients, by which the image is described. This will greatly save the space of the file system in which the biometric person identification system is situated.

After this we are to restore the fingerprint image using the coefficients of the polynomial and to make the final identification. To restore the fingerprint image, we should convert the plot into the matrix. As a result there are five arrays of coordinates of each curve on the plot. After this the restoring of the fingerprint image is possible.

The restored image is showed on the pict. 7.

Pict. 7. The restored fingerprint image

After getting the restored fingerprint image, we can make the correlation of the snippet with the incoming fingerprint image. As a result, we are getting the graphical correlation coefficient (pict. 8).
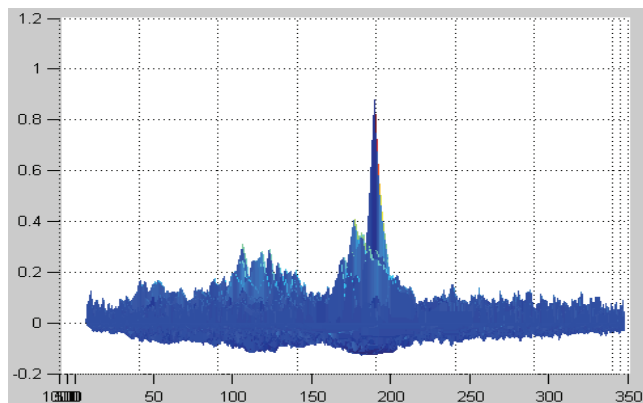
Pict. 8. The graphical correlation coefficient

It's obvious, that at some point in time, the correlation coefficient acquired value 0.9, indicating that the restored fingerprint snippet is part of the incoming fingerprint image, and hence the capacity of the algorithm is proved.

References

1. *Maslennikov M.A.* The practical cryptography / M.A. Maslennikov. – StPb.: BHV-Petersburg, 2003. – 464 p.
2. *Vorona V.A.* Access control systems / V.A. Vorona, V.A. Tihonov. – M.: Hot-line telecom, 2010. – 272 p.
3. *Barsukov V.S.* Modern security technologies / V.S. Barsukov, V.V. Vodolazkiy. — M.: Knowledge, 2000. – 496 p.
4. *The* organization and modern metods of information security / Edited by S.A. Diev, A.G. Shavaev / S.A. Diev, A.G. Shavaev. – M.: Concern "Bank Business Centre", 1998. – 472 p.
5. *The* official Institute of Cryptography, Telecommunications and Informatics. – Http://www.fssr.ru.
6. *LAN-crypto*. Information security. Algorithms. – Http://www.lancrypto.com/ index_ie_rus .html.

UDC 004.056.5(043.2)

V.A. Temnikov, PhD, A.V. Peteichuk
(National Aviation University, Ukraine)

THE VOICE OPERATORS AUTHENTIFICATION BY CONTINUOUS SPEECH CONSIDERING THE PHONEMES FEATURE CHARACTERISTICS

In article introduced an approach for the automatic voice operator's (the ergatic systems subjects) authentication on continuous speech with intermediate recognition of keywords based on the feature characteristics analysis of the different phonemes representations on speech signals spectrograms. Application of the developed approach can improve the quality performance of the voice control systems, which designed to prevent unauthorized operators access to control systems ergatic systems.

Published in the literature statistics of economic and social costs causes of transport (including aviation) companies indicate that the majority of accidents and violations of process conditions are caused by operational staff. [1].

One of the ways to improve the transport security (including aviation) is continuous monitoring of actions of human operator as the subject of ergatic systems (ES), that allow to significantly reduce the amount of accidents and incidents due to human error.

Considering that work of operational staff of ergatic system (the system "man - machine") connect with necessity quickly making informed decisions in different, including, unusual situations, such monitoring should be implement remotely, without contact [2].

The control of operators proposed to run automatically on a voice by analyzing the parameters of speech signals which received during the information exchange process between operators and takes into account that, as we know, when operators of their duties, in particular air traffic control, use standard fixed phraseology.

The authentification process comprises the following steps: preliminary speech signal processing, the keyword recognition (separation) and properly the human-operator keyword authentification

The functional scheme of operator authentification by automatic words recognition is depicted on figure 1.
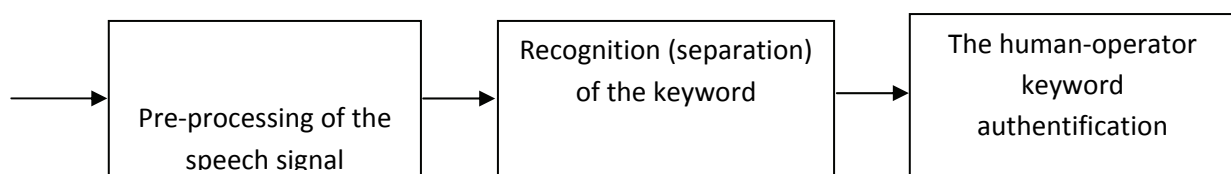
Fig 1. The functional scheme of operator authentification system with automatic keyword recognition

The speech signal that is fed to the microphone during the exchange information process is subject to preliminary treatment, in which implement the removal of noise and extraneous signals.

The keyword recognition (separation) from continuous speech, in developed authors system, based on a comparison basing pattern (model) of the keyword which is a clear sequence of consonant and vowel phonemes. An initial comparison of the phonemes required sequence can improve the quality of keyword selection.

The authors have system of criteria for the compilation of the dictionary patterns keywords developed.

Spectrogram of Russian fraise «переключитесь» from used air traffic controller's Russian command «Переключитесь на высоту» is depicted on figure 2. Each phoneme on spectrogram is

characteristically present. For example, sequence of consonant and vowel phonemes can be determined by the presence or absence of pitch. The area without pitch is voiceless Russian consonants «Ч», «П», «К». On the spectrogram each voiceless consonant phoneme has a gap in the pitch area determination. That is, the criteria for determining.
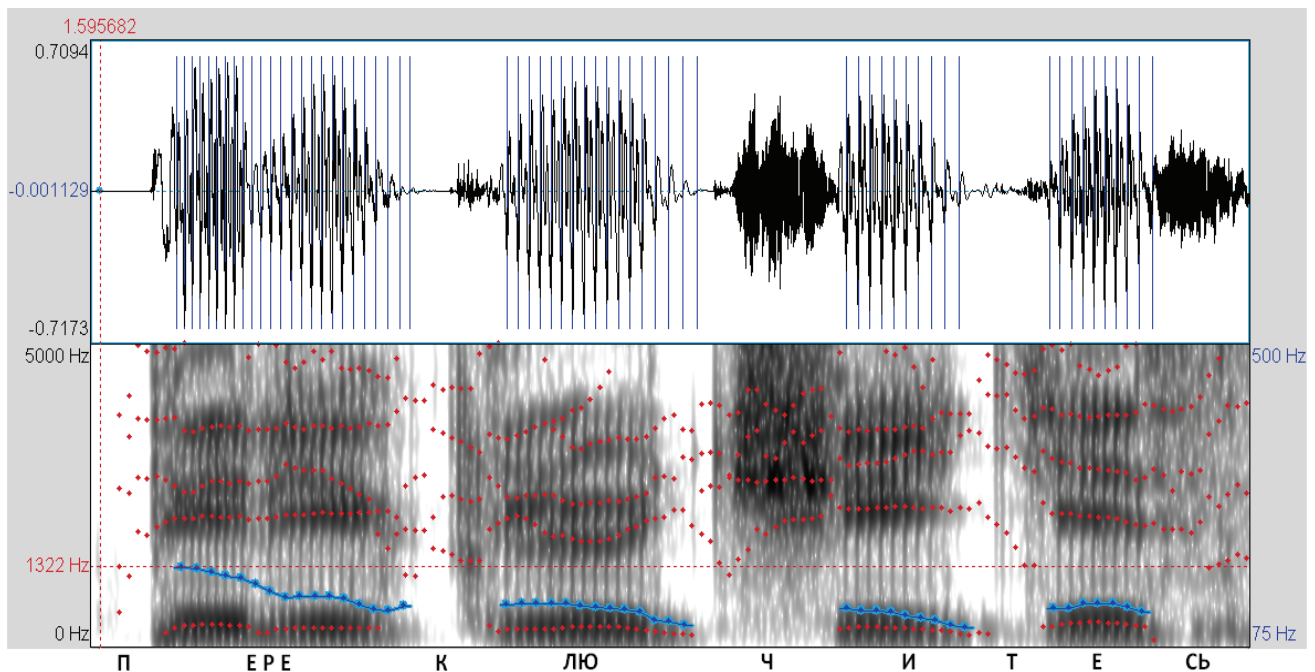
Fig 2. Word spectrogram «Переключитесь» (solid line denotes the time dependence of pith, dotted line – time dependence of formant frequencies)

If we pay attention to the area of the sequence of Russian phonemes "ЕРЕ" and "ЛЮ", the criterion with pitch is not appropriate. But the distinguishing criterion of consonants of this type can be the fact that pith of vowel occurs without noise.

The best recognition for vibrating sound "Р" for a very short (30 ms) breaks in the sound. Should take into account that the phoneme "Р" in both sides surrounded by the phoneme "Е" which is known as an allophone "ЙЭ". In phonetic theory phoneme «Й» (or "и" no syllable ") refers to a specific type of sonorant, but mostly it is used as "mitigation". So in this case, as in the case of the combination of "ЛЮ", can be guided by the criterion that the vowels a voice channel is opened, so that the stream of air coming out is not encounters obstacles. When the consonants in the way of exhaled air flow is always formed in a certain place the voice channel barrier of some form, which affects the values of formant frequencies of higher order, and vowels are characterized nonfocal (unfocused) articulation, consonants - localized articulation.

One of generalizing criteria that define the essential difference between consonants and vowels are transients from consonant to vowel phonemes and vice versa. These processes are manifested as changes of the vowels amplitude and frequency.

Recognition and separating the pieces of speech (words) from the air traffic controllers continuous speech are the basis for subsequent authenticate air traffic controller.

Since at the recognition keyword stage, we estimated different parameters, such as pitch and formant frequencies, by the time the determining that a desired human operator is on the work place, the system will have all data, which reducing processing time and results.

Being that a pitch depends on the person physiological condition, the proposed authentication operators based on analysis of the estimation of the fourth formant frequency.

This is evidenced by the relative values of the fourth formant frequencies for different phonemes which uttered by different speakers. Figure 3 shows the data for the three speakers.
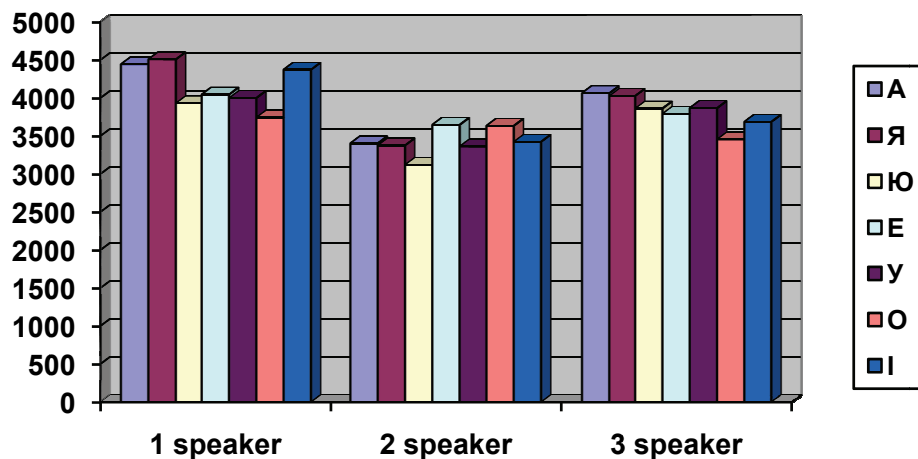
Fig. 3. The value comparing of the fourth formant frequencies for different phonemes of three speakers

All speech recordings were made in a studio.

The speech signal processing and calculations have been implemented with «Adobe Audition», «Praat» and «Speech Analyzer» software.

Conclusion

In article introduced an approach for the automatic voice operator's authentication on continuous speech with intermediate recognition of keywords based on the feature characteristics analysis of the different representations of phonemes. It makes possible to authentificate the human-operator in real time, can significantly reduce the processing of speech signals and increase the probability of correct recognition of operators.

References

1.   Burov O. U. Ergonomic foundations systems development forecasting performance of human - operator based on physiological models of activities: dis., DPhil: 05.01.04/NDI of Military Medicine problems of the Armed Forces of Ukraine. — K., 2006. — 329 p.

2.   Temnikov V.O., Peteichuk O.V. Control of the air traffic controllers using speech signal in real time // X International Scientific Conference «AVIA-2011».Proceedings. – V.1. – K.:NAU, 2011. –P.2.105-2.108

UDC 004.056 (043.2)

Khanko Yaroslav (National Aviation University, Ukraine)

METHODS AND MEANS OF BANKIG PAYMENT SYSTEMS PROTECTION

In this paper the general anal analysis of existing threats and vulnerabilities of payment systems is carried out. Their influence on development of protection means of payment systems and Ukrainian legislation are shown.

Introduction. The dynamic development of e-commerce leads to increase usage of cash flow via electronic payment systems, which, in its turn, increases the number of cyber crimes. Taking in consideration the above, the main focus of this research is to find existing technical and organizational measures to provide the protection of electronic payment systems.

Economic sector of Ukraine is goes through a revolutionary development. Rapid transition from a planned economy to market-driven economy discovered the imperfection of the current legislation for new vulnerabilities and threats of information security. The following laws specifying the main requirements for information security in the banking sector: Act of Ukraine "About banks and banking activity", Act of Ukraine "About protection of information in automated systems", Act of Ukraine "About electronic digital signature". National Bank of Ukraine (hereinafter - NBU) developed a set of regulations, specifying the requirements for information security and protection measures for payment transactions, namely: Decree of the NBU № 112 "About approval of the Order of organizations of protection of electronic bank' documents with usage of protection means of the National Bank of Ukraine ", Decree of the NBU № 223 "About carrying out of operations with the use of special payment means", Decree of the NBU № 243 "About approval of the Rules of technical protection of information in the bank' premises, in which electronic documents are processing", Decree of the NBU № 254 "About approval of the Order of the organization of operating activity in banks of Ukraine", Decree of the NBU № 267 "About approval of the Order of storage, protection, use and disclosure of bank secrecy", Decree of the NBU № 357 "About approval of the Order of creation, storage and destroying of electronic archives in the National Bank of Ukraine and banks of Ukraine ", and the revolutionary Decree of the NBU № 474 "About approval of standards of information security management in the banking system of Ukraine ", which was based on international standards of information security management series ISO/IEC 27000.

Review of IS threats and protection measures of cards payment systems. The migration to electronic banking services primarily subjected to efficiency of the transactions and the convenience for the end user. In addition, it is important that it is economically reasonable for banks to develop electronic payment systems. For example, at average, to serve one client on the branch it is needed to spend 20 Euros, to serve one client using ATM 5 Euros, and via Internet banking only 1 Euro. Conditionally, payment systems can be divided into two categories: payment systems using credit cards and Internet banking systems. Let's consider the most actual and popular, among cyber criminals, threats to payment systems with using credit cards, as well as methods and protection means, aimed to reduce the probability of vulnerabilities realization. The aim of cyber criminals are: number of payment card, expired date and Card Verification Value 2 (CVV2) code, and the data from the magnetic strip. Figure 1 shows the most likely ways to get this information:
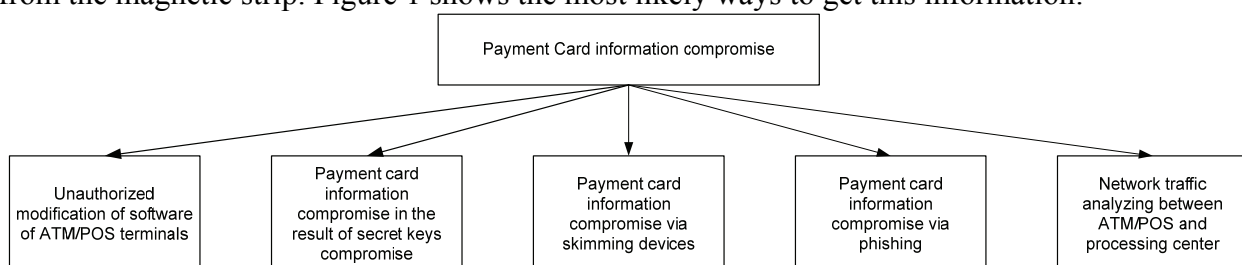
Fig.1. Classification of threats payment systems

Most often, cases of modification of software are detected on the ATM due to objective reasons. Access to the ATM' software is become possible through physical penetration (usually employees of ATM service company) or through unprotected data channels and using known vulnerabilities of Operating System. To protect ATM' software from modification is possible only in a comprehensive approach. The first way, is to use specialized software for integrity control or systems of behavior analyzing, which could block and inform the security of banks about all suspicious activity on the ATM. Increasing of the overall security of ATM' could provide usage of the virtual machine technology, which represents closed, highly secure software container, in which executes part of the ATM' applications. One more effective measure is so called obfuscation. This method can significantly complicate the analysis of algorithms of ATM' software operating for attacker and subsequent modification of software. Finally, protection of data transmission channels between the ATM and the processing center through encryption using strong cryptographic algorithms.

One of the most critical cardholder data is PIN code. According to the PCI PIN Security Requirements, PIN code must be processed only in protected form. To protect PIN code applies hardware encryption means known as HSM (Host Security Module) modules for generating, encryption and verification of PIN codes. These modules use strong cryptography, for example, 3DES (Triple DES) with a key length at least 112 bits, and in case of unauthorized physical penetration into the module (tampering, laser treatment, etc.), instantly destroys all secret information (PIN blocks, keys, etc.) stored in cryptographic module. In addition, the PCI DSS standard is strictly regulates the prohibition of writing of PIN code into log files. Despite this, the log files contain a complete PC numbers, which needed for investigations in the case event of questioned transaction. To provide confidentiality and integrity of log files applies encryption and usage of digital signature. For example, ProSecure system (developed by Netgear), uses 3DES encryption algorithm with 160-bit key length, and DSA algorithm for digital signature with key lengths 2048 bits. To ensure the protection of data transmission channels, there are wide verity of high performance solutions from Cisco, Check Point or Juniper, which using a strong cryptographic algorithm, such as AES. Let's consider measures to protect the PC information against compromising through skimming devices. It could be divided into passive and active antiskimming device. As concerns passive devices, they represent a pad on the card reader slot, made of durable material (plastic or metal).Thankstof its form, it makes it impossible to install skimming devices and at the same time does not prevent normal operation of the ATM. More interesting solution is active antiskimming devices. Its represents electronic device with detectors and the various components, that allow to analyze the gradient of the electromagnetic field in the zone of the PIN keyboard, monitor, and card reader slot of the ATM. In the case of change of the intensity of the field, the device initiates a lock of ATM.

Review of IS threats and protection measures of Internet banking systems. To increase security of payments using PC in the Internet, Visa developed 3D Secure protocol, which provides an additional level of authentication (e.g. notification by SMS to PC holder with a randomly generated code for the confirmation of the operation). Virtually, this protocol is shift responsibility on the bank, that issued the card instead merchant for carrying out transactions using stolen PC.

Let's consider the most actual and popular threats to threat of Internet banking systems, as well as methods and protection means, aimed to provide secure transactions in the Internet banking systems. Table 1 shows the most probable threats and risks for Internet banking systems.

Attacks are often go in the following scenario. Attacker steals, using malware, private keys and passwords for access to Internet banking systems. It should be noted that, up to date, for such activity, by organized crime group was wide variety of specialized malicious software with high versatility. For example, Win32/Spy.Shiz.NAL bot has the following functionality: lock/unlock Internet banking system, it could work as proxy server, it could search secret keys, disrupt the operating system, it could gather complete information about computer, lock/brake access of users to the client side of Internet banking system. It could be used as for popular systems ("BIFIT», WebMoney, HandyBank) and for specialized Internet banking systems of individual banks.

Gathered all necessary information, the attacker transfers funds on accounts of legal or physical bodies, which was specially specifically for fraud. Since all of these operations are carried out, client can detect suspicious payment and inform the bank to block this transaction. To restrict client access to Internet banking system, attacker usually uses malware, as mentioned above or performs DoS attack on a Internet banking system server.

Tab.1. Classification of threats and risks of Internet banking systems

Threat	Secret key of digital signature compromise		Replacement of transfer order		Unauthorized of secret key	
Risk	Secret key thievery from unprotected storage	Secret key thievery from RAM	Malware activity	Interception and modification of transfer order	Thievery of guaranteed storage means	Remote management of user workstation
Probability	70%	5%	1%	10%	10%	14%
Decision	Usage of guaranteed storage means of secret keys, which performs all operation with secret key entirely inside the electronic key.		Usage of update antivirus systems.	Protection of data transmission channels by means with strong cryptographic algorithms.	Usage of additional authentication (OTP token, SMS notification) for access to guaranteed storage means of secret keys.	1. Usage of additional authentication factor (OTP token, SMS notification). 2. Usage of secure virtual environment.

The most effective way to provide security of payment transactions via Internet banking system – use of guaranteed storage means of secret keys. As an example, an electronic key "Crystal-1", which has expert judgment, and therefore, according to the laws of Ukraine, can be used in the banking sector for protection the bank secrecy. Hardware-software means of cryptographic protection Electronic key "Crystal-1" is developed using the following cryptographic algorithms: Encryption - ДСТУ ГОСТ 28147:2009, Digital signature – ДСТУ 4145-2002, hashing – ГОСТ 34.311-95. In addition, the secret key is generated and processed secret key entirely inside the electronic key, eliminating the interception of secret key, including RAM. To increase security, the bank uses the efficient and cost-effective solutions as one-time, as additional authentication factor. Deserves special attention new approach for protection transactions via Internet banking systems, which represents using secure virtual environment for payments. The principle is simple: on the client workstation runs a virtual environment, pre-loaded from a reliable source (bank service providers), which by default is authoritative. This technology is relatively new and only tested in some Israel banks and does not give accurate information about the vulnerabilities and its advantages or disadvantages over existing protections systems.

Conclusion. This paper represents the general analysis of the main threats and vulnerabilities to payment systems and defined the most effective ways for its elimination. The next research will be aimed on development of new and improvement of existing protection means of payment systems.

References

1. Loginov A., Elhimov N. General principals of operating of electronic payment systems and providing protection measures against fraudulent // Confident. – 1995. – № 4. – P. 48–54.
2. Korolyov D. Korolyov M. Information systems in banking industry // Belgorod, 2004. P. 158
3. Tony Bradley. PCI Compliance. Understanding and Implement Effective PCI Data Security Standard Compliance. // Syngress Publishing. – 2007. P. 329.
4. http://iit.com.ua/index.php?page=getcontent&p=3

UDC 681.5.042

K.Y. Ohrimenko, c.t.s., honorable professor of ChDTU, A.V. Manziura
(Cherkassy State Technological University, Ukraine)
K. Eichhorn (K.K. Ohrimenko), c.t.s., docent.
(German Society of International Cooperation, Germany)
D.P. Ornadsky, c.t.s., docent.
(National Aviation University, Ukraine)

THE ERROR ACCURACY OF THE OUTPUT LINK OF ASSOCIATED MOVEMENTS OF THE KINEMATIC CHAIN

The accuracy probabilistic assessment method of a kinematic chain for screw displacement formation of a differential spacing terminal link at simulation modeling taking into account the equipartition law of random numbers is considered.

The helical surfaces of differential spacing find a wide application in various transporters, extruders and other mechanisms where either positioning accuracy achievement or high-speed conditional change of a terminal segment on the example of industrial robots manipulators is required. The solution of a research problem of kinematic accuracy of kinematic chains of differential spacing helical motion in this article is considered on the example of the general purpose lathe. For helical surface cutting of a differential spacing one of possible pitch control mechanisms is in addition entered into the construction of the machine axis drive.

The mathematical model of shaping at the helical surface generation of differential spacing in matrix form looks like:

$$\overline{r_0} = \prod_{\ell=1}^{n} A_{o\ell} \cdot \overline{r_\ell} = \begin{vmatrix} \cos\theta & -\sin\theta & 0 & 0 \\ \sin\theta & \cos\theta & 0 & 0 \\ 0 & 0 & 1 & 0 \\ 0 & 0 & 0 & 1 \end{vmatrix} \times \begin{vmatrix} 1 & 0 & 0 & 0 \\ 0 & 1 & 0 & 0 \\ 0 & 0 & 1 & z \\ 0 & 0 & 0 & 1 \end{vmatrix} \times \begin{vmatrix} 1 & 0 & 0 & x \\ 0 & 1 & 0 & 0 \\ 0 & 0 & 1 & 0 \\ 0 & 0 & 0 & 1 \end{vmatrix} \cdot \overline{r_\ell} , \tag{1}$$

where $\overline{r_0}, \overline{r_\ell}$ – respectively the equations of an ideal treated surface and the tool in a vector form, $\prod_{\ell=1}^{n} A_{o\ell}$ – product of shaping motion array of moving coordinates connected to elements of a kinematic chain; x, z – coordinate of in-out and longitudinal machine axis, $z = A_n x^n + A_{n-1} x^{n-1} + ... + A_2 x^2 + A_1 x + A_0$ – a polynomial n-ht degree, defining the function type of curve scan of the differential spacing helical line.

Using Lagrangian interpolation polynomial at a tabular coordinate assignment

$$L_n(x) = \sum_{i=0}^{n} y_i \frac{(x-x_1)(x-x_2)...(x-x_{i-1})(x-x_{i+1})...(x-x_n)}{(x_i-x_0)(x_i-x_1)...(x_i-x_{i-1})(x_i-x_{i+1})...(x_i-x_n)} , \tag{2}$$

we come to the system of algebraic equations defining a polynomial ratio for the functional dependence of curve scan of any kind set by coordinates numerical values. The curve scan of the helical line of differential spacing can be created by sections fitting of straight lines and curves in junction points from a condition of set laws of movement taking into account values of speed and acceleration. Structurally-kinematic and kinematic schemes of the general purpose lathe with the pitch control mechanism to the offered configuration are considered in fig. 1.

According to the kinematic scheme of the machine fig. 1a, the equation of kinematic balance of an axis drive elements taking into account the additional pitch control mechanism looks like:

$$1об.шп. \cdot \frac{60}{60}\frac{30}{45}\frac{40}{86} \cdot \frac{86}{64}\frac{28}{28}\frac{28}{35}\frac{35}{35}\frac{20}{30}\frac{30}{35} \cdot 12\frac{22}{30} \cdot 12\frac{36}{12}\frac{32}{15}\frac{36}{16} \cdot u_д \cdot \frac{28}{28}\frac{18}{40}\frac{15}{48} \cdot 12 = p_{н.в.}$$

Fig. 1 - a) Kinematic scheme of the general purpose lathe; b) Block kinematic diagram of the general purpose lathe

The kinematic chain contains 33 links from which $z_1,...,z_4$ - links of spindle group, $z_5,...,z_{11}$ - group of replacement wheels; $z_{12},...,z_{28}$ - group of links of differential spacing cutting; $z_{29},...,z_{33}$ - separatory group. For determining of influence of each link in error formation of a cut pitch on the basis of the transfer relations of the kinematic balance equation the numbers of turns of each chain elements for one turn of the motion screw are defined.

For the accuracy assessment of positioning of kinematic chain terminal links of industrial robots manipulators similarly to the shaping accuracy of helical surface from an error effect of each element of kinematic chain of an axis drive the method of statistical tests is used. As opposed to the research of A.V. Levashov and A.S. Pluzhnikov [1,2] in this research [3,4] on the basis of the equipartition law of probability density of random quantities the statistical method of simulation modeling is applied. The vector nature of operating errors of kinematic chain elements, taking into account the direction, is estimated by quadratic means. The developed determination technique of the greatest accumulated error of a helical surface cutting pitch considers its importance for each of discrete intervals within one turn of the motion screw and all links of the additional kinematic chain. It allows to determine the influence of each element of a kinematic chain in limits as of one turn of the motion screw, and at repeated passes from a condition of a statistical sample of a kinematic chain on output accuracy. Setting discrete values of turn of the motion screw on $9°$ and repeating this procedure during a turn, we will receive a statistical sample of a set of discrete values of the pitch cumulative error of a kinematic chain. The received sample allows to get probabilistic value of a differential spacing of a cut helical surface. The pitch total cumulated error of a cut s helical surface at turn of the motion screw on each $9°$ is calculated with the accounting of all links on a formula, micron:

$$\Delta p_{\Sigma} = \sum_{i=1}^{33} \left(\Delta p_{\Sigma 1} + \Delta p_{\Sigma 2} + ... + \Delta p_{\Sigma 33} \right), \qquad (3)$$

where the cumulative error of each i-th of a link changes according to the harmonic law:

$$\Delta p_{\Sigma} = \sum_{i=1}^{33} \left[A_i \sin\left(k_i \varphi_j + \psi_i\right) \right] + \delta T_{\Sigma i}. \qquad (4)$$

In this formula i – the number of a kinematic chain link; A_i – the amplitude value of kinematic accuracy standard of i-th of a link depending on a rotation angle of the motion screw; φ_i – rotation angles of the motion screw; ψ_i – phases shift of errors i-th link; k_i – the number of turns of a gear i-th link at turn of the motion screw on the selected angle; $\delta T_{\Sigma i}$ – a permissible variation of the helical line of the motion screw for a rotation angle φ_i.

Within carried-out research the angle of phase shift ψ_i is a random variable which accepts different values for each i-th turn of the motion screw. Shift of phases is defined as $\psi_i = 360° \cdot C$ and changes in limits $0 \div 360°$, where C – the numbers of equipartition in the interval $0 \div 1$ which are programmatically oscillated by the generator in the form of pseudo-random numbers.

From a condition of cutting modes calculation the spindle rotation frequency is accepted 1500min^{-1}. The fragment of calculation dependence compiling technique for determining of the total cumulative error of a pitch of a cut thread at turn of the screw on $9°$ within the first turn out of forty intervals of the motion screw turn, we will present in the form:

$$\Delta p_{\Sigma 9°} = 0{,}625 \sin\left(0{,}6 \cdot 9° + 360 \cdot 0{,}9355\right) + 0{,}625 \sin\left(0{,}6 \cdot 9° + 360 \cdot 0{,}3973\right) +$$
$$+ 0{,}625 \sin\left(0{,}6 \cdot 9° + 360 \cdot 0{,}23955\right) + 0{,}625 \sin\left(0{,}4 \cdot 9° + 360 \cdot 0{,}2133\right) +$$
$$+ 0{,}625 \sin\left(0{,}4 \cdot 9° + 360 \cdot 0{,}9035\right) + 0{,}625 \sin\left(0{,}25 \cdot 9° + 360 \cdot 0{,}4693\right) +$$
$$+ 0{,}625 \sin\left(0{,}25 \cdot 9° + 360 \cdot 0{,}3275\right) + 0{,}625 \sin\left(0{,}25 \cdot 9° + 360 \cdot 0{,}7653\right) +$$
$$+ 0{,}625 \sin\left(0{,}25 \cdot 9° + 360 \cdot 0{,}9115\right) + 0{,}625 \sin\left(0{,}2 \cdot 9° + 360 \cdot 0{,}7013\right) +$$
$$+ 0{,}625 \sin\left(0{,}2 \cdot 9° + 360 \cdot 0{,}555\right) + 0{,}625 \sin\left(0{,}2 \cdot 9° + 360 \cdot 0{,}0877\right) +$$
$$+ 0{,}625 \sin\left(0{,}15 \cdot 9° + 360 \cdot 0{,}0159\right) + 0{,}625 \sin\left(0{,}15 \cdot 9° + 360 \cdot 0{,}8933\right) +$$
$$+ 0{,}625 \sin\left(0{,}15 \cdot 9° + 360 \cdot 0{,}6235\right) + 0{,}625 \sin\left(0{,}1 \cdot 9° + 360 \cdot 0{,}3493\right) +$$
$$+ 0{,}625 \sin\left(0{,}1 \cdot 9° + 360 \cdot 0{,}8475\right) + 0{,}625 \sin\left(0{,}95 \cdot 9° + 360 \cdot 0{,}8453\right) +$$
$$+ 0{,}625 \sin\left(0{,}95 \cdot 9° + 360 \cdot 0{,}2315\right) + 0{,}625 \sin\left(0{,}08 \cdot 9° + 360 \cdot 0{,}9813\right) +$$
$$+ 0{,}625 \sin\left(0{,}08 \cdot 9° + 360 \cdot 0{,}1755\right) + 0{,}625 \sin\left(0{,}05 \cdot 9° + 360 \cdot 0{,}3573\right) +$$
$$+ 0{,}625 \sin\left(0{,}05 \cdot 9° + 360 \cdot 0{,}795\right) + 0{,}625 \sin\left(0{,}03 \cdot 9° + 360 \cdot 0{,}5733\right) +$$
$$+ 0{,}625 \sin\left(0{,}03 \cdot 9° + 360 \cdot 0{,}3435\right) + 0{,}625 \sin\left(0{,}03 \cdot 9° + 360 \cdot 0{,}2293\right) +$$
$$+ 0{,}625 \sin\left(0{,}03 \cdot 9° + 360 \cdot 0{,}3675\right) + 0{,}625 \sin\left(0{,}02 \cdot 9° + 360 \cdot 0{,}9253\right) +$$
$$+ 0{,}625 \sin\left(0{,}02 \cdot 9° + 360 \cdot 0{,}5515\right) + 0{,}625 \sin\left(0{,}014 \cdot 9° + 360 \cdot 0{,}2613\right) +$$
$$+ 0{,}625 \sin\left(0{,}014 \cdot 9° + 360 \cdot 0{,}2955\right) + 0{,}625 \sin\left(0{,}009 \cdot 9° + 360 \cdot 0{,}8373\right) +$$
$$+ 0{,}625 \sin\left(0{,}009 \cdot 9° + 360 \cdot 0{,}9995\right) + 0{,}9 = 1{,}8598, \, micron$$

Where $A_i = 25/40 = 0{,}625$ micron (25 microns – standard of kinematic accuracy of a gear for diameter of a separatory circle $d = 125$ mm; 40 – the number of intervals within a screw turn through $9°$); 0,6, 0,4,…, 0,08,…,0,009 – numbers of turns of each link of a kinematic chain for turn of the motion screw on $9°$; 0,9 microns – the pitch cumulative error limit of the motion screw at turn on $9°$ according to the standards of accuracy.

The reliability of the total cumulative error assessment is reached at the expense of increase in a statistical sample of calculation of 5 hundred passes of a helical surface cutting for dependence.

$$\Delta p_{\Sigma r} = \sum_{i=1}^{500} \Delta p_i. \tag{5}$$

The carried-out calculations allow to draw the histogram of value distribution range of the accumulated error where all dispersion values range $\Delta p_{\Sigma \max}$ is divided into sixteen categories

(a_{i-1}, a_i) with the length of Δa and the number of hits m in i-th category is counted up. The total accumulated error of a pitch for 500 passes, allows to define a mathematical expectation of the greatest accumulated error $\Delta p_{\Sigma 500} = \Delta p_1 + \Delta p_2 + \Delta p_3 + ... + \Delta p_{500}$, micron:

$$M\left|\Delta p_{\Sigma \max}\right| = \sum_1^{500} \left(\Delta p_\Sigma\right)_r \Big/ 500 \text{ , micron.}$$

Some values of specific influence of separate links on the cumulative error of the kinematic chain, calculated according to the formula f. (7) are presented in the table.

$$E_i = \frac{M\left|\Delta p_{\Sigma \max}\right| - M\left|\Delta p_{\Sigma \max}\right|_i}{M\left|\Delta p_{\Sigma \max}\right|} \cdot 100\% . \tag{7}$$

Процент влияния	E_1	E_2	E_3	E_4	E_5	E_6	E_7	E_8	E_9
%	2,94	2,93	2,76	2,91	2,92	2,94	2,96	2,94	2,93
Influence percent	E_{10}	E_{11}	E_{12}	E_{13}	E_{14}	E_{15}	E_{16}	E_{17}	E_{18}
%	2,9	2,93	2,92	2,95	2,68	2,9	2,92	2,94	0,001
Influence percent	E_{19}	E_{20}	E_{21}	E_{22}	E_{23}	E_{24}	E_{25}	E_{26}	E_{27}
%	3,02	2,86	2,89	2,87	2,94	2,92	2,92	2,96	2,88

According to four groups of links of a kinematic chain, their influence made for: spindle – 11,77 %; groups of replacement wheels – 20,54 %; groups of the wheels providing differential spacing cutting – 49,76 % and separatory group – 14,73 %.

Conclusions

The developed technique allows to calculate the cumulative error of a cut helical surface of a differential spacing and by analogy of positioning accuracy of a terminal function element of the industrial robot manipulator depending on a kinematic error of wheel gear and the pitch control mechanism.

The technique of simulation modeling is considered on the example of cumulative error determining of one and repeated turns of the motion screw. The specific influence on helical surface forming accuracy of each separate link of a thread-cutting kinematic chain is found.

With use of computer means the offered technique can be used at design of kinematic chains of drives and will allow to standardize the helical surface cutting accuracy of a differential spacing or the point-to-point accuracy of terminal links of industrial robots manipulators.

References

1. *Плужников А.С.* Расчёт точности зубо-резьбообрабатывающих станков. ЦБТИ, М.:1968, 75 с.

2. *Левашов А.В.* Основы расчёта точности кинематических цепей металлорежущих станков. М.: Изд. Машиностроение,1966, 212с.

3. *Охрименко К.Я., Манзюра А.В., К. Eichhorn (К.К. Охрименко).* Исследование оценки точности кинематической цепи станка при нарезании винтовых поверхностей постоянного шага. К.: Вістник інженерної академії України №2, 2011, С.245-250.

4. *Ohrimenko K.Y., Eichhorn K.K., Manziura O.V.* Simulation modelling of accumulated error of discrete drive kinematic chain. The fourth world congress "Aviation in the XXI-st century" – 2010, С.15.1-15.4.

P. Pavlenko, d.t.s. (National Aviation University, Kyiv, Ukraine)

METHOD OF OPTIMIZING DYNAMIC CONTROL RE-ENGINEERING PROCESSES OF INTEGRATED AUTOMATED INDUSTRIAL SYSTEMS

In this article the author gives the main results of optimizing control re-engineering processes of of integrated automated industrial systems which are the basis for algorithms and software of "RAIN" subsystem.

The control re-engineering process of integrated automated industrial systems (IAIS) in the *expanded* production conditions and integrated information environment should take into account many factors, that is characterized by the planty number of elements and connections between them and is varied in space and with time. Thus, there is a problem of choosing from a variety of management options according to given performance criterion, that is the solution of optimization [1, 2].

Under the optimization is implied the process of finding the *extremum of* quantitative control variable (parameter) , which is given by a function. By an optimal solution is assumed the best solution from the set of solutions that provides the specified characteristics of the re-engineering project with the most productive method at minimum costs, that is fulfilling the main criteria of maximizing the effectiveness of the re-engineering project [3].

During the re-engineering method development of a specific production the primary task is to determine the minimum necessary information that will allow to effectively solve the problem of re-engineering management.

Integrated and effective solution of industrial function re-engineering problem management production is largely dependent upon the coordinated systems interaction of these systems. Traditional formulation of the problem can be reduced to a nonlinear programming problem [4]. That is, $\min\limits_{d,x} \Phi(d,x,\theta)$ with limitations

$$h(d,x,\theta)=0, \; g(d,x,\theta)\leq 0,$$

where Φ – is a total objective function, which expresses economical efficiency of management; d– is the vector of design objectives; x– is a state vector of control function; θ–is a vector of control parameters; h– is a vector–function of management models; management model; g –is a vector–function of system's limitations.

With such formulation of the problem the vector of control parameters is supposed as invariable. Supposition that θ has the probability distribution is one of the possibilities of inclusion of variable parameters of control problem. But such approach doesn't give guarantees of finding of x state in accessible region, which is defined by a model h and by restrictions of g.

The task solution $\{d^*,\theta^*\}$ provides the admissibility of states only for θ^* parameters value. In practice, if $\theta=\theta^*$ arises a situation, when re-engineering project states will be located in an inadmissible area, which will lead to destruction certain restrictions and the failure of certain control re-engineering process functions .

Thus the duration of the task of this class increases significantly even with a small increase in the dimension of the project. However, in the dynamics of the modern production, however, in the dynamics of contemporary production, as determined by the competitiveness of its ability to respond quickly to any changes in markets and reorganize manufacturing according to the market requirements, operatively making changes in to the range of manufactured products, CIAS for production purposes should be modular with the ability to increase their functional functions.

Should be noted that the choice of the functional quality for the purposes of the management's optimization depends on the specific problems of production, but its a general view, in terms of optimizing the costs of the reengineering project may provide with an integral control function in

the field to maximize effectiveness of the re-engineering project based on limitations of costs and the time limitations and of expenses [5]: – $\max E_{ik}^{int}$,

$$E_{ik}^{int} = \sum_{q=1}^{N}\sum_{i=1}^{n_q} x_{i_q} e_{i_q} + \sum_{q=1}^{N}\sum_{k=1}^{u_q} x_{k_q} e_{k_q} ,$$

taking into account limitations costs: $C_{ik}^{int} \leq C_{ik}^{int*}$,

$$C_{ik}^{int} = \sum_{q=1}^{N}\sum_{i=1}^{n_q} x_{i_q} \cdot c_{i_q} + \sum_{q=1}^{N}\sum_{k=1}^{u_q} x_{k_q} \cdot c_{k_q} , \qquad (1.1)$$

and time limitations: $T_{ik}^{int} \leq T_{ik}^{int*}$,

$$T_{ik}^{int} = \sum_{q=1}^{N}\sum_{i=1}^{n_q} x_{i_q} t_{i_q} + \sum_{q=1}^{N}\sum_{k=1}^{u_q} x_{k_q} \Delta t_{k_q} , \qquad (1.2)$$

where $x_{i_q} -$ is avariable which is link with the use of i-y of CIAS in the q-y subsystem of re–engineering control: $x_{i_q} \in \{0,1\}$;

$x_{k_q} -$ is avariable which is related to creation k-y CIAS in the q-y subsystem of reengineering control: $x_{e_k} \in \{0,1\}$;

e_{i_q} - is a quantitative constituent of predictable efficiency of reengineering control of i-y of CIAS in the q-y subsystem of reengineering control;

e_{k_q} - is the quantitative constituent of predictable efficiency of reengineering project k-y CIAS for the q-y subsystem of reengineering control;

c_{i_q} - charges are on programmatic-vehicle facilities of i-y of CIAS in the q-y subsystem of management;

c_{k_q} - organizational charges after k-y CIAS for to the q-y subsystem of management;

t_{i_q} - charges of time are on modification of i-y of CIAS for the q-y subsystem of reengineering control;

t_{k_q} - charges of time on modification k-y CIAS for the q-y subsystem of reengineering control.

It is needed to expect probability of event P_1^T , at which the reengineering project will be executed at set σ- algebra in space t so, that time of project will be $T_{ik}^{int} \leq T_{ik}^{int*}$. That it is necessary to provide the optimum of parameters t_{i_q} and t_{k_q} , which will provide the maximal value of probability of $P^T(t)$, which is the task of optimum dynamic management.

Let us that P_1^T is the probability that space parameters t in the select re-engineering project are in an interval $\mu(T_1, T_M^3) = |T_1 - T_M^3|$. Then

$$P_1 = \frac{\mu(T_M^3, T_1)}{\mu(T_M^3, T_K)}$$

1.8.2

where μ - is a *sign* for measure in space $T = \left\{ t_{i_q} ; \ t_{k_q} \right\}$, and $\mu\left(T_M^3, T_K\right) = T \le T_M^3$; T_K − time, which is given by a specialist that manages the components of $T_{ik}^{int_1}$ and $T_{ik}^{int_2}$ on each of reengineering steps.

Obviously, project will be carried out optimally only when

$$g_i = 1 - P_i^T = 1 - \frac{\mu\left(T_M^3, T_i\right)}{\mu\left(T_M^3, T_K\right)}. \tag{1.3}$$

Then we can write, that

$$g_K = 1 - P_M^T = 1 - \frac{\mu\left(T_{K-1}, T_K\right)}{\mu\left(T_M^3, T_K\right)}. \tag{1.4}$$

A sequence $\left\{ g_K, \ k = \overline{1, K} \right\}$ in this case is a measure that characterizes the quality of control re-engineering process of CIAS. Thus, we can talk about the completion of re-engineering control process and about probability of this event θ.

Taking into account a theorem about the sum of probabilities [6], the generalized description that describes the quality of re-engineering control process of CIAS of optimum efficiency can be calculated by the formula:

$$\theta = g_{i1} + g_{i2} + ... + g_{ih} - \sum_{i_1 < i_2}^{k} g_{i1} g_{i2} + \sum_{i_1 < i_2}^{k} g_{i1} g_{i2} g_{i3} + (-1) \sum_{l=1}^{k} i_{l-1} \sum_{i_1 < ... < i_k}^{k} g_{i1} \cdots g_{ik}. \tag{1.5}$$

Consequently, this functional (1.5) is the function of its arguments and can be considered as a criterion that characterizes the σ- algebra defined on the set T by correlations (1.3) and (1.4). Now, operating parameters α_1 and α_2 it is necessary to maximize the value of the K_{ik}^{int} function. For solving this problem it is used the following compromise criterion in the form of additive convolution:

$$K_{ik}^{int} = \alpha_1 \hat{C}_{ik}^{int} + \alpha_2 \hat{T}_{ik}^{int}, \tag{1.6}$$

where $\hat{C}_{ik}^{int} = C_{ik}^{int} \big/ C_{ik}^{int*}$; $\hat{T}_{ik}^{int} = T_{ik}^{int} \big/ T_{ik}^{int*}$;

α_1 - the significance criteria of cost of re-engineering project $\left(0 < \alpha_1 < 1 \right)$;

α_2 - the significance time criteria of re-engineering project $\left(0 < \alpha_2 < 1 \right)$;

where $\alpha_1 + \alpha_2 = 1$.

Values α_1 and are given by a specialist of re-engineering control process.

During the re-engineering control process the time t_i is determined by a specialist, assigning time for modification of the system. For the mathematical solution of this optimization problem we introduce a function:

$$I_K = \theta^2. \tag{1.7}$$

Then for a given quality criterion of re-engineering control (1.4) and limitations (1.1) and (1.2) on the parameters of re-engineering project can be obtained a control process, the optimum in terms of probability of obtaining the maximum efficiency of the reengineering control process of CIAS. Set of correlations (1.1), (1.2) and (1.5) determines an optimum model of re-engineering process of integrated automated industrial systems for the concrete tasks of enterprise.

As shown by the authors of scientific works [6, 7], is the only solution of obtained correlations. Thus decision is seeking by sorting out variants of the values of C_{ik}^{int} and T_{ik}^{int}. For each fixed managing parameters the problem was solved in the theory of dynamic optimal control.

Setting the variants of managed parameters C_{ik}^{int} and T_{ik}^{int}, we will obtain the maximum value of functional (1.7) and therefore optimum of re- engineering control process of IAS effectiveness. Also it may be used various methods of optimization problem solution (1.1), (1.2) and (1.6).

Obtained effectiveness of engineering control process of IAS is the optimal under constraints and industrial conditions. Thus it has been fulfilled mathematical target setting and it has been proposed a method of IAS's dynamic optimal industrial control re-engineering process.

The realization of the IAS's reengineering control method is produced by "Varian" software module. System administrator of the re-engineering project using the control of the time value provides the maximum effectiveness of the re-engineering control process according to adaptive furl (1.6) and (1.7).

The same approach can be used for the others problem solving of IAS's re-engineering control. For example, at the level of the aggregate value of holding IAS. minimum criterion of the aggregate value of holding IAS, which are equipped in the re–engineering project is presented in a next kind – $\min TCO_{ik}^{int}$:

$$TCO_{ik}^{int} = \sum_{q=1}^{N}\sum_{i=1}^{n_q} x_{i_q} tso_{i_q} - \sum_{q=1}^{N}\sum_{k=1}^{u_q} x_{k_q} tso_{k_q},$$

taking into account limits on charges: $C_{ik}^{int} \leq C_{ik}^{int*}$,

$$C_{ik}^{int} = \sum_{q=1}^{N}\sum_{i=1}^{n_q} x_{i_q} \cdot c_{i_q} + \sum_{q=1}^{N}\sum_{k=1}^{u_q} x_{k_q} \cdot c_{k_q},$$

and time limitations: $T_{ik}^{int} \leq T_{ik}^{int*}$,

$$T_{ik}^{int} = \sum_{q=1}^{N}\sum_{i=1}^{n_q} x_{i_q} t_{i_q} + \sum_{q=1}^{N}\sum_{k=1}^{u_q} x_{k_q} \Delta t_{k_q}.$$

Obviously, all that problems are set in general view. At the time of realization of the presented method of the re-engineering control method IAS production purposes it is necessary to solve that problem with the help of step by step method, using the optimization method for each of the indicators of equity costs separately.

Thus, the essence of the method of the re-engineering control is the step-by-step task solution of optimizing re-engineering project with taking into account the costs of all restrictions of time and funds. System administrator inputs information about re-engineering project in the subsystem of "RAIN". Specialised software module of "VARIAN" configures optional variants of control parameters (costs, time, number of participants in the re-engineering process)to the subsystem. At the following stage the software module of "REIND" processes the input data using possible variants of controlled parameters and maximal effectiveness of re-engineering process (according to 1.4) with taking into account the costs of all restrictions of time and funds (according to 1.1 and 1.2).

Conclusions

The developeped method of optimizing dynamic control re-engineering processes of integrated automated industrial systems may be used by IT employees in the re-engineering process both in the enterprise and in the subsystem structure.

References

1. Balakhonova I. Logistic: Integration of processes by the ERP-system / I. Balakhonova, S. Volchkov, V. Kapiturov // M. : Priority, 2006. – 464 p.

2. Loginovskiy O. Management an industrial enterprise / O. Loginovskiy, A. Maksimov // M. : Engineer-1, 2006. – 576 p.

3. Torshin D. Methods of integration of these computer systems on the basis of universal format of exchange by information : avtoref. dis. on the competition of graduate degree of kand. tekhn. sciences : special. 05.13.11 the «Mathematical and programmatic providing of calculable machines, complexes and computer networks» / D. Troshin ; GOU VPO the «Ufimskiy state aviation technical university», Ufa, 2009. – 16 p.

4. Bernus P., Nemes L. Modeling and Methodologies for Enterprise Integration. – London: Chapman and Hall, 1996. – P. 112-135.

5. Hammer M., Champy J. Reengineering the Corporation a Manifesto for Business Revolution. – New York: HarperCollins, 1993. – 273 p.

6. Gikhman I. The Guided casual processes. / I. Gikhman, A. Skorokhod // – K.: Sciences thinking, 1977. – 250 p.

7. Propoy A. Elements of theory of optimum discrete processes. – M.: The Main release of fiz-mathem literary publishing house "Science", 1973. – 256 p.

K.S. Babich (National Aviation University, Ukraine)

COMPLEX APPROACH FOR TECHNICAL PREPRODUCTION PROCESS CONTROL

The development of products in machinery industry involves numerous engineers from different disciplines working on independent components. Thus, the main objective is to develop an approach that can manage complexity in technical preproduction (TP) process reduce the cycle time, the product development cost and the product quality. The design structure matrix (DSM) and criterion optimization in couple is a simple tool to perform both analysis and management of complex systems.

The engineering technical preproduction (TP) is union of design, technological and organization processes. Therefore, major portion of information from common information environment of enterprise must be used for effective TP process implementation. This information is the mean for TP process control. Control automation and TP process optimization reduces design and development stage duration of product lifecycle.

Development time is an important factor in production and marketing in engineering. So Blackburn [1] highlighted the inefficiency of sequential product design. He showed that sequential design creates a continuous cycle of development time and design changes. To overcome the continuous cycle, Nevins and Whitney [2] introduced parallel processing (concurrent engineering). Brett et al. [3] showed a significant development time saving as compared to sequential design. Linghua Kong et al. [4] evaluated the sequential engineering and concurrent engineering and pointed out that concurrent engineering processes were more valuable, when the intensity of interaction was high. Ford and Bloebaum [5] showed that concurrent engineering increases feedback and decreases design changes in aircraft design and development.

Ross et al. showed that to reduce development time and parallelize product and process development, the designers had to proceed with partial information and subjective interpretation [6]. Eppinger et al. [7] showed that project evaluation review technique/critical path management (PERT/CPM) assumes that no activity can begin until all preceding activities have been completed. Mayer, Painter, and Witte [8] stated that the integrated definition (IDEF) methodology is inefficient to address the task dependencies in concurrent engineering.

To analyze the task dependencies in concurrent engineering, Steward [9] introduced design structure matrix (DSM). Ali Yassine and Dan Braha [10] summarized the four principles of DSM.

Kusiak and Wang [11] decomposed design tasks in DSM to identify serial, parallel, and coupled ordering of tasks using cluster analysis. Eppinger et al. [12] analyzed task interactions to create design task groupings using DSM in order to find alternative sequence and task dependency of a project. Gonzalez-Zugasti et al. [13] developed an algorithm for DSM to carry out the task grouping and sequencing.

Studies reported in the literature have identified limitation of sequential engineering and concurrent engineering. Also, the studies reported in the literature have pointed out the limitation of PERT/CPM and IDEF methods in addressing the complex information flow in design and development of aircraft. To overcome this limitation, DSM is recommended for engineering design based on some recent studies.

The engineering product development has a large number of functional groups (decision-making activities) that combine creative thinking, experience and quantitative analysis, the characteristics of which are iterative, cooperative and uncertain. This results in information interpretation asymmetries between the experts involved. These characteristics make the TP process complex. To overcome the complexity of information flow in TP a DSM method comprising of five-step analysis is used [14]. The design process begins with the building of the DSM and results in the definition of architectural chunks and/or team chunks ready for resource allocation and detail design.

DSM five-step analysis methods for design:

1. Building the DSM for design.
2. Document the interactions between elements.
3. Partitioning.
4. Clustering.
5. DSM tearing [15].

In DSM, the subsystem/activity elements are listed as rows and also as columns in the same order.

The DSM identifies those elements that are involved in information feedback cycles and potential rework. As the project unfolds, these assumptions are revised in the light of the new information and the dependent task is reexecuted. Dependencies above the diagonal also impact all those elements that are dependent on the outputs from an element that has to be repeated or redesigned.

Partitioning is the process of manipulating (reordering) the DSM rows and columns such that the new DSM arrangement does not contain any feedback marks, thus transforming the DSM into a lower triangular form [15]. In partitioning, the main objective was to move the feedback marks from above the diagonal to below the diagonal, given that the DSM elements were tasks to be executed.

The next step is to cluster the elements into chunks. Clustering can be used to define not only the physical architecture of the product but also the product development team structure. This may be done on the basis of the interactions alone. Clustering can significantly impact the coordination complexity of the TP process. The interactions documented in the previous step describe, at the system level, the TP issues, which the engineering teams must resolve.

Coordination complexity can be reduced, if the elements are clustered such that the interactions predominately occur within chunks, rather than between chunks. During the process of clustering, for example in Figure 1, row A having cross below the diagonal is being influenced by column B in unidirectional fashion and are considered sequential. The system elements that do not interact with each other are considered parallel. For example, column F and column D is independent of each other. Finally, in the coupled system, the flow of information is intertwined. For example, column C influences row E and column E influences row C.

a – primary DSM

	A	B	C	D	E	F
A	•	×				
B		•				
C		×	•		×	
D	×			•		
E	×		×		•	×
F		×				•

b – DSM after analysis

	B	A	F	D	C	E
B	•					
A	×	•				
F	×		•			
D		×		•		
C	×				•	×
E		×	×		×	•
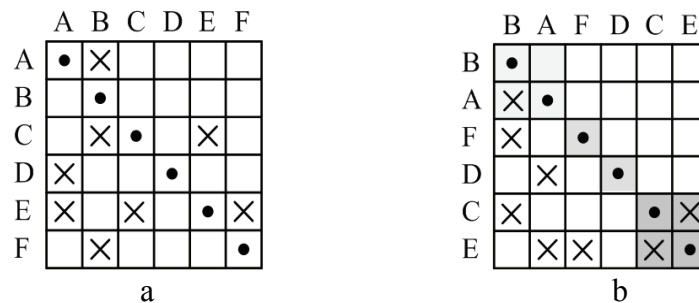
Figure 1. DSM process model:
a – primary DSM, b – DSM after analysis.

DSM tearing is the process of choosing the set of feedback marks such that if it is removed from the matrix (and then the matrix is repartitioned), it will render the matrix to be lower triangular. Identifying the marks that are removed from the matrix in coupled tasks result in identification of assumptions that need to be made in order to start design process iterations. Once the DSM for design is clustered, tasks in parallel are identified and executed concurrently. For the coupled ones upfront planning is necessary.

The next step after DSM tearing is the parametrical optimization of the obtained TP workflow.

The expertise for optimization parameters identification was conducted at basic machinery enterprises of Ukraine – Motor Sich JSC (Zaporozhye) and PJSC «Sumy Frunze NPO» (Sumy). As result, it was noted that product parameters and resource parameters define process parameters such as whole process duration and part process durations. It was decided to separate TP process control parameters into two groups: parameters of TP process elements and executor parameters.

Next parameters were included to the set of TP process element's parameters $P = \{ d, k, l, t_z, r \}$:

– output document type $d \in \{ 1, 2, \ldots, m_d \}$, where m_d - quantity of possible output document types at present enterprise (for example, 1 – drawing, 2 – assembly, 3 – 3D-model, 4 – technological process, etc.);

– task performance complexity coefficient $k \in \{ 1, 2, \ldots, m_k \}$, where m_k - quantity of possible complexity levels for every task type;

– task modification level $l \in \{ 0, 1, 2, 3, 4 \}$, where, for example, 0 – modification is not required for the task, 1 – error correction, 2 – update, 3 – improvement, 4 – development;

– average task executing time $t_z(d, k, l) = \dfrac{1}{N} \sum\limits_{i=1}^{N} t_{z_i}(d, k, l)$, where N – current quantity of tasks, having certain type, complexity and modification level in database ;

– task executing priority $r \in (1, 2, \ldots, m_r)$, where m_r - quantity of levels in TP project structure.

As executor parameters $E = \{ k_e, D, k_{max}, t_f, q \}$ where defined next values:

– executor's qualification $k_e \in \{1, 2, \ldots, m_{k_e}\}$, where m_{k_e} - quantity of possible qualification levels;

– executing task types $D = \{d_i\}$, $d_i \in \{1, 2, \ldots, m_d\}$, where m_d - possible quantity of task types at present enterprise;

– the highest level of task performance complexity k_{max};

– quantity of free time t_f;

– task performance quality $q = n_{in} / n_\Sigma$, where n_{in} - unique task quantity, $n_\Sigma = n_{in} + n_{cor}$ - total quantity of executed tasks; n_{cor} - quantity of returned for error correction tasks.

On the base of enterprises expertise, it was decided to use combined vector criterion for optimization TP process task distribution. It consists of next partial criteria:

1) criterion of total TP process duration minimization – reducing workflow area on Gantt diagram. This criterion also known as integral criterion;
2) averaging of executor's loading;
3) minimax criterion – minimization of loading maximal loaded executor;
4) executors quantity minimization;
5) increasing of work capacity – in task distribution process two factors are discounting: the maximal executor qualification level and his average performance time for certain type and complexity tasks;
6) quality improvement of TP task performance – in this case the aim of task performance is to execute TP process tasks with the highest possible quality, but not in minimal time. So two parameters are discounting: task performance quality and task performance complexity coefficient;
7) performance priority;
8) TP process cost minimization.

With specified parameters and selected criteria the quasioptimal composition T of TP process elements executes:

$$T = f(P, E, \overline{K}),$$

where P - the set of TP process element parameters;

E - the set of executor parameters;

$\overline{K} = \{K_1, K_2, \ldots, K_N\}$ - the optimization criteria vector,

N - the quantity of possible criteria of task performance optimization.

As result of program executing, we get TP process task distribution.

Conclusion

The effective TP process implementation demands the unification and accessibility of information about whole development cycle in information environment. This is beneficial to decrease the duration of the development lifecycle and increase the quality of the product. But at the same time, it will increase the complexity and the coupling process during the product development. Thus, the TP process should be seen as a multi-objective decision-making process. We should use different criteria and different control parameters at different stages. TP process must be planned very carefully to unearth the structure of the process. Parameters and criteria given above simplify and make more adaptable implementation and control of TP process on machinery enterprises.

References

1. *Blackburn J.D.* Time-Based Competition. The Next Battleground in American Manufacturing // Homewood, IL: Business one Irwin – 1991. – 352 p.

2. *Nevins J.L.,Whitney D.E.* Concurrent Design of Products and Processes: A Strategy for the Next Generation in Manufacturing // New York: McGraw-Hill. – 1989. – 254 p.

3. *Wujek B.A., Renaud J.E., Batill S.M., Brockman J.B.* Concurrent subspace optimization using design variable sharing in a distributed computing environment // Concurrent Engineering, 4 (1) – 1996. – pp. 361–377.

4. *Kong L., Bhuiyan N., Thomson V.* Determining the Value of Sequential and Concurrent NPD Processes // Sage Publications, 16(3). - 2008. – pp. 201–211.

5. *Ford, J.F. and Bloebaum, C.L.* A Decomposition Method for Concurrent Design of Mixed Discrete/Continuous Systems // Advances in Design Automation ASME, 65(2). - 1993. – pp. 367–376.

6. *Prasad B., Morenc R.S., Rangan R.M.* Information Management for Concurrent Engineering: Research Issues // Sage Publications, (1). - 1993. – pp. 3–20.

7. *Eppinger S.D., Whitney D.E., Smith R.P., Gebala D.A.* A Model-Based Method for Organizing Tasks in Product Development // Research in Engineering Design, 6(1).-1994.–pp.1–13.

8. *Mayer R., Painter M., Witte P.* IDEF Family of Methods for Concurrent Engineering and Business Re-Engineering Applications // College Station, TX: Knowledge Based Systems – 1993. – 652p.

9. *Steward D.* The Design Structure System: A Method for Modelling the Design of Complex Systems // IEEE Transactions on Engineering Management, 3. - 1981. – pp.71–74.

10. *Yassine A., Braha D.* Complex Concurrent Engineering and the Design Structure Matrix Method // Concurrent Engineering: Research and Applications, 11(3). - 2003. – pp.165–176.

11. *Kusiak A., Wang J.* Efficient Organizing of Design Activities // International Journal of Production Research, 31(4) - 1993. – pp. 753–769.

12. *Eppinger S.D., Whitney D.E., Smith R.P., Gebala D.A.* Organizing the Tasks in Complex Design Projects // ASME Design Theory and Methodology, 27. - 1990. – pp. 39–46.

13. *Gonzalez-Zugasti J.P., Otto K.N., Whitcomb C.A.* Options-Based Multi-Objective Evaluation of Product Platforms // Naval Engineers Journal, 119(3). - 2007. – pp. 89–106.

14. *Shekar B.., Venkataram R., Satish B.M.* Managing Complexity in Aircraft Design Using Design Structure Matrix // Concurrent Engineering: Research and Applications, 19 (4). – 2011. - pp. 283-294.

15. *Browning T.* Applying the Design StructureMatrix to System Decomposition and Integration Problems: A Review and New Directions // IEEE Transactions on Engineering Management, 48(3). - 2001. – pp. 292–306.

UDC 004:65.011 (045)

V. Treityak (National Aviation University, Ukraine.)
S. Doroshenko (JSC «SNPO» Summy, Ukraine.)
V. Kovacs (DME Europe, Vsetin, Czech Republic.)

TECHNOLOGY OF INFORMATION SUPPORT OF MANAGEMENT PRODUCTION PROCESSES OF MACHINE-BUILDING ENTERPRISE

In work the technology of information support of management is offered by productions of machine-building enterprises. It is proved that formation of the knowledge base and management of knowledge this important direction of development of automation of management of modern machine-building enterprise.

Complication of production tasks of management needs informative support as at strategic so at the operative planning. Especially it shows up in the conditions of unstable economic situation, instabilities of supplying with acquisition, absence of necessary financial resources and other.

In the process of operative management of machine-building operations a shop or area foreman, master, technologist, controller, et cetera, that, it will be a person which makes decision (PMD) at workshop level to settle the semi structured problems. And here the programmatic modules of information technology (IT) of support of processes of management in computer-integrated automated system (CIAS) of the production setting have an important value as: Computer-Aided Design (CAD) / Computer-Aided Manufacturing (CAM) / Computer-Aided Engineering (CAE) / Computer-Aided Process Planning (CAPP) / Product Data Management (PDM) / Enterprise Resource Planning System (ERP) / Manufacturing Enterprise Solutions (MES)-systems and other, what will allow to prompt the variants of operating on the process of production for achievement of the put aims and the end-point are possible. The modules of the programs of IT of support of management processes in CIAS must be in a position to adapt oneself to the change of calculable models, «socialize» with an user on specific for the guided area a «language», present results in such form which would be instrumental in more deep understanding of results. That, the function of IT of support of management processes consists not in that, to replace a leader, but in that, to promote his efficiency. IT of support of management processes must support intuition, able to recognize ambiguity and incompleteness of information, and have facilities for their overcoming. Except for the known requirements to the informative systems (powerful SMDB which provides effective access to information, their integrity and defense; developed analytical and calculable procedures which provide treatment and analysis of data; transportability, reliability, flexibility, possibility of including of new technological procedures), IT of support of management processes must have such specific lines, as:

- possibility of forming of variants of decisions in the special, unexpected for PMD situations;

 -models, applied in the system, must be in a position to adapt oneself to concrete, specific reality as a result of dialog with an user;

- a subsystem must interactively generate models in the process of their exploitation.

Thus, developed of IT of support of management processes in management information is computer-integrated, that arose up as natural development and continuation of the administrative informative systems and control system by bases information, must decide the unstructured and semi structured multicriterion tasks.

A decision of such tasks presently is in majority cases by the prerogative of consulting models or systems of support of making decision [1-2]. At the same time, existent developments for allow to put the bases of knowledge's and decide the project tasks of including of the programmatic modules and bases of knowledge's in the created system of informative support of management processes.

Will formulate raising of task of development of project procedure of acceptance of administrative decisions for poorly formalization and nonpermanent production situations.

For the decision of problem production situations it is offered it is formalized to describe the actions of PMD, which consist in that its activity is presented by the task of plural of Gu of possible variants of decisions of ui $(i = 1,...,N)$, accepted them in the process of management of operations.

Under a decision the sequence is understood of $ui = (ui1 ...., uin)$, that uij – local decisions, characteristic for given and, are i-y situations.

The plural of Gu is broken up on the variants of production situation on the subsets of $G_u^{(S)}$, where s – amount of possible variants of production situation.

Thus the known aggregate of H of indexes of Yi of efficiency of decisions

$$H^S(u_{is}) \rightarrow H(Y_1, Y_2, ... Y_N), \tag{1}$$

in accordance with the values of which the decision of PMD of ui can be attributed to the area of possible, if the aggregate of the set private indexes appears in an area G_Y^S:

$$Y_i \in G_Y^S. \tag{2}$$

The aggregate of indexes (1) allows to define the concept of optimum decision of $uis = u*is$, if $Hs(u*is)$ arrives at a maximal value. The basic task of PMD is folded in the selection of some subset of $G_u^{(S)}$ of decisions, in which, on its opinion, feasible or optimum solutions can appear with most probability, it accepts some suppositions about a situation, classifies a dynamic production situation and does ranging of subsets of $G_u^{(S)}$ where $(s = 1, 2, ..., m)$ with the use of one of types of practical estimation of perspective of subsequent actions, which is expressed as a function:

$$F_i[H_u^S(u_{is})], s=1,...,m. \tag{3}$$

Then for the subset of $G_u^{(S)}$, which a maximal estimation (3) is arrived at on, the area of applicable indexes of efficiency (2) is calculated and estimated, it is whereupon determined better in all from them. The formalized sequence of project procedure of acceptance of administrative decisions of PMD is resulted on fig. 1.

Thus, the formal raising of task of acceptance of administrative decisions, the decision of which becomes possible due to a rapid reaction on events which take place directly in a production is realized, due to application of mathematical methods of indemnification of deviations from a production time-table and programmatic modules of IT of support of management processes in CIAS, will allow to optimize a production and do him more cost-effective.
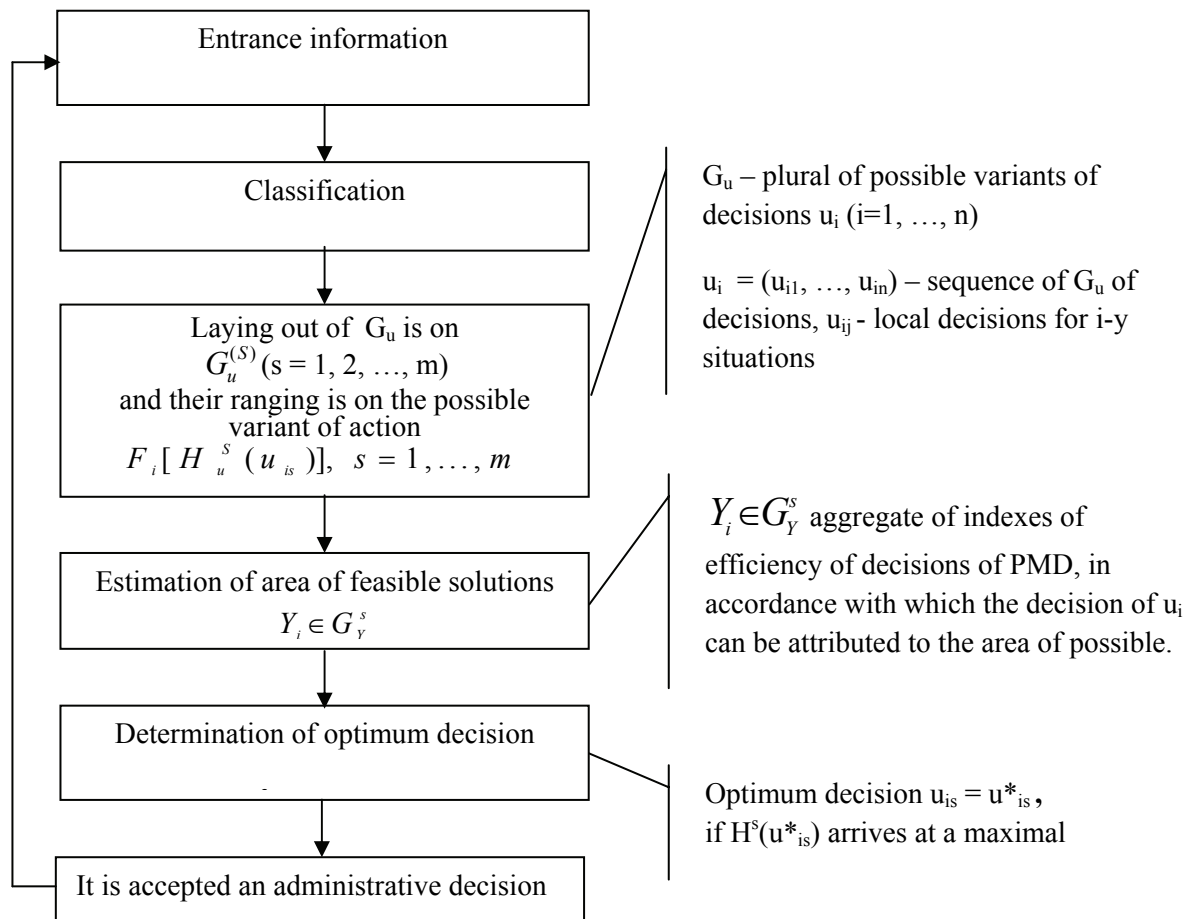
Figure 1. Formalized project procedure of acceptance of administrative decision declaration

At the same time, one of major resources of machine-building enterprise, the more so in the conditions of large nomenclature of wares of enterprise, knowledge is. The competitiveness of enterprise straight depends on organization of management these knowledge's. The wide use of information technologies is provided by the transfer of source of knowledge's from paper transmitters in electronic databases technological setting of industrial enterprises [3]. Databases grew into the basic mean of management information, and consequently and by knowledge's. A management knowledge's in the conditions of multitop-level machine-building production can part on three parts: forming, search and distribution of knowledge's.

Due to appearance sufficiently of big databases application of processing of data, which got the name of «getting of information, became possible» (Data Mining). The process of getting of knowledge's focuses on application of algorithms of search of templates, that allows to attain higher results in comparing to traditional the methods of treatment of information [2].

Knowledge about technological processes is one of the most meaningful areas of knowledge's for a modern production. For providing of complexity of knowledge's there is necessary intervention from a man in dear industry. At the same time with it introduction of the informative systems of the automated management draws the rapid enough piling up of information in bases given. Providing of receipt and treatments of knowledge's without intervention from a man is one of the most substantial problems in development of CIAS.

The area of knowledge's about production resources, processes and objects of production, contains plenty of heterogeneous knowledge's. In general case they can part on five types:
- certificate knowledge's;
- knowledge is about production resources;
- knowledge is about making decision;
- knowledge about the models of technological processes;
- knowledge about the models of object of production.

Knowledge has the manned analysis and interpretation the traditional method of transformation of information. By a key figure at processing of data and knowledge's about technological processes for today there is an expert. For example, on oversea machine-building enterprises there is practice of periodic analysis of tendencies in an engineer, and documents which regulate a production. On the basis of it an expert forms a document in which on the whole describes the results of analysis [3]. Influence of such document on the process of making decision in a sufficient degree limitedly, the form of analysis requires substantial temporal and financial charges, in a considerable measure depends on an expert. In a final result, with reason considerable growth of volume of information such method of analysis is not optimum.

With introduction of IT of support of management processes in IAS on the enterprise of knowledge about the processes of management these bases accumulate in bases given can become the basic source of knowledge's. A receipt of information is about the process of management, based on the models of production process can be the effective mean of automation of processes of management of operations. A process of forming of knowledge's on the basis of getting (extraction) of information from a database IT of support of management processes in CIAS is specific is the process of application of specific algorithms for the receipt of information from bases given (DB). All stages of this process (for example, preparation, selection, and revision of information, and also interpretation of results) are key for the receipt of complete knowledge's, got from DB.

For complete description of knowledge's the informative model of management process must be based on the thorough analysis of in-use information. An informative model contains an all basic objects process: good, details, production resources, route of making, et cetera An informative model is the made structure and formed from well-organized combination of information and knowledge's about details, production and human resources, organization of production processes. An informative model sets protocol of receipt of knowledge's in a database IT of support of management processes in CIAS by standardization of description of elements of process in DB.

Realization of IT of support of management processes is in CIAS, in basis of which there are the guided models of the object-oriented platform, creation of upgradable universal and adaptive CIAS guarantees. Such CIAS can dynamically change the structure of presentation of this DB and source of data. In-use in such system a general informative model changes the object-oriented approach as design method. This approach is a fundamental mean for formalization of area of knowledge's and description of elements of informative model in style of human thought.

The processes of planning and management use plenty of production information and knowledge's [4]. In traditional control system the base of knowledge's mainly contains information for making decision. At offered IT of support of management processes in CIAS a database contains the system informative model of the specialized additions – base of these administrative decisions also (fig. 2).

In DB model-oriented IT of support of processes of management in IAS of knowledge and information is kept as copies of objects. The informative model of additions of IT of support of management processes in IAS can be presented in different presentations. Different presentations can represent different information, for example, of fame about organization of working process, about a personnel, about a technical document et al. A class of objects is basis of description of information and knowledge's. The copy of object shows by itself real information. Methods and rule objects describe knowledge about the process of making decision and system configuration.

Process of the use of IT of support of management processes in CIAS it is possible to divide into three parts: introduction of IT of support of management processes is in CIAS, accumulation of information receipt of knowledge's. The process of receipt of knowledge's, built on the combined application of informative models and specialized methods of the use of software, allows to realize the computer analysis of data selection of knowledge's. The applied tool of process of receipt of knowledge's is given algorithm and rule to the search. The modern generation of bases given is created mainly for support of business-additions. Success of language, applied in all modern SMDB, is based on the use of two-bit of simple elements, sufficient for description majority of production-additions.
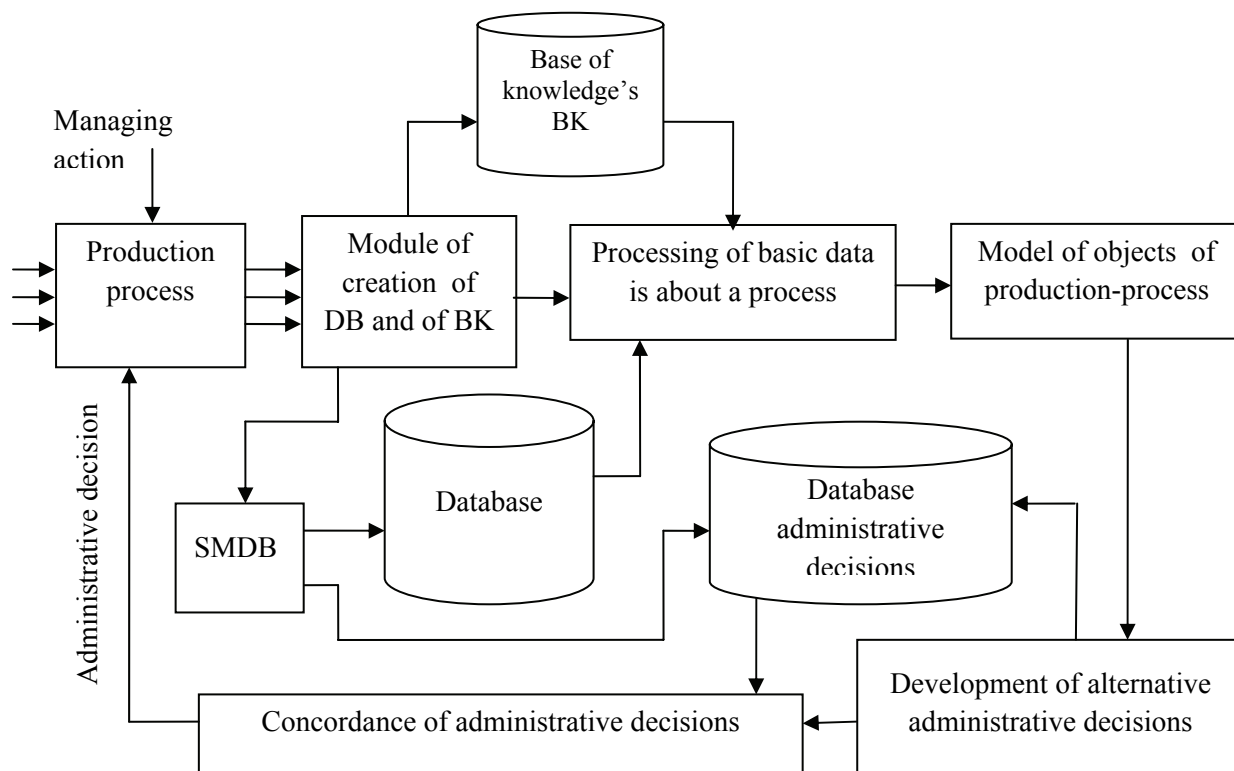
Figure 2. Structurally functional chart of informative support of processes of management in CIAS of the production setting

Unfortunately, to the set of these elements not enough for description of class of the systems, that appears, which (systems) work with knowledge's. The process of extraction of knowledge's from bases given must inherit basic principles which modern SMDB is based on, must be more concrete, what process of creation of queries. It links with that objects bases of knowledge's are more complex in comparing to the records in DB.

Thus, there is a necessity of creation of language, alike from SQL and intended for description of objects knowledge's. Such language must be semantically alike with the language of SQL and to be in a position to translate the elements of language in the elements of SQL for the language of knowledge's in DB.

Conclusions

Forming of base of knowledge's and management knowledge's is important direction of development of automation of management a modern machine-building enterprise. Next to it forming of base of knowledge's is a difficult and complex process which requires considerable charges. The process of forming of base of knowledge's can not be successfully completed only by programmatic facilities, however much application of new methods of construction of software will allow to standardize the sets of data and will allow to use facilities of automation for forming of bases of knowledge's.

References

1 Boyko V. Computer-integrated systems planning and management / V. Boyko, G. Boltunov, O. Mansurova − SPb. : SPBGU ITMO, 2010. – 162 p.

2 Pavlenko P. Automated systems of technological preparation of the extended productions. Methods of construction and management: Monograph / P. Pavlenko − K.: Book publishing house of NAU,2005.–280 s.

3 Terelyanskiy P. Systems of support of making decision. Planning experience: monograph / P. Terelyanskiy − Volgograd : VOLGGTU, 2009. – 127 p.

4 Kulga K. Models and methods of creation of the computer-integrated informative system for automation of technical preparation and management of aviation and machine-building operations: monograph. / K. Kulga, I. Krivosheev. − M.: Engineer, 2011. – 377 p.

UDC 004.94:378.14 (043.2)

Y. Vlasenko (National Aviation University, Ukraine)

METHOD OF ESTIMATING OF THE INTEGRATED COMPETENCE OF IT-SPECIALIST

The article describes the method of estimation and visualization of the results of evaluations of groups (sub-) attributes, which allows you to compare equal competence of experts and expect a generalized index - a compliance rate.

The method of estimating the integrated competency specialist technical profile is based on using a model of individual competence of staff, which includes as components of feature vector knowledge, skills and abilities (KSA), professionally important qualities (PIQ), and motivation (MT), each of which may in turn be viewed as a collection of sub- attributes. Attributes can be measured using different scales. In particular, the biomedical and physical dimensions characteristic of PIC be measured using the scale intervals and / or absolute scale, for which there are computerized methods of treatment. The results of these measurements can be included in the data on which the decision is made regarding the level of competence of the specialist technical, directly or subject to changes in the value of the average four-point scale.

Thus, consistent processing results are subject to performance during the acquisition of appropriate technical profile - profession (marks in the diploma), the expert survey, testing, and certification, expressed the average estimates. The result of applying the model of individual competence of the employee to be a reliable conclusion as to compliance with the competence of the expert (the object of diagnosis), the reference value corresponding to the technical standard profile or the negative result.

To solve this problem, developed an automated system of evaluation of competence (ASEC), which actually is an expert decision support system (ESPPR) constructed on the basis of the shell and the tool is designed for state estimation of complex systems (objects) in the presence of a significant number of important factors or on the basis of the personnel management system. At the same time provide the linkages and interdependencies between the factors that are beginning to use the system can be clearly defined. Scheme information links in the application of ASEC shown in Fig. 1.

1 The baseline data for evaluation
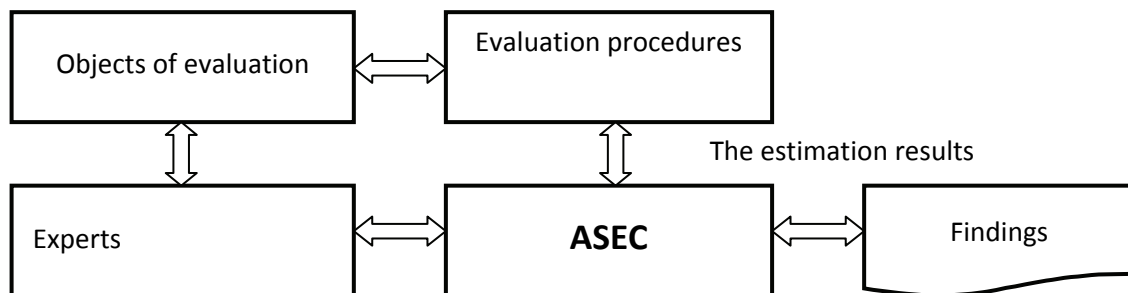
Figure 1 -The scheme links to the information ASEC

For each of the technical specialists (object reference), passing competency assessment completed personogramma, which contains a set of attributes - three of the estimates obtained from the average four-point scale (AFPS), or converted to its values.

The first group - the overall results of expert evaluation specialist, which indirectly determine the level of knowledge, skills and abilities. This group of data reflects the personality traits such as intelligence, creative approach to business, independent thinking, good memory, diligence and patience in achieving the goal, the ability to implement its KSA in practice.

The second group of estimates - the results of expert evaluation of professionally important qualities (STC) is estimated by experts. An example of a source of such assessments may be the so-called factor of sixteen test signs Cattell - questionnaire is a subjective level of control.

The third group of estimates - the results of expert assessment of the motivational component. The most common methods for identifying motifs include staff interviews, tests and questionnaires. The interview may be conducted by the method of STAR When tested in domestic practice are most commonly used tests such as the method of estimation Smeykla - Kucera, the method of "career anchors" E. Shane,

method of diagnosis of labor motifs V. Gerchikova, etc.

The number of groups of attributes and, accordingly, the estimates are generally not limited and can be expanded by, for example, data relating to the definition of an emotional type of worker, physiognomic data, graphological, fingerprint and others, are widely studied in the present methods of identifying the qualities individuals

2 Visualization of the results of evaluation evidence

Take a circle and divide it into n (number of partial indicators) sectors. For each of the objects of comparison (OC) postpone the distance along the radius proportional to the values of the partial indicators v_i and obtain a polygon. In the graphical representation of results of calculations by means of the Excel application of MS in the form of so-called radar chart this polygon (Fig. 2) is a visualized way personogrammy expert who evaluated or any one of the components of its feature vector. The area of a polygon can be calculated by the formula:

$$S_P = \sum_{i=1}^{n} S_i , \qquad (1)$$

where S_i - the area of a triangle which is formed by connecting adjacent values v_i and v_{i+1}.

To calculate the area of a triangle of an arbitrary orientation of the calculation formula is applicable in a rectangular coordinate system:

$$S_\Delta = \left[x_1(y_2 - y_3) + x_2(y_3 - y_1) + x_3(y_1 - y_2) \right]/2 . \qquad (2)$$

If one of the vertices of a triangle, for example, the third, placed at the origin, then (2) simplified:

$$S_\Delta = \left| x_1 y_2 + x_2(-y_1) \right|/2 . \qquad (3)$$

In the general case

$$S_i = \left| x_i y_{i+1} + x_{i+1}(-y_i) \right|/2 , \qquad (4)$$

where $x_i = v_i \sin[\alpha(i-1)]; \quad y_i = v_i \cos[\alpha(i-1)]; \quad \alpha = 2\pi/n$.

The reference space in the form of a regular polygon inscribed in a circle with a radius corresponding to the maximum value for the selected v_{max} scale, is an ideal way formalized technical specialists - a benchmark. His area of S_R can be calculated by the formula (4) provided $v_i = v_{max}$.

Compliance rate of the j-th expert estimated to the ideal image, calculated as:

$$K_{CB_j} = S_{P_j} / S_R \qquad (5)$$

For example, for technical specialists - M., the level of KSA is the best on the results of testing (the test is made up of 13 questions) an arithmetic mean of the estimates (AME) is equal to 4.38, the value estimates, measured by means of the average four-point scale presented in Table 1, visualized results - shown in Fig. 2.

Table 1

The results of estimating the level of specialist KSA

№ job	1	2	3	4	5	6	7	8	9	10	11	12	13
E_{AFPS}	5,00	5,00	5,00	3,66	4,66	4,33	3,00	4,23	5,00	4,66	4,66	3,67	4,04
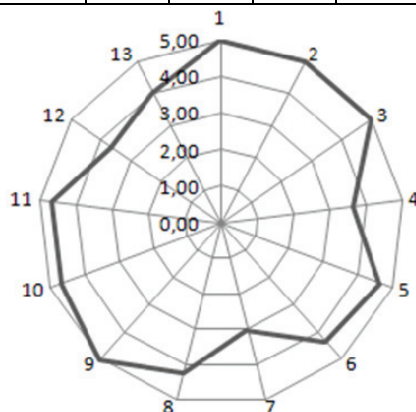
Fig. 2 – Radar estimation of the level of KSA

Calculated according to formula (5) The value of the coefficient of conformity $K_{cBj} \approx 0,77$.

3 Data processing

Preprocessing of the collected and accumulated data is estimated by experts to provide analysis of all sources of information, its arrangement, and preparation for computer

processing means applications that are part of the system software staffing companies.

We use logical methods describe the subject area and represent a model of the data processing specialists evaluated the language of predicate calculus.

Let $M = \{m_j\}$, $j = 1 ...$, m - a lot measured at the level of competence of technical specialists, power or cardinal number which is equal to m. Each of the elements mj, this set is a set of properties (attributes). Select them from the top and represent them as a set of attributes $V = \{v_i\}$, $i = 1...,n$, For example, professionally important qualities (PIQ) specialist: v_1 - discipline, v_2 - perseverance, v_3 - determination and so on. Then the set-theoretic language can be written: $m_j \in M$ and has the property $m_j|V(m_j)$.

In essence, each attribute - it is a linguistic variable - "discipline," "perseverance," "resolve," and so on, which can be estimated in the range of the average four-point scale [2.00 ... 5.00].

We assume that the limiting value of the estimated fuzzy values is a number $\alpha \geq 4,00$, which in the theory of fuzzy sets is called α-cut of the membership function. In other words, we assume that the assessment $m_j \in M$ of an attribute v_i, the value $\alpha \geq 4,00$ characterizes the best of professional and $\alpha < 4,00$ - vice versa.

Consider the predicate $G(m_j(v_i))$ which means that a specialist $m_j \in M$ has all n properties $v_i \in V$, that can be measured in the range [2,00... 5,00]. Then the axioms that define a group of competent and incompetent professionals, respectively:

Axiom 1. $\forall m_j G\big(m_j\big(v_1 \wedge v_2 \wedge ... \wedge v_n\big) \geq 4,00\big) \rightarrow 1$;

Axiom 2. $\forall m_j G\big(m_j\big(v_1 \wedge v_2 \wedge ... \wedge v_n\big) < 4,00\big) \rightarrow 0$.

For the group of the required level of competence of specialists processing continues. We write predicates on the model:

Predicate 1. $\exists m_j \exists v_i G\big(m_j, v_1\big) \rightarrow 1$;

Predicate 2. $\exists m_j \exists v_i G\big(m_j, v_1 \wedge v_2\big) \rightarrow 1$;

....

Predicate n. $\exists m_j \exists v_i G\big(m_j, v_1 \wedge v_2 \wedge ... \wedge v_n\big) \rightarrow 1$

The sequence of subsequent processing is as follows:

1.   For each group (subgroup) of the equilibrium properties (attributes) to calculate the matching competencies j-th expert in the formula (5):

$$K_{CB_j} = S_{\Pi_j} / S_{\Im}$$

2.   Forming a matrix V of dimension m × k, where m - number of objects of comparison; k - number of groups (sub-) attributes (partial characteristics) of the objects of comparison.

3.   Calculate the column vector R, is the vector whose components $(r_1...r_n)$ calculated by the expression: $R = V \times W$,

where W - column vector of values of the weighting characteristics, as determined by experts.

4.   Chosen specialist expertise which corresponds to the maximum value of the element column vector R or more objects in order of decreasing values of the estimates of r_j.

In the case of coincidence of assessments of the competence of the individual estimated rj experts on the elements of the set of quasi-formed, for example, five experts who evaluated:

$$\big(m_1(R) = m_3(R)\big) > \big(m_2(R) = m_4(R)\big) > m_5(R).$$

The final rankings with some additional conditions will be presented as a series of advantages (for the same example):

$$m_1(R) \succ m_3(R) \succ m_2(R) \succ m_4(R) \succ m_5(R) \tag{6}$$

Here the sign "$\succ$" notes the ratio of benefits.

5. A series of advantages (6) and the final statement about each of the estimated relative levels of their professional competence granted to the decision, as the output.

4. Assessing the adequacy of the characteristics of the developed technic

To estimate the accuracy of the proposed method using a reduced error limits of permissible basic error:

$$p = \Delta / X_N \tag{7}$$

where Δ - absolute error of estimation results; X_N -- scale length.

In our case, the result of evaluation contained four significant digits, that is, any evaluation of the results (the coefficients of compliance) may be varied 0,6400... 0,9999 (X_N = 0,9999 - 0,6400 = 0.3500) with an absolute error $\Delta \leq 0,0001$, and reduced error is:

$$p = 0,0001 / 0,3500 \approx \pm 0,0003.$$

With the same number of significant digits of the weight handling medium and median estimates of comparison sites (results of the evaluation may vary in the range 4.000 ... 5.000) gives

$$p = 0,001 / 1,000 \approx \pm 0,001.$$

Obviously a three-fold advantage in the accuracy of the method that is proposed.

The sensitivity S characterizes the ability of any transmitter measurements respond to changing input values and estimated by the ratio of signal change Y_{out} output to a change in the signal at the input X_{in}. Sensitivity - is usually a dimensional quantity, which serves a variety of units that depend on the nature of input and output variables.

In general, the sensitivity S is defined as the derivative of the transformation:

$$S = dY / dX \approx \Delta Y_{out} / \Delta X_{in} . \tag{8}$$

It is obvious that the sensitivity decreases with increasing number of features (partial performance), but is sufficient for the differences in their professional competences, any one of the estimates which differ by $\pm$ 0,01 points.

Calculated values of similar characteristics of other methodologies for assessing the competence of an integrated specialist technical profile analyzed in the literature available.

Conclusion

1. Developed a method for the quantitative assessment and visualization of results of evaluation groups (subgroups) signs, which allows you to compare the equal competence of professionals and expect a generalized index - a compliance rate.

2. A method for estimating the rating technical specialists on a formal model based on data about the employee being evaluated, which may reduce the subjectivity in assessing and comparing the selection of personalized data personogramm (the values of the results of expert estimation of individual parameters) according to certain rules and formulation of recommendations for decision makers.

3. Carried out performance testing of integrated assessment methods competency technical specialists and software implementations on real data, which confirmed the possibility of ensuring objectivity during the proficiency test to determine the level of specialist.

4. Evaluated characteristics of the proposed methodology - given uncertainty and sensitivity - which is sufficient for the application of techniques in practice.

UDC 005.311.2:004.94

V. Kudryakov, m.n.s.
(National Aviation University, Kyiv, Ukraine)

FORECASTING OF DYNAMICS OF PRODUCTIVITY OF THE EQUIPMENT OF THE ENTERPRISE BY MEANS OF INFORMATION SYSTEM OF TECHNICAL OPERATION MANAGEMENT.

In the reports considered by the requirements to the information of the automated control system of technical exploitation, the introduction of which will allow us to greatly increase the efficiency of production and the capitalization of the industrial enterprises.

Domestic industrial enterprises during the current crisis, are in a difficult situation: the high level of demolition of fixed assets, a shortage or lack of investments for its renewal, low production efficiency, run-down technology, the lack of qualified specialists. The worst of it is accounted for the enterprises which are engaged in science-intensive production. This is connected with the high cost of equipment, and with serious requirements to qualification of the personnel, and to strong competition from foreign enterprises. Such a situation makes the issue of improving efficiency of production and the competitiveness of the enterprises on the domestic and external markets. For the decision of these problems in recent years more and more often use methods of re-engineering the business processes of the enterprise. Properly conducted reengineering of the business processes allows to tens of percent increase efficiency of work of industrial enterprises, but often reengineering projects do not achieve planned results from the shortage of working capital and investment, which is directly connected with the capitalization of the enterprise. Consider the possibility of solving these problems, on the basis of the experience of the developed countries and the opportunities of modern information technologies.

Capitalization of the industrial enterprise - the quantitative characteristics of the effectiveness of its use. Capitalization of characterizes not so much the asset as a thing, as an asset, which works. The cost of the asset can be represented as the multiplication of the value of an in-demand product, produced assets in a unit of time, the expected time of its functioning. The cost of domestic tangible assets compared with their foreign counterparts is very low. Many of the engineering industry market value is less than a hundred times or even close to zero. These assets need to upgrade and replace because the end of their life cycle. Replace the dilapidated assets preferably at a more efficient. But to solve the problem of low value assets, it is important that modernized assets belonged to a qualitatively new type, which is amenable to digitization. Digital production assets allow to determine exactly how much and what kind of resources they consume on the input, how many products and services are provided for the output. And the most important thing, digital asset quality provide a forecast of dynamics of their productivity. Only then it becomes possible attraction of investments on modernization projects.

The project of re-engineering to increase capitalization of the company shall be at least three different project level:
- at the level of production technologies it is necessary due to a partial, limited modernization or replacement of assets add them additional digital quality;
- at the level of information technologies it is necessary to carry out such processing of digital data, to ensure the monitoring and forecast of dynamics of productivity of our assets;

Get the investments under the project of modernization of the enterprise is possible only in case, if this project is compliant with stringent standards of financial technologies, so that a potential investor will be able to clearly calculate how much time will you need to return the loan and how it will be done. In order to make the forecast estimation of capitalization, it is first necessary to digitize the performance of the production of the Fund and to build the expected dynamics of its change. We must turn the replacement of each unit of equipment in the attractive investment project with specific parameters and terms of repayment. To increase the investments involved, need to be projected capitalization of each asset, based on the most accurate assessment of his working resource, which remains, and a forecast of the dynamics of its performance. In the developed countries of the world for preparation of such

forecasts are used by system type EAM (Enterprise Asset Management - management of the main funds of an enterprise, allows to reduce the downtime costs for maintenance, repair and logistics).

Thus, the project reengineering needs to be divided into several stages. The first stage is the shortest, it requires a relatively small funds and is to optimize the functioning of the asset. Optimization is achieved by the installation of a special automation and software, which allow to partially copy the asset. As a result accumulates and summarizes the information about the peculiarities of its functioning. Information portrait of the asset allows, improving regulation, achieve gains in productivity by 2-3%. The second stage - the transition from the planned-preventive, typical repairs to address configured precisely to the asset. For this is being developed or obtained special software [1]. Due to this reduced downtime in the repair and possible productivity gains already on 10-12%. It allows to increase revenue, build a credit history, to increase the degree of digitalization of the asset. Then at the third stage it is possible, by increasing the capitalization of the asset, raise funds for a project of the modernization and full replacement.

The second problem of industrial enterprises in the fact that the assets недогружены. In order to maximally use the assets necessary to go beyond the enterprise, construct a chain, schemes, networks of production of new products and services, the new value at which the asset after it should be built to its full load. This means that most of the resources, which are needed for the implementation of this chain, and outside of the enterprise: in the system of public needs, human institutions, the network of suppliers, in the transport infrastructure, the organization of public safety, standardization bodies, communication networks and the like

The activity of the asset, or the means of production, can be divided into some groups. Firstly, to know how he will behave further, it is necessary to understand, that it is, its technical characteristics, parameters. Secondly, you need to understand the modes in which he worked, what events had been happening to him and that is the cause of these events. Under the events are meant a different kind of failure, stop, the non-extradition of the staff parameters up. All these details are recorded in the repair records, defective data. For each group of assets is detailed plan of operation on the basis of the technical characteristics of the production plant and the history of each unit, that, according to statistics, gives the reduction of expenses for maintenance of two to four percent.

Thirdly, you need to take into account the so-called surroundings of the asset, where he is located. One and the same equipment, the product in different chains of production process on a different effect on the rate of return. Need to take account of all the activities associated with the technique of security: the need to perform certain procedures in the repair, in some cases, innocent be a certain way prepared working. All of the listed groups of settings you need to know and in a convenient for themselves the form of have before my eyes in order to predict the production of the asset in the coming years. For assets management according to the methodology it is necessary to collect and take account of the great number of data - on the running time, idle time, the dynamics of the technical condition of assets, costs of material and financial resources for the operation, on carrying out of capital repairs and so on. The collection of these data manual in paper form is not possible. The use of the primary means of automation, such as Excel spreadsheets, does not allow to organize the collection of information from several sources. As a rule, the primary sources of necessary data are in different subsections of the enterprise, territorially remote from the main office. Therefore, the processes of collection and processing of information can be organized only means integrated the automated control system of technical exploitation (IAS), which provides a common information space for all participants of THOSE, irrespective of their location, which supports the convenient system of diagnostics of the technical parameters of the production of the asset and that has a system of controls to monitor all parameters of the assets of

On the basis of computer modeling in the integrated automated control system for THE opportunity to compare the costs, which requires one or the other of the asset, with the incomes, which he can hold, that will allow to compare them and to фондоотдачей new means of production, which appear on the market today [2]. If the parameters of the new assets more profitable (low operating costs, better performance, greater productivity of an asset according to its technical characteristics), then is there a possibility to make the business-plan of the investment project for replacement of equipment,

under which it is possible to attract funds, or to draw up a similar business-plan on repair of the equipment, if in this case repair the asset is profitable, than to replace it. Making information portrait of each asset, you can move it in the direction of not priority service or excess of maintenance, depending on its location in the processing chain. Managing these moments, you can again actively manage value for the cost of repairs and maintenance. Asset management is carried out with the purpose of obtaining specified indicators of their functioning according to the operating conditions and the system of maintenance of efficiency. Indicators can be reliable (failure rate, availability and technical and economic (production volume, cost, profit margin). The optimal duration of life of the asset can be determined for a minimum of specific expenditures, which are machine-hour work, the maximum of the profit per unit, given the level of profitability. Model of the terms of service for a minimum of unit costs and maximum profit per unit (optimal values of approximately the same) it is advisable to apply in case the operating organization funds for the renewal of assets. Model minimum level of profitability applies to businesses that feel the deficit of funds for modernization of the assets [3].

Thus, IAS should contain: the software modules, carrying out planning and accounting of the activities to ensure the assets, the calculation of the indicators in accordance with the methodology, the optimization of business processes, including the definition of the period of service; electronic parts catalog, a database of suppliers of products and services, customers, personnel, market, technology and so on. The basis for the functioning of the integrated automated control system for THAT is the base of data, which contain information on spare parts and materials of each unit of the asset, the types of maintenance and repairs, repair existing equipment, technical and repair documentation, and so on. Because to every object in the maintenance and repair (TM & R) are all maintenance work on it and the necessary resources for them all, the plans of future work and the need for spare parts and materials should be formed in CIASM automatically. On the basis of the accumulated in the integrated automated control system for THE data and in order to implement the above-described methods, in CIASM IT must be formed by analytical forms, which show the results, and also the forecast of performance of technical operations for a given period of time within a given section, for a specific kind of equipment and so forth On the basis of operational data in CIASM IT should be also reliable indicators for each unit of the asset with the use of data, which characterize the operation of this unit. To other tasks CIASM THEN take the optimization of the structure of production assets, control and improve the quality of maintenance and repair, realization of methods of planning of TMR for the development, the technical state, for the minimization of organizational financial expenses for technical maintenance and repair, and so on [4].

Conclusion

In carrying out reengineering of the industrial enterprises should take into account that one of the problems that may hinder the increase of production efficiency is the low capitalization of the enterprises, connected from not download assets and complexity of forecasting of the dynamics of their performance. For the decision of these problems it is necessary to spend the automation of the enterprises with the help of the special information of the automated control system of technical exploitation. The CIAS should be not only the software or database, but also a flexible tool for the improvement of the system of operation of complex technical objects and systems, effective as for small enterprises, and also for large production associations.

References

1. N.M. Kapustin, P.M.. Kuznetsov, A.. Схиртладзе, etc.; Under ed. N.M. Kapustina. Automation of production processes in machine-building / - M.: Vyssh. SHK., 2004. - 415 p.

2. Tomaszewski VM. Modeling of systems. / - SPb.: Articles group BHV, 2004. 352 p.

3. Pavlenko P.M.. Автоматизовані system технологічної following розширених виробництв. Methods побудови the management of: Monograph. - К.: Книжкове view - in the NAU, 2005. - 280p.

4. С.В.Репин, К.В.Рулис, А.В.Зазыкин, Н.К.Ховалыг. Development of information databases of equipment for use in the automated control system of technical maintenance and repair of construction machines. International electronic library (electronic resource: interlibrary.narod.ru) .- 2007. –12p.

UDC 004:377.1

S.V. *Kozyakov, graduate student (National Aviation University, Ukraine)*

FORMALIZATION SUBJECT AREA PROCESSES OF MOTIVATION IT-SPECIALISTS

The article gives the results of researching the interdependence between the needs of IT-specialists, types of their activities and motivators as well as their formalization.

The terms of introducing IT systems as well as the success of their operation depends on the effectiveness of a modern IT-specialist's work. In its turn the efficiency of an IT-worker depends on his motivation which must be individual for every specialist. Nowadays there are many different methods to form the systems of motivators at work, but the three-side dependence between the types of activities, the needs of an IT-worker and motivators is not taken into account.

The existance of a priori dependence between the types of activities, the needs of an IT-worker and motivators which are meant to meet those needs, causes the necessity to formalize this dependence with an aim to solve the task of making the process of managing motivation automatic in future.

The existing interdependeces mentioned above are formalized poorly and are not taken into account in modern information systems of personnel managing (HRM – systems) and ERP – systems (running an enterprise). The solving of this scientific and technical problem is an urgent point, as for the management of an enterprise and for the developers of HRM and ERP systems.

Any pattern of a human behaviour may be explained by internal and external reasons. In the first case, the beginning and the end of explanation lies in psychological features of a person, in the former case — external conditions and the circumstances of his activity. In the first case we talk about the motives, needs, aims, intentions, wishes, and etc., in the former — about the stimulus or motivators which are caused by the current situation.

To develop an IT for managing motivation it is necessary to formalize, which means to describe mathematically, basic notions, objects and their interconnections in this subject area.

Needs — the state of needing of a human being or animal in certain circumstances which are not enough to exist and develop normally. Any need as a state of a person is always connected with the person's feeling of dissatisfaction which is due to the shortage of something necessary for the person. The needs of a person are marked on illustration 1 according to A. Maslow's classification [1].
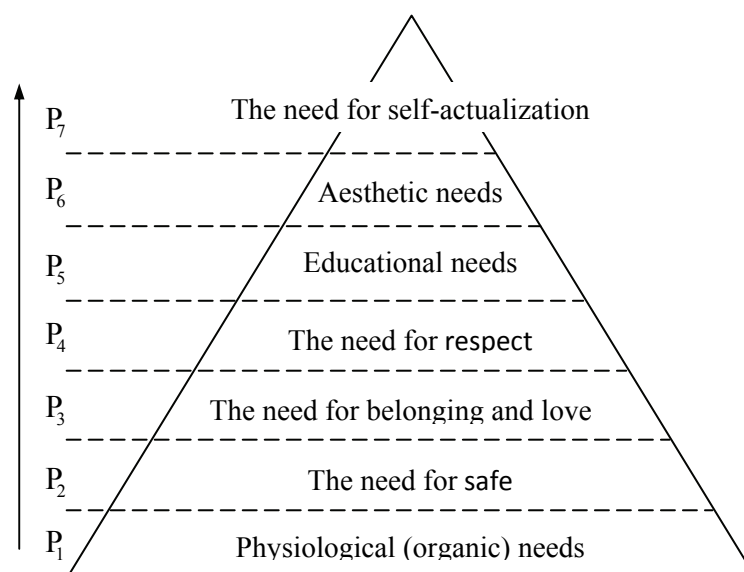
Ilus. 1. A. Maslow's pyramid of needs.

The key point in A. Maslow's pyramid of needs is the idea that the needs are not satisfied by the principle all or nothing. One may say about any healthy personthat he or she is satisfied and not satisfied at the same time in his or her basic needs. The lower needs are always satisfied in a fuller degree than the upper ones. An average person's physiological needs must be satisfied up to 85%, the need of safety up to 70%, the need of belonging, loving and being loved – up to 50%, the need of respect – up to 40%, cognitive – up to 30%, aesthetic – up to 20%, and the need of self-actualization – up to 10%» [2].

The dependence between the needs of an IT-specialist and tje types of his activities while performing his duties at work may be shown as a matrix [1, 2]:
:

$$
M_p = \begin{vmatrix}
P_{11} & P_{12} & P_{13} & P_{14} & P_{15} & P_{16} & P_{17} \\
P_{21} & P_{22} & P_{23} & P_{24} & P_{25} & P_{26} & P_{27} \\
P_{31} & P_{32} & P_{33} & P_{34} & P_{35} & P_{36} & P_{37} \\
P_{41} & P_{42} & P_{43} & P_{44} & P_{45} & P_{46} & P_{47} \\
P_{51} & P_{52} & P_{53} & P_{54} & P_{55} & P_{56} & P_{57} \\
P_{61} & P_{62} & P_{63} & P_{64} & P_{65} & P_{66} & P_{67}
\end{vmatrix}, \qquad (1)
$$

where every element of it means a subset of a certain set of needs, every line forms a set of needs for different activities (ensuring vital functions, work, studying, free time, communication, carreer [3]); $M_P = |P_{ij}|$, $i = \overline{1,6}$, $j = \overline{1,7}$, де $P_{ij} \subseteq P_j$, where , 6 – the number of activities, 7 – the number of needs.

To define the set of needs which are fulfilled in different activities questionaires were designed for expert evaluation. The interview of 50 IT experts at a basic for this research enterprise "Motor Sich" (the city of Zaporizhya) allowed to single out the needs which are not used in certain types of activities, $P_{31} = \varnothing$, $P_{41} = \varnothing$, $P_{51} = \varnothing$, $P_{61} = \varnothing$, $P_{32} = \varnothing$, $P_{62} = \varnothing$, $P_{13} = \varnothing$, $P_{14} = \varnothing$, $P_{15} = \varnothing$, $P_{16} = \varnothing$, $P_{17} = \varnothing$, which in its turn allows us to show matrix (1) as follows:

$$
M_p = \begin{vmatrix}
P_{11} & P_{12} & 0 & 0 & 0 & 0 & 0 \\
P_{21} & P_{22} & P_{23} & P_{24} & P_{25} & P_{26} & P_{27} \\
0 & 0 & P_{33} & P_{34} & P_{35} & P_{36} & P_{37} \\
0 & P_{42} & P_{43} & P_{44} & P_{45} & P_{46} & P_{47} \\
0 & P_{52} & P_{53} & P_{54} & P_{55} & P_{56} & P_{57} \\
0 & 0 & P_{63} & P_{64} & P_{65} & P_{66} & P_{67}
\end{vmatrix}, \qquad (2)
$$

The presence of empty sets is caused by the fact that each type of an IT-worker's activity has a certain type of needs to match, and which in their turn were determined experimentally.

Using (2) is possible to formally show the interconnection between the motivators and needs of an IT – specialists. The analysis and diagnostics of these motives connected with different types (factors) of stimulating work and the results achieved by IT-specialists are also necessary.

The methods of stimulating IT-specialists may be various and depend on the stimulating system's quality at an enterprise, the general system of managment and characteristic features of the activities of the enterprise. The methods of stimulation may be split into material, adminisrative, social and psychological, informational. Such classification is one of the widely-spread and is based on motivational orientation of managing methods [3]

The system of motivator sets for IT-specialists, which are aimed to satisfy the needs of a worker may be shown as follows

$$M_M = \left| M_{ij} \right|, \quad i = \overline{1,6}, \quad j = \overline{1,7}, \qquad (3)$$

where M_{ij} - the set of motivators aimed at satisfying the needs of a j-type worker, and they are realised in the process of i-type activity, in this case $M_{ij} = \left\{ M_{ij}^h \right\}, \quad h = \overline{1,4}, \qquad (4)$

where M_{ij}^h – the set of h-type motivators, which are aimed at satisfying the needs of a j-type worker, and are realised in the process of i-type activity, $M_{ij}^h \subseteq M^h$.

As a visual aid the system of motivator sets of IT-specialists may be presented as a matrix :

$$M_M = \begin{vmatrix} M_{11} & M_{12} & M_{13} & M_{14} & M_{15} & M_{16} & M_{17} \\ M_{21} & M_{22} & M_{23} & M_{24} & M_{25} & M_{26} & M_{27} \\ M_{31} & M_{32} & M_{33} & M_{34} & M_{35} & M_{36} & M_{37} \\ M_{41} & M_{42} & M_{43} & M_{44} & M_{45} & M_{46} & M_{47} \\ M_{51} & M_{52} & M_{53} & M_{54} & M_{55} & M_{56} & M_{57} \\ M_{61} & M_{62} & M_{63} & M_{64} & M_{65} & M_{66} & M_{67} \end{vmatrix}, \qquad (5)$$

where every column means a set of motivators which satisfy certain needs in the Maslow pyramid depending on the type of their activity..

To define the sets of motivators for IT-specialists, which satisfy the needs of a person and a fulfilled in different types of his or her activity an expert interview was conducted and it was based on the form given in table 1

Table 1 — A fragment of the form for the expert interview which was meant to define a set of motivators for IT-specialists, which satisfy the needs of a person satisfied in different types of his activity

P24→M24 Motivators that meet the need for respect in the process of labor

	M1						M2												
	m_{11}	m_{12}	m_{13}	m_{14}	m_{15}	m_{16}	m_{21}	m_{22}	m_{23}	m_{24}	m_{25}	m_{26}	m_{27}	m_{28}	m_{29}	m_{210}	m_{211}	m_{212}	m_{315}
p_{41}	+		+	+	+									+	+		+	+	
p_{42}																			
p_{43}				+														+	
p_{44}				+														+	
p_{45}				+														+	
p_{46}	+	+	+	+	+	+											+	+	+
p_{47}				+	+														
p_{48}																		+	+
p_{412}													+						

P34→M34 Motivators that meet the need for respect in the learning process

	M1						M2												
	m_{11}	m_{12}	m_{13}	m_{14}	m_{15}	m_{16}	m_{21}	m_{22}	m_{23}	m_{24}	m_{25}	m_{26}	m_{27}	m_{28}	m_{29}	m_{210}	m_{211}	m_{212}	m_{315}
p_{41}														+	+		+	+	
p_{42}																			
p_{43}																		+	
p_{44}																		+	
p_{45}																		+	
p_{46}																	+	+	+
p_{47}																			
p_{48}																		+	+

All the points were given by the experts individually, relying upon their personal experience in managing motivation at an enterprise.

As a result of the interview 32 questionaires were received with the expert marks. The processing of the forms allowed to get a system of motivator sets for IT-specialists, the mentioned sets satisfy the needs of a person and are fulfilled in different activities.

The system of motivator sets got from the interview (5) is aimed at satisfying the needs of a worker and is described by the following sets:

– motivators which satisfy physiological needs;

$$M_{11} = \left\{M_{11}^1, M_{11}^2\right\} = \left\{m_3^1, m_2^2, m_3^2\right\}, \quad M_{21} = \left\{M_{21}^1\right\} = \left\{m_1^1, m_3^1, m_4^1\right\}, \quad M_{31} = \varnothing, \quad M_{41} = \varnothing, \quad M_{51} = \varnothing,$$
$$M_{61} = \varnothing;$$

– motivators which satisfy the need of safety;

$$M_{12} = \left\{M_{12}^1, M_{12}^2\right\} = \left\{m_6^1, m_3^2, m_4^2\right\}, \quad M_{22} = \left\{M_{22}^1, M_{22}^2\right\} = \left\{m_2^1, m_3^1, m_3^2, m_4^2\right\}, \quad M_{32} = \varnothing$$
$$M_{42} = \left\{M_{42}^1, M_{42}^3\right\} = \left\{m_6^1, m_{12}^3, u_{13}^3\right\}, \quad M_{52} = \left\{M_{52}^2, M_{52}^3, M_{52}^4\right\} = \left\{m_3^2, m_{12}^3, m_{13}^3, m_2^4\right\}, \quad M_{62} = \varnothing;$$

– motivators which satisfy the need of belonging, loving and being loved;

$$M_{13} = \varnothing,$$
$$M_{23} = \left\{M_{23}^1, M_{23}^2, M_{23}^3, M_{23}^4\right\} = \left\{m_1^1, m_2^1, m_3^1, m_6^1, m_1^2, m_2^2, m_6^2, m_{11}^2, m_{12}^2, m_3^3, m_4^3, m_{10}^3, m_{14}^3, m_{15}^3, m_3^4, m_4^4, m_6^4\right\}$$
$$M_{33} = \left\{M_{33}^3, M_{33}^4\right\} = \left\{m_{10}^3, m_{14}^3, m_3^4, m_4^4, m_6^4\right\}, \quad M_{43} = \left\{M_{43}^3, M_{43}^4\right\} = \left\{m_{10}^3, m_{11}^3, m_{12}^3, m_{13}^3, m_3^4, m_4^4\right\},$$
$$M_{53} = \left\{M_{53}^3, M_{53}^4\right\} = \left\{m_3^3, m_{10}^3, m_{12}^3, m_{13}^3, m_2^4, m_3^4, m_4^4, m_7^4\right\}, \quad M_{63} = \left\{M_{63}^2, M_{63}^4\right\} = \left\{m_3^2, m_{10}^2, m_{11}^2, m_{12}^2, m_6^4\right\};$$

– motivators which satisfy the need of respect;

$$M_{14} = \varnothing, \quad M_{44} = \left\{M_{44}^3\right\} = \left\{m_{10}^3, m_{12}^3, m_{13}^3\right\}, \quad M_{54} = \left\{M_{54}^3, M_{54}^4\right\} = \left\{m_{10}^3, m_4^4\right\},$$
$$M_{24} = \left\{M_{24}^1, M_{24}^2, M_{24}^3, M_{24}^4\right\} == \left\{ \begin{matrix} m_1^1, m_2^1, m_3^1, m_4^1, m_5^1, m_6^1, m_7^2, m_8^2, m_9^2, m_{11}^2, m_{12}^2, \\ m_1^3, m_2^3, m_3^3, m_5^3, m_6^3, m_7^3, m_8^3, m_9^3, m_{10}^3, m_{14}^3, m_{15}^3, m_1^4, m_3^4, m_4^4 \end{matrix} \right\},$$
$$M_{34} = \left\{M_{34}^2, M_{34}^3, M_{34}^4\right\} = \left\{m_8^2, m_9^2, m_{11}^2, m_{12}^2, m_1^3, m_2^3, m_3^3, m_5^3, m_6^3, m_7^3, m_8^3, m_9^3, m_{10}^3\right\},$$
$$M_{64} = \left\{M_{64}^1, M_{64}^2, M_{64}^3, M_{64}^4\right\} = \left\{m_1^1, m_4^1, m_5^1, m_{11}^2, m_{12}^2, m_5^3, m_7^3, m_8^3, m_9^3, m_{10}^3, m_{14}^3, m_{15}^3, m_1^4, m_6^4\right\};$$

– motivators which satisfy cognitive needs;

$$M_{15} = \varnothing,$$
$$M_{25} = \left\{M_{25}^2, M_{25}^3, M_{25}^4\right\} = \left\{m_1^2, m_7^2, m_8^2, m_9^2, m_{15}^3, m_1^4, m_2^4, m_3^4, m_4^4, m_5^4, m_7^4\right\},$$
$$M_{35} = \left\{M_{35}^3, M_{35}^4\right\} = \left\{m_{14}^3, m_{15}^3, m_5^4\right\}, \quad M_{45} = \left\{M_{45}^3\right\} = \left\{m_{10}^3, m_{13}^3\right\},$$
$$M_{55} = \left\{M_{55}^3, M_{55}^4\right\} = \left\{m_{10}^3, m_{11}^3, m_{13}^3, m_{15}^3, m_7^4\right\},$$
$$M_{65} = \left\{M_{65}^2, M_{65}^3, M_{65}^4\right\} = \left\{m_7^2, m_{12}^2, m_{14}^3, m_{15}^3, m_5^4, m_6^4, m_7^4\right\};$$

– motivators which satisfy aesthetic needs;

$$M_{16} = \varnothing, \quad M_{46} = \left\{M_{46}^1, M_{46}^2, M_{46}^3\right\} = \left\{m_4^1, m_6^1, m_5^2, m_6^2, m_{12}^3, m_{13}^3, m_{14}^3\right\},$$
$$M_{26} = \left\{M_{26}^1, M_{26}^2, M_{26}^3\right\} = \left\{m_1^1, m_3^1, m_4^1, m_5^1, m_6^1, m_3^2, m_6^2, m_9^2, m_{11}^2, m_1^3, m_2^3, m_7^3\right\},$$
$$M_{36} = \left\{M_{36}^3, M_{36}^4\right\} = \left\{m_{15}^3, m_6^4\right\}, \quad M_{56} = \left\{M_{56}^3\right\} = \left\{m_{10}^3\right\}, \quad M_{66} = \left\{M_{66}^2\right\} = \left\{m_{12}^2\right\};$$

– motivators which satisfy the need of self-actualization;

$$M_{17} = \varnothing, \ M_{67} = \left\{ M_{67}^2, M_{67}^3, M_{67}^4 \right\} = \left\{ m_{11}^2, m_{12}^2, m_{10}^3, m_{14}^3, m_6^4 \right\},$$

$$M_{27} = \left\{ M_{27}^1, M_{27}^2, M_{27}^3 \right\} = \left\{ m_5^1, m_7^2, m_8^2, m_9^2, m_{10}^2, m_{11}^2, m_{12}^2, m_1^3, m_2^3, m_3^3, m_5^3, m_6^3, m_7^3, m_{14}^3, m_{15}^3 \right\},$$

$$M_{37} = \left\{ M_{37}^3, M_{37}^4 \right\} = \left\{ m_{14}^3, m_{15}^3, m_7^4 \right\}, \ M_{47} = \left\{ M_{47}^3 \right\} = \left\{ m_{10}^3 \right\}, \ M_{57} = \left\{ M_{57}^3 \right\} = \left\{ m_{10}^3 \right\}.$$

The empty sets which were got allow to show matrix (5) as follows:

$$M_m = \begin{vmatrix} M_{11} & M_{12} & 0 & 0 & 0 & 0 & 0 \\ M_{21} & M_{22} & M_{23} & M_{24} & M_{25} & M_{26} & M_{27} \\ 0 & 0 & M_{33} & M_{34} & M_{35} & M_{36} & M_{37} \\ 0 & M_{42} & M_{43} & M_{44} & M_{45} & M_{46} & M_{47} \\ 0 & M_{52} & M_{53} & M_{54} & M_{55} & M_{56} & M_{57} \\ 0 & 0 & M_{63} & M_{64} & M_{65} & M_{66} & M_{67} \end{vmatrix}, \qquad (6)$$

The presence of zero elements in matrix (6) is caused by the absence of needs which are characteristic for this activity and as a result the motivators which could satisfy the empty sets of needs are not necessary.

Conclusion

The achieved results of decomposition of motivators for IT – specialist according to the types of activity (6) provide the following algorhithmization of the motivator sets' analysis, which in its turn will make the formalization of a three side dependence between types of activities , the needs and motivators of an IT – specialist simplier. As a result – the formalization of in-let data forfurther automatization of the motivation management for IT – specialists at industrial enterprises.

References

1. *Maslow A.* The Farther Reaches of Human Nature / Translated from English. Moscow.: Smysl, 1999. — 425p.

2. *Argyris C.* (1965). Organization and innovation. Homewood, IL: Irwin. Aronoff J. (1962). Freud's conception of the origin of curiosity.Journal of Psychology, 54,39–45.

3. *McClelland D.* Human motivation / Translated from English.- "Peter Press"; edited by prof. E.P. Ilyina. — StP.: St Petersburg, 2007. – 672p.

UDC 005.311.2:004.94

A. O. Khlevnyi (Nation Aviation University, Ukraine)

INFORMATION TECHNOLOGY OF DESIGN ENGINEERING WORKS MANAGING OF INDUSTRIAL COMPANIES

Two basic methods of technological preparation of production are examined; the advantages and disadvantages of each in the allocation of tasks for the design and technological documentation are analyzed. The ways of improving information technology for production purposes is determined.

Rigid industrial competition forces domestic firms to adapt to the market needs and to move from mass production to small-scale or customized production. However, the demands for quality products and terms of their release increased significantly. These demands are realized , to some extent, with modern integrated automated system for production purposes, which automates the process life cycle of products. Especially relevant is the problem of automation of Ukrainian enterprises of aviation and engineering industries, for the phase of technological preparation. Automated system of technological preparation of production must be based not only on modern software tools for solving engineering and technological problems, but also have to use effective methods of management of technological preparation of production.

Currently, two methods are used for managing of engineering work in industrial production. The first (the earlier one) – is a method based on project management. The second is the method, product lifecycle management, based on CALS and PLM-technology.

Project management – is the traditional method of preparation of new products based on the preparation of work plans, the allocation of resources, expenditure and control over it. By carrying out complex projects more problem are solved - the coordination of the parameters of products with the customer, integrating the designing results of the separate parts of the product, the organization of the cooperation of the specialists from different departments and others.

To use the experience of industrialized countries in addressing these issues the standard project management PM BOK (Project Management Book of Knowledge) is developed is being used. Organization of projects based on this standard allows the company to improve the coordination of project work, improve their quality, and shorten deadlines and costs. To implement the project approach in the enterprise it is necessary to adapt PM BOK standard, taking into account the characteristics of organizational structure and the products to produce.

However, this approach is static, it is not flexible and does not take into account the uncertainties, which occur by developing of new products. For example, the customer gives new product requirements during the process of developing, but the engineers do not have time to make necessary changes in product design and finish the project on time. As a result, according to statistics nonprofit organization with affiliates in 170 countries - PMI (Project Management Institute) the production term are not met for 60% of project, the budgets exceed in 80%, and the results require improvements in 75% [1, 2].

Product Lifecycle Management (Product Life Manadement-PLM) expects the usage of technology to create an integrated information environment (ICI). It is necessary to combine jobs of designers and engineers with the help of the system of production to the PDM (Product Data Management) and create a single database, which will combine three applied field data - products, processes, resources. This approach reduces costs (material, time) for the creation and for the establishment of a new product. World experience shows that the manufacturing of products using PLM technology significantly reduces the time of technological preparation of production (TPP), minimizes errors, thus reduces the time to market exit.

These methods will be considered in the example of distribution of work on planning processes in the technology office of the enterprise and the monitoring of their implementation.

The main quality parameters of efficiency of the process of TPP is the time spent on preparing technical documentation (T_{TD}), and its quality, which must meet the requirements of the customer.

To compare two methods of controlling will be used T_{TD}, which in turn consists of the following components:

t_r - time spent in reception (transfer) the design documentation in Technology Bureau;

t_{an} - time spent on analysis of the design documentation and dividing of works on creation of technical documentation among the groups of technologists;

t_{dis} - time for discussing and dividing the tasks among the team leaders, then the leaders of groups give them to each technologist separately;

t_{dev}- the development of technical documentation and changes in product design;

t_{chec} - checking and approval of technical documentation;

t_{tr} - time spent on the transfer documents into the production.

Implementation of the project method in the enterprise and the process of distribution are as follows: when the Technology Bureau receives the design documentation (DD) to a product with the terms of completion of TPP, a manager allocates work on the design of technical documentation (TD) between the groups of engineers.

By analyzing the distribution of tasks will be relied only on engineers own knowledge, skills and qualifications. The process of tasks' dividing will be carried out of the leaders of groups at the meeting. Assignments are given in a written form with the established deadline of each of them, or (if the computer network) electronic copies stored by the leader of each group, or are stored in digital form (floppy disks, CD, flash).

The above described process is extremely laborious and is accompanied with the disputes between the leaders of groups, because everyone is trying to get a better paid job. [3,4].

It is very difficult for the manager of the processing office to take control of the works in accordance with the plan of TPP. It is necessary to analyze information from subordinates, often given in written form, and to calculate the probable completion time of all the work. The process of coordination and approval of changes in product design is very difficult. It is often the reason why the planned schedule fails, and as a result of it - disruption f the terms of product supply.

Thus, the time spent on TPP by the using the project approach and local systems of automation CAD/CAM/CAE and other, will be defined as following:

$$T_{TD\ I} = t_r + t_{an} + t_{dis} + t_{dev} + t_{chec} + t_{tr} \qquad (1)$$

Using the capabilities of modern PDM-systems, and the method of managing of the product's life cycle, the process of getting the DD and the distribution of tasks in designing TD occurs in an integrated information environment. A letter comes to the Head of Technology Office through the corporate mail (in the PDM-system) with technical tasks which indicates the number of products, time and location of TPP on the product DD. Then the head looks DD in electronic format (3D-model drawings) through, plans, allocates tasks between the engineers groups, and sends letters of engagement with the plan for the design of the TD on the product for the teams leaders. In turn, the head of the group divides the work between the technologists.

In such a way is the process of making and approving changes to the design of the product simpler. Due to the integrated information environment of the enterprise, there is a direct exchange of information between its units, and clear business processes of making and approving of the changes. They allow you to make quickly adjustments to product design and not to exceed the planned completion dates MSW. The example of such a business process is shown in Fig. 1.

So t_r, t_{dis}, t_{chec}, t_{tr} reaches zero, or become part of t_{dev} through parallel processes of development and corrections, approval and transfer to the production, and the time of the development of TD in an integrated information environment PDM-system will be determined by the formula:

$$T_{TD\ II} = t_{an} + t_{dev} \qquad (2)$$

The disadvantage of this design work distribution is the distance of the head of Technology Bureau from his subordinates. Much responsibility is on the managers of all levels. Although a

single information base simplifies the process of obtaining the necessary data for the manager, but he must analyze it himself.

By comparing the formula (1) and (2), we conclude that ICI has allowed cutting the development time TD, by automating a number of processes. That's why the majority of domestic enterprises in mechanical engineering, aerospace, automotive industries use the method of managing of the product lifecycle.
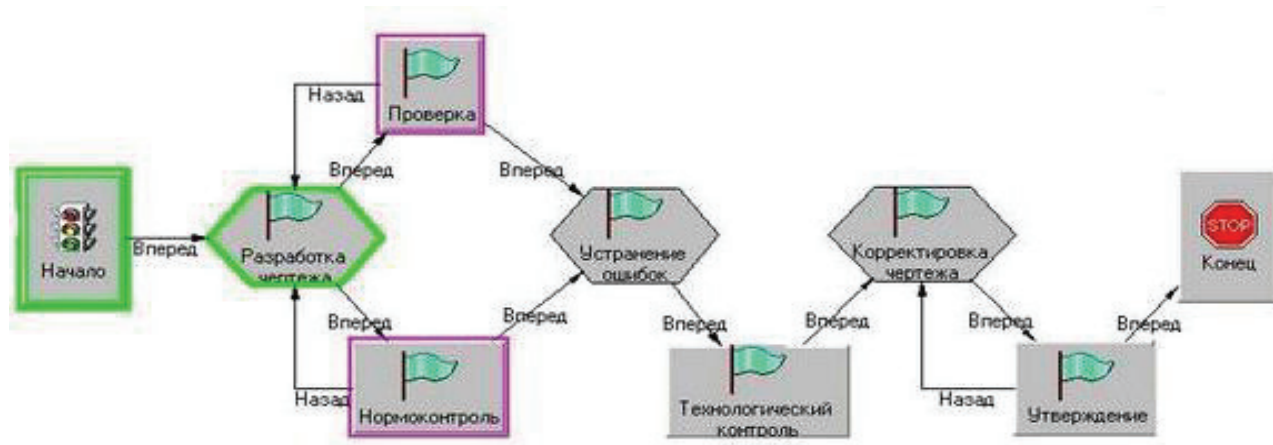
Fig. 1 Representation of the approval process of the developed document in PDM - the system of ENOVIA SmarTeam V5

Automated managing PDM-system such as: ENOVIA SmarTeam, Windchill, Teamcenter, ЛОЦМАН:PLM and others do not have modules that would assist the head of technology office to distribute the work properly among his subordinates, and quickly assess at what level of designing of TD is each group of technologists. Now the head must analyze the information from the PDM-system for the timely detection of failure of plans. It is difficult to do, when you have several hundred of documents.

Modern scientific and technological challenge is to create an information technology, that would expand functionality of the PDM-system, and that would automatically distribute tasks in designing of TD among the technologists, and that would automatically generate routine controlling reports over their implementation.

To solve the task will be use the 3D-model of products. 3D-modeling is widely used for modern industrial production. It can reduce errors by designing; quickly analyze the amount of required resources for the manufacture of products, develop programs for machines with numerical program controlling, present products to the buyer after the completion of the designing work without waiting for producing of products and more.

The domestic enterprises use different designing CAD-systems (SolidWorks, CATIA, Компас, and other), that is why the subsystem, which would analyze and allocate work for the design of TD, must use universal 3D-formats such as STEP.

So, for the work of the subsystem must be generate together with the original 3D-model a copy in a universal format. For this purpose must be used the features of PDM-system, such as ENOVIA SmarTeam V5 (developer Dassault Systemes, France). This system has the ability to automatical generation along with the original model, the file with the same name, but in the STEP format. The Subsystem wills compare the model of 3D-patterns of each technologist with the models of parts of the new product, using the properties of 3D-models: volume, dimensions (width, height), material and mathematical description of geometric shapes. Patterns would be model of the components on which the technologist developed previously TD. Previously dividing the 3D-models and forming the task letters the subsystem will be waiting for the confirmation from the head of the technology office, for sending the tasks to the technologists.

The subsystem controlling the works on the design and technological documentation would use a common database of the company as a source of objective data for analysis. The subsystem would calculate controlling time, which depends on the total (planned) time, allocated for preparation of TD, and would compare the number of design documents issued for the technologist (N_{DD}) for the developing of TD, with the number of approved technical documents (N_{TDd}). According to the formula (3) the percentage of work performed would be calculated and the results of calculation would be displayed graphically in the form of diagrams.

$$K = N_{TDd} / N_{DD} \times 100\% \tag{3}$$

Thus the use of this subsystem presented above will reduce the decision-making process of the head of the managing office for technological preparation of production.

Conclusion

The usage of the product life cycle management is the key to successful competition of the company that produces complex, scientific products. To increase the efficiency of integrated information environment in the process of TPP, must be partially extend the functionality of PDM-systems through the use of the developed subsystem of the automated analysis and distribution of tasks among the technologists, and the controlling over their execution.

References

1. *Бирбраер Р.А., Альтшулер И.Г.* Основы інженерного консалтинга: Технология, экономика,организация / Бирбраер Р.А., Альтшулер И.Г. – 2-е узд.,перераб., доп., – М.: Дело, 2007. – 232с.
2. *Лягушкин А.* От программных продуктов – к отраслевым решениям/*А.Лягушкин*//САПР и графика. – 2008 – №4. – С.54-58
3. Управление жизненым циклом продукции/*А.Ф.Колчин, М.В.Овсянников, А.Ф.Стрекалов, С.В.Сумароков;* Под ред. А.Пальчикова. – М.:Анахарсис, 2002. – 304с.
4. *Павленко П.М.* Автоматизовані системи технологічної підготовки розширених виробництв. Методи побудови та управління: монографія / П.М. Павленко. – К.: Кн. вид-во НАУ, 2005. – 280 с.

UDC 004.67

P. Pavlenko, Dr. of Technical sciences,
(Nation Aviation University, Ukraine),
A. Avedyan (Corp. Dassault Systemes , Suresnes Cedex, France),
O. Cherednikov Cand. of Technical sciences, A. Borisov,
(Chernihiv State Technological University, Ukraine).

THE TECHNOLOGY OF INFORMATION SUPPORT OF THE SIZED ANALYSIS OF TECHNICAL SYSTEMS

Is provided information technology of the sized analysis of technical system, methods of control over analysis process, practical implementations are this.

Any technical system, as well as each element making it, is three-dimensional spatial object, and is characterized by a complex of the sizes and geometrical parameters. In build process the complex of the sizes of one element of a product interacts with complexes of the sizes of other elements therefore there are sized communications. Spatial character of elements of the product, difficult volume configuration of products on the basis of these elements leads to formation of spatial system of sized communications of geometrical parameters – systems of communications of complexes of the sizes of spatial elements. The perspective direction of increase of efficiency of technical systems is use of the approaches based on the analysis of sized communications of surfaces, details and nodes by creation and calculation of spatial sized circuits [1,2].

Support of reliability of the sized analysis (SA) of technical systems at the present stage of development of production is possible only on the basis of creation of the optimized computer technologies. Formalization and mathematical simulation of the sized analysis, development of methods and criteria are for this purpose necessary for their optimization on the basis of computer technologies, creation of the optimized technological processes of an automated assembly and the solution of other tasks.

Development of the computer integrated production is connected to creation of the generalized electronic model of a product which is created, stored, changes and is transferred in a common information space and includes different local models. Thus the data received at one production phase, are used and are available on all subsequent [3,4].

Therefore need for repeated obtaining the same data disappears and time of passing of information flows decreases. Observance of a principle of eligibility of information allows to create models of technological processes of the machine-assembling production, describing not only structure of operations of transitions, but also the mechanism of their impact on a product.

For the purpose of control of SA it is necessary to create control link of U, which is connected to the purposes of control of Z *, through the control algorithm φ, which represents specifying how to achieve a goal, having of information on environment X statuses, nodes Y and the purposes Z^*:

$$U = \varphi\left(X, Y, Z^*\right).$$

Control purposes {Z*} resources of sized communications of technical systems: increase in a resource, lowering of influence of a human factor, lowering of repair costs and maintenance. Control objects closing links of a sized circuit of an element and administrative process by assembly in this case appear.

When reviewing difficult technical systems we always face a discrepancy between nominal and actual parameter values. Owing to the different reasons these parameters represent different random functions on time. The vector of the current or actual structural parameters $Y(t)=(Y_1(t),...,Y_n(t))$, naturally, differs from the initial, initial vector of the structural parameters $Y_0(t)=(Y_{01}(t),...,Y_{0n}(t))$. Let's designate through $\Delta_m(Y_0,Y)$ closing links of sized communications of difficult technical system (aggregate). They depend both on initial Y_0, and from the current vector of

Y of parameters and define operability of system.

The system is efficient, if everyone shorting a link, from all array Δ_m, satisfies to certain conditions. For our researches, this condition if they change in certain boundaries (upper lower deviations of the nominal sizes of closing links) or is accepted by the values close in this or that sense to some in advance set fixed values, defined through coordinate of the middle of a tolerance zone.

One of the main stages arising in case of design of difficult technical systems, consists in support of their working capacity. It is reached for the new aggregate by a set of an initial vector of the structural parameters $Y_0(t)$, and for the aggregate which has looked down on repair, working capacity is influenced by implementation of the current vector of parameters $Y(t)$ which depend on system structure.

Thus, there is a task of a choice of a vector of structural parameters $Y(t)$, for the purpose of array restoration Δ_m which would provide optimum operability of system.

Therefore, operability of system can be described as probability of that any of array parameters Δ_m, doesn't quit for tolerable limits (lower limit α_m, upper limit β_m,), i.e.

$$J(x) = P\{\alpha_m \leq \Delta_m\ (Y_0,\ Y) < \beta_m\}.$$

Many tasks of the queuing theory which is engaged in the quantitative study of processes and quality of servicing systems, are provided to models which, in essence, can be considered from the point of view of the adaptive approach.

Let's consider theoretical premises of an offered technique of increase of the quality level of major repair of aggregates of cars optimization of repair sized communications.

The technique is based on use of the theory of the sized analysis in case of carrying out repair of aggregates of cars, on a choice optimum, from the point of view of restoration of accuracy of closing links, strategy of restoration of sized communications, on acceptance of reasonable decisions in case of restoration of repair sized communications, «decisions» are understood as the sizes of component links providing accuracy of a closing link after repair equal or close to accuracy of the new aggregate.

The objective is solved in four main stages. At the first stage the structural model of the considered aggregate provided in the form of hierarchical structure is created. Aggregate representation in the form of hierarchy gives the chance to us to trace correlation between elements of different levels of system, levels of system are: car as a whole, car system, aggregate, assembly unit, assembly node, detail. Creation of structural model is necessary for executing I use directories of the appropriate aggregates for the purpose of creation of the enlarged model enveloping all array of details, assembly nodes etc.

At the second stage the sized model of the considered aggregate is created. Creation of such model provides the description of details as set of the sizes which in turn are component links of sized communications of the appropriate aggregate. Further there is a compilation of sized communications with the accounting of links entering into them.

At the third stage there is a creation of basis of closing links of the aggregate for comparing – calculation of sized communications for the sizes of the new aggregate (the solution of the reverse task). I use this basis, there is an optimization of repair sized communications as by results of the carried-out researches by us it was revealed that it is possible to take accuracy of the new aggregate for an optimum measure of accuracy of the repaired aggregates.

At the fourth stage there is a choice of an optimum combination of replaced details taking into account their correlations in sized circuits and acceptance of decisions on the sizes of component links, taking into account an array of closing links of the new aggregate.

To evaluate efficiency of the developed technique it is necessary to decide on an index, using which it is possible to evaluate the repair quality level. Such criterion it was selected by L – a resource of a sized circuit after repair, and as an aggregate resource.

Taking into account the carried-out researches it is revealed that the resource of a sized circuit can be evaluated through residual accuracy of a sized circuit. As residual accuracy it is understood – the residual tolerance on the closing link, received in use or calculated after restoration of a closing

link.

The basis of a database of information technology is made by two models: structural and sized. These both models filled with data on the new aggregate are necessary for operation of algorithm of optimization for us.

After implementation of this procedure we have the array of size connections of new aggregate, expressed through the surfaces of details, and set of closing links of new aggregate. These data are constants and mainly does not suffer changes, except for the cases of change of construction of aggregate.

Forming of model of actual sizes of closing links of size connections of aggregate goes the next stage. In the database of size model of aggregate there are sizes as actual (real sizes of details of aggregate, suitable without repair) and sizes of details being on storage of enterprise. Having a base of sizes of details being on storage and plugging in itself all three groups of sizes – new, recovered and suitable without repair, it is necessary to form real-time for the concrete repaired aggregate such combination of commutable in him details, i.e. set into place not suitable, at that a resource of all aggregate will be maximal.

The main functions of the software and information center (SIC) are:

1. creation of structural and dimensional models of the car (unit), which can also be used as electronic catalogs on the unit;

2. completion of these various information models;

3. calculations of state parameters of units before and after repair;

4. formation evaluation and distribution functions of the random variables (size of parts, the rate of wear surfaces of units and others);

5. and the simulation of random events and values of the random variables;

6. resource modeling RC renovated units;

7. selection of the most reasonable solutions to restore ties sized units;

8. search for the best replacement parts list for a given structural characteristics.

Software and information complex consists of several modules (fig. 1).
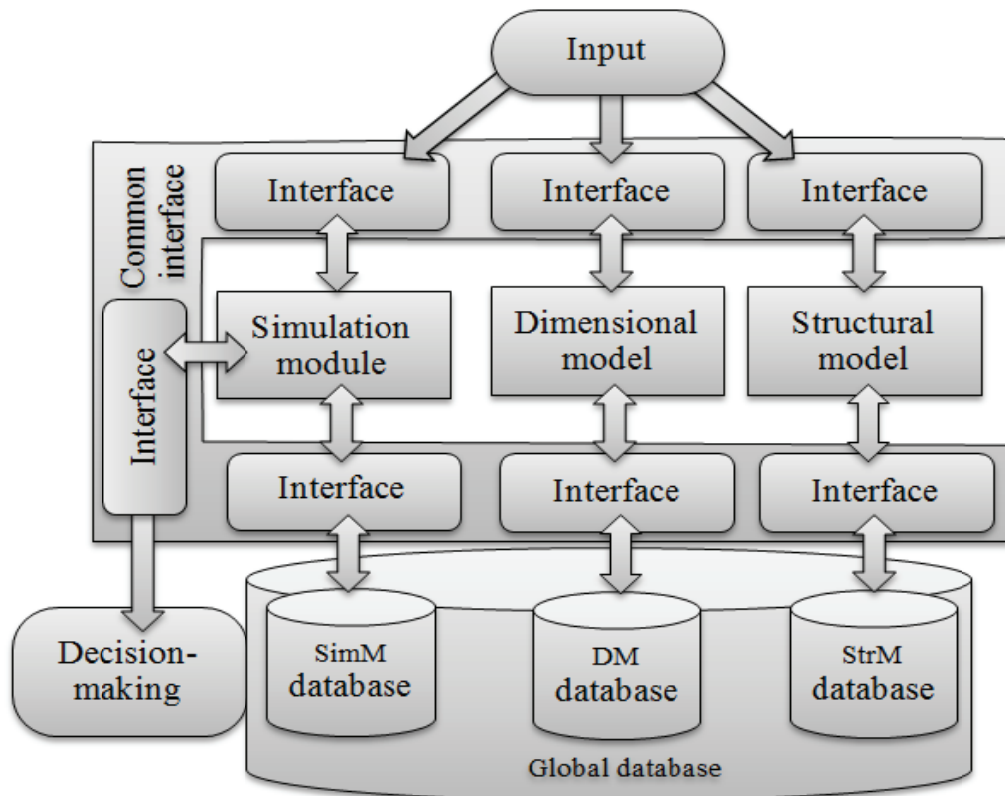
Fig. 1. The general structure and software information center

1.8.33

The main ones are: a structural model of the module (StrM), module dimensional model (DM) and simulation module (SimM). Each module performs its specific objectives, methods, implementation of which will be discussed below.

To ensure that you have input, which can be obtained in different ways, from different sources. To be able to exchange information between the sources of the input modules and the SIC is the interface, and each of his module. Interface enables the exchange of information between the database and the modules and files between simulation module and the simulation results. The set of all interfaces are common interface.

Conclusion

Research has concluded that to improve the quality of assemblies of complex engineering systems can be achieved through better decision-making to restore the dimensional relationships of the unit, determines the accuracy of the output parameters, using the apparatus of the dimensional analysis.

However, the application of the proposed approach has a number of problems associated with the processing of a large amount of diverse and heterogeneous information. The solution to many problems is possible only in case of the use of modern information technology. To this end have been developed:
  ➢ the mathematical model the relationships between the states of the technical system with master links the size of chains,
  ➢ the method of operational control of the dimensional analysis of technological systems,
  ➢ information technology

References

1. *Бондаренко С.Г.* / Особливості розрахунку розмірних ланцюгів спеціальних машин./ С.Г. Бондаренко.// "Вісник ЧТІ". – № 1. – Чернігів: ЧТІ, 1996. – С. 39-41.

2. *Paul J. Drake* /Dimensioning and Tolerancing Handbook / Paul J. Drake, Jr. // Printed and bound by Quebecor. – Martinsburg, – 1995 – 773 p.

3. *Павленко П.М.* Автоматизовані системи технологічної підготовки розосереджених виробництв. Методи побудови та управління: Монографія. – К.: Книжкове вид-во НАУ, 2005. – 280 с.

4. *Чередніков О.М.* Модуль-алгоритм формування баз даних оцифровки поверхонь / О. М. Чередніков, О. О. Борисов, В. І. Канюка // Вісник Чернігівського державного технологічного університету: зб. – Чернігів: ЧДТУ, 2010. – № 45 . – С. 87 – 89.С

UDC 005.311.2:004.94

P. Pavlenko, Dr. of Technical sciences
(Nation Aviation University, Ukraine)
A.V. Tolbatov (Sumy State University, Ukraine)

INFORMATION TECHNOLOGY SUPPORT FOR THE FUNCTIONING OF THE GAS TURBINE POWER

The results of studies of gas turbine power plant processes are represented in this article. An information technology of the predicted time series loads, which significantly increase the stability of gas turbine power plant is proposed.

Information technology of gas turbine power station (GTP) (Fig. 1) performs the following functions: data collection with a block input and output block synthesis plan; data analysis for decision making; storage and retrieval of information using a database (DB), and system database management.
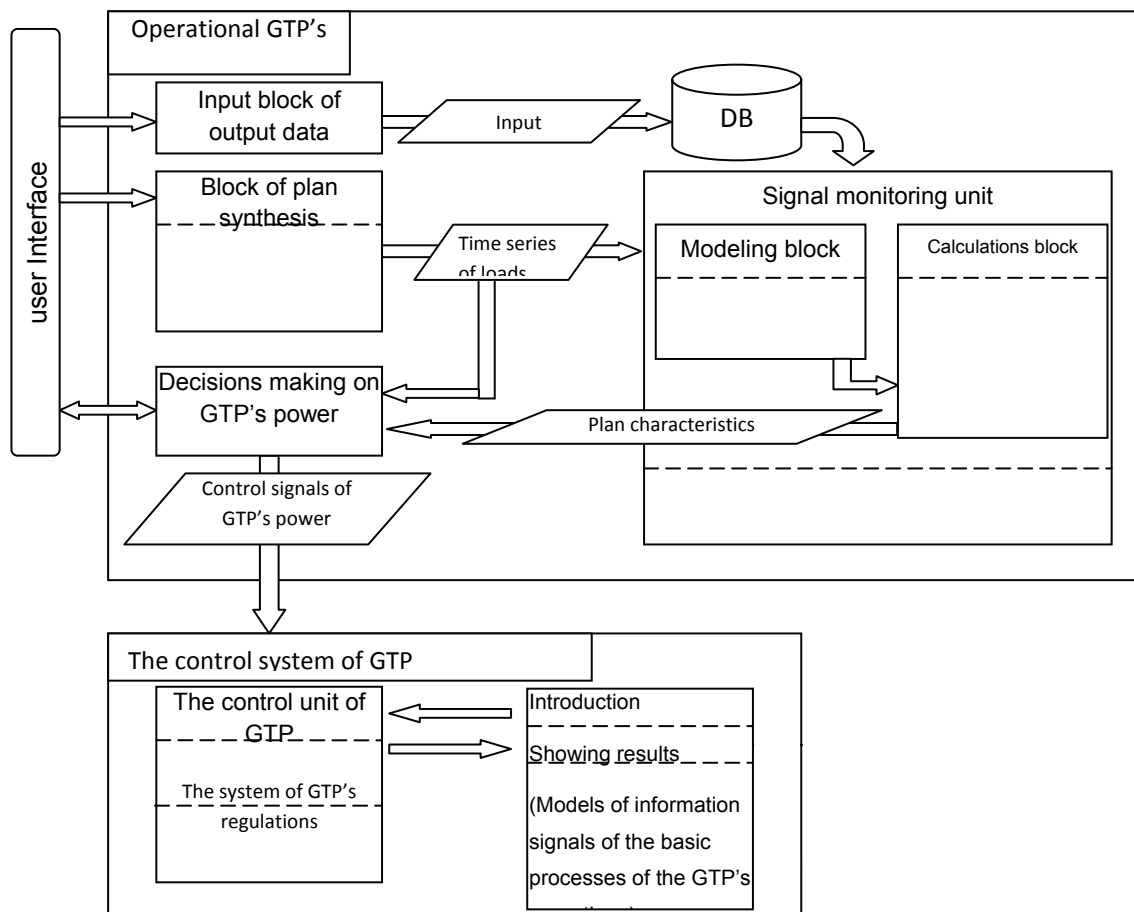
Fig. 1. Architecture of information technology support of the GTP

The person who decides whether to monitor the functioning of GTPs, performs the following functions:
1. Entering the initial data required for calculations.
2. Making decision concerning data processing expediency.
3. GTP power plan synthesis [1].
After GTP's power plan synthesis, plan option goes to the analysis module, which determines the power level of GTP by the way of process modeling. The resulting prediction of GTP power level points to

the possibility or impossibility of monitoring signals and allows to perform automatic calculations of the efficiency of power [2].

Fuel governor controller (FGC) is the software application. The technical novelty of the developed management system is based on FGC module presence, which includes 8 proportional integral difirentiating (PID) controllers which allow to regulate the GTPs power with higher sensitivity and a wider ranges than the automated control system (ACS) of GTP that does not have such module. FGC interacts with the ACS GTPs grogram that solves the problem of motor control sequence diagram forming and its protection by limiting parameters. FGC is used to adjust the power turbine, depending on the load supply. The use of FGC allows GTPs to operate on small loads without compromising the quality of electricity by means of software calculation of control action in real time and impact on dosing gas.

GTPs schedules with electrohydraulic fuel regulator and programmable controller are presented in Fig. 2 and 3, respectively. This GTPs with FGC at rapid changes in the external load up to 100% in 0.25 sec is still in working state. GTPs with electrohydraulic controller at sudden load change over 25% goes to the emergency stop, which is not acceptable in the systems of electricity for local power plants.
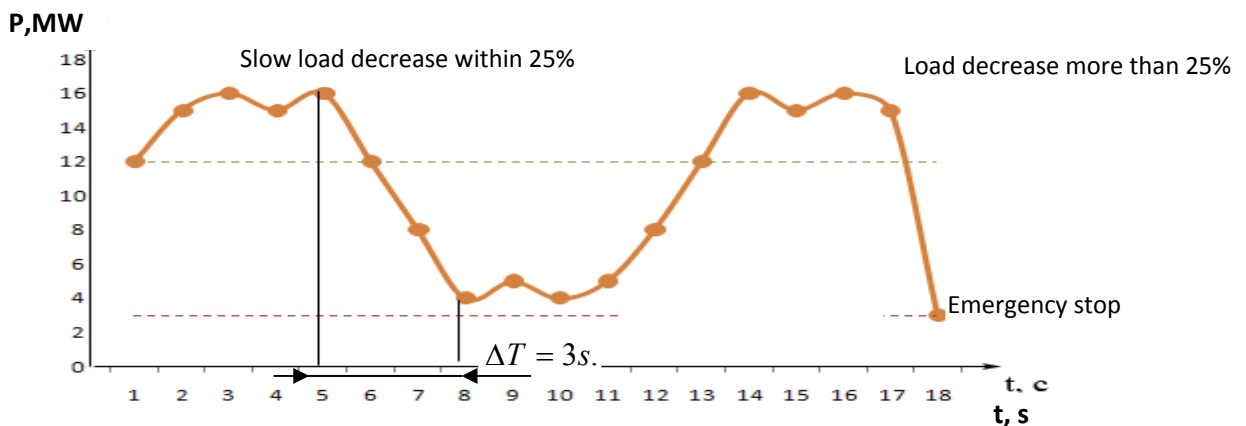
Fig. 2. power consumption Schedule when GTPs with electrohydraulic fuel control is running
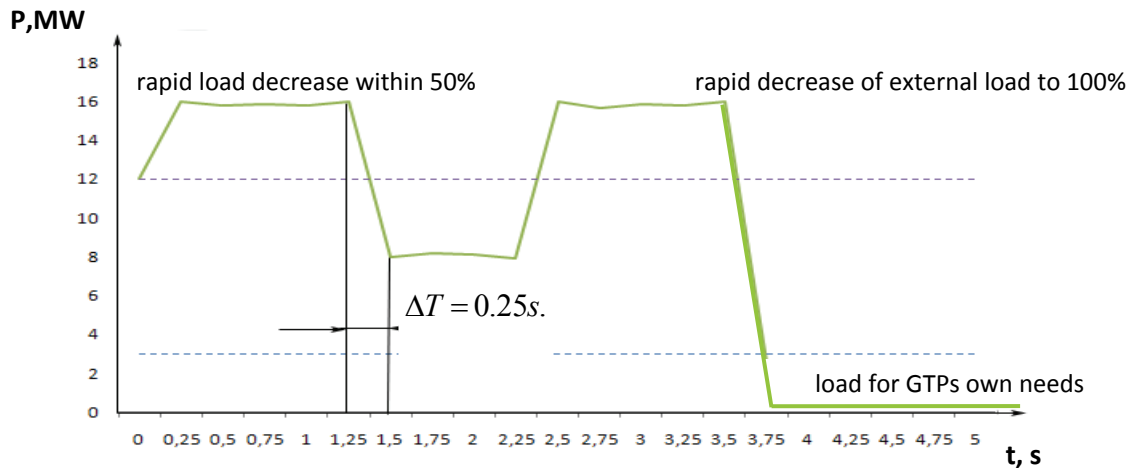
Fig. 3. Power consumption schedule when GTP with fuel governor controller is running

.NET technology was chosen from the wide tapestry of the known distributed development tools, which is developed by Microsoft Company and is one of the most progressive and powerful means. .NET technology is neutral with respect to programming languages, most importantly, that they are compatible with .NET. Net function invocation is possible using different programming languages: Visual Basic, C #, C ++ and others. To increase efficiency of .NET technology, developers introduced new software design. Main programming languages of Microsoft company, such as Visual Basic and Visual C ++ were also reviewed.

Logical database design - information (logical) model design process based on existing data base models, regardless of the target database management system and other physical conditions of implementation. To develop the database relational model was chosen as the most common one. The basic

concepts which determine the relational model are following: domain, relation, tuple, cardinality, attributes, degree, primary key.

General methodology was used to move from the logical data model to physical model:

1. Denormalization of the relational model.

2. Converting relational model into physical model. Each relation is converted to a table. Each attribute becomes a table column. A primary key relationship becomes the primary key table. For columns, if necessary, values ranges can be set.

3. Renaming of tables and attributes of the physical model.

4. Generation of physical models using CASE-method.

5. Renaming the keys, referral relationships.

6. The development of the virtual relationships.

7. Procedures and user functions writing.

The GTP's main operational processes and place of the proposed information technology is shown in Fig.4.
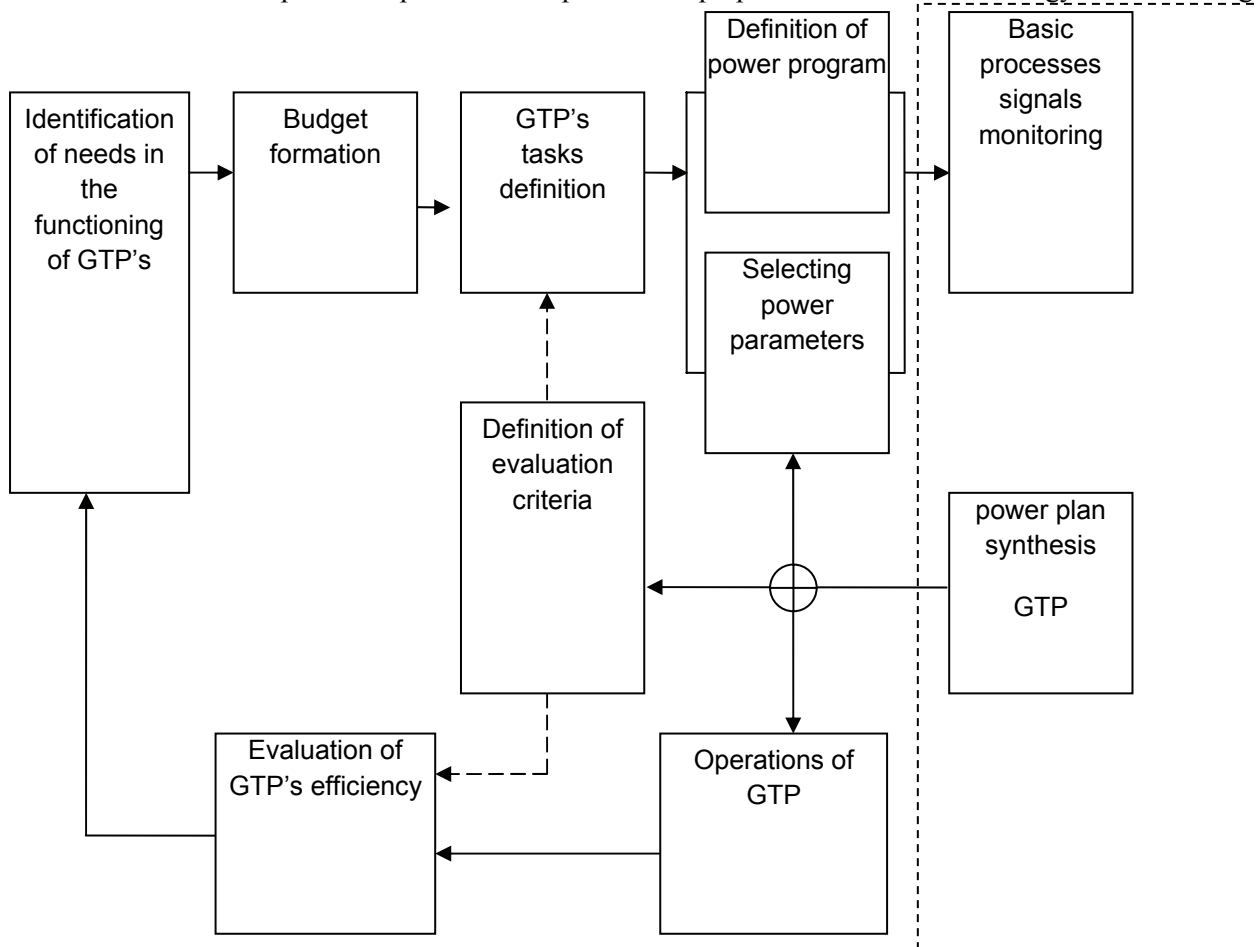
Fig. 4. GTP's operations using data processing information technology

Conclusions

The proposed information technology of the GTP's loads time period prediction with fuel governor controller usage allows to provide stable functioning of power plant in case of external load abrupt changes.

References

1. *Tolbatov A.V.* Control system for gas turbine plant equipment GE Fanuc / Measurings and computer science in technological processes. Hmelnytskyy.-2008. - № 1 p.72-75.

2. *Tolbatov A.V. Shcherbak T.L.* Stochastic model of rhythmic load power plants / Bulletin of the National Technical University "KPI". - Kharkov: NTU "KPI" - 2005. - № .57. - p. 104-112.

K.Y. Ohrimenko, c.t.s., honorable professor of ChSTU
(Cherkassy State Technological University, Ukraine)
K. Eichhorn (K.K. Ohrimenko), c.t.s., docent.
(German Society of International Cooperation, Germany)
V.P. Kvasnikov, d.t.s., prof.
(National Aviation University, Ukraine)

RESEARCHES OF KINEMATIC ACCURACY OF THE KINEMATIC CHAIN TAKING INTO ACCOUNT THE PLANETARY SCREW ROLLER MECHANISM

The technique of simulation modeling on the basis of the equal probability distribution statistical law for definition of the given error of a drive kinematic chain of mechanisms drive when using planetary drive of screw-nut rolling motion is considered in the article.

The calculation procedure of running accuracy of kinematic chains function elements of industrial robots, various mechanisms and, in particular, of metal-cutting tools axis drives, with the use of new perspective planetary drive screw-nut rolling motion with thread rollers while cutting the helical surfaces is offered in the article. Advantages and disadvantages of planetary roller screw drives converting rotary axis motion into progressive one against ballscrew mechanisms and the screw-nut sliding differ from with compactness of a design, high precision of positioning, high loading, dynamic and static characteristics, work possibility at big speeds up to 3000 min^{-1}. For point-to-point accuracy evaluating of actuators output links of industrial robots, similarly to forming accuracy of a cut helical surface from errors effect of each kinematic chain element of axis drive, the synthetic sampling is used. As opposed to the research of accumulated error of spiral gear kinematic chains [1,2] in this research [3,4], when using the planetary roller screw mechanism, on the basis of equipartition law of probability density of random quantities, the statistical method of simulation modeling is applied. With this method the vector nature of the errors defining the direction of their effect, is estimated by quadratic mean. The defining role in kinematic spacing error of the cut helical line forms the accumulated error of intermediate train of gears and the planetary roller mechanism of a kinematic chain. From a condition of the conjugate arcs lengths equality, the worm gear turn $d_{x6} = 40$ mm on the angle $9°$ corresponds $36°$ of roller turn $d_p = 10$ mm and $6°$ of nut turn $d_2 = 60$ mm. The developed determination technique of the greatest cumulative error of helical surface cutting takes into account its importance for each pass within one turn of motion screw and multiple passes from statistical sample, defining influence of each kinematic chain segment on output accuracy. A total cumulative error of cut screw pitch with motion screw turn on the given angle taking into account all kinematic chain segments of the general purpose lathe fig. 1 (in this case 14 links of the cogwheels, four rollers and a nut), accepting harmonious response of change is defined by dependence:

$$\Delta p_{\Sigma} = \sum_{i=1}^{14}\left[A_i \sin\left(k_i\varphi_j + \psi_i\right)\right] + \sum_{j=1}^{4}\left[A_{ip}\sin\left(k_{ip}\varphi_{jp} + \varphi_{jp}\right)\right] + \Delta p_{\Sigma 2} + \delta T_{\Sigma j}, \qquad (1)$$

where i − cogwheel number; A_i, A_{ip} − respectively amplitudes of cumulative kinematic error of cogwheel pitch and rollers motion error; φ_j, φ_{jp} − rotation angles of the motion screw and rollers; k_i, k_{ip} − number of pinion gear revolutions i-th of pinion and rollers; ψ_i, ψ_{ip} − errors phases shift i-th and j_p-th of kinematic chain segments; $\delta T_{\Sigma i}$ − accumulated error limit of motion screw pitch for one screw turn; $\Delta p_{\Sigma i}, \Delta p_{\Sigma j}, \Delta p_{\Sigma 2}$ − accumulated error of a cut helical surface pitch on selected angle and cumulative error of nut helical surface pitch.
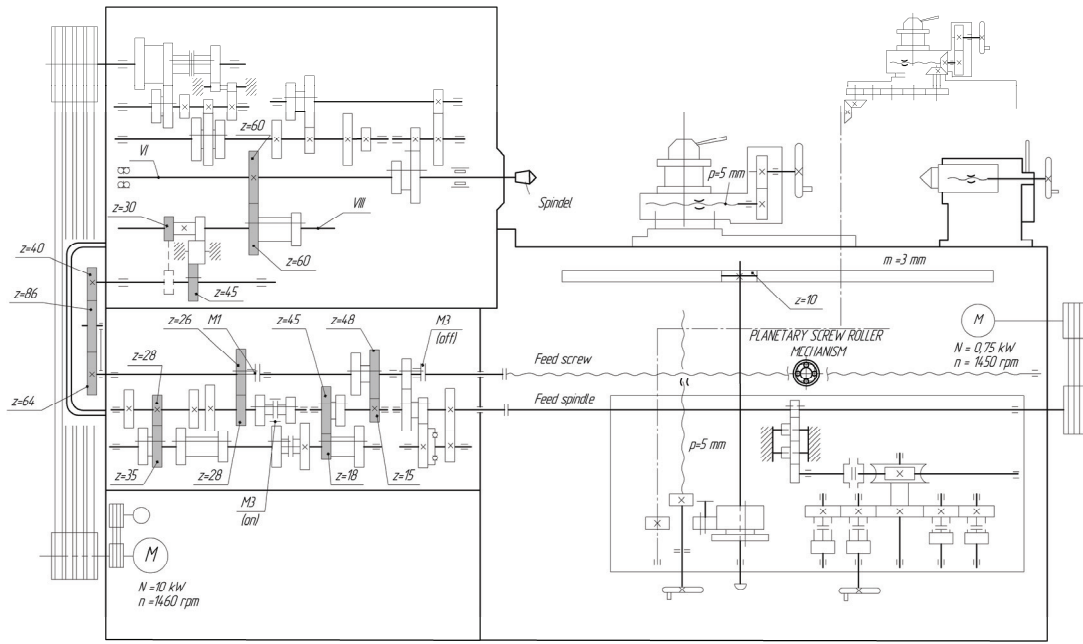
Fig. 1. Kinematic chain of the general purpose lathe

For each pass in this research the accumulated error is defined in nine degrees of the motion screw turn $\varphi_j = 9°$ (where number of samples $j = 40$). And each angle corresponds φ_j a certain portion of cumulative error limit of pitch for one motion screw turn $\delta T_{\Sigma j}$. Phases shift ψ_i, ψ_j are random quantities which accept different values for each i-th, j_p-th link, and each r of pass. In this cases the kinematic chain consists of a number of cogwheels segments $i = 14$, a number of rollers $j = 4$ and calculation is executed for a number of passes $r = 500$. Phases shift ψ_i, ψ_{jp} lies in limits $0 \div 360°$ and is defined as ψ_{ir}, where $-$ C equipartition numbers in interval $0 \div 1$ which are programmatically generated in the form of pseudo-random numbers ($\psi_{ir,jr} = 360° \cdot C$). Using velocity ratio of kinematic balance equation of a kinematic chain, angles of turns of each link for one motion screw turn are determined. From a calculation condition of cutting rate the rotation frequency of spindle is assumed as 1500 min^{-1}. For a statistical assessment of cumulative error effect of a step at a helical surface cutting the random quantity distribution law of equal probability for initial phases of error display by each kinematic chain element is used. For example, rated dependence of the pitch total cumulative error of a cut thread with the motion screw turn for $144°$ according to f. (1) looks like:

$$\Delta p_{\Sigma 144°} = 10\sin(9,6 \cdot 144° + 360° \cdot 0,489314) + 10\sin(9,6 \cdot 144° + 360° \cdot 0,21229) +$$
$$+ 10\sin(9,6 \cdot 144° + 360° \cdot 0,1096) + 10\sin(6,4 \cdot 144° + 360° \cdot 0,2254) + 10\sin(6,4 \cdot 144° + 360° \cdot 0,8503) +$$
$$+ 10\sin(4 \cdot 144° + 360° \cdot 0,02873) + 10\sin(4 \cdot 144° + 360° \cdot 0,49883) + 10\sin(4 \cdot 144° + 360° \cdot 0,1969) +$$
$$+ 10\sin(4 \cdot 144° + 360° \cdot 0,4195) + 10\sin(3,2 \cdot 144° + 360° \cdot 0,3319) + 10\sin(3,2 \cdot 144° + 360° \cdot 0,3608) +$$
$$+ 10\sin(1,28 \cdot 144° + 360° \cdot 0,4621) + 10\sin(1,28 \cdot 144° + 360° \cdot 0,6381) + 10\sin(0,4 \cdot 144° + 360° \cdot 0,3574) +$$
$$+ 10\sin(1,6 \cdot 576° + 360° \cdot 0,9564) + 10\sin(1,6 \cdot 666° + 360° \cdot 0,9376) + 10\sin(1,6 \cdot 756° + 360° \cdot 0,9226) +$$
$$+ 10\sin(1,6 \cdot 846° + 360° \cdot 0,0747) + 10\sin(0,267 \cdot 96° + 360° \cdot 0,0175) + 5,2 = -4,04461 \quad micron,$$

where $A_i = 16 \cdot 25/40 = 10$ micron (25 microns – standard of kinematic accuracy of each link, for diameter of a reference circle of gear wheels no more than a $d = 125$ mm; 40 – number of intervals within a screw turn through 9°); 9,6, 6,4, 4, 3,2, 1,28, 0,4 , 1,6 – numbers of turns of each of

fourteen cogwheels of a kinematic chain for turn of the motion screw on $144°$; numbers $576°, 666°, 756°, 846°$ – correspond the position angles of four rollers of the planetary roller screw mechanism; 0,267 – number of turns of a roller from a condition of its turn on $36°$ for $9°$ turn of the motion screw; 5,2 microns – the cumulative error limit of the motion screw pitch at the turn on $9°$, according to an acceptable cyclic deviation of the helical line of 13 microns.

Calculations of the total accumulated error of a step of a helical surface for each of forty intervals within one turn of the motion screw which results are presented on fig. 2 are carried out similarly.
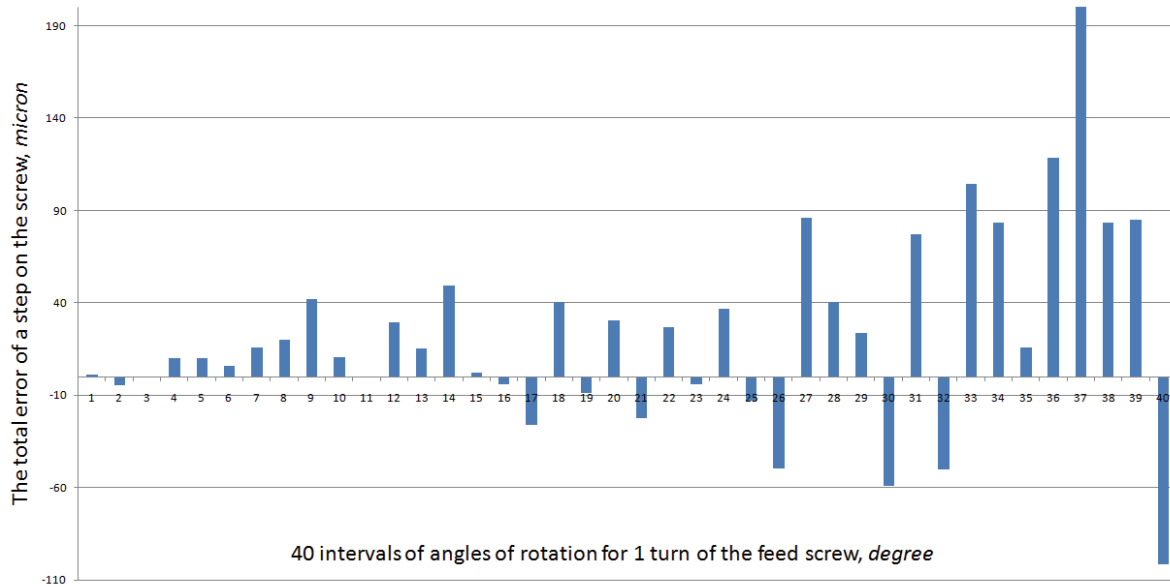
Fig. 2. The components, the accumulated errors of a step for a turn of the motion screw

For obtaining confidential information, the assessment of the total accumulated error is carried out by methods of mathematical statistics from a sample of 5 hundred passes of a helical surface cutting on dependence:

$$\Delta p_{\Sigma r} = \sum_{i=1}^{500} \Delta p_i .$$ (2)

The spectrogram of fluctuations of the total accumulated error of a step of a cut helical surface, is presented on fig. 3.
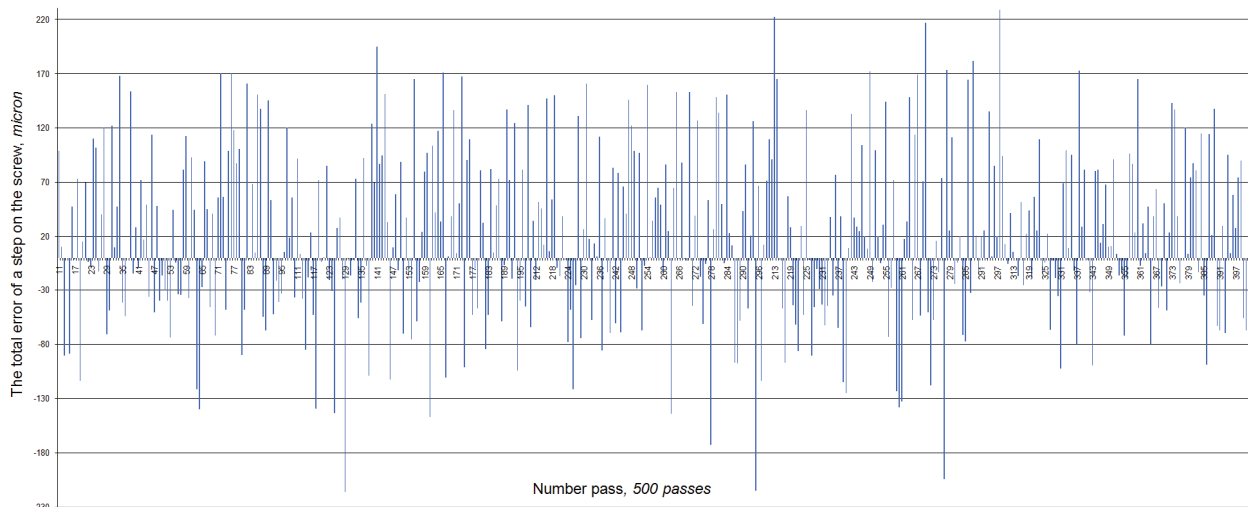
Fig. 3. The spectrogram of change of pitch error at five hundred passes.

1.9.3

The total cumulative error of a step for 500 passes calculated according to f. (2), it is equal to $\Delta p_{\Sigma 500} = \Delta p_1 + \Delta p_2 + \Delta p_3 + ... + \Delta p_{500} = 9667{,}76$ micron, from where the mathematical expectation of the greatest accumulated error of a step of the cut cumulative error of a step of a cut helical surface makes:

$$M\left|\Delta p_{\Sigma \max}\right| = \sum_{1}^{500} \left(\Delta p_{\Sigma}\right)_r \Big/ 500 = \frac{9667{,}76}{500} = 19{,}3355 \text{, micron.}$$

Error specific effect distribution of each separate link on the cumulative error of a kinematic chain is determined by the formula:

$$E_i = \frac{M\left|\Delta p_{\Sigma \max}\right| - M\left|\Delta p_{\Sigma \max}\right|_i}{M\left|\Delta p_{\Sigma \max}\right|} \cdot 100\% , \tag{3}$$

is presented in the table according to which the greatest influence on the total accumulated error exerts the tenth link.

Influence percent	E_1	E_2	E_3	E_4	E_5	E_6	E_7	E_8	E_9
%	1,02	0,27	3,31	3,44	5,31	6,35	3,13	1,9	1,25

Influence percent	E_{10}	E_{11}	E_{12}	E_{13}	E_{14}	E_{IP}	E_{IIP}	E_{IIIP}	E_{IVP}	E_{VP}
%	8,1	0,34	3,28	2,13	0,26	4,61	1,19	1,27	3,32	0,78

According to the carried-out research, influence of the planetary roller screw drive on output accuracy of a helical surface forming made 14,49 %.

Conclusions

The developed technique allows to calculate cumulative error of a cut helical surface depending on a kinematic error of tooth gearings and the accumulated error of the planetary roller screw mechanism.

Taking into account the error statistical distribution sample, the technique allows to determine the error specific effect of each link of the thread-cutting chain within one turn and repeated passes of the motion screw.

The technique of simulation modeling considered on the example of multiple gearings of a feed drive of the screw-cutting lathe 16К20, can be used at design of real drives, definition of terminal segments displacement of robots and various mechanisms. With the use of computer means the technique allows to define quickly enough and adequately an output error at any stage of calculations for any link and to normalize accuracy of a step of a cut helical surface, taking measures of increasing the accuracy of its manufacturing.

References

1. *Плужников А.С.* Расчёт точности зубо-резьбообрабатывающих станков. ЦБТИ, М.:1968, 75 с.

2. *Левашов А.В.* Основы расчёта точности кинематических цепей металлорежущих станков. М.: Изд. Машиностроение,1966, 212с.

3. *Охрименко К.Я., Манзюра А.В., К. Eichhorn (К.К. Охрименко).* Исследование оценки точности кинематической цепи станка при нарезании винтовых поверхностей постоянного шага. К.: Вісник інженерної академії України №2, 2011, С.245-250.

4. *Ohrimenko K.Y., Eichhorn K.K., Manziura O.V.* Simulation modelling of accumulated error of discrete drive kinematic chain. The fourth world congress "Aviation in the XXI-st century" – 2010, С.15.1-15.4.

UDC 681.2.083:555.7

V.V. Drevetskiy, D.Sc., M.M. Klepach
(National University of Water Management and Natural Resources Use, Ukraine)
O.I. Osmolovskyi, Ph.D (National Aviation University, Ukraine)

THE AUTOMATIC ANALYZER OF QUALITY FOR MOTOR FUELS AND OILS

This article refers to the development of methods and devices for determining the quality characteristics of motor fuels and oils in real time mode

One of the most important criteria in service and support of the auxiliary machines park at the airports is the quality of motor fuels and oils usage. The products, that are present on market, do not always satisfy the regulatory requirements, what reduces exploitation characteristics, increases the consumption of materials, affects the quality and completeness of fuel combustion, increases the opacity of exhaust gases, and aggravates the engines work conditions [1]. As result, the parts and units of machines untimely failure and the harmful substance emissions are increasing. Therefore, it is necessary to control such important parameters as density, viscosity and viscosity-temperature characteristics of the fuel and lubricants, gasoline octane number, cetane number and cetane index of diesel fuels at all stages of use. Special attention should be paid to the biodiesel storage, which eventually loses its quality characteristics.

To solve these problems, by combination of classical methods of hydrodynamics and advanced information technologies, the automatic analyzer of motor fuels and oils has been developed. The measurement process is based on hydrodynamic methods of kinematic viscosity and density definition. Sensing element is a throttle bridge converter (TBC), formed by two laminar and two turbulent throttles through which the substance is pumped continuously.

Due to applying modern unified microprocessor automation tools there are two ways of using the analyzer – in offline mode, or with integration to the enterprise resource planning systems (ERP). In general, the structure of the automatic analyzer can be divided into three parts (fig.1):
- measurement process control and automatic TBC state control systems;
- programmable logic controller (PLC);
- operator's graphic touch panel.
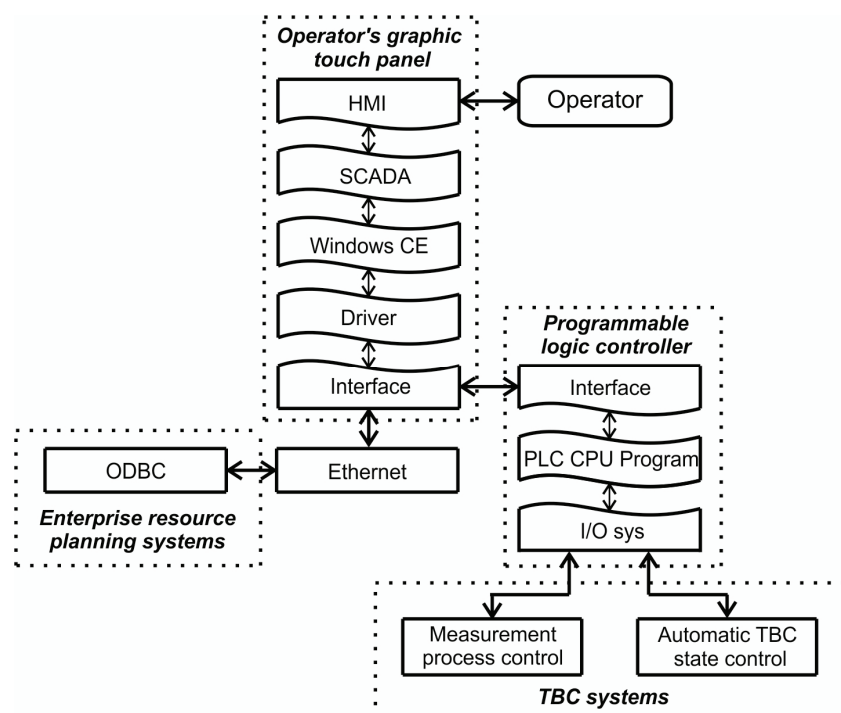
Fig. 1 Structure diagram of automatic analyzer

Measurement process control system provides balanced state of TBS by changing of volumetric flow and temperature stabilization of the substance. The optimization of this system was made by means of computer modeling, using MatLab software, that provided high speed and accuracy of measurements [3]. Information signals from the TBS sensors are perceiving and retranslating to a higher level by the automatic TBC state control system.

As a programmable logic controller, "VIPA PLC System 100V" is used, which, by means of analog and discrete inputs and outputs, is connected to the TBC systems, collects and processes the primary information. Information exchange between PLC and operator's graphic touch panel is realized via MPI interface.

Operator's graphic touch panel "VIPA Touch Panel", with Windows CE and Movicon SCADA-system preinstalled, provides graphical user interface (GUI) for the comfortable representation of measured data, graphic screens changing and trends previewing. On Fig.2 is represented GUI during the quality characteristics of diesel fuel measurement. Management of measurement process performed by means of the resistive screen of graphic panel. By tools, which are provided by SCADA-system, all data can be stored on external memory (USB-Flash device or CF/SD/MMC memory card). Connection to the remote databases of ERP-systems is realized by using the Open Database Connectivity (ODBC) technology via Ethernet.
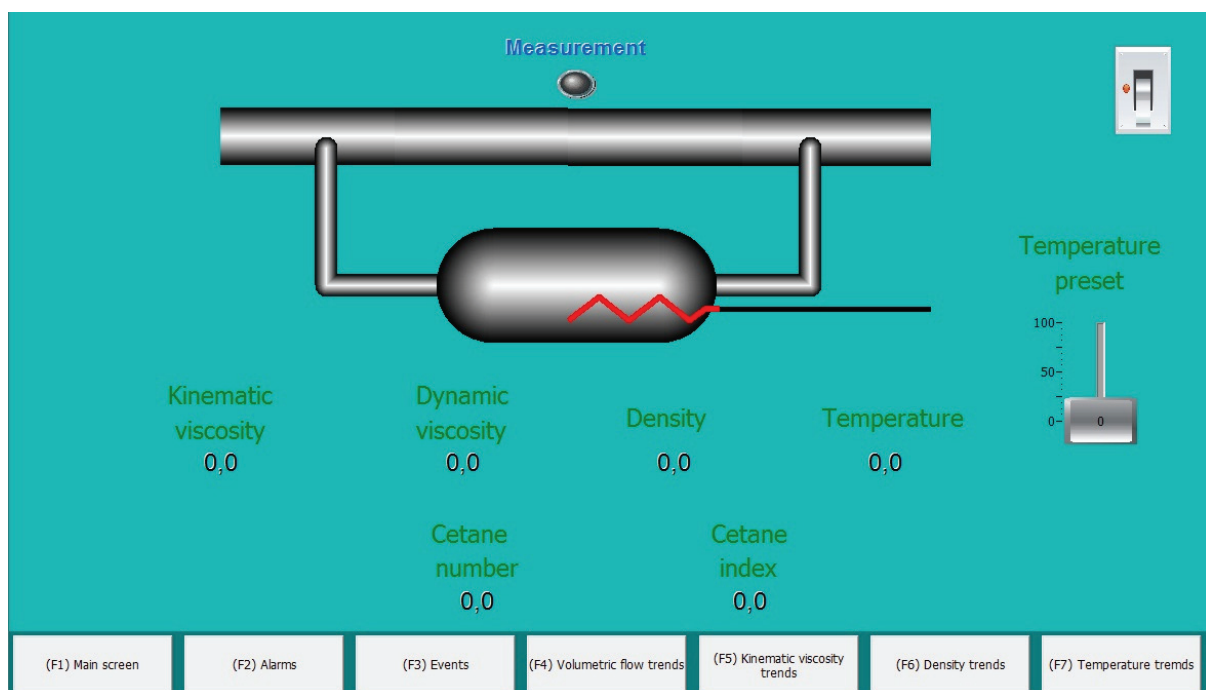
Fig. 2 GUI of the automatic analyzer

The principle of analyzer's work is next. After powering on, after nearly 1 minute, the measurement process control system leads the TBS to a balanced state, and then the measurement process starts (Fig. 3). By signals, received from the automatic TBC state control system, the values of the kinematic viscosity (υ) and density (ρ) are defined, the dynamic viscosity (μ) is calculated and the temperature (T) is being registered in PLC. This data is retranslated to the operator's panel. By means of SCADA-system the base of the artificial neural networks (ANN) is realized. Depending on chosen type of substance the appropriate algorithms of ANN are processed. The received value of quality parameters are represented on the screen, archived on the external device, and, if necessary, written to the remote database.

The separate regime of analyzer's work is a definition of viscosity-temperature characteristic. In this case, the product is periodically heated. Based on appropriate values of temperature and kinematic viscosity, the viscosity-temperature characteristics are calculated.

| Product → | Measurement process control system | → | Automatic TBC state control system | ΔP T ΔP$_\Sigma$ Q | → | Primary information processing system | T ρ ν μ | → | Base of artificial neural networks | ν, μ ρ, T CN, CI ON | → | Visua-lization |
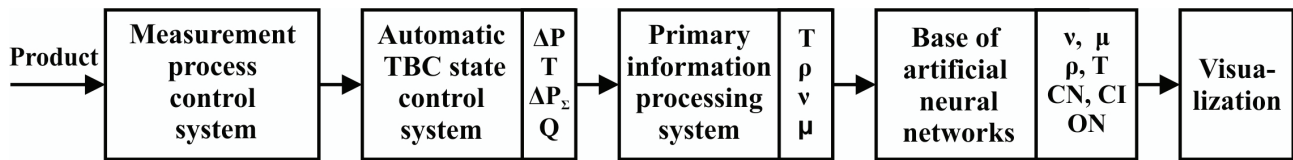
Fig. 3 The information flow diagram of automatic analyzer, where: ΔP – pressure drops in the TBS's indicator diagonal; ΔP$_\Sigma$ – total pressure drops on TBC; Q – volumetric flow of product through TBC; CN – cetane number; CI – cetane index; ON – octane number

There are 4 artificial neural networks realized at the base (Table 1). For building them, we used data, received during laboratory analysis of automobile gasolines and diesel fuels of different sorts, and from quality certificates of biodiesel. The ANN models were created and trained by means of Matlab software.

Table 1

Base of artificial neural networks

№	Input	Number of neu-rons	Output	Substance
1	density, viscosity	20	cetane number	diesel fuel
2	density, viscosity	10	cetane index	diesel fuel
3	density	20	octane number	gasoline
4	density, viscosity	8	cetane number	biodiesel

As the example, one of neural networks for gasoline octane number definition by measured density is represented on fig. 4.
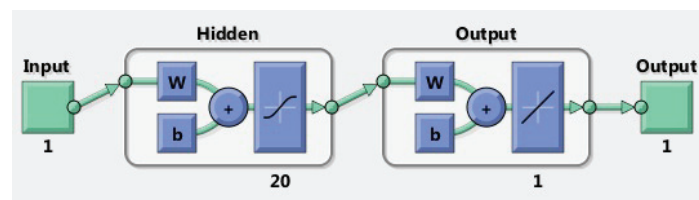
Fig. 4 ANN for octane number definition

It is a two-layer feed-forward network with 20 sigmoid hidden neurons and 1 linear output neuron. Density used as input and octane number as output. Comparative diagram of octane number values defined with standard motor method and with ANN is represented on fig. 5.
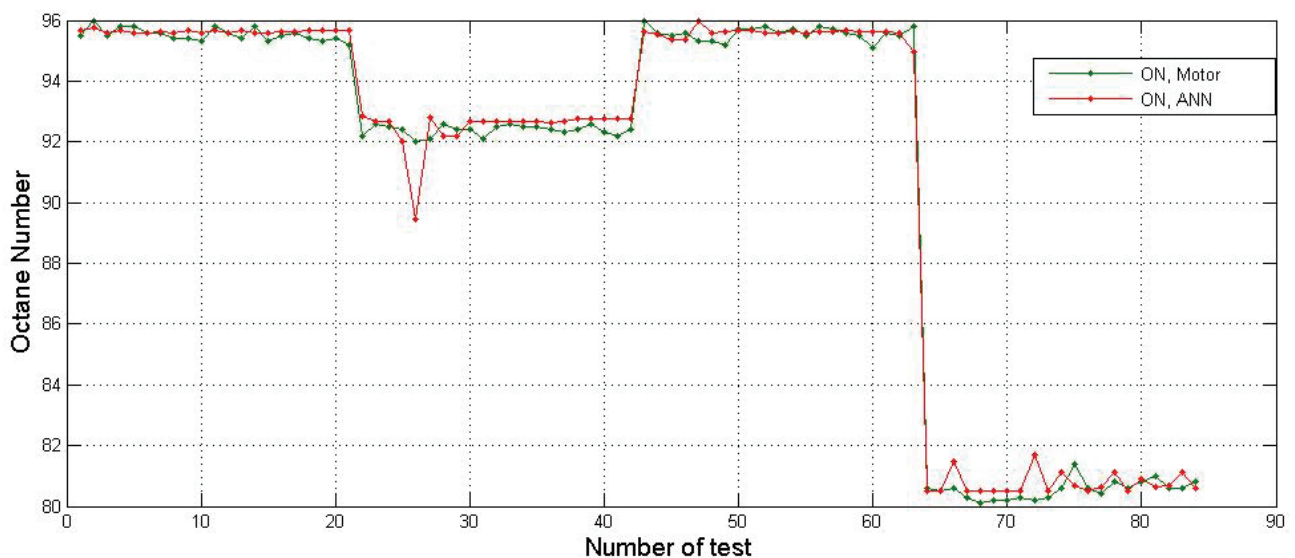
Fig. 5 Comparative diagram of octane number values defined with standard motor method (green line) and with ANN (red line)

The results of evaluation ANN performances using mean square error (MSE) and regression analysis (R) are represented in table 2.

Table 2

Evaluation of ANN performances

№	Parameter	MSE	R
1	cetane number, diesel fuel	0,12	0,93
2	cetane index, diesel fuel	0,18	0,7
3	octane number, gasoline	0,45	0,99
4	cetane number, biodiesel	2,17	0,78

Errors can also be reduced by retraining neural networks on lager data sets. Received values of MSE shows that automatic analyser is accurate enough to define quality characteristics of motor fuels and oils in real time mode.

The photos of developed automatic analyser are represented on pic.6.
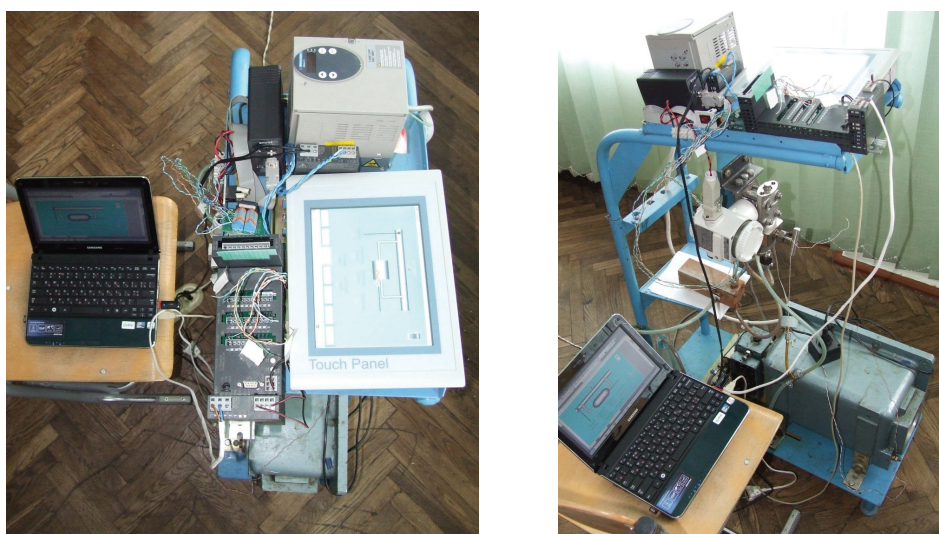
Fig. 6 Photos of developed automatic analyzer

Conclusions

The researches have practically and scientific value. Developed automatic analyzer for motor fuels and oils can be used both, singly and as a part of automated technological process control systems or technological monitoring systems of ERP class. The developed base of the artificial neural networks, that realize the methods of fuels and oils quality characteristics definition by measured density and kinematic viscosity, may have usage at the laboratory analysis as the additional software without TBC-based measurement system.

References

1. *SV Boychenko, SV Ivanov, VG Burlaka*. Motor fuels and oils for modern technology / Kiev: NAU, 2005. -216p.

2. *Drevetskiy V. V., Klepach M. M., Vorobjuk S. P.* Automatic analyzer of physical-chemical parameters of oil products / Bulleting of Engineering Academy of Ukraine. – Kiev. - 2009. P. 82-86.

3. *Drevetskiy V. V., Klepach M. M.* Real-time modeling of the information-measurement system for physical-chemical parameters of oil products / Mathematical machines and systems. – 2011. – N 2. – P. 81-84.

Yu.I. Yevdokymenko C. of Ph. and M. Sc., s.s.s
(Kharkiv Trade and Economic Institute of Kyiv National Trade
and Economic University, Ukraine)
A.P. Narezhnyi, N.I. Svitenko, C. of Eng. Sc (Metrological Center of Military Measurement
Standards of the Armed Forces of Ukraine, Ukraine)
V. P. Kvasnikov, Doctor of Technical Sciences (National Aviation University, Ukraine)
D.A. Filisteev (Central Department of Metrology and Standardization of the Armed Forces
of Ukraine of Armaments of the Armed Forces of Ukraine, Ukraine)

APPLICATION OF THE CORRELATION-EXTREME METHOD OF MEASURING THE PHASE SHIFT ANGLE BETWEEN TWO HARMONIC SIGNALS IN AUTOMATION OF CALIBRATION WORKS IN MOBILE MEASUREMENT EQUIPMENT LABORATORIES

The correlation-extreme method of measuring a phase shift angle between two harmonic signals, which permits to determine current values of amplitudes and output signal phases of a phase shift calibrator based on the linear equation system solution obtained by means of minimization of the functional containing discrepancies between the results of immediate measurements of output signals and a priori calibration signals is proposed.

    Problem statement and literature analysis.

At present, armies of the world leading countries give much attention to creation of mobile calibration laboratories (PLIT) for provision of metrological support of armament and military equipment at their dislocation place. The following PLITs are developed and put into service in armed forces of NATO countries, Japan, Russia and Ukraine: Messi (USA, Fluke, Tektrat), MCRU (FRG, Rohde Schwarz), DOMAT (Франция, Alkotel), AN/GSM-421, AN/GSM- 705 (USA), комплекс SMRV (FRG), Terminal-10 system (USA, Fluke), Matsushita (Japan), system 9550 (USA, Hewett Packard), PLIT-A3-2M, PLIT-A2-4/1-4 , PLIT A2-6/1-2 (Russia), basic container set PLIT-U2-1 (Russia), PLVT UA2-4 /A,B (Ukraine).

Now, PLVT UA2-4 /A,B mobile measurement laboratory modernization works are in progress in Ukraine. At the same time, one of the most actual aspects is the issues related to automation of calibration works. In particular, processes of automation of harmonic signals phase shift measurements widely used in calibration of radar and sonar stations, glideslope aircraft landing systems during ground tests and operation of armament and military equipment samples. For this purposes, a definite phase shift measuring method should be chosen for representation of a phase shift angle unit size by a working standard providing the required accuracy and possibility of automation of phase measurements.

In the work [2] the classification of harmonic signal phase shift measuring methods is represented.

Analysis of special phase measurement equipment showed that for measurement uniformity and accuracy assurance Ukraine needs a system of transfer of a unit of phase shift angle between two electrical oscillations with error limits (0,1–0,01)° in the frequency range from 5 Hz to 10 MHz and amplitude dynamic range 40-50 dB. In this case, formation of a phase shift angle with given parameters cause no difficulties in digital calibrators of signal phase shifts as opposed to measurement of given parameters. In this connection, the search of a phase measurement method permitting to provide the required accuracy and automation of phase measurements has become critical.

As a model of standard signal for phase shift calibrators, the model of harmonic signal which parameters are not changed in the infinite time interval. Such model is idealized and used in practice only with a finite time window in taking measurements. Analysis of potential capabilities and basic errors of the known correlation method of valuation of a phase shift angle between two harmonic signals has been performed in a number of works [2-9]. Disadvantages of the correlation method include: the higher frequency range limited by a several kilohertz value; the necessity of mu-

tual frequency synchronization of a clock generator for an analog-digital transducer (ADT) of a digital correlator and output signals of a phase shift calibrator; cosine-ideal nature of the scale; unambiguity of indication only in the range $0 \div 180°$; low accuracy of measurements of phase shift angles close to the value of $0°$ and $180°$.

The work [10] contains description of a correlation phase meter with the simplified working algorithm of an arithmetic unit. There are variants of realization, in which the scale [8] is linearized but low accuracy of measurements of phase shift angles close to $0°$ and $180°$ is a critical for this method and it cannot be compensated.

Averaging of measurements of a phase shift angle between two harmonic signals by means of mathematical treatment of results of immediate measurements of tension of harmonic signals being studied leads to errors of different types conditioned by availability of method dead zone to phase changes. This dead zone is related to manifestation of nonlinear functional links between instantaneous voltage values and harmonic signal phase. This circumstance results in the necessity to search such methods of conversion of measurement results of instantaneous voltage measurements of two harmonic signals to the angle of their phase shift, which wouldn't contain dead zones.

Aim of the article. Increase of the phase measurement accuracy in modern special phase measuring equipment based on the development of the phase shift angle measurement in the range from 5 Hz to 10 MHz with an absolute error not more than $\pm 0,01°$ and dynamic range of signal levels 40-50 dB.

Basic material

The main point of the proposed correlation-extreme method of phase shift angle measurement between two harmonic signals consists in the following. A signal being measured, which may be described by a certain function $f(t)$, is compared with a standard signal which may be described by the function $F(t, \vec{P})$, where t − current time, $\vec{P}$ − vector of standard signal parameters to be determined. Then mutual correlation is determined

$$R(\tau, \vec{P}) = \int_0^\infty \left[f(t) - F(t, \vec{P}) \right] \times \left[f(t - \tau) - F(t - \tau, \vec{P}) \right] dt, \qquad (1)$$

where $\tau = \varphi T / 2\pi$ − delay time, φ − phase shift angle, definitely determined only in the interval $[0, 2\pi)$, and T − reference frequency oscillation period.

Mutual correlation as a function from parameters $\vec{P}$ and τ, will have a global extremum in case of such values of the given parameters, where the function $F(t, \vec{P})$ reflects the function $f(t)$ with the best accuracy.

It is known that the function derivative in the point of its extremum amounts to zero. According to the foregoing we can state that solution of the equation system made by setting equal to zero of partial derivatives for all elements of the vector $\vec{P}$ and the parameter τ makes possible to obtain unique estimates of elements of $\vec{P}$ vector and τ parameters at which the standard signal will reflect the signal being measured with the best accuracy.

If a function class, which includes the signal being measured, is known, then the identification task of the measured signal with help of a standard one is solved in an optimal way.

Under such task statement $R(\tau, \vec{P})$ is deemed to be a functional to be minimized. In this case, the condition of area minimum between graphs of both functions, in other words the quadratic form minimum [3].

A phase calibrator reproduces two harmonic signals with a given phase shift angle between them, thus function measurement belong to the harmonic functions class.

In this case, signals from phase calibrator terminals may be represented as follows:

$$f_1(t) = A_R \cos \omega t + A_I \sin \omega t + \xi_1(t); \qquad (2)$$

$$f_2(t) = B_R \cos \omega t + B_I \sin \omega t + \xi_2(t), \qquad (3)$$

where A_R, A_I, B_R, B_I − signal parameters to be determined, $\xi_1(t), \xi_2(t)$ − noise terms of signals

of the phase calibrator having the following characteristics: mathematical expectations $M[\xi_1(t)] = 0$, $M[\xi_2(t)] = 0$ and dispersion $D[\xi_1(t)] = \sigma_1^2$, $D[\xi_2(t)] = \sigma_2^2$ accordingly; $\omega = 2\pi/T$ – reference frequency of the phase shift calibrator (a priory known value).

In this case for signals (2) and (3) the following functions may be chosen as standard ones:

$$F_1(t, \omega, X_R, X_I) = X_R \cos\omega t + X_I \sin\omega t . \tag{4}$$

$$F_2(t, \omega, Y_R, Y_I) = Y_R \cos\omega t + Y_I \sin\omega t . \tag{5}$$

Taking into account (4) and (5) expression of (1) for the functional $\Phi(\vec{P})$ for two channels of the phase calibrator may be presented as follows

$$\Phi_1(X_R, X_I, \omega) = \int_0^\infty [f_1(t) - X_R \cos\omega t - X_I \sin\omega t]^2 dt ; \tag{6}$$

$$\Phi_2(Y_R, Y_I, \omega) = \int_0^\infty [f_2(t) - Y_R \cos\omega t - Y_I \sin\omega t]^2 dt . \tag{7}$$

Function value $f_1(t)$ and $f_2(t)$ can be changed with ADT at the discrete points of time t_j. At that, in the final observation interval one can obtain only finite samples $f_1(t_j)$ and $f_2(t_j)$ with $j \in 1...N$. In this case, expressions (6) and (7) are transformed into the final sums.

Prior to obtain the equation system concerning standard signal parameters lets pay attention to the following aspects. First: frequency of signals in the expressions (2) and (3) is set by the phase shift calibrator and its value may be specified more precisely by measuring by a frequency meter. That's why this parameter of the standard signal may be deemed as known. Second: the time interval $\Delta t = t_{j+1} - t_j$ between two adjacent indications of the measured signals $f_1(t)$ and $f_2(t)$ is also known and determined by the sample frequency of ADT. That's why unknown parameters of standard signals are X_R, X_I, Y_R, Y_I amplitudes concerning which the equation system should be formed. Third: with known frequency ω, the equation system concerning the parameters being searched, is broken into two independent equation systems:

$$\begin{cases} \dfrac{\partial}{\partial X_R}\Phi_1(X_R, X_I) = 0 \\ \dfrac{\partial}{\partial X_I}\Phi_1(X_R, X_I) = 0 \end{cases} \text{и} \begin{cases} \dfrac{\partial}{\partial Y_R}\Phi_1(Y_R, Y_I) = 0 \\ \dfrac{\partial}{\partial Y_i}\Phi_1(Y_R, Y_I) = 0 \end{cases} . \tag{8}$$

After fulfillment of differentiation operations (8) the systems acquire the following form:

$$\begin{cases} (N-a)X_R + bX_I = 2c_I; \\ bX_R + (N+a)X_I = 2c_R, \end{cases} \begin{cases} (N-a)Y_R + bY_I = 2g_I; \\ bY_R + (N+a)Y_I = 2g_R, \end{cases} \tag{9}$$

where $a = \sum\limits_{j=1}^{N} \cos(j\omega\Delta t)$; $\qquad b = \sum\limits_{j=1}^{N} \sin(j\omega\Delta t)$;

$c_R = \sum\limits_{j=1}^{N} f_1(t_j)\cos(j\omega\Delta t)$; $\quad c_I = \sum\limits_{j=1}^{N} f_1(t_j)\sin(j\omega\Delta t)$;

$g_R = \sum\limits_{j=1}^{N} f_2(t_j)\cos(j\omega\Delta t)$; $\quad g_I = \sum\limits_{j=1}^{N} f_2(t_j)\sin(j\omega\Delta t)$,

N – a number of measurements of output signals used for determining the standard signals parameters.

The systems (9) have the following way of solution:

$$X_R = \frac{2[bc_R - (N+a)c_I]}{b^2 + a^2 - N^2}; \quad X_i = \frac{2[bc_I - (N-a)c_R]}{b^2 + a^2 - N^2};$$

$$Y_R = \frac{2[bg_R - (N+a)g_I]}{b^2 + a^2 - N^2}; \quad Y_i = \frac{2[bg_I - (N+a)g_R]}{b^2 + a^2 - N^2}. \tag{10}$$

Amplitude pairs X_R and $\underline{X_I}$, Y_R and Y_I represents real and imaginary components of complex amplitudes, which can help to present harmonic signals at terminals of the phase shift angle calibrator, i.e.

$$X = X_R + jX_I = X_0 \exp(j\varphi_1);$$
$$Y = Y_R + jY_I = Y_0 \exp(j\varphi_2).$$

Taking into account the given value, phases in the first channel φ_1 and in the second channel φ_2 may be represented as follows.

$$\varphi_1 = \begin{cases} \operatorname{arctg}\left(\left|\dfrac{X_I}{X_R}\right|\right), & \text{при } X_R > 0, X_I > 0; \\[2mm] \operatorname{arctg}\left(\left|\dfrac{X_I}{X_R}\right|\right) + \dfrac{\pi}{2}, & \text{при } X_R < 0, X_I > 0; \\[2mm] \operatorname{arctg}\left(\left|\dfrac{X_I}{X_R}\right|\right) + \pi, & \text{при } X_R < 0, X_I < 0; \\[2mm] \operatorname{arctg}\left(\left|\dfrac{X_I}{X_R}\right|\right) + \dfrac{3\pi}{2}, & \text{при } X_R > 0, X_I > 0. \end{cases} \tag{11}$$

$$\varphi_2 = \begin{cases} \operatorname{arctg}\left(\left|\dfrac{Y_I}{Y_R}\right|\right), & \text{при } Y_R > 0, Y_I > 0; \\[2mm] \operatorname{arctg}\left(\left|\dfrac{Y_I}{Y_R}\right|\right) + \dfrac{\pi}{2}, & \text{при } Y_R < 0, Y_I > 0; \\[2mm] \operatorname{arctg}\left(\left|\dfrac{Y_I}{Y_R}\right|\right) + \pi, & \text{при } Y_R < 0, Y_I < 0; \\[2mm] \operatorname{arctg}\left(\left|\dfrac{Y_I}{Y_R}\right|\right) + \dfrac{3\pi}{2}, & \text{при } Y_R > 0, Y_I > 0. \end{cases} \tag{12}$$

Thus, the task of phase difference determination $\Delta\varphi = \varphi_2 - \varphi_1$ between two output signals of the phase calibrator is solved.

Conclusion

In the article the correlation-extreme method of measuring a phase shift angle between two harmonic signals based on the use of modern ADTs, developed to provide automation of phase measurements while transferring a phase shift angle unit size to the working standards in points of their operation by means of mobile laboratories.

References

Results of determination of the main directions of modernization of mobile measuring equipment laboratory PLVT UA 2-4/A,B. KhNURE Scientific-production magazine "Metrology and devices" №6, 2010 pp.47-52.

1. *Yu.V. Kuts, L.M. Scherbak.* Statistical Phasometry. Edited by L.M. Scherbak. – Ternopil: TNTU, 2009. – 384 p. (Monograph).
2. *Volkov V.M., Ivanko.* Nonstationary processes in phasometrical system elements. – K.: Equipment, 1977. – 120 p.

3. *Chmyh M.K.* Digital Phasometry. – M.: Radio and liasion, 1993. – 184 p.

4. *Ganzing K.I.* Measuring of phase characteristics by the correlation method. – "Radio electronics issues". Series VI. "Radio metering equipment", 1962, issue 4, p.87-96.

5. *Molodov V.D.* Correlation method of phase shift measurement. – Book: Control equipment. Issue 6. Lviv, 1969, p. 40-43.

6. *Molodov V.D.* Correlation phase meters. – Book: Control equipment. Issue 6. Lviv, 1969, p. 44-48.

7. *Molodov V.D.* Interference and curve shape influence on the two-channel correlation phase meter error. – Book: Control equipment. Issue 10. lviv, 1971, p. 25-29.

8. *Koltik Ye.D., Korovkin Ye.I.* Correlation method of phase shift measurement. – "Requirements of USSR metrological institutes" 1971, issue 126 (186), p. 26-34.

9. *Tsydelko V.D., Kuznietsov V.I., Ivanov B.R.* Digital Correlation phase meter. Author's certificate № 423066. – "Image Bulletin", 1974, №13.

UDC 621.7.044+621.313

M.K. Knyazyev, PhD (National Aerospace University "KhAI", Ukraine)
Yu.V. Protsan (Laboratory of Alternative and Renewable Energy, Ukraine)
O.I. Osmolovsky, PhD (National Aviation University, Ukraine)

DEVELOPMENT OF CONTROL SYSTEM FOR SMART ELECTROHYDRAULIC PRESS

Factors that determine low stability of electrohydraulic forming processes are analysed. Parameters of forming processes and electrohydraulic impulse presses to be automatically controlled and corrected are revealed. Types of systems suitable for control of electrohydraulic presses are analysed. Composition of control system that is able to measure actual form of sheet blank and make corrections in loading pressure fields for the next forming step is proposed.

Impulse sheet-forming methods are most suitable for conditions of small-batch production and the shortest pre-production periods for manufacturing of sheet-formed items. Electrohydraulic impulse forming (EHF) method proved its high efficiency under market conditions of economy development and limitations applied to the use of explosives in industry connected with their storage, transportation and utilization [1]. EHF is based on the use of "safety" type of energy – electric energy and allows reducing significantly application of manual labour in manufacture of complicated sheet parts with ensuring the specified accuracy at the expense of one hard shape-determining surface (die or punch) and positive effects of metal deformation under the impulse loading.

Now EHF manufacturing processes find the increasing application in various branches of industry for production of components from sheet blanks, especially taking into account rise of volume of small-batch production of sheet parts that, in its turn, determines increased interest of specialists to seeking new ways and the most economical means for manufacture of parts with methods of sheet-metal stamping.

But widest application of EHF technology in industry is limited by low stability of forming processes and, hence, low stability of geometric shape of final sheet products. For high-voltage non-initiated discharges low stability has two aspects. The first one is connected with large non-uniformity of impact pressure distribution along a sheet blank surface [2]. Another aspect is low repeatability of pressure fields generated by high-voltage discharges under the same conditions [3].

Low uniformity of pressure distribution is because of nature of non-initiated discharges: discharge channel can randomly select any position in a relatively large volume in the spark gap between electrodes. This volume has a shape of near to lentil surface with axis connecting two work surfaces of electrodes including areas nearby their tips. It is generally accepted that the length of the discharge channel is approximately 2 times larger than length of spark gap.

The position of discharge channel in this volume depends on many hard to predict and to control parameters: surface condition of electrodes, geometry of discharge surfaces of electrodes, area of electrodes open surfaces, condition and wear of electrode insulator, local conductivity of water in the volume of spark gap, presence of some mechanical particles and gas bubble content in water and on the surfaces of electrodes, etc. At the same time electrodes create barriers for shock waves propagations and this effect forms "shadowed zones", if discharge channel is located over electrodes. Position and shape of discharge channel determine the configuration of isobars on the surface of blank, the location of zones of the highest and the lowest pressure, the location of "shadowed zones", value of maximal pressure in the zones nearby the side walls, that is, pressure distribution along blank surface [2].

For multi-electrode discharge blocks the problem of low stability becomes more acute because of large quantities of spark gaps, discharge channels generated non-simultaneously, shock waves and those factors listed above.

Present EHF processes are controlled by on the basis of probabilistic theory. An EHF specialist makes calculations and specifies quantity and voltage (energy) of discharges at the condition of the poorest pressure distribution and their repeatability. This approach gives good results for single-

step forming processes, when final shape of a sheet part is obtained in one final tool. But even in this case the approach leads to over-consuming of electric energy up to 50 % and process time up to 30 %.

The situation is more complicated when forming process is performed in several steps. Here the forming should be stopped at some moment, when geometric shape of a formed blank is good for inserting or removal additional special elements of die and making the next forming step. In this case an operator of EHF press should stop the process after several preliminary discharges to inspect shape of a formed blank and to estimate quantity and voltage (energy) of the following discharges to strike into proper blank shape. And this procedure is repeated for each forming step. Therefore multi-step processes are so long, not stable, requiring participation of a skilled EHF specialist.

Beside of functions of impact loading and controlling pressure fields, EHF presses should provide the following auxiliary functions: travel of table to work position, clamping of tooling, filling discharged chamber with water, charge-discharge cycles, pouring water out of discharged chamber, unclamping of tooling, travel of table to auxiliary position. Other functions can be applied, if necessary: vacuuming of die cavity, supply of compressed air into die, check of electrodes insulators condition, check for water presence in vacuum pipes, check for a sheet blank fracture, heating of sheet blank and check of temperature, check of proper operation of high-voltage safety units, etc.

Improvements of EHF presses design, their units and systems are directed to facilitate control of sheet blank shapes during forming process at the expense of automation level rise. Higher level of automation causes application of more complicated systems of measurements and control. At the same time complicated control systems need more progressive and adequate mathematical tools and models.

It is significantly difficult task to create a complete simulation model of an EHF press operation. Many interrelations are not easy to describe in terms of ordinary logic: many actual technical solutions are based on expert knowledge and practical experience to be difficult to formalise.

Experience of the leading press- and machine-building companies shows that control systems are developed in one direction – increase of their adaptability, that is, ability to change their parameters depend on control tasks or signals of an operators and production conditions [4].

The three stages in development of automatic control systems can be defined.

At the first stage specialists used classical approaches of automatic control theory and created devices with two-valued (definite) logic based on relay-type elements. But such devices working on principle "inhibition-permission" has no ability of operating re-programming, that is, even of their forced adaptation to the changed conditions.

At the second stage microprocessor control systems with electronic programming components appeared. Computing devices, airborne computers and microcomputers allowed to input various control programs into their memory units and to adapt in some measure to changing production conditions.

At the third, current, stage in order to take into consideration a huge variety of information about an item, various influences and conditions, characteristics of control signals of an operator, actions of operating environment and mechanisms directed to a work blank it is reasonable to create intelligent control systems, which are based on algorithms with fuzzy logic similar to a human thinking process [5]. These are adaptive control systems in their classical understanding.

The sequence of listed stages is not chronologically precise. Elements of each next stage were conceived in a previous stage. Moreover, the stages exist simultaneously.

Technologies of the highest adaptability level for control of EHF press operation include creation of complex systems possessing the functions of estimation, diagnostics, check and protection of all press systems. Such systems should have elements of artificial intelligence in order to control all subsystems, units, pumps, counters, electrodes, etc. starting from the energy receiving stage, its transformation and delivering to a sheet blank.

As a variant, the complex system can be equipped with 32-bit processor-computer with satis-

factory operating speed, for example, of 300 MHz, which operates in a mode of permanent dialog and data exchange with devices, subsystems and controls. When making some motion or operating environment changes occur, computer identifies the situation, analyses it, makes prognosis and selects such a variant of mutual actions of all subsystems, which optimises a shape of sheet blank and energy consumption.

Besides of a main computer the system can be equipped with additional computing modules of a smaller size responsible for the operation of separate devices. For example, one of such modules can solve the task of check of a sheet blank shape after each discharge, another – can check conditions of electrodes in each discharge contours, etc.

Adaptive subsystem for check of a blank shape after discharge should include measuring system or sensors in order to identify actual shape of a sheet blank, reveal unsatisfactory segments of shape, calculate difference between actual and specified bank shape at a certain stage of forming process. Local processor with the given algorithms of fuzzy logic processes the incoming data and generates a signal to the main processor of EHF press and to local processors of electrodes in order to make or not to make additional discharge of an assigned voltage (energy). Operator, which checks the forming process, can cancel this decision of control system, if he considers it to be incorrect. Otherwise the control system will realise its decision automatically. And in the most of cases the system does control motions more precisely than operator due to the system obtains and processes data of many sensors, discharge curves of many electrodes, etc., and operator takes into account only limited volume of information and makes decisions approximately on a basis of his experience and intuition.

Such a system can have the general structure shown in Figure 1. Its modules perform the following functions:

- Control object includes EFH system sensors and actuators;
- Control system includes specific units of Fuzzy Logics operations (Fazification and DeFazification) and other necessary units to implement the necessary tasks of control;
- Sensors unit collects and transmits parameters data to Control System;
- Charge Electrodes and Actuators unit implements functions of control by signals from Con-
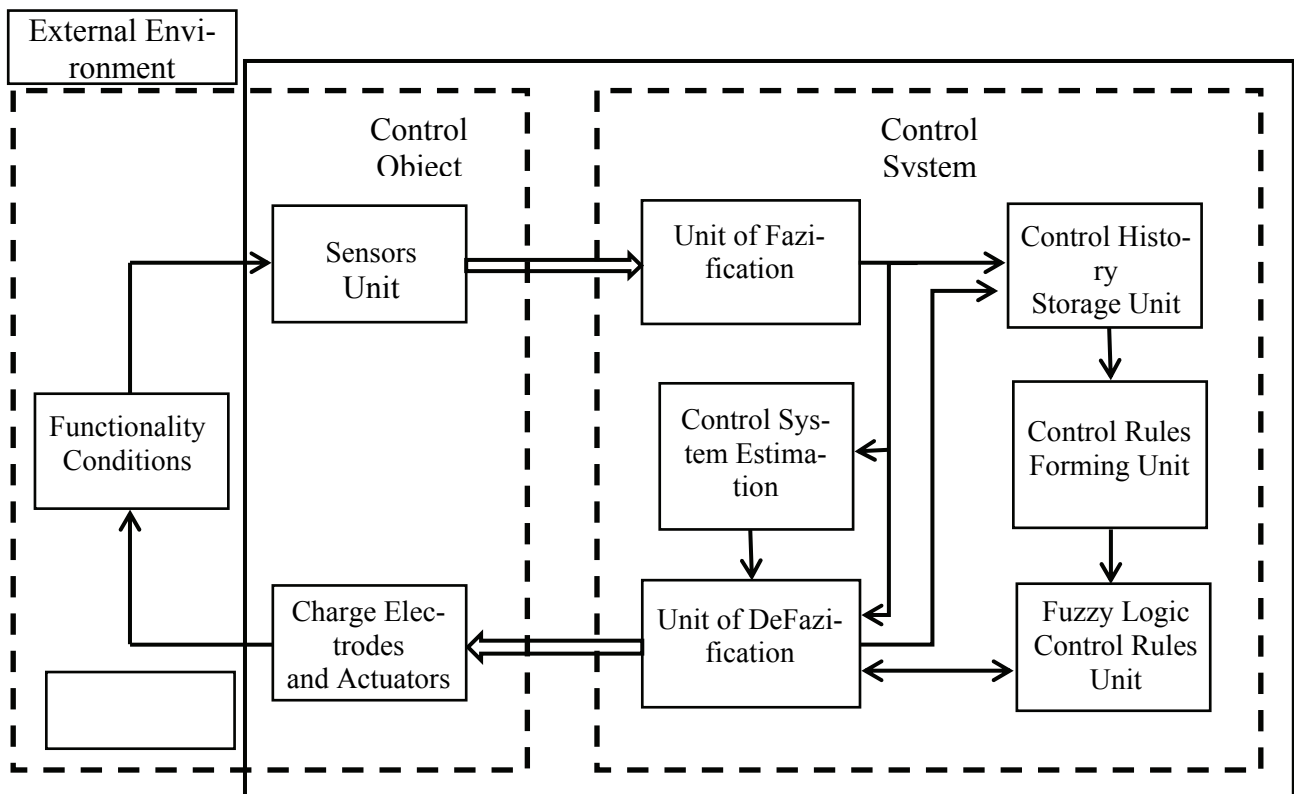
Figure 1. General structure of a complex intelligent system for control of EHF press

trol System.

Thus, in order to solve the specified problem the combined method of automatic control of EHF press is proposed. The task of sheet blank shape optimization is solved by control method based on fuzzy logic, and control of peripheral elements (auxiliary functions) is planned to perform with classical control method by servo-loop systems.

Conclusions

In this work the factors that determine low stability of electrohydraulic forming processes have been analysed. Parameters of forming processes and motions of electrohydraulic impulse presses are revealed. Conclusion about necessity of automatic control is made. Types of systems suitable for control of electrohydraulic presses are analysed taking into account results of the performed analyses. Composition of intelligent control system that is able to measure actual form of sheet blank and make corrections in loading pressure fields for the next forming step is proposed. The accuracy and efficiency of EHF press control with such a system is expected to be higher than control by a human operator.

References

1. *Голованова М.А.*, *Гонсалес Б.*, *Князев М.К.* Efficiency improvements of batch production of sheet parts with method of electrohydroimpulse forming // Авиационно-космическая техника и технология. – 2007. – № 11 (47). – С. 232-239.

2. *Eguia I.*, *San José J.*, *Knyazyev M.K.*, *Zhovnovatyuk Ya.S.* Pressure Field Stabilization in High-Voltage Underwater Pulsed Metal Forming Using Wire-Initiated Discharges // Key Engineering Materials, Vol. 473, 2011. – pp. 965-972.

3. *San José J.*, *Perez I.*, *Knyazyev M.K.*, *Zhovnovatyuk Ya.S.* Pressure Fields Repeatability at Electrohydraulic Pulse Loading in Discharge Chamber with Single Electrode Pair. Proceedings of the 5th International Conference on High Speed Forming "ICHSF2012", Dortmund, Germany, April 24-26, (2012), p. 33-42.

4. *Антипов С.И.*, *Дементьев Ю.В.*, *Калинин А.Е.* Нечеткая логика и возможности ее применения в системах управления современного автомобиля // Материалы международной научно-технической конференции. – М: МГТУ «МАМИ», 2009. – С. 38-42.

5. *Дорф Р.*, *Бишоп Р.* Современные системы управления / Пер. с англ. Б.И. Копылова. – М.: Лаборатория Базовых Знаний, 2002. – 832 с.

UDC 629.7

D.P. Kucherov, d.s.
(National Aviation University, Ukraine)

MODELING TRAFFIC IN CONTROL PROBLEMS OF ROBOTIC SYSTEMS

In the report the general approach of the modeling traffic for control problems of robotic systems is considered.

Recently, the possibility to use mobile robotic systems expanded. At the same time one of the most interesting trends developed in the world, is the direction associated with the provision of group motion of robots in the performance of collective operations, including a possible action in hostile environments, and game problems, which for various reasons can not be fulfilled by individual devices [1].

A number of issues management group movements of mobile devices that operate on land, water, air space has been studied by researchers at different times, as evidenced by numerous sources.

It is assumed that the simulation system will take into account the possibility of a variable group of robotic control systems, the group acts as to realize one or more goals (objectives), as the action of the operator, or independently.

The structure of the system based on modern concepts of management capabilities as well as the construction of the system. Structurally, the system consists of a human operator formative elements of the task group, the control panel, control over the communication channel is both open and closed, and the direct object control - robotic systems. Robotic system is composed of both traffic management and the means to accomplish the task.

The main object of management is considered a separate unit that performs a task in the group. So naturally arises the problem of an adequate mathematical model of the robotic system, as part of the group.

To control the robotic systems use a different number of control algorithms. In these algorithms, it is usually assumed that the structure of the control system consists of two parts, one of which is responsible for planning the route (the so-called scheduler), the second for the management of the route (the regulator). In this control sets the value of such speed and acceleration of the manipulator (gripper, a camera), which provide the desired type of motion.

Note that the trajectory of the manipulator is not unique and must be submitted to a smooth curve satisfying some constraints on the position and orientation of the gripper and the camera on the initial and final parts of the trajectory. Of course the route to provide an analytic function defined, for example, in Cartesian coordinates. An alternative approach is to present a set of points of the route, the path between them can be selected from a class of functions subject to the restrictions on the position, and velocity and acceleration of the manipulator are known. Given the complexity of choosing the form of an analytic function satisfying the desired route, the second approach to the selection of the route seems more appropriate.

Ensure effective management of mobile robotic systems (robots) is an important problem of automatic control theory. Depending on the nature of the problems solved by robots, can be generated by different criteria for evaluating their performance, but in the first place stands the problem of minimizing the time move the robot or its separate parts (gripper) from one point, seen as the starting point of the trajectory to another destination. The task of minimizing the time to test the route appears as the planning phase of the trajectory, and the process of working out.

The task of route planning robotic system is well known and remains a subject of current research in recent years in connection with the planning of the trajectories of several complexes.

The requirements for this task include safety in difficult driving conditions, the minimum time of arrival at destination, precision castings route, smooth curve route [1-3]. The motion of the robot

to be controlled on-board control system in real time, with the route planning algorithm should be able to reroute traffic in the process.

Under the conditions of the problem is a trajectory of a curve joining two fixed points: the beginning of the route and destination. There are different approaches to the construction of the curve. For example, an approach based on the construction of curves of minimal length (Dubins curves) [3, 4], which construct a pair of arched curves and linear section connecting them. As the path chosen is the curve which has minimal length.

The planning method based on the construction of Voronoi diagrams, it is proposed in [4]. Lots of robots paths between adjacent points whose coordinates depend on the relative positions of the sources of threats, determine the trajectory of the robot on the ground. This trajectory is determined by solving a system of differential equations for the body. The method requires a certain spatial arrangement of the sources of threats, which is routed between the UAV.

An alternative to the methods discussed is a campaign in which the route of the UAV s (t) is based on the control points $p_k = (x_k, y_k)$ as a Bezier curve, according to the expression

$$s(\bar{t}) = \sum_{k=0}^{2} p_k \frac{n!}{k!(n-k)!} \bar{t}^k (1-\bar{t})^{(n-k)},$$

(1)

where $k = 0, 1, 2$, and the setting $\bar{t}$ has a sense of relative of time, $0 \le \bar{t} \le 1$.

At the same Bezier curve is a quadratic function of the phase plane, starting at coordinates $P_0 = (x_0, y_0)$ and ends at coordinates $P_2 = (x_2, y_2)$, through the points $P_1 = (x_1, y_1)$ is determined by the vertex of the parabola of the form

$$s(\bar{t}) = \bar{t}^2 (P_2 - 2P_1 - P_0) + 2\bar{t} + P_0.$$

(2)

Last, the point P_1, determines the curvature of the parabola, and may be associated with the "depth" circumvent obstacles to the robot, which allows you to choose the path with the smallest curvature (Fig. 1).
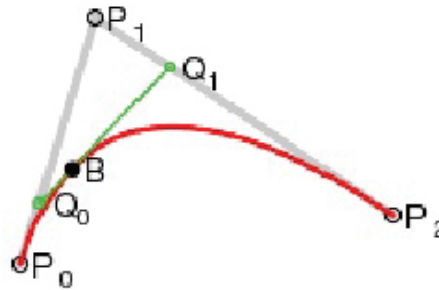
Fig. 1. View of the functions in the phase plane.

Point B in Fig. 1 represents the position of the managed object at a time on the trajectory, the points Q_0, Q_1 subsidiary. The choice of the curve depends on the complexity of the route, while the number of control points may be increased, but the highest power of polynomial (1) is always one less than the number of control points.

To solve the problem of traffic gripper (camera) is traditionally [3-6] is selected from the PID controller's law of the form:

$$\delta_в = \frac{1}{p}\left[k_\theta(\theta - \theta_3) + k_{\dot\theta} p\theta + k_{\ddot\theta} p^2\theta\right],$$

(3)

where $\delta_в$ - given the value of the spatial coordinates of the gripper, a camera, θ - the current value of the coordinates, $k_\theta, k_{\dot\theta}, k_{\ddot\theta}$ - transfer of control of the output coordinate, angular velocity and acceleration. The transfer of control ratios $k_\theta, k_{\dot\theta}, k_{\ddot\theta}$ is supposed to determine on the results of standard setting in the mining impacts.

Efficiency controller's is determined by the quality of master control system. Because of ambiguities in the standard configuration control of movements, depending on the initial and final positions (orientations) of the controlled element, should apply adaptive configuration settings controlled by the regulator. The assignment of this class of problems to the terminal allows you to automate configuration of the controller (see for example [4, 6]).

A common feature of the terminal control problem is the case when the parameters of the control object exactly unknown in measuring the coordinates of the object of control channels have the nuisance, limited by amplitude noise, the statistical parameters of which are unknown. An effective way to eliminate this factor is to introduce a control law of a signum function, which leads to an increase in the target area.

In the case where the control object parameters unknown, it is advisable to use an adaptive approach. You may notice that all the possible phase states of the control object is responsible only two possible values of the control signal $\{1, -1\}$, then the terminal control problem in the terminology of pattern recognition learning (classes) can be interpreted as a problem of pattern recognition of two classes (types) of the signals. At the same teaching methods that have been developed for pattern recognition problems, can be used to solve the problems of terminal control. An example of such a task is given in [8]. Education has two negative cases. This "rolling" mode (Fig. 2, Fig. 3) and the mode of misses in the target area for a certain number of sign changes of the control signal, which allows it to use this information as a training and guidance to implement it as an external teacher.
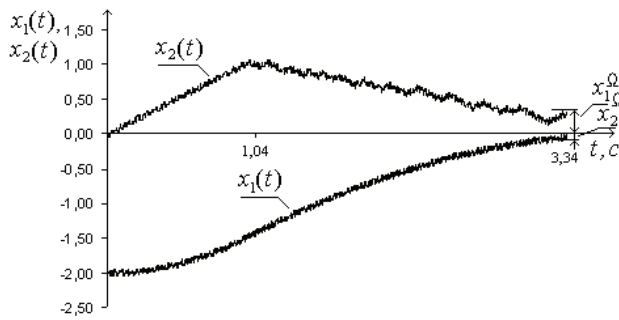
Fig. 2. Sliding mode in the time plane   Fig. 3. The signal $u(t)$ in the sliding mode
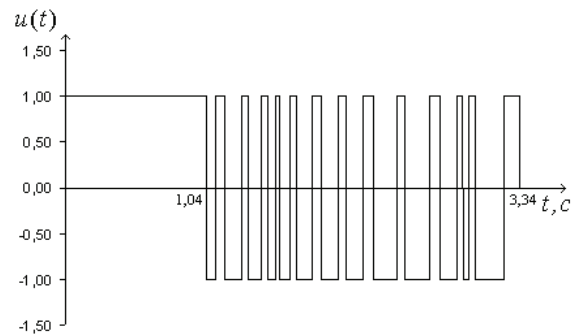
Using as a training point of the first switching control signal, it is possible to organize training procedure for the control system

$$c_n = \begin{cases} c_{n-1}, & \text{if } process \text{ ended occasion 1;} \\ \Pr_\Omega\{c_{n-1} \pm w(t_n)\}, & \text{if process ended occasion 2} \end{cases}$$

(4)

based on solving systems of infinite inequalities recurrence.

Learning algorithm (4) allows excluding sliding modes of permissible modes of operation, there is converging, but at the same time, has one deficiency - there are quite long.

As part of the identification approach to solving the problems of adaptive control algorithms are applied modular solutions targeted recurrent inequalities in discrete time of the "strip"

$$\text{в}_j(n) = \left\langle \left\| \hat{x}_j - x_j \right\| \le \text{e} \right\rangle (\text{в}_{j-1}(n)).$$

(5)

These algorithms need to develop a discrete model of the managed object. In the case of a dynamic object, which is considered a model of the object can be obtained by converting the differential equations in their discrete form. The application of these algorithms, since the sampling signal source control object allows to organize the process of training the system terminal management in a single step training system terminal control. The procedure of training (5) is a modular difference between the original signal model and object management. The training is carried out gating model

parameters, which are then translated into the parameters of the switching function, taking into account the known sampling period. The algorithm does not require knowledge about the negative consequences of learning, it focuses on the error introduced by the designer of the system, which is in the interest rate of coincidences should be large enough. This fact does not exclude the possibility of sliding mode of the number of allowable modes of operation, and therefore can not be used in the problem of self-learning system, the terminal management. The identification procedure (5) can be supplemented by the above method of Terminal Control on the basis of the theory of learning to recognize patterns of control signals. The effectiveness of integrated teaching method allows a 1,5 - 2 times to reduce the number of successive steps of learning.

An alternative approach is the identification of methods of point identification method of multi-proposed in [7]. According to this method of tuning parameters selected from the sets that are specified in each step of the next instruction

$$B_j = \left[\underset{-j}{\text{в}}^1, \ \overset{-1}{\text{в}}_j \right] \times ... \times \left[\underset{-j}{\text{в}}^N, \ \overset{-N}{\text{в}}_j \right]. \tag{6}$$

The initial set is formed set of subsets of the initial values of the parameters that are bounded by certain values of the lower and upper bounds. At each next step is clarification of the boundaries of permissible parameter sets so that each successive set of admissible parameters is a subset of it, that is, completely in the previous set.

Such a procedure definition of borders is possible, if during step training to get a set of parameters, among which we can determine their minimum and maximum values. The procedure for identifying multiple (6) gives the guaranteed best estimates than the previous ones. But the choice of the parameter estimates from the resulting set of arbitrary rank does not preclude the establishment of a sliding mode of the system. Therefore, this method is also used alone is not advisable.

Conclusions

The peculiarity of the developed technique is that for the synthesis of terminal controls is not necessary to have full information about the parameters of the managed object model. This feature is due to the synthesis procedure, i.e. technology of building controls. A new training algorithm of terminal control system has better convergence properties due to the parallel operation of the methods considered. For this reason, the approach outlined deserves research and development as applied to various problems of practical importance.

References

1. *Кунцевич В.М.* Некоторые задачи управления групповым движением подвижных роботов // Automatics-2011. XVIII Міжнародна конференція з автоматичного управління, 28-30 вересня 2011 року: матеріали конференції. – Львів: видавництво Львівської політехніки, 2011. – 430 с.

2. *Dubins L.E.* On curves of minimal lengthwith a constrainton overage curvature, and with prescribed initial and terminal positions and tangents / Dubins L.E. // AM. J. Math. – 1957. - 79. – P. 497-516.

3. *Borrof S.A.* Path Planning for UAVs / Borrof S.A. // Proceedings of the American Control Conference, June 2000, Chicago, Illinois, p. 364-368.

4. . *Крутько П.Д.* Алгоритмы терминального управления линейных динамических систем / Крутько П.Д. // Известия РАН. Теория и системы управления. - №6. – 1998. - С. 33-45.

5. *Kim T.-H.* Time optimal control of a single-DOF mechanical system with friction / Kim T.-H., Ha In.J. // IEEE Transactions on automatic control. – Vol. 46. - №5. – 2001. – P.751-755.

6. *Кучеров Д.П.* О двух подходах к задаче синтеза системы управления курсом корабля: оптимальность по времени и ПД-регулятор / Кучеров Д.П., Василенко О.В., Іванов Б.П. // Системи управління, навігації та зв'язку. - № 3 (11).– 2009. – С. 80-85.

7. *Кунцевич В.М.* Управление в условиях неопределенности: гарантированные результаты в задачах управления и идентификации / Кунцевич В.М. - К.: Наук. думка, 2006. 264 с.

UDC 531.004

L.V. Kolomiets, rector OSATAQ d.t.s., professor
(Odesa State Academy of the Technical Adjustment and Quality, Ukraine),
Y.P. Leschenko, post-graduate student
(National Aviation University, Ukraine)

MEASURING SYSTEMS OF COORDINATE MOVINGS OF MEASURING ROBOTS

It is described factors which are used at a choice of measuring systems. Namely the error of measurement and step-type behavior of counting, a design, operational features are described. Photo-electric measuring systems with raster measuring rulers, inductive measuring systems, measuring systems with mechanical knots of transformation of linear moving to rotation and laser interferometers are presented.

Measuring systems are intended for counting of moving mobile knots of measuring robots when changed coordinates of the points. At a choice of measuring systems for measuring robots it is considered: error of measurement and step-type behavior of counting; design; operational features.

The measuring channel (Fig.1) contains: the analog measuring converter (AMC), the analog digitizer (AD) and digital measuring means (DMM).

In the process of measuring size X to the measurement canal is affected by external random factors φ (electric hindrances, temperature change, humidity, etc.) on which the result of measurement of Y depends.
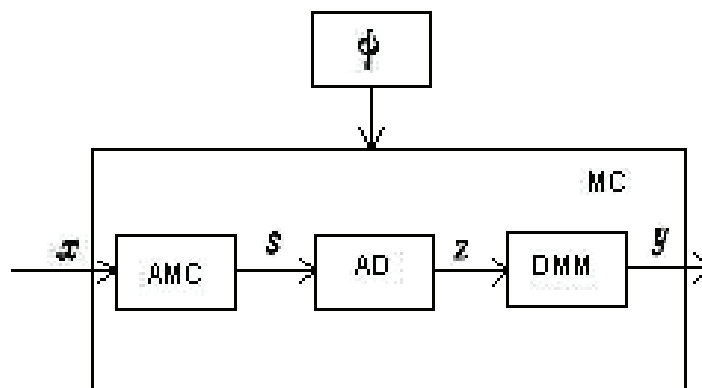
Fig.1 The structure of the measuring channel

Error of measurement and step-type behavior of counting.
Practically the error of measuring systems makes 0,3-0,5 errors measurement of length on measuring robots along coordinate axes. Thus, for high-precision measuring robots the error of measuring systems shouldn't exceed 2 microns/m.

Considering possibility of compensation systematic errors of measurement on measuring robots by means of the computer entering into its structure, an important factor is the ratio of values of systematic and random components of an error of measuring system and character of the first. Compensation of the errors having linearly changing character, is carried out by simple multiplication of indications of measuring system on constant factor.

For compensation of the errors having nonlinear character, amendments for certain shifts of rather initial point are entered. The number of amendments increases with increase in accuracy of compensation and frequency of harmonious components errors of measuring system. Step-type behavior of counting, as a rule, doesn't exceed 0,1-0,2 errors measurement of length along coordinate axes of measuring robots.

The design should correspond to the following requirements:
small overall dimensions and mass of the measuring converter;
absence in the measuring converter of sources of intensive thermal radiation and vibrations;
existence of digital indication and automatic conclusion of information;
the necessary form of information deduced and value of target signals.

The weight and overall dimensions of the measuring converters established on the measuring robots easy high-speed mobile hubs, which weight doesn't exceed 30 kg, make essential impact on a choice of type of measuring system.

At small movings it is more convenient to fix motionlessly a display head, and to move a measuring ruler; at the big - on the contrary. The free choice of a zero point of system of coordinates and other systems of coordinates by position of the calibrator and base surfaces of details gives opportunity to use in measuring robots cyclic measuring systems.

Advantage of measuring system with code measuring rulers consists in saving of the known provision of mobile knots after its repeated inclusion and the convenience of input of compensatory values of errors of measuring system connected with it or errors of measurement of measuring robots.

The question of input of necessary amendments conveniently is solved in the cyclic measuring systems having sequence impulses on which introduction of amendments is carried out.

Operational features.
The following demands are made to them:

necessary sensitivity to temperature change, tolerance to pressure and humidity change, and also to a dust content of environment and existence in it cooling liquids, to external electric and magnetic hindrances;

necessary speed and value of measured moving;

small electric lag effect and high speed of a conclusion of information;

reliability, simplicity of adjustment and service, absence of rigid connections between rather mobile and motionless knots;

a little requirements to accuracy of moving of mutually mobile knots.

Factor of linear expansion of measuring rulers choose close to factor of linear expansion of a measured detail at the expense of what errors from temperature deformations decrease. For measuring robots of universal appointment speed of measured movings doesn't exceed 10 m/mines, for measuring robots of the increased speed reaches 33 m/minutes. The electric lag effect of measuring systems at various speeds of calibration of measuring head and measurements of a detail leads to measurement errors. The measuring robots having precision mobile knots of coordinate movings, always provide specific requirements to accuracy of movings of knots of measuring system.

Separately consider the most widespread linear measuring systems. Angular measuring systems are a part of rotary tables or rotary devices and as separate independent system in measuring robots aren't used. Measuring converters of measuring system are a part of a base unit. The vast majority of measuring robots (to 90 %) is equipped with the photo-electric measuring systems having raster measuring rulers. Besides, the following measuring systems are used: the inductive; containing mechanical knots of transformation of linear moving to the angular; the laser.

Photo-electric measuring systems with raster measuring rulers most fully correspond to the specified requirements of measuring robots. The principle of their work is based on modulation of the light stream passing through two rasters, and its transformation into electric signals.

The basic element defining first of all accuracy of measuring system, the raster measuring ruler having periodically changing structure with sites of equal width, giving a different transmission or light reflection is. The measuring systems working in passable and reflected light are used.

The minimum value of an error of measuring systems of this type makes 1-2 microns/m. The error has monotonously changing character from a low-frequency dominating component. The error within a step, being a high-frequency component, is equal 0,02-0,05 steps which for precision measuring systems makes 8-20 microns. The step-type behavior of counting depending on a step and number of interpolation, reaches 0,1 microns. The gap between measuring and display rulers doesn't exceed 0,1 mm, and its admissible change which is not influencing yet accuracy of measurement, makes ±10 % from a gap.

The measuring systems providing the highest accuracy, have glass measuring rulers, the factor of which linear expansion is close to factor of linear expansion of steel, and work in passable light. The program software of a number of measuring robots gives opportunity of compensation of errors of measurement of length on known temperature and factor of linear expansion of measuring rulers and measured details. The cross-section section of measuring rulers makes from 2x200 mm to 15x40 mm. The maximum length of glass rulers to 2000 mm. For providing bigger length of measurement of a ruler are joined.

However thus there are considerable difficulties as rulers should be established so that to provide distance between strokes a number of the standing rulers, equal to multiple number of steps, to within ±2,5 step %. Therefore in practice joining more than two glass rulers are used only in exceptional cases. Big limits of measurement are provided with the measuring systems working in reflected light with metal measuring rulers, executed in the form of a level or a tape. Besides, such rulers simplify a design of knots of measuring robots as the ruler can be established with an insignificant ledge on knot of measuring robots.

Using more difficult optical system, possibility to increase a gap in raster interface to 5 mm is represented and respectively to increase its admissible change. The minimum value of an error of photo-electric angular measuring systems makes to 2".

Inductive measuring systems are used in average and large-sized measuring robots, first of all the production. Thanks to the constructive device and in most cases used phase principle of work they are less sensitive, than photo-electric measuring systems with raster rulers, to an adverse effect of environment; they are strong, don't wear out, are easy-to-work, as don't demand special leaving, frequent adjustment, are convenient for installation.

The measuring scale is carried out in the form of the separate rulers produced, as a rule, from a material, the factor of which linear expansion is close to factor of linear expansion of steel. Separate scales can be joined conveniently for formation of the compound scales intended for measurement of big movings. Accuracy is less, than photo-electric measuring systems. Their minimum error makes ±3 a micron on length of 1 m, and step-type behavior of counting of 0,5 microns.

On overall dimensions also concedes to photo-electric measuring systems a little. With a scale executed on a metal tape with an insulating cover, have smaller in comparison with considered overall dimensions, but also are less exact. Their error makes to ±10 a micron on length of 1 m.

Errors angular make to ±2". Now searches of new designs with a view of increase of their accuracy and resistance to influence of environment, reduction of the sizes are conducted. Measuring systems with mechanical knots of transformation of linear moving to rotation are used for measurement of movings of knots low-exact average and large-sized measuring robots.

In it the measuring systems containing a lath and a cogwheel, established on a converter axis are used. A lath produce from steel or brass, and a cogwheel - from steel. The module gets out such that the step of gradation was equal to multiple number of millimeters. The minimum value - 1 mm. Laths are produced in the length to 750 mm.

In need of bigger length of measurement of a lath are joined: "Mobility" of a lath or a cogwheel decides on the converter of measurement of angular movings proceeding from convenience of their installation. Inductive and photo-electric small-sized measuring converters are used. The error of such measuring systems makes to 50 microns/m, step-type behavior of counting - 10 microns. These measuring systems are sensitive to a contamination a dust, oil, cooling substances and consequently demand good protection against their hit and periodic cleaning. Besides, in, operation process they wear out.

For transportation and measurement of moving of knots precision measuring robots are used transfer the screw - a nut and precision measuring systems of angular movings. For reduction of negative impact of environment the screw is located in an oil bath. The error at length to 450 mm can make to 6 microns. Precision screws use in measuring robots with movings to 1200 mm. For a case of transportation of knots the second end of the screw incorporates to a drive. It is recommended to make measurements for increase of accuracy of measurement with an approach on the

one hand. Because of insufficient accuracy, inconvenience of operation, complexity of manufacturing and wear process these measuring systems of a wide circulation didn't receive.

The laser interferometers applied as measuring systems of measuring robots at the present stage of their development, also it is necessary to consider as a special case. Laser interferometers provide the highest accuracy.

The measurement error practically makes about 1 micron on length of 1 m, has linearly changing character. Step-type behavior of counting can be 0,01 microns. They are convenient for installation in large-sized measuring robots as there is no long mechanical measure for counting of movings.

Conclusions

However interferometers are difficult in operation, are sensitive to change of temperature, humidity and pressure of air, is several times more expensive than photo-electric or inductive measuring systems.

It is possible to assume that precision large-sized measuring robots will be the closest perspective scopes of such measuring systems.

Thanks to high precision and use possibility for the automated measurement of other parameters of movement of knots of measuring robots they already now are one of fixed assets of check of accuracy of the majority of measuring robots.

It is more favorable to go by the way of creation of deserted technology and use of reprogrammed industrial robots. But in this case often exact positioning, for example, controllable details is required. Serially let out robots provide accuracy of positioning of-0,1 mm.

On the basis of use of measuring robots it is possible:

to carry out metrological processes which on conditions of production are impossible with participation of the person (a toxic, dusty, gas polluted, explosive environment, a high radiation level of working space, ultrahigh speed, monotonous and heavy operations, etc.);

to reach high efficiency of control in the conditions of fast removability of production (the flexible automated production), reduction of terms of training to metrological receptions at release of new production.

Measuring robot can carry out:

quality standard of structure of a working environment;

to establish presence of certain objects, their account, a possible arrangement, to state quality standard, sorting;

an assessment of value of parameters of available or produced subjects (details);

determination of correctness of functioning of separate objects or their parts.

References

1. *A.A. Gapshis, A.Y. Kasparaitis, M.B. Modestov* Coordinate measuring machines and their application / A.A. Gapshis, A.Y. Kasparaitis, M.B. Modestov - M: Mechanical engineering, 1988. – 328 pages.

2. *Presnukhin L.N.* Photo-electric converters of information / Presnukhin L.N. M: Mechanical engineering, 1984. – 362 pages.

3. *Zhdankin V. K.* Absolute sensors of angular situation with the SSI interface Modern technologies of automation, 2004, No. 1. – 36-54 pages.

UDC 621.314.26

V. P. Kvasnikov, Doctor of Technical Sciences (National Aviation University, Ukraine)
O.V. Kvashina, PhD, O.G. Barakin, PhD
(Academy of Fire Safety, Ukraine)

THE PROBLEM OF RIGIDITY OF MATHEMATICAL MODEL IN THE ANALYSIS OF ROBOTIC SYSTEMS

Numerical methods that concern the electrotechnical systems analysis characteried by the SMM have been analysed. The main attention is paid to the opportunity of using the "predictor-corrector" methodes to solve this task.

The need for sustainability and the required accuracy of calculations with the lowest labor determines the choice of a method of numerical integration. The rigidity of the system of differential equations is the main factor that influences these characteristics of the computational process in the analysis of robotic systems.

Explicit and implicit methods for the numerical integration are traditionally used for solving differential equations which describe processes in robotic system But the problem of numerical stability and accuracy with an increase in the integration steps occurs during the application of the first methods. And the need, in general, the treatment of the Jacobian matrix, which causes difficulties in the case of large order matrix or bad condition of its, when we use the second method.

Diakoptichesky methods are used to solve the robotic systems, which contain valve converters and electrical machines. This is shown in [1]. In these methods, the separation of the system into subsystems is possible at the level of the mathematical model. The subsystems correspond to the fast and slow variables. In [1], this separation is performed at the level of the mathematical model of the system, given its properties, taking into account the presence of small parameters in the right parts of differential equations. Such a system of differential equations robotic system can be represented in the form of

$$x'_1 = f(x_1, x_2, t) \tag{1}$$
$$x'_2 = \sigma g(x_1, x_2, t). \tag{2}$$

The presence of small parameters in the form of a diagonal matrix σ determines the existence of fast (x_1) and slow (x_2) component in the solution of vector and determines the rate of change of variables within the range of search solutions.

Small parameters can serve as basic elements and elements of equivalent circuits, reflecting the various parasitic effects. Subsystem integration step (2) may be much higher than the subsystem (1). This reduces the amount of computation compared to the direct solution of the complete system with the same numerical method.

The principle of quasi-stationary derivatives (fast component filtering solutions) is one of the methods of solving stiff Cauchy problems, which suggested by Y. Rakitskiy [2]. The specific properties inherent in rigid systems are used in this case. Rapidly decaying components of the rigid linear systems are leading to the establishment outside the boundary layer nearly the exact algebraic relations between the components of the vector solutions. These relations coincide with number of decreasing partial solutions. So, we can construct the radically different asymptotic model which preserves the order of differential equations. This model allows us to apply to the entire system a single explicit method of numerical integration. The algorithm selection step discretization of method provides the required accuracy and the ability to increase the step without losing stability.

But after filtration, the members of the larger eigenvalues and increasing the integration step as a result of accidental causes, components with large derivatives may again appear in the solution. At the same time there are growing fluctuations in the solution. This leads to an automatic reduction of the integration step and the exclusion of members of the re-, which correspond to large eigenvalues. This reduces the performance of the method. This maintains the real model with filtering members with large derivatives. It is the main advantages of the method.

The following method of calculation systems, described by stiff differential equations, was offered by Y. Rakitskiy. It received the name of the system [2].

In rigid systems, the eigenvalues of the coefficient matrix **A** are grouped so that value of their real parts in some groups $a_1...a_i$, differ significantly from the values of those parts of an a_{i+1}, a_j, other groups. At the same time within a given group, these values differ slightly.

Assume that the largest absolute value a_{i+1} (a_{j+1}) followed by a group of about one order of magnitude smaller than the smallest value of $a_i(a_j)$ of the previous group. Then we can allocate a certain amount of time τ_{psi} (τ_{psj}), after which the influence of exponents, which correspond to these groups of eigenvalues can be neglected. After time τ_{psi} can neglect the terms corresponding to $a_1...a_i$ and after time τ_{psj} can neglect the terms that correspond to $a_{i+1}...a_j$.

In terms of the use of computer technology it is necessary to increase the integration step as the exponential decay which correspond to large eigenvalues, which define a small integration step. But this can not be done because the disturbed condition of stability of the numerical method. This gradual increase in the integration step can be obtained by applying a systematic method.

The system method allows us to solve systems of differential equations of arbitrary stiffness. It is especially effective for solving stiff systems of equations. This is its universality.

Increasing the efficiency of solving systems of stiff differential equations without dividing it into any subsystem can be the methods of problematic adaptation. The essence of the methods of problematic adaptation is to use to solve the same system as an explicit (at sites quickly change the decision) and implicit (in areas of slow changes in the solution) methods. This allows you to select the appropriate criteria at each step of the calculation method, which provides a minimal amount of computation. Problem adaptation allows to separate use of methods or combining them in a combination formula. Using the problem of adaptation requires careful formulation of criteria for selecting methods that enhance the efficiency analysis in general.

One of the principles of these methods is the principle of modularity [3]. This allows us to consistently complicate the calculation algorithm based on simple standard formulas. Thus, the multimodular algorithms can be shaped so that the less accurate modules used on the smaller steps of numerical integration.

In [4] is proposed a method of constructing a new class of numerical methods with directional formed of the area of computer stability.

As noted, the rigid system of differential equations that describes complex systems are characterized by a strong scatter of the coefficient matrix. In explicit methods of integration in this case, the restriction is imposed on the computational stability, it is necessary that all values $h\lambda$ were within the area stability of the numerical method.

Usually, the eigenvalues of the coefficient matrix formed unique domain in the complex plane $h\lambda$ in a rigid system. Rapidly decaying components of the free process, no interest, present a selection of a sufficiently small integration step for sustainability. You must create a method that allows the extension of the stability region only in the direction of the domain, which causes instability of the eigenvalues. This allows you to do this method.

The method allows to form a region of stability appropriate to a task. This makes it very mobile in the application. Explicit formulas are obtained, provide a relatively high speed. Exclusion of stability problems in the integration of stiff systems of differential equation, can further improve the performance of methods with a controlled resistance compared to conventional explicit methods the stronger the greater rigidity of the system.

Methods of "predictor-corrector" are among the methods of analysis of stiff systems separately. They are among other things that allow us easy by control of the local error in the calculations. They are powerful methods Gere-Nordsieck; methods that use higher derivatives in the calculation based on a formula Obreshkova [5], [6]:

$$\sum_{j=0}^{k} \alpha_j y_{n+1} = \sum_{i+1}^{l} h^j (\sum_{j=0}^{k} \beta_{ij} y_{n+1}^{(i)}). \qquad (3)$$

Methods (3) have been implemented according to the 1st, 2nd, 3rd, and derivatives were tested in a software package for analyzing complex systems:

$$y_{n+1} = y_n + (h/2) \cdot (y_{n+1}^{(1)} + y_n^{(1)}) - (h/12) \cdot (y_{n+1}^{(2)} - y_n^{(2)}),$$ (4)

$$y_{n+1} = y_{n-1} + 2hy^{(1)} + 7hL^2 y_n^{(1)}/15 - (h^2/15) \cdot (y_{n+1}^{(2)} - y_{n-1}^{(2)}),$$ (5)

$$y_n = y_{n-1} + (h/2) \cdot (y_n^{(1)} + y_{n-1}^{(1)}) - (h^2/10) \cdot (y_n^{(2)} - y_{n-1}^{(2)}) + (h^3/120) \cdot (y_n^{(3)} - y_{n-1}^{(3)}).$$ (6)

They are effective in the case where a combination of system parameters is such, that it is difficult to separate large and small time constants.

Methods were compared with the explicit Runge-Kutta method, Runge-Kutta-Merson fourth-order. The methods allow to obtain a stable solution. The methods are of the order of accuracy from 5-th to 7-th.

Findings. Methods can provide control of local error a step and automatic integration step until any further is obtained in the process of calculating the values. Methods allow to reduce the number of arithmetic operations at each integration step, the number of calls to the subroutine computing the right parts. Methods yield gains over time in the 2-8 times depending on the type of system and method.

References

1. *Заруба Н.И., Михалевич Г.А., Ющенко В.А.* Машинный метод анализа электромагнитных процессов на основе разделения быстрых и медленных переменных. — В кн.: Проблемы нелинейной электротехники.— 4.1. — Киев: Наукова думка, 1981. — С.188—191.

2. *Ракитский Ю. В., Устинов С.М., Черноруцкий И. Г.* Численные методы решения жестких систем. — М.: Наука, 1979. — 208 с.

3. *Башарин С.А., Матханов П.Н.* Применение многомодульных методов численного интегрирования к задачам анализа и синтеза сложных динамических цепей // Электричество. — 1988. — №12. — С.63—65.

4. *Бородулин М.Ю., Дижур Д.П., Кадомский Д.Е.* Точность численного интегрирования дифференциальных уравнений, описывающих переходные процессы в электрических цепях // Электричество. — 1988.
— №6. — С.45-51.

5. *Остапчук Т.Е., Пузаков А.В., Семенова О.В.* Повышение эффективности процедуры анализа электромагнитных процессов в импульсных преобразователях // Техн. электродинамика. — 1995. —№3. — С.19—21.

6. *Квашнина О.В.* Усовершенствование метода "предиктор-корректор" с использованием высших производных для анализа динамических режимов в импульсных преобразователях // Техн. електродинаміка. — 1998. —№5. — С.22—24.

UDC 681.3.07

I.G. Kisil, Prof., Doctor of technical sciences
(Ivano-Frankivsk National Technical University
of Oil and Gas, Ukraine)
O.I. Osmolovskyi, PhD (National Aviation University, Ukraine)
Y.M. Kuchirka, PhD student
(Ivano-Frankivsk National Technical University of Oil and Gas, Ukraine)

IMPROVEMENT OF TECHNIQUE OF MEASUREMENT OF SURFACE TENSION OF SURFACTANTS SOLUTIONS BY MAXIMUM BUBBLE PRESSURE METHOD

This article presents improved technique of measuring surface tension of surfactants solutions by the maximum bubble pressure method (MBPM), which allows automated measurement of equilibrium and dynamic surface tension of surfactants solutions without measuring the density of surfactants solution and system of precision immersion of capillaries at a depth of this surfactant solution.

Introduction. Measurement and control of surface tension of surfactants solutions in the production of surfactant solutions for oil and gas, aviation, space and other industries of Ukraine, environmental control of water, including water used in the extraction of shale gas, medical research of biological fluids of the human body have an acute need to develop reliable methods for measuring of surface tension of surfactants solutions and production on the basis of automated measuring instruments.

Problem definition. Existing technique of measuring surface tension by the MBPM based on the use of one or two measuring capillaries with different radii. Technique based on single capillary tube [1] requires precise installation depth of immersion of the capillary in the liquid by means of precision mechanical or pneumatic system. The presence of such moving systems which directly affect the outcome measuring of surface tension considerably reduces the reliability of the device during its long operation and precision of measurement of surface tension. Using for measuring surface tension two capillaries with different radii at the same depth of immersion [2] or its modifications [3-5] can eliminate the need for mentioned precision systems, but even the same bubbles frequency or the lifetime of the meniscus surface does not guarantee the identity conditions of dynamic surface tension for capillaries of different radius due to a different area of meniscus in the process of bubbles formation and different initial accumulation of surfactant on the surface of the meniscus after bubble separation [6]. The disadvantages of one-capillary technique also include the need for proper selection of the radius and length measuring capillaries depending on the desired time range measurement of dynamic surface tension [7].

In order to determine the surface tension of surfactant solution when used one or two capillaries must first measure the difference in density between the surfactant solution and gas to determine the value of hydrostatic pressure on the bubble. Density of fluid can not measure if one of capillaries will be movable or two capillaries simultaneously immerse at two different depths and to determine the pressure difference at two different positions. However, this approach still requires a precision system of immersion of capillaries at a depth that significantly eliminates the benefits.

Problem solution. In contrast to mentioned it is proposed the method for measuring surface tension, which is based on three immersed on an arbitrary depth fixed capillaries: two capillaries with the same inner radius but located at different depths of immersion and third capillary, which has a different radius, but is located on the same depth of immersion that the second capillary (Figure 1) [5].
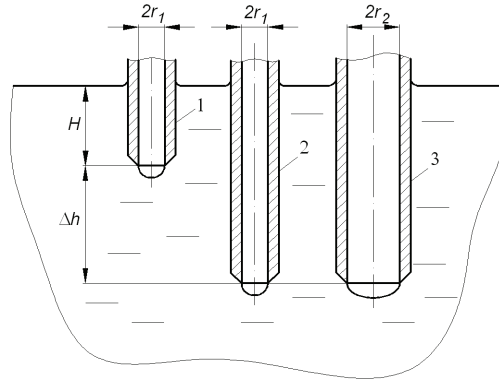
Figure 1. Measurement of surface tension by the MBPM with three capillaries

Scope of this technique is as follows. Maximum capillary pressure is measured for each of three capillaries (pressure at which the bubble is formed). The maximum pressure for the first, second and third capillaries $P_{max.1}$, $P_{max.2}$, $P_{max.3}$ are determined by formulas [10]:

$$P_{max.1} = 2\text{y}/R_{o1} + \Delta c g(H + z_{o1}),\qquad(1)$$

$$P_{max.2} = 2\text{y}/R_{o1} + \Delta c g(H + \Delta h + z_{o1}),\qquad(2)$$

$$P_{max.3} = 2\text{y}/R_{o2} + \Delta c g(H + \Delta h + z_{o2}),\qquad(3)$$

where R_{o1}, R_{o2}, z_{o1}, z_{o2} - respectively the radii of curvature in the embolic point of meniscus and distance in the vertical direction from that point to end the first, second and third capillaries in maximum pressure moment; Δc - the difference density of the investigated liquid and gas; g - gravity; Δh - strictly fixed distance between second and third ends of capillaries that immersed to arbitrary, but the same depth and the first capillary. Subtracting $P_{max.1}$ from $P_{max.2}$ can receive the difference densities of investigated liquid and gas (or density of the fluid relative to air) by the formula:

$$\Delta c = \left(P_{max.2} - P_{max.1}\right)/\Delta h\, g\,.\qquad(4)$$

Using equation (1-4) iterative method allows to determine the surface tension of pure fluids or equilibrium surface tension of surfactant solutions by the formula:

$$\sigma_{equilibrium} = \frac{P_{max.3} - P_{max.2} - \left(P_{max.2} - P_{max.1}\right)\left(z_{o2} - z_{o1}\right)/\Delta h}{2\left(1/R_{o2} - 1/R_{o1}\right)}\;.\qquad(5)$$

Parameters R_{o1}, R_{o2}, z_{o1}, z_{o2} can not be determined at the moment of maximum bubble pressure and these parameters are received in the form of approximable dependencies as a functions of σ, Δc, the radius of the corresponding capillary r by the method [8]. To get dynamic surface tension of surfactant solution maximum pressure values are automatically measured with specified step by turns from the minimum lifetime of the surface of the meniscus until the equilibrium maximum pressure for each of three capillaries. The values of maximum pressure and the lifetime of the surface meniscus obtained by the analysis of real-time curves of pressure and gas flow through the system, as a result, received three curves for maximum pressure on the lifetime of the surface of the meniscus for each of three capillaries (Figure 2):
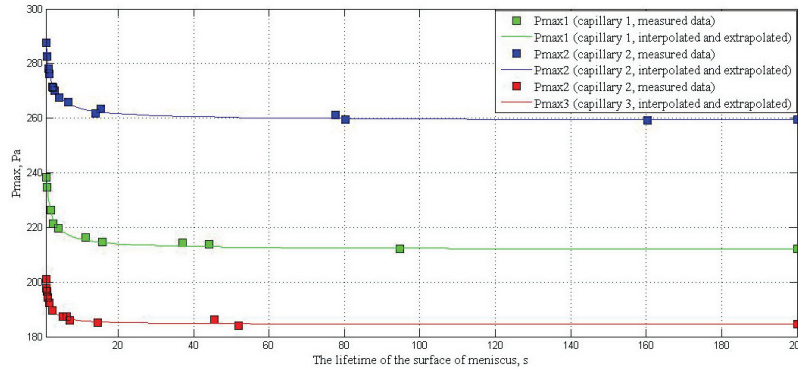
Figure 2. Dependence curves of maximum pressure tension on the lifetime of the surface of meniscus of surfactants solution for three fixed capillaries

A moment of maximum pressure equilibrium is established when you reach the minimum value for $\Delta P_{\max}/\Delta t_{lifetime}$, where $\Delta P_{\max}$ - change in the magnitude of the curve maximum pressure during the change of lifetime of meniscus $\Delta t_{lifetime}$. The acceptable value is set based on the balance of the established acceptable error of measurement and the duration of the experiment. These measured values of maximum pressure are automatically interpolated and extrapolated using precision-based procedures "cubic splines" [9]. Last allows to determine the intermediate value of surface tension and to calculate the point of maximum pressure equilibrium at which the condition $\Delta P_{\max}/\Delta t_{lifetime} \rightarrow 0$. Values of the maximum pressure equilibrium for each capillary are used to determine the surface tension equilibrium by the formula (5).

Calculated equilibrium surface tension and the maximum pressure for each of three capillaries allows to determine the density of the surfactants solution by the formula (4) and the depth of capillaries immersion (or level of liquid relative to fixed capillaries) by the formula:

$$H = \frac{(P_{\max})_n}{\Delta \rho g} - \frac{2 y_{equilibrium}}{a \cdot R_o \cdot \Delta \rho g} - a \cdot z_o,$$ (6)

where a - capillary constant of liquid ($a^2 = \dfrac{\sigma}{\Delta \rho g}$); n - number of the corresponding capillary.

Determined $\Delta \rho$, H, and measured or interpolated $P_{\max}(t_{lifetime})$ allow to calculate the dependencies of surface tension $\sigma(t_{lifetime})_n$ on the lifetime of the surface of meniscus $t_{lifetime}$ for three capillaries of different radii and depth of immersion (Fig. 3) for the same surfactant solution by the formula:

$$\sigma(t_{lifetime})_n = \frac{R_{On}}{2}\left(P_{\max n}(t_{lifetime}) - \Delta \rho g(H_n + z_{On})\right)$$ (7)

These curves $\sigma(t)_n$ allow investigate the influence of dynamic effects, depth of immersion of capillaries, of various radii of capillaries on the measured surface tension and correct the its value.
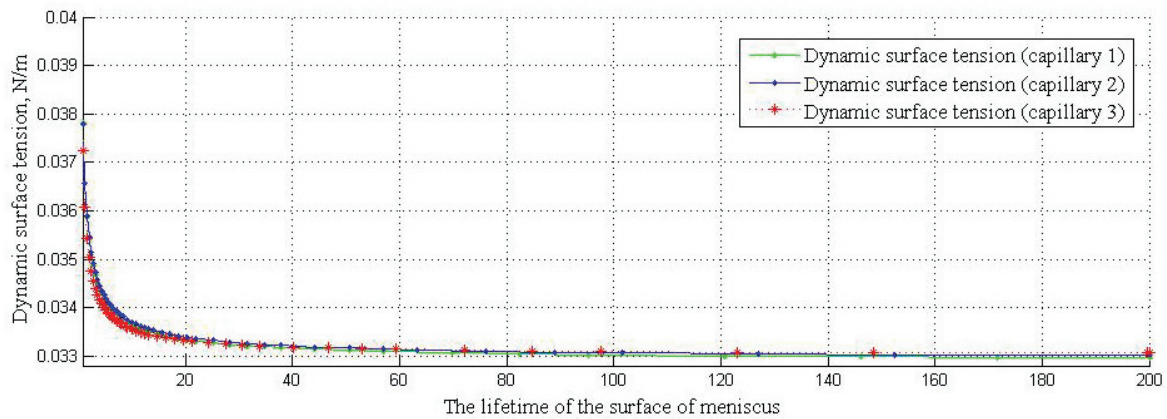
Figure 3. Dependence curves of dynamic surface tension on the lifetime of the surface of meniscus for three fixed capillaries

To implement the described techniques we have designed and manufactured model device, which consists of a source gas (compressor), a stabilization pressure gas system, a through-flow capillary with fixed at its ends a differential pressure transducer for measuring gas flow through the system, electro-pneumatic valves for switching the gas flow in the system, a stepper motor with a pressure regulator to set a given gas pressure in the system, a pressure transducer to measure pressure in the system, two temperature sensors to measure temperature of gas and surfactant solution investigated, a thermal stabilization system to maintain the desired temperature of the surfactants solution. The entire system is based on the MCU Analog Devices ADUC 834, which includes two

high-precision ADC and is controlled by PC. The system can perform all operations of calibration and measurement of surface tension of the surfactants solution automatically and remotely in real time. It allows minimize human impact on the measurement result and measurement of in an environmentally adverse to human environments.

Conclusions

Presented technique of measuring surface tension of surfactant solutions by the MBPM on the basis of three capillaries allows automated measurement of equilibrium and dynamic surface tension of surfactant solutions without measuring the density of the solution and system of precision immersion of capillaries at a depth of this surfactant solution. Determination of equilibrium surface tension by iterative method is based on differences of maximum pressure for each of three capillaries. The using of three capillaries to determine the dynamic surface tension in a long time range allows to improve the accuracy of measuring of surface tension of surfactant solution in comparison to single - or two-capillary methods.

The obtained curves of surface tension (Fig. 3) on the lifetime surface meniscus show the difference of surface tension, which measured for capillaries of different radius (radii of the first and second capillaries are equal, the radius of third capillary is different) in short-term range of lifetime surface meniscus. This phenomenon is due to the influence of aerodynamic resistance of capillaries, and various area and volume of meniscus for capillaries of different radius. Thus, when comparing the results of measurements of surface tension by the MBPM in short-term range of lifetime of surface meniscus by different instruments should take into account a different radius and aerodynamic resistance of capillaries of these instruments, if such has place, and lead all results to capillary with standard radius. Using of three capillaries with different radii (from respectively different surface area and volume of meniscus at the moment of maximum pressure) and depth of immersion in the same surfactants solution will allow to evaluate and consider these factors on the measured dynamic surface tension in short-time range of lifetime of surface meniscus. Corrected dependence of surface tension on the lifetime with calculated surface area and volume of meniscus at the moment of maximum pressure by method [10] can be used to calculate the dependence of surface tension on the effective time of adsorption [11] $y(t_{ef})$, which in turn will allow to compare the results measurement by the MBPM with other methods of determination of dynamic surface tension of surfactants solution.

References

1. *M. Simon, Ann. Chim.* Phys. 32 (1851) 5.
2. *S. Sugden, J. Chem.* Soc. 121 (1922) 858.
3. *Cuny, K. H.* ; and *Wolf, W. L.* : Development of the Bubble-Pressure Method for Determination of the Surface Tension of Liquids. Annalen der Physik, vol. 17, 1956, pp. 57-77.
4. *Pugachevich, P.P.*, Zh. Fiz. Khim., 38(1964) 758.
5. *Jaeger, F.M., Z.* Anorg.Chem., 101 (1917).
6. *V.B.Fainerman, V.D.Mys, A.V.Makievski, R.Miller*, J.Colloid Interface Sci. 304(2006) 222.
7. *V.I. Kovalchuk, S.S. Dukhin*, Dynamic effects in maximum bubble pressure experiments / Colloids and Surfaces A: Physicochem. Eng. Aspects 192 (2001) 131–155.
8. *Кісіль І.С., Кулиняк А.В., Кучірка Ю.М.* Удосконалена методика і прилад для вимірювання поверхневого натягу рідин методом максимального тиску в газовій бульбашці // Методи та прилади контролю якості, № 17. - 2006. - С.47-52.
9. *De Boor, C.*, A Practical Guide to Splines, Springer-Verlag, 1978.
10. *Кісіль І.С.* Визначення поверхневого натягу рідин на основі виміряного максимального тиску в газовому меніску // Методи та прилади контролю якості, №1.- 1997.- С.50-55.
11. *J. Kloubek, J.* Colloid Interface Sci., 41 (1972) 1.

UDC 681.5.62-5(043.2)

L.N. Pokydko (National Aviation University, Ukraine)
V.Yr. Moskovka (National Aviation University, Ukraine)
V.L. Shkuratnik, DS (Moscow mountain institute, Russia)

CONTROLLING METHOD OF THE LASER RADIATION IN TECHNOLOGICAL PROCESSES WITH THE HELP OF PIEZOELECTRIC DRIVE

The control unit of piezodriver in the laser ray control system is considered. The unit realized by high voltage switch elements and microcontroller with built-in width-pulse modulator is offered. Simulation of impulse control unit of piezodriver is carried out.

Lasers are widely and extremely effectively used in various technological processes. In most of their applications lasers functionate as sources (generators) of controlled powerful coherent optical radiation. Control and transformation in such cases mean deflection, switching on and switching off, separation and unification, synchronization, intensity modulation and stages, regulation of length and frequency of wave, change of laser oscillations' polarization.

Direct control of optical radiation of solid and gas lasers acting in severe physical conditions and technical structures, is difficult. Various tasks of controlled transformation of optical radiation in such laser systems are performed by special equipment, primarily the elements of geometrical optics, modulators and deflectors.

The maximum oscillation angle of electromagnetic deflectors (figure 1) is equal to ±12,5. Electromagnetic deflectors are used for production of surface with dimensions from 50.50 to 250.250 mm with the width of track from 0,05 to 0,1 mm.
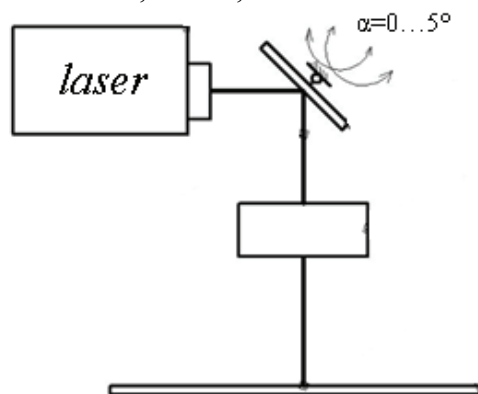
Figure 1. Pattern of electromagnetic deflector

In such systems, laser beam transfers on two coordinates with the help of two high-precision electric motors with the mirrors fixed on their axes – scanners (figure 2.).

Galvanometric scanners are the most frequently used. Laser beam is directed to the first folding mirror, fixed on the shaft of *X*-scanner, and deflects along the axis *x*. Consequently, the deflected beam gets to the second mirror of *Y*-scanner, which is set to an angle of 90° in relation to the first one. *Y*-scanner performs the rotation of the beam along the axis *y*. Such deflecting systems require the usage of very light mirrors.

It makes sense to use deflecting system on the basis of piezoelectric drive for small-angle deflection of laser beam. It is connected with the fact that reverse piezoeffect is lineal when values of electric field's tension are little and the speed of piezoelectric drives is higher than electromagnetic.

In most of the cases deflectors with the piezoelectric drives are used for ±5-degree deflection angles of the laser beam during the production of surface with dimensions not more than 10.10 mm and width of track 0,015 mm. The main manufacturers of such systems are such companies as "Microvision", "Motion Instruments Piezo Systems" (both – USA) and "Physik Instrumente" (PI), "Piezosystem Jena" (both – Germany). Although, when these systems are of high quality they are expensive.
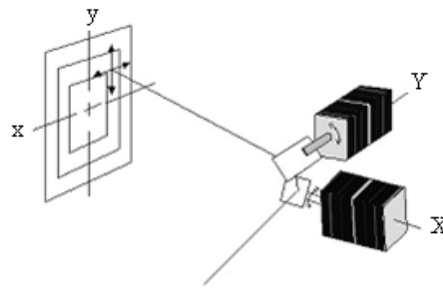
Figure 2. Pattern of electromagnetic deflector's scanner

Structural scheme of two-axis deflecting system with bimorph piezoelectric actuators is reflected on the figure 3, where *1* — body frame; *2* — flexible element; *3* — four bimorph piezoelements (CB), rigidly fixed to the body frame; *4* — glass swinging; *5* — reflecting mirror; *6* — rectifying screw; *7* — barrel positioning screw; *8* — barrels.
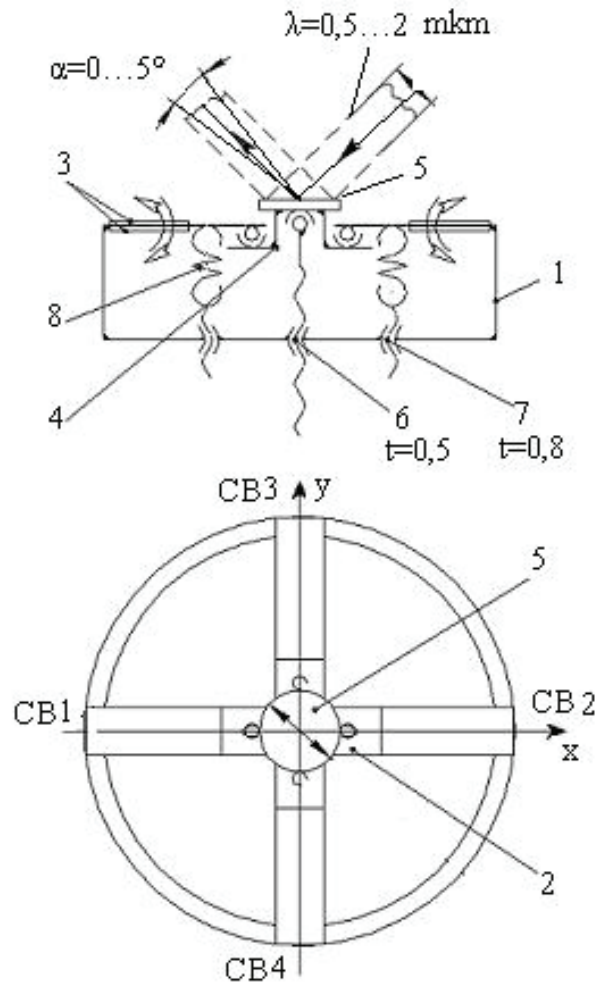
Figure.3. Pattern of two-axis deflecting system with bimorph piezoelectric actuators

During the application of voltage to the bimorph piezoelectric actuators, free end begins to bend, flexible element presses on joint, bending down glass swinging together with reflecting mirror. During the voltage application of opposite polarity to two symmetrically placed bimorph piezoelements (e.g. CB 1 and 2), they deflect right-about increasing the swing amplitude of the mirror in comparison with the pattern which contains only one CB for each coordinate.

Test bench (figure. 4) contains deflecting system 1 which is under investigation and semiconductor laser *3* (length of wave λ=0,64 micron of visible spectrum, red colour). Radiation gets in the middle of the deflecting mirror *2*, than projects to the sheet of paper *4*, placed over a distance *L* =3 m and fixed on the wall. With the oscillation angle (α), the picture with development A appears on the surface.
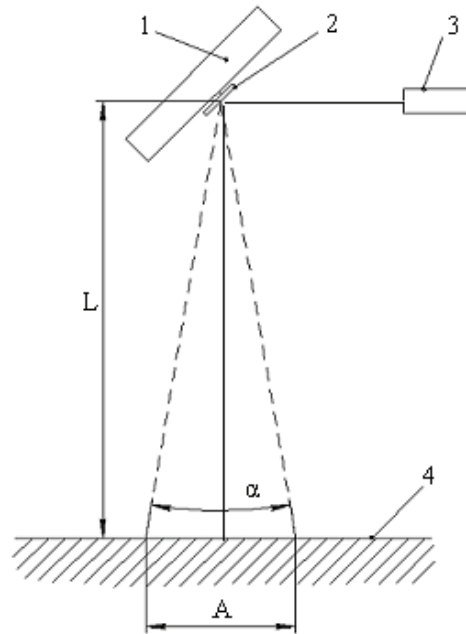
Figure 4. Test bench pattern of investigation of laser beams deflection system

The main task of investigations included the valuation of performance capabilities of developed deflector. In the process of experiments, the work of each piezoelement, in pairs and all four together, was analyzed. The application of voltage U was performed step-by-step 15-40 V and 40-15 V with the frequency of supply voltage 30 hz. When the voltage was changed, the width of development on the surface A was measured. When the distance L (3 m) is known, we can define the angle α. In accordance with the data of the experiment, diagrams of dependence of mirror's oscillation angle on the voltage applying to the one (*a*), two (*б*) and four (*в*) bimorph piezoelectric actuators were made (figure 5, *a—в*). In the process of analyzing of the diagrams, we can make a conclusion that angle α changes when the voltage increases (curve *1*) and decreases (curve *2*).
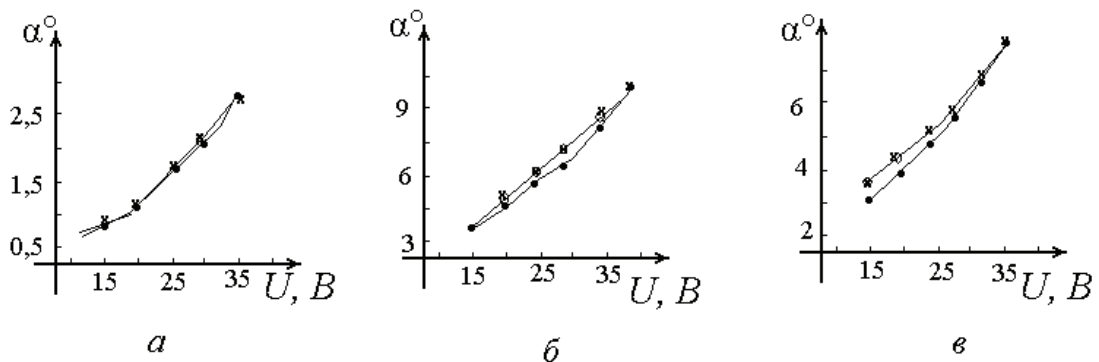
Figure. 5. Diagrams of dependence of mirror's oscillation angle on the voltage applying to the one (*a*), two (*б*) and four (*в*) bimorph piezoelectric actuators.

When the frequency of voltage changes, the geometrical forms of the projected picture remained unchanged. Investigations when $U = 3$ V showed the following: resonance frequency of the system when BP *1* and *2* are switched on turned out to be equal 580 hz; BP *3* and *4* are switched on — 560 hz.

When the voltage is 30 V and frequency is 50 hz the power input of one piezoelement made up 0,9W, and of four piezoelements — 3,6W.

The figure 6 shows the development of the picture on surface *A*, which demonstrates the divergence between direct and reverse beam path.

Such hysteresis loop is connected with inaccuracy of manufacturing of mechanical engineering assemblies, which can be compensated by control system with the help of feedback circuit.
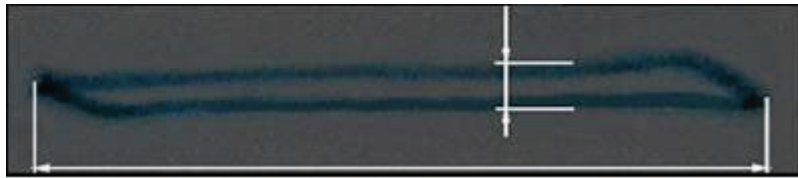
Figure 6. Development of the picture on the surface A

Work mode of deflective system is realized by method of line development with the help of control system (figure 7). For it's realization, the harmonic voltage is applying along the coordinate *x* to BP *1* and *2*, and along the coordinate *y* to BP *3* and *4*, step change voltage for line displacement is applying.
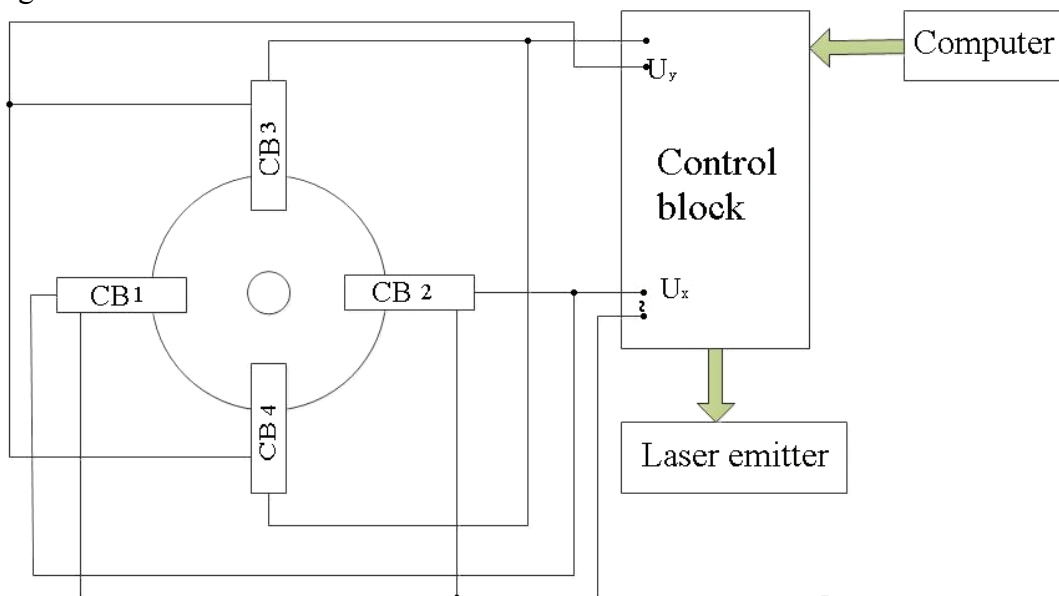
Figure 7. Scanning deflective system

Creating the jump of the voltage which is applied to *3* and *4*, to quantity $Uy1$ and $Uy2$, the direct and reverse beam path can be united (figure 8).
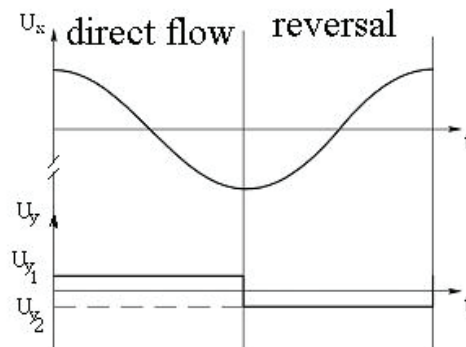
Figure 8. Diagram of dependence of voltage on time when
the laser beam is direct (a) and reverse (б)

Proposed scanning system provides scanning which is quick enough and also precision of model construction of the scanning object. The usage of piezoelectric deflector makes it possible to gain measurable increase of productivity of details' control of difficult shape (1000 measures for 2 hours). It would have taken approximately one month to perform this work if we used the old methods. Piezo managed deflectors in most of the cases are used for ±5-degree deflection angles of laser beam. The investigations of the proposed scanning system showed the high stability of parameters of development and high precision of positioning of the beam on the surface of scanning object. Disadvantage of such item is a great dependence on vibrations and drawbacks in the work of the system of phase deflection of the voltage.

E.N. Bezvesilnaya, D.E., prof.
(National Technical University of Ukraine "KPI", Ukraine)
V.P. Kvasnikov, D.E., prof. (National Aviation University, Ukraine)
Koval A.V., graduate (Zhytomyr State Technological University, Ukraine)

TWO GYROSCOPE GRAVIMETER OF AVIATION GRAVIMETRIC SYSTEM

It is offered and investigated two gyroscope gravimeter of aviation gravimetric system which provides higher accuracy of measurements, than known gravimeters, at the expense of elimination of errors from cross angular speeds of the basis and angular speed of rotation of the Earth and measurement of a full vector of acceleration of gravity.

Problem statement. Today modern devices in the field of air gravimetry (string GS and quartz GAL-S) have significant lapses from agency of cross angular rates of the basis and angular rate of twirl of the Earth (only last lapse makes 584 mGl). The gyroscopic one-spool gravimeter also has above indicated lapses.

Demands to accuracy of measurements of a gravitational field of the Earth, correction of inertial navigational systems on a gravitational field of the Earth and other precision problems of space area increase every year.

Therefore the problem of raising accuracy of air gravity measurements by compensation of lapses from agency of cross angular rates of the basis and angular rate of twirl of the Earth is the actual.

The analysis of researches. The conducted researches showed that the big contribution to the theory and practice of land gravity measurements has been made by a row of outstanding scientists: V.O. Bagromjantsa, J.D. Bulanzhe, K.E. Veselov, A.M. Lozinskoy, A.A. Mihajlova, S.A. Poddubny, Y.I Popova, V.A. Tulina, V.V. Fedinsky, M.Y. Heifetz and others.

The big role in working out of gravitational measurements was played by activities of foreign scientists: L. La-Kosta, D. Garrison, A. Graf, J. Tomodi, M. Golvani and others.

Intensively conduct gravimetric researches in many big technological centres: NNC "metrology Institute" (Kharkov) under the direction of G.S.Sidorenko; CSII "Azimuth" (St.-Petersburg) under the direction of L.P.Nesenjuka, G.B.Volfsona, B.A.Blazhnova; VVIAU (Moscow) under the direction of A.A. Krasovsky, A.I. Soroki; RV VIAU (Riga) under the direction of A.A. Veselov.

At present there is a numerous literature in the field of methods and gauges of gravity anomalies (GA) [1] which contains both a principle of operation, and technical datas of modern devices for measurement of GA. The great attention is given to one gyroscope gravimeters [1, 2] on which the basic methods of definition of acceleration are based. The information about two gyroscope gravimeters is absent.

Purpose: to offer and investigate two gyroscope gravimeter (TG) of aviation gravimetric system (AGS) which provides the higher accuracy of measurements, than known systems, at the expense of elimination of lapses from cross angular rates of the basis and angular rate of twirl of the Earth and measurement of full gravitational vector (instead of one component, as in gravimeters GAL-S, GS and one gyroscope).

The basic part. For measurement of gravity anomalies it is offered aviation gravimetric system (fig. 1) which has bigger accuracy and response, than known, and consists of the two-degree-of-freedom gyro 1 which have been installed in internal 2 and external 3 frameworks, provided with systems of interframe correction which contains 4 internal framework of the gyro installed on an axis 1 angle-date transmitter (AT) 5 and the torque sensor (TS) 6 connected to its exit which have been installed on an axis of 7 external framework 3. To exit AT 8 it is connected the TS 9 which have been installed on an axis 4 of internal framework 2. In observed AGS it is injected additional, identical first, the two-degree-of-freedom gyro 1, which rotor is twirled in an opposite side from the basic gyro 1. Additional gyro AGS is provided also with analogous systems of correction which consist from AT 5, with 4 internal framework 2 had on an axis, and the TS 6 connected to its exit

which have been had on an axis of 7 external framework 3, AT 8, 7 external framework 3 to which exit it is connected the TS 9 which have been installed on an axis 4 of the internal framework 2. Centers of weight of two equal (basic and additional) gyros 1 are displaced on equal distance l In one side along axes 10 twirl of rotors of gyros 1 concerning axes of 7 external frameworks 3. Vectors of an angular momentum of two gyros are opposite directed.

In two gyroscope gravimeter two proceeding signals of linear acceleration f_z, f_x are formed as the sum of signals from AT 8 of two gyros concerning one axis z And as the sum of signals from AT 5 of two gyros concerning the second axis x. Proceeding signals f_z, f_x move into airborne digital counting machine (ADCM). Both gyros are installed on a platform 11 which angular position is ruled by engine 12, installed on an axis x and engine 13 — on an axis z. The signal of linear acceleration f_z moves to engine 12 and the signal f_x — into engine 13. Both engines operate an angular rule of a platform 11 on signals f_x, f_z. In ADCM signals from system of definition of navigational parametres and from the altitude metre also arrive.
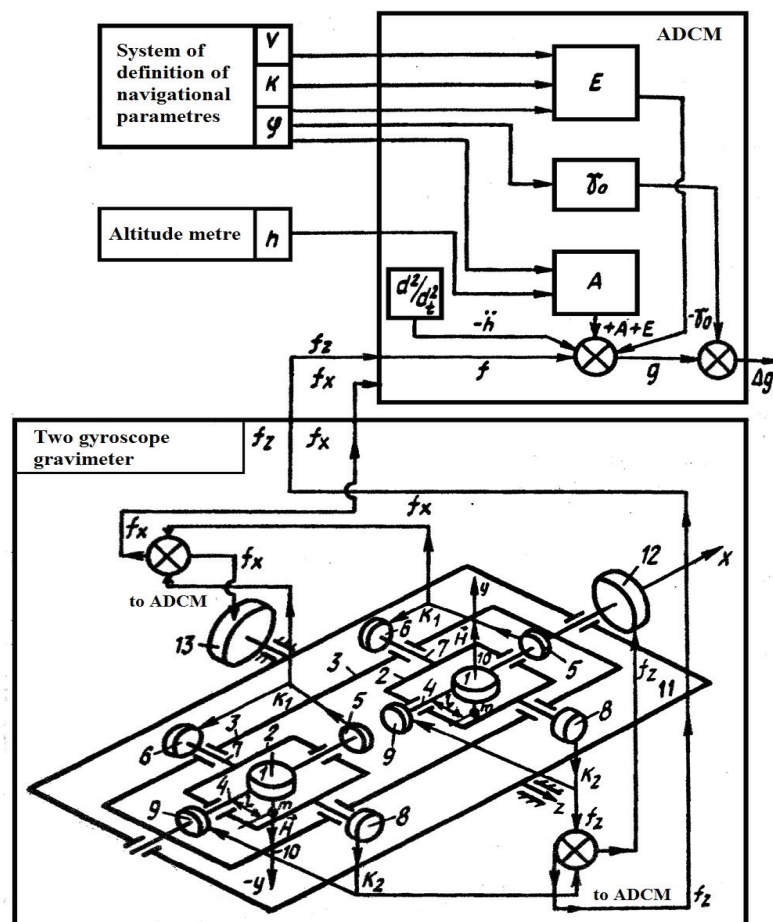
Fig. 1. Aviation gravimetric system with two gyroscope gravimeter

In the presence of a component g_x linear acceleration along axes 4 of internal frameworks of 2 gyros, frameworks start to be twirled round axes of 4 internal frameworks 2 under the influence of the pendulum moment $ml\,g_x$ (ml — a pendulosity), 7 external frameworks directed on axes 3. Refund of gyros under the influence of this moment serves as the reason of emersion of electric signals from two equal AT 5, 4 internal frameworks 2 had on axes which exits are connected to control windings of two equal TS 6 which have been had on axes of 7 external frameworks 3. Two TS 6 create the moments which compensate the pendulum moments $ml\,g_x$, on axes 7 of external frameworks 3. Under the influence of the pendulum moment $ml\,g_z$, the linear acceleration caused by a component g_z along axes of 7 external frameworks and 4 internal frameworks of 2 gyros directed along axes, two two-degree-of-freedom gyroes start to be twirled round axes of 7 external frameworks 3. Twirl of two gyros under the influence of the moment $ml\,g_z$ serves as the reason of emer-

sion of electric signals from two equal AT 8, 7 external frameworks 3 had on axes which exits are connected to control windings of two equal TS 9 which have been had on axes of 4 internal frameworks 2. Two equal TS 9 create the moments which compensate the pendulum moments $ml\,g_z$ which act on axes of 4 internal frameworks of 2 gyros. In two gyroscope gravimeter starting signals f_z and f_x of linear acceleration, as the sum of signals from AT 8 of two gyros on one z-axis as the sum of signals from AT 5 of two gyros on the second x-axis are formed. Starting signals f_z, f_x move in ADCM. Signals of linear acceleration f_z, f_x arrive on engine 12, 13, installed on axes x, z. Both engines operate an angular rule of a platform 11 on which installed the device. In ADCM initial signals v, k, ϕ from system of definition of navigational parametres and an initial signal h from the altitude metre move also. ADCM computes gravity anomalies.

Let's explain operating principle of AGS using system of the precision motion equations of one of two equal gyros of gravimetric system:

$$\begin{cases} H\dot{\beta} + k_1\beta + n_1\dot{\alpha} = ml\,w_x - ml\,g_x - H(\omega_x + \omega_y\alpha) - A\dot{\omega}_z - H\omega_3\cos\phi, \\ H\dot{\alpha} + k_2\alpha + n_2\dot{\beta} = ml\,w_z - ml\,g_z - ml(w_x\alpha - w_y)\beta - B(\dot{\omega}_x + \dot{\omega}_y\alpha) - \\ -H\omega_y\beta - H\omega_3\sin\phi, \end{cases} \qquad (1)$$

where H – a gyro angular momentum; α, β – turn angles of an external framework concerning installation and a casing of the gyro concerning an external framework; k_1, k_2 – factors which are equated to product of transfer factors matching AT and TS of two correction channels; n_1, n_2 – factors of forces of a viscous friction concerning matching axes; w_x, w_y, w_z – projections of a translatory acceleration of the airplane to axes Ox, Oy, Oz of reference axes $xOyz$, connected with the airplane (its beginning O coincides with centre of mass of a loose port of the device; axis Ox is directed in parallel an installation longitudinal axis, axis Oy – in parallel cross-section; axis Oz – in parallel normal axis); $\omega_x, \omega_y, \omega_z$ – projections of angular rate of installation to the axes connected with it; A – shown to a spinning ax of an external framework a system moment of inertia "the gyro in кардановом a suspension"; B – a moment of inertia "a rotor and an internal framework of the gyro"; g_z, g_x – a vertical and horizontal component of acceleration of a gravity which act on the gyro; ω_3 – angular rate of revolution of the Earth; ϕ – latitude.

Marked out a disturbing moment of obstructions concerning axes of a suspension of frameworks of the gyro

$$M_1 = ml\,w_x - H(\omega_x + \omega_y\alpha) - A\dot{\omega}_z - H\omega_3\cos\phi,$$

$$M_2 = ml\,w_z - ml(w_x\alpha - \omega_y)\beta - B(\dot{\omega}_x + \dot{\omega}_y\alpha) - H\omega_y\beta - H\omega_3\sin\phi,$$

let's transcribe system (1) in an aspect

$$\begin{cases} H\dot{\beta} + k_1\beta + n_1\dot{\alpha} = M_1 - ml\,g_x, \\ H\dot{\alpha} + k_2\alpha + n_2\dot{\beta} = M_2 - ml\,g_z. \end{cases} \qquad (2)$$

Let's find the solution of the equations (2):

$$\alpha(p) = \left[n_2 p(M_1 - ml\,g_x) - (Hp + k_1)(M_2 - ml\,g_z)\right]\left[n_1 n_2 p^2 - (Hp + k_1)(Hp + k_2)\right]^{-1}; \qquad (3)$$

$$\beta(p) = \left[n_1 p(M_2 - ml\,g_z) - (Hp + k_2)(M_1 - ml\,g_x)\right]\left[n_1 n_2 p^2 - (Hp + k_1)(Hp + k_2)\right]^{-1}. \qquad (4)$$

Let's record expressions of resistant to values of turn angles of one of gyros, using (3), (4):

$$\alpha_{ycm} = k_2^{-1}\left[-ml\,g_z + ml\,w_z - ml(w_x\alpha - w_y)\beta - B(\dot{\omega}_x + \dot{\omega}_y\alpha) - H\omega_y\beta - H\omega_3\sin\phi\right];$$

$$\beta_{ycm} = k_1^{-1}\left[-ml\,g_x + ml\,w_x - H(\omega_x + \omega_y\alpha)\beta - A\dot{\omega}_z - H\omega_3\cos\phi\right].$$

Let's generate signals, proportional to the sum of turn angles of two gyros. It is for this purpose used two equal gyros with opposite directed vectors of an angular momentum. Signals of two gyros look like accordingly:

$$\alpha_{1ycm} = k_2^{-1}\left[-ml\,g_z + ml\,w_z - ml(w_x\alpha - w_y)\beta - B(\dot{\omega}_x + \dot{\omega}_y\alpha) - H\omega_y\beta - H\omega_3\sin\phi\right],$$

$$\alpha_{2\,ycm} = k_2^{-1}\left[-m\lg_z + ml w_z - ml\left(w_x\alpha - w_y\right)\beta - B\left(\dot\omega_x + \dot\omega_y\alpha\right) + H\omega_y\beta + H\omega_3\sin\phi\right];$$

$$\beta_{1\,ycm} = k_1^{-1}\left[-ml\,g_x + ml\,w_x - H\left(w_x + w_y\alpha\right)\beta - A\dot\omega_z - H\omega_3\cos\phi\right],$$

$$\beta_{2\,ycm} = k_1^{-1}\left[-ml\,g_x + ml\,w_x + H\left(w_x + w_y\alpha\right) - A\dot\omega_z + H\omega_3\cos\phi\right].$$

Let's find two proceeding signals two gyroscope gravimeter:

$$f_z = \alpha_{1\,ycm} + \alpha_{2\,ycm} = k_2^{-1}\left[-2ml\,g_z + 2ml\,w_z - 2ml\left(w_x\alpha - w_y\right)\beta - 2B\left(\dot\omega_x + \dot\omega_y\alpha\right)\right]; \qquad (5)$$

$$f_x = \beta_{1\,ycm} + \beta_{2\,ycm} = k_1^{-1}\left[-2ml\,g_x + 2ml\,w_x - 2A\dot\omega_z\right]. \qquad (6)$$

From expressions (5) and (6) proceeding signals AGS one can see that:

• compound of a wanted signal $-2ml\,g_z, -2ml\,g_x$ double;

• two gyroscope gravimeter AGS can measure a total direction and the module gravity acceleration under formulas

$$\vec g = \vec g_z + \vec g_x, \; |g| = \sqrt{g_z^2 + g_x^2},$$

that provides the higher accuracy of measurements and alignment of two gyroscope gravimeter AGS. For this output signals s $f_z \equiv 2g_z$ and $f_x \equiv 2g_x$ (expressions (5) and (6)) of two gyroscope the gravimeter use for control of two additional engines of in addition injected platform on which the basic and additional gyross are instaled;

• some moments of an obstruction owing to cross linear and angular accelerations double $\left[2ml\,w_z - 2ml\left(w_x\alpha - w_y\right)\beta - 2B\left(\dot\omega_x + \dot\omega_y\alpha\right); 2ml\,w_x - 2A\dot\omega_z\right]$. Here it is possible to consider only agency of the moments $-2ml\,w_z, -2ml\,w_x$. Therefore it is possible to consider that

$$f_z \cong k_2^{-1}\left(-2ml\,g_z + 2ml\,w_z\right),$$

$$f_x \cong k_1^{-1}\left(-2ml\,g_x + 2ml\,w_x\right).$$

Let's notice that the moments-obstructions indicated above (in the sum with the moments-obstacles which agency in two gyroscope gravimeter is expelled) influence equally on activity of one gyroscope gravimeter of AGS;

• lapses called by the gyroscopic moments-obstacles from cross angular rates are eliminated $\left[H\omega_y\beta, H\left(\omega_x + \omega_y\alpha\right)\right]$ and from angular rate of twirl of the Earth $\left(H\omega_3\sin\phi, H\omega_3\cos\phi\right)$, which can be significant (namely, last – 584 mGl).

Conclusions

Offered TG AGS has certain advantages compared with other known gravimeters:

1. Observed TG AGS provides the higher accuracy of measurements, than with one gyroscope gravimeter thanks to compensation of lapses in a consequence of cross angular rates and angular rate of twirl of the Earth.

2. In TG AGS compound a legitimate signal double.

3. Two gyroscope gravimeter AGS can measure a total direction and the module of acceleration of a gravity which provides the higher accuracy as directly measurements Δg, and alignment of two gyroscope gravimeter system thanks to application of two additional engines and an additional platform.

References

1. *Bezvesilnaya E.N.* Measurement of accelerations: the Textbook. - K: Lybid', 2001. – 254 p.

2. *Bezvesilnaya E.N.* Air gravimetric systems and gravimeters: the Monography. – Zhitomir: ZSTU, 2007. – 604 p.

O.V. Kovanko, Master
(National University of Water Management and Nature Resources Use, Rivne, Ukraine)
M.V. Michalko, Vice-Rector (National Aviation University, Ukraine)

UNDERGROUND MOVING DEVICES WITH INTELLIGENT CONTROL SYSTEM

In this article described the functionality and construction of underground moving devices with intelligent control system. Also it shows a possibility to use such devises to solve different kinds of problems related to providing underground technologies

In modern conditions the further development of underground space, its raw and power potential the development of geotechnology, increasing need of placing various underground manufactures and storage of toxic materials and specialized objects of a scientific and applied character is extremely urgent need to increase efficiency, particularly energy savings of hardware for laying and flaw detection of underground engineering communications.

Analysis of modern technical means for such work has shown feasibility and perspectives of hybrid devices development, that can move both in soil space and through pipelines of various purpose to their cleaning and flaw detection.

Such controlled multifunction devices can find a wide application in many fields of economy of Ukraine, particularly in mining, agriculture and public services, geological survey, geotechnology, as a means of underground space monitoring, as well as gas and oil transport systems.

At the first stage of this problem solution through bionic synthesis have been developed multifunctional worms like underground mobile devices (UMD) [1]. The second stage involves intellectualization of such devices based on the synergetic combination of mechanical component with electronic, electrical and computer components that provide these moving control devices.

First achievements in this area have been done [2-4] a logical extension of which is the UMD presented in Fig. 1 and 3.
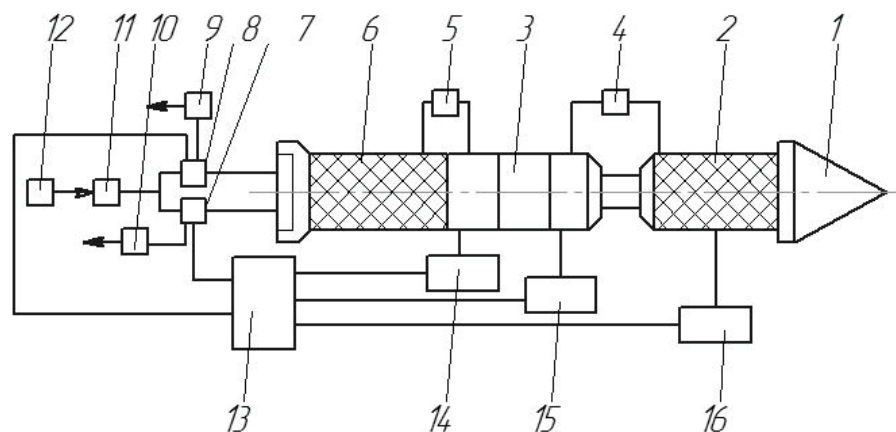
Fig. 1. Schematic diagram of the UMD with automatic movement control systems

The device consists of nose part 1, the front fixing chamber, covered by the elastic cover 2, the power module (linear multistage hidropneumoengine 3), valves 4 and 5, the rear fixing chamber, covered by the elastic cover 6, the electromagnetic valves 7 and 8 with 9 and 10 indicators of their operation, locking mechanism 11, the pneumatic or hydraulic block of energy 12, intelligent programmable microcontroller 13, sensors 14, 15, 16 of extreme left and right position of nose part 1 pressure and energy in the front fixing chamber.

Elastic membrane 6 is increased in volume to the contact with the wall cavity of soil or pipe and, due to friction forces, fixed when receiving energy carrier from the power unit 12 through the locking mechanism 11. It is possible only at achievement a given pressure. After that energy carrier served through valve 5 to the power module 3. As a result, the nose will move forward by some part of the path. Thus in its rightmost position activated the valve 4 and the energy carrier is directed to the front fixing chamber. Its elastic cover 2, after increasing in volume, fixes nose of the device.

The cover of rear fixing chamber simultaneously decreases in volume to its original state so the energy carrier arrives to the opposite cavities of power module 3. As a result, the tail part is moved forward up to the fixed nose part at the path, which is equal to its previous movement. Information about the pressure in the nose fixing chamber and about the extreme left and right nose part 1 position is transmitted using the pressure sensors 16 and position sensors 14 and 15 to intelligent programmable microcontroller 13 which manages electromagnetic valves 7 and 8, providing a incremental wall anchors, discrete movement of the device (Fig. 2)
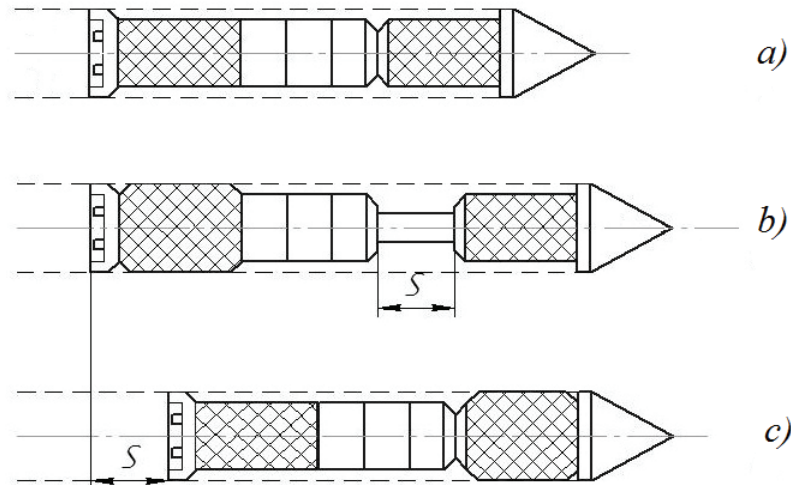
Fig. 2. Discrete device movement: a) starting position; b) fixation of the tail and move forward of the nose part to the path S; c) fixation of nose part and pulling up to it the tail part

In the development of this principal scheme of the UMD with automatic trajectory stabilization system is developed (Fig. 3)
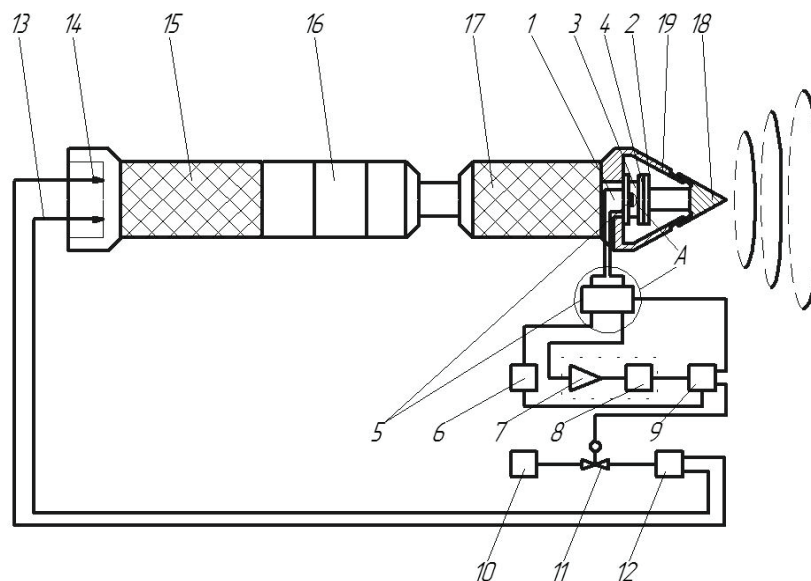
Fig. 3. Principle scheme of the UMD with intellectual control system:
1 - nose, 2 - frustum, 3 - body of ultrasound vibrator 4 - membrane 5 - piezo pack 6 - high frequency electronic generator, 7 - electronic amplifier, 8 - normalizing converter, 9 - intelligent programmable microcontroller, 10 - energetic unit of hydraulic or pneumatic energy; 11 - actuating mechanism, 12 - reverse distributor, 13 and 14 - flexible pipes, 15 - rear fixing camera, 16 - linear hidropnevmo engine, 17 - the front fixing chamber, 18 - bit, 19 - plate base

Following describes mentioned device's the principle of action. Working fluid from the power unit 10 comes to UMD through actuating mechanism 11, reversible distributor 12 and flexible pipes 13 and 14. If the working fluid supplied by the pipeline 13, then the pressure in the pipeline 14 is always equal to atmospheric. Under the influence of working fluid elastic cover of the rear fixing chamber 15, increasing in volume up to the contact the wall of pre-formed by the nose part 1 frag-

ment of soil cavity is fixed, and the nose is moved by hidropneumatic engine 16 forward to the given part of the path ("step") . Then working fluid is supplied by the pipeline 14. Spent working fluid is given out by the pipeline 13. This would mean that the elastic cover of the rear fixing chamber 15 will decrease up to its previous size, and elastic cover of front fixing chamber 17 increases in volume up to the contact with the wall cavities of soil and the tail part will pull up to the fixed nose part to the length of "step ". At the same time the device also will move forward to this "step" length. Then the process will be repeated and the device discretely will "step" forward.

During its motion the following happens. When the tail of device is fixed and the nose part is moving relative to it forward, intelligent programmable microcontroller 9 gives the command to enable high frequence electron generator 6, which generates electrical fluctuations of ultrasound frequency. They are converted by piezo battery pack 5, which is in the body of ultrasound vibrator 3, closed with the membrane 4, which contact with the plate base 19 of tip 18 of the nose part 1, into the mechanical vibrations of ultrasound frequency. During high-frequency oscillations of the tip 18 relative to truncated conical element 2, the mechanical waves of ultrasound frequency (ultrasound beam) emitted into the soil. When the tail part pull's up to its fixed nose part, microcontroller 9 gives command to disconnect the generator 6 and piezo battery pack 5. At the same reflected by the border of two environments of different density, mechanical waves of ultrasound frequency will act through the tip 18 (which can fluctuate relative to truncated cone 2), its plate base 19 and the membrane 4 on piezo battery pack 5, which converts reflected mechanical waves of ultrasound frequencies in the electrical signal of the same frequency. This electrical signal is amplified by the amplifier 7, and using normalizing converter 8 is reduced to a standard signal. The latter is directed to the input of microcontroller 9, which based on the difference Δt measured time t_1 (direct) and t_2 (reverse) passing the ultrasound beam and known velocity v of ultrasound in the soil, determines the distance S an obstruction ($S=v\Delta t/2$) and by the intensity of the reflected signal - the nature of obstacles. Accordingly, by the microcontroller 9 forming the command electrical signal that comes up to the actuator 11. It changes the pressure of energy carrier, that influences on the strength of the nose part to act on the obstacle. Also it influences on the strength of fixing nose and tail parts. This provides a guaranteed overcoming barrier's reactive forces of resistance and stabilization trajectory.

The above can increase energy saving of the UMD and its penetrating ability, maintain the required speed and stabilize the desired trajectory and increase the action radius without replenishment of energy.

Conclusion

The device is multi-purpose and can be used for probing and clearing linearly extended objects, laying all sorts of of underground engineering communications, search for minerals also can be used as a vehicle to deliver a given point of soil space corresponding material and technical means, such as underground means of the object "Shelter" monitoring.

References

1. *Kovanko V.V.* Біомеханічні основи створення підземно рухомих пристроїв підвищеної ефективності.– Рівне: Вид-во НУВГП, 2011. – 198 с.

2. *Drevetskiy V.V., Kovanko O.V.* Підземнорухомий пристрій з автоматичною системою стабілізації траєкторії у вертикальній площині // Вісник Інженерної академій України (ІАУ): Теоретичний і науково-практичний журнал ІАУ. – Київ, 2009. – Вип. 3-4. – С. 212 – 214.

3. *Drevetskiy V.V., Kovanko O.V.* Підземнорухомий пристрій з автоматичною системою регулювання швидкості руху // Вісник Інженерної академій України (ІАУ): Теоретичний і науково-практичний журнал ІАУ. – Київ, 2009. – Вип. 2. – С. 205 – 208.

4. *Kovanko O.V.* Підземнорухомий пристрій // Патент України на корисну модель №41889 E02F 5/18. – Бюл. №11 від 10.06.2009.

UDC 621.512.011.56.001.115

V.P. Kvasnikov, Dr.of Eng.
(National Aviation University, Ukraine)
G.M. Kleschov, Cand. of Eng.
(State Academy of the Technical Adjusting and Quality, Odesa, Ukraine)

COMPUTER-INTEGRATED THROUGH SYSTEM OF COMPUTER-AIDED DESIGN WITH EXTENSION OF «LIFE CYCLE» OF STAMP INSTRUMENT

Summary. Reduction of time of planning and making of details of stamps is examined as a result of application of computer-integrated through computer technology of preproduction, and also new technology with the extension of «life cycle» of stamps.

Preproduction one of labour intensive constituents of productive process. On preparation productions depend: labour intensiveness, terms of making, increase of efficiency, costs and quality of wares. By the issues of the day of preproduction in industry and, in particular, in aviation, machine-tool, motor-car and agricultural industries I am: introduction of modern mathematical methods and facilities of the computing engineering, creations intellectual computer-integrated adaptive through computer designer - technological systems of preproduction, and also creation of flexible CASS : machine-tools, instruments (stamps) and automatic transfer lines.

Stamps of the cold sheet stamping in preproduction of modern productive process are:

1) one of the most widespread methods, which allows to make the most various in a due form details in short spaces with minimum expenses;

2) perspective as specific gravity of the details stamped from a sheet for basic industries of industry made from 60% to 85%;

3) necessary as a nomenclature of cold-stamped details broadens due to hard-deformed and little-plastic metals, alloys and non-metal details;

4) expedient as present taking about the tendency of translation of row of processes of casting and forging on the cold sheet stamping, that reduces weight of detail on 50% and diminishes the expense of metal to 70%.

The analysis of existing in area of automation directions and their research was shown expediency of further automation of preproduction and making of wares, first of all, stamp rigging and automatic transfer lines as making components of all industries of national economy, having a mass production, and lately, in the conditions of conversion, the stake of small-serial and single production increased. In also time at a single (individual) or small-serial production the questions of cost and economy occupy a basic place in market relations.

From a rangeability and amount of the produced products foregoing indexes depend considerably. In this connection there was a necessity for technically flexible mechanisms and control system, allowing to promote the productivity at a small-serial production, which the traditional methods of automation are useless for.

The tendency of height of market to the small-serial (single) production of wares compelled many producers to call to more flexible methods of treatment, to allowing more frequent to reconstruct a production, expending on it minimum time and labauroxpenditure.

Research aim: reduction of time of planning and labour expenses of making of details of stamps, and also introduction of new technology of production and extension of «life cycle» of stamps.

Taking into account the stated the model of computer-integrated through computer technology of management is worked out and investigational preproduction and making of details of stamps [1]

presented on Fig..1. (PATENT № 48027, request 27.07.2009, publication. 10.03.2010, Bulletin. № 5, research Methodology is approved in a process experienced - industrial introduction.

A model works as follows.. On an entrance the draft of the stamped detail of customer is given. The draft of customer is encoded on instruction and passed in a computer-integrated computer-aided of stamps design. Computer-integrated system of consists from:

systems «Entrance» : control of initial task with visual verification on Plotter; systems «Cutting» out : drafts of cutting (mode) out of contours of details of customer and taking of technological character; systems «Designer» : information about the projected details of stamp (drafts); system «Technologist» : information for the automated managing program development for machine-tools with By numerical control, (flowsheets); CALS -technology for managing program [2, 3].

Productive block on making stamp- ready-to-cook foods: blocks and packages and revision of packages (shape-generating instrument and attended details) on the detail of customer.

Suggestion new technology of production of stamps in Ukraine. The scientific novelty of new technology consists in theoretical and mathematical fundamental works of authors of this article, transferred in the used literature. A productive process includes two enterprises - doubler (in case of blowing off a productive process on one of them), informatively constrained inter se and carrying out both planning and making of stamps in a metal through COMPUTER and machine-tools with By numerical control.

On new technology to the plants - orders are given out manufacturers on planning and making, and to the plants - stamps are given out customers in a metal with stamps - doublers without the complete sets of drafts and flowsheets on the detail of stamps. In the process of exploitation stamps wear (fall out) out and replaced by stamps - doublers. Stamps, requiring repair (extension of «life cycle» of stamps), are not repaired on plants customers, and leave on enterprises are doublers manufacturers of stamps, for the centralized repair, utilizarion system of data-bases and knowledge in which data are kept about the before projected stamps. Enterprises - doublers make repairs out-of-commission details stamps.

As a result of enterprise - doublers free ten of designers and technologists, preparing documentation for a customer, Customer frees ten of designers and technologists, and also workers of high qualification, т. of e also. does not make repairs for itself.

As a result the customers of stamps do not contain for itself a workshop (areas) on repair of stamps out-of-commission, does not occupy an area under an equipment for repair, does not spend a mean on concomitant materials and on different family power mediums. In also time large economy on the salary of designers, technologists and on the workers of high level of proficiency, and basic customer for which the pressed details are made on: combines, machine-tools, tractors, airplanes and details, for industry of instrument-making will be got by details considerably cheaply. A transferred unit cost also will be cheaper and thus more competitor ability of market.

Enterprises are doublers designers and manufacturers of stamps, giving out customer stamps only in a metal without drafts and flowsheets for repair of stamps does not prepare this documentation for the customer of stamps does not get, accordingly, the money withholdings, because planning is executed by Computer (without the hand planning), and drafts in India ink on a tracing paper are executed by Plotter (passing the hand copying). Applying new technology of planning and making of stamps considerably time and labour intensiveness grow short, efficiency rises.
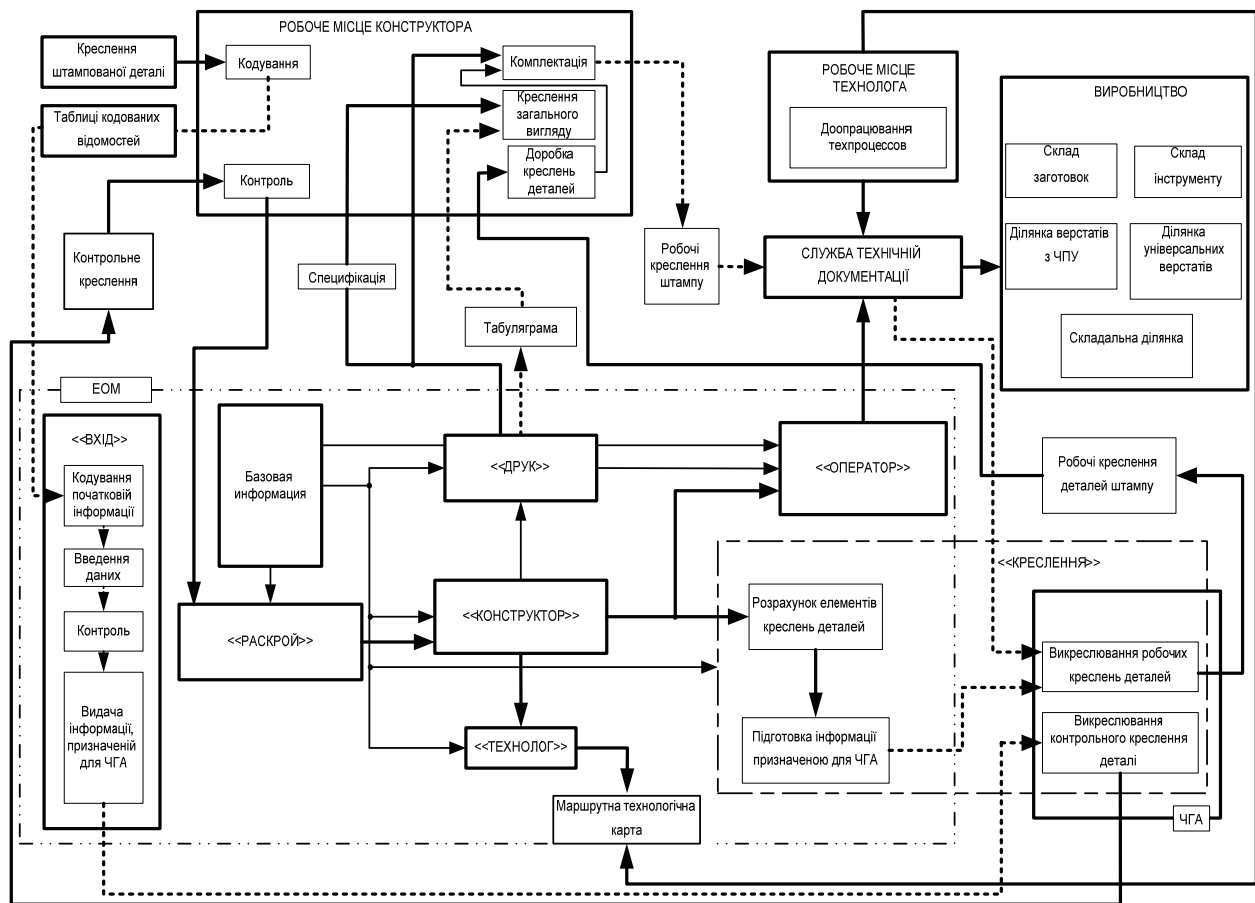
Fig. 1 Model of computer-integrated through computer technology of management preproduction and making of details of stamps

Conclusions

The considered conception of the intellectual computer-integrated through system of preproduction and flexible production are most advantageously in an individual, small-serial and serial production which embraces now to 85 % and more than all productions of agricultural machinery industry and instrument-making. Model of computer-integrated through computer technology of management presented in the article preproduction and making of details of stamps and also new technology of production of stamps provide the decline of temporal, labour and cost expenses, promote efficiency and quality of stamps.

References

1. *Квасников В.П.* Патент «Метод інтегрованої наскрізної підготовки виробництва та виготовлення деталей штампів», № 48027 від 10.03.2010 Бюл.№5 / В.П.Квасников, Л.В. Коломиец, Г. М. Клещев и др. – К.: 2010.

2. *Клещов Г.М.* Адаптивна наскрізна комп'ютерна технологія управління підготовкою виробництва та виготовлення деталей штампів на базі штамп - напівфабрикатів/ Г.М. Клещов. – Одеса // Під загальною редакцією доктора технічних наук, професора Л.В. Коломійця. 2010 – 283 с.

3. *Клещев Г.М.* Наскрізна комп'ютер на технологія керування підготовкою виробництва штампів ХЛШ на базі стандартизованих та уніфікованих штамп- напівфабрикатів у сільгоспвиробництві / Г.М. Клещов, Л.В. Коломієц Л.В. Сборник Международных научно-технических трудов MOTROL' 2010, Том 12 LUBLIN, Польша, 2010, С.54 – 58.

UDC 517.983:519.2:539.25:620.187:519.711.3

Ju.E. Gagarin, Ph. D. (Kaluga Branch of Bauman Moscow State Technical University, Russia,
S.A. Dvoretsky, Ph. D. (Rzhanov Institute of Physics of Semiconductors of the Siberian Branch of
the Russian Academy of Sciences, Russia),
Ju.N. Dolganin, Ph. D. (Moscow Plant "Sapphire", Russia),
V.V. Karpov, Ph. D. (Moscow Plant "Sapphire", Russia),
N.N. Mikhailov, Ph. D. (Rzhanov Institute of Physics of Semiconductors of the Siberian Branch of
the Russian Academy of Sciences, Russia),
N.N. Mikheev, Ph. D. (Branch of the Shubnikov Institute of Crystallography of the Russian Acade-
my of Sciences – the Research Center «Space Materialce Science», Russia),
A.I. Osmolovsky, Ph.D. (National Aviation University, Ukraine),
A.N. Polyakov, Ph.D. (Tsiolkovsky Kaluga State University, Russia),
M.A. Stepovich, Dr.Sci. (Tsiolkovsky Kaluga State University, Russia)

SOME ASPECTS OF MANUFACTURING AND DIAGNOSTICS OF STRUCTURES ON THE BASIS OF THE HgCdTe-SOLID SOLUTIONS INTENDED FOR USE IN PHOTODETECTORS OF INFRARED RADIATION OF 3…5 AND 8…12 MICRONS

Some results of the researches devoted to the development of technology of reception high-quality he-teroepitaxial structures HgCdTe with buffer layers from wide-gap semiconductors CdTe and ZnTe and their solid solutions for manufacturing on their basis of photodetectors for registration of infrared radiation of ranges 3…5 and 8…12 microns are described.

Introduction. Solid solutions cadmium-mercury-tellurium (CMT) are widely used for detecting infrared radiation of a range 8…12 microns. The base manufacturing techniques of such photodetectors are well fulfilled, therefore devices with parameters necessary for practical use can be produced. To a lesser degree it is known about manufacturing heteroepitaxial structures HgCdTe for registration of infrared radiation of a range 3…5 microns and use of such structures for manufacturing the two-band photoreceivers, allowing to register infrared radiation in both above-stated ranges, in particular, enables to solve various problems of air navigation [1].

One of perspective directions of reception of high-quality CMT-structures is using in photodetector structures buffer layers from wide-gap semiconductors: CdTe, ZnTe and their solid solutions, – which should provide necessary perfection of layers of the basic material [2]. In the present work some aspects of manufacturing and diagnostics of the structures with buffer layers are considered and some information about parameters of the photodetectors produced on developed technology are cited.

Manufacturing of HgCdTe-structures with buffer layers. Buffer layers from CdTe and ZnTe can be made by a method of molecular-beam epitaxy (MBE) with use of the modes corresponding to the requirements for manufacture of multielement photodetectors. The unique process of fabricating of CMT-structures by a MBE-method on substrates from GaAs and Si with buffer layers ZnTe and CdTe is developed and realized in Russia in Rzhanov Institute of Physics of Semiconductors of the Siberian Branch of the Russian Academy of Science. Studying mechanisms of formation of defects and their nature is lead by development of technology of fabricating of such structures, researches optical and electrophysical properties of the materials received on used MBE-installation are carried out. The technique of growing of epitaxial MBE-structures with change of composition of a growing layer in a real time which allows to grow up layers with the set profile on thickness of a film is developed. This technique has allowed to develop and realize measures for prevention of mercury volumetric migration. The essence of the problem is as follows. Dielectric films create areas of a volumetric charge in a working layer of the semiconductor which change electrophysical parameters of structure which is undesirable for stable work of the device [3]. Besides in multicomponent structures with Hg presence volumetric charge can stimulate formation of sites of a semiconductor material with the changed width of the forbidden zone due to change of molar composi-

tion of a structure, especially at significant thermal loadings, that also destabilizes the work of devices using them. The layers with variable width of vorbidden-gap creating an internal electric field in frontier areas of structure, allow to reduce speed of surface recombination and to limit migration of mercury to a surface [4]. However the migration of mercury does not suppress in the working narrow-gap material of such structure, and it leads to thermal instability of the material, down to the change of stehiometric composition of a solid solution and discharges of the second phase that changes electrophysical and photo-electric parameters of structure, and, finally, destabilizes the work of the devices designed on their basis.

The working layer of photosensitive structure (with defined width of the forbidden zone) alternates with intermediate layers (identical thickness) in which the width of the forbidden zone is more defined for at least 50 % for overcoming intravolumetric migration of mercury [5]. For compensation the influence of consecutive resistance of intermediate layers (at passage of current through volume of the photoresistor) the thickness of working layers is doubled in process of removal from the surface layer with variable width of vorbidden-gap (fig. 1a).
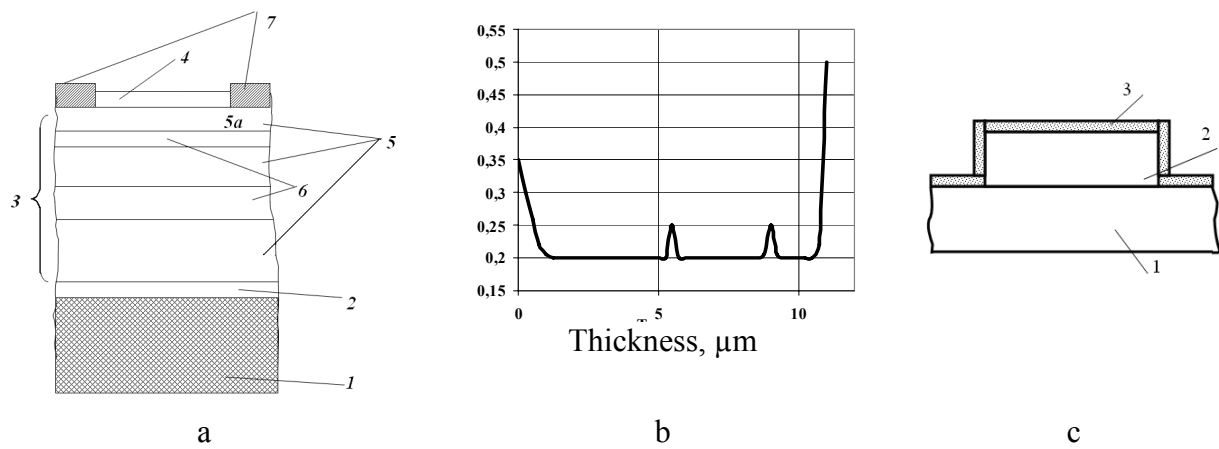
Fig. 1. The schematic image (a and c) and the information on composition (b) CMT-structures:
a – a substrate 1, boundary layer with variable width of vorbidden-gap 2, working area 3 and the surface layer with variable width of vorbidden-gap 4, working layers 5, an intermediate layers 6, contact area 7;
b – the structure of molar composition of CdTe as a function of thickness of layered structure;
c – a substrate 1, a working layer 2, a protective layer 3 made in the form of a layer of solid solution $Cd_xHg_{1-x}Te$ with variable width of vorbidden-gap.

Presence of more wide-gap intermediate layers in working area (fig. 1b) limits the migration of mercury to the surface due to embedding in structure of layers with stable crystal lattice. The use of wide-gap material also allows to realize protection of a lateral area of mesa-structure by forming the CRT-layer with variable width of vorbidden-gap on it with increased of working layer composition CdTe in relation to structure. It reduces deficiency and shunting influence of the layer disturbed by ionic bombardment, improves lateral surfaces of photosensitive structure, providing small surface currents of outflow, increase resistance and constraining leaving of mercury from the material of a working layer (fig. 1c).

Diagnostics of local parameters of wide-gap semiconductors can be carried out with use of the cathodoluminescence (CL) microscopy methods allowing in some cases to receive necessary information about the object of the research which is rather difficult or impossible to receive by the other methods.

The required estimations of parameters of the functional dependence $I = I(E_0, \Theta)$ connecting intensity I of monochromatic CL direct-gap semiconductor with electron beam energy E_0 and required parameters Θ (diffusion length of minority carriers of a charge (MCC) L, depth l_s subsurface area which has been impoverished by the majority charge carriers, the coefficient of diffu-

sion D, the coefficient of absorption α, etc.), can be found by minimization of some functional as which they often choose the sum of squares is nonviscous. Many methods used are reduced to the method of the least squares (MLS) or to its development – to the method of confluence analysis (MCA) [6] – to the iterative method, allowing to receive dot and interval estimations of parameters in view of an error both of functional dependence, and its arguments. Minimized functional in such a problem looks like this [7]:

$$F = \frac{1}{2}\sum_{i=1}^{n}\left\{\frac{\left(E_{0i} - E_0^{(i)}\right)^2}{\sigma^2(E_{0i})} + \frac{\left[I_i - I\left(E_0^{(i)}, \Theta\right)\right]^2}{\sigma^2(I_i)}\right\}.$$

Here E_{0i} and I_i – measured (at modeling – set) values of an energy of electron beam and an intensity of monochromatic CL of the semiconductor accordingly, $\sigma(E_{0i})$ and $\sigma(I_i)$ – their dispersions.

Some results of modelling are resulted on fig. 2.
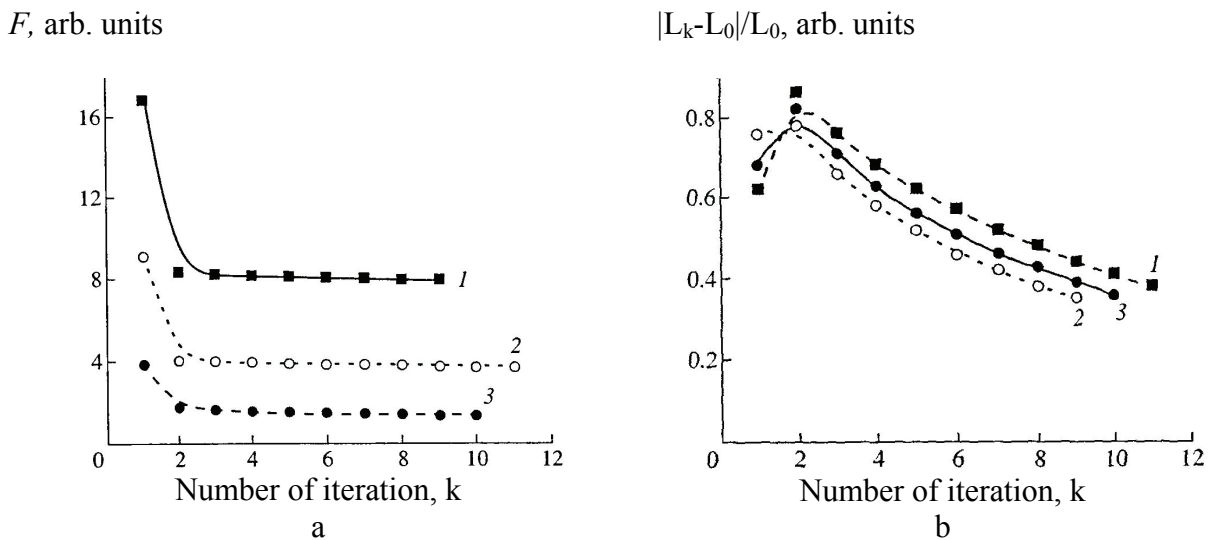
Fig. 2. Results of mathematical modelling: in the left figure – changes of value of functional F and in the right figure – changes of relative value of diffusion lengths of MCC - depending on number of steps k iterative process. The value of accuracy of measurement of electron beam energy makes: 1 – 0,2 keV; 2 – 0,3 keV; 3 – 0,5 keV.

From the received data it follows, that at $k > 2$ value of the functional F practically does not vary, while the change of diffusion lengths on each step for $2 \le k \le 10$ essential.

As a whole as show results of the lead researches, use of methods of mathematical modelling allows both to optimize conditions of carrying out of experiment, and to realize correct identification of parameters of semiconductors [7, 8].

The results of photodetectors' parameters measurements. Parameters of the photodetector produced according to the developed technology for registration of infra-red radiation of a range 3…5 micron, following:

1) a range of spectral sensitivity 1,0…5,2 microns;
2) number of photosensitive elements 5;
3) size of photosensitive elements 500×500 microns, a backlash 100 microns;
4) specific detectability in a maximum of spectral sensitivity $(5...9) \times 10^{10}\ \mathrm{W}^{-1} \times \mathrm{cm} \times \mathrm{Hz}^{1/2}$;
5) cooling – a two-cascade thermoelectric cooler;
6) a range of working ambient temperatures from -60°C up to +60°C.

The looks of the photodetector and its spectral characteristics are resulted on fig. 3 [9].
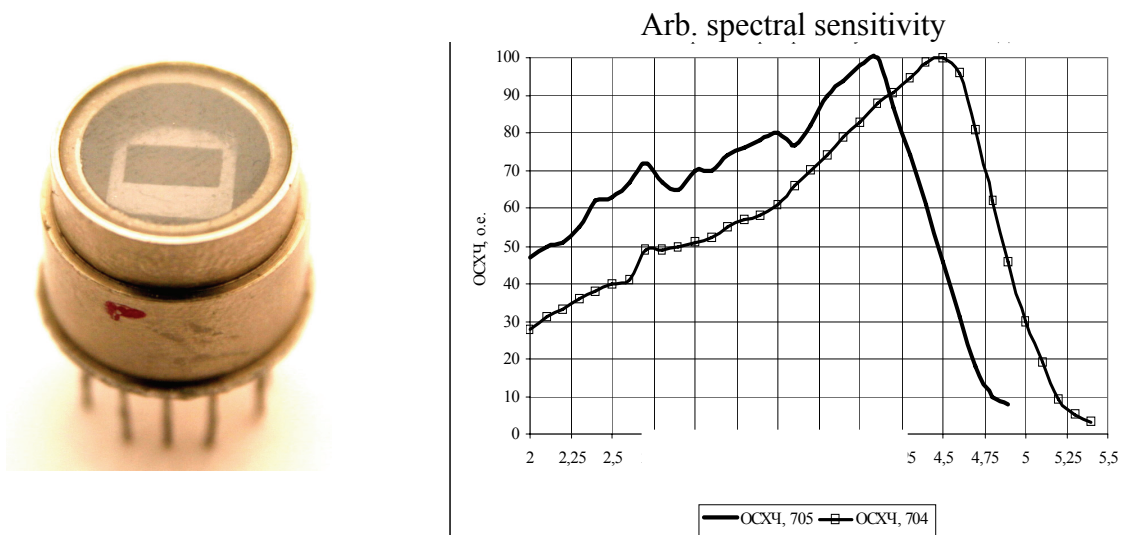
Fig. 3. The photodetector on the basis of solid solution HgCdTe and typical characteristics of its spectral sensitivity

Conclusion. The analysis of available information and the received results of experimental researches have confirmed the perspectivity of the works development, devoted to development of the reception high-quality heteroepitaxial structures HgCdTe technology with the buffer layers from wide-gap semiconductors CdTe, ZnTe and their solid solutions for creating of photodetectors on their basis for registration of infra-red radiation of ranges 3…5 and 8…12 microns.

References

1. *Filachyov A.M., Taubkin I.I., Trishenkov M.A. Modern* condition and the main directions of development of modern photoelectronics. – Moscow: Fizmatkniga, 2010. 128 p. (in Russian).

2. *Guzev A.A., Varavin V.S., Dvoretskij S.A., at al.* // Rus. J. Applied Physics. 2009. No. 2. P. 92-95. (in Russian).

3. *Nemirovsky J., Bahir G.* // J. Vac. Tecnol. A. 1989. Vol. 7. No. 2. P. 450-459.

4. *Bhan R.K. at all.* // Appl. Phys. Lett. 1996. Vol. 68. P. 2453-2458.

5. The Way of manufacturing of CdHgTe-mesa-structures. The decision on delivery of the patent under the application No. 2007116341 from 3/21/2008 Photosensitive structure. The patent of the Russian Federation No. 49361. (in Russian).

6. *Greshilov A.A, Stakun V.A., Stakun A.A.* Mathematical methods of construction of forecasts. – Moscow: Radio and Communication, 1997. 112 p. (in Russian).

7. *Gagarin Yu.E., Stepovich M.A.* // Proc. SPIE. 2004. V. 5398. P.179-185.

8. *Mikheev N.N., Polyakov A.N., Stepovich M.A.* // J. of Surface Investigation. X-ray, Synchrotron and Neutron Techniques. 2009. Vol. 3. No. 5. P.820-825.

9. *Dvoretskii S.A., Dolganin Yu.N., Karpov V.V. at all.* // J. of Surface Investigation. X-ray, Synchrotron and Neutron Techniques. 2011. Vol. 5. No. 5. P. 934-940.

UDC 621:891

S.V. Golub, Ph.D., professor, S.G. Palash, post-graduate student
(Cherkasy Bogdan Khmelnytskyi National University, Ukraine)
M.V. Michalko, vice-rector
(National Aviation University, Ukraine)

TRANSFORMATION OF A PHOTOGRAPHIC IMAGE INTO AN INPUT DATA ARRAY FOR MULTI-LAYER MODELING OF COMPLEX OBJECTS

We would like to describe the process of information transformation from an image of the photographic file into a form of the two-dimensional table of input data array necessary for synthesis of multi-layer models of complex objects. Results of this work are used as an additional source of information for modeling of complex objects.

As information technologies get more and more developed there is a numerous variety of different program means of information processing and transformation written in different programming languages. This variety emerged due to the specific features of each branch in which information processing takes place. For instance, during processing of graphic images we widely use methods of image identification. The process of information transformation presented in the form of electronic photographs provides a great number of possibilities for getting information about properties of the pictured images by means of the technology of multi-layer information transformation [1].

In any task of information transformation formation of the initial description is very important. While working with graphic images they should be brought to necessary conditions. If we consider a scheme of graphic image transformation, particularly of electronic photographs into initial description, this scheme can be presented as the one shown in Picture 1.
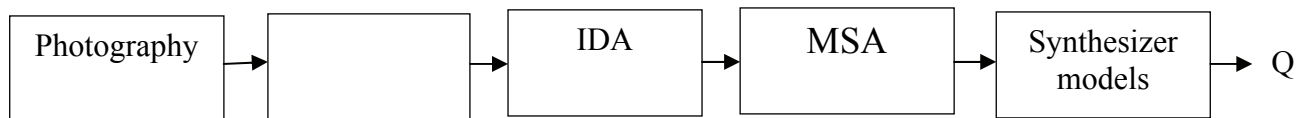
Picture 1. The scheme of transformation of a graphic image into an initial description

where ID – initial description in the form of a table with necessary data for further transformation:
IDA – input data array formed at the previous stage necessary for further modeling;
MSA – model synthesis algorithm;
Q – interpretation of transformation results.

This scheme, for instance, has been used in medicine for diagnosis of problematic features in mammograms and for forecasting of treatment results.

We took mammograms in the form of electronic pictures – a file in jpeg graphic format. Pictures were divided into windows and windows were separated into clusters. The window size was defined by the user. Observations featuring a damaged issue were identified as FRIEND. Other observations were termed as FOE. Characteristics of a definite number of clusters of the specific window formed a separate observation. Characteristics of the sequence of observations formed up an initial description of the object under observation. After transformation of graphic images of information we obtained 8602 observations for teaching.

8252 observations were used for teaching models and 348 observations were used for model testing. As a result of information transformation we got a table of the array of numerical characteristics imported in file xls format. In such a way we formed up an initial description of the object under examination for synthesis of an inductive model which is able to identify a part of the photographic picture which has pathology.

Picture 2 features modeling results
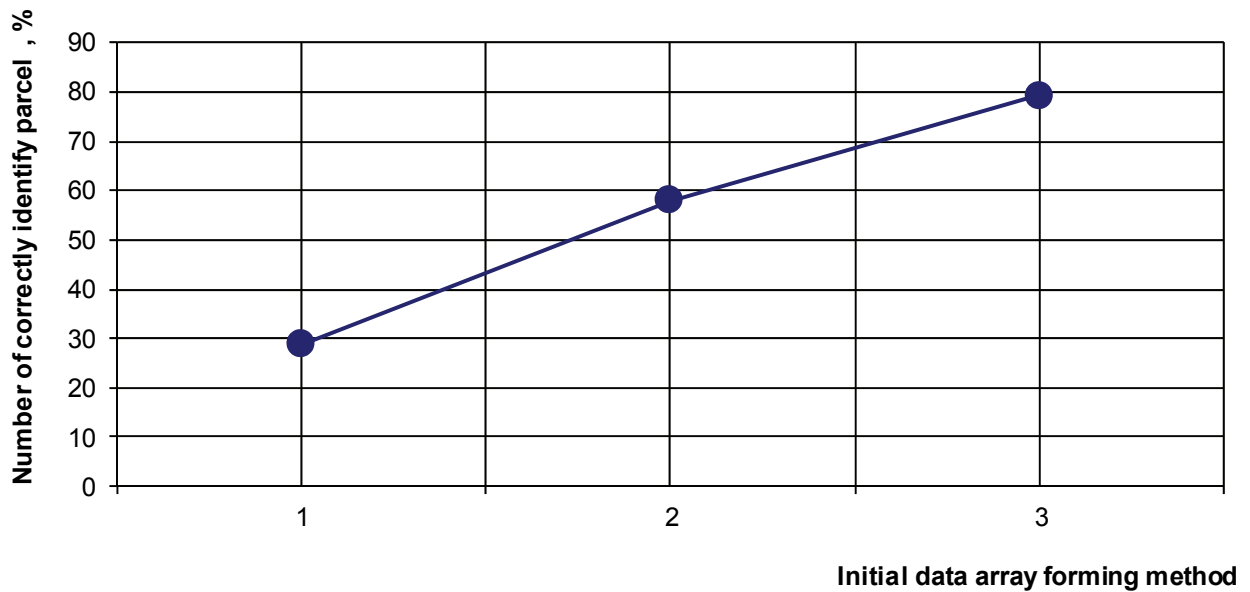
Picture 2. Initial Data Array Forming Method
Characteristics of the initial data array forming method:
1 – one-level inductive models synthesized according to multi-row algorithm element grouping me-
thod based on initial description having all cluster characteristics which form up an observation; 2 –
one-level inductive models synthesized on initial description basis after initial data processing; 3 –
two-level inductive models synthesized according to ascending element synthesis method [3] on the
basis of initial description after initial data processing.

The element group accounting method which is a multi-level information transformation pro-
cedure is used for multi-layer modeling of complex objects. this is a method of inductive modeling
and one of the most effective methods of structural and parametric identification of complex objects
processes and system as a result of observation in conditions when information is incomplete. The
element group accounting method has a variety of opportunities at all stages of the process of mod-
eling of complex systems as compared with other methods of setting up of models. it pertains first
of all model generators and quality criteria of structures used as well as model classes (basic func-
tions). this method differs from other means by active employment of the principles of automatic
generation of variants, consequent selection of models and other criteria for setting up of optimal
complex models. the element group accounting method is well known and it quickly develops both
in this country and abroad. experts developed fundamentals of the theory of structural model identi-
fication with minimum range of mistakes in forecasting. the effective means of this theory is the
critical dispersion method which for the first time gives a possibility to analytically solve the fol-
lowing tasks – comparative criteria analysis of structural identification, experiment planning and
method property analysis. in this case the conditions of selection of optimal model structure are be-
ing studied depending on dispersion (level) of noise, selection length, input influence (experiment
plan) and object parameters with close interrelation between them. the means of this theory have
established that the element group accounting method is a method of setting up of models with a
minimum range in mistakes forecasting and its effectiveness was compared with other methods. the
explanation is that the element group accounting method is the main tool of the theory of inductive
modeling and is the most modern method of computing intellect.This method is an original and ef-
fective means of solving of a wide range of problems of artificial intellect - identification and fore-
casting, image learning and clustering, information intellectual analysis and rule finding.
During last decade the interest in element group accounting method have grown throughout
the world and this is explained by the already acknowledged effectiveness of this method and by
growing popularity of the technologies of artificial neuron networks. The fact is that the structure of
the element group accounting method can be interpreted as a neuron network which can self-

organize the structure and its parameters. It appears that the advantages of the element group accounting method are the automatic setting up of the network structure, simplicity and speed of adjustment of its parameters as well as the possibility of transformation of the created network into a definite mathematic form. Neuron networks are used in medicine, particularly in diagnostics, for multi-level information transformation. They can be regarded as modern computing systems which transform information to some extent using the process images similarly to a human mind. Processed information has a numerical form permitting to use a neuron network, for instance, as a model of the object with absolutely unknown characteristics. Other standard programs of neuron networks are used to solve the tasks of image identification, classification, analysis or compression. For the sake of high output performance neuron networks are used for storage of information having numerous interlinks between elementary edges of numerous calculations. With view of getting of a necessary structure of interlinks between neurons in a neuron network a certain procedure called a teaching algorythm is used. This method differs from other methods of mathematic analysis by the fact that a task is not solved by selection of mathematic methods strictly chosen but by the repetition of deductive methods of task solution peculiar to the work of an expert.

Moreover, neuron networks can include practically the unrestricted number of factors of forecasting formation and these factors can be added to the model if an experimentator decides that new factors are useful for result improvement. This method can also be advantageous from the point of view of the level of forecasting importance and counter action of new factors with the available selection of choice. That is why this method is different from the traditional statistic methods. The peculiar feature of the method of neuron networks is that it is simpler to learn and to use the technologies of these networks than to study mathematic statistics or indefinite logic.

Conclusions

Initial processing of information transformation results permits to increase as much as twice the number of correctly identified portions of various types of mammograms. Employment of a multi-level information transformation system enables to provide the number of the correctly identified portions of mammograms to a specific accepted level. Test results showed that under research conditions this technology allows to identify correctly more than 79% of portions of various types of mammograms. So, for a multi-layer modeling of complex objects experts use more often element group accounting method as well as the method of neuron networks in order to create adequate models for further modeling and functioning of complex objects.

References

1. *Ивахненко А.Г.* Долгосрочное прогнозирование и управление сложными системами. – Киев «Техника», 1975 – 311 с.

2. *Голуб С.В.* «Багаторівневе моделювання в технологіях моніторингу оточуючого середовища». С.В.Голуб - Черкаси, Вид. від ЧНУ імені Богдана Хмельницького, 2007 – 220 ст.

UDC 004.896

R.N. Kvetny (Vinnitsa National Technical University, Ukraine),
O.V. Bisikalo (Vinnitsa National Technical University, Ukraine),
O.I. Osmolovsky (National Aviation University, Ukraine),
I.A. Kravchuk (Vinnitsa National Technical University, Ukraine)

MORPHOLOGICAL ANALYSIS OF INPUT INFORMATION IN INTELLIGENT ROBOTIC SYSTEMS

This article analyzes the construction of robotic systems with elements of artificial intelligence and processing information within such systems. A methodology for morphological analysis as a first stage of processing of natural language information is suggested.

Technological operations of control, measurement, diagnostics, which are widespread in the industry, are the most difficult to automate. Without automation of such operations a flexible manufacturing systems and automated production of a limited number of workers cannot be created. To complete the automation of entire production cycle control-measuring robotic systems are applied.

Interaction of advanced robotic systems with real external environment should be based on elements of adaptation, i.e. taking into account information on the status and position of working and processing equipment, state of the environment and objects in the working area. Such information is provided by information-measuring system that is a part of the control robot device. It is the "feelings" of a robot as a part of the work of the technical complex and it largely determines its functionality, operational efficiency and reliability, the complexity of tasks, and security staff. The robot, which has the ability to "feel" can easier to perform complex actions to adapt the performance of a wide range of tasks. This increases the degree of universality of the robot that ultimately, despite the increasing cost of their own work, leading to lower cost of production and service operation.

Structure of the robotic systems is shown in Fig. 1 [1].

The external environment
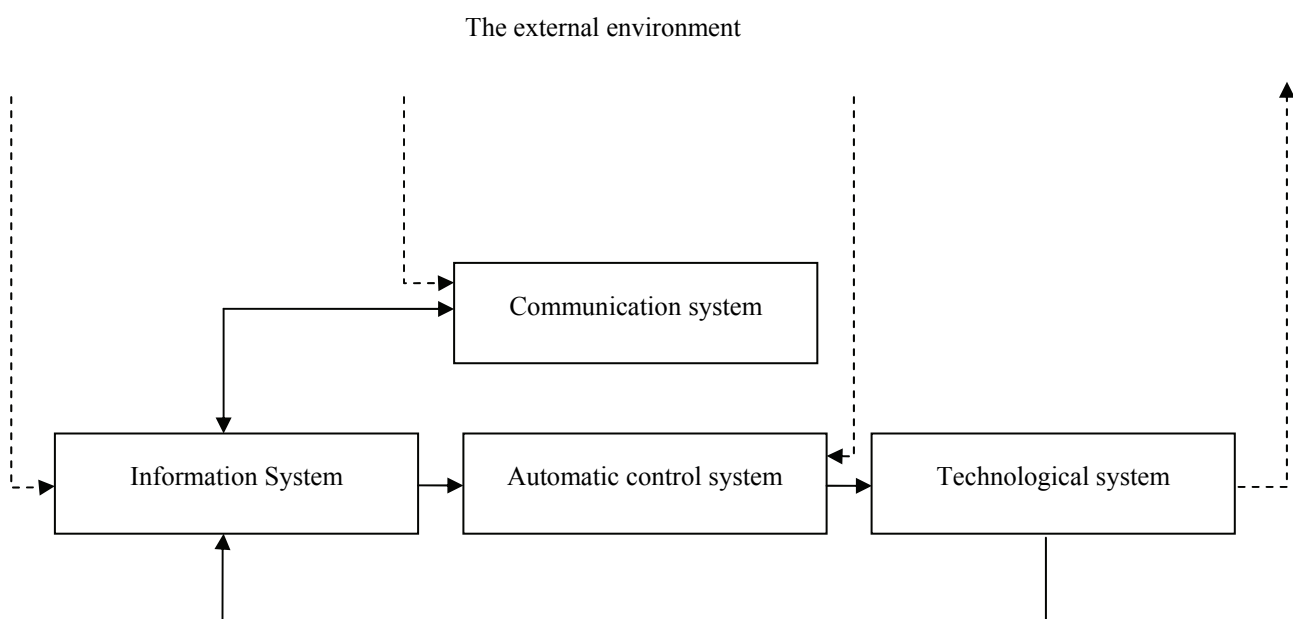
Figure 1 – Block diagram of robotic systems

Information and measurement (or sensor) system of a robot is indicated in the diagram as two parts - information system and communication system. They are designed for automatic acceptance,

collection and conversion of information about the internal state of a robot and the environment and transfer it into the management system.

Intelligent robotic systems have algorithmic and software of adaptive control systems to automate the operation of intellectual character.

Distinctive features of such systems are the availability of databases and knowledge bases of problems of interpretation and planning of solutions and algorithms for the formation of concepts, recognition of situations and decisions.

Intelligent of the robotic system is the ability of its management system to solve technological problems by intelligent character conversion signifies our strong information and knowledge, experience and training to adapt to an environment variable.

This made it possible to create an interface for communicating with the robot in natural language.

Scheme of control system intelligent robotic systems is presented in Fig. 2.
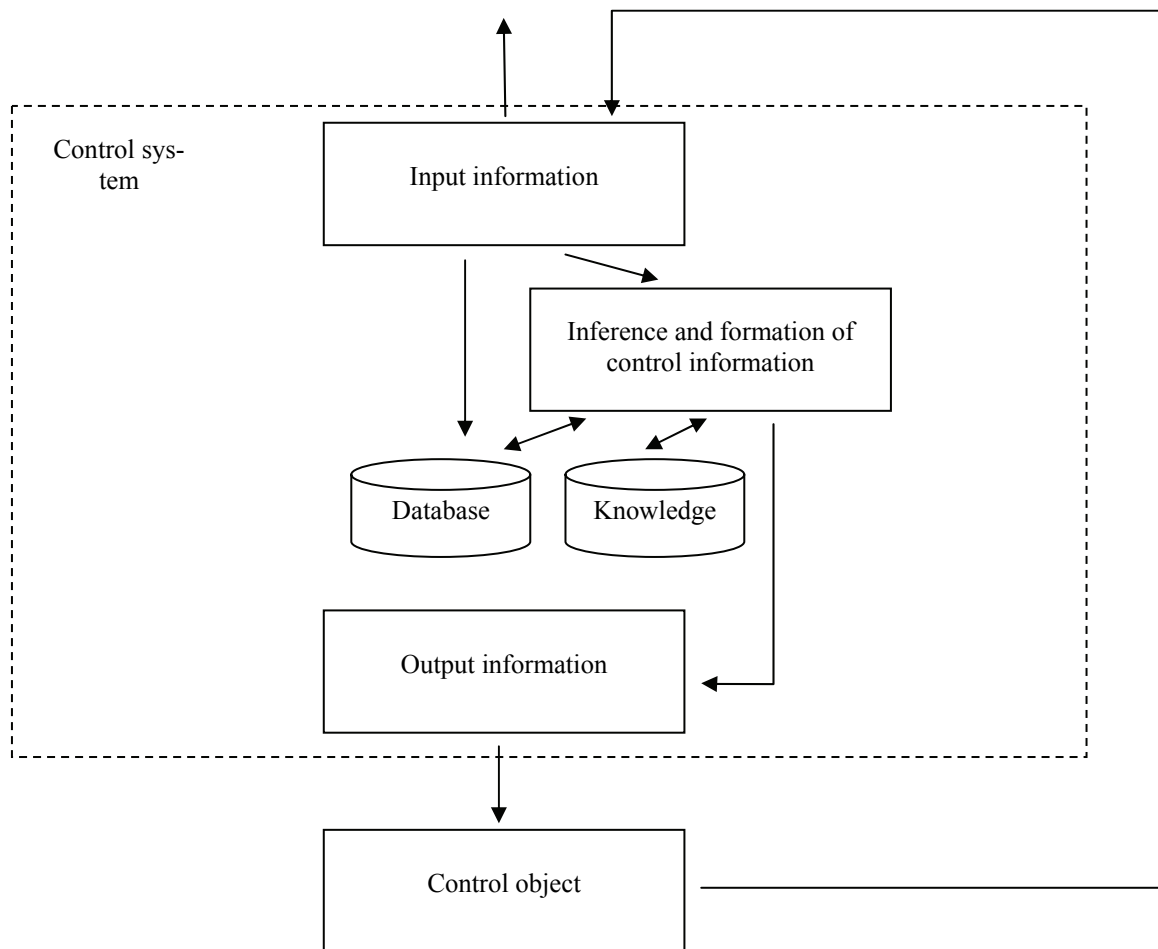
Figure 2 – Scheme of the control system

Input information may come from the user, the environment, management object. Then input information supplied to the unit inference, or directly into the database – a set of tables that store is usually character and numeric information about the objects of the domain.

Block of inference and formation of control information to find solutions to problems clearly formalized, provides action planning and formation control information to guide or control object based on the knowledge base and database. Knowledge Base is a set of knowledge, for example, the system of production rules of the laws of the domain.

Information received on the input must be linguistic processing before get into the knowledge base or database.

The first stage of linguistic processing is morphological analysis. A suggested morphologic analysis is based on associative-statistical approach to gain knowledge from natural language texts.

For the purpose of morphological analysis of linguistic patterns apply context-free grammar that recognizes words:

$$G = (V_T, V_N, S, P),\qquad(1)$$

where V_T – alphabet of terminal (main) characters (morphemes);

V_N – nonterminal alphabet characters (metavariables), and $V_T \cap V_N = \varnothing$;

S – starting symbol;

P – finite set of rules $\varphi \to \psi$, where $\varphi \in V_N$, and $\psi \in F(V)$ – arbitrary word free semi-group of words over the alphabet $F = V_T \cup V_N$.

Considered Grammar (1) generates the language L as a set $L(G)$ of all correct words in the grammar G.

A formal model of speech, is based on analysis of morphological structure of words fleksible language is:

$$w = xyz\nu\qquad(2),$$

where w – word,

x – prefix,

y – root,

z – suffix,

ν – end.

Apply the model used for modeling of speech with a prefix, suffix and the ending, although not eliminated variation of the word with multiple prefixes and / or suffixes [2]. The approach to the definition of morphemes in words with prefixes and suffixes more based on the use of statistical evaluation found morphemes, after which finally determined affixes [3].

Conclusions

Suggested method of morphological analysis is based on associative-statistical method of obtaining knowledge from natural language texts and will improve the processing of natural language information to the input control system of intelligent robotic systems.

References

1. *Nazarov H. N.* Robotic systems and complexes / *H. N. Nazarov*. – TGTU, 2004. – 102 p.

2. *Kvetny R.N.* Morphological analysis of words based on the associative-statistical approach / *R. N. Kvetny, O. V. Bisikalo, I. A. Kravchuk* // Bulletin of Cherkasy State Technological University. – 2010. – № 3. – Pp. 132 – 135.

3. *Bisikalo O. V.* The conceptual separation of morphemes algorithms for implementing information technology for processing natural language texts / *O. V. Bisikalo, I. A. Kravchuk* // Information processing systems. – 2011. – № 3. – Pp. 7 – 9.

E.N. Bezvesilnaya, D.E., prof.,
(National Technical University of Ukraine "KPI", Ukraine)
V.P. Kvasnikov, D.E., prof.,
(National Aviation University, Ukraine)
Podchashinsky Yu.A., Ph.D., dotsent,
(Zhytomyr State Technological University, Ukraine)

MEASUREMENTS OF OF LINEAR ACCELERATIONS BECAUSE OF ARTIFICIAL NEURAL NETWORK

In the article the algorithmic method of increase of accuracy of linear accelerometers is considered. In the gyroscopic accelerometer the angle of deviation of a sensing element consists of a constant and variable making. The constant making is proportional to acceleration, which is considered constant on an interval of one measurement. Variable making is determined by precessions of a sensing element. In conditions of presence of correlated distortion of determined and random character it is necessary with high accuracy to define values of a constant making. This problem is solved in the article because of method of a maximum probability. The realization of algorithm of identification of an angular rule of a sensing element because of artificial neural network is offered. This network contains a delay line and three adaptive linear neurons. The procedures of training and adaptation of a network provide additional error reduction in non-stationary and unfavorable conditions. The obtained outcomes can be used for a construction of high-precision navigational and gravimetric systems.

Introduction

For perfecting high-precision gravimetric and navigational systems the broad application of algorithmic methods of processing of measuring signals is necessary. Let's consider algorithmic methods of identification of a condition of a gyroscopic sensing element in linear accelerometers. By an outcome of an evaluation the condition is identification of an angular position and parameters of an attitude of a sensing element $\alpha(t) = \alpha_{\Pi} + \alpha_{3M}(t)$. Thus amplitude useful making α_{Π} Is considered by a constant on an interval of observation. This amplitude is proportional to linear acceleration, which is measured. The parameters variable making $\alpha_{3M}(t)$ Motion of a sensing element are necessary in further procedures of algorithmic processing for compensation of errors of an evaluation of a condition and increase accuracy of linear accelerometers.

Variable making $\alpha_{3M}(t)$ is determined by the solution of a non-linear differential equation [1]

$$\ddot{\alpha}_{3M} + 2\xi_{3M}\dot{\alpha}_{3M} + \omega_0^2 \sin\alpha_{3M} = 0,$$ (1)

where ω_0, ξ_{3M} − circular frequency and decay coefficient of precessions of a sensing element.

In case of small oscillations $\sin(\alpha_{3M}) \approx \alpha_{3M}$, and the solution of an equation (1) has a kind [1]: $\alpha_{3M}(t) = A_{3M}e^{-\xi_{3M}t}\sin(\omega_{3M}t + \varphi_{3M})$, where $\omega_{3M} = \sqrt{\omega_0^2 - \xi_{3M}^2}$, A_{3M}, φ_{3M} − amplitude and initial phase of precessions of a sensing element. If $\xi_{3M} \to 0$, mathematical model of ideal trajectory of motion of a sensing element

$$\alpha(t) = \alpha_{\Pi} + \alpha_{3M}(t), \quad \alpha_{\Pi} = const, \quad \alpha_{3M}(t) = \alpha_C \sin\omega_{3M}t + \alpha_S \cos\omega_{3M}t,$$ (2)

where $\alpha_C = A_{3M}\cos\varphi_{3M}$, $\alpha_S = A_{3M}\sin\varphi_{3M}$. In this case state vector of a sensing element, which is necessary for identifying, is equaled: $Z_\alpha = (\alpha_{\Pi}, \alpha_C, \alpha_S)^T$.

The evaluation is executed because of data processing α_i^* from the sensor of an angular position of a sensing element. Thus

$$\alpha_i^* = \alpha(t_i) + \delta_\alpha(t_i), \quad i = \overline{1,K}, \quad t_i = i \cdot \delta_\text{д}, \quad T_c = K \cdot \delta_\text{д},$$

where $\alpha(t_i)$ – value, which correspond of ideal trajectory of motion of a sensing element, $\delta_\alpha(t_i)$ – errors of the measured trajectory of motion in view of handicaps which are operational on a sensing element, and errors of the sensor of a angle, K – quantity of references, which go from the sensor of a angle and are used for an evaluation of a condition, T_c – time of observation behind a sensing element, $\delta_\text{д}$ – the interval of time between references.

Generally errors $\delta_\alpha(t_i)$ measured trajectory of motion can be correlated. It is stipulated by presence of handicaps of determined character and kinematics nonlinearities of a sensing element. For example, the operation of a harmonic handicap is stipulated by a non-stationary thermal mode of a sensing element and influence of periodic motions on frequency of oscillations of this element [1]. It is possible to consider distribution of amplitude of an error normal, proceeding from presence of a set of the factors calling these errors. Therefore it is necessary to apply a method of a maximum probability to an evaluation of a condition of a sensing element.

Identification of an angular position of a sensing element

For an evaluation of a condition of a sensing element we shall make a functional because of of method of a maximum probability [3]:

$$J(Z_\alpha) = \frac{1}{(2\pi)^{K/2}(\det(R_\alpha))^{1/2}} \cdot \exp\left(-\frac{1}{2}\Delta_\alpha^\mathrm{T} \cdot R_\alpha^{-1} \cdot \Delta_\alpha\right), \tag{3}$$

where

$$R_\alpha = \sigma_\text{ДК}^2 \cdot I_K + R_\text{чE} \tag{4}$$

– correlation matrix of errors of the measured trajectory of motion of a sensing element, $\sigma_\text{ДК}^2$ – dispersion of an error of the sensor of a angle, I_K – unit matrix by the size $K \times K$, $R_\text{чE}$ – correlation matrix of errors stipulated by an operation of correlated handicaps on a sensing element, $\Delta_\alpha = \left(\delta_\alpha(t_1),...,\delta_\alpha(t_K)\right)^\mathrm{T}$ – vector of errors of the measured trajectory of motion of a sensing element.

For simplification of further evaluations we shall pass to a log of a functional (3):

$$\ln J(Z_\alpha) = \ln\left(\frac{1}{(2\pi)^{K/2}(\det(R_\alpha))^{1/2}}\right) - \frac{1}{2}\Delta_\alpha^\mathrm{T} \cdot R_\alpha^{-1} \cdot \Delta_\alpha. \tag{5}$$

The evaluation of a maximum probability Z_α for state vector Z_α because of (5) is determined from an equation [3]

$$\frac{d(\ln J(Z_\alpha))}{dZ_\alpha} = A^T \cdot R_\alpha^{-1}\left(\alpha^* - \alpha(Z_\alpha, T)\right) = 0, \tag{6}$$

where

$$A^T = \begin{bmatrix} \dfrac{\partial\alpha(Z_\alpha, t_1)}{\partial\alpha_\Pi} & \dfrac{\partial\alpha(Z_\alpha, t_2)}{\partial\alpha_\Pi} & ... & \dfrac{\partial\alpha(Z_\alpha, t_K)}{\partial\alpha_\Pi} \\ \dfrac{\partial\alpha(Z_\alpha, t_1)}{\partial\alpha_C} & \dfrac{\partial\alpha(Z_\alpha, t_2)}{\partial\alpha_C} & ... & \dfrac{\partial\alpha(Z_\alpha, t_K)}{\partial\alpha_C} \\ \dfrac{\partial\alpha(Z_\alpha, t_1)}{\partial\alpha_S} & \dfrac{\partial\alpha(Z_\alpha, t_2)}{\partial\alpha_S} & ... & \dfrac{\partial\alpha(Z_\alpha, t_K)}{\partial\alpha_S} \end{bmatrix},$$

$\alpha^* = \left(\alpha_1^*,...,\alpha_K^*\right)^\mathrm{T}$ – vector of outcomes of measurement of trajectory of motion of a sensing element, $\alpha(Z_\alpha, T) = \left(\alpha(Z_\alpha, t_1),...,\alpha(Z_\alpha, t_K)\right)^T$ – vector of values of a angle of deviation of a sensing element calculated for mathematical model (2) because of ideal trajectory of motion in view of an

evaluation Z_α state vector, $T = (t_1, ..., t_K)^T$ – vector of instants, for which the references of the measured trajectory of motion are obtained.

In this case

$$\alpha(Z_\alpha, t_i) = \alpha_\Pi + \alpha_C \sin(\omega_{3M} t_i) + \alpha_S \cos(\omega_{3M} t_i), \tag{7}$$

$$A^T = \begin{bmatrix} 1 & 1 & ... & 1 \\ \sin(\omega_{3M}\delta_д) & \sin(2\omega_{3M}\delta_д) & ... & \sin(K\omega_{3M}\delta_д) \\ \cos(\omega_{3M}\delta_д) & \cos(2\omega_{3M}\delta_д) & ... & \cos(K\omega_{3M}\delta_д) \end{bmatrix}. \tag{8}$$

In an equation (6) return correlation matrixes of errors of the measured trajectory of motion are calculated according to (4) and numerically is equaled

$$R_\alpha^{-1} = [w_{ji}], \; i, j = \overline{1, K}. \tag{9}$$

Let's calculate an evaluation of a maximum probability for state vector of a sensing element because of (6) with the registration (7), (8) and (9):

$$\begin{cases} \alpha_\Pi \displaystyle\sum_{i=1}^{K}\sum_{j=1}^{K} w_{ji} + \alpha_C \sum_{i=1}^{K}\left(\sin(i\omega_{3M}\delta_д)\sum_{j=1}^{K} w_{ji} \right) + \\ + \alpha_S \displaystyle\sum_{i=1}^{K}\left(\cos(i\omega_{3M}\delta_д)\sum_{j=1}^{K} w_{ji} \right) = \sum_{i=1}^{K}\left(\alpha_i^* \sum_{j=1}^{K} w_{ji} \right), \\ \alpha_\Pi \displaystyle\sum_{i=1}^{K}\left(\sin(i\omega_{3M}\delta_д)\sum_{j=1}^{K} w_{ji} \right) + \alpha_C \sum_{i=1}^{K}\left(\sin^2(i\omega_{3M}\delta_д)\sum_{j=1}^{K} w_{ji} \right) + \\ + \alpha_S \displaystyle\sum_{i=1}^{K}\left(\sin(i\omega_{3M}\delta_д)\cos(i\omega_{3M}\delta_д)\sum_{j=1}^{K} w_{ji} \right) = \sum_{i=1}^{K}\left(\alpha_i^* \sin(i\omega_{3M}\delta_д)\sum_{j=1}^{K} w_{ji} \right), \\ \alpha_\Pi \displaystyle\sum_{i=1}^{K}\left(\cos(i\omega_{3M}\delta_д)\sum_{j=1}^{K} w_{ji} \right) + \alpha_C \sum_{i=1}^{K}\left(\sin(i\omega_{3M}\delta_д)\cos(i\omega_{3M}\delta_д)\sum_{j=1}^{K} w_{ji} \right) + \\ + \alpha_S \displaystyle\sum_{i=1}^{K}\left(\cos^2(i\omega_{3M}\delta_д)\sum_{j=1}^{K} w_{ji} \right) = \sum_{i=1}^{K}\left(\alpha_i^* \cos(i\omega_{3M}\delta_д)\sum_{j=1}^{K} w_{ji} \right). \end{cases} \tag{10}$$

The solution of a system (10) concerning an evaluation of state vector Z_α also is by an outcome of identification of parameters of motion of a sensing element in the linear accelerometers. This solution can be obtained because of known rules of the solution of systems of linear algebraic equations. Thus, the solution of a problem of identification because of method of a maximum probability has a kind:

$$\alpha_\Pi = \sum_{i=1}^{K} \alpha_i^* \cdot l_{\alpha\Pi,i}, \quad \alpha_C = \sum_{i=1}^{K} \alpha_i^* \cdot l_{\alpha C,i}, \quad \alpha_S = \sum_{i=1}^{K} \alpha_i^* \cdot l_{\alpha S,i}.$$

In this case for definition of state vector of a sensing element the constants factors $l_{\alpha\Pi,j}$, $l_{\alpha C,j}$, $l_{\alpha S,j}$, $j = \overline{(n-k+1), n}$ are used. These factors depend on frequency of oscillations of a sensing element ω_0, decay coefficient ξ_1, frequency $\omega = \sqrt{\omega_0^2 - \xi_1^2}$, which is used in algorithm of identification, slice of time $\delta_д$ between references acting from the sensor of a angle.

Realization of algorithm of identification because of artificial neural network

All listed values can be certain with some error and the means of measurements can vary on some interests under an operation of the various destabilizing factors while in service. All this requires adaptation and optimum set-up of parameters in algorithms of an evaluation. In an outcome the additional error of linear accelerometers, stipulated by unfavorable and non-stationary conditions of measurements decreases. The adaptation and optimum set-up of parameters of algorithm

of an evaluation can be executed during adaptation and training artificial neural network. Because of such network is offered to realize algorithms of an evaluation of a condition of the linear accelerometers. The built-in algorithms and methods of set-up of weight factors are essential advantage artificial neural network on a comparison with usual means of processing of the measuring information [4].

For an evaluation of state vector of a sensing element we shall use artificial neural network, which consists of delay lines and three adaptive linear neurons (Fig. 1). Training of such network and set-up it of weight factors we shall execute because of modifications of a method of least squares [4].
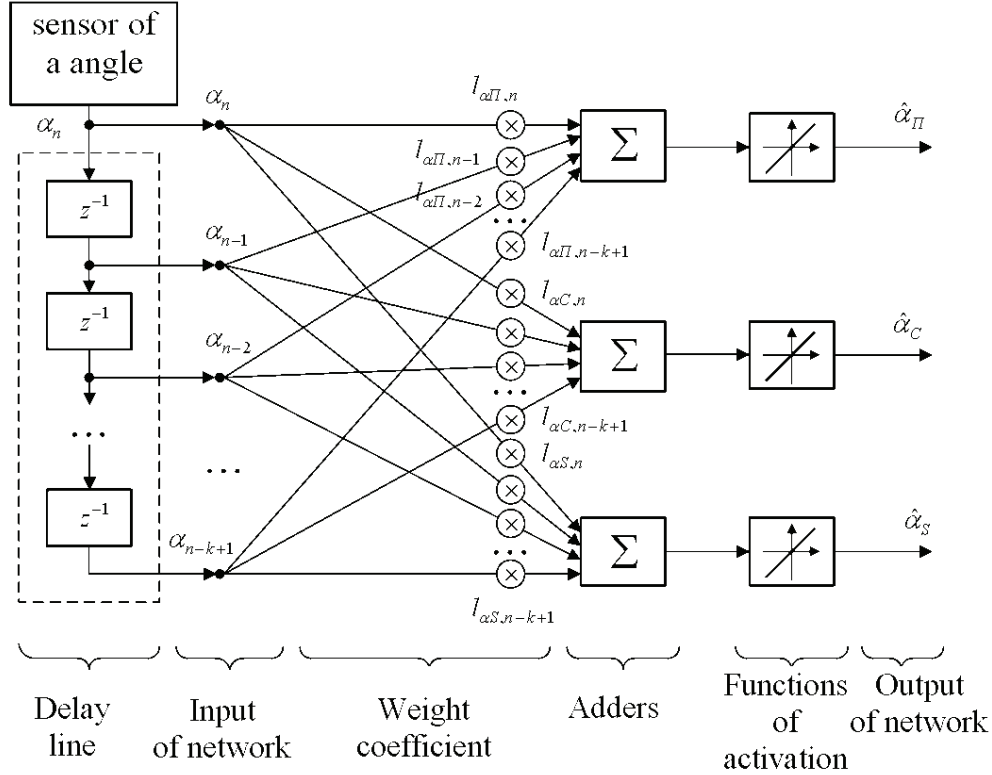
Fig. 1. Block Diagram of an evaluation of state vector of linear accelerometer
because of artificial neural network

The degree of approximation of an output signal of a network $Z_N = (\alpha_\Pi, \alpha_C, \alpha_S)^T$ to precisiouly value $Z_N = (\alpha_\Pi, \alpha_C, \alpha_S)^T$ can be appreciated by a functional of quality of activity of a network. For example, for the first output of a network this functional $J_{\alpha\Pi} = E[F(\Delta_{\alpha\Pi}(\alpha_н, \alpha_\Pi, \tilde{c}))] \to \min$, where $E[.]$ – expectation of a loss function $F(\Delta_{\alpha\Pi}) = (\Delta_{\alpha\Pi})^2$ from an error $\Delta_{\alpha\Pi} = \alpha_\Pi - \alpha_\Pi$ network. The outcome of training is optimum vector of weight factors $c^* = (l^*_{\alpha\Pi,n}, l^*_{\alpha\Pi,n-1}, ..., l^*_{\alpha\Pi,n-k+1})^T$, which minimizes a functional $J_{\alpha\Pi}$. This vector takes into account influence of the destabilizing factors and non-stationary conditions of measurements. The value $\tilde{c} = c^*$ can be obtained from an equation

$$\nabla J_{\alpha\Pi}(\tilde{c}) = E[\nabla F(\Delta_{\alpha\Pi}(\tilde{c}))] = 0.$$

Recurrent algorithm of training artificial neural network:

$$\tilde{c}(q) = \tilde{c}(q-1) - \Gamma(q) \cdot \nabla F(\Delta_{\alpha\Pi}(\alpha_{н\Pi}, \alpha_\Pi, \tilde{c}(q-1)), \tilde{c}(q-1)), \qquad (11)$$

where $q = \overline{1, N_{навч}}$ – number of a step of recurrent algorithm of training because of signal $\alpha_{н\Pi}$, $N_{навч}$ – duration of a procedure of training (total of steps), $\Gamma(q)$ – matrix of amplification, which determines speed of a procedure of training,

$$\frac{\partial F}{\partial l_{\alpha\Pi,n}} = \frac{\partial(\Delta^2_{\alpha\Pi})}{\partial l_{\alpha\Pi,n}} = -2\alpha_{\text{н},r}\left(\alpha_{\text{н}\Pi} - \sum_{j=n-k+1}^{n}\alpha_{\text{н},j}l_{\alpha\Pi,j}\right) = -2\alpha_{\text{н},r}\left(\alpha_{\text{н}\Pi} - \alpha_{\Pi}\right). \tag{12}$$

Because of (12) and (11) is obtained:

$$\widetilde{c}(q) = \widetilde{c}(q-1) + \Gamma(q)\cdot 2\alpha_{\text{н},r}\cdot\left(\alpha_{\text{н}\Pi} - \alpha_{\Pi}\right), \tag{13}$$

Because of (13) is obtained a resultant expression for an evaluation of weight factors of neurons in learning process:

$$\widetilde{l}_{\alpha\Pi,j}(q) = \widetilde{l}_{\alpha\Pi,j}(q-1) + 2\alpha_{\text{н},r}\cdot\left(\alpha_{\text{н}\Pi} - \alpha_{\Pi}\right)\cdot\gamma_{\text{н}}/\|\alpha_{\text{н}}\|,$$

$$\widetilde{l}_{\alpha C,j}(q) = \widetilde{l}_{\alpha C,j}(q-1) + 2\alpha_{\text{н},r}\cdot\left(\alpha_{\text{н}C} - \alpha_{C}\right)\cdot\gamma_{\text{н}}/\|\alpha_{\text{н}}\|,$$

$$\widetilde{l}_{\alpha S,j}(q) = \widetilde{l}_{\alpha S,j}(q-1) + 2\alpha_{\text{н},r}\cdot\left(\alpha_{\text{н}S} - \alpha_{S}\right)\cdot\gamma_{\text{н}}/\|\alpha_{\text{н}}\|,$$

where $\|\alpha_{\text{н}}\| = \alpha_{\text{н}}^{\mathrm{T}}\cdot\alpha_{\text{н}}$ – Euclidean norm of vector of references of a test signal on an input of a network.

Indication of the ending of a procedure of training is the fulfillment of conditions

$$\alpha_{\text{н}\Pi} - \alpha_{\text{н}\Pi}(q) \le \varepsilon_{\alpha\Pi}, \ \alpha_{\text{н}C} - \alpha_{\text{н}C}(q) \le \varepsilon_{\alpha C}, \ \alpha_{\text{н}S} - \alpha_{\text{н}S}(q) \le \varepsilon_{\alpha S}, \tag{14}$$

where $\varepsilon_{\alpha\Pi}, \varepsilon_{\alpha C}, \varepsilon_{\alpha S}$ – allowed values of an error of an evaluation of state vector for the linear accelerometer (error of an output artificial neural network). Let's consider, that $\varepsilon_{\alpha\Pi} = \varepsilon_{\alpha C} = \varepsilon_{\alpha S}$. Then for mathematical model (2) the root-mean-square value of an error of a signal $\alpha(t)$, stipulated by errors (14), is equaled $\sigma_{\alpha} = \varepsilon_{\alpha\Pi}/\sqrt{3} \le \sigma_{\text{ДК}}/3$, where $\sigma_{\text{ДК}}$ – root-mean-square value of an error of the sensor of a angle. From here

$$\alpha_{\text{н}\Pi} - \alpha_{\text{н}\Pi}(q) \le \sigma_{\text{ДК}}/\sqrt{3}, \ \alpha_{\text{н}C} - \alpha_{\text{н}C}(q) \le \sigma_{\text{ДК}}/\sqrt{3}, \ \alpha_{\text{н}S} - \alpha_{\text{н}S}(q) \le \sigma_{\text{ДК}}/\sqrt{3}.$$

These ratios determine the ending of a procedure of training artificial neural network. These ratios also guaranteeing theoretically calculated accuracy of assessments of state vector for the linear accelerometer in unfavorable and non-stationary conditions of measurements.

Conclusions

The algorithmic method of increase of accuracy of linear accelerometers is considered. In conditions of presence of correlated distortion of determined and random character it is necessary with high accuracy to define values of a constant making. This problem is solved in the article because of method of a maximum probability.

The realization of algorithm of identification of an angular rule of a sensing element because of artificial neural network is offered. This network contains a delay line and three adaptive linear neurons. The procedures of training and adaptation of a network provide additional error reduction in non-stationary and unfavorable conditions.

The obtained outcomes can be used for a construction of high-precision navigational and gravimetric systems.

References

1. *Безвесільна О. М.* Авіаційні гравіметричні системи та гравіметри : підручник / *О. М. Безвесільна*. – Житомир : ЖДТУ, 2007. – 604 с.

2. *Синицын И. Н.* Фильтры Калмана и Пугачева : учебное пособие / *И. Н. Синицын*. – М. : Университетская книга ; Логос, 2006. – 640 с.

3. *Кузьмин С. З.* Основы теории цифровой обработки радиолокационной информации / *С. З. Кузьмин*. – М. : Советское радио, 1974. – 432 с.

4. *Руденко О. Г.* Штучні нейронні мережі : навчальний посібник / *О. Г. Руденко, Є. В. Бодянський*. – Харків : ТОВ "Компанія СМІТ", 2006. – 404 с.

A.N. Sirotenko, V.V. Kovalchuk, G.V. Trushkov (Military Academy, Odessa, Ukraine)
V.M. Ilchenko, candidate of technical science (National Aviation University, Ukraine)

CONFINEMENT AND OPTICAL PROPERTIES OF THE STRUCTURE AS ELEMENTS OF THE ROBOT

In this paper, we have discussed in detail the theoretical results using local functional density method in parameterized modification of silicon clusters. One of the main conclusions is that the comparison between theory and experiments shows the possibility of different radiative channels for the recombination in porous silicon.

Motivation of the study. Research into semiconductor clusters is focused on the properties of quantum dots (QD) - fragments of semiconductor (for example, Si) consisting of some to hundreds of atoms - with the bulk bonding geometry and with surface states eliminated by enclosure. QD exhibit strongly size-dependent optical and electrical properties [1-3]. Two peculiar characteristics of semiconductors influence the ways in which we think of an ideal semiconductor cluster, which is often called a QD. First, it is important to realize that in any material, substantial variation of fundamental electrical and optical properties with reduced size will be observed when the electronic energy level spacing exceeds the temperature. In semiconductors, this transition occurs for a given temperature at a relatively large size compared to metals, insulators, or molecular crystals.

The luminescence observed for por-Si raises an interesting problem related to the possibility of using Si in optoelectronics [2]. One likely explanation is *quantum confinement*, induced by the formation of nanocrystallites, whose effect is to break partially the optical selection rules and allow the material to luminesce.

The most striking property of semiconductor nanocrysials is the massive change in optical properties as a function of size. As size is reduced, the electronic excitations shift to higher energy, and the oscillator strength is concentrated into just a few transitions. These basic physical phenomena of *quantum confinement* arise as a result of changes in the density of electronic states and can be understood by considering the relation between position and momentum in free and confined particles. For a free particle, or a particle in the periodic potential of an extended solid, the energy and the crystal momentum can both be precisely defined, whereas the position cannot. For a localized particle, the energy may still be well defined, but the uncertainty in position decreases, so that momentum is no longer well defined.

For example, the kinetic stability of tetrasilatetrahedrane (Si_4H_4), hexasilaprismane (Si_6H_6) and octasilacubane (Si_8H_8) depends strongly on the steric bulkiness of the substituents (matrix). The silyl-substituted Si_nY_m ($Y=t-Bu$) is stable in an inert atmosphere, but is oxidized in air to give colourless solids. The 1,1,2-trimethylpropyl-substituted Si_nY_m ($Y=C\,Me_2 CH\,Me_2$) is very stable even in air and survives for two weeks in the solid state. The prismanes with Si and Ge skeletons are yellow to orange. These prismanes have absorptions tailing into the visible region. So, Si_6H_6 has an absorption band with a maximum at 241 *nm* tailing to *ca* 500 *nm*. The absorption band of Ge_6Y_6 ($Y=2,6-i-Pr_2 C_6 H_3$) has a maximum at 261 *nm*, which is red-shifted compared to that of Ge_6Y_6 because of the higher-lying orbitals of the Ge-Ge bonds [4].

The discrete energy eigenfunctions of the particle may then be viewed as superpositions of bulk momentum states. Given the relation between energy and momentum in the bulk solid, one can see how a series of nearby transitions occurring at slightly different energies in the bulk be compressed by quantum confinement into a single, intense transition in a QD.

The experimental data reveal a more complex situation probably characteristic of several radiative channels. Our main aim of this paper is to review the relevant theoretical information in order to identify radiative channels.

Calculations of quantum confinement effect. A number of calculations have been performed over the last few years, as for quantum dots as for silicon clusters since both possibilities

have been invoked for porous silicon. They essentially belong to four classes: effective mass approximation (EMA), empirical tight binding (ETB), empirical pseudopotential (EPS) and finally ab initio local density functional theory (LDFT).

In Fig. 1 we give the predicted band gaps versus size as obtained from LDFT calculations compiled in Ref. [5] for hydrogen-terminated Si-clusters, wires and slabs.
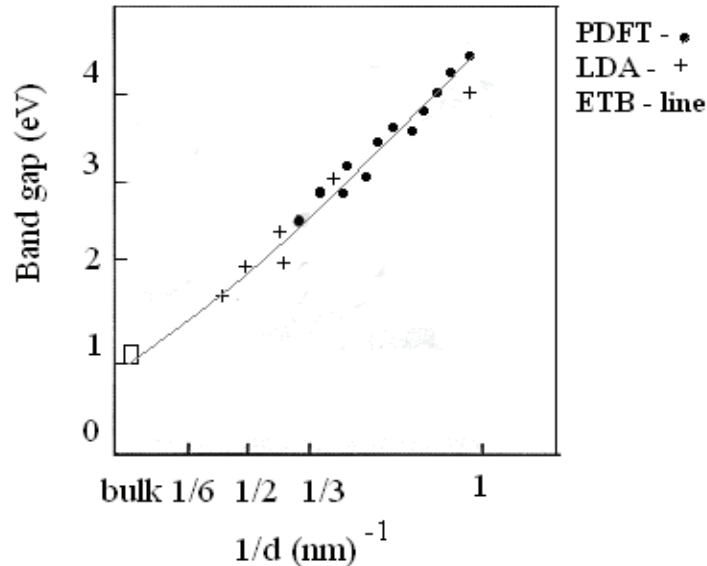
Fig. 1. Energy gap versus confinement parameter 1/d for hydrogen-terminated Si clusters
($d = a(0,75\ N\pi)^{1/3}$ for clusters, $d = a(0,75\ N\pi)^{1/2}$ for wires; $a = 0.54$ nm and N is the number
of Si atoms in the unit cell).

They are compared to the results obtained in our group using DFT approach with parameters (PDFT [3]) providing an extremely good fit to the bulk band structure. One can notice a good agreement between the LDFT and PDFT predictions which gives some confidence into the reliability of these theoretical values. At this stage it is important to notice that the LDFT gap values include a rigid shift of 0,6 eV since it is known that LDFT underestimates the bulk band gap by this amount. Note that the theoretical calculation grossly overestimate the blueshift.

They must then be discarded since EMA can be considered as an approximation to the best ETB or EPS descriptions which match the effective masses. One can, however, wonder why parameterized techniques should provide quantitative estimates of the one-electron gap. The basic point is that they are based on the postulate of transferability of the parameters from the known bulk band structure (to which they are fitted) to the unknown crystallite case. If this is accepted, then an essential criterion by which a particular semi-empirical model can be judged is how well it describes the bulk band structure. So from Fig. 1 we could conclude that PDFT as well as corrected LDA techniques are likely to give reliable predictions for crystallites.

Channels for the radiative recombination. Fig. 2 presents a compilation of data showing that observed luminescence energies on porous silicon or silicon nanocrystals in an oxide matrix are consistently lower that the predicted optical gaps of Fig. 1. On the other hand, they qualitatively agree with optical absorption data. Recent results also show that the luminescence of fresh porous silicon samples is subject to a large red shift when it is exposed to air and when the average size of the nanocrystals is smaller than 3 nm (Fig 3). On the other hand, recent luminescence measurements on silicon crystals obtained by silane decomposition are in good agreement with theory, but the luminescence is only observed for the largest crystallites. The situation is thus complex, even if it seems that the degree of oxidation of the samples plays an important role in the recombination mechanisms. All these results suggest that other channels for the radiative recombination are possible. Large Stokes shifts might be consistent with the eventual existence of deep luminescent centers. The problem is that nothing is presently known regarding the nature and origin of these states. Both from PDFT and LDA calculations that such states indeed exist under the form of self-trapped exci-

tons, most probably at the surface. A possible situation is the trapping of an exciton on a Si-Si bond of a surface dimer whose dangling bonds are saturated by hydrogen atoms. We have found another interesting situation with very small crystals, containing less than about 50 silicon atoms, where we systematically obtain a large atomic relaxation in the excited state which induces an important reorganization of the bonds in the cluster. The consequence is a large Stokes shift between the absorption and the emission energies. Therefore, small nanocrystals could play a role in the luminescence of porous silicon.
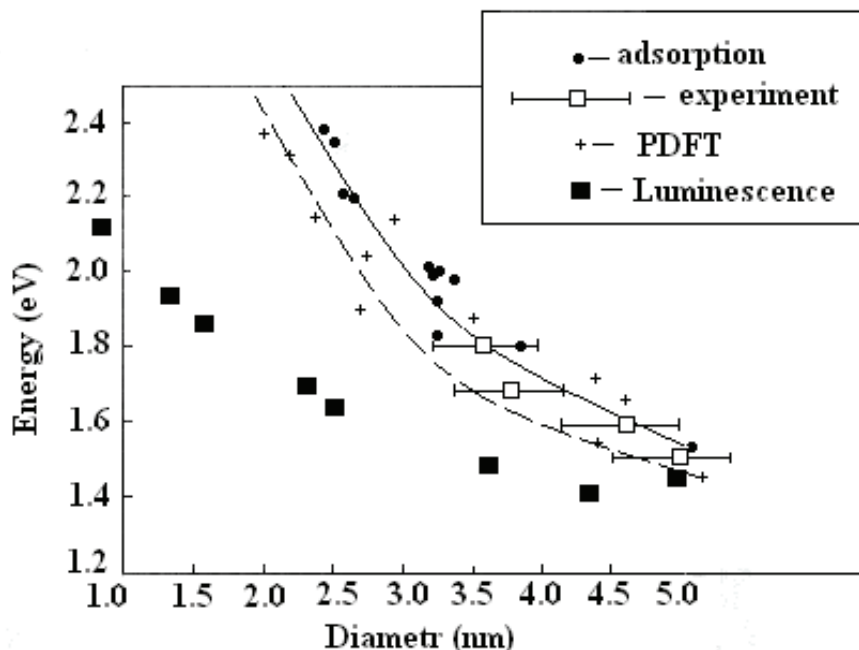
Fig. 2. Compilation of optical band gaps of silicon crystallites and porous silicon samples obtained from optical absorption and luminescence (filled symbols and also the more experimental results of B.Kohn group with error bars). Dashed and continuous lines: calculated values with and without the excitonic correction.

We are presently investigating the possible existence of defect states in the band gap induced by the oxidation of the surface. Among different systems that we have studied, preliminary results show that an oxygen atom doubly bonded to a silicon atom (Si=O) at a nanocrystal surface is a good candidate to be involved in the luminescence of porous silicon. It gives rise to a deep level below the conduction band minimum which could explain the evolution with size of the luminescence peak in Fig. 3.
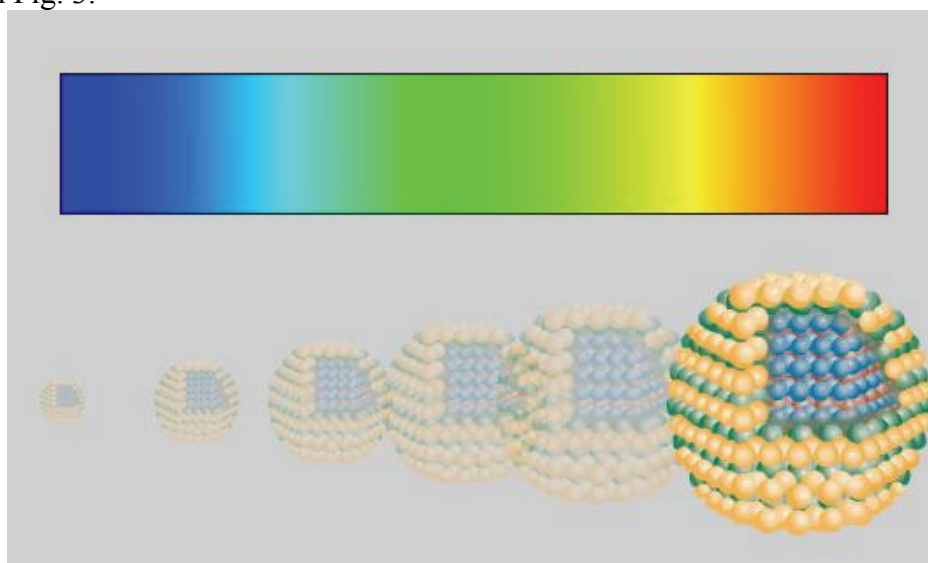
Fig. 3. Illustration of the large red shift for ball-like clusters

Structural dependence of the band gap. G. Allan with coworker's shows that the radiative recombination rate in spherical silicon nanocrystals (calculated as in Ref. [4]). It is low and it decreases for smaller band gap because of the indirect bulk band gap. In this regard, it would be of interest to use a direct gap phase of silicon such as Si-III (BC8) or to use materials like SiGe alloys or amorphous silicon because the disorder breaks the selection rules. But an essential question arises about the existence of quantum confinement effects in disordered materials. Here we describe recent results that we have obtained on these problems.

The Si-III (BC-8) crystal phase is obtained for *t* bulk samples by releasing the pressure on the high-pressure *betta-tin* phase (Si-II) [**5**]. Existing theoretical calculations show that the valence band maximum and the conduction band minimum occur at the same H point in the Brillouin zone. BC-8 silicon is thus a direct gap material but the calculations conclude that it is close to a zero gap semiconductor. To calculate the electronic structure of BC-8 crystallites with size in the 1-3 nm range, we have chosen the same non-orthogonal ETB technique as used for silicon crystallites with the diamond structure but we have developed a specific parameterization for that structure.

Our results show that the confinement effect is quite similar for BC-8 and diamond clusters. The only difference when one goes from the BC-8 cluster to the diamond one with the same size comes from the bulk gap value which simply shifts the cluster gap energy. We have also performed PDFT calculations. One can see that the values calculated with PDFT for two small clusters and shifted by 0.6 eV to take into account the underestimation of the bulk gap, are in very good agreement with our ETB calculation. This confirms the transfer-ability of the ETB parameters from the bulk material to clusters.

Experimentally, it was shown [2, 6, 7] than the BC-8 structure is obtained upon release of a high pressure on porous silicon. But the luminescence band remains practically unchanged except perhaps for a small shift (of order 0.1 - 0.2 eV) after release of the pressure. This finding completely disagrees with our predictions, where this redshift should amount to ~ 1 eV for crystallites of the same size. This would rule out quantum confinement as the origin of the observed luminescence band and favor other possibilities.

We compare the variation of the recombination rate as a function of the cluster gap for the BC-8 [**5**] and the diamond structures [8]. Because it has a direct bulk band gap, the recombination rate in the BC-8 phase remains constant and pretty high) when the cluster size increases and the blue shift decreases. It is of the order of a few ms^{-1} (*i.e.* more then 10^3 times larger than in the diamond phase below 2 eV), but remains however lower than the result for GaAs (~ ns^{-1}) which is also a direct gap semiconductor. However, the luminescence yield must be strongly improved for the BC-8 structure compared to the diamond structure.

With improved optical properties compared to silicon, Si_xGe_{1-x} alloys are also interesting materials. We have studied the strong confinement effects in SiGe clusters performing ETB calculations with the parameters. We consider spherical clusters passivated by hydrogen atom where the atomic sites are occupied randomly by Si or Ge atoms following the composition *x*. Our results shows that the band gaps of $Si_{0.8}Ge_{0.2}$ and Si clusters are quite close, with comparable blue-shift. This is due to the fact that the electronic states in bulk SiGe alloys are still delocalized, so they experience the full confinement effect as for crystalline Si (c-Si).

We now analyze the case of stronger disorder as obtained in amorphous silicon (a-Si). It raises extremely interesting problems related to the confinement induced blue shift of the energy gap: (a) does it exist in clusters of a-Si and is it comparable to what is obtained for c-Si; (b) what is the behavior of disorder-induced localized states in this regard. It has been often assumed that quantum confinements effects are small in a-Si nanostructures due to the short coherence length of free carriers in these materials. We will see that it is not true.

We calculate the electronic structure of a-Si and a-Si:H spherical clusters using the ETB and PDFT model. The interaction parameters are limited to first-nearest neighbors and the usual d^{-2} Harrison law can be used to calculate their variation with interatomic distance *d*. The starting structure for the a-Si or a-Si: H clusters is obtained by selecting the atoms belonging to the respective atoms

unit cell. Due to the new boundary conditions the structure is no more in equilibrium and we have thus relaxed the atomic positions using a Keating potential.

A generally accepted picture of the electronic structure of a-Si is that it is still composed of valence and conduction bands separated by an energy gap but with bandtails of defect or disorder-induced localized states extending into the gap. For what follows we find it useful to classify the electronic states into three categories: delocalized states, experiencing the full confinement effect as for c-Si;   strongly localized states with extension in space much smaller than the cluster diameter and energies deep in the gap, insensitive to the confinement effect and showing no blue shift; weakly localized states with extension in space of the order of the cluster diameter and energies near the gap limits, subject to an intermediate blue shift.

To characterize the luminescence of our a-Si clusters with 1-2.5 nm size we have first computed their fundamental gap, i.e. the distance in energy between the HOMO (highest occupied molecular orbital) and the LUMO (lowest unoccupied molecular orbital). There is a substantial blue shift in both cases, more important for a-Si than for a-Si:H. Furthermore, our larger a-Si clusters give rise to a two-peak distribution. We have checked that the lower and upper peaks are, respectively, due to strongly and weakly localized or delocalized states. The relative intensity of the upper peak thus corresponds to the proportion of clusters which do not contain strongly localized states. The apparent blue shift in a-Si clusters has thus two origins: (a) the varying proportion of clusters with strongly localized states and (b) the normal confinement effect on the other states. This is confirmed on the sapie figure by the a-Si: H clusters which show only the second type of behavior.

Thus we have discussed in detail the theoretical calculations on the band gap of Si clusters. One of the main conclusions is that the comparison between theory and experiments shows the possibility of different radiative channels for the recombination in porous silicon which is a complex material.

References

1.   *Drozdov V.A., Kovalchuk V.V.* Electronic processes in nanostructures with silicon sub-phase // J.of Phys.Studies.-2003.-v.4, № 7.-p.393-401.

2.   *Chen X., Zhao J., Wang G., Shen X.* The effect of size distributions of Si nanoclusters on photoluminescence from ensembles of Si nanoclusters // Phys. Lett. A.-1999.-v.212.-p.285-289

3.   *Kovalchuk V.V., Drozdov V.A., Moiseev L.M., Osipenko O.V.* Quantum Confinement and Optical Properties of Clusters // Photoelectronics.-2007.-№ 16. -P.3-6

4.   *Delerue C., Allan G., Lannoo M.* Optical band gap of Si nanoclusters// J. Lum.- 1999.-v.80.-p.65-73.

5.   *Kovalchuk V.V.* The optical properties, stability and reactivity of solid nanocluster sub-system // Photoelectronics.-2011.-№ 20.- p.53-58

6.   *Pavesi L., Dal Negro L., Mazzoleni C., Franzo G., Priolo F.* Optical gain in silicon nano-crystals // Nature. –2000. - v.408.- p.440-444

7.   *Kanzawa Y., Kageyama, Takeoka S., Fujii M., Hayashi S., Yamamoto K.* Size-dependent near-infrared photoluminescence spectra of Si nanocrystal embedded in SiO_2 matrices // Sol.St.Com.- 2007.- v.102.- p.533-537

8.   *Marsen B., Lonfat M., Scheiier P., Sattler K.* The energy gap of pristine silicon clusters // J.Electr.Sp.Rel. Ph. - 2000. - v.109. - p.157-168

V.V. Kovalchuk, O.V. Afanas'eva, V.O. Rats (Military Academy, Odessa, Ukraine)
M.V. Michalko, vice-rector (National Aviation University, Ukraine)

NANOPARTICLE'S MORPHOLOGY FOR THE ROBOT INTELECTUAL SYSTEMS

It is proposed that polyhedral nanocluster are "bricks" of core of the nanometers particles. A parameterisation density functional theory scheme for calculations of atomic and electronic structure of these clusters is presented. The accuracy of the method is illustrated by the results of calculations for robot intelectual systems with nanometer sizes.

In recent years, optical properties of silicon nano structures (Si-NS) have been the subject of intense investigations, because the quantum confinement of electrons and holes leads to linear and non-linear optical properties, much different from those of bulk crystals. Besides, optical data indicated the existence of nanoclusters (NC) in films and was mediated by the localized electronic states associated with the clusters. In particular, there were observed peculiar Raman spectra in Si-SiO_2 systems, being different from those of bulk c-Si, a-Si, and micro - crystalline Si, but very similar to the density of state spectra of Si_{33} and Si_{45} [1]. The experimental data strongly suggest that these films are the systems of AC much smaller than about 2 *nm* embedded in SiO_x matrices. Although the size and size distribution of the clusters are not known, introduction of various size of clusters randomly into SiO_2 thin films may generate localized electronic states. If these previous results are taken into account, it is rather straightforward to attribute the presently observed $\ln \sigma$ (σ-conductivity) versus $T^{-1/4}$ (T - temperature) behaviour to the VRH (variable range hopping) conduction through the localized electronic states associated with the C, Si, and Ge clusters. As the Si concentration increases, the slopes *(B)* of $\ln \sigma$ versus $T^{-1/4}$ straight lines decrease. Since the increases in the Si concentration lead to the increases in the size and/or number of Si - NC, the decreases in *B* may be attributed to the increase in the size and/or number of Si - NC. Thus optical data indicated the existence of clusters in the films, the present VRH conduction was thought to be mediated by the localized electronic states associated with the clusters.

In the other hand, small Si-NC are the subjects of intense study in the hope that their properties can provide new insight to the physical and chemical behaviour of the nanodimensional materials [2,3]. Probably, the Si-NS consists from Si-NC structures. The large surface-to-volume ratio and the large step and defect density are expected small Si-NC to be highly reactive. Moreover, the flexibility afforded by the small number of atoms could give rise to novel structures, which can possibly lead to the synthesis of artificial materials with uncommon properties.

In this paper a new approach to the study of Si-NCS consists small and intermediate-size Si-NC is proposed as the components of the robot intelectual systems.

The nature of the Si-NS and reconstruction of Si-NC in the range size $1 < n \leq 100$ (n is a number of atoms in NC) remains open to intense debate too. Si-NC is a small piece of the nature in the range of nanometers and is not molecule, and it can not to represent itself as the bulk material also. For example, Chelikowsky J.R. and Phillips J.C. [see ref. 1] has suggested that the small Si-AC was metallic rather than covalent in nature. This is due to of their physical size. Clusters of covalently bound non-metals usually have more open geometries that satisfy the specific highly-directional bonding requirements of silicon and germanium. Si-AC form prolate structures up to $n \approx 25 \div 35$, but then rearrange to more polyhedral morphologies. In fact the Si-AC appears to be more closely related to the high-pressure metallic phases of bulk silicon than to the diamond structure. These works appears to define metallic clusters as those, which have bond angles of 60°.

The absorption spectra from 0,94-5,58 eV are obtained for gas-phase neutral Si-NC containing 18-41 atoms. The spectra of all clusters are essentially identical. The optical signature of these clusters has much in common with that of c-Si. These spectra are unexpected: theoretical calculations predict a wide variation in structure over the size range, but experimentally a Si-NC has numerous strong sharp absorption which does not shift in energy over Si-NC size range. Furthermore,

the partial spectra of Si-NC are smaller than Si_{18} and larger than Si_{41}. The spectral signature common to Si_{18} - Si_{41} persists for sizes up to at least 70 atoms. This spectral similarity is completely unexpected. Because of a molecular point of view, these clusters span a sufficiently large size range to have structural differences, which should show up in their optical spectra.

From these data follows that Si-NC in this size range are expected to undergo rapid structural change because of the large surface/volume atom ratio. Nonetheless, major changes occur in the geometric structures of Si-NC as a function of size below 50 atoms. Such changes are mirrored in the photoelectron spectra measured for Si-NC anions containing 3-12 atoms [3]. Structural differences of Si-NC (similar size range) for positively charged NC have also been inferred from mobility and chemical reactivity data [1]. Thus, the electronic spectra of neutral Si-NC larger than Si_{18} do not any show evidence for any structural changes. This leads us to conclude that all of these small silicon clusters share one or more common structural entities. One possibility is that small Si-NC shares a common bonding network, which persists and extends as the cluster grows in size.

Yet, the absorption spectrum of crystalline silicon has much in common with the silicon cluster spectra. Strong absorption features at energies above 3 eV dominate both Si-NC and c-Si spectra. The 800 K bulk spectrum, which is red shifted by the thermal expansion of the lattice, more closely corresponds to the cluster spectrum. Nonetheless, a number of discrepancies between the bulk and cluster spectrum should still be explained. For instance, the cluster spectrum has six peaks between 3,0 and 5,6 eV whereas the bulk spectrum contains only three features. Furthermore, a comparison with the 800 K bulk spectrum neglects effects of lattice contraction and quantum confinement which are known for Si-NS and these characteristics do not change as a function of NC size range.

Given that Si-NC containing only few tens of atoms are too small to have either band structures or bulk excitations, the similarity of their optical signature to crystalline silicon is unexpected. Moreover, these spectra are far more similar to the spectrum of the most stable crystalline form of Si than to the spectra of other Si forms.

These experimental and theoretical data showing the spectral regularity of Si-NC challenge all known theoretical models, which used for the construction of the space structures in the size range $10 < n \leq 100$. This leads to the intriguing conclusion that silicon clusters containing tens of atoms are derived from a common structural entity. We do not know the nature of this entity but its spectral similarities to the bulk crystalline spectrum provide a proving ground for further theoretical investigation. However, this is not optimal practical procedure for cluster with larger sizes: for a system with many degrees of freedom, the problem of identifying the lowest-energy configuration becomes computationally difficult and depends on the sizes of clusters. Si-NC with size range $10 < n \leq 100$ requires to search the possible new calculation schemes. In addition to this, in order to elucidate the properties of their NC, the development of different specific models has the great importance.

These facts became the motivation of our computer researches. To attack this problem we investigated electronic and geometry structures of Si-NC theoretically using parameterised density-functional theory (DFT) [1-3].

The use of only a few parameters minimises the effort for the determination of the parameters, it yields a close relation to full ab initio DFT schemes (for example, GAMESS [1]). This is guarantee of the good "transferability" of the parameters, going from one system to another. On the other hand, the use of some approximations in connection with a few empirical parameters makes the scheme computation extremely fast. PDFT allows also the study of dynamical processes through the coupling with molecular dynamics (MD).

The calculated geometry of the clusters is in good agreement with results from corresponding DFT ab initio calculations, provided using GAMESS algorithm. The nearest neighbour distances in Si lattice are obtained correctly. The energetic positions and equilibrium distances of high-pressure modifications of silicon are described rather well.

In the next step, the Si-NS was constructed. For inter Si-polyhedral clusters (Si-PC) interaction the pairwise additive approximation (PAA) [2] was used. The calculation analyses of Si-PC,

which has spherical symmetry, were performed. Formally, the total energy of an ensemble of N Si-AC can be written as:

$$E_N = \sum_{i<j}^{N} E_{ij}(r_{ij}, \Omega_{ij}) + \sum_{i<j<k}^{N} E_{ijk}(r_{ij}, r_{ik}, r_{jk}, \Omega_{ijk}) + \dots ,$$

$$+ \dots \sum_{i<j<k<l}^{N} E_{ijkl}(r_{ij}, r_{ik}, r_{il}, r_{jk}, r_{jl}, r_{lk}, \Omega_{ijkl}) + \dots . \tag{1}$$

where the first term is the sum of all two-body (pair, E_{ij}) interactions (each as function of the separation r_{ij} and relative orientation Ω_{ij} of the two "ball"). The three-body term E_{ijk} provides the difference between the actual energy for a trio of Si-PC in a given orientation and the sum of the three pair potential terms; similarly, E_{ijkl} is the corresponding correction to give the correct energy for a quartet of "ball"; and so on. For the system which consist of the Si-PC, the pairwise additive approximation by only using the first term in this expansion was used. NS consists of Si-PC with an average diameter d (as shown in **Fig.1**). For choice of a potential (E_{ij}, E_{ijk}) in stick and ball model may be recommend.

stucture	geometry	calculation scheme
NDSP *particle*		
N S *surface structure*		PAA
Polyhedral Si-AC		MD PDFT MIEHT-α

Fig.1 [1]
Nanocluster as a blocks of the nanodimensional structure

Summary

We have tested the modified DFT scheme to the total energy of a complicated atomic geometry, which included some useful simplicity. Due to the neglect of all three-centre integrals and the use of a short-range repulsive interaction potential in the energy calculations, the method is computationally extremely fast. It gives reliable results for geometry's, binding energies and vibration frequencies for different NC. The method is applied to the building of the Si-NS from the Si-surface "blocks" reconstructed as planar. The bond lengths and angles are obtained with an error less than 5%.

Three important reconstruction steps have been considered: 1) the isolated Si-cyclic NC (with 5-, 6- and 7-atoms), 2) the Si-PC which consists from Si-cyclic NC, and 3) the cluster model of Si-NS. We found reasonable agreement of the different structures for the $i-$fold Si-NC rings per sur-

face elementary cell. However, there are also characteristic discrepancies with respect to the order of magnitude for several effects and quantities: buckling amplitude and bond length in the chain, relaxation in the first and second atomic layer, bond angles. But these problems will be argued in the following publications

The PDFT scheme may be viewed as a "hybrid" between pure ab initio method - based on DFT - and the use of purely empirical potentials. It has the advantage over the latter in overcoming the "transferability" problem, and it requires much less computational effort than full "ab initio" methods. And even in comparison to traditional TB schemes, which are computationally as fast as our method, the transferability is much better, since only very few parameters are used and their determination is straightforward.

References

1. *Kovalchuk V.V.* Cluster Modification of the semiconductor hetrostructure. - Kiev: Hi-Tech Press, 2007.-309 p.

2. *Rinnen K.-D., Mandich M.L.* Spectroscopy of neutral silicon clusters, Si_{18}-Si_{41}: Spectra are remarkably size independent // Phys.Rev.Lett. - 2002. - **v.69**. - P.1823-1826

3. *Kovalchuk V.V., Hrabovskiy O.V., Chizhikov Yu.S.*The optical properties of the clusters at the solid state matrix // Photoelectronics.- 2010.-№ 19. – P.22-25

UDC 681.518:681.3.08

Yuriy D. Zhukov, D.E., Prof., Boris N. Gordeev, D.E., Alexey V. Zivenko, postgraduate
(National Shipbuilding University, Nikolaev, Ukraine)
V.M. Ilchenko, candidate of technical science (National Aviation University, Ukraine)

POLYMETRIC METHOD OF OPERATIONAL CONTROL OF QUALITATIVE AND QUANTITATIVE CHARACTERISTICS OF AVIATION FUELS

A complex fuel quality/quantity control method has been developed. Industrial application of developed method to control the quantity and quality of aviation fuels is proposed.

Modern aircraft require high quality standards for fuel. As specified by safety rules, fuel quality parameters are checked at each stage of fuel's existence – from production through distribution and consumption process in the air. Quantity control is also important, as it comprises the amount and weight of fuel both on the ground and in the air. As we can see, fuel quality/quantity control is a very important task and a highly topical issue.

The most important aviation fuel quality parameters are: detonation resistance, fractional composition and chemical stability [1]. Detonation resistance characterizes fuel's usability in engines with high compression ratios without the possibility of explosive combustion and hence without the risk of excess shock load on pistons and cylinder head overheating, and it is characterized by octane number. Fractional composition affects fuel's volatility and therefore reflects its ability to produce air-fuel mixture. Chemical stability characterizes its ability to retain its chemical composition during storage, transportation and usage. The most important jet fuel quality parameters are the mass/volumetric heat of combustion, thermostability, saturated vapor pressure, negative temperature viscosity and density [1]. Nowadays, measuring any of these characteristics is technically difficult and requires specific tools and equipment with different principles of operation [2]. Complex estimation, which implies combined measurement of quality/quantity characteristics, is better suited for operating control. This is possible in cases whereby highly informative and approachable methods of measurement are used.

The purpose of this work is to develop a method of operative industrial quantity/quality control for aviation fuels.

Let us consider control procedures for quality/quantity parameters of various fuel types at the stage of distribution at the airport or at the storage/distribution facility. Once fuel is brought to a storage unit, which is usually located at a distance from the airport, it is tested with expensive high end equipment provided by the storage laboratory. To avoid errors, selection of several samples of fuel and independent tests for each sample are made and then it is stored in huge storage tanks. There are various types of tanks intended for various types of fuel, which differ in size and structure, equipment for level measurement, leak and overflow detection.

Then the fuel is pumped or shipped to the airport's distribution base and there it is stored in smaller tanks. It is absolutely imperative that the fuel is operatively checked for impurities and water before flight.

Distribution facilities with a large number of tanks intended for different types of fuel require a huge fleet of fuel quality control equipment, including complex machinery not intended for operative quality evaluation. In order to promptly receive information about the quality of fuels, special high speed measurement tools and methods must be used to speed up the perception of fuel quality. Although such methods and equipment cannot replace the well-known state standart established methods, but they can operatively obtain information about fuel's compliance with regulatory requirements and as a result - suggest that this sample of fuel must be lab-tested. These methods are applied to define the most important (informative) parameters, which can be used to determine fuel quality within a short period of time.

The authors have developed an pulse polimetry measurement method, which helps to promptly evaluate the amount of fuel in a tank with high precision and provides a complex estimate

of fuel quality parameters.

In general, polymetric measurements is the process of obtaining the values of several (> = 2) measured values characterizing the state of the controllable object at the current time, via a highly informative signal received from one specialized sensor. The impulse polymetry method consists in:

– generation of the special shape pulses;
– probing of generated pulses in a special transmission line (n-wire);
– receiving and initial processing of the polymetric signal;
– interpretation of the received signal to determine the values of the measured characteristics.

According to the developed method special low power pulse (duration $10^{-12}...10^{-9}$ sec, voltage amplitude 1V) is probed to the object (controlled media) through a contact sensor - a long line (transmission line or measuring line). Passing the object and interacting with its inner discontinuities (changes of wave impedance) impulse can be partially or completely reflected. In case of partial impulses reflection, it creates refracted impulse which continues to pass further in the object. The delay time between probed and reflected pulses defines level of the controllable liquid (amount of liquid in the tank).

The complex spectrums calculated on the polymetric signals carry information about quality characteristics of the fuel. This creates an opportunity for operative quality/quantity analysis of fuels.

Here is a brief presentation of fuels quality/quantity evaluation algorithm based on the method described above. Figure 1 shows a typical polymetric signal when sensor is partly immersed into controllable liquid, which represents the dependence of voltage U_i expressed in analog-digital conversion units at the times $t_i = i \cdot \Delta t$ (nanoseconds), where i stands for the time step number, Δt stands for time sampling interval.
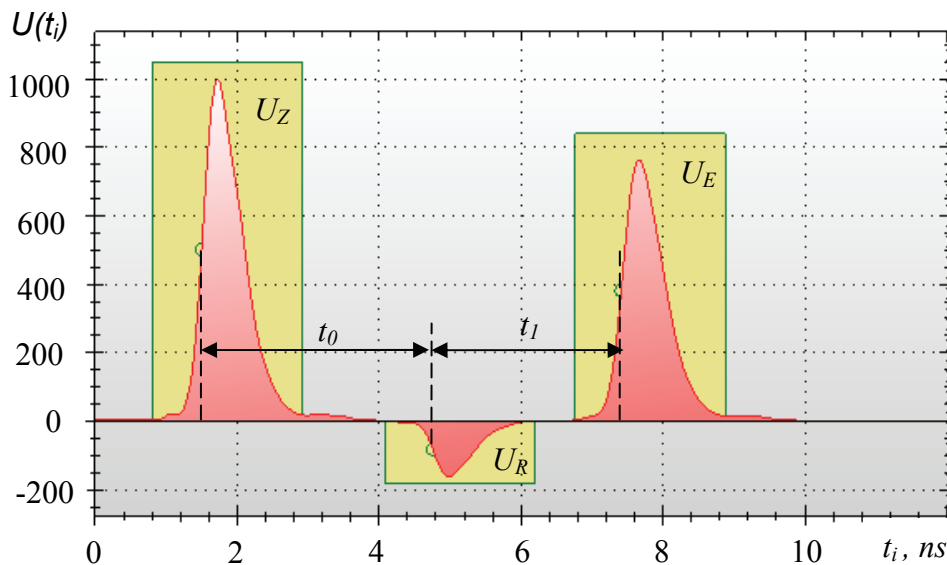
Fig. 1. Typical polymetric signal corresponding the situation when sensor is partly immersed into controllable liquid. U_Z – main pulse; U_R – pulse reflected from fuel; U_E – pulse reflected from the end of the measurement line; t_0 – time delay between points of of U_Z and U_R pulses (half of a max amplitude values); t_1 – time delay between points of U_R and U_E pulses (half of a max amplitude values).

Processing of such signal in time and frequency domains gives the information about temporal parameters, dispersion and reflection coefficients, which characterize electrophysical properties of fuels. The complex reflection coefficient $G(\omega)$ is defined according to the frequency spectrums of the probed $U_Z(\omega)$ and reflected $U_R(\omega)$ pulses:

$$G(\omega) = \frac{U_O(\omega)}{U_Z(\omega)}.$$

Simultaneously, the reflection coefficient is related to the dielectric permittivity spectrum $\varepsilon(\omega)$ through the following equation [5]:

$$G(\omega) = \frac{1 - \sqrt{\varepsilon(\omega)}}{1 + \sqrt{\varepsilon(\omega)}}.$$

It should be noted, there is another method of evaluation of permittivity frequency spectrum [6], which is more relevant to use because it takes into account reflected and transmitted waves.

The main advantage of this method over the other ones is that the sought-for fuel quality parameter are functionally related with several operatively evaluated from signal parameters (complex dielectric permittivat at different frequencies, amplitudes of reflected pulses, delays between reflected pulses, etc.). Combined use of operatively evaluated spectral and temporal parameters q allows to correctly calculate basic fuel quality parameter Q. The fuel quality parameter Q is related to several operatively evaluated from signal parameters q through generalized functional dependence [7]:

$$Q = F[q_1, q_2, \ldots q_n],$$

where q_j ($j=1,2..n$) stands for a set of n operatively evaluated from signal parameters.

Generally, there is no information about this dependence for various kinds of fuels. The main purpose of calibration is estimation of this function. Calibration is a group of processes: selection of fuels samples with known quality parameters and composition of sample database, determination of the informative parameters in time and frequency domains and estimation of unknown function (3) . Increasing the amount of samples in database and use of appropriate classification algorithms leads to more accurate and reliable measurements.

These measurements are provided by the SADKO™ system, which uses impulse polimetry techniques.

Conclusions. Described measurement method enables operative evaluation of fuel quantity/quality parameters without using complex equipment. Use of the set of evaluated from polymetric signal parameters ensures higher precision and reliability of fuel quality measurements. Instrumentation based on described measurement technique is flexible and can be used at stationary or mobile objects, with various types of media (including aggressive) and various types of tanks.

References

1. Авиация: Энциклопедия [Текст] / Гл. ред. Г.П. Свищев //— М.: Науч. изд-во «Большая росийская энциклопедия» : Центральный аэрогидродинамический институт им. Н.Е. Жуковского, 1994. — 736 с.:ил.

2. *Скворцов, Б. В.* Приборы и системы контроля качества углеводородных топлив [Текст] / Б.В. Скворцов, Н.Е. Конюхов, В.Н. Астахов.// - М.: Энергоатомиздат, 2000. –264 с.

3. *Гордеев, Б. Н.* Развитие теории и практическое применение компьютеризированных полиметрических систем оперативного контроля количественных и качественных характеристик жидких сред (энергоносителей) [Текст] дис. докт. техн. наук: 05.13.05: защ. 29.03.2011; утв. 11.11.2011 / Гордеев Борис Николаевич. – К., 2011. – 422с.

4. *Жуков, Ю. Д.* Теория полиметрических измерений [Текст] // Инновации в судостроении и океанотехнике. Материалы первой международной научно-технической конференции. – Николаев : НУК, 2010. – С. 387–389.

5. *Глебович, Г. В.* Исследование объектов с помощью пикосекундных импульсов [Текст] / Г.В. Глебович, А.В. Андриянов и др. // - М.: Радио и связь, 1984. – 256 с.

6. *Зивенко, А. В.* Оперативная оценка спектра диэлектрической проницаемости в полиметрических системах [Електронний ресурс] / Ю. Д. Жуков, Б. Н. Гордеев, А. В. Зивенко // Електронне видання «Вісник Національного університету кораблебудування». – Миколаїв : НУК, 2010. – № 2. – Режим доступу – http://ev.nuos.edu.ua.

7. *Зивенко, А. В.* Алгоритм калибровки полиметрической системы на основе спектров элктрофизических параметров жидких сред [Текст] / Б.Н. Гордеев, А.В. Зивенко // Зб. наук. праць Національного університету кораблебудування им. адм. Макарова. – 2010. – № 2 (431). – С. 112 – 117.

UDC 531.7

L.O. Borkovsjka, cand.tech.sci., O.V Borkovskiy, assistant
(National Aviation University, Kyiv, Ukraine)

QUALITY CONTROL PROCESSES IN COMPUTERIZED ROBOTIC VISION SYSTEMS

In modern industrial assembly and quality control processes, that provides one of the crucial factors for the competitiveness of industry in general, there is a strong need for advanced robot-based object detection and recognition, object grasping and for the capability to perform assembling operations in non-structured environments with randomly positioned objects. Vision-based robotic assembly and quality control systems, which have been a topic of continued research interest for almost four decades, have now matured to a point where they can be effectively applied to advanced robot-based assembly and quality control tasks.

As advanced robotic systems are becoming more popular and widespread in many industrial assembly settings, the need for reliable operation with the least possible amount of downtime is a common, expected demand. Traditional assembly robots are programmed to pick up a part from the exact same location every time and if the part is even slightly out of the place, the robot will fail to pick that part. Significant advantages can be realized when these robots are coupled with vision systems.

Modern robot vision configurations with advanced recognition systems are used more often in later time to adjust the coordinates from where the robot expected to find the object to where it actually is located. This can be achieved with using only a single camera, multiple cameras or different combination systems. Cameras, computer and software work together with the robot to adjust the robot's position, allowing retrieval of the part. One of the examples in this direction is the continued improvements to 3D robot vision. The advances in 3D vision have made robots adept at recognizing a changing environment and adapting to it. This flexibility has allowed robots to work on projects that lack precise consistency, something that was very difficult for a robot to do in the past. Nowadays, robotic vision research is expanding into many new areas. Robots can now pick variously shaped objects from an indexing conveyor, eliminating the need for part designated in-feed systems and machines

Many current vision systems require extensive support from trained experts and are less reliable due to their complexity. This is the main reason why a fundamental step change to simplify the programming and mechanical complexity of robotic guidance applications is necessary. An innovative vision scheme is only half the battle. Mechanical reliability also plays an important role.

Implementation of robot vision in assembly and quality control processes is a multilayer problem and demands therefore expert knowledge, experiences, innovations and most often a problem specific solution. Usually, the procedure of the planning and development of a process of an assembly, inspection and measurement equipment using machine vision is split into precise determination of tasks and goals like detection, recognition, grasping, handling, measurement, fault detection, etc. and into machine vision component selection and working conditions determination like camera, computer, lenses and optics, illumination, position determination, etc. With regard to the automatic assembly part handling, robotic handling and assembly systems offer good prospects for the rationalization and flexibilisation of assembly and quality control processes.

Machine vision will certainly help take robot based assembly to the next level, and machine vision will probably be a part of the next generation safety solution. Off-the-shelf products already offer work cell protection based on 360-degree vision technology, and more robot controllers now come with built-in machine vision capability.

Industrial assembly is a part of the production process (figure 1) and can be defined as an ordered sequence of physical handling tasks in which discrete parts and components are brought together and joined or mated to form a specified configuration. Assembly is a production process operation that provides a crucial factor for the competitiveness of industry in general. It is surprising,

that such an important manufacturing process, that can take up to 30% of the manufacturing cost of an end product (Rowland & Lee, 1995), is still mainly performed by hand. Manual assembly becomes expensive, if high levels of quality are to be achieved, because it involves highly skilled human laborers. Also much verification and inspection is needed to compensate for potential human insufficiencies. Manual assembly is often difficult, tedious and time consuming.

Figure 1. Production process of the computerized robotic vision system

Robot or machine vision is the application of computer vision to industry and manufacturing, mainly in robots. As computer vision is mainly focused on machine-based image processing, robot vision most often requires also digital input/output devices and computer networks to control other manufacturing equipment such as robotic arms. Specific advantages of robot vision systems include precision, consistency, cost effectiveness and flexibility.

In a robot vision system, a variety of components are included. The systems layout mainly depends on factors like the environment, the application and the budget. Nevertheless, there are several common ingredients to all vision systems. A typical robot or machine vision system for assembly tasks consists of several of the following components:

- ✓ one or more digital or analogue cameras (black-and-white or color) with suitable optics for acquiring images;
- ✓ a camera interface for digitizing images (frame grabber) – depends on the application;
- ✓ a processor (often a PC or embedded processor, such as a DSP) – when processors and frame grabbers are integrated into the camera itself, such cameras are called "smart cameras";
- ✓ input/Output hardware or communication links;
- ✓ optics - lenses to focus the desired field of view onto the image sensor;
- ✓ light source (LED, fluorescent or halogen lamps etc.);
- ✓ a program to process images and detect relevant features;
- ✓ a synchronizing sensor for part detection to trigger image acquisition and processing;
- ✓ actuators to sort or reject the processed parts.

Digital technology has some significant advantages in comparison to the analog one: digital image-processing systems allow significantly better image quality, up to 12-bit dynamic range, the camera's parameters can be set using software, the camera's availability, as well as its properties, can be maintained remotely, upgrading the camera in the field is easily achieved etc.

In the computerized robotic vision system a vision recognition system aims to mimic the human sense of vision and must be capable of perceiving and detecting assembly parts as good as the humans can. Three-dimensional object recognition entails representation of a 3-D object, identification of the object from its image, estimation of its position and orientation and registration of multiple views of the object for automatic model construction. Important stages in the design and development of a recognition system
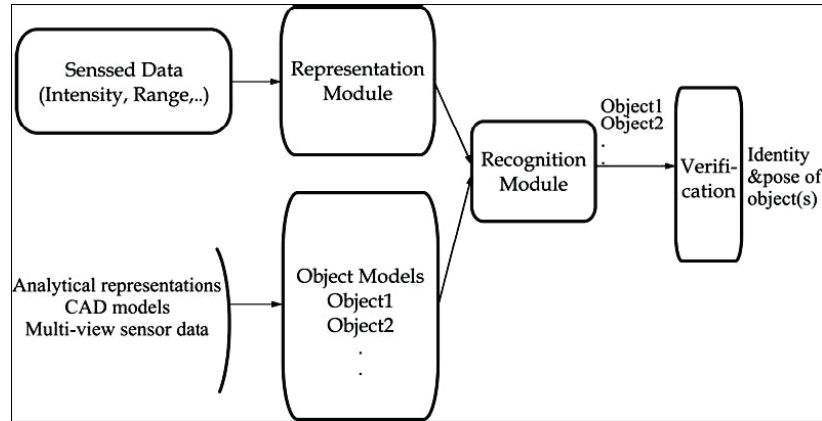
Figure 2. Recognition system of the computerized robotic vision system

A typical approach for handling the object recognition tasks using traditional image processing and computer vision methods usually consists of five steps:

- ✓ Detection or pre-processing – is the low level signal processing which extracts information from the scene and represents it as some form of primitive symbols;
- ✓ Grouping or segmentation – is based on the low level symbols, the primitive features are grouped into higher order features, which give more information for the selection and matching in the next steps;
- ✓ Indexing or feature extraction – selecting from the stable object features the most likely model from a library of models (model base) and finding a way of quickly comparing a set of features with a model, avoiding a search through all models. As a critical component, a stable, representative feature extraction system should be developed to extract key features for a specific problem domain in the feature extraction stage. The result of feature extraction is normally a feature vector. There is usually one of two methods of representation applied:
    - appearance-based approach – information about appearance of the object is used;
    - model-based methods – information about geometrical features, type and spatial relations of the object is used.
- ✓ Matching or classification – finding the best fitting between the scene features and the model features and solving the localization problem. In this stage, a classifier system uses extracted key features to distinguish the classes of the objects of interest. The algorithms or methods for these stages are generally domain dependent, particularly when using traditional image processing and computer vision techniques;
- ✓ Verification – verifying the estimated identity and location of an object.

In many assembly processes, the control process is still undertaken by the operators. They are capable of making an estimation and judgment about the accuracy and shape faults of a product or part using their acquired skills for quick and accurate decisions based on the human vision system. These tasks are usually complex and the accuracy and speed depend on the operator's psychological and physical condition. The consequences are unreliable results and a very serious possibility of overlooking faults. The reliability of human decisions is also reduced by the monotony of the task and by tiredness.

Today's robot vision and identification systems are more and more reliable and robust, and therefore convenient for industrial applications and are becoming indispensable to the assembly or

disassembly process Control systems, based on robot vision, are capable of maintaining a control process even more efficiently than a human if the conditions for an appropriate use of the technical benefits of robot vision are ensured.

Inspection, measurement and fault detection, has to be a robust and very reliable system. For this reason, the development of measurement equipment using robot vision has to follow a fixed procedure. Usually, the procedure is split into a precise determination of tasks (measuring, fault detection) and goals, into the robot vision selection and working conditions (illumination and position determination), component selection of the robot vision (camera, computer, lenses and optics), and finally, the development of an automatic robot handling system for the parts.

When using a robot vision system for fault detection and dimension control, lighting is always a critical component and should be treated as one of the first steps of component selection. The effectiveness of an illuminating source in an inspection and fault detection process is determined by the direction at which light strikes an object and the direction of the reflected light into, or away from the camera. Suitable illumination covers the required field of view, creates a consistently measurable degree of contrast and does not cause reflected glare. Different light types are required to provide successful illumination for the broad range of products being inspected by automated systems.

Conclusions

The application of robot vision in robot assembly and control processes provides immense potential and challenges, at the same time, for both research and industrial applications, as can be seen by the recent developments summarized in this chapter. It can easily be perceived that the next generation of assembly technology will include versatile robot vision systems with a high level of versatility and robustness. The chapter provides a brief overview of the most recent research efforts in the area of machine vision in assembly and control processes. Various approaches and issues relating assembly, robot assembly, robot vision and object recognition including the bin picking problem are addressed.

References

1. Trucco E., Introductory Techniques for 3-D Computer Vision / E Trucco, A. Verri, // M. : Prentice Hall, 2008. – 464 p.

2. Faugeras O. Three-Dimensional Computer Vision, / O. Faugeras // M. : MIT Press, 2003. – 325 p.

3. Fischler M., Perceptual organization and curve partitioning / M. Fischler, R. Bolles, // M. : PAMI, 1986. – 155 p.

UDC 621.37:621.391

Y.G.Lega, Dr.Tech.Sci. (Cherkasy State Technological University, Ukraine)
V.P.Kvasnikov, Dr.Tech.Sci (National Aviation University, Ukraine)
V.V.Palahin, Ph.D.. (Cherkasy State Technological University, Ukraine)
T.A.Zabochen (Cherkasy State Technological University, Ukraine)

POLYNOMIAL SIGNALS DETECTION IN BACKGROUND ADDITIVE-MULTIPLICATIVE NON-GAUSSIAN NOISE

The adaptation of moment criterion minimum upper limit probability of errors for signals detection on a background additive - multiplicative Non-Gaussian noise at the use of polynomials decision rules and moment-cumulant description of random variable is considered. The analysis of efficiency of the got results is conducted.

The most complete model of the interaction of signal and noise are additive - multiplicative model, which is typical for many practical cases of signals in communication channels. Additive-multiplicative noise arise when the parameters of the transmission system or the properties of the environment in which distributed signals undergo random changes in time [1].

One example of additive-multiplicative noise is fading signal at the reception of short waves. Interference mechanism of this phenomenon is extremely sensitive to small changes in signal propagation conditions. For example, used in cellular radio decimeter slightly curve around obstacles while experiencing multiple reflections from surrounding objects and surfaces. The consequences of such multiradiate distribution is the rapid decrease of the intensity of the received signal with distance, fading and distortion resulting signal [2].

Set the problem of signal processing is much more difficult when considering non-Gaussian noise, both additive and multiplicative character. Therefore, actual task is to develop methods and tools of statistical signal processing in the background of additive-multiplicative non-Gaussian noise in robotic systems, radar, sonar, geophysics, cellular communication systems.

For the solution of the problem is well-developed theory test statistical hypotheses based on the use of probabilistic criterions of quality [3]. In practice, the widespread Gaussian model of random processes on the one hand, is a convenient mathematical idealization, on the other hand, do not reflect the fine structure of real natural processes [4]. Therefore, to improve the accuracy of detection, to use it non-Gaussian model signal and noise. However, the use of classical quality criterions for processing non-Gaussian signals and processes, causes a number of difficulties associated with the construction of complex algorithms and their practical implementation. As a solution to this problem is possible to use an alternative approach to the description of random variables, in particular moment and kumulate description [5]. Based on this description of the moment developed quality criterion that allow to successfully solve the problem of signal detecting on background non-Gaussian noise [6 - 10].

A moment adaptation criterion minimum upper limit of probability of errors [7], based on the use of stochastic power series polynomials. The purpose of paper is to improve systems to signals detect on background asymmetric non-Gaussian noise on the basis of polynomial decision rules, moment criterion of quality test of statistical hypotheses and moment-kumulate describe random variables for additive-multiplicative models non-Gaussian noise.

Let the input of observed random signal $\xi(t)$. Processing is subject to sampling $\vec{x} = \{x_1, x_2, \dots x_n\}$ volume n of a sequence of independent and identically distributed random variables on the results of which should make the decision to perform one of two hypotheses: H_1 - received signal $\xi(t) = (a_0 + \Delta)S + \eta$, and H_0 - received noise $\xi(t) = \eta$, where S - useful constant signal, additively associated with asymmetric non-Gaussian noise that has zero mathematical expec-

tation, is characterized by variance χ_2, cumulate coefficient γ_3 and multiplicative associated with Gaussian noise Δ, which is different from zero expectation a_0 and is characterized by variance μ_2.

Decision Rule (DR) of signals detection on background of additive-multiplicative non-Gaussian noise is synthesized by moment minimum criterion for the upper limit of probability of errors is the stochastic polynomial of finite order s:

$$\Lambda\left(\vec{x}\right)_{ns} = \sum_{i=1}^{s} k_i \sum_{v=1}^{n} x_v^i + k_0 \underset{H_0}{\overset{H_1}{\underset{<}{\overset{>}{}}}} 0. \tag{1}$$

where the unknown coefficients k_0 are set as:

$$k_0 = -\frac{1}{2}\left(E_{1(sn)} + E_{0(sn)}\right). \tag{2}$$

and coefficients k_i are provided with a minimum criterion upper probability of errors:

$$Ku_{sn}\left[G, E\right] = \frac{G_{1(sn)} + G_{0(sn)}}{\left(E_{1(sn)} - E_{0(sn)}\right)^2}. \tag{3}$$

where $E_{i(sn)}$, $G_{i(sn)}$ - the mathematical expectation and variance of DR (1), $i = \overline{0,1}$, which depend on the number of sample values n, degree polynomial s and have the form:

$$E_{0(sn)} = n\sum_{i=1}^{s} k_i u_i, \quad E_{1(sn)} = n\sum_{i=1}^{s} k_i m_i, \tag{4}$$

$$G_{0(sn)} = n\sum_{i=1}^{s}\sum_{j=1}^{s} k_i k_j F_{i,j}\left(H_0\right), \quad G_{1(sn)} = n\sum_{i=1}^{s}\sum_{j=1}^{s} k_i k_j F_{i,j}\left(H_1\right), \tag{5}$$

where $F_{i,j}\left(H_0\right)$, $F_{i,j}\left(H_1\right)$ - korelyanty with size $\left(i, j\right)$ for hypothesis H_0 and H_1, m_i, u_i - at the initial moments for hypotheses H_1 and H_0.

The system of equations to determine the unknown coefficients k_i DR (1) is find from minimize the functional (3) and has the form:

$$\sum_{j=1}^{s} k_j \left[F_{i,j}\left(H_0\right) + F_{i,j}\left(H_1\right)\right] = m_i - u_i, \quad i = 1, s. \tag{6}$$

The adaptation is to find the optimal coefficients DR, according to the presented model signal and noise.

To evaluate the effectiveness of the synthesized DR is used value of the criterion $Ku_{sn}\left[G, E\right]$ (3). The smaller the value of $Ku_{sn}\left[G, E\right]$, the less of upper limits of errors of first and second order type DR (1) and therefore, the best algorithm for processing sample values.

Using this approach, the synthesis of nonlinear signal detection algorithms based on stochastic polynomials $s = 1...3$ is obtained. Consider the problem of synthesis of nonlinear DR for signals detection on background asymmetric non-Gaussian noise.

Priori information about the constant signal S, additive η and multiplicative Δ noise are based on the use of moment-kumulate description signals, that received on background non-Gaussian noise.

Moment and cumulate description for the hypothesis H_0 is:

$$u_1 = 0, \ u_2 = \chi_2, \ u_3 = \gamma_3 \chi_2^{3/2}, \ u_4 = 3\chi_2^2, \ u_5 = 10\gamma_3 \chi_2^{5/2}, \ u_6 = 5\chi_2^3\left(2\gamma_3^2 + 3\right),$$

where γ_3 - kumulate coefficient of additive noise η, which characterizes the asymmetry non-Gaussian noise.

The initial moments for hypotheses H_1 will be the form:

$$m_1 = a_0 q^{1/2} \chi_2^{1/2}, \quad m_2 = \chi_2 \left(1 + a_0^2 q + q\mu_2\right), \quad m_3 = \chi_2^{3/2} \left(3a_0 q^{1/2} + a_0^3 q^{3/2} + \gamma_3 + 3a_0 q^{3/2} \mu_2\right),$$

$$m_4 = \chi_2^2 \left(3 + 6a_0^2 q + a_0^4 q^2 + 4a_0 q^{1/2} \gamma_3 + 6q\mu_2 + 6a_0^2 q^2 \mu_2 + 3q^2 \mu_2^2\right),$$

$$m_5 = \chi_2^{5/2} \left(15a_0 q^{1/2} + 10a_0^3 q^{3/2} + a_0^5 q^{5/2} + 10\gamma_3 + 10a_0^2 q\gamma_3 + 30a_0 q^{3/2} \mu_2 + 10a_0^3 q^{5/2} \mu_2 + 10q\gamma_3\mu_2 + \right.$$
$$\left. + 15a_0 q^{5/2} \mu_2^2\right),$$

$$m_6 = \chi_2^3 \left(15 + 45a_0^2 q + 15a_0^4 q^2 + a_0^6 q^3 + 60a_0 q^{1/2} \gamma_3 + 20a_0^3 q^{3/2} \gamma_3 + 10\gamma_3^2 + \right.$$
$$\left. + 45q\mu_2 + 90a_0^2 q^2 \mu_2 + 15a_0^4 q^3 \mu_2 + 60a_0 q^{3/2} \gamma_3\mu_2 + 45q^2 \mu_2^2 + 45a_0^2 q^3 \mu_2^2 + 15q^3 \mu_2^3\right),$$

where $q = \dfrac{S^2}{\chi_2}$ - the ratio signal / noise on power.

Centered korelyanty $F_{i,j}$ that are find from $F_{i,j}(H_0) = u_{i+j} - u_i \, u_j$ and $F_{i,j}(H_1) = m_{i+j} - m_i \, m_j$, $i, j = \overline{1, n}$, for the hypothesis a H_0, are as follows:

$$F_{1,1}(H_0) = \chi_2, \quad F_{1,2}(H_0) = F_{2,1}(H_0) = \gamma_3 \chi_2^{3/2}, \quad F_{2,2}(H_0) = 2\chi_2^2, \quad F_{3,1}(H_0) = F_{1,3}(H_0) = 3\chi_2^2,$$

$$F_{3,2}(H_0) = F_{2,3}(H_0) = 9\gamma_3 \chi_2^{5/2}, \quad F_{3,3}(H_0) = \chi_2^3 \left(9\gamma_3^2 + 15\right).$$

Similarly, for hypothesis H_1 centered korelyanty can be written as:

$$F_{1,1}(H_1) = \chi_2 \left(1 + q\mu_2\right), \quad F_{1,2}(H_1) = F_{2,1}(H_1) = \chi_2^{3/2} \left(\gamma_3 + 2a_0 q^{1/2} \left(1 + q\mu_2\right)\right),$$

$$F_{2,2}(H_1) = 2\chi_2^2 \left(2a_0 q^{1/2} \gamma_3 + \left(1 + q\mu_2\right)\left(1 + 2a_0^2 q + q\mu_2\right)\right),$$

$$F_{3,1}(H_1) = F_{1,3}(H_1) = 3\chi_2^2 \left(a_0 q^{1/2} \gamma_3 + \left(1 + q\mu_2\right)\left(1 + a_0^2 q + q\mu_2\right)\right),$$

$$F_{3,2}(H_1) = F_{2,3}(H_1) = 3\chi_2^{5/2} \left[3\gamma_3 \left(1 + a_0^2 q + q\mu_2\right) + 2a_0 q^{1/2} \left(1 + q\mu_2\right)\left(2 + a_0^2 q + 2q\mu_2\right)\right],$$

$$F_{3,3}(H_1) = 3\chi_2^3 \left[3\gamma_3^2 + 6a_0 q^{1/2} \gamma_3 \left(3 + a_0^2 q + 3q\mu_2\right) + \left(1 + q\mu_2\right)\begin{pmatrix} 5 + 3a_0^2 q\left(4 + a_0^2 q\right) + \\ q\mu_2\left(10 + 12a_0^2 q + 5q\mu_2\right) \end{pmatrix}\right].$$

Here is a synthesis algorithm for DR degree stochastic polynomial $s = 1$, which in general will look like:

$$\Lambda(\vec{x})_{1n} = k_1 \sum_{v=1}^{n} x_v + k_0 \underset{H_0}{\overset{H_1}{\underset{<}{>}}} 0.$$

Shown that k_1 is find from the system of equations (6) and has the form:

$$k_1 = \frac{a_0 \, q^{1/2}}{(2 + q\mu_2)\chi_2^{1/2}}.$$

Mathematical expectation and variance of DR for hypotheses H_0 and H_1 are find from the expressions (4), (5) and have the form:

$$E_0 = 0, \quad E_1 = \frac{a_0^2 nq}{2 + q\mu_2}, \quad G_0 = \frac{a_0^2 nq}{\left(2 + q\mu_2\right)^2}, \quad G_1 = \frac{a_0^2 nq(1 + q\mu_2)}{\left(2 + q\mu_2\right)^2}.$$

Thus, the DR (1) for $s = 1$ has the form:

$$\Lambda(\vec{x})_{1n} = \frac{1}{n}\sum_{v=1}^{n} x_v - \frac{a_0 S}{2} \underset{H_0}{\overset{H_1}{\underset{<}{>}}} 0.$$

1.9.80

Shown that the upper limit of probability of errors of first and second kind DR value criterion Ku_{1n} is find from the expression (3) and has the form:

$$Ku_{1n} = \frac{2 + q\mu_2}{a_0^2 nq}.$$

When power the stochastic polynomial is $s = 2$, we obtain DR, which in general will look like:

$$\Lambda(\vec{x})_{2n} = k_1 \sum_{\nu=1}^{n} x_\nu + k_2 \sum_{\nu=1}^{n} x_\nu^2 + k_0 \underset{H_0}{\overset{H_1}{\underset{<}{\overset{>}{}}}} 0.$$

Unknown coefficients k_1, k_2 are found from system of equations (6) and have the form:

$$k_1 = \frac{q^{1/2}\left(q^{1/2}\gamma_3\left(a_0^2 - \mu_2\right) + a_0\left(2 + a_0^2 q + q\left(1 + a_0^2 q\right)\mu_2\right)\right)}{\left(4 + 2a_0^2 q - 2\gamma_3^2 - 2a_0 q^{3/2}\gamma_3\mu_2 + q\mu_2\left(6 + 2a_0^2 q + q\mu_2\left(4 + q\mu_2\right)\right)\right)\chi_2^{1/2}},$$

$$k_2 = \frac{-2a_0 q^{1/2}\gamma_3 + q\mu_2\left(2 - a_0^2 q + q\mu_2\right)}{2\left(4 + 2a_0^2 q - 2\gamma_3^2 - 2a_0 q^{3/2}\gamma_3\mu_2 + q\mu_2\left(6 + 2a_0^2 q + q\mu_2\left(4 + q\mu_2\right)\right)\right)\chi_2}.$$

The value of the criterion Ku_{2n} is find from the expression (3) and has the form:

$$Ku_{2n} = \frac{8 + 4a_0^2 q - 4\gamma_3^2 - 4a_0 q^{3/2}\gamma_3\mu_2 + 2q\mu_2\left(6 + 2a_0^2 q + q\mu_2\left(4 + q\mu_2\right)\right)}{nq\left(2a_0^2\left(2 + a_0^2 q\right) + \mu_2\left(a_0^2 q\left(4 + a_0^2 q\right) - 4a_0 q^{1/2}\gamma_3 + q\mu_2\left(2 + q\mu_2\right)\right)\right)}. \tag{7}$$

Analyzing the expression (7), we can say that the value of the criterion Ku_{2n} depends not only on the ratio signal/noise q and multiplicative noise variance μ_2 but also from the asymmetry coefficient of additive noise γ_3. Similarly, DR for degree polynomial $s = 3$ are obtained

The effectiveness of the obtained signals detection DR is estimated by value ratio criterions Ku_s / Ku_1. In analyzing the effectiveness of synthesized DR shows that taking into account the asymmetry coefficient γ_3 and increasing degree polynomial DR to the $s = 2...3$ received a fundamentally new results. The results show that the synthesized nonlinear DR are characterized by lower values of the upper limit of probability of errors in comparison with linear DR, obtained for Gaussian noise model. In Fig. 1 the results compare the effectiveness of nonlinear signal detection $(s = 2...3)$ with linear signal detection $(s = 1)$ for specific values q, μ_2 and variable coefficient of asymmetry γ_3 are obtained.

Shown that the value criterions Ku_{2n} and Ku_{3n} less than value criterion Ku_{1n}, depending on the parameters of signal and noise. Especially, this tendency appears for the account of the fine structure non-Gaissian noise, that is different from zero coefficient of asymmetry γ_3.
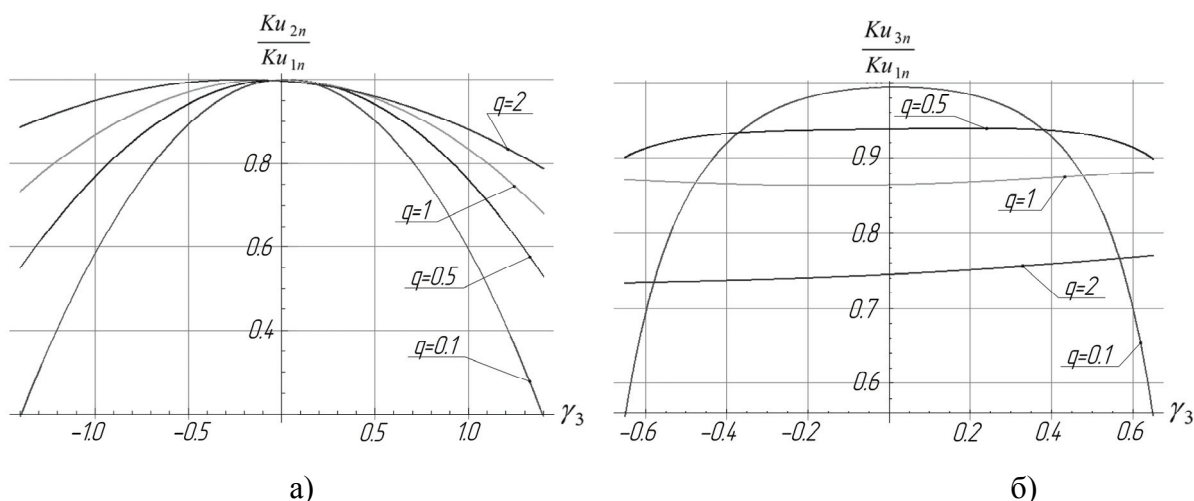
Fig. 1. The dependence of the efficiency signal detection the nonlinear DR for $s = 2$ a) and for $s = 3$ b) against linear DR ($s = 1$) when $a_0 = 2$, $\mu_2 = 0,1$ from the coefficient of asymmetry γ_3.

Conclusion

Were synthesized DR constant signal detection on background non-Gussian asymmetric noise by used stochastic degree polynomial $s = 3$. Is shown, that with increasing degree of stochastic polynomial and taking into account non-Gaussian noise, the criterion value upper limit of probability of errors of first and second kind Ku_{sn} decreases, that indicate increase their effectiveness in comparison with known linear results. The results may find their application in software realizations of algorithms precision devices signal processing (in modern robotic systems, telecommunication systems, radar systems and others.

References

1. *Tuzlukov V. P.* Signal Processing Noise. – USA, Florida: CRC Press LLC, 2002. – 688 р.

2. *Ратынский М.В.* Основы сотовой связи. – М.: Радио и связь, 1998. – 248 с.

3. *Левин Б.Р.* Теоретические основы статистической радиотехники. 3-е изд., перераб. и доп. – М.: Радио и связь, 1989. – 656 с.

4. *Шелухин О.И.* Негауссовские процессы в радиотехнике. – М.: Радио и связь, 1999. – 310 с.

5. *Малахов А.Н.* Кумулянтный анализ негауссовых процессов и их преобразований. – М.: Сов. радио, 1978. – 376 с.

6. *Кунченко Ю.П.* Проверка статистических гіпотез при использовании полиномиальных решающих правил, оптимальних по моментному критерию суммы асимптотических вероятностей ошибок / Кунченко Ю.П., Палагин В.В. // Радиоэлектроника и автоматика. – 2006. – № 3(34). – С. 4 – 11.

7. *Кунченко Ю.П.* Разработка нелинейных обнаружителей сигналов при негауссовых помехах, оптимальных по дисперсионных критериям. / Кунченко Ю.П., Палагин В.В., Мартыненко С.С. // Тр. 2-й междунар. конф. по радиосвязи, звуковому и телевиз. вещанию (УкрТелеком-95). – Одесса, 1995. – С. 440 – 443.

8. *Палагін В.В.* Синтез поліноміальних алгоритмів розпізнавання сигналів на тлі асиметричних негауссівських завад. / Палагін В.В., Жила О.М. // Труды Одесского политехнического университета. – 2007. – № 2(28). – С. 171 – 176.

9. *Палагин В.В.* Адаптация моментного критерия качества для многоальтернативной проверки гипотез при спользовании полиномиальных решающих правил. // Электронное моделирование – 2010. – Т.32. №4. – С. 17 – 33.

10. *Кунченко Ю.П.* Стохастические полиномы. – К.: Наук. думка, 2006. – 267 с.

UDC 004.413:338.5(045)

METHOD OF CALIBRATION OF COCOMO MODEL VIA REDUCTION OF THE MAIN EQUATION

This article reviews method of calibration of COCOMO software cost estimation model by reduction of the main equation as well as scientific and mathematical method that lied foundations for it.

Introduction.

With the significant growth of software complexity methods for software cost estimation became necessary condition of the success of any software project. But over the years of software cost estimation models' improvement still most of the models are not generalized and that is the reason for the appearance of various calibration techniques and methods aiming to improve the quality of software cost estimation results of a given model for a specific company domain.

This article presents the results of scientific research in the field of software cost estimation model calibration and proposes the special method of calibration of COCOMO model via reduction of the main equation of the model.

The mathematical model

In this method, a number of ideas are taken from the relevance of features that were discussed in [1], and the evaluation criteria for prediction models in [2], [3] and [4]. This method aims to find the optimal feature subset that enables higher accuracy and lower variability of results than the general model with the full feature set. Therefore it is important to build the mathematical model and define corresponding terminology. The optimal feature subset not always includes all relevant feature subsets but generally it shouldn't include the irrelevant feature subset.

$PM = a * (KSLOC^b) * (\prod EM_j)$ (Equation 1)

Where PM – person months; EM – effort multipliers; KSLOC – size as thousand lines of code, is estimated or converted from a function point metric; a and b – domain-specific constants;

$PM = A * \left(KSLOC^{B+1.01*\sum_{i=1}^{5} SF_i}\right) * (\prod_{j=1}^{17} EM_j)$ (Equation 2)

Where A – baseline multiplicative constant; B – baseline exponential constant; Size – size of the software project measured in terms of KSLOC (thousand of source lines of code) or function points related to programming language; SF – scale factor; EM – effort multiplier.

Definition 1. Model. These models are the same as the ordinary COCOMO 81 model shown in Equation 1 or the COCOMO II model shown in equation 2 except that it uses fewer model parameters (calibration features, e.g. effort multipliers).

Definition 2. Feature. A feature, sometimes called a parameter, an attribute, a factor, or a cost driver, describes some characteristics of a project instance.

Definition 3. Feature Subset. A feature subset includes one or more than one but not all parameters of the model.

Definition 4. Full Feature Set. A full feature set includes all parameters of the model.

Definition 5. Accuracy. COCOMO's performance is often measured in terms of PRED(30). PRED(N) is calculated from the relative error, or RE (shown in equation 3), which is the relative size of the difference between the actual and estimated value. Given a data set of size D, a Training set of size (Train=|Train|) ≤ D, and a test set of size T=D- |Train|, then the mean magnitude of the relative error, or MMRE (the mean magnitude of relative error, shown in equation 5), is the percentage of the absolute values of the relative errors, or MRE (the magnitude of relative error shown in equation 4), averaged over the T items in the test set. PRED(N) for each hold-out experiment is calculated with equation 6.

$RE_i = \frac{estimate_i - actual_i}{actual_i}$ (Equation 3)

$MRE_i = abc(RE_i)$ (Equation 4)

$MMRE = \frac{100}{T}\sum_{i=1}^{T} MRE_i$ (Equation 5)

$PRED(N)_h = \frac{100}{T}\sum_{i=1}^{T}\begin{cases} 1 \; if \; MRE_i \leq \frac{N}{100} \\ 0 \; otherwise \end{cases}$ (Equation 6)

In this approach, Hold-out experiments are conducted; the accuracy of the model is defined in equation 7 as the mean of PRED(N) in all hold-out experiments in the same calibration dataset:

$PRED(N) = \frac{1}{n}\sum_{i=1}^{n} PRED(N)_h^i$ (Equation 7)

The results are reported in terms of PRED(N), not MMRE. This is a pragmatic decision as PRED(N) is easier understood by business users than MMRE. Also, there are more PRED(N) in reports in the literature than MMRE, possibly due to the influence of the COCOMO researchers who reported their 1999 study using PRED(N) [5].

Definition 6. Variability. PRED(N) is calculated for different "holdout" samplings of the calibration data. Holdout samplings use randomized subsamples of the data to calibrate PRED value and the unsampled data to calculate PRED value. Variability of the estimation in the model, denoted as V in equation 9, shows how much spread is in the estimation. Standard deviation σ in Equation 10 is used to measure the variability of the accuracy of the model in this approach:

$\mu(x) = \frac{1}{N}\sum_{i=1}^{N} x_i$ (Equation 8)

$\mu(x) = \frac{1}{N}\sum_{i=1}^{N} x_i$ (Equation 9)

$\sigma = \sqrt{V}$ (Equation 10)

Definition 7. Better feature subset. Given a learner L, a training dataset and a test dataset with the feature subsets X_1, X_2, ..., X_n, a better feature subset, X_{bet}, is the feature subset X^i that provides higher accuracy without increasing variability than those of the full feature set X of the general the model:

$Accuracy(X^i) > Accuracy(X)$ i $Variability(X^i) < Variability(X)$ for any $1 \leq j \leq n$ (Equation 12)

Definition 8. The best accuracy feature subset. Given a learner L, a training dataset and a test set with the better feature subsets X^1_{bet}, X^2_{bet}, ..., X^n_{bet}, the best accuracy feature subset, X_{acc}, is the better subset X^i_{bet} that maximizes the accuracy among the better feature subsets:

$Accuracy(X^i_{bet}) Accuracy(X^j_{bet})$ for any $1 \leq j \leq n$ (Equation 13)

Definition 9. The least variability feature subset. Given a learner L, a training dataset and a test set with the better feature subsets X^1_{bet}, X^2_{bet}, ..., X^n_{bet}, the least variability feature subset, X_{sd}, is the better subset X^i_{bet} that minimizes the SD (standard deviation) among the better feature subsets:

$SD(X^i_{bet}) \leq SD(X^j_{bet})$ for any $1 \leq j \leq n$ (Equation 14)

Definition 10. The optimal feature subset. Given a learner L, a training dataset and a test set with the better feature subsets X^1_{bet}, X^2_{bet}, ..., X^n_{bet}, an optimal feature subset, X_{opt}, is the better subset X^i_{bet} that maximizes the accuracy among the better feature subsets:

$Accuracy(X^i_{bet}) Accuracy(X^j_{bet})$ for any $1 \leq j \leq n$ (Equation 15)

Definition 11. The relevance of a feature. If adding a feature X_i into any feature subset that does not include X_i, or removing X_i from any feature subset that includes X_i will change the accuracy of the model, the feature X_i is strongly relevant to the model. If a feature X_i is not strongly relevant and there exists such a feature subset, adding X_i into the feature subset that does not include X_i or removing X_i from the feature subset that
includes X_i will change the accuracy of the model, the feature X_i is weakly relevant to the model. If a feature X_i is strongly relevant or weakly relevant, X_i is relevant to the model. If a feature X_i is neither strongly relevant nor weakly relevant, X_i is irrelevant to the model. This approach apply the Wrapper – feature subset selection implementation method with k-fold cross validation to evaluate the features of the model and N is the number of how many times a feature X_i is selected in the k-fold cross validation experiments:

1) X_i is strongly relevant if and only if $N = k$ (such as Size);
2) X_i is weakly relevant if $1 \leq N < k$;

3) X_i is relevant if $1 \leq N \leq k$;
4) X_i is irrelevant if and only if $N = 0$. (Equation 16)

Methods Applied in the Approach. Machine Learning is defined as the study of computer algorithms that improves automatically through experience [6]. Applications with machine learning techniques learn when they change their behavior in a way that makes them perform better in the future [7]. A number of research applied machine learning and statistical methods in software cost estimation [8], [9], [10], [11], [5], [12], [13], [14], and [15]. The most successful approach is [5], which has been used to calibrate COCOMO II from 1998. In this research approach shown in Figure 1 for software cost estimation, machine learning techniques are used to formulate the process and build the model from the training data, and statistical methods are used to test, validate and evaluate the process and the model built by machine learning on the test set.
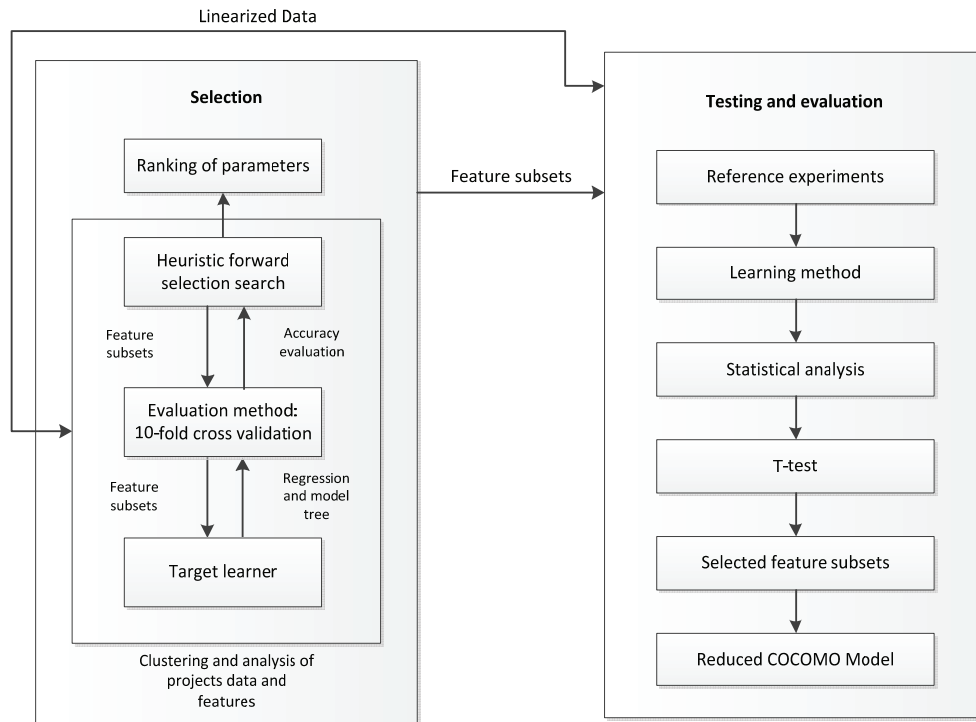
Figure 1. The integration of different techniques and methods in the approach

Linearization
Ordinary least squares regression and M5 model tree are linear models. COCOMO 81 shown in Equation 17 and COCOMO II shown in Equation 18 are exponential models. The logarithmic transformation were used to transform COCOMO 81 and COCOMO II into linear models.
Linearized COCOMO 81 model:
$ln(PM) = \beta_0 + \beta_1 * \ln(Size) + \beta_2 * \ln(EM_2) + \cdots + \beta_{16} * \ln(EM_{16})$ (Equation 17)
Linearized COCOMO II model:
$ln(PM) = \beta_0 + \beta_1 * \ln(Size) + \beta_2 * 0.01 * SF_1 * \ln(EM_2) + \cdots + \beta_6 * 0.01 * SF_5 * \ln(Size) + \beta_7 * \ln(EM_1) + \cdots + \beta_{23} * \ln(EM_{17})$ (Equation 18)

All these transformations create new parameters that are full mathematical equivalents to the original parameters, but are expressed in different measurement.

Clustering and Analyzing Project Features
In this approach, the most promising features in a given dataset are identified with learning algorithm - FSS (Feature subset selection). As the data sets may contain several extraneous features which can reduce the efficiency of the model, this approach helps us identify the important attributes and remove redundant ones.
In this study, the WRAPPER FSS method is applied, which is a FSS method evaluating parameter sets by using a learning scheme and statistical re-sampling technique such as cross validation to

estimate the accuracy of the learning scheme for a set of attributes, and implemented in WEKA [7] (which is a data mining toolkit, free, open source, well documented, compatible on many platforms, and easy to install).
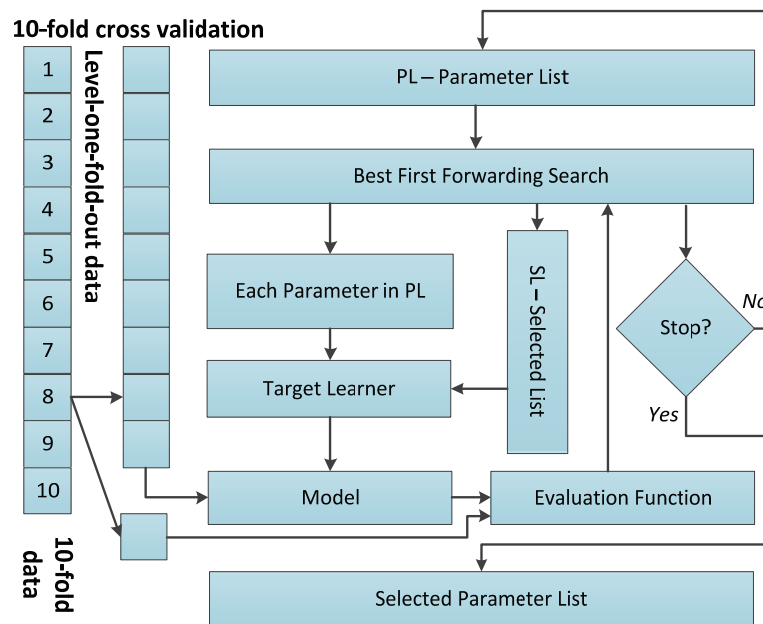
Figure 2. The Wrapper in RPM

In their comparative evaluation of feature subset selection techniques [16], Hall and Holmes conclude that WRAPPER is the best FSS mechanism, if the data set is not too large.

Table 1. Wrapper Results for the NASA 60 Project Data

NASA 60 data with LSR Approach: 60 Instances						
Parameter	60 Folds	50 Folds	40 Folds	30 Folds	20 Folds	10 Folds
TURN	100	98	100	100	100	100
ACAP	100	100	100	97	100	100
TIME	100	100	100	100	100	100
LOC	100	100	100	100	100	100
STOR	95	92	93	87	90	80
VEXP	60	60	65	67	70	70
DATA	23	14	20	20	20	40
AEXP	8	2	5	3	0	20
PCAP	5	10	5	7	0	10
MODP	0	14	3	3	5	10
VIRT	0	0	8	3	20	10
RELY	3	2	5	7	0	0
TOOL	0	0	0	3	10	0
CPLX	3	10	5	7	5	0
LEXP	2	10	0	0	5	0
SCED	5	4	3	3	0	0

NASA effort data used in this study are available on-line at the PROMOSE repository of public domain software engineering data set: http://promise.site.uottawa.ca/SERepository/datasets/cocomonasa.arff.

Summary

Presented mathematical model for the calibration of COCOMO model via reduction of it's main equation increases the accuracy of the model for specific company domain, but decreseas the accuracy of the model for the generalized case. The accuracy of calibration depends on the amount of historical data in the company that is used to calibrate the model. Some variation in calibrated

model results may appear if the company changes the specifics of the software projects being developed. This may require recalibration of the model to accont for new specifics, or otherwise accuracy may be even worse than for the generalized COCOMO model.

References
1. R. Kohavi, G. John, "Feature Extraction, Construction and Selection : A Data Mining Perspective", edited by H. Liu and H. Motoda.
2. Foss, T.; Stensrud, E.; Kitchenham, B.; Myrtveit, I. "A Simulation Study of the Model Evaluation Criterion MMRE", IEEE Transactions on Software Engineering, 29(2003)11, pp. 985-995
3. M. Jørgensen, D. I. K. Sjøberg. "An effort prediction interval approach based on the empirical distribution of previous estimation accuracy", Journal of Information and Software Technology, 45 (3), March 2003, pp. 123-136.
4. K. J. Moløkken-Østvold. "Effort and Schedule Estimation of Software Development Projects", PhD-thesis, 2004, http://www.simula.no/photo/effort_and_schedule_estimation_of_software_development_projects.pdf
5. S. Chulani, B. Boehm, B. Steece. "Bayesian analysis of empirical software engineering cost models". IEEE Transactions on Software Engineering, 25(4), July/August 1999.
6. T. Mitchell. "Machine Learning", McGraw Hill, ISBN 0070428077, 1997.
7. I. H. Witten, E. Frank, "Data Mining: Practical Machine Learning Tools and Techniques with Java Implementations". Morgan Kaufmann, 1999.
8. M. Shepperd and C. Schofield., "Estimating Software Project Effort Using Analogies", IEEE Transactions on Software Engineering, Nov 1997, Vol. 23, No. 12. http://www.utdallas.edu/~rbanker/SE_XII.pdf
9. K. Srinivasan and D. Fisher. "Machine learning approaches to estimating software development effort", IEEE Trans. Soft. Eng., pages 126–137, February 1995.
10. G. Wittig, G. Finnie. "Estimating software development effort with connectionist models", Information and Software Technology, 39(7):469–476, 1997.
11. L. C. Briand, Kh. El Emam, D. Surmann, I. Wieczorek. "An assessment and comparison of common software cost estimation modeling techniques", The 21st International Conference on Software Engineering, May 1999.
12. C. Mair, G. Kadoda, M. Lefley. "An Investigation of Machine Learning Based Prediction Systems", Journal of software systems, vol. 53, pp. pp23-29, July 2000.
13. S. Bibi, I. Stamelos, L. Aggelis. "Bayesian Belief Networks as a Software Productivity Estimation Tool", 1st Balkan Conference in Informatics, Thessaloniki, Greece, November 2003.
14. G. Boetticher. "When will it be done? the 300 billion dollar question, machine learner answers", IEEE Intelligent Systems, June 2003.
15. T. Menzies, D. Port, Z. Chen, J. Hihn, S. Stukes. "Validation Methods for Calibrating Software Effort Models", ICSE 2005, May 15–21, 2005
16. M.A. Hall and G. Holmes. "Benchmarking attribute selection techniques for discrete class data mining". IEEE Transactions On Knowledge And Data Engineering, 15(6):1437– 1447, 2003.

UDC 004.413:338.5

E.V. Chebanyuk, Associate professor (National Aviation University, Ukraine)
V.I. Chuprinka, Doctor of engineering
(Kyiv National University of Technologies and Design, Ukraine)

METHOD DETERMINING OF SOFTWARE COMPONENT REUSE

The method of determining software components for reuse is represented in this article. The peculiarity of this method that it's necessary to determine design patterns, when domain model is built, and integrate them into framework model. Such model can be used in application engineering stage for mapping software requirements to design patterns. Then we can found the software components which responsible for the particular task and use them for designing new applications. The metalanguage of design pattern description is also given.

Actual Requirement analysis during software product lifecycle is one of the application engineering stages. The main tasks of requirement analysis are the next: exclusion of contradictory or coinciding requirement, to reduce the project budget and developers efforts. Known methods of requirement analysis can be divided on three large groups: making software prototypes [1,2], software modeling [2,3] and interviews with the customer [4]. They are regulated by standards of requirement engineering and methodic guide of management requirements IEEE Std 830-1998, "IEEE Recommended Practice for Software Requirements Specifications"

Widespread software products such as IBM Rational group (IBM Rational Requisite Pro, Telelogic Doors, Sybase Power Designer, IBM Requirement Composer and Team Concert), Borland Caliber RM and others support activity of requirements analysis. They allow to consider problem tracing changes in software and compose artifacts, such as product backlogs, software requirement specification, platform specific models and others. But the difficulties of usage such kind of solutions are the next: they required high quality personal, volume deployment and high cost.
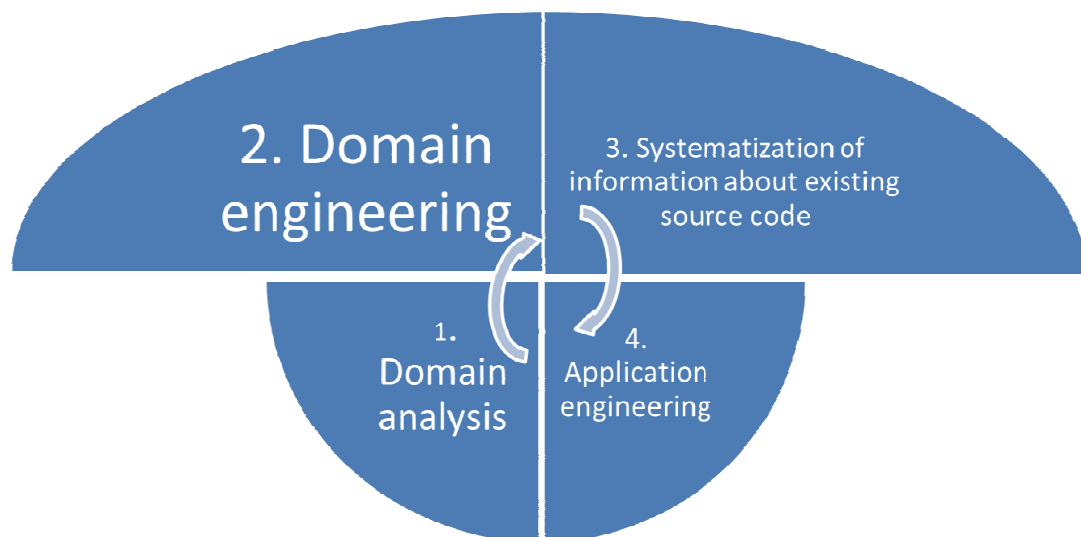
Pict. 1 The phases of method requirement reuse

But the mentioned methods of requirement analysis don't focus on effective reuse of existing software components. The proposed method of determination software reuse components while requirements analysis, is grounded on mapping of application domain tasks and design patterns structure and functionality. Method cover four phases (pict. 1).

The iterative character of determining of reusable components explains by the fact that some artifacts (for example domain model) produced in the way "step by step" and they need continues

refinement. Such method can be implemented for designing like small software products and large software complexes like CAD components for aviation or car-building industries.

Steps of methods for implementation

The proposed method covers the next phases: domain analysis, domain engineering systematization information about existing code and also application engineering (pict. 1). Let consider purposes of every phase.

Domain analysis It's necessary to build domain model which be adopted for borrowing components from the framework during application engineering. For the constructing of effective frameworks it is necessary to consider application domain at the task level. The task analysis is made by domain analytics. During constructing the model of framework it is necessary to use object oriented techniques in order to raise quality of framework and separate components with the purpose to facilitate reuse process. One of perspective techniques is usage design patterns for projecting class and package diagrams.

Domain engineering Mapping design pattern description with the tasks, entities and relationships of application domain. Constructing and refining the framework detail with patterns. One more task – it's to create metalanguage of design patterns description.

Systematization of information about previous developments Finding correspondence between task of application domain and existing software. A separate task for this phase is to develop criteria for finding correspondence between existing code and

Application engineering Determining reusable components or software modules according to requirement specifications. Using components engineering in order to integrate components into future applications.

Basic denotations of metalanguage for pattern description
We introduce the following notation.

Class – C. Class represents like set of properties α, fields χ and methods β $C = \{\alpha \cap \chi \cap \beta\}$.

Interface – I. Interface represent like set of methods β^i, $I = \{\beta^i\}$, with condition that the realization of this methods is empty $m_j = \varnothing, m_j \in \beta^i$, $j = 1...n$, where n – number of methods in interface.

Inheritance

Interface inheritance

When class inherited interface it's mean, that class realize all interface methods. It's denoted as: $C = \{C \cap I\} = \{\alpha^c \cap \chi^c \cap \beta^c \cap \beta^i\}$, where every method should satisfy the condition - $m_j \neq \varnothing, m_j \in \beta^i$, $j = 1...n$ (Method shouldn't be empty).

When class use multiple inheritance of interfaces it's denoted as $C = \{C \cap \partial_m\} = \{\alpha^c \cap \chi^c \cap \beta^c \cap \beta_0^{\,i} \cap \beta_1^{\,i} \cap ... \cap \beta_m^{\,i}\}$, where ∂_m -is set of m interfaces (the index in the bottom – is the number of interface).

Class inheritance

Denote - C_1 heir of class C_0. Thus the functionality of class C_1 will be described in the next way– $C_1 = \{C_0 \cap C_1\} = \{\alpha_0^{\,c} \cap \alpha_1^{\,c} \cap \beta_0^{\,c} \cap \beta_1^{\,c} \cap \chi_1^{\,c}\}$.

If several classes inherited class C_0 the set of this classes denotes like $\phi = \{C_{11}, C_{12}, ..., C_{1k}\}$, where k – number of classes in that set.

Hierarchy of inheritance

The heir of class C_1 is class C_2 and so on. Generalize – the hierarchy of inheritance C_j - the heir of the class C_0 level j. (For instance, $j=7$, C_1 is the heir of class C_0, C_2 is the heir of class C_1, and so on, C_7 the heir of class C_6)

Polymorphism

Denote ε, as set of polymorphic methods of class C_j. Number of methods of this set is equal to t. For every method m_i^{c1} from set ε for all methods of class C_1, which are polymorphic (they contained *override* in their signature) the condition $m_i^{c1} = m_i^{c0} \cup m_i^{c1}$ (1) is proved and just one (no more) constituent of (1) is equal to one and signature of the methods m_i^{c0} and m_i^{c1} differs just with modificators (virtual and override).

Functionality of every method m^{cj} of class C_j from the set ε is defined by the next expression $m^{cj} = m^{ci}$, where $i = \max\{m^{ct}\}$ if $m^{ct} \neq \varnothing$ .i=0,...,j-1.

Composition

Consider two entities of one level (entities not interconnected by relationships of inheritance). Every entity represented like separate class. Denote them like $C_0^|$ and $C_0^{||}$. The relationships of composition are denotes by the next way: $C_0^| = \{C_0^| \cap C_0^{||}\}$

Aggregation

The relationships of aggregation are denoted in the next way: $C_0^| = \{C_0^| \cup C_0^{||}\}$

Association

Every relationship of association is described in the next way^
$C_0^| = \{C_0^| + C_0^{||}\} = \{\alpha_0^| \cup \beta_0^| \cup \chi_0^| + m_0^{||}\}$

Examples of pattern description
Strategy

The entity $C_0^|$ and set of k entities $\phi = \{C_{11}, C_{12},...,C_{1k}\}$ are given. For every entity from set ϕ exist at least one method, witch satisfy condition $m_j^{ci} = m_j^{c0} \cup m_j^{ci}$, де $i=1,...,k$. The purpose of this methods – is to make the same operation with the help of different algorithms. The interaction between entities in strategy pattern organized in the next way: entity $C_0^{||}$ use methods m_j^{ci} for making some actions in a different way.

Observer

The entity $C_0^|$ and not empty set from independent entities $\gamma = \{C_1^{||}, C_2^{||},...,C_p^{||}\}$ are given. For every entity from γ it's necessary to make some action when the state of entity $C_0^|$ occurs. In order to realize such a schema the next structural elements are used:

Interface $I_0^|$ inherits entity $C_0^|$. $C_0^| = \{C_0^| \cap I_0\} = \{\alpha_0^c \cap \chi_0^c \cap \beta_0^c \cap \beta^i\}$

Interface $I_0^{||}$, inherits all classes from γ. Than, for every class from γ, the condition $C_0^{||} = \{C_0^{||} \cap I_0^{||}\} = \{\alpha_0^c \cap \chi_0^c \cap \beta_0^c \cap \beta^i\}$ is proved.

The interaction of entities in pattern strategy When state of entity $C_0^|$ happened the message about this event is sent to every entity from γ. For executing action of adding entity into $\gamma = \gamma + C_0^{||}$ it should inherit interface $I_0^{||}$ and override its methods $C_0^{||} = \{C_0^| \cap I_0^{||}\} = \{\alpha_0^c \cap \chi_0^c \cap \beta_0^c \cap \beta^i\}$.

Stages of code reuse
1. Phase of Domain Engineering
1.1. Phase domain analysis
- Determining objects, processes and task of application domain.
- Building a domain model in a class diagram [5].
- Refine the relationship between objects (composition, association, aggregation, inheritance).
2. Defining artifacts for reuse
  - Analyzing application domain activities and relationships between objects distinguish design
    patterns.
  - Determine the existing software components which are suitable for reuse.
3. Phase engineering applications

- The customer formulate the task.
- Requirements are refining with a list of questions that reflect certain properties of existing components. Getting information helps to design the architecture of a particular software product. Also, there is an additional opportunity to clarify requirements and to predict future maintenance or development software.

Conclusions The advantages of the proposed method in comparison with classical approach of requirements engineering are the next:
1   Using special rules for building models of framework allows quickly determining of reusable components on framework in the application engineering stage.
2   It can be used without modification both for developing small software product as for large software complexes.
3   Mapping business processes and design pattern allow to use reliable constructions for making and distribution of software components.
4   Proposal mathematical apparatus let formalize rules of mapping business processes to desing patterns.

References

1   Carlos Cetina , Joan Fons , Vicente Pelechano, Applying Software Product Lines to Build Autonomic Pervasive Systems, Proceedings of the 2008 12th International Software Product Line Conference, p.117-126, September 08-12, 2008
2   Hiroyuki Nakagawa, Akihiko Ohsuga, and Shinichi Honiden. gocc: A Configuration Compiler for Selfadaptive Systems Using Goal-oriented Requirements Description. In Proc. of the 6 The International Symposium on Software Engineering for Adaptive and Self-Managing Systems, pages 40–49. ACM, 2011.
3   V´ıtor E. S. Souza, Alexei Lapouchnian, and John Mylopoulos. (Requirement) Evolution Requirements for Adaptive Systems. In Proc. of the 7 the International Symposium on Software Engineering for Adaptive and Self-Managing Systems , 2012.
4   Axel van Lamsweerde. Requirements Engineering: From System Goals to UML Models to Software Specifications. Wiley, 1 edition, 2009.
5   Чебанюк О.В. Метод доменного аналізу для ефективного моделювання процесів при проведенні експериментів з використанням програмного забезпечення / О.В. Чебанюк, В.І. Чупринка // Проблеми програмування. - 2012. – №2-3. – С. 168-173.

V.A. Khomenko, Ph.D. (National Aviation University, Ukraine)

SOFTWARE CONSTRUCTOR OF NOISE SIMULATORS FOR FLIGHT SIMULATORS

The constructor enables to build the noise simulators using the widely accessible aircrafts cockpits sound records. This approach and tool can be applied at the low-budget projects under inaccessible aircraft condition. The case study of the two-engine turboprop airplane noise simulator development is given.

Introduction

Noise simulator is the integral part of the any modern flight simulator that provides the imitation of the real sound environment [1, 2] during the training. The simulator creation is the complex and expensive process that requires studying and analysis of the object aircraft noises in the different work modes, synthesis of the single noises generators, matching the sound dependencies on the flight parameters and verification of adequacy. Under the inaccessible object aircraft condition the sound characteristics analysis and adequacy checking are impossible if the traditional approaches are used. But simulator developer now is able to get easy the flight audio (and video) records from the aircraft cockpit made by any appropriate compact record device.

The idea of the aircraft sound record usage for the sound environment imitation is not new but is not applied for the professional simulator owing to different reasons [1], particularly because perfect digital audio technologies became accessible for simulator developers later than advanced analog noise generation. Here is proposed the simulator constructor, based on the playback of the aircraft sound digital record samples. These samples are played once or iteratively with the control parameters depend on the work mode of the noise sources.

Approach. The model M of the sound environment usually is presented as the additive set of noises; each of them is created by single source (aircraft mechanism or the environment factor):

$$M = \sum_{i=1}^{n} m_i ,$$

where m_i – model of the single noise.

For each model m_i should be described the noise characteristics and their dependencies on set of the noise source parameters. Noise control can be described by the functional that defines sound parameters dependencies $Y = \{y_1, y_2, ... y_k\}$ on the input parameters of source $X = \{x_1, x_2, ... x_l\}$:

$$m_i(Y) = F(X) .$$

It is useful to cast the functional F to the set of the independent functions; each of them describes the one output parameter changing depending on input set:

$$y_i = f_i(x_1, x_2, ... x_m) .$$

Sound environment model for the controlled samples set differs from the above model because the single noise models cannot be independent, owing to difficulties of the "pure" samples extraction from the "live" record. Hereby, one model is depended the several other noises:

$$m_i(Y) = F(X, \{m_k\}, k \neq i) ,$$

where m_i – selected model,

Y – noise parameters set,

X – noise source parameters set,

$\{m_k\}$ – set of the other noises models.

This problem should be solved by the extraction of maximum disconnected samples and correction of dependencies during the parameters control rules definition.

Implementation. The simulator structure is similar to traditional (fig.1) and includes set of the controlled noise generators that output signals are summarized [2]. The main difference is controlled players instead generators (fig.2).
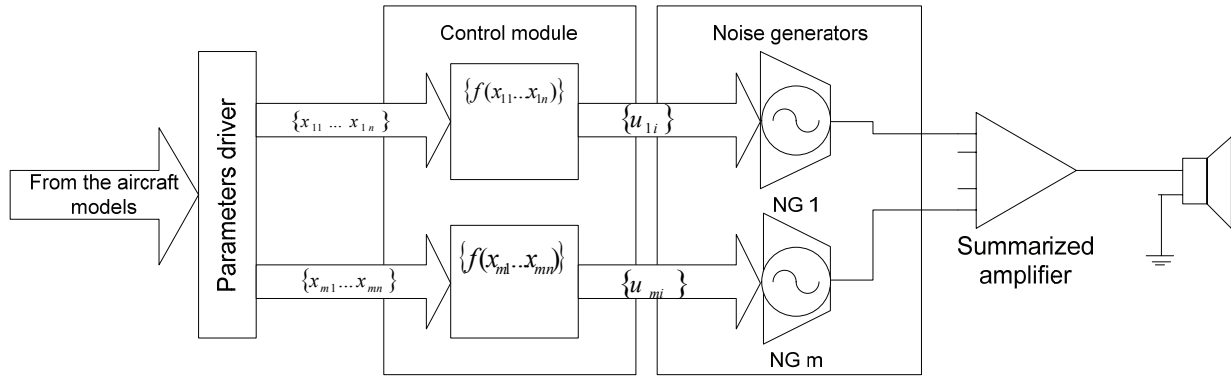
Fig.1. Traditional noise simulator structure

The playback can be controlled by speed for the frequency change effect, by volume and by several additional parameters, as the flange-effect, echo, etc. The playback mode can be one-time (for the one-time sounds, similar gear extension/retraction) and looped (for continuous, similar turbine or screw noise). The dependencies between the controlled players parameters and modeled aircraft parameters are executed by the special converters. Each converter can realize the function of the one parameter of player from the one or several parameters of the model. Usually, the playback speed is the function of the one parameter. The volume can be product of the single functions:

$$V = V_{\max} \times \prod_{i=1}^{n} f_i(x_i),$$

where V – playback volume;

$V_{\max}$ – maximum noise volume;

$f_i(x_i)$ – normalized function of parameter V from model parameter x_i.
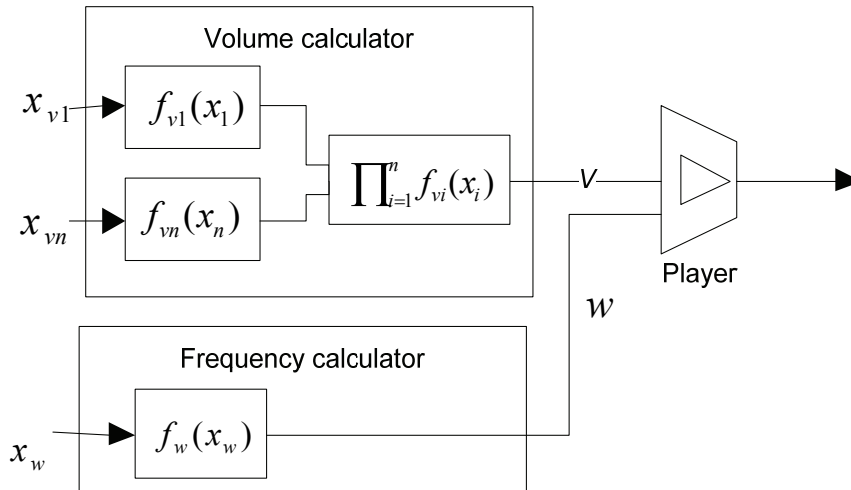
Fig.2. Structure of the controlled player – the noise simulator element

This elaboration is possible due to multiplicative character of the mechanisms volume dependencies. For example, the air screw volume depends multiplicatively on the rotor frequency and pitch (blade angle); wheel touch volume – on horizontal and vertical landing speeds. In these cases the control function can be realized as the product of the normalized approximation functions, defined for the each parameter. This approach enables to create the suitable user tool for the control function specification as the set of the aircraft parameters $\{x_i\}$ and functions $f_i(x_i)$, (fig.2) defined by the piecewise-linear approximation.

Noise simulator constructor provides the following:
- creation of the random number of the noise players;
- association the noise samples with players;
- definition of the dependencies of the noise players with the aircraft model parameters by the piecewise-linear approximation;
- tuning of the additional playback effects;
- noise players testing;
- GUI for the noise simulator developers;
- complex noise imitation testing with the parameters receiving;
- simulator compilation to the ready to use console application.

The constructor is implemented on the .NET platform by the C# language (fig.3). Software architecture is based on the «Model–View–Presenter» [3]. The division of model and presentation requires additional development effort but enables the separation the model and GUI, simplify the testing and permits to replace the GUI or model components.
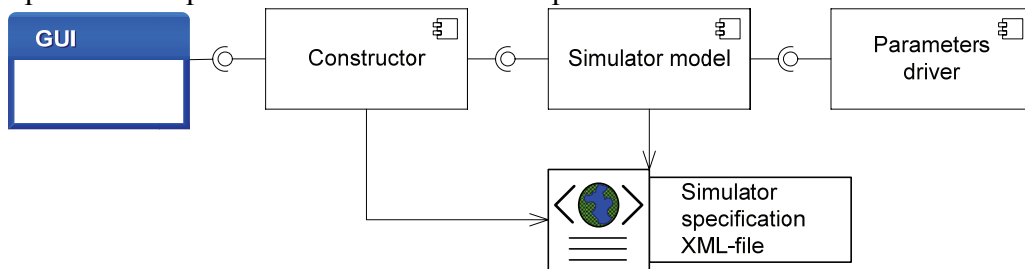
Fig.3. Architecture of the noise simulator constructor software

The simulator specification file example is shown on the fig. 4 and includes the airplane right screw noise description.

```xml
…
<sound name="Right screw" type="Continuous">
  <!—Sample file -->
  <soundFile>C:\sound-system\Sounds\Screw_1896.wav</soundFile>
  <!—Sound channel (Left/Right) -->
  <position>"Right"</position>
  <!-- Set of input volume parameters -->
  <volumeParameters>
   <parameter name ="R_SCREW_RPM">
   <!-- Volume approximation points table for the screw rotation -->
   <tableOfValues>
      <entry x ="0.0" y ="0.0"/>
      <entry x ="2700" y ="0.9"/>
      <entry x ="3800" y ="1.0"/>
    </tableOfValues>
   </parameter>
   <parameter name ="R_SCREW_PITCH">
   <!-- Volume approximation points table for the screw pitch -->
    <tableOfValues>
      <entry x ="0" y ="0.5"/>
      <entry x ="90" y ="1.0"/>
    </tableOfValues>
   </parameter>
  </volumeParameters>
   <!—Playback speed input parameter -->
  <frequencyParameter name ="R_SCREW_RPM">
   <!-- Frequency approximation points table for the screw rotation -->
   <tableOfValues>
      <entry x ="0" y ="0.0"/>
      <entry x ="1896" y ="1.0"/>
      <entry x ="3800" y ="2.0"/>
    </tableOfValues>
   </frequencyParameter>
  </sound>
       …
```

Fig.4. The part of the simulator specification XML-file

Simulator model is realizing the initialization and functioning of simulator and includes the samples players, control module and approximator.

The GUI permits to engineer to add/delete the noise sources, define their attributes and dependencies, and test them.

The parameters driver receives the required aircraft model parameters and notifies the simulator model.

Case study. This approach and constructor were applied during the reengineering of the flight simulator TL410M of National Aviation University [4]. The original pure hardware noise simulator [5] was out of order. Under the low-budget and aircraft inaccessible condition the developers (teachers, engineers and students of the computer science department) used the audio and video records from the L410 airplane cockpit [6] and proposed constructor. The result is the fully functional noise simulator that extends the features of original simulator [7].

Summaries

Formalization of the noise simulator enabled to create the software tools for the rapid construction of the flight simulator noise simulators, supporting their creation, testing and system integration.

The National Aviation University TL410 flight simulator reengineering case study demonstrates the approach and tool operability.

Approach requires the next research for the methods of the preliminary sample processing (influence filtering, spectral correction etc) and automation of the detection and correction of the samples interference.

References

1. *Alfred T. Lee.* Flight simulation: virtual environments in aviation. – Ashgate Publishing Limited. – 2005. – 147 p.
2. *David Allerton.* Principles of flight simulation. – *John Wiley and Sons Ltd. – 2009. – 457p.*
3. *Fowler, Martin.* Patterns of Enterprise Application Architecture . – Addison-Wesley Professional, 2002 – 560p.
4. *Сидоров Н.А., Хоменко В.А., Недоводеев В.Т., Сердюк И.П.* Реинженерия программного обеспечения информационно-моделирующих тренажерных комплексов. Управляющие системы и машины. – 2008. – № 4. – С.68-74.
5. Тренажер TL410. Техническое описание и инструкция по эксплуатации. Книга 5. – Praha, Rudy Letov. – 1979. – 75 с.
6. Audio and video records of L410 aircraft on AVSIM.SU site – http://www.avsim.su/files.phtml?uploader=2860.
7. Сайт тренажера TL410 Национального авиационного университета – https://sites.google.com/site/tl410nau/home.

UDC 378.1:004:303.732.4(477)

V. Dudnyk, U. Ryabokin, I. Mendzebrovskiy (National Aviation University, Ukraine)

METHOD OF DOMAIN ANALYSIS TO INFORMATION SUPPORT OF AIRCRAFT

We are presented method of domain analysis construction. The method is demonstrated an example of building a software remote instructor's aviation training system.

The task of re-use of software by identifying the objects or class of the same systems in a domain is solved by methods of domain analysis [1]. There are many methods of domain analysis and its implementation. But experience shows that the ways of domain analysis depend on the task, the experience of experts, the nature and state of the domain availability information for the domain analysis. This feature makes impossible the total automation of domain analysis and creation the design of the universal ways of its execution. On the other hand experience shows that there are actions performed by domain analysis and performed of any domain and for any original problem. A method that provides a domain analysis tools for solving a particular problem, given the specified characteristics.

Common objects and operations are likely to occur in multiple applications within a domain and thus are candidates for reusable components. A domain is analyzed by studying several of its representative systems and by developing an initial view of the structure and functionality of these systems. When familiarity with the domain has been achieved and the representative systems are understood, information used in developing these systems as well as their common and variable parts are identified, captured and organized for later reuse in developing new systems in that domain.

Domain analysis stresses the reusability of analysis and design, not code. This is done by deriving common architectures, generic models or specialized languages that substantially increase the power of the software development process in the specific problem area of the domain. Domain analysis can be seen as a continuing process of creating and maintaining the reuse infrastructure in a certain domain. Fig.1 shows the inputs, outputs, controls and mechanisms of domain analysis. A vertical domain is a specific class of systems. A horizontal domain contains general software parts being used across multiple vertical domains. Examples of horizontal reuse are mathematical function libraries, container classes.

Domain-specific reuse is usually accomplished by separating domain engineering and application engineering. The goal of domain engineering is to Domain Analysis identify objects and operations of a class of similar systems in a particular problem domain. Typical activities in domain engineering are domain analysis, architecture development, reusable component creation and component recovery and component management. Application engineering means software engineering taking the results of the domain engineering process into consideration, i.e., identifying reuse opportunities and providing feedback to the domain engineering process.

The essence of the method is that on the basis of the formalized description of processes of the domain analysis which should be carried out and by application of the created software tool means of the domain analysis are under construction are directed on its performance for a specific objective in the domain. Formalization of description processes is carried out by means of Real Time Process Algebra (RTPA) [2]
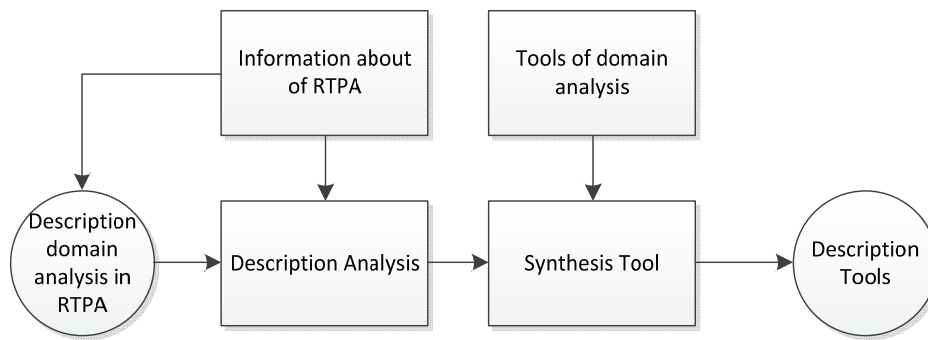
Fig. 1 Schema of method realization

The architecture of tools is presented in Fig. 1. In implementation of software tool used MS Office 2010, as part of the implementation of domain analysis. The work of tool consists of three steps.

The first step – formalized representation processes of domain analysis using RTPA.

The second step – analysis of process description and creation description of domain analysis processes which represented in MS Visio 2010

The third step – synthesis tool components in product dependency diagram on the set of components of MS Office 2010.

An example of tools for creating software remote trainers aviation training system.

The console of instructor is an integral part of aviation training system. It displays the information about the flight simulator and state. Existing consoles of most legacy simulators implemented hardware, outdated and physically worm out. This is the reason for replacement hardware control instructor for new hardware and software tools based on modern computer technology. When developing software remote trainer aircraft simulator, software development is one of the main problem.

To increase the flexibility of building interface elements and configure remote interface for different kinds of tasks used domain analysis.

The interface for the role of instructor is synthesized by selecting and setting certain interface elements: $r_{instr} = RV_{instr} \subseteq \{ei_i = (it\ , pf) \,|\, i = 1..l\}$ [3].

To build a software instructor indicator stand different types was used design pattern "Composite". The indicators are constructed as compositions of elements such as circular unit includes dial, arrow label and signature division of the scale. To create a specific interface element to determine the composition of elements and set the value of their attributes.

Based on domain analysis, classification and properties of elements based the specification hierarchy of classes. Pattern "Composite" is used as the basic architectural concept hierarchy. On the basis of hierarchy developed class library.

The class library is implemented using the technology of Windows Presentation Foundation, which is a part of .NET Framework 3.0. To create a remote interface element used markup language XAML, which is part of the Windows Presentation Foundation. The developer can build indicators of that type, including compositions for a variety of items from the library.

Software engineering is a unique discipline in which the objects of their studies require new forms of mathematics known as denotation mathematics in the treatment, modeling, description, specification, development, implementation, and maintenance of software systems. RTPA (Real-time process algebra) is developed as a coherent notation system and a formal engineering methodology for addressing the 3-D problem in software system specification, refinement, and implementation for both real-time and nonrelative systems. The type system, process notations, process relations, and process composing rules of RTPA are described. The system specification and refinement methodology of RTPA and case studies on real-world problems that demonstrate the descriptive power of RTAP as a powerful software engineering notation system will be provided in the following sections.

Real-Time Process Algebra (RTPA) is a set of formal notations and rules for describing algebraic and real-time relations of software processes [3].

A process is an abstract model of a unit of meaningful software behavior that represents a transition procedure of the system from one state to another by changing values of its inputs $\{I\}$, outputs $\{O\}$, controls $\{C\}$, requires $\{R\}$.

RTPA is designed as a coherent algebraic software engineering notation system and a formal engineering methodology for addressing RTPA can be used to describe both logical and physical models of a system. Therefore, logic views of the architecture of a software system and its operational platform can be described using the same set of RTPA notations as that for system behaviors. When the system architecture is formally specified, the static and dynamic behaviors that perform on the system architectural models can be rigorously described by a three-level refinement scheme at the system, class, and object levels in a top-down approach.

The software composing rules state that the RTPA *process relation system* R encompasses fundamental algebraic and relational operations elicited from basic computing needs, i.e.:

$$R = \{\rightarrow, |, |\ldots|\ldots, * R, R, i R, \|, \oint, \|\|, \gg,$$

A sequence, denoted by $\rightarrow$, is a process relation in which two meta processes P and Q are executed one by one, i.e.:

$$P \rightarrow Q$$

A *jump*, denoted by , is a process relation in which, on the termination of a process P, the system exits the linear sequence of processes, and invokes a designated process Q, i.e.:

$$P \curvearrowright Q$$

where Q is usually identified as a label or a logical address.

S - Name of process
N - Number of process
I - Input
O - Output
R - Require
C - Control
$\curvearrowright$ - Jump
$\rightarrow$ - Sequence

Considered the an example domain analysis which presented by one process (Fig. 2)[1]
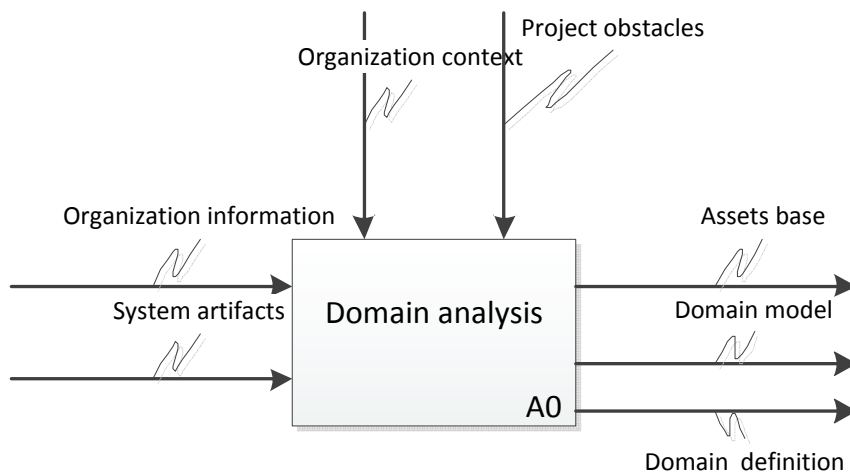
Fig. 2 Domain analysis

Output for this process are: organizational information – I1; system artifacts – I2; definition domain – O1; domain model – O2; base assets – O3; organizational context – R1; project obstacles– R2; plan domain – DP1; model domain – DP2; base assets engineering – DP3

Description of the process in RTPA is as follows:

Static
description

(Process Schema DOMAIN ENGINEERING = PN 0 ‖ { ProcessID: DOMAIN ENGEERING ({I:I1,I2};{O:O1,O2,O3};{R:R1,R2})} ‖ { DetailedProcesses: DP1, DP2, DP3 })

Dynamic
description

Process Dispatch ≙ § → (@Event1 DOMAIN ENGINEERING → {PN0:DP1,DP2,DP3})→ §
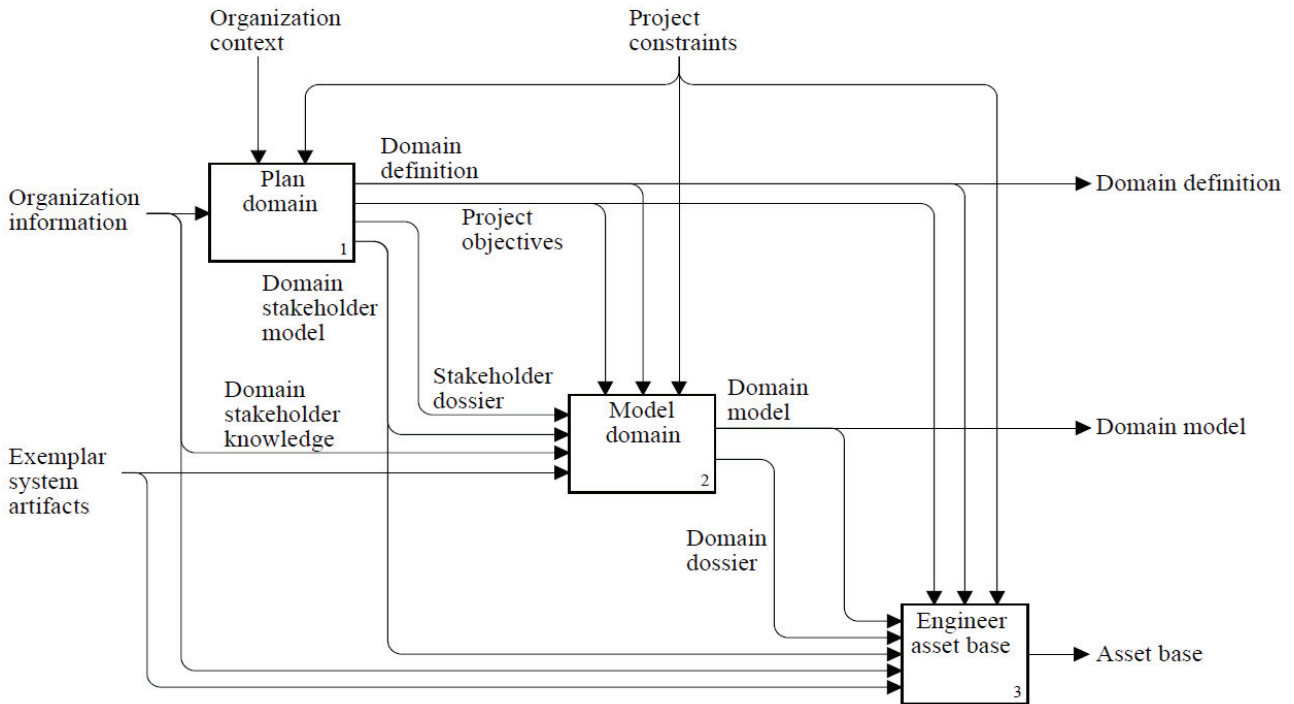
Fig.3 Domain analysis detailed diagram

Static
description

(Process Schema PLAN DOMAIN = PN 1
‖ {ProcessID: PLAN DOMAIN ({I: Organization information};{O: Domain definition, Project objectives, Stakeholder dossier, Domain stakeholder model};{R: Organization context, Project constrains})}
‖ {DetailedProcesses: DP1, DP2, DP3, DP4}
)
(Process Schema MODEL DOMAIN = PN 2
‖ {ProcessID: MODEL DOMAIN ({I: Stakeholder dossier, Domain stakeholder model, Domain stakeholder knowledge, Exemplar system artifacts};{O: Domain model, Domain dossier};{R: Domain definition, Project constraints, Project objectives})}
‖ {DetailedProcesses: DP1, DP2, DP3}
)
(Process Schema ENGINEER ASSET BASE = PN 3
‖ {ProcessID: ENGINEER ASSET BASE ({I: Domain model, Domain dossier, Domain stakeholder model, Organization information, Exemplar system artifacts};{O: Asset base};{R: Domain definition, Project constraints, Project objectives})}
‖ {DetailedProcesses: DP1, DP2, DP3 }
)
(Process DOMAIN ENGINEERING Relations = PN1:O1→PN2:R1; PN1:O2→PN2:R3; PN1:O3→PN2:I1;PN1:O3→PN2:I2; PN1:O1∼PN3:R1; PN1:O2∼PN3:R3; PN2:O1→PN3:I1; PN2:O2→PN3:I2
)

Dynamic
description

Process Dispatch ≙ § →
(@Event1 DOMAIN ENGINEERING → {PN1:DP1,DP2,DP3}
| @Event2 DOMAIN ENGINEERING → {PN2:DP1,DP2,DP3}
| @Event3 DOMAIN ENGINEERING → {PN3:DP1,DP2,DP3}
)
→ §

Diagram in graphical notation IDEF0 given in Fig.3. Diagram dependencies of components of MS Office 2010 shown in Fig.4
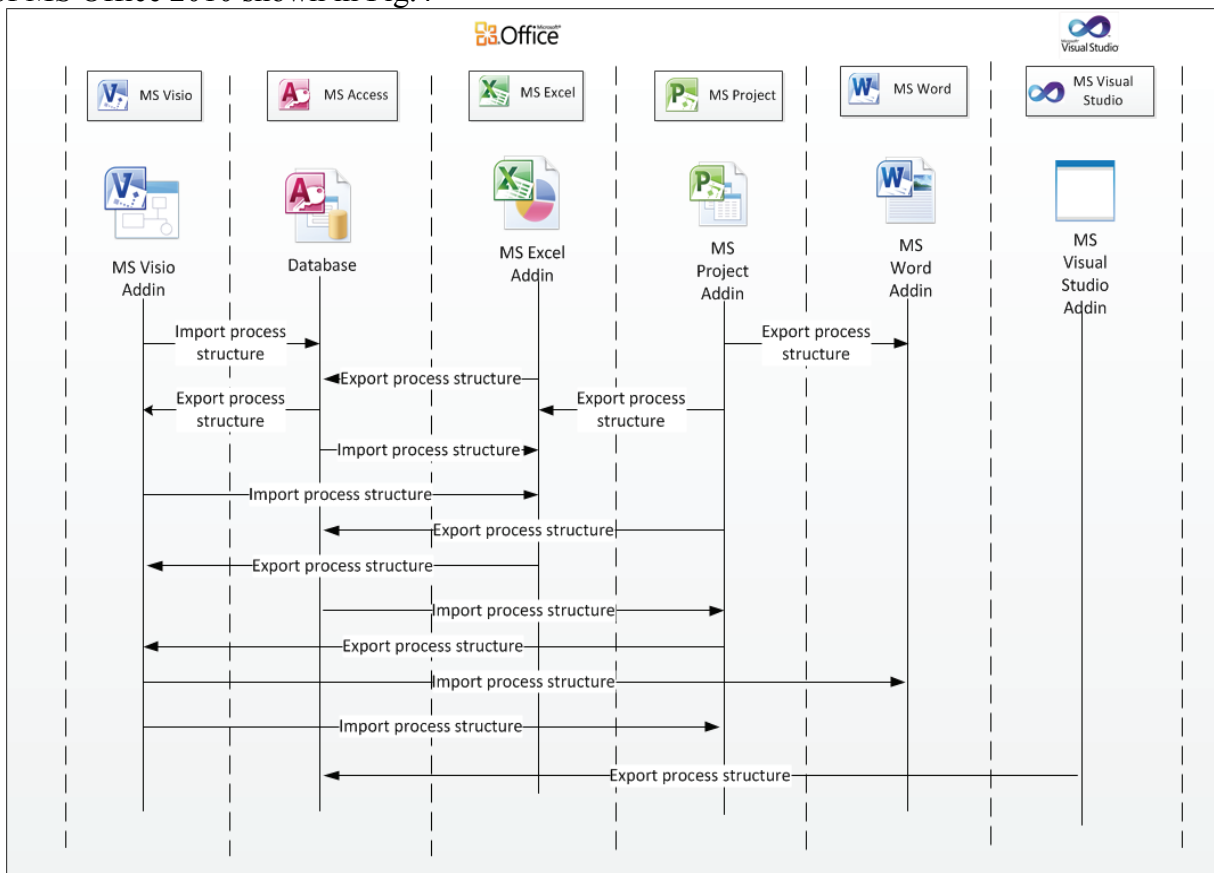
Fig. 4. Dependencies of MS Office 2010 components

We are presented method of construction of domain analysis. The method is demonstrated an example of building a software remote instructor's aviation training system. We have described aspects of domain analysis, benefits, activities and methods. The results of this work –developed MS Visio Add in, MS Project Add in, MS Excel Add in, MS Word Add in used MS Visual Studio 2010 and .NET Framework 4.0 and description of domain analysis processes used RTPA.

References

1. STARS. Organization Domain Modeling (ODM) Guidebook Version 2.0. STARS Technical Report D613-55159, STARS Technology Center, Arlington VA, July 1996.
2. Метод доменного аналізу в інженерії програмного забезпечення, *Дудник Валентин,* с.13, 2010 р.
3. Software Engineering Foundations, *Yingxu Wang,* pp. 217-271, 2008.

UDC 004.413

G.Y. Goloborodko (National Aviation University, Ukraine)

SOFTWARE OF THE GREEN INFORMATION SYSTEMS

Several aspects of the energy-saving approach in the information systems development are reviewed. The energy-saving standards APM and ACPI are described with examples of their efficient usage for hardware power management. Basic techniques for efficient usage of the system resources in development of software part of information systems are described. Recommendations for developers to write programs that ensure the optimal use of electricity and computer resource are given.

Introduction

The purpose of this report is the overview of existing standards and technolohies, that can be applied for the software development and can be applied for the implementation of the main aspect of the green information systems – energy conservation, making the recommendations for the application of the ACPI technology for the software in green information systems on the particular examples and making recommendations that can be used by developers in design and development of the information systems, that meet the requirements of greenness

Green information systems

Greenness of information systems is defined in three dimensions [4]:

1. Energy Conservation
2. Reduction of the harmful effects on the environment.
3. Making "green" data centers.

The object of this report is the first aspect of the green information systems – energy efficiency. In the context of the information system the energy saving is possible by reducing computer's power consumption by transferring it into a low power mode when it's not loaded. One of the mechanisms that provide lower power consumption is to increase the computational efficiency of the algorithms used in the information system, which leads to smaller loads on the computer, and accordingly, reduces the electricity spending. Computational efficiency is the computational complexity of the algorithm divided on the number of elements in the input data [14]

The implementation of the energy saving technologies is one of the areas, which is actualized by the so-called "green" software. Within this trend, the emphasis is on using software as a means of reducing the direct or indirect harmful effects on the environment. From the standpoint of Green Software is also important to minimize the use of primary (the amount of memory, time and speed) and secondary (the amount of external storage, distribution channels) computing resources [1], which will also be discussed and illustrated by examples in the context of the report.

Power interfaces

For the software control of the computer's hardware we need to have some interface that is implemented on the operation system level that will provide an oportunity to manage power consumption of the whole system or particular devices by calling methods of this interface – the power consumption inteface. This interface should be standardized for device manufacturers. Since 1992, created two similar interfaces - APM and ACPI. Currently, APM interface is deprecated and is no longer developed and supported in new operation systems.

ACPI Interface

ACPI (Advanced Configuration and Power Management) is an open industry standard that defines a common interface for detection of hardware, power management and configuration of the motherboard and devices. At the moment, the latest version of the ACPI specification is version 5.0, released on December 6, 2011. The task of ACPI is to provide interaction between the operating system, hardware and motherboard BIOS [7]. Standard ACPI was developed specifically to support

the technology OnNow. OnNow is the ideology of a computer device that is ready to resume the fast speed and get to work at any time [8].

ACPI defines the notion of a global system state. Every system state is characterized by a level of performance and energy consumption. The global system states are determined by the following criteria [7]:

- does the application work;
- what is the delay of their response to external events;
- what is the level of electricity consumption;
- whether to restart the operating system to return to normal functionality.

In addition, ACPI standard introduces the concept of the system system. System context is all the current data in systems that have not been saved to the hard drive [7].

List of states ACPI is shown in Table 1.

State name	State description
G0 (S0) (Working)	Normal operation. Average power consumption, maximum performance
G1 (Suspend, Sleeping, Sleeping Legacy)	Computer is turned off, but the current system context is saved, the work can be continued without a reboot. For each device is determined the "the degree of the information loss " in the process of falling asleep, and where information should be stored and from where it will be read upon awakening and time to wake up from one state to another (such as from a sleep state to working state).
G2 (S5) (soft-off)	The system is completely stopped, but energized and ready to wake up at any time. The system context is lost
G3 (mechanical off)	The mechanical system shutdown, ATX power supply is turned of

Table 1. Global system states in ACPI

The G1 state (Sleep) provides 4 substates that vary the level of energy consumption as well as the way to store and restore the system context.

In the ACPI there are separate states for the central processor (CPU) and all other devices – modems, monitors, network cards, video cards, etc. In each group, states are always present: the full functionality state, two states with limited functionality and reduced power consumption and physical turn-off state.

The software in green information systems should provide the efficient switching between the modes described by the power management interface (APM, ACPI) in the context of the whole system – switching the global system state, and in the context of a specific device – switching the device state.

Let us consider some possibilities for optimizing the use of certain computer components. Examples of specific software implementation of an interface to communicate with ACPI on a C ++ can be found in [9].

CPU

The CPU and video card are the major consumers of electricity in Dive Computers. It is obvious that during the idle processor must go to sleep state (G1 in the standard ACPI). In the case of multi-core processor with unused kernels they must go into low power mode until there will be nessessary to paralellize the task to be performed on multiple cores (Core Scheduling) [10].

RAM

During long idle of the memory the hibernatio technology can be used. It writes the contents of RAM to the drive for later retrieval and ability transite memory in sleep mode or low power consumption mode. This technology should be used, weighing the energy consumption associated with the writing and reading data from the hard drive. Energy costs can be compared, for example, using a PowerExecutive utility from IBM [11] or the eXtreme Power Supply Calculator utility [12].

Network

During the downtime, or a long-running data processing operations the unused devices can fall asleep for short periods of time. For real-time systems the transition into sleep states also can be done in the least busiest time of day. For systems that responds to the network requests, transition of the drives into sleep state can be done until the next network request (this technology is called "Wake On Lan"). In this case, obviously, there will be a certain delay for devices to wake, but the energy savings justifies these delays [10].

The Software level

Effective use of computer resources at the program level information system makes it possible to work while the computer or individual devices operate in low power mode ACPI. One of the ways of effective resources management is the use of specialized data processing algorithms, which can be difficult in the initial implementation, but provide fewer resources for the specific task. Examples are:
- fast sorting algothitms instead of those what are easier in implementation
- binary search instead of simple search where all the elements in the data input are analyzed;
- Shell sorting instead of QuickSort (QuickSort uses stack)
- list-based scattered matrix instead of array-based
- characteristic array sorting when sorted objects consume big amount of memory and their copying and transferring will be costly task

Also as the recommendations for programmers who are involved development of information systems we can give the following suggestions to make the information systems greener:
- Establish effective power consumption via ACPI.
- If the information system is the main executable program on the computer, the computer should be transited into low powe modes during the intervals when the IP does not receive data for processing.
- Use a multi-threaded processing.
- Ensure efficient heap allocation to prevent the memory leaks and dangling references.

Conclusion

The ACPI power interface thar is described in this report allows the developers of information systems, to use these interfaces to provide the first aspect of information systems greenness for their products. It is illustrated with specific examples. In addition to energy conservation aspect of the information system greenness another way is to minimize the use of basic and additional computing resources, so the recommendations that are given in this report allow the developers to ensure the efficient use of computing resources. "Greenness" of information systems is a topical and demanded area and requires further development. The above provisions may be used to ensure the sustainability of the offices within the "green office" project.

References

1. [Murugesan, 2011] San Murugesan. Green IT: helping to create a sustainable planet. [Электронный ресурс]: May, 2011. Режим доступа: http://www.computer.org/portal/web/computingnow/archive/may2011 .

2. [Chen, 2008] Adela J.W. Chen, Marie-Claude Boudreau, Richard T. Watson, (2008) "Information systems and ecological sustainability", Journal of Systems and Information Technology, Vol. 10 Iss: 3, pp.186 - 201

3. [Сидоров, 2010] Н.А. Сидоров. Экология программного обеспечения. Інженерія програмного забезпечення №1, 2010.

4. [Velte, 2008] Toby Velte, Anthony Velte, Robert Elsenpeter. Green IT [Электронный ресурс]: McGraw-Hill Prof Med/Tech, 2008, p. 45-62. Режим доступа:

http://books.google.com.ua/books?id=xPQZqKrJN7oC&printsec=frontcover&hl=ru&source=gbs_ge_summary_r&cad=0#v=onepage&q&f=false

5. [WWF Finland, 2011]: WWF, Finland. Green Office: Environmental Management System For Sustainable Organisations. [Электронный ресурс]: 2011. Режим доступа: wwf.fi/mediabank/1414.pdf

6. [Intel, 1996] Intel Corporation. Microsoft Corporation. Advanced Power Management (APM). BIOS Interface Specification. [Электронный ресурс]: February, 1996. Режим доступа: http://download.microsoft.com/download/1/6/1/161ba512-40e2-4cc9-843a-923143f3456c/APMV12.rtf

7. [HP, 2011] ADVANCED CONFIGURATION AND POWER INTERFACE SPECIFICATION. Revision 5.0, [Электронный ресурс]: December 6, 2011. Режим доступа: www.acpi.info/DOWNLOADS/ACPIspec50.pdf .

8. [Михайлов, 2000] Дмитрий Михайлов. Управление питанием и реализация ACPI в Windows 2000 - теория и практика. [Электронный ресурс]: 2000. Режим доступа: http://www.ixbt.com/mainboard/acpi-win2000-pract.html

9. [MSDN, 2001] MSDN. Windows Instrumentation: WMI and ACPI [Электронный ресурс]: December 4, 2001. Режим доступа: http://msdn.microsoft.com/en-us/windows/hardware/gg463463.aspx#EQE .

10. [Webber, 2009] Lawrence Webber, Michael Wallace. Green Tech: How to plan and implement sustainable IT solutions, AMACOM, 305 p. 2009, p. 54-100.

11. IBM Power Executive. [Електронний ресурс]. Режим доступу: http://www-03.ibm.com/systems/management/director/about/director52/extensions/powerexec.html .

12. eXtreme Power Supply Calculator v2.5 [Электронный ресурс]. Режим доступа: http://www.extreme.outervision.com/psucalculator.jsp

13. [Visser, 2010] Joost Visser. What could be green about software? [Электронный ресурс]: 2010. Режим доступа http://www.slideshare.net/jvlasveld/presentation-joost-visser-sig-what-can-be-green-about-software-workshop-green-software-architecture-green-it-amsterdam-and-sig.

14. [Разборов, 1999] А. А. Разборов О сложности вычислений // Математическое просвещение. — МЦНМО, 1999. — № 3. — С. 127-141.

15. [Рихтер, 2007] Джеффри Рихтер. CLR via C#. Программирование на платформе Microsoft .NET Framework 2.0 на языке C#, Питер, 2007 г, 656 с., с.573-607.

16. [Мэттсон, 2006] Тим Мэттсон. Введение в технологии паралельного программирования. [Электронный ресурс]: 2006. Режим доступа: http://software.intel.com/ru-ru/articles/writing-parallel-programs-a-multi-language-tutorial-introduction/ .

17. [Erikson, 2010] Cal Erikson. Memory Leak Detection in C++ [Электронный ресурс]: Linux Journal #110, June 2003. Режим доступа: http://www.linuxjournal.com/article/6556 .

18. [Асеев, 2007] Асеев Г.Г. Электронный документооборот. Учебник. – К.: Кондор, – 2007. – 500 с.

19. [Server Technology, Inc., 2008] Measuring Power & Efficiency in the "Green" Data Center [Электронный ресурс]: 2010. Режим доступа: http://www.missioncriticalmagazine.com/ext/resources/MC/Home/Files/PDFs/WP_MeasuringPowerAndEfficiency.pdf

20. [Schulz, 2009] Greg Schulz, The Green And Virtual Data Center, 2009, Taylor & Francis Group, LLC, 398 p..

21. [Stanley, 2007] J.R.Stanley, K.G.Brill, J.Koomey, Four Metrics Define Data Center "Greenness". [Электронный ресурс]: 2007. Режим доступа:http://uptimeinstitute.org/wp_pdf/(TUI3009F)FourMetricsDefineDataCenter.pdf .

22. [The Green Grid, 2007] The Green Grid Data Center Power Efficiency Metrics: PUE and DCiE,.

23. [Greenpeace, 2010] Как сделать офис зеленым. Рекомендации Гринпис России. - М.: ОМННО «Совет Гринпис», 2010, 68 с.

24. [Portaland Office of Sustainable Development, 2001] Portaland Office of Sustainable Development, Green Office Guide. [Электронный ресурс]: 2001. Режим доступа: http://www.oregon.gov/ENERGY/CONS/BUS/docs/Green_Office_Guide.pdf .

UDC 004.413 (043.2)

O.O. Grinenko, Postgraduate student (National Aviation University, Ukraine)

MODELS OF SOFTWARE ECOSYSTEMS

The definition of the software ecosystem as part of software ecology, models of software ecosystem, the main types of elements of software ecosystems are considered.

Introduction

Recently, the term "ecosystem" was adopted in the software to identify the socio-technical objects and subjects that are formed during its creation, operation and maintenance. In the context of the ecological approach, software is considered as a technical object that interacts with the environment, and development of software products subject to study Ecology Engineering.

Software Ecosystems

The notion of ecosystems originates from ecology and means a community of living organisms (plants, animals and microbes) in conjunction with the nonliving components of their environment (things like air, water and mineral soil), interacting as a system. The concept of "software ecosystem" is widely used by companies and researchers of the software. Researches into software ecosystems are represented by several works. Throughout this thesis we will consider a few definitions of software ecosystems. In [8] software ecosystem is a set of actors functioning as a unit and interacting with a shared market for software and services, together with the relationships among them. These relationships are frequently underpinned by a common technological platform or market and operate through the exchange of information, resources and artifacts. The transaction between two software vendors is centered around software components and software services. In this thesis a definition of software components is used: software component a bundle of software functions accessible through a single interface or carrying a single name which is or can be used as an element in other software packages but of which the core functionality is developed separate from these packages. A software service is a software component accessible via communications outside the users native environment. User can be both human and non-human. Native environment changes depending on the user. If the user is human, the native environment is most probably his or her own computer. If the user is a software package, the native environment consists of the compiled or interpreted code.

Another definition of software ecosystem is given in [7]. The discussion of software ecosystems is started from the notion of human ecosystem. A human ecosystem consists of actors, the connections between the actors, the activities by these actors and the transactions along these connections concerning physical or non-physical factors. For the discussion in this paper, we further distinguish between commercial and social ecosystems. In a commercial ecosystem the actors are businesses, suppliers and customers, the factors are goods and services and the transactions include financial transactions, but also information and knowledge sharing, inquiries, pre- and post-sales contacts, etc. Social ecosystems consist of users, their social connections and the exchanges of various forms of information. A software ecosystem consists of the set of software solutions that enable, support and automate the activities and transactions by the actors in the associated social or business ecosystem and the organizations that provide these solutions. Of course, a software ecosystem is also an ecosystem, specifically a commercial ecosystem, and hence the goods and services are the software solutions and software services that enable, provide support for or automate activities and transactions.

Corporation "Microsoft" defines software ecosystem as a set of interactions and mutual influences of organizations (public, educational and commercial) and individuals that work with software [6].

In thesis "Reverse Engineering Software Ecosystems" [11] software ecosystem is considered as a abstraction level of software products and projects that can be described by analyzing the lower

levels. The author proposes a method and means for reverse engineering of ecosystems, which essence is to analyze the information components of projects for high-levels ideas that characterize the organization of software components and determined by the social structure.

In [15] the authors describe software ecosystems and the typical elements of ecosystems and their context, namely:
- software and its role in IT;
- users of software;
- software creating processes;
- management of the establishment and maintenance of software;
- supply and support of software;
- communication network of state agencies;
- software economy.

In the report of the Software Engineering Institute [14], dedicated Ultra-Large-Scale Systems, the authors consider that the industry tends to use concepts of ecosystems to describe the socio-technical systems of software. The authors explain this image of modern software Ultra-Large-Scale Systems scale dynamic communities of independent and competing organisms in a complex changing environment, where people, computing devices and organizations are organisms.

Considering the software as ecosystem it is necessary to consider internal and external interaction. External interaction is characterized by the presence of other ecosystems that are part of the software or are related to other software. The main objective is to create models of ecosystem models and their evolution. Internal interactions are characterized by the presence in the software program-clone, software agents and others. The objective of this study is its software operation, principles of cooperation programs, etc.

Models of Software Ecosystems

Ecosystem software is an artificial complex that includes the software, environment of its development, operation, maintenance and utilization associated with each exchange of software and intelligence. A software products and services, producers of products and services, customers, contacts are the main elements of ecosystem. It is important to create models of software ecosystems. We use the following representation for describing the software ecosystem: i*(figure 1), UML and Petri nets.
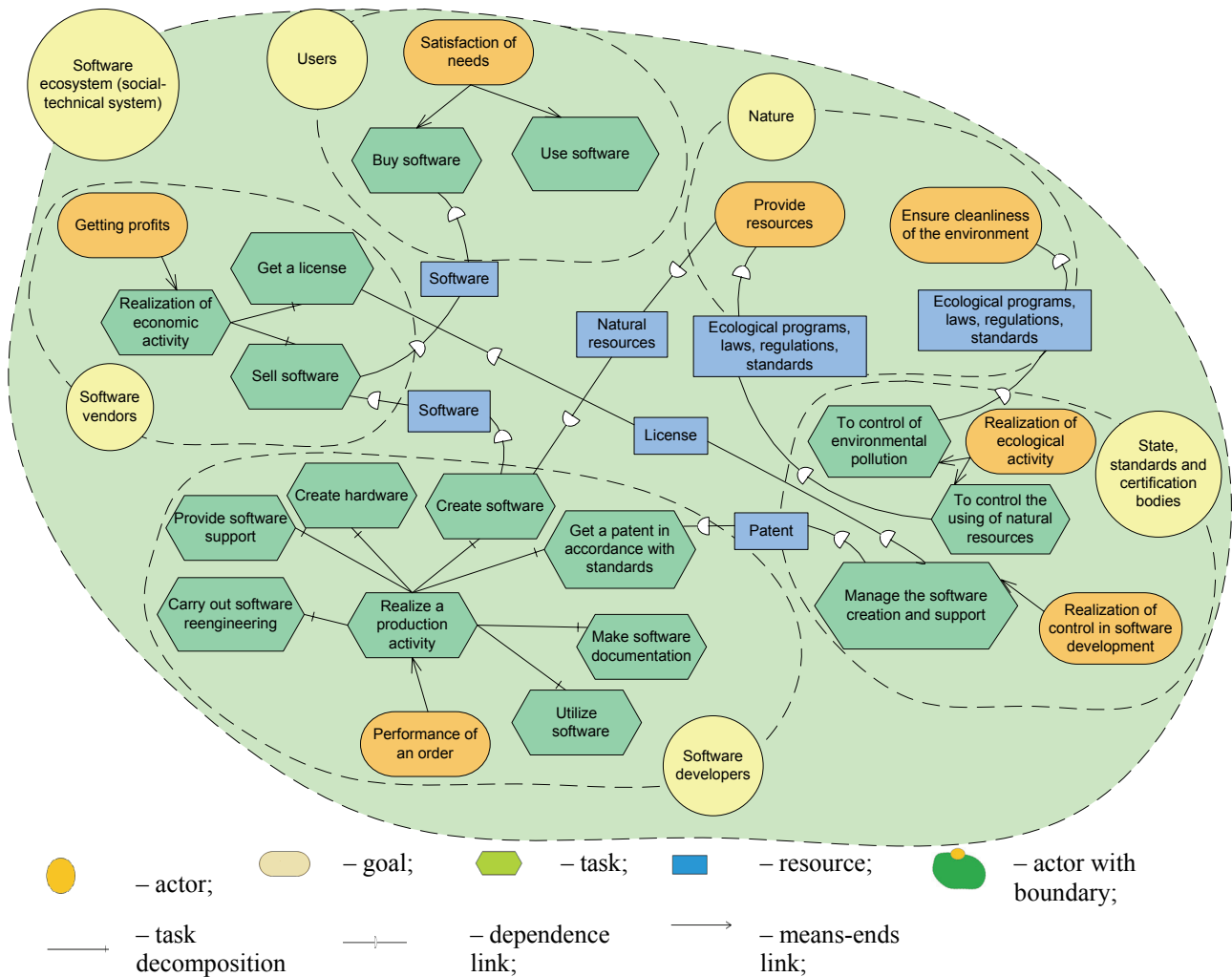
Figure 1. I* software ecosystem model

In practice, modeling systems have often to solve problems related to formalize description and analysis of cause-effect relationships in complex systems, in which several parallel processes are run. The most common currently formalism that describes the structure and interaction of parallel systems and processes is a Petri net.

Formally, Petri net is given as 4-tuple:

$$G(V, E, I, O), \text{ where}$$

V – set of positions, $V \neq \emptyset$,

E – set of transitions, $E \neq \emptyset$, $V \cap E \neq \emptyset$,

I – input function (direct function of incidence)

$I: V \times E \rightarrow \{0,1\}$,

O – output function (the inverse function of incidence)

$O: E \times V \rightarrow \{0,1\}$.

$I(e_j) = \{v_i \in V | I(v_i, e_j) = 1\}$,

$O(e_j) = \{v_i \in V | O(e_j, v_i) = 1\}$,

$I(v_i) = \{e_j \in E | I(e_j, v_i) = 1\}$,

$O(v_i) = \{e_j \in E | O(v_i, e_j) = 1\}$, $i = 1, \ldots, n$, $j = 1, \ldots, m$, $n = |V|, m = |E|$.

For this system the goals and objectives will be presented by a set of positions, and relationships between objects will be a set of transitions. Analytical representation of system, using Petri nets, has the following form:

$$V = \{n_i, d_j, r_s, p_q, k_t | i = \overline{1,2}; j = \overline{1,5}; s = \overline{1,10}; q = \overline{1,4}; t = \overline{1,3}\};$$
$$E = \{t_m | m = \overline{1,6}\};$$

$$I(t_1) = \{n_1\} \qquad\qquad O(t_1) = \{r_4\}$$
$$I(t_2) = \{1\} \qquad\qquad O(t_2) = \{d_2, d_3\}$$
$$I(t_3) = \{d_2\} \qquad\qquad O(t_3) = \{n_2\}$$
$$I(t_4) = \{d_3\} \qquad\qquad O(t_4) = \{n_1\}$$
$$I(t_5) = \{d_4\} \qquad\qquad O(t_5) = \{d_5\}$$
$$I(t_6) = \{d_5\} \qquad\qquad O(t_6) = \{r_3\}$$
$$I(t_7) = \{r_1\} \qquad\qquad O(t_7) = \{r_2\}$$
$$I(t_8) = \{r_2\} \qquad O(t_8) = \{r_3, r_4, r_5, r_6, r_7, r_8, r_9, r_{10}\}$$
$$I(t_9) = \{r_4\} \qquad\qquad O(t_9) = \{p_3\}$$
$$I(t_{10}) = \{p_1\} \qquad\qquad O(t_{10}) = \{p_2\}$$
$$I(t_{11}) = \{p_2\} \qquad\qquad O(t_{11}) = \{p_3, p_4\}$$
$$I(t_{12}) = \{p_3\} \qquad\qquad O(t_{12}) = \{k_2\}$$
$$I(t_{13}) = \{k_1\} \qquad\qquad O(t_{13}) = \{k_2, k_3\}$$

Petri nets are used to describe the modeling of events of arbitrary duration. In this case, the model was built using Petri nets, reflects only the order of occurrence of events in the studied system. To display the time parameters of the system that is modeled using Petri nets, extension staff Petri nets: temporal nets, E - nets, Merlin nets, etc [5].

Model of software ecosystems can be represented in UML by Use Case Diagram. Use Case Diagram is a graphical tool of specification requirements, which used to determine the following:
- overall limits and context of the domain,
- general requirements for the functional behavior of the projected;
- interaction of the proposed project and with the outside world.

Conclusion

The software creates organizational and technical systems, which appear, develop and degrade like natural biological systems. Software ecology is a term that affects the exploration properties, behavior and laws of software systems and their impact on environment and human activities. Software ecosystems play a key role in the study of software ecology. Further investigation of ecosystems software may be associated with the identification and formalization of software ecosystem types and with development of recommendations for the establishment and maintenance of software ecosystems.

References

1. [*Любимский, 2009*] Любимский Э.З. На пути к построению общества программ //Программирование. – 2009. - №1. – С. 4 – 10.

2. [*Мазур, 1999*] Мазур И.И., Молданов О.И. Курс инженерной экологии. – М.: Высшая школа, 1999. – 447 с.

3. [*Кондратюк, 1987*] Кондратюк Є. М., Хархота Г. І. Словник-довідник з екології. — К.: Урожай, 1987. — 160с.

4. [*Сидоров, 2010*] Сидоров Н.А. Экология программного обеспечения //Інженерія програмного забезпечення. – Київ. – 2010. – № 2. – С. 1 – 9.

5. [*Советов, 2001*] Советов Б.Я., Яковлев С.А. Моделирование систем. – М.: Высшая школа, 2001. – 344 с.

6. [*Хоменко, 2011*] Хоменко В.А. Экосистемы програмного обеспечения// Вісник НТУ. – Київ, 2011. - № 23. – С. 114 – 118.

7. [*Bosh, 2009*] Bosch J. From Software Product Lines to Software Ecosystems// 13th International Software Product Line Conference. – San Francisco, August 24 – 28, 2009. – P. 1–10.

8. [*Duinkerken, 2009*] Duinkerken W. Transaction Cost Economics in Software Ecosystems: some empirical evidence. – April 20, 2009. – P. 22 – 37.

9. [*Florina, 2000*] C. Florina. The digital ecosystem – creating digital divides. – Conf. Proc. – oct. 16. 2000.

10. [*Jansen, 2009*] Jansen S., Finkelstein A., Brinkkemper. A sense of community: A research agenda for software ecosystems// 31th International Conference on Software Engineering, New and Emerging Research Track. – 2009.

11. [*Lungu, 2009*] M.F. Lungu. Reverse Engineering Software Ecosystems. – Doct. Diss. – USI. – 2009. – 208 p.

12. [*Messershmitt, 2003*] D.G. Messershmitt, C. Szyperski. Software Ecosystems: Understanding an Indispensable Technology and Industry. – London: MIT press, 2003. – 233 p.

13. [*Schulz, 2009*] G. Schulz. The Green and Virtual Data Center. // Taylors Francis G. – 2009. – 218 p.

14. [*Veley, 2008*] Y. Velye, A. Velye, R. Elsenpeter Green IT: Rednee your Information systems Environmental input while adding to the bottom line. – 2008.

15. [*Webber, 2009*] L. Webber, M. Wallance Green Tech: thow two and to plan implement sustain – able IT solutions. – FBACOM. – 2009. – 29 p.

I.O. Kovrizhkin (National Aviation University, Ukraine)

DEFINING THE "TRIANGLE OF VELOCITIES" ON INDIRECT INFORMATION FROM THE GPS

The article presents a method of indirect determination of the vector of wind speed and airspeed through the data obtained only from the GPS system. This method is recommended for use in a light unmanned aerial machines class micro or mini, does not require installation of additional equipment.

The problem of determining the wind speed in aircraft is generally solved by using the "triangle of velocities."

$$\mathbf{W} = \mathbf{V} + \mathbf{U}$$

Where $\mathbf{W}$ – the aircraft speed over ground, $\mathbf{V}$ – airspeed (the aircraft speed in relation to atmosphere) and $\mathbf{U}$ – the wind speed.

With a seemingly simple solution, the practical realization of its demands serious hardware support. Let us note that all values are the vectors, which implies the need to determine not only the modulus of air velocity $|\mathbf{V}|$, and the angular orientation of the aircraft. Pay attention to the fact that all vector quantities, which in turn implies the need to determine not only the modulus of the air velocity $|\mathbf{V}|$, but the angular orientation of the aircraft. Only for the determination of the $\mathbf{V}$ – vector, we need a system of air signals (SAF) and the system of angles (roll, pitch, course).

To determine the ground speed of aircraft the expensive Doppler meters (DISS) and / or dead reckoning system are used. The use of traditional methods for UAV of "small" classes (mini, micro) is problematic. First of all, these are unacceptable on the UAV because of the size and weight specifications of the equipment and according to their energy supply and high cost. However, the definition of air speed and wind speed on the aircraft of such classes is rather important, for example for the uncontrolled delivery of cargo by parachute landing on a limited surface area.

Typically, the UAVs of mentioned classes use relatively inexpensive system of satellite navigation (SSN) as the primary navigation device. Along with the geographical coordinates, the speed over ground $|\mathbf{W}|$ and the angle of the course (azimuth ψ) is sent from the output of the GPS receiver.

Let us consider the possibility of determining the wind velocity at such minimum of information support. The problem can be solved with two main assumptions that are quite acceptable for a number of practical problems.

1. The wind speed is constant and the horizontal (no vertical component).
2. The aircraft does a turn (non-rectilinear flight) in horizontal control surface, with a constant (for the time of maneuver, 5 ... 40 seconds) air velocity.

Thus, to determine the wind immediately before use (for example, when approaching to discharge cargo) the aircraft has to make a turn. Note that the assumption 1 is generally accepted in solving the ballistic task [2].

Let's examine the aircraft movement in the horizontal plane. We denote the horizontal plane with axes XgYg (index g denotes horizontal earth coordinate system that doesn't spin). Direction of axes is unprincipled, but certainty Xg can be considered as axis directed to north. Let's assume that two vectors of speed over groung are known (we know the module of speed and angle of the course) $\mathbf{W1}$ and $\mathbf{W2}$.
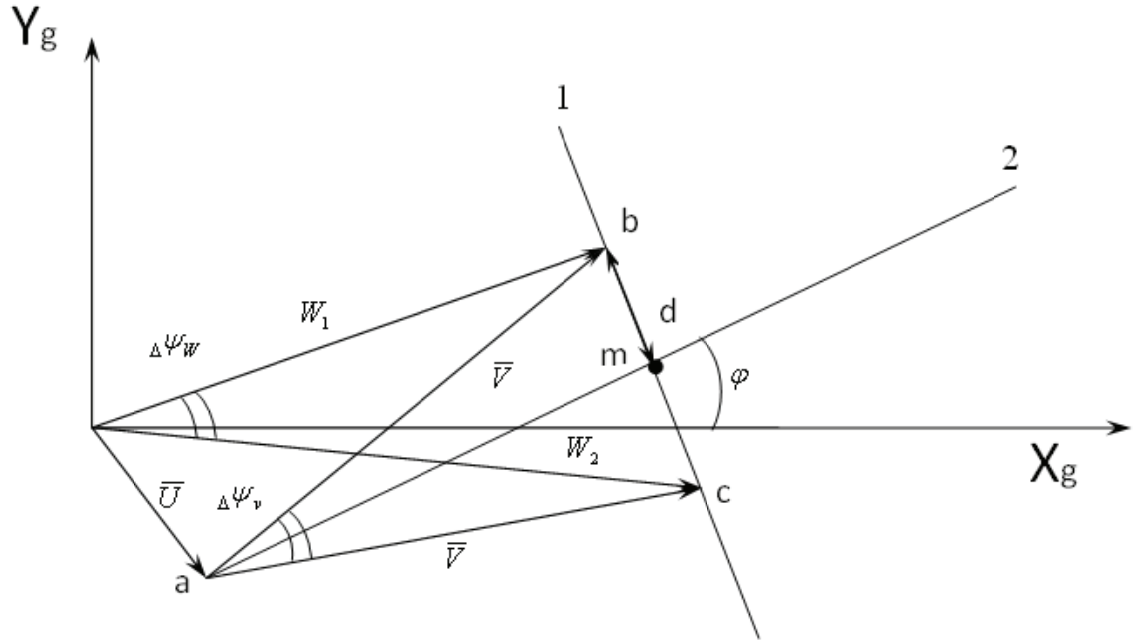
Pic. 1.

Let us join two ends of the vectors **W1** and **W2** – this is the **bc** segment that is situated on the straight line **1**. (Pic. 1).

The triangle **abc** is isosceles because of the assumption **2**. Let's mark the point in the middle of the **bc** segment with letter **m**. And draw the straight line **2** through the a and m points.

Let's find the equation of the line **1** in **A1x+B1y+C1=0** form. Substituting the values of the coefficients we get:

$$\overbrace{(W_1y - W_2y)}^{A_1}x + \overbrace{(W_2x - W_1x)}^{B_1}y + \overbrace{(W_1x \times W_2y - W_2 \times W_2y)}^{C_1} = 0;$$

The other form of the line is **y=kx+b** (where **k** is tangent of the angle between the axis of abscissas and the line). So the equation for the line **1** will be:

$$k_1 = -\frac{A_1}{B_1}$$

Let us find the equation of line 2, it goes through the point m, which coordinates are:

$$m = \begin{bmatrix} \frac{1}{2}(W_2x - W_1x) + W_1x \\ \frac{1}{2}(W_1y - W_2y) + W_2y \end{bmatrix} = \begin{bmatrix} m_x \\ m_y \end{bmatrix}$$

And is perpendicular to line **1**:

$$k_2 = -\frac{1}{k_1} = \frac{B_1}{A_1}$$

1.10.29

Let's find the coefficient b_2 of the line **2**: $y_2 = k_2 x_2 + b_2$;

$$b_2 = y_2 - k_2 x_2 = m_y - k_2 m_x;$$

So the angle will be: $\varphi = arctg(k_2)$.

And the equation of line 2 will take the next form:

$$y_2 = \frac{B_1}{A_1} x + (m_y - \frac{B_1}{A_1} m_x);$$

Now let's define the distance of |ma| (height) and V - Sidebar of the triangle:

$$d = \frac{|bc|}{2} = \frac{1}{2}\sqrt{(W_{1x} - W_{2x})^2 + (W_{1y} - W_{2y})^2};$$

Then: $\dfrac{d}{V} = \sin\left|\dfrac{\Delta\psi_v}{2}\right|; \qquad V = \dfrac{1}{\sin(\Delta\psi_v/2)} \times d \qquad (|\Delta\psi_v| > 0);$

$$p = |ma| = \frac{1}{tg(\Delta\psi_v/2)} \times d = \sqrt{V^2 - d^2};$$

The projection of a segment ma on the x and y axes:

$$p_x = p \cdot \cos\varphi = p \cdot \cos(arctg(k_2))$$
$$p_y = p \cdot \sin\varphi = p \cdot \sin\varphi$$

Finally we can get the obtained value:

$$U = \begin{bmatrix} U_x \\ U_y \end{bmatrix} = \begin{bmatrix} a_x \\ a_y \end{bmatrix} = \begin{bmatrix} m_x - p_x \\ m_y - p_y \end{bmatrix}$$

Note that, by virtue of the hypotheses adopted, the proposed method of determination of the components of the wind is accepted only in the horizontal plane. By itself, this fact is acceptable for most practical purposes with the use of UAVs. Since the vertical wind component is significant only in mountainous terrain at relatively small heights above the surface. Usually in such cases the technique is not acceptable.

Another feature of the practical side of the above approach is the fact that aircraft follow a horizontal maneuver type "right bank". For guided fly right bank is the main "classical" element of piloting and does not cause difficulties. However, analysis of UAV flights that were available to the author shows that the performance of superelevation on some samples UAV is plot "failure height" in the first seconds of rotation. This is because in the automatic control system (ACS) UAV equipped control the rate and pitch (height) are autonomous. And elimination of loss of height

caused by the appearance of rotation offset from the delay. Very little law of ACS can compensate for this fact.

Another feature of the practical side of described the approach is the fact that aircraft is necessary to perform a horizontal maneuver type of "the correct turn". For guided flights the correct turn is the main "classical" element of piloting and does not cause difficulties. However, analysis of the UAV flights that were available to the author shows that the performance of super elevation on some samples of Drones has the area with "failure in height" on the first seconds of rotation. This is because of the automatic control system (ACS) that UAV is equipped with. Control of the rate and pitch (height) are autonomous.

The analysis confirms the efficiency of simulation methods, the performance of the UAV turning at the rate of about 30 degrees showed that the wind speed estimation error was the about 3 ... 5%.

So we brought the method of estimating the vector of wind speed measurements from GPS. We must bear in mind the following observations:

Method determines the definition of 2-components of the wind vector;

Method reports wind in real-time; Individual assessment of wind can be used for making calculations in real time, or it has to be filtered (averaged) to provide a generalized assessment of wind;

In order to the make method work, the aircraft must change the course of flight.

References:

1. *Горелин И.С., Коврижкин О.Г., Королев В.В.* - Авиационные прицельно-навигационные системы. К.: КИВВС, 1996. – 475 с.

2. *Коврижкин О.Г., Коврижкин И.О.* - Блок аеродинамічного корегування польотом авіаційної бомби з використанням сигналів супутникової навігації. Тез. доп. «Створення та модернізація озброєння і військової техніки в сучасних умовах», Киев, 2010, С. 170-171.

A.G. Petruk (National Aviation University, Ukraine)

HIGH-AVAILABILITY SOFTWARE ARCHITECTURE STYLES

Availability are important quality attributes of today's software. So it is necessary to address these aspects at the architectural level. Architectural styles enable reuse for create high-availability software. This paper presents the basic notions and explains why it's convenient to focus on styles.

1. Introduction

Architecture software – this view isthe main structural, functional properties and consumer software. Software architectureis composed ofthree types ofelements- components, connectorsand data. Components encapsulate some functionality and connectors make the interaction between components[1].

The main task of the architect in the development of mission critical systems (on-board aircraft systems, financial and banking systems, enterprise level systems) are provide availability of software system.

Availability is concerned with system failure and its associated consequences. A system failure occurs when the system no longer delivers a service consistent with its specification[2]. Such a failure is observable by the system's users – either humans or other systems.

Among the areas of concern are how system failure is detected, how frequently system failure may occur, what happens when a failure occurs, how long a system is allowed to be out of operation, when failures may occur safely, how failures can be prevented, and what kinds of notifications are required when a failure occurs.

We need to differentiate between failures and faults. A fault may become a failure if not corrected or masked. That is, a failure is observable by the system's user and a fault is not. When a fault does become observable, it becomes a failure. For example, a fault can be choosing the wrong algorithm for a computation, resulting in a miscalculation that causes the system to fail.

Once a system fails, an important related concept becomes the time it takes to repair it. Since a system failure is observable by users, the time to repair is the time until the failure is no longer observable. This may be a brief delay in the response time or it may be the time it takes someone to fly to a remote location in the mountains of Peru to repair a piece of mining machinery.

The distinction between faults and failures allows discussion of automatic repair strategies. That is, if code containing a fault is executed but the system is able to recover from the fault without it being observable, there is no failure.

The availability of a system is the probability that it will be operational when it is needed. This is typically defined as

$$\text{Availability} = \frac{\text{mean time to failure}}{\text{mean time to failure} + \text{mean time to repair}}$$

2. Availability tactics.

Architectural properties can be divided into functional properties achieved by the system, and non-functional properties such as ease of expansion, the ability to reuse components, efficiency, often called the qualitative features[3].

The properties are the result of architectural constraints. Restrictions are often motivated by the properties of architectural elements. For example, pipe and filter style obtains property of reusable components and configuration flexibility of applications using common interfaces for its components - limiting components to a single type of interface.

Achieving quality attributes must be considered throughout design, implementation, and deployment. No quality attribute is entirely dependent on design, nor is it entirely dependent on implementation or deployment.

Quality attributes are divided intothree classes: Qualities of the system (availability, modifiability, performance, security, testability, and usability); Business qualities; Qualities of the the architecture.

For the implementation of quality attributes in software architecture used - tactic. Tactics - is afundamental design decisions that affect the management response to the attributes of quality [3].Illustration of the tactics available is presented in Figure 1. The collectionof tactics called - an architectural strategy[4].All approaches to maintaining availability involve some type of redundancy, some type of healthmonitoring to detect a failure, and some type of recovery when a failure is detected. In some cases, the monitoring or recovery isautomatic and in others it is manual.
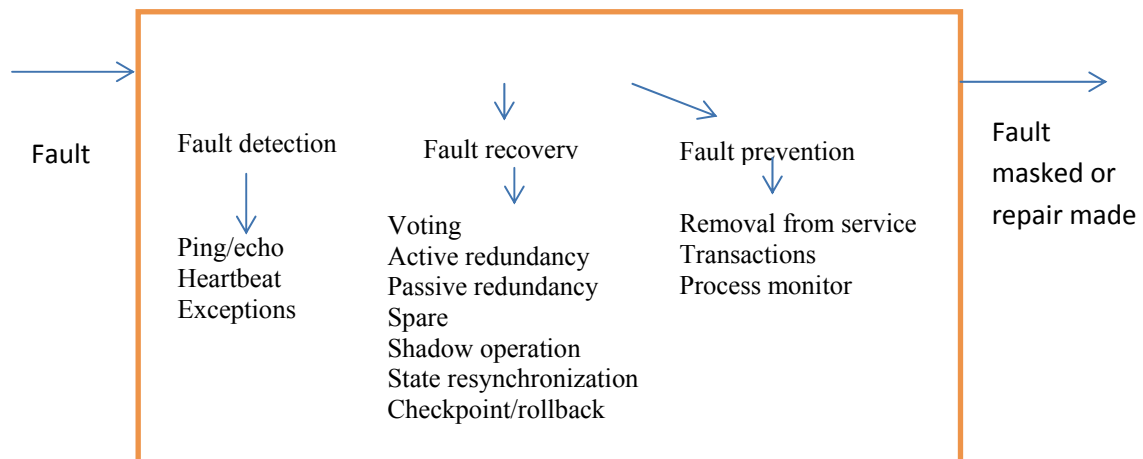
Fault

Fault detection

Ping/echo
Heartbeat
Exceptions

Fault recovery

Voting
Active redundancy
Passive redundancy
Spare
Shadow operation
State resynchronization
Checkpoint/rollback

Fault prevention

Removal from service
Transactions
Process monitor

Fault
masked or
repair made

Figure 1.

3. Fault detection

Three widely used tactics for recognizing faults are ping/echo, heartbeat, and exceptions.

Ping/echo. One component issues a ping and expects to receive back an echo, within a predefined time, from the componentunder scrutiny. This can be used within a group of components mutually responsible for one task. It can also used be used byclients to ensure that a server object and the communication path to the server are operating within the expected performancebounds. "Ping/echo" fault detectors can be organized in a hierarchy, in which a lowest-level detector pings the softwareprocesses with which it shares a processor, and the higher-level fault detectors ping lower-level ones. This uses lesscommunications bandwidth than a remote fault detector that pings all processes.

Heartbeat. In this case one component emits a heartbeat message periodically and another componentlistens for it. If the heartbeat fails, the originating component is assumed to have failed and a fault correction component isnotified. The heartbeat can also carry data. For example, an automated teller machine can periodically send the log of the lasttransaction to a server. This message not only acts as a heartbeat but also carries data to be processed.

Exceptions. One method for recognizing faults is to encounter an exception, which is raised when one of the fault. The exception handler typically executes in the same process that introduced theexception.

4. Fault recovery

Fault recovery consists of preparing for recovery and making the system repair. Some preparation and repair tactics follow.

Voting. Processes running on redundant processors each take equivalent input and compute a simple output value that is sentto a voter. If the voter detects deviant behavior from a single processor, it fails it. The voting algorithm can be "majority rules" or "preferred component" or some other algorithm. This method is used to correct faulty operation of algorithms or failure of a

processor and is often used in control systems. If all of the processors utilize the same algorithms, the redundancy detects only a processor fault and not an algorithm fault. Thus, if the consequence of a failure is extreme, such as potential loss of life, the redundant components can be diverse.

Active redundancy. All redundant components respond to events in parallel. Consequently, they are all in the samestate. The response from only one component is used (usually the first to respond), and the rest are discarded. When a fault occurs, the downtime of systems using this tactic is usually milliseconds since the backup is current and the only time to recover is the switching time. Active redundancy is often used in a client/server configuration, such as database managementsystems, where quick responses are necessary even when a fault occurs. In a highly available distributed system, theredundancy may be in the communication paths. For example, it may be desirable to use a LAN with a number of parallel paths and place each redundant component in a separate path. In this case, a single bridge or path failure will not make all of the system's components unavailable.Synchronization is performed by ensuring that all messages to any redundant component are sent to all redundant components. If communication has a possibility of being lost, a reliable transmission protocol can be used to recover. A reliable transmission protocol requires all recipients to acknowledge receipt together with some integrity indication such as a checksum. If the sender cannot verify that all recipients have received the message, it will resend the message to those components not acknowledging receipt. The resending of unreceived messagescontinues until the sender marks the recipient as out of service.

Passive redundancy.One component responds to events and informs the other components (the standbys) of state updates they must make. When a fault occurs, the system must first ensure that the backup state is sufficiently fresh before resuming services. This approach is also used in control systems, often when the inputs come over communication channels or from sensors and have to be switched from the primary to the backupon failure.

Spare. A standby spare computing platform is configured to replace many different failed components. It must be rebooted to the appropriate software configuration and have its state initialized when a failure occurs. Making a checkpoint of the systemstate to a persistent device periodically and logging all state changes to a persistent device allows for the spare to be set to the appropriate state. This is often used as the standby client workstation, where the user can move when a failure occurs. The downtime for this tactic is usually minutes.

Shadow operation. A previously failed component may be run in "shadow mode" for a short time to make sure that it mimics thebehavior of the working components before restoring it to service.

State resynchronization. The passive and active redundancy tactics require the component being restored to have its state upgraded before its return to service. The updating approach will depend on the downtime that can be sustained, the size ofthe update, and the number of messages required for the update. A single message containing the state is preferable, ifpossible. Incremental state upgrades, with periods of service between increments, lead to complicated software.

Checkpoint/rollback. A checkpoint is a recording of a consistent state created either periodically or in response to specific events. Sometimes a system fails in an unusual manner, with a detectably inconsistent state. In this case, the system should berestored using a previous checkpoint of a consistent state and a log of the transactions that occurred since the snapshot wastaken.

5. Fault prevention

The following are some fault prevention tactics.

Removal from service. This tactic removes a component of the system from operation to undergo some activities to prevent anticipated failures. One example is rebooting a component to prevent memory leaks from causing a failure. If this removal from service is automatic, an architectural strategy can be designed to support it. If it is manual, the system must be designed to support it.

Transactions. A transaction is the bundling of several sequential steps such that the entire bundle can be undone at once.Transactions are used to prevent any data from being affected if one step in a process fails and also to prevent collisions among several simultaneous threads accessing the same data.

Process monitor. Once a fault in a process has been detected, a monitoring process can delete the nonperforming process andcreate a new instance of it, initialized to some appropriate state as in the spare tactic.

6. Architectural design high-availability systems

Inarchitectural design method based onthe style use das attributesto selectthe architectural style that definesthe configuration architecture, based on functional requirements of thear chitectselects the architectural components and there by forms the architecture of the system. Application ofarchitectural designbased onstyleallowsreuseof architecture, whichreducesthe design architecture.Thus, using the availability tactics as future property of the system to determine the behavior when a fault is detected, or after repairing the case of faults[5]. The ping/echo tactic for example can be used when a system is distributed over several network nodes but is apparently useless for building desktop applications. Redundancy is also suitable for large distributed systems. Embedded systems are another domain where it can be used. For example some values couldbe computed or measured. Having components for both approaches would be a form of analytic redundancy.

7. Conclusion

Software architecture isan important level ofimplementation ofsystem availability. The article deals with concepts suchas architecture, quality attributes, tactics and styles. Each selected property item sand important architectura llimit ationss hould be consideredas a sign, which should or should notapply thearchitecturefor the systembeing developed. Styles help to simplify the reuse of architectural knowledge by specifying building blocks for architectural qualitypatterns.The main criterionin the design ofsoftware systemswith highavailability requirementsis an effectiveuse ofarchitecturaltactics.There are a number of styles addressing improve availability and thesetactics are well known and well structured. So there is the possibility for reuse of ideas as tactics mainly structure ideas for design decisions.

References

[1] A. G.Petruk, Architectural styles of software/ / Softwareengineering conference. Proceedings graduate students. - K.: NAU, 2005. - P. 20-24.

[2] IEEE Standard Glossary of Software Engineering Terminology (1990), http://ieeexplore.ieee.org/ISOL/standardstoc.jsp?punumber=2238

[2] Bass, L., Clemens, P., Kazman, R.: Software Architecture in Practice. SEI Series in Software Engineering, Addison-Wesley, 2 edn. (2003)

[3] Wu, W., Kelly, T.: Safety Tactics for Software Architecture Design. In: Proc. 28th Annual International Computer Software and Applications Conference COMPSAC 2004. pp. 368{375 (2004)

[4] Buschmann, F., Meunier, R., Rohnert, H., Sommerlad, P., Stal, M.: Pattern-Oriented Software Architecture, vol. 1: A System of Patterns. John Wiley &Sons (1996)

[5] Alexander, C., Ishikawa, S., Silverstein, M., Jacobson, M., Fiksdahl-King, I., Angel, S.: A Pattern Language. Oxford University Press (1977)

UDC 378.1:004:303.732.4(477)

I.M. Sydorov (National Aviation University, Ukraine)

ARCHITECTURE OF A CLOUD-ENABLED SERVICE ORIENTED PLATFORM.

The problems of building PaaS and SaaS applications are covered. Reference architecture is offered for building cloud-enabled platform to host a number of SaaS applications and support general characteristics of a cloud such as rapid elasticity, on-demand self-service, multi-tenancy, resource pooling and measured service. General directions of adopting cloud computing in aviation industry are mentioned.

During recent years the term "Cloud" just exploded the internet and became a very popular, not to say fashionable, trend in IT industry. Most influential vendors like Microsoft, Google and Amazon presented their platforms for building cloud application. In this article discussed and proposed a pattern for building cloud enabled applications built on concepts of Service Oriented Architecture.

The term "cloud" is used as a metaphor for the Internet, based on the cloud drawing used in the past to represent the telephone network [1], and later to depict the Internet in computer network diagrams as an abstraction of the underlying infrastructure it represents. Today cloud is widely used to represent an abstraction of technology, resources and its location used build integrated computer infrastructure, including networks, systems and applications. In 80s and 90s during the pre-web enterprise era, applications where very monolithic. Companies had a number of very complex and self-reliable systems; any interfacing between those was basically done via batch dumps.

Seems that web changed it all, but not really. Yes most enterprises are now using web based application, but still they are inherently monolithic and very tricky to change, extend and integrate with each other. The answer to that challenge is Service Oriented Architecture, which is about building an application based on set of services that can be easily extended, reorganized to meet ever-changing business requirements. As we know the maintenance stage of a software development lifecycle takes up to 60% of effort and SOA that provides atomic enterprise building blocks can significantly reduce future cost on software adaptation.

So as for Cloud applications, most of them are fundamentally built with the same "monolithic" architectural principles with a little concern of Enterprise Architectural patterns.

One of the key characteristics for cloud application is the ability to manage resources efficiently. Such efficiency should be translated into natural elasticity of the resources, where in a given moment you will need to scale up or down, based on unplanned peak of work, but minimizing investments in infrastructure.

Traditional capacity planning assumes that customer has a certain infrastructure capacity. During most of the day the service may remain sub-utilized, wasting capacity because demand is less than requirements. In any given moment capacity could be exceeded, ending up with frustration for end users because of slowness and application errors. Typically to solve this, more resources are added to the data center, which means more cost and waste of valuable resources.

In a cloud deployment scenario a minimum resources are provisioned to the customer. As the demand increases additional on-demand resources are added and as soon as the need in resources decreases the data center capacity decreased.

Cloud deployment in turn can be classified as:
- private –deployed in a customer's own datacenter [2];
- public – deployed on a public cloud provider [3];
- hybrid – is a combination of both public and private with a secure bridge between them [2].

No matter the type of deployment the company decides on for the future, the cloud services platform should enforce the core characteristics of cloud architecture. Those characteristics are defined by the National Institute of Standards and Technology [2]:

- on-demand self-service: A consumer can unilaterally provision computing capabilities such as server time, network storage, as needed automatically without requiring human interaction with a service provider;
- broad network access: Capabilities are available over the network and accessed through standard mechanisms that promote use by heterogeneous thin or thick clients such as workstations, laptops, slates, mobile phones etc. as well as other traditional or cloud-based software services;
- resource pooling: The provider's computing resources are pooled to serve multiple consumers using multi-tenant model. Different physical and virtual resources are dynamically assigned and reassigned according to demand. There is a certain degree of location independence so customer is often has no control over exact location of resources but may have an ability to specify location at a higher level of abstraction, for example county, region or datacenter;
- rapid elasticity: capabilities can be rapidly and elastically provisioned (in some cases automatically) to quickly scale up and shrink down;
- measured service: Cloud systems automatically control and optimize resources usage by leveraging a metering capability at some level of abstraction appropriate to the type of a service (storage, processing, bandwidth, or active users). Resources usage can be monitored, controlled and reported, providing transparency for both provider and consumer;
- multi-tenancy: Many organizations (tenants) can use cloud with mechanisms to protect and isolate each tenant from all others securing company's sensitive information.

Although this seems to be straightforward, this requires a different application architecture paradigm that can leverage these characteristics. Proposed architecture option is based on Event-Driven architecture framework, as well as use of Message-Oriented middleware to interconnect processes and ensure:

- extreme loose coupling and well distributed workload;
- horizontal scalability;
- shared-nothing processes.

The component of the architecture that enables this capability is named Controller and has the following characteristics:

- is able to post and receive notifications;
- is able to receive remote configuration parameters;
- has embedded security components;
- is able to notify every event or transaction for auditing purposes;
- is able to run multiple processes at the same time, without conflicting with the management of the requirements (self-balanced);
- is able to support multi-tenancy;
- if needed is able to interact with external applications in their native form or based on the provided integration mechanisms.
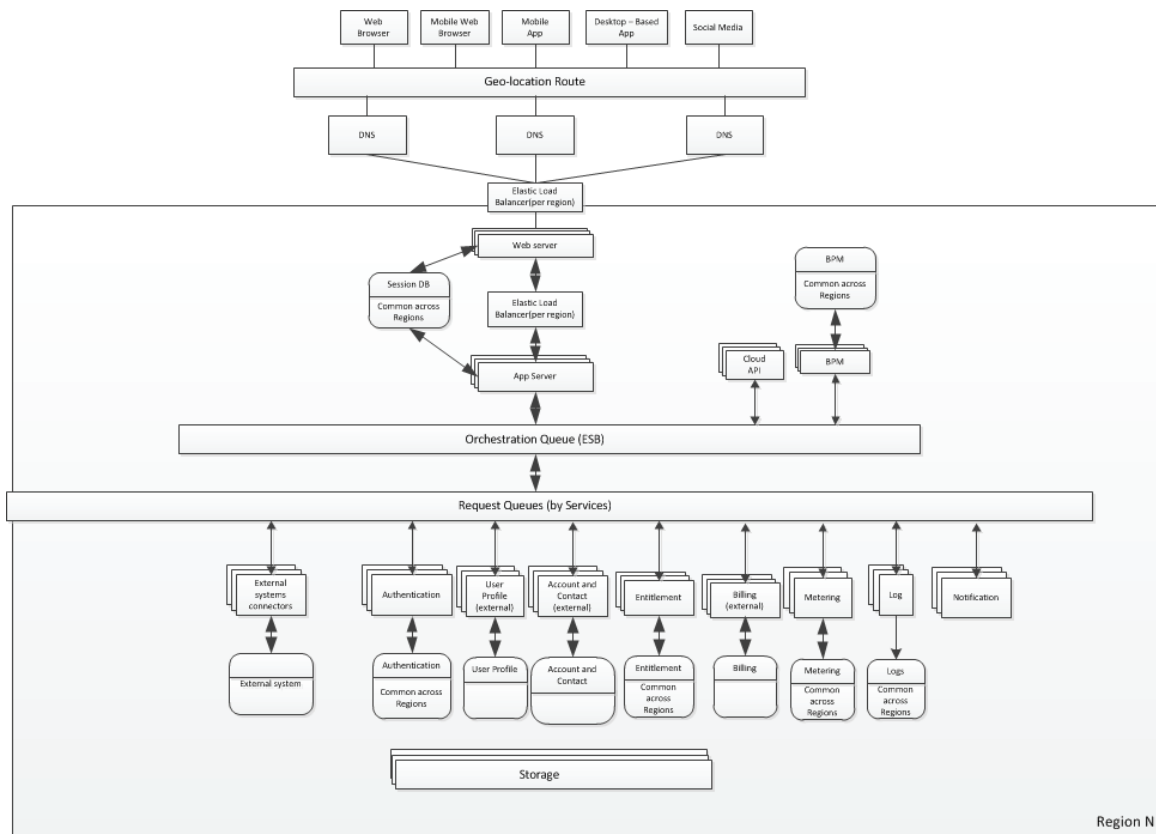
Figure 1 Platform components diagram.

So the platform consists from small atomic business components - controllers. Each controller is responsible for a subset of business operations (e.g. user management, logging, billing, etc.). Interaction between controllers is done via message bus. Message bus implementation can be different according particular project needs. It can be privately deployed Apache ActiveMQ or public cloud services can be used such as Amazon Simple Queue Service or Windows Azure Queue Storage. An orchestration layer makes it possible to apply custom business rules to enrich application capabilities. Application and web servers hidden behind elastic load balancers provide access to the system by heterogeneous clients such as web browsers, mobile phones, thick and thin clients. Unified message format for the bus and abstracted API for interaction with the bus makes it possible to develop controllers in a various programming languages (such as C#, Java, C++, NodeJs) host them on various platforms (Windows, Linux). This flexibility is also very beneficial in integration scenarios so the best approach can be chosen for a particular system.

Aviation industry is slow to change, very risk averse. Software solutions are complex and not easily tackled [4]. Therefore some companies started adoption of a cloud computing for the need of aviation industry. Xerox is launching its cloud platform to help airlines to seamlessly share important data and key transmissions from airline to other carriers and flight authorities [5]. In areas where data sharing, instant and effective distribution is important cloud platforms and applications can be very beneficial. Seamless integration between systems, B2B interaction, scalability and fault tolerance can help cloud computing to make its way into aviation industry.

References

1. Cloud symbol 49 in Figure 1, "Internet cloud 106", US Patent 6,069,890, column 7, line 64
2. National Institute Of Standards And Technology, Special publication 800-145, "The NIST definition of cloud computing".- 2010.-175 p.
3. IDC 2008.09.23 "Defining Cloud Services and Cloud Computing"
4. I. Sydorov Software Engineering Conference, 2008/I. Sydorov, "Architecture of an instructor's board software for aircraft simulators".- Kiev.- 2008.- P.45.
5. http://news.xeros.com

UDC 378.1:004:303.732.4(477)

Nika Sydorova, postgraduate (National Aviation University, Ukraine)

ONTOLOGY OF GENERATION OF PROFESSIONAL COMMUNICATION OF BACHELORS IN SOFTWARE ENGINEERING

Approach to the generation of professional communication competence of specialists in software engineering is proposed. Ontology of generation of bachelors' preparedness is elaborated.

Problem statement

Industry of software development in Ukraine is constantly evolving. That is why there is a need in specialists. In 2006 in Ukraine there was established a new education direction in training of software engineers 6.050103 «Software engineering» in correspondence with the international standard [1], the standard was developed and the education process started [2]. Five years of this direction existence proved that the issue of development of an integrated approach to the generation of preparedness of future bachelors for the professional communication in realization of software development processes should be solved.

The **objective** of the work lies in elaboration of ontology of bachelors' professional communication.

The ontology may be applied as an instrument in education of professional communication as far as it contains knowledge in corresponding matters and terms. One of the steps in ontology evaluation is conceptualization, which requires the definition of scope of ontology, concepts, description of each of them, e.g. glossary, specification of features and relations.

Ontology

Considering the place of bachelor in working process according to the software engineering general ontology was considered in four aspects in correspondence with the IDEF5 standard: (pic.1).
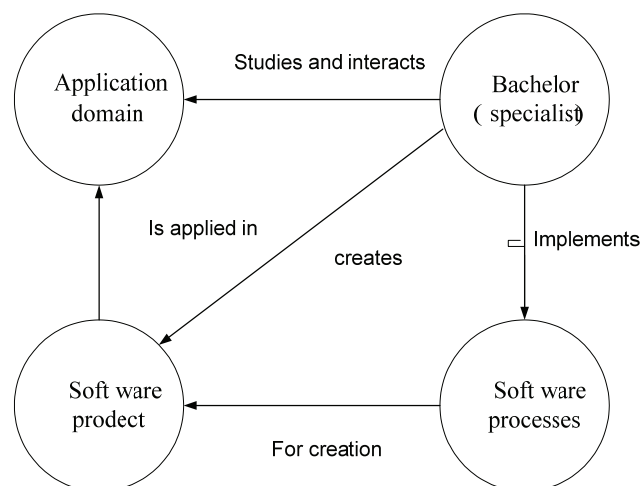
Pic. 1. General ontology

Specialist implements software processes, which are aimed at the creation of software product, for its use in application domain. Specialist interacts with the subjects of application domain and should have relevant communication knowledge and skills.

Description of general ontology contains:
− Verbal description;
− Graphic image;

– Analytic description.

Verbal description contains:

– bachelor (specialist) – graduate of the institution of higher education of corresponding education direction;

– application domain – area of real world, for which software product is created;

– software processes – processes, which are performed within the life cycle and are aimed at the creation of software product;

– software product – software, which is used in the application domain and meets the requirements.

Graphic image is shown in the PIC.

Analytic description:

– systems and elements;

– unique identifiers;

– connectors of elements;

– observations and information;

– correctness;

– axioms.

In analytic description the method described in the work is applied [10].

System and its elements. There is observed the system s:S with bachelor (specialist) a:A, with application domain a1:A1, with software product a2:A2, with application processes a3:A3, where S, A, A1, A2, A3 – types.

Elements u:U, де U – universal set, is either a bachelor (specialist), or application domain, or software product, or software processes, i.e.:U=A|A1|A2|A3.

Elements are explained in terms of unrelated types: bachelor (specialist) AA, application domain AO, software product AB, software processes AC:

A=mkA (aa: AA)

A1=mkA1(ao:AO)

A2=mkA2(ab: AB)

A3=mkA3(ac:AC)

Unique identifiers. Each element is linked with unique identifier ui:UI, де UI – type.

It is possible to track from the element its unique identifier, i.e. obsUI:U->UI.

Thereby from the element there may be tracked either a bachelor (specialist), or application domain, or software product, or software processes:

is_A:U->Bool

is_A(u)≡case 1 of mkA(_)->true,_->false end

is_A1:U->Bool

is_A1(u)≡case 1 of mkA1(_)->true,_->false end

is_A2:U->Bool

is_A2(u)≡case 1 of mkA2(_)->true,_->false end

is_A3:U->Bool

is_A3(u)≡case 1 of mkA3(_)->true,_->false end

Connectors of elements. Bachelor (specialist) is associated with maximal quantity of incoming connectionsm, which exceeds unity and zero of incoming connections:

obs_inCs:A->{0:Nat}

obs_outCs:A->Nat

Application domain is associated with maximal quantity of incoming connectionsc, which exceeds unity and zero of outgoing connections:

obs_inCs:A1->Nat

obs_outCs:A1->{0:Nat}

Software product is associated with maximal quantity of incoming connectionsd, which exceeds unity and one outgoing connections:

obs_inCs:A2->Nat

obs_outCs:A2->{1:Nat}

Software processes are associated with one incoming connection and one outgoing connection:

obs_inCs:A3->{1:Nat}

obs_outCs:A3->{1:Nat}

Axioms:

$\forall$ a:A (obs_outCs(a) $\geq$2)

$\forall$ a1:A1 (obs_inCs(a1) $\geq$2)

$\forall$ a2:A2 (obs_inCs(a2) $\geq$2)

Observations and connections. All elements of the system may be tracked from it:

obs_Us:S->U-set

From the element there may be observed pairs of incoming and outgoing elements, which are not crossing, and with which they are connected:

obs_cUIs:U->UI-set×UI-set

wf_Conns:U->Bool

wf_Conns(u) $\equiv$ let(iuis,ouis)=obs_cUIs(u)
in iuis $\cap$ ouis={0} $\wedge$ case u of

a) bachelor (specialist) may be connected with zero of incoming elements and all outgoing elements:

mkA (_)->card iuis $\in$ {0} $\wedge$ card ouis $\in$
{2… obs_outCs(a)}

б) application domain may be connected with elements from bachelor (specialist) and software product (incoming) and zero of outgoing elements:

mkA1(_)->card iuis $\in$ {2… obs_inCs(a1)} $\wedge$ card ouis $\in$ {0}

в) software product may be connected with elements from bachelor (specialist) and software processes (incoming) and with zero or one element of the application domain (outgoing):

mkA2(_)->card iuis $\in$ {2… obs_inCs(a2)} $\wedge$ card ouis $\in$ {0,1}

г) software processes may be connected with zero or one incoming element from bachelor (specialist) and with zero or one element from software product (outgoing):

mkA3(_)->card iuis $\in$ {0,1} $\wedge$ card ouis $\in$ {0,1}

end end

Correctness. Elements of identifiers obtained by observation from obs_cUIs should be identified, as the elements from S.

Axiom:

$\forall$ s:S,u:U•u $\in$
obs_Us(s)$\Rightarrow$let(iuis,ouis)=obs_cUIs(s) in

$\forall$ ui:UI•ui$\in$iuis $\cup$ ouis$\Rightarrow$ u':U $\in$
obs_Us(s)$\wedge$ u'$\neq$u$\wedge$obs_UI(u')=ui

end

Graphic images of two subontologies according to the aspects of application domain and bachelor are shown in PIC 2, 3.

Analytic description of subontologies may be done the way it is described above.

Subontology of application domain is a state of knowledge of the part of real world, where software product shall be used. In communication with specialists of application domain the software engineer shall possess corresponding knowledge (PIC 2).
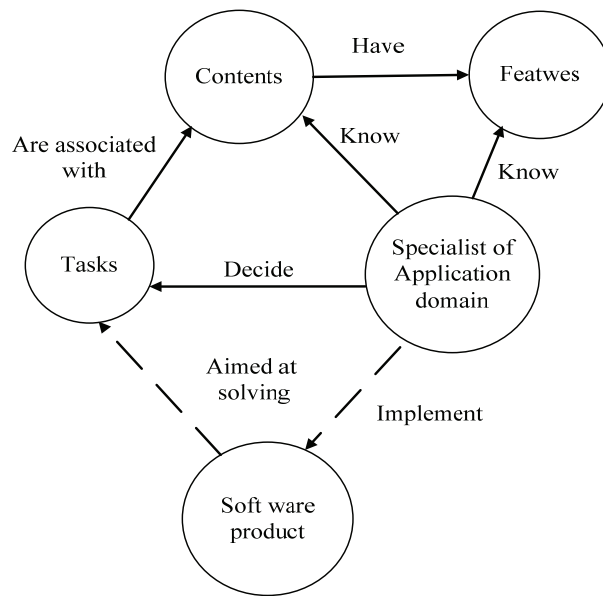
PIC 2. Subontology of application domain

Apart from the knowledge of domain a bachelor shall have skills of group dynamics, which enables him to realize relevant professional communication (PIC 3).
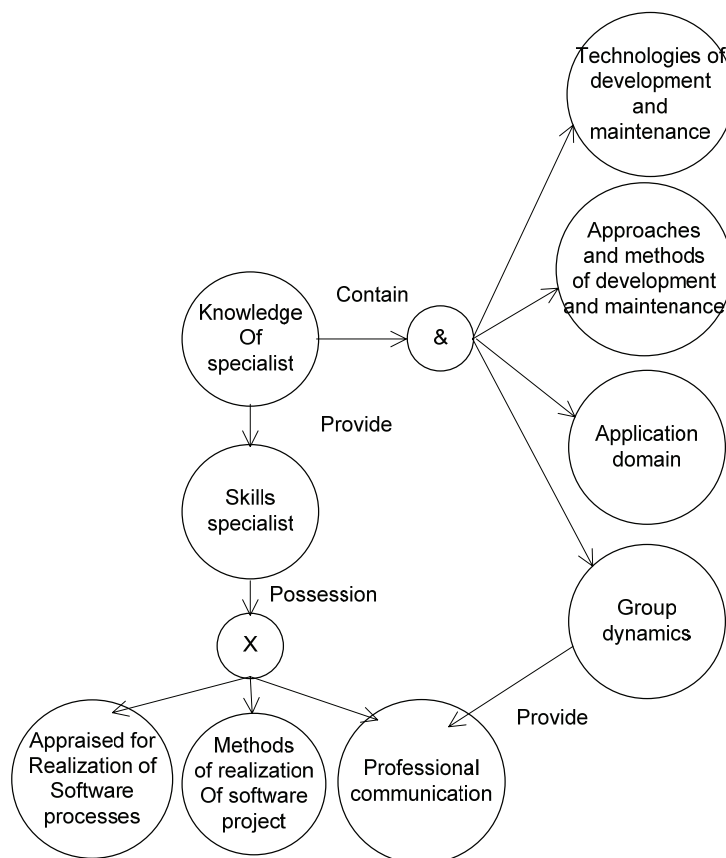
PIC 3. Subontology of bachelor (specialist)

Summary

Professional communications are important component of group dynamics in the processes of software development. Ontology is a consolidating component of methods of training of software specialists.

References

1. *Software Engineering 2004.* Curriculum Guidelines for Undergraduate Degree Programs in *Software Engineering.* A volume of the Computing Curricula Series. August 23, 2004. – 128 p.

2. *Бондаренко М.* Модель випускника бакалаврату "Програмна інженерія" (3 досвіду роботи науково-методичної підкомісії 050103) / М. Бондаренко, М. Сидоров, Т. Морозова, І. Мендзебровський // Вища школа. – 2009. – № 4. – С. 50–61.

3. *Сидорова Н.Н.* Навчання інженерії прог-рамного забезпечення – системний огляд літератури / Н.Н. Сидорова // Інженерія програмного забезпечення. – К.: НАУ. – 2011. – № 2 (6). – С. 56–67.

4. *Сидорова Н.М.* / Формування готовності бакалаврів з інженерії програмного забезпечення до професійної комунікації / Н.М. Сидорова // Вісник НАУ.- 2012.-№3.- с.94 – 100.

O. Zudov, PhD (National Aviation University, Ukraine)

GRADIENT CROSSOVER FOR REAL-CODE GENETIC ALGORITHMS

The new approach in evolution optimization is suggested as modifying of genetic algorithm with real-code solution space. The method combines gradient and genetic algorithms to extract the advantages of both ones. Multi-modal target function can be analyzed without loosing of global extremum. The suggested method has better convergence in multi-dimensional space in comparison with standard genetic algorithms.

All gradient optimization methods have one disadvantage. They cannot find the global extreme of objective if there are local ones (fig.1) [1, 2].

To solve such poly-modal optimization problems the genetic algorithms are often used. These algorithms suggested by Holand [3] simulate natural evolution.

Fig. 1
Gradient search

To solve such poly-modal optimization problems the genetic algorithms are often used. These algorithms suggested by Holland [3] simulate natural evolution.

The main steps of genetic algorithm are:

1) coding of solution set by binary code (genome forming);
2) the initial array of solution forming (initial generation);
3) calculating of target function values for current generation (fitness level);
4) selection of solutions pairs for crossing (competition);
5) crossover (genes exchange) and new solution points generation;
6) random change of some bits in genome (mutation);
7) new circle (go to step 3).

Genetic algorithms require the very long binary codes especially for big number of space dimensions. For example, target function with 4 parameters $f(x_1, x_2, x_3, x_4)$, $-1 < x_i < 1$, with accuracy 10^{-6} needs $2 \cdot 10^{24}$ solution points that corresponds to $\log_2(2 \cdot 1024) \approx 81$ bits word.

Also criteria of selection and crossing, i.e. hereditary characters, must be defined. Usually these are the best genes (bits combinations) of parents which have small distance between them. It can go to premature convergence around local extremum (fig. 2).
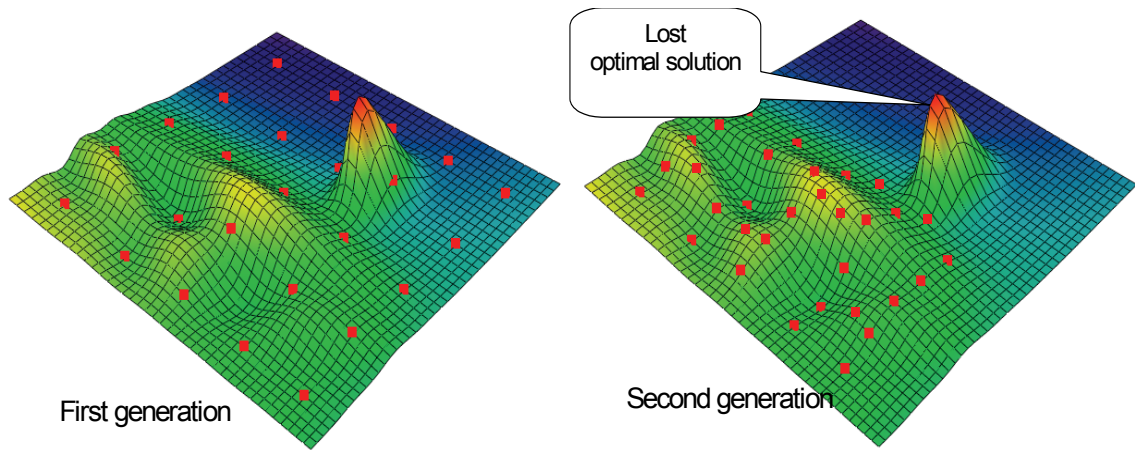
Fig. 2
Example of genetic search

Instead binary coding solution can be represented by real number vector. Such methods are called evolution strategy or real-code genetic algorithms [1, 4].

We suggest to combine gradient and genetic optimization algorithms. It gives advantages of both methods. The main idea is using gradient directions of target function in parent pair points for estimation of their crossing suitableness and for determining of descendant point coordinates.

Let us consider 2-dimention case of suggested methods (fig.3).

1. The uniform grid of points is selected in search space (initial generation). Number points is N. For these points gradients are calculated.

2. The new generation of pointes is found by "crossing" of gradients in all pairs. For 2D case this is crossing of two rays that go from the points of parent pair in gradient directions.

3. The number of crossings is C_N^2. From this array (excepting points out of range) new generation is selected. The new generation population size is also N.

4. In each iteration for the best points of generation usual gradient search of extremum is used.
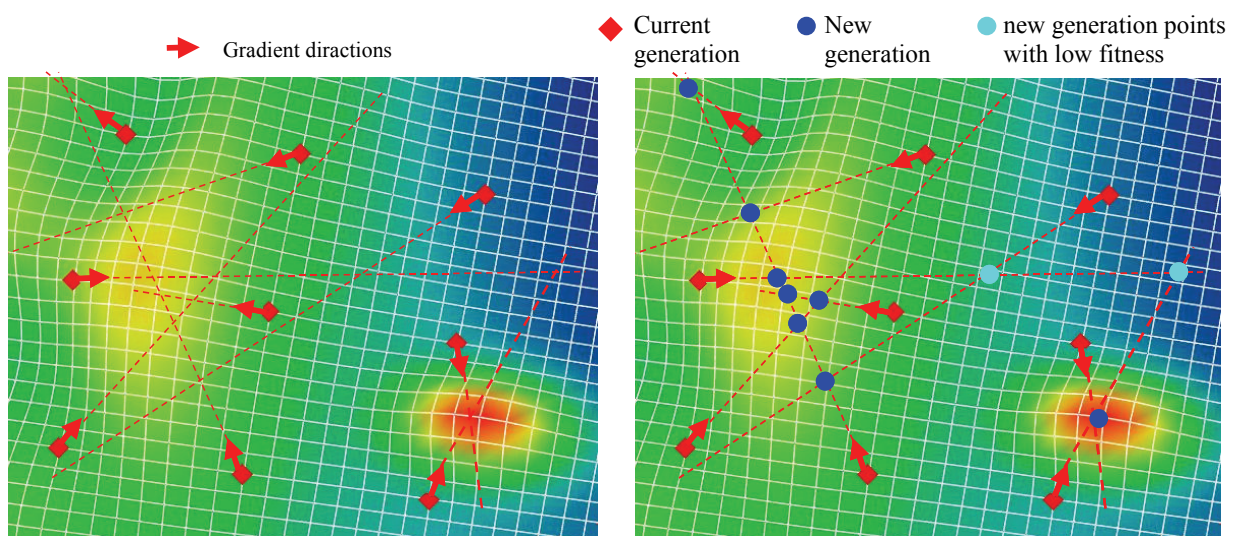
Fig. 3
Gradient crossover

Suggested method can be developed for multi-dimentional case. If the target function depends on n parameters the gradient rays are on skew lines in many-dimensional space. In this case descendant points is so called convergence center of these lines (fig.4). This is the central points of shortest segment connecting these lines.
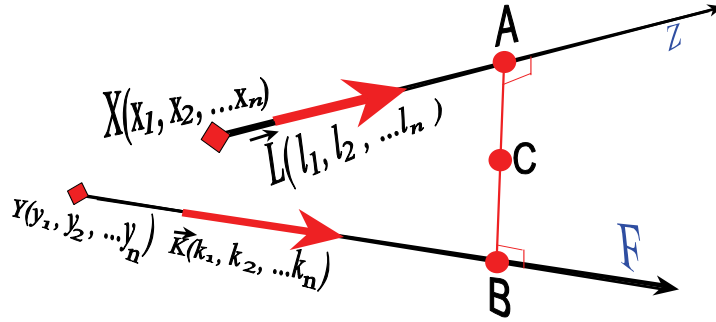
Fig. 4

Search of convergence center for gradient rays in many-dimensional space

Let's consider the lines F and Z equations that are defined in vector-parametrical form:

$$Z = X + s \cdot L,$$
$$F = Y + t \cdot K,$$

where $X(x_1, x_2, ... x_n)$ and $Y(y_1, y_2, ... y_n)$ are known points (parent pair of current generation); $L(l_1, l_2, ... l_n)$ and $K(k_1, k_2, ... k_n)$ are direction vectors of these lines (gradients of parent point); s and t are real parameters.

To find the points A ϵ Z and Bϵ F the distance function must be minimized:

$$D\,(s,t) = \|AB\|^2 = (X + s \cdot L - Y - t \cdot K)^2.$$

The linear system

$$\begin{cases} \dfrac{\partial D}{\partial s} = 0, \\[2mm] \dfrac{\partial D}{\partial t} = 0 \end{cases}$$

gives next parameters values:

$$s_o = \frac{(K,\,L) \cdot (XY,\,K) - \|K\|^2 \cdot (XY,\,L)}{\|K\|^2 \cdot \|L\|^2 - (K,\,L)^2}\,,$$

$$t_o = \frac{\|L\|^2 \cdot (XY,\,K) - (K,\,L) \cdot (XY,\,L)}{\|K\|^2 \cdot \|L\|^2 - (K,\,L)^2}$$

and corresponding coordinates of shortest segment ends:

$$A = X + s_o \cdot L,$$
$$B = Y + t_o \cdot K$$

Point C is found as the center of AB.

The shortest distance $\|AB\|$ between rays is the criterion of crossing reasonability. If this distance is big (more or about the distance between crossed parents) there is no sense to cross them. This criterion improves genetic algorithm because it shows not only the rang of separate points in generation but defines fitness of pair pretending to common descendant.

Another important characteristic is the sign of *s* and *t* parameters. Negative parameters indicate points *A* and *B* lying in directions that are opposite to gradients.

In conglomerations of points in current population the traditional gradient search is reasonable because this conglomeration indicates the high probability of global extremum nearby.

Conclusion

Suggested modifying of genetic algorithm with real-code solution space allows to make the optimization problem calculation faster due to the better convergence. This is achieved by using specific crossover method which allows to estimate the potential efficiency of crossing for each couple of parent solutions. The gradient crossover improves the real-code genetic algorithm since it uses advantages of gradient search but has no risk to loose the global extremum.

References

1. *Goldberg David E.* Genetic Algorithms in Search, Optimization and Machine Learning. Addison-Wesley Publishing Company, Inc. 1989. - 412p.
2. *Субботін С. О., Олійник А. О., Олійник О. О.* Неітеративні, еволюційні та мультиагентні методи синтезу нечіткологічних і нейромережних моделей: Монографія // Під заг. ред. С. О. Субботіна. – Запоріжжя: ЗНТУ, 2009. -375 с.
3. *Holand J.H.* Genetic algoritms and the optimal allocations of trials. SIAM Journal Computing, 2(2), 1973 - P. 88-105.
4. *Herrera F., Lozano M., Verdegay J.L.* Tackling real-coded Genetic algorithms: operators and tools for the behaviour analysis // Artificial Intelligence Review, Vol. 12, No. 4, 1998. – P. 265-319.
5. *Сабанин В. Р., Смирнов Н. И., Репин А. И.* Модифицированный генетический алгоритм для задач оптимизации в управлении // Exponenta Pro, №3-4 (7-8), 2004. – С.78-85.

I.V. Misharin, I.I.Rudnyk
(National Aviation University, Ukraine).

GLOBAL AIR NAVIGATION PLAN FOR CNS/ATM SYSTEMS. TECHNOLOGY SOLUTIONS FOR IMPLEMENTATION OF THE NEXT GENERATION OF AIR TRAFFIC MANAGEMENT.

Air traffic management (ATM) is about the process, procedures and resources which come into play to make sure that aircraft are safely guided in the skies and on the ground. Ensuring of flight safety and saving of airlines costs are the number one priority topics. FDT in collaboration with Head Enterprise for Flight Data Processing Company has developed a new approach – the FlightLink complex for solution of these problems.

The main targets of the project:
- Support the Implementation of Global Air Navigation Plan for CNS/ATM Systems;
- Fulfill requirements of amendments 34 to Annex 6 Part I, 29 to Annex 6 Part II and 15 to Annex 6 Part III to discontinue use of magnetic tape, photographic film recorders, etc.;
- Upgrade old generation aircrafts' navigation systems;
- Optimize fuel efficiency via improved flight trajectories and recommended modes;
- Accomplish ICAO Annex 6 requirement 3.3.6 regarding "flight data analysis program as part of…safety management system";
- Substitute "black box" outdated technology with "white box" concept.

FlightLink complex is developed by evolving Canadian company Flight Data Technologies - **FDT** in collaboration with *Head Enterprise for Flight Data Processing company.* **FDT** is led by best experts in aircraft accident investigations, together comprising more than 55 years of experience in flight safety management.

FlightLink complex includes the following equipment:
1. Antennas for satellite signal– the size is 20mm x 20mm x 4mm;
2. Modems;
3. FIFO buffer and multiplexor;
4. FDR- increased memory size - 16 Gb, wireless information readout, corresponds to the requirements EUROCAE ED-112;
5. Software.

Pic.1. Flight Data Recorder.

Pic.2. Modem.

FDT provides the following service:
1. Installation of equipment and Flight Data Analysis software on the aircraft
2. Data traffic channel between airplane and ground station (PC)
3. Analysis of flight information with identification of threats and hazards
4. Real-time visualization of aircraft environment
5. Air-ground voice connection and data transferring – the service is provided 24/7 worldwide
6. Advising pilots on any stage of flight on flight trajectory, speed and flight modes to optimize fuel efficiency and reduce noise exposure
7. Real-time quality assured electronic information (aeronautical, terrain and obstacle).

In order to ensure all those targets and provide services mentioned above a reliable communication channel must be used. IRIDIUM is a choice of satellite communication
IRIDIUM Benefits:

- Iridium is the world's only truly global mobile communications company, with coverage of the entire Earth, including oceans, airways and Polar Regions.
- The unique Iridium constellation of 66 Low Earth Orbiting (LEO) cross-linked provides the necessary transmission speed
- Due to the low orbiting satellites location above the Earth, acceptance antennas installed on the aircraft will have small size and can be installed on a few locations on fuselage, therefore in case of unstable aircraft positioning, the satellite signal will not be lost
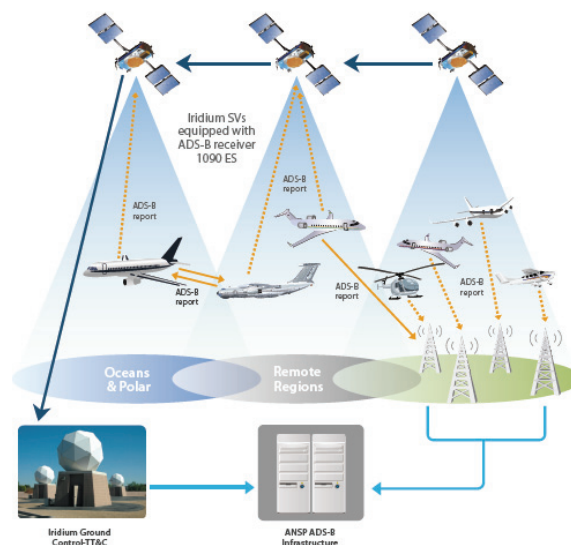
Pic.3.Scheme of connection between Ground stations, Aircraft and Satellites.

1.10.49

IRIDIUM disadvantages and their solutions:
- Speed for data transfer -2400 bps is low;
- Applying the unique technology, FDT&IRIDIUM will increase the speed of data transmission to 1MBps by:
  - wrapping information via compressing algorithm, at the same time providing the required security protocol;
  - optimization of available resources by using unique controller;
  - applying combined antenna;
  - dynamic traffic redistribution among participants, etc.
- Currently Iridium suggests high prices for low speed and the pay-per-time-use concept.

FDT&IRIDIUM suggests technologies allowing to increase the speed and provide the pay-per-data-transferred approach.

FlightLink complex will help to implement the main concepts of ICAO Global Air navigation plan:
1. Dynamic and Flexible ATS Route Management
2. Operational implementation of data link-based surveillance
3. Functional integration of ground systems with airborne system
4. Decision Support and Alerting Systems
5. Data link application
6. Flexible use of airspaces
7. Aeronautical Information - To make available in real-time quality assured electronic information (aeronautical, terrain and obstacle).
8. Navigation Systems
9. Communication Infrastructure

ICAO Global Air Navigation plan – proposed solution
- The suggested approach is a bottom-up - to pilot the system in regions, starting from one state
- To retrofit aircrafts located on the territory of one state
- Establish ATM system on the territory of the same state
- Develop procedures and protocols
- While the system undergoes testing, the current means of communication will remain in place
- The suggested product is generic and can be installed on different types of aircrafts.

Airlines will get a lot of benefits from this complex. They are:
- Increasing the flight safety by means of additional visualization of aircraft environment;
- The suggested solution doesn't require major changes to the aircraft and its avionics as well as there are no needs in significant training to pilots;
- Aircraft retrofit will be performed during check form;
- *FDT* gives the warranty on installed equipment for 3 years;
- Reduction of fuel consumption – **FDT** guarantees the saving of 500 kg of fuel per one hour of flight for aircrafts with MTOW in excess of 27000 kg;
- Decrease the cost of data traffic – Sharing flight data among all participants will improve the aircraft status through "turn-around" process and reduce cost of aircrafts operation;
- Increase the flight safety via additional visualization of aircraft environment (installation of the system will allow to better prevent accidents similar to Tupolev 154 crash with Polish president on board);
- Reduce FOQA program expenses;
- Discontinuing the use of magnetic tape, photographic film recorders, etc. without considerable costs;

- Monitoring on all stages of flight on flight trajectory, speed and flight modes to optimize fuel efficiency, reduce fuel burn penalty, CO_2 emission and the noise levels;
- Cost savings on rescue services and search of recorders (Air France spent €100 millions to find A330 FDR crashed in 2009);
- Making profit by providing data traffic service to passengers;

Profit on launching the initiative:
- 5000 USD per equipment installed on one aircraft;
- 10 USD per flight data analysis per one flight with providing recommendations to "turn-around" process, flight modes and FOQA;
- Flight data acquisition (GSIC feed).

Achievements on launching the initiative:
- Lead the industry to successful implementation of new ATM generation and realization of Future Air Navigation System (FANS);
- Assist to airlines to comply with amendments 34 to Annex 6 Part I, 29 to Annex 6 Part II and 15 to Annex 6 Part III - to discontinue use of magnetic tape, photographic film recorders, etc. by equipping aircrafts with digital FDR and CVR;
- Support the industry in ATM equipment renovation and increase the level of flight safety.

Conclusions

IRIDIUM & FDT satisfies 9 out of 11 main expectations that have been included in operational concept (Doc 9854) which was endorsed at the Eleventh Air Navigation Conference (Montreal, September,22 to October,3 2003): *safety, security, environment, efficiency, cost-effectiveness, capacity, access and equity, flexibility, predictability* and could help to implement two others: *global interoperability* and *participation by the entire aviation community.*

References

1. www.eurocontrol.int/articles/what-air-traffic-management
2. www.airtrafficmanagement.net/
3. www.thalesgroup.com/Markets/Aerospace/
4. www.iridium.com/
5. www.icao.int/Pages/default.aspx
6. www.iata.org/Pages/default.aspx

UDC: 532.13 (045)

O.M. Glazok, candidate of technical sciences
(National Aviation University, Ukraine)

MATHEMATICAL MODEL OF FRICTION AT PRESENCE
OF ANISOTROPIC ADMIXTURES IN THE COMPOSITION OIL

The mathematical model of process of friction in presence of a lubricant con-taining rigid particles with anisotropic properties is examined. The model is oriented to the numerical experiment. For solving the problem of numerical modeling the modified method of solving of systems of linear equations is applied.

The mathematical modeling of friction phenomena have large value in modern aviation science. On the one hand, the friction is inherent for all moving mechanical parts of the aerial vehicle, such as the parts of the engines. On the other hand, understanding of the nature of the inner friction in the environment would help to build aerodynamic models of the flight.

Boric acid, widely known as an antiseptic tool, possesses unique tribologic characteristics due to its crystalline structure. The solid (crystallized) matter of boric acid consists of separate flat layers in which atoms are located close and densely combined between itself. At the same time, the distance between the nearby levels of this structure is relatively large. Hereupon intermolecular connections between levels, which result from the actions of the Van der Vaals forces – are comparatively weak. Being placed under sliding loadings, these layers can easily slide on each other. Thus the presence of strong connections within the limits of every level prevents a direct contact between sliding parts, reduces a friction and minimizes a wear. Exactly on this effect the use of boric acid is based as a component matter of admixtures to lubricating oils and film coverages of metallic surfaces of friction. A graphite which also is widely utillized in composition lubricating materials has a similar level structure.

As a result of scientific researches new materials are developed and synthesized with the properties similar to those of the graphite and boric acid. Introduction of new materials needs difficult and of long duration process of their research, which includes the study of properties of the matter, development, creation and practical test of the proper technological materials and processes on its basis. Therefore development of mathematical models which will allow the tools of numerical experiment to estimate perspective of certain direction of practical researches is expedient [1].

The purpose of the article is development of mathematical model of process of friction in the presence of liquid lubricating material in the complement of which enter in quality the admixture of particle with anisotropic properties.

As the basis of the offered mathematical model, the classic models of processes of dry and hydrodynamic friction [2] are taken, and also hydrodynamic processes [3]. For the conducting of numerical experiment the method of solving of the systems of linear algebraic equations is utillized [4].

As surfaces of friction are real always have inevenness, the area of contact between them can be divided into areas (fig. 1) in which their co-operation has different character:

1) Area of direct contact of materials of the two surfaces (fig.1, position 1). In this area the friction of surfaces takes place without painting (dry friction, solid friction).

2) Area of contact of materials through oxidizing film which is present on the spot metal surfaces (fig. 1, position 2).

3) Area of contact of materials through the olive film the thickness of which is equal to a few molecules of olive (fig. 1, position 3).

4) Area, where materials are parted by thick (comparatively to the characteristic size of molecules) tape of olive (fig. 1, position 4). This area can be named the area of the hydrodynamic greasing.
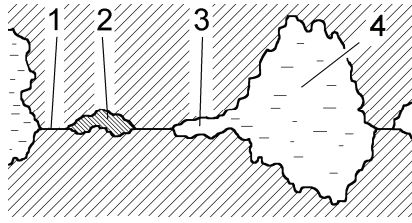
Fig. 1. Chart of contact of the two surfaces: 1 – the area of friction without painting; 2 – the area of contact through oxidizing film; 3 – the area of contact through the olive film of molecular thickness; 4 – the area of the hydrodynamic greasing.

At different terms there can be different friction condition in between the volumes of the corresponding areas. In the first and second areas the olive does not take participation in the process of friction. From the point of view of the hydrodynamic laws we should examine influence of olive sense only in a fourth area, and in the third area inter-molecular interaction plays the primary role.

For development of the basic simplified mathematical model of the process of friction in the fourth area let us consider the two flat and parallel surfaces of friction, one of which moves in parallell to the other (Fig.2). The space between surfaces is filled with liquid lubricating material which contains anisotropic particles in composition. Their anisotropy appears in that force of sliding the parts of a «granule» of admixture in one of directions is insignificant.
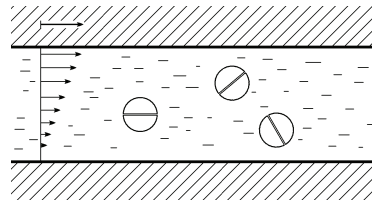

Fig. 2. Between surfaces of friction there is liquid lubricating
material with anisotropic particles.

For simplification let us suppose that the anisotropic particles have a bullet form, their density is equal to the density of liquid environment; for every particle the radius of R_i and the coefficient *of s* are set, that determines the effort of shift S_i :

$$S_i = sR_i^2 . \qquad (1)$$

Given the viscosity of the olive, equal to μ , and the coefficients of friction between the olive and the material of surfaces of friction f_1 , and between the olive and the surface of anisotropic particle – f_2.

For mathematical description of the problem the following relationships are utillized:
1) The Navier-Stokes equations

$$\rho \frac{du}{dt} = \rho X - \frac{\partial p}{\partial x} + \frac{\partial}{\partial x}\left(\mu\left(2\frac{\partial u}{\partial x} - \frac{2}{3}\left(\frac{\partial u}{\partial x} + \frac{\partial v}{\partial y} + \frac{\partial w}{\partial z} \right) \right) \right) + \frac{\partial}{\partial y}\left(\mu\left(\frac{\partial u}{\partial y} + \frac{\partial v}{\partial x} \right) \right) + \frac{\partial}{\partial z}\left(\mu\left(\frac{\partial w}{\partial x} + \frac{\partial u}{\partial z} \right) \right) \ ;$$

$$\rho \frac{dv}{dt} = \rho Y - \frac{\partial p}{\partial y} + \frac{\partial}{\partial x}\left(\mu\left(2\frac{\partial v}{\partial y} - \frac{2}{3}\left(\frac{\partial u}{\partial x} + \frac{\partial v}{\partial y} + \frac{\partial w}{\partial z} \right) \right) \right) + \frac{\partial}{\partial z}\left(\mu\left(\frac{\partial v}{\partial z} + \frac{\partial w}{\partial y} \right) \right) + \frac{\partial}{\partial x}\left(\mu\left(\frac{\partial u}{\partial y} + \frac{\partial v}{\partial x} \right) \right) \ ;$$

$$\rho \frac{dw}{dt} = \rho Z - \frac{\partial p}{\partial z} + \frac{\partial}{\partial z}\left(\mu\left(2\frac{\partial w}{\partial z} - \frac{2}{3}\left(\frac{\partial u}{\partial x} + \frac{\partial v}{\partial y} + \frac{\partial w}{\partial z} \right) \right) \right) + \frac{\partial}{\partial x}\left(\mu\left(\frac{\partial w}{\partial x} + \frac{\partial u}{\partial z} \right) \right) + \frac{\partial}{\partial y}\left(\mu\left(\frac{\partial v}{\partial z} + \frac{\partial w}{\partial y} \right) \right) \ ,$$

where ρ is the density of the liquid, μ is viscosity of the liquid, p is pressure; u,v,w are components of speed of an elementary volume of the liquid; X,Y,Z are the components of force which operates on the elementary volume of the liquid.

2) Maximum terms, which stipulate nonbreakability of the thread of liquid from the hard walls and determine forces of frictions which operate between a hard matter and liquid. Simply enough to set maximum terms for flat surfaces:

$$v = 0, \quad \boldsymbol{F} = f_1 (\boldsymbol{V_1} - \boldsymbol{U})/(V_1 - U) \quad \text{(for the top surface)},$$

$$v = 0, \quad \boldsymbol{F} = f_1 \, \boldsymbol{U}/U \quad \text{(for the bottom surface)}$$

where $\boldsymbol{F}$ is the vector of force which operates on the elementary volume of liquid; $\boldsymbol{V1}$ is a vector of speed of flat topside, $\boldsymbol{U}$ is a vector of speed of elementary volume of liquid, $V1$ and U are the proper modules of these vectors.

Setting the maximum terms for flowing around the anisotropic particles a liquid it is though possible as equations, however much their use in a numeral experiment causes calculable difficulties because the size of particles is relatively small, and that is why for the correct calculation of conduct of liquid round every particle it is necessary to introduce the calculable net round every particle and considerably to increase the dimension of task. It is therefore expedient to separate equation of motion of liquid round a large spherical particle, oriented in relation to the system properly, and, drawing on the got result as the model problem, to scale it to the sizes of this particle.

3) Correlations which determine effort of shift (slide) and operates on the border of elementary volume of liquid (considering an olive a newtonian liquid):

$$\tau_x = \mu \frac{du}{dy} ; \tau_z = \mu \frac{dw}{dy} .$$

Conclusions

In the article the mathematical model of process of friction between flat surfaces which move flat and parallel is considered, in the presence of liquid lubricating material in the complement of which introduced the admixture of particles with anisotropic properties. A numerical experiment is conducted from the design of hydrodynamic processes in the oil taking into account influence of anisotropic particles and nanoparticles. As a result of numerical experiment the examples of dependences of equivalent viscosity of olive with admixtures on concentration of admixtures and other parameters are got. The purpose of the conducted numerical experiment was determination of the force of friction. In order to disengage oneself from the geometrical parameters of the experiment, it is expedient to take the relative force of friction to the area of surfaces and to the gradient of speed, and to examine the value $\mu' = \dfrac{F}{S \cdot (u/h)}$, where F is force of friction, S is an area of surfaces of friction, h is distance between them, u is speed of motion of one of the surfaces in relation to other.

Perspective directions of research can be solving the tasks of numeral design of processes of friction in other configurations of surfaces, for example – to the process of hydrodynamic friction.

References

1. *Васильев Ю.Н.* Математическая модель трения и изнашивания поликристаллических твердых тел /Ю.Н.Васильев, В.А. Фуголь. – Трение и износ. – 2010. – Т. 31, вып. 2. – С. 127-143.

2. *Hori Y.* Hydrodynamic lubrication /Y. Hori. – Springer, 2006. – 238 p.

3. *Белоцерковский О.М.* Численное моделирование в механике сплошных сред / О.М.Белоцерковский. – М.: Наука, 1984. – 520 с.

4. *Glazok O.M.* Method of solving systems of linear algebraic equations in the distributed calculating environment /O.M.Glazok. //Proceedings of the NAU. – 2010. – № 3 (44). – Pp. 50-55.

Y.B. Artamonov, candidate of technical sciences,
O.S. Vasyliev,
(National Aviation University, Ukraine)

USE OF ANALYTICAL TECHNOLOGIES FOR RECOGNITION OF IMAGES

In this article method of recognition system is defined using RGB-format. Using facilities of Microsoft Visual Studio represented methods on aerial photo. On this base make conclusion about fault rates and opportunity of next researching. Proposed goals which can be reached using system of recognition on unmanned aerial vehicles.

Introduction

Analytical technologies - a method that based on some models, algorithms, mathematical theorems, which allow for known data to estimate the value of unknown characteristics and parameters.

Analytical technologies in the first place are needed people who make important decisions - managers, analysts, experts and consultants. Company profit in most cases depends on the quality of those decisions - the accuracy of forecasts, optimally chosen strategies.

The question of pattern recognition is relevant past 40 years and relevance does not decrease so far. So when developing software to control unmanned aerial vehicles (UAV) pattern recognition problem faced in the development of autopilot.

Pattern recognition has a wide range of use in the autopilot:

1) problem of determining the location of the UAV;
2) search certain objects on the ground, and so on;
3) patrolling moving objects;
4) analysis of area.

As test data we use an arbitrary image area. It should be images of acceptable quality and resolution. But given that arbitrary image, you need to take into account the uncertainty analysis. As a model for search you must select a unique part of the picture. This object has characteristics very well and clearly visible to the human eye.

1. Description of method.

With the image selected sample of size 375x300 pixels. This size is not significant and is equal to the size of fields in program analysis.

Data Format - 32 bits per pixel in RGB-format. This format allows you to submit any color as three components (red, green, blue). This format is used for many sources of color are light sources such as screens monitors, TVs and more.

Software tools can track each color separately in 8 bit format. This can significantly reduce the required memory for storing images.

Also, depending on the character set can be present such as setting transparency. Length - 8 bits. The lower the number - the transparent image.

To start, load an image and draw a complex component that is a decimal display format code in RGB. This means Microsoft Visual Studio let us operate image as an array of points. For simpler processing transform each pixel in the array, because array access faster than taking the color of each pixel. Thus we get an array of colors for each point on the screen. For the first attempt selected image areas of road junction (Fig. 1), and the search is performed on the image of the road (Fig. 2).

The way a simple search of both arrays, we compare the full image of an image search. The comparison is for an integrated color value of the point.

Since the color format consists of 24 bits, according have 2^{24} colors. It is 16 million colors. The human eye does not distinguish neighboring colors. And even colors with a difference of 10 is also difficult to distinguish. Therefore, there is the first option - sensitivity.

Fig. 1. Original image

Fig. 2. Search image

It appears first "reef." For example, the colors # 969600 and # 96960A with a difference of 10. But this difference is actually blue. In decimal form this number 9868800 and 9868810 respectively. But if you take the colors # 969600 and #909600 is a significant difference in the concept of decimal 9,868,800 and 9,475,584. The difference of 400 thousand, but a difference of 6 units of red. Thus, we can conclude that the need process each color separately. Etalon has options 27x54 points. It is 1458 points for comparison. Original image has 375x300 points. To find the right bulkhead will need about 140 million cycles. Even with modern methods of computer technology it is very bulky volume and process.

Having considered the color values of neighboring pixels can be seen that they are very similar. And after 2 or 3 pixels color is not significantly changed. So should not conduct an analysis of each area, such as every second or third. This will increase the speed to 2 or 3 times, respectively.

Can we expect 100% match in this case? Of course not. But we get some suspicious sites and rate increases at times.

Fig. 3. Result of searching

Thus we have 35 million plus 109 checks on suspicious similarity plots. All areas are in close proximity to the original and may be the correct result.

Increase the sensitivity and reduce the chance to match: We have 208 squares, half of which are obviously untrue and have a very low coefficient of coincidence. Hence we can conclude that the increase in step with decreasing test sensitivity and threshold matching can speed up the algorithm and reduces the probability of the result.

Recognition only contrasting polygons.

Another way to find a piece of road is to subscribe it as a polygon of low contrast. Low-contrasting polygon has a little difference between two neighboring pixels. That's why find a diagram which represent difference by one of RGB-colors. For example red. Result is shown on fig.4.
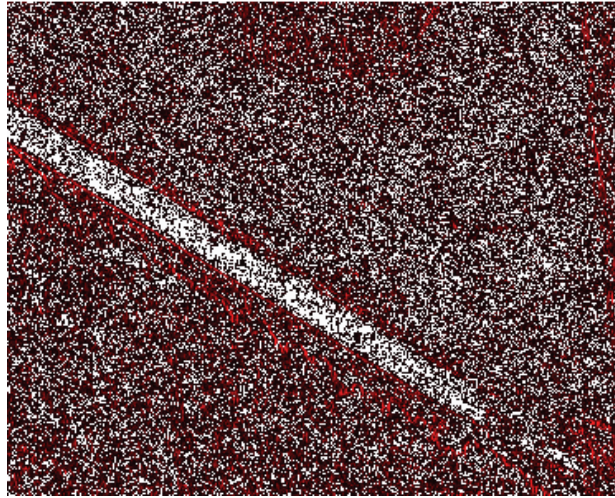
Fig. 4. Image of differences between two pixels in row

On this figure low-contrast (less 3) is shown as white color and another differences is multiplied by 5. For human it is evident where the road is (most white color) and we can see contrast places (saturated red color)

Contrasting and low contrasting polygons (10x10) is shown on fig.5 and fig.6.

Fig. 5. Low contrasting polygons   Fig. 6. High contrasting polygons

All systems for pattern recognition with a rate coefficient as a false alarm and failure rate.

Coefficient of wear - the ratio of false positives to the total number of inspections. For the first case it is 0, the second - 0, for the third $3 * 10^{-6}$. It is supposedly good, but believe that some nuances not taken into account as it complexity image and an array of test images is small.

Bounce rate - the ratio of failures to the total number of inspections. In all three cases, it is 0. This indicates a lack of the original.

In practical problems the system has some standards. This may be the faces of people, photos of products, objects on the map. Man thinks images. This enables identification of different shape, parameters. For each group of products is desirable to find the model parameters. For example, a set of lines.

One measure is the difference brightness points. When the point of equal brightness with the background, it merges with the background. Therefore, the difference brightness or color, we can build a model of standards.

Creating an album of samples increases stability, but increases the rate of false positives. A large number of elements of the album considerably slows down the algorithm is a generalized model is to simplify the search.

To investigate polygons it is recommended another system, for example neurosystem.

Proposed method is a method of pre-processing data to recognition on another system.

Conclusions

1. Using full-color images requires significant memory and performance. The shorter operands for comparison, the more operations are compared.

2. Analyzing the results must take into account data representation format #RRGGBB and highlight the prevailing color in this type of image.

3. Determination of sensitivity is determined by external conditions and the experimental method.

4. Step movement of the image is greater than unity - this will increase performance. But the maximum value should be set up according to the image. In this experiment used a 1/10 of the sample.

5. Lowering the percentage of matches with the standard gives false results, but allows you to define the image of some disabilities or differences.

6. A simple neurosystem can complete this method for powerful instrument in UAV-software.

References

5. *Айзерман М. А., Браверман Э.М., Розоноэр Л. И.* Метод потенциальных функций в теории обучения машин. М., «Наука», 1990.

6. *Андерсон Т.* Введение в многомерный статистический анализ. М., Физматгиз, 1993.

7. *Фисенко В.Т., Фисенко Т.Ю.* Компьютерная обработка и распознавание изображений: Учебное пособие. - СПб.: СПбГУ ИТМО, 2008. - 192 с.

B.G. Maslovskiy, candidate of technical sciences,
O.M. Glazok, candidate of technical sciences,
(National Aviation University, Ukraine)

MODELING THE OPERATION OF AN AIRCRAFT ON THE BASIS
OF TEST-DRIVEN DEVELOPMENT

The way of building the model of the aircraft operation is considered. The approach of test-driven development proposes the possibility to garantee the quality of the code and its easy maintenance and upgrading afterwards. The fee for these features has the form of some additional labour that the developer needs to put in his or her work during coding.

A programmatic code is considered as bad code, if it does not work. However, if a program performs, at least, some activity tat seems to be correct, and the programmer believes that his code works well and is good, what is his confidence based on? Developers often run into a number of problems: there can be errors in the programs, a code can be heavy for understanding, et cetera. And majority from these problems can reveal themselves not immediately, but after weeks, months and even years of work with a project.

Further, even if a programmer is sure that there are no errors in a code, it can happen that it will be necessary to do refactoring, that is, to change something in the code, or, maybe, split large functions into smaller ones. How is it possible after bringing of such changes to acquire the confidence that the obtained code still works? For such a confidence it is necessary to have warranties; these warranties may have a form of successful realization of certain tests. Among the stages of the software lifecycle, such as analysis and forming of requirements, development of specification of product, coding, testing of the product, maintaining the prepared product and correction of the errors discovered in it – the stage of testing takes at least 40-45% of the developer's working time.

Therefore modern developers consider even working code as a bad one, if it is not easily subject to testing. The automatic testing is here implied, that is, the use of testing programs, checking out code in the automatic mode. If it is required to modify the code somehow in order that it can be tested, – it means that the code is written in a bad manner. Why? Because, again, after these changes there is no guarantee that the code is able to continue working exactly as it was working before these changes. Thus, here is the closed circle.

Methods of improvement of this situation are all based on various kinds of testing. The most known of them are manual code testing, automatic code testing, module testing, integration testing. Any professional programmer pays to testing more or less attention.

In a simple case, a test may consist in the «manual» start of the tested programmatic system with application of some (test) data inputs. The manual testing of the program is a very labour intensive process; the bigger the program becomes, the more difficult is to test it by hand. The manual testing works well for the student programs which consist of 300-400 code lines. But, if you develop the program that occupies a million lines, to test all its features by hand during reasonable time is impossible. And, even if you succeeded in doing that, any improvement or alteration in the program done thereafter will introduce probability to break something, so after the alteration you need to repeat all labour-intensive testing again. Finally, your customer or client purchases the program and notices that there are some situations where the program does not work as it should, while you was not able to cover these situation in your program of manual testing.

It is why there appeared technologies which allow to test the program automatically. One of such technologies is the module testing. Module testing is an automatic process of verification of program units for correctness of their work. Essentially, the developer needs to write for every class with non-trivial functionality the set of tests which check up work of methods of this class. For the facilitation of development of tests the special frameworks has been created. Various code-driven

testing frameworks have come to be known collectively as xUnit. These frameworks allow testing of different elements (units) of software, such as functions and classes. The main advantage of xUnit frameworks is that they provide an automated solution with no need to write the same tests many times, and no need to remember what should be the result of each test. Such frameworks are based on the design by Kent Beck, originally implemented for Smalltalk as SUnit. Later SUnit was ported to Java, where it turned into JUnit. From there, the framework was also ported to other programming languages and development platforms, e.g., CppUnit (for C++), NUnit (for .NET). They are all referred to as xUnit and are usually free, open source software.

Extensions are available to extend xUnit frameworks with additional specialized functionality. Examples of such extensions include XMLUnit, XmlUnit.Xunit, DbUnit, HtmlUnit and HttpUnit.

There are also some other popukar testing frameworks, such as CxxTest and TestNG.

All test frameworks share the following basic component architecture, with some varied implementation details:

1) *Test case* is the most elementary concept or class. All unit tests are inherited from it.

2) *Test fixture* (also known as a test context) is the set of preconditions or state needed to run a test. The developer should set up a known good state before the tests, and return to the original state after the tests.

3) *Test suite* is a set of tests that all share the same fixture. The order of the tests shouldn't matter.

4) *Assertions* are functions or macroses that verify the behavior or the state of the unit under test. Failure of an assertion typically throws an exception, aborting the execution of the current test.

The execution of an individual unit test is described in the code as follows:

setup(); /* First, we should prepare the program's environment to make an isolated sandbox for testing. */

...

/* Body of the test; */

...

teardown(); /* Finally, whether the test succeeds or fails, we should clean up the program's environment to not disturb the operation of the other tests or code. */

The setup() and teardown() methods serve to initialize and clean up test fixtures.

Together with the module testing, the technique of development through testing, or test-driven development (TDD), is widely used. It is a technique of programming, at which at first tests are written for the module, and then the programmer adds to the module functionality which corresponds to these tests. Such an approach allows to substantially promote the quality of the code. The tests manage development, and partially appear as formal requirements to the module. At first we create a test which describes the desired behaviour of the class, and then implement the functionality of class, which satisfies these requirements. These tests can be developed in obedience to a specification, or, occasionally, just the test can play the role of specification.

Another practice of programming that lies close to test-driven development is referred to as test-driving. The test-drive development consists of short cycles, not longer that 10-20 minutes.

Development in the test-driven style includes the followings stages [1].

At the first step a developer extracts a program code from repository. This step guarantees that a developer always deals with the latest version of programmatic code.

The second step is adding of a new test to the set of tests which are already present. If some framework is utillized for writing a test, the test is a function or a method which checks whether the system will realize a new conduct, or whether it contains some error about which the testing command reported. The purpose of test is either to reproduce an error, or specify by means of the programming language some new requirements to the programmatic system. It is very important to write the test before making the corresponding alteration in the code; thus, the test places formally new requirements to the code.

Since a new test is written, the third step is executed – the program is compiled and the tests are run. All of the tests must be executed successfully, except for the latest one, which has been just written, because it imposes a new requirement to the system which it does not satisfy yet.

This step is needed in order to make sure, that our test is successfully integrated in the general system of testing, and indeed allows to reproduce an error. That is, a new test reflects new system requirements correctly.

On the fourth step we must correct a mistake or add new functionality with a minimum of efforts. It is important to add the simplest possible solution which will demand from us to write a minimum of code. The less code is written, the less chances, that we will break something with it. Well, it is difficult enough to make an error at writing 3-4 lines of code; at least, it is more difficult, than to make an error while you write 50-60 lines of code.

On the next step it is necessary to do refactoring – a process of change of underlying structure of the program without the change of its conduct. Naturally, refactoring means that we introduce some changes to the code, together with a new probability to break something in the construction of the program. Therefore further it is again necessary to start a test and make sure that our changes pass them, so we have not broken anything. If something goes wrong at this stage, the problem should be fixed, until the tests are run successfully.

And the last step is uploading of our changes into the repository.

Let us consider this approach on the example of development of class which describes the state of an airplane. It is necessary to realize the Airplane class, possessing the following properties: amount of fuel, amount of passengers onboard, presence of pilots and stewardesses onboard, current state (on earth, sets to flight, flight, landing), passengers seats capacity

A class must support the followings methods: fueling, entering and exit of passengers, entering and exit of members of crew, being on the flight, landing. Prior to writing any actual airplane code, we need to create a set of tests for the class of airplane. Let us create a new test with the use of the CxxTest library, that checks up the correctness of creation of an instance of the Airplane() in terms of correct operation of the class constructor. The code of the test case will be as simple as the following:

```
class AirplaneTestSuite : public CxxTest::TestSuite
{
public:
  void TestAirplaneConstruction()
  {
          Airplane airplane;
  }
};
```

Here we call the constructor of the Airplane class. Obviously, this code will not work, because we did not yet write the Airplane class; but, nevertheless, we must try to compile our program and make sure that it is not compiled. This result tells us that our test is correctly plugged into the program, and its compiling is executed, though it is finishes in an abortive manner. In order to comple the test successfully, we need to add the Airplane class to the program. Now, after the necessary changes in the code and inclusion of the header file, our tests get an access to the source code of the Airplane class. Now the test passes successively.

One of the following CxxTest test suits produced for the purproses of testing of such a class may have the following form:

```
class AirplaneTestSuite : public CxxTest::TestSuite
{
public:
  void TestAirplaneConstruction()
  {
          // 100 – number of seats, 500.0 – fuel tank capacity
```

```
        Airplane airplane(100, 500.0);

        TS_ASSERT_EQUALS(airplane.GetFuel(), 0);
        TS_ASSERT_EQUALS(airplane.GetNumberOfPassengers(), 0);
        TS_ASSERT_EQUALS(airplane.GetNumberOfSeats(), 100);
        TS_ASSERT_EQUALS(airplane.GetNumberOfPilots(), 0);
        TS_ASSERT_EQUALS(airplane.GetNumberOfStewardess(), 0);
        TS_ASSERT_EQUALS(airplane.GetFuelTankCapacity(), 500.0);

        // 50 – number of seats, 400.3 – fuel tank capacity
        Airplane airplane1(50, 400.3);
        TS_ASSERT_EQUALS(airplane1.GetNumberOfSeats(), 50);
        TS_ASSERT_EQUALS(airplane.GetFuelTankCapacity(), 400.3);
    }
};
```

It is easy to notice that this test suite includes a bunch of tests that check the necessary values of the instance's properties. Now, among the other features, we took into account the possibility of fueling of the airplane. Again, we must start with creation tests that check up the state of fueling of airplane, taking into account that the airplane must have another additional property – the capacity of the fuel tank. The airplane can take in some amount of fuel, but not more than the fuel tank allows. So, the amount of fuel will be passed as the parameter of a constructor. Now we need to have for testing at least two instances of airplanes with the fuel tanks of different capacity. At running of the tests, it will immediately turn out that the returned amount of fuel is not equal to the expected value, so the initialisation of the property value is performed in a wrong way, possibly due to some garbage information in the memory. Now this error is easily detected and corrected. Now, when we believe that the code is correct, we run the tests again, and there is again an error, now it is in the assertion TS_ASSERT_EQUALS(airplane.GetFuelTankCapacity(), 400.3). The method of GetFuel() should return the 400,3 litre for the second airplane, while in fact it returned 500 for some reason. It is the very realistic situation, though. So, our test suite allows us to find the errors one after another, until the Airplane has the desired behaviour.

Conclusions

The report describes an example of building the model of the on-flight filling the aircraft tanks with fuel on the basis of the test driven development paradigm. The power of the test driven development lies in the fact that the organization of the process guarantees that the code remains correct in the logical sense at almost any point of the development process. As an addition to the correct code logic, the developer acquires a bunch of automatic tests that may help him to maintain the correctness level at any further work on the code. Also, the manner of solving the problem completely changes, as the developer actually considers and produces a solution at developing the tests, prior to the developing of the tested code.

Nevertheless, any conveniences should be payed for. In this case, the payment is the need to write the tests – and it is just the developer who must wear this burden. Behind that, there is another, more valuable sacrifice – the developer must change the approaches to the problem consideration in his or her mind.

And, finally, as Dijkstra said, "Testing may be utillized for demonstration of presence of errors in programs, but it is not able to prove their absence".

References

1. *Stephens M.* Design driven testing: test smarter, not harder /Matt Stephens, Doug Rosenberg. – Apress, 2010. – 368 p.

UDC: 004.78 (045)

Artamonova V.O.,
Zholdakov O.O.,
(National Aviation University, Ukraine)

A SOFTWARE ENVIRONMENT FOR AUTOMATED TEXT MANIPULATION

The basic concepts which have been used in the new program environment of texts editing "Intelligent book" were considered. The Primary goal of program environment is creation of electronic books with the content which automatically changes according to the level of information presentation depth. The basic mechanism of program work is settled on creation certain connections between text blocks, which allow to correct view of questions representation, which are revealed in the given text, automatically.

Preamble

The problem of automated detection the text content is not new. For over than 30 years both separate scientists (Leont'eva N.M.) and scientific departments of number of institutes, primarily in Russia (The Institute of Linguistics of the Russian State Liberal University, The Institute of informatics problems of RAS, Russian SRI of Artificial Intelligence, The Kazan's state University [1] etc.) are engaged by this problem. The results of scientific researches became separate programmatic developments – Dialing, Politext, Galaxy-ZOOM, and even open-source projects (one of the most known is the Automatic text processing [2]).

But there is a task which has no decision until now – it is creation of adequate to the necessities of concrete user electronic variant of book product by the help of computer programs in the automatic mode. Even approaches to the decision of this scientific task are not enough formalized or take contradictory character until nowadays.

That, as soon as work reaches to recognition of text sense or even logical construction of connections between heterogeneous information in the book text, one have to use knowledge and ability of experts from the proper field of knowledge and bibliography. The necessity of personnel training, mediocre speed of information treatment, subjectivism, possibility of errors, and on the whole – a high cost of treatment the large volumes of text, does expedient development and use of software for automation of this process.

Exactly on crossing of these two directions – automatic text processing and development of bibliography-robot, – lies the idea of creation the software environment «Intelligent book».

The basic task of this software environment is creation of electronic books with content which automatically changes according to the level of information presentation depth. This product on nowadays design time needs «hand» tuning (what in course of time possibly will be transferable on automatic) and provides the performance of the followings objectives:

1. Creation of the book itself;

2. Determination of the complete plural of connections between the book's text and it' content;

3. Filtration of the given information on the basis of the personal interest of user of questions which are lighted up in a book.

The basic mechanism of the program work is based on creation of certain connections between the blocks of text in the electronic book environment, which allow to correct the presentation of subject of this text in the automated mode.

Conception of the «Intelligence book» software product construction

The given problem needs the decision of the followings two questions:

1) Correct fastening of text elements, what will allow to represent information both in a complete form and as an abstract; thus an abstract form must maximally pass the common content and, at a necessity, ex-pose the separate fragments of text, which can interest a reader;

2) Adjusting the flexible mechanism of watching the personal interest of reader, this will allow him to give the timely access to necessary information.

The personal "interest" concept does not have a clear determination in psychology until now. There is a point of view, that attention is determined as an arbitrary or involuntary orientation and concentration of psychical activity on some object of perception. And this concentration does not appear in a "clean" kind.

Unlike cognitive processes (perception, memory, thought, etc.) attention does not have the special sense (determination); it appears as being inside of these processes and inseparably from them. Basic properties of attention in this case are volume, concentration, firmness, oscillation, switching. The volume of attention is measured by the amount of objects which are perceived simultaneously. The objects incorporated according to their sense are perceived in a greater amount, than not incorporated. For the grown man the volume of attention is equal to 6-8 objects. Separately here distinguish involuntary and arbitrary attention [3].

First who made an attempt to expose the concept of attention from the mechanical point of view was Ribo in the motive theory of attention, and later this approach was developed in behaviorists and reflexologists. In this case attention is taken to the reflex options. The second attempt was related to the theory of Gestalt psychology and reduced the phenomenon of attention to the structures of the sensory field [7]. There can be no doubt that reflex options act substantial part in initial, most primitive forms of attention. It is well known that influence on the organism of some irritant usually cause organism to reflexly adapt to its best perception. Thus, for example, influence of sound on the ear-drum irritant cause a reflexive turn toward the source of sound.

Obviously, that using this principle it is possible to watch and general signs of attention to the text for a reader. As basic elements for attention control were select:

1) Time of being on a page (only a middle area gets out, because a very rapid transition means absolute incuriosity, and large time of revision can mean the loss of the personal interest) is a basic parameter of control which relates to direct properties of attention. (In subsequent modifications of the system this parameter must change automatically, depending on the features of concrete user);

2) Motions of manipulator (for every reader there is a scenario of the interested transition – transition without the rapid returning on the page of content – in which the set of motions enters by a manipulator during the revision of text). This parameter needs the special tuning on a user and relates to the second proper-ties of attention.

Technology of the correct text elements fastening

For the correct fastening of text elements, which will allow representing information both in a complete form and as an abstract, it was decided to present content of book text after a chart, represented on Fig. 1. From this chart it is evidently, that there are three levels information presentations in the program. They are intended to grant the information to concrete user in the volume in which it is needed on the first stage of the personal interest.

The first level: it is a text without any reductions and treatments. This level is intended for use of readers who are only introduced the thematic of a book.

The second level: at this level the text of book passes certain processing (more detailed it is described below) which will allow the user with a shallow or middle knowledge of book subject to obtain most exact information, without a necessity to read what he already know.

The third level: information at this level passes the detailed treatment. User at this level has only a common picture of the book subject and requires just separate exact theorems and formulas without any explanations. On each of these three levels it is necessary to give user the possibility of access to the searching sys-tem, which allows finding all necessary connections in a book, which could not get to the authors needed connections.

Inserting own semantic connections can be presented as a separate branch of the program development. But this mechanism will require not only grant permission for user to the management of semantic connections, but also requires creation of separate instrument for verification contradictory connections of absence.
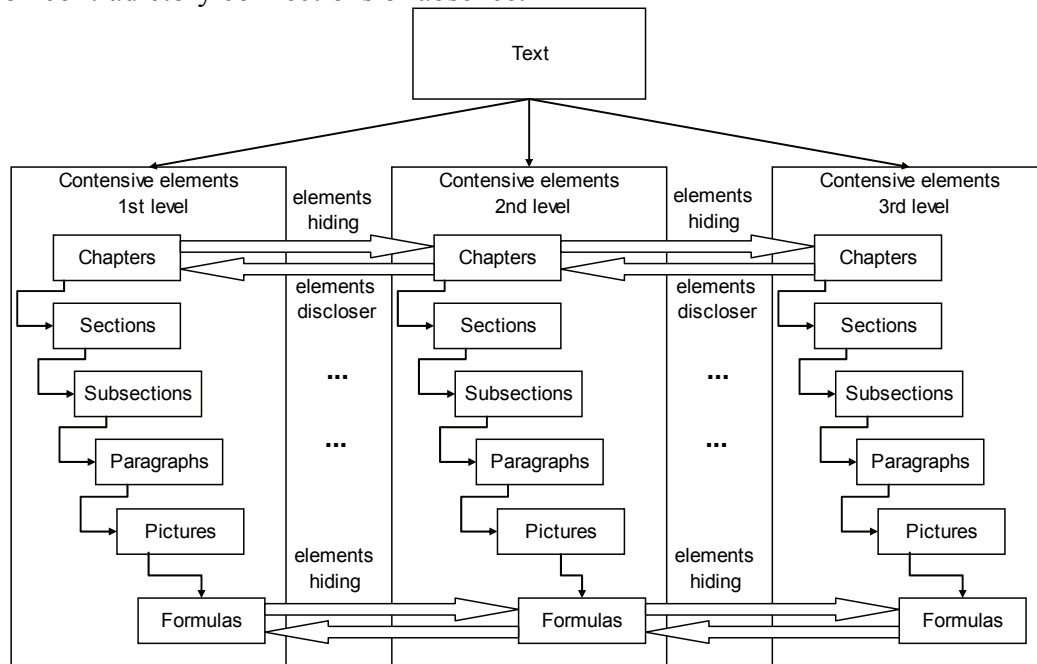

Fig. 1. Schema of book content division on 3 levels

Programmatic facilities of watching the personal interest by text contents

The question of watching personal interest of reader needs programmatic realization of such functions:

1) Control of time being on the page which automatically translates all elements of this page on the proper level of representation (also all elements of text, which are richly in content related to the elements of this page, get greater status);

2) Control of transitions between elements, which have rich in content copulas (this control requires the flexible extra charge of opening the separate text elements status marks);

3) Control of indirect user actions, such as manipulator moves, keys pressing, copying and insertion of text elements into other programs.

Obviously time have to be a basic control parameter, what reader outlays on an acquaintance with the text element. But even the book author cannot exactly present the expected time of reading the select group of text fragments.

That is why the next formula of nominal presentation time calculation of the group of selected for showing elements was selected as a standard measure:

$$T_N = \sum_{i=1}^{A} (K_i \cdot T_T) + \cdot T_F \cdot F + T_P \cdot P,$$

where T_N – is normative time for consideration of selected text fragment which consists of A indentions, F of formulas and P of pictures,

K_i – is amount of letters in an i indention,

T_T – is mean time on reading of single character,

T_F – is mean time on understanding of one formula,

T_P – is mean time for consideration of one picture.

For determination of mean values of T_T, T_F, T_P, which can be different for different users, is used program unit, at reading of text from screen, requires to push the button upon termination of reading, and at consideration of formulas and pictures – to answer question to them (time is taken

into account only in the case of positive answers).

After determination of time, necessary for mastering of this text element, all elements related to him are opened for access and the additional opening marks begin to be counted for all connections of the first and second levels (after achieving the proper amount of total marks they also will open).

Thus user does not manipulate transitions from one level to other. But he gets possibilities to preliminary define the level of opening the text contents or specify on erroneous, according to his opinion, copulas.

As was said higher, user can get possibility of creation his own connections for adjusting of material opening procedure in obedience to own desires.

The use of network mechanisms for the improvement of the program quality work

On the initial stage of using any new book in the described environment the basic problem is determination of possible time being on a page.

The mechanism of determination of mean time is described in a previous section. However, it is almost impossible to define limit values (maximum and minimum) according to this scheme. But exactly these values with greater authenticity specify on the personal interest in the selected fragment of text.

For the decision of this task a network version, which foresees work with the electronic book of not one user, but whole group, was developed. Thus working with an electronic book is possible not only in the conditions of network usage. Connection to the server can be made only for sending of data about own statistics and receiving of updates about statistics of other users.

Every user passes registration and gets unique type which will be saved not only for current electronic book, but also for all next books with which this user will work in this software environment.

Having possibility of collecting the statistical information, it is possible to move from the evaluation of normal time of reading a fragment after a middle formula which is used for all fragments, to determination of this time for every text element.

Conclusions

Potential of the use of similar software environment of books with internal semantic copulas is very high; in fact everyone would like to get necessary data quickly, without the considerable charges of time on an information retrieval, as in an ordinary book, and what is main – consistently.

Also a question of common acquaintance and receiving of the initial understanding of textbook or book content is important. Taking into account the large volume of information exactly the mode of acquaintance can be most used for work with materials of books in this software environment.

It is obviously expedient to consider possibility of application of this software product in the controlled from distance education at creation of electronic courses and books.

Certain application this program will also be able to get in works of bibliographies of scientific editions in matters of automation.

References

1. *Биряльцев Е.В.* Особенности лексико-семантической структуры наименований артефактов реляционных баз данных/ *Биряльцев Е.В., Гусенков А.М., Галимов М.Р.* // Тр. Казанской школы по компьютерной и когнитивной лингвистике TEL-2005, Казань: Изд-во Казан. гос. у-т, 2006, Вып.9. С.4-12.

2. Project of automated text process - www.aot.ru

3. *Вопросы* развития познавательных интересов учащихся в процессе обучения /Под общей ред. Д.К. Гилева.- Свердловск, 1970.–143с.

4. Світ психології - www.psychology.net.ru.

UDC: 004.78 (045)

G.M. Kremenetskiy, candidate of technical sciences,
(National Aviation University, Ukraine)

GROWING ARTIFICIAL NEURAL NETWORKS IN DYNAMIC ENVIRONMENT

This article is a review of recent growing and pruning strategies in Artificial Neural Networks (ANN). Artificial Neural Networks which adjust own capacity and structure according to data in use are the cutting edge of science in this area. For the last time such kind of growing and pruning ANN strategies was developed: Adaptive Growing Neural Gas (GNG), Growing Cell Structures (GCS). These strategies were described in article taking in consideration dynamic Internet environment. Network traffic decreasing is the important task in distributed Internet applications. For this purposes the possibility of clustering such kind of ANN was analyzed. Also, there proposed WEB services as standard for ANN clusters interconnections.

The Artificial Neural Networks (ANN) fast growing last ten years. We can highlight the main properties, which initiates this growing: computation possibilities, usage scope increasing, ANN simplicity increasing for wide users. The network structure chooses is one of biggest problem in ANN. Many static structures exist: back propagation networks, self-organizing maps etc, but in that case the dynamic development of ANN is a weights change only. ANNs with dynamic structure are not such spreaded because of small count of their realization as software or hardware.

Growing Cell Structures

This model [1] is rather similar to the growing neural gas model. The main difference is that the network topology is constrained to consist of k-dimensional simplexes whereby k is some positive integer chosen in advance. The basic building block and also the initial configuration of each network is a k-dimensional simplex. This is, e.g., a line for k=1, a triangle for k=2, and a tetrahedron for k=3.

For a given network configuration a number of adaptation steps are used to update the reference vectors of the nodes and to gather local error information at each node.

This error information is used to decide where to insert new nodes. A new node is always inserted by splitting the longest edge emanating from the node q with maximum accumulated error. In doing this, additional edges are inserted such that the resulting structure consists exclusively of k-dimensional simplexes again.

The growing cell structures learning procedure is described in the following:

1. Choose a network dimensionality k. Initialize the set A to contain $k+1$ units c_i:

$$A = \{c_1, c_2, ..., c_{k+1}\}$$

with reference vectors $w_{c_i} \in R^n$ chosen randomly according to $p(\xi)$.

Initialize the connection set $C, C \subset A \times A$ such that each unit is connected to each other unit, i.e., such that the network has the topology of a k-dimensional simplex.

2. Generate at random an input signal ξ according to $p(\xi)$

3. Determine the winner s:

$$s(\xi) = \arg\min_{c \in A} \|\xi - w_c\|.$$

4. Add the squared distance between the input signal and the winner unit s to a local error variable E_s

$$\Delta E_s = \|\xi - w_s\|^2$$

5. Adapt the reference vectors of s and its direct topological neighbors towards ξ by fractions e_b and e_n, respectively, of the total distance:

$$\Delta w_s = e_b(\xi - w_s)$$
$$\Delta w_i = e_n(\xi - w_i) \ (\forall i \in N_s)$$

Thereby, we denote with N_s the set of direct topological neighbours of s.

6.   If the number of input signals generated so far is an integer multiple of a parameter λ, insert a new unit as follows:

• Determine the unit q with the maximum accumulated error:
$$q = \arg\max_{c \in A} E_c$$

• Insert a new unit r by splitting the longest edge emanating from q, say an edge leading to a unit f. Insert the connections (q,r) and (r,f) and remove the original connection (q,f). To re-build the structure such that it again consists only of k-dimensional simplices, the new unit r is also connected with all common neighbors of q and f, i.e., with all units in the set $N_q \cap N_f$.

• Interpolate the reference vector of r from the reference vectors of q and f: $w_r = \dfrac{(w_q - w_f)}{2}$

• Decrease the error variables of all neighbors of r by a fraction which depends on the number of neighbors of r:
$$\Delta E_i = -\frac{a}{|N_r|} E_i (\forall i \in N_r).$$

• Set the error variable of the new unit r to the mean value of its neighbors:
$$\Delta E_r = -\frac{a}{|N_r|} \sum_{i \in N_r} E_i .$$

7.   Decrease the error variables of all units:
$$\Delta E_c = -\beta E_c (\forall c \in A).$$

8.   If a stopping criterion (e.g., net size or some performance measure) is not yet fulfilled continue with step 2.

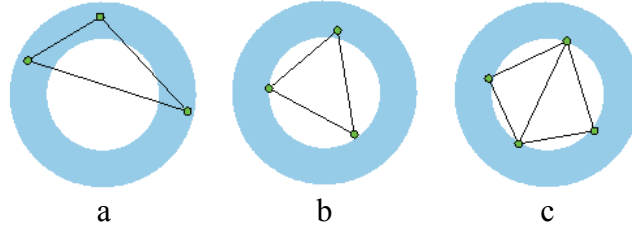Neural network structure for this algorithm You can see on Fig. 1

a   b   c

Fig. 1. GCS growing process for ring-shaped probability distribution
(a – 0 signals, b – 100 signals, c – 300 signals)

Growing Neural Gas

This method [2,3] is different from the previously described models since the number of units is changed (mostly increased) during the self-organization process. The growth mechanism from the earlier proposed growing cell structures [1] and the topology generation of competitive Hebbian learning [4] are combined to a new model. Starting with very few units new units are inserted successively. To determine where to insert new units, local error measures are gathered during the adaptation process. Each new unit is inserted near the unit which has accumulated most error. The complete growing neural gas algorithm is the following:

1.   Initialize the set A to contain two units c_1 and c_2
$$A = \{c_1, c_2\}$$
with reference vectors chosen randomly according to $p(\xi)$.

Initialize the connection set $C, C \subset A \times A$, to the empty set: $C = 0$.

2.   Generate at random an input signal ξ according to $p(\xi)$

3.   Determine the winner s_1 and the second-nearest unit $s_2\,(s_1, s_2 \in A)$ by

$$s_1 = \arg\min_{c \in A}\|\xi - w_c\| \text{ and } s_2 = \arg\min_{c \in A\backslash\{s_1\}}\|\xi - w_c\|.$$

4.   If a connection between s_1 and s_2 does not exist already, create it: $C = C \cup \{(s_1, s_2)\}$

Set the age of the connection between s_1 and s_2 to zero (``refresh'' the edge): $age_{(s_1,s_2)} = 0$.

5.   Add the squared distance between the input signal and the winner to a local error variable:

$$\Delta E_{s_1} = \left\|\xi - w_{s_1}\right\|^2.$$

6.   Adapt the reference vectors of the winner and its direct topological neighbors by fractions e_b and e_n, respectively, of the total distance to the input signal:

$$\Delta w_{s_1} = e_b(\xi - w_{s_1}), \ \Delta w_i = e_n(\xi - w_i) \ (\forall i \in N_{s_1})$$

Thereby N_{s_1} is the set of direct topological neighbors of s_1.

7.   Increment the age of all edges emanating from s_1:

$$age_{(s_1,i)} = age_{(s_1,i)} + 1(\forall i \in N_{s_1})$$

8.   Remove edges with an age larger than $a_{\max}$. If this results in units having no more emanating edges, remove those units as well.

9.   If the number of input signals generated so far is an integer multiple of a parameter λ, insert a new unit as follows:

• Determine the unit q with the maximum accumulated error: $q = \arg\max_{c \in A} E_c$

• Determine among the neighbours of q the unit f with the maximum accumulated error:

$$f = \arg\max_{c \in N_q} E_c$$

• Add a new unit r to the network and interpolate its reference vector from q and f

$$A = A \cup \{r\}, w_r = \frac{(w_q - w_f)}{2}$$

• Insert edges connecting the new unit r with units q and f, and remove the original edge between q and f: $C = C \cup \{(r,q),(r,f)\} \ C = C \backslash \{(q,f)\}$

• Decrease the error variables of q and f by a fraction a: $\Delta E_q = -aE_q$, $\Delta E_f = -aE_f$.

• Interpolate the error variable of r from q and f: $\Delta E_r = \dfrac{E_q + E_f}{2}$.

10.   Decrease the error variables of all units:

$$\Delta E_c = -\beta \Delta E_c, (\forall c \in A).$$

11.   If a stopping criterion (e.g., net size or some performance measure) is not yet fulfilled continue with step 2.

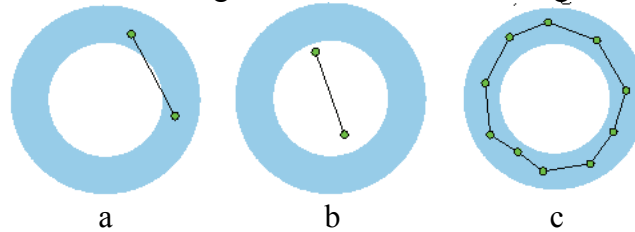Neural network structure for this algorithm You can see on Fig. 2

Fig. 2. GNG growing process for ring-shaped probability distribution
(a – 0 signals, b – 100 signals, c – 2500 signals)

Artificial neural network clustering in Internet environment

The modern collaborative environment as Internet makes some restriction for ANN growing among separate computers. One way is to use some GRID or cluster software which represents set of computers as one power node. In such situation we should take into account signal transmitting between ANN parts which situated on different computers. In most cases it will decrease ANN speed much. According to this we should develop different kind of software which will be suitable for ANN.

For example we could add condition for growing process which represents real Internet environment. In such way we will see such picture Fig. 3 of ANN clusters growing.
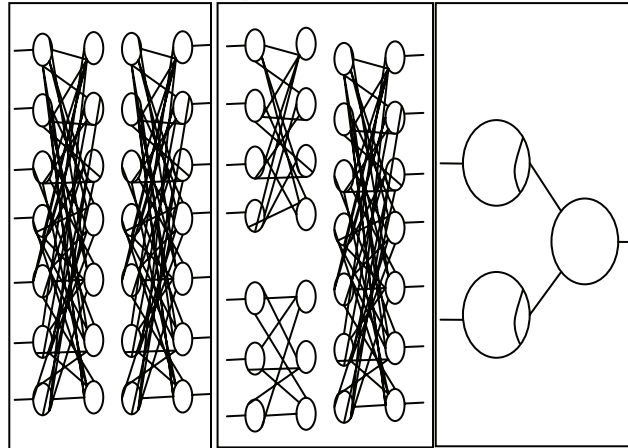

Fig. 3 ANN clusters growing process

On this picture we see few stages. On first stage ANN starts growing on one computer and on next stage it's continue to grow on different computers. In such way we can separate few different ANN growing nodes. This nodes are interconnect with less count of edges (neurons connection) than inside computer. Such nodes named clusters.

The real life tasks approve such possibility. For example currency courses prognoses creation. This task needs as input information trade prognoses, the currency prognosis which based on historical data, many other additional market trends. All this input information could be calculated by ANNs which situated in different clusters. Such clusters could be located on servers in different financial structures.

The additional problem is interconnection protocols. We can develop some special application level protocols which based on TCP/IP. But we can have problems with distribution of such technology. Because many computers and networks have hardware and software firewalls. And a lot of administrator and end-users should change their configuration files. In other way we can use standard named WEB-services.

This is a kind of distributed application building standards such as DCOM, CORBA etc. Fortunately WEB-services standard have had developed for Internet specific environment.

The WEB-services works smooth for program modules. Developer use modules which situated on other computers in same way as local. It is simplify distributed application development process. The WEB-services technology uses such protocols: Universal Description Discovery and Integration (UDDI), Simple Object Access Protocol (SOAP).

The UDDI are application level protocol based on TCP/IP stack. It used for WEB services discovery requests. This requests sends application server when it tries to find suitable object for application which started on. For example when some application which situated on current application server needs some class application server sends such request to UDDI registry. The application server receives information about requested object location.

After location information and WSDL (Web Services Description Language) description have had received main application server starts SOAP session with target application server (Application server where situated requested class). For the main application it is no any difference between local and distance target class location. The main application uses proxy class for object method and properties onvocation.

On the Fig. 4 described clustered ANN architecture which based on WEB-services technology.
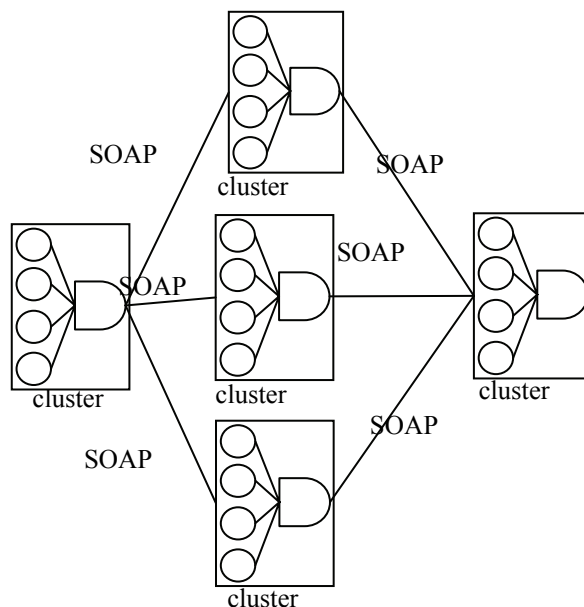

Fig. 4. Clustered ANN WEB-services architecture

Any cluster in that architecture could by located on the same computer with others or on some application server in Internet. Such architecture create possibility for new types of services in Internet – the ANN WEB-services. This services could be created on some information sources or resource sources. Eg it could be created on some brokers' board, weather forecasts, physical labs, telescopes etc.

This ANN WEB-services could be charged or free. They could be used for other services creation.

Conclusion

This paper is a first step for developing ANN testing environment. Using ideas which are proposed here we can build WEB-services environment which simplify testing of different clustering methods. Also we can simple use different development languages for different ANN types. It is increase a possibility to find some already developed modules and classes. But for main language we plan to use Java as platform independent language. This language has biggest support in such kind application.

References

1. *Губинский А.И., Кобзев В.В.* Оценка надежности деятельности человека-оператора в системах управления. – М.: «Машиностроение», 1975. – 52 с.

2. *Ложкин Г.В., Повякель Н.И.* Практическая психология в системах «человек-техника»: Учеб. пособие. – К.: МАУП, 2003. – 296 с.

3. *Fritzke B.* Growing cell structures - a self-organizing network for unsupervised and supervised learning // Neural Networks. - №7(9):1460. - 1994.

4. *Fritzke B.* A growing neural gas network learns topologies // Advances in Neural Information Processing Systems, MIT Press, Cambridge MA.-1995,- №7. - P. 625-632.

5. *Кременецький Г.М.* Кластеризація у модульних нейронних мережах / Г.М. Кременецький // Журнал обчислювальної та прикладної математики. - К.2009,- №3(99). – С. 57-62.

6. *Кременецкий Г.Н.* Аппаратные и программные средства реализации системы передачи новостей абонентам // Проблеми інформатизації та управління. – Вип. 7. – К.: НАУ, 2003. – С. 111-113.

UDC: 044.82 (045)

A.I. Vavilenkova, candidate of technical sciences
(National Aviation University, Ukraine)

METHOD OF THE AUTOMATED FORMATION OF LOGIC-LINGUISTIC MODELS

In this article it is offered the primary goals for which decision formalisation of the text information is necessary are considered, the method of the automated formation of logic-linguistic models which transforms syntactic designs of a natural language to formulas of logic of predicates of the first order that allows to take the knowledge formalized according to structural rules from the initial text information.

Introduction

Essentially new possibilities of computers and networks are the reason of occurrence of absolutely new ways of processing of the information which will develop first of all in an intellectualization direction. The necessity of working out of effective linguistic technologies on which technologies of operating by knowledge will be based, demands creation of universal system of support of linguistic development and researches [1].

So, for possibility of comparison of texts and search in them for logic contradictions, it is necessary to learn how to represent the text information in the formalized form. One of approaches of creation of such system is based on construction of logic-linguistic model of the text which is exposed to check on the logic contradiction concerning other texts. The basic problem on this way is automation of process of construction of such model that will allow to apply further to logic-linguistic models algorithms of the proof of logic contradictions as to the formal models presented by predicates of the first order [2].

For the decision described above a problem the method of the automated formation of logic-linguistic models of the text information which consists in automation of process of transformation of syntactic designs (sentences) of a natural language (NL) in formulas of logic of predicates of the first order [3] is sentenceed. The method allows to take from the initial text information the knowledge formalized according to structural rules and which the computer can independently use for the decision of problems on in advance chosen algorithms, such, as a logic conclusion. The mechanism for realization of process of transformation of the sentence in formulas of logic of predicates is the automated parser on the basis of which results the logic-linguistic model is formed.

The method of the automated formation of logic-linguistic models of the text information consists of consecutive performance of certain actions on each of method stages. The general algorithm of a method is presented in drawing of a Fig. 1, where

B^{d1} - Set of words of a database;

B^{d1}_{t1} - Set of words of the table of a database, $B^{d1} \in B^{d1}_{t1}$;

B^{t1} - Set of tables of a database;

S^{t1}_{rh} - Word of t_1-table of set of tables of a database B^{t1};

B^{d2} - Set of words of a database;

B^{d2}_{t2} - Set of words of the table of a database, $B^{d2} \in B^{d2}_{t2}$;

B^{t2} - Set of tables of a database;

S^{t2}_{rh} - Word of t_2- table of set of tables of a database B^{t2}.

Identification of the initial text

Let the sentence represents system which consists of elements (word forms): simple (words) and difficult (word-combinations which automatically include words). Then the control object will be complex organizational system which consists of simple n cooperating elements $S_i, \overline{i=1,n}$ and complex m cooperating elements ($S^i_j, \overline{i=1,n}; \overline{j=1,m}$).
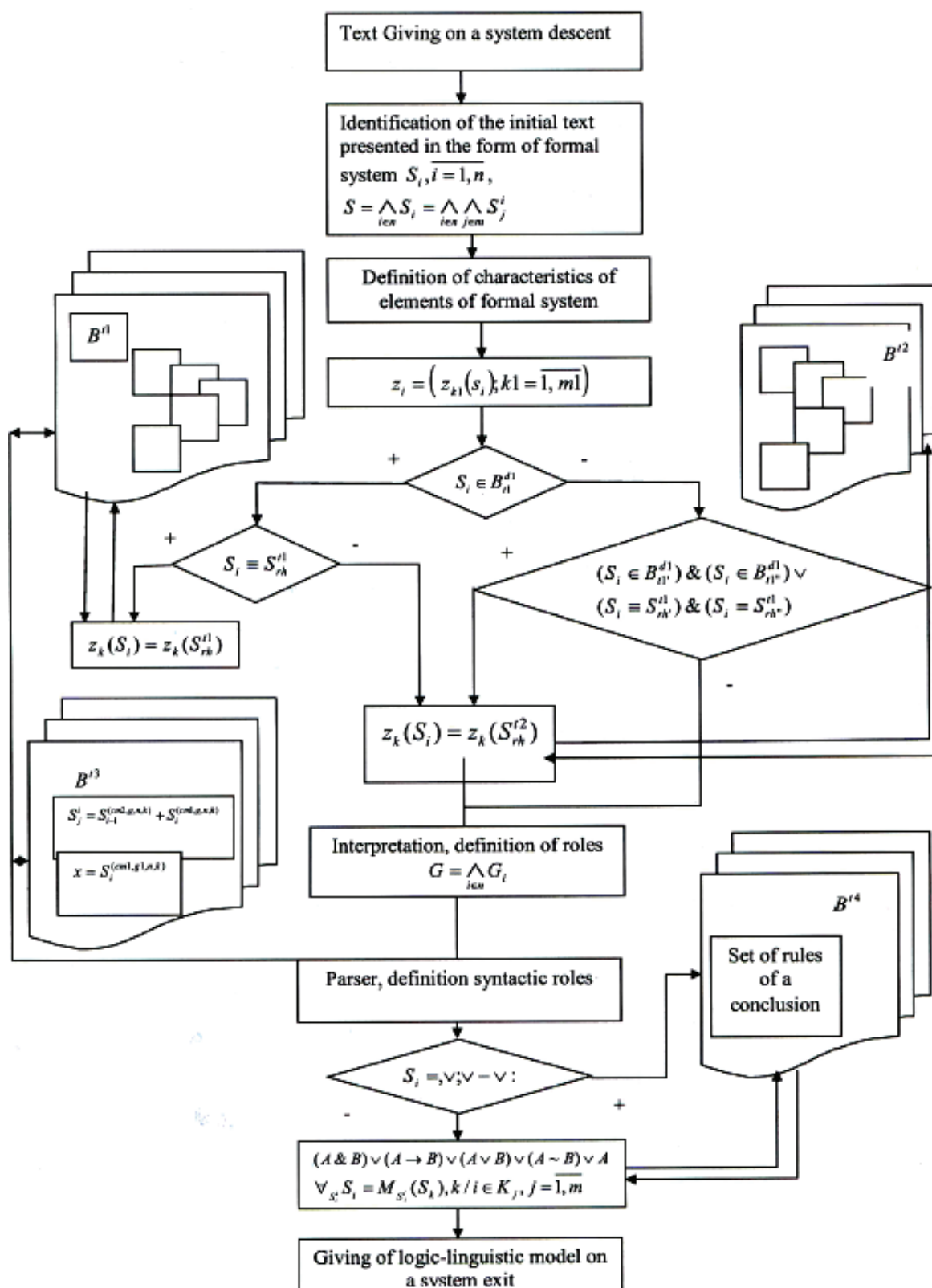
Fig. 1 – The Generalized algorithm of a method of the automated formation of logic-linguistic models of the text information

Communications between system elements can be tracked only after performance of following stages of algorithm according to a method of the automated formation of logic-linguistic models of the text as for each concrete communication system will be different.

$S_i, \overline{i = 1, n}$ - Simple elements of system (word) which can enter or not enter into structure of complex elements;

$S_j^i, \overline{i=1,n}; \overline{j=1,m}$ - complex elements of the system (word-combination), which main component is the simple element $S_i, \overline{i=1,n}$.

That is, at an identification stage the initial text information which represents set of syntactic units of a natural language, is identified with formal system $S = \underset{i \in n}{\wedge} S_i = \underset{i \in n}{\wedge} \underset{j \in m}{\wedge} S_j^i$.

Such transformation gives the chance to consider any sentence (somehow difficult structure) as system of operations over sequences of symbols, and operations – it is formal, without semantic interpretation.

I.e. at an identification stage occurs splitting the entrance text on word forms by means of application of logic reception of decomposition to signs on components to research the text information (sentences) and communications between word forms making it and also to take knowledge (essence) which systems on an exit will be transformed to logic-linguistic models.

Conceptualism, definition of characteristics of elements of formal system

At the given stage, it is necessary to explicate key concepts, relations and communications between elements about which it was spoken at an identification stage, and also are defined the characteristics of these elements necessary for the description of the further process of the decision of a task in view. Conceptualism of data represents procedure of introduction of ontological representations in an array of empirical data; the primary theoretical form which provides the theoretical organization of a material; the scheme of connection of concepts which allows producing hypotheses about the nature and character of communications. At this stage the way of the organization of the further work that will allow to move from initial theoretical concepts to more abstract "constructs" is defined [4].

The basic role at definition of characteristics of elements of formal system is played by a database which contains the dictionary of the Ukrainian language and the dictionary of morphemes that gives the chance to receive the information on a concrete element of system $S_i, \overline{i=1,n}$.

The database is organized in the form of set of the tables realized in the form of relational model thanks to what the structural aspect is provided – data represent a set of relations, aspect of integrity – relations (table) answer conditions of integrity and aspect of processing – possibility to manipulate data. All information filling of a database is presented by one way, namely through the obvious task of values of attributes in corteges of relations, in particular on what value of attribute is answered with a system element, $S_i, \overline{i=1,n}$ in what little table of the table of a database it its grammatical characteristics are defined: a case, a sort, number, the form etc.

The grammar of any language studies appropriateness of development and functioning of grammatical units, forms system of rules how it is necessary to use them, of morphemes to form words and to change them, to search for the necessary forms and to unite them in word-combinations, how to find for words and word-combinations common correct order and to form of them sentences for thought expression. Language units are characterized in grammar by that have grammatical value. To understand the nature of grammatical value, it is necessary to consider it in comparison with lexical which corresponds with subjects or the phenomena of the real world, with concepts and their names. The grammatical word meaning is expressed in their grammatical forms which will be called as grammatical characteristics of element NL $z_i = \left(z_{k1}(s_i); k1 = \overline{1,m1} \right)$.

Each simple element of system is described by a vector of values of characteristics, $z_i = \left(z_{k1}(s_i); k1 = \overline{1,m1} \right)$ where $m1$-quantity of grammatical characteristics of i-element of system $i = \overline{1,n}$. Size of $m1$ is defined as a constant for all elements of formal system as each word in the Ukrainian language has a number of morphological signs, characteristic for other words, for example, a part of speech, a case, a sort, number etc.

Morphological analysis assumes the word characteristic as parts of speech. For definition of a part of speech it is necessary to use some factors: semantic (expressed value), morphological

(expressiveness of certain grammatical categories) and syntactic (a concrete syntactic role in the sentence).

During morphological analysis not all characteristics will be peculiar to each word, therefore in the absence of morphological signs of this or that element, such characteristics will be replaced by zero that will give more than the theoretical information for the further establishment of interrelations between elements in a complex syntactic designs.

So, that means that the definition of characteristics of elements of system gives a primary conceptual explanation which carries character of interpretation (recognition).

Process of definition of characteristics of each element of formal system represents the conceptual scheme which sets set of possible modes of work at theoretical level, assumptions of the nature and properties of elements which are researched.

Interpretation, definition of roles

All problem of understanding of statements is divided into two stages: the analysis and interpretation. At a stage of conceptualism it has been analyzed each element of system and it has been defined its properties. On the basis of the received data at an interpretation stage the inquiry in the knowledge base which is presented in the form of axioms of formal system owing to what the structure of difficult elements of system is defined is transferred $S_j^i, \overline{i=1,n}; \overline{j=1,m}$.

The set of axioms of the given formal system is a set of rules of the Ukrainian language, agrees which words unite in word-combinations. Rules of formation of word-combinations are taken from the Ukrainian language (natural language) and interpreted in formulas of logic of predicates of the first order. Definition of roles is carried out on the basis of data, received from a database and the knowledge base.

The stage of conceptualism and interpretation serves as original preparation for parse of formal system and creation of new data file. Dimension of such file answers quantity of elements of system, n and value of elements – names of syntactic roles of each of simple or (if at a stage of interpretation it becomes possible) complex elements of FS.

Each sentence of a natural language is characterized by the grammatical organization: a structure of the sentence and grammatical expression (registration) of sentence parts.

In the sentence we allocate a grammatical basis (the centre, a kernel) without which any sentence cannot exist. A grammatical basis the main sentence parts (make a subject and a predicate) or only one main sentence part. It is considered, that the relation between a subject and a predicate, and also their general relation to that they express actually, and form the most basic grammatical property of the sentence (its essence) – predicativity [5].

Acts as what sentence part a word (element FS) and defines its role in the sentence:
- Subject – grammatical independent sentence part which means a subject about which it is spoken in the sentence;
- The predicate – the main sentence part which designates action, a condition or property of a subject and grammatical submits to it;
- Addition – a minor sentence part which means a subject on which action is directed, a condition;
- Definition – a minor sentence part which names property;
- Circumstance – a minor sentence part which names circumstances of action, process, a condition.

Formally role of a word in the sentence is defined by value of an element of set $G = \bigwedge_{i \in n} G_i$.

A parser

On the basis of data received at the previous stages of performance of a method of the automated formation of logic-linguistic models of the text information, namely grammatical characteristics of simple and difficult elements of system, the analyzer defines a syntactic role of each element. In the Ukrainian language exists five sentence parts: a subject, a predicate, addition,

definition, circumstance. Such values can accept elements of a file of roles for G which elements of formal system are $S_i, \overline{i = 1, n}$ prototypes.

The syntactic role of some elements can be defined at a stage of conceptualism (a Fig. 1), having received result of inquiry to a database B^{t1}. But the basic complexity of a method which is considered, is that the text information which is transformed to logic-linguistic model, can concerns different subject domains, accordingly types of sentences and interrelation between them can be various. Therefore for universal definition of syntactic roles of elements axioms of the knowledge base which B^{d3} represent rules of the Ukrainian language according to which it is defined are used as what sentence part this or that word or a word-combination acts. The main sentence parts are the subject and a predicate, in the knowledge base B^{d3} the set of axioms for their accurate definition contains.

On the basis of the received data the file of roles $G = \bigwedge_{i \in n} G_i$ is formed, where each element of a file G_i is put in conformity the element of formal system $S_i, \overline{i = 1, n}$.

After definition of syntactic roles it is necessary to pay attention to punctuation signs in the initial text information, and also the unions and allied words. Here the reference with a database B^{d1} and the knowledge base B^{d4} is carried out - sets the conclusion of formal system corrected S.

Formalization of process of construction of logic-linguistic model

The logic-linguistic model in a general view for any difficult syntactic design (sentence) represents a set of axioms (1) - (2):

$$(A \& B) \vee (A \to B) \vee (A \vee B) \vee (A \sim B) \vee A, \tag{1}$$

$$\forall_{S_i^i} S_i = M_{S_j^i}(S_k), k / i \in K_j, j = \overline{1, m}, \tag{2}$$

where A - the difficult logic statement which describes a simple sentence which is a part difficult, and is the main thing or describes any terse sentence;

B - The complex statement which describes a simple sentence which is a part complex and is dependent;

K_j - Set of elements (words) which are a part of a difficult element, S_j^i i.e. each j - word-combination;

$M_{S_j^i}$ - The set of values which property of a dependent word in a word-combination (additional parts of a difficult element S_j^i) can accept, S_j^i for example, the main word can designate object, quantity, quality that depends on word-combination type;

k - Part of a complex element S_j^i.

The quantity of components of logic-linguistic model is equaled, $(m + 1)$ i.e. each axiom (2) for displays $j = \overline{2, m + 1}$ sense of a word-combination.

The given set of axioms gives the chance to construct logic-linguistic model of any sentence by accurately certain rules.

Difficult statements A and B represent the sequence of simple elements of formal system structured by certain rules.

At the heart of structurization lays ontology that on the basis of characteristics of each of system elements, and also values of elements of a file, $G = \bigwedge_{i \in n} G_i$ interrelations between sentence parts are described:

$$P(x, U(x), Y(\{D(x)\}\{Y(\{D(x)\}, \{Q(D(x))\})\}, \{O(x)\})$$

where - P a predicate which means a predicate;

x - Subject;

$\{U(x)\}$ - Set of definitions which characterize a subject;

$\{D(x)\}$ - Set of additions;

$\{Q(D\ (x))\}$ - Set of definitions which characterize sentence additions;

$\{Y(\{D(x)\},\{Q\ (D(x))\})\}$ - Set of lexical-connected additions and definitions;

$\{O(x)\}$ - Set of circumstances.

Conclusions

From the point of view of constructive semantics (a science which is engaged in studying and formation of rules of synthesis of sign systems which provide process of display of the objective world in its models) formalization means transition to operating by symbols at which it is not necessary the additional analysis of things of the objective world and all theory develops in sign area, without the reference to experience.

The formalized form of representation of text documents can be logic-linguistic models which are capable to display sense of the sentence [3]. Taken as a principle process of automation the idea of use of syntactic parsing of the sentence, gives the chance to standartize logic-linguistic model under all types of sentences.

References

1. *E.V. Popov* Speaking with PC in a natural language. – M: the Science. The main edition of the physical and mathematical literature, 1982. – 360p.

2. *D. Jarratano,* Expert systems: principles of working out and programming, 4 edition.: the lane with English – M: Open Company "Williams", 2007. – 1152p.

3. *V.N. Vagin.,* Deduction and generalization in decision-making system. – M: the Science, 1988. – 384p.

4. *K. Taunsand, D. Foxt,* Designing and program realization of expert systems on personal computer :Transl. With English/Predisl. G.S.Osipova. – M.:Finance and statistics, 1990. – 320p.

5. *R.G. Buharaev., D.S. Sulaymanov,* Semantic analysis in question-answer systems. – Kazan.: Publishing of the Kazan university, 1990. – 124p.

UDC 519.21: 681.518

E.P. Nechyporuk, candidate of technical sciences
N.B. Marchenko, candidate of technical sciences,
(National Aviation University, Kiev, Ukraine)

SPECTRAL-TIME MODELS OF DATA SIGNALS UNDER THE ACTION OF INTERFERENCES IN THE TASKS RELATED TO ELECTRIC AND MAGNETIC VALUES MEASURING

Spectral-time models based on the use of linear and harmonizable random processes allow to describe and study a wide range of data signals and influencing interferences during measuring of the parameters and characteristics of electric and magnetic values not only in terms of correlation theory but taking into account higher-order moments.

While measuring mechanical, light, heat, acoustical and other physical values their conversion into electrical and magnetic values always occurs. That is why functioning of many information measuring systems is based on the measuring of electric and magnetic values parameters and characteristics. It is known, that the achieved measurement precision is limited for a number of reasons, including the action of interferences. Further increase of measurement precision is connected with both, systems enhancement and deeper analysis of signals and interferences based on the development of new mathematical models and their description.

Models based on the use of linear random process and a field are called time models; spectral models considered to be used for harmonizable random process and a field.

Definition: Hilbert random processes $\{o(t) \in L_2(-\infty; \infty)\}$ that simultaneously allow view representation

$$\xi(t) = \int_{-\infty}^{\infty} \varphi(\tau, t) d\eta(\tau), \quad t \in T \tag{1}$$

and

$$\xi(t) = \int_0^{\infty} \cos 2\pi f t dR_C(f) + \int_0^{\infty} \sin 2\pi f t dR_S(f), \quad t \in T \tag{2}$$

create the class of LG-models.

The view representations (1) in which non-random function $\varphi(\tau, t) \in L_2$ at all conditions and $\{\eta(\tau), \eta(0), \tau \in (-\infty; \infty)\}$ is a non-uniform random process with independent increments and infinitely divisible distribution law create the class of linear random processes [4, 5]. The view representations (2) where correlation functions of random functions $R_C(f)$ and $R_S(f)$ have limited variation create the class of harmonizable random processes [1, 3]. In this study we will consider only one-dimensional case.

Thereby, the class of LG-models is formed by the intersection of linear and harmonizable random processes classes. Using the results of study [1, 3-5] we can define the main statistical characteristics of LG-models and consider the examples of their use for the description of particular signals in measurement technology.

1. Multidimensional characteristic function of a non-stationary non-Gaussian linear process [1] received with the use of the results [4,5] is described by the following expression:

$$f_\xi(U_1,...,U_n;t_1,...,t_n) = \exp\left\{ i\sum_{j=1}^{n} U_j \int_{-\infty}^{\infty} \varphi(\tau,t_j)d\mu(\tau) - \frac{1}{2}\sum_{j=1}^{n}\sum_{k=1}^{n} U_j U_k \times \right.$$

$$\left. \times \int_{-\infty}^{\infty} \varphi(\tau,t_j)\varphi(\tau,t_k)dD(\tau) + \int_{-\infty}^{\infty}\int_{-\infty}^{\infty}\left[e^{ix\sum\limits_{j=1}^{n} U_j\varphi(\tau_1 t_j)} - 1 - \frac{ix}{1+x^2} \times \right. \right.$$

$$\left. \left. \times \sum_{j=1}^{n} U_j\varphi(\tau,t_j) \right]\frac{1+x^2}{x}d_x d_\tau G(\tau,x) \right\},$$

(3)

where $\mu(\tau)$, $D(\tau)$, $G(\tau,x)$ are τ-function continuous. They categorize completely divisible distribution law of generating random process with $\eta(\tau)$ independent increments.

The expression (3) clearly describes the structure of the linear process. Gaussian and Poisson components of the generating process $\eta(\tau) = \omega(\tau) + \pi(\tau)$ form the correspondent components of the linear process. If Poisson component is not found, i.e. when $G(\tau,x) = 0$ the linear process is considered to be Gaussian one. In the case, when generating process $\eta(\tau)$ doesn't include Gaussian component, i.e. when $D(\tau) \equiv 0$, the linear process will not have it too. Realizations of Gaussian linear process are continuous with probability one. The behaviour of realization of the linear process $\xi(t)$ with only Poisson component of the process $\pi(\tau)$ is defined by the functions $G(\tau,x)$ and $\varphi(\tau,t)$ behaviour in any particular case.

For the solution of practical tasks the following formulae for defining of compound cumulants of n-degree ($n > 2$) linear process is of considerable importance

(4)

$$\chi_n\left[\xi^{k_1}(t_1)...\xi^{k_n}(t_n)\right] = \int_{-\infty}^{\infty}\prod_{j=1}^{n}\varphi^{k_j}(\tau,t_j)dH_n(\tau), \quad t_j \in T$$

where k_j are integer nonnegative numbers that fit the equations $\sum_{j=1}^{n}k_j = n$, and

$$dH_n(\tau) = \begin{cases} d\mu(\tau) + \int_{-\infty}^{\infty}x^2 d_\tau d_x G(\tau,x), & n=1 \\[2mm] dD(\tau) + \int_{-\infty}^{\infty}x(1+x^2)d_\tau d_x G(\tau,x), & n=2 \\[2mm] \int_{-\infty}^{\infty}x^{n-1}(1+x^2)d_\tau d_x G(\tau,x), & n>2 \end{cases}$$

Linear processes as time models of signals are widely used for the tasks of signal conversion analysis and design in linear and non-linear transmission channels of measuring systems.

2. As a basis of spectral representation of random processes is the representation (2) that is considered to be the limit of integral sum of elementary harmonic vibrations with random amplitudes and phases. The analysis of harmonizable processes is usually conducted in terms of two initial moments. We can use the results [3] to demonstrate that correlation function of non-stationary harmonizable process (2) at a condition $M\{R_C(f)\} = M\{R_S(f)\} = 0$ is described by the following expression

$$R(t_1,t_2) = \int_{0}^{\infty}\int_{0}^{\infty}\left[(\cos 2\pi f_1 t_1 \cos 2\pi f_2 t_2)d_{f_1}d_{f_2}Q(f_1,f_2) + (\cos 2\pi f_1 t_1 \sin f_2 t_2) \times \right.$$

$$\left. \times d_{f_1}d_{f_2}D_{cs}(f_1,f_2) + (\sin 2\pi f_1 t_1 \cos 2\pi f_2 t_2)d_{f_1}d_{f_2}D_{cs}(f_1,f_2) + \right.$$

(5)

$$\left. + (\sin 2\pi f_1 t_1 \sin f_2 t_2)d_{f_1}d_{f_2}I(f_1,f_2)\right],$$

1.11.28

where

$$\mathrm{M}\{R_c(f_1)R_c(f_2)\} = Q(f_1,f_2),\ \mathrm{M}\{R_s(f_1)R_s(f_2)\} = I(f_1,f_2),$$
$$D_{cs}(f_1 f_2) = \mathrm{M}\{R_c(f_1)R_s(f_2)\} = D_{sc}(f_2,f_1).$$

Functions $Q(f_1,f_2)$ and $I(f_1,f_2)$, are also called spectral ones, and $D_{cs}(f_1 f_2)$, $D_{sc}(f_2,f_1)$ are called mutual spectral functions of generating random functions $R_C(f)$, $R_S(f)$ of the harmonizable process (2).

Practical importance of the results of a harmonizable process analysis considerably increases when we define a narrower subset with additional properties from this class of processes.

      3.   Here are the examples of electric and magnetic signals described by LG-models.

Modulated signals with harmonic carrier are most widely used for the transmission of measurable signals. It is assumed that modulated desired signals, as well as the value of frequency carriers and other parameters of the signal are already known.

So, amplitude-modulated signal that is described by the expression

$$x(t) = A[1 + m_{AM} a_1(t)]\cos(2\pi f_{\text{н}} t + \theta), \quad t \in T$$

on the output of a transmitter will represent the signal of another type, namely $\xi(t)$ on a receiver with the action of

$$y(t) = A\{1 + m_{AM}[a_1(t) + \xi(t)]\}\cos(\omega_{\text{н}}(t) + \theta), \quad t \in T$$

interference.

$y(t) = x(t) + \xi(t)$ or $y(t) = x(t)\xi(t)$, where $\alpha(t)$ is a modulated signal, random in general case, and $\xi(t)$ is an interference that allow the description by the representation (1) or (2), i.e. by LG-models. $A, \theta, \omega_H, m_{AM}$ — are numerical coefficients.

At angle modulation

$$x(t) = A\cos(\varpi_{\text{н}} t + m_{YM}\int_{t_1}^{t_2} a(\tau)d\tau + \theta), \quad t \in T$$

we receive respectively

$$y(t) = A\cos\left(\omega_{\text{н}} t + m_{YM}\int_{t_1}^{t_2}[a(\tau) + \xi(\tau)]d\tau + \theta\right), \quad t \in T$$

or depending on the initial conditions in combinations specified for amplitude-modulated signal.

At associated amplitude and angle modulations of a signal

$$x(t) = A\left[1 + m_{AM} a_1(t)\cos\left(\omega_{\text{н}} t + m_{YM}\int_{t_1}^{t_2} a_2(\tau)d\tau + \theta\right)\right], \quad t < T$$

different combinations of a signal and an interference can occur on the receiver. For example,

$$y(t) = A\{1 + m_{AM}[a_1(t) + \xi_1(t)]\}\cos\left(\omega_{\text{н}} t + m_{YM}\int_{t_1}^{t_2}[a_2(\tau) + \xi_2(\tau)]d\tau + \theta\right), \quad t \in T$$

$y(t) = x(t) + \xi(t)$ or $R(t) = y(t)| + \xi(t)$ or $R(t) = y(t)\xi(t)$, where linear and harmonizable random processes $\xi(t)$, $\xi_1(t)$, $\xi_2(t)$ can be both non-correlated (independent) and dependent.

Modulated signals with noise carrier have more noise immunity as compared to signals with harmonic carrier, and the task of transmission and reception of modulated signals research is more physically based, as all the measuring devices generate signals with the definite number of harmonic components or continuous spectrum.

Receiving of the noise carrier as the random process can be described in two ways:
      a)   as a result of linear filtering

$$\xi(t) = \int\limits_{-\infty}^{\infty} \varphi(t-\tau)\,d\eta(\tau), \quad t \in T$$

representing stationary linear process, where homogeneous process with independent increments $\eta(\tau)$ is considered to be generating one;

b) stationary harmonizable process

$$\xi(t) = \int\limits_{0}^{\infty} \cos 2\pi ft\, dZ_c(f) + \int\limits_{0}^{\infty} \sin 2\pi ft\, dZ_s(f), \quad t \in T,$$

where $Z_c(f)$ and $Z_s(f)$ are random functions with non-correlated (orthogonal) increments, and spectral densities of both representations coincide.

Noise processes occurring in physical medium (magnetic noises in ferromagnetic materials, electromagnetic noises in semiconductors or insulators), electronic systems (shot noise, thermal noise, flicker noise) and other noises can be described by a unified mathematical model represented by linear mathematical process [4,5]. The application of this process for noise processes description allows using of initial physical prerequisites of process forming more widely if to compare it with harmonizable process. So, describing shot noise in semiconducting and electronic devices we can define three modes of a noise source and choose three kinds of generating process $\eta(\tau)$ respectively:

saturation mode is characterized by the similar charge carrier velocities (generating process is Poisson one);

saturation mode is characterized by the considerably different charge carrier velocities (complex generic generating process);

extreme case, when the average number of charge carriers increases indefinitely (Wiener Gaussian process).

Function $\varphi(\tau,t)$ as the kernel of integral representation (1) describing the thermal noise by the linear stationary Gaussian process is defined by the kind of desired spectral density $S(f)$

at continual Wiener generating process $\omega(\tau)$. So, if $S(f)$ is constant in all the frequency band (white noise) , then $\varphi(t)$ is delta function. For band noise $S(f)$ is constant and differs from zero only in finite frequency interval $f \in [-f_0, f_0)$ function $\varphi(t)$ is $\dfrac{\sin 2\pi f_0 t}{2\pi f_0 t}$.

Reverberatory process that characterizes distribution of electromagnetic vibrations in conducting continuum connected with reflection, refraction and reradiating from radiators discretely distributed in medium can be described by the discrete linear process

$$\xi(t) = \sum_{\{j|\tau_j(t)\}} \alpha(\tau_j) s(\tau_j, t), \quad t \subset T,$$

where $\{\alpha(\tau_j), j = \dots, -1, 0, 1, \dots\}$ — is a sequence of random quantities, that characterize the state of j radiators in the moment of time τ_j; $s(\tau_j, t)$ is elementary diffuse signal caused by radiated non-stochastic signal $s(t)$ and received by the receiving point in τ_j moment.

The latter expression can be represented as (1) i.e.

$$\xi(t) = \int\limits_{-\infty}^{\infty} s(\tau, t)\, d\pi(\tau), \quad t \subset T,$$

where Poisson process $\pi(\tau)$ is generating one.

Impulse signals represent a wide range of data signals in measurement technology. Whereas the description of non-stochastic video and radio impulses sequence is conventional, there are no structural models for describing random signal impulses that overlap in time.

The use of linear processes allows solving the problem, notably using the representation (1) as mathematical models of random impulse signals where Poisson component is a generating process in a common case of a heterogeneous stochastically continuous random process with independent

increments $\eta(\tau)$ and infinitely divisible laws of distribution, i.e. Gaussian component $\omega(\tau)$ is missed. The kernel of integral representation (1) can selectively describe:

impulse transition function of a linear channel of distribution of an explored signal from its source to the input of a receiver;

impulse transition function of a linear system during the conversion of an impulse signal;

analytic description of an elementary impulse form.

Particularly, linear process describes impulse interferences of reception caused by lightings, industrial-scale plants, ignition systems of internal-combustion engines, atmospheric interferences, and output electric signals of rectifying and gated installations at a random action.

Thereby, suggested spectral-time models based on the use of linear and harmonizable random processes can be used for describing a wide range of data signals and acting interferences in measuring electric and magnetic values. LG-models class enables to receive more grounded integral representations of signals and interferences as all the conditions of generating are used in there definition, as well as time and frequency responses and the characteristics of analysed signals. Received characteristics of LG-models allow analysing not only in terms of correlation theory but taking into consideration higher-order moments.

References

1. *Ya. P. Dragan*. Structure and representation of stochastic signal models. – Kiev: Naukova Dumka, 1980. – 384 p.

2. *Ya. P. Dragan, I. N. Yavorsky*. The rhythmics of rough sea and underwater acoustic signals. – Kiev. Naukova Dumka, 1982. – 248 p.

3. *M. Loev*. Probability theory.- M. Foreign literature publishing house, 1962. – 720 p.

4. *B. G. Marchenko*. The method of stochastic integral representations and their application in radio engineering. – Kiev: Naukova Dumka, 1973. – 191 p.

5. *B. G. Marchenko, L.N. Shcherbak*. Linear random processes and their application.- Kiev: Naukova Dumka, 1975. – 143 p.

UDC 519.872 (045)

O.V. Koba, doctor of p.-m. sciences,
S.V. Pustova, candidate of technical sciences,
*O.M. Dyshliuk,*
(National Aviation University, Ukraine)

MODELING QUEUEING SYSTEM WITH DUAL REQUESTS AND DETERMINED SERVICE TIMES

Single-channel queueing system with Poisson flow of dual requests is considered. An average waiting time for the first and second operations of the request is determined analytically in the case of determined duration of operations and a gap between them. A Laplase-Stiltjes transform of virtual waiting time is found.

Mathematical models of present-day information systems, which are described by means of queueing theory, have both complex discipline of selecting the requests for servicing and complex structure of requests itself. Under request's complex structure we understand its multiplicity, that is, a request is divided into unconnected impulses, every of which needs corresponding service on the same server. For example, in air traffic control systems request's duplicity occurs due to intermittence of taking the information from aircrafts and transmission of control information to aircraft by flying control officer. Some problems on dual requests were considered in [1, 2].
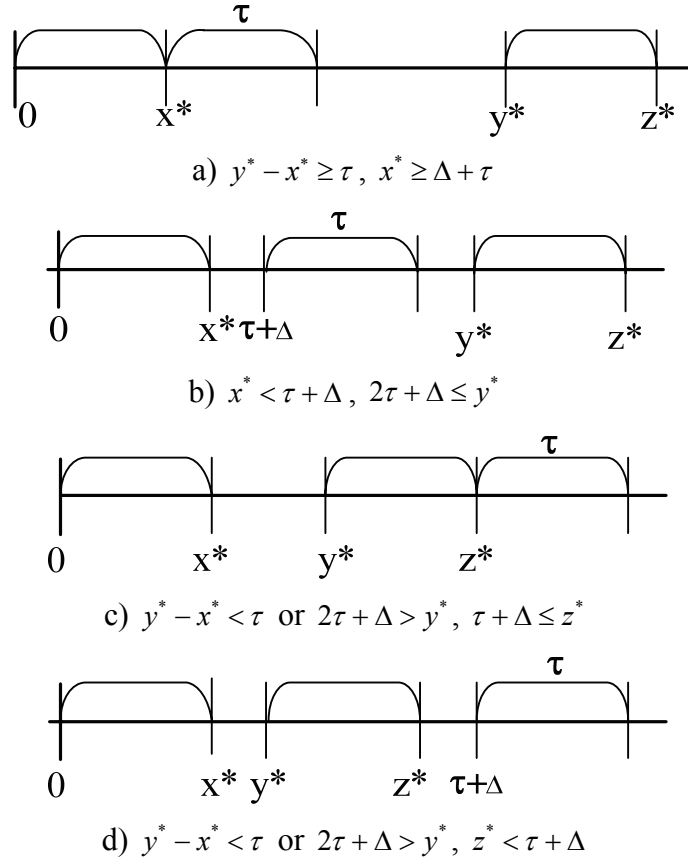
Queueing system. Consider a single-channel queueing system in which Poisson flow of requests arrives with rate λ. The service for each request consists of two servicing operations with constant duration τ, but the second operation can be started only after the first one is completed and after time $\tau + \Delta$ after the request entered a system. Splitting up the fulfillment of operations is prohibited. As soon as request enters a system, times for the first and second operations can be planned.

For example, let at moment of request's arrival, taken as a zero, intervals $(0, x)$ and (y, z) are already chosen for servicing the requests that have come earlier. If $y - x \geq \tau$ then the first operation of the new request occupies interval $(x, x + \tau)$, otherwise $(z, z + \tau)$ (pic. 1 a), 1 b)).

a) $y - x \geq \tau$

b) $y - x < \tau$
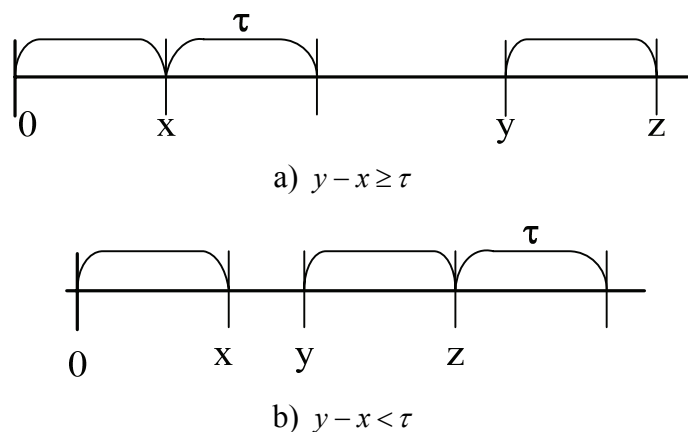
Pic. 1. Allocation of intervals for operations

After the first request's time is planned, two intervals $(0, x^*)$ and (y, z^*) would be occupied, where there may be two cases, where a) $x^* = x + \tau$, $y^* = y$, $z^* = z$, and b) $x^* = x$, $y^* = y$, $z^* = z + \tau$. Then 4 cases are possible (pic. 2): a) when $y^* - x^* \geq \tau$ and $x^* \geq \Delta + \tau$; b) when $x^* < \tau + \Delta$, $2\tau + \Delta \leq y^*$; c) when either $y^* - x^* < \tau$, or $2\tau + \Delta > y^*$, and $\tau + \Delta \leq z^*$; d) when either $y^* - x^* < \tau$, or $2\tau + \Delta > y^*$, and $z^* < \tau + \Delta$.

a) $y^* - x^* \geq \tau$, $x^* \geq \Delta + \tau$

b) $x^* < \tau + \Delta$, $2\tau + \Delta \leq y^*$

c) $y^* - x^* < \tau$ or $2\tau + \Delta > y^*$, $\tau + \Delta \leq z^*$

d) $y^* - x^* < \tau$ or $2\tau + \Delta > y^*$, $z^* < \tau + \Delta$

Pic. 2. Allocation of intervals for the next operations

Problem statement:
1) to find ergodicity conditions;
2) to find distribution function $F(x)$ of virtual waiting time of double request and distribution functions $F_1(x)$ and $F_2(x)$ of waiting times w_1 and w_2 of the first and second operations of random request, counting waiting time of the second operation from the moment $\tau + \Delta$ after request entered a system;
3) to find average waiting times of the first and second operations.

Ergodicity conditions
Theorem 1. At $2\lambda\tau \geq 1$ the total waiting time $w_1^{(n)} + w_2^{(n)}$ of the first and second operations of the n-th request tends by probability to ∞ at n tends to ∞.
Theorem 2. At $2\lambda\tau < 1$ random vector $(w_1^{(n)}, w_2^{(n)})$ has ergodic distribution.

Average waiting time of the first and second operations of the double request at $\Delta < \tau$
Let's consider $\Delta < \tau$. In this case it is impossible to allocate operation of another request between two operations of the given request; this simplifies analytical research.
Let's use the method of virtual waiting time $w(t)$. So, $w(t)$ is the virtual waiting time: so much request will be waiting, if it enters the system at moment t. Many queueing system problems have been solved by using this method, invented by Takach [3].
The structure of the process $w(t)$ in our case is as followed. If in the range dt requests doesn't enter the system, then $w(t + dt) = w(t) - dt$ at $w(t) > 0$ and $w(t + dt) = 0$ at $w(t) = 0$. If a request entered the system in the state $w(t) = x$, then the new value y of the variable $w(t)$ is defined by formula:

$$y = \begin{cases} 2\tau + \Delta \;\; at \;\; x \le \Delta \\ x + 2\tau \;\; at \;\; x > \Delta. \end{cases} \tag{1}$$

Let $F(t)$ be the distribution function of the random variable $w(t)$ in stationary case. Then

$$P\{w(t) < z\} = P\{w(t+dt) < z\} = F(z).$$

Event $\{w(t+dt) < z\}$ may occur in two cases:

1) $w(t) < z + dt$ and there were no requests for the time dt. Probability of such event

$$(1 - \lambda dt)F(z+dt) + o(dt).$$

2) for the time dt a request entered. Denote $w(t) = x$, $w(t+dt) = y$, on the base of formula (1) we get the next condition for x: $x < z < 2\tau$ at $z \ge 2\tau + \Delta$.

This event isn't possible at $z < 2\tau + \Delta$.

So,

$$F(z) = (1 - \lambda dt)F(z+dt) + \lambda dt F(z+2\tau) \;\; at \;\; z \ge 2\tau + \Delta;$$
$$F(z) = (1 - \lambda dt)F(z+dt) \;\; at \;\; z < 2\tau + \Delta.$$

From this we get equations

$$F'(z) - \lambda F(z) + \lambda F(z-2\tau) = 0 \;\; at \;\; z \ge 2\tau + \Delta, \tag{2}$$
$$F'(z) - \lambda F(z) = 0 \;\; at \;\; z < 2\tau + \Delta. \tag{3}$$

Solving (3):

$$F(z) = Ce^{\lambda z}, \;\; 0 \le z \le 2\tau + \Delta. \tag{4}$$

After some computations we get constant C:

$$C = (1 - 2\tau\lambda)e^{-\lambda\Delta}.$$

From formula (4)

$$F(z) = (1 - 2\tau\lambda)e^{\lambda(z-\Delta)}, \;\; at \;\; 0 \le z \le 2\tau + \Delta \tag{5}$$

In the range $2\tau + \Delta < z < \infty$ equation (2) can be solved by numerical method.

But $Ew(t) = \int\limits_0^\infty zF'(z)dz$ can be found in the explicit form:

$$Ew(t) = \frac{2\tau^2\lambda}{1 - 2\tau\lambda} + \Delta - \frac{1 - 2\tau\lambda}{\lambda}(1 - e^{-\lambda\Delta}). \tag{6}$$

Let's consider special cases, in which this formula is easy to explain.

1. At $\Delta = 0$ we get

$$Ew(t) = \frac{2\tau^2\lambda}{1 - 2\tau\lambda},$$

which corresponds to the Khinchin formula [3] for the average waiting time in queueing system $M/G/1$ at load $\rho = 2\tau\lambda$ and fixed servicing time 2τ.

2. At $\lambda \to 0$ we get

$$Ew(t) \sim \lambda(2\tau^2 + 2\tau\Delta + \frac{\Delta^2}{2}) = \frac{\lambda}{2}(2\tau + \Delta)^2.$$

This formula can easily be interpreted by intuition: at low load requests will overlap only with very little probability. Random request may enter at the system's busy period with probability $\lambda(2\tau + \Delta)$, and it would have to wait for service averagely half of this period, i.e. $\lambda(2\tau + \Delta)/2$.

3. At $\rho = 2\lambda\tau \to 1$ from (6) we get

$$Ew(t) \sim \frac{\tau}{1 - \rho}.$$

At the same time from Khinchin formulas [3] an average time in queueing sustem $M/G/1$ with constant (-2τ) service time equals

$$(2\tau)^2 \lambda / (2(1-\rho)) \sim \tau / (1 - \rho) \;\; at \;\; 2\lambda\tau \to 1,$$

i.e. the same asymptotics. This can be explained by the fact that at high load ($\rho \to 1$) virtual waiting time usually will be large and the effect of the gap Δ between operations will vanish.

Now let's find formulas for the distribution of the waiting time via distribution of the virtual waiting time. Let's define distribution functions $F_1(x)$, $F_2(x)$ of waiting the first and the second operations of request in steady-state condition. If a request enters at moment t, when virtual waiting time $w(t) = x$, then waiting time of the first operation is also equals to x, and the second one 0 at $x \leq \Delta$ and $x - \Delta$ at $x > \Delta$ (the first operation will end at moment $t + x + \tau$, and for the second one the observation of waiting time will start at moment $t + \tau + \Delta$; $(t + x + \tau) - (t + \tau + \Delta) = x - \Delta$).

$$F_1(z) = P\{w_1 < z\} = F(z); \tag{7}$$

$$F_2(z) = P\{w_2 < z\} = P\{w < z + \Delta\} = F(z + \Delta) \text{ at } z > 0. \tag{8}$$

Average waiting time, based on formulas (7) and (8),

$$Ew_1 = Ew = \frac{2\tau^2 \lambda}{1 - 2\tau\lambda} + \Delta - \frac{1 - 2\tau\lambda}{\lambda}(1 - e^{-\lambda\Delta}),$$

$$Ew_2 = \int_0^\infty z dF(z + \Delta) = \int_\Delta^\infty (x - \Delta) dF(x). \tag{9}$$

As a result of some computations

$$Ew_2 = \frac{2\tau^2 \lambda}{1 - 2\tau\lambda}.$$

Analysis of the virtual waiting time distribution of dual request

We've obtained the main equations (2-3) for the distribution function $F(x)$ of virtual waiting time of double request. $F(x)$ is continuous at $x > 0$.

Let's denote

$$F(2k\tau + \Delta + x) = F_k(x). \tag{10}$$

Then (2-3) can be rewritten as

$$F'(x) - \lambda F_k(x) + \lambda F_{k-1}(x) = 0, \ 0 < x < 2\tau, k \geq 1, \tag{11}$$

$$F'(x) - \lambda F_0(x) = 0, \ -\Delta < x < 2\tau. \tag{12}$$

Equation (12) has already been solved as

$$F(x) = (1 - \rho)e^{-\lambda\Delta + \lambda x}, 0 < x \leq 2\tau + \Delta,$$

then from (10)

$$F_0(x) = (1 - \rho)e^{\lambda x},$$

where $\rho = 2\lambda\tau$, it is expected that $\rho < 1$.

Let's find an expression for Laplase-Stiltjes transform

$$\phi(s) = \int_0^\infty e^{-sx} dF(x), \ \text{Re } s \geq 0.$$

Denote $G(x)$ as decision of the equation

$$G'(x) - \lambda G(x) + \lambda G(x - 2\tau) = 0, \ x > 2\tau$$

under condition

$$G(x) = (1 - \rho)e^{\lambda x}, \ -\infty < x \leq 2\tau,$$

continuous at $x > 0$. Then

$$F(x) = G(x - \Delta), \ x > 0.$$

It can be noticed that $G(x)$ at $x > 0$ coincides with distribution function $F_0(x)$ of virtual waiting time in queueing system $M / D / 1$ with waiting time, which with probability 1 equals 2τ.

By Khinchin formula, denoting

$$\phi_0(s) = \int\limits_0^\infty e^{-sx} dF_0(x),$$

we get

$$\phi_0(s) = \frac{1-\rho}{1 - \dfrac{\lambda}{s}(1 - e^{-2\tau s})}, \tag{13}$$

as waiting time always equals 2τ and its Laplase-Stiltjes transform is $\exp(-2\tau s)$. For relative distribution function $F_0(x)$ we can write, using symbols $\delta(x)$ of Dirac's delta function and $\eta(x)$ of Heaviside step function, which equals to 0 at $x \le 0$ and 1 at $x > 1$:

$$F_0'(x) = (1-\rho)\delta(x) + G'(x)\eta(x).$$

So,

$$\phi_0(s) = \int\limits_{-\infty}^\infty e^{-sx} F_0'(x) dx.$$

By the shift theorem

$$\phi_0(s)e^{-s\Delta} = \int\limits_{-\infty}^\infty e^{-sx} F_0'(x-\Delta) dx.$$

Changing to Laplase-Stiltjes transforms, we get

$$\phi(s) = \phi_0(s)e^{-s\Delta} + (1-\rho)\frac{s}{\lambda - s}(e^{-s\Delta} - e^{-\lambda\Delta}) \tag{14}$$

Substituting (13), we get

$$\phi(s) = \frac{(1-\rho)e^{-s\Delta}}{1 - \dfrac{\lambda}{s}(1 - e^{-2\tau s})} + (1-\rho)\frac{s}{\lambda - s}(e^{-s\Delta} - e^{-\lambda\Delta}). \tag{15}$$

By formulas (14) and (15) we can define moments of virtual waiting time distribution. Therefore, as $Ew = -\phi'(0),$ then from (14), having taken from Khinchin's formula that

$$\phi_0'(0) = -\frac{\rho\tau}{1-\rho},$$

we get

$$Ew = -\phi_0'(0) + \Delta - \frac{(1-\rho)(1-e^{-\lambda\Delta})}{\lambda} = \frac{\rho\tau}{1-\rho} + \Delta - \frac{(1-\rho)(1-e^{-\lambda\Delta})}{\lambda}.$$

References

1. *Dyshliuk O.N., Koba E.V., Pustova S.V.* Investigation of the distribution of waiting time in a queueing system with dual demands // J. Autom. Inf. Sci. – v.43, i.7 – 2011. – P.29–39.

2. *Dyshlyuk O.M., Koba O.V., Pustova S.V.* Investigation of Distribution of Waiting Time in Queueing System with Dual Demands by the Method of Statistical Modeling // J. Autom. Inf. Sci. – v.43, i.10 – 2011. – P.10–18.

3. *Гнеденко Б.В., Коваленко И.Н.* Введение в теорию массового обслуживания / Изд. 3-е, испр. и доп. – М.: КомКнига, 2005. – 400с.

Lytvynenko O.E., doctor of technical sciences
(National Aviation University, Ukraine)

THE SOLUTION METHOD OF THE NONLINEAR EQUATIONS' SYSTEMS WITH BOOLEAN VARIABLES (THE COMBINATORY EQUATIONS)

The solution method of the nonlinear equations' systems with boolean variables, which realizes the strategy of the directed enumeration of variants, is stated. Necessary and sufficient conditions of existence of feasible plans are formalized. Procedure of the formal analysis of subsets of variants is described. The structure of the algorithm that possesses the completeness property is resulted. Special cases of systems of equations under consideration are considered.

Introduction

The necessity of research of the nonlinear equations systems with boolean variables (the combinatory equations) appears during solution derivation in expert control systems of complex organizational and technological processes, and also in diagnosing systems of complex technical objects, in which there can be plural refusals with the effect of "imposing" of their consequences [1] - [2].

Besides, the equations systems with boolean variables are part of mathematical models of numerous applied combinatory optimization problems, to which belong the problems of traffic streams routing, scheduling problems, the problems of ordering and scheduling of a complex of the interconnected works, complex objects design, etc. [3] - [7].

For the solution of similar problems various heuristic algorithms are traditionally used. It is known, that such algorithms have a number of grave disadvantages that restrict their practical application. First of all, these include the weak action purposefulness and completeness property absence. As a result, there are unfairly high machine time expenses, and also situations, when there is no success in resolving a problem though the solution obviously exists.

The aspiration to set the solution process of the nonlinear equations systems with boolean variables on a strict mathematical basis has lead to the development of the new method, which realizes the strategy of the directed enumeration of variants. The statement of this method is the purpose of this article.

Problem Statement

The nonlinear equations system with boolean variables can be represented in the following general view:

$$g_j(x) = b_j; \; j = \overline{1,n}, \qquad (1)$$

Where x is the m-dimensional vector of the independent boolean variables:

$$x = (x_i; \; i = \overline{1,m}); \; x_i \in \{0,1\};$$

where $g_j(x)$ is the function of independent variables, which has a nonlinear structure:

$$g_j(x) = \sum_{r \in R_j} a_{jr} \varphi_r(x); \; j = \overline{1,n};$$

$\varphi_r(x)$ is a product of independent variables (x-product):

$$\varphi_r(x) = \prod_{i \in I_r} x_i; \; r = \overline{1,q};$$

R_j is a set of numbers of x-products, which are included in j-th equation; $j = \overline{1,n}$;

I_r is a set of numbers of the independent variables, which form the r-th x-product; $r = \overline{1,q}$;

a_{jr}, b_j are the rational numbers, which aren't periodic fractions; $j = \overline{1,n}$; $r \in R_j$.

It is necessary to define a vector of the bivalent variables' values $x = (x_i;\ i = \overline{1,m})$, satisfying the equations system (1).

The problem has a combinatorial nature and belongs to the class of the NP-full problems, which require huge (and, in some practical cases, unacceptable high) expenses of machine time for their solution.

The suggested method allows to minimize the number of algorithm's realization steps and, hence, duration of the equations system's solution due to high direction and maximal narrowing of the search area of the vector of a boolean variables' values $(x_i;\ i = \overline{1,m})$ that satisfy the given system.

The method is based on consecutive breaking of the initial set of variants until the optimum plan or the incompatibility of system of restrictions is established. Allocated subsets of variants are subjected to the formal analysis, the purpose of which is:

- the revealing and exclusion from further consideration the subsets, which do not contain feasible plans;
- the revealing and exclusion from further consideration the equations, which have lost the property of activity with respect to the plans of the analyzed subset of variants during problem solution;
- the revealing and fixing the variables, which can accept only non-alternative values (only 0 or only 1) to provide the permissibility of supplemental plans of the analyzed subset of variants.

The Basic Notions and Conventional Signs

Let at the beginning of certain step of the problem's (1) solution λ not crossed subsets G_k, containing feasible plans, are allocated in full set of variants G; $k = \overline{1,\lambda}$.

Let I_k^0 and I_k^1 be sets of numbers of the decision variables, which received values 0 and 1 in plans of k-th subset of variants, and I_k be a set of variables' numbers, the values of which are not fixed in G_k.

The set of variables' values $x_i,\ i \in I_k^0 \cup I_k^1$ such as $(\forall i \in I_k^0)(x_i = 0)$ and $(\forall i \in I_k^1)(x_i = 1)$ is called the partial plan of k-th subset of variants. Any set of variables' values $x_i,\ i \in I_k$ satisfying the bivalent condition $x_i \in \{0,1\}$ is called the supplemental plan of the subset G_k.

Let's introduce the following signs:

R_k^0 and R_k^1 - the sets of numbers of functions $\varphi_r(x)$ converted by the partial plan of the k-th subset of variants accordingly to 0 and 1:

$$R_k^0 = \left\{ r : I_r \bigcap I_k^0 \neq \varnothing \right\};\ R_k^1 = \left\{ r : I_r \subseteq I_k^1 \right\};$$

R_k - the set of numbers of functions $\varphi_r(x)$, which aren't converted by the partial plan of subset G_k to a constant:

$$R_k = \{1,...,q\} \setminus (R_k^0 \bigcup R_k^1).$$

The constitution of sets R_{jk} and R_{jk}^1, $j = \overline{1,n}$, similar to the named above, but relating to the j-th equation of system (1), is defined according to formulas:

$$R_{jk} = R_j \bigcap R_k;\quad R_{jk}^1 = R_j \bigcap R_k^1.$$

The system's (1) equation, in case when even one of the subset's G_k supplemental plans doesn't satisfy it, is called active with respect to plans of the given subset. A set of numbers of such restrictions we shall designate as J_k; $J_k \subseteq \{1, 2, ..., n\}$.

The equations' system (1) brought into accord with the k-th subset of variants will have the following form:

$$g_{jk}(x) = b_{jk};\ j \in J_k;\qquad\qquad (2)$$

where

$$g_{jk}(x) = \sum_{r \in R_{jk}} a_{jr} \varphi_{rk}(x);$$

$$\varphi_{rk}(x) = \prod_{i \in I_{rk}} x_i; \quad I_{rk} = I_r \cap I_k; \quad r \in R_k;$$

$$x_i \in \{0,1\}; \quad i \in I_k;$$

$$b_{jk} = b_j - \sum_{r \in R_{jk}^1} a_{jr}.$$

On sets R_{jk} and I_{jk}, $j \in J_k$ the following subsets are defined:

$$R_{jk}^2 = \{r \in R_{jk} : a_{jr} < 0\}; \qquad\qquad R_{jk}^2(r') = \{r'\} \cup \{r \in R_{jk}^2 : a_{jr} \le a_{jr'}\};$$

$$R_{jk}^3 = \{r \in R_{jk} : a_{jr} > 0\}; \qquad\qquad R_{jk}^3(r'') = \{r''\} \cup \{r \in R_{jk}^3 : a_{jr} \ge a_{jr''}\}$$

$$R_{jk}^4(r') = \{r \in R_{jk}^3 : I_{rk} \subseteq I_{jk}^2(r')\}; \qquad R_{jk}^5(r'') = \{r \in R_{jk}^2 : I_{rk} \subseteq I_{jk}^3(r'')\};$$

$$R_{jk}^6(r'') = \{r \in R_{jk}^2 : I_{rk} \cap I_{jk}^8(r'') \ne \varnothing\}; \quad R_{jk}^7(r') = \{r \in R_{jk}^3 : I_{rk} \cap I_{jk}^9(r') \ne \varnothing\};$$

$$R_{jk}^8(r'') = \{r \in R_{jk}^3(r'') : m_{rk} = 1\}; \qquad R_{jk}^9(r') = \{r \in R_{jk}^2(r') : m_{rk} = 1\};$$

$$I_{jk}^v(r') = \bigcup_{r \in R_{jk}^v(r')} I_{rk}; \quad v \in \{2,9\}; \qquad I_{jk}^v(r'') = \bigcup_{r \in R_{jk}^v(r'')} I_{rk}; \quad v \in \{3,8\},$$

where $m_{rk} = |I_{rk}|$.

Let's introduce the following signs:

$$s_{jk}^v = \begin{cases} \displaystyle\sum_{r \in R_{jk}^v} a_{jr}, \text{if } R_{jk}^v \ne \varnothing \\ 0, \text{if } R_{jk}^v = \varnothing \end{cases}; \quad v \in \{2,3\};$$

$$s_{jk}^v(r^*) = \begin{cases} \displaystyle\sum_{r \in R_{jk}^v(r^*)} a_{jr}, \text{if } R_{jk}^v(r^*) \ne \varnothing \\ 0, \text{if } R_{jk}^v(r^*) = \varnothing \end{cases},$$

where $r^* = \begin{cases} r' \text{ at } v \in \{4,7\} \\ r'' \text{ at } v \in \{5,6\} \end{cases}$.

For each j-th ($j \in J_k$) equation of the system (2) the necessary and sufficient conditions of its performance can be formulated. The necessary condition is the belonging of the free member b_{jk} to the numerical axis' segment restricted to minimal and maximal values of the left part of the equation:

$$\min g_{jk}(x) \le b_{jk} \le \max g_{jk}(x).$$

With the certain approximation degree as $\min g_{jk}(x)$ and $\max g_{jk}(x)$ the sum of negative and positive coefficients of function $g_{jk}(x)$ accordingly can be accepted:

$$s_{jk}^2 = \min g_{jk}(x); \ s_{jk}^3 = \max g_{jk}(x)$$

The sufficient condition of performance of the jth ($j \in J_k$) equation of system (2) should be the existence of such combination of its coefficients, the sum of which exactly equals to b_{jk}. Presence or absence of such combination we shall reflect as value "true" (1) or "false" (0) of the predicate $P_j(G_k)$ accordingly:

$$P_j(G_k) = \begin{cases} 1, \text{ if } \displaystyle\sum_{r \in R_o(G_k)} a_{jr} = b_{jk} \\ 0, \text{otherwise} \end{cases},$$

where $R_j(G_k)$ is some subset of x-products' numbers, which are included in the j-th equation of system (2); $R_j(G_k) \subseteq R_{jk}$.

The establishment of the fact of fulfillment or non-fulfillment of a sufficient condition of the system's (2) j-th equation solution existence is generally equivalent to the solution of the unique linear equation with ρ_{jk} boolean variables:

$$\sum_{r \in R_{jk}} a_{jr} y_r = b_{jk} , \qquad\qquad (3)$$

where $y_r \in \{0,1\}$; $r = \overline{1, \rho_{jk}}$; $\rho_{rk} = |R_{jk}|$.

Becase the given equation can be considered as special case of system (1), the simplified modification of the method for its solution is used in this article. Obviously, the presence of a bivalent vector of variables' values y_r ; $r = \overline{1, \rho_{jk}}$, satisfying the equation (3), indicates the fulfillment of a sufficient condition of the system's (2) j-th equation solution existence, absence – the non-fulfillment.

The Structure of the Algorithm

The solution algorithm of the equations' system (1), which realizes the strategy of the directed enumeration of variants, provides the performance at each computing process stage the following sequence of actions:
  - choosing a subset of variants subject to further splitting;
  - choosing a variable, the values of which are subject to fixing;
  - splitting a subset of variants into two not crossed subsets;
  - analysis of received subsets of variants;
  - checking the conditions of computing process ending.
  1. Choosing a Subset of Variants Subject to Splitting.

As the considered problem is not the optimization one, it is expedient to use the number of variables, which in subsets G_k , $k = \overline{1, \lambda}$ have the fixed values, as criterion of choosing a subset of variants for further splitting. It means, that for further splitting the subset of variants G_{k*}, $1 \le k* \le \lambda$ is chosen, to which the partial plan of the maximal capacity corresponds:

$$\mu_{k*} = \max\left\{\mu_k, k = \overline{1, \lambda}\right\},$$

where $\mu_k = \left|I_k^0 \cup I_k^1\right|$.

Such criterion responds aspiration to achieve required calculations' result for minimum quantity of algorithm steps.
  2. Choosing a Variable, the Values of which are Subject to Fixing.

According to the given reasons in the previous step, it is expedient for the given operation to choose a variable, the fixing of values of which can lead to essential simplification of the system (2), corresponding to the subset of variants G_{k*}. Any variable of that x-product, which belongs to equations set (2) with the maximal coefficient in absolute value, can have such property.

Hence, for giving values 0 and 1 an arbitrary variable $x_{i*} \in I_{r*k*}$ is chosen, which belongs to the x-product $\varphi_{r*k*}(x)$, so that

$$\left|a_{jr*}\right| = \max\{\left|a_{jr}\right|; \ j \in J_{k*}; r \in R_{jk*}\} .$$

  3. Splitting a Subset of Variants G_{k*}.

By fixing values of the variable x_{i*} the subset G_{k*} is broken into two not crossed subsets of variants G_{k*}^0 and G_{k*}^1. In all plans of the first of them $x_{i*} = 0$, of the second $x_{i*} = 1$. These values are serially substituted in equations of the system (2), with the help of which two new systems of equations, corresponding to the two new subsets of variants G_{k*}^0 and G_{k*}^1, are formed.
  4. The Analysis of Subsets of Variants G_{k*}^0 and G_{k*}^1.

New subsets G_{k*}^0 and G_{k*}^1 are serially exposed to the formal analysis according to the procedure stated above. After that (if the required solution is not found) all considerations left in the variants' subset are renumbered again, starting with one.

5. Checking the Conditions of Computing Process Ending.

Computing process ends after finding a solution (a set of solutions) of the equations set (1) or after establishing its incompatability.

Conclusion

The problems, which require solving the nonlinear equations systems with boolean variables, are widely used in the automated control systems, the design and diagnostic complex objects' systems.

In order to solve such problems various heuristic algorithms are traditionally used, which have the limited practical application due to their known disadvantages.

In given article the mathematical solution method of the nonlinear equations' systems with boolean variables, which realizes the strategy of the directed enumeration of variants, is stated.

The given algorithm has completeness property, because none of allocated subsets of variants is excluded from the consideration, until the fact of incompatibility of the corresponding equations set is established.

Computer realization of the method is carried out in operational environment UNIX IP with the use of language C ++.

References

1. *Литвиненко А.Е.* Комбинаторный метод выработки решений в экспертных системах управления сложными объектами. – Кибернетика и системный анализ, 1992. – № 5. – с.81-86.

2. *Литвиненко О.Є.* Математичний метод визначення множинних відмов в складних технічних системах. – Вісник НАУ, 2002. – №4. – с. 143-150.

3. *Пападимитриу Х., Стайглиц К.* Комбинаторная оптимизация. Алгоритмы и сложность. – М.: Мир, 1985. – 512 с.

4. *Литвиненко А.Е.* Метод решения экстремальных комбинаторных задач с нелинейной структурой. – Кибернетика, 1983.– № 5.– с.83-87.

5. *Frederick S. Hillier, Gerald J. Lieberman.* Introduction to Operations Research. – McGraw-Hill Science/Engineering/Math; 8 edition (August 10, 2005). –1061 p.

6. *Wayne L. Winston.* Operations Research: Applications and Algorithms. – Duxbury Press; 4 edition (July 25, 2003). – 1440 p.

7. *Hamdy A. Taha.* Operations Research: An Introduction (8th Edition). – Prentice Hall; 8 edition (April 4, 2006). – 813 p.

S.M. Stanko,
O.M. Glazok, candidate of technical sciences,
(National Aviation University, Ukraine)

USING THE FUNCTIONAL APPROACH FOR DETERMINING PARAMETERS OF DYNAMIC MODELS OF FLYING APPARATUSES

The possibility of using the functional approach to the solving problem of determination of the characteristiscs of dynamic models of flying apparatuses is explored. The greater power of the functional approach lies in the idea that the operations may be treated just in the same way as data. The strengthes, weaknesses and problematic questions of functional approach application are discussed.

Quality of automatic control of an aircraft is one of important factors of safety of flights and competitiveness of the flying apparatus. Success of developing of the system of automatic control for an aircraft, as well as quality of its work, depend on exactness of model of aircraft as a dynamic object, which is used for creation of the control system, on plenitude and authenticity of information about the object of control (plant). The more complete and more exact is the mathematical description (mathematical model) of object, the greater effect can be got as a result of its automation and optimization. Thus, determination of parameters of mathematical model of object on the basis of watching its behaviour makes substantial part of work of designer of a control system, as well as the engineer who performs adjustment and maintenance of such a system. [1]

Mathematical models are formalized mathematical descriptions of objects, control systems and their parts, and also of their intercommunications. A model of any kind is the simplified reflection of the actual object, but it must reflect all its substantial features, that is, that complex of properties of object, the taking account of which is important for the supposed application of model. Model's closeness to the object in terms of these properties is estimated with adequacy criteria which are based on different quantitative estimations of deviations of the state variables of the obtained model from the available experimental information. In researches, related to the construction of models of complicated objects, questions of adequacy have the special significance. Plenty of the real objects – nonlinear, non-stationary, multidimensional, with many internal reverse connections, having the distributed parameters, owning a large inertance and delay, are characterized by the large number of input and initial parameters, much from which are uncontrolled variables and/or subject to intensive disturbances. These reasons complicate building of the mathematical model, considerably adequate to the real object, in this connection there arises a requirement of model simplification.

Nowadays, there are two selected different approaches to the construction of models of the controlled objects. One approach consists in an attempt to penetrate into the "deeps" of the object operation and to set its properties and intercommunications to comprehensive physical and mathematical analysis of the phenomena and processes which take a place at its functioning. Such analytical path is very labour intensive and justifies itself only at the construction of cognitive models. Other path consists in watching and registering changes of values at the object inputs and outputs in the process of its exploitation, on its initial co-ordinates, etc, and, finally, making conclusions about the object properties and creating its mathematical model, or consistently specifying the adjustable hardware or programmatic model. Such approach, unlike the first one, is based not on theoretical, but on experimental researches of object.

Wide prospects for modification and perfection of processes of determination of parameters of models of the run-time systems are given by application of the functional approach. Usually people remember about functional approaches at the periods of technology changes, when the role of analytical and research tasks grows. It is not an accident that nowadays one often uses the term «functionality» at comparative description of the information systems.

Functional approach, and its practical mapping, functional programming, is a paradigm that originated from ideas older than the first computers. The first functional programming language celebrated its 50th birthday in 2008. Functional languages are very expressible, yet everything is achieved using a minimal number of concepts. Despite their elegance, functional languages have largely been ignored by mainstream developers until now.

Today we are facing new challenges and trends that open the door to functional approaches. We need to design systems and write programs that process large sets of data and scale to a large number of processors or computers. We want to create components that can be easily tested. We want to be able to express our logic in a declarative way which expresses results without explicitly specifying execution details – making the created structure easier to understand and reason about.

The common complication of solving problems by means of functional determinations may be overcome by aiming at formalization of basic set of objects and determination of the complete semantic system of operations applied to them. It allows to present the classes of tasks and their solutions in the form of strict formulas, which, for the sake of evidency, may be simplified by means of introduction of the extended functional characters. If necessary such characters are brought into the determination of the system of algebra which results in its expansion, and new functions are introduced, like proving lemmas and other auxiliary constructions in mathematics. Recursive and character denotations of both information and actions and any formulas, comfortable at determination functions is actively utilized.

Let us consider a procedure for determination of frequency characteristics of an aircraft directly from the records of the measured signals. Basicly, the dynamic system is supposed to be linear, with the differential equation of the following form in the time domain [2]:

$$a_n \overset{(n)}{y}(t) + a_{n-1} \overset{(n-1)}{y}(t) + ... + a_0 y(t) = b_m \overset{(m)}{x}(t) + b_{m-1} \overset{(m-1)}{x}(t) + ... + b_0 x(t) \quad.$$

For such signals let us apply the Laplace transform to both parts of the diferential equalization of the system:

$$L\{y_n(t)\} = Y_n(s) \ ; \ \ L\{x_m(t)\} = X_m(s) ;$$

$$W_{n,m}(s) = \frac{Y_n(s)}{X_m(s)} = \frac{\sum_{j=0}^{k} b_j s^j}{\sum_{j=0}^{r} a_j s^j}.$$

Let us introduce into the consideration the followings functions and operators:

the functions $F_{mn}(x_m(t), y_n(t))$, which characterize the system's identificability;

the functions $V_{mn}(x_m(t), y_n(t))$, which characterize the speed of fading of the process of identification;

the functions (functionals) $P_{mnp}(x_m(t), y_n(t))$, which characterize the errors of the values of the identified parameters of the system;

the functions (functionals) $E_{mnp}(x_m(t), y_n(t))$, which characterize the errors of control (by the output values), provided that the control is performed on the basis of the identified parameters of the system;

the identification operators $I_m(y_n(t))$;

the operator $R\{\}$ of recursive application of identification procedure;

the operator of the Laplace transform $L\{\}$;

the operator of the reverse Laplace transform $L^{-1}\{\}$;

the operators of modification of the input data $M^d{}_j\{\}$, $j = 1...J_1$;

the operators of modification of the penalty functions $M^f{}_j\{\}$, $j = 1...J_2$;

With the use of these denotions the problem of determination of parameters may be formulated as the problem of search of such functional operators I_m, $R\{\}$, $M^d_j\{\}$, $M^f_j\{\}$, that for the given set of input data allow to minimize the norms of functions of $P_{mnp}(x_m(t), y_n(t))$ and $E_{mnp}(x_m(t), y_n(t))$. This problem setting may be further expanded, according to the actual needs of the control system developers and their customers. Such formal expansion is conservative (every new character is determined through the old ones), while it guarantees the maintenance of all of functional properties of the source system. The minimum set of denotations in which it is possible to describe all the correct (calculated) formulas of the system, plays the role of the base of the system, realization of which is a minimum version of the system.

In realisation of such an approach, we face several problematic questions [3]. The first of them is about the effectiveness of the composed system, in comparison to the systems in which the traditional principles are applied. In order to compare the efficiencies of algorithms meaningfully, the time requirements of an algorithm must first be quantified. Although it is theoretically possible to predict the exact time taken to perform many operations, such an approach quickly becomes intractable as the system gets more complicated.

Consequently, one should sacrifice exactness in favour of an approximate but still quantitative measure of the time taken for an algorithm to execute. This approximation, the conventional notion of algorithmic complexity, is derived as an upper- or lower-bound or average-case of the amount of computation required, measured in units of some suitably-chosen primitive operations. Furthermore, asymptotic algorithmic efficiency is derived by considering these forms in the limit of infinite algorithmic complexity.

Another significant issue is interoperability. Modem scientific computing often requires many separate components to interact. These components typically use different styles, are written in different languages and sometimes even run on separate platforms or architectures. The functional approach allows programs to interact easily with other systems and even other platforms across the internet. As an example, the F# functional programming language provides a unique combination of expressive power and easy interoperability.

There is a wide variety of different software used by scientists. As the practice shows, COM and .NET applications can easily be set for interoperation with most important applications, such as Microsoft Excel, The Mathwork's MATLAB and Wolfram Research's Mathematica.

Conclusions

The power of the functional approach lies in the idea that the operations may be treated just in the same way as data. The concept of a function, unlike the classic concept of a set, partially includes a concept of time: at first arguments are calculated in order of their introduction, then in accordance with the approved algorithm the value of the function is determined – possibly, its result is obviously dependent upon the results of other functions or of the same function, but at other, before calculated, values of arguments. As usual, the values of the arguments are calculated till to them a function is used. But if in quality information not only a value but also character forms is assumed for the calculation of these values, question about time of calculation of arguments it is possible to decide not so categorically. This leads to the extended possibility of the use of recursive functions and methods of their realization.

References

1. *Зеленков А.А.* Бортовые системы автоматического управления. Оценка точности по результатам испытаний /А.А.Зеленков, В.М.Синеглазов. – К., НАУ-друк, 2009. – 264 с.

2. *Артюшин Л.М.* Теорія автоматичного керування /Л.М.Артюшин, О.А.Машков, Б.В.Дурняк, М.С.Сівов. – К.: «Атіка», 2003. – 270 с.

3. *Petricek T.* Real World. Functional programming with examples on F# and C# /Tomas Petricek, Jon Skeet. – Manning Publications, 2010. – 500 p.

V.V. Klobukov, V.A. Ryabokon, L.P. Klobukova,
(National Aviation University, Ukraine)

INTEGRATION VIRTUAL DESKTOP INFRASTRUCTURE IN THE LEARNING PROCESS

The possibility of using virtualization technology to increase IT efficiency in the modern PC learning. The use of modern technology hardware and software virtualization for building IT infrastructure of the educational process.

Personal Computer (PC) today is an inherent part of the learning process and the means of most of the learning objectives. A real tool of the student in the learning process is the software, which is only linked to a PC, making it an intermediate corporate information system. As a result, the active development of cloud computing where users have access to their own data, but do not run and do not think about the infrastructure, operating system and its own software with which they work.

Basic service issues a large number of PCs
• High transaction costs to support a local area network;
• The complexity associated with managing desktops;
• Providing users with secure and reliable access to the software and applications you need to work;
• Technical support for users;
• Install and update software licenses and maintenance costs;
• Backup, etc.

Solve most of the problems arise due to the use of technology desktop virtualization based Virtual Desktop Infrastructure (VDI). VDI allows the user to separate the software from the hardware - PC - and access to client applications via terminal devices.

IT virtualization is the process of isolation of computer resources from each other, which allows reduce the dependencies between them. Distinguish between hardware and software virtualization. Hardware virtualization - virtualization with hardware. Not differ fundamentally from the software virtualization, hardware virtualization is to deliver performance, comparable to that of non-virtualized machines, giving the possibility of practical use of virtualization and its caused widespread.

The most common virtualization technology Intel VT and AMD-V, which differ primarily by the manufacturer.

- In the Intel VT (Intel Virtualization Technology) implemented virtualization real address (compatibility with 8086). Appropriate hardware virtualization IO - VT-d. Often abbreviated VMX (Virtual Machine eXtension). Codename - Vanderpool.

- AMD-V is often abbreviated as SVM (Secure Virtual Machines). Codename - Pacifica. Appropriate technology virtualization IO - IOMMU. AMD-V is easier and more efficient than Intel VT. Supports AMD-V appeared in Xen 3.3 .

The use of such terms as virtualization implies - the process of presenting a set of computing resources, or logical association that gives any advantage over the original configuration. This new virtual view of the resources, the realization of unlimited, geographical location, or physical configuration of parts. Typically virtualized resources include computing power and data storage.

At the moment, actively develop various virtualization technologies: applications, presentations, business PCs, servers, and so on. Such variety allows you to virtualize almost all processes and resources of the company, which will undoubtedly help save not only on hardware, software, and human resources previously consolidate and reduce the power consumption of your

infrastructure by more than 50% (currently one of the main criteria or reasons the use of virtualization technology).

Benefits of Virtualization:
• Consolidation of resources and services.
• Reduction of energy consumption.
• Lower cost of ownership.
• Increased resiliency.
• IT Service Continuity.
• Dynamic allocation of resources.
• Cost of hardware and software.
• Security.
• Planning and management of infrastructure.
• The ability to create distributed services (Cloud).

Desktop computers are the backbone of any IT infrastructure including the learning process, as they provide the flexibility and mobility, for which, however, have to pay high transaction costs on IT support, user support, maintenance, and purchase of software licenses (software).

Technology VDI, makes it possible to create virtual IT infrastructure that provides high-performance management tools, without having in significant changes in the user's workflow. VDI technology allows you to create virtual desktops (virtual computer labs, virtual labs), which can be centrally deployed based on a single hosting server. This reduces operating costs and improving the safety and requires no end-user training work with the new interface. VDI - it's a win-win solution that provides benefits such as:
• Minimize costs.
• Environmentally friendly business.
• Flexible management.

Thanks to VDI, users have at their disposal a virtual PC, which look exactly like regular PCs, and you can work not only in the classroom but also in the library or from home. All data and settings are stored on the server, so there is no need to carry information with you.

In terms of optimizing IT VDI allows you to consolidate multiple servers, supporting virtual PC, which results in significant cost savings. Additional cost savings are also due to centralized management and deployment of applications and updates, and hence reduce the burden on system administrators and department support users.

With VDI, IT services and training facilities in schools can improve the flexibility and manageability of a local area network and infrastructure in general.

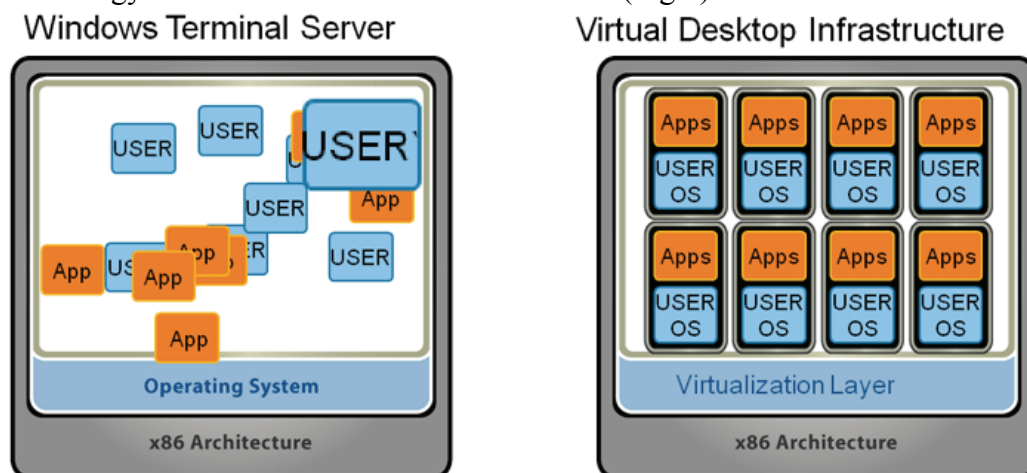VDI technology is an extension of terminal solutions (Fig.1).

Fig. 1 Windows Terminal Server and VDI

In contrast to the classical approach, using VDI server resources are shared between users is not due to a session on Wednesday, the same operating system, and by starting the virtual machine

interface using transmission system users on PCs and thin clients.

VDI provides technology: the use of the client operating system in terminal mode, the presence of administrative rights in the terminal environment for the user, the ability to save the state of the working environment and resume, increased isolation of user work environments from one another, the crucial issue of instability in the application or the possible peak loads on the hardware server resources, affecting other users; transfer fluid to the local computer by copying the virtual hard disk.

Economic benefits of VDI technology:

Reduction of investment costs in the workplace:

• Thin clients are at least 2 times cheaper PC

• The use of a single license for the server instead of the 100 anti-virus anti-virus licenses for PC

Reduced administration:

• All jobs are located on servers data center.

• Instant "creation of new jobs

• Instant "install applications

Reduced operating costs:

• Power consumption thin client is 10 times smaller than a standard PC

• Monitoring, Backup, cheaper accommodation in more than 5 times

Data Protection:

• Corporate information never leaves the data center.

• Performing regular backups.

• a centralized anti-virus protection system.

High availability and compatibility:

• Supports standard clustering solutions for Windows and Linux.

• Decision VDI support most business applications of different vendors.

VDI software:

VDI-solution Microsoft - helping companies to reduce total cost of ownership, business agility and continuity, accessibility anywhere, improved security. For companies, the new means of desktop virtualization, using Microsoft Application Virtualization, in the initial stage can provide a quick cost savings. Cooperate closely with Citrix's virtualization.

VDI-decision Parallels - is an effective way to reduce the cost of maintaining a local area network without making any significant changes to the workflow users. The basis formed Parallels VDI solution based on Parallels patented container technology.

VDI-decision VMware - offers medium and large organizations, a new approach to building the infrastructure of desktop PC users in the concept of virtual desktops (Virtual Desktop Infrastructure, VDI). This solution, formerly bore the name of VMware VDI, now called VMware View. However, this is not just a name change - it is completely finished concept of providing a reliable, secure infrastructure and mobile desktops.

Conclusions

Using the new virtualization technologies will create classes for different subjects, which at one and the same time, it will be possible to study and use of any software in any operating environment. Students and university staff will receive a powerful tool to provide a modern learning process all the necessary IT services.

References

1. *Haletky E.* VMware ESX Server in the Enterprise. Planning and Securing Virtualization Servers.Prentice.[ENG,576p.,2008]

2. *Goldworm B.* Blade Servers and Virtualization.Wiley.[ENG,384p.,2007]

3. *Макалистер Н.* Виртуализация серверов.[RUS,2007]

4. *Azad T.* Securing Citrix XenApp Server in the Enterprise.Syngress.[ENG,739p.,2008]

5. *Хики Э.* ИТ «в облаке».100 лучших вендоров.[RUS,2010]

UDC 621.45.038

A.A. Khalatov, Academician of NASU, Dr.Sci., S.D.Severin, Ph.D.
(*Institute of Engineering Thermophysics NAS, Ukraine*),
M.V.Bezlyudnaya, Post graduate student (*National Technical University «KPI», Ukraine*)

NUMERICAL MODELING OF FLAT PLATE FILM COOLING WITH COOLANT INJECTION INTO SPHERICAL DIMPLES

The numeral modeling of film cooling over a flat plate has been studied where a coolant supplies into two rows of inclined cylindrical holes arranged in spherical dimples. Two rows traditional film cooling has also been studied for comparisons. The numerical and experimental results have been compared to select the turbulence model providing the best results. The commercial ANSYS CFX 14 software was employed in all numerical calculations.

Introduction

The tendency of gas turbine inlet temperature growth in modern gas turbine engines to 1600…1800 K level leads to the necessity of the gas turbines blades film cooling, as at such high temperatures the using of only traditional internal convective cooling does not provide the blade wall temperature maximum limit.

In this connection the main problem of gas turbines blade cooling systems development is to provide the higher values of blowing ratio with the high values of film cooling efficiency. In the ordinary film cooling systems with coolant blowing through one or two rows of holes maximal film cooling efficiency arrives at the blowing ratio value $m \approx 0,6...0,7$ [1]. For providing of high values of film cooling efficiency at the acceptable values of blowing ratio, the different ways of film cooling intensification are used (blowing coolant through the shaped holes, into craters, trenches, application of anti-vortex systems, double jet system and other). In these paper the numeral modeling of flat plate film cooling with coolant injection through two rows of the cylindrical inclined holes into the spherical dimples and through the ordinary double-row holes configuration are presented. Comparison of numerical results and experimental data, as well as comparison of film cooling efficiency for both studied configuration are presented. The commercial software ANSYS CFX 14 was employed for CFD-modeling.

### Geometrical 3D - models and computational grids

The geometrical 3D-models of flat plate film cooling with coolant injection through two rows of holes into spherical dimples and ordinary double-row configuration with inclined holes located in a staggered order with incline angle $\gamma = 30^0$ were built in the ANSYS Design Manager 14, thus all geometrical parameters of investigational models were corresponded to the sizes of experimental test rig [2]. The lengths of models main and pre-included channels were $x/d = 35$ and $x/d = 10$ accordingly.

For CFD-modeling the unstructured combined computational grids built in ANSYS CFX Mesh 14 grid generator were used (Fig.1). The computational grids structure was a combination of tetrahedral elements in main flow area, with prismatic elements near solid walls.

The parameters of the computational grids used for numerical modeling and its dimensions are presented in a table 1.
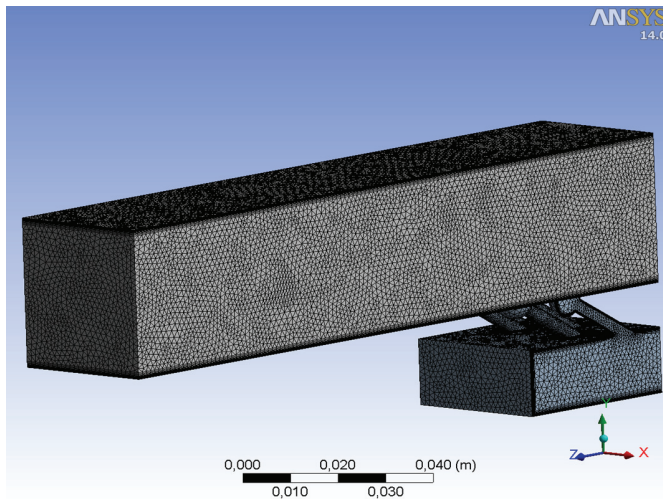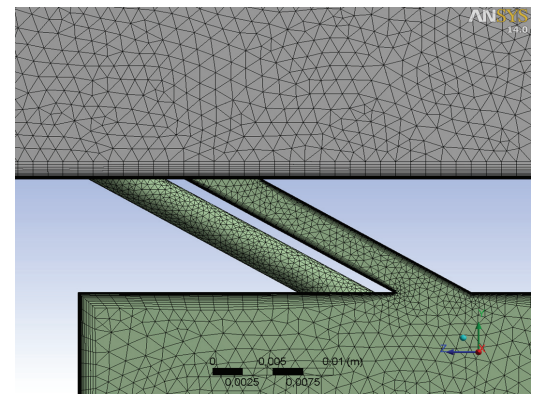
Model №1
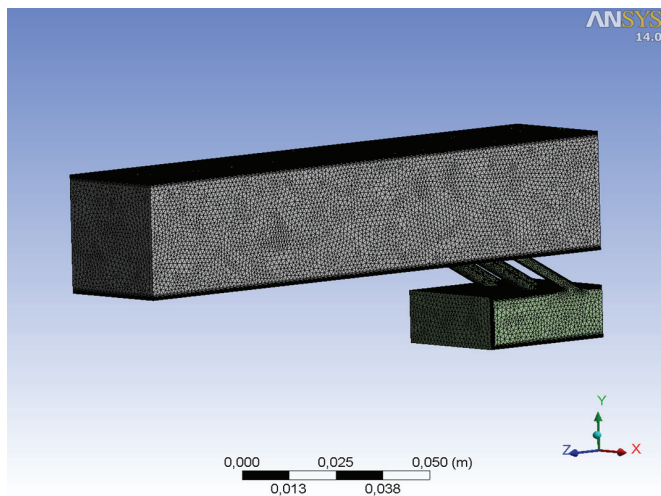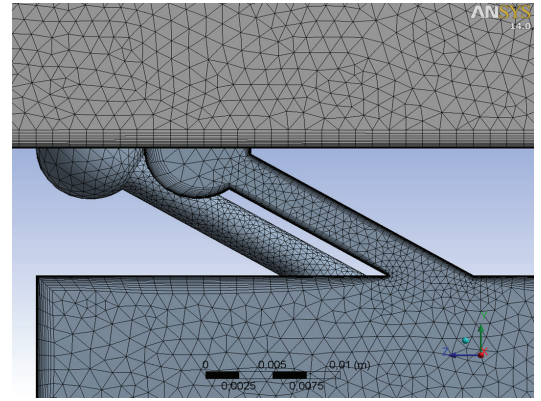
Model №2

Fig.1 Computational grids**.**

Table 1

Model	Number of tetrahedral elements	Number of prismatic elements	Number of grid nodes	Number of cells near the walls
№1	812730	396330	**353716**	15
	In all the elements	**1209060**		
№2	810552	801540	**564980**	30
	In all the elements	**1612092**		

Physical model and boundary condition

The atmospheric air was considered to be the ideal gas (the equation of the state is $P = \rho R T$) with temperature dependent of thermophysical properties. In particular, dependence of the heat capacity from temperature at the constant pressure was described as the following polynomial function:

$$\frac{C_p}{R} = a_o + a_1 \cdot T + a_2 \cdot T^2 + a_3 \cdot T^3 + a_4 \cdot T^4, \qquad (1)$$

where R is the gas constant; $a_0 ... a_4$ are coefficients of polynomial.

Dependence of the dynamic viscosity coefficient and the air heat conductivity on a temperature set by means of the Satherlend correlation:

$$\mu = \mu_0 \left(\frac{T}{T_0} \right)^n \frac{T_o + C_S}{T + C_S}, \tag{2}$$

$$\lambda = \lambda_0 \left(\frac{T}{T_0} \right)^n \frac{T_o + C_{S1}}{T + C_{S1}}, \tag{3}$$

where μ_0, λ_0 is the reference dynamic viscosity and heat conductivity accordingly.

The boundary conditions on an inlet and outlet of calculation area were set close to the experimental conditions. The solid walls of calculation area were set as being adiabatic walls $(q=0)$. On the side surfaces of calculation area the symmetry conditions were set. The Reynolds averaged Navie-Stoks equations were solved for viscous heat-conductive gas along with the total energy equation at stationary conditions. The boundary conditions set up in the calculations, were corresponded to the values of blowing ratio $m=0,5$; $1,0$; $1,5$, $2,0$ and presented in the Table 2.

Table 2

Area	Average static pressure, Pa	Average velocity, m/s	Static temperature, ^{0}C	Mass flow ratio, kg/s	Turbulence intensity
Inlet №1	-	30	15	-	-
Inlet №2	-	-	70	0,0005955	1%
				0,001191	
				0,0017865	
				0,0021438	
Выход	101300	-	-	-	-

Turbulence models testing

To selection the mostly suitable turbulence model the preliminary test calculations were carried out using various turbulence models. Two models of *k-e* group (the classic *k-e* model and *RNG k-e* model), two models of *k-ω* group (classic *k- ω -model* and Menter's SST - turbulence model) were used in these calculations. Testing of turbulence models was performed at identical boundary conditions at the inlets and outlet of calculation area, corresponding to the blowing ratio $m = 1,007$ (inlet №1 - $w = 30$ m/s; inlet №2 – $G_2 = 0,001191$ kg/s; outlet - $P = 101300$ Pa).

The testing of turbulence models was made by means of comparison with experimental data on the adiabatic film cooling effectiveness [2], taking into account the heat capacity temperature dependence $C_p = f(T)$. The correlation for the adiabatic film cooling effectiveness can be written as [1]:

$$\eta_{film} = \frac{i_g^* - i_{film}^*}{i_{film}^* - i_{wall}}. \tag{4}$$

Here, i_g^*, i_{film}^* — is the total enthalpy of gas and coolant on the injection plane accordingly; i_{wall} — is the adiabatic wall enthalpy.

The results of different turbulence models testing for the blowing ratio $m = 1,007$ are presented in Fig. 2, 3.

On the Fig. 2, 3 the dependence of local adiabatic film cooling efficiency from the relative axial distance (x/d) is given for the double row film cooling configuration. The calculations are presented for the different relative transversal coordinate y/D. Here D is the dimple diameter, coordinate $y/D = 0$ corresponds to the central line after the second row holes, $y/D = 1,0$ is the central line after the first row holes.

The following conclusions can be extracted from the obtained data. The best agreement with the experimental results provides the classic $k - \omega$ - model and Menter's SST- turbulence model. In the range of $x/d = 2,5...25$ the maximal deviation of the predicted local adiabatic film cooling

efficiency from experimental data for these two turbulence models does not exceed 5…10%. As can be seen from Fig. 2, 3 the most deviation from experimental data provides *k-e* and *RNG k-e* turbulence models.
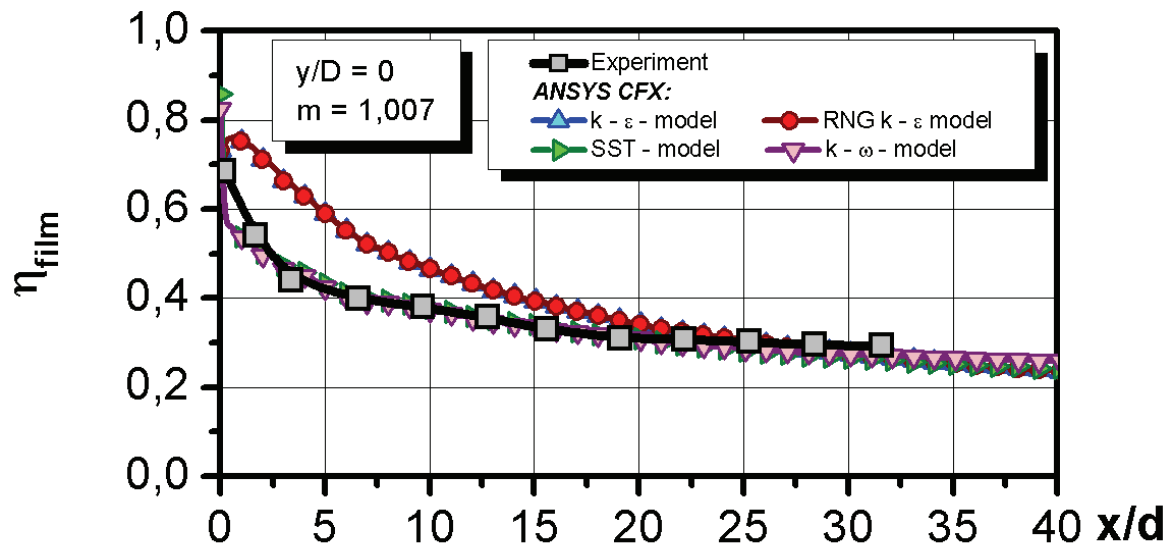

Fig. 2 Dependences of film cooling adiabatic efficiency local values from the relative distance for central line after the second row of holes.
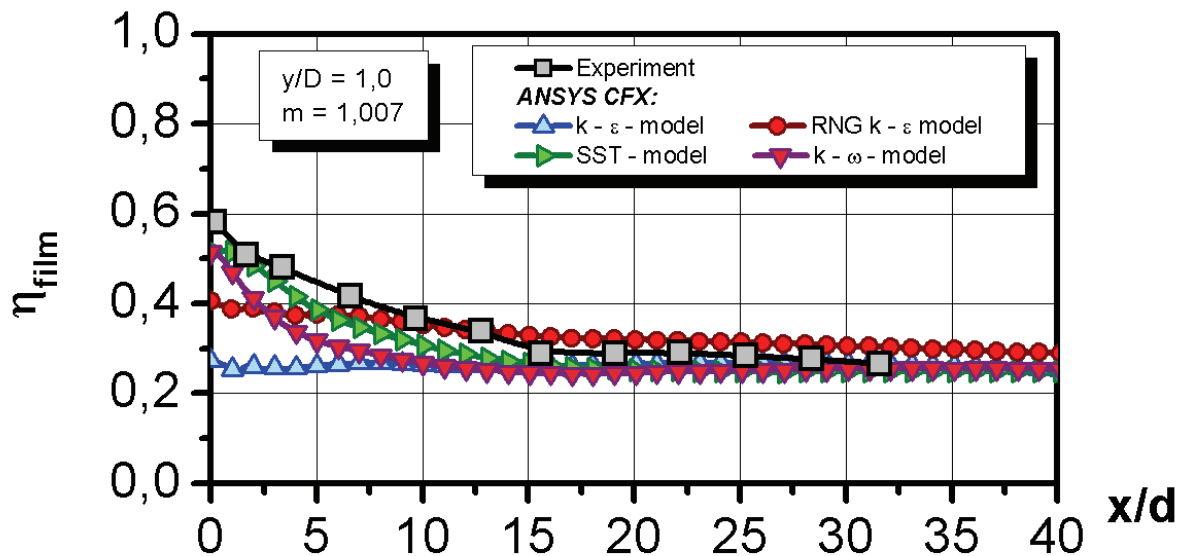

Fig. 3 Dependences of film cooling adiabatic efficiency local values versus relative distance for central line after the first row of holes.

Thus, for the further calculations the SST – model of the *k-ω* group can be used as the basic turbulence model, which uses the same as *k - ω* – model the near wall automatic adaptation. The selection of SST - turbulence model was also based as this model takes into account the share stress transport and, as experimental data show, provides more precise prediction of jet and separated flows. For all calculations carried out the near wall computational grid adaptation provided $y^+ < 2$ condition.

Averaged film cooling adiabatic effectiveness

On the Fig. 4 the laterally averaged adiabatic film cooling effectiveness as a function of the relative axial distance is given for different blowing ratios. The experimental data for the blowing ratio $m = 2,0$ is given here for comparisons.
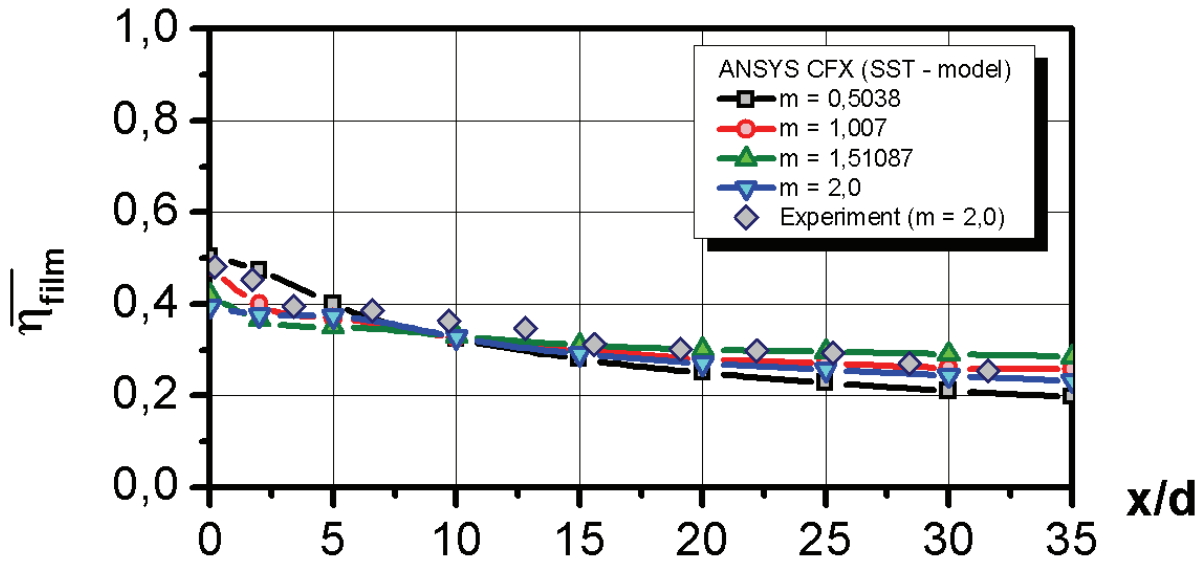

Fig. 4 Laterally averaged adiabatic film cooling effectiveness versus relative axial distance for different blowing ratios.
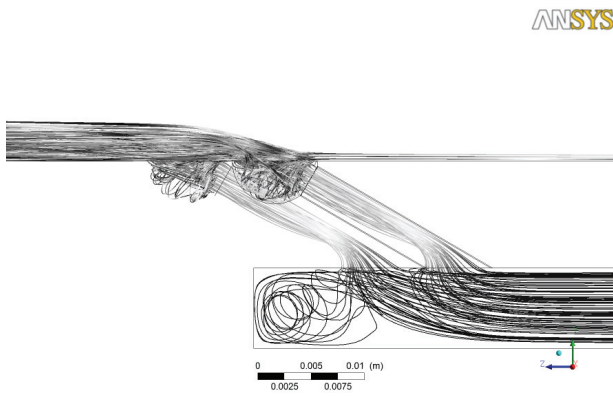

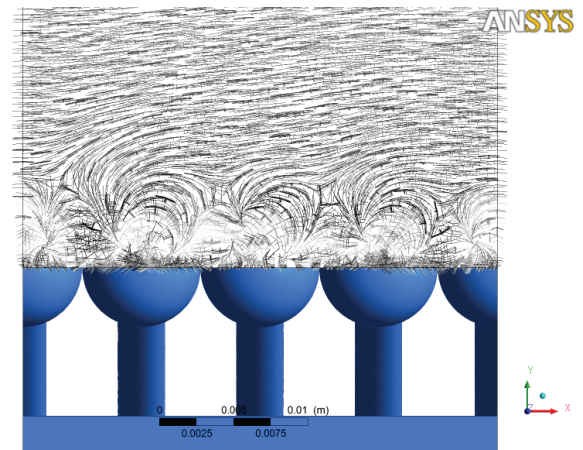Fig.5 The flow structure in spherical dimples (m=1,007).

Fig. 6 Vortex structure upstream of spherical dimples.

As can be seen from Fig. 4 the numerical results on the averaged adiabatic film cooling effectiveness, obtained with using of SST turbulence model, demonstrate good agreement with experimental data. As follows from this figure for two rows configuration with coolant injection into spherical dimples, the film cooling effectiveness depend weakly from the blowing ratio. At $x/d > 20$ the blowing ratio actually does not influence on the film cooling effectiveness.

Such a character of $\overline{\eta}_{film} = f(x/d, m)$ behavior can be explained by two basic physical reasons. First reason is that due to the jet flow in dimple the preliminary expansion effect occurs at the holes outlet. Second reason is formation of low pressure areas in the vortex kernels, appearing in the dimple under coming out jet (Fig. 5) preventing jets separation from the cooled flat plate

surface. Such a situation is different to the case of standard two rows cooling configuration with coolant injection through the inclined holes at great blowing ratios.

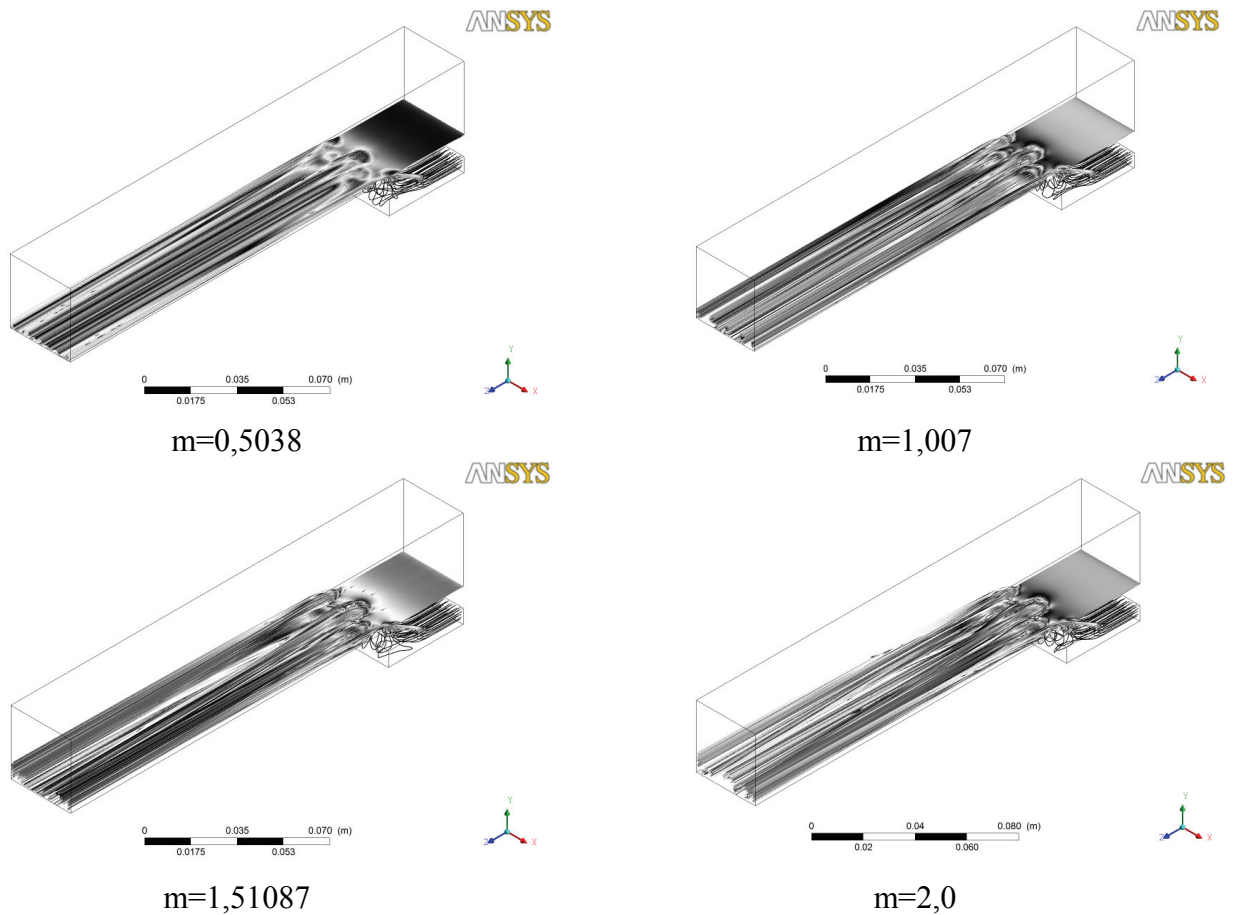
m=0,5038

m=1,007

m=1,51087

m=2,0

Fig. 7 Streamlines on flat plate with coolant blowing through two rows of holes into spherical dimples.

At the same time, in-dimple low pressure area, caused by vortex formation under the coolant jet, leads to the mixing of hot gas transported from the boundary layer and coolant in dimple (it is clearly seen from Fig. 4) resulting in some decrease of the adiabatic film cooling effectiveness on the initial area at the increase of blowing ratio, but does not influence on the film cooling effectiveness on a main area for the wide range of blowing ratio.

As CFD-modeling shows, the coolant blowing into spherical dimple does not destroy «kidney» vortices at the dimple outlet (Fig. 6). Their intensity increases with the blowing ratio growth, however interaction of jets from the first and second rows destroys their classic pair structure. As can be seen from Fig. 7 the increase in blowing ratio leads to the growth of the first and second row jet interactions and their decline from plate axis. Jets mutual interaction and jets interaction with the main flow leads to formation of complicated twisted structures and irregularity in film cooling effectiveness field. This effect is not predictable in cases of using *k-e* group of turbulence models.

In Fig. 8 the comparison of the laterally averaged film cooling adiabatic effectiveness for two considered film cooling configuration is given. As seen from Fig. 8, in the range of blowing ratio studied the film cooling configuration with coolant blowing spherical dimple demonstrates higher averaged film cooling effectiveness, namely in 2…2,2 times at $0<x/d< 10$, and in 1,5…1,7 times at $x/d >10$.
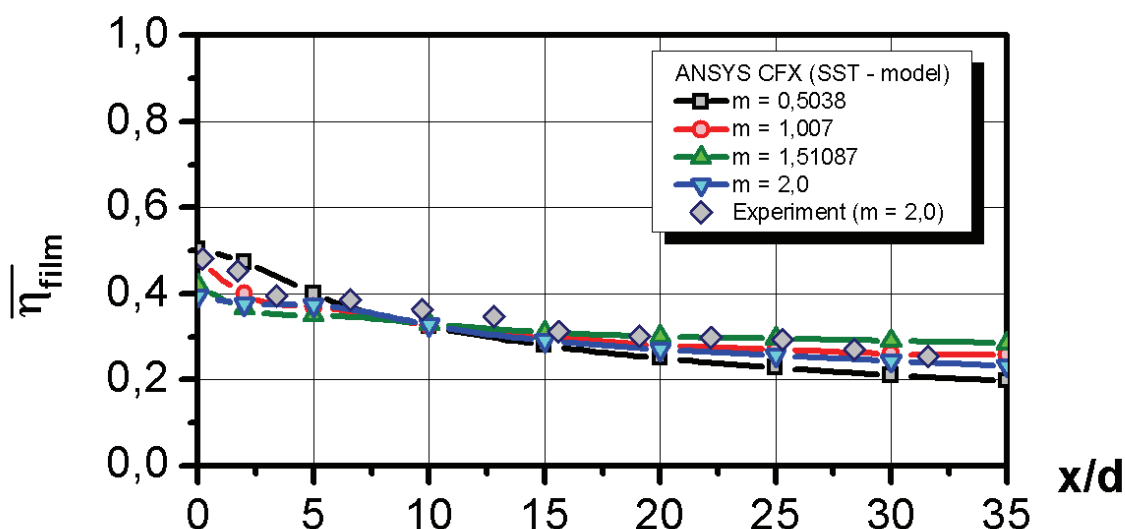
Fig. 8 Comparison of the laterally averaged adiabatic film cooling
effectiveness for two studied film cooling configurations.

Conclusions

1. The commercial CFD package ANSYS CFX was successfully used at the modeling of flow and film cooling effectiveness of two configurations with coolant blowing into surface dimple (one and tow rows). The numeral results of the film cooling effectiveness prediction well agrees with experimental data when using the classic k - ω - model and Menter's SST- turbulence model.

2. Results of numeral modeling confirmed basic conclusions from experimental studies regarding application of two rows of in-dimple film cooling systems for gas turbines blade cooling.

3. In the range of blowing ratio $0,5 < m < 2,0$ two rows film cooling system with coolant blowing into the spherical dimple provides the averaged film cooling effectiveness that is $1, 5…2,2$ times greater of that for the standard film cooling configuration.

References

1. *Repukhov V.M.* "Theory of wall thermal defense by gas injection". - Kiev: Naukova dumka, 1980. - 296 p.

2. *Khalatov A.A., Borisov I.I., Kovalenko A.S., Dashevskiy U.Y., Severin S.D., Shevtsov S.V., Bezlyudnaya M.V.* "T*he flat plate film cooling by double-row holes system in the spherical dimples". - East-European Journal of Advance Technologies., №3/10 (57) 2012. - 4-8 p.

T. Donyk, Post graduate (Institute of Engineering Thermophysics, NAS, Ukraine),
A. Zinchenko, Research engineer (LTD of GK of «Tekhinservis», Ukraine),
A. Khalatov, Academician of NASU, Dr.Sci.
(Institute of Engineering Thermophysics, NAS, Ukraine)

THE NUMERAL SIMULATION OF AN AIR FLOW STRUCTURE WITH PARTIAL SWIRL

The numeral simulation of an air flow structure in tube with partial flow swirl has been carried out. The flow swirl angle near the tube wall changed from 30° to 45°. The new calculated data have been obtained characterizing the swirling flow vortex structure.

Introduction

The problem of heat transfer enhancement in channels attracts attention of researchers and engineers aimed to develop new energy and power systems, intensive technological equipment, industrial heat exchangers, heat recuperators and chemical reactors.

Currently, to enhance internal heat transfer various methods are employed including the flow swirl, flow turbulization, surface ribbing, pimples and dimples of different shape, channel shape variation in the axial direction, and some other methods [1, 2]. One of effective and simple methods of heat transfer enhancement is the flow swirl, in particular the partial flow swirl. Such a swirl generators are simpler in production, they demonstrate the self-cleaning feature from industrial contaminations, provide a wide heat transfer variation at the constant flow rate due to partial flow swirl.

In paper [3] the cruciform insert with bendable petals (Fig. 1) is considered due to those the partial flow swirl is generated, while results of heat transfer and pressure drop studies are presented in [3]. The present paper goal is to study numerically in-tube flow structure using such a swirl generator. The ANSYS CFX 14 commercial package was employed in all calculations..

A computer design was started with design of calculation area geometry which is the cylinder with a diameter of 69 mm and length of 380 mm, as well as cruciform insert with bendable petals. The basic dimensions are as follows: $l = 380$ mm; $d = 69$ mm; $a = 10$ mm; $b = 30$ mm; $\varphi = 30°$, $35°$ and $45°$ (Fig. 1). For this insert the designed flow swirl angle φ is $33°$ [4].
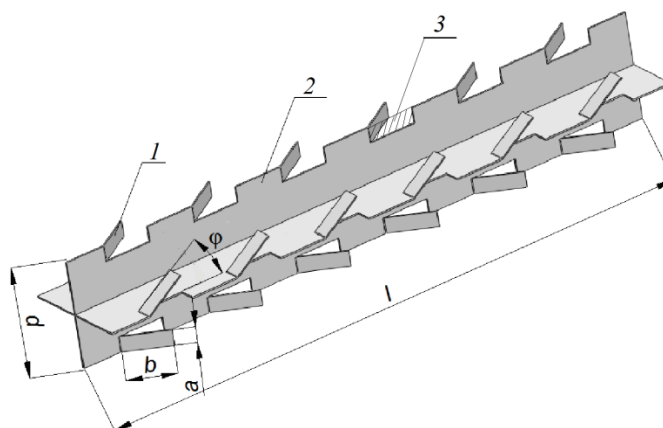

Fig. 1 – Cruciform insert with partial flow swirl.

The digitization of computational area was made using the built-in grid editor ANSYS ICEM CFX. The tetrahedron elements were used at the grid development. The prismatic elements were used on the channel wall providing more exact description of the boundary layer hydrodynamics. The thermophysical air properties were set by means of the empiric correlations in the pre-processor

ANSYS CFX. The boundary conditions are as follows: the constant velocity at the inlet, atmospheric pressure at the outlet, adiabatic channel wall.

The time of one test calculation took about 3 hours, while basic calculation took about 8 hours. The calculations were stopped when the difference between two iterations did not exceed 10^{-4}.

The test calculations were conducted at the Reynolds numbers Re_d of 30000; 74000; 101000; 175000 using four different turbulence models, namely k-ε, k-ω, RNG k-ε, SST k-ω models. The results obtained have shown the velocity profile is not developed within the tube. Based on these the pressure losses in tube and the hydraulic resistance coefficient were determined from Darsi correlation:

$$ f = \frac{\Delta P}{\dfrac{l}{d}\dfrac{\rho w^2}{2}} $$

Here: ΔP is the pressure losses, Pa; l, d is the tube length and internal diameter, m; ρ is the air density, kg/m^3; w is the average flow velocity, m/s. The results of calculations showed that exact prediction of axial in-tube flow demonstrates the k-ε turbulence model, providing the deviation from the basic correlation for the un-developed turbulent not more than 4%.

The basic calculations were further conducted, using the same procedure of calculated data processing. The Fig. 2 shows dependence of the averaged pressure drop coefficient from the Reynolds number for four turbulence models (k-ε, k-ω, RNG k-ε, SST k-ω) and three swirl angles (φ = 30°, 35°, 45°).
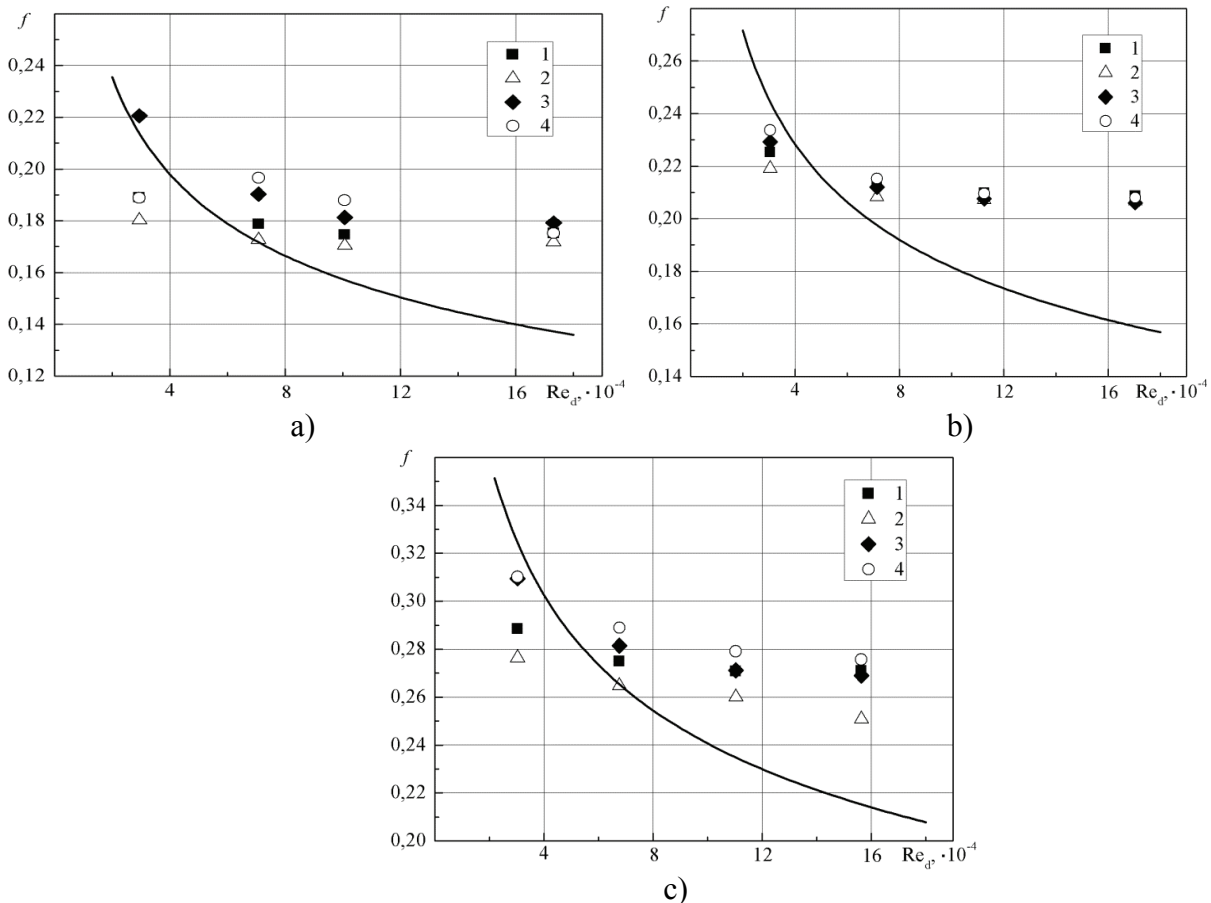
Fig. 2 − Pressure drop at φ = 30° (a), φ = 35° (b) and φ=45° (c); Line 1 is the experimental data for φ = 30°, φ = 35° and φ = 45° accordingly [3]; Turbulent model: 1 – k-ε; 2 − k-ω; 3 − RNG k-ε; 4 − SST k-ω.

As follows from these figures, with growth of Reynolds number the pressure drop coefficient falls down, but in the computer modeling this falling down is not such a rapid, as in experiments.

Moreover, for the swirl generator φ =35° and RNG model, the constant behavior of the pressure drop coefficient is occurred. For the swirl generator φ = 35° the small difference between calculated data are occurred for the Reynolds number range from 60000 to 160000. The general error of computer modeling data is within 20%.

From all turbulence models studied, the SST model is most exactly describes swirling flow at various flow swirl angles. Therefore, for further basic calculations the SST turbulence model was employed in the range of Reynolds number from $3 \cdot 10^4$ to 10^5. The results of calculations made for the SST turbulence model are given in Fig. 3.
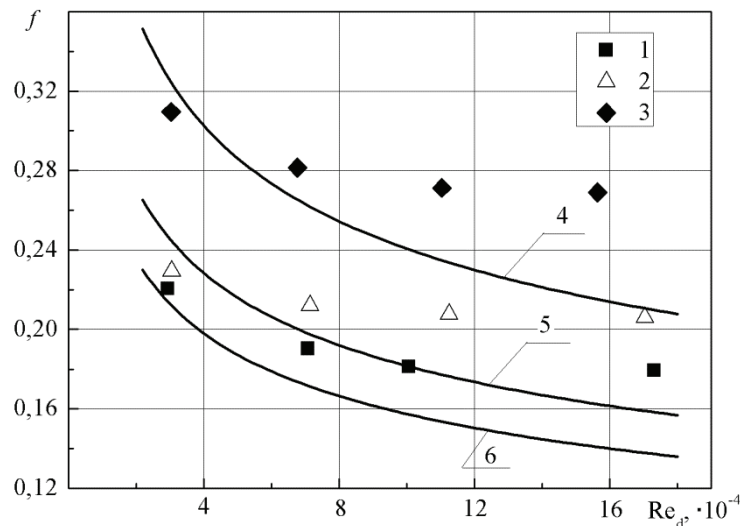

Fig. 3 − In-tube pressure drop; the SST turbulence model: 1, 2, 3 – computer modeling, φ = 30°, φ=35° and φ=45° accordingly; 6, 5, 4 − experimental data, φ = 30°, φ = 35°and φ = 45° accordingly [3].

As seen from this figure the SST turbulence model provides the minimum deviation from the experimental data (up to 5%) at Reynolds number $Re_d = 5 \cdot 10^4$.

Flow structure.

The in-tube air swirl flow with partial swirl has a complex three-dimensional structure. It can be divided as an axial flow (r from 0 mm to 24,5 mm) and flow near the wall (r from 24,5 mm to 34,5 mm). As follows from Fig. 4 for this swirl generator the set of discrete rectangular shape are formed near the tube surface. At φ = 35° (Fig. 4, b) the air comes out from the rib rectangular hole and gets into the hole of adjacent rib, thus providing swirl generator design conditions (φ =33°). At φ = 30° the air jet from the rib hole does not exactly get into adjacent rib hole, it strikes against the adjacent rib surface, slides over it and then gets into the rib hole. This flow type can be characterized as the «un-swirl» flow mode. If the swirl angle increases to 45° the «over-swirl» mode can be occurred when the part of jet strikes against the rib surface, reflects of it to generate the complex vortical structure.

The in-tube distribution of total velocity streamlines at the non-dimensional distance *x/d* of 2,3 is given in Fig. 5 for all swirl generators studied (φ = 30°, 35°, 45°). As seen, zones of increased velocity are formed near the tube surface, while immediately beyond the rectangular hole of swirl generator the large-scale secondary flows of different shape and configuration are seen, the intensity of which depends on the swirl flow angle. Both factors lead to the heat transfer augmentation.
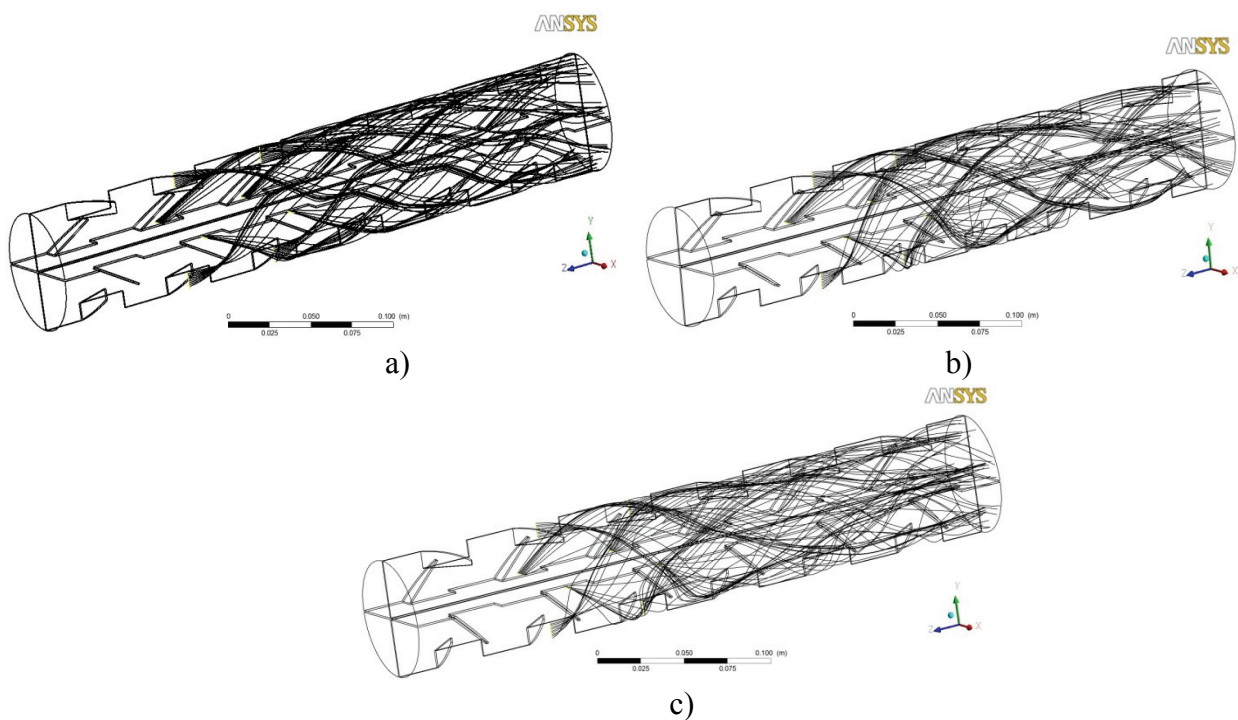
Fig. 4 − Total velocity steam-lines over the tube surface:
a − φ = 30°; b − φ = 35°; c − φ = 45°
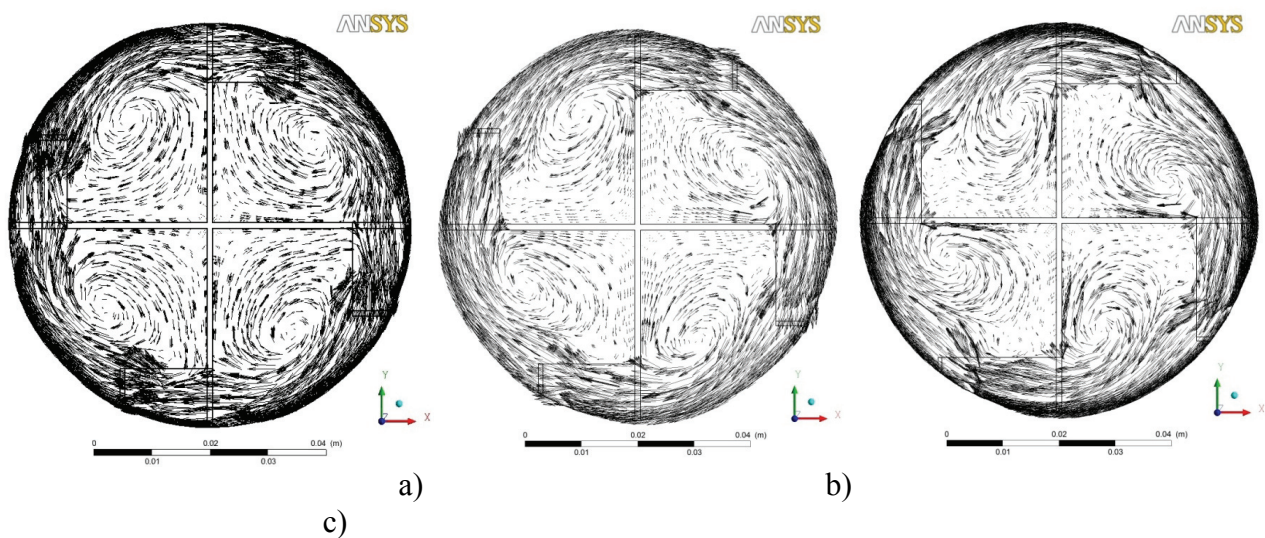
Fig. 5 − The total velocity distribution at the distance *x/d* of *2,3:* a − φ = 30°; b − φ = 35°; c −
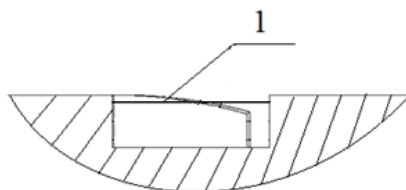φ = 45°.

Fig. 6 − Determination of averaged velocity in the swirl generator hole: 1 − the line of average.
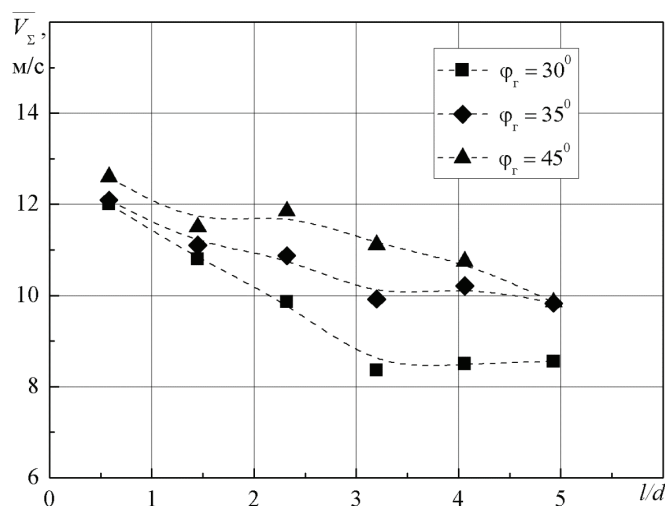
Fig. 7 − Averaged total velocity in the swirl generator hole.

For the quantitative analysis of the flow structure the graphs of total velocity in the swirl generator hole were constructed. The average velocity in each hole was determined on the line located on the distance of 1,5 mm from the tube surface (Fig. 6). This operation was realized in the post-processor of ANSYS CFX package, where the number of points taken for the velocity average was specified (100 points).

Results of the averaged velocity in the opens of swirl generator for three swirl flow angles (φ = 30°, 35°, 45°) are presented in Fig. 7. As seen, the total velocity in the swirl generator holes reduces along the tube axial distance moreover this velocity grows with the swirl flow angle elevation.

The total velocity change over the β angle characterizes the flow non-uniformity rate in the swirl generator hole. For this purpose the axially averaged velocity was determined for different β angles, located at the distance of 1,5 mm from the tube surface. The results of calculations are given in Fig. 9. As it can be seen from Fig. 9 the total velocity increase occurs in the space between swirl generator ribs with a further insignificant reduction. For all swirl generator studied the total velocity at the inlet hole (β = 75°) is 10…15% greater than that at the outlet hole (β = 15°). As follows, for all swirl generators in the area β from 15 to 30° the average total velocity is actually identical, while at β>30° the velocity grows with swirl angle elevation. For β >75° in front of the swirl generator inlet the tendency of velocity alignment can be seen. For all swirl generators tested the maximal total velocity magnitude is occurred in the area β from 45 to 55°.
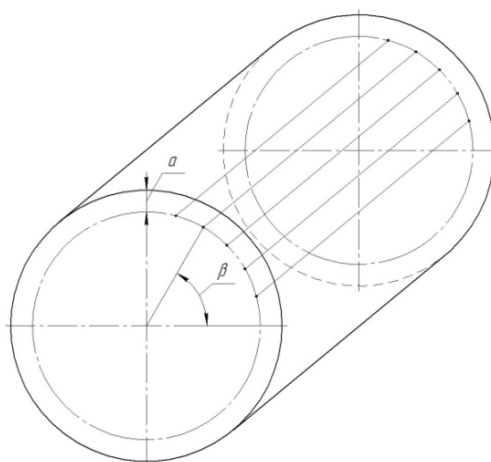

Fig. 8 − Specification of the β angle: a − distance from the wall;
β − angle between tube radius and the circle axis.
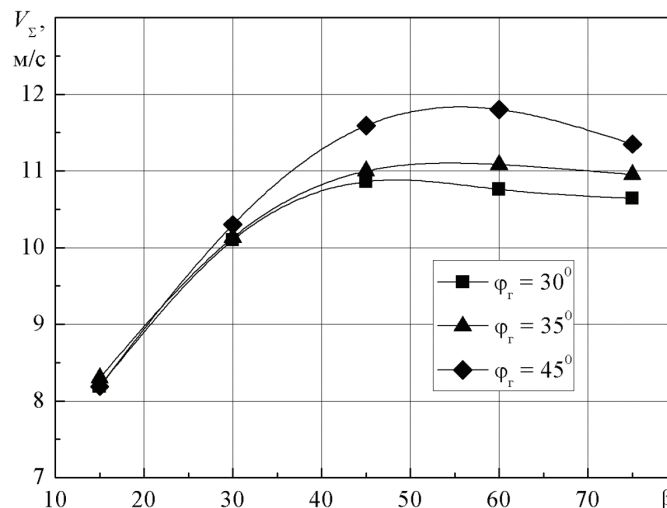
Fig. 9 − Change of the average total velocity in the tube space
between adjacent swirl generator ribs (a = 1,5мм)

Conclusions

1. The computer model of the partial flow swirl generator has been developed and comprehensively tested. As found, at Re_d = 50000 the SST turbulence model provides the best results compared with experimental data.

2. The calculations has shown at φ = 30° the «un-swirl» flow scheme occurs with flow sliding over the swirl generator rib. At φ = 35° all jets come through swirl generator holes, i. g. corresponding to the designed swirl angle φ of 33°. At φ = 45° there is the «over-swirl» flow mode with flow impingement over the rib surface and separated flow appearance.

3. The averaged total flow velocity in holes of swirl generator reduces along the axial distance, but grows with φ angle increase. At β = 15…30° and at $\beta \rightarrow$90° the total flow velocity is actually identical for all swirl generators tested. At the swirl generator hole inlet (β=75°) the total flow velocity is around 10...15% greater than that at the hole outlet (β=15°).

References

1. *Isachenko V., Osipova V., Sukomel A.* «Heat-transfer».– M.: Energy, 1975. – 488 p.

2. *Kalinin E., Dreycer A., Yarkho S.* «Intensification of heat exchange is in channels».– M.: Engineer, 1972. – 220 p.

3. *Donyk T., Khalatov A.* «Heat transfer and hydraulic resistance in a tube with a cruciform insert and partial flow swirl».– Industrial Heating Engineering. Vol. 34, №2, – 2012., P. 28-32.

4. *Donyk T., Khalatov A. Patent* of Ukraine №68122 «Device for heat transfer enhancement» 12.03.2012.

UDC 532.526.4

S.A. Isaev, Dr.Sci. (Saint-Petersburg State University of Civil Aviation, Russia),
G.A. Voropaiev, Dr.Sci. (Institute of Hydromechanics, NAS, Ukraine),
V.T. Movchan, Dr.Sci., E.A. Shkvar, Dr.Sci. (National Aviation University, Ukraine)

MATHEMATICAL MODELING OF TURBULENT VORTICAL FLOWS – THE FUNDAMENTAL DIRECTION OF MODERN FLUID DYNAMICS: DIFFERENT APPROACHES, PROBLEMS, OUTCOMES AND PERSPECTIVES

The advantages and weak sides of different levels of basic approaches for wall turbulent shear flows mathematical modeling have been analyzed. The principles of turbulence modeling, based on the understanding the necessity and importance to account the vortical dynamics phenomena, have been worked out. The further actual directions of elaborating the methods of turbulent structure analysis and the basic requirements for constructing the corresponding mathematical models are determined.

In flow of air or liquid near the solid on its surface a thin boundary layer with significant gradients of basic parameters is forming. The aero- or hydrodynamic drag of the body is significantly determined by the type and structure of this boundary layer (laminar, turbulent or transitional). The disturbances, generated in the boundary layer by different nature factors (internal instability of fluid flow, local inhomogeneities of a surface, the effect of mass forces, external disturbances etc.), lead to the development of both coherent and stochastic vortical structures, if their intensity exceeds a certain stability threshold under the given fluid flow conditions. As a result, these structures change the distribution of energy in the boundary layer and affect the integral characteristics of the flow near the streamlined surface. It is important to investigate whether the number, scale and intensity of the coherent structures are independent or how they are dependent on the parameters of the disturbing factors. The development of small disturbances in the initial stage determines not only the transition zone in the boundary layer, but also the structure of finite disturbances in the final stage of transition and the initial structure of the turbulent boundary layer.

The present report deals with the modeling of a turbulent boundary layer developing with the accounting the influence of significant spatial structuring of quasi-periodic vortical structures and nonlinearity of the physical processes of energy exchange between the components of the Reynolds stress tensor. So, the Reynolds stress transport model was taken as the basis of mathematical modeling. Therefore, as a first step of the closure hypotheses, formulating at low Reynolds numbers up to 10^4, the analysis of the vortical structures formation has been made with the use of solutions of the fully unsteady Navier-Stokes equations. On the base of information about the structure of the vortical flow for specific flows (temporal and spatial scales, intensity) in modeling the mechanisms of generation, dissipation, turbulent diffusion, energy redistribution among the components of the stress tensor the scales of coherent structures and their local energy capacity in comparison with the amount of Reynolds stresses tensor components were taken into account [1-4]. In case of the Reynolds number increasing this ideology can be extrapolated to arbitrary Reynolds numbers, but as a first step, the unsteady Reynolds equations must be solved with a standard form of closure hypotheses (for complex flow fields with the use of flow geometry). The second step of modeling suggests making the changes in the hypothesis depending on the parameters of the local vortical structures.

This approach differs from the LES technology because the energy transfer between structures of various sizes doesn't conserve itself on a fixed grid and allow the following iterations for closure hypotheses modification. In frames of this method the direct numerical simulation of the formation and development of vortical structures in the wall flows under the simultaneous action of distributed mass forces and local inhomogeneities (geometric, temperature) is elaborating on the base of solving the full unsteady Navier-Stokes and unsteady Reynolds equations for stage of the turbulent flow regime development.

The study of peculiarities of formation of the flow structure in boundary layers under certain conditions and factors, allows to evaluate their effect on the integral characteristics of boundary layers

for different flow regimes and identify those of them, that can be used to control the structure of the layer in the required directions, that is, for hydrodynamic drag reduction, lift increasing, heat exchange intensification in the vicinity of the surface.

The next section of the report is dedicated to turbulence models improving in close connection with the development of numerical simulation technique. Despite the actualizing the models of large and detached eddies simulation as well as considerable interest in the world to the direct numerical simulation, fueled by advances in computer multiprocessor systems, it is shown that the Reynolds approach, based on the concept of eddy viscosity, successfully applied by Prandtl to interpret the turbulent boundary layer, still works well and has significant resources for development. Attention also focuses on the computational side of this outstanding physical problem, closely connected with the development of methods of applied mathematics, implemented in tools of primarily engineering analysis – packaging technologies.

The base of Reynolds approach is the averaging in time scales the Navier-Stokes equations, describing the instantaneous flow characteristics, and further obtaining the generalized transport equation for the mean flow, which is not closed, since it includes so-called tensor of Reynolds stresses, recorded with respect to fluctuating velocity components. Dissatisfaction with this approach is associated with the inability to reflect on its base the real time-dependent nature of turbulence, in contrast to large-eddy simulation, creating largely illusory prediction of this complicated physical process. At the same time, measurements of integral and local characteristics which are traditionally used to verify the numerical predictions, in principle, carried out by averaging their measuring instruments. It should also be accounted that computational methods, numerical discretization of the process being modeled and numerical implementation on computers bring to the obtained results not only quantitative errors similar to measurement, but also the systematic errors associated with the artificially imposed "scheme" mechanisms.

The problem of the Reynolds equations closure is solved on different levels of complexity of constructing models of turbulence, representing the algebraic relations for the eddy viscosity (for one- and two-parametric models), balance differential equation for modeled characteristics of turbulence and, in general case, for the Reynolds stresses tensor components, together with empirical constants, selected on the base of special experimental and numerical testing. Such models although are built for fairly wide classes of problems, but, obviously, do not cover all kinds of physical processes. Thus, it does not make sense to design a universal turbulence models. At the same time, a certain freewill in assigning the empirical constants, associated with the existence of ranges of their variation (by the way, quite narrow) and arising from the physical model situations, should not create the illusion of their unreasonableness and possible adjustment with the particular experiment for the best agreement between predictions with measured data. The necessity for revision of the constants actually cancels out the applied semi-empirical model and in this case we have to work, in fact, with the new model, for which we need to perform an extensive verification study. On the other side, it does not mean that we cannot modify the semi-empirical models. For example, it is known that the current models (Menter and Spalart-Allmaras) in their standard form cannot be used for calculation of separated flows, because they lead to the generation of false eddy viscosity inside vortex cores. In particular, this circumstance initiates the necessity of introducing the corrections for the streamlines curvature and rotation, promoting the correct modeling of large-scale vortical structures [5].

As already noted, the numerical solution of Reynolds equations and the closing them differential equations of the chosen turbulence model, it is important to take into account the "scheme" errors, associated with equation terms approximation, grid choice, including the shape and sizes of cells. At the present time the discretization schemes of order below then the 2-nd are not in use, but at the same time the grids are rather rude and aren't able to reflect the hydrodynamic peculiarities of small scales. Usually, the well-known requirement for dimensionless according to wall scaling normal to streamlined surface coordinate y^+ ($y^+ = y\upsilon_* / \nu$, $\upsilon_* = \sqrt{\tau_w / \rho}$ – shear velocity, ν – kinematic viscosity coefficient, τ_w – wall shear stress, ρ – density) is satisfied near the wall, but the presence of high-gradient zones outside the walls that need to be resolved on the grid at the appropriate scale is

unreasonably ignored. On the other side, it is wrongly assume that the total reduction of grid cells sizes is able to save the situation. In addition, unstructured grids, commonly used in engineering calculations, produce difficulties on the way of achieving the accurate solution. Alternative way is to apply the multi-block different scales grids with overlap [1, 5]. They allow not only solve problems in multilinked domains on grids with simple topology, close to orthogonal, but tune them for the hydrodynamic characteristics scales capturing and the high-gradient zones resolving of flow with high eddy viscosity.

Testing of turbulence models is carried out after their tuning on a set of testing cases, and the expansion of the range of tasks and their complexity increases their acceptability and level of confidence to them. In general, the testing tasks are different by dimensionality, complexity of geometry, necessity of taking into account in addition to turbulence some other mechanisms, such as compressibility effects, physical heterogeneity of moving media, scaling factor. There are classical two-dimensional problems, such as the circulating flow in a cavity with a movable cover, flow in the turning channel, facing and backward facing steps channel flows, diffuser channel flow, flow around a circular cylinder etc. There is a significant database of calculations obtained by different methods, packages on the base of different semi-empirical models in corresponding scientific literature. Some data about these classical testing cases are collected in the library of European Research Community On Flow, Turbulence and Combustion – ERCOFTAC. Also a significant amount of material on three-dimensional problems is accumulated, for example, about the modeling of flow around a cube inside a narrow channel (Martinuzzi experiment, 1992). There was a tendency to test models, based on calculations of full-scale aero- and hydrodynamical testing stands, beginning from pre-combustion chamber and considering the further flow development inside the flow path, including the nozzle block and output of the working part with located testing streamlined body. Fig. 1 represents the computing analog (*b*) of wind tunnel at the Italian Aerospace Research Center – CIRA (*a*). Illustration Fig. 1 (*c*) shows the results of comparison of the pressure coefficient distributions along the testing airfoil obtained experimentally and predicted numerically with taking into account the streamlines curvature effect in frames of the Shear Stress Transport (SST) Menter's model of turbulence.
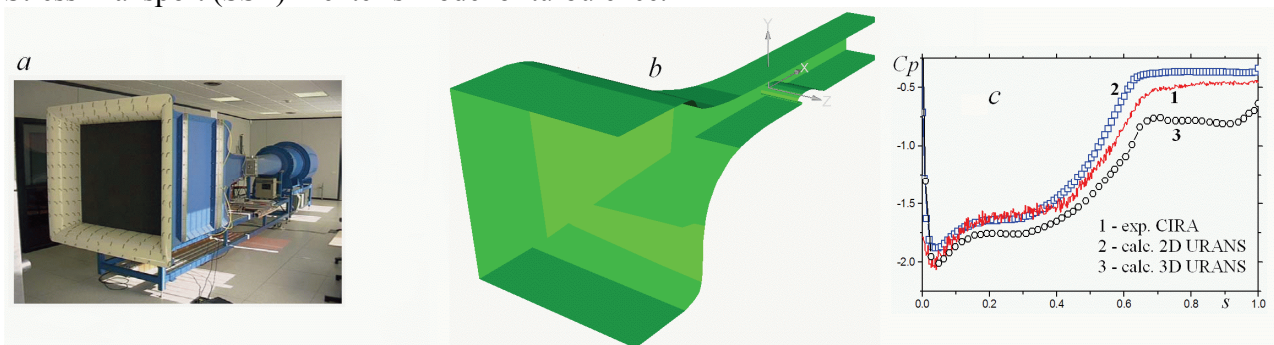

Fig. 1. Wind tunnel at the CIRA (*a*), its computing analog (*b*) and comparison of experimental and calculated distributions of C_P along the contour of the airfoil (*c*)

Another perspective direction in shear flow modeling, based on the Reynolds approach, is connected with the idea to combine several different types of turbulence model in frames of hybrid one with more universal possibilities than each of its elements. This idea corresponds to well-known zonal method and it allows using effectively advantages and minimizing weaknesses of the model components due to their local application. By the way, this approach can be tuned and improved like considered earlier other models depending on required set of modeling conditions, prevailing flow properties and, in particular, in case of necessity, it is possible to introduce the mentioned above corrections for the streamlines curvature, rotation etc. In addition to this the hybrid models of turbulence can be more flexible and adaptive in comparison with traditional clearly algebraic or differential models in case of their application to different problems of flow control and, in particular, to drag reduction problems. It is important to note the fact of very important advantage, connected with ability of hybrid models to simulate effectively different combined schemes of drag reduction, directed simultaneously on different scales of vortical structure of turbulence. Here we represent one of possible realizations of this approach [6-11], based on the well-known fact of a good level of relevance of algebraic models for

descripting the small-scale turbulence properties in the inner region of boundary layer and qualitative enough possibilities of differential models and, in particular, $k - \varepsilon$ one to predict the inertial dynamics of large-scale vortical structures in the outer region.

The developed method is based on the Reynolds equations together with the following turbulence model:

$$\nu_t = \nu_{t\,wake} \tanh \frac{\nu_{t\,wall}}{\nu_{t\,wake}}, \qquad \nu_{t\,wall} = \chi y \upsilon_* \sqrt{\tau} D_m,$$

$$D_m = \tanh \frac{\sinh^2 (\varkappa_1 y_1^+ \sqrt{\phi}) \tanh [\sinh^2 (\varkappa_2 y_1^+ \sqrt{\phi})]}{\chi y_1^+ \sqrt{\phi}}, \qquad \nu_{t\,wake} = C_\mu \frac{k^2}{\varepsilon},$$

where χ, χ_1, χ_2, C_μ – model coefficients. The proposed model has a hybrid structure. Its internal part $\nu_{t\,wall}$ is an algebraic representation of a turbulent viscosity, developed by Movchan [10] and the outer part $\nu_{t\,wake}$ is a traditional Jones-Launder $k - \varepsilon$ model in its standard high-Reynolds-number form. The algebraic approach is well-adjusted for description of small-scale turbulence structure in the vicinity of a wall. Besides, it was expanded for the cases of accounting the effects of surface relief and polymer injection in the near-wall region due to introducing the shifting functions $\varDelta y_{rel}^+$ [6, 7] and $\varDelta y_{pol}^+$ [8] of semi-empirical nature, so $y_1^+ = y^+ + \varDelta y_{rel}^+ + \varDelta y_{pol}^+$. These functions reflect a well-known effect of a shift the logarithmic part of a wall law scaled velocity profile in a semi-logarithmic representation $u^+ = f(y^+)$ on some value $\varDelta u^+$ up or down depending on presence of polymer additive solutions or surface relief influence respectively. There are many sources of experimental data, establishing the dependencies between $\varDelta u^+$ and parameters of surface relief or polymer additives. The advantage of the proposed approach is possibility to connect $\varDelta u^+$ with $\varDelta y^+$ analytically. In particular, for a surface with riblets and in case of near-wall polymeric injection the following dependence can be applied $\varDelta y^+ = \chi_1^{-1} \text{th} (\chi_1 \varDelta u^+)$. Due to the additive property of shifting functions $\varDelta y_{rel}^+$, $\varDelta y_{pol}^+$, and a structure of a model form of a turbulent viscosity for the inner region, it allows to account effectively in calculations the data, obtained experimentally for any special type of a surface relief or polymeric solution injection both separately and in any combinations. On the other side, in the outer region the two-equation differential $k - \varepsilon$ turbulence model is used. It describes well the different aspects of evolution of large-scale turbulent vortical structures. In particular, this model has been successfully applied for prediction of Large Eddy Breakup devices (LEBU) effect [9]. That is why the $k - \varepsilon$ model is more adopted for turbulence description in the outer region versus algebraic model. Nevertheless, it is not physically valid near the wall, but this disadvantage is effectively eliminated by the structure of the proposed approach, namely, the algebraic model works near the wall as a damping function for a differential component of constructing model. Different application of this model for predicted the characteristics of turbulent boundary layers, modified by different near-wall flow control methods like polymer injection, longitudinal and lateral surface riffling, wall jets, LEBU both in single use and in different combinations can be found in [6-10]. In addition to this it is important to note the successful applicability of the developed model, used in generalized form in frames of algebraic Reynolds stress model for predicting the vortical structure of secondary flow inside streamlined corner [11], which is one of traditional classical space configurations for turbulence models testing.

Conclusions and perspectives

1. Perspectives of turbulence development models are connected, first of all, with the account of the laminar-turbulent transition, and expanding the models, built on the describing the typical steady flows, for essentially unsteady periodic flow. In many cases the prevalent prejudices against Reynolds' approach are associated with the unjustified use of two-dimensional models. Thus, a well-known problem of reflecting the velocity defect in the wake behind the body is one of illustrative examples.

There is no doubt that some problems can be successfully removed in frames of the correct formulation of spatial tasks.

2. The proposed variant of turbulence model with the hybrid algebraically-differential structure is developed for flexible accounting the turbulent boundary layer control methods, oriented on different scales of turbulent vortical structures in single and combined forms. The structural model elements are effective locally in the regions, where they have the greatest level of physical correctness and ability to describe an action of the considered flow control methods. The further perspectives of this turbulence model development will be connected with extending the number of flow control factors, which can be accounted, and searching some other more adoptive and more universal possibilities of linking the inner and outer model representations of the elaborated approach.

References

1. *Гринченко В.Т.* Управление ламинарным пограничным слоем вихрями, генерируемыми овальной лункой / В.Т. Гринченко, Г.А. Воропаев, С.А. Исаев, В.А. Воскобойник, А.А. Воскобойник, А.В. Воскобойник // Вісник Донецького національного університету. – Сер. А: Прир. науки. – 2009. – вип. 1. – С. 191-198.

2. *Воропаев Г.А.* Динамические и кинематические характеристики вязкоупругого слоя переменной толщины под действием импульсной нагрузки / Г.А. Воропаев, Я.В. Загуменный // Акустичний вісник – 2005. – Т. 8, N 4. – С. 29-37.

3. *Воропаев Г.А.* Турбулентный пограничный слой на деформирующейся поверхности / Г.А. Воропаев // Прикладна гідромеханіка. – 2005. – Т. 7, № 3-4. – С. 35-43.

4. *Воропаев Г.А.* Модель переноса напряжений рейнольдса для турбулентных течений слабоконцентрированных растворов полимеров / Г.А.Воропаев, Н.Ф.Димитриева // Вісник Донецького національного університету. – Сер. А: Прир. науки. – 2009. – вип. 2. – С. 89-95.

5. *Быстров Ю.А.* Численное моделирование вихревой интенсификации теплообмена в пакетах труб. / Ю.А. Быстров, С.А. Исаев, Н.А. Кудрявцев, А.И. Леонтьев // – СПб: Судостроение, 2005. – 398с.

6. *Шквар Є.О.* Фізичне та математичне моделювання напівобмежених турбулентних струменевих течій на оребрених поверхнях / Є.О. Шквар, Т.В. Козлова, А.О. Бондарець // "Промислова гідравліка і пневматика". – 2011. – №1 (31) – С. 35-41.

7. *Шквар Є.О.* Математичне моделювання турбулентних пристінних струменів на рифленій поверхні / Є.О. Шквар // Системи управління, навігації та зв'язку. – К.: ЦНДІНУ. – 2010. – Вип. 2 (14). – С. 152–157.

8. *Shkvar E.A.* Mathematical Simulation of the Admixture Transfer by Turbulent Boundary Layer / E.A. Shkvar // Int. J. of Fluid Mech. Research. – Vol. 29, Issue 6. – 2002. – P. 798–810).

9. *Корнилов В.И.* Моделирование турбулентных пограничных слоев на теле вращения при наличии разрушителей крупных вихрей / В.И. Корнилов, Е.А. Шквар // Теплофизика и аэромеханика. – Изд-во ИТТФ СО РАН №3. – 2010. – С. 335–348.

10. *Мовчан В.Т.* Різнорівневі математичні моделі коефіцієнта турбулентної в'язкості / В.Т. Мовчан, Є.О. Шквар // Прикл. гідромех. – К.: ІГМ. – 2010. – Т. 12 (84), №1. – С. 55–67.

11. *Шквар Є.О.* Математичне моделювання регулярних вихрових структур у кутових конфігураціях обтічних поверхонь / Є.О. Шквар // Наукоємні технології – 2011. – № 1-2 (9-10). – С. 106-110.

O.A. Prykhodko, Dr.Sci. (Dnepropetrovsk National University, Ukraine),
A.V. Sokhatsky, Dr.Sci. (Ukrainian Academy of Customs, Ukraine),
T.V. Kozlova,Cand.Sci. (National Aviation University, Ukraine)

NUMERICAL SIMULATION IN HIGH-SPEED GROUND VEHICLE AERODYNAMICS

HSGT aerodynamic characteristics are obtained on the base of numerical simulation. Computational techniques for magnetically levitated transport vehicles are developed on the base of Navier-Stokes equations. Aerodynamic analysis of an up-to-date HSGT configuration made it possible to propose the aircraft- type shape for designing the promising magnetically levitated transport vehicles.

Introduction

Technological and commercial success of the HSGT "MAGLEV" like most of aerospace systems greatly depends on successful aerodynamic configuration. Determination of the aerodynamic loads is a key moment at designing the HSGT, as at high speeds the overall power cost of order from 70% to 90% is necessary to overcome air drag. This in turn significantly influences the determination of linear driver, track structure and controlling equipment characteristics. Besides, it seems to be worthwhile to use aerodynamic forces for increasing the technical and economical performance of MAGLEV transport. One of the ways is to produce the additional lift force using the wing- type configuration of a car.

1. Methods of numerical simulation

Navier–Stokes equations. To obtain discrete analogues with the use of control volume method computational domain is divided into uncrossing cells. Nonstationary compressible gas Navier–Stokes equations are written in the vector integral form:

$$\frac{\partial \mathbf{q}}{\partial t} + \frac{1}{A}\oint_{\Omega} \left(\mathbf{F}\cdot\overline{\mathbf{n}} - \mathbf{F}_v\cdot\overline{\mathbf{n}} \right) d\Omega \;=\; 0 \;, \tag{1}$$

Here A is cell volume, Ω is surface area, $\mathbf{q}$ is vector of conservative variables, $\overline{\mathbf{F}}\cdot\overline{\mathbf{n}}$ is convective flux vectors and viscous flux vectors $\mathbf{F}_v\cdot\overline{\mathbf{n}}$ in the thin layer approximation have the form

$$\mathbf{q} = \begin{bmatrix} c \\ cu \\ cv \\ cw \\ e \end{bmatrix} \;,\quad \mathbf{F}\cdot\overline{\mathbf{n}} = \begin{bmatrix} cU \\ cUu + n_x p \\ cUv + n_y p \\ cUw + n_z p \\ (e+p)U \end{bmatrix},\quad \mathbf{F}_v\cdot\overline{\mathbf{n}} = \frac{1}{\mathrm{Re}} \begin{bmatrix} 0 \\ \mathrm{M}\left(u_n + \frac{1}{3}n_x U_n\right) \\ \mathrm{M}\left(v_n + \frac{1}{3}n_y U_n\right) \\ \mathrm{M}\left(w_n + \frac{1}{3}n_z U_n\right) \\ f_{5v} \end{bmatrix}.$$

with $f_{5v} = \frac{k}{\Pr(\Gamma-1)}\left(a^2\right)_n + \frac{\mathrm{M}}{2}\left(u^2+v^2+w^2\right)_n + \frac{\mathrm{M}}{3}UU_n;\quad U = n_x u + n_y v + n_z w$ – velocity in the direction to the external singular normal to the cell surface; $n_x,\ n_y,\ n_z$ – single vector components of external normal to the control volume face; $U_n = n_x u_n + n_y v_n + n_z w_n$.

Turbulence model. Mathematical simulation of turbulence remains one of the week fields in the present-day computational fluid dynamics, especially at the background of general progress in numerical methods, computer power, grid generation and flow visualization methods.

The cause/effect mechanism of turbulent instability still remains hypothetical. Turbulent viscosity models, which are based on the empirical data-bases, obtained as a rule for the free shear flows, do not take into account external pressure gradient, surface curvature and other important parameters properly. At the same time approaches based on the large-scale turbulence and direct numerical simulation of turbulence give an extremely high cost of design work.

The applied program package developed includes algebraic, one- and two-parameter models of turbulent viscosity for Reynolds averaged Navier-Stokes equations. Among numerous algebraic closure methods Baldwin-Lomax, Cebeci-Smith and Sovershenny models demonstrate good behavior. Among one-parametric models Glushko-Rubesin and Spalart-Allamaras ones should be highlighted. To close Navier-Stokes equations with two additional turbulent transport equations $k - \varepsilon$ model by Johns-Launder and its modification $k - \omega$ model by Menter show high reliability.

2. Numerical algorithm

To calculate the convective flux vector in (1) the splitting technique is usually used. Flux vectors in the paper are written depending on the normal to the face Mach number $\mathrm{M}_n = U/a$. For the supersonic flow in the direction $\mathrm{M}_n \geq 1$ we have

$$\mathbf{F}^+ = (\mathbf{F} \cdot \overline{\mathbf{n}})^+ = \mathbf{F}, \qquad \mathbf{F}^- = (\mathbf{F} \cdot \overline{\mathbf{n}})^- = 0, \qquad (2)$$

and for the supersonic flow in the backward direction $\mathrm{M}_n \leq -1$ we have

$$\mathbf{F}^- = (\mathbf{F} \cdot \overline{\mathbf{n}})^- = \mathbf{F}, \qquad \mathbf{F}^+ = (\mathbf{F} \cdot \overline{\mathbf{n}})^+ = 0. \qquad (3)$$

or the subsonic flow $|\mathrm{M}_n| < 1$ convective flow are splitted into two components $\mathbf{F}^+$ and $\mathbf{F}^-$, similarly like Jacobs matrix $\mathbf{F}^+$ has positive eigenvalues and Jacobs matrix $\mathbf{F}^-$ has negative eigenvalues.
Fluxes are defined using the relations

$$\mathbf{F}^\pm = (\mathbf{F} \cdot \overline{\mathbf{n}})^\pm = \begin{bmatrix} f^\pm_{\mathrm{mass}} \\ f^\pm_{\mathrm{mass}}\{[n_x(-U \pm 2a)/\gamma]+u\} \\ f^\pm_{\mathrm{mass}}\{[n_y(-U \pm 2a)/\gamma]+v\} \\ f^\pm_{\mathrm{mass}}\{[n_z(-U \pm 2a)/\gamma]+w\} \\ f^\pm_{\mathrm{energy}} \end{bmatrix} \qquad (4)$$

where

$$f^\pm_{\mathrm{mass}} = \pm c\, a\, (\mathrm{M}_n \pm 1)^2 / 4, \qquad (5)$$

$$f^\pm_{\mathrm{mass}} = f^\pm_{\mathrm{mass}} \left[\frac{(1-\Gamma)\, U^2 \pm 2\, (\Gamma-1)\, Ua + 2\, a^2}{\Gamma^2 - 1} + \frac{u^2+v^2+w^2}{2} \right]. \qquad (6)$$

Residual $\mathbf{R}$ is calculated by integration, using the trapezium method of fluxes through each face of the control volume. Residual for convective flux is calculated using the relation

$$\mathbf{R} = -\oint_\Omega \mathbf{F} \cdot \overline{\mathbf{n}}\, d\Omega = -\sum_i \left[\mathbf{F}^+(q_i^-) + \mathbf{F}^-(q_i^+) \right] \Omega_i \qquad (7)$$

Here $\mathbf{F}^\pm(\mathbf{q}^\pm)$ are convective fluxes though the cell faces. To construct the scheme of the first order values of variables are assumed to be constant in the volumes, which are divided by the face. To construct the scheme of higher order variables are extrapolated over the cell surfaces using the special interpolative relation, which give TVD properties to the algorithm.

To obtain an implicit algorithm the equation system (7) is linearized using the splitting of the flux vectors in a Taylor series, then we have

$$[A]^n \{\Delta\mathbf{q}\}^n = \{\mathbf{R}\}^n, \qquad (8)$$

$$[A]^n = \frac{S}{\Delta t}\, \mathbf{I} + \frac{\partial \mathbf{R}^n}{\partial q} \tag{9}$$

which at each time step are solved using the Gauss-Seidel procedure or conjugated gradients method.

Initial and boundary conditions. On the body surface the conditions of attachment and thermally insulation are set. On the outer boundary undisturbed mainstream parameters are ensured using the Riemann invariants. On other boundaries symmetry and non-reflection or zero-gradient conditions are set depending on a body in consideration.

Realization. Realization of the approach used has been carried out in the framework of the unified package of applied programs. All the stages where numerical methods are extended for the calculation of transport vehicle aerodynamics are realized: choice of the initial statement of a problem; choice of the governing equations; generation of the computational grid; solution of developed numerical algorithm; visualization and analysis of data obtained.

3. Numerical results

Calculations on the base of Navier-Stokes equations. Numerical investigation of flow around the transport vehicle profile in the vicinity of track structure is carried out. Two configurations of HSGT were chosen for investigation MLU and TRANSMAG. Transport vehicle MLU type was wedge-tailed and wedge-nosed and had a bended bottom to create the effusive diffusive effect. Transmag type vehicle had an aircraft-type configuration with a flat bottom. After solving the Navier-Stokes equations, pressure fields and Cartesian velocity vector components, pressure distribution and distribution of friction coefficients over the profile surfaces of HSGT have been received. Parametric investigation of a flow structure around two configurations of HSGT is accomplished. The first (unwinged) configuration corresponds to the type of magnetically-levitated transport TRANSRAPID (Germany) and MLU (Japany). The second one is characterized by the presence of finite-span low-aspect-ratio wing and corresponds to the design of the Institute of Transport Systems and Technologies "TRANSMAG".

Wing arrangement has a V-type form with wing inclination -36°. Such shape allows both to reinforce the ground effect and to minimize the losses of aerodynamic quality.

Calculations are carried out for different aerodynamic gaps h $h/L=0.01$, 0.1, 0.2, 0.5 and for the isolated body ($h/L=\infty$). Figures 5, 6 give numerical results at $h/L=0.1$. The overall picture of flow around the HSGT corresponds to the known data on flow around bodies of high aspect ratio (rockets, aircrafts). Mainstream decelerates immediately in front of the body then there occurs the pressure drop on the nose and a "plateau" forms along of the body. In a bottom area (domain) the pressure is somewhat increased due to flow interference. The growth in the boundary layer is taking place along the body and separation occurs in a bottom area.

As the body of HSGT approaches the track structure (aerodynamic gaps h/L decreases) the flow field begins to change. Its outer part remains virtually unchanged but an air stream is forming underneath the bottom with its maximum intensity near the aft part of the body. Such location of the flow peak velocity in the aerodynamic gap is explained by the growth in a boundary layer on a bottom and a track structure, by increasing in the thickness of displacement and accordingly by decreasing in the effective cross section of the aerodynamic gaps.

Overall intensity of the flow in a gaps between the HSGT and a track structure essentially depends on the nose shape. "Lifted" aircraft type configuration assists in catching air mass into the gap (clearance) and in strengthening the air current underneath the bottom resulting in decreasing the pressure on the lower part of the body and in appearing a negative vertical aerodynamic force.

In other words, additional retaining force, counteracting the magnet suspension appears instead lift force. That brings up the need of further investigations to understand how the shapes of nose and aft parts influence aerodynamic characteristics of HSGT.

Including the wing into arrangement of HSGT allows not only to compensate the negative retaining force but to create positive lift force comparable in magnitude with a magnet linear driver. At the same time the choice of wing profile and its location on the body is an isolated problem. In the configuration considered wings are somewhat displaced to the aft to compensate the unfavorable pitching moment which appears in the case of unwinged type of HSGT. That in turn leads to additional intensification of air current in a gap and to formation of powerful vortex structures in a bottom domain (Fig. 1-2).
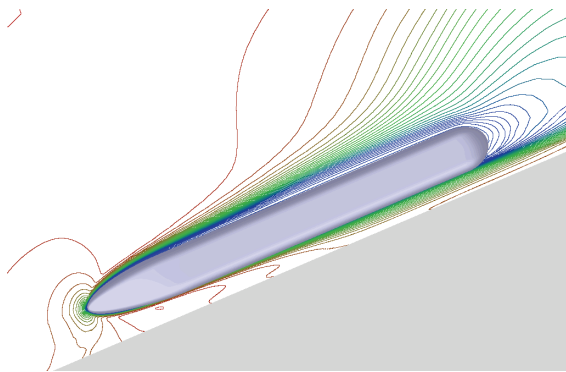
a)
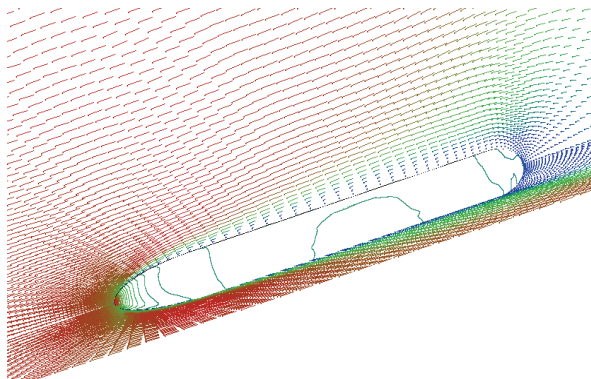
b)
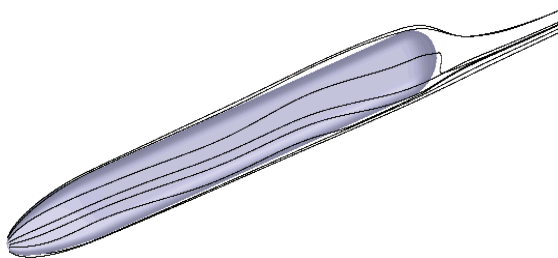
c)

Fig. 1. Distribution of Mach number contours (a), velocity vectors and pressure contours over the surface (b) and spatial streamlines (c) at the unwinged HSGT body in ground proximity.
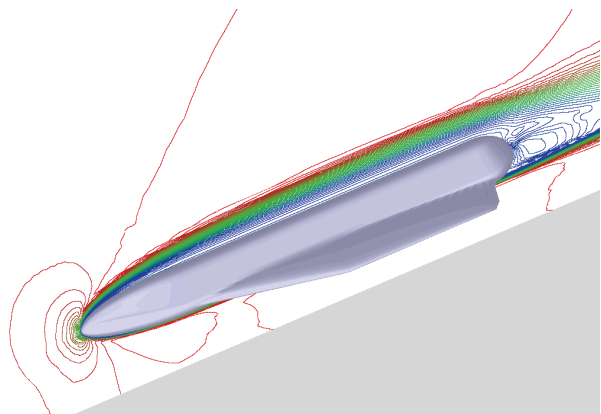

a)

b)

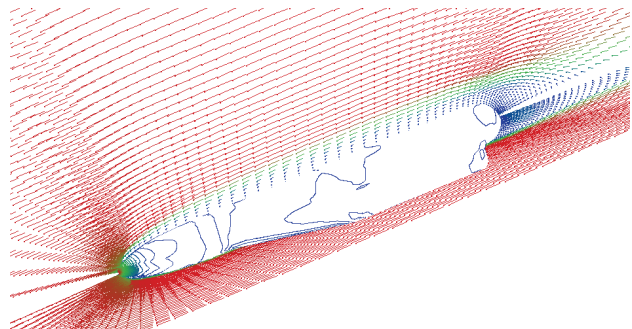
c)
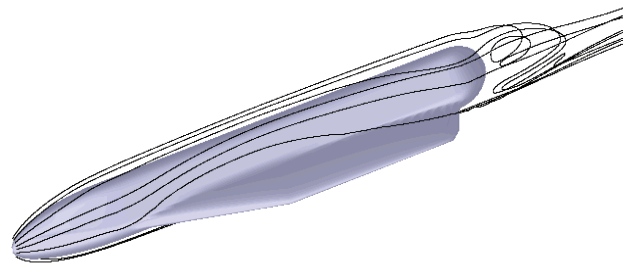
Fig. 2. Distribution of Mach number contours (a), velocity vectors and pressure contours over the surface (b) and spatial streamlines (c) at the winged HSGT body in ground proximity.

Conclusions

- Computational techniques based on Navier–Stokes equations have been developed to calculate aerodynamics of magnetically levitated transport vehicles.
- Algorithms and programs for approximation of HSGT surface and generation of computational grid for HSGT in the vicinity of track structure have been developed.
- Verification and testing of the techniques and algorithms developed have been carried out.
- Analysis of the up-to-date aircraft type HSGT aerodynamic configurations gives possibility to propose to apply the aircraft type configuration at designing the promising magnetically levitated transport vehicles.
- To improve technical and economical parameters of HSGT it is suggested to apply trapezoidal low aspect ratio arrowhead wing. Investigation showed that lifting properties of the arrowhead wing in ground proximity are sufficient at low drag.
- Aerodynamical analysis of winged profiles testifies that CLARK–Y profile families with flat bottom surface and sufficient lifting abilities at low relative thickness have an advantage.

References

1. *Prykhodko O.A.* On the Calculation of Aerodynamic Characteristics of High-Speed Ground Vehicles on the Base of Three-Dimensional Navier-Stokes Equations / O.A. Prykhodko., O.B. Polevoy, A.V. Mendriy // Proceedings of 18th International Conference on Magnetically Levitated Systems and Linear Drives. China, Shanghai, 25-29 October 2004.- P. 575-583.

2. *Prykhodko O.* On the aerodynamic calculation of high-speed ground transport vehicles / O. Prykhodko, A. Sokhatsky // 17th international conference on magnetically levitated systems and linear drives. Swiss Federal Institute of technology.- Lausanne, 2002. N PP05201. - 11 pp.

UDC 532.526

Y.A. Krashanytsya, Dr.Sci. (National aerospace university «KHAI», Ukraine)
V.T. Movchan, Dr.Sci. (National Aviation University, Ukraine)

DEVELOPMENT OF THE THEORY OF HYDRODYNAMIC POTENTIALS AND THE METHOD OF BOUNDARY INTEGRAL EQUATIONS IN BOUNDARY VALUE PROBLEMS OF HYDRODYNAMICS

The results of some generalizations of the original vector and tensor analysis and its applications in terms of the method of boundary integral equations and its numerical implementation for solving nonlinear boundary value problems of hydrodynamics are presented.

By characteristics manifold nonlinearity and fundamental problems of continuum mechanics, a significant development, along with the physical, got a computer experiment. Significant achievements were obtained in numerical analysis and, especially, in the numerical implementation of specific mathematical models of mechanics, gas dynamics in a significant development of computational fluid dynamics was given the physical-chemical processes that allow us to offer our customers develop methodical software determining the aerodynamic characteristics of aircraft operated on transonic flight regimes, create engineering calculation methods based on the typical computer-PC in real time the dynamics of a viscous incompressible fluid, the main attention is paid to a new qualitative research methods initial-boundary value problems, which in turn make it possible to formulate realistic mathematical problems and outline some of the ways their permission, give rise to new formulations of mathematical models and solutions of the motion of a viscous fluid and for small and medium Reynolds numbers that are crucial in matters of livelihood and ecology in the complex aerodynamics of lifting surfaces based on the systematic use of the method of boundary integral equations and numerical implementation options obtained and distributed the total nonlinear aerodynamic characteristics of load-bearing forms, plane and space, and studied the processes that accompany flow separation, formation and stability of vortex structures, which allows for extensive theoretical and experimental study of the problems of livelihood and safety, as well as creating an inexhaustible source of energy in the form aero-and hydroxyl units with high efficiency and a wide range of capacities.

The most reliable and proven mathematical model of a viscous fluid is the initial-boundary value problem for systems of differential equations in partial derivatives of the Navier-Stokes equations. This system was built in 1826 and so far not found a general method for investigating and solving this nonlinear system, and are known only to some, usually obtained by chance, the particular solutions of this system. Particular exact solutions are valuable for the study of viscous liquids, because they can figure out the error results when the assumptions made, or another numerical method to verify. Methodological value of such solutions is also great.

Initial-boundary value problems for systems of differential equations in partial derivatives of the Navier-Stokes equations are important and challenging task in applied mathematics and mechanics and their decision will significantly change the way of the hydro-and aerodynamic calculations, improve the quality of these calculations and increase the reliability of the results that may be and also the real economic value.

The boundary integral approach has obvious advantages over finite difference and finite element methods. This is why nowadays this method is being successfully applied for solving complex engineering problems – on surface and in space, stationary and time-dependent.

The stationary problem [1] for the flow of the incompressible viscous fluid around a body is shown in Fig. 1. The most effective method for solving a wide spectrum of boundary value problems of continuum mechanics is the method of boundary integral equations [2]. In the absence of internal moments and temperature effects, a mathematical model of the dynamics of an incompressible fluid flow is described using a well-known system of conservation laws:

- mass

$$(\nabla, \mathbf{V}) = 0, \tag{1}$$

where V is velocity of fluid flow;
- momentum

$$\left(\nabla, (\mathbf{V} * \mathbf{V})\right) = \left(\nabla, \left(-\mathbf{I}\frac{p}{\rho} + \nu\left(\nabla\mathbf{V} + \nabla^*\mathbf{V}\right)\right)\right), \tag{2}$$

where $\nabla^*\mathbf{V}$ is the dual tensor $\nabla\mathbf{V}$, and ρ is density of the medium, p is pressure, ν is kinematical viscosity and $\mathbf{I}$ is an identity tensor.

In addition, it is advisable to investigate the conservation of vortices $\mathbf{Щ} = [\nabla, \mathbf{V}]$

$$\left[\nabla, [\mathbf{Щ}, \mathbf{V}]\right] + \nu\left[\nabla, [\nabla, \mathbf{Щ}]\right] = 0 \tag{3}$$

as a critical kinematics characteristics of the interaction of viscous flow with a streamlined body.

Solution of the system of differential equations of the conservation laws (1 - 3) is subject to the natural boundary condition

Fig.1. Fixed body (S) in a steady flow of a viscous incompressible fluid inside the control volume (Σ)

$$\mathbf{V}\big|_{S+\Sigma} = \mathbf{U}^{S+\Sigma}(s, \tau), \quad p\big|_{\Sigma} = p_\infty, \quad \mathbf{Щ}_n\big|_S = 0, \quad \mathbf{Щ}\big|_{\Sigma} = 0, \tag{4}$$

where $\mathbf{V}\big|_S$ is the velocity of points on the liquid surface of the body and is a boundary condition that may depend on the surface coordinates (s, τ) in some particular cases.

The main objective of the vector analysis is the determination of the vector field V on the set of divergence

$$(\nabla, \mathbf{V}) = q \tag{5}$$

and vorticity

$$[\nabla, \mathbf{V}] = \mathbf{Щ}, \tag{6}$$

where the intensity function of the density of mass flow q - known as the vortices vector $\mathbf{\Omega}$ - near-contains the definition.

Thus, in accordance with the theorems of vector analysis [3] and with the theory of boundary value problems of mathematical physics [4], solutions must be consistent with the natural boundary conditions of the mathematical model (1 - 4). Therefore, it is necessary to solve the boundary value problem (1 - 4), for example, in R³.

Then equations (5 - 6) can be constructed using the differential operators of second order:

$$\nabla(\nabla, \mathbf{V}) = \nabla q, \quad \nabla(\nabla, \mathbf{Щ}) = 0. \tag{7}$$

It is not difficult to prove [4-5] that the tensor $\mathbf{\Gamma} = \mathbf{I}\varphi - [\mathbf{I}, \mathbf{G}]$, where $\varphi(|\mathbf{x} - \mathbf{y}|) = \dfrac{1}{4\pi|\mathbf{x} - \mathbf{y}|}$ is the

fundamental solution of Laplace's equation in R³, and the vector $\mathbf{G} \in C^2(E)$ defined by the conservative condition

$$(\nabla, \mathbf{\Gamma}) = 0 \Leftrightarrow \nabla\varphi = [\nabla, \mathbf{G}] \tag{8}$$

is the fundamental solution of differential operators in (7), i.e.

$$\nabla(\nabla, \mathbf{\Gamma}) = \mathbf{I}\delta(|\mathbf{x} - \mathbf{y}|), \tag{9}$$

where $\delta(|\mathbf{x} - \mathbf{y}|)$ is the Dirac delta function, which depends on two points in space.

Conservative nature of the law of conservation of the momentum (2) allows us to write the generalized D.Bernoulli integral:
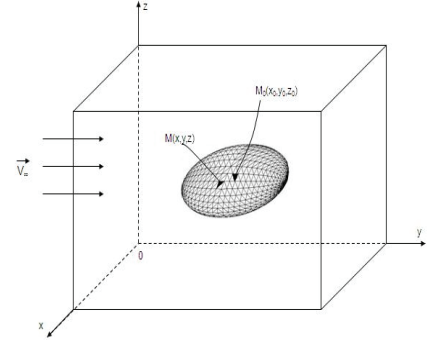
$$\mathbf{V} * \mathbf{V} + \mathbf{I}\frac{p}{\rho} + \nu\left(\nabla^{*}\mathbf{V} - \nabla\mathbf{V}\right) = \nabla^{*}\mathbf{Ш}, \tag{10}$$

where the choice of the vector potential **Ш**, by virtue of conservatism of the left side of expression (2) will be governed by the condition

$$\nabla\left(\nabla, \mathbf{Ш}\right) = 0, \tag{11}$$

i.e. vector **Ш** belongs to the class of solutions of equations (7).

Similarly, the law of conservation of vortices $\mathbf{\Omega}$ (see (3)) has an integral representation

$$\left[\mathbf{I}, [\mathbf{Ш}, \mathbf{V}]\right] + \nu\left(\nabla^{*}\mathbf{Щ} - \nabla\mathbf{Щ}\right) = \nabla^{*}\mathbf{Ц}, \tag{12}$$

which is a vector potential and it is a solution of equation (11)

$$\nabla\left(\nabla, \mathbf{Ц}\right) = 0. \tag{13}$$

Integrating in space (τ) a combination of differential operators (9, 7, 11, 13) (for an arbitrary vector **a**), taking the standard limit, and also taking into account the properties of the double-layer potential [4], the fundamental solution of Laplace's equation in R^3, we have an integral representation solutions

$$\mathbf{a} = \oiint_{(S+\Sigma)} \left\{ \left(\left(\frac{\partial \mathbf{a}}{\partial n} + [\mathbf{n}, [\nabla, \mathbf{a}]]\right), \mathbf{\Gamma} \right) - \left(\mathbf{a}, \left(\frac{\partial \mathbf{\Gamma}}{\partial n} + [\mathbf{n}, [\nabla, \mathbf{\Gamma}]]\right) \right) \right\} dS. \tag{14}$$

This expression is the source of the integral representations of solutions of the definition of basic kinematics and dynamic characteristics of the interaction of a moving viscous fluid and a solid. And here all the differential operations are linear combinations of the characteristics of the problem and potentials **Ш** and **Ц** .

Numerical solution of linear systems of boundary integral equations type (14) for kinematics and dynamic characteristics can be obtained using the classical quadrature integration on each element of the triangulated surface (Fig. 2).

Some results of calculations for the distribution and total hydrodynamic characteristics, as well as the convergence of the computational method are shown in Fig. 3-5.

Fig. 2. Elements of a triangulated surface
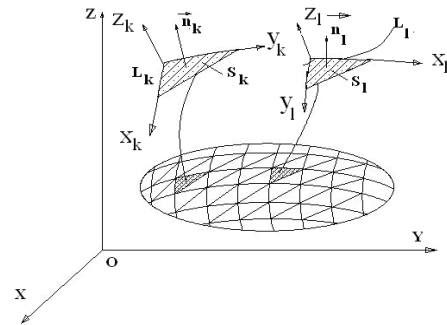

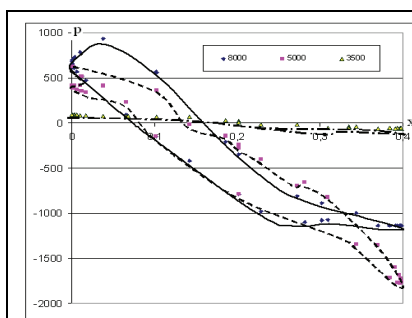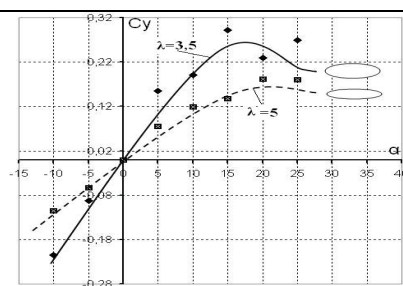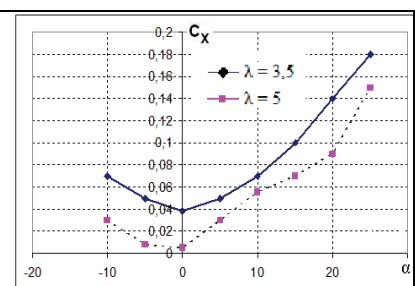| Fig. 3. Influence of the number of cells of the triangulation surface of ellipsoid (1.0, 1.0, 0.3) on the calculation quality at $\alpha = 5^0$ [5]	Fig. 4. The dependence of the lift coefficient of an ellipsoid with different elongation [5]	Fig.5. The dependence of the drag coefficient on the angle of attack ellipsoid at different extensions and Re = 4.9•10^6 [5]

Results and discussions

This approach has the absolute advantage over finite difference methods and finite element method. That is why at the present time this method has been successfully applied to solve complex engineering problems - flat and spatial, stationary and time dependent. Shown in Fig. 3-5 results illustrate the wide range of capabilities of the developed method in terms of computing as distributed and total hydrodynamic characteristics of flow around bodies of arbitrary space configuration real stream media including theology and any external influences.

Conclusions

A new generalized approach to obtain analytical and numerical solutions for a wide class of nonlinear problems in continuum mechanics is presented. New approach and required formal apparatus for the formulation of the boundary integral equations, equivalent to the initial-boundary problems of the basic mathematical models in mechanics of fluid and gas, are developed.

References

1. *Loytsyanskiy, L.* Mechanics of liquid and gas. M.: Nauka, 1970. – 904 p.

2. Boundary-integral equation method: computational applications in applied mechanics (ed. T. Ruse, F. Rizzo). The American Society of Mechanical Engineers, N.Y., 1975. – 178 p.

3. *Krashanitsa, Yu.A.* Basic task of vector analysis in continuum mechanics / Yu.A. Krashanitsa // Visnik Dnipropetrovskogo universitetu. V.3, t.1. 2000. 52 – 56.

4. *Vladimirov, V.S.* Equations of mathematical physics. - M.: Science, 1981. – 512 p.

5. *Krashanitsa Y.* Triangulation method of numerical realization of the spatial boundary value problems of viscous fluid dynamics / Y.A. Krashanitsa, M.T. Ngo // Proceedings of the Academy of Engineering Sciences of Ukraine. Special Issue. Mechanical engineering and advanced technology. - 2009 - № 1 (38) / - S. 158 - 161.

V.M. Lapotko, Cand.Sci., Yu.P. Kukhtin, Cand.Sci.,
I.F. Kravchenko, Cand.Sci. (SE Ivchenko Progress, Ukraine)

"CLOCKING" – AN EFFECT OF ACOUSTICAL INTERACTION OF TURBOMACHINE BLADE RIMS

An analysis of acoustical interaction of non-adjacent working wheels at various relative angular positions rotating at an equal angular velocity and having equal number of blades was carried out. A method of tracking gas flow filaments by example of an experimental two-stage low pressure turbine was used. Existence of a relative circumferential position of the working wheels, at which minimal levels of wide-bend and tonal noise in the source can be expected, was shown.

Introduction

The rotor and stator interaction in turbo-machines is a very important part of the phenomena specific for a stationary flow, including noise generation. In the study [1] it was shown that, if the rotor-blade wakes passing through the adjacent stator vane channels reach the rotor blades of the stage located downstream, then both in the boundary lays of these blades and in the wakes increase of the turbulence level, i. e. growth of the wide-bend noise is observed.

Such a phenomenon is of a regular nature when the number of blades in the non-adjacent blade rims is equal or multiple to each another. This phenomenon was called "acoustical clocking-effect of turbo-machine".

During a certain time after the study [1] was published a number of works ensuring improvement of the calculation method concerning both the taking account of the flow three-dimensionality and the improvement of the tonal noise calculation were carried out. These works were reflected in the publication [2].

Designations

Tu, α – turbulence level and flow inlet angle, respectively;

P_0^0, T_0^0 - total pressure and total temperature at the inlet section, respectively;

P_a, T_a – static pressure and static temperature at the inlet section, respectively;

ω, W – rotor speed and gas flow velocity, respectively;

k – pulsating motion energy;

PK, CA – working wheel and N.G.V. assembly, respectively.

Object of researches

As an object of computational researches served are the experimental low pressure turbine 1.5 stages and the downstream located rim of aerodynamic struts that can be conventionally considered as a N.G.V. assembly (Fig. 1).

For the structure under consideration, is of interest the possibility for minimization in the source both the broad-bend and the tonal noise in 73-d harmonics at the expense of relative mutual change of the circumferential arrangement of non-adjacent working rotor blade rims rotating at similar rotational speed and consisting of equal number of blades.

The turbine operation conditions corresponded to the engine takeoff operation conditions. All values were reduced to the dimensionless form. As a length standard taken was the general extent of computational space which was equal to 650 mm. As pressure and temperature standards taken were the values P_a = 132700.0 Pa and T_a = 802.5 K at the turbine outlet. The adiabatic index κ = 1.325, the gas constant R = 287.0 J/(kg·K). As a velocity standard served was the isothermal sound velocity $\sqrt{RT_a}$. The Reynolds number determined on the basis of the general axial extent of

computational space and the physical gas viscosity at the turbine length made up 4940000.0. The background flow turbulence at the computational space inlet $T_{U0} = 2\%$.
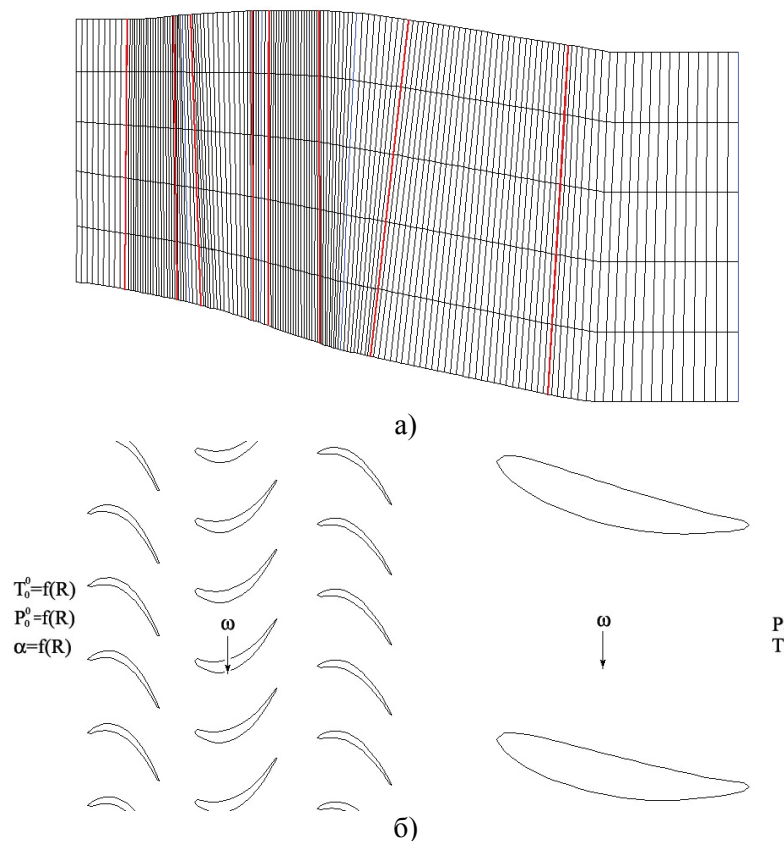

а)

$T_0^0 = f(R)$
$P_0^0 = f(R)$
$\alpha = f(R)$

ω

ω

P_a
T_a

б)

Fig 1. Researched 2.0 stages of experimental low pressure turbine,
a) turbine gas flow path б) circumferential development of height-averaged layer

Subject of researches

The reason of wide-bend (swirling-type) noise lies on the wide spectrum of micro-vortices associated with the flow turbulent disturbances in the blade boundary layer and in the aerodynamic wakes. A physical quantity, which reflects the level of turbulent pulsation and, as a sequence, the wide-bend noise level, is the pulsating motion energy, which is presented in calculations as a definable value of the turbulence k-ε model.

The reason of tonal noise appearance is in the periodical pressure pulsations on the blade surfaces caused by ingress of the flow aerodynamic irregularities, generated by the upstream blades, on them.

The non-stationary pressure fields, obtained on the surfaces under investigation in the issue of timing calculations, were subjected to Fourier analysis. Hereby a possibility for analyzing the most essential harmonics of acoustic vibrations appeared.

Thus, the specified values – the pulsating motion energy field in the computational space and the results of Fourier analysis of non-stationary pressure on the surfaces of straightening struts – were the subject of researches in this study.

Results of calculations

The calculations were carried out in the relative coordinate system connected with the rotor. The cases under consideration corresponded to various relative positions of the rotors:
    1 – the wheel blades are located in front relative to one another (displacement 0.0˚);
    2 – the blades of the second wheel are displaced by 1.75˚ relative to those of the first wheel;
    3 - the blades of the second wheel are displaced by 2.41˚ relative to those of the first wheel;
    4 - the blades of the second wheel are displaced by 3.17˚ relative to those of the first wheel.

At the takeoff power rating under consideration the most advantageous disposition of rotors corresponding to minimal wide-band noise and minimal pulsating pressure on the surfaces of straightening struts, that specifies the 73-d harmonic of tonal noise, is the position 0.0°.

As shown in the Fig. 2, the maximal level of the pulsating motion energy of the last blade rims in cases of 1.75°, 2.41°, 3.17° is higher by ≈ 1.3 fold as compared with the case of 0.0 due to generation of additional energy of pulsating motion in the boundary layer of the third rim blades during their interaction with the wakes descended from the first rim blades.

a)

б)
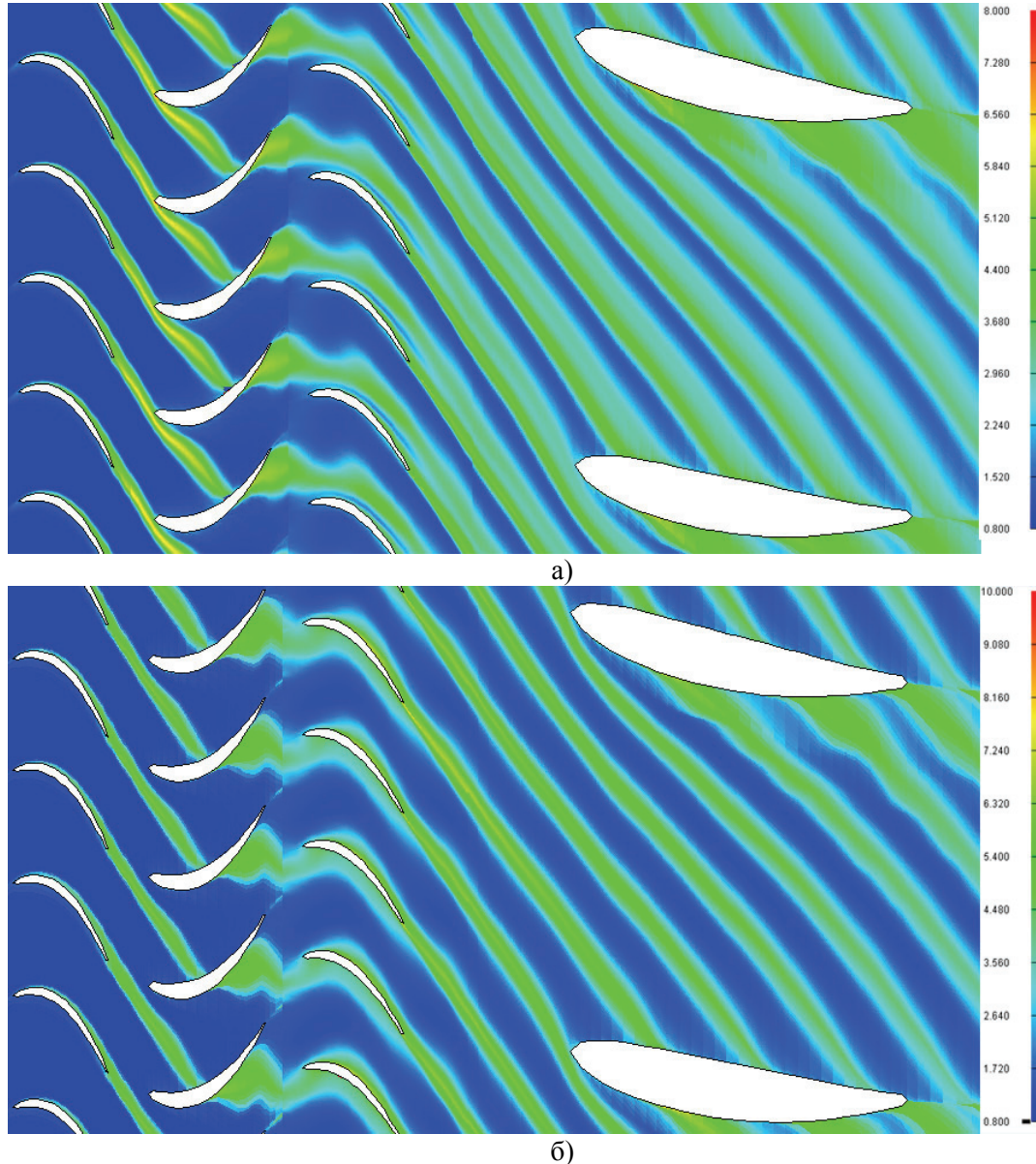
Fig. 2. Instantaneous field of pulsating motion energy in the layer distant from the flow-path root by 0.7 of the blade height: a) case of 0.0° (the 1st and 3rd rims are in front relative to each other); б) the 1st and 3rd rims are displaced by 1.75° relative to each other

The relative position 0.0° is an advantageous position corresponding to the 73rd harmonic of tonal noise (see Fig. 3a, 3б), in comparison with the disadvantageous position of 1.75° (see Fig. 3в, 3г).
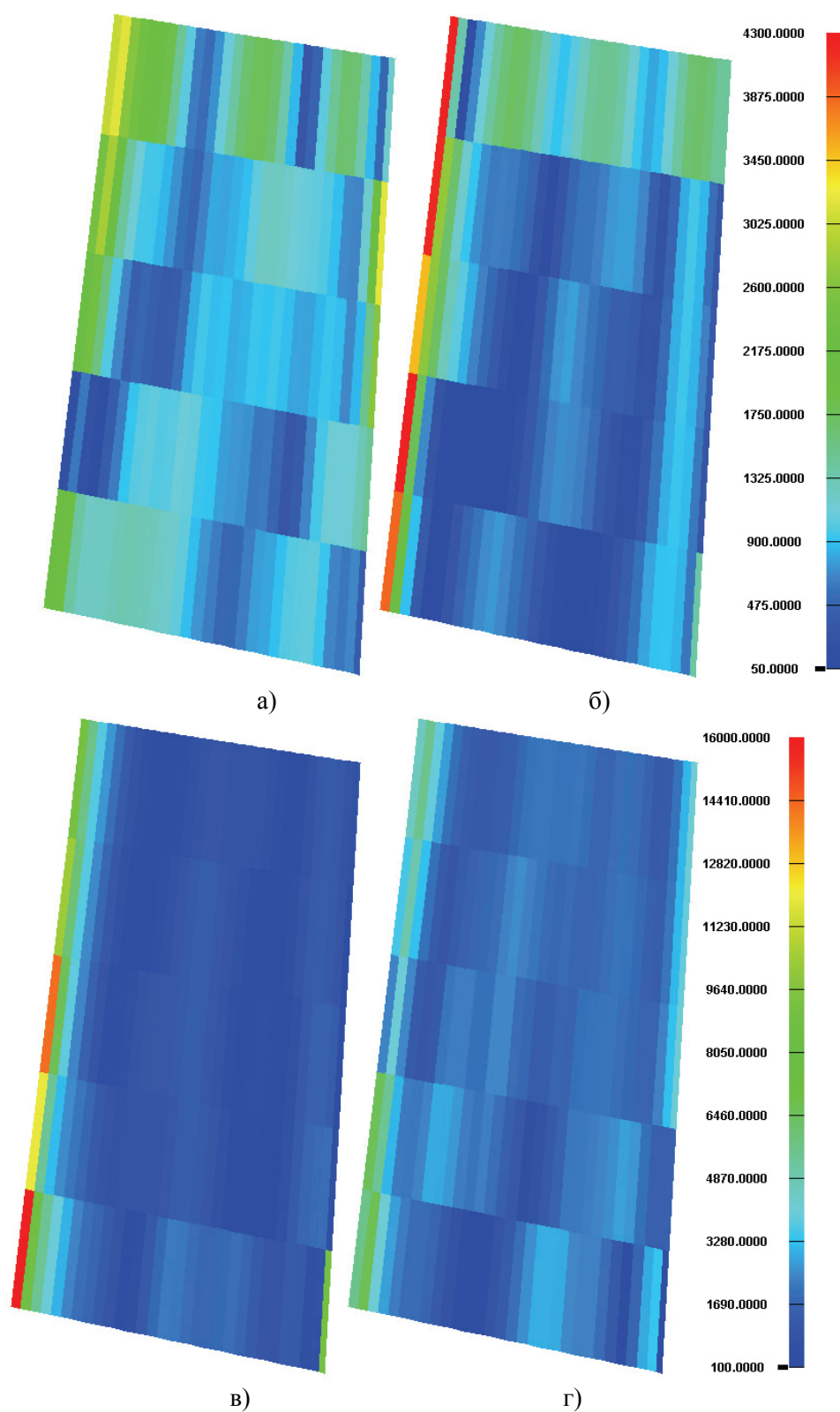
Fig. 3. Distribution of pulsating pressure corresponding to the 73rd harmonic on the surfaces of diffuser grids: for the relative position 0.0 a) upper surface, б) lower surface; for the relative position 1.75 в) upper surface, г) lower surface

This is explained by the fact that in cases of 1.75°, 2.41° and, partially, 3.29°, where the wakes from the first working rim blades hit the surfaces of the second working rim blades, the velocity valleys in the wakes become greater (see Fig. 4).
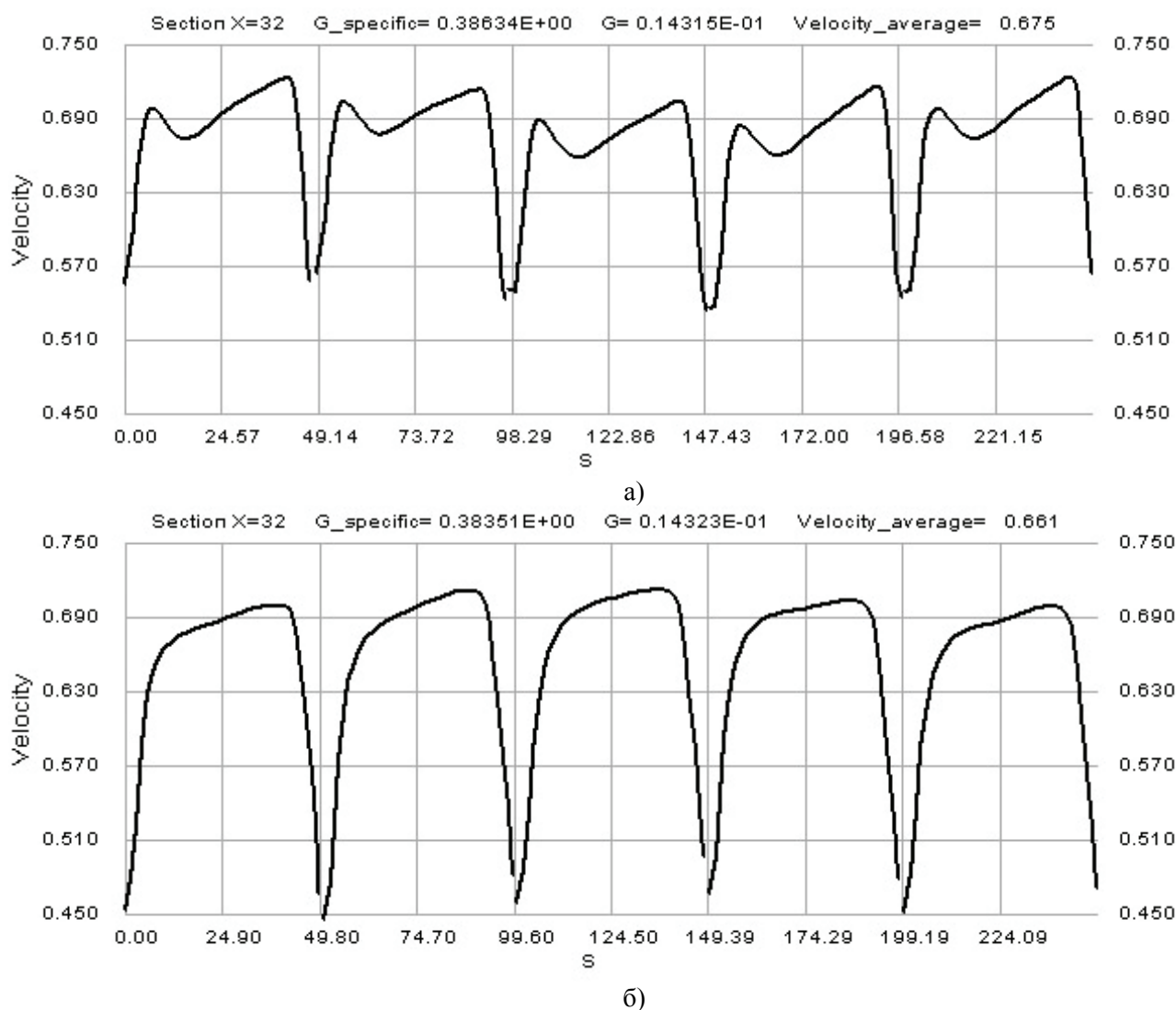
Fig. 4. Change of the velocity after the second working wheel: a) alternate calculation 0.0˚ - non-displaced rims; б) alternate calculation 1.73˚ - alternate calculation

Conclusions

On the basis of the results of this study obtained is a possibility for establishing optimal characteristics of turbo-machines, as well as decreasing the sources of aerodynamic noise generated by them.

References

1. *Muravchenko F.M.* "Estimating the acoustical interaction of the D-18T engine fan turbine rims" / *F.M. Muravchenko, V.M. Lapotko, Yu.P. Kukhtin,S.B. Reznik, A.I. Popuga* // S&T Journal "Вестник двигателестроения" (Herald of Propulsion Engineering), Zaporozhye: Motor Sich. – No. 1. – 2006. – P. 8-13.

2. *Lapotko V.M.* "Method of numerical evaluation of tonal noise level in the source in case of non-stationary interaction of turbo-machine rims", / *Lapotko V.M., Yu.P. Kukhtin, G.I. Slynko* // S&T Journal "Авиационно-космическая техника и технология" (Aerospace engineering and technology), Kharkov: KhAI. – 2012, 10 p. (in press)

A.E. Aslanyan, Dr.Sci., A.A. Belskaya, Cand.Sci.
(National Aviation University, Ukraine)

SINGULARITIES OF MATHEMATICAL MODELING THE DYNAMICS OF ENERGY OBJECTS

The linear dynamic model of energy object in vector-matrix form is proposed, based on which is synthesized the automatic system for continuous monitoring parameters, which characterize its current technical condition

Analysis of results theoretical and experimental studies wide class of energy objects (EO), such as gas turbine engines of aircraft and ships, compressor stations, gas turbines and mobile power plants, steam-turbine plant, diesel power units, pumps, etc., confirms that in most cases their analytical description is possible in a system of ordinary nonlinear differential equations of the form:

$$\dot{x}_i = F_i(x_1, x_2, ..., x_q, u_1, u_2, ..., u_r), \ i = \overline{1, n}, \ (n < q), \tag{1}$$

$$G_j(x_1, x_2, ..., x_q, u_1, u_2, ..., u_r) = 0, \ j = \overline{1, q - n}. \tag{2}$$

Here: $\mathbf{x} = (x_1, x_2, ..., x_q)'$ − vector of EO condition parameters; $\mathbf{u} = (u_1, u_2, ..., u_r)'$ − control vector; $\mathbf{F} = (F_1, F_2, ..., F_n)'$ − nonlinear vector-function which characterizes the inlet (outlet) power to the drive; $\mathbf{G} = (G_1, G_2, ..., G_{q-n})'$ − nonlinear vector-function of EO condition parameters and controls.

Functions $\mathbf{F}(\mathbf{x}, \mathbf{u})$ and $\mathbf{G}(\mathbf{x}, \mathbf{u})$ are exist and continuously differentiable in space $\mathbf{X} \times \mathbf{U}$, i.e. for the entire set of admissible controls and condition parameters of EO. Coordinates of EO condition vector $\mathbf{x} = (x_1, x_2, ..., x_q)'$ are the set of controlled parameters, choice of which is ambiguous, but requirements for this vector are general in nature, namely: measured parameters must have acceptable accuracy and stability of readings over time, must have greatest diagnostic value among other parameters, must base on regular measurements, must ensure simplicity and ease using of measurement means. Under coordinates of control vector $\mathbf{u} = (u_1, u_2, ..., u_r)'$ refers inertial control actions, which have definite physical meaning (fuel consumption, steam flow, the angle of guide vanes, the cross-sectional area of jet, etc.).

Depending on the nature of control tasks and properties of the energy object is an acceptable use of its linear dynamic model, i.e. use of mathematical model that derived from linearization equations (1) - (2). It is obvious that linear dynamic model can be no appropriate to describe very fast processes in the energy object, or processes, associated with large changes in load, i.e. its scope is limited. However, we know that the conclusion about stability or instability of solution the original system nonlinear differential equations, in accordance with first method A.M. Lyapunov, can be made based on analysis system of equations first approximation.

Equally important the linear dynamic models of energy objects in synthesis the automatic system of continuous monitoring their technical condition [1]. The synthesis of such system is a major step in organization of exploitation "on condition" of EO.

In general, the linearized system of equations (1) - (2), written in deviations in dimensionless form, is given by:

$$\dot{x}_i = \sum_{k=1}^{q} a_{ik}(t) x_k + \sum_{m=1}^{r} b_{im}(t) u_m, \ i = \overline{1, n}, \ (n < q), \tag{3}$$

$$\sum_{k=1}^{q} c_{jk}(t) x_k + \sum_{m=1}^{r} d_{jm}(t) u_m = 0, \ j = \overline{1, q - n}. \tag{4}$$

In stationary case, (3) - (4) can be written in vector-matrix form as follows:

$$\mathbf{T}\dot{\mathbf{x}} + \mathbf{x} = \mathbf{Ku}, \tag{5}$$

where $\mathbf{T}$ − singular square matrix of generalized time constant, size $q \times q$, and $\mathbf{K}$ − a matrix of gain coefficients, size $q \times r$.

Define matrix $\mathbf{T}$ and $\mathbf{K}$ for single-shaft turbojet engine with a fixed jet without influence of fuel system at nominal mode of the engine.

It is known [2], for engines with fixed jet, adjustable parameters are: $x_1(t)$ − speed of rotation, $x_2(t)$ − temperature of gases before the turbine, $x_3(t)$ − temperature of gases after the turbine, and control factor $u(t)$ − fuel consumption. Taking into account that among energy storage devices (rotating mass, the volume of jet pipe filled with pressurized gas, the volume between compressor and turbine, the volume of input device filled with compressed air, battery thermal energy) determines energy storage is rotating weight, which includes the turbine, the compressor, the connecting shaft and moving mass of auxiliary units, powered by the turbine shaft, at first approximation we can confine ourselves to considering only one energy storage in form of rotating masses, i.e. limited to only one degree of movement freedom. Energy conversion in the combustion process, resulting in heat, in a first approximation can be regard as inertialess process that takes place with negligible time lag.

Choosing as initial data a moment of inertia rotating masses of the engine $J = 5,88 \ \ N \cdot m \cdot sec.^2$ and other necessary data from thermal design of the engine, given in [2], we obtain the linear dynamic model of single-shaft turbojet engine with fixed jet in form of equations (3) - (4):

$$\begin{cases} \dot{x}_1 = -2x_1 + 0.667u, \\ 0.889x_1 + x_2 - 0.667u = 0, \\ 1.583x_1 + x_3 - 0.585u = 0. \end{cases} \qquad (6)$$

The system of equations (6) can be written in vector-matrix form (5), and

$$\mathbf{T} = \begin{pmatrix} 0.5 & 0 & 0 \\ -0.445 & 0 & 0 \\ -0.792 & 0 & 0 \end{pmatrix}, \ \mathbf{K} = \begin{pmatrix} 0.334 \\ 0.370 \\ 0.058 \end{pmatrix}.$$

The mathematical model of turbojet engine presented in form (5) allows us analytically carry out the synthesis of automatic system for continuous monitoring its technical condition, herewith, as shown in [3], the matrix of transfer functions for system of continuous monitoring has next form:

$$\mathbf{H}(p) = \mathbf{E} - (\mathbf{T}p + \mathbf{E})^{-1} \mathbf{K} \left[\mathbf{K}' \left(\mathbf{TT}'p^2 + (\mathbf{T} + \mathbf{T}')p + \mathbf{E} \right) \mathbf{K} \right]^{-1} \mathbf{K}' (\mathbf{T}'p + \mathbf{E})^{-1}, \qquad (7)$$

where $\mathbf{E}$ − identity matrix, size 3×3, $'$ − the symbol of transposition.

It can be shown that the matrix of transfer functions is symmetric, i.e. $\mathbf{H}'(p) = \mathbf{H}(p)$ and $\mathbf{H}^2(p) = \mathbf{H}(p)$.

Substituting values the matrix of generalized time constancies $\mathbf{T}$ and the matrix of gains $\mathbf{K}$, founded for single-shaft turbojet engine with fixed jet, into expression (7) we obtain an expression the matrix of transfer functions for system of control:

$$\mathbf{H}(p) = \begin{pmatrix} \dfrac{0.197p^2 + 0.281p + 0.141}{0.197p^2 + 0.281p + 0.252} & -\dfrac{0.111p + 0.123}{0.197p^2 + 0.281p + 0.252} & -\dfrac{0.098p + 0.020}{0.197p^2 + 0.281p + 0.252} \\ -\dfrac{0.111p + 0.123}{0.197p^2 + 0.281p + 0.252} & \dfrac{0.086p^2 + 0.035p + 0.115}{0.197p^2 + 0.281p + 0.252} & -\dfrac{0.098p^2 + 0.128p + 0.022}{0.197p^2 + 0.281p + 0.252} \\ -\dfrac{0.098p + 0.020}{0.197p^2 + 0.281p + 0.252} & -\dfrac{0.098p^2 + 0.128p + 0.022}{0.197p^2 + 0.281p + 0.252} & \dfrac{0.111p^2 + 0.246p + 0.248}{0.197p^2 + 0.281p + 0.252} \end{pmatrix}.$$

An effectiveness of synthesized system of turbojet engine technical condition monitoring illustrates by performing the simulation in a software MATLAB. Assume that on output of control-

measurement system is observed vector $\mathbf{x}(t) = \left(x_1(t), x_2(t), x_3(t)\right)'$. Three variants of the vector $\mathbf{x}(t)$ graphs are given by Fig. 1.
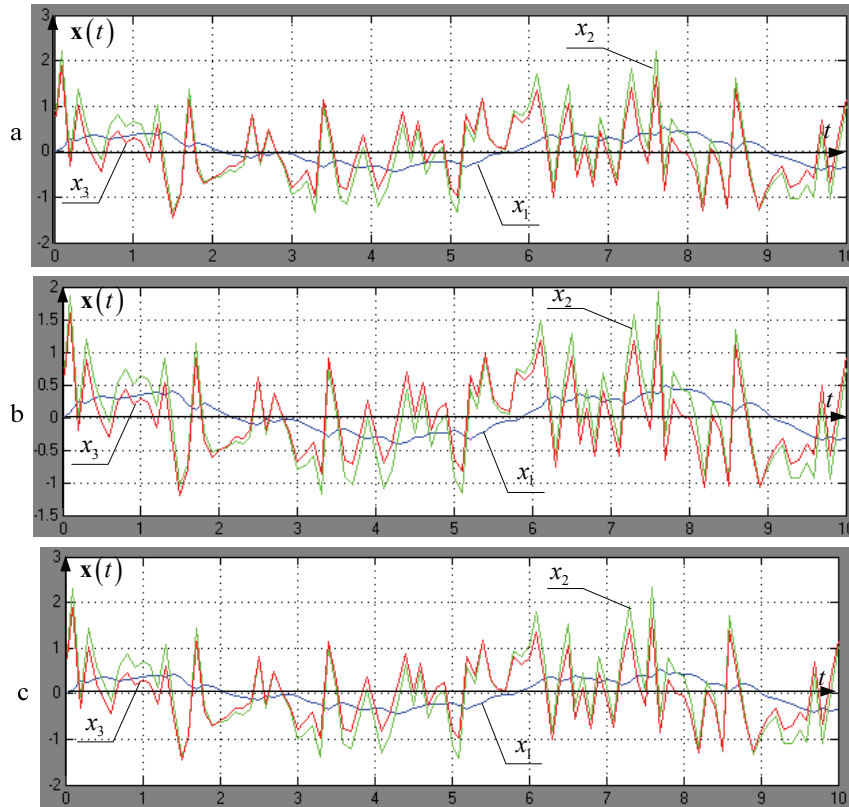

Fig. 1. Variations of observed output vector $\mathbf{x}(t)$

On automatic control system output have seen a vector $\mathbf{x}^*(t) = \left(x_1^*(t), x_2^*(t), x_3^*(t)\right)'$, corresponding graphs of its coordinates shown on Fig. 2.

If in Fig. 1, the corresponding coordinates of the observed parameters $\mathbf{x}(t)$ for all three models do not differ, the output of the synthesized control system (Fig. 2) corresponding coordinates of vector $\mathbf{x}^*(t)$ are significantly different.

In Fig. 2 (a), each coordinate of the vector $\mathbf{x}^*(t)$ deviates from zero by no more than $\varepsilon = 3 \times 10^{-4}$ that is within the accepted error of computation $\delta = 10^{-3}$, so in this case there is no reason to assume that the parameters of a linear dynamic model of serviceable objects do not correspond to the current technical condition of turbojet engine.

The maximum deviation of the first coordinate vector $\mathbf{x}^*(t)$ on Fig. 2 (b) is $\varepsilon = 9 \times 10^{-2}$ that substantially exceeds the error of calculation adopted $\delta = 10^{-3}$, so the coordinates deviation of vector $\mathbf{x}^*(t)$ from zero is a consequence of the fact that some of parameters linear dynamic model does not correspond to the current technical condition of turbojet engine. As a result, we identify the new value of time constant $T = 0.6\,sec.$ (previous value $T = 0.5\,sec.$).

The maximum deviation of the third coordinate vector $\mathbf{x}^*(t)$ on Fig. 2 (c) is $\varepsilon = 6 \times 10^{-2}$ that significantly exceeds the error of calculation adopted $\delta = 10^{-3}$, so this deviation is a consequence of non-compliance certain parameters of linear dynamic model to current technical condition of turbojet engine. Using the procedure of finding rows of transfer functions matrix, containing elements whose parameters do not correspond to the current technical condition of the object [4], we determine that the correction is subject to the second element of the matrix $\mathbf{K}$. As a result of identification we have a new value $k_2 = 0.400$ (the previous value is $k_2 = 0.370$).
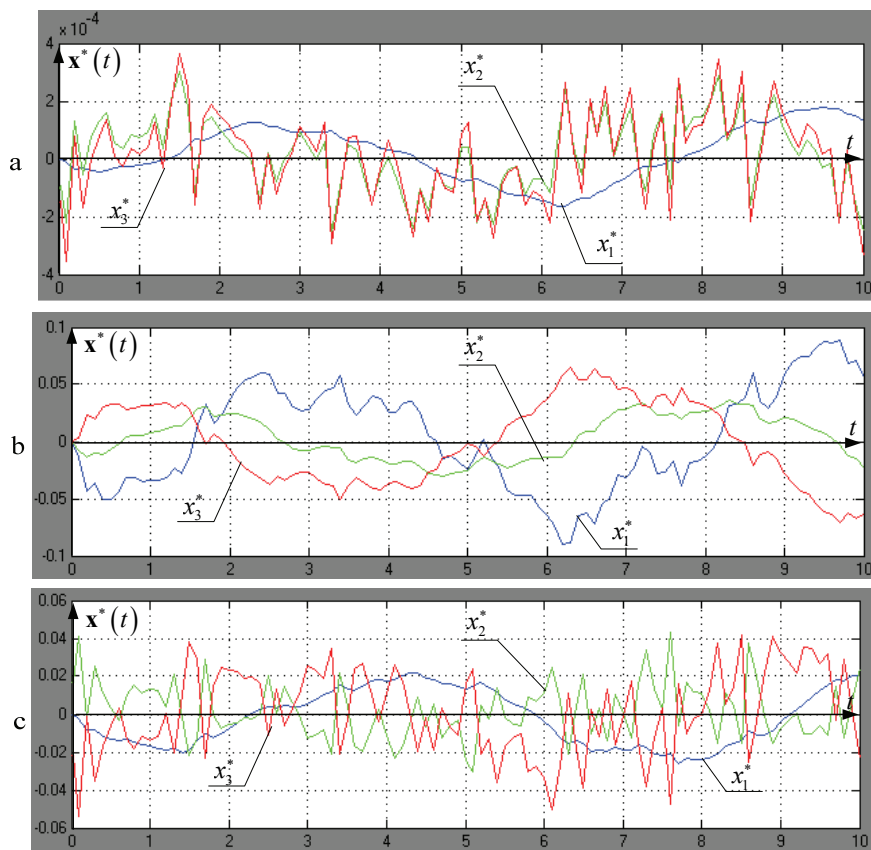
Fig. 2. Variations for output vector $\mathbf{x}^*(t)$ of monitoring system

Conclusions

1. A singularity mathematical models of energy object is the presence as non-linear ordinary differential equations and nonlinear algebraic equations, due to the presence of energy object both inertial and noninertial elements.

2. Using the parameters linear dynamic models of energy object (gain, time constant) to characterize the current technical condition is justified for a wide class of objects, a control system which operates in the mode of stabilization, herewith matrix of the generalized time constants is always singular. The consequence is the presence in the matrix of transfer functions at least one element that has the degree of the numerator and denominator polynomials are the same.

References

1. *Асланян А.Э., Бельская А.А.* Математические проблемы технической эксплуатации по состоянию / Науковий вісник Академії муніципального управління. Серія «Техніка».– К.: АМУ, 2009. – Вип. 2. – С. 94-99.

2. *Шевяков А.А.* Автоматика авиационных и ракетных силовых установок. – М.: Машиностроение, 1970. – 548с.

3. *Бєльська О.А.* Синтез автоматичної системи неперервного моніторингу технічного стану динамічних об'єктів / Проблеми інформатизації та управління: зб. наук. праць.– К.: НАУ, 2011. – №2(34). – С. 23-30.

4. *Бельская А.А.* Локализация неисправностей в линейных системах большой размерности при отсутствии информации о входном сигнале // Матеріали VII міжнародної науково-технічної конференції «Авіа-2006». – К.: НАУ, 2006, –Т. II. – С. 3.1–3.4

UDC 532.526.4

Ye.O. Shkvar, Dr.Sci., V.V. Kravchenko, O.V. Samusenko,
S.O. Shevchenko (National Aviation University, Ukraine)

METHODS OF VORTICAL STRUCTURE CONTROL IN TURBULENT FLOWS AND THEIR MATHEMATICAL MODELS

The actuality of control of turbulent shear flows, developing on the external surfaces of perspective transport vehicles and great-scale buildings is justified from the standpoint of energy efficiency in the transport industry and, in particular, for aviation, as well as in planning the of modern cities development. The perspective directions of elaborating the methods of turbulent structure control are identified and the actuality of constructing the corresponding mathematical models is proved.

Argumentation of near-wall turbulent flow control actuality. Nowadays the world energy consumption of natural resources is growing exponentially and its dominating part belongs to oil and natural gas. However, their stocks are steadily exhausted, and this fact rapidly increases the urgency for development and implementation of various resource-saving technologies. One of the largest consumers of fuel is the transport industry, particularly aviation, and under the necessity to increase continuously the traffic volumes, energy saving is one of the most effective possibilities to prevent a fast aggravation of an imminent crisis together with simultaneous reducing the atmospheric pollutions. It is a known fact, that aviation fuel losses correspond to 22% of direct operational costs [1] and, for example, consumption of fuel for the largest mass transport aircraft like An-124 at maximum payload equals 12,600 kg of fuel per flight hour. If due to some actions it will be possible to reduce the drag by 1%, the costs be reduced by 0.2% that it is equivalent to an extra transportation of 10 passengers or 1.6 tons of cargo. At the same time it will reduce harmful emissions. The European Commission requires decreasing till 2020 in a half of carbon dioxide emissions by aviation, which, in turn, will help to reduce the fuel consumption [2].

The overwhelming majority of drag of transport vehicles belongs to friction drag and if we take into consideration sizes of modern vehicles and their typical speed, we can specify that this friction drag occurs under the turbulent flow regime. It is known that this component of resistance composes relatively to the full drag about 50% for the aircraft, up to 60% for submarines and up to 90% for gas transferring equipment, so its reduction should be seen as a powerful instrument for energy saving both for aviation and other types of transport. At the same time it should be noted that the shape of modern aircrafts and other vehicles, aircraft propellers and flow path components of aircraft engines have already very high level of optimization of the streamlined surfaces geometry. Therefore, taking into account primarily turbulent flow regimes, the most actual direction of drag reduction possibilities investigation can be associated, first of all, with friction drag reduction, aimed primarily at regularization of the turbulent motion and its vortical structures organizing. The complexity of the turbulent motion processes, difficulties of their theoretical description and problems of practical implementation of control methods and absence of optimal strategies, inadequate or lack of appropriate mathematical models for physical description of turbulent flow formation and possibilities for its control cause mainly experimental type of researches in this field. These circumstances define the **scientific actuality and practical importance** of mathematical models creation for turbulent vorticity control.

The aim of this research is the study the turbulent flow properties and constructing the appropriate mathematical models of some modern turbulent flow control methods, which are based on knowledge about extremely complex physical mechanisms of turbulent exchange processes and well-known successful attempts to organize them. **The object** of research is the vortical structures of turbulent motion, which arises in flows around surfaces with different geometries and varied relief. **The subject** of study and modeling is methods, which are focused on the influence of mechanisms of generation, diffusion and convection of vortical structures in turbulent near-wall shear flows.

Priority tasks and corresponding approaches of vorticity control. One of investigated workable methods of control is microprofiling the streamlined surface, which is widely distributed in nature (Fig. 1). The most common in technical implementations is a surface microprofiling by longitudinal microgrooves with the triangular, trapezoidal or hemispherical shape of cross-section and sizes, comparable with the viscous sublayer thickness of boundary layer (Fig. 2). These microgrooves have their traditional name – riblets.
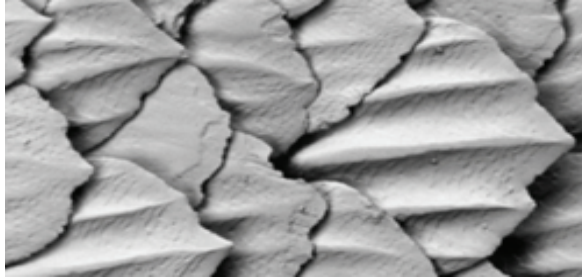

Fig. 1 Skin of adult shark with regular grooved surface – natural realization of microprofile
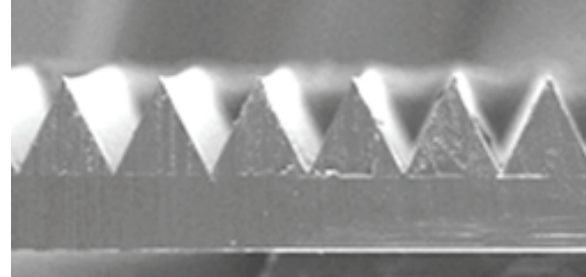

Fig. 2 Riblets – technical implementation of streamlined surface profiling technology

Riblets effect is aimed on modification of small-scale near-wall vortical component of turbulent motion. One explanation of the riblets mechanism is that the regular structure of the surface relief with ribs forms a regularized vortical system (Fig. 3), which damps the transverse components of the disturb pulsating motion [3-5]. The ribbing of streamlined surface with properly selected parameters, accounting the expected modes of operation of the transport vehicle is able to provide a stable reduction of friction drag up to 8% (Fig. 4), and for some conditions even to 15% and more, but the process of optimizing the microrelief geometry requires not only the generalization of experience of experimental studies of different configurations, but also constructing the appropriate mathematical models. These models should be based on the fundamental physical laws, represented in the form of fluid-dynamic equations, reliable approaches for description of the turbulent exchange and vortex generation processes and available information about the delicate effects of interaction of surface microriffling and turbulent flow over it. There are different kinds of algebraic and differential models, which are able to describe some elements of these processes. Thus, the problem of detail mathematical description of this control method is relevant and is considered by authors as one of the main priorities in their further researches.
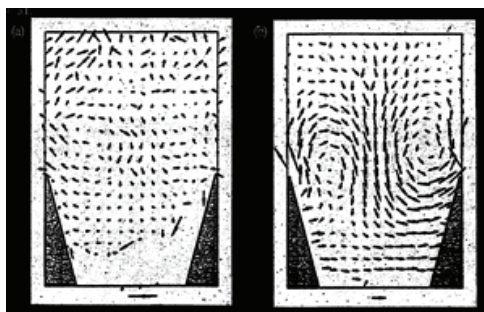
Fig. 3. Secondary vortex structures near the surface with ribs for different flow conditions [3–5]
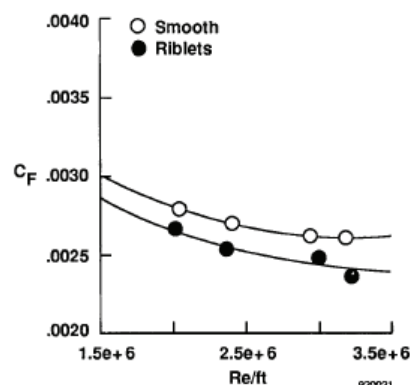
Fig. 4. Reduction of the friction coefficient depending on the aircraft speed at M=1.4 [6]

Another preferred control method, which is investigated by authors, is microelectromechanical systems (MEMS). These systems are steadily gain popularity in various fields of engineering due to the rapid development of electronics, its components miniaturization and steady production costs fall. For transport vehicles MEMS can be considered as one of the

newest and the most promising methods of control due to their abilities to realization of adaptive principle of real time fixing and damping the appearing turbulent disturbances due to simultaneous presence of microsensors, actuators and microprocessors. So, MEMS allow responding immediately on unwanted additional vorticity production processes. Adaptive control principle gives to MEMS a set of more universal abilities for modification of turbulent flows in comparison with other methods, which significantly expands the range of its effectiveness on various modes of transport vehicle motion. The potential benefits of MEMS usage are: improving of efficiency, stall effects preventing, lift increasing and drag reduction. In particular, Fig. 5 demonstrates the experimentally fixed positive effect of MEMS implementation, which is connected with the ability of MEMS significantly reduce drag of streamlined surface with mounted on it vortex generators depending on the frequency and phase of the operation of actuators. As it can be seen that even for some correlations of frequency and phase it is possible to reach such level of drag for this complicated turbulent flow, which is smaller than drag in laminar flow. Therefore, it is apparent that the key to effective MEMS functioning is developing the physically correct algorithm of their operation, which is impossible without understanding the deep principles of turbulent disturb motion together with corresponding mathematical description. On the other side, MEMS, like any complex technology, also have disadvantages that hinder their implementation in life. The basic of them are: the high price at the current stage of development, when it is necessary to cover by small-sizes MEMS devices a significant area of streamlined surface; significant cost and duration of the experimental investigations and as a result, few amount of relevant experimental results. This in turn creates another problem – unknown range of optimal operating conditions in which the positive effect can be achieved; indirect type of influence on the flow through the inhibition of near-wall turbulent disturbances and the need to develop universal and effective control algorithms; the need of MEMS for additional energy consumption can reduce or completely neutralize the positive effect of their use that must be accounted in the process of designing and evaluating the effectiveness of the whole system. In addition, choosing the optimal size of these devices, it is important to consider the balance between their inertial characteristics and frequency range, which preserves their sensitivity and to consider complexity of control performance, reliability and service. So it is possible to conclude that the costs on the research to overcome these problems and time on implementation and optimization can be significantly reduced with the help of application of the mathematical modeling technologies.

Therefore, the development of appropriate mathematical models of turbulent flows, modified by MEMS, is considered by the authors as one of the important areas of their research.

One more important and perspective direction of authors researches, which is also linked with problems of adverse vorticity production and directly related to the objectives of energy and resource saving is a flow around modern urban relief. Constantly increasing of urban density causes to ventilation problems in large cities. This problem is significantly aggravated due to the rapid growth of floors number of modern buildings and the real need to integrate them with the

Fig. 5. Reducing the friction drag coefficient due to MEMS usage [7]

existing building structure, which leads to the formation of complex turbulent vortical structures. So only the existence of mathematical prediction is the key to avoiding mistakes, which are inevitable when using traditional building norms. Experimental methods are based on the use of both precious wind tunnels and test equipment, they require careful and stretched in time models manufacturing
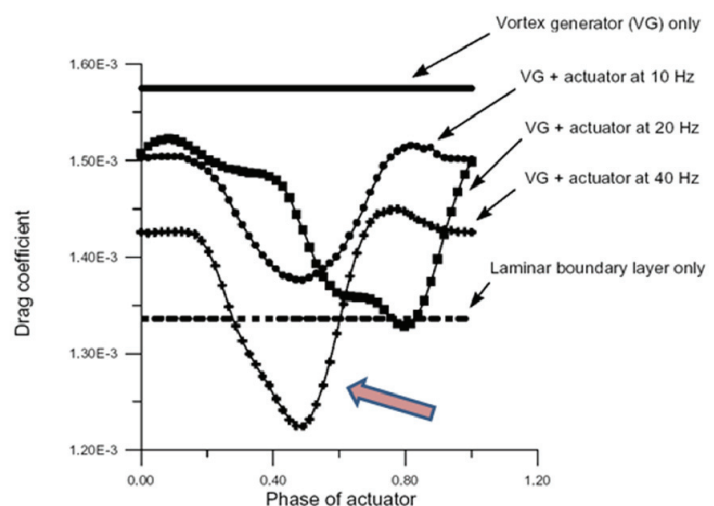
and enforcement of similarity principles during the measurements. All these requirements cannot be realized completely at the same time. These circumstances do not only increase the cost estimate and the project execution of experimental researches, but also force to develop alternative theoretical technologies, which are based on numerical solution of fluid-dynamics governing differential equations. Taking into account the scale of the planetary boundary layer and sizes of the constituent elements of the surface relief the flow mode must be considered as developed turbulent one. These facts and mode complexity greatly increase the level of difficulty of theoretical solving the considering problem and significantly limit and reduce the reliability of experimental methods due to impossibility to recalculate correctly the obtained experimental data to natural conditions. This factor suggests a priority the need to develop appropriate mathematical models of turbulent motion and the corresponding numerical methods for calculating the characteristics of flows developing near the surfaces with complex irregular relief in order to ensure proper accuracy and efficiency of the mathematical simulation of vortical structures and their interaction with both relief peculiarities and each-other, that is a significant scientific problem.

Thus, the authors offer a unique approach to solve a wide range of different problems of classical and industrial aerodynamics, which are combined by presence of turbulent vorticity generating and needs to reduce it with the help of specially designed control methods. This effectively leads to the development of competitive transport vehicles, economical consumption of fuel resources and environmental safety.

Basic principles and foundations of mathematical modeling of the investigated effects.

The basis of mathematical modeling of flows, having the dominant direction of development, is a system of differential equations in the boundary layer approximation:

$$\frac{\partial \overline{u}}{\partial \overline{x}} + \frac{1}{r^{\chi}} \frac{\partial r^{\chi} \overline{v}}{\partial \overline{y}} + \frac{\overline{u}}{u_h} \frac{du_h}{dx} = 0 ; \tag{1}$$

$$\overline{u} \frac{\partial \overline{u}}{\partial \overline{x}} + \overline{v} \frac{1}{r^{\chi}} \frac{\partial r^{\chi} \overline{u}}{\partial \overline{y}} + \overline{u}^2 \frac{1}{u_h} \frac{\partial u_h}{\partial \overline{x}} = -\frac{d\overline{p}}{dx} + \frac{2}{3} \frac{\partial k}{\partial x} + \frac{1}{r^{\chi}} \frac{\partial r^{\chi} \overline{\tau}}{\partial \overline{y}} ; \tag{2}$$

$$\overline{u} \frac{\partial \overline{k}}{\partial \overline{x}} + \overline{v} \frac{1}{r^{\chi}} \frac{\partial r^{\chi} \overline{k}}{\partial \overline{y}} + 2\overline{u}\overline{k} \frac{1}{u_h} \frac{\partial u_h}{\partial \overline{x}} = \frac{1}{r^{\chi}} \frac{\partial}{\partial \overline{y}} \left(r^{\chi} \overline{D}_k^{eff} \frac{\partial \overline{k}}{\partial \overline{y}} \right) + \mathrm{P} - \overline{\varepsilon} ; \tag{3}$$

$$\overline{u} \frac{\partial \overline{\varepsilon}}{\partial \overline{x}} + \overline{v} \frac{1}{r^{\chi}} \frac{\partial r^{\chi} \overline{\varepsilon}}{\partial \overline{y}} + 3\overline{u}\overline{\varepsilon} \frac{1}{u_h} \frac{\partial u_h}{\partial \overline{x}} = \frac{1}{r^{\chi}} \frac{\partial}{\partial \overline{y}} \left(r^{\chi} \overline{D}_{\varepsilon}^{eff} \frac{\partial \overline{\varepsilon}}{\partial \overline{y}} \right) + (C_{\varepsilon 1}\mathrm{P} - C_{\varepsilon 2} f_{\varepsilon} \widetilde{\varepsilon}) \frac{\overline{\varepsilon}}{\overline{k}} , \tag{4}$$

where (1) is continuity equation; (2-4) – transfer equations of the longitudinal velocity component u, kinetic energy of turbulence k and its dissipation rate ε; $C_{\varepsilon 1} = 1.44$, $C_{\varepsilon 2} = 1.92$ – model coefficients; f_{ε} – damping function [10]. Longitudinal axis x is associated with the streamlined surface and has the same direction as the direction of the external flow, and the axis y is perpendicular to the streamlined surface; $r = r_w + y$, where r_w – the radius of the streamlined body; $\chi = 1$ – for bodies of revolution, $\chi = 0$ – for plane surface flow. Equations (1-4) are presented in dimensionless form; $\overline{x} = x/L$, $\overline{y} = y/L$; L – typical linear scale. External flow velocity u_h is a known function of coordinate x; gradient of dimensionless pressure $\overline{p} = p/(\rho u_h^2)$ is determined by the distribution of external velocity u_h according to Bernoulli's equation; ρ – density; v – the normal component of velocity; $\overline{u} = u/u_h$, $\overline{v} = v/u_h$. Dimensionless friction stress $\overline{\tau} = \tau/(\rho u_h^2)$ is modeled by the Boussinesq formula $\overline{\tau} = \overline{V}_{eff} \frac{\partial \overline{u}}{\partial \overline{y}}$, where $\overline{V}_{eff} = \frac{(v + v_t)}{u_h L}$ – dimensionless kinematic coefficient of effective viscosity; v, v_t – kinematic coefficients of molecular and turbulent viscosity respectively. The kinetic energy of turbulence k and its dissipation rate ε were made dimensionless in the following way: $\overline{k} = k/(\rho u_h^2)$, $\overline{\varepsilon} = \varepsilon L/(\rho u_h^3)$. The coefficients of diffusion for

k and ε are: $\overline{D}_{k\,eff} = \dfrac{(v + v_t/\sigma_k)}{u_h L}$, $\overline{D}_{\varepsilon\,eff} = \dfrac{(v + v_t/\sigma_\varepsilon)}{u_h L}$, $\sigma_k = 1.0$, $\sigma_\varepsilon = 1.3$, $P = v_t \left(\dfrac{\partial \overline{u}}{\partial \overline{y}} \right)^2$ – a term

of generation k. The system (1-4) is solved under the following boundary conditions.

On the streamlined surface ($\overline{y} = 0$) or its vicinity ($\overline{y}_* = 30v/(\upsilon_* L)$) for equations (3, 4):

$$\overline{u} = 0, \quad \overline{v} = 0, \quad \overline{k} = \dfrac{\upsilon_*^2}{u_h^2 \sqrt{C_\mu}}, \quad \overline{\varepsilon} = \dfrac{\upsilon_*^3}{u_h^3 k \overline{y}_*}, \quad C_\mu = 0.09; \tag{5}$$

On the external boundary δ, which is determined as $\overline{u} = 0.995 u_h$ ($\overline{y} = \delta$):

$$\overline{u} \to u_h(\overline{x}), \quad \dfrac{\partial \overline{k}}{\partial \overline{y}} \to 0, \quad \dfrac{\partial \overline{\varepsilon}}{\partial \overline{y}} \to 0; \tag{6}$$

In the initial counting cross section ($\overline{x} = \overline{x}_o$):

$$\overline{u} = f(\overline{y}), \quad \overline{k} = \varphi(\overline{y}), \quad \overline{\varepsilon} = \psi(\overline{y}). \tag{7}$$

Functions (7) set the initial profile of the design characteristics, whose source in this study were found by interpolating the available experimental data for $\overline{u}(\overline{y}), \overline{k}(\overline{y})$ with recalculations for $\overline{\varepsilon}(\overline{y})$.

Hybrid turbulence model. Diffusion coefficients for the problems mentioned above are proposed to determine on the basis of hybrid differential-algebraic models of turbulence, which was built by Shkvar [8] on the base of Movchan's algebraic model [9] and differential two-parametric Jones-Launder model [10]. It is important to properly describe the vorticity dynamics for these problems. From the first of these models the basic principle of relationships association for inner and outer regions of the near-wall flow was applied together with well adapted for the turbulent viscosity description in the inner region formula

$$v_t = v_{twake} \,\mathrm{th}\, \dfrac{v_{twall}}{v_{twake}} \tag{8}$$

$$v_{twall} = \chi y_1^+ v \sqrt{\overline{\tau}} D_m, \qquad D_m = \mathrm{th} \dfrac{\mathrm{sh}^2 [\,\chi_1 y_1^+ \sqrt{\overline{\phi}}\,]\,\mathrm{th}[\,\mathrm{sh}^2(\,\chi_2 y_1^+ \sqrt{\overline{\phi}})\,]}{\chi y_1^+ \sqrt{\overline{\phi}}}, \tag{9}$$

where $\overline{\tau} = 1 + \dfrac{dp}{dx} y$ for $\dfrac{dp}{dx} \geq 0$ and $\overline{\tau} = 1 \left/ \left(1 - \dfrac{dp}{dx} y \right) \right.$ for $\dfrac{dp}{dx} < 0$; $\upsilon_* = \sqrt{\tau_w/\rho}$ – shear velocity; $k = 0.4$, $\chi_1 = 0.072$, $\chi_2 = 0.223$ – model coefficients; $y_1^+ = y^+ + \Delta y_{rh}^+$; Δy_{rh}^+ – generalized parameter that takes into account the influence of any kind of streamlined surface roughness and, in particular, regular microrelief. It is expected to account at a sufficient level for practical needs some similar changes in flow properties like modified surface relief due to MEMS installing. The second, differential $k - \varepsilon$ model is locally applied for the outer region, where it is able to predict the characteristics of dynamics of large-scale turbulent vortical structures, namely:

$$v_{twake} = C_\mu k^2 / \varepsilon. \tag{10}$$

Class of differential models in comparison with the algebraic level of turbulence modeling is more reasonable for description of the inertial properties of large-scale turbulent structures in outer region and its response to controlling factors, directed to the large-scale vortices due to modeling processes of the energy balance at the level of corresponding differential transfer equations (3, 4).

It should be noted that the $k - \varepsilon$ model is based on the principle of local equilibrium of turbulence, which loses its validity in approaching to the streamlined surface. So, consequently, the $k - \varepsilon$ model also has low validity in the vicinity of the surface that is a traditional reason for insertion of damping functions f_μ and f_ε together with modifications of the right sides of equations (3, 4) by special additional source terms, which are significant only near the wall. This approach due to the lack of physical background of the damping has been realized in several different low-Reynolds versions of the $k - \varepsilon$ model. Primarily, they allow achieving the required mathematical asymptotic of characteristics, modeled near the streamlined surface. In the proposed approach the factor $\mathrm{th}(v_{twall}/v_{twake})$ of algebraic model (9) can also be considered as a damper of

$k - \varepsilon$ model (similar to traditionally used functions f_μ [10]), but this damper has much more intelligent features that allow to reproduce the effects of several methods of near-wall control of small-scale vortical structures.

Thus, the proposed combination of two different approaches provides only the local intervals of use for each of the combined models, where they are most reasonable and applicable according to their structures. This gives the reason to hope that the proposed hybrid model will be able to realize its advantages for discussed above problems, where the dynamics of turbulent vortical structures is one of the most important factors.

Conclusions

3. The set of actual problems of turbulent near-wall flows modeling and their control has been highlighted and analyzed. The most significant common physical mechanism has been selected - the generation and further dynamics of turbulent vortical structures.

4. The efficiency of traditional experimental and perspective numerical methods of flow analysis has been examined for three different realizations of vortical motion, including regular and irregular relief of streamlined surface and MEMS. The difficulties of practical implementation of modern methods of flow control have been analyzed. The actuality of elaborating the appropriate mathematical models has been justified from the standpoint of efficient optimization of geometry and operating parameters of facilities that provide the technical implementation of boundary layer control technique.

5. The basis for the mathematical model description of the considered flow control methods is proposed in the form of a method of constructing the hybrid differentially-algebraic turbulence models, which effectively combines two different approaches of turbulent viscosity modeling and the most adapted for describing the different scale properties in the inner and outer regions of the near-wall shear flows.

References

1. *Reneaux J.* Overview of drag reduction technologies for civil transport aircraft. / J. Reneaux // ECCOMAS. – 2004. – 18 p.

2. *Argüelles P.* Report of the group of personalities. European Aeronautics: a vision for 2020. / P. Argüelles, J. Lumsden, M. Bischoff et al. // European Aeronautics. – 2001. – 26 p.

3. *Suzuki Y.* Turbulent Drag Reduction Mechanism above a Riblet Surface / Y. Suzuki, N. Kasagi // AIAA Journal. – September, 1994. – Vol. 32, № 9. – P. 1781–1790.

4. *Suzuki Y.* Drag Reduction Mechanism on Micro-grooved Riblet Surface / Y. Suzuki, N. Kasagi // Proc. of the Int. Conf. on Near-Wall Turbulent Flows, Temple. – 1993. – 10 p.

5. *Suzuki Y.* On the Turbulent Drag Reduction Mechanism above a Riblet Surface / Y. Suzuki, N. Kasagi // AIAA 93-3257 AIAA Shear Flow Conference, Orlando. – 1993. – 11 p.

6. *Zuniga F.A.* Flight test results of riblets at supersonic speeds / F.A. Zuniga, B. T. Anderson, A. Bertelrud. // NASA technical memorandum 4387. – June 1992. – 37 p.

7. *Tsao T.* An integrated MEMS system for turbulent boundary layer control / T. Tsao, F. Jiang, Y. Tai et al. // Int. conf. on solid-state sensors and actuators. – 1997. – P. 315 – 318.

8. *Шквар Є.О.* Фізичне та математичне моделювання напівобмежених турбулентних струменевих течій на оребрених поверхнях / Є.О. Шквар, Т.В. Козлова, А.О. Бондарець // "Промислова гідравліка і пневматика". – 2011. – №1(31) – С. 35-41.

9. *Мовчан В.Т.,* Математические модели турбулентной вязкости в расчетах пристенных течений / В.Т. Мовчан // Сб. науч. трудов "Аэрогидродинамика: Проблемы и перспективы", Национальный аэрокосмический университет "ХАИ", 2006. – с. 272-286

10. *Launder B.E.* Mathematical Models of Turbulence / B.E. Launder, D.B. Spalding // Academic Press London and New Work. – 1972. – 162 p.

M.S. Kulyk, Dr.,Pr., NAU,Ukraine,
O.G. Kucher, Dr.,Pr., NAU,Ukraine,
M.O. Koveshnikov, PhD, NAU,Ukraine,
S.S. Dubrovsky, PhD, Kryvyi Rih NTU,Ukraine,
Y.A. Petruk, Ukraine

MATHEMATICAL MODEL OF LONG-TERM STRENGTH OF MATERIALS HEAT RESISTANT AIRCRAFT ENGINES

The characteristics of the long-term strength of heat-resistant materials ЕІ437БВД, ЖС6К, ЖС6У, ЕП99 and Х18Н10Т are in the article. These characteristics are often used for manufacturing details of the "hot part" of gas turbine engines. Analytically described characteristics can be used for the calculation of estimation of durability of parts of aircraft engines and other power plants working in high and slowly varying temperature conditions, as well as in conditions of cyclic "starts and stops".

Problem statement

The calculations of long-term durability of parts "hot parts", operating under conditions of thermal changes is not always easy to use reference characteristics of long-term durability data presented linear, long-term strength of the level of pressure at fixed temperature level. Therefore the main task of the paper is an analytical approximation of long-term strength characteristics that allow them to be used for any intermediate and variable temperatures and significantly improve the accuracy of calculations on durability of parts "hot parts" GTE.

The method of statistical analysis and processing characteristics of long-term strength of materials

The equation of the family long-term strength curves for different material constant temperature can be obtained by analytical description of the experimental data.

In figure 1 shows data of experimental studies of long-term strength of alloy ЭИ437Б borrowed from [1-6]. As this figure comes from the results of the experiment are significant variation that leads to the need for statistical processing methods. To use these methods to establish the law of distribution of material durability.

In accordance with the guidelines given in [1-7], the distribution of material durability in long-term static load should describe the logarithmically normal law.

Log normal distribution density durability τ is expressed following relation:

$$\varphi\left(\tau\right) = \frac{\lg e}{\tau\sqrt{2\pi D_{\lg\tau}}}\exp\left[-\frac{\left(\lg\tau - M_{\lg\tau}\right)^2}{2D_{\lg\tau}}\right] \tag{1}$$

Parameters of this distribution depend on the level of stress. In particular, (as follows from fig. 1), Expectation logarithm of durability can take a linear function of stress $\sigma_{\partial m}$:

$$M_{\lg\tau} = a + b\sigma_{\partial m}, \tag{2}$$

where a, b – coefficients.

Variance of the logarithm of durability for the data presented in figure 1, should be considered independent of strain, i.e. take

$$D_{\lg\tau} = S^2 = \text{const} \tag{3}$$

Combining equation (11) and (12), we find

$$\varphi\left(\tau\!\!\diagup\!\!_{\sigma_{\partial m}}, a, b, S\right) = \frac{\lg e}{\tau\cdot S\sqrt{2\pi}}\times\exp\left[-\frac{\left(\lg\tau - a - b\cdot\sigma_{\partial m}\right)}{2S^2}\right]. \tag{4}$$

The most effective method for estimation of parameters a, b, S distribution (4) is the method of maximum likelihood [7], which involves minimizing dependent on these parameters likelihood function:

$$L = \prod_{i=1}^{n} \varphi_i (a, b, S) \to \min ,\qquad\qquad (5)$$

where n is number of experimental values of durability of the material for some temperature.
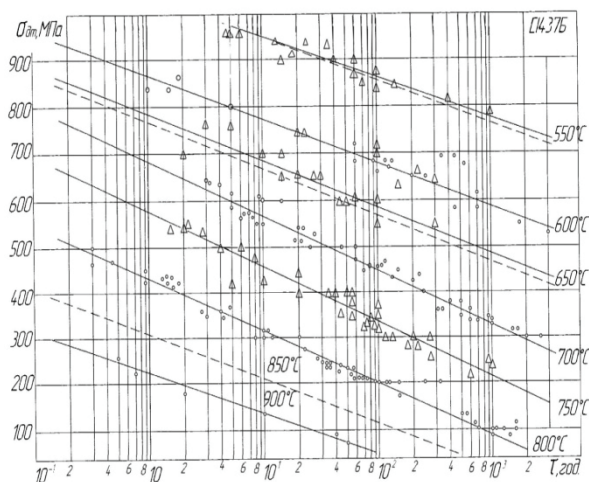
Figure 1– Characteristics of long-term strength of alloy ЭИ437Б; data for temperature, ^{0}C:

Figure 2 – Dependence of distribution parameters for the temperature alloy ЭИ437Б Δ –550, 650, 750, ∘ - 600, 700, 800, 900; —— – experimental depending; – – – calculation dependence

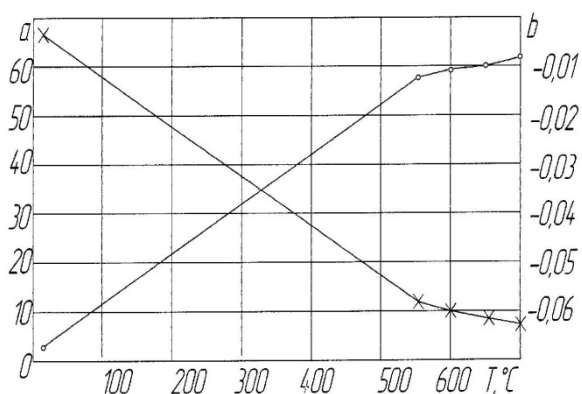Figure 3 – Dependence of parameters of the equation long-term strength curves of the temperature alloy ЭИ437Б
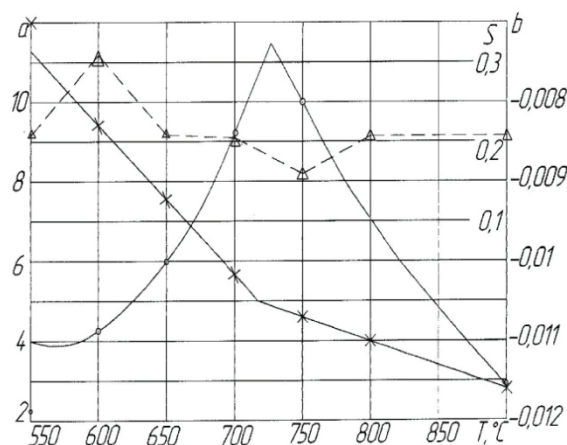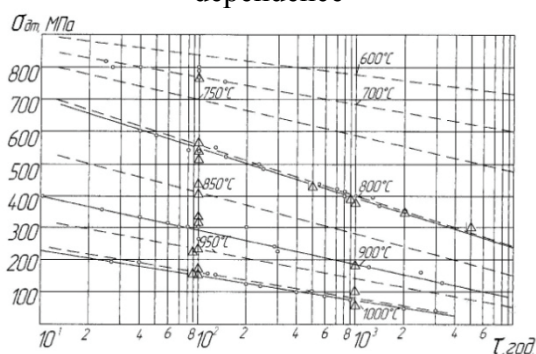

Figure 4 – Characteristics of long-term strength of alloy ЖС6К; data for temperature, °C:
∘ - taken from [12,13]; Δ - taken from [6,7] ; —— experimental curves; – – – calculation curves

Requirement (5) equality is equivalent to:

$$\frac{\partial \ln L}{\partial a} = \frac{\partial \ln L}{\partial b} = \frac{\partial \ln L}{\partial S} = 0, \qquad (6)$$

this is a system of equations for the parameters a, b, S.

For distribution (4) system (6) has the form:

$$\left. \begin{array}{l} \sum_{i=1}^{n} \lg \tau_i - na - b\sum_{i=1}^{n}(\sigma_{\partial m})_i = 0; \\[2mm] \sum_{i=1}^{n}(\sigma_{\partial m})_i \lg \tau_i - a\sum_{i=1}^{n}(\sigma_{\partial m})_i - b\sum_{i=1}^{n}(\sigma_{\partial m})_i^2 = 0; \\[2mm] \sum_{i=1}^{n}\left[\lg \tau_i - a - b(\sigma_{\partial m})_i\right]^2 - n \cdot S^2 = 0. \end{array} \right\} \qquad (7)$$

Solving system of equations (7), we find

$$b = \frac{n\sum_{i=1}^{n}(\sigma_{\partial m})_i \lg \tau_i - \sum_{i=1}^{n}(\sigma_{\partial m})_i \cdot \sum_{i=1}^{n}\lg \tau_i}{n\sum_{i=1}^{n}(\sigma_{\partial m})_i^2 - \left[\sum_{i=1}^{n}(\sigma_{\partial m})_i\right]^2}; \qquad (8)$$

$$a = \frac{1}{n}\left[\sum_{i=1}^{n}\lg \tau_i - b\sum_{i=1}^{n}(\sigma_{\partial m})\right]; \qquad (9)$$

$$S^2 = \frac{1}{n}\sum_{i=1}^{n}\left[\lg \tau_i - a - b(\sigma_{\partial m})_i\right]^2. \qquad (10)$$

The formula (8) - (10) using the data in figure 1 parameters of distribution (4) for alloy ЭИ437Б shown in figure 2 with corresponding temperature dependences. As follows from figure 1, standard deviation of the logarithm of longevity S with the change of temperature shows no trend to change, and therefore this option can be taken constant in the considered range of temperature and equal to S ≈ 0.2. In the temperature dependences of parameters of equation (2) *a* and *b* there are clear trends, and these dependencies are fractures in the temperature region 720 ÷ 725 ° C. specified fractures reflect a sharp change in strength properties of the material, due, perhaps, phase transformations.

In figure 2. turns out that the dependence of a on temperature can be approximated by equations of the two segments of straight lines. However, using the absolute value of the property, these segments can be described by one common equation that has the form (8)

$$a = 23,1815 - 0,025255\,T + |8,6915 - 0,012135\,T|. \qquad (11)$$

Presented in figure 2. dependence $b(T)$ should be approximated by two polynomials of the second order, or by using the absolute value of the property, one equation of the form:

$$b = \left(383,473 - 1,338474T + 9,79304\cdot10^{-4}\cdot T^2 - |5,49486\cdot10^{-4}T^2 - 0,392786T - 3,711|\right)\cdot10^{-4} \qquad (12)$$

The obtained value (11) (12) together with equation (12) describe a family of long-term strength curves ЭИ437Б alloy in the temperature range 550÷900 °C. With these correlations in figure 1. calculated curves based long-term strength are indicated by dashed lines for temperatures 550, 650 and 850 °C.

In the temperature range 20 ÷ 550 °C depending on parameters of equation (2) Adopted for the temperature alloy ЭИ437Б linear (see fig. 3). For these dependences obtained the following relation:

$$\left. \begin{array}{l} a = 71,2 - 0,11T; \\[2mm] b = -0,688 + 0,001036T \end{array} \right\} \qquad (13)$$

The method of constructing mathematical models of long-term strength characteristics was used in the work for the rest of the studied materials: ЖС6К, ЖС6У, ЭП99ВД, Х18Н10Т.

Results of experimental studies long-term strength alloy ЖС6К collected according to the papers [6, 7] shown in figure 4.

These data, using the parameters of distribution (4), indicated in figure 5 points on the

respective temperature dependences. As a result of the analysis show the relationship between *a*(*T*) and *b*(*T*) is approximated by linear equation (11). These equations are presented in table 1, which also indicated the limits for deviations medium square aqueous logarithm of durability.

Experimental data of long-term strength of alloy ЖС6У taken from. The data presented in figure 6, and the corresponding parameters of the distribution (4) – figure 7.

Approximating formulas for the dependences *a (T)* and *b (T)*, and the extent of change of parameter S are summarized in Table. 1.

In figure 8 built long-term strength curves for alloy ЭП99ВД this work [3].

Dependences of *a (T)*, *b (T)* and *S (T)* for this alloy are shown in figure 9. Approximating functions for parameters of long-term strength curves of equation (2) are as in figure 1.

Table 1

Approximating functions for parameters of the equation
long-term strength curves

| Material	The equations for the parameters *a* and *b*	S
ЭИ437Б	$a = 71,2 - 0,11T; b = -0,688 + 0,001036\,T$ (at T = 20÷550 °C); $a = 23,1815 - 0,025255T + \left\|8,6915 - 0,012135T\right\|$ (at T = 550÷900 °C); $b = \left(\begin{array}{c} 383,473 - 1,338474T + 9,79304\cdot10^{-4}\cdot T^2 - \\ -\left\|5,49486\cdot10^{-4}T^2 - 0,392786T - 3,711\right\| \end{array} \right)\cdot10^{-4}$	0,15÷0,3
ЖС6К	$a = 31,03602 - 0,0319973T \div \left\|19,70507 - 0,0246871T\right\|$ $b = \left(0,0123598T - 16,0853 - \left\|0,0433511T - 34,6767\right\|\right)\cdot10^{-3}$ (at T = 600÷1000°C);	0,075÷0,15
ЖС6У	$a = 20,12495 - 0,016589T \div \left\|7,86305 - 0,0087368T\right\|$ $b = \left(9,7805 - 0,0205985T - \left\|0,0351485T - 31,6335\right\|\right)\cdot10^{-3}$ (at T = 800÷1100°C);	0,1÷0,2
ЭП99ВД	$a = 30,0697 - 29,4057\cdot10^{-3}T - \left\|4,5412\cdot10^{-3}T - 4,0871\right\|$ $b = -\left(10,4385 \div 3,19\cdot10^{-3}T \div \left\|8,2843\cdot10^{-3}T - 7,45585\right\|\right)\cdot10^{-3}$ (at T = 700÷1000°C);	0,2÷0,25
X18H10T	$a = 38,1925 - 0,0564443T \div \left\|22,0271 - 0,0402606T\right\|$ $b = \left(0,0975971T - 69,3924 - \left\|0,129843T - 71,4136\right\|\right)\cdot10^{-3}$ (at T = 500÷900°C);	0,12÷0,24
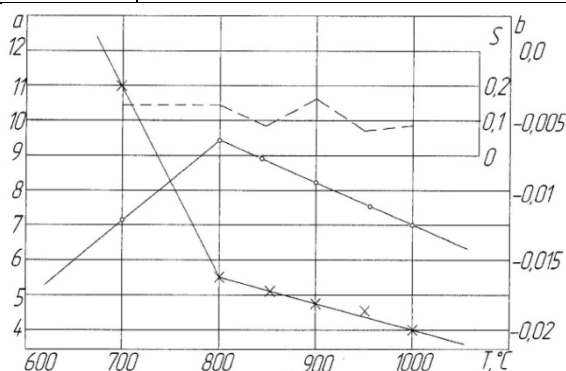
Figure 5 – Dependences of the parameters
for the distribution of temperature alloy
ЖС6К
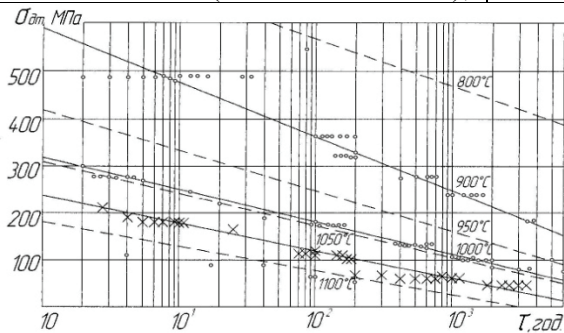
Figure 6 – Characteristics of long-term strength
of alloy ЖС6У: data for temperature, °C:
° - 800, 900, 1000, 1100; × - 1050;—— experimental
curves; – – – calculated curves

For stainless steel X18H10T (fig. 10) experimental data from long-term strength borrowed from [3]. Temperature dependences of the parameters of equation (11) are the same as for previous materials approximated by linear functions (see table 1).

With the help given in table 1 equations and correlation (11) figure 4, *c*, figure 6, figure 8, figure 10 calculated curves based long-term strength of materials, which, as it shows good agreement with experimental data.
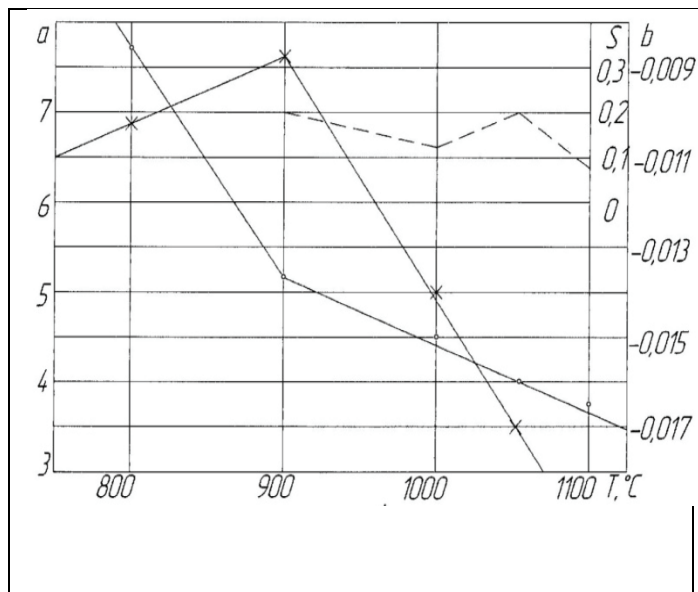
Figure 7 – Dependence of distribution parameters for the temperature alloy ЖС6У	Figure 8. Characteristics of long-term strength of alloy ЭП99ВД: ——— experimental curves; – – – calculated curves
Figure 9 – Dependence of parameters for the distribution rafting ЭП99ВД temperature	Figure 10 Characteristics of long-term strength of alloy X18H10T: ——— experimental curves; – – – calculation curves
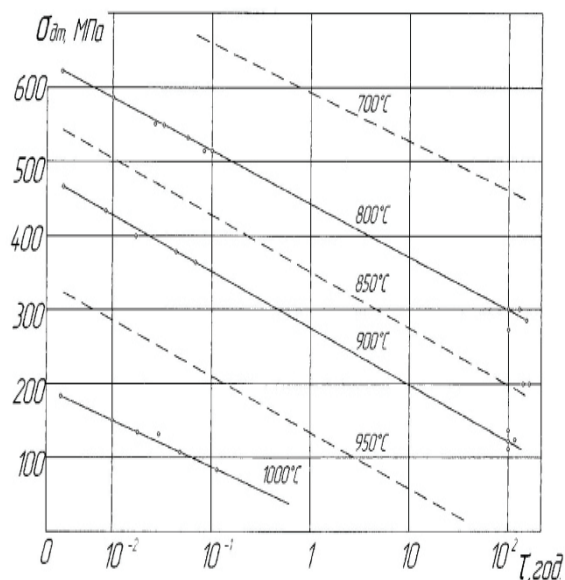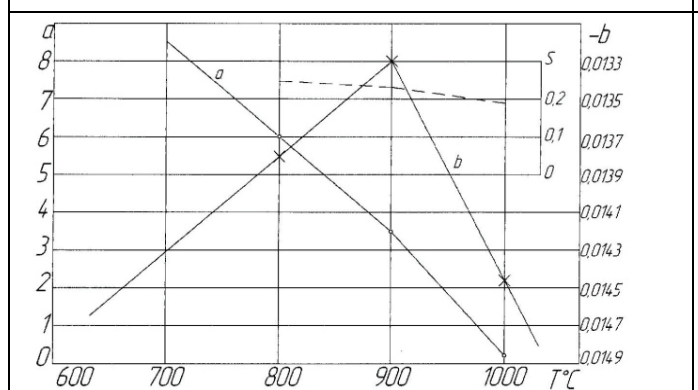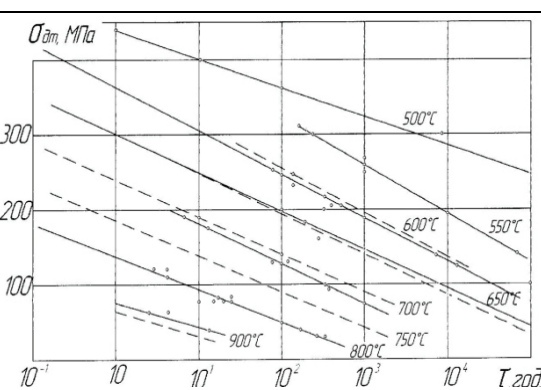
Conclusions

1. These equations of curves long-term durability can be used to implement proposed in the article method of calculating the durability of materials thermocyclic hypothesis of linear damage sum for the approximate evaluation of the resource details "hot parts" of aviation GTE.

2. These equations and extrapolation characteristics of long-term durability may be used for accurate assessment of durability of parts "hot parts" GTU operating in the stationary or quasistationary modes in a wide range of operating temperatures.

3. The method of analytical approximations of the characteristics of long-term durability also can be used to describe new high-temperature materials.

References

1. *Справочник* по авиационным материалам. – М.: Машиностроение, 1965. – 632 с.
2. *Химушин Ф.Ф.* Жаропрочные стали и сплавы/ Ф.Ф. Химушин. – М.: Металлургия, 1969. 2-е изд. – 752 с.
3. *Дульнев Р.А.* Термическая усталость материалов /Р.А. Дульнев. – М.: Машиностроение, 1971. – 63 с.
4. *Справочник* по авиационным материалам и технологии их применения. – М.: Транспорт, 1979. – 242 с.
5. *Веронский А.И.* Термическая усталость материалов / А.И. Веронский. – М.: Машиностроение, 1986. – 129 с.
6. *Арзамасов Б.Н.* Конструкционные материалы / Б.Н. Арзамасов, В.А. Бростем, Н.А. Буше и др.; Под общ. ред. Б.Н. Арзамасова. – М.: Машиностроение, 1990. – 688 с.
7. *Адамович В.К.* Сопоставление методов экстраполяции длительной прочности / В.К. Адамович, Я.Ф. Фридман, М.Б. Ревзюк, А.В. Станюкович. – К.: Пробл. прочности, 1975. – № 11. – С. 26.–29.

UDC 629.735.083.02.06(045)

Y. Tereshchenko, Dr. of Sci (Engineering) (National Aviation University, Ukraine)
Y. Tereshchenko, Ph. D. of NAU (Engineering) (National Aviation University, Ukraine)
K. Doroshenko, Ph. D.(Engineering) (National Aviation University, Ukraine)
L.Volyanskaya, Ph. D.(Engineering) (National Aviation University, Ukraine)

CRITICAL MODES OF FLOW IN AIRFOIL CASCADE

Flow of viscous compressible gas is considered in the airfoil cascade with big negative angles of attack. Influence of wall boundary layer upon the flow stall modes is estimated in the article.

Introduction

Aerodynamic research of the compressor stages begins with calculation of the air flow in elementary stages, are designed as airfoil cascades.

Characteristics of the axial-flow compressor stages and modes' of operation typical restrictions, are determined by using cascade aerodynamic characteristics.

The modes of operation main restrictions are of such types: restrictions for gasdynamic stability, are caused by flow separation under big positive angles of attack, and compressor stage stall modes for the air consumption.

Separation flows are widely spread in nature and practice, description of them plays important role in engineering calculations. Separation appears in the result of viscous-nonviscous interaction between flow layers, that is why viscous processes, as well as nonviscous should be exactly modeled to foresee flow separation. Processes interact nonlinear, this fact have to take into account.

It is well known, that position of a separation point depends on boundary layer condition in front of interaction zone.

Turbulent boundary layer is more stable for separation than laminar, because viscous displacing tension, that has counteracted to pressure gradient is higher. Therefore, during separation flows research it is necessary to consider and to model at quite exactly level condition of boundary layer.

Researches and publications analysis

On the Fig. 1 airfoil cascade characteristic in the ideal gas flow was represented. It allows to evaluate an appearance of the flow stall modes depend upon the relation of the throat crosscut flow area to the normal crosscut flow area at the entry into cascade (F_{Γ} / F_1).
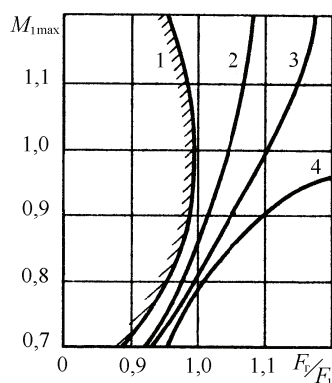
Fig. 1. Dependence of the M_{max} values from the relation of F_{Γ} / F_1: 1 – theoretical attitude(experiment); 2 – supersonic cascade(experiment); 3 – transonic cascade(experiment); 4 – subsonic cascade(experiment).

The wall boundary layer is formed on a plates surface under real gas flow. Throat crosscut flow area of the blade channel becomes lower, this influences on flow mode and appearance of the stall mode.

Target setting

Influence of flow compressibility and viscousity is taking into account to foresee need of quite exact definition of the separation zones' arrangement and intention, also to correct pitch angle and the cascade density, which is calculated for nonviscous flow under different M numbers.

The goal of this research was to define real flow viscosity influence level on stall modes. Target setting like this allows to analyze exactly viscosity influence on stall modes of the airfoil cascade without taking features of aerodynamic plates form into account(plates "bodily").

Geometrical parameters of the airfoil cascade(cascade density $\dfrac{t}{b}$; plates pitch angle γ), are corresponded to similar parameters for aerodynamic plates cascade. Choking modes overall performance. Air flow under this modes can be divided into confusor (up to throat) and diffuser (after throat) sections (Fig. 2). If the air flow in the blade channel's throat area corresponds to condition $w_T = a_{cr}$, there will be stall mode with maximum possible air consumption.
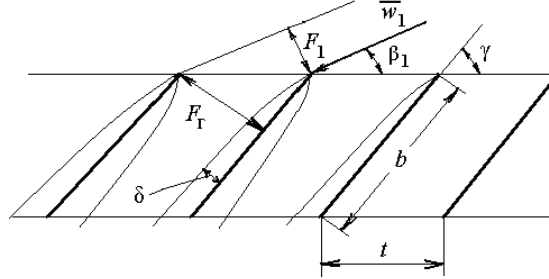
Fig. 2. The airfoil gratings scheme

On the Fig. 2 flow parameters are designated: w_1– is the velocity vector on cascade input; γ– is the plate pitch angle; β_1 – is the angle of attack; b – is the plate chord; t – is the grid spacing; F_1 – is the normal crosscut flow area at the entry into cascade; F_r –is the blade channel throat flow area; δ – is the boundary layer thickness on the profile surface.

Analysis of viscous compressible gas flow in the airfoil cascade

Let's examine gas flow in the cascade of the thin plates (Fig. 1) for two cases: nonviscous compressible gas flow and viscous compressible gas flow.

To the first case consumption equation for sections F_1 and F_r is written down in the form of:

$$mF_1 \frac{P_1^*}{\sqrt{T_1^*}} q(\lambda_1) = mF_r \frac{P_D^*}{\sqrt{T_D^*}} q(\lambda_D),$$

where m – air consumption coefficient, considers features of actuating fluid's physical property,

equal: $m = \left(\dfrac{2}{k+1}\right)^{\frac{k+1}{2[k-1]}} \sqrt{\dfrac{k}{R}}$; R – is the gas constant; F_1 – is the normal crosscut flow area at the entry into cascade; F_D –is the blade channel throat flow area; P_1^*, T_1^* – is the impact pressure and temperature in F_1 crosscut; P_r^*, T_r^* – is the impact pressure and temperature in F_D crosscut; $q(\lambda_1)$, $q(\lambda_r)$ –relative current density in characteristic crosscut.

From equality $P_1^* = P_r^*$ and $T_1^* = T_r^*$ we get:

$$\frac{q(\lambda_r)}{q(\lambda_1)} = \frac{F_1}{F_r} = \frac{t \cdot \sin \beta_1}{t \cdot \sin \gamma} \; ; \quad \frac{q(\lambda_r)}{q(\lambda_1)} = \frac{\sin \beta_1}{\sin \gamma}; \quad q(\lambda_1) = q(\lambda_r) \frac{\sin \gamma}{\sin \beta_1}.$$

Value of the consumption function in F_1 crosscut, corresponds to the flow stall mode in throat F_T is written down in the form of: $q(\lambda_1) = \dfrac{\sin \gamma}{\sin \beta_1}$.

Quantity $M_{max} = \dfrac{w_1}{a}$, corresponds to the appearance of stall flow in the blade channel throat, is written down in the form of:

$$M_{max} = \left(\frac{\frac{k+1}{2}}{1 + \frac{k-1}{2} M_{max}^2} \right)^{\frac{k+1}{2(k-1)}} = \frac{\sin \gamma}{\sin \beta_1}.$$

To the second case equation of continuity with taking boundary layer into account, is written

down in the form of: $mF_1 \dfrac{P_1^*}{\sqrt{T_1^*}} q(\lambda_1) = m(F_r - \delta^*) \dfrac{P_r^*}{\sqrt{T_r^*}} q(\lambda_r)$, where $\delta^* -$ boundary layer displacement thickness in F_t cross section.

From equality $P_1^* = P_r^*$ and $T_1^* = T_r^*$ we get:

$$\frac{F_1}{(F_r - \delta^*)} = \frac{q(\lambda_r)}{q(\lambda_1)}; \quad \frac{t \cdot \sin \beta_1}{(t \cdot \sin \gamma - \delta^*)} = \frac{q(\lambda_r)}{q(\lambda_1)}; \quad \frac{\sin \beta_1}{\left(\sin \gamma - \dfrac{\delta^*}{t}\right)} = \frac{q(\lambda_r)}{q(\lambda_1)}.$$

To the stall mode under: $q(\lambda_r)=1$ Derivable:

$$q(\lambda_1) = \frac{\left(\sin \gamma - \dfrac{\delta^*}{t}\right)}{\sin \beta_1}. \tag{1}$$

where $\dfrac{\delta^*}{t}$ is the relative boundary layer displacement thickness on the profile surface in the throat area; t - the grid spacing $\left(t = b \cdot \left(\dfrac{t}{b}\right)\right)$; b - the profile chord; $\dfrac{t}{b}$ is the cascade density.

For the viscous gas flow the cascade stall mode is defined by algebraical expression:

$$M_{max} = \left(\frac{\dfrac{k+1}{2}}{1 + \dfrac{k-1}{2} M_{max}^2}\right)^{\frac{k+1}{2(k-1)}} = \frac{\sin \gamma - \dfrac{\delta^*}{t}}{\sin \beta_1}. \tag{2}$$

To evaluate the influence of the boundary layer parameters on the stall modes, we use the determination method of turbulent boundary layer's integral characteristics in the blade channel throat. Calculation formula:

$$\delta_r = kx_r \cdot \frac{1}{\sqrt[5]{Re_r}}.$$

Where: x_r is the coordinate of the throat channel (from the profile nose); k is the coefficient characterizing geometric parameters of the cascade and is defined by data of experimental researches (for cascade of the thin plates with grating density of $\dfrac{b}{t} < 1.5$ and the coefficient of $k \approx$ 0.37); $Re_r = \dfrac{w \cdot x_r}{v}$ is the Reynolds criterion for the point with coordinate of x_r.

The displacement thickness for crosscut in the blade channel throat can be defined by formula:

$\delta_r^* = \delta_r \cdot \dfrac{1}{n+1}$, where the coefficient $n = 1.43 \ldots 2.5$.

For the cascades with grating solidity $\dfrac{b}{t} = 0.8 \ldots 1.5$ chord $b = 80 \ldots 120$ mm, angle of pitch $\gamma = 38 \ldots 45°$, flow parameters correspond to the numbers of $Re = 3 \ldots 5 \cdot 10^5$, impulse losses thickness $\delta = 0.3 \ldots 0.4$ mm. Based on the fact, that boundary layer integral characteristics are interrelated by formula:

$$\frac{\delta^*}{\delta^{**}} = \frac{2+n}{n}, \tag{3}$$

The displacement thickness of the boundary layer in the cross section of the blade channel throat is: $\delta^* = \delta^{**} \cdot \dfrac{2+n}{n} = 0,76 \ldots 0,92$ mm.

We receive the M_{max} values by formula (2) taking into consideration displacement thickness of the boundary layer by formula (3) and can evaluate gas viscosity influence on stall of axial-flow compressor stages. Fig. 2 shows the M_{max} values, are calculated for nonviscous gas flow in the airfoil cascade by following dependence:

$$M_{max} = f\left(\frac{F_{\text{г}}}{F_1}\right).$$

Fig. 3 shows calculation dependences of M_{max} values for the flow without taking boundary layer into consideration, and M^*_{max} values with taking boundary layer into consideration

Analysis of these dependences proves that throat channel stall under significant reduction of speed values at the cascade entrance takes place, as a result of the viscous real flow influence. In the airfoil cascade, discrepancy of M_{max} and M^*_{max} values is from 5 to 15%.
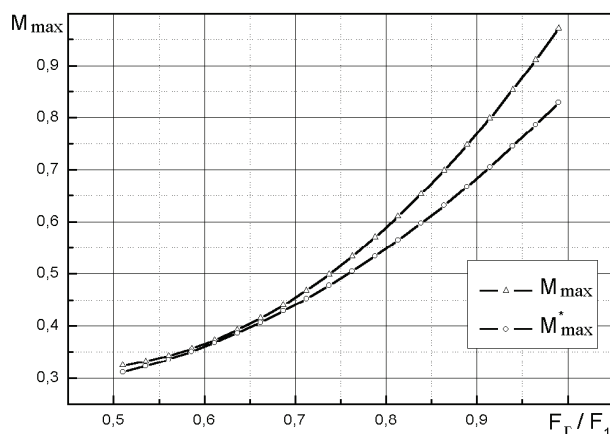
Fig. 3. Dependence of the M_{max} values from the relation of F_{T}/F_1

The M^*_{max} values had defined with the help of the formulas (1) and (2) under quality signs contemporized with the experimental research results, that are shown on Fig. 1 (curves 2-4). Continuation of researches in this direction should be oriented to determine the calculation dependences to evaluate flow viscosity influence on subsonic and supersonic airfoil cascades characteristics.

Conclusions

1. Offered method allows evaluating the estimation of the flow viscosity influence on cascade aerodynamic characteristics during streamline of them with the big negative angles of attack. Comparison of stall modes characteristics for the airfoil cascade and experimental data for aerodynamic profiles proves that offered method of calculation is correct enough.

2. Taking into account flow viscosity leads to lowering the M_{max} calculation value, corresponds to the compressor cascade stall mode for the air consumption. For the airfoil cascade the M_{max} and M^*_{max} values discrepancy is from 5 to 15%.

3. The aim of the further research is to obtain results and to analyze the influence of peculiarities of the aerodynamic form of cascade blades profiles on the grating blocking modes in the viscid gas flow.

<div align="center">Reference</div>

1. *Терещенко Ю.М., Мітрахович М.М.* Авіаційні газотурбінні двигуни. – К.: КВІЦ, 2001. – 312с.

2. *Терещенко Ю.М.* Аэродинамика компрессорных решеток. – М.: Машиностроение, 1979. – 120с.

3. *Терещенко Ю.М.* Аэродинамическое совершенствование лопаточных аппаратов компрессоров. – М.: Машиностроение, 1987. – 168с.

UDC 629.7.036(075.8)

Y. Tereshchenko, Dr. of Sci. (Engineering), (NAU, Ukraine),
L. Volyanskaya., Ph.D.(Engineering), (NAU, Ukraine),
E. Doroshenko, Ph.D.(Engineering), (NAU, Ukraine)
I. Lastivka, Ph.D.(Engineering), (NAU, Ukraine)

AERODYNAMIC CHARACTERISTICS OF TANDEM SUBSONIC COMPRESSOR CASCADE

Method determination of aerodynamic forces by direct measurement using three-component aerodynamic balance is given in the article. Investigation of separated airfoils and foil cascades were carried out for a given range of the angle of attack. Comparison flow around the airfoils displays increase of non-stalling flow range

Introduction

Improvement of compressor parameters and characteristics is based on understanding of physical processes which determine aerodynamic characteristics of compressor cascade. From correlation of Howell [1] to present day the using of correct model (physical model, mathematical model) and assumptions in studies of compressor cascade aerodynamic characteristics allow to estimate efficiency of different effects on flow.

One of interesting and important ways to increase compressor efficiency and range of no stall flow is tandem compressor cascade application. Effect of boundary layer control in the channel with adverse pressure gradient is used in this compressor cascade.

The geometry and aerodynamic parameters for a tandem blade row are almost the same as those used for single airfoils, but the problem of cascade parameter and operation mode optimization has simple solution for single airfoils. It is solved such that efficiency of cascade $\eta_{\text{реш}}$ is maximum or lift-drag ratio $k_{\max}=\dfrac{c_y}{c_x}$ is maximum. The problem of parameter and mode operation optimization is intricate problem for tandem compressor cascade because there are flow interactions in the blade passage.

The purpose of this investigation was experimental determination of aerodynamic characteristics of tandem subsonic compressor cascade by direct measurement of forces and moments acting on the airfoil under subsonic cascade flow and evaluations various aerodynamic performance of a single and a tandem cascade for a wide range of inlet angles.

Experimental equipment, method of investigation.

Experiments were carried out in wind tunnel UTAD-2 of National Aviation University. The experimental facility is closed atmospheric wind tunnel. Open working area is elliptical and this zone size is 750×450×900mm, general view of working area with test object is given on fig.1. The fan with direct current motor is after diffuser. The motor power is 2 kWatt. The motor has system of continuously adjustable rotational speed. The system maintains air flow of constant velocity (within the limits of 5-30 m/s) in the working area.

Wind tunnel UTAD-2 is equipped 3-component mechanical wind-tunnel balance with dipstick and manual control for measuring aerodynamic loads. The wind-tunnel balance allows measuring three components of aerodynamic force in vertical plane acting upon a body tested in wind tunnel. There is embedded mechanism for measuring angle of attack. The range of angle of attack is i=-20 ... +40°. Dynamic head is measured with a liquid manometer having inclined tube MMN-240.

Unlike usual procedures in this research aerodynamic forces were determined by means of direct measurement in three-component balance. Research was carried out for separate airfoils and for cascades to ascertain flow features in the channel between blades of first and second rows and influence of air stream coming from blade channel on streamline character.
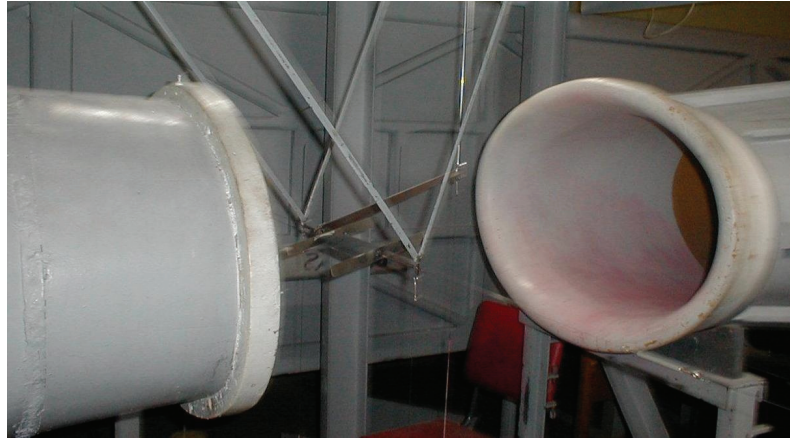
Fig.1. General view of working area with test object

Though aerodynamic parameters for a tandem blade row are the same as those used for single airfoils, but two additional variables appear in the arrangement. These variables are the axial displacement and the tangential displacement and a tandem airfoil can be treated in two different ways:
- single blade specification: the single blade parameters corresponding to the front and rear profiles of a tandem blade and a notation of the relative position between the blades (axial and tangential displacement) are used to characterize the tandem cascades when the focus of the study is the interaction between both profiles ;
- overall parameters: the overall tandem parameters, derived from the single blades quantities, represent the tandem blade as an equivalent single one. Therefore, they are used to compare a single cascade with a correspondent tandem blade row.

The optimal blade location in a tandem cascade was studied in [2], [3], [4]. The authors concluded that the axial and tangential displacement have to be set experimentally because they depend highly on the flow parameters and the geometry of the profiles. Therefore, there is no an established rule to assure an optimum blade performance for a tandem arrangement. The authors coincide in the fact that when the second blade is positioned in such a way that a gap nozzle area is formed in the interference zone between the two profiles, there is an advantage in terms of total losses.

Experimental investigations of the airflow were performed for reference classical profile separate blades and for equivalent tandem blade. All models were made equivalent. Chord reference profile airfoil length was taken as characteristic geometrical feature for calculation parameters tandem blade.

Experimental results
Results of model test in wind tunnel were integrated as functional dependence of profile drag coefficient c_x on attack angle i. This dependence for reference classical profile separate blade and for equivalent tandem blade is given of the fig.2.

General behavior of profile drag coefficient c_x on attack angle i is identical for reference classical profile separate blade and for equivalent tandem blade. But this dependence for tandem blade is flat in wide range of airflow modes. The attack angle for reference profile separate blade is well-defined at minimum value of profile drag coefficient. The graph for tandem blade has two minimum values. Viscous layer interaction on some airfoil elements brings to change of pressure distribution along the airfoil, it generates pressure gradient, which prevents the second element of tandem blade from possible stall.

The experiment was replicated on cascades, because there is distinction between flow separation from separate blade and stall in cascade. Investigations were performed for equivalent models. One row cascade and two row cascade have 5 blades. Cascades were made up of airfoils having parabola center line, angle of center line bending was $\theta=30°$. The geometry of cascade

airfoils was determined by equivalence condition: single airfoil chord and total tandem blade chord was $b=b_\Sigma=70mm$. The front and rear profiles in the tandem cascade have the same chord. The number of blades in the front and rear row of the cascades is the same. That means that the solidity of the front blade row is equal to the solidity of the second blade row. The solidity of cascades was $b/t=b_\Sigma/t=1$. Relative axial and tangential displacements of two row blades were $l/b_\Sigma=0.08$, $f/b_\Sigma=0.07$. Quasi-three-dimension airflow was modeled by leading-edge sweep, which changed over the range 0…15°.

Fig.2. Aerodynamic characteristics
of separate blades
−o− - classical profile blade; −◇− - tandem blade

Compressor cascade was made up in the form of turn package of blades. All cascade blades except of one (central) are rigid in the swing holder. The central blade is independent of the rest and is installed in the aerodynamic balance. The configuration of model allows realizing direct measuring of aerodynamic forces acting upon the blade in the cascade. This increases the accuracy of determination of foil aerodynamic parameters.

Results of wind-tunnel tests were integrated as dependence of aerodynamic coefficients c_y and c_x or flow parameters flow angle of deviation $_\Delta\beta$ and total pressure loss coefficient ξ on attack angel. Getting characteristics of one row blade cascade are given on fig.3, characteristics of tandem cascade are given on fig.4.
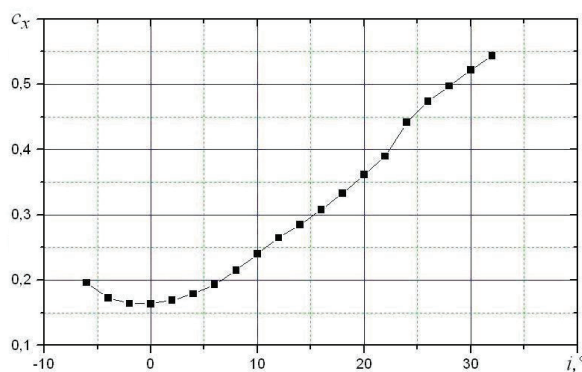
a
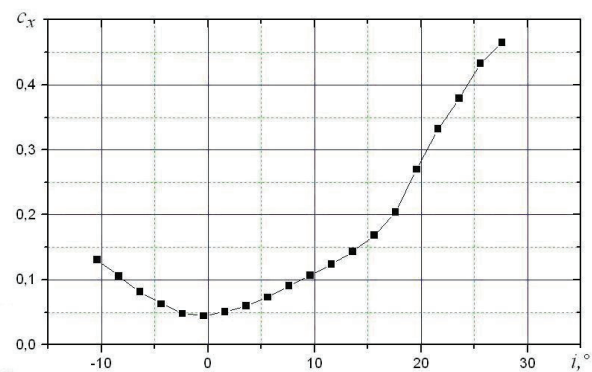
b

Fig.3. Aerodynamic characteristics of one row blade cascade
a – straight blades; b – blades with leading-edge sweep
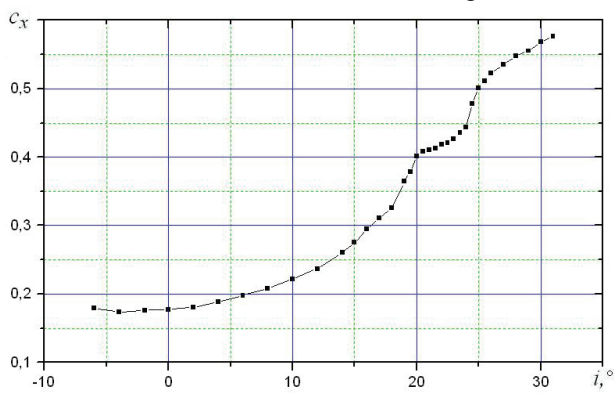
a
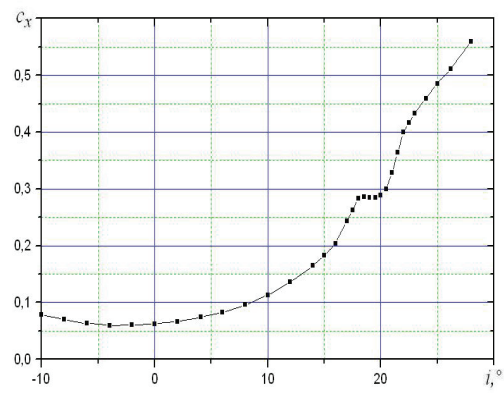
b

Fig.4. Aerodynamic characteristics of tandem cascade
a – straight blades; b– blades with leading-edge sweep

1.13.13

It is seen from graph that dependences profile drag coefficient on attack angle for cascades and for separate blades are identical. Like for tandem blade tandem cascade experimental data show that there is range extension of minimum value of drag coefficient on attack angle towards the positive angles and double minimum, capable of steady flow at wide attack angles.

Gap area in a tandem blade leads to pressure redistribution and variation of interaction between viscous layers of first and second airfoils, besides the rate of flow deceleration, consequently the diffusion factor, is less in two row blades than in one row blades [5], [6].

Spatial structure of flow in tandem cascade in general is similar to flow structure in equivalent one row cascade. Analysis of flow spatial structure in rotating tandem cascade of axial compressor shows that redistribution of energy between different flow regions takes place so it is possible to increase limit of aerodynamic load and decrease losses by flow control in tandem blades. The stream coming out of tandem blade slot goes along the second profiles without separation that sustains steady flow through tandem cascades at wide attack angels. However a range of airflow around the foils without stalls and low level of losses depends essentially on the relative position of the blades first and second rows. Results of researches [1], [7] show that effect of control flow around the second row foils appears at increase of critical attack angels, which are in several times greater then in equivalent one row cascades. Using tandem cascades at the same operating process design parameters can alloy to improve specific parameters and dynamic characteristics of gas turbine engines.

Conclusions

The flow behaviour was investigated along the two profiles which conform a tandem arrangement. The interaction mechanism between both profiles was studied as a comparison with the results obtained for the separate tandem blade and tandem cascade.

Based on the obtained results the following conclusions can be done:

– spatial structure of air flow in tandem compressor cascade is identical flow structure in equivalent one raw cascade;

– research of flow through tandem compressor cascade confirmed that main aerodynamic performance relations determined for one raw cascade are valid for tandem cascade;

– tandem cascade's dependence of profile losses on attack angel has double minimum and is sufficiently flat in wide range of airflow modes.

References

1. Терещенко Ю.М., Митрахович М.М. Аэродинамика компрессоров с управлением отрывом потока. –Киев.: Институт математики НАН Украины, 1996. –250 с.

2. Bammert, K., Staude, R., Experimentelle Untersuchungen an ebenen verzögernden Tandemgittern, 1976, VDI-Berichte Nr. 264, Pg. 81 – 89, Hannover.

3. Sachmann, J., Fottner, L., Highly Loaded Tandem Compressor Cascade with Variable Camber and Stagger, 1993, ASME paper number 93-GT-235.

4. Weber, A., Steinert, W., Design, Optimization, and Analysis of a High-Turning Transonic Tandem Compressor Cascade, 1997, ASME paper number 97-GT-412.

5. Bammert K., Staude R. Optimization for rotor blades of tandem design for axial flow compressors// Trans. ASME: J. Eng. for Gas Turbines and Power, 1980. Vol. 102, №2.–P. 369-375.

6. Бунимович А.И. Обтекание двухрядных компрессорных решеток при дозвуковых скоростях. – Некоторые результаты экспериментального исследования плоских компрессорных решеток. //Труды ЦИАМ. –М.: ЦИАМ, 1957, вып. № 307. – С. 16-30.

7. Бунимович А.И., Святогоров А.И. Обобщение результатов исследования плоских компрессорных решеток// Лопаточные машины и струйные аппараты.– М.: Машиностроение, 1967, вып.2. – С. 36-64.

P.I. Grekov Ph.D., associate professor
K.I. Kapitanchuk Ph.D., associate professor
V.V. Kozlov Ph.D., associate professor
E.P. Yasinitskyi Ph.D., associate professor
G.N. Nikitina Ph.D., associate professor
(National Aviation University, Ukraine)

PICK UP THE QUESTION OF DEFINITION GAS-DYNAMIC PARAMETERS OF SUBSONIC EJECTORS

The article tells us about one of the way of definition (agreement) gas-dynamic parameters high-pressure and low-pressure gases of subsonic ejector and sentence of necessity of using diffusers in subsonic gas ejectors.

Gas ejectors have been widely used in different branches of technique, particularly in aviation, gas, chemical and vacuum industry. Capability in result of the flow interaction have the mix of medium pressure that higher then environment pressure attracts scientists and create incentives for further research study. The main advantage of gas ejector as jet compressor is the lack of motion parts. Technique and technical simplicity, capability of using in corrosive and high-temperature medium are the decisive in choosing of gas ejector in role of pressure fluid-jet amplifier at compressor inlet of energy machine [1].

Research of ejectors that help to mix the flows of incompressible liquid started at about 80th ears ago [2]. The main difficulties of ejector theoretical determination are the describing the process of turbulent flows mix, their interaction in space, limited by solid walls that called "mix chamber" but, that definition is generally accepted. The presence of solid walls of ejector helps have the internal presence that differs from low-pressure gas and gas mix.

One of the terms that make cause easily is static pressure equality of low-head and high-head gases at the inlet for mix chamber. This condition is fair for flows with subsonic speeds and it is always truest for the supersonic ejectors [2].

For calculation of ejector total characteristics apply an equation of environment movement between initial and final cross section of cylindrical mixing chamber. At Soviet literature [3, 4 and 5] for calculation flow at ejector using semiempirical theory of turbulent flow G.A. Abramovicha.

Researches and improvements gas ejectors carried out activity in our times [2 and 6], besides most research varied out at the sector gas production and gas processing technique which is important for present economy.

Subsonic ejectors have the specific purpose for decreasing the temperature of helicopter engine exhaust devices, ventilation of flying machine hood space and gas turbine plant containers of gas compressor units. At this cause flow high-pressure gas is subsonic at low pressure drops at high-pressure gas nozzle $\pi_c = p_c^* / p_h = 1{,}03\ldots1{,}1$.

Disadvantage of using an ejector for ventilation of hood space at the low speed mode and pressure drops perhaps unstable modes of ejector operation and as a rule entering exhaust gases through the nozzle of passive gas into the hood space or gas turbine plant containers. This leads to increase the temperature at hood space more than alarm level and as a result – to damages the GTU system control operation sensors.

Irrespective of the gas flow during mixing we have the alignment of the gas velocity by the cross section of the chamber with the help of exchanges pulses between the parts that velocity is high and low.

This process is accompanied by loses. Besides simple hydraulic losses for friction between the walls of nozzle and mixing chamber there are losses during ejector operating process because of mixing process nature.

So, the pressure of ejector leads for additional energy losses that caused by flows mixing of high-pressure and low-pressure gases. Presence in exhaust device of GTE (GTU) flow reversal at 90th degrees leads to additional energy losses caused by secondary flow. So, ensuring minimum energy loss and GTE safety operation with exhaust devices ejectors type possible in the presence of reliable methods of calculation subsonic gas ejectors and methodology agreed with their characteristics with elements of GTE (GTU). Special place is occupied by the question of irregularity of flow at the nozzle inlet of high-pressure gas at characteristics of gas ejector.

Irregularity of flow could be caused by presence at the nozzle inlet high-pressure gas knee, shaft transmission of torque to the screw for GTE and supercharger for GTU.

The well known ways for calculation subsonic gas ejector with mixing chamber variable shape and divided gas flow that mixing haven't been considered or require clarification. Calculation of the ejector with the help of gas-dynamic function and theory of turbulent flows [3] in cause when all flow parameters are given at the nozzle inlet there is the problem from the point of view similarity with the experiment.

But in many causes necessary to provide preliminary calculation of gas ejector that has the form mixing chamber that almost looks like cylinder. In the presence of the gas ejector average characteristics gas ejector could make to calculation of amendment that take into account irregularity of flow, friction the presence of the flow turns (rotations) etc.

During calculation of gas ejectors with the help of gas-dynamic and theory of flows the main difficulties helps during static pressure on nozzle cross-section high-pressure and low-pressure gases, respectively and velocity at nozzle cross section low-pressure gas. In cause of known flow parameters at nozzle cross-section high-pressure gas we couldn't define arbitrarily λ_2 because define pressure have the same coefficient of ejection.

Calculation of gas ejector is simplified if we take the following values:
- flow of ideal gas is one-dimensional and stationary;
- friction of the walls with out mixing;
- velocity on nozzle cross-section high-pressure gas is subsonic (M<0,7);
- nature and temperature of high-pressure and low-pressure gases are the same;
- flow mode at the mixing chamber exhaust corresponds to the complete expansion.

The scheme of gas ejector and cross-section location that define gas-dynamic parameters of ejector shows at fig.1.

All the reflections and conclusions are through for subsonic barometric ejector. An approach to the coordination modes of flow through the first and second circuit ejector when its calculation is presented in [3 and 5] doesn't establish the first and second circuit. In scientific research [5] tells if two flows at the initial cross-section mixing chamber and that are we can assume that the static pressure is constant throughout the area input sector of the chamber. This condition is links to each other the values λ_1 and λ_2, so at pressure $p_1 = p_2$, we have $p_1^* \cdot \pi(\lambda_1) = p_2^* \cdot \pi(\lambda_2)$ (1).
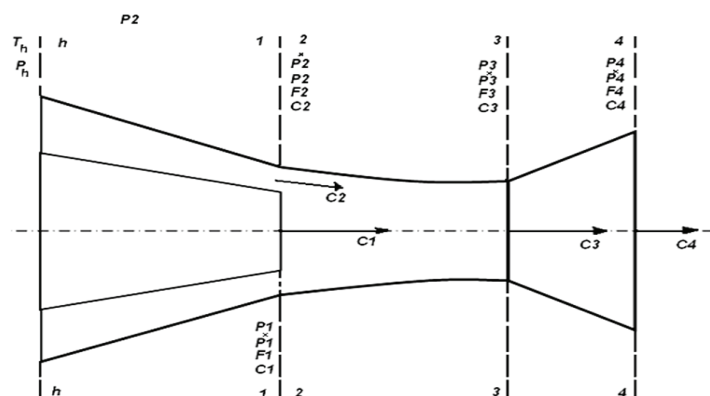
Fig.1. Scheme of gas ejector and location cross-section
at what we define gas dynamic parameters of ejector

So, at subsonic velocity of the flows optionally you can specify velocity reproduced only one of them, the velocity of them define like ration of total gas pressure [5].

In this cause, value $\pi(\lambda_2)$ define from the formula (1) doesn't allow to find all necessary gas-dynamic parameters on the nozzle cross-section another part even in the first approximation.

It's caused by that velocity on the nozzle cross-section of high-pressure gas defines like

$$c_1 = \sqrt{2\frac{k}{k-1}RT_1^*\left(1 - \left(\frac{p_h}{p_1^*}\right)^{\frac{k-1}{k}}\right)} \quad (2).$$

The value C_1 and $\pi(\lambda_1)$ depends from the ratio $\dfrac{p_h}{p_1^*}$, the value $c_2(\pi(\lambda_2))$ depends from ratio of parameters $\dfrac{p_2}{p_h}$. Because $p_1^* \cdot \pi(\lambda_1) \neq p_2^* \cdot \pi(\lambda_2)$. So, the static pressure $p_2 = p_1$ at the initial cross-section of mixing chamber would remain undefined.

Iterative methods for define the static pressure at the inlet to the mixing chamber of ejector doesn't provide any positive results. In literature there are suggestions to define the static pressure at the inlet of mixing chamber iterative methods, however, ways to solve this problem with the help of iterative methods doesn't specified.

As shown in research [3 and 5] and take into account the above assumption of mix movement should be equal to the initial amount sum of flow moving $(G_1 + G_2)c_3 = G_1c_1 + G_2c_2$ where

$$c_3 = \frac{G_1c_1 + G_2c_2}{G_1 + G_2} \quad (3).$$

This value is less than the finite sum of kinetic energy flows to mix equal

$$\Delta E = E_1 + E_2 - E_3 = \frac{G_1 G_2}{G_1 + G_2}\frac{(c_1 - c_2)^2}{2}.$$

The value ΔE is the loss of kinetic energy that connected to the mixing process [5].

But, if we lose energy ΔE equivalent energy consumption high-pressure gas by kinetic energy low-pressure gas, then energy losses of high-pressure gas provides with the help of static pressure at mixing chamber inlet.

Therefore, you can get the following equation: $\dfrac{G_1 G_2}{G_1 + G_2}\dfrac{(c_1 - c_2)^2}{2} = G_2\dfrac{c_2^2}{2} \quad (4).$

After appropriate transformations and taking into account, that $n = G_2/G_1$, we have: $nc_2^2 + 2c_1c_2 - c_1^2 = 0$.

The resulting quadratic equation has the following real solution:

$$c_2 = \frac{c_1}{n} \cdot (\sqrt{1+n} - 1). \quad (5)$$

So, velocity on the nozzle cross-section of low-pressure gas depends on the velocity at nozzle cross-section velocity of high-pressure gas and ratio of gas consumption through the nozzle (ejection factor).

According to dependence (4) formula (3) looks like $c_3 = \dfrac{c_1}{\sqrt{1+n}} \quad (6).$

Velocity at nozzle cross-section of high-pressure gas C_1 depends by formula (1). Using dependence for definition gas velocity at nozzle outlet at defines pressure drops

$$c_2 = \sqrt{2\frac{k}{k-1}RT_h\left(1-\left(\frac{p_2}{p_h}\right)^{\frac{k-1}{k}}\right)} \text{ could define static pressure } P_2 \quad p_2 = p_h\left(1-\frac{c_2^{\,2}}{2\frac{k}{k-1}RT_h}\right)^{\frac{k}{k-1}} \quad (7).$$

After changing C_2 to it value at dependence (5) we have $p_2 = p_h\left(1-\dfrac{\dfrac{c_1^2}{n^2}\cdot(\sqrt{1+n}-1)^2}{2\dfrac{k}{k-1}RT_h}\right)^{\frac{k}{k-1}}$.

So, $\displaystyle Lim_{n\to\infty}\frac{c_1^2}{n^2}\cdot(\sqrt{1+n}-1)^2 = 0$, then $p_2 = p_h$ at $n\to\infty$.

This suggests that the high coefficients of high-pressure ejection gas flows in practically unlimited space and there is degeneration of ejector as well as the correctness of assumptions adopted by equation (4). Equation (2), (5), (6) and (7) allows defining at first approximation the absolute velocity of low and high-head gas on the nozzle outlet and the velocity from mixing cameras output at our assumption and according $\lambda_1, \lambda_2, \lambda_3$ static pressure $p_2 = p_1$.

Consideration of possible assumptions adopted by the recommendations given in [3, 5 and 6].

An important place is occupied by problem of intensification of the process of mixing the purpose of obtaining a uniform velocity field at the output of the mixing chamber with loss of its length. This is true for aircraft gas turbine engines. For example, an experimental chamber with exacerbation of mixing [7] is shown in fig. 2. Exhaust devices GTU ground with a large enough length ($L_{вн} >> d_{вн}$), so for them the process of intensification of the process of mixing isn't important.

Another problem in the calculation of subsonic gas ejector is a form of mixing chamber and the necessary of presence the diffuser, with is behind the mixing camera.

In source [5] available mixing chamber of various geometries form (mixing chamber is expanding, shrinking, isostatic and other) which have their advantages and disadvantages. Often, there are no specified limits of certain form of mixing chambers with different modes of the gas ejector.

a)   b)

Fig. 2. Prototype of ejector
a) with the external and internal nozzles of second contour
b) with leafed mixing chamber

In cause of subsonic barometric gas ejector, with the full extension the output flow, there are needs to use the diffuser after mixing chamber. Geometric form of mixing chamber should meet the requrenments of the calculated gas expantions at known velocties at nozzles cross-section and second contour and also mixing chamber. The main reason is that on the cross-section of subsonic nozzle there are no unexpanion operation. For subsonic nozzle at the taken subcritical pressure drop, only possible maximum velocity that correspond to the full expansion of gas in the nozzle. Future reduction of the inlet cross-section leads to redusing gas flow through the nozzle.

For helicopter turbine engine allowed uncalcukated mode that allows pert of kinetic energy of the exhaust gases trousform to compression operation and as conclusion increase pressure drop on the free turvine and consequently the engine power. Power and economic increasing can be quite big, as in modern engines kinetic energy of exhaust gases by a free turbine at about 10…20% from received performance operation. It all indicates, that the mixing chamber of gas ejector for "EVP" and ventilation of hoot space never be cylindrical. Shape of mixing chamber should meet the optimal value of energy saving at the exhaust of GTE.

Conclusions

At susonic flow high pressure and low-pressure gas ejector define reduced velocity of one of them by the ratio of total pressure of these gases isn't true. Its caused by the fact that real velocity at the cross-section of high-pressure and low-pressure gas are defined by the condition when $p_1^* \cdot \pi(\lambda_1) \neq p_2^* \cdot \pi(\lambda_2)$.

However, if the problem considered from the point of view that energy losses equivalent energy consumption of high-head gas to change kinetic energy of low pressure gas then energy losses of high-head gas occur by reducing the static pressure at the inlet to the mixing chamber. Taking into account show that the velocity of low-head nozzle gas depends on the velocity on the nozzle exhaust high-head gas determine as (2) at the ratio of gas consumption through the nozzle.

References

1. *Kulyk M.S., Kapitanchuk K.I., Grekov P.I., Onischenko S.P.,* Gas ejector as a pressure stabilizer at the inlet compressor power installation

2. *Аркадов Ю.К.* Новые газовые эжекторы и эжекционные процессы. – М.: Физматлит, 2001. – 334 с.

3. *Г.Н. Абрамович.* Теория турбулентных струй. М., Гос. изд. ФМЛ, 1960.

4. *Абрамович Г.Н.* Прикладная газовая динамика. М., Гостехиздат, 1953.

5. *Абрамович Г.Н.* Прикладная газовая динамика. ч.1: Учеб. Руководство: Для втузов. - М.: Наука, 1991. – 600 с.

6. *Маланичев В. А.* Исследование работы газового эжектора при различных параметрах смешиваемых газов //Труды ЦАГИ, 1994, №2519.

7. *П.І. Греков, І.О. Ластівка, К.І. Капітанчук* Газові ежектори для екранно-вихлопних пристроїв ГТД.:Матеріали IX Міжнародної науково-технічної конференції «АВІА-2009», 21-23 вересня, ТОМ II.-Київ-2009. с.13.12-13.15.

UDC 629.735.017.1:629.735.33(043.2)

O.A.Tamargazin, doctor science of engineering, O.S.Yakushenko, PhD
P.O.Vlasenko, postgraduate student (National Aviation University, Ukraine)

FORMING OF INSTALLERS FOR AIRLINE'S FLEET RELIABILITY CONTROL AUTOMATED SYSTEM

Expediency of creating the reliability control automated system is approved on the basis of analysis of questions related to airline's fleet reliability control. General structure and main functions of automated system are considered. Content of software installers that could be used for installing to company's server, system administrator, expert and operator workplaces is described.

Problem

One of the most effective modern means for supporting, controlling and optimizing maintenance and technical activities of airline is the reliability control system of aircraft functional systems and components.

The general reliability control circuit of airline park consists of data collecting, data processing and control actions. Initial data for reliability control is faults and failures detected by pilots or during maintenance process, unscheduled components removal, flight delays and cancellations, scheduled maintenance reports, flying time of airplane mainstay products and components, scheduled check and check reports. On the base of these data the reliability parameters estimation, control and monitoring is provided. The prognostication of reliability parameters, analysis and control of components life state, preparation of evidence info are conducted. Control of Airline Maintenance Program and Reliability Program is provided by making the necessary changes in Maintenance program. These changes are made for increasing (saving) the reliability and reducing costs for maintenance, airworthiness and flight safety necessary level support.

Information concerning only flight or maintenance personnel comments is put in Logpage. For a large company that has 20-30 aircraft there are 4000 - 6000 Logpages. Airlines need to process information for three last years at least. Firstly this work should be done by some persons and the results of this work must be given to appropriate workers of the Airline. Secondly this work can not be done with a high quality without special software even if it would be done with a significant staff.

All this data points to necessity of creating specialized automated system for reliability control of aircraft park and mainstay products (plane, engine, auxiliary power unit, propeller, gear) of airline.

Research and publications analysis

In recent years numerous papers such as [1-4], which focusing on the creation of automated systems pay much attention to development of reliability control methodologies and methods. But not enough papers pay attention to development of software for automated systems. Also, taking in account that these automated systems must agree with international and national Authorities requirements and regulations (ICAO, the State Department of Aviation Transport of Ukraine) and airline manufacturers. Herewith the requirements and procedures of these organizations are constantly improving and changing.

Taking into account this the aim of this paper is to consider questions connected with development of the general structure of reliability control automated system at the airline level.

General structure of reliability control automated system of Airline fleet

Automated system that can provide simultaneous work of some users with information should be based on the use of relational database management systems. Such systems are designed to work in local networks and in the Internet. They include:

- the database (a file or files on hard disk that contain data);

- server (standard software system for database management, which is installed on the server computer and provides database control);

- ODBC - drivers (Open Database Connectivity, a software interface for databases accessing) that are installed on each computer of end users and provide interaction of application (automated system) with the server;

- automated system software.

Possible structure of such system is shown on Figure 1.

Fig. 1. The structure of reliability control automated system of Airline fleet

Main functions of reliability control automated system of Airline fleet and purpose of it's main modules

Analysis of stated information shows that the automated system should provide at least three fundamentally different groups of functions for operation with the database:
- entering of data;
- creation of output forms, reports and their expert analysis;
- maintenance of automated systems database.

Thus software installer should provide four types of system installation:
- database server, that should be installed only at one computer (usually at network server computer);
- operators' workplace;
- experts' workplace;
- system administrator's workplace.

At all workplaces except server computer should be installed ODBC-drivers. At the server these drivers are installed only in case if both database software and end user software are installed there. Such variant of installation is possible for example if automated system and database are installed at one personal computer.

Key features of software that is installed at operator's workplace should provide input to the system and modification of the following information:

- failures and faults detected on the airplane by crew or maintenance staff;
- flight delays;
- flight cancellation (by technical reasons);
- delay maintenance;
- corrective actions of maintenance personnel;
- types of airline's aircrafts and their characteristics;
- airline's aircrafts and their characteristics;
- monthly fling time of aircraft;
- long time maintenance;
- periodical maintenance and checks of functional systems (high altitude starting of auxiliary power unit, check of auto landing system);
- codifiers and classifiers of systems.

Key features of software that is installed at expert's workplace should provide analyzing of processed input data:
- samples of specified type failures for determined period;
- reliability parameters for the whole aircraft park, individual airplanes and for individual systems;
- flight delays and cancelations;
- summary report of the aircraft operation;
- summary report of the engines operation;
- failures of individual components;
- long time maintenance;
- periodic checks of individual systems;
- contextual search of information;
- batch creation of reports for aircraft manufacturer and Department of Aviation Transport.

Key features of software that is installed at administrator's workplace should provide such database control functions:
- creation/deletion of users, controlling of information access rights (view parts of database, information modifying, records deleting);
- system database maintenance (cleaning, reindexing, analyzing of database and its tables);
- the database backup and restore of the database from a previous backups;
- change of database structure and features;
- service functions.

Conclusions

The analysis of the main functions of reliability control automated system of Airline fleet was conducted. Reasonable dividing of functions to the parts depending on operation (expert, operator, administrator) was considered.

References

1. *Кучер О.Г.* Контроль та аналіз стану надійності систем і агрегатів повітряних суден в експлуатації/ Кучер О.Г., Власенко П.О.// Наукоємні технології. – 2010. – № 1. – С. 15–26.

2. *Кучер О.Г.* Експлуатаційна надійність авіаційних двигунів. Її контроль та аналіз в авіакомпанії/Кучер О.Г., Власенко П.О.// Авиационно-космическая техника и технология. – 2011. – № 9(86). – С. 108–115.

3. *Кучер О.Г.* Модель експлуатаційної надійності повітряних суден/ Кучер О.Г., Власенко П.О. // Наукоємні технології. – 2010. – № 2. – С. 10–17.

4. *Кучер О.Г.* Порівняльний аналіз показників надійності і ефективності іноземної та вітчизняної техніки/ Кучер О.Г., Власенко П.О.// Наукоємні технології – 2009.- № 2.– С. 9-17.

5. *Хоменко А.Д.* Работа с базами данных в Delphi. 3 изд./ Хоменко А.Д., Гофман В.Э.// - СПб.: БХВ-Петербург, 2005. -640 с

6. *Князьков П.В.* Анализ и обеспечение надежности воздушных судов гражданской авиации в процессе их эксплуатации СПб.: 2001. -110 с

I.I. Gvozdetskyi, Ph.d. (National Aviation University, Ukraine)

METHOD OF ACCOUNT OF STATIC AND CYCLIC DAMAGES MUTUAL INTERACTION ON DURABILITY OF GAS TURBINE HEATPROOF MATERIALS

Components of gas turbines, made of heatproof alloys in the operation process are subject to influence of the static and cyclic loadings. The cyclic loadings are largely caused by rapid variation of gas and component temperature, in particular during the engine start, rapid variation of gas turbine engine operation mode, and during engine shutoff /1/.

Because of an action each mentioned types of loadings of specific kinds of damages of material are appeared and are accumulated gradually /2/ . In research paper /3/ on the basis of experimental information, obtained as results of specimen test in the conditions of thermocycling with curing at the maximal temperature of cycle (fig.1), it was shown up that the mentioned damages are accumulated in material not independently of each other, but act with a certain interference.
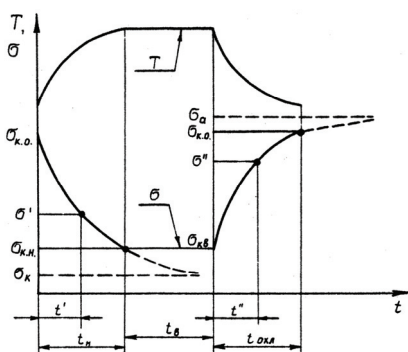
Fig.1 Variation of temperature and tension at the long-term thermal fatique test of specimens in conditions of cyclic creep

Thus mutual interaction of these two types of damages results in the decline of longevity of all examined heatproof alloys at influence on them of the alternating cyclic and static loadings. It is evident evidently from the graph (Fig. 2), built on results long-term thermal fatique tests of three heatproof alloys specimens in the conditions of cyclic creep and in the conditions of cyclic stress relaxation , performed in our laboratory on testing stands, described in research papers /4,5/. Here on axes the values of the maximum destructive static D_τ and cyclic D_n damages accumulated to the moment of destruction as result of thermal fatique tests with curing times t_c =0, 1, 5,15 and 30 minutes are set aside. From the graph it is evidently, that at all of the modes of tests a sum of the ultimate accumulated maximum damages that corresponds material destruction was less then one , unlike the cases of simple single-component loading separately static loading and cyclic loading, when $D_\tau=1$ and Dn =1. Analogical results were got as results of the tests of several other heatproof alloys both in our laboratory and by other researchers / 7 /.
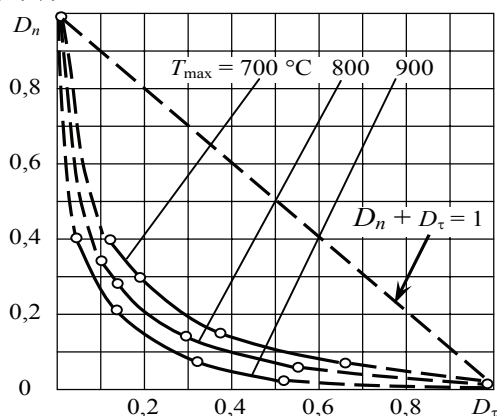
Fig.2 Variation of maximum static and cyclic damages at the test of ЭИ-437Б alloy thermal fatique tests with curing times t_c =0, 1, 5,15 and 30 minutes in the conditions of cyclic creep

Taking into account this mutual interaction of two types of damages we proposed /6/ the formula for the calculation estimation of materials longevity in the examined conditions of loading:

$$N_r = \frac{1 - D_{n,\tau}}{\dfrac{1}{N_0} + \dfrac{t_c}{\tau_{d,st}}}, \qquad (1)$$

where Nr is longevity of material (number of destruction cycles) at a thermo-cycling with self-controls with time of curing duration of t_c; N_0 is longevity of material (number of cycles to destruction) at the cyclic variation of temperature on a "saw-tooth cycle" in range from T_{max} to T_{min} ; $\tau_{d,st}$ is longevity of material (time to destruction) at a stationary temperature, which equals to maximal temperature in the cycle T_{max}; $D_{n,\tau}$ is a function of mutual interaction of static and cyclic damages.

Values of function of mutual interaction of static and cyclic damages $D_{n,\tau}$ and also values of number of cycles to destruction at the "saw-tooth cycle" N_0 were determined as sesults of experimental investigations under corresponding thermocyclies conditions, and indexes of longevity $\tau_{d,st}$ at a static ladening at maximal temperature of cycle T_{max} were determined from reference data / 8 /.

At treatment of results of the conducted experiments value of function of mutual interaction of static and cyclic damages $D_{n,\tau}$ was determined in accordance with expression :

$$D_{n,\tau} = 1 - \frac{N_r}{N_0} - \frac{N_r * t_c}{\tau_{d,st}} \quad , \quad (2)$$

where all conditional denotations correspond accepted in the formula (1).

The analysis of experimental data, represented in fig. 3 and fig. 4, allowed to make conclusion that function of mutual interaction of static and cyclic damages $D_{n,\tau}$ depends on the row of indexes of thermocycle and may be in a general view considered as follows:

$$D_{n,\tau} = D_{n,t}\left(t_c, T_{max}, \sigma_{st}, K_0, \Delta T\right),$$

where T_{max} and ΔT are parameters of thermal cycle, σ_{st} it is static tension, acting in a specimen in the process of curing, K_0 is a jamming rigidity coefficient of specimen, determining the range of cyclic thermo-stresses $\Delta\sigma$ that appear in a specimen in the thermo-cycle, t_c is duration of curing at the maximal temperature of cycle.
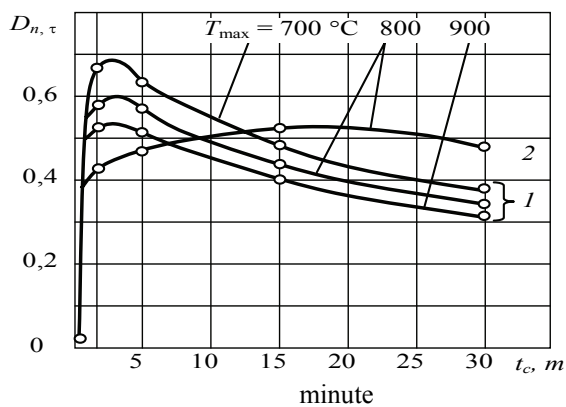
Fig.3. Dependence of function of mutual interaction of static and cyclic damages $D_{n,\tau}$ versus duration of curing at the maximal temperature of cycle t_c for ЭИ437Б alloy specimens in the conditions of cyclic creep at different values of T_{max}, constant value of double-amplitude peak of thermocycle ΔT =600 $^{\circ}$C and different values of jamming rigidity coefficient of specimen K_0 (1- K_0 = 0.35, 2- K_0 = 0.65)
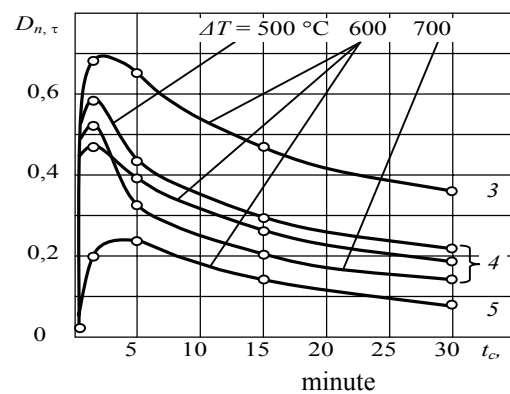
Fig. 4. Dependence of function of mutual interaction of static and cyclic damages $D_{n,\tau}$ versus duration of curing at the maximal temperature of cycle t_c for ЭИ437Б alloy specimens tested in the conditions of cyclic creep at different values of double-amplitude peak of thermocycle ΔT, constant value of maximal temperature T_{max} = 800°C and different values of jamming rigidity coefficient of specimen K_0 (3 - K_0 = 0.62, 4- K_0 = 0.72, 5 - K_0 = 0.805)

The similar graphs were got as results of the specimen tests on the protracted thermo-cicle fatique in condition of cyclic stress relaxation of several heatproof materials /6/.

From the graphs evidently, that in a most degree the function of mutual interaction of static and cyclic damages $D_{n,\tau}$ depends on duration of time curing at a maximal temperature. Thus flowing of curves $D_{n,\tau}$ depending on duration of curing at all of investigated conditions of loading is characterized by presence of ascending branch, peak-points and descending branch, containing an inflection point.

Noted identity of curves, proper the different modes of tests and different modes of loading allowed for their analytical description to use single approximating expression as exponentially-model function of kind :

$$D_{n,\tau} = a\left(t_c\right)^b e^{c(t_c)}, \qquad (3)$$

where *a, b, c* are permanent coefficients, for these temperature and power conditions of tests.

By taking the logarithm expression (3) can be resulted to the linear kind, whereupon finding of values of his coefficients on results the conducted tests does not present complication.

It is necessary to mark that exactness of approximation of function (3) substantially depends on the choice of knots of approximation. In this case the knots of approximation got out so that one of them lay on the upleg of curve (fig. of 2 and рис.3), second – on a downleg to the inflectionpoint, and third – after an inflectionpoint.

Analysis of the got values of coefficients *and, b, with* rotined that they substantially depended on the basic indexes of термоцикла. In particular, dependences of the indicated coefficients on the maximal temperature of cycle at the fixed values of scope of термоцикла can be approximated equalizations of parabolas:

$$a = a_0 + a_1 T_{\max} + a_2 \left(T_{\max}\right)^2;$$
$$b = b_0 + b_1 T_{\max} + b_2 \left(T_{\max}\right)^2; \qquad (4)$$
$$c = c_0 + c_1 T_{\max} + c_2 \left(T_{\max}\right)^2$$

The coefficients of equalizations (4) depend on the scope of thermo-cycle ΔT.

The indicated dependence, as the conducted analysis rotined, can be described by linear equalizations of such kind:

$$a_0 = a_0' + a_0'' \Delta T;$$
$$a_1 = a_1' + a_1'' \Delta T; \qquad (5)$$
$$a_2 = a_2' + a_2'' \Delta T$$

Analogical equations may be worked out for other coefficients of equalization (4).

Values of permanent coefficients a_0', a_0'', a_1, a_1', a_1'' et cetera, approximating equalizations (5), calculated on results of the tests of ЭИ437Б alloy specimens are represented in the table below.

Values of coefficients for the calculation of function of взаимовлияния of $D_{n,\tau}$ for the ЭИ437Б alloy (tests in the conditions of cyclic creep at $K_0 = 0.35$ is the mode I, at $K_0 = 0.35$ is the mode II)

Denotation of coefficients	Mode of tests		Denotation of coefficients	Mode of tests	
	I	II		I	II
a_0'	2,3649	1,6183	b_1''	$-0,7498 \cdot 10^{-6}$	0,161210–4
a_0''	$-0,6249 \cdot 10^{-2}$	$-0,1350 \cdot 10^{-2}$	b_2'	$-0,1499 \cdot 10^{-5}$	0,212410–5
a_1'	$-0,3366 \cdot 10^{-2}$	$-0,2624 \cdot 10^{-2}$	b_2''	0,499810–9	$-0,8749 \cdot 10^{-7}$
a_1''	0,159910–4	$-0,3750 \cdot 10^{-5}$	c_0'	$-0,0756$	0,2144
a_2'	0,166610–5	0,141610–5	c_0''	0,864910–4	0,210910–3
a_2''	$-0,9997 \cdot 10^{-7}$	$-0,2501 \cdot 10^{-8}$	c_1'	0,161110–3	0,4769
b_0'	-1,1635	2,2033	c_1''	$-0,1775 \cdot 10^{-6}$	$-0,4896 \cdot 10^{-6}$
b_0''	0,154910–3	$-0,7469 \cdot 10^{-2}$	c_2'	$-0,9083 \cdot 10^{-7}$	$-0,2762 \cdot 10^{-6}$
b_1'	0,274610–2	$-0,3937 \cdot 10^{-2}$	c_2''	0,749910–10	$-0,2997 \cdot 10^{-9}$

Using these values of permanent coefficients, we can determine by equalizations (5), (4) and (3) values of function $D_{n,\tau}$, if the values of basic parameters of thermal cycle as well as static tension σ_{st}, acting in a specimen in the process of curing are known.

Values of function $D_{n,\tau}$ got thus, are necessary for calculation of a material longevity concordantly to described above approach on a formula (1), These values of function $D_{n,\tau}$ also will be useful for the analysis features of accumulation of thermal cycle and static damages at a thermo cycling

with curing at maximal temperature. Main of these features, as it is obvious from a fig. 2 , fig. 3 and fig. 4, are the followings:

– maximum values of the accumulated thermal-cycle and static damages, and also intensity of their mutual interaction very substantially depend on duration of curing time at the maximal temperature of cycle;

– for every combination of temperature indexes of cycle there is duration of curing time t_C', at which mutual interaction of static and thermal-cycle damages appears most substantially ($Dn_{,\tau} = Dn_{,\tau\ max}$). For the ЭИ437Б alloy in the investigated range loading modes the indicated values of duration of curing time t_C', lies within the range of 1–5 minbtes, here a lower limit corresponds the low values of T_{max}, and overhead limit corresponds to higher values of T_{max} ;

– degree of mutual interaction of static and thermal-cycle damages is the more considerable when value of temperature and power indexes of cycle are minimal (it means that when absolute value of material longevity is maximal).

Conclusions

The resulted information about the features of accumulation process of thermal cyclic and static damages of investigated heatproof materials may be used for :

- planning of tests of other heatproof alloys in the conditions of the protracted thermal cycling in order to reduce the extent of tests;

- calculation prognostication of longevity of gas turbine engines hot part components;

- setting of the steady and transient operational modes of gas turbine engines,

- programming of their equivalent tests and decision of other tasks, related to durability and longevity of heatproof materials.

References

1. *Технический отчет №198/68*. О температурном состоянии узла горячей части двигателя АИ-20 К. Предприятие п-я 57, 1973 г.- 40 с.

2. *Третьяченко Г.Н.* Исследование разрушения лопаток газовых турбин под воздействием теплосмен. «Проблемы прочности», 1971, №2. с. 36-40.

3. *Гвоздецкий И.И.* К расчету долговечности жаропрочных материалов в условиях длительной термической усталости. – В кн.: Надежность и долговечность авиационных газотурбинных двигателей Сб.науч.тр. Вып. 4, стр.103-109, – К.: КИИГА, 1973 -175 с.

4. *Лапшов В.Ф., ТАРАСЕНКО А.В., ГВОЗДЕЦКИЙ И.И.* и др. Установка для исследования прочности материалов в условиях постоянных и переменных температур. – В кн.: Надежность и долговечность авиационных газотурбинных двигателей. Сб. науч.тр. Вып.3, стр .89-94. – К.: КИИГА, 1972.

5. Гвоздецкий И.И., ЛАПШОВ В.Ф., КУДРЯШОВ Б.Я. и др. Установка для исследования влияния временного показателя верхнего предела температурного цикла на термоусталостные характеристики материалов. – В кн.: Надежность и долговечность авиационных газотурбинных двигателей. Сб.науч.тр. Вып. 1., стр 56-61, – К.: КИИГА, 1971.

6. Гвоздецкий И.И. Приближенный расчет долговечности жаропрочных материалов при длительном термоциклировании. В кн.: Надежность и долговечность авиационных газотурбинных двигателей. Сб.науч.тр. Вып. 1., стр 103-109, – К.: КИИГА, 1979.

7. Дульнев Р.А. Суммирование повреждений и условие прочности при циклическом нагружении. «Проблемы прочности», 1971, №10. с. 32-36.

8. Виам, Справочник по авиационным материалам.том.3 М.: Машиностроение, 1970 - 380 с.

UDC 629.735.03

F.Kirchu, PhD (National Aviation University, Ukraine)

NUMERICAL FLOW STUDY IN A COMPRESSOR CASCADES USING DIFFERENT TURBULENCE MODELS

In the article investigated the influence of turbulent viscosity models on the characteristics of the compressor cascades. The dependence of the angle of flow and total pressure losses in the compressor cascades from models of turbulent viscosity "k-ε", and "SST". The advantages and disadvantages of these models with respect to modeling the flow in the compressor cascade.

The study of gas flow in planar compressor cascades is a necessary preliminary step for a rational calculation and design of blade machines. There are several methods for obtaining the characteristics of the compressor cascades, namely the experimental and calculated (numerical). Numerical methods [1] allow us to study the flow at all possible modes of arrays operating at all Mach and Reynolds numbers. And, very importantly, the cost of the application of numerical methods is relatively low because the cost of software and computer technology is constantly decreasing.

But, if you have obvious advantages, there is also a number of problems when using numerical methods. One such problem is not possible (limited due to the very high demands on computer resources), the direct solution of the Navier - Stokes equations. Therefore, the solution of engineering problems by methods of numerical equations of gas dynamics are averaged Reynolds, which closed models of turbulent viscosity. Widely used in turbomachinery are two-parameter model of turbulent viscosity " $k-\varepsilon$ ", " $k-\omega$ " and " SST "

In 1942 Kolmogorov [2] proposed a model of turbulent viscosity with two differential equations. This model includes the transport equation of turbulent kinetic energy k and the specific energy dissipation rate ω. Below is one of the most common models of k-ω type proposed by Wilcox [3]:

$$\rho \frac{\partial k}{\partial t} + \rho \overline{u}_j \frac{\partial k}{\partial x_j} = \tau_{ij} \frac{\partial \overline{u}_i}{\partial x_j} - \rho \beta^* k\omega + \frac{\partial}{\partial x_j}\left[(\mu + \sigma^* \mu_t)\frac{\partial k}{\partial x_j}\right],$$

$$\rho \frac{\partial \omega}{\partial t} + \rho \overline{u}_j \frac{\partial \omega}{\partial x_j} = \alpha \frac{\omega}{k} - \tau_{ij} \frac{\partial \overline{u}_i}{\partial x_j} - \beta^* \omega^2 + \frac{\partial}{\partial x_j}\left[(\mu + \sigma \mu_t)\frac{\partial \omega}{\partial x_j}\right],$$

$$\mu_t = \rho \frac{k}{\omega},$$

$$\tau_{ij} = -\rho \overline{u_i' u_j'} = \rho \mu_t \left(\frac{\delta \overline{u}_j}{\delta x_j} - \frac{\delta \overline{u}_j}{\delta x_i}\right) - \frac{2}{3}\rho k \delta_{ij},$$

The model constants are:
$\beta^* = 9/100; \beta = 3/40; \alpha = 5/9; \sigma^* = 1/2; \sigma = 1/2.$
The most popular model with two differential equations is the k-ε model [4].

$$\rho \frac{\partial k}{\partial t} + \rho \overline{u}_j \frac{\partial k}{\partial x_j} = \tau_{ij} \frac{\partial \overline{u}_i}{\partial x_j} - \rho \varepsilon + \frac{\partial}{\partial x_j}\left[\left(\mu + \frac{\mu_t}{\sigma_k}\right)\frac{\partial k}{\partial x_j}\right],$$

$$\rho \frac{\partial \varepsilon}{\partial t} + \rho \overline{u}_j \frac{\partial k}{\partial x_j} = c_{\varepsilon 1}\frac{\varepsilon}{k}\tau_{ij}\frac{\partial \overline{u}_i}{\partial x_j} - c_{\varepsilon 2}\frac{\varepsilon^2}{k} + \frac{\partial}{\partial x_j}\left[\left(\mu + \frac{\mu_t}{\sigma_\varepsilon}\right)\frac{\partial \varepsilon}{\partial x_j}\right],$$

The model constants are:
$$c_{\varepsilon 1} = 1.44; \; c_{\varepsilon 2} = 1.92; \; c_\mu = 0.09; \; \sigma_k = 1.0; \; \sigma_\varepsilon = 1.3.$$

Since the type of turbulence model k-ε better describe the properties of shear flows, and models such as k-ω have advantages in modeling near-wall functions, Menter modified the standard relationship between k, ε, and turbulent viscosity μt. In this connection introduced a special delimiter (SST), which provides a transition from it to the formula Bradshaw [5] according to which

stress are proportional to the turbulent kinetic energy of turbulence. This technique, called SST (shearstresstransport), later widely used in other models of turbulence with two equations. Thus, the main objective of this study was to numerically study the characteristics of the compressor cascades using two models of eddy viscosity k-ε and SST, and compare these results with the experimental results. In this paper, to simulate gas flow in the compressor cascades used a modern computer system "ANSYS-CFX",

The object of investigation was chosen compressor cascades KP-33 (Fig. 1) [6], which consisted of a series helical profiles of the BC-10 average line, which was bent in an arc of a circle with a relative thickness profile 0.087, the basic geometric characteristics are given in Fig. 1.

Structural angle of profile: β_{1k} =43°, β_{2k} =111°.

Bending angle profile $\theta = \beta_{2k} - \beta_{1k}$ =68°.

Angle of incidence γ =76,5°.

Hord b =52 mm.

Relative array pitch t / b =0,385.
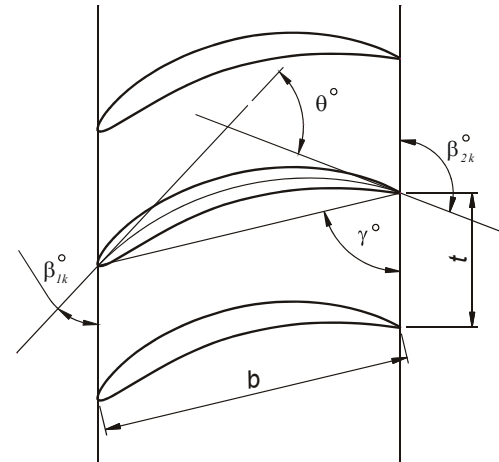
Fig. 1 Geometrical characteristics of the compressor cascades KP-33

In studies of the compressor cascades number Re, calculated from the rate before the cascades and the chord blades changed within $3*10^5$ <Re<$5*10^5$.

As the computational domain was chosen as part of a periodic cascade containing a single blade (Fig. 2), in which using the ICEM CFD computational grid was applied.
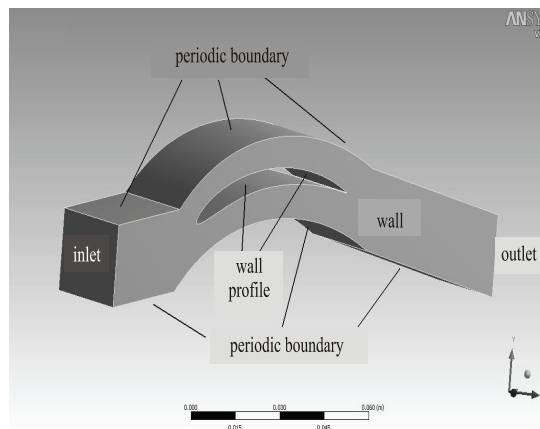
Fig.2 The computational domain

The computational grid in its structure a block-structured. The total number of elements of the computational grid is 1116747.

Boundary conditions were determined on all surfaces of the computational domain, and include conditions on the solid walls of the conditions at the inlet and outlet and periodiccal conditions. Boundary conditions on solid walls (blade surface) have been identified as a condition of sticking to a smooth adiabatic wall.

The boundary conditions at the entrance to the grid were set to fixation a static pressure (101325 Pa) static temperature (300 K), and the flow rate calculated by the number of λ

$$\lambda = \frac{c}{c_{\kappa p}} = \frac{c}{18,3\sqrt{T^*}}$$

The boundary conditions at the outlet of the cascade were set with the extrapolation of the flow parameters of the input parameters ("free outlet"). In the periodic boundaries of the computational domain, determined by the conditions of a periodic interface between the lateral sides of the computational domain of the cascade. Used for the calculation of viscous compressible gas model, which takes into account the viscosity of the flow and compressibility.

The criterion for convergence of the numerical calculations was the achievement of the residual mean square value at 10^{-5}, which was achieved in about 600 ... 800 time steps. The smaller value corresponded to steady airflow around the cascade, and the a great advanced in the presence of flow around the separation.

Studies were carried out at numbers Lambda $\lambda = 0,5$ and $\lambda = 0,6$. The results of calculations of characteristics of the cascades are shown in Fig. 3 and 4 in the form of dependency, where the *i*- the angle of attack, for models of turbulent viscosity *k-ε* (3a, 4a) and *SST* (Fig. 3b, 4b). The results of numerical simulations were compared with experimental data [7].
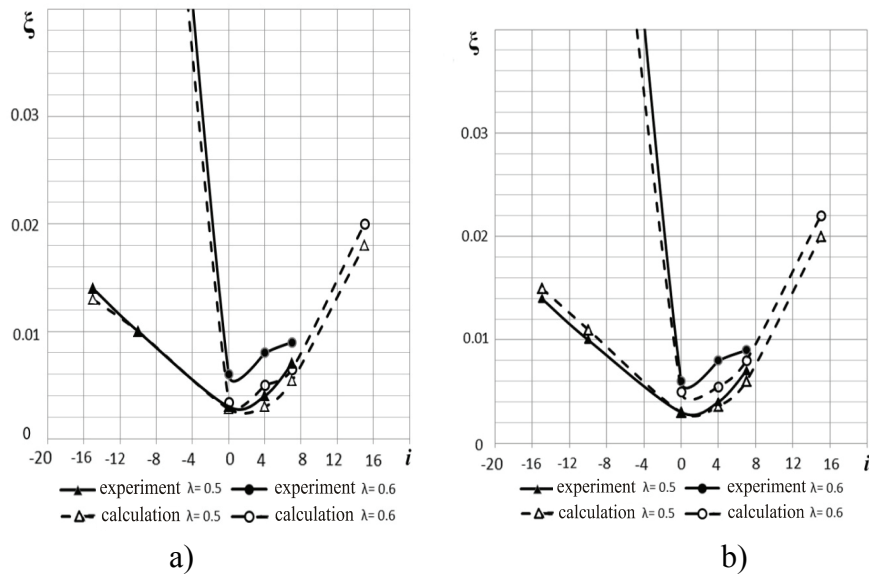
Fig. 3. The dependence of the total pressure losses on the angle of attack
a) turbulence model k-ε, b) the SST turbulence model
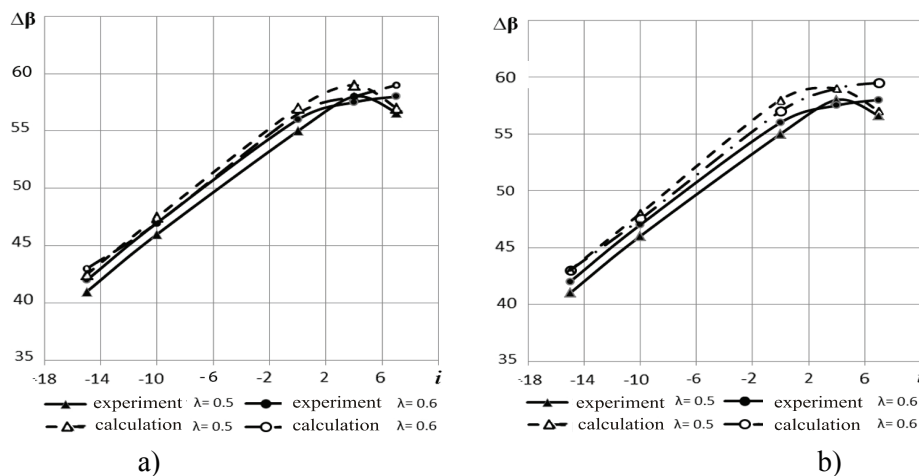
Fig. 4. The dependence of the angle of flow from the angle of attack
a)   turbulence model k-ε, b) the SST turbulence model

$i=-5^{\circ}$ $i=-5^{\circ}$

$i=0^{\circ}$ $i=0^{\circ}$

$i=7^{\circ}$ $i=7^{\circ}$

a)   b)
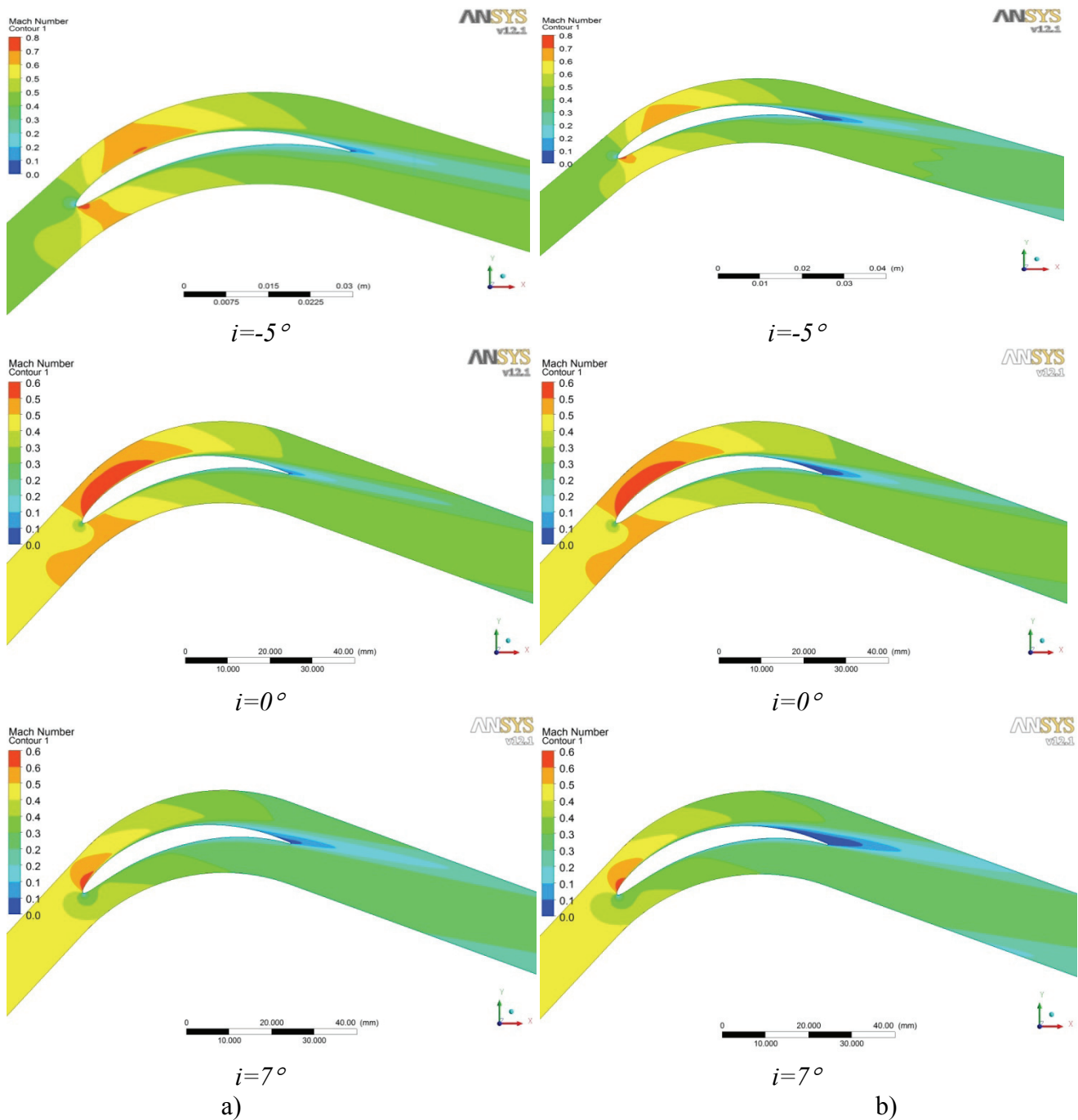
Fig. 5 Change of Mach number in blade channel
a) turbulence model k-ε, b) the SST turbulence model

Analysis of the results of the study showed that, in general, the use of a k-ε and SST model gives adequate results. The maximum error in estimating the total pressure loss in the case of λ = 0,5 and k-ε model was 34%, when using the SST model - 28%. In both cases the underestimation of the total pressure losses in comparison with experimental data on the positive angles of attack and the overstatement of losses on negative angles of attack (Fig. 3). With increasing number of λ there is a reduction of error. Thus, at λ = 0,6 and k-ε model, the maximum error was 12% and 14% SST model.

In assessing the angle of rotation of the flow is observed over-values compared with the experimental data using a k-ε model and SST. The maximum error at λ = 0,5 for k-ε model was 1.75% for the SST-1.1%. Change the number of λ on the error has almost no effect. Comparison of flow patterns in the blade channels showed that the use of SST eddy viscosity model is more intense eddies in the boundary layer (Fig. 5), and the nature of the flow close to the best of reality.

We also assessed the costs of temporary resources to perform the calculations of Table 1. The calculations were performed on a computer with the following parameters: CPU - CORE^{TM}i5; RAM -4 GB bit operating system - 64 bit.

Table 1

Estimated completion time to complete the calculations for a single angle of attack

Parameters	The model of turbulent viscosity	
	$k-\varepsilon$	SST
Number of steps	950	950
Time, h	22,8	32,5

From Table 1 shows that in modeling the flow in the compressor cascades using SST eddy viscosity model requires an average of 30% of the time compared with the k-ε model. Moreover, with increasing angle of attack increases time spent.

Conclusions

From the analysis of the results of modeling the flow in the compressor gratings using two known models of eddy viscosity k-ε and SST, it is clear that the use of SST model gives better agreement with experimental results. However, this increases by an average of 30% of calculation time. Thus, it can be used to approximate calculations of the initial k-ε model of turbulent viscosity (due to less time-consuming and fairly accurate), and for more detailed calculations - the model SST.

References

1. Аэродинамический расчет и оптимальное проектирование проточной части турбомашин / *Бойко А.В., Говорущенко Ю.Н., Ершов С.В., Русанов А.В., Северин С.Д.* – Х.: НТУ "ХПГ", 2002. – 356 с.

2. *Kolmogorov A.N.* Equations of turbulent motion of an incompressible fluid // Izvestia Academy of Sciences, USSR. – 1942. - Physics № 6. - P. 56-58.

3. *Wilcox D.C.* Reassessment of the scale-determining equation for advanced turbulence models // AIAA J. - 1988. - 26, № 11. - P. 1299-1310

4. *Jones W.P.* The calculation of low-Reynolds number phenomena with a two-equation model of turbulence / W.P. Jones, B.E. Launder // Int. J. Heat and Mass Transfer. - 1973. - 16, № 10. - P. 1119-1130.

5. *Bradshaw P., Ferris D.H., Atwell N.P.* Calculation of Boundary Layer Development Using the Turbulent Energy Equation // Journal of Fluid Mechanics. – 1967. - Vol. 28, Pt.3. - P. 593-616.

6. *СвечниковВ.С., КирилловА.Б.,* Аэродинамические характеристики компрессорных решёток // Труды ЦАГИ. –М.:БНТЦАГИ, 1957. – вып. № 142. – 56 с.

UDC 629.735.083.03(045)

V.V. Kozlov, Ph.D. (eng.), Y.M. Chokha, FullDoctor (eng.)
(National Aviation University, Ukraine)

METHODS AND PROBLEMS OF OPERATIONAL DIAGNOSING OF MODERN GAS-TURBINE ENGINES IN OPERATION

Analysis of existing methods of on-line diagnostics of gas turbine engines is given. Definition of methods of important scientific and applied problem of parametric control efficiency quality of parametric analysis is decrypted.

Introduction

Continuous improvement of the design of aircraft power plants (PP) of modern airplanes (AP), which include several engines of functional systems, intensification of work processes, which occurs whithin them, significantly exacerbates the problem of improving the efficiency of the processes of airplane operation (APO) and technical maintenance (TM).The most important role is played by the possibility of adequate operational evaluation by professionals of current technical condition (TC) of each instance of aircraft engine and deciding on the expediency of its further operation.

Diagnosis of airplane PP through a number of specific features of their design and operation has its own characteristic differences in determining the interaction of objects with methods and means of diagnosis, ie in construction of the control parameters and their analysis in APO and TM.The study of science and technology is subject of the work of many authors, among which pride place occupied by representatives of the research school of prof. L.P.Lozytskiy[1-7]. They are classical in the development of new methods of diagnosing modern gas turbine engines (GTE) using mathematical models and automated diagnostic systems in diagnosing PPin operation.Such attention to the problem of improving the efficiency of diagnosing complex dynamic aircraft technic (AT) objects is associated primarily with their high functional importance of ensuring the necessary level of flight safety and AP airworthiness.

Ways of GTE diagnosis improvement

Modern aircraft engines and their functional systems are complex dynamic technical objects.After their manufacturing and during regular use there is need for continuous monitoring of the current TC of each instance of the engine and making specific technical solutions.

Among the large number of existing methods and means of monitoring and diagnosing PP used in the process of APOand maintenance for the evaluation and management of the current TC, the most common is the constant parametric control of the registration data from embedded systems staff, followed by trend-controlled parameters of probabilistic methods of statistics. Collection and processing of information provided at this through the use of aviation board (such as MSRP, BASK, BUR, etc.), land (such as "Luch," "Analys", "Control", etc.) or land-board (type EIDS, HMAN, EXPERT, etc.) control and diagnostics systems (CDS) for typical AT objects.However, despite the fact that the vast majority of modern gas turbine engine is equipped with a small number of means of direct parametric measurement
[8] the efficiency of existing standard CDS and quality of analysis of parametric data remains high enough (Fig. 1 and 2).
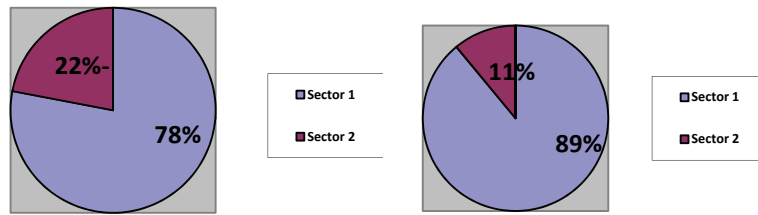
Fig.1. Level of control capability of considered types GTE: Sector 1 - low level, sector 2 - high level.

Fig.2. The degree of automation of diagnostics of aircraft gas turbine engines: Sector 1 - low, sector 2 - increased.

This leads to late detection of defects specific node (element) of these AT and to inability of personellto make adequate operational maintenance decisions.

The result is an increase in the number of failures and early termination of operation of aircraft engines and reduce of airplane safety. Methods of diagnosing turbine engine in flight, using the measured parameters [1,2,3] allows for the depth of their diagnosis only on the 1st level, ie the PP as a whole, without assessment of TC of units and elements of turbine engines and their functional systems.

Therefore particularly important and urgent issues for the aviation industry is to solve scientific and applied problems of efficiency and quality control parameters of the analysis of parametric data by creating theoretical foundations of decision support for operational in-depth diagnostics of modern power plants that are using automated tools and technologies providing support for the adoption of personnel technical solutions both in flight and in between flights while performing maintenance. Continuous degradation of unit and element TC of PP makes the implementation of the automated monitoring of their current level of airworthiness throughout the period of intended use very important. Possible solutions of this scientific and applied problem (SAP) with no significant structural PP improvements are the following: For radical increasing of control capability level:

• Increasing the number of direct measurements of parameters via embedded control systems, as well as technological covers of AT objects for the use of machine vision and methods of nondestructive testing;

• Using modular design in the design of PP;

• Widespread using of indirect methods of measurement in analytical modeling workflow;

• the optimal combination of direct and indirect measurements of parameters that characterize the work of nodes and elements of AT;

• use complex criteria informative and diagnostic indicators of AT TC and TC of its components and elements.

To significantly improve the quality of the analysis of parametric data and operational evaluation of TC of AT:

• Development and application of integrated land-board automated control systems;

• Develop and implement automated systems for diagnosing, monitoring of TC decisions using new software tools for providing information;

• evelopment of new calculation and information methods and means of automation of the process fo evaluation and management by personnel of aviation technical condition of AT.

Model of a comprehensive approach to diagnosing GTE

At the same time it provides a high level parametric informativeness and efficiency of management processes TC of specific instances of GTE, which are diagnosed at the expense of a more complete assessment of their individual characteristics. Evaluation of application of this approach shows the possibility of achieving a significant increase (by 50-80%) efficiency of

aviation facilities operation and the level of safety while significantly reducing (by 30-60%) the cost of their maintenance [1,3,4].

Modern methods, means and technologies of control and diagnostics GTE provides general control of TC in the APO and maintenance by continuous direct measurement of control parameters that characterize the modes of operation, evaluation of current TC of these objects and the adoption of appropriate personnel maintenance and technology solutions who sold it to specific instances of GTE during the whole period of operation. But this approach does not allow to fully ensure the airworthiness PP, and thus support a given level of reliability and safety. That is why the question of improving the methods and means of monitoring and diagnosing aircraft PP devoted considerable number of scientific and technical work [4]. However, insufficient attention is paid to the development and implementation of new methods of synthesis of the settlement and information control algorithm parameters, the expansion of informative and diagnostic framework CDS staff without their structural improvements, technology assessment of current operational node deep TC, the element of choice of effective representation of diagnostic information and airline personnel ensure a high level of automation and efficiency of operational technical solutions to ensure practical implementation of the strategy guide for the GTE technical condition with the parameter level control. The existing operational methods of diagnosing air vymirennym PP on the flight parameters is quite bulky, non-operational and do not fully take into account the complex influence of operational factors on the dynamics of degradation of the TS for each instance of the engine, which is diagnosed. This is primarily due to low control capability and parametric informativeness of majority GTE PP, operated on aircrafts of airlines of Ukraine and CIS countries, and low-aided information management processes of ensurace of their TC. n addition, one of the reasons that limited the possibilities of using new analytical methods for assessing TC, decision support and advanced information technologies that they are implemented, was the lack of on-board most aircraft automated CDS-based microelectronic computers. Therefore, commissioning of AP with modern means of objective control parameters, equipped with electronic systems for collecting and processing diagnostic information and the availability of workstations with PC at the airlines, offers prospects of new accounting methods and information depth operative diagnosis of GTE, technology and indicative of early reporting of malfunctioning units and elements of the PP and its implementation guide for the technical state of the control level parameters or to control the level of airworthiness [4].

Therefore particularly important and urgent issues for the aviation industry is the problem of diagnosing GTE. In this regard, proposed methodological model of complex computation-information approach (Figure 3) which provides for development of new automated diagnostic systems based on the knowledge base logical analytical methods, techniques, models and indicative of that realized by modern analytical technology knowledge engineering, testing and evaluation of their performance on specific types of gas turbine engines that are in operation, without significant structural improvements.
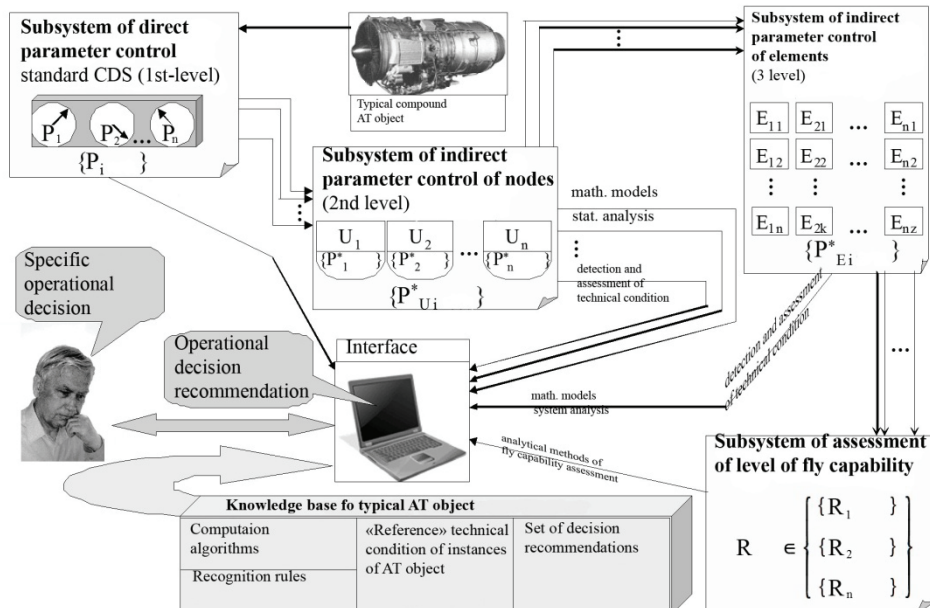
Subsystem of direct parameter control standard CDS (1st-level)

P_1 P_2 ... P_n
$\{P_i\}$

Typical compound AT object

Subsystem of indirect parameter control of nodes (2nd level)

U_1 U_2 ... U_n
$\{P^*_1\}$ $\{P^*_2\}$ ... $\{P^*_n\}$
$\{P^*_{Ui}\}$

math. models
stat. analysis
:
detection and assessment of technical condition

Subsystem of indirect parameter control of elements (3 level)

E_{11}	E_{21}	...	E_{n1}
E_{12}	E_{22}	...	E_{n2}
:	:		:
E_{1n}	E_{2k}	...	E_{nz}
$\{P^*_{Ei}\}$

detection and assessment of technical condition

Specific operational decision

Operational decision recommendation

Interface

math. models system analysis

analytical methods of fly capability assessment

Subsystem of assessment of level of fly capability

$$R \in \begin{bmatrix} \{R_1\} \\ \{R_2\} \\ \{R_n\} \end{bmatrix}$$

Knowledge base fo typical AT object

| Computaion algorithms | «Reference» technical condition of instances of AT object | Set of decision recommendations |
| Recognition rules | | |

Fig.3. Methodological model of an integrated approach to address the operational depth diagnosis of TC of GTE

Model of integrated assessment of technical condition of aircraft power plant in operation

Development and implementation of conceptual and methodological approaches to the implementation of new processes operative diagnosis of deep levels of modern gas turbine engines and their functional systems involves solving a series of scientific, technical and organizational problems. The first group of problems connected with the need to develop adequate analytical information and diagnostic models based on expert analysis of business processes and their regular services, the creation of new practices and technologies of identification of this type of TC structural units (elements) and their effective use in real operating conditions . It is clear that the growing technical diagnosis and improving its quality and efficiency associated with the use of methods (procedures), proposed for analyzing the fixed non-random small variations of values of controlled and calculated parameters and diagnostic features of structural units of individual instances of PP that are diagnosed. You must also solve a number of methodological issues related to linking depth diagnosis of the computational and information (CI) methods, modern technologies and means of displaying information and providing high quality analysis parameters.

Very important is the next group of problems related to the rationale for increasing existing levels of information and automation of processes and APO and maintenance of aviation facilities and the organizational ability to implement new techniques and technologies in the structure of their operational support. The most effective is an integrated approach [1,3,8]. On the one hand, it has already determined that the process of diagnosing depth parameter, which is a mandatory part of the process of operation of any modern aircraft objects (AT), to build on the basis of the most progressive strategy guide for AT TC that provides the closest relationship between the processes of APO and maintenance of each facility AT. This specificity of these tasks is the best use of airborne and ground-based automated regular CDS. It allows you to receive adequate initial amount of parametric information necessary to support the adoption of adequate aviation operational decision as to possible future safe use of each object AT, and ensuring the reduction of operating costs to support a given level of its airworthiness (AW).

On the other hand, the complexity of connections should be provided to facilitate regular operation of the processes of designing and producing these AT objects. It is well known that the current rating object's operation TC is a major factor in ensuring its security and maintain the level of AW, which are taken in the design process are provided in the process of mass production and are controlled and maintained in the process of regular use. Therefore, incorporation of these features when developing the conceptual model of the new computation and information

(integrated control and calculation - ICC) method operative in-depth diagnosis of complex dynamic object by using AT medium automated diagnosis and decision support (ASD PPR) as "EXPERT object AT "[3] provides the necessary complexity to solve these scientific-technical and organizational problems.

So one of the most promising and effective ways to solve existing problems to improve the quality analysis of parametric information in the course of current in-depth diagnostics of modern aviation PP low control capability and provide high speed adoption of adequate aviation maintenance solutions is the development of new complex RI methods of diagnosing the depth of a constructive node (item) that is realized in media specialized hybrid dynamic ASD PPR [9]. Given the above drawbacks of existing methods applied parametric diagnostics, offer new conceptual model (Fig. 4) of ICC method [3] operational depth evaluation of the current TC of a modern PP. It is based on the use of calculation algorithms informative diagnostic model (IDM) business processes common types of PP, as determined for the conditions of their serviceable TC, and for current conditions and faulty TC. This model serviceable TC instance PP, which is diagnosed, characterized by "reference" set of values of its parameters $\{P^*_{i\,\text{o}}\}$. Current TC of the same instance of PP is characterized by a set of current values of the same parameters $\{P^*_{i\,\text{пот}}\}$. When comparing the current and "reference" populations that are registered in certain well-established diagnostic modes copy of PP calculated a set of variations ("residuals") values of these parameters $\{\delta P^*_{i\,\text{пот}} = P^*_{i\,\text{пот}} / P^*_{i\,\text{о}}\}$. It used a special type of decision rules identify the current TC as this instance of PP as a whole ($K_{\Sigma\,\text{пот}}$) and its individual structural units (elements) by the sign of extremes and review the information ("portrait") diagnostic indicator of an individual node (item) ($K_{i\,\text{max/min}}$). As a result of this analysis produced specific operational solutions for aviation, which is based on the obtained current results identify the type of TC of diagnosed PP.

Thus, one of the main differences of the considered model of the existing approaches parametric trend diagnostic method is the use of conditional comparison IDM workflow object AT, which is in good ("a reference") TC with IDM workflow of the same object is in the current TC (Fig. 5).
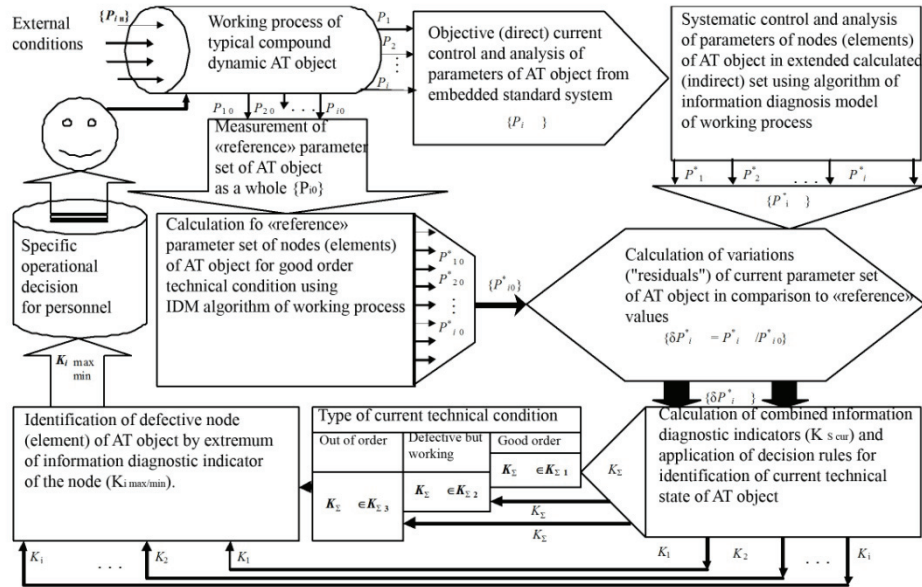
Fig. 4. A new conceptual model of integrated advanced surgical diagnosis of modern aircraft power plants
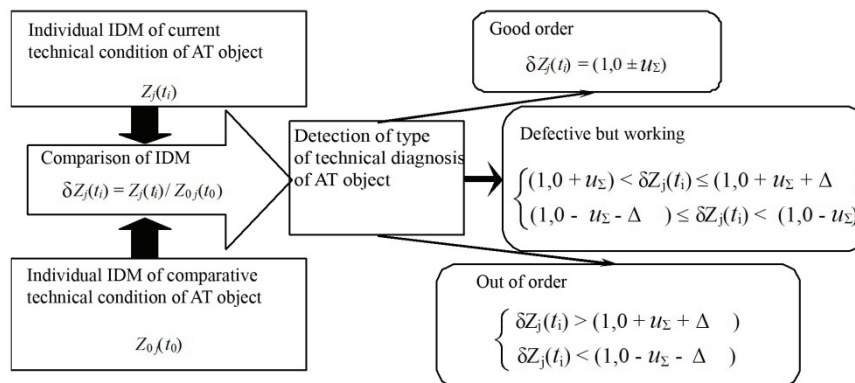
Fig. 5. Scheme of the method of conditional comparison IDM workflow instance of a typical PP

Analytic structure of the model conditional comparison of current IDM and "Reference" TC model object AT is the following:

$$\delta Z_j(t_i) = Z_j(t_i)/Z_0(t_0) = \delta\varphi_j\left[\delta x_j + \delta y_j + u_z\right],$$

where δx_j, δy_j – correspondingly the relative deviation of the current values measured and calculated parameters of the controlled object AO from their original ("standard") values corresponding to the specifications; u_z – total systematic error of measurement (calculation) of j-paramater of IDM.

Conclusion

Development and implementation of fundamentally new informative diagnostic automated systems currently in-depth monitoring and diagnosis of complex dynamic aviation facilities like power plants, can significantly enhance the implementation of more effective operational decision support technology aviation. Implementation of new accounting methods and information identifying specific performance damages units and elements of modern gas turbine engines running and functional systems to ensure their work in the early stages of development, can significantly improve the quality of the analysis of large amounts of parametric data and the effectiveness of specialized environments such as ASD CPD "Expert-GTE" and application of new instrumental and technological means of prevention and treatment of identified faults without structural improvements and demolition of power plants in regular operation.

References

1. *Лозицкий Л.П.* Оценка технического состояния авиационных ГТД /Л.П.Лозицкий, А.К.Янко, В.Ф.Лапшов. – М.: Транспорт, 1982. – 160 с.

2. *Лозицкий Л.П.* Автоматизированная система диагностирования ГТД АСД «Контроль-8-2У» /Л.П.Лозицкий, М.Д.Авдошко, И.И.Марченко. – Киев: КИИГА, 1986.-230 с.

3. *Кулик Н.С.* Параметрические методы оценки технического состояния ГТД в эксплуатации. /Н.С.Кулик. – Киев: КИИГА, 1993. – 139 с.

4.*Дмитриев С.А.*. Исследование влияния забоин на характеристики плоской охлаждаемой турбинной решетки. /С.А.Дмитриев, Н.С.Кулик, В.В.Козлов. //Обеспечение надежности авиационных двигателей в эксплуатации: Сб.научн.тр. –К.: КИИГА,1993.-С.40-43.

5. *Кулик М.С.* Математичне моделювання робочого процесу турбореактивного двигуна. /М.С.Кулик, В.В.Козлов, В.В.Пуляєвський, С.О.Осадчий. //Вісник Національного авіаційного університету. - 2001.-№3(10). - С.5-9.

6. *Козлов В.В.* До оцінювання технічного стану осьових компресорів газотурбінних ГПА. /В.В.Козлов, Л.Г.Волянська, С.О.Осадчий, С.В.Ізбаш. //Нафтова і газова промисловість.- 2002.-№3.-С.32-34.

7. *Чоха Ю.М.* Прикладні автоматизовані системи діагностування та підтримки прийняття експлуатаційних рішень: Методи, моделі, інформаційні технології: Монографія /Ю.М.Чоха, В.В.Кретов. – Київ: Ун-т Україна, 2010. – 488 с.

8. *Гаврилова Т.А.* Базы знаний интеллектуальных систем /Т.А. Гаврилова, В.Ф. Хорошевский. – С.-ПБ.: Питер, 2001. – 384 с.

UDC 629.7.036(075.8)

Y.Tereshchenko, Dr. of Sci. (Engineering) (National Aviation University, Ukraine)
V.Panin, Dr. of Sci. (Engineering) (Kyiv State Maritime Academy, Ukraine)
L.Volyanska., Ph.D.(Engineering) (National Aviation University, Ukraine)

METHOD OF DETERMINATION COMPRESSOR PERFORMANCES WITH AIR BLEED FROM MIDDLE STAGES

Method is proposed for calculating the compressor performances, in which parameters of tow groups of stages with different mass flow rate are considered instead separately consideration of a single spool compressor performance at an open bleed valves. The performances are shown as relation of head to flow coefficient. The method also allows to define the operation conditions of compressor cascade and other elements of gas turbine engine (GTE).

Introduction

Air release is an effective way to reduce the low-speed and starting effects. Air release basically is used when you start the engine. For air supply to the auxiliary units at cruising modes air is bled from the middle stages of the compressor of ships' power plants with gas turbine engine "Водолей".

At design the marine gas turbine engines it is needed to take into account such important parameters as the power output and dynamic stability. These parameters changes are a consequence of compressor performance changes.

At the present time to obtain the characteristics of compressors the closure of the bleed air valve BV known is accepted and a common characteristic for all modes that use the release air are built. Sometime two different characteristics (one - in the case of BV open, the other - case closed BV [1]) are built.

Review of existing methods for obtaining the characteristics of compressors with their changes in the release air flow path geometry changes is shown below.

In software systems GSR and GASTURB compressor characteristics are presented in tabular form and in system «ГРАД» parameter calculation of the axial compressor and a gas turbine is based on mathematical models of the third level of complexity. In calculation all the parameters are averaged over the cross section and are defined for the average diameter. The calculation of the compressor in system «ГРАД» is performed according to the fourth level mathematical model [2] which describes the working process in the compressor. The geometry of compressor is given at several radii. Influence of air bleeding from intermediate stages are taken into account in the mathematical model [3,4]. Two independent parameters are given as table, one for closed air bleed valve, the other - for the open valve. An open valve position sign i_{bv} is input parameter for the compressor calculation.

Formulation of the problem

The above methods of compressor parameters calculation the compressor spools were considered as one unit. But the air mass flow rate at the inlet and outlet compressor sections is not constant because there is air bleeding from the intermediate compressor stages. It is not possible to draw compressor characteristic then air bleed valve is open [5]. That's why it is necessary to consider separately the characteristics of two stage groups with different air mass flow rate.

Characteristics of the two consecutive compressors are considered instead of the single characteristic of a multistage compressor.

The characteristics of a multistage axial compressor with operating line and characteristics of the group stages with bypass air from the middle stages are shown on Fig.1. The design mode corresponds to a point P in Fig. la.

While in throttling the operating point moves through the operating mode line and reaches the position 0 corresponding to the minimum gasdynamic stability margin. Air bleeding starts at the point 0 and under further engine throttling the change of air parameters in the compressor is defined by two characteristics. The first characteristic is characteristic of first group formed from the first stages and second characteristic is characteristic of second group formed from last stages

(Fig. lb). At constant rotational speed the opening of compressor bleed ports leads to increase of air mass flow rate by ΔG in first group of stages and the working point on the characteristic moves from point 0 to point A in the line n_{np0}=const. The pressure ratio in the group of first stages π_{K1}^{*} decreases, gasdynamic stability margin increases.
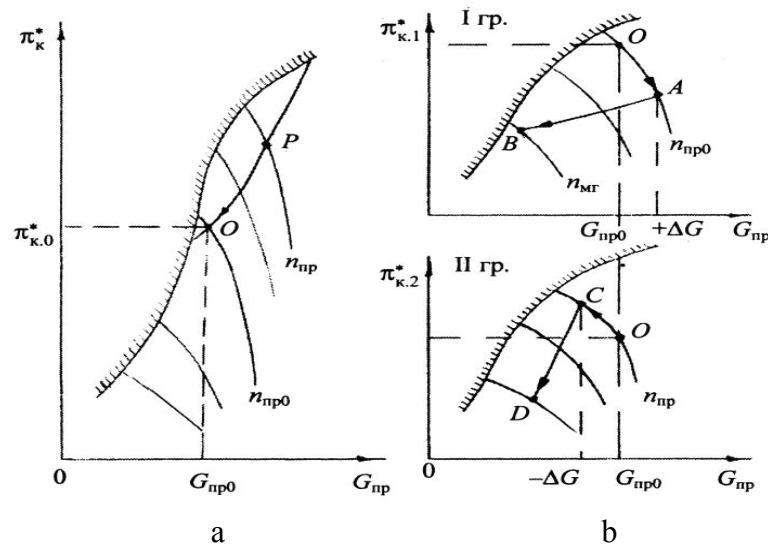

Fig.1. Characteristics of multistage compressors:
a – compressor characteristics without air bleeding; b – the characteristics of groups compressor stages
with air bleeding from the middle stages

The operating point 0 on the characteristic line of last stages group shifts into point C. The pressure ratio of this group π_{K2}^{*} increases and gasdynamic stability margin decreases. While operating mode reduces to idling power parameters of group of first stages shift through the line AB, parameters of last group of stages shift through the line DC.

The purpose of this paper is development of compressor characteristic calculation method at the air bleeding presence.

Compressor characteristic calculation method

To calculate characteristics of GTE with open compressor bleed ports it is necessary to determine conditions of joint operation of compressor spool and other elements of engine. So the characteristics of first and second stages must be determined.

The axial velocity at the compressor inlet increases after open bleeding valves. Increase of axial velocity leads to decrease pressure ratio in this stage π_{cTI}^{*}, that produces additional increase of axial velocity at the inlet of second stage. The axial velocity at the inlet of second stage increases by ΔC_{aII}

$$\Delta C_{\text{aII}} = C^{`}_{\text{aII}} - C_{\text{aII}} = C_{\text{aII}} \left[ (\pi^{`}_{\text{cTI}}/\pi_{\text{cTIp}})^{1/\,k-1} \right],$$

where $C^{`}_{\text{aII}}$, $C_{\text{aII}}$ – axial velocity of previous and current stages; $\pi^{`}_{\text{cTI}}, \pi_{\text{cTIp}}$ – actual and estimated values of the pressure ratio of fist stage.

Increase of the axial velocity produces decrease of flow swirl in compressor rotor wheel of second stage by

$$\Delta(\Delta W_{\text{uII}}) = \Delta C_{\text{aII}} (ctg\beta_2 - ctg\alpha_1),$$

where β_2– relative flow angle, α_1 – absolute flow angle.

The work of second stage decreases by $\Delta L_{\text{cTII}} = U\Delta(\Delta W_{\text{uII}})$, where U is blade speed. In other words, change of parameters next stage is caused not only by deformation of initial characteristic,

but air mass flow change $\Delta \overline{C}_a = \dfrac{\Delta \overline{C}_a i}{U}$ caused by previous stage parameter changes. Change temperature of stagnated flow brings to change reduce circumferential tip speed next stage $U_{\text{кпр}}$. Since small change of value U does not bring to change stage characteristics [6] then parameters of each compressor stage are related with next function dependences $\overline{H} = f(\overline{C}_a, \gamma)$, $\eta^* = f(\overline{C}_a, \overline{H})$; where $\overline{H} = L_{\text{см}} / u_{\text{к}}^2$ – coefficient of expended work; γ – parameter characterizing change of stage characters.

For calculation the initial and changed parameters of compressor stages are used as relations $H = f(\overline{C}_a)$ and $\eta^* = f(\overline{C}_a)$. Initial compressor parameters $\left(\pi_{\text{к}}^*\right)_{\text{вих}}$, $\left(\tau_{\text{к}}^*\right)_{\text{вих}}$, $\left(G_{\text{впр}}\right)_{\text{вих}}$, $\left(n_{\text{пр}}\right)_{\text{вих}}$ and geometry and kinematic ($D_{\text{кi}}$, F_i, $\alpha_{\text{вхi}}$) parameters are got from gasdynamic compressor calculation. Calculation consists of two parts. Changes of compressor stage parameters under air bleeding are calculated first then calculation is performed with changed parameters.

Then characteristics of two groups of compressor stages are obtained and states of operating points are determined from engine mathematical model, the total pressure ratio and efficiency of compressor spool are calculated. The total pressure ratio is product of pressure ratios of stage groups. Efficiency is determined from formula:

$$\eta_{\text{к}}^* = \frac{L_{\text{ад.к}}}{\left(\dfrac{L_{\text{ад.к1}}}{\eta_{\text{к1}}^*} + \dfrac{L_{\text{ад.к2}}}{\eta_{\text{к2}}^*}\right)},$$

where $L_{\text{ад.к}}, L_{\text{ад.к1}}, L_{\text{ад.к2}}$ –adiabatic work of compressor and stage groups respectively.

If air bleeding is in one section then efficiency is calculated as

$$\eta_{\text{к}}^* = \frac{T_{\text{в}}^*\left(T_{\text{к}}^{*\frac{k-1}{k}} - 1\right)}{\left(T_{\text{к}}^* - T_{\text{в}}^*\right) + \dfrac{\Delta G_B}{G_{\text{в}} + \Delta G_{\text{в}}}\left(T_{\text{пер}}^* - T_{\text{в}}^*\right)},$$

where где $T_{\text{к}}^*$ - stagnation flow temperature behind compressor; $\Delta G_{\text{в}}$ - mass of bleeding air; $T_{\text{пер}}^*$ - stagnation flow temperature of bleeding air.

Conclusions

The method alloys to obtain characteristics of multistage compressor then bleed valves open. Consider compressor composed of two groups of stages the total pressure ratio and efficiency of multistage compressor with air bleeding are determined.

References
I. Романовський Г.Ф., Тарасенко А. А., Построение характеристик компрессоров с устройствами перепуска воздуха с помощью обобщенных зависимостей / Г.Ф. Романовський, А.А. Тарасенко // Авиационно - космическая техника и технология.-2011.- № 9 (86)- С. 51-54.
2. Програмный комплекс ГРАД (Газодинамические Расчеты Авиационных Двигателей) [Электронный ресурс]. - Режим доступа: http: //grad. kai.ru.
3. Проектирование авиационных газотурбинных двигателей: учебник для вузов / А.М. Ахмедзянов, Ю. С. Алексеев, Х.С. Гумеров и др.; под. Ред. А.М. Ахмедзянова. - М.: Машиностроение, 2000. - 454с.
5. Терещенко Ю.М. Теория авиационных газотурбинных двигателей. /Ю.М. Терещенко, Л.Г. Волянская, М.С. Кулик, В.В. Панин. - К: Книжное издательство НАУ, 2005. - 500с.
6. Казанчан П.П. Метод расчета параметров многоступенчатого компрессора при заданном изменении характеристик его ступеней // ЦИАМ. I960. Технический отчет № 144. - 11 с.

Voznyuk A.P.
(National Aviation University, Ukraine)

RADIAL CLEARANCES INFLUENCE ON GAS TURBINE ENGINES OF AIR AND GROUND APPLICATION MAIN PARAMETERS.

The paper deals with gas turbine engine flow channel geometrical parameters changes due to radial clearance in the compressor and turbine during the long operation. The proposed method of assessing the impact of these changes on engines transit modes and practical measures to eliminate adverse effects.

Entry

During extended service live of gas turbine engine the process of geometric parameters change results a shift of workflow characteristics.

Diagnosing and troubleshooting that arise due to these processes is very difficult due to slow percolation of degradation processes and the complexity of the altered characteristics. Despite the slow progress and relative obscurity degradation processes take effect on almost all engine characteristics.

Problem

It is known that the most informative in terms of diagnosis are transitional modes turbine engine.

To date, relatively little attention paid to modeling of transient modes of gas-turbine engines. But we know that the signs of engine characteristics change at the first place shown on transition mode. This contradiction is explained by the fact that transiency transients prevented obtaining the necessary diagnostic information using on-board systems of accumulation and control. The situation began to change after the emergence of digital control systems and storage media, which replaced the old on-board tools.

Get information in real time with high frequency and short period of processing options allows the use of dynamic models of aircraft gas turbine engines to meet the challenges of diagnosis. For improving the accuracy of the diagnosis requires consideration of factors such as changes in geometrical parameters of the flow during prolonged use.

Solution

Analysis of modified engines the same structural scheme, but with different absolute values of their parameters, shows that the relative deviation of key data on their values specifications are the same. The above enables use of statistics of different engines to establish general patterns of parameters changes during operating time [2].

These geometric parameters as nozzle area turbine units are essential, those that directly affect the data base engine (thrust and specific fuel consumption). The value of radial clearance is not affected directly based engine data, and their impact on defining parameters such as compressor efficiency and turbine stages.

Foreign companies and airlines, since GTE earlier generations, carefully study the impact of attrition on the performance and operational reliability of the engines. For example, the company "Pratt-Whitney" surveyed the effects of wear on the compressor motor JT3D characteristics and stability on engine starting mode [3].

To determine the radial changes during operation we use exponential regression equation:

$$\Delta\delta(\tau) = Ae^{\frac{\alpha}{\tau}},$$

(1)

where A and α - constant coefficient.
To find the constant coefficients A and α least-squares method to minimize the expression:

$$Q = \sum_{i=1}^{n} \left[\lg \Delta\delta(\tau) - \lg A + \alpha \frac{1}{\tau_i} \lg e \right]^2 \quad (2)$$

After differentiation cut Equations (2) and the corresponding transformations we obtain relations for the determination of lg A and α.

$$\lg A = \cfrac{\cfrac{\sum\limits_{i=1}^{n} \lg \Delta\Pi(\eta)}{n - \cfrac{\left(\sum\limits_{i=1}^{n} \cfrac{1}{\eta}\right)^2}{\sum\limits_{i=1}^{n} \cfrac{1}{\tau_i^2}}}}{} \left[1 - \cfrac{\sum\limits_{i=1}^{n} \cfrac{1}{\tau_i} \lg \Delta\Pi(\tau_i)}{\sum\limits_{i=1}^{n} \lg \Delta\Pi(\tau_i)} \cdot \cfrac{\sum\limits_{i=1}^{n} \cfrac{1}{\tau_i}}{\sum\limits_{i=1}^{n} \cfrac{1}{\tau_i^1}} \right];$$

$$z = 2{,}302 \cfrac{1}{\sum\limits_{i=1}^{n} \cfrac{1}{\tau_i}} \left[n \lg A - \sum\limits_{i=1}^{n-1} \lg \Delta\Pi(\tau_i) \right], \quad (3)$$

The values included in equations (3), carried out by the number of experimental points n.

It is necessary to establish a link between changes in the value of radial clearance and defining parameters (efficiency compressor stages). .

To solve this problem use the relation given in [1]

$$\delta\eta_K^* = -K_1 z_K \left(2{,}8 \frac{(\overline{\delta} - 0{,}01)}{\eta_{cn.o}^*} + \frac{\delta\varepsilon_{TP}}{K_2} \right), \quad (4)$$

where K_1 and K_2 - coefficients of influence [6]; Z_K – number of stages in cascade; $\overline{\delta}$ - the relative value of radial clearance; $\delta\varepsilon_{TP}$ - relative deviation ratio of losses by increasing the degree of surface roughness of blades. Value of $\delta\varepsilon_{TP}$ associated with the relative roughness of blades the following relation:

$$\delta\varepsilon_{TP} = \frac{(0{,}05 - 0{,}08)\varepsilon^{0{,}25}\left(\frac{b}{A}\right)}{\varepsilon_{TP.0}} - 1, \quad (5)$$

Where b - blade chord; A – width between blade channel; $\delta\varepsilon_{TP}$ - Initial value of the coefficient of losses.

Using formulas (4) and (5), we can continue to evaluate how changing the basic parameters of the engine and workflow options for stationary and transient conditions of GTE.

Due to the properties of materials radial gaps between the shoulder blades and stator compressor and turbine are changed as a result of heating units running of the engine. It is important to remember that largest thermal load acting on the turbine blades and nozzle apparatus. It is very important is the development and application of methods of cooling blades and stator parts of the compressor and turbine.

In most cases, the cooling air in the turbine taken from low pressure compressor. The following relation is important: larger selection of air from the internal circuit, the lower the efficiency of the engine. It is therefore necessary to take cooling air from an external circuit. This pre-compression of cooling air can be made in some compressors. Design and development of such

systems, the selection is not yet complete. But raising fuel efficiency by reducing engine bleed air for cooling can be achieved by improving turbine blades cooling. In patent No US 2004/0151587A1. authors suggest instead of the traditional method of cooling and design of turbine blades, use "micro-circulation" cooling system.

In the traditional method of cooling air carts through the holes in blade shank, served in the internal longitudinal profile, and then goes partly to the holes in the final section, later in the tract for gas (convective cooling method). However, the convective efficiency of the method is not enough high, as 90-s of the last century began to use film cooling. This method of cooling air is derived through the holes in the front and creates a film to avoid direct contact of hot gases with the surface of the blade.

Despite the high efficiency cooling, this method has a significant drawback: the effective thickness of the profile increases the thickness of film cooling. Consequently, the degree of efficiency decreases, which affects the fuel efficiency of the engine. Therefore, there appropriateness of use of convective cooling method in, but at a new level: instead of 3.4 radial canals, as was the traditional method (Fig. 1.1), using highly developed system of "micro-circulation" channels below the surface of the blade (Figure 1.2).
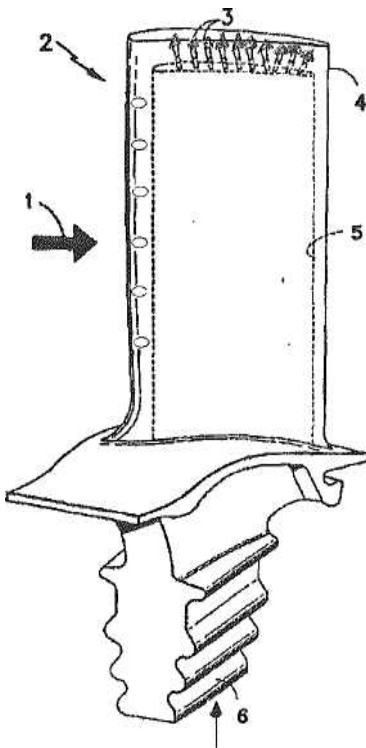
Fig. 1.1 Example of rotor blade with traditional cooling system
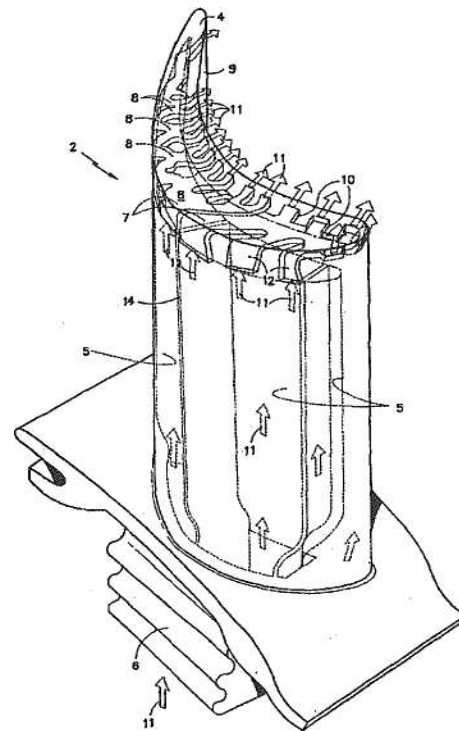
Fig. 1.2 Example of rotor blade with "micro-circulation" cooling system

This method of cooling avoids shortcomings of traditional methods (convection and film), to provide reliable cooling blades without increasing the effective thickness profile and the resulting gain increasing efficiency of the turbine. Analytical expressions to describe the impact the efficiency of stages based on GTE working process parameters may be obtained by solving systems of equations describing the motion of the rotors and the conditions of operation elements engine transient conditions[6].

$$\frac{dn_j}{dt} = \frac{N_{Tj} - N_{Kj} - \Delta N_j}{(\pi/30)^2 J_{zj} n_j};$$

$$G_{Kj} - G_K (j+1) - \Delta G_{Kj} = 0;$$ \hfill (6)

$$G_{K.3.} + \sum_{i=j}^{N} \Delta G_{c.a.i} + \sum_{i=j+1}^{N} \Delta G_{pKi} - G_{rj}\left(\pi_{Tj}, \tau_{uj}\right) = 0;$$

$\Phi\left(F_C\right)=0$; $\Phi_1\left(g_n\right)=0$;   } control laws in the transition process.

where n_j - rotational speed of the j-s rotor; N_T and N_{Kj} - power turbine and compressor rotor j- s rotor; ΔN_j - Power of the shaft shown in the j-s rotor; J_{zj} - Moment of inertia of the j-s rotor; G_{Kj} and G_{K3} - air losses in compressor j-s stage and in combustion chamber; $G_{rj}\left(\pi_{Tj}, \tau_{uj}\right)$ - gas losses determined by the characteristics of each turbine stage; $\Delta G_{CA.j}$ and ΔG_{pKj} - amount of air flow for cooling blades of the machine nozzle and impeller j-s stage turbine; g_Π - relative fuel consumption; F_C - area of the nozzle.

Solutions of equations are carried out after setting the initial conditions, such as options on the idle power by using a standard program of integration of differential equations.

Changes in efficiency of stages directly affect the output value of these stages, which are a system of equations (6).

Conclusions

The suggested approach allows to take into account and numerically describe the effects of changes in radial clearance in GTE compressor and turbine on degradation processes. Integrated application of the proposed method and technical solutions allows you to create the conditions for significant improvement in engine parameters during continuous operation.

References

1.*Панин В.В., Чумак О.Ч., Ратынский В.В., Шевченко М.А.* Анализ корреляционных связей термодинамических и геометричиских параметров ГТД// Авиационно-космическая техника и технология

2.*Бутончников А.П.* О влиянии нароботки в летной эксплуатации на ухудшение параметров двухконтурных турбореактивных двигателей /*А.П.,.Бутончиков, Е.Д.Нестеров, С.С. Акимов, Э.Л.Симкин*// Труды ЦИАМ №:731, 1976. – 11 с.

3. *Arnold B.R., Gast J.R.* A cooperative airline program to evaluate engine parts aging effect on a current turbofan engine model.SAE «Preprints»,s.a., №700329,10 pp.,ill. Экспресс-информация ВИНИТИ, Воздушный транспорт, 1971, №16

4.Инженерные расчеты газотурбинных двигателей методом малых отклонений /А.Я.Черкез - М.: Машиностроение, 1975.-380 с.

5. Динамика авиационных ГТД / *Г.В.Добрянский, Т.С.Марьянова* – М.: Машиностроение, 1989.-240 с.

6. Неустановившиеся режимы работы авиационных газотурбинных двигателей / *Сосунов В.А.,Литвинов Ю.А.* – М.: Машиностроение, 1975.-216 с.

UDC 621.452.3 (045)

M.Y. Bogdanov
I.A. Lastivka Ph.D., associate professor
I.F. Kinaschuk Ph.D., associate professor
G.N. Nikitina Ph.D., associate professor
(National Aviation University, Ukraine)

ANALITICAL METHOD OF AN EXPERIMENTAL COMPRESSOR STAGE BLADE ROW CONSTRUCTION

In research presented methodology of blade row construction according to the gas-dynamic calculation. This methodology permit at first approximation obtain coordinate of section face and tray of blade row subject to angles of setting, profile curvature, profile thickness ration by height o blade row.

Introduction

This article tells us about one of the approaches of axial flow compressor blade row construction. The idea of the analytical method of calculation is the geometry of given profile specified with the help of some primary profile size definition. By blade row height calculation data made primary profile geometry calculation, subject to angles of setting, profile curvature, profile thickness ratio by height of blade row.

Analysis of researches and publications

Up-to-date methods of blade rows flow calculation of axial-flow compressor allows basically define only qualitative figure of process that take in channel of interscapular row. That's why definition of inverse problem on basis of gas-dynamic calculation data doesn't allows getting a scape of blade row that satisfied actual aerodynamic properties.

Data of gas-dynamic calculation, for example, by the help of finite-difference equation is used in general for the account some physical events those are difficult and sometimes impossible to investigate by experiment. Practically in all cases are required an experimental researches for finishing prototype models of impeller machine elements.

Pretty much all optimization problem of axial-flow compressor air-gas channels design consist of at the prime with inverse one-dimensional calculations and radius calculations of blade row parameters with the subsequent organization of blade row. At the heart of axial-flow compressor blade row profile geometry organization as often as not base original profile with task geometry that profile can be symmetrical or asymmetrical [1].

Methods of blade row profiles design considered in works [1, 2 and 3] and others. All of them are based on graphic and grapho-analytical methods of axial-flow compressor stage can be based summarized characteristics of axial-flow compressor planar gratings or mode stage. Also provide blades smoothing blade rows geometry during the research. In any cause for take an experiment we need to have blade rows with technical characteristics satisfied the performance specification.

Profiling of blade rows could have done by gas-dynamic calculation of axial-flow compressor, by arbitrary diameter and calculation of the flow parameter by blade height.

During a blades design we can take as design section (fig.1) at the blade tips and at the root usually take section that locate on 2…4 mm by the exit edge of blade from radial flow section to the direction of pitch diameters [1].

Centerline of reference profile bent so that bend angles leading and trailing edges χ_1 and χ_2 (fig.2) are fit with calculation. The bent of centerline can be performed on a circle arch, a parabola or some other selected law.

In elementary compressor blade rows with consists of profiles, distinguish the following angles:

- constructive angle at the inlet, β_1';
- inlet flow angle, β_1;
- constructive outlet angle, β_2';
- outlet flow angle, β_2;
- bend profile angle, Θ;
- delay profile angle, δ;
- angle of flow alteration in row, $\Delta\beta$;
- angle of profile setting, γ;
- attack angle, i;
- angle between tangent to the profile centerline at the leading edge and chord, χ_1;
- angle between tangent to the profile centerline at the trailing edge and chord, χ_2.
Also the important parameters of a cascade are:
- profile chord, b;
- array spacing, t;
- distance between grate forward and back front edge, S.

Problem statement

The idea of analytical method of calculation lies in the fact that geometry of desired profile defined by the way of some desired profile size recalculation.

Task solution

The task of preliminary profiling of compressor blades with the help of reference aerodynamic profiles could be divided on two parts: profile centerline construction and blade row construction at its height. Analytic construction of blade profile centerline that curved along the arc of parabola is done using the equation

$$y(i) = \frac{bx(i) - x(i)^2}{2Ax(i) + c}, \qquad (1)$$

where $A = 0,5(ctg\chi_2 - ctg\chi_1)$, $c = b \cdot ctg\chi_1$, i – the number of original symmetrical profile sections to coordinate χ.

In some cause of blade centerline design provide by circular arc with the help of equation

$$y(i) = a(x(i) - x(i)^2), \qquad (2)$$

where $a = tang\left(\frac{\Theta}{2}\right)$, Θ – angle of centerline profile.

Next, we need to specify the reference symmetrical profile. For example, on fig.3 showed reference symmetrical profile №2$\left(\bar{C}_{\text{пр}} = 12\%\right)$ [1].

Coordinate of section face of profile and profile and profile tray can calculate, using following procedure. Definition of profile suction face and profile tray possible by the way of normal equation using to curve in points $\{x(i); y(i)\}$

$$y - y(i) = -\frac{x - x(i)}{f'x(i)}, \qquad (3)$$

where y, x – straight line current value that is normal to profile centerline in point $\{x(i); y(i)\}$.

Fig.1. Calculation scheme of blade row

Fig.2. Gas-dynamics and kinematics parameters of plane grating

x	y_c	y_x	y_{cp}	h
0	0	0	0	0
1,25	1,89	-1,89	0	5,78
2,5	2,62	-2,62	0	5,24
…	…	…	…	…
…	…	…	…	…
90	1,45	-1,45	0	2,90
95	0,81	-0,81	0	1,62
100	0	0	0	0

Fig.3. Scheme and geometry characteristics of original symmetrical airfoil section

1.13.48

The first derivative of equation (2) will have the appearance

$$. \qquad (4)$$

Then equation (3), take $\qquad$, have another view

$$. \qquad (5)$$

Distance from centerline along the normal to profile section face (fig. 4) could define from equation

$$, \qquad (6)$$

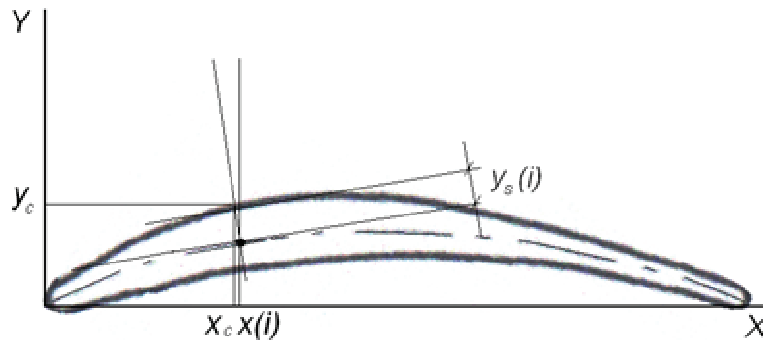where $\qquad$ – value of i^{-th} ordinate of symmetrical profile.

Fig.4. Scheme of arc-shaped airfoil profile

In cause when an original profile is asymmetrical, then perpendicular to the chord isn't simultaneously a perpendicular to the centerline. This observation is easily taken into account during arc-shaped airfoil profile design.

Solving the equations (5) and (6) we can obtain a value of arc-shaped airfoil profile suction and tray coordinate

$$\overline{\qquad} ;$$

$$\overline{\qquad} ;$$

$$\overline{\qquad} ;$$

$$\overline{\qquad} .$$

After transfer coordinate system in the center of gravity of arc-shaped airfoil profile (fig.5) or axis system, that is used during blade machining, suction face and tray define like

$$;$$
$$;$$
$$;$$
$$.$$

Knowing the angles of setting of the height blade rows profiles, coordinates suction faces and trays sections of blade rows define with the help of equations

$$,$$
$$,$$
$$,$$
$$,$$

where – angle of setting of a profile on blade row height, – number of section of blade row on a height.

If thickness of blade row profile changes in blade height, for example, by linear law

$$\overline{\hspace{3cm}},$$

then coordinates of symmetrical profile suction face and tray by the row section define from equation and should be accounted during the definition of profile coordinate on blade row height
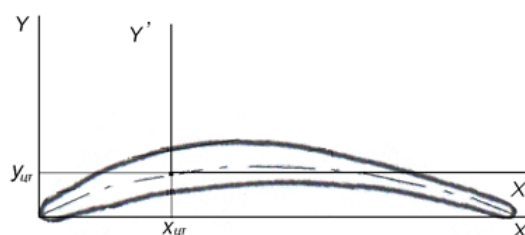

Fig.5. Scheme of coordinate grid transfer

During experimental stage design of axial-flow compressor we could also provide blades rows of stage rotor and guide vanes with the help of staples that are installed to the platform with cavities (fig. 6). Using the graphite powder can help us to design the model of blades row oven which in consequence form is designed and by the form we can get the necessary quality of guide vanes blade row and stage rotor for blading of axial-flow compressor experimental plant stage.

Conclusion

Proposed methodology of blades row design could get coordinates of blade row back and

launder with account of profile row angles of setting at every one radius and also could help to design the example we can design form for producing necessary quantity of blades for blading, for example, experimental axial-flow compressor stage.

a)

b)

Fig.6. Platform with staples for turbomachine blades row design

References

1. *Холщевников К.В.* Теория и расчет авиационных лопаточных машин. – М.: Машиностроение, 1970 г., 610 с.

2. *Терещенко Ю.М.* Газодинамический расчет ступени компрессора и турбины газотурбинного двигателя. – К.: КВВАИУ, 1974., 78 с.

3. *Юрин А.В.* Выбор основных параметров и расчет осевого многоступенчатого компрессора. – Куйбышев: КАИ, 1970., 103с.

UDC 621.43.018

D.V. Kondratiev (National Aviation University, Ukraine),

THE ESTIMATION OF THE TECHNICAL CONDITION OF THE POWER TURBINE OF THE CONVERTIBLE AIRCRAFT ENGINE

In this paper the authors proposed to make the estimate of the technical condition of the power turbine's flowing part of the gas turbine power plant with a convertible aircraft engine using the adiabatic turbine efficiency.

Introduction

Currently, one of the solutions to create gas turbine plants (GTP) to drive the gas compressor units (GCU), widely used conversion of the aircraft gas turbine engines. This is effected by changing the nodes associated with the appointment of a new product (front-line unit of the combustion chamber, fuel and control system), change type of the fuel and the appearance a power turbine in a converted engine, with about 70 ... 75% of the basic units and parts of the base engine remains [1].

A changing of the power turbine efficiency directly affects the power output of the GPT. This turbine is designed to drive a centrifugal compressor.

A case of the changing the value of the power turbine efficiency is a deterioration of the technical condition of the turbine's flowing part.

Given the above, assessment of technical condition of the power turbine is important.

The estimation of the technical condition of the power turbine's the flowing part of the GPT is conveniently performed by means of adiabatic efficiency. It only takes into account the internal losses in the turbine that is characterized by the perfection of gas-dynamic flow of the turbine [2].

Statement of the Problem

The formula for the adiabatic turbine efficiency is of the form [3-5]:

$$\eta_{ts} = \frac{T_1^* - T_2}{T_1^* \left[1 - \left(\dfrac{P_2}{P_1^*} \right)^{\frac{k-1}{k}} \right]}, \qquad (1)$$

where T_1^*, P_1^* - stagnation temperature and pressure at a turbine inlet; T_2, P_2 - static temperature and pressure at an outlet of the turbine.

Equation (1) is not very convenient for GCU mark: GCU-C-6.3 (a convertible engine D-336-2, NK-12ST and DT71), GCU-C1-16S (with convertible engine DG-90) and other, because at these types of the GCU of the pressure measurement is not made of the gas flow at the inlet and the outlet of the power turbine. Therefore, adapting the formula (1) for the gas turbine where no measurements on the pressure of the gas flow before and after the power turbine [6, 7].

Determination of the adiabatic turbine efficiency on temperature ratio

The relationship between temperature and pressure in the polytropic (real) expansion process is as follows:

$$\frac{T_1}{T_2} = \left(\frac{P_1}{P_2} \right)^{\frac{n-1}{n}}, \qquad (2)$$

where T_1, P_1 - temperature and pressure at the beginning of the polytropic process, T_2, P_2 - temperature and pressure at the end of polytropic expansion; n - the polytropic index.

Assume that the parameters of the gas flow, P and T have got the elementary increment in the process of adiabatic expansion. Then we'd have [2]:

$$\frac{P+dP}{P} = \left(\frac{T+dT_{ad}}{T}\right)^{\frac{k}{k-1}}. \tag{3}$$

Lay out the right-hand side of (3) in a series and neglecting terms of second and higher order terms, we obtain

$$\frac{dP}{P} = \frac{k}{k-1} \cdot \frac{dT_{ad}}{T}. \tag{3'}$$

Denote the efficiency of the elementary process by η. Then, substituting $\dfrac{dT_{ad}}{T} = \dfrac{dT}{\eta}$ in (3'):

$$\frac{dP}{P} = \frac{k}{k-1} \cdot \frac{dT}{T \cdot \eta} \tag{4}$$

or after integration (with $k = $ const and $\eta = $ const):

$$\frac{P_2}{P_1} = \left(\frac{T_2}{T_1}\right)^{\frac{k}{(k-1)\eta}}. \tag{5}$$

For the power turbine (5) with (2) will be written as follows [2, 8]:

$$\frac{P_2}{P_1^*} = \left(\frac{T_2}{T_1^*}\right)^{\frac{k}{(k-1)\eta_{TS}}}. \tag{6}$$

Substituting (6) in (1):

$$\eta_{TS} = \frac{T_1^* - T_2}{T_1^*\left[1 - \left(\left(\dfrac{T_2}{T_1^*}\right)^{\frac{k}{(k-1)\eta_{TS}}}\right)^{\frac{k-1}{k}}\right]} = \frac{T_1^* - T_2}{T_1^*\left[1 - \dfrac{T_2}{T_1^*}^{\frac{1}{\eta_{TS}}}\right]}.$$

Finally,

$$\eta_{TS} = \frac{1 - \dfrac{T_2}{T_1^*}}{1 - \left(\dfrac{T_2}{T_1^*}\right)^{\frac{1}{\eta_{TS}}}}. \tag{7}$$

Equation (7) is quite difficult to apply in practice, since the right-hand side of the equation lies in the degree of the adiabatic turbine efficiency.

We'll introduce a coefficient $a = 1/\eta_{TS}$ and will make some assumptions. Taking into account that according to the gas turbine theory, the adiabatic turbine efficiency for the gas turbine plant for terrestrial applications in the range of 0,88-0,92 [5], will accepted it averaged value of the coefficient:

$$a = \frac{1}{0,9} = 1,111.$$

Given this assumption, equation (7) becomes:

$$\eta_{TS} = \frac{1 - \dfrac{T_2}{T_1^*}}{1 - \left(\dfrac{T_2}{T_1^*}\right)^{a}}. \tag{8}$$

Adiabatic efficiency in small deviations
Logarithm of expression (8):

1.13.53

$$\ln(\eta_{TS}) = \ln\left(1 - \frac{T_2}{T_1^*}\right) - \ln\left(1 - \left(\frac{T_2}{T_1^*}\right)^a\right);$$

After differentiate and converting the expression to determine $d\eta_{TS}/\eta_{TS} = \delta\eta_{TS}$ obtain:

$$\delta\eta_{TS} = K_1\left(\delta T_1^* - \delta T_2\right), \tag{9}$$

where $K_1 = \dfrac{\dfrac{T_2}{T_1^*}\cdot\left[1 - \left(\dfrac{T_2}{T_1^*}\right)^a\right] - a\cdot\left(\dfrac{T_2}{T_1^*}\right)^a\left(1 - \dfrac{T_2}{T_1^*}\right)}{\left(1 - \dfrac{T_2}{T_1^*}\right)\cdot\left[1 - \left(\dfrac{T_2}{T_1^*}\right)^a\right]}.$

Thus, the expression (9) describes the effect of temperature at the turbine inlet and the outlet turbine, on change the adiabatic power turbine efficiency.

A method of the estimate of the technical condition of the power turbine's flowing part

The estimate of the flowing part of the power turbine is carried out by comparing the actual value of the adiabatic power turbine efficiency to the baseline (standard) by its value. In another words, compared the technical condition of the reduced flowing part of the power turbine to the technical condition, defined as the standard.

In this case, proposed to use the coefficient of the technical condition of the power turbine based on the adiabatic turbine efficiency ($K\eta_{TS}$).

During the deterioration of the technical condition of the gas turbine plant is a reduction of its rated power, then to account for this fact we introduce the coefficient of the technical condition based on power of the gas turbine plant (K_{Ne}).

The coefficient of the technical condition of the power is the ratio of the actual power of the gas turbine plant (N_e^a) to its standard value (N_e^s):

$$K_{Ne} = \frac{N_e^a}{N_e^s}.$$

Thus, the coefficient of the technical condition based on the adiabatic power turbine efficiency will be:

$$K\eta_{TS} = \frac{\eta_{TS}^a}{\eta_{TS}^s}\cdot\frac{1}{K_{Ne}},$$

where η_{TS}^a - the actual value of the adiabatic power turbine efficiency; η_{TS}^s - the standard (base) value of the adiabatic power turbine efficiency.

Calculation of errors

The relative error inherent in the coefficient a will defined, based on the fact that the range of the adiabatic turbine efficiency is from 0.88 till 0.92:

1) $\delta a = \dfrac{(0,88 - 0,9)}{0,9}\cdot 100 = -2,22\%$;

2) $\delta a = \dfrac{(0,92 - 0,9)}{0,9}\cdot 100 = 2,22\%$.

Thus, the error is embedded in the coefficient a is $\pm 2,22\%$.

We define a relative error of the adiabatic turbine efficiency of the measurer. A temperature of the gas flow at the turbine inlet and the outlet of it are measured by thermocouples TCA during the operation of the GTP, according to [7]. Absolute error of the thermocouple TCA is $2 \div 3$ degrees.

The formula for determine the relative error of the adiabatic turbine efficiency is as follows:

$$\delta\eta_{ts} = \sqrt{\left[100\cdot\Delta T_1^* \cdot\frac{\partial}{\partial T_1^*}\ln\left(\frac{1-\dfrac{T_2}{T_1^*}}{1-\left(\dfrac{T_2}{T_1^*}\right)^a}\right)\right]^2 + \left[100\cdot\Delta T_2 \cdot\frac{\partial}{\partial T_2}\ln\left(\frac{1-\dfrac{T_2}{T_1^*}}{1-\left(\dfrac{T_2}{T_1^*}\right)^a}\right)\right]^2} \ .$$

After differentiate and converting the expression to determine $d\eta_{\text{TS}}/\eta_{\text{TS}} = \delta\eta_{\text{TS}}$ obtain:

$$\delta\eta_{ts} = \sqrt{\left(100\cdot\Delta T_1^* \cdot K_2\right)^2 + \left(100\cdot\Delta T_2 \cdot K_3\right)^2} \ , \tag{10}$$

where $K_2 = \dfrac{a\cdot\left(\dfrac{T_2}{T_1^*}\right)^a\left(1-\dfrac{T_2}{T_1^*}\right) - \dfrac{T_2}{T_1^*}\cdot\left[1-\left(\dfrac{T_2}{T_1^*}\right)^a\right]}{\left[1-\left(\dfrac{T_2}{T_1^*}\right)^a\right]\left(T_1^* - T_2\right)}$; $K_3 = K_2 \cdot \dfrac{T_1^*}{T_2}$.

Checking the adequacy

As mentioned above, the gas compressor units with convertible aircraft gas turbine engines is not possible to measure the pressure of the gas flow at the inlet and the outlet of the power turbine, so to verify the adequacy and accuracy of all previous assumptions perform a comparative analysis for the GCP type GT-750 with a nominal power 6 MW. The parameters at the nominal operation of the power turbine of this type of the GCU are presented in Table 1.

Table 1

Parameters of the power turbine of the GCU grade GT-6-750

Parameter	Value
The temperature at the inlet (T_1^*), ^{0}K	803
The outlet temperature (T_2), ^{0}K	693
Inlet pressure (P_1^*), MPa	0,2
The temperature at the outlet (P_2), MPa	0,103

The results of the calculation of the adiabatic power turbine efficiency by (1) and (8), where were adopted by the assumptions presented in Table 2. In determining the relative error of the measuring instruments it was assumed that the temperature measured by a thermocouple TCA with a maximum absolute error of 3^0, and the pressure measured using a digital pressure-vacuum gauge with an adapter with an absolute error of 0.2 kPa [6, 7].

Table 2

Comparative analysis

Parameter	is defined by:	
	(1)	(8)
The adiabatic efficiency of the power turbine	0,902	0,907
The relative error of the measuring instruments	3,6%	0,03%

The relative error of the adiabatic power turbine efficiency GCU type GT-6-750 from the accepted assumptions will be:

$$\delta\eta_{\text{TS}} = \frac{|0,902 - 0,907|}{0,902}\cdot 100\% = 0,6\% \ .$$

The relative deviation of the adiabatic power turbine efficiency is defined to the adopted coefficient a (see (8)) from the adiabatic power turbine efficiency to its true value (see (7)) for the GCU type GT-6-750. The value of η_{TS} (7) will be:

$$\eta_{\text{тs}} = \frac{1 - \dfrac{693}{803}}{1 - \left(\dfrac{693}{803}\right)^{\frac{1}{0,902}}} = 0,909 \ .$$

Thus, the deviation will be:

$$\delta\eta_{\text{тs}} = \frac{\left|0,909 - 0,907\right|}{0,909} \cdot 100\% = 0,22\%$$

An error in the determination of the adiabatic power turbine efficiency of the GCU type GT-6-750, taking into account the deviation and the coefficient, which was previously calculated and is equal to ± 2.2%, will be:

$$\delta\eta_{\text{тs}} = \sqrt{0,03^2 + 0,6^2 + 2,2^2} = 2,2\%$$

As can be seen from the last calculation, the error in the determination is not large and is approximately 2% for the power turbine of the GCP type GT-6-750, while the relative error of the measuring instruments for the adiabatic power turbine efficiency is 3.6 %, which determined by (1).

Conclusion

1. The formula for determining the adiabatic turbine efficiency by using the temperature ratio at a power turbine input and an output of it was obtained.

2. The influence of temperature on the inlet and the outlet of the power turbine to the change in the adiabatic turbine efficiency in small deviations was taken into consideration.

3. The method for estimate of the technical condition of the power turbine of the GTP with converted aircraft engine was developed. This method based on the adiabatic turbine efficiency as a diagnostic criterion.

4. The formula for determining accuracy of the adiabatic power turbine efficiency of the measurer was obtained

5. The errors on accepted assumptions in determining the adiabatic power turbine efficiency with the temperature at the inlet and the outlet of the turbine were determined.

References

1. *Гриценко Е.А.* Конвертирование авиационных ГТД в газотурбинные установки наземного применения / *Е.А. Гриценко, В.Л. Данильченко, С.В. Лукачев, В.Е. Резник и др.* – Самара: СНЦ РАН, 2004. – 266 с.

2. *Абианц В.Х.* Теория авиационных газовых турбин [Текст] / *В.Х. Абианц* – М.: Оборонгиз, 1953. – 216 с.

3. *Антонюк Л.М..* Теория газотурбинных двигателей [Текст]: Учеб. пособие. Часть 1: Газогенераторы, входные и выходные устройства / *Л.М. Антонюк, В.С. Марусенко* – М:1998, - 161с.

4. *Кулик М.С.* Теорія компресорів і газотурбінних установок [Текст] : Навч. посібник. / *М.С. Кулик, В.Г. Моца, М.І. Шпакович* – К.: НАУ, 2002.– 219 с.

5. *Михальцев В.Е.* Теория и проектирование газовой турбины [Текст]: Учеб. пособие. Часть 1: Теория и проектирование ступени газовой турбины / *В.Е. Михальцев, В.Д. Моляков.* – М.: МГТУ им. Н.Э. Баумана, 2006. – 104 с.

6. Компресорні станції. Контроль теплотехнічних та екологічних характеристик газоперекачувальних агрегатів: СОУ 60.3-30019801-011:2004. – [Чинний від 2004 – 12 – 22]. – К. : ДК «Укртрансгаз», 2004. – 117 с.

7. *Гаврилків В.М.* Теплотехнічне діагностування газоперекачувальних агрегатів з газотурбінним приводом / *В.М. Гаврилків, С.Л. Левченко, С.О. Цуркан* – К.: Четверта хвиля, 2009. – 88 с.

8. *Поршаков Б.П.* Газотурбинные установки / *Б.П. Поршаков, А.А. Апостолов, В.И. Никишин* – М.: ГУП «Нефть и газ» РГУ нефти и газа им. И.М. Губкина, 2003. – 240 с.

CONGRESS SECRETARIAT
National Aviation University,
1, Kosmonavta Komarova ave.,
Kyiv, 03680, Ukraine
Tel: +38044 406-71-56
Fax: +38044 406-72-12
e-mail: aviacon@nau.edu.ua
Congress homepage: